BNL-104423-2014

RIKEN/RBRC Workshop
Approach to Equilibrium in Strongly Interacting Matter
April 2-4, 2014

Proceedings of RIKEN BNL Research Center Workshop

Volume 118

RBRC
RIKEN BNL Research Center

Disclaimer

This work was prepared as an account of work sponsored by an agency of the United States Government. Neither the United States Government nor any agency thereof, nor any of their employees, nor any of their contractors, subcontractors or their employees, makes any warranty, express or implied, or assumes any legal liability or responsibility for the accuracy, completeness, or any third party's use or the results of such use of any information, apparatus, product, or process disclosed, or represents that its use would not infringe privately owned rights. Reference herein to any specific commercial product, process, or service by trade name, trademark, manufacturer, or otherwise, does not necessarily constitute or imply its endorsement, recommendation, or favoring by the United States Government or any agency thereof or its contractors or subcontractors. The views and opinions of authors expressed herein do not necessarily state or reflect those of the United States Government or any agency thereof.

Notice: This manuscript has been authored by employees of Brookhaven Science Associates, LLC under Contract No. DE-AC02-98CH10886 with the U.S. Department of Energy. The publisher by accepting the manuscript for publication acknowledges that the United States Government retains a non-exclusive, paid-up, irrevocable, world-wide license to publish or reproduce the published form of this manuscript, or allow others to do so, for United States Government purposes.

Preface to the Series

The RIKEN BNL Research Center (RBRC) was established in April 1997 at Brookhaven National Laboratory*. It is funded by the "Rikagaku Kenkyusho" (RIKEN, The Institute of Physical and Chemical Research) of Japan and the U. S. Department of Energy's Office of Science.

The Memorandum of Understanding between RIKEN and BNL, initiated in 1997, has been renewed in 2002, 2007 and 2012.

The Center is dedicated to the study of strong interactions, including spin physics, lattice QCD, and RHIC physics through the nurturing of a new generation of young physicists.

In April 2013, Dr. Samuel Aronson was named Director of the Center, preceded by Nicholas Samios and T.D. Lee.

The RBRC has theory, lattice gauge computing and experimental components. It is presently exploring the possibility of an astrophysics component being added to the program. The RBRC Theory, Computing and Experimental Groups comprise a total of approximately 42 researchers. Positions include the following: full-time RBRC Fellow, half-time RHIC Physics Fellow, and full-time Postdoctoral Research Associate. The RHIC Physics Fellows hold joint appointments with RBRC and other institutions and have tenure track positions at their respective institutions. To date, RBRC has over 10 graduates (Fellows and Post-docs) of whom approximately 70 percent have already attained tenure positions at major institutions worldwide.

Beginning in 2001 a new RIKEN Spin Program (RSP) category was implemented at RBRC. These appointments are joint positions of RBRC and RIKEN and include the following positions in theory and experiment: RSP Researchers, RSP Research Associates, and Young Researchers, who are mentored by senior RBRC Scientists. A number of RIKEN Jr. Research Associates and Visiting Scientists also contribute to the physics program at the Center.

RBRC has an active workshop program on strong interaction physics with each workshop focused on a specific physics problem. In most cases all the talks are made available on the RBRC website. To date there are over 100 proceedings volumes available.

A series of high performance computers has been designed and built by individuals from Columbia University, IBM, BNL, RBRC, and University of Edinburgh, with the U.S. DOE Office of Science providing infrastructure support at BNL. QCDSP, a 0.6 teraflops parallel processor, dedicated to lattice QCD, was begun at the Center in February 1998, was completed in August 1998, and was decommissioned in 2006. It was awarded the Gordon Bell Prize for price performance in 1998. A 10 teraflops RBRC QCDOC computer funded by RIKEN, Japan was unveiled on May 26, 2005. QCDOC was decommissioned in May 2012. The next generation computer in this sequence, QCDCQ (600 Teraflops), is currently operational and is producing important simulations of fundamental processes in nuclear and particle physics. Recent $K^0 \rightarrow pp$ results were awarded the Ken Wilson Prize in 2012.

Samuel H. Aronson, Director
April 2014

* Work performed under the auspices of U.S.D.O.E. Contract No. DE-AC02-98CH10886.

Introduction

The purpose of this Workshop is to critically review the recent progress on the theory and phenomenology of early time dynamics in relativistic heavy ion collisions from RHIC to LHC energies, to examine the various approaches on thermalization and existing issues, and to formulate new research efforts for the future.

Specific topics we plan to address include:

- **Experimental evidence for equilibration/isotropization**. What do the latest experimental results say about these questions? How model (in)dependent are these conclusions? Since the pressure isotropization is important for hydrodynamics, is there a way to assess the longitudinal pressure from measurements?
- **Comparison of various approaches**. Various tools and approaches have been employed to study thermalization: kinetic theory, 2-particle irreducible formalism, classical statistical field theory, strong coupling techniques such as AdS/CFT,... Do their range of applicability overlap? How do they compare (in terms of ease of application, and in their results)?
- **Dependence on the initial conditions and couplings**. Typically, the late time behavior of a system confined in a fixed volume will only depend on the conserved quantities, regardless of the details of the initial conditions. However, transient regimes will differ in general. When a system is free to expand in empty space, is there still a (partial) loss of details about the intial conditions? Are there various limiting regimes, depending on initial conditions and/or values of couplings? In heavy ion collisions, the initial conditions just after the collision are characterized by a strong coherent color field surrounded by small fluctuations. What is the role played by this coherent field? What is the role of plasma instabilities, in particular, at later stages of the evolution?
- **Turbulent cascades and Bose-Einstein condensation**. Various studies performed in toy scalar models have shown that, if the initial condition is overpopulated, turbulent cascades may form and the particle excess can condense in the zero mode. This excess is gradually destroyed later on by inelastic processes. In heavy ion collisions, the initial condition is similarly overpopulated, but elastic and inelastic processes are parametrically of the same order in the coupling in contrast to the scalar field theory case. How does the formation of turbulent cascades and the question under which conditions a Bose-Einstein condensate could form compare between scalar and non-Abelian gauge field theory? What roles do the inelastic processes play during the evolution of a non-Abelian gauge field system with initial overpopulation?

Contents

Presentations:

Maximilian Attems .....*Instabilities in non-Abelian expanding plasmas*
Jean-Paul Blaizot.....*Jets in quark-gluon plasmas; Turbulent QCD cascade; Bottom-up thermalization*
Kirill Boguslavski.....*Universality far from equilibrium and the range of validity of classical-statistical simulations*
Thomas Epelbaum.....*Early isotropization of the quark gluon plasma*
Stefan Floerchinger.....*Isotropization from color field condensate in heavy ion collisions*
Kenji Fukushima .....*Real-time stochastic quantization: Problems and simulations*
Vicenze Greco .....*Isotropization, condensation and elliptic flow in a kinetic approach with a Q_s scale*
Ulrich Heinz.....*Viscous fluid dynamics for anisotropically expanding fireballs*
Michal Heller.....*The approach to hydrodynamics in holographic gauge theories*
Xu-Guang Huang.....*Thermalization and transient BEC: Effect of the inelastic processes*
Barbara Jacak.....*Thermalization: An experimentalist's view*
Yin Jiang.....*Medium effect on glasma evolution*
Aleksi Kurkela.....*UV cascade of over-occupied gluons*
Tuomas Lappi .....*Spatial Wilson loops in the glasma*
Larry McLerran.....*The glasma and thermalization: Ups and downs*
Akira Ohnishi.....*Entropy production in the classical Yang-Mills theory as the coherent-state dynamics*
Jan Pawlowski .....*Non-equilibrium dynamics of gauge theories, and transport coefficients*
Owe Philipsen.....*Lattice calculation of a second order transport coefficient of hydrodynamics*
Paul Romatschke .....*Strong coupling far-from-equilibrium thermalization for 'nuclei'*
Bjoern Schenke .....*Geometry and fluctuations in large and small nuclear collision systems*
Soeren Schlichting.....*Turbulent thermalization process in heavy-ion collisions*
Denes Sexty.....*Non-equilibrium Bose-Einstein condensation in scalar and gauge systems*
Edward Shuryak.....*QCD strings and equilibration in high multiplicity pA,pp collisions*
Michael Strickland .....*Anisotropic hydrodynamics: Recent progress*
Naoto Tanji .....*Quark production in classical statistical field theory*
Derek Teaney.....*Fluctuation-dissipation in equilibrating SYM plasma*
Bin Wu .....*Quark production, Bose-Einstein condensates and thermalization of the quark-gluon plasma*
Bin Zhang.....*The roles of elastic vs inelastic scatterings in thermalization*

Agenda

List of Registered Participants

Additional RIKEN BNL Research Center Proceeding Volumes

Presentations

Back to Contents

Instabilities in non-Abelian expanding plasmas

Maximilian Attems

University of Barcelona

The Approach to Equilibrium in Strongly Interacting Matter

Motivation

Filamentation instability

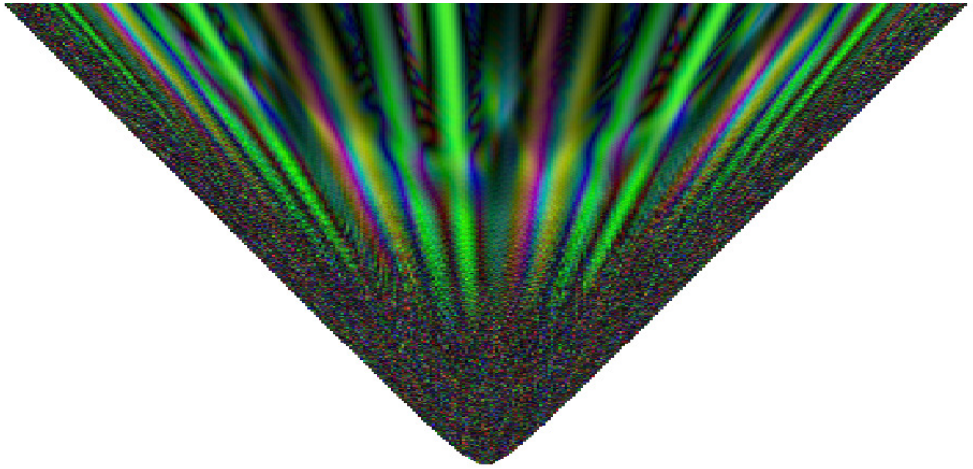

[MA, Rebhan, Strickland 2008]

Motivation

Filamentation instability

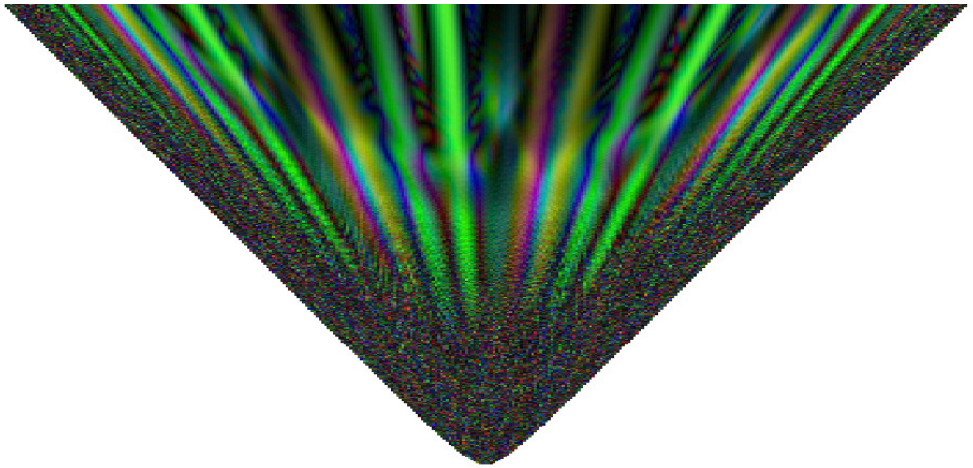

[MA, Rebhan, Strickland 2008]

- Hard Thermal Loop (HTL)
  $\alpha_s \approx 0.3$

Motivation

Filamentation instability

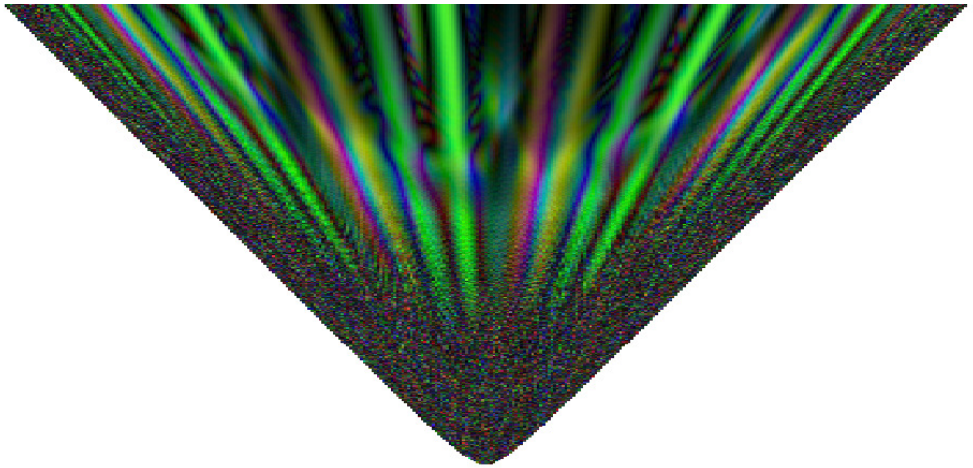

[MA, Rebhan, Strickland 2008]

- Hard ~~Thermal~~ Loop (H~~T~~L)
  $\alpha_s \approx 0.3$
- Real-time physical quantities of non-equilibrium processes

Motivation

Filamentation instability

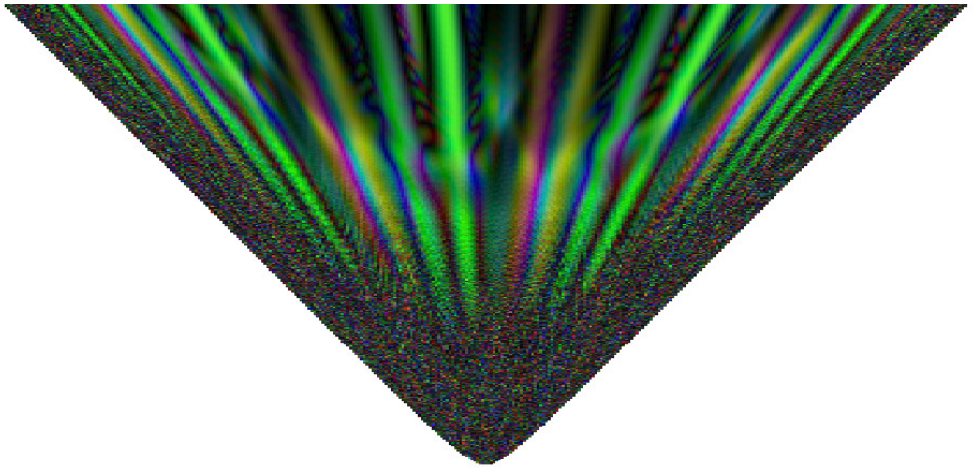

[MA, Rebhan, Strickland 2008]

- Hard ~~Thermal~~ Loop (H~~T~~L) $\alpha_s \approx 0.3$
- Real-time physical quantities of non-equilibrium processes
- Plasma turbulence affects parton transport (isotropization, jet energy loss, viscosity,..)
- Derivation of time scales for isotropization, thermalization

Stages of an heavy ion collision

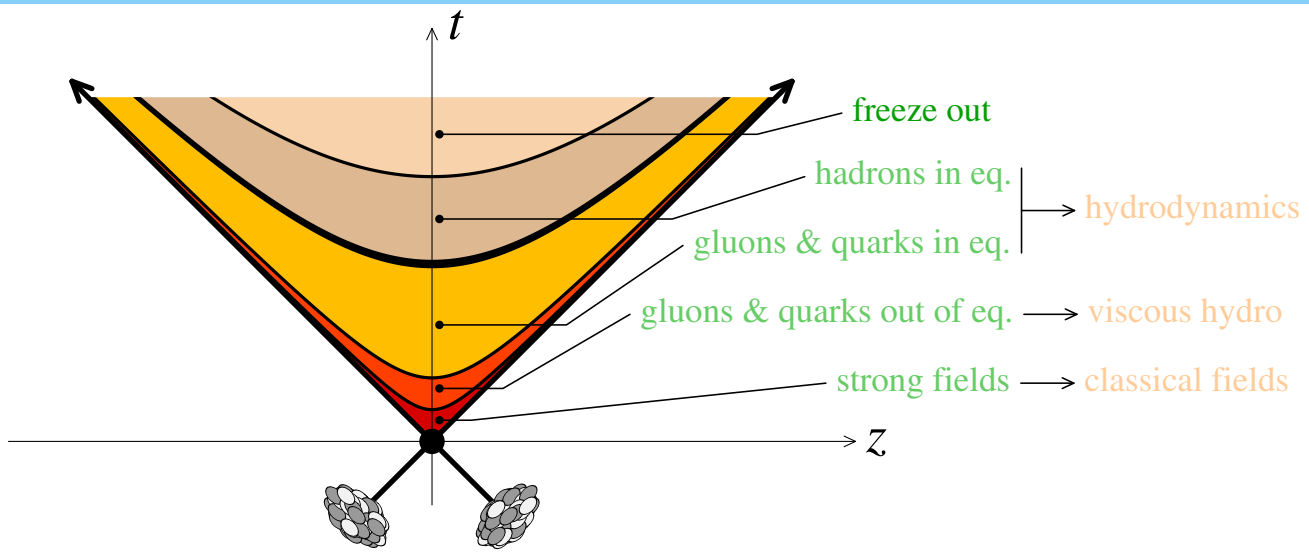

[Gelis 2006] Illustration of the stages of a heavy ion collision.

Stages of an heavy ion collision

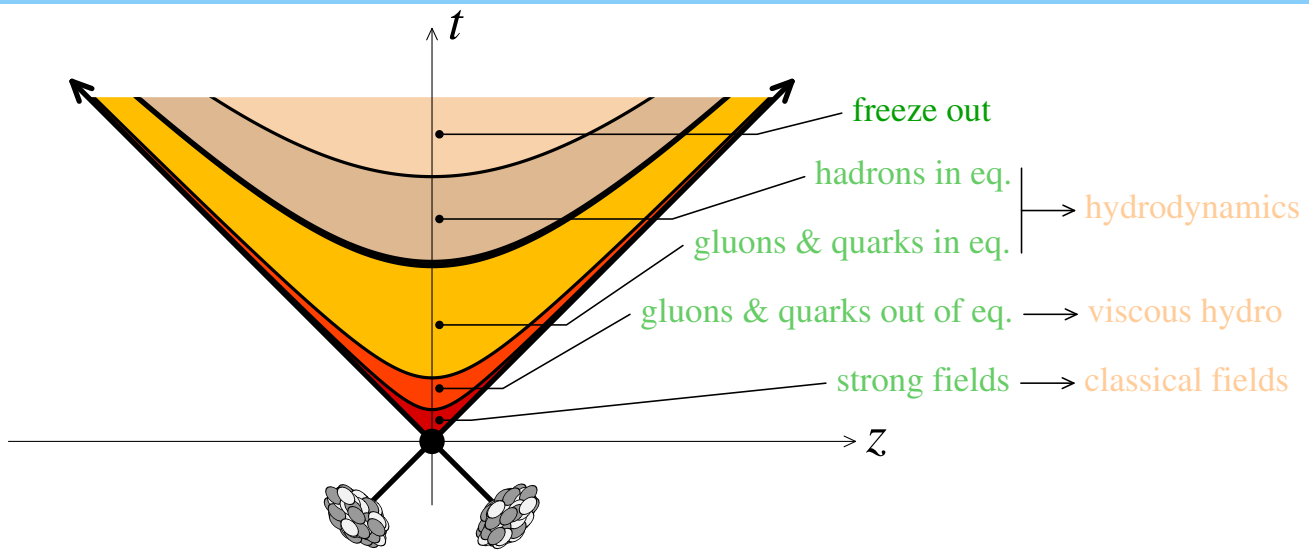

[Gelis 2006] Illustration of the stages of a heavy ion collision.

Numerical approaches to early phase with strong fields:

1. Numerical solution of Yang Mills equations in real-time: [Romatschke, Venugopalan; Berges, Sexty; Gelis, Fukushima; Dusling; Dumitru, Nara, Schenke; Moore, Kurkela; Sexty; Epelbaum; Schlichting, Boguslavski]
2. Hard Loop Simulation (Eikonalized particles): [Strickland, Romatschke, Rebhan; Arnold, Lenaghan, Moore; Mrowczynski; Rummukainen, Bödeker; Ipp, Attems; Deja]

Outline

1 SU(3) Yang Mills Box
- Stages of a heavy ion collision
- Equation of motions
- Energy density
- Pressure
- Energy density spectra
- SU(2) versus SU(3)

2 Chromo-Weibel instability
- Scales of wQGP
- Weibel instabilities
- Bjorken expansion
- Unstable modes growth rate
- Yang-Mills Vlasov
- Energy densities
- Pressures
- Spectra

EOM

Yang-Mills equations in conjugate field momenta $E^\mu = \partial_t A_\mu$

$$\begin{aligned} \partial_t E^3 &= -D_i F^i{}_3 \,, \\ \partial_t E_i &= -D_j F^{ji} - D_3 F^{3i} \,. \end{aligned}$$

with the Gauss law constraint

$$0 = D_3 E^3 + D^i E_i \,.$$

Gauge symmetry check with $g \in \mathrm{SU}(3)$

$$U_\mu(x) \to g(x) U_\mu(x) g^{-1}(x + a_\mu)$$

Energy density

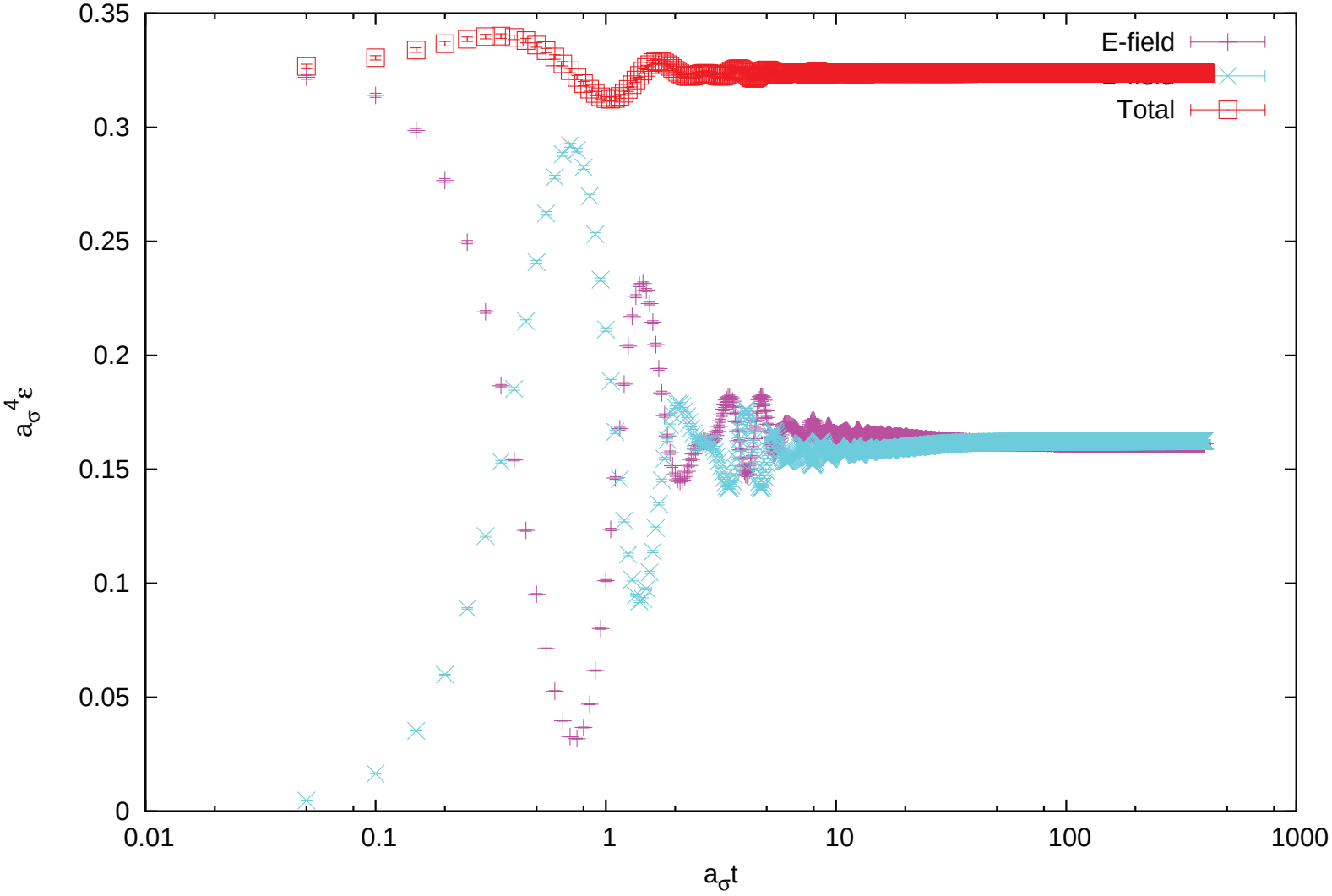

CGC IC Yang-Mills box [MA, Philipsen, Schäfer 2014]

Pressure

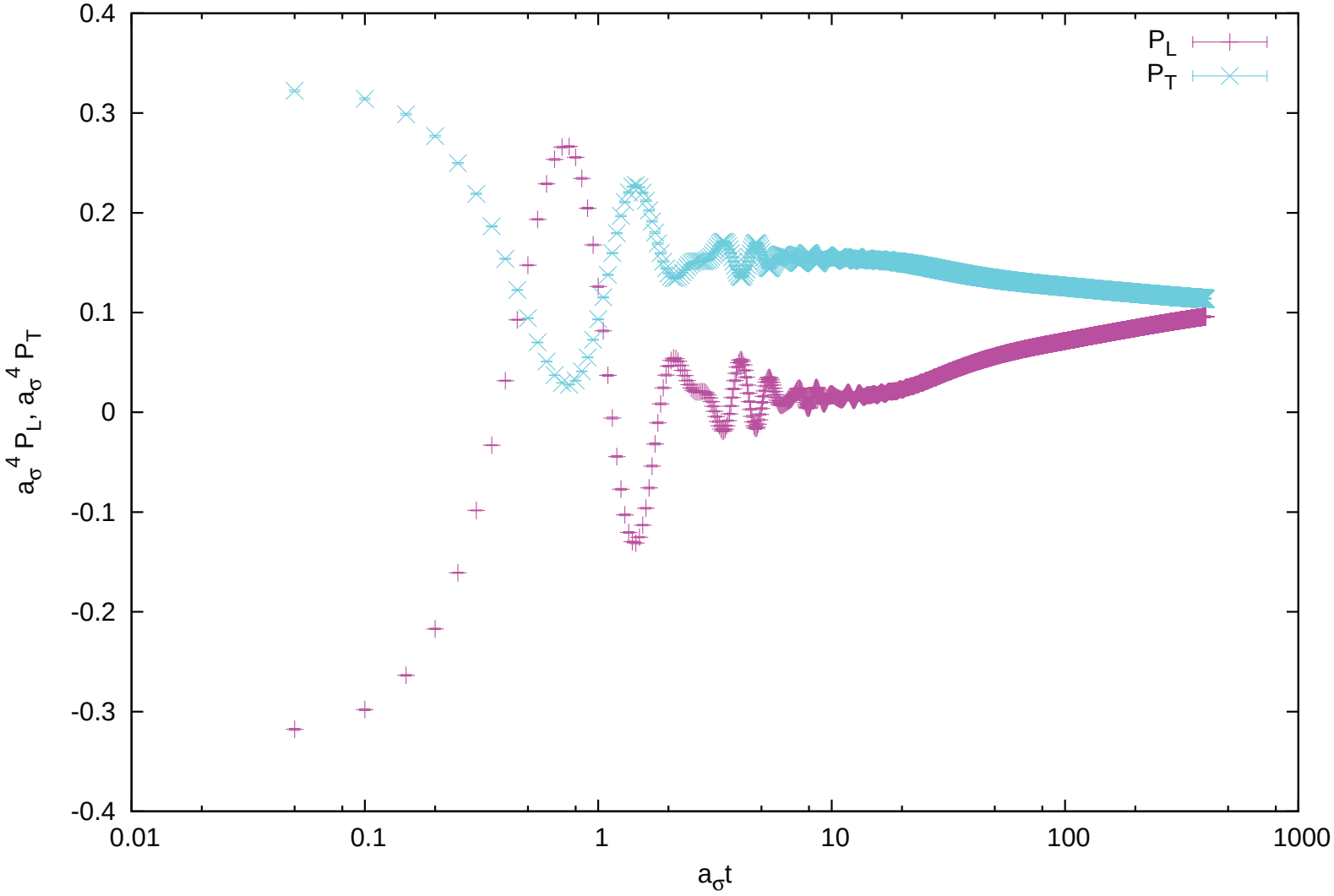

Pressure evolution [MA, Philipsen, Schäfer 2014]

Pressure

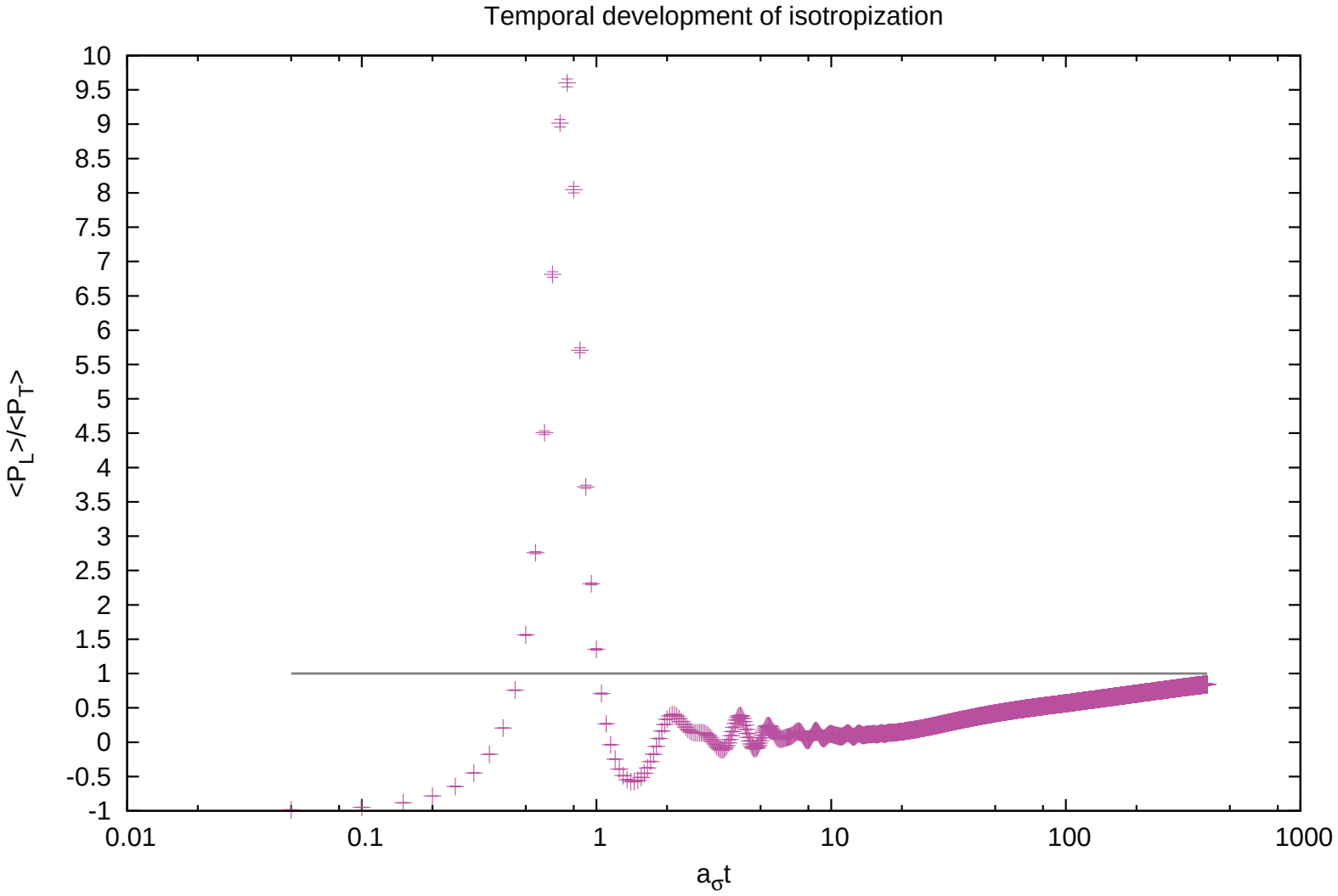

Pressure evolution [MA, Philipsen, Schäfer 2014]

Energy density spectra

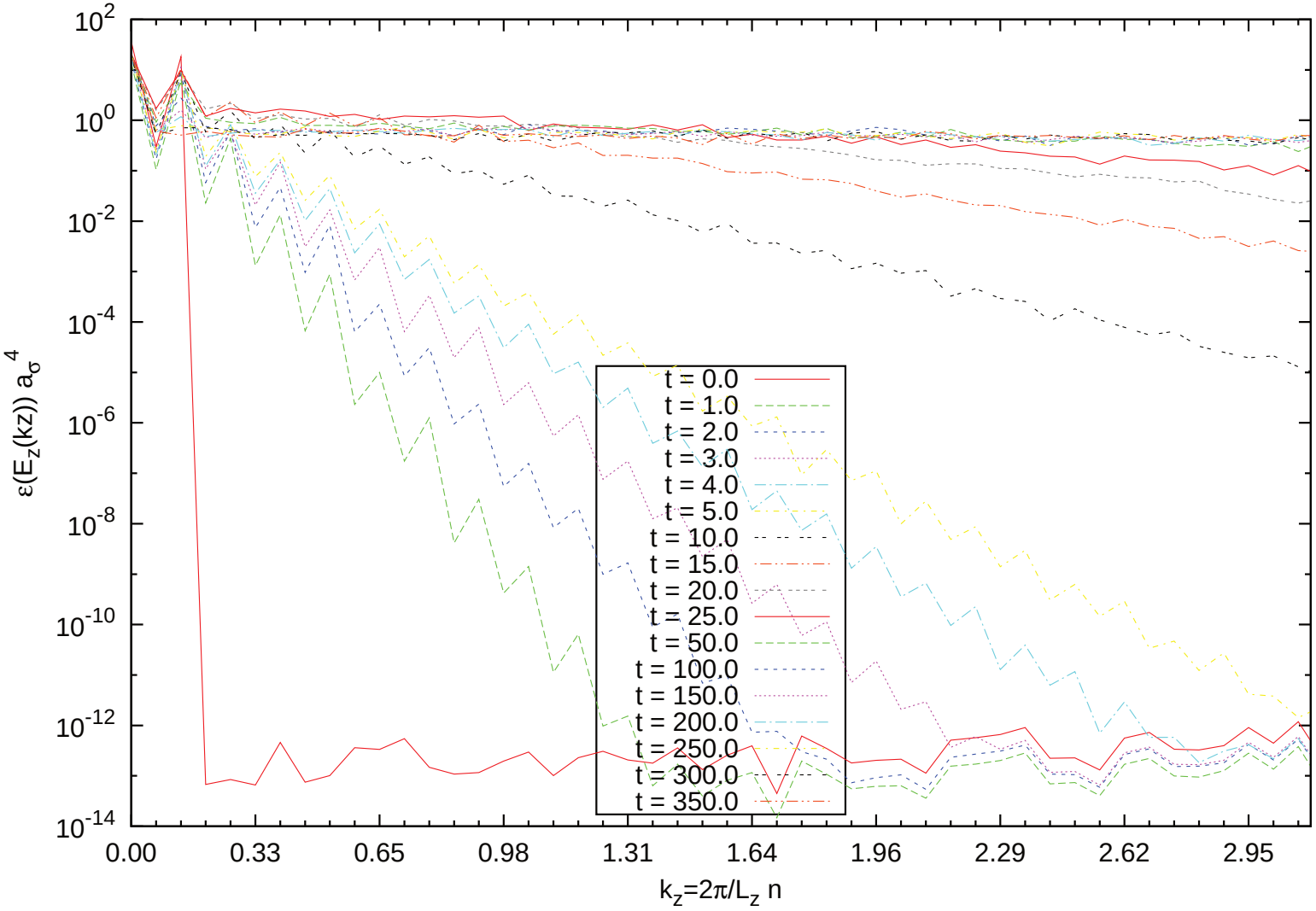

Chromo-electric spectra [MA, Philipsen, Schäfer 2014]

Energy density spectra

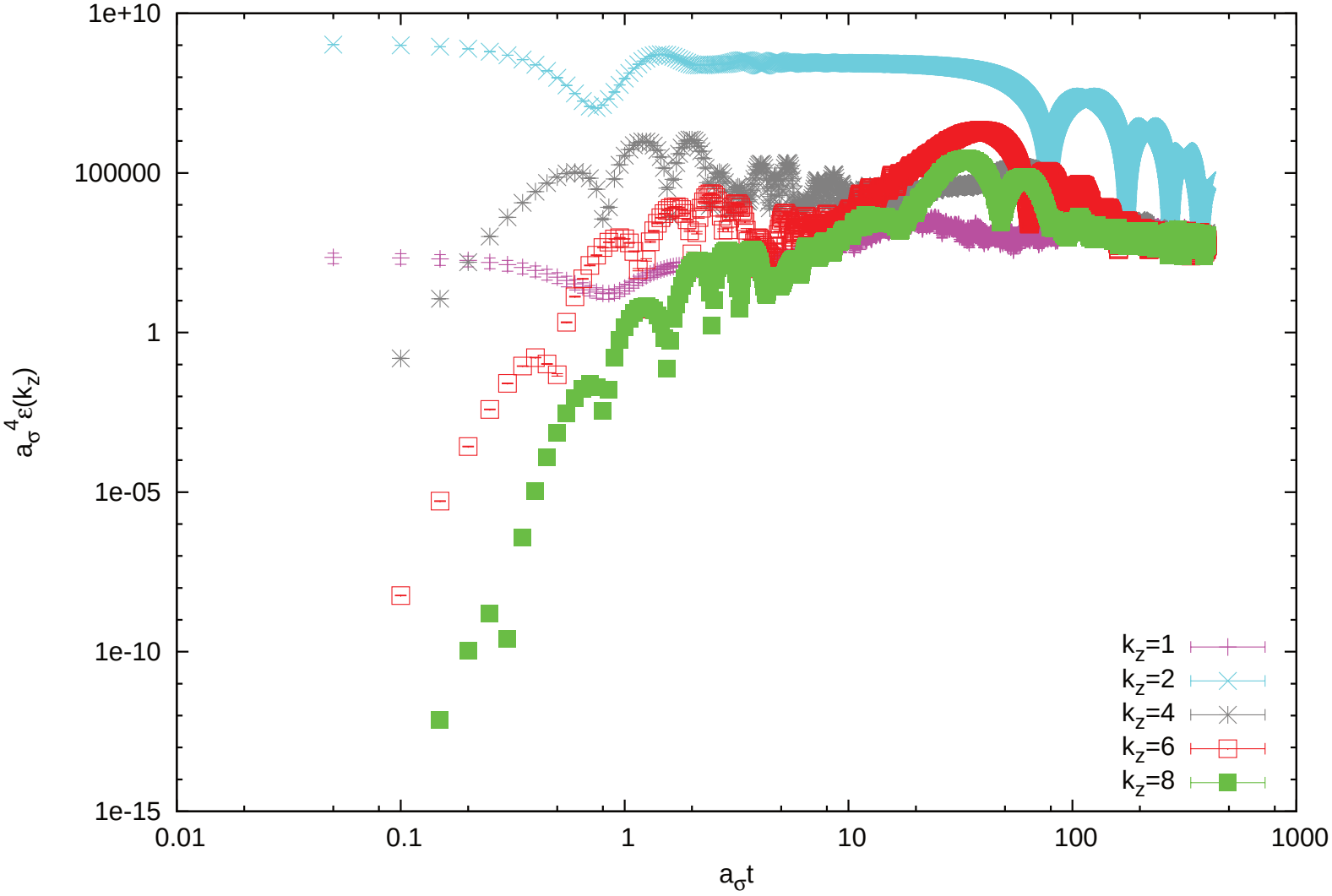

Chromo-electric spectra [MA, Philipsen, Schäfer 2014]

CGC IC Yang-Mills Box

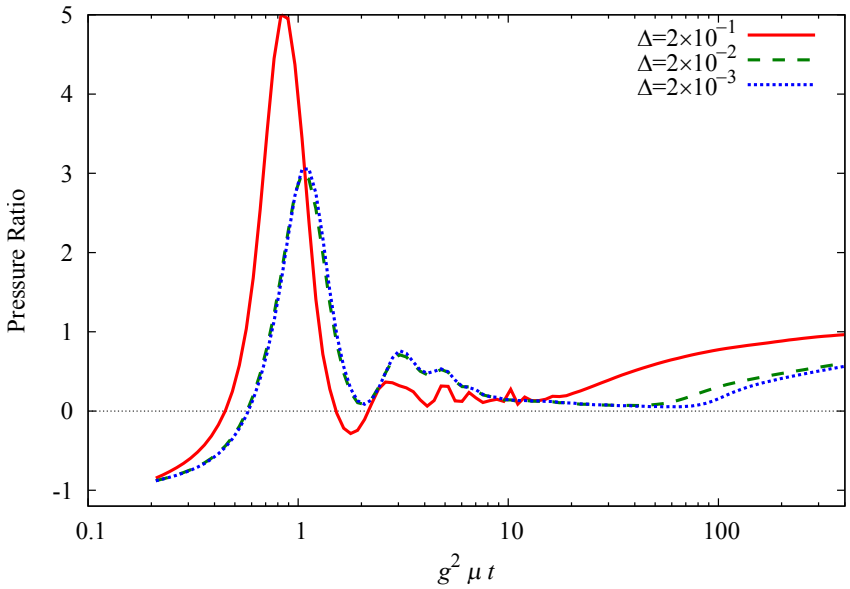

SU(2) [Fukushima 2013]

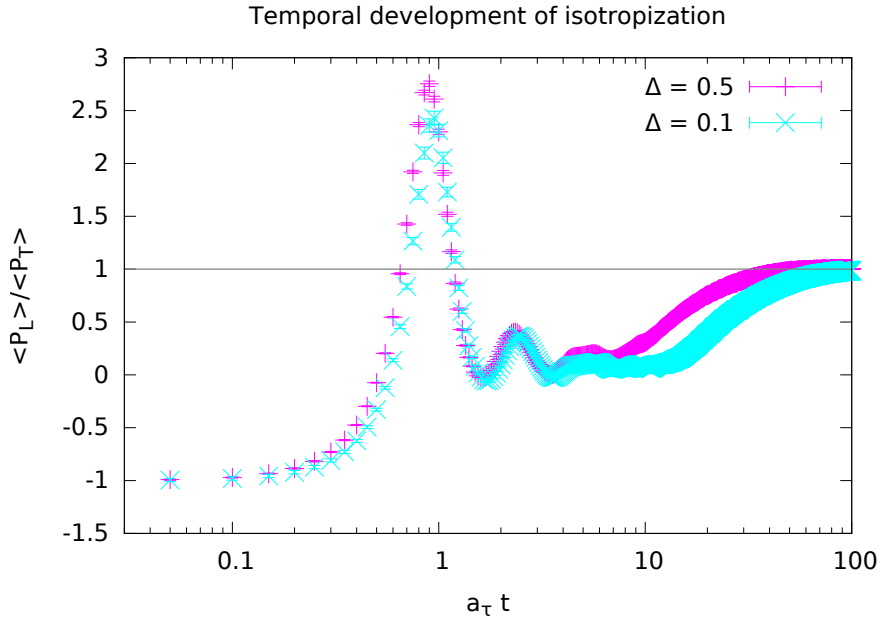

SU(3) [MA, Philipsen, Schäfer 2014]

Isotropization at later time is a very slow process even in a non-expanding and symmetric box.

Outline

1 SU(3) Yang Mills Box
- Stages of a heavy ion collision
- Equation of motions
- Energy density
- Pressure
- Energy density spectra
- SU(2) versus SU(3)

2 Chromo-Weibel instability
- Scales of wQGP
- Weibel instabilities
- Bjorken expansion
- Unstable modes growth rate
- Yang-Mills Vlasov
- Energy densities
- Pressures
- Spectra

Scales of wQGP

Equilibrium:

- T: energy of hard particles
- gT: thermal masses, Debye screening mass,
- $g^2 T$: magnetic confinement, color relaxation, rate for small angle scattering
- $g^4 T$: rate for large angle scattering, $\eta^{-1} T^4$

Scales of wQGP

Non-Equilibrium:

- p_{hard}: energy of hard particles
- gA_μ: thermal masses, Debye screening mass, plasma instabilities [Mrowczynski 1988, 1993, ..]

Weibel instabilities

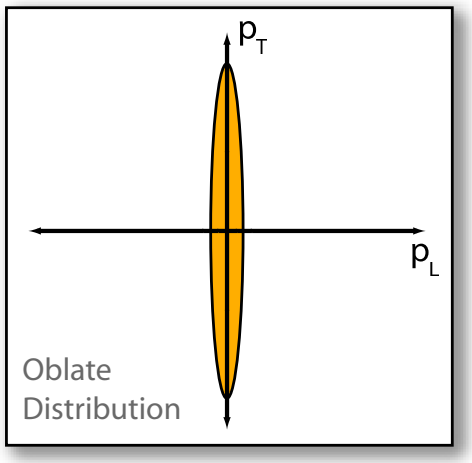

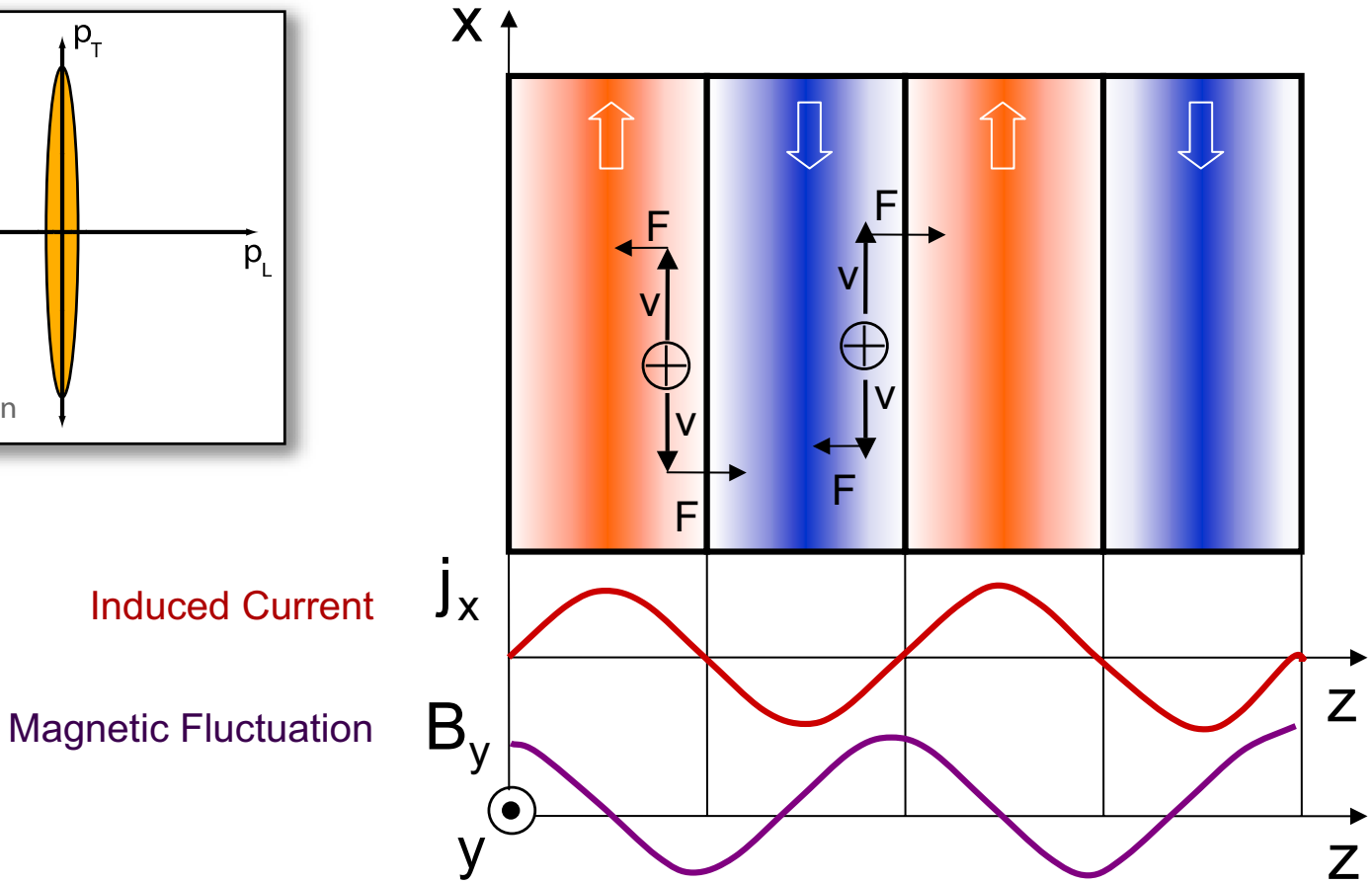

[Mrowczynski 1993; Strickland 2006]: Illustration of the mechanism of filamentation instabilities with Lorentz force.

Bjorken expansion

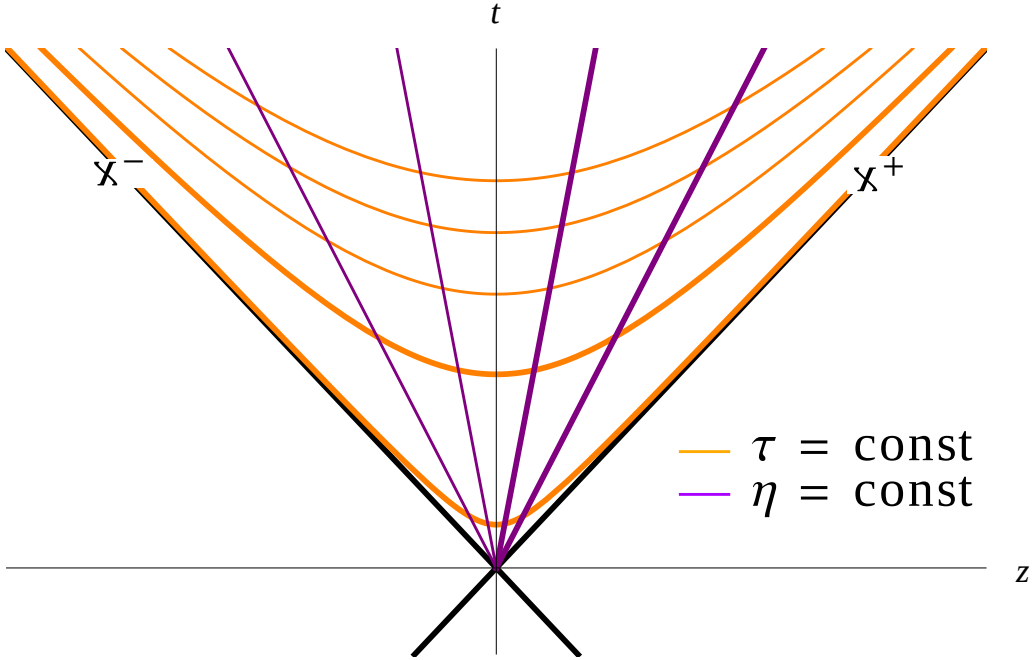

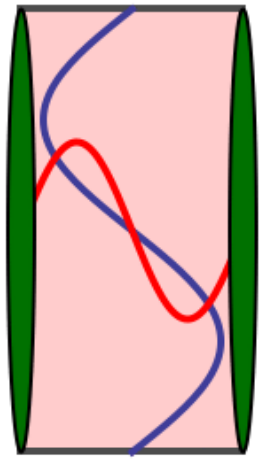

It is convenient to switch to comoving coordinates

$$t = \tau \cosh \eta \,, \qquad \tau = \sqrt{t^2 - z^2} \,,$$

$$z = \tau \sinh \eta \,, \qquad \eta = \operatorname{arctanh} \frac{z}{t} \,,$$

with the corresponding metric

$$ds^2 = d\tau^2 - d\mathbf{x}_\perp^2 - \tau^2 d\eta^2 \,.$$

Unstable modes growth rate

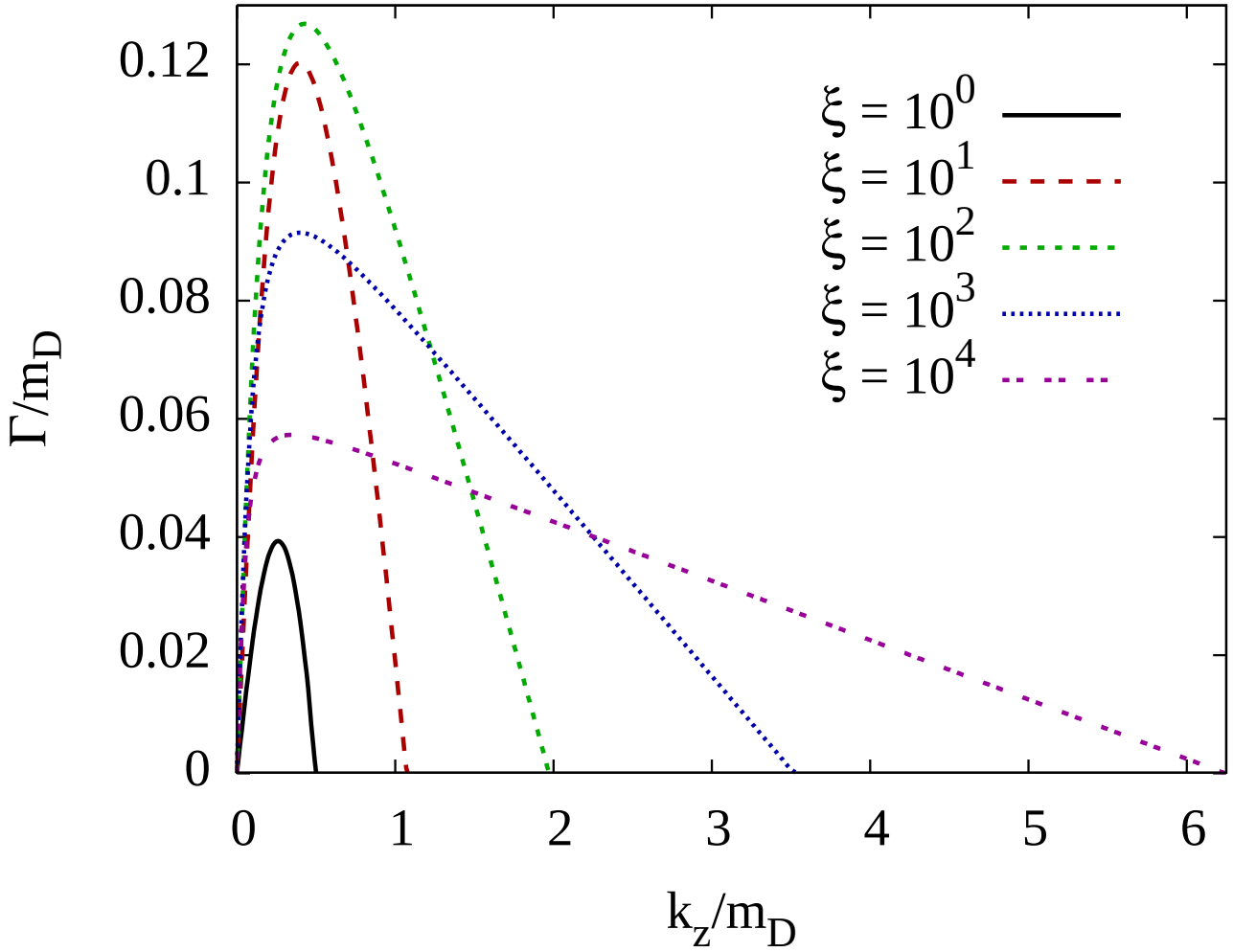

[Romatschke, Strickland 2003] Unstable mode spectra of purely longitudinal modes: $N(\tau) \approx \exp(2m_D\sqrt{\tau\tau_{\rm ISO}})$.

Filamentation instability

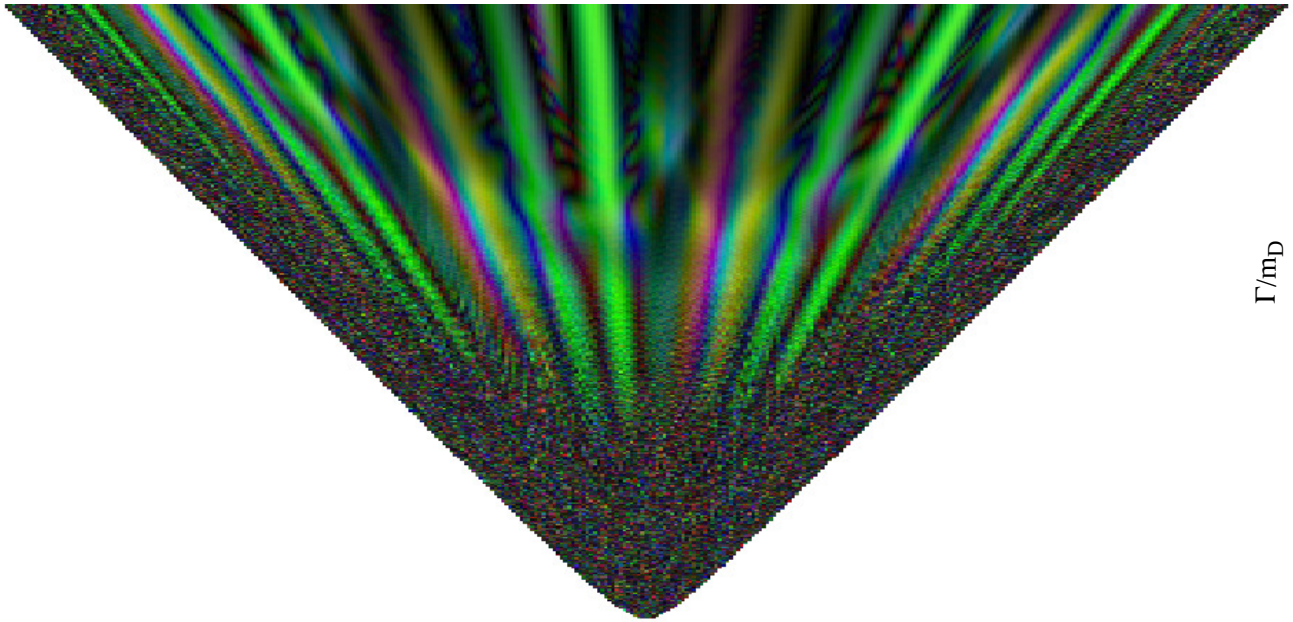

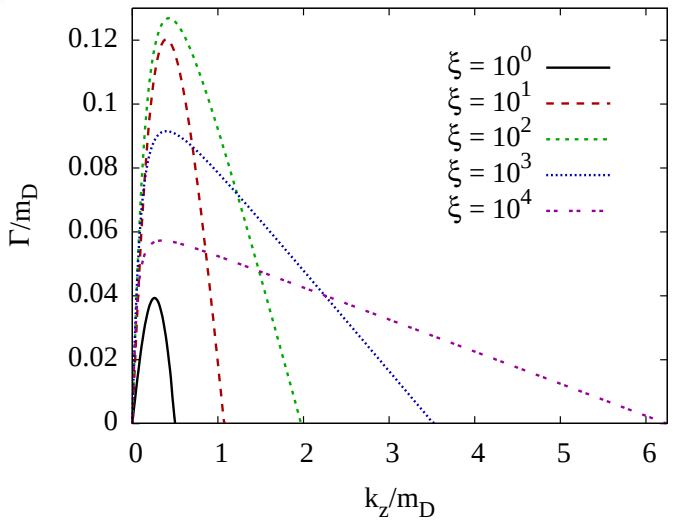

[2008 MA, Rebhan, Strickland.] Visualization of the 1D+3V space-time development of color correlations in a non-Abelian plasma instabilities in Bjorken expansion.

Yang-Mills Vlasov

[Heinz 1985; Blaizot, Iancu 1993] One solves the covariant Vlasov

$$V \cdot D\, \delta f^a \Big|_{p^\mu} = g V^\mu F^a_{\mu\nu} \partial^\nu_{(p)} f_0(\mathbf{p}_\perp, p_\eta)$$

Yang-Mills Vlasov

[Heinz 1985; Blaizot, Iancu 1993] One solves the covariant Vlasov

$$V \cdot D\, \delta f^a \Big|_{p^\mu} = g V^\mu F^a_{\mu\nu} \partial^\nu_{(p)} f_0(\mathbf{p}_\perp, p_\eta)$$

coupled to Yang-Mills

$$D_\mu F^{\mu\nu}_a = j^\nu_a = g\, t_R \int \frac{d^3p}{(2\pi)^3} \frac{p^\mu}{2p^0} \delta f_a(\mathbf{p}, \mathbf{x}, t)$$

with the Ansatz $\delta f(x; p) = -g W_\beta(x; \phi, y) \partial^\beta_{(p)} f_0(p_\perp, p_\eta)$

Yang-Mills Vlasov

[Heinz 1985; Blaizot, Iancu 1993] One solves the covariant Vlasov

$$V \cdot D\, \delta f^a \big|_{p^\mu} = g V^\mu F^a_{\mu\nu} \partial^\nu_{(p)} f_0(\mathbf{p}_\perp, p_\eta)$$

coupled to Yang-Mills

$$D_\mu F^{\mu\nu}_a = j^\nu_a = g\, t_R \int \frac{d^3p}{(2\pi)^3} \frac{p^\mu}{2p^0} \delta f_a(\mathbf{p}, \mathbf{x}, t)$$

with the Ansatz $\delta f(x;p) = -gW_\beta(x;\phi,y)\partial^\beta_{(p)} f_0(p_\perp, p_\eta)$ using the longitudinal free streaming background distribution function

$$f_0(\mathbf{p}, x) = f_{\rm iso}\left(\sqrt{p_\perp^2 + (\frac{p'^z \tau}{\tau_{\rm iso}})^2}\right)$$

resulting in the plasma anisotropy

$$\xi = \frac{1}{2}\frac{\langle p_T^2 \rangle}{\langle p_z^2 \rangle} - 1\,, \quad \xi = (\tau/\tau_{\rm iso})^2 - 1.$$

Numerical setup

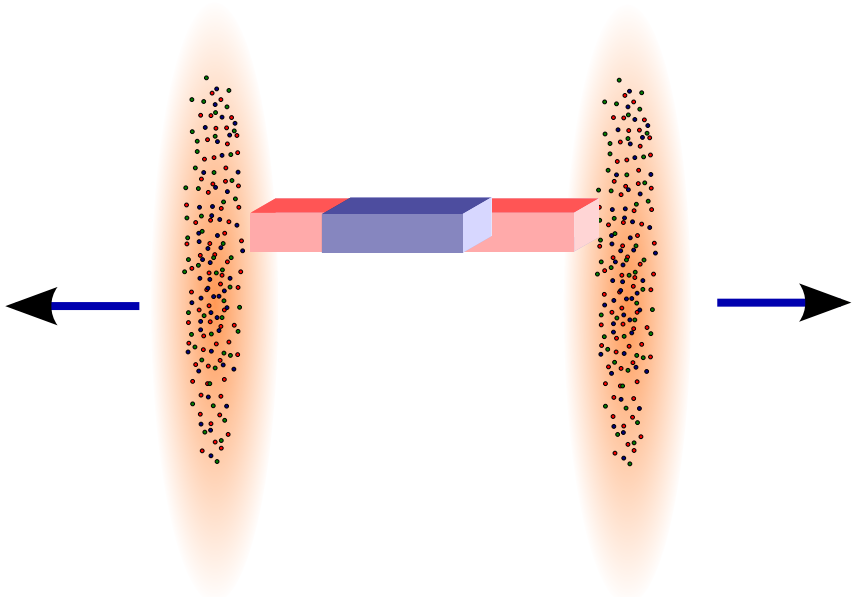

SU(2) particle content

$Q_s = 2\mathrm{GeV}$
Extrapolate to $\alpha_s \sim 0.3$

Initial gluon densities given by the gluon liberation factor $c = 2\ln 2$ [Kovchegov 2001].

lattice size for leapfrog EOM:

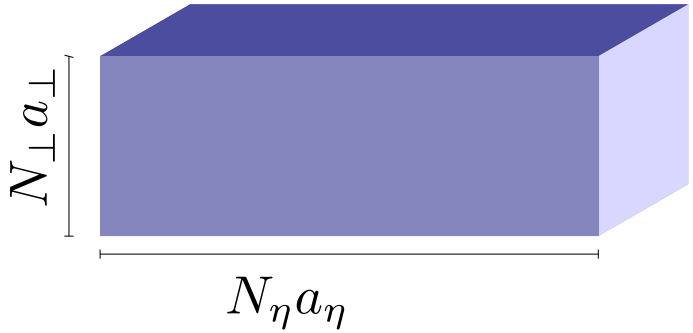

$N_\eta \times {N_\perp}^2 \times N_u \times N_\phi =$
$128 \times 40^2 \times 128 \times 32$
$a_\eta = 0.025,\ a_\perp Q_s = 1$
$\tau_0 = 1/Q_s$
$a_\tau = 10^{-2}\tau_0$

$$n(\tau_0) = c\frac{N_g Q_s^3}{4\pi^2 N_c \alpha_s(Q_s\tau_0)}$$

Energy densities fields

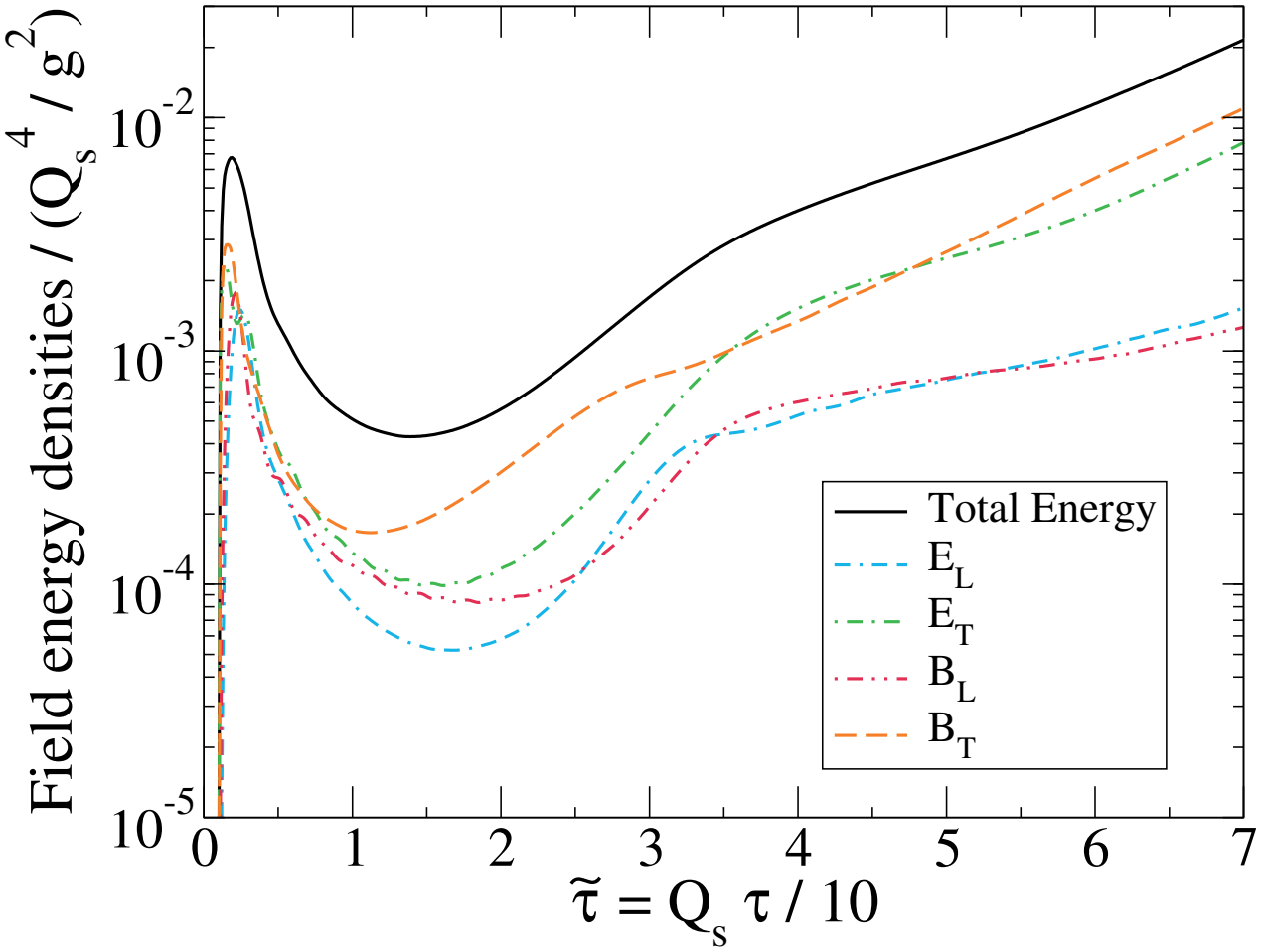

50 averaged runs $N_\perp * N_\eta * N_u * N_\phi = 40^2 * 128 * 128 * 32$: after onset one sees **rapid growth** of $\mathbf{B}_T$ and $\mathbf{E}_T$ **fields**, followed by non-Abelian interactions kicking in.

Energy densities fields

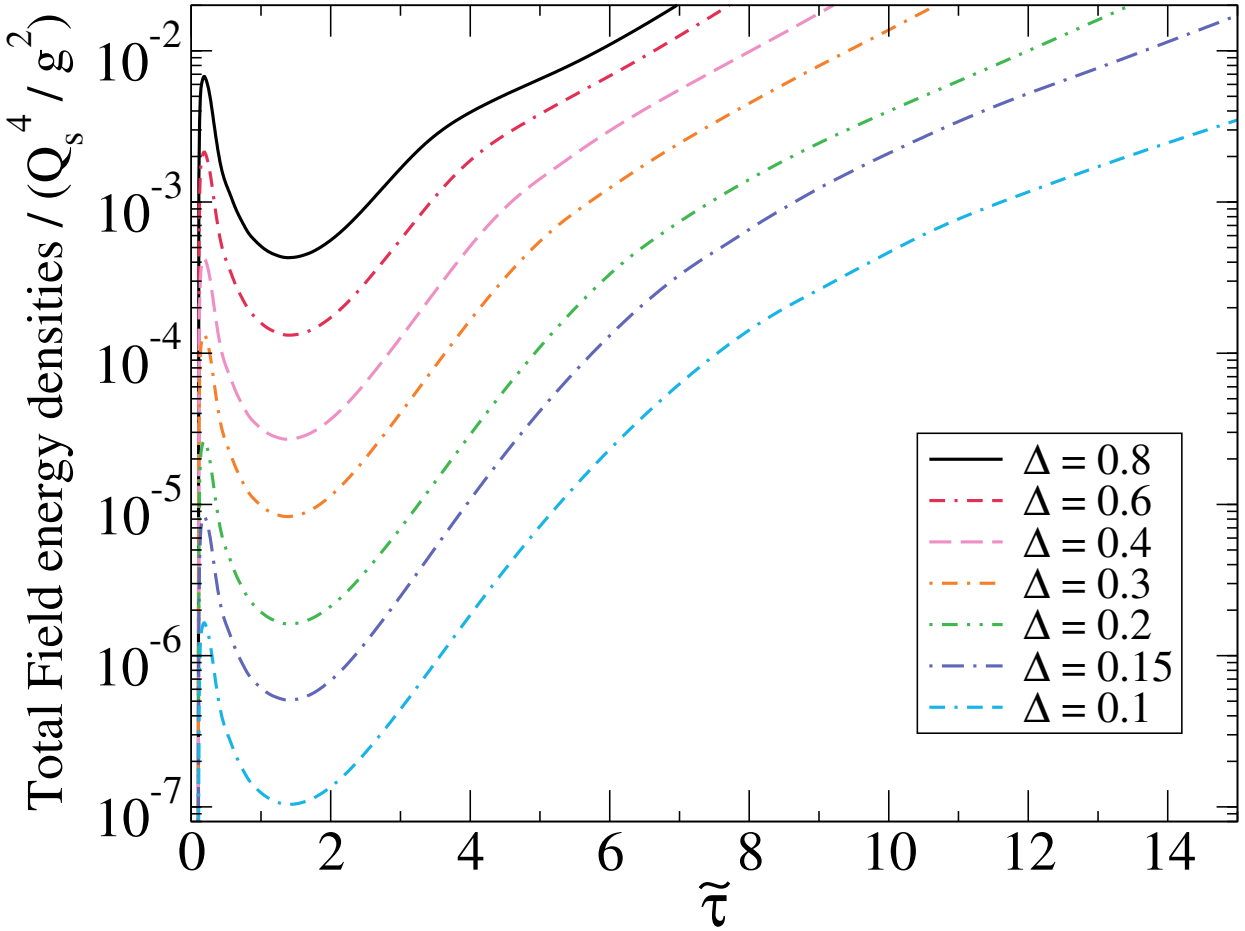

Total field energy density for different initial current fluctuation magnitudes.

Pressures

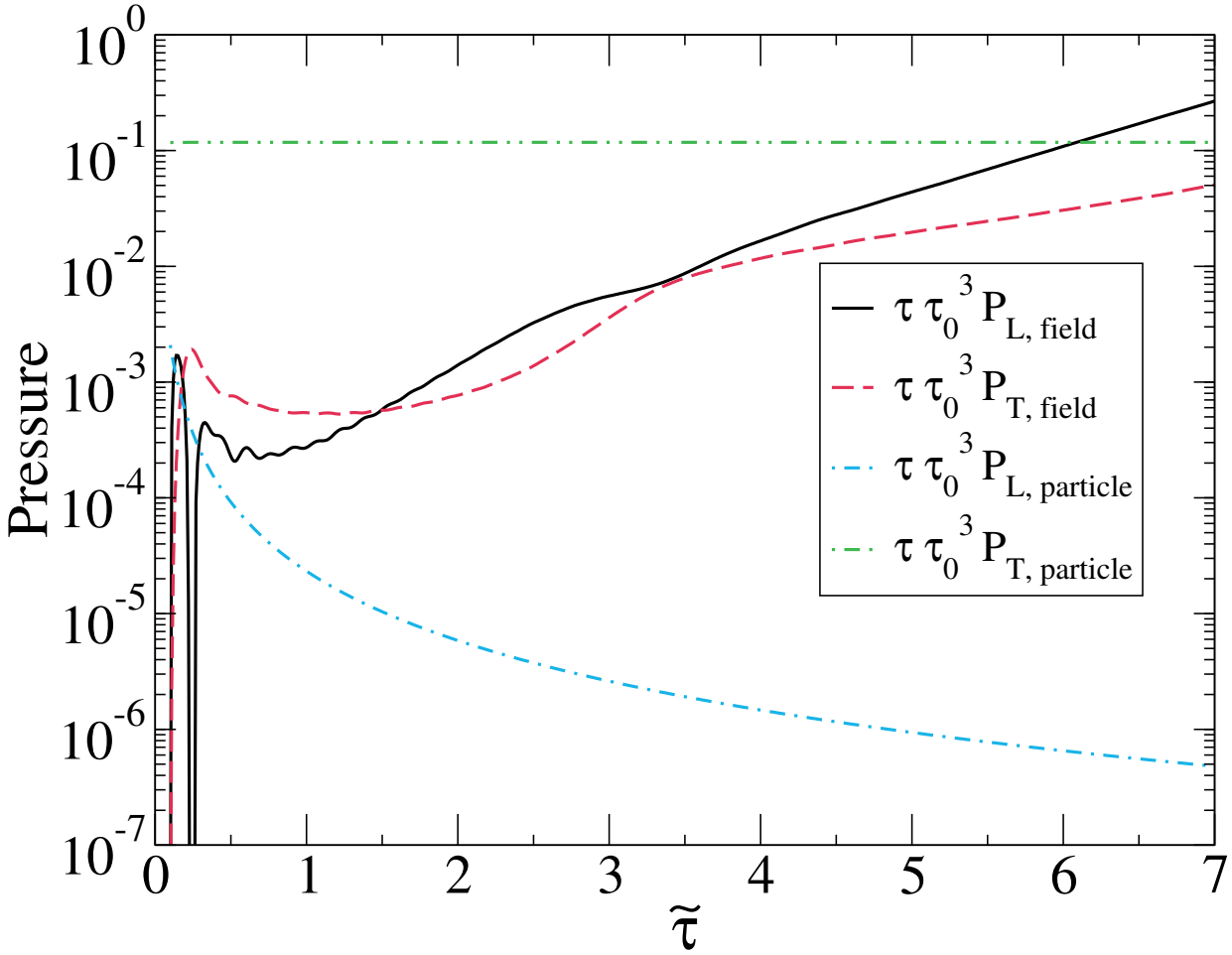

Initially highly anisotropic, note $P_{L,\mathrm{field}}(\tau = 0.3) < 0$, **growing field pressures**, $P_{L,\mathrm{field}}$ dominates at late times, $\tilde{\tau}$ scaled P_L drops $\propto 1/\tilde{\tau}^2$.

Pressure ratios

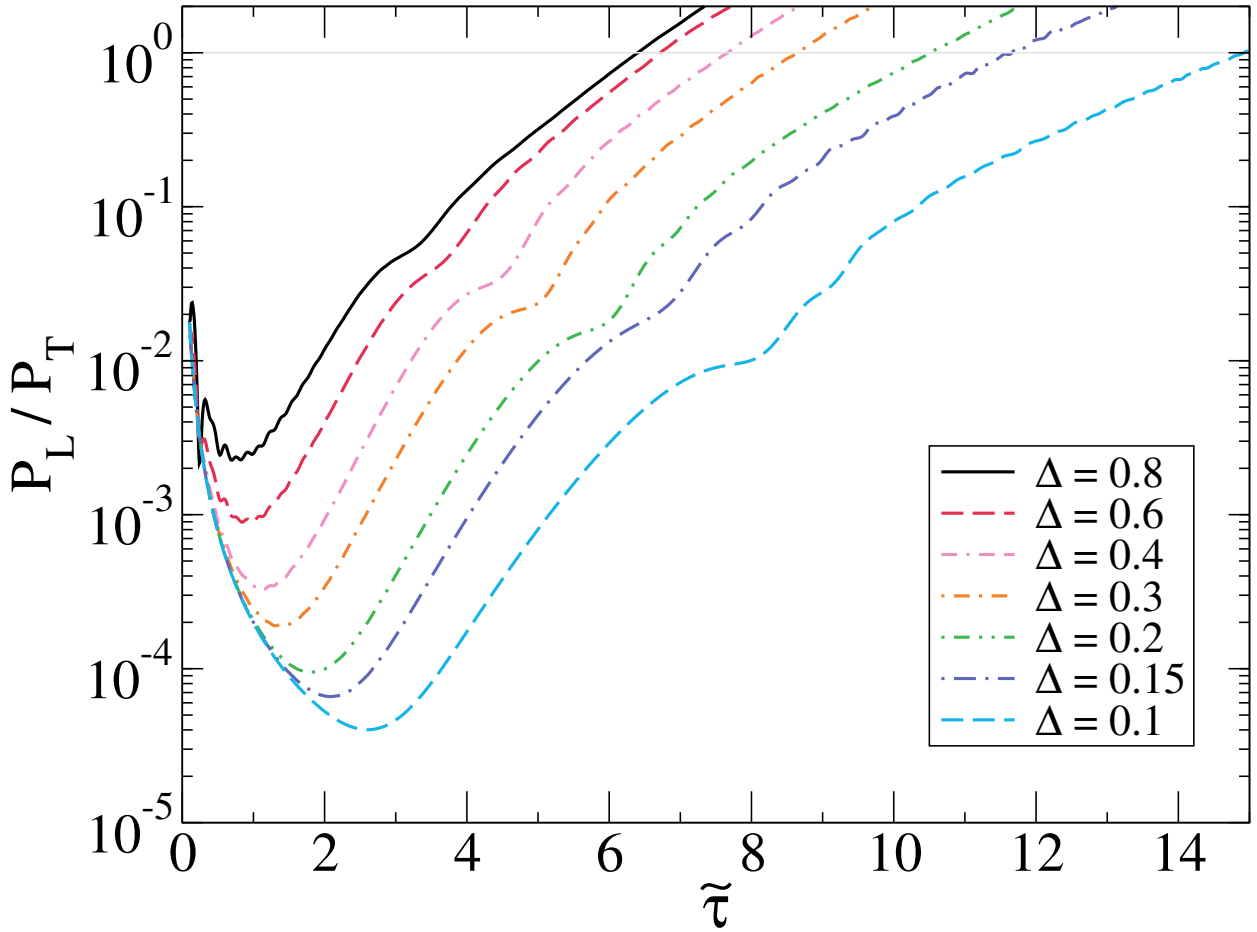

The evolution of the total longitudinal pressure over the total transverse pressure for different initial current fluctuation magnitudes Δ.

Spectra

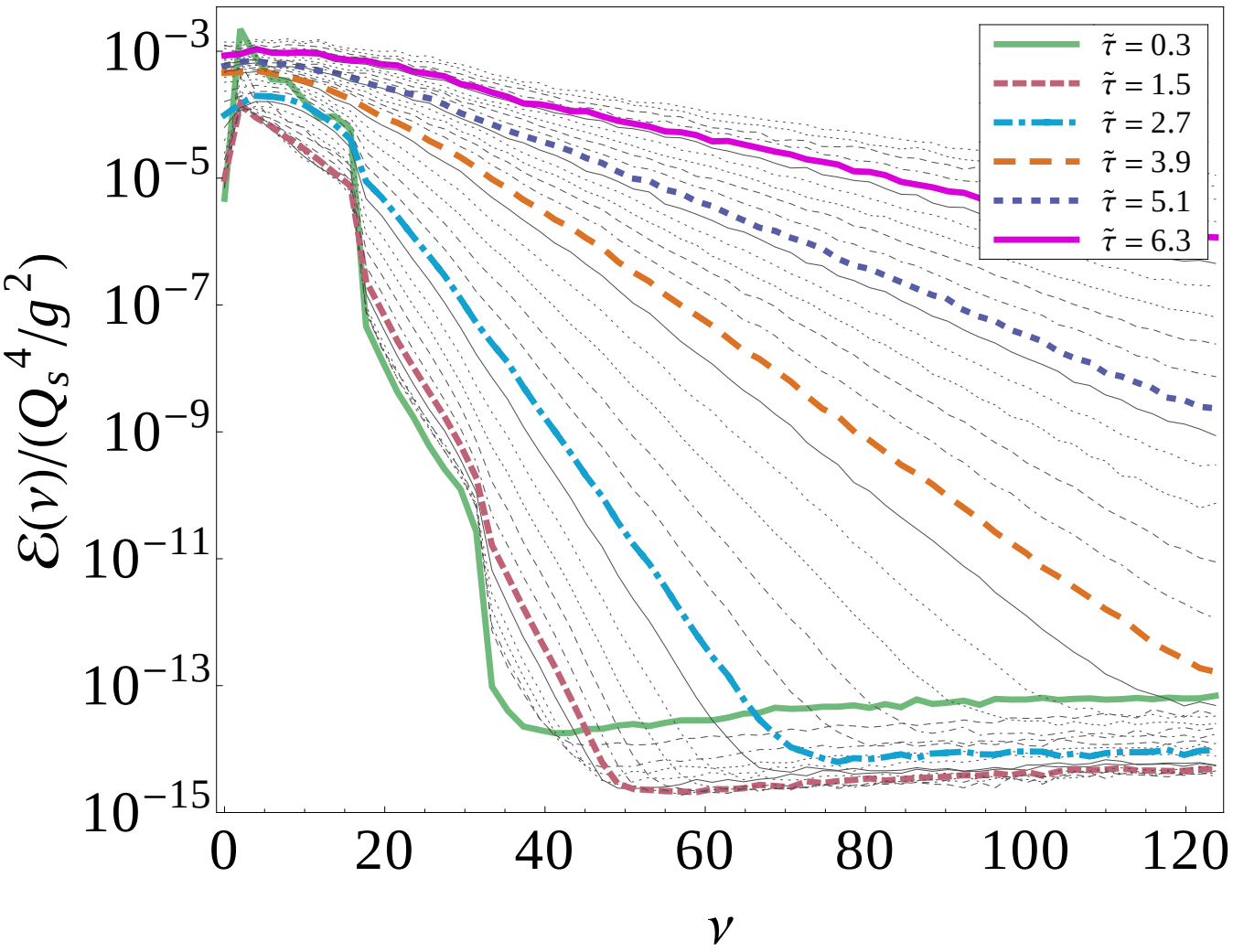

The longitudinal energy spectra at various proper times over the longitudinal wavenumber $\nu = k_z * \tau$: **rapid emergence of an exponential distribution of longitudinal energy**.

Spectra

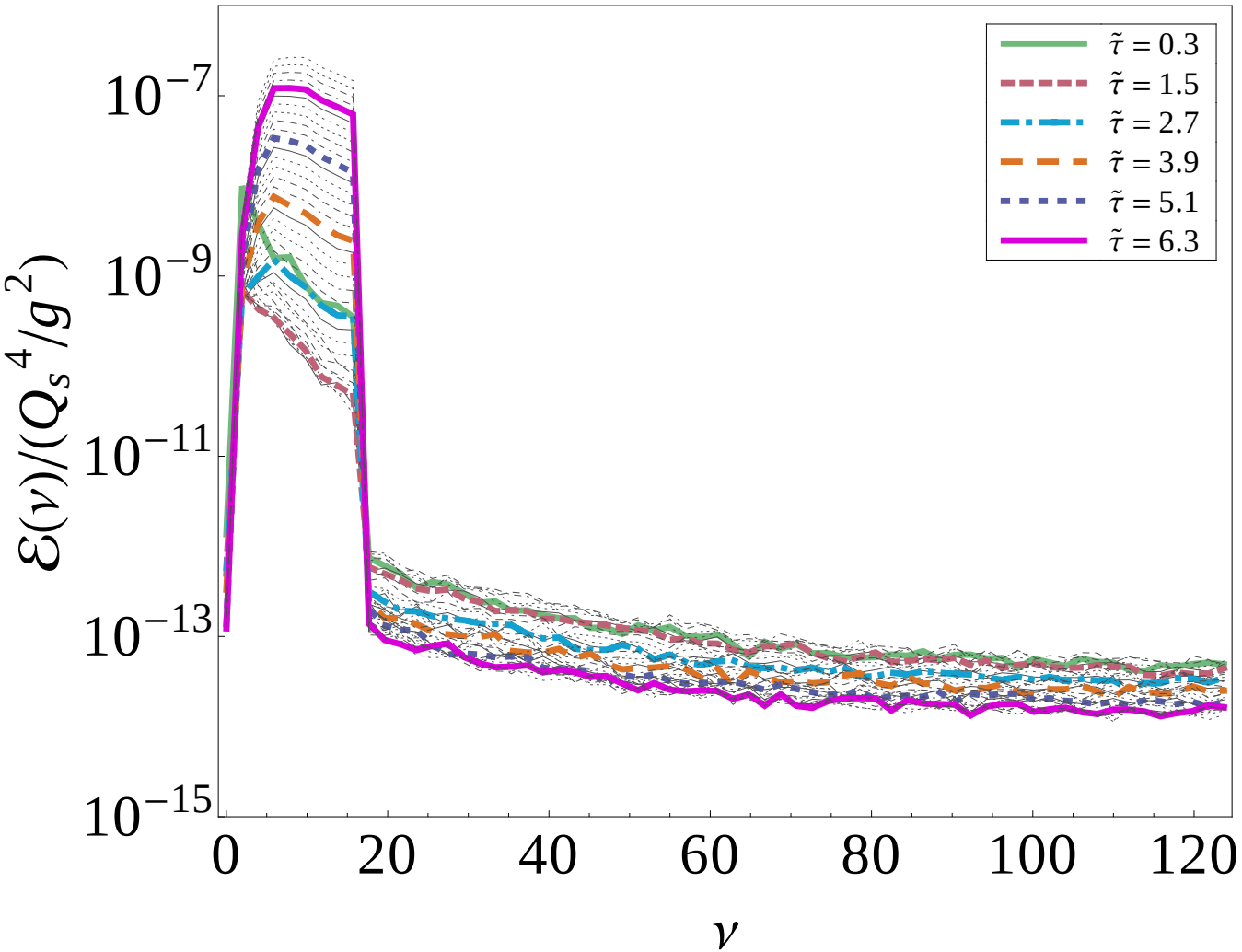

Longitudinal spectra for **abelian** runs shows amplification of the initial seeded modes.

Spectra

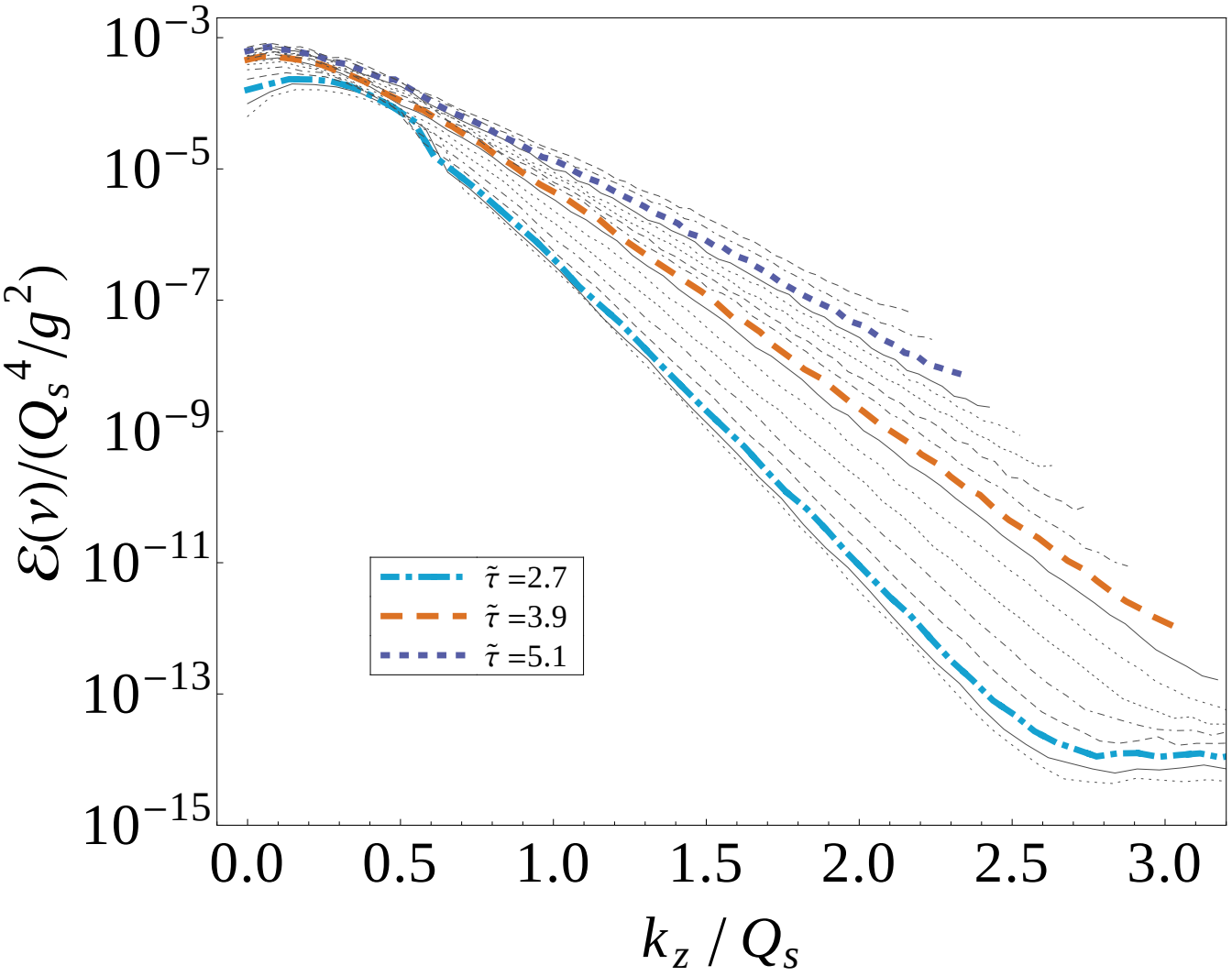

The **red-shifting** is even more visible in the k_z plot. Nonlinear mode-mode coupling is vital in order to populate high momentum modes.

Longitudinal thermalization

Massless Boltzmann distribution fits the longitudinal spectra:

$$\mathcal{E}_{\text{fit}}(k_z) = A\left(k_z^2 + 2|k_z|T + 2T^2\right)\exp\left(-|k_z|/T\right) \qquad (1)$$

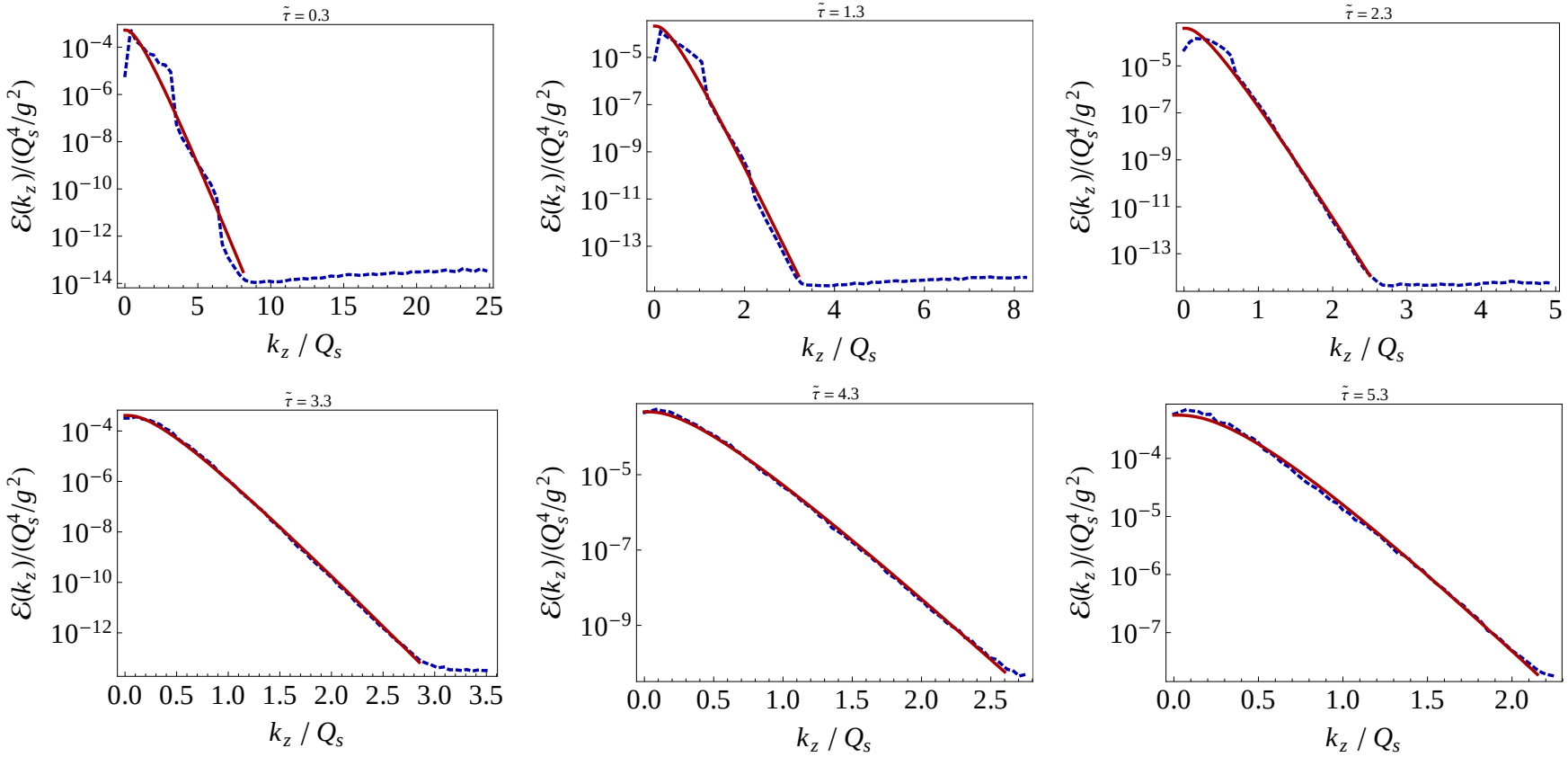

Comparison of Vlasov simulation and fit function at six different $\tilde{\tau}$.

[MA, Rebhan Strickland 2012]

Longitudinal thermalization

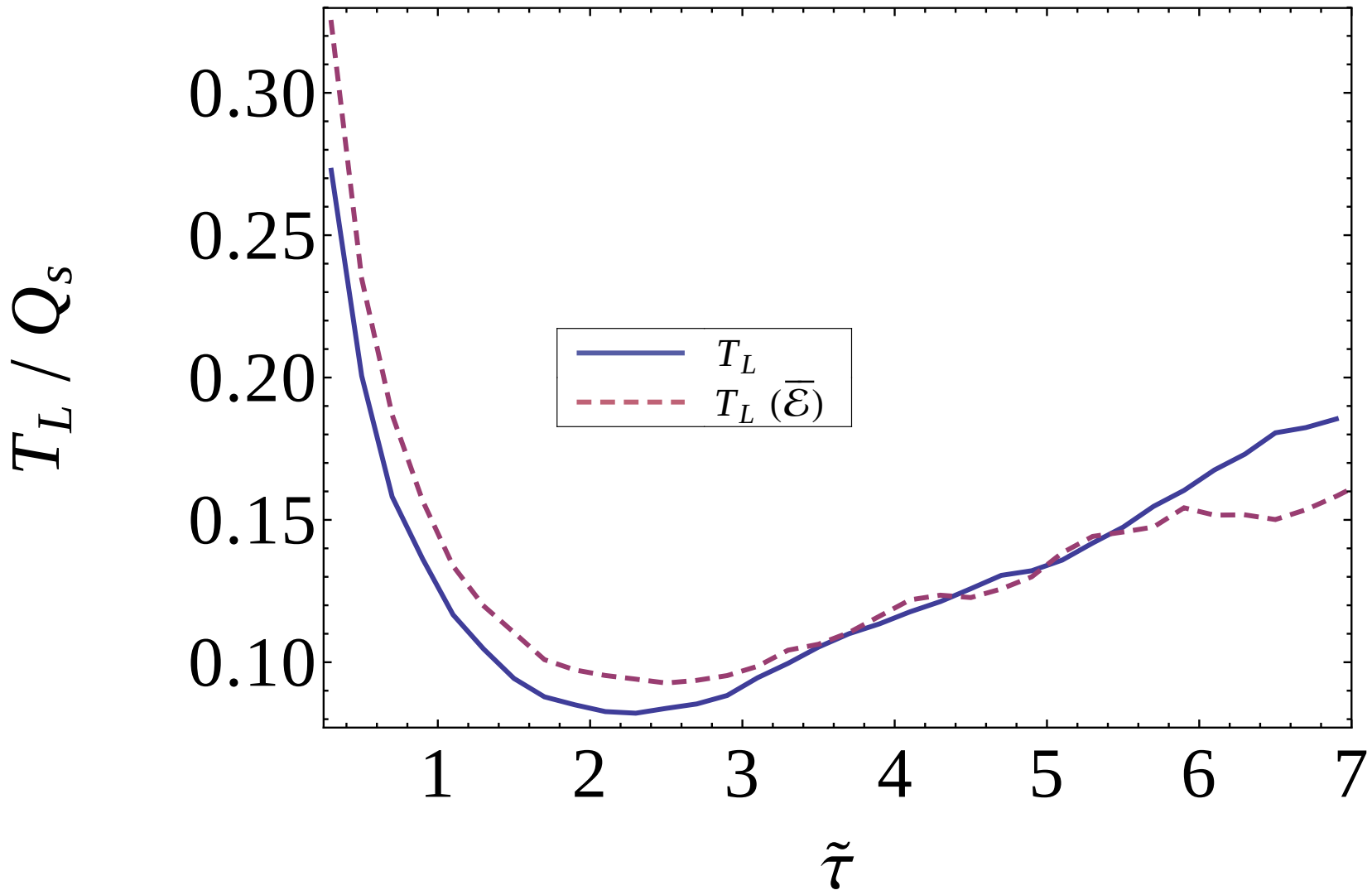

After initial cool down **instabilities reheat** longitudinal soft fields.

Conclusions

- We performed the **first real-time 3d numerical** study of non-Abelian plasma in a longitudinally expanding system within the discretized hard loop framework:
  hard expanding loops HEL.

- Extrapolating our results to energies probed in ultrarelativistic heavy-ion collisions we find, however, that a **pressure anisotropy** persists for a few fm/c.

- The longitudinal spectra seem to be well described by a Boltzmann distribution indicating **rapid longitudinal thermalization of the gauge fields** $\tau_{\mathrm{thermal}} \sim 1 \quad \mathrm{fm/c}$.

- We compute first **SU(3)** 3d real-time Yang-Mills of non-Abelian plasma with some persisting anisotropy. We are implementing the NLO CGC Initial condition.

Computational challenge

Real-time lattice simulations distributed on the cluster:

Loewe Scientific Computing:

Vienna Scientific Cluster:

The code scales to 1-4k CPU's using OpenMPI for $> 10^{10}$ auxiliary fields organised in 5-dimensional matrices on sites.

Unstable mode comparison

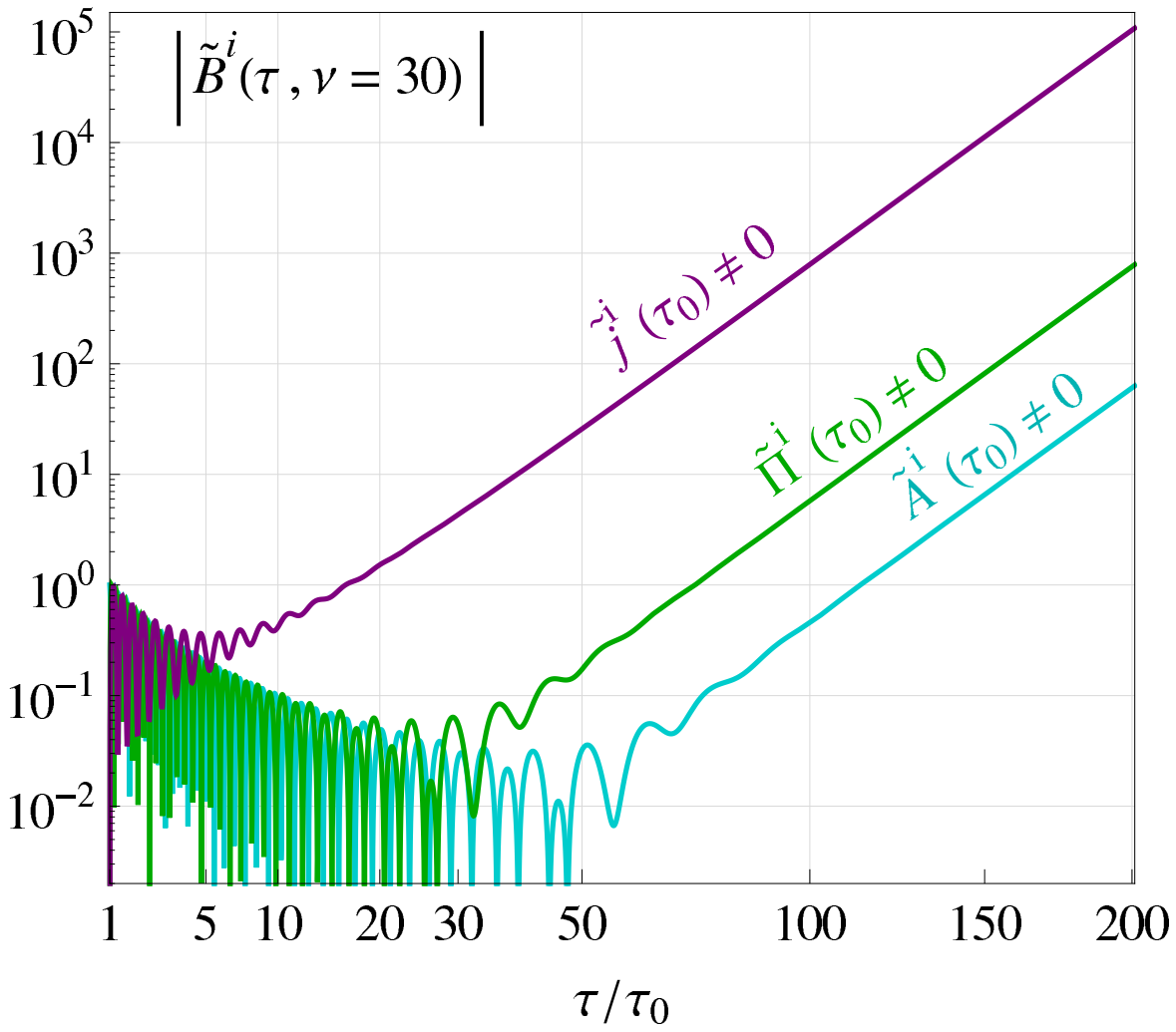

[Rebhan, Steineder 2009] IC variation for specific mode $\nu = 30$

HEL 1d test

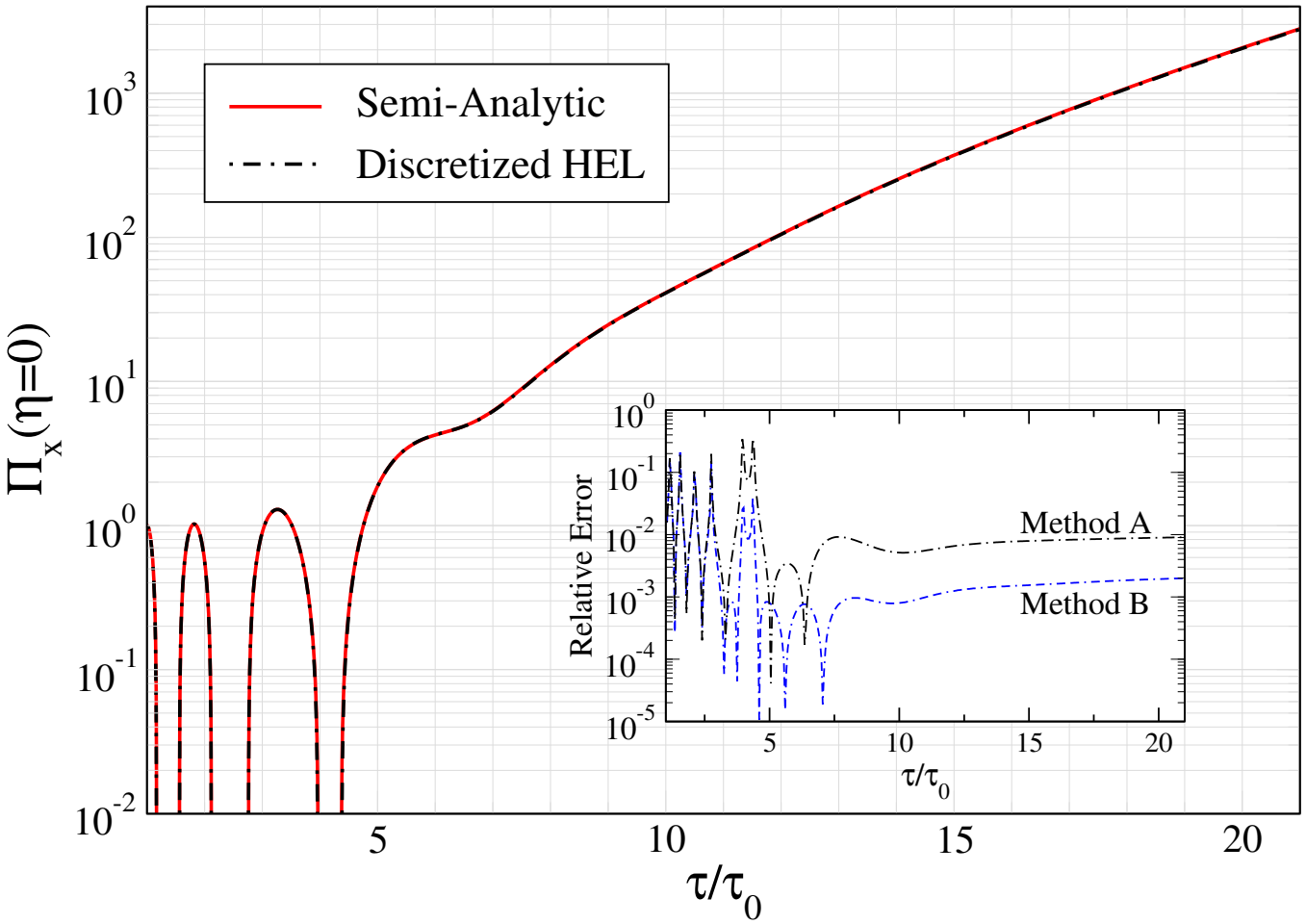

[MA, Rebhan, Strickland 2008] Abelian single mode evolution the conjugate momentum comparison with [Romatschke, Rebhan 2006]

High occupancy

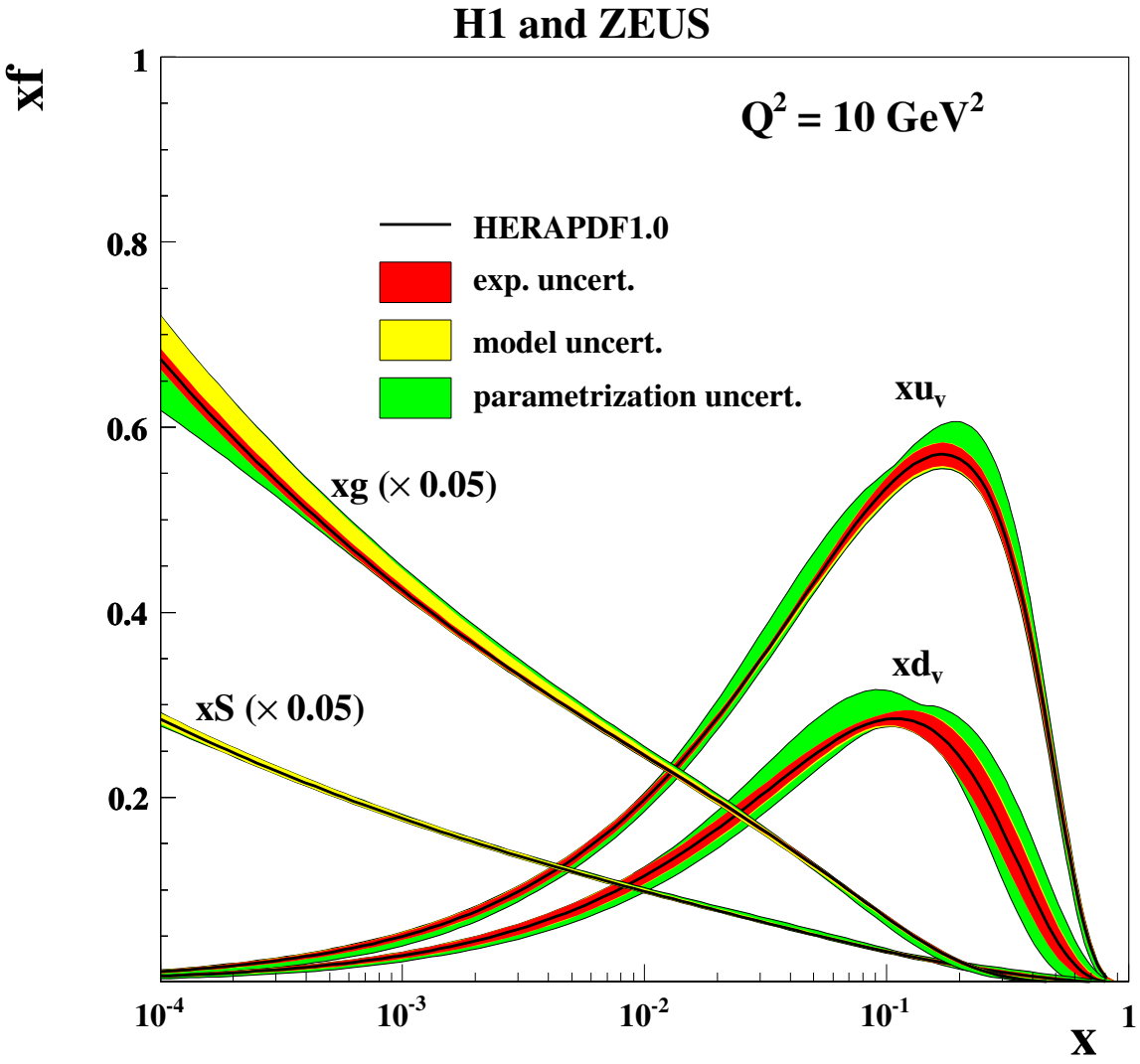

[H1, ZEUS Collaborations 2010] parton distribution functions

Transverse thermalization

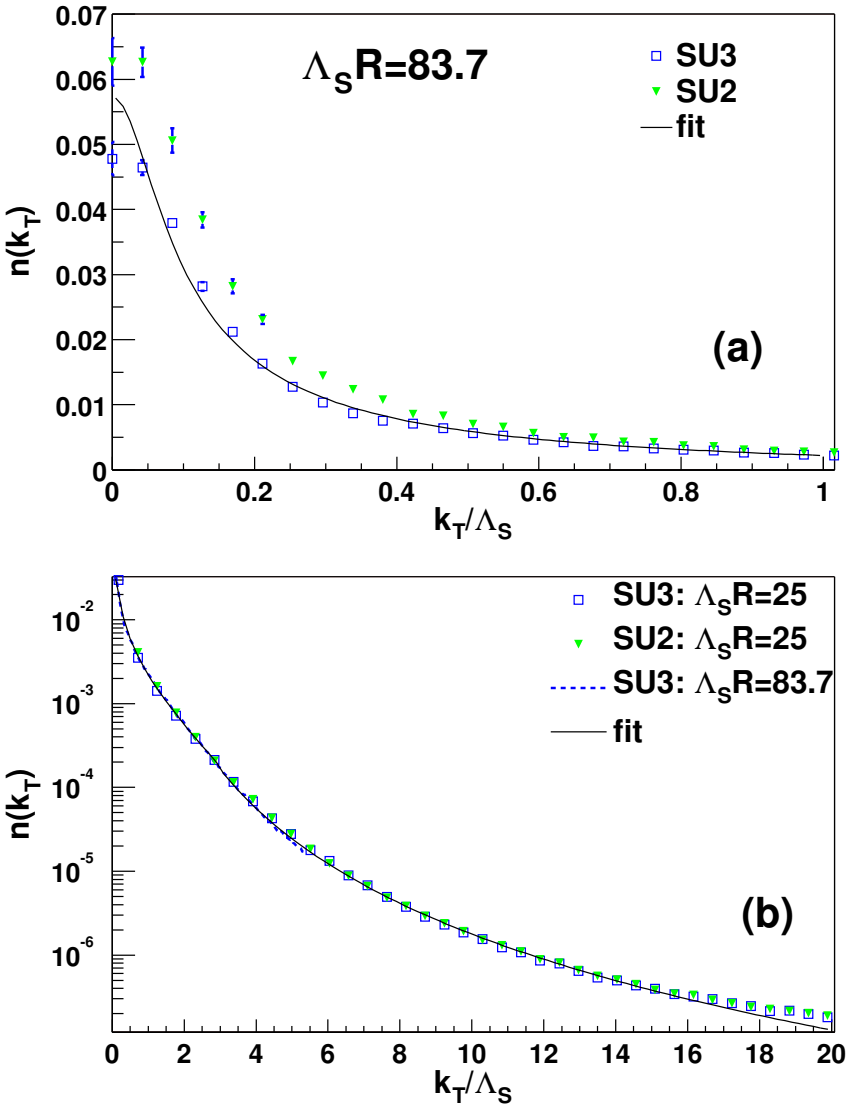

CGC setup at time scales Q_s^{-1} [Krasnitz, Nara, Venugopalan 2001]

Unstable Color Glass Condensate

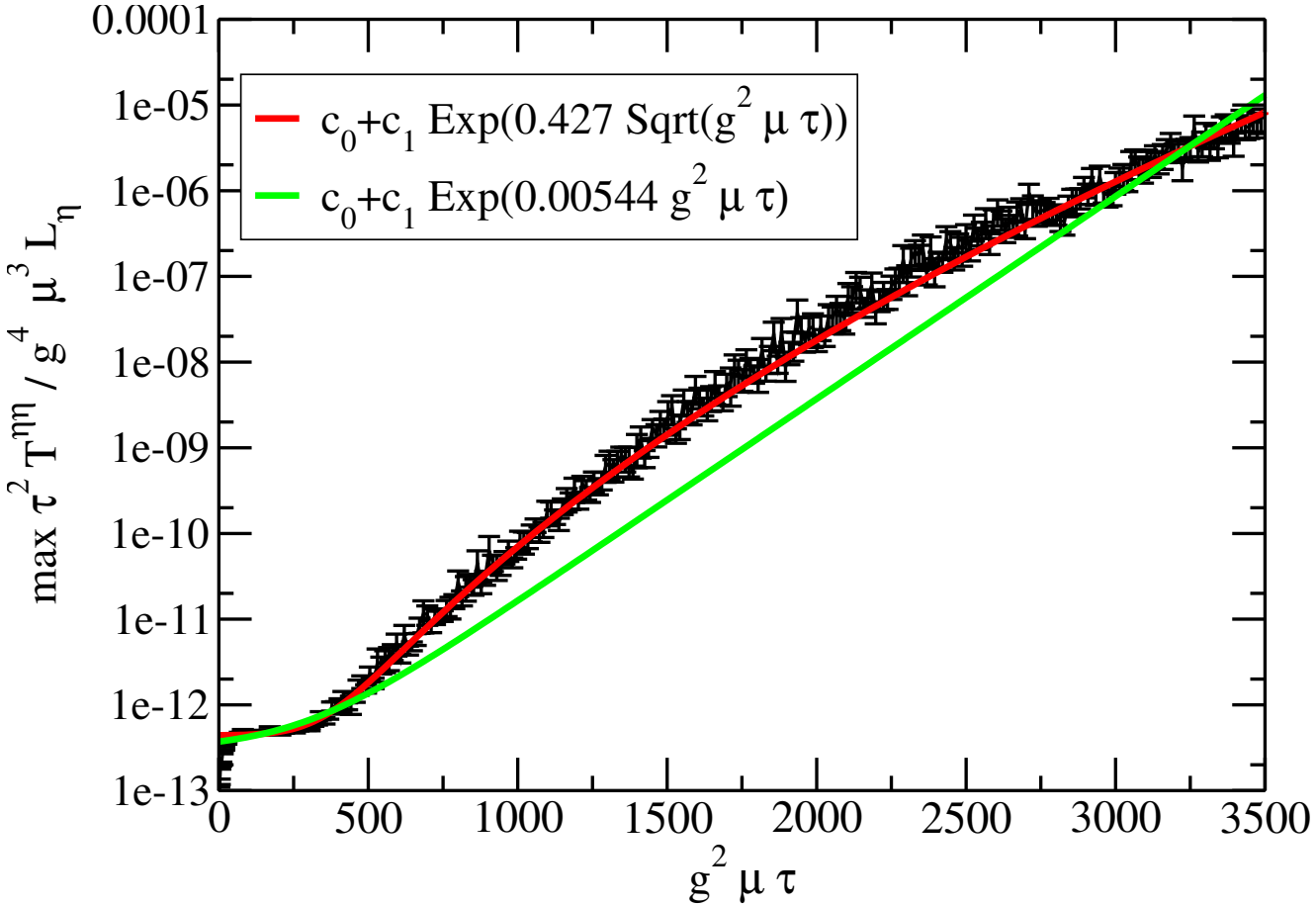

[Romatschke, Venugopalan 2006] NLO Color Glass Condensate (CGC) longitudinal pressure sees chromo-Weibel exp growth.

Unstable Color Glass Condensate

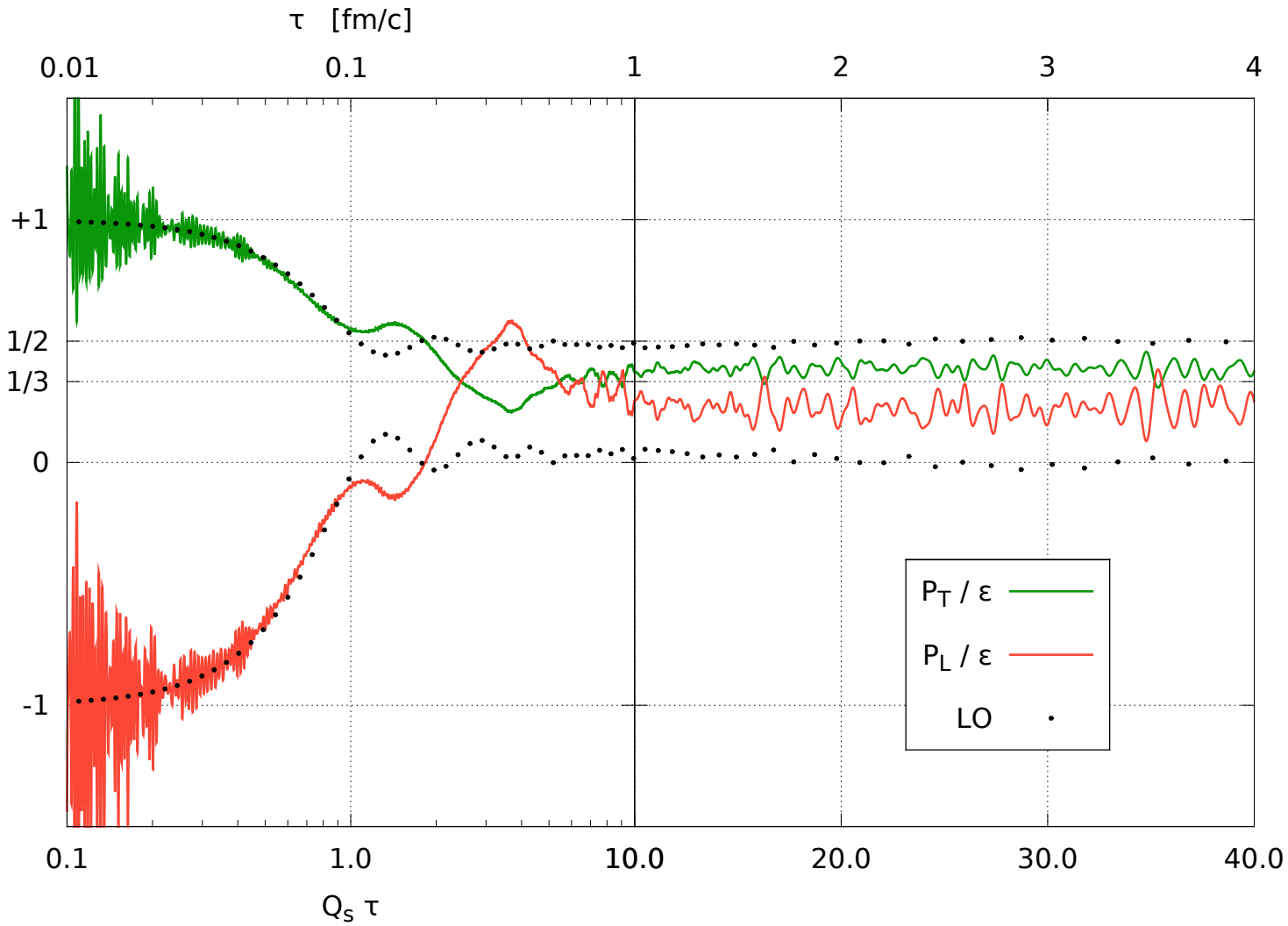

[Epelbaum, Gelis 2013] CGC NLO spectrum pressure evolution
[McLerran, Venugopalan (1993)]

Jets in quark-gluon plasmas
Turbulent QCD cascade
Bottom-up thermalization

« Approach to Equilibrium in Strongly Interacting Matter »
BNL, April 2, 2014

European Research Council

Jean-Paul Blaizot, IPhT- Saclay

IPhT SACLAY

Outline

- Phenomenological motivations
- Jets in quark-gluon plasmas: loss of coherence, medium-induced gluon branching
- Turbulent in-medium QCD cascade
- Bottom-up thermalization scenario
- Summary

Work done in collaboration with F. Dominguez, E. Iancu and Y. Mehtar-Tani (arXiv:1209.4585, 1301.6102, 1311.5823)

Jets in a quark-gluon plasma

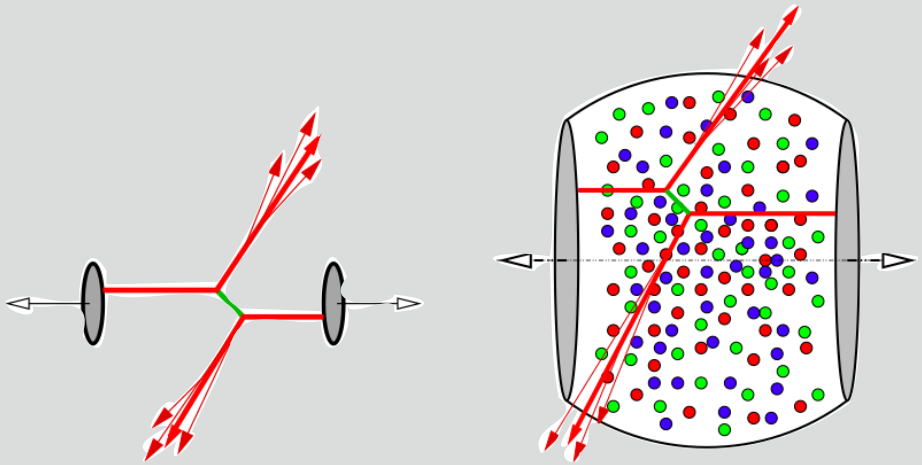

Jets are **quenched** due to interactions with the QGP

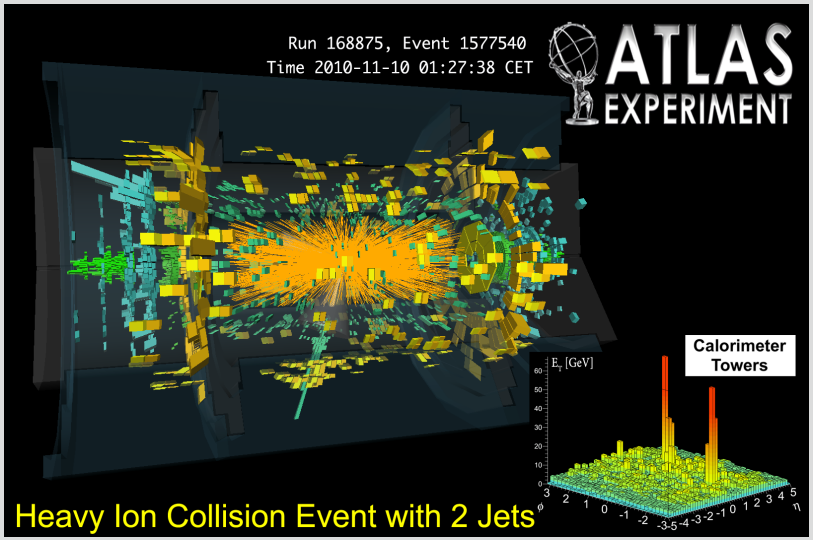

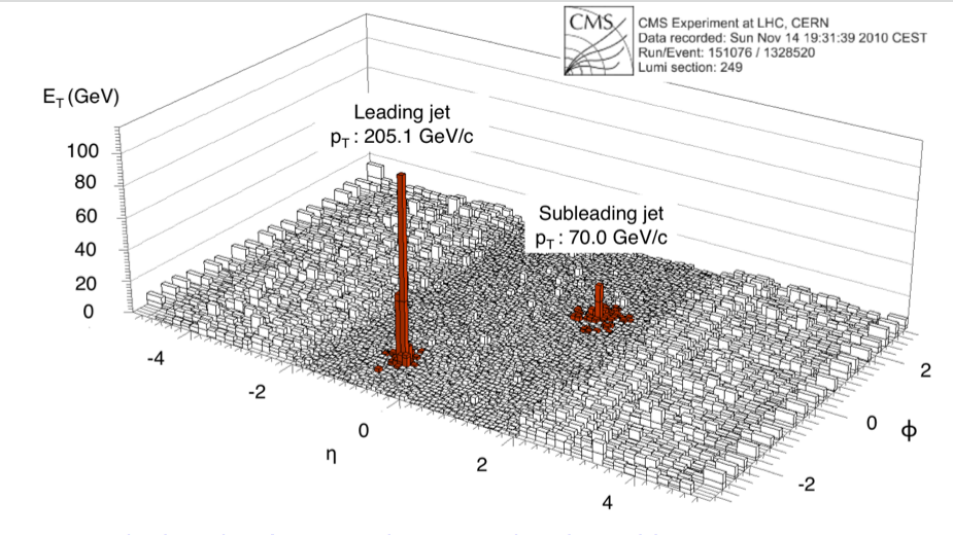

Di-jet asymmetry

there is more to it than just 'jet quenching'...

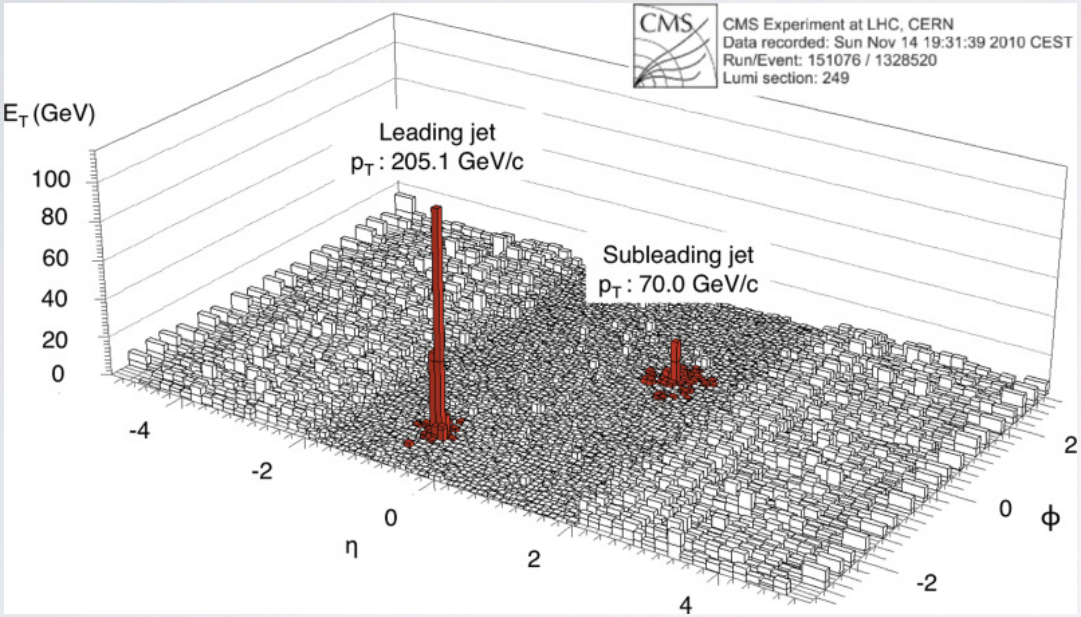

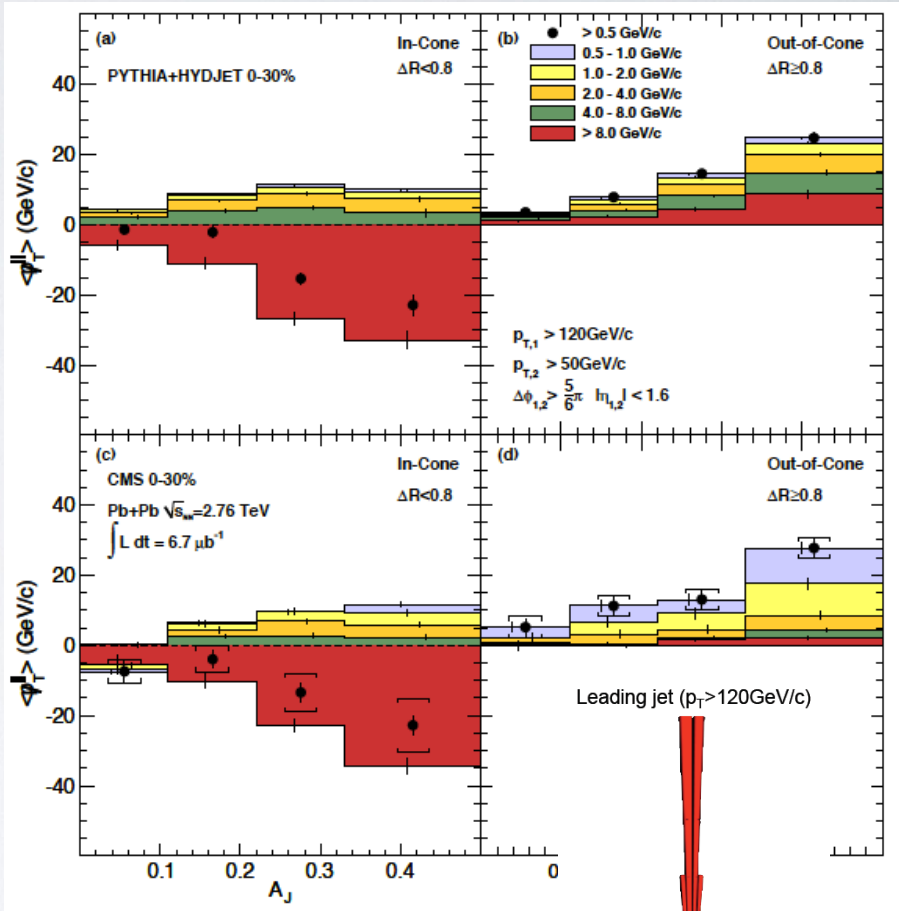

Missing energy is associated with additional **radiation of many soft quanta at large angles**

We argue that this reflects a **genuine feature of the in-medium QCD cascade** (JPB, E. Iancu and Y. Mehtar-Tani, arXiv: 1301.6102, PRL)

$$A_J = \frac{p_{T,1} - p_{T,2}}{p_{T,1} + p_{T,2}}$$

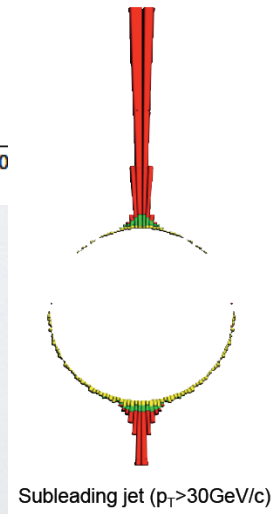

Jets in a quark-gluon plasma

How does the jet interacts with the medium?

- **Color coherence is altered inside a colored medium**

Y. Mehtar-Tani, K. Tywoniuk, C. A. Salgado, PRL (2011)

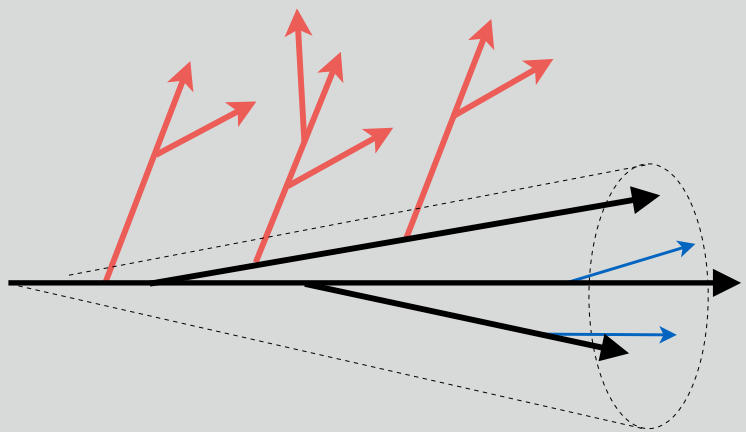

For collimated jets the medium only resolves the total color charge $\langle C_{jet} \rangle \neq 0$

- **Medium-induced radiation off the total jet charge at large angles**

J. -P. B, F. Dominguez, E. Iancu, Y. Mehtar-Tani. (2012-2013)

Medium-induced radiation

- Scatterings with the medium can induce gluon radiation
- The radiation mechanism is linked to transverse momentum broadening

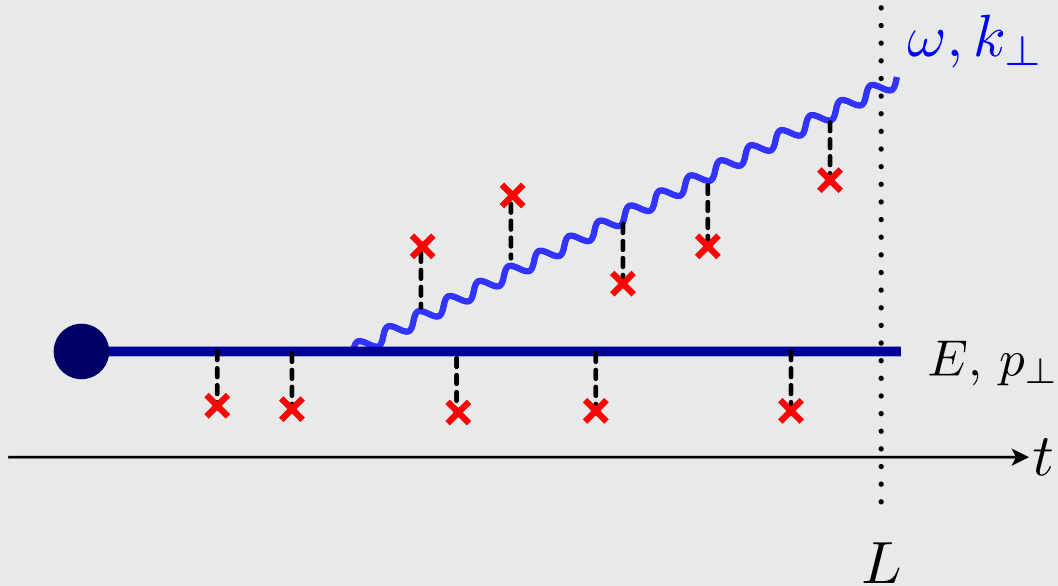

$$\Delta k_\perp^2 \simeq \hat{q}\,\Delta t$$

jet quenching parameter

$$\hat{q} \equiv \frac{\Delta k_\perp^2}{\Delta t} \simeq \frac{m_D^2}{\lambda} = \frac{(\text{Debye mass})^2}{\text{mean free path}}$$

[Baier, Dokshitzer, Mueller, Peigné, Schiff (1995-2000) Zakharov (1996)]

The BDMPSZ mechanism

Gluon emission is linked to momentum broadening

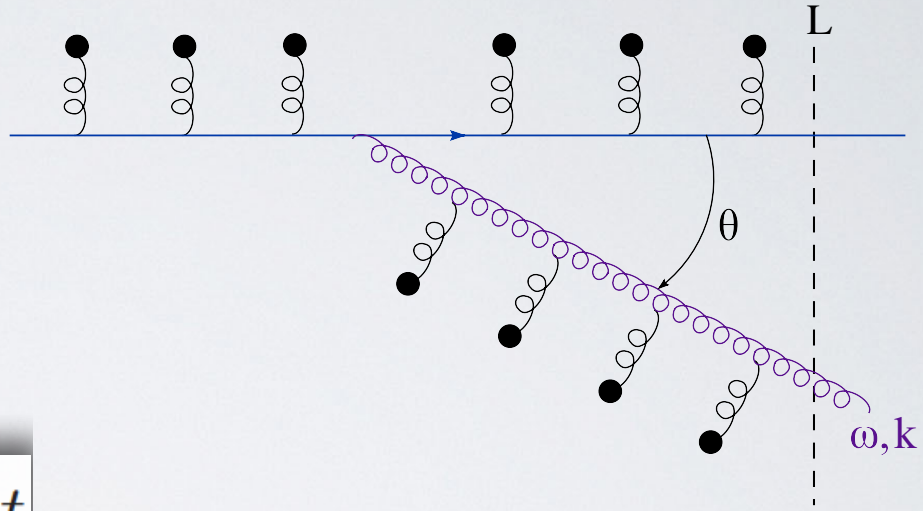

$$\frac{1}{\tau_{\rm f}} \sim \frac{k_\perp^2}{2\omega}$$

$$\Delta k_\perp^2 = \hat{q}\Delta t$$

Time scale for the branching process

$$\tau_{\rm br}(\omega) \sim \sqrt{\frac{2\omega}{\hat{q}}}$$

Medium of finite extent

$$\tau_{\rm br} \lesssim L \Rightarrow \omega \lesssim \omega_c \qquad \omega_c \sim \hat{q}L^2$$

Formation time and emission angle

Typical branching kT and angle

$$k_{\rm br}^2 = \hat{q}\tau_{\rm br}$$

$$\theta_{\rm br} \sim k_{\rm br}/\omega \sim \left(\hat{q}/\omega^3\right)^{1/4}$$

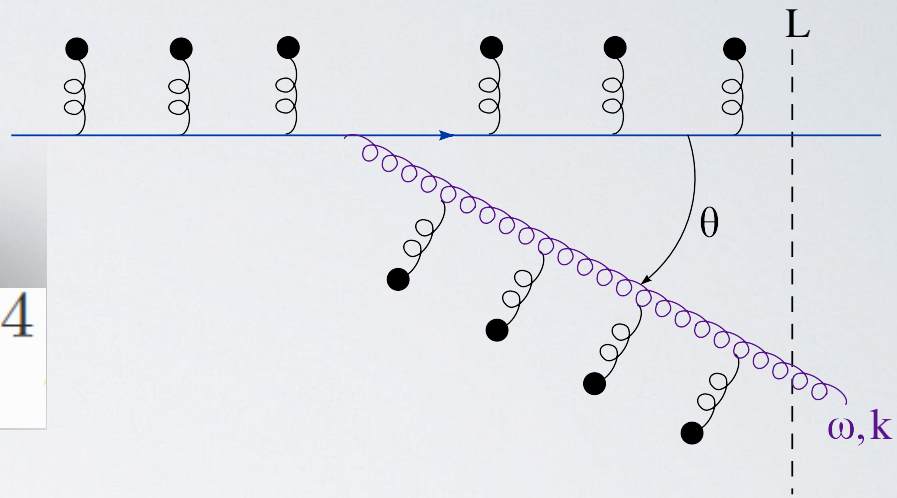

Hard gluon: small angle, long time

$$\tau_{\rm br} \lesssim L \qquad \omega \lesssim \omega_c \qquad \theta_{\rm br} \gtrsim \theta_c$$

Soft gluon: large angle, short time

$$\tau_{\rm br} \ll L \qquad \omega \ll \omega_c \qquad \theta_{\rm br} \gg \theta_c$$

Multiple branchings in-medium cascade

$$\omega \frac{\mathrm{d}N}{\mathrm{d}\omega} \simeq \frac{\alpha_s N_c}{\pi} \sqrt{\frac{\omega_c}{\omega}} \equiv \bar{\alpha} \sqrt{\frac{\omega_c}{\omega}} = \bar{\alpha} \frac{L}{\tau_{\mathrm{br}}(\omega)}$$

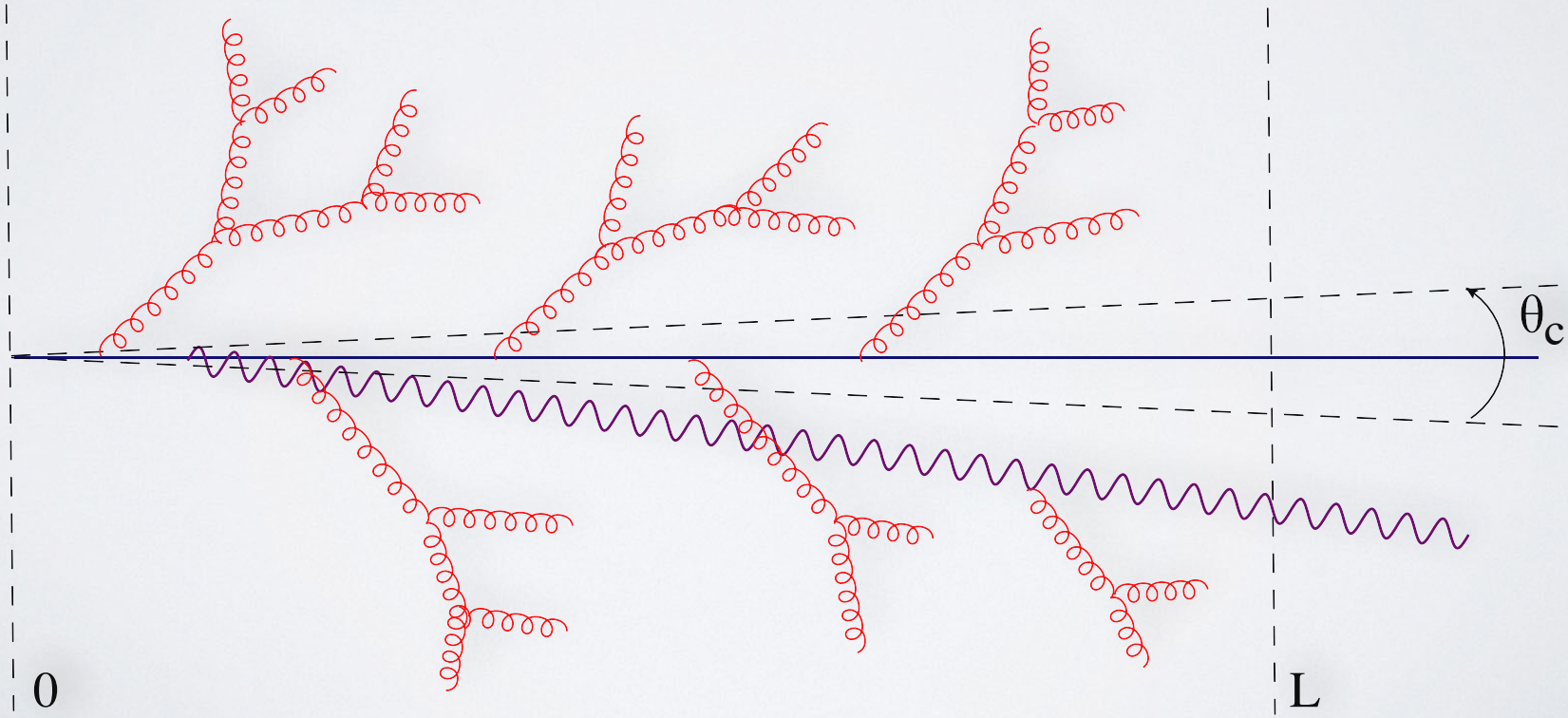

Multiple emissions

In medium, interference effects are subleading, and independent emissions are enhanced by a factor L/τ_f

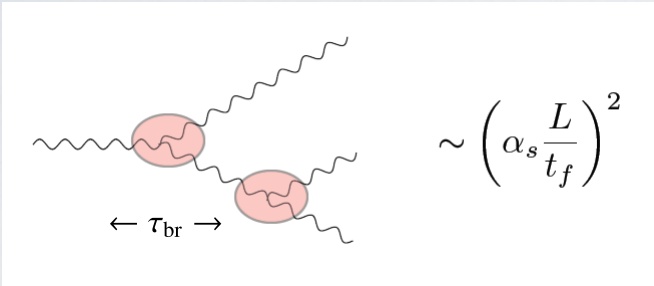

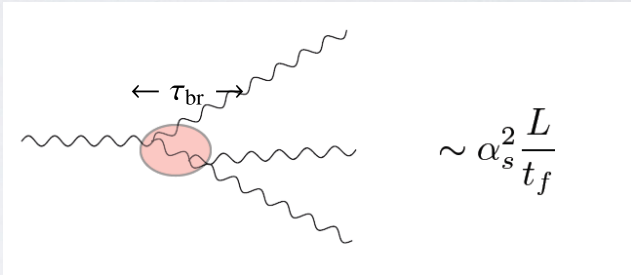

When $\bar{\alpha} L/\tau_{br} \sim 1$ all powers of $\bar{\alpha} L/\tau_{br} \sim 1$ need to be resummed.

Since independent emissions dominate, the leading order resummation is equivalent to a probabilistic cascade, with nearly local branchings

JPB, F. Dominguez, E. Iancu, Y. Mehtar-Tani, arXiv: 1209.4585

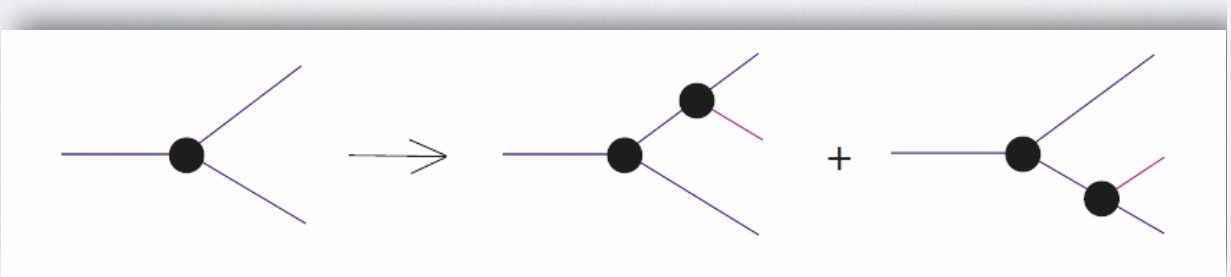

Note: already implemented in some Monte Carlo codes (MARTINI, Q_Pythia, etc)

Inclusive Gluon Distribution

Density of gluons with momentum k inside a parton with momentum p:

$$x\frac{dN}{dx\,d^2\boldsymbol{k}} \equiv D(x,\boldsymbol{k},t)$$

$$x = \omega/E$$

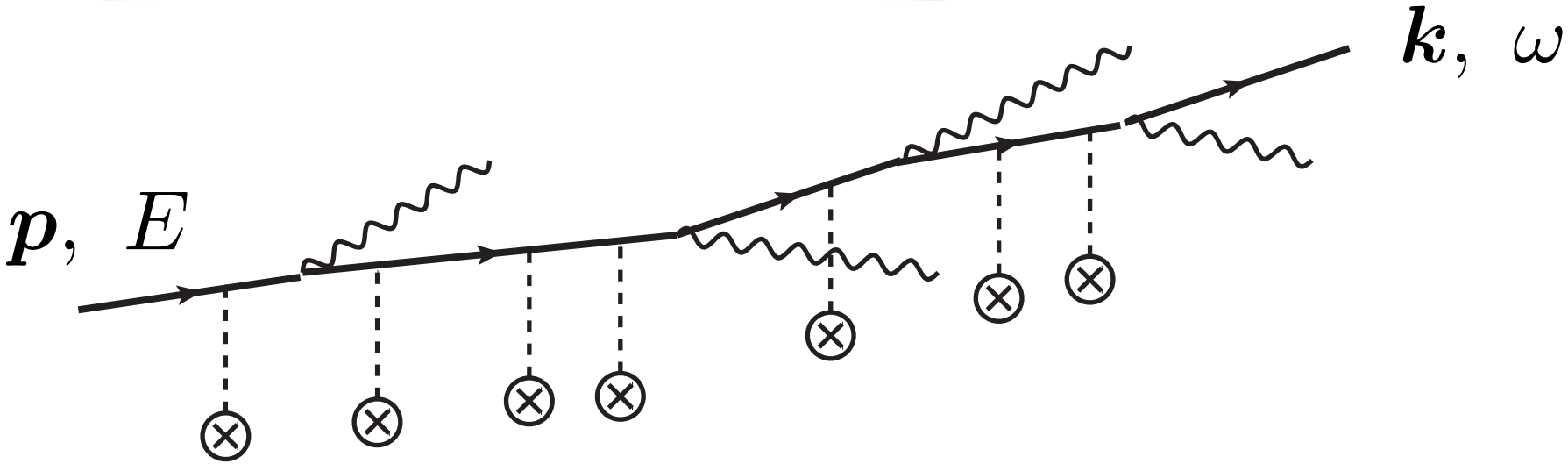

Inclusive one-gluon distribution

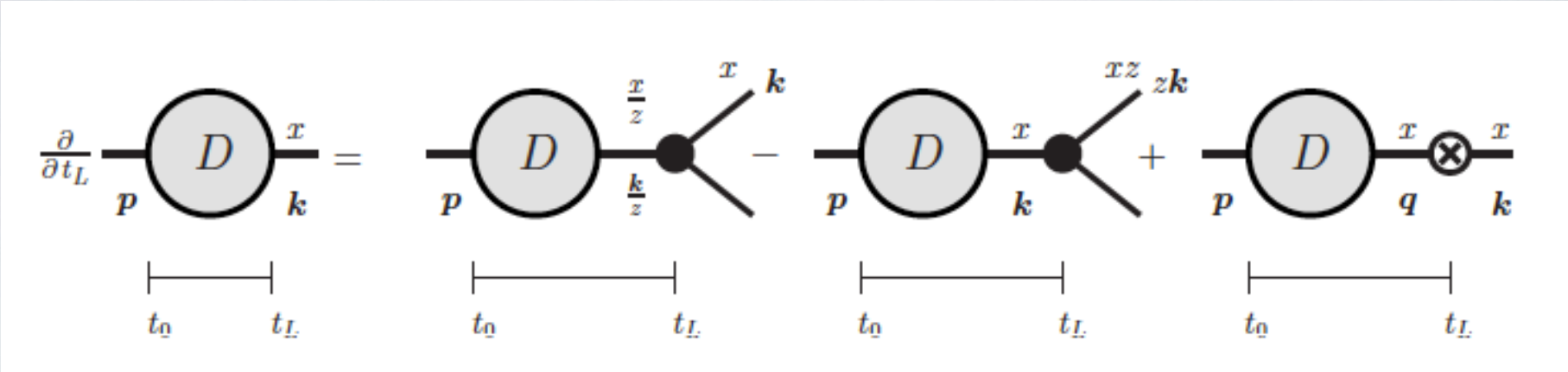

Leading order equation

$$\frac{\partial}{\partial t} D(x, \boldsymbol{k}, t) = \int_{\boldsymbol{l}} \mathcal{C}(\boldsymbol{l}, t) D(x, \boldsymbol{k} - \boldsymbol{l}, t)$$
$$+ \alpha_s \int_0^1 \mathrm{d}z \left[\frac{2}{z^2} \mathcal{K}\left(z, \frac{x}{z} p_0^+; t\right) D\left(\frac{x}{z}, \frac{\boldsymbol{k}}{z}, t\right) - \mathcal{K}\left(z, x p_0^+; t\right) D(x, \boldsymbol{k}, t) \right]$$

Di-jet asymmetry and turbulence

soft particles
large angles

Richardson cascade 1921

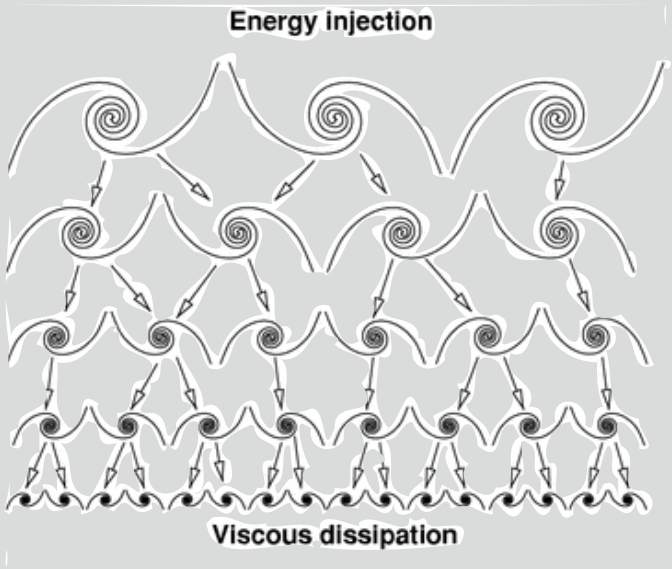

- gain = loss $\Longrightarrow$ the energy flux is independent of x
- energy flows from large to low frequencies and large angles without accumulating (signature of wave turbulence)

Efficient mechanism for energy transport at large angles

Energy flow through democratic branching

Integrating over transverse momentum yields equation for energy flow

$$\frac{\partial D(x,\tau)}{\partial \tau} = \int \mathrm{d}z\, \mathcal{K}(z) \left[\sqrt{\frac{z}{x}} D\left(\frac{x}{z},\tau\right) - \frac{z}{\sqrt{x}} D(x,\tau) \right]$$

$$\mathcal{K}(z) = \frac{\bar{\alpha}}{2} \frac{f(z)}{[z(1-z)]^{3/2}}, \qquad f(z) = \left[1 - z(1-z)\right]^{5/2}$$

Similar eq. postulated: R. Baier, A. H. Mueller, D. Schiff, D.T. Son (2001) S. Jeon, G. D. Moore(2003)

Formally analogous to DGLAP. But very different kernel... and physics.

→ A QCD cascade of a new type

Exhibits wave turbulence

One finds (exact result) $$D(x,t) \simeq \frac{t}{\sqrt{x}}\, \mathrm{e}^{-\pi t^2} \qquad \text{for } x \ll 1$$

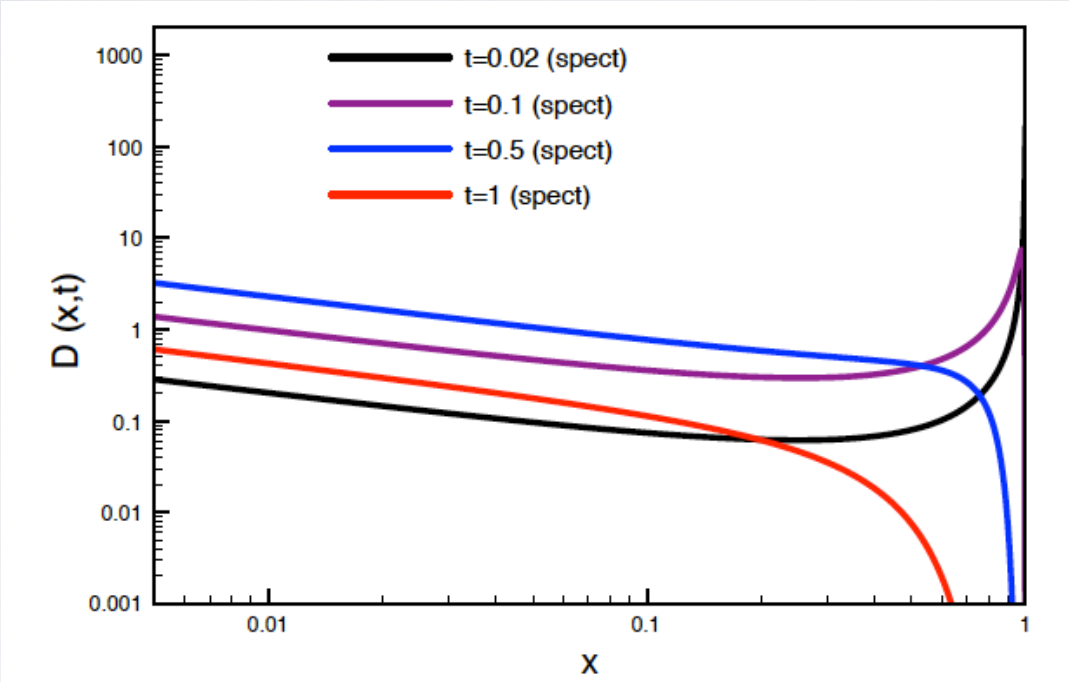

Fine (local) cancellations between gain and loss terms

BDMPS spectrum emerges as a fixed point, scaling, spectrum

Characteristic features of wave turbulence (Kolmogorov, Zakharov)

Kolmogorov exponent 1/2

Digresssion: source problem

At this (fixed) point ALL the energy flows through the whole system

Energy is injected at x=1, at a constant rate

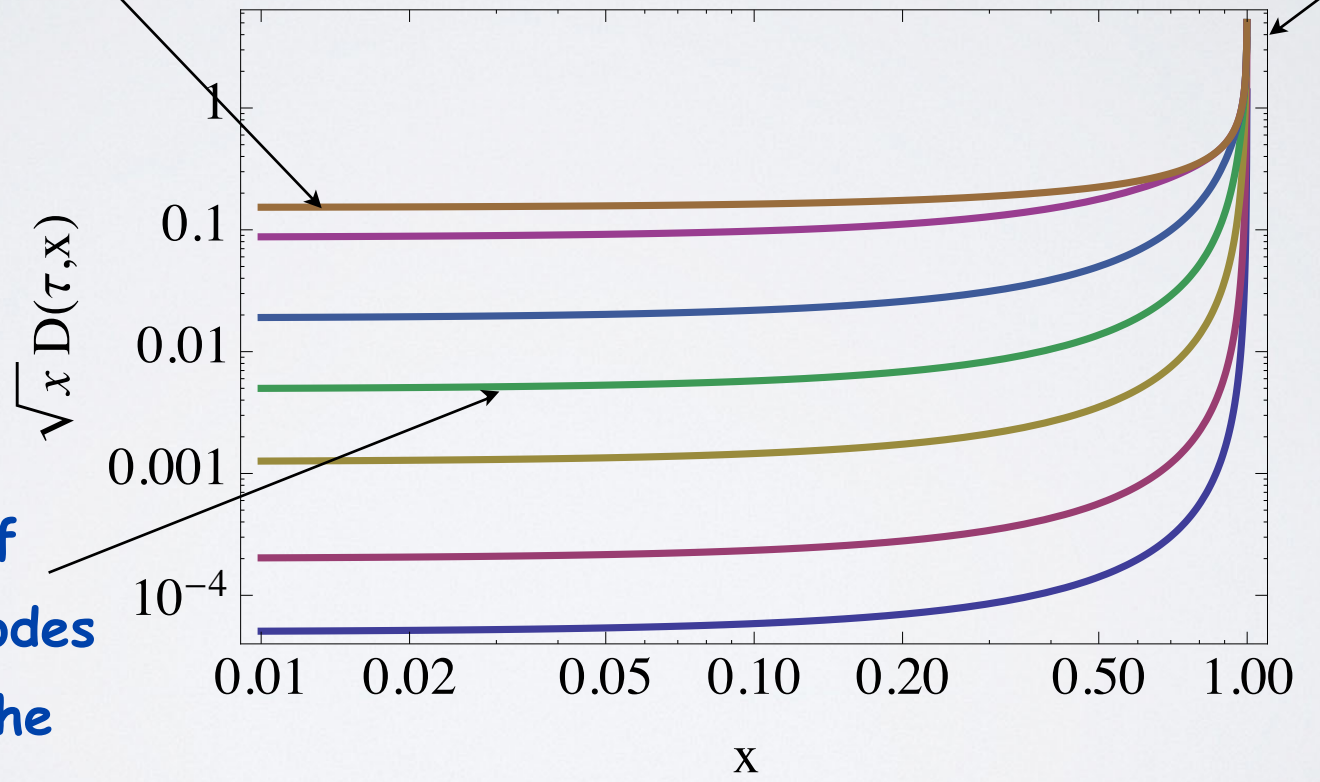

The population of the various x-modes grows, keeping the shape of the spectrum at small x

Relevance to di-jet asymmetry

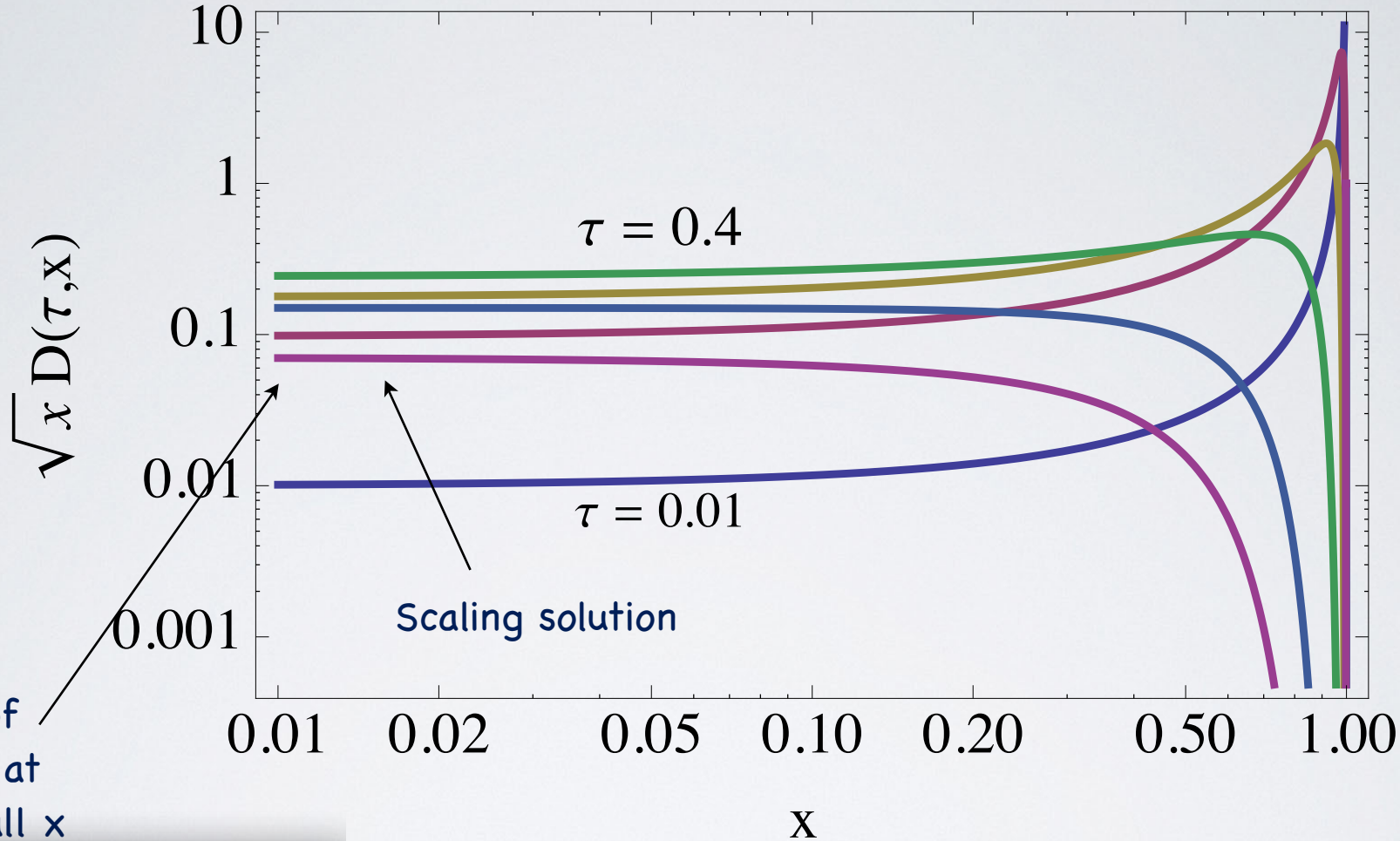

Flow of energy at very small x

$$\mathcal{E}_{\rm flow} = E\frac{\upsilon\tau^2}{2} = \frac{\upsilon}{2}\,\bar{\alpha}^2\omega_c \qquad \omega_c \equiv \frac{\hat{q}L^2}{2} \qquad \upsilon \simeq 5$$

Estimate $\hat{q} = 1\,\mathrm{GeV}^2/\mathrm{fm}$ $\quad \omega_c \simeq 40$ Gev $\quad \bar{\alpha}^2 \simeq 0.1$ $\quad \mathcal{E}_{\rm flow} \simeq 15$ GeV

$L = 4$ fm

J.-P. B., E. Iancu, Y. Mehtar-Tani, PRL 2013

Energy flow at large angle

$E_{\rm in}$ energy in the jet with x>xo

$E_{\rm out}$ energy in the spectrum with x<xo

$E_{\rm out} + E_{\rm flow}$ energy out of the jet cone

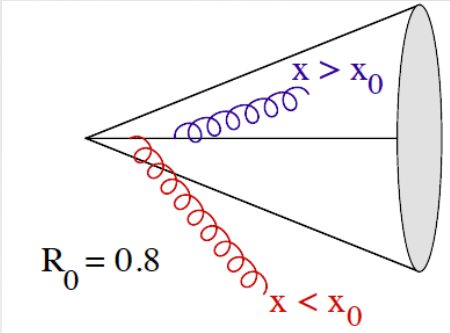

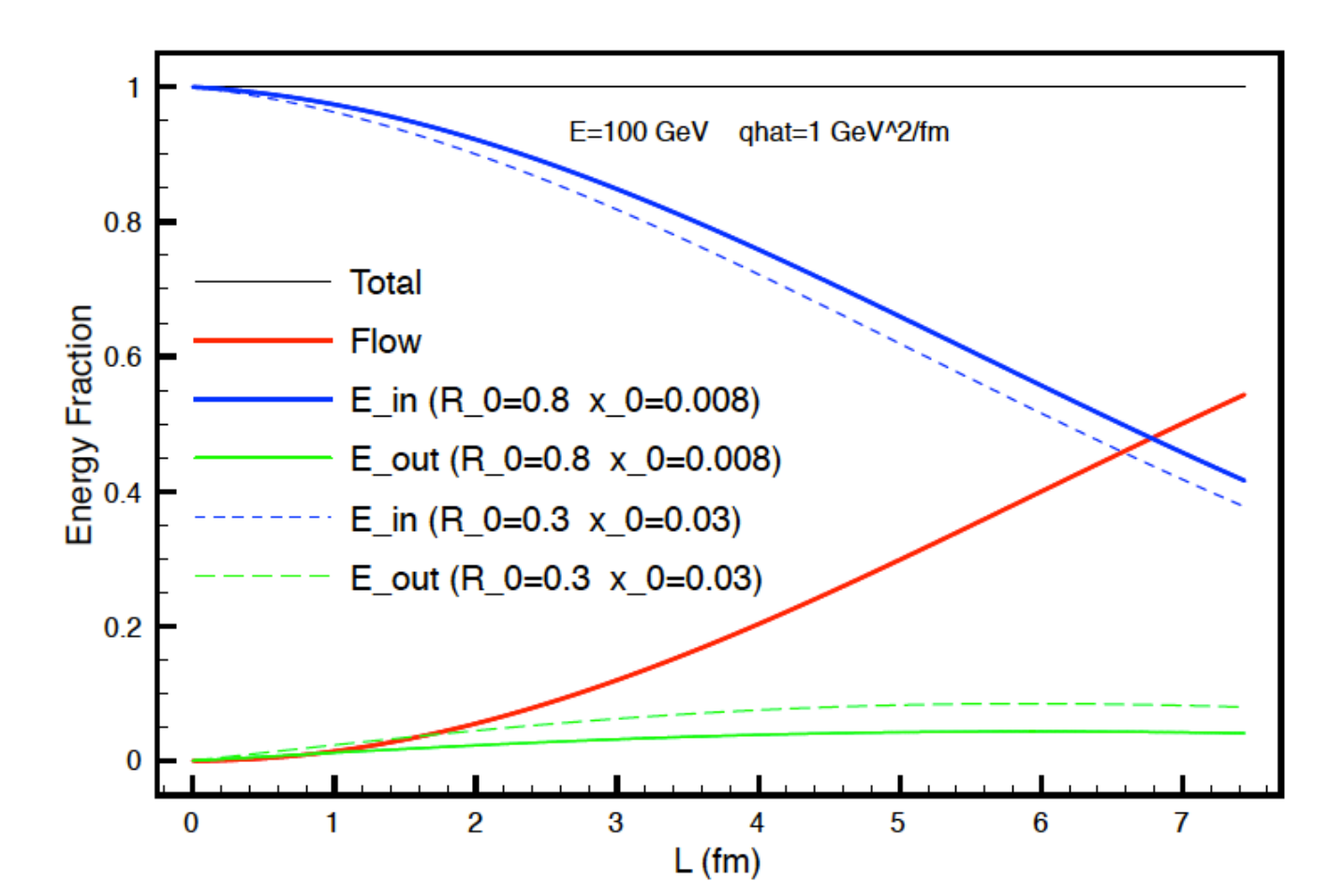

Thermalization
Classical-statistical simulations

Fixed point analysis of classical-statistical (real-time) simulations

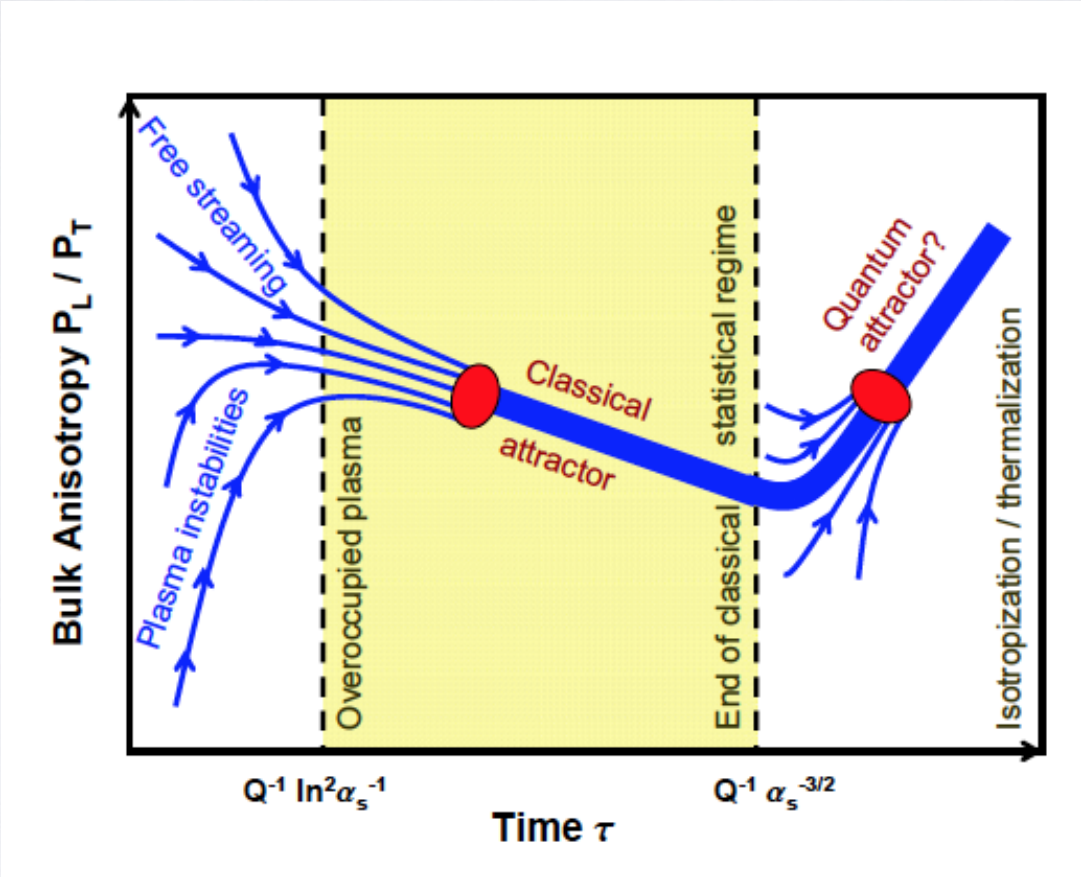

J. Berges, K. Bogulavski, S. Schlichting and R. Venugopalan, arXiv: 1303.5650

Bottom-up thermalization

R. Baier, A. H. Mueller, D. Schiff and D. T. Son, Phys. Lett. B 502, 51 (2001)

Based on kinetics after time $\tau \gtrsim Q_s^{-1}$

Assumes initial gluon density of the form $\frac{\mathrm{d}N}{\mathrm{d}y\mathrm{d}k_\perp^2} = \frac{1}{\alpha} f\left(\frac{k_\perp}{Q_s}\right)$

1. Fast emission of soft gluons

2. Quick equilibration of the soft gluons which form a thermal bath

3. Hard gluons loose their energy to the soft bath, till complete thermalization

This last phase shares common features with the in-medium QCD cascade described earlier.

Bottom-up last stage

analysis using kinetic theory

$$\left(\frac{\partial}{\partial\tau} - \frac{p_z}{\tau}\frac{\partial}{\partial p_z}\right) f(\vec{p}) = C_{\rm el} + C_{\rm prod}$$

inelastic contributions are like gain and loss term in the branching processes

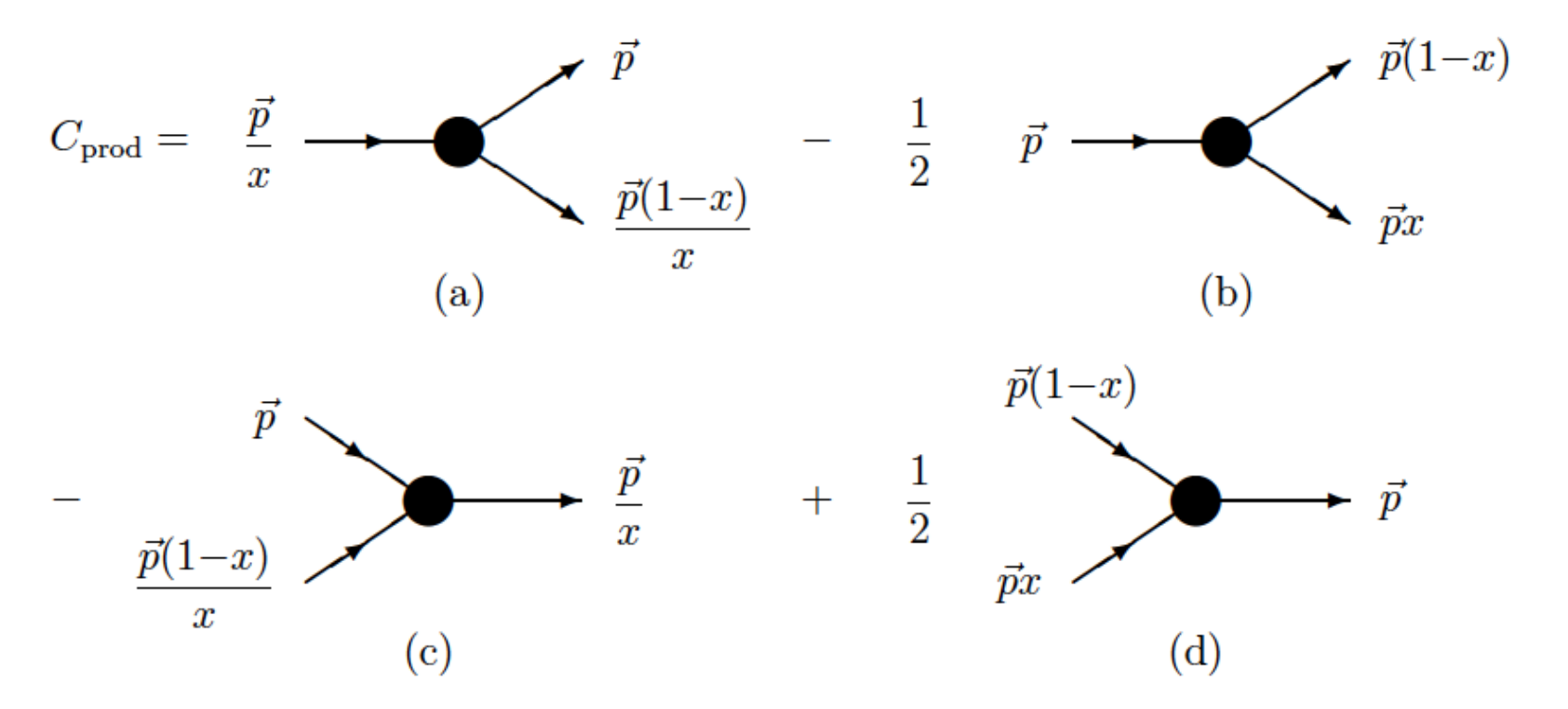

Bottom-up last stage

energy carried by hard gluons $\int dp_\perp \epsilon(p_\perp)$

$$\epsilon(p_\perp) = 2\pi p_\perp^2 \int dp_z\, f(\vec{p})$$

kinetic equation reduces to

$$\frac{1}{\tau}\frac{\partial}{\partial\tau}(\tau\epsilon(p_\perp)) = \frac{\alpha^2 N^{1/2}}{p_\perp^{1/2}} \int dx\, h(x)\left[x^{1/2}\epsilon\left(\frac{p_\perp}{x}\right) - \frac{1}{2}\epsilon(p_\perp)\right]$$

$$h(x) = h_0 \frac{(1-x+x^2)^{5/2}}{(x-x^2)^{3/2}}$$

analogous to the equation controlling the evolution of the spectrum for the in-medium QCD cascade. Same fixed point (stationary solution) with

$$\epsilon(p) \sim 1/\sqrt{p}$$

Summary

In a medium of large size, the successive branchings can be treated as independent, giving rise to a cascade that is very different from the vacuum cascade (no angular ordering, turbulent flow)

This turbulent cascade provides a simple and natural mechanism for the transfer of jet energy towards very large angles. The mechanism is intrinsic, not related to a specific coupling between the jet and the medium.

This turbulent cascade may play a role in the latest stages of the thermalization of the quark-gluon plasma produced in ultra-relativistic heavy ion collisions

Universality far from equilibrium and the range of validity of classical-statistical simulations

Kirill Boguslavski

Ruprecht-Karls
University Heidelberg

In collaboration with:
Jürgen Berges
Sören Schlichting
Raju Venugopalan

Based on:
arXiv:1312.5216
arXiv:1311.3005
arXiv:1303.5650

The Approach to Equilibrium in Strongly Interacting Matter
RIKEN BNL Research Center Workshop

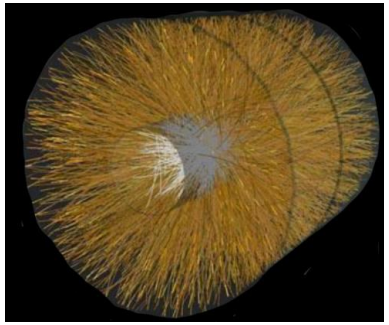

Alice, LHC, Cern

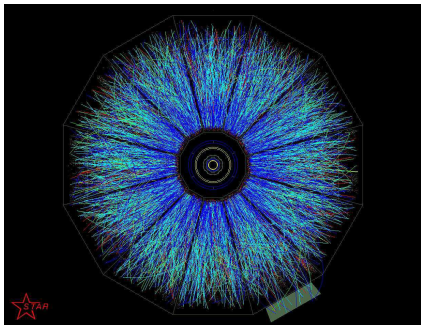

STAR Collaboration, RHIC, BNL

Table of Contents

1. Introduction

2. Turbulent thermalization process in scalar field theory

3. Comparison of scalar and gauge theories with longitudinal expansion

4. Conclusion and Outlook

Introduction

Heavy-ion collisions at early times

(Ultrarelativistic energies, weak-coupling limit)

Glasma + vacuum fluctuations → Plasma instabilities → Overoccupied plasma

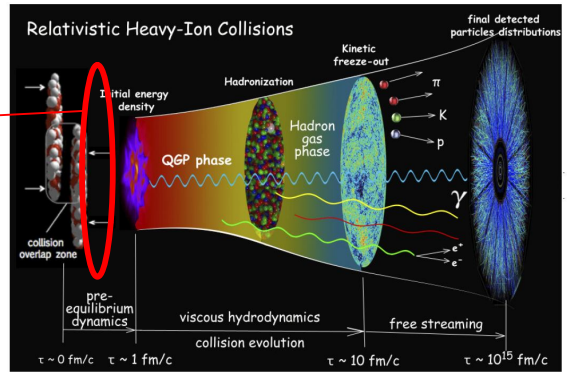

Little Bang by P. Sorensen and C. Shen

Early universe cosmology

($\lambda\phi^4$ -theory at weak couplings)

Large condensate $\phi \sim 1/\sqrt{\lambda}$ + vacuum fluctuations → Instabilities (e.g. Parametric resonance) → Overoccupied system $f(p \lesssim Q) \sim 1/\lambda$

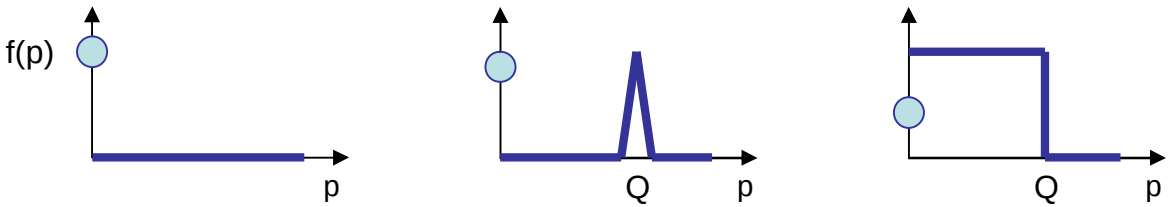

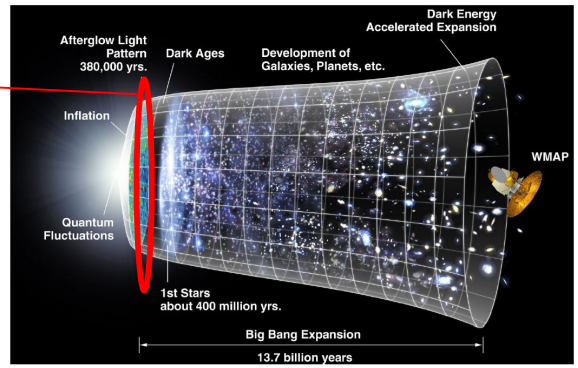

Big Bang by NASA

Turbulent thermalization process of the overoccupied scalar system

System approaches self-similar attractor

$$f(t,p) = t^{\alpha} f_s(t^{\beta} p)$$

Large occupancies

$$f(p \lesssim p_{\rm ch}) \sim 1/\lambda \gg 1$$

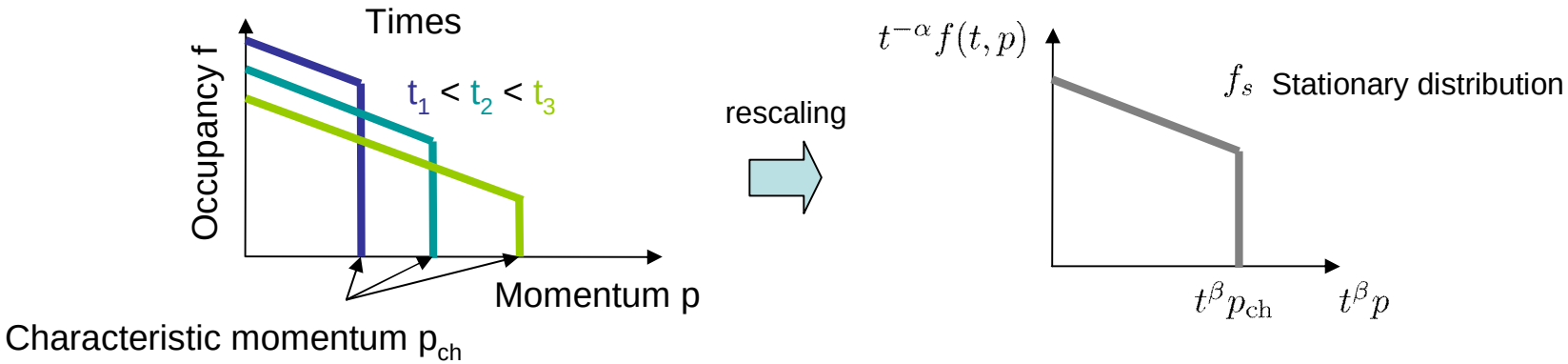

Dynamical scaling exponents: $\alpha = -\frac{4}{5}\,, \quad \beta = -\frac{1}{5}$

Micha, Tkachev (2004)

Dual cascade: Wave turbulence

Turbulent thermalization process in scalar theory

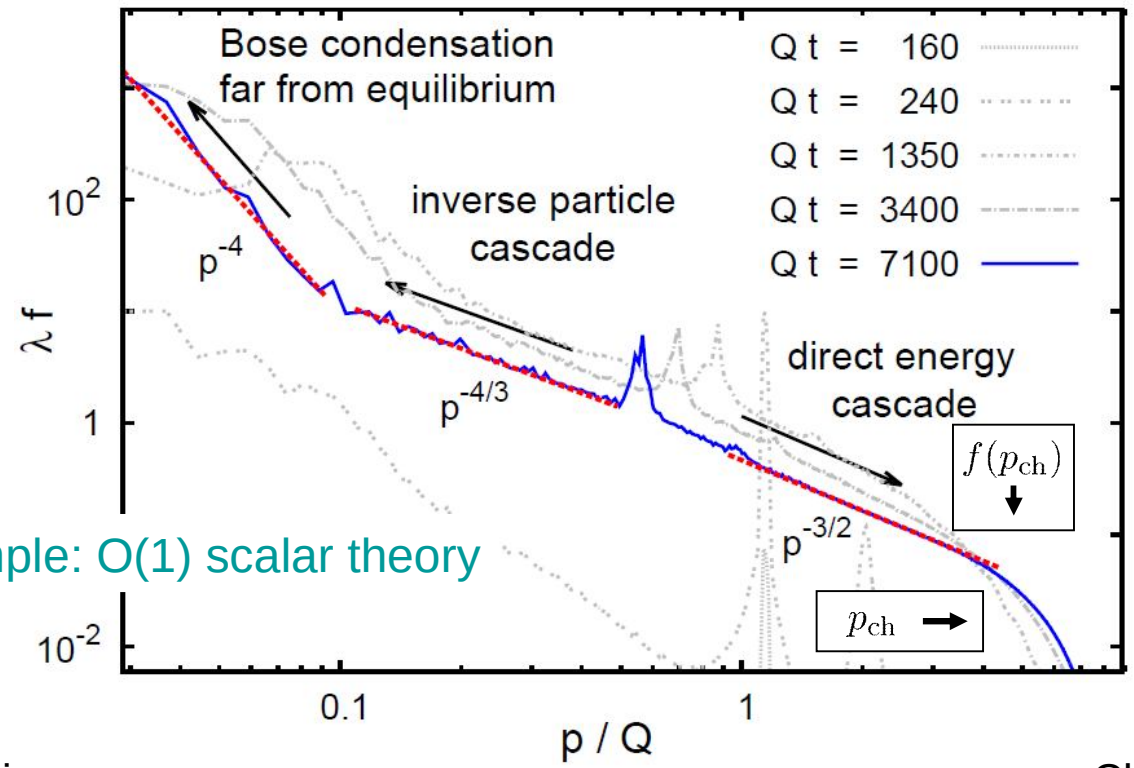

Example: O(1) scalar theory

Scale $Q = (\lambda\epsilon)^{1/4}$

with energy density ϵ

Bose Condensation:
Berges, Sexty (2012)

Energy cascade:
Micha, Tkachev (2004)

Particle cascade:
Berges, Rothkopf, Schmidt (2008)

Berges, KB, Schlichting, Venugopalan (2013)

Kinetic Processes:

$2 \leftrightarrow 2$ $\quad$ $2 \leftrightarrow 2$ $\quad$ $2 \leftrightarrow (1 + \text{soft})$

Characterized by exponents α, β and functional form f_s

Attractor approached for different initial conditions

Turbulent thermalization process in scalar theory

Condensate driven IC

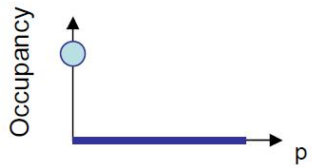

$\phi_0 \sim 1/\sqrt{\lambda}$ $\quad f = 0$

Fluctuation dominated IC

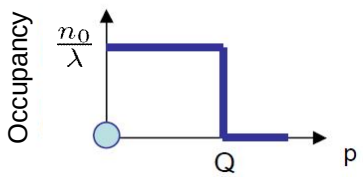

initial occupancy

$\phi_0 = 0$ $\quad f(p \leq Q_0) = n_0/\lambda$

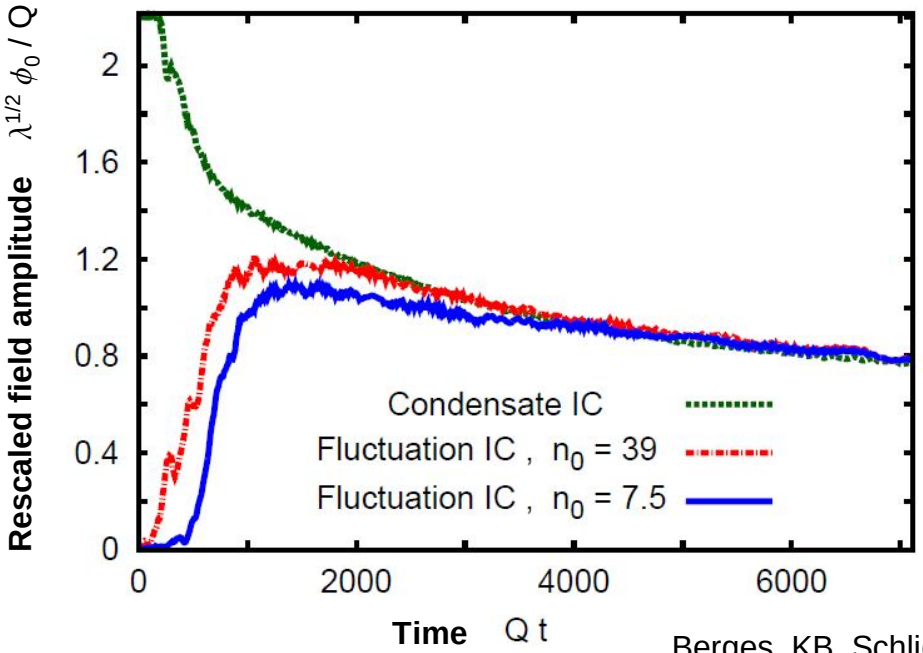

$(\ Q = (\lambda\epsilon)^{1/4}\ )$

Berges, KB, Schlichting, Venugopalan (2013) arXiv:1312.5216

Approach to the nonthermal attractor provides a partial memory loss!
Both sets of initial conditions lie in its basin of attraction.

Range of validity of classical-statistical simulations

Turbulent thermalization process in scalar theory

Method:
- Solve classical EOM on the lattice, e.g. $\Box\,\varphi + \frac{\lambda}{6}\varphi^3 = 0$
- Sampling with quantum initial conditions introduces fluctuations

Decades of research in cosmology: Klebnikov, Micha, Tkachev; Smit, Tranberg; Berges, Sexty; …

Classicality condition: $\langle\{\Phi,\Phi\}\rangle \gg \langle[\Phi,\Phi]\rangle$ or $f \gg 1$ Aarts, Berges (2001)

→ Accurate low-energy description of quantum theory!

Break-down time t_{quant} of classicality condition when $f(t_{\rm quant}, p_{\rm ch}) \approx 1$:

Onset time of attractor, self-similar evolution ⟶ $Q t_{\rm quant} \sim \boxed{15\ln(\lambda^{-1})}\,\lambda^{-5/4}$

Range of validity of classical-statistical simulations

Turbulent thermalization process in scalar theory

Rescaling: $\Box\,\varphi + \frac{\lambda}{6}\varphi^3 = 0 \xrightarrow{\varphi=\tilde{\varphi}/\sqrt{\lambda}} \Box\,\tilde{\varphi} + \frac{1}{6}\tilde{\varphi}^3 = 0$

Coupling drops out of classical dynamics

→ enters initial conditions, e.g. $\langle\tilde{\varphi}\tilde{\varphi}\rangle(t=0,p) = \frac{\tilde{f}(p)+\frac{\lambda}{2}}{\omega(p)}$

Coupling controls „quantum-$\frac{1}{2}$"

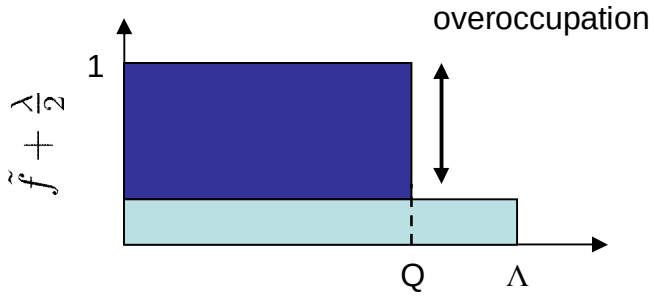

Break-down time t_* due to non-renormalizability of classical-statistical theory

$$Qt_* \sim 2048\pi^3\lambda^{-2}(Q/\Lambda)^{-2}$$

Epelbaum, Gelis (2014)

For finite cutoff $\Lambda \gg Q$
accurate low-energy description
for sufficiently small coupling λ

For $\Lambda \lesssim 15Q$ and $\lambda \lesssim 0.1$

$$Qt_* \gg 15\ln(\lambda^{-1})\,\lambda^{-5/4} \sim Qt_{\rm quant}$$

Comparison of scalar and gauge theories
with longitudinal expansion

Heavy-ion collisions in large nuclei, high energy, weak coupling limit

Change coordinates to proper time and rapidity

In new coordinates:
longitudinal expansion (in beam direction)

Compare simulations

Non-Abelian gauge theory (SU(2))

Berges, KB, Schlichting and Venugopalan (2013): arXiv:1311.3005, arXiv:1303.5650

Scalar field theory (O(4))

Berges, KB, Schlichting and Venugopalan

Thermalization process of expanding gauge theory: Nonthermal fixed-point for $f \gg 1$

Transverse shape of distribution

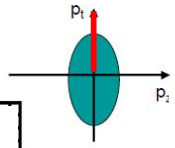

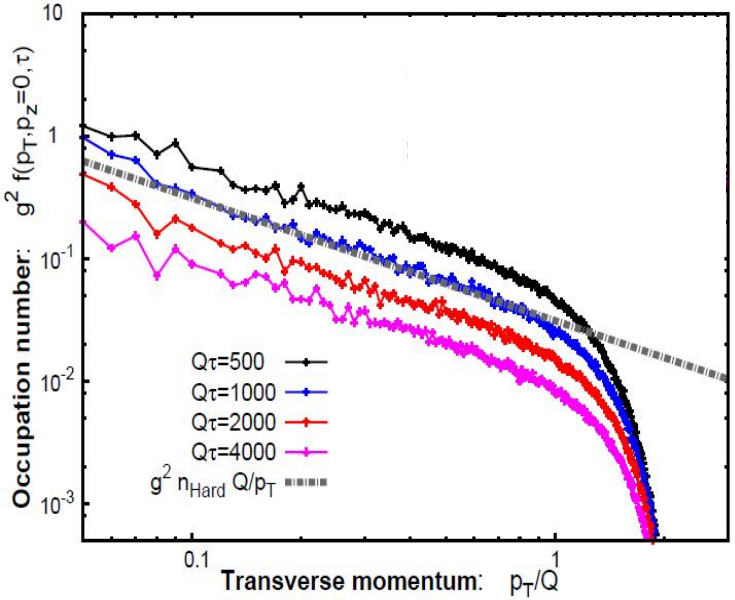

Berges, KB, Schlichting, Venugopalan (2013)
arXiv: **1311.3005**

Longitudinal shape of distribution

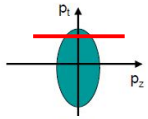

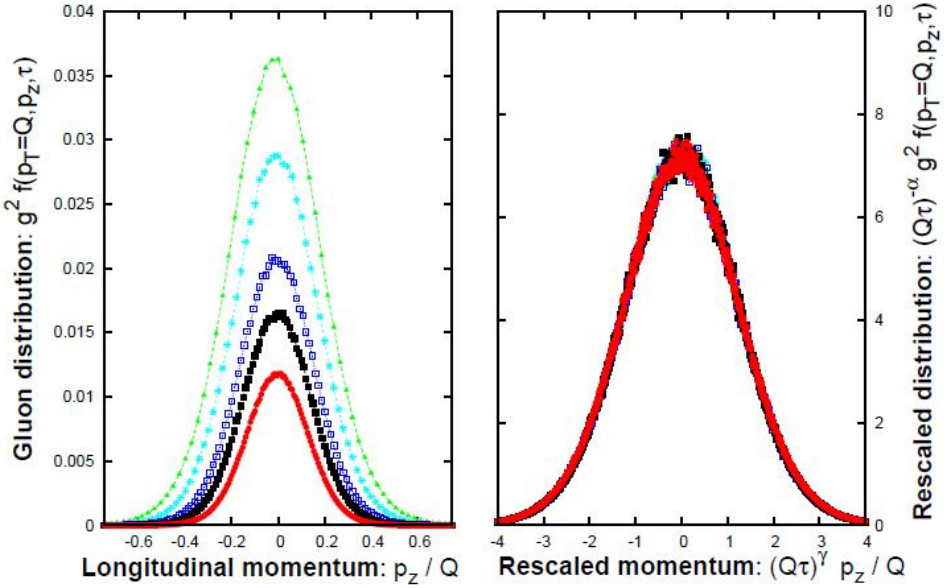

Berges, KB, Schlichting, Venugopalan (2013)
arXiv: **1303.5650**

Self-similar evolution

$$f(p_t, p_z, \tau) = \tau^{\alpha} f_s(\tau^{\beta} p_t, \tau^{\gamma} p_z)$$

Stationary function

Scaling exponents

$$\begin{array}{lcr} \alpha & \simeq & -2/3 \\ \beta & \simeq & 0 \\ \gamma & \simeq & 1/3 \end{array} \longrightarrow \alpha - \gamma = -1$$

Effective direction of scatterings

Comparison of expanding scalar and gauge theories

Scalars for harder momenta:

Thermal-like integrated distribution

Reminder: Self-similarity

$$f(p_t, p_z, \tau) = \tau^{\alpha} f_s(\tau^{\beta} p_t, \tau^{\gamma} p_z)$$

Relations

$$\boxed{\begin{aligned} \alpha - \gamma &\approx -1 \\ \beta &\approx 0 \end{aligned}}$$

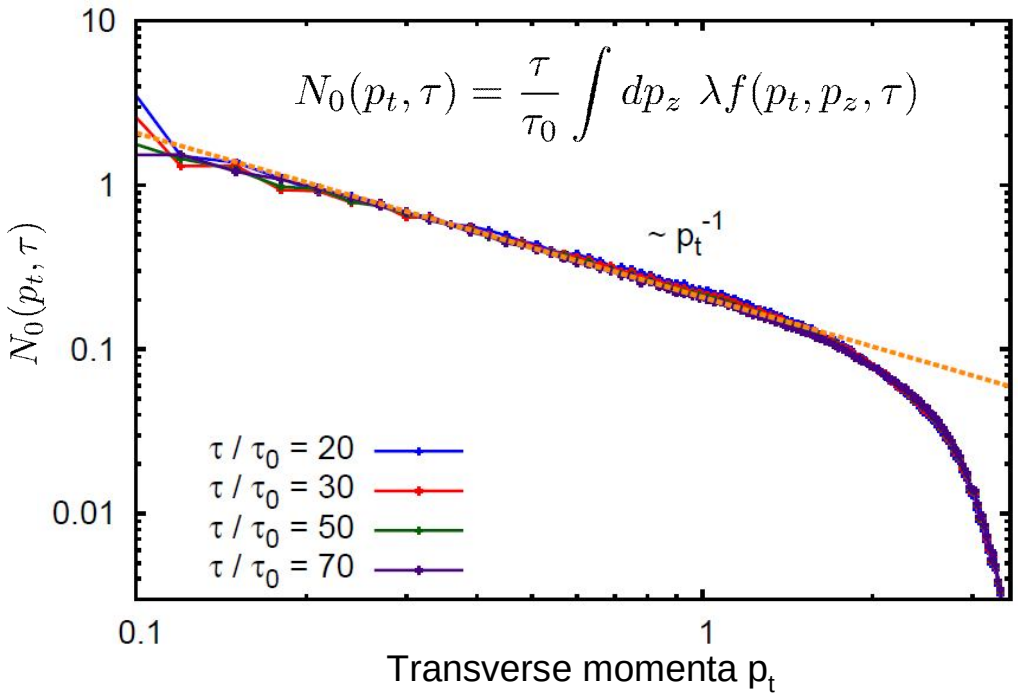

Effectively no flow into transverse direction.

Comparison: Also in expanding gauge theory scattering effectively proceeds in longitudinal direction

$$\left[\partial_\tau - \frac{p_z}{\tau}\partial_{p_z}\right] f(p_t, p_z, \tau) \; = \hat{q} \; \partial^2_{p_z} f(p_t, p_z, \tau)$$

for $2 \leftrightarrow 2$ elastic processes

Baier, Mueller, Schiff, Son (BMSS) (2001)

Universal scaling function for both theories

Comparison of expanding scalar and gauge theories

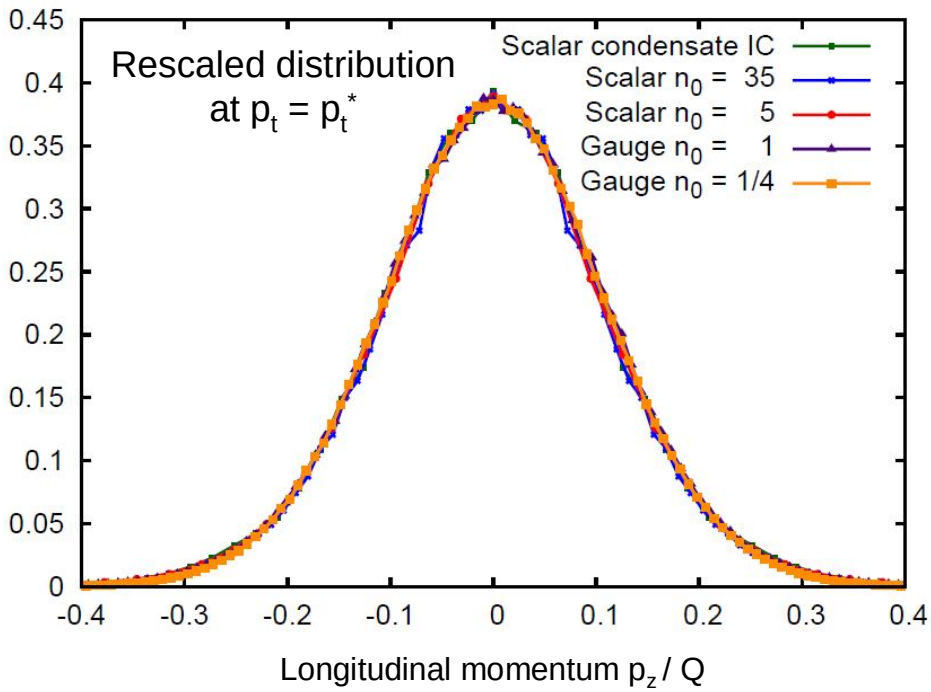

Scalars: Characteristic transverse momentum p_t^*

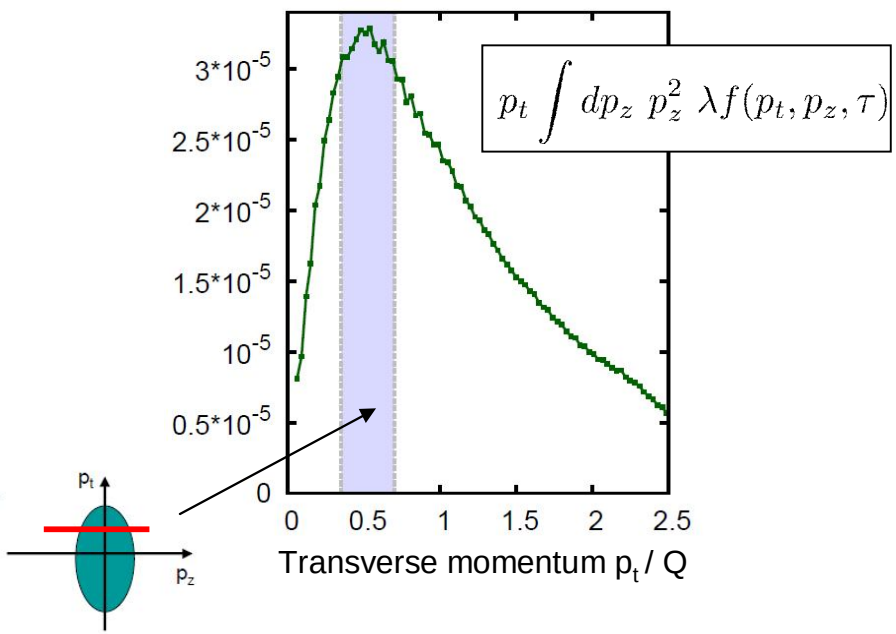

Universal scaling function: At characteristic momentum p_t^*, distribution functions for different initial conditions of scalar and gauge theories lie on top of each other!

Scalars: Insensitivity to different initial conditions

Comparison of expanding scalar and gauge theories

Scalars: Occupation number $\lambda f(p_t^*, p_z = 0)$

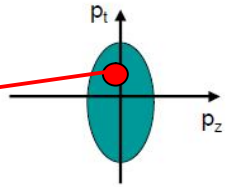

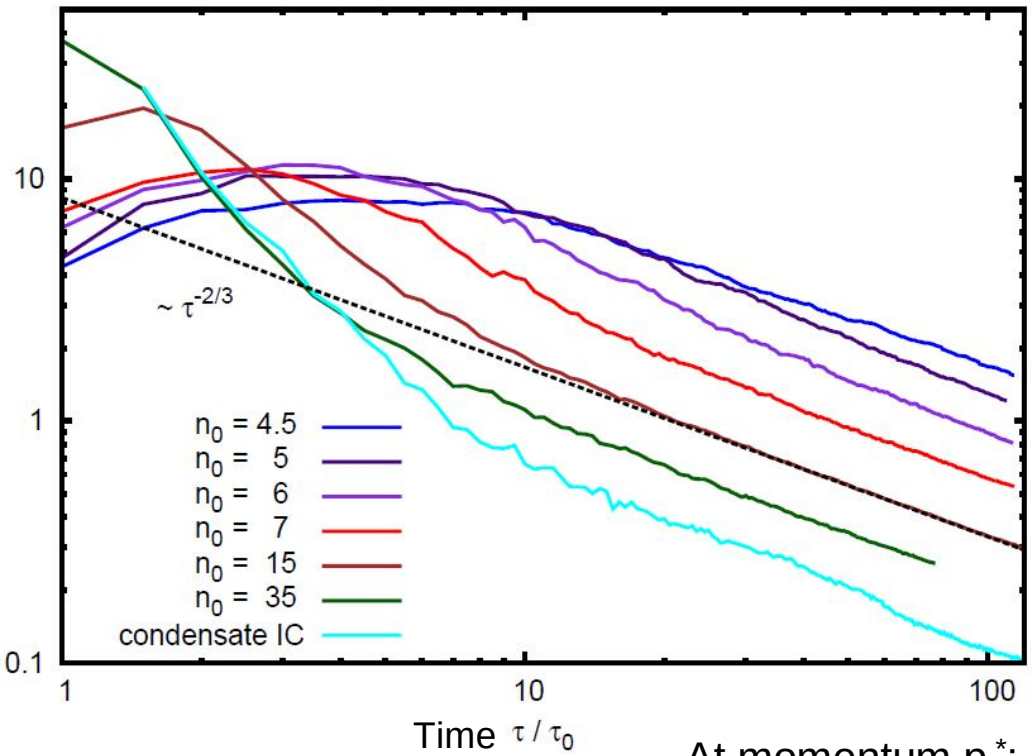

At momentum p_t^*:

Different IC

Fluctuation IC

Condensate IC

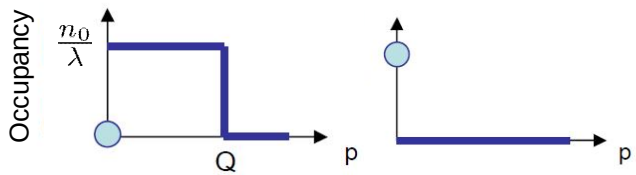

Reminder: Self-similarity

$$f(p_t, p_z, \tau) = \tau^{\alpha} f_s(\tau^{\beta} p_t, \tau^{\gamma} p_z)$$

$$\Rightarrow \lambda f(p_t^*, p_z = 0) \sim \tau^{\alpha}$$

Universal exponent $\alpha \simeq -2/3$
in scalar and gauge theories.

Insensitive to initial conditions!

Universal dynamical scaling exponents

Comparison of expanding scalar and gauge theories

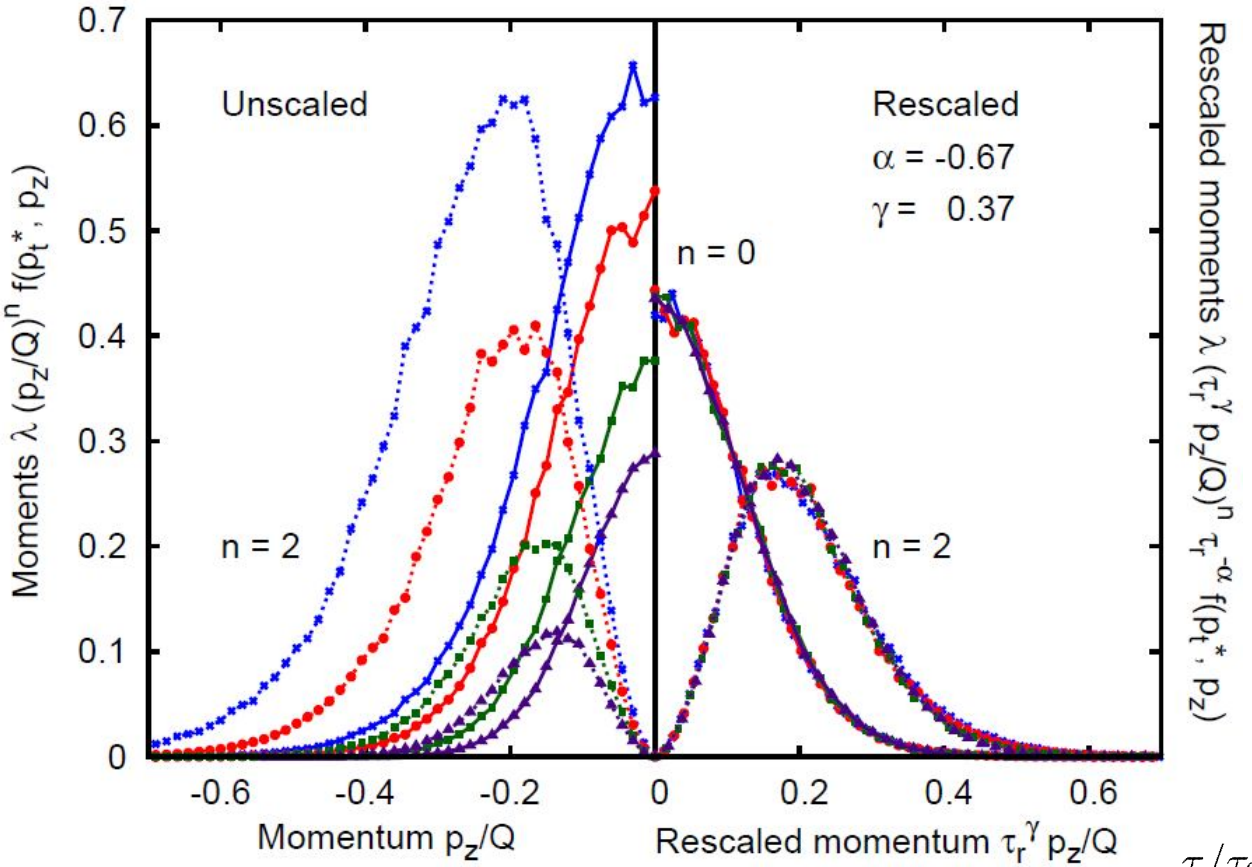

Scalars: Dynamical scaling exponents:

$$\alpha \simeq -2/3$$
$$\gamma \simeq 1/3$$

Self-similar evolution with same exponents as in gauge theory!

At momentum $p_t = p_t^*$

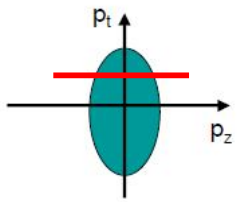

Times

$$\tau/\tau_0 = 22 - 74$$

Conclusion and Outlook

Conclusion:

- Nonthermal fixed points in non-expanding and expanding scalar field theories
  → Characterized by self-similarity, insensitive to different sets of initial conditions.

- Universality far from equilibrium in longitudinally expanding systems
  → Same scaling exponents and scaling function in characteristic momentum range!

Outlook:

- How can this strong similarity between scalar and gauge theories be explained in detail? → Currently under investigation.

- Direct calculations at stronger couplings with classical techniques?
  → Known to fail for scalars *Berges, KB, Schlichting, Venugopalan (2013) ; Epelbaum, Gelis, Wu (2014)*

- How do the systems evolve in the under-occupied regime $f \lesssim 1$ where the classical-statistical approach is no longer valid? Is there a (quantum) attractor?

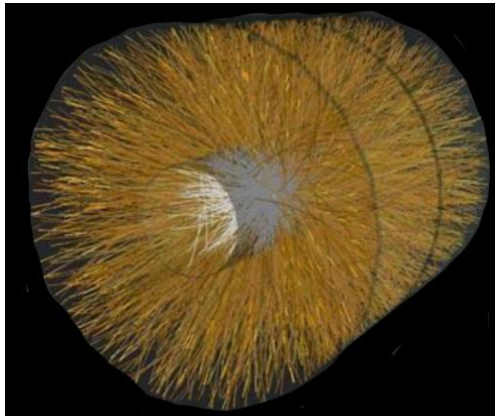

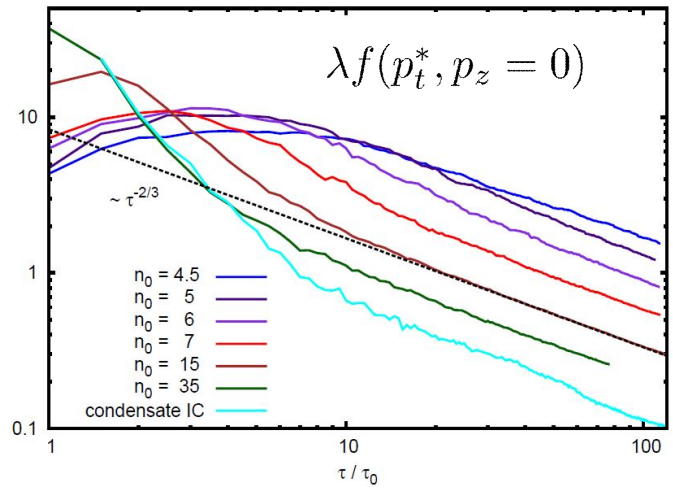

Thank you for your attention!

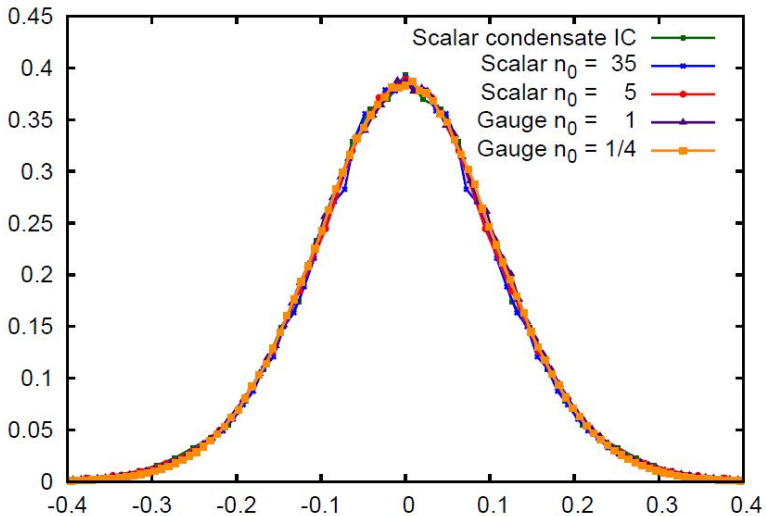

BACKUP SLIDES

Range of validity of classical-statistical simulations

Increasing the coupling

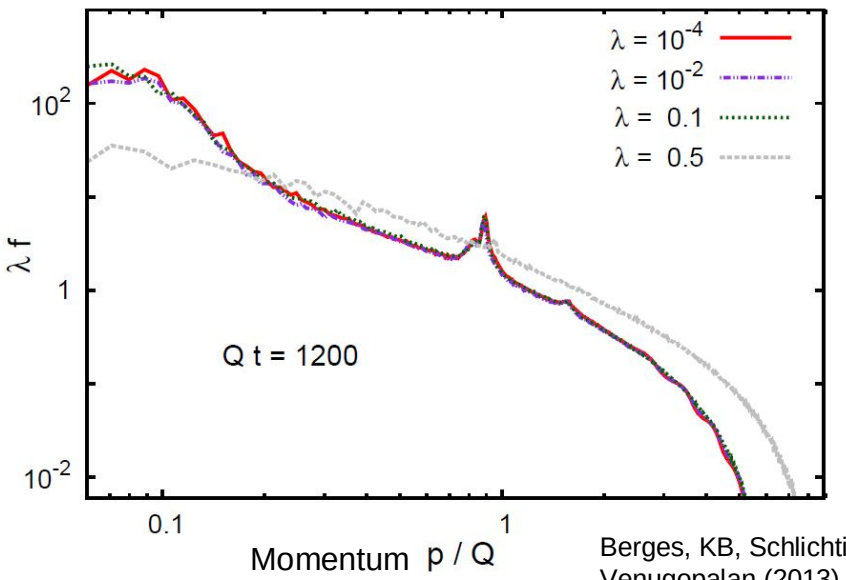

Berges, KB, Schlichting, Venugopalan (2013) arXiv:1312.5216

Up to some coupling no deviations visible. For larger couplings, validity tests needed.

Occupying just unstable modes

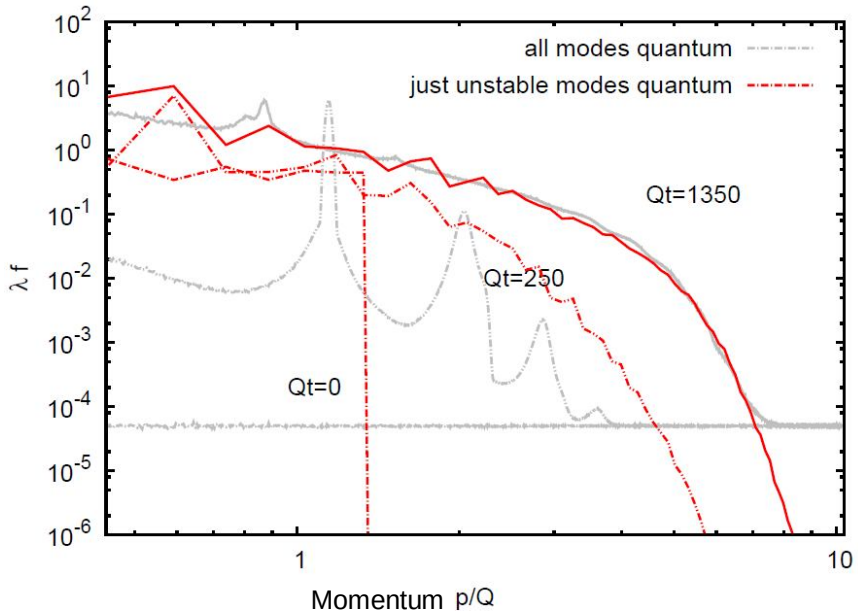

Evolution at later times as for weak coupling.

Range of validity of classical-statistical simulations

Turbulent thermalization process in scalar theory

Check cutoff dependence for small coupling, e.g. $\lambda = 10^{-4}$

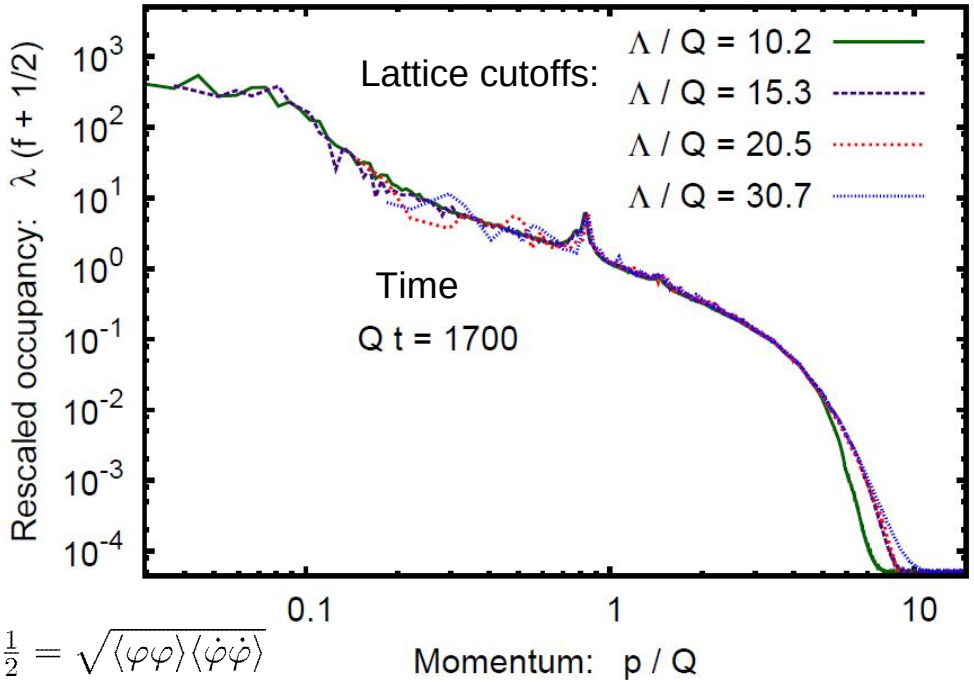

$f + \frac{1}{2} = \sqrt{\langle\varphi\varphi\rangle\langle\dot{\varphi}\dot{\varphi}\rangle}$

Maximum cutoff exists, for which results are still accurate.

But small cutoffs lead to lattice artifacts.

→ Cutoffs limited to time dependent finite window.

Relevant modes p / Q < 5 insensitive to the shown cutoffs at this time.

Range of validity of classical-statistical simulations

Testing simulations for same cutoff

Classicality condition

$$f \gg 1$$

Energy parts

$$\epsilon_\phi = \lambda \phi_0^4/24 \quad \text{(Condensate)}$$

$$\epsilon_{\text{part}} = \int_{\boldsymbol{p}} \omega f \quad \text{(Particles)}$$

$$\epsilon_{\text{quant}} = \int_{\boldsymbol{p}} \omega f \; \Theta(1-f)$$

(Estimate for modes not satisfying condition)

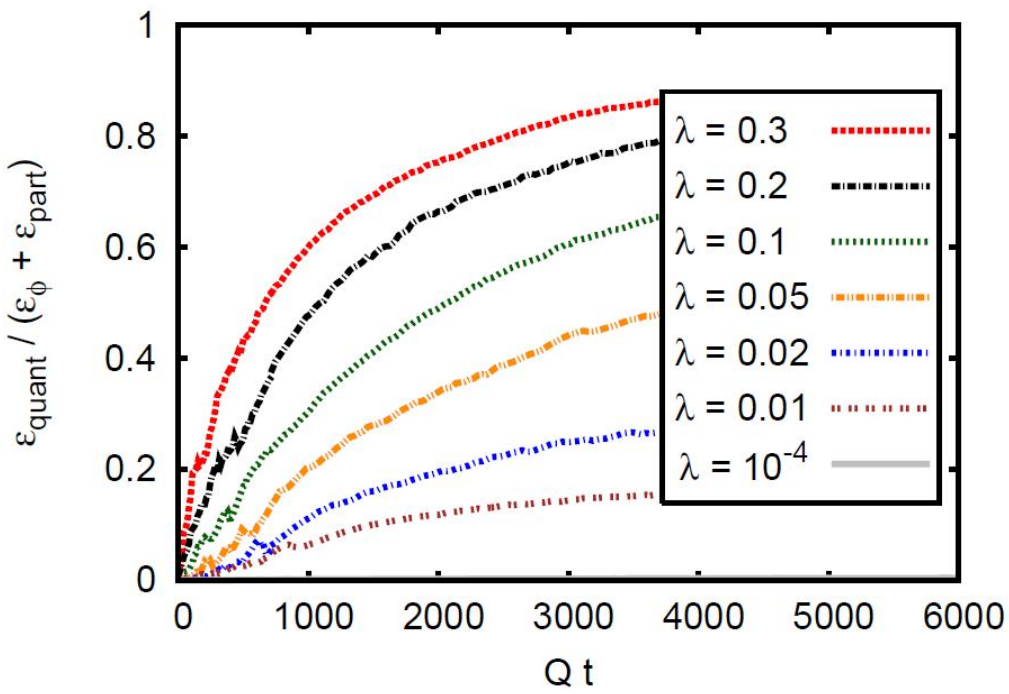

Estimate: Classical-statistical method breaks down when this ratio is large.

Beyond range of validity of classical-statistical simulations

Cutoff dependence

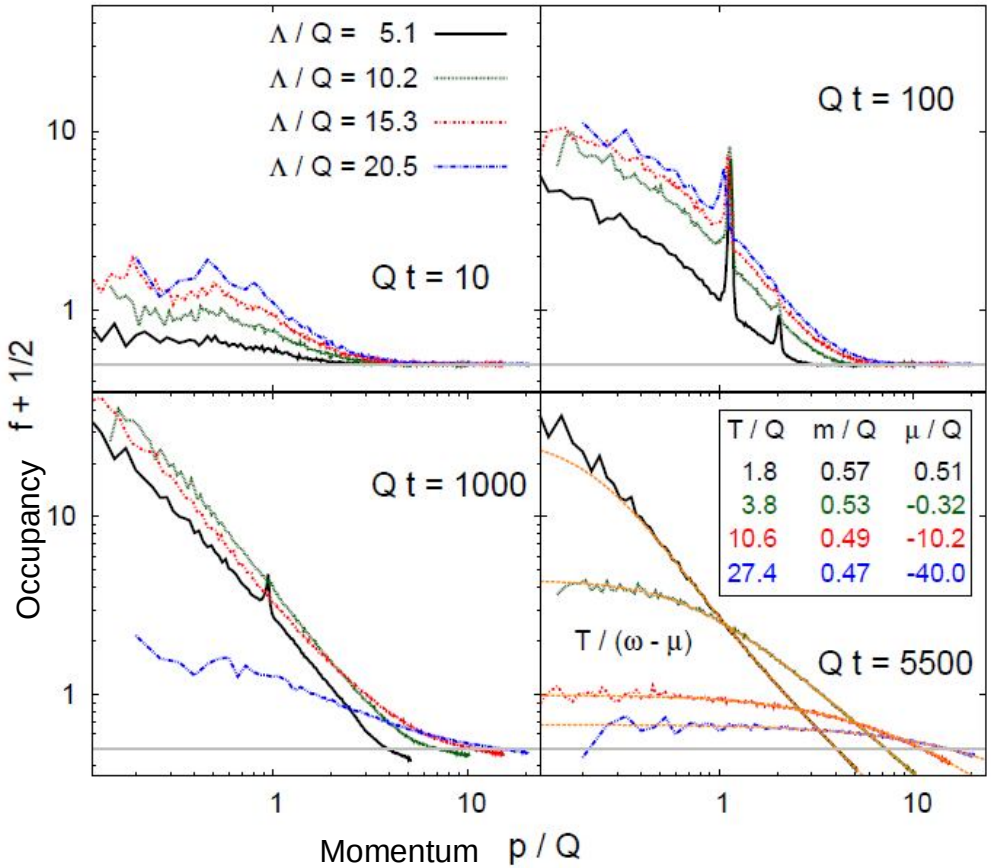

Negative occupation numbers

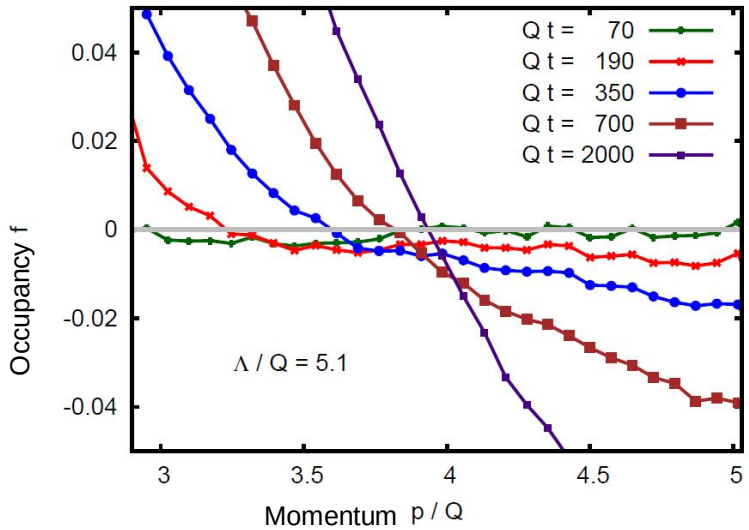

Examples: O(1) scalars, $\lambda = 1$

Berges, KB, Schlichting, Venugopalan (2013) arXiv:1312.5216

Kinetic analysis of expanding systems I

Self-similar evolution

$$f(p_t, p_z, \tau) = \tau^{\alpha} f_s(\tau^{\beta} p_t, \tau^{\gamma} p_z)$$

Constraints

Energy conservation

$$\epsilon \sim \int_{\boldsymbol{p}} \omega_p \, f(\boldsymbol{p}) \, , \qquad \partial_\tau \epsilon = -\frac{\epsilon + P_L}{\tau} \quad \Rightarrow \quad \alpha - 3\beta - \gamma = -1$$

Large anisotropy

$$\begin{aligned} \omega_p &\simeq p_t \\ P_L/\epsilon &\ll 1 \end{aligned}$$

Particle number conservation

$$N \sim \int_{\boldsymbol{p}} f(\boldsymbol{p}) \, , \qquad \partial_\tau N = -\frac{N}{\tau} \quad \Rightarrow \quad \alpha - 2\beta - \gamma = -1$$

Both conserved

$$\begin{aligned} \alpha - 3\beta - \gamma &= -1 \\ \alpha - 2\beta - \gamma &= -1 \end{aligned} \quad \Rightarrow \quad \boxed{\begin{aligned} \alpha - \gamma &= -1 \\ \beta &= 0 \end{aligned}}$$

Kinetic analysis of expanding systems II

Self-similar evolution

$$f(p_t, p_z, \tau) = \tau^{\alpha} f_s(\tau^{\beta} p_t, \tau^{\gamma} p_z)$$

Kinetic equation

$$\left[\partial_\tau - \frac{p_z}{\tau}\partial_{p_z}\right] f(p_t, p_z, \tau) = \hat{q}\, \partial^2_{p_z} f(p_t, p_z, \tau)$$

Diffusion parameter $\hat{q} \sim \tau^{2\alpha - 2\beta - \gamma}$

Complete set of equations:

$$\begin{aligned} \alpha - 3\beta - \gamma &= -1 \\ \alpha - 2\beta - \gamma &= -1 \\ 3\alpha - 2\beta + \gamma &= \alpha - 1 \end{aligned}$$

$$\Rightarrow \quad \boxed{\begin{aligned} \alpha &= -2/3 \\ \beta &= 0 \\ \gamma &= 1/3 \end{aligned}}$$

Baier, Mueller, Schiff, Son (BMSS), PLB 502 (2001) 51-58

Insensitivity to different initial conditions

Comparison of expanding scalar and gauge theories

Characteristic longitudinal momentum

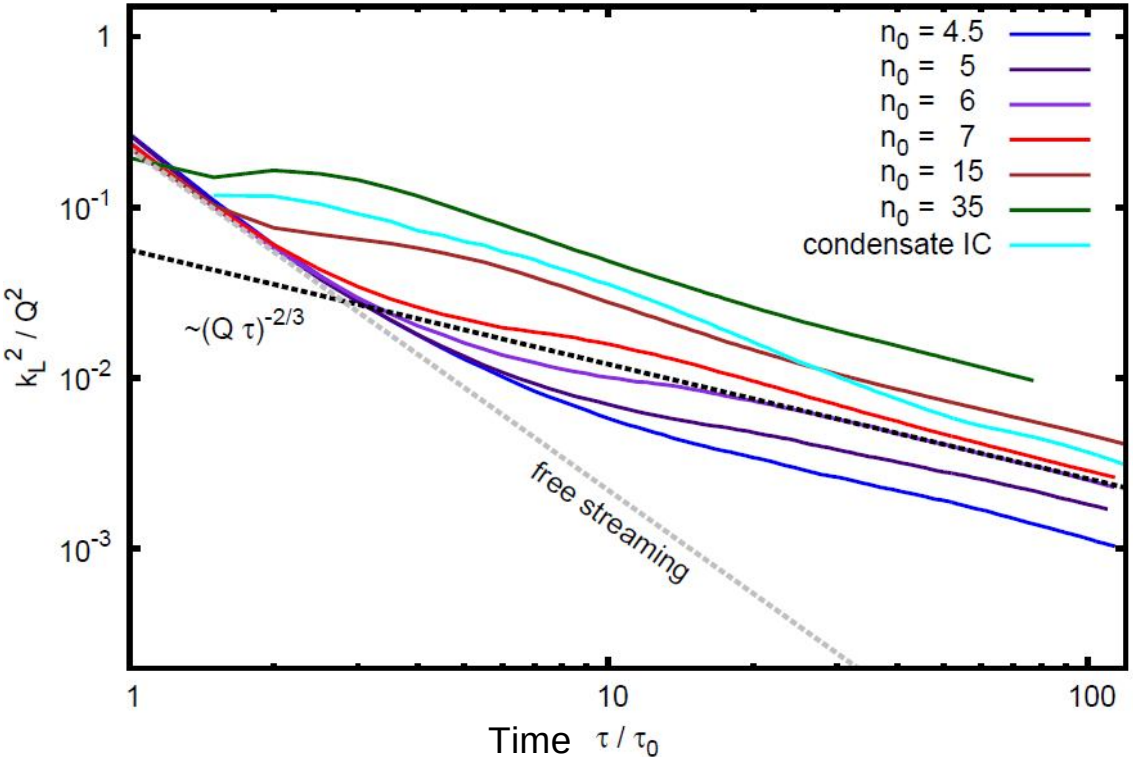

Different IC

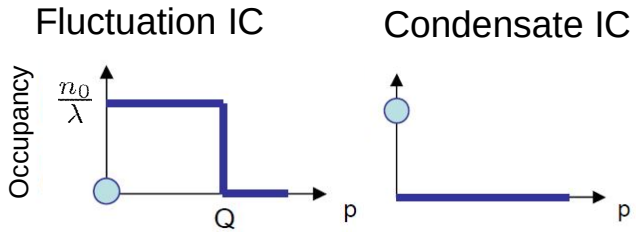

$$k_L^2 = \frac{\int dp_z \; p_z^2 f(p_t^*, p_z)}{\int dp_z \, f(p_t^*, p_z)}$$

Universal scaling!

$$k_L^2 \sim \tau^{-2\gamma}$$

$$\gamma \simeq 1/3$$

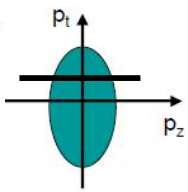

Same exponent as in gauge theory!

Universal behavior of expanding scalar fields

Hard scales $\Lambda_T^2/Q^2 \sim \tau^{-2\beta_{\rm H}}$ $\Lambda_L^2/Q^2 \sim \tau^{-2\gamma_{\rm H}}$

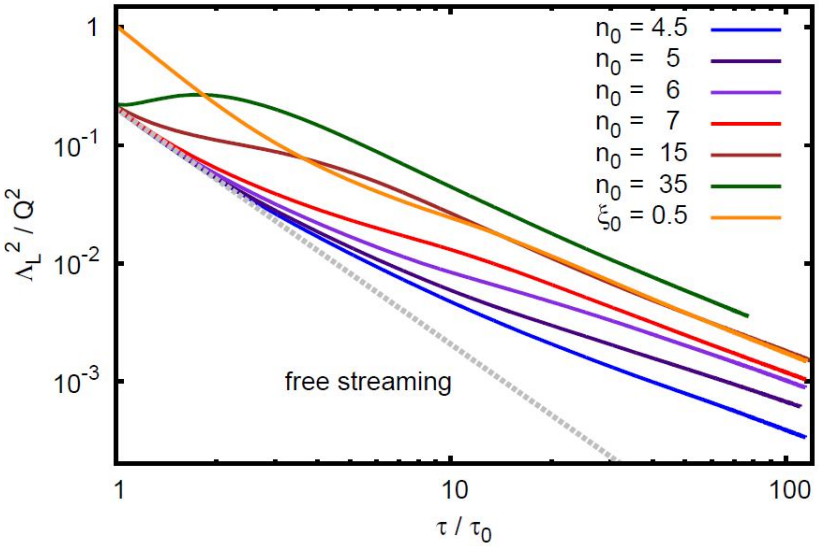

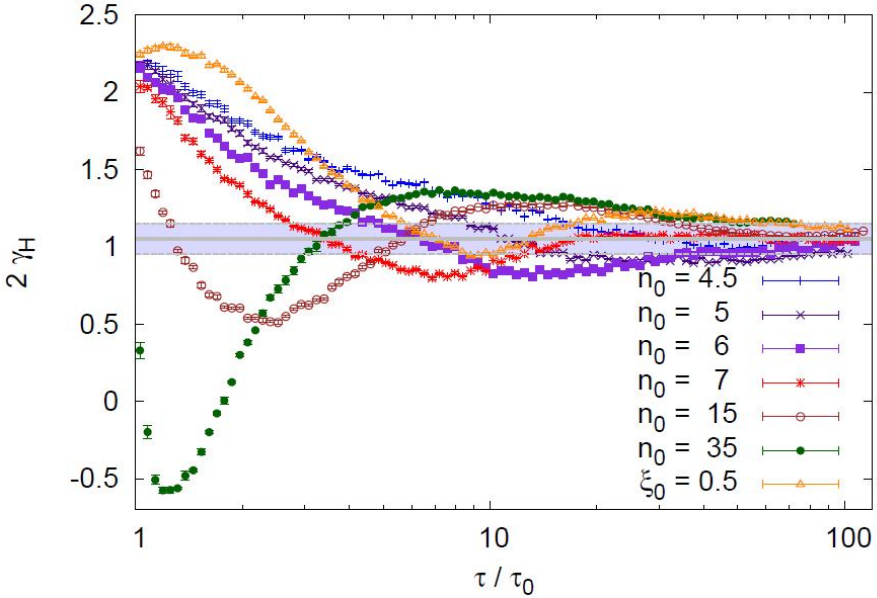

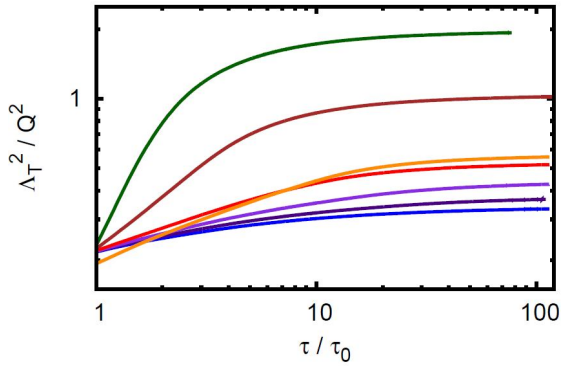

Scaling exponents

$$\boxed{\begin{aligned} 2\beta_{\rm H} &= 0 + \delta \\ 2\gamma_{\rm H} &= 1.05 \pm 0.1 \end{aligned}}$$

$\delta \lesssim 0.06$

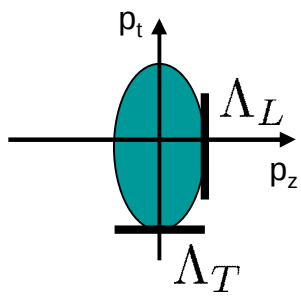

Turbulent thermalization of expanding gauge theory

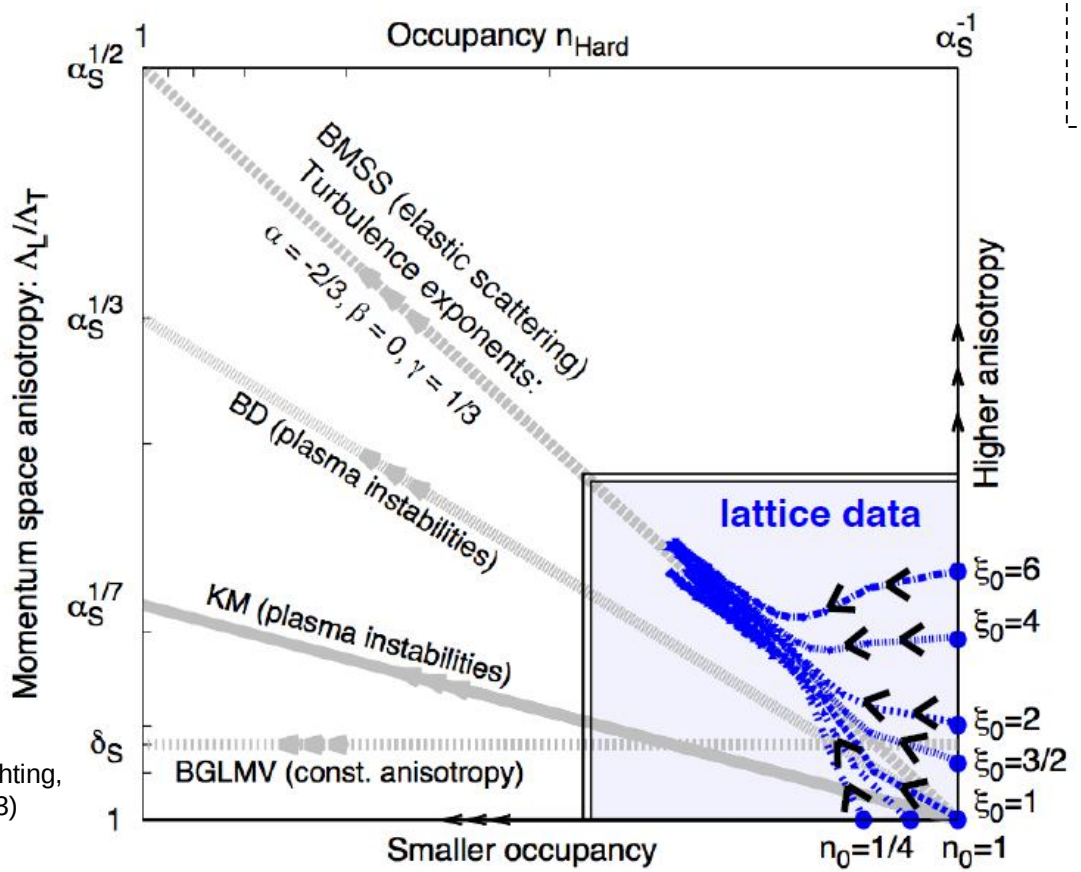

Berges, KB, Schlichting, Venugopalan (2013)
arXiv: **1303.5650**

Reminder: Self-similar evolution

$$f(p_T, p_z, t) = t^\alpha f_S(t^\beta p_T, t^\gamma p_z)$$

Simulations approach nonthermal fixed point with universal scaling exponents

$$\begin{aligned} \alpha &= -2/3 \\ \beta &= 0 \\ \gamma &= 1/3 \end{aligned}$$

Nonthermal fixed point matches the BMSS scenario!

Thermalization scenarios

Baier, Mueller, Schiff, Son (BMSS), (2001)

Bodeker (BD), (2005)

Kurkela, Moore (KM), (2011)

Blaizot, Gelis, Liao, McLerran, Venugopalan (BGLMV), (2012)

Early isotropization of the Quark-Gluon Plasma

Brookhaven RBRC workshop, 2nd April 2014

Thomas EPELBAUM

IPhT

Viscous Hydrodynamics

I) Macroscopic theory
II) Few parameters: P_L, P_T, ϵ, $\vec{u}$
III) Need input:

1) Equation of state $f(P_L, P_T) = \epsilon$
2) Small anisotropy
3) Initialization: $\epsilon(\tau_0)$, $P_L(\tau_0)$? ...
4) viscous coefficients: shear viscosity η,...
5) Short isotropization time

Viscous Hydrodynamics

I) Macroscopic theory
II) Few parameters: P_L, P_T, ϵ, $\vec{u}$
III) Need input:

1) Equation of state $f(P_L, P_T) = \epsilon$
2) Small anisotropy
3) Initialization: $\epsilon(\tau_0)$, $P_L(\tau_0)$? ...
4) viscous coefficients: shear viscosity η,...
5) Short isotropization time

None of this is easy to get from QCD

Early transition: the problem

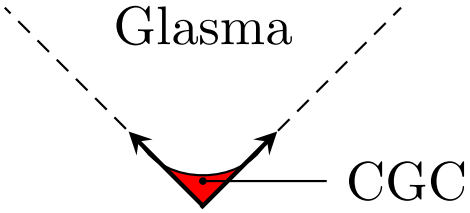

Isotropization?
Time scale?

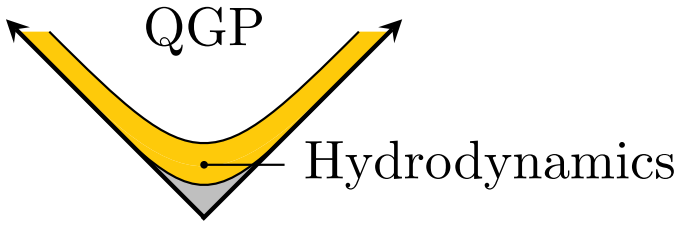

Huge anisotropy
(negative P_L)

Small anisotropy

Long time puzzle: Does (fast) hydrodynamization occur?

LO CGC initial conditions at $\tau = 0^+$: $\mathcal{A} \sim \frac{Q_s}{g}$

$$\mathcal{A}^i(\boldsymbol{x}_\perp) = \alpha_1{}^i(\boldsymbol{x}_\perp) + \alpha_2{}^i(\boldsymbol{x}_\perp) \qquad \mathcal{A}^{\eta a}(\boldsymbol{x}_\perp) = \frac{ig}{2}\left[\alpha_1{}^i(\boldsymbol{x}_\perp), \alpha_2{}^i(\boldsymbol{x}_\perp)\right]$$

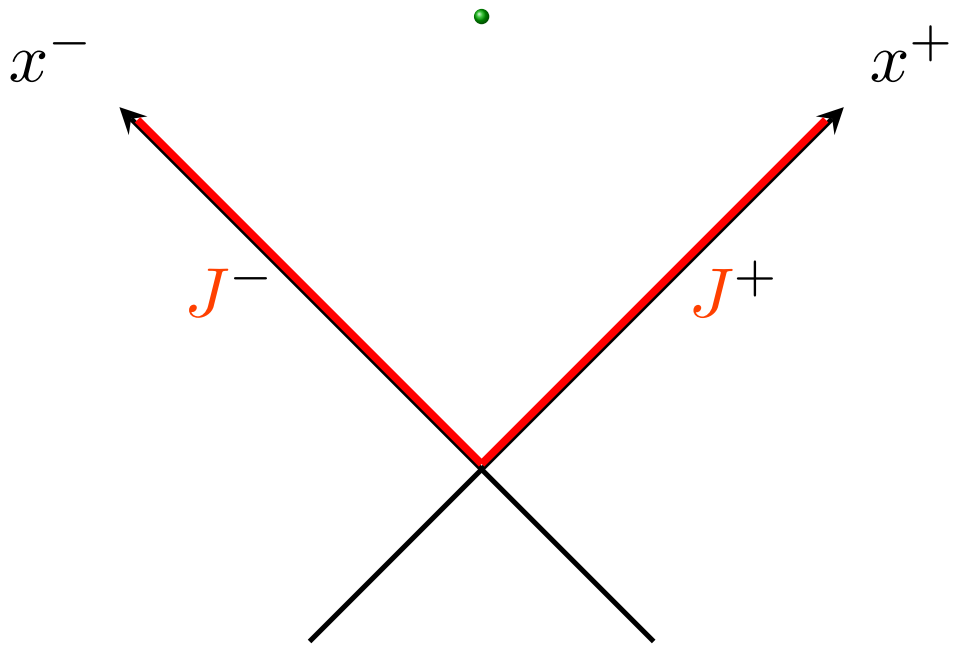

$$\alpha_n{}^i(\boldsymbol{x}_\perp) = \frac{i}{g}\mathcal{U}_n{}^\dagger(\boldsymbol{x}_\perp)\partial^i\mathcal{U}_n(\boldsymbol{x}_\perp) \qquad \mathcal{U}_n(\boldsymbol{x}_\perp) = e^{-ig\frac{1}{\nabla_\perp^2}J^\pm(\boldsymbol{x}_\perp)}$$

Classical time evolution

$$\left[\mathcal{D}_\mu(\boldsymbol{x}_\perp), F^{\mu\nu}(\boldsymbol{x}_\perp)\right] = 0 \,,$$

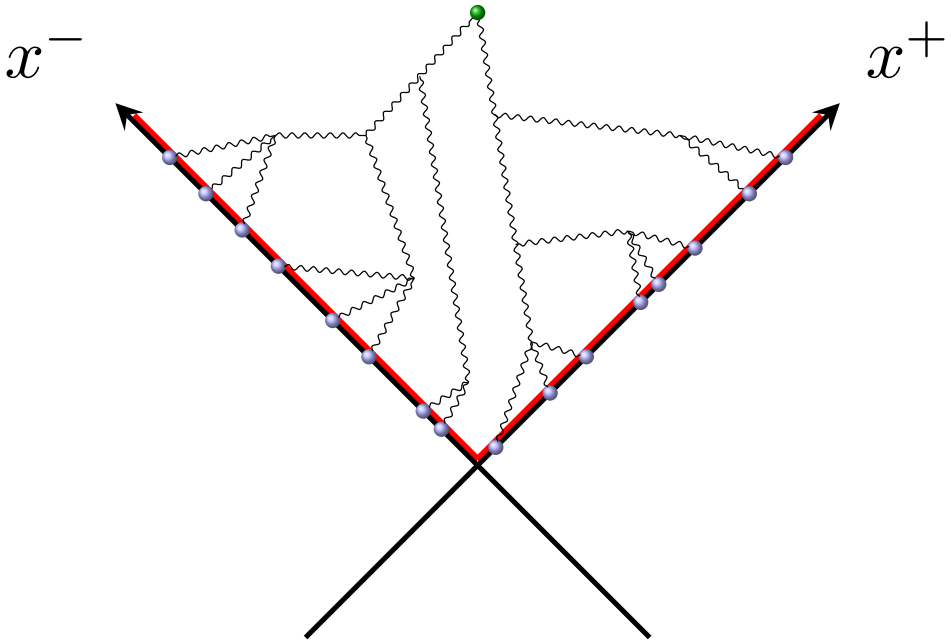

LO result: Strong anisotropy at all times

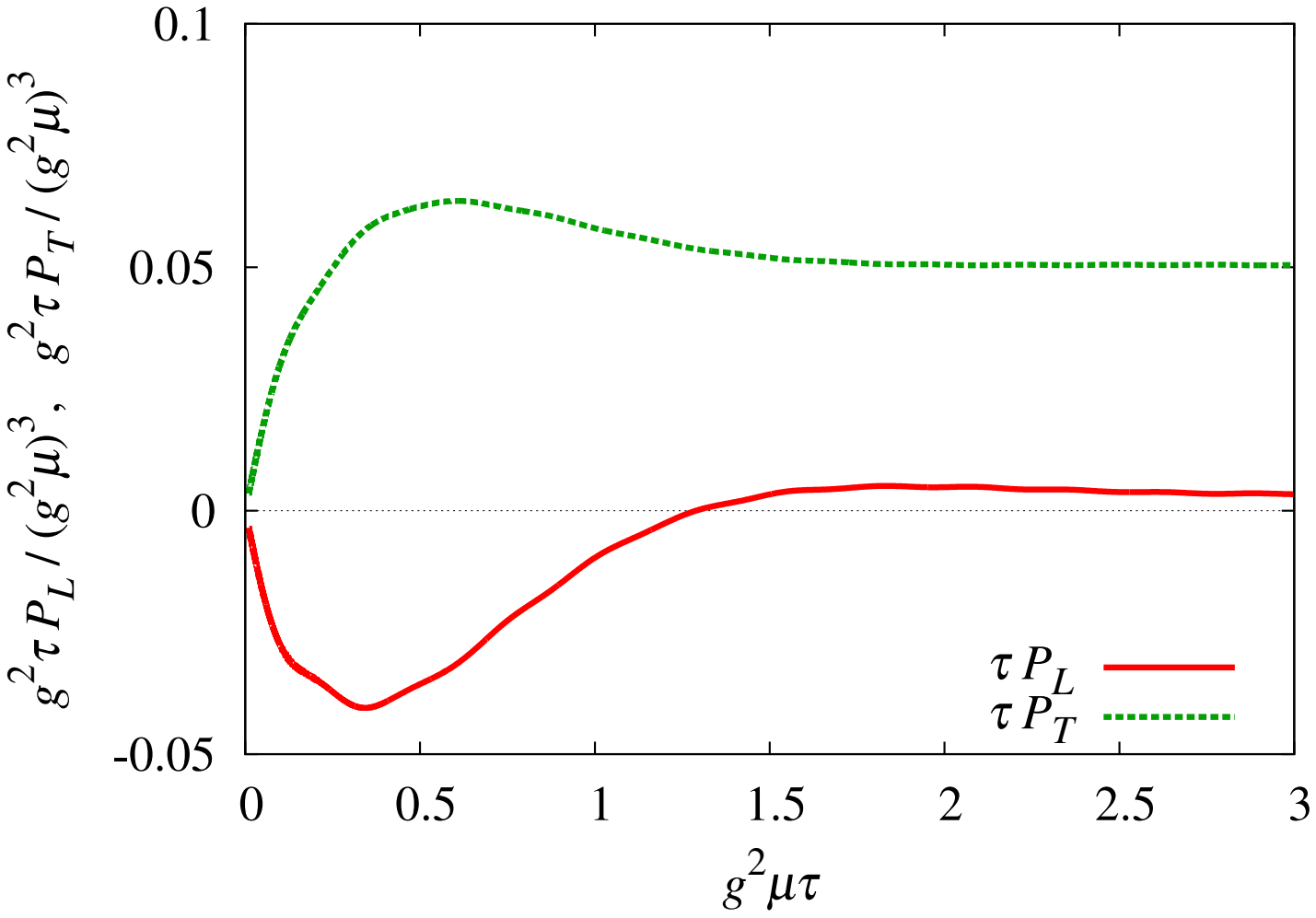

Understanding the initial strong anisotropy

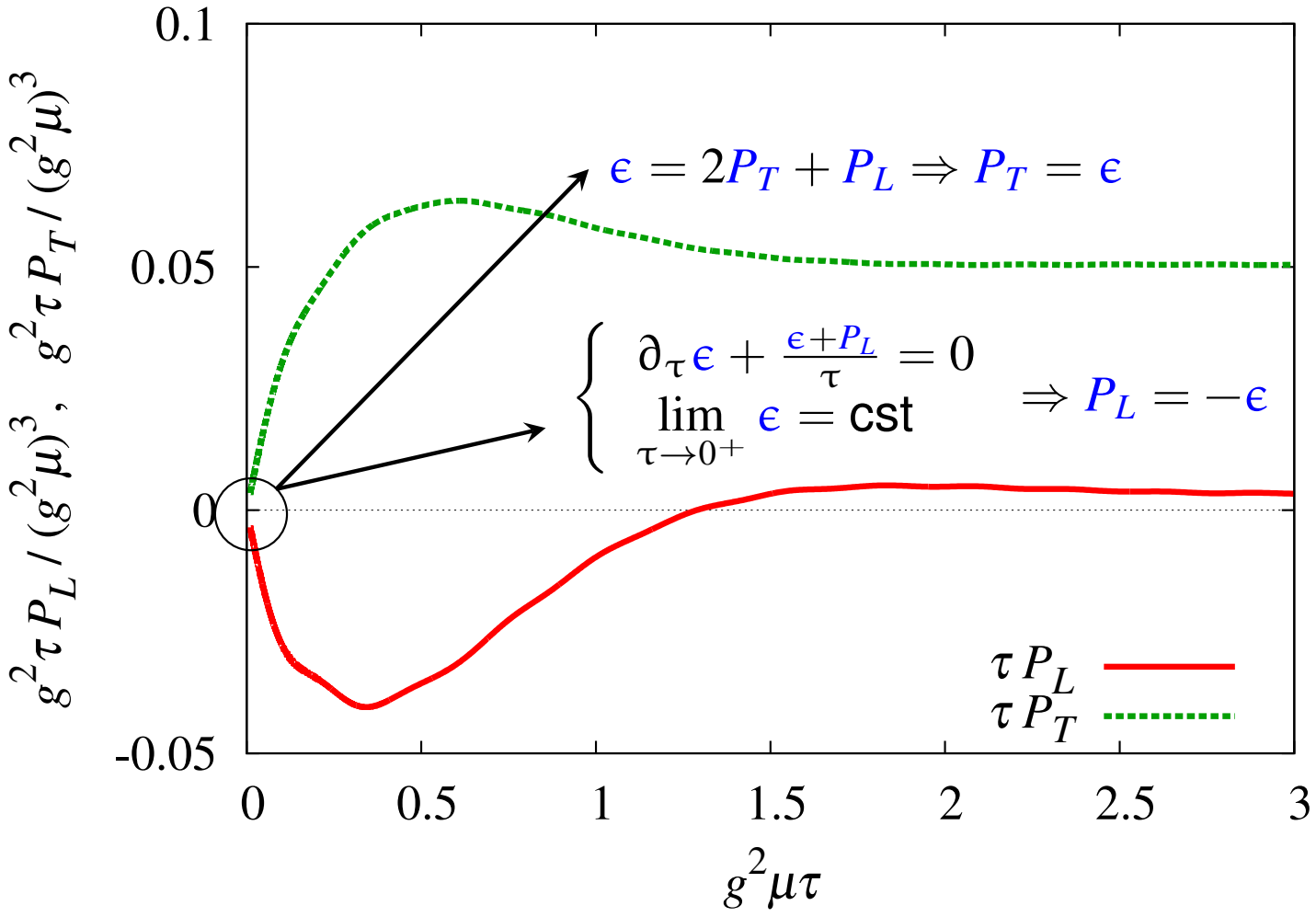

The Color Glass Condensate at NLO (1)

$$A^{\mu a}(x) = \underbrace{\mathcal{A}^{\mu a}(\boldsymbol{x}_\perp)}_{\text{LO}} + \underbrace{\sum_{\lambda,c} \int_{\boldsymbol{k}} a^{\mu a}_{\boldsymbol{k}\lambda c}(x)}_{\text{NLO}}$$

$a^{\mu a}_{\boldsymbol{k}\lambda c}(x)$ perturbation to $\mathcal{A}^{\mu a}$ created by a plane wave in the remote past.

$a^{\mu a}_{\boldsymbol{k}\lambda c}(x)$ obeys to the linear Equation Of Motion

THE COLOR GLASS CONDENSATE AT NLO (2)

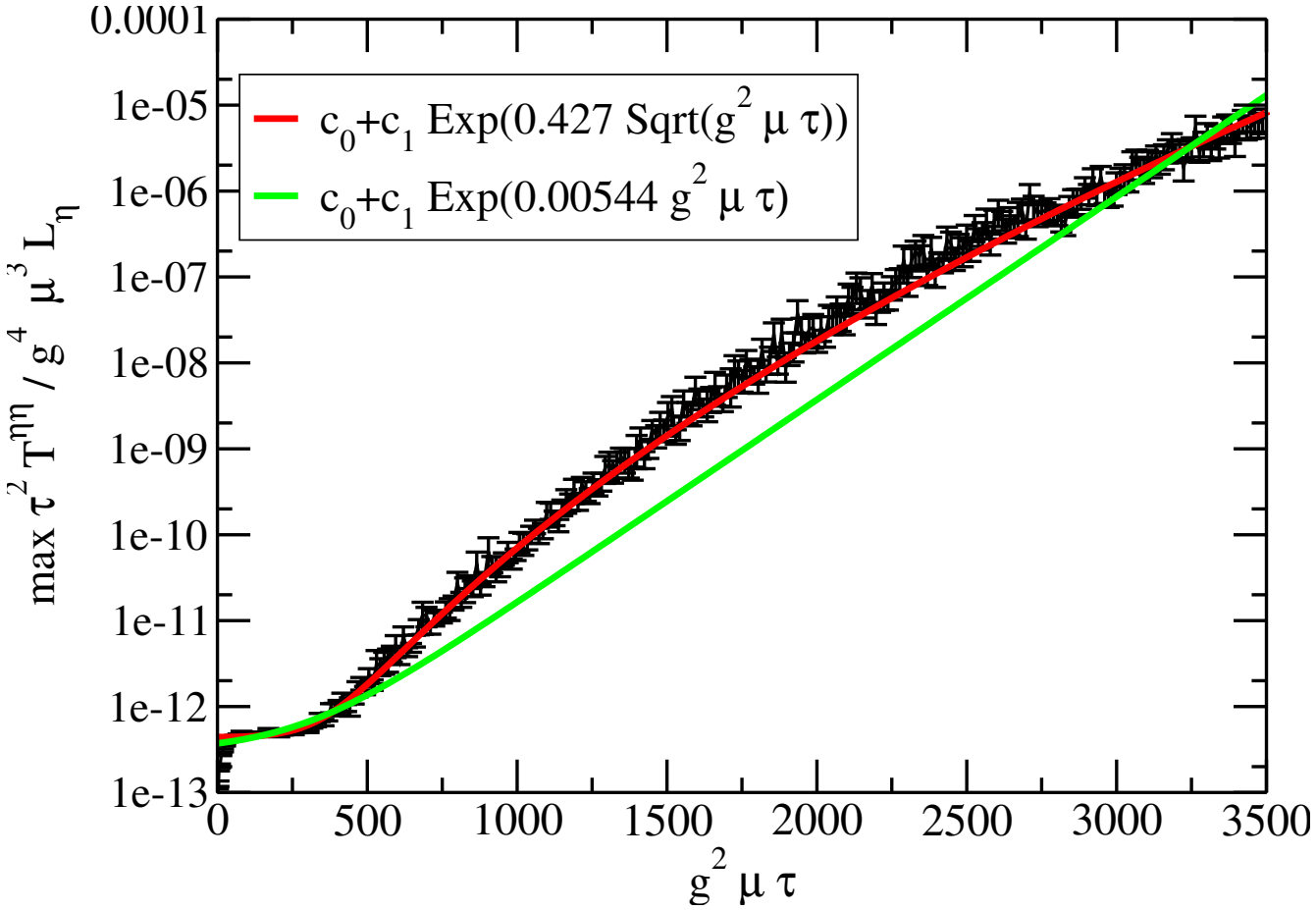

[ROMATSCHKE, VENUGOPALAN (2006)]

Small Fluctuations grow exponentially (Weibel instability)

The Color Glass Condensate at NLO (3)

- Because of instabilities, the NLO correction eventually becomes as large as the LO $\Rightarrow$ Important effect, should be included

- NLO alone will grow forever $\Rightarrow$ unphysical effect, should be taken care of

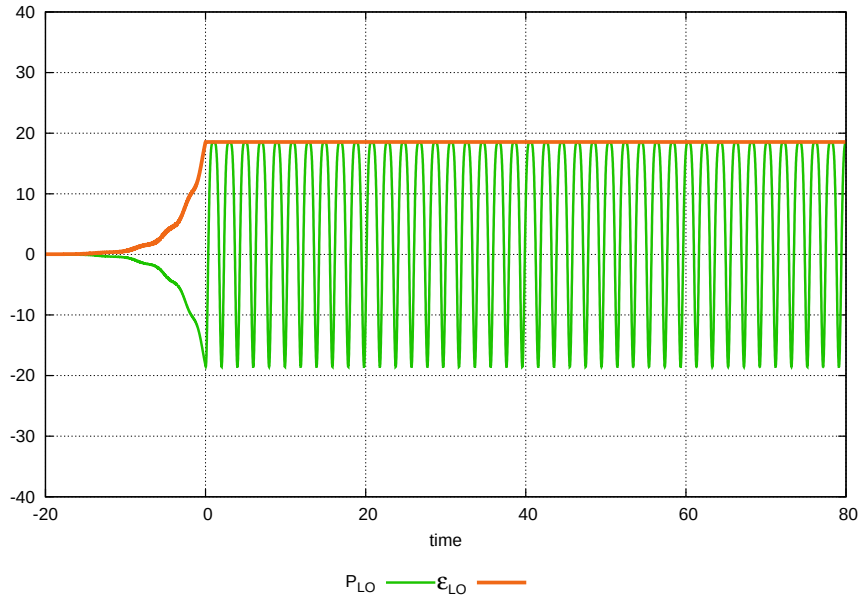

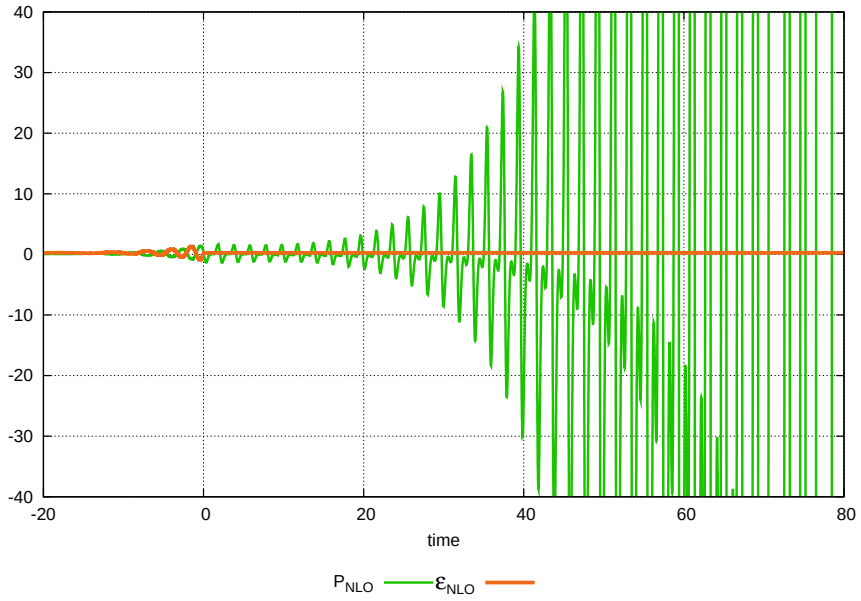

- Such growing contributions are present at all orders of the perturbative expansion

How to deal with them?

Key step

$$T^{\mu\nu}_{\text{NLO}} = \underbrace{\frac{1}{2} \int_{\tau_{x,y}=0^+} \mathrm{d}^3\boldsymbol{x}\, \mathrm{d}^3\boldsymbol{y}\, G(x,y)\, \mathbb{T}_x\, \mathbb{T}_y}_{\mathcal{O}}\, T^{\mu\nu}_{\text{LO}}\left[\mathcal{A}(0^+, \boldsymbol{x}_\perp)\right]$$

where

$$G(x,y) \sim \sum_{\lambda c} \int_{\boldsymbol{k}} a_{\boldsymbol{k}\lambda c}(x) a^*_{\boldsymbol{k}\lambda c}(y)$$

and

$$\mathbb{T}_x \sim \frac{\delta}{\delta \mathcal{A}(x)} \sim e^{\sqrt{\mu\tau}}$$

Resummation technique

$$T^{\mu\nu}_{\text{resum}} = e^{\mathcal{O}}\, T^{\mu\nu}_{\text{LO}}\left[\mathcal{A}(0^+, \boldsymbol{x}_\perp)\right] = T^{\mu\nu}_{\text{LO}} + T^{\mu\nu}_{\text{NLO}} + \ldots$$

Numerical implementable way to express $T^{\mu\nu}_{\text{resum}}$

$$T^{\mu\nu}_{\text{resum}} = \int [Da] \exp\left[-\frac{1}{2}\int_{x,y} \mathrm{d}^3\boldsymbol{x}\, \mathrm{d}^3\boldsymbol{y}\; a(x)\, G^{-1}(x,y)\, a(y)\right] T^{\mu\nu}_{\text{LO}}\left[\mathcal{A} + a\right]$$

- At the initial time $\tau = \tau_0$:

$$A^{\mu a}(\tau_0, \boldsymbol{x}_\perp, \eta) = \mathcal{A}^{\mu a}(\boldsymbol{x}_\perp) + \sum_{\lambda, c} \int_{\boldsymbol{k}} c_{\boldsymbol{k}\lambda c}\, a^{\mu a}_{\boldsymbol{k}\lambda c}(\tau_0, \boldsymbol{x}_\perp, \eta)$$

  where $c_{\vec{k}}$ are random coefficients: $\left\langle c_{\vec{k}} c_{\vec{k}'} \right\rangle \sim \delta_{\vec{k}\vec{k}'}$

- Solve the **Classical** equation of motion $D_\mu F^{\mu\nu} = 0$
- Compute $\left\langle T^{\mu\nu}_{\text{resum}}(\tau, \boldsymbol{x}_\perp, \eta) \right\rangle$, where $\langle\rangle$ is the average on the $c_{\vec{k}}$

This gives: LO+NLO+Subset of higher orders

All the tree diagrams (LO)

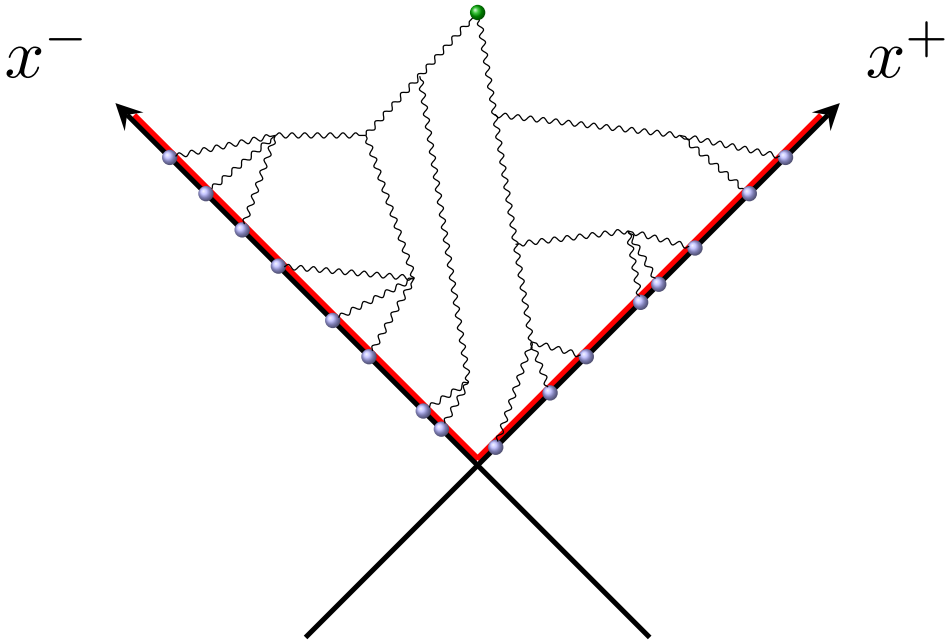

All the one loop diagrams (NLO): $\times \left(g e^{\sqrt{\mu\tau}}\right)^2$ the LO

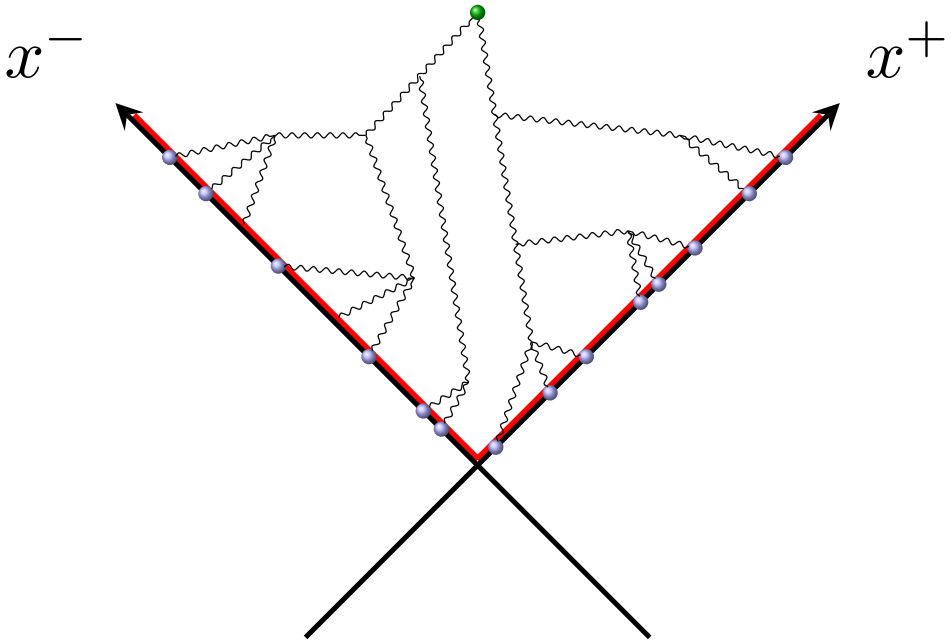

$$\mathcal{O} = \frac{1}{2}\int_{x,y} G(x,y)\,\mathbb{T}_x\,\mathbb{T}_y \sim \frac{1}{2}\int_{x,y}\sum_{\lambda c}\int_{\boldsymbol{k}} a_{\boldsymbol{k}\lambda c}(x)\,a^*_{\boldsymbol{k}\lambda c}(y)\,\frac{\delta}{\delta\mathcal{A}(x)}\,\frac{\delta}{\delta\mathcal{A}(y)}$$

All the one loop diagrams (NLO): $\times \left(g e^{\sqrt{\mu\tau}}\right)^2$ the LO

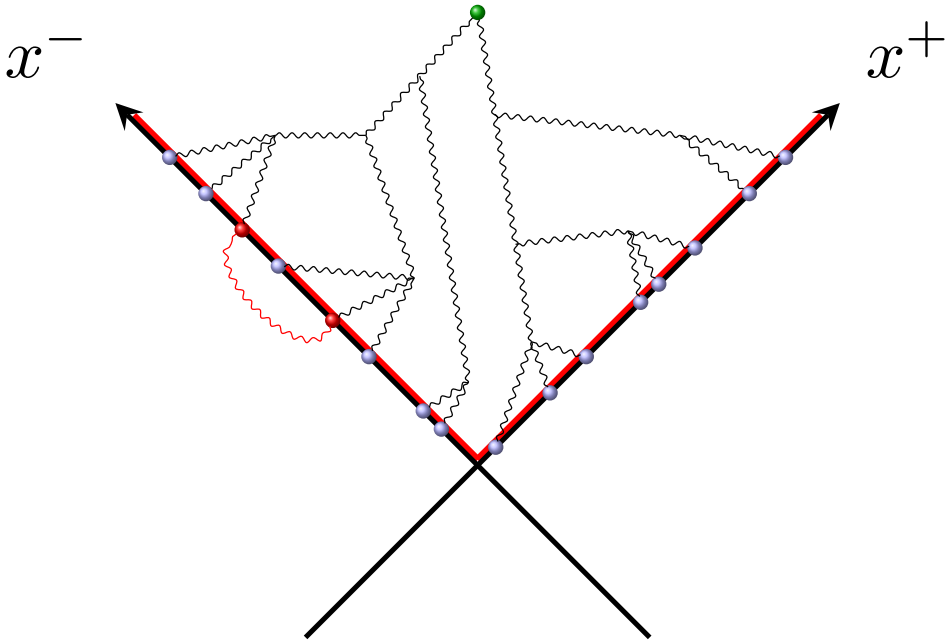

$$\mathcal{O} = \frac{1}{2}\int_{x,y} G(x,y)\,\mathbb{T}_x\,\mathbb{T}_y \sim \frac{1}{2}\int_{x,y}\sum_{\lambda c}\int_{\boldsymbol{k}} a_{\boldsymbol{k}\lambda c}(x)\,a^*_{\boldsymbol{k}\lambda c}(y)\,\frac{\delta}{\delta\mathcal{A}(x)}\,\frac{\delta}{\delta\mathcal{A}(y)}$$

Subset of NNLO included: $\times \left(ge^{\sqrt{\mu\tau}}\right)^4$ the LO

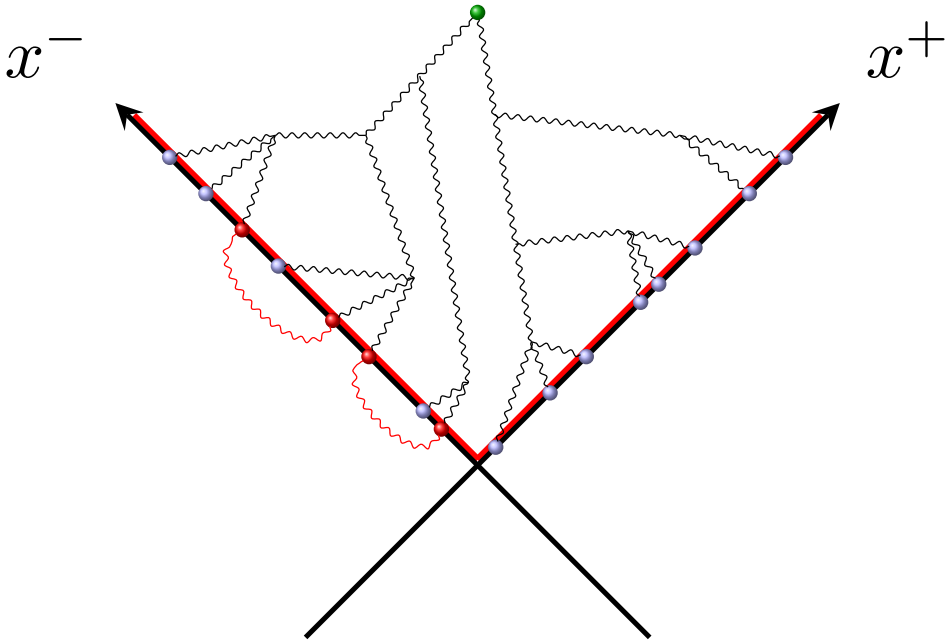

Subset of NNLO not included: $\times g \left(g e^{\sqrt{\mu\tau}}\right)^3$ the LO

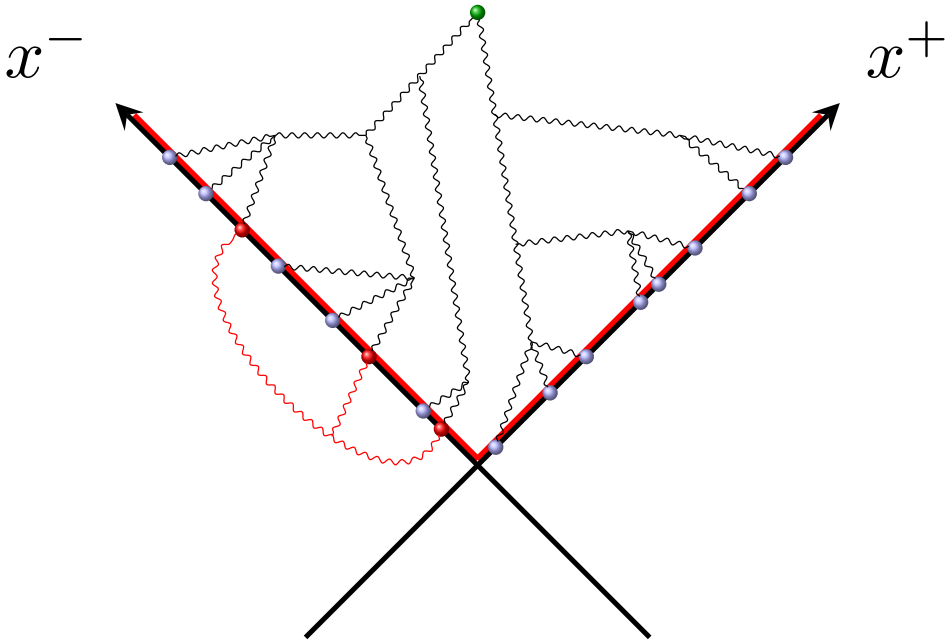

Subleading!

Finding the small fluctuations at $\tau = 0^+$

$$\mathcal{D}^{ab}_{\mu}\left(\mathcal{D}^{\mu bc}a^{\nu c} - \mathcal{D}^{\nu bc}_{\beta}a^{\mu c}\right) - ig\mathcal{F}^{\nu\mu ab}a^{b}_{\mu} = j^{\nu a}$$

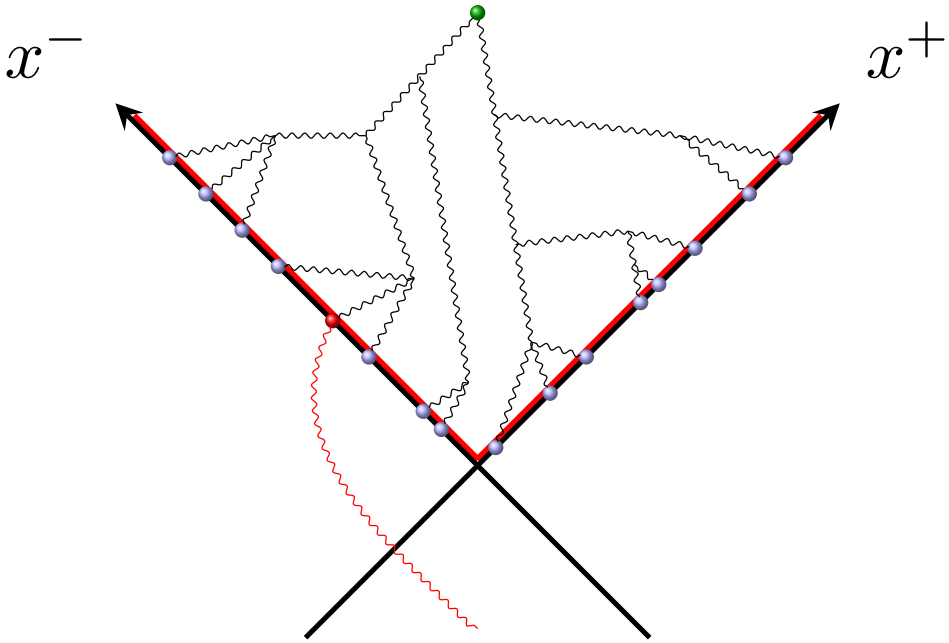

$$a^{\mu a}_{\boldsymbol{k}\lambda c} = \delta^a_c \epsilon^{\mu}_{\boldsymbol{k}\lambda} e^{ikx}$$

Result of [TE,GELIS (2013)]

$$a_\eta^{\boldsymbol{k}_\perp \nu\lambda c} = \tau^2 \mathcal{D}^{iab} \left(\frac{F^{-,ia}_{\boldsymbol{k}_\perp \nu\lambda c}}{2-i\nu} - \frac{F^{+,ia}_{\boldsymbol{k}_\perp \nu\lambda c}}{2+i\nu} \right) \qquad a_i^{\boldsymbol{k}_\perp \nu\lambda c} = -\left(F^{-,ia}_{\boldsymbol{k}_\perp \nu\lambda c} + F^{+,ia}_{\boldsymbol{k}_\perp \nu\lambda c} \right)$$

$$e^{\eta a}_{\boldsymbol{k}_\perp \nu\lambda c} = \mathcal{D}^{iab} \left(F^{-,ia}_{\boldsymbol{k}_\perp \nu\lambda c} - F^{+,ia}_{\boldsymbol{k}_\perp \nu\lambda c} \right) \qquad e^{ia}_{\boldsymbol{k}_\perp \nu\lambda c} = i\nu \left(F^{-,ia}_{\boldsymbol{k}_\perp \nu\lambda c} - F^{+,ia}_{\boldsymbol{k}_\perp \nu\lambda c} \right)$$

with

$$F^{\pm,ia}_{\boldsymbol{k}_\perp \nu\lambda c}(x) = e^{i\nu\eta} \Gamma(\mp i\nu) e^{\frac{\pm\nu\pi}{2}} \int \frac{\mathrm{d}^2\boldsymbol{p}_\perp}{(2\pi)^2} e^{i\boldsymbol{p}_\perp \cdot \boldsymbol{x}_\perp} \left(\frac{p^2\tau}{2k} \right)^{\pm i\nu} \left(\delta^{ij} - \frac{2p^i p^j}{p^2} \right) \mathcal{V}^{ja}_{1,2\boldsymbol{k}_\perp \lambda c}$$

and

$$\mathcal{V}^{ja}_{1,2\boldsymbol{k}_\perp \lambda c}(\boldsymbol{x}_\perp, \boldsymbol{p}_\perp) = \mathcal{U}^{ab\dagger}_{1,2}(\boldsymbol{x}_\perp) \int \mathrm{d}^2\boldsymbol{y}_\perp \, e^{-i(\boldsymbol{p}_\perp + \boldsymbol{k}_\perp)\cdot \boldsymbol{y}_\perp} \, \mathcal{U}^{bc}_{1,2}(\boldsymbol{y}_\perp) \left(\delta^{ij} - \frac{2k^i k^j}{k^2} \right) \epsilon^i_{\boldsymbol{k}_\perp \lambda} \, .$$

Gauge potential $A^\mu \to$ link variables (exact gauge invariance on the lattice)

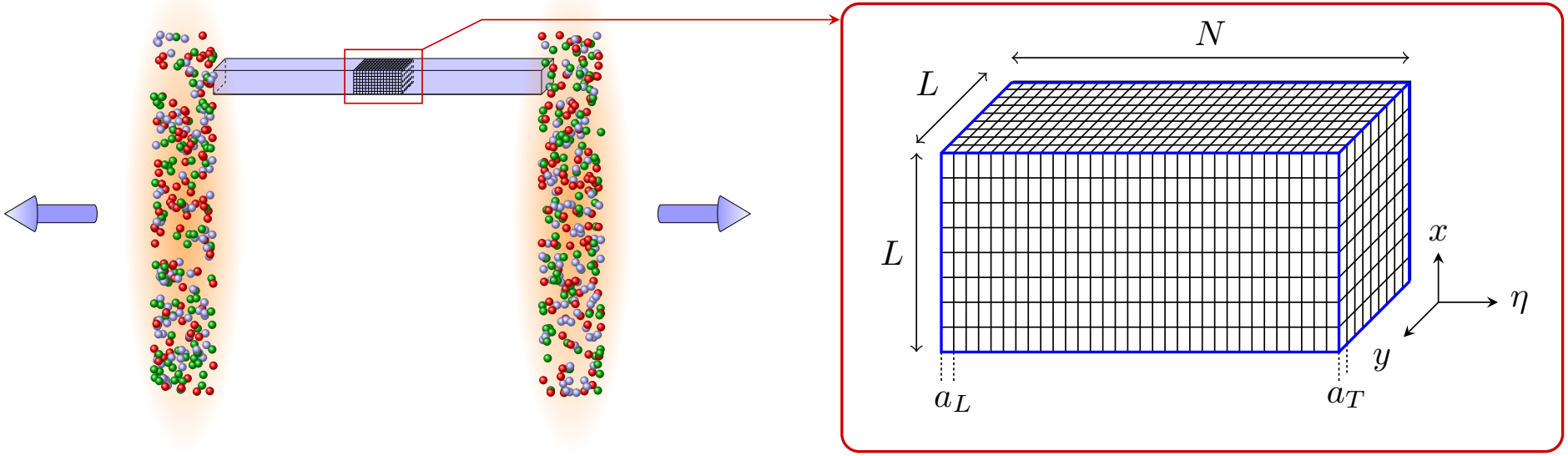

Numerical parameters

- Transverse lattice size $L = 64$, transverse lattice spacing $Q_s a_T = 1$
- Longitudinal lattice size $N = 128$, longitudinal lattice spacing $a_L = 0.016$
- Number of configurations for the Monte-Carlo $N_{\text{conf}} = 200$ to 2000
- Initial time $Q_s \tau_0 = 0.01$

NUMERICAL RESULTS [TE,GELIS (2013)]

$$\alpha_s = 8\,10^{-4}\ (g = 0.1)$$

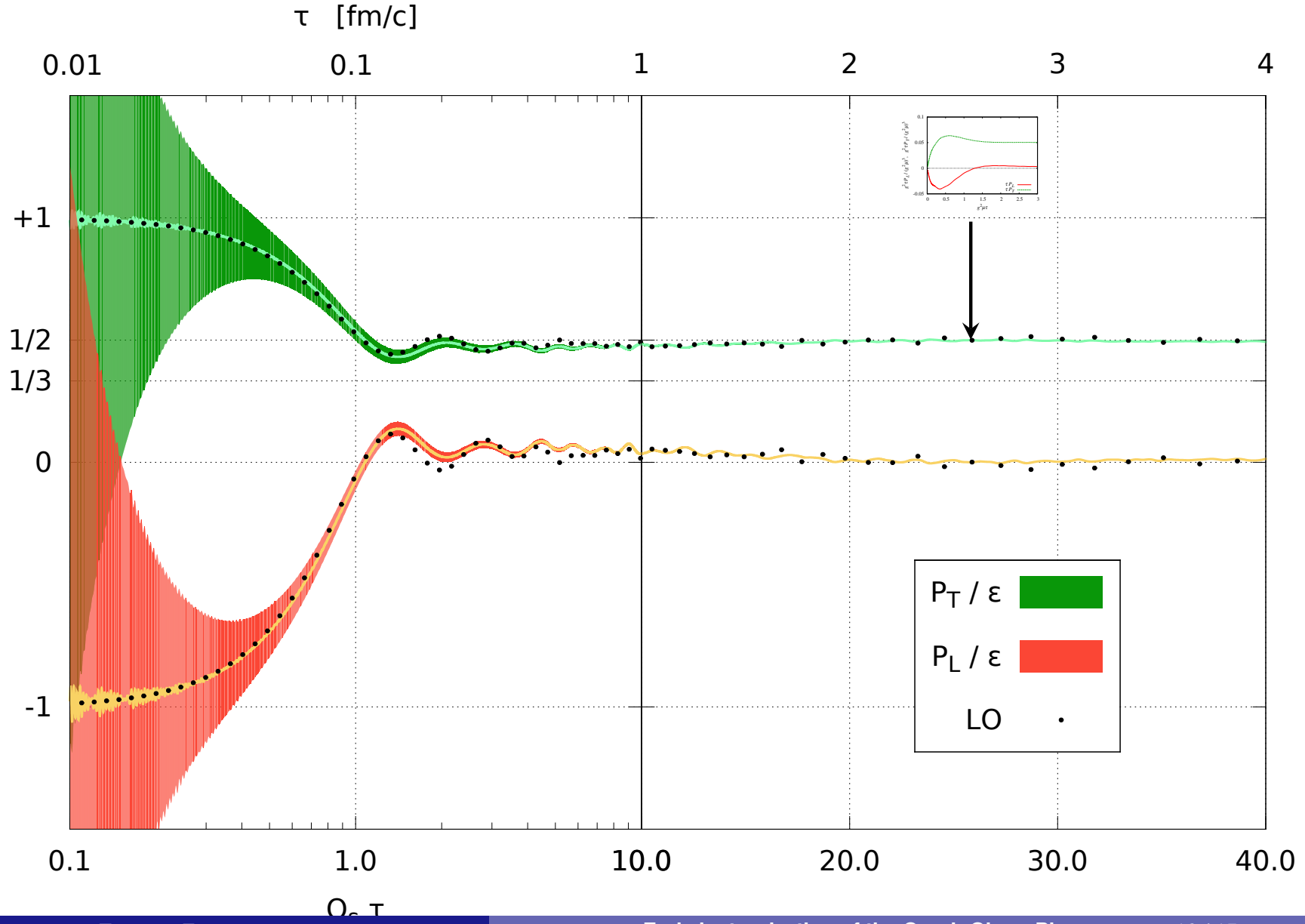

Renormalization procedure

$$T^{\mu\nu}_{\text{resum}} \sim \frac{Q_s^4}{g^2} + c_0\Lambda^4 + c_2(Q_s)\Lambda^2 + ...$$

Quartic divergences can be subtracted with a simulation where

$$A^{\mu a}(x) = 0 + \sum_{\lambda,c} \int_{\boldsymbol{k}} c_{\boldsymbol{k}\lambda c}\, a^{\mu a}_{\boldsymbol{k}\lambda c}(\tau_0, \boldsymbol{x}_\perp, \eta)$$

Gives a $T^{\mu\nu}_{\text{part renor}} = T^{\mu\nu}_{\text{resum}} - T^{\mu\nu}_{\text{vac}}$

Renormalization procedure

$$\epsilon_{\text{part renor}} \sim \frac{Q_s^4}{g^2} + \frac{Q_s^2 \nu_{\max}^2}{\tau^2} + \ldots$$

$$P_{L_{\text{part renor}}} \sim \frac{Q_s^4}{g^2} + \frac{Q_s^2 \nu_{\max}^2}{\tau^2} + \ldots$$

$$P_{T_{\text{part renor}}} \sim \frac{Q_s^4}{g^2} + Q_s^2 k_{\perp,\max}^2 + \ldots$$

How to deal with the $\frac{Q_s^2 \nu_{\max}^2}{\tau^2}$ terms $\rightarrow$ fitted for the time being.

Otherwise $\epsilon_{\text{part renor}}$ and $P_{L_{\text{part renor}}}$ behaves as τ^{-2} at early time.

RENORMALIZATION PROCEDURE

$$\langle P_T \rangle_{\text{phys.}} = \langle P_T \rangle_{\substack{\text{backgd.} \\ + \text{ fluct.}}} - \langle P_T \rangle_{\substack{\text{fluct.} \\ \text{only}}}$$

$$\langle \epsilon, P_L \rangle_{\text{phys.}} = \underbrace{\langle \epsilon, P_L \rangle_{\substack{\text{backgd.} \\ + \text{ fluct.}}}}_{\text{computed}} - \underbrace{\langle \epsilon, P_L \rangle_{\substack{\text{fluct.} \\ \text{only}}}}_{\text{computed}} + \underbrace{A\,\tau^{-2}}_{\text{fitted}} \,.$$

The additional term is the only one that can satisfy Bjorken's law

$$\partial_\tau \epsilon + \frac{\epsilon + P_L}{\tau} = 0$$

and the Equation Of State:

$$\epsilon = 2P_T + P_L$$

NUMERICAL RESULTS [TE,GELIS (2013)]

$$\alpha_s = 2\,10^{-2}\ (g = 0.5)$$

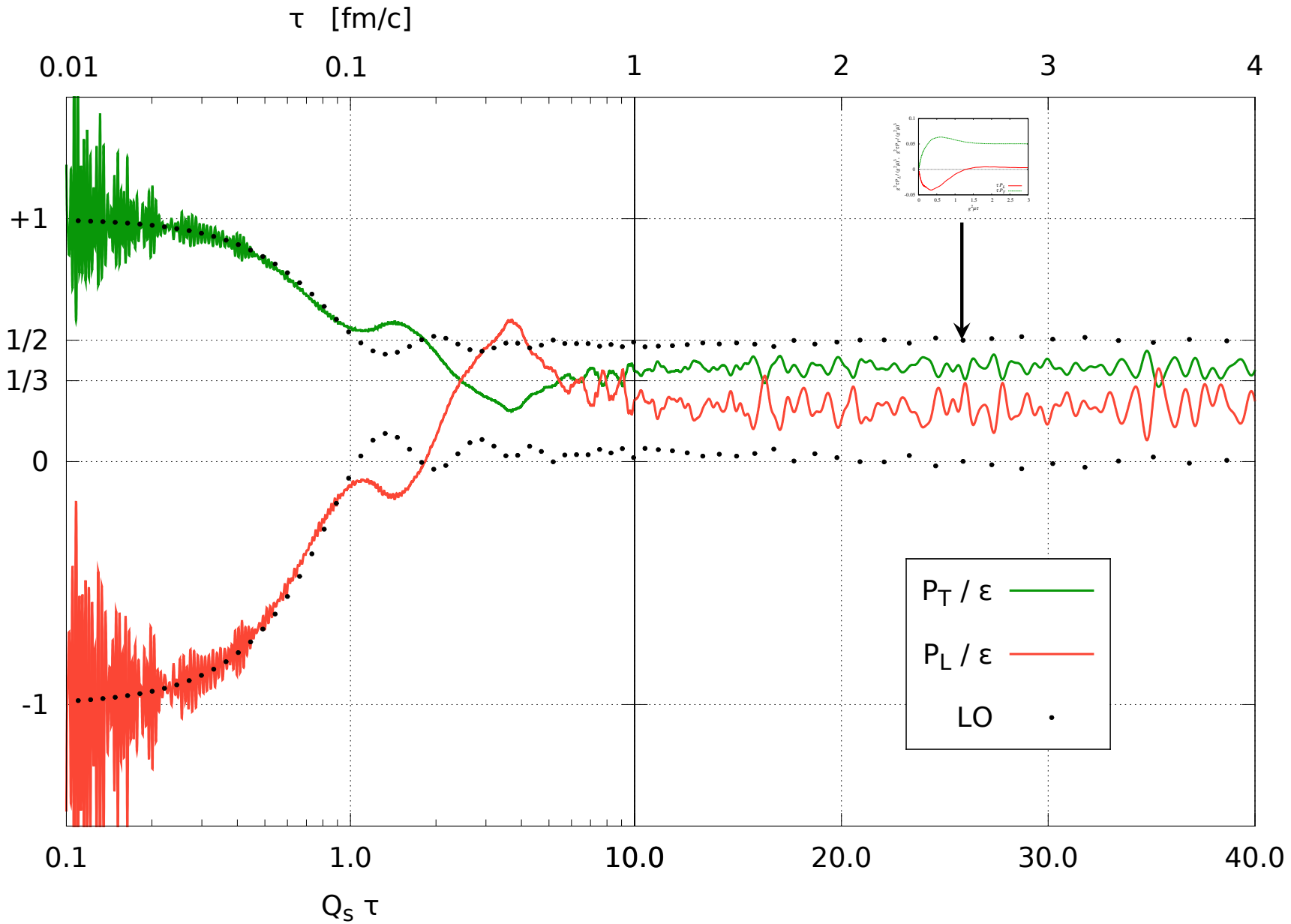

NUMERICAL RESULTS [TE,GELIS (2013)]

$$\alpha_s = 2\,10^{-2}\ (g = 0.5)$$

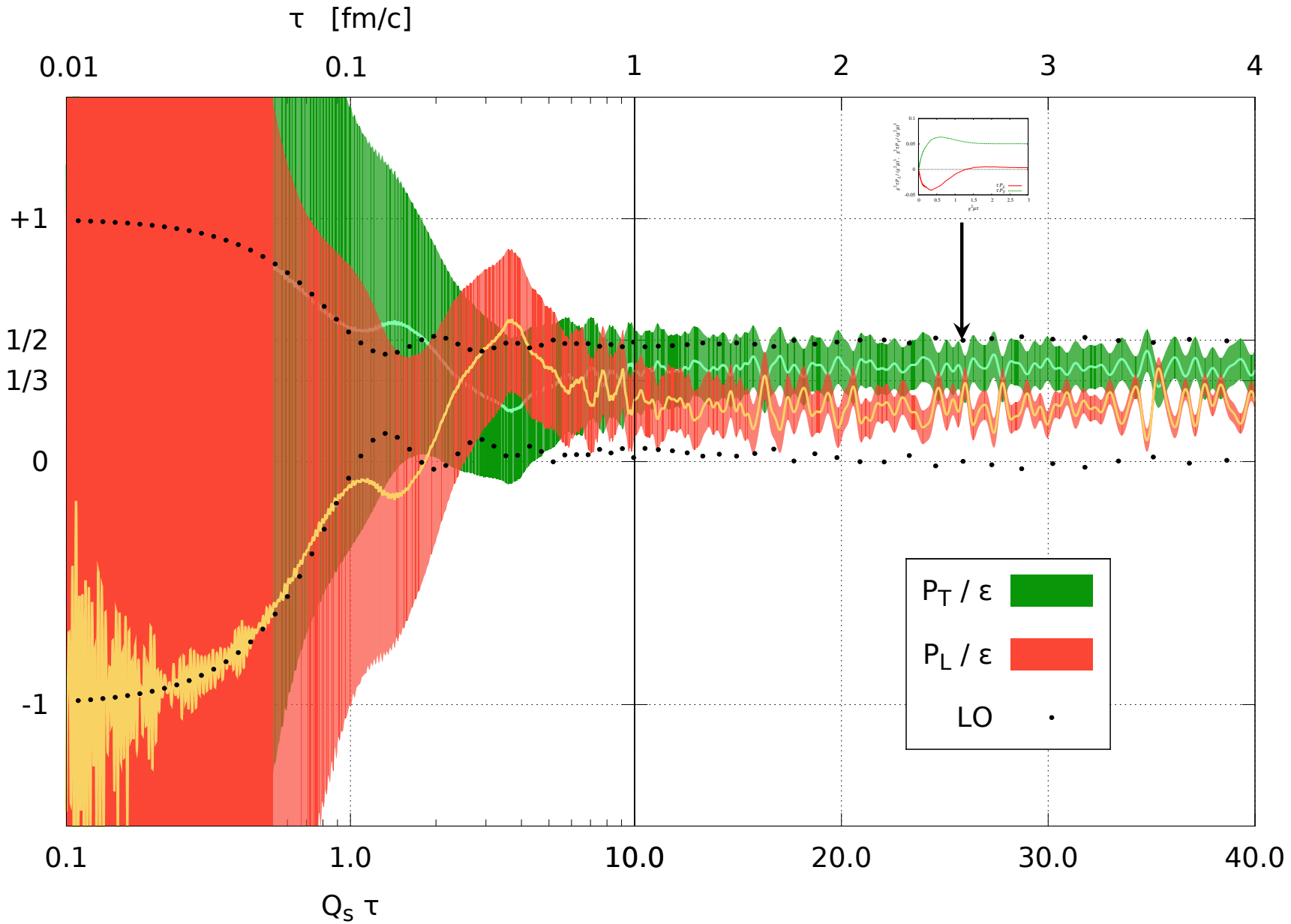

Assuming simple first order viscous hydrodynamics

$$\epsilon \approx \underbrace{\epsilon_0 \tau^{-\frac{4}{3}}}_{\text{Ideal hydro}} - \underbrace{2\eta_0 \tau^{-2}}_{\text{first order correction}}$$

we can compute the dimensionless ratio ($\eta = \eta_0 \tau^{-1}$)

$$\eta \epsilon^{-\frac{3}{4}} \lesssim 1$$

In contrast, perturbation theory at LO gives $\eta \epsilon^{-\frac{3}{4}} \sim 300$.

If the system is closed from being thermal

$$\epsilon^{\frac{3}{4}} \sim s \Longrightarrow \frac{\eta}{s} \text{ same magnitude as } \frac{1}{4\pi}$$

Conclusion

- Correct NLO spectrum from first principles
- $\frac{P_L}{P_T} \approx 0.6$ for $g = 0.5$ at $\tau \sim 1 fm/c$
- No need for strong coupling to get isotropization
- Assuming simple first order viscous hydrodynamics

$$\eta \epsilon^{-\frac{3}{4}} \lesssim 1$$

Backup: CGC initial conditions vs completely decoherent fields

$\langle A \rangle \sim 0$, $\langle E \rangle \sim 0$
$\langle A^2 \rangle - \langle A \rangle^2 \sim \frac{Q_s^2}{g^2}$
$\langle E^2 \rangle - \langle E \rangle^2 \sim \frac{Q_s^4}{g^2}$
May give correct answer at LO
Not correct at NLO

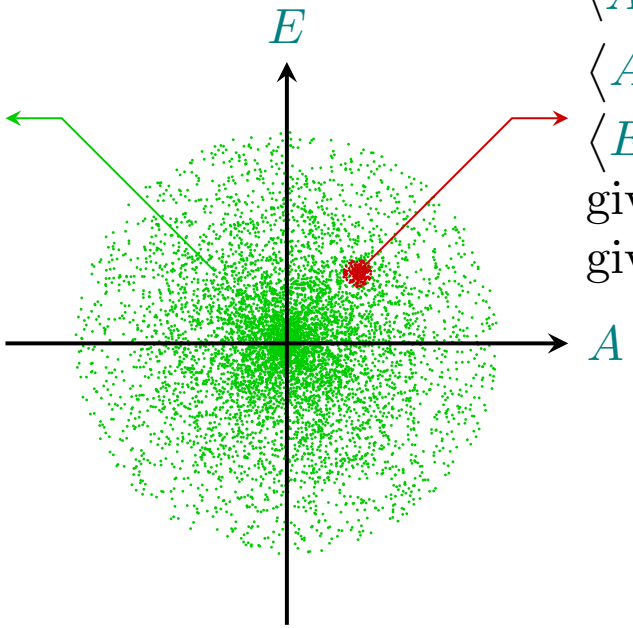

$\langle A \rangle \sim \frac{Q_s}{g}$, $\langle E \rangle \sim \frac{Q_s^2}{g}$
$\langle A^2 \rangle - \langle A \rangle^2 \sim Q_s^2$
$\langle E^2 \rangle - \langle E \rangle^2 \sim Q_s^4$
give correct answer at LO
give correct answer at NLO

Isotropization from Color Field Condensate in heavy ion collisions

Stefan Flörchinger (CERN)

RBRC Workshop on "The Approach to Equilibrium in Strongly Interacting Matter", BNL, April 2, 2014.

based on:
S. Floerchinger and C. Wetterich, *Isotropization from Color Field Condensate in heavy ion collisions*, [JHEP 03 (2014) 121].

Heavy Ion Collisions

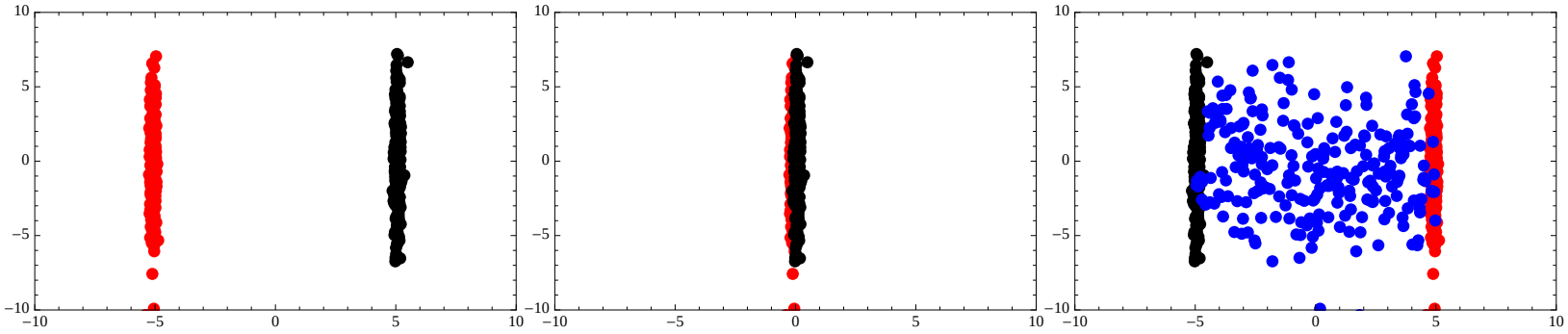

- ions are strongly Lorentz-contracted
- *some* medium is produced after collision
- medium expands in longitudinal direction and gets diluted

Evolution in time

- Non-equilibrium evolution at early times
  - initial state at from QCD? Color Glass Condensate? ...
  - thermalization via strong interactions, plasma instabilities, particle production, ...
- Local thermal and chemical equilibrium
  - strong interactions lead to short thermalization times
  - evolution from relativistic fluid dynamics
  - expansion, dilution, cool-down
- Chemical freeze-out
  - for small temperatures one has mesons and baryons
  - inelastic collision rates become small
  - particle species do not change any more
- Thermal freeze-out
  - elastic collision rates become small
  - particles stop interacting
  - particle momenta do not change any more

The puzzle of thermalization / isotropization

- Hydrodynamic description works well when started at $\tau_0 \approx 0.5\,\mathrm{fm/c}$.
- Perturbative time-scale for thermalization is much longer [Baier, Mueller, Schiff, Son (2001)].
- Effective hydrodynamic description for some quantities may also be possible without local equilibrium and detailed balance.
- Some quantities e.g. pressure may thermalize faster than others: "Prethermalization" [Berges, Borsanyi, Wetterich (2004)].
- In praxis hydro description *does* assume early local equilibrium and it works rather well with that.
- There must be some nontrivial mechanism of thermalization / isotropization to be understood.
- Another puzzle is: How does entropy and particle production work?

Could macroscopic / classical fields be the solution?

- Field expectation value or "classical field" has influence on quasi-particle excitations and leads to
  - modified vertices
  - modified dispersion relations / self energies
- That could lead to higher scattering rates and faster thermalization.
- Dynamical evolution of classical fields itself might also contribute to isotropization.
- Classical fields can also induce instabilities / particle production.

Large occupation numbers versus condensate

- In thermodynamic limit (stationary, infinite volume) a classical field corresponds to large occupation number of zero-mode: a *condensate*.
- For realistic heavy-ion collision one may have
  - non-equilibrium situation
  - finite size
  - finite number of gluons.
- Distinction between condensate and large occupation numbers for a few modes is not so clear.
- Nevertheless, condensate picture may be easiest way to capture important features of situation with large occupation numbers.
- Gluon condensate were also discussed in kinetic theory framework. [Blaizot, Gelis, Liao, McLerran, Venugopalan, Epelbaum, Berges, Schlichting, Sexty, Kurkela, Moore,...]

Is a homogeneous and isotropic color field possible?

- Expectation value for vector field $\langle \mathbf{A}_\mu \rangle$ breaks rotation invariance except for $\mu = 0$ component.
- But $\mathbf{A_0}$ is gauge degree of freedom.
- One can choose Weyl or temporal gauge, $\mathbf{A_0} = \mathbf{0}$.
- Seems to suggest that homogeneous and isotropic color field is *not* possible.

Modified rotation symmetry

- One can combine rotations with gauge transformations into a modified rotation transformation [Reuter, Wetterich (1994)].
- Group theoretic: embed $SU(2) \in SU(3)$.
- Gauge singlets rotate in the normal way.
- There are two inequivalent embeddings of this type. For one of them Lie algebra of $SU(2)$ spanned by Gell-Mann matrices $\lambda_2, \lambda_5, \lambda_7$.
- Contains a singlet

$$(A_j)_{mn} = \sigma\, \epsilon_{jmn}$$

- More general, temporal part $\mathbf{A}_0$ transforms like

$$\mathbf{8} = \mathbf{5} + \mathbf{3},$$

and spatial part $\mathbf{A}_j$ like

$$\mathbf{24} = \mathbf{7} + 2 \times \mathbf{5} + 2 \times \mathbf{3} + \mathbf{1}.$$

Field configurations with cylindrical symmetry

- There is only one candidate for isotropic condensate σ, i.e. a singlet under three-dimensional rotations.
- For cylindrical symmetry, i.e. reduced symmetry under
  - rotations in the transverse plane of x_1, x_2,
  - rotations of 180° around x_1 or x_2 axis,

  one has two more condensate candidates, $\tilde{\gamma}^A$ and $\tilde{\gamma}^B$.
- For space parity transformations $\mathsf{P}(\mathbf{A_0}, \mathbf{A_j}) = (\mathbf{A_0}, -\mathbf{A_j})$ one has

$$\mathsf{P}\,\sigma = -\sigma, \qquad \mathsf{P}\,\tilde{\gamma}^{\mathsf{A}} = -\tilde{\gamma}^{\mathsf{A}}, \qquad \mathsf{P}\,\tilde{\gamma}^{\mathsf{B}} = -\tilde{\gamma}^{\mathsf{B}}.$$

- For color charge conjugation $\mathsf{C}\,\mathbf{A}_\mu = -\mathbf{A}_\mu^*$ one has

$$\mathsf{C}\,\sigma = \sigma, \qquad \mathsf{C}\,\tilde{\gamma}^{\mathsf{A}} = -\tilde{\gamma}^{\mathsf{A}}, \qquad \mathsf{C}\,\tilde{\gamma}^{\mathsf{B}} = \tilde{\gamma}^{\mathsf{B}}.$$

  and accordingly for CP

$$\mathsf{CP}\,\sigma = -\sigma, \qquad \mathsf{CP}\,\tilde{\gamma}^{\mathsf{A}} = \tilde{\gamma}^{\mathsf{A}}, \qquad \mathsf{CP}\,\tilde{\gamma}^{\mathsf{B}} = -\tilde{\gamma}^{\mathsf{B}}.$$

Time evolution of condensates 1

- Time evolution of condensate in general quite complicated due to quantum effects.
- Qualitative guiding from classical Yang-Mills equations.
- For isotropic and homogeneous condensate σ

$$\partial_t^2 \sigma = -2g^2\sigma^3.$$

Anharmonic oscillator, solution in terms of Jacobi elliptic functions.

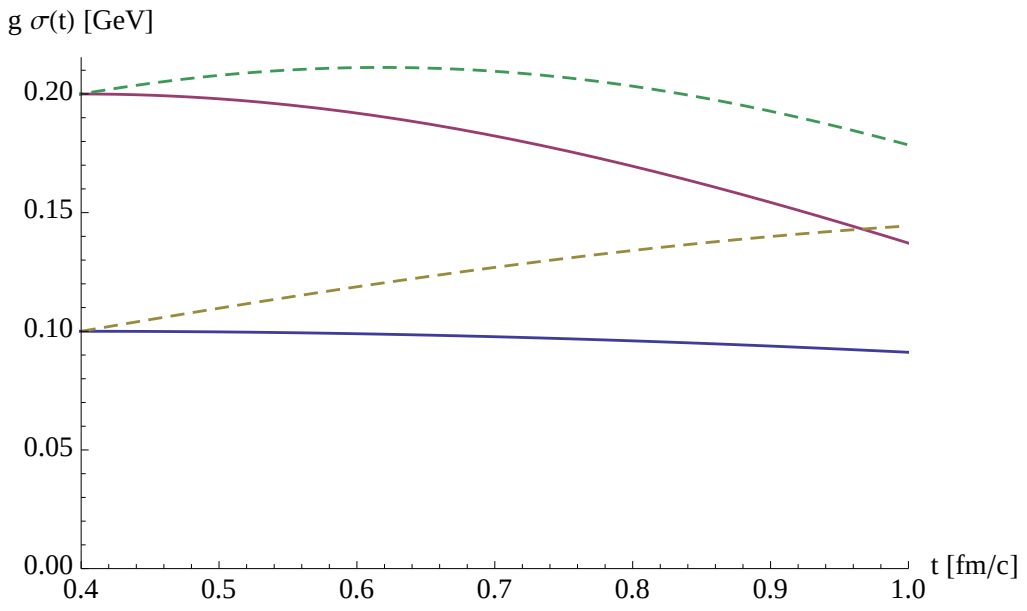

Time evolution of condensate 2

- Isotropic and cylindric condensates have coupled evolution equations.
- Can be easily solved numerically.
- Isotropic condensate σ can be generated from $\tilde{\gamma}^A$, $\tilde{\gamma}^B$. For example:

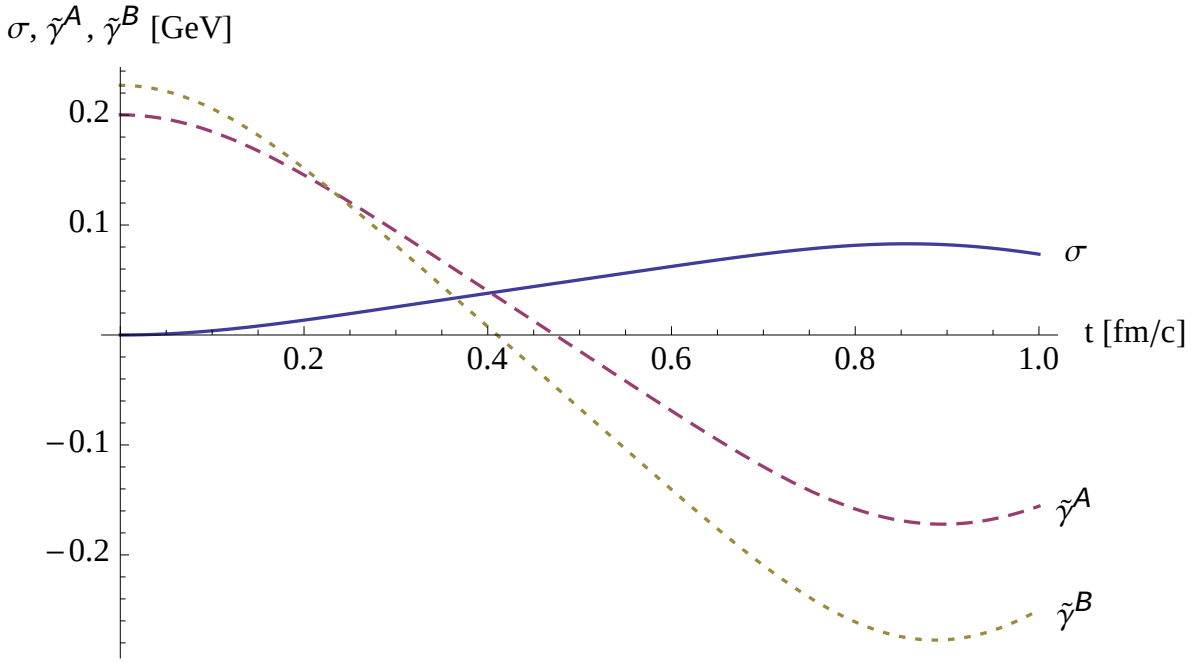

Energy-momentum tensor due to condensates

- Energy-momentum tensor due to condensates

$$T^{\mu\nu} = 2\text{tr}\ \mathbf{F}^{\rho\mu}\mathbf{F}_{\rho}{}^{\nu} - \frac{1}{2}g^{\mu\nu}\ \text{tr}\ \mathbf{F}^{\alpha\beta}\mathbf{F}_{\alpha\beta}.$$

- Assume that energy and momentum are dominated by this.

$$T^{\mu\nu} = \text{diag}(\epsilon, p_{tr}, p_{tr}, p_l).$$

For same example as above:

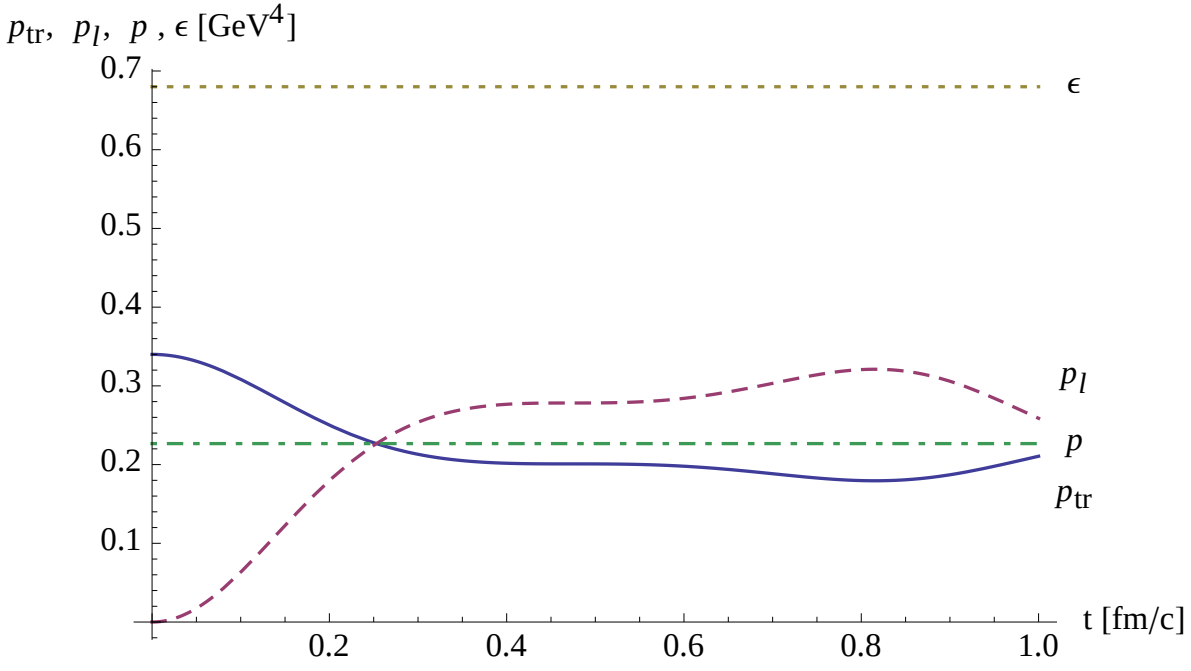

- Condensates can contribute to quick isotropization!

CP-*even cylindrical condensate*

- Initial condition with only $\tilde{\gamma}^A$ is CP symmetric.
- CP-breaking isotropic condensate σ not generated.
- Initial energy momentum tensor of the form

$$T^{\mu\nu} = \text{diag}(\epsilon, p_{tr}, p_{tr}, p_l) = \text{diag}(\epsilon, \epsilon, \epsilon, -\epsilon).$$

- Leads to oscillations between p_{tr} and p_l

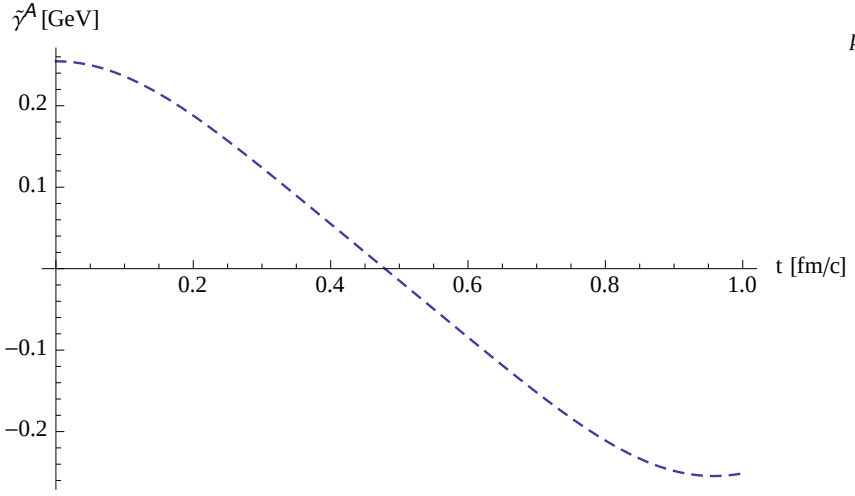

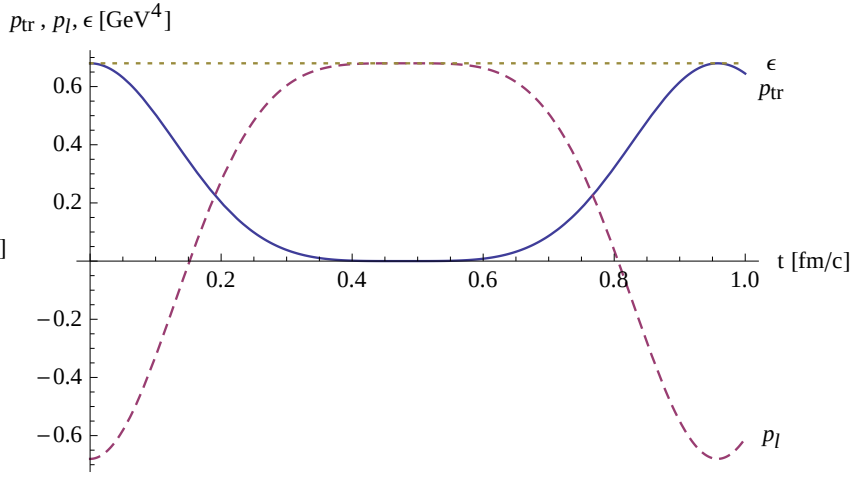

Longitudinal expansion

- In realistic heavy ion collision the time evolution is modified by several effects, in particular by longitudinal expansion.
- Condensates will be diluted.
- That will probably hinder oscillations.
- Compare here only different scenarios for time evolution to $1/\tau^{1/3}$ dilution.

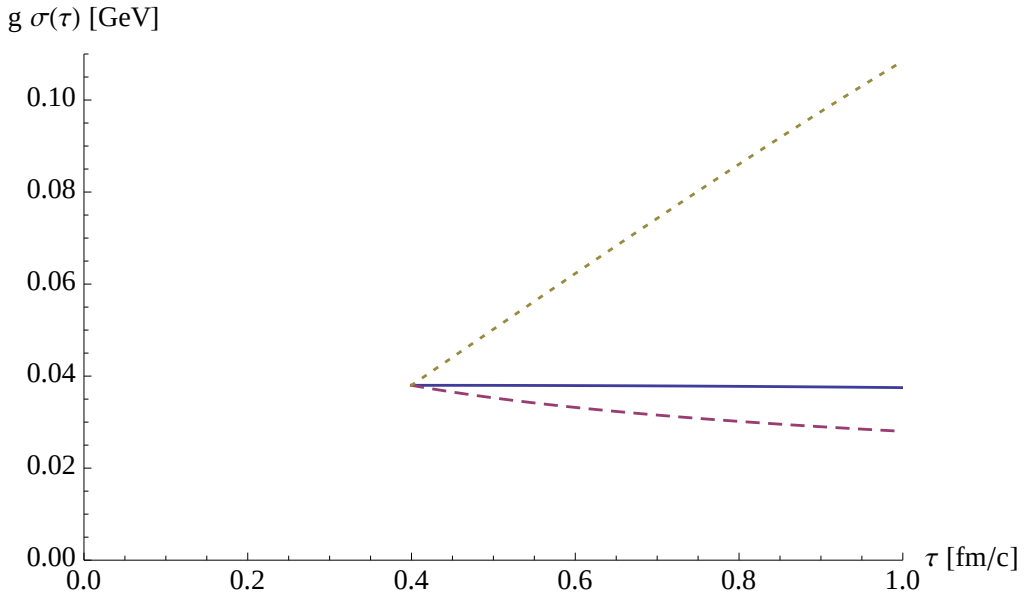

Excitations

- Consider now excitations of other field modes in the presence of isotropic condensate σ.
- Classify them according to the transformation behavior under modified rotations.
- Investigate in particular dispersion relations for excitations in the presence of isotropic condensate σ

Decomposition of gauge field 1

Write spatial and temporal parts of gauge field

$$
\begin{aligned}
(A_j)_{mn} =& \kappa_{jmn} + \gamma^A_{mk}\epsilon_{kjn} + \gamma^A_{nk}\epsilon_{kjm} + i\,\gamma^B_{jk}\epsilon_{kmn} \\
&+ (\beta^A_m + i\,\beta^B_m)\,\delta_{jn} + (\beta^A_n - i\,\beta^B_n)\,\delta_{jm} - \frac{2}{3}\beta^A_j\delta_{mn} + i\,\sigma\,\epsilon_{jmn} \\
(A_0)_{mn} =& \gamma^C_{mn} + i\,\beta^C_l\,\epsilon_{lmn}
\end{aligned}
$$

with

- κ_{jmn} is real, completely symmetric, three-dimensional tensor of rank three, traceless with respect to all contractions,
- γ^A_{jk}, γ^B_{jk} and γ^C_{jk} are real, symmetric and traceless three-dimensional tensors,
- β^A_m, β^B_m and β^C_m are real, three-dimensional vectors.

In summary

$$
\begin{aligned}
\mathbf{24} =& \mathbf{7} + 2\times\mathbf{5} + 2\times\mathbf{3} + \mathbf{1}, \\
\mathbf{8} =& \mathbf{5} + \mathbf{3}.
\end{aligned}
$$

Decomposition of gauge field 2

To analyze dispersion relations it is useful to decompose further

- vectors

$$\beta_m = \partial_m \beta + \hat{\beta}_m$$

  - β is a real scalar,
  - $\hat{\beta}_m$ is a real, divergence-less vector.

- tensors of rank two

$$\gamma_{mn} = \hat{\gamma}_{mn} + \partial_m \hat{\gamma}_n + \partial_n \hat{\gamma}_m + (\partial_m \partial_n - \frac{1}{3}\delta_{mn}\partial_j^2)\gamma$$

  - $\hat{\gamma}_{mn}$ is real, traceless and divergence-less tensor
  - $\hat{\gamma}_m$ is real, divergence-less vector
  - γ is a real scalar.

- and tensors of rank three

$$\kappa_{jmn} = \hat{\kappa}_{jmn} + \partial_j \hat{\kappa}_{mn} + \partial_m \hat{\kappa}_{jn} + \partial_n \hat{\kappa}_{jm} + \ldots$$

Decomposition of gauge field 3

- Discrete symmetries C and P classify fields further.
- Fields in different representations du not mix on linear level.
- Gauge fixing to Weyl gauge implies $\mathbf{A}_0 = 0$ or $\gamma^C_{mn} = \beta^C_m = 0$.
- At this point we are left with
  - C-even scalars $\sigma, \beta^B, \gamma^B$
  - C-odd scalars $\beta^A, \gamma^A, \kappa$
  - C-even vectors $\hat{\beta}^B_m, \hat{\gamma}^B_m$
  - C-odd vectors $\hat{\beta}^A_m, \hat{\gamma}^A_m, \hat{\kappa}_m$
  - C-even rank-two tensors $\hat{\gamma}^B_{mn}$
  - C-odd rank-two tensors $\hat{\gamma}^A_{mn}, \hat{\kappa}_{mn}$
  - C-odd rank-three tensor $\hat{\gamma}_{jmn}$

  which makes 24 real degrees of freedom.
- To reduce to 16 d.o.f. one needs the Gauss constraint.

Constraint equations

Variation of action with respect to $\mathbf{A}_0$ yields the Gauss constraint

$$\partial_j (E_j)_{mn} - ig(A_j)_{mk}(E_j)_{kn} + ig(E_j)_{mk}(A_j)_{kn} = D_j(E_j)_{mn} = 0.$$

Linearize this around constant background σ and decomposed further

- tensor constraint

$$\partial_0 \Big[\partial_j \, \kappa_{jmn} + \epsilon_{kjn}(\partial_j \gamma^A_{mk}) + \epsilon_{kjm}(\partial_j \gamma^A_{nk}) + \partial_m \beta^A_n + \partial_n \beta^A_m - \frac{2}{3} \partial_j \beta^A_j \, \delta_{mn} - 6 \, g\sigma \, \gamma^A_{mn} \Big] = 0,$$

- vector constraint

$$\partial_0 \Big[\partial_k \gamma^B_{jk} + \epsilon_{jmn} \partial_n \beta^B_m + \partial_j \delta\sigma - 2 \, g\sigma \, \beta^B_j \Big] = 0.$$

Instabilities and particle production

One can now determine the dispersion relations for independent excitation modes. For example, for symmetric tensor of rank three $\hat{\kappa}_{jmn}$

$$p_0^2 = \vec{p}^2 + 2g^2\sigma^2 \pm 4pg\sigma,$$

- One mode gapped with $\Delta = \sqrt{2g^2\sigma^2}$.
- Other mode has Nielsen-Olesen instability for intermediate momenta.
- Particles will be produced in that momentum regime.
- Time scale for particle production $\tau_{\text{pp}} \approx 1/\sqrt{g^2\sigma^2} \approx 1\,\text{fm/c}$.

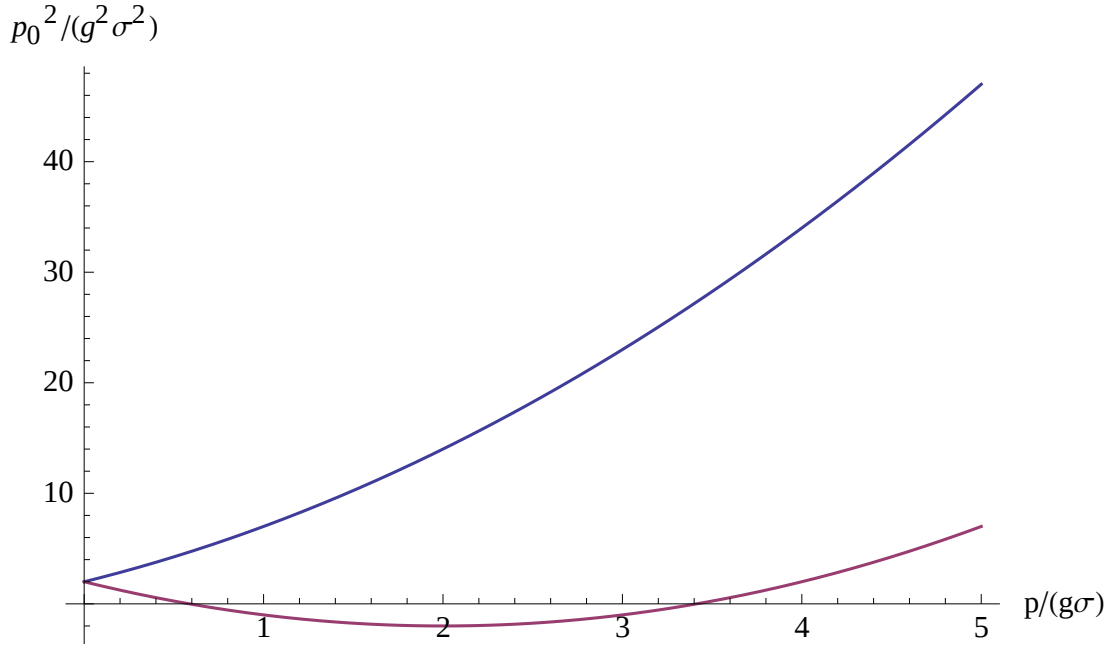

Dispersion relations 1

C-odd tensors of rank two

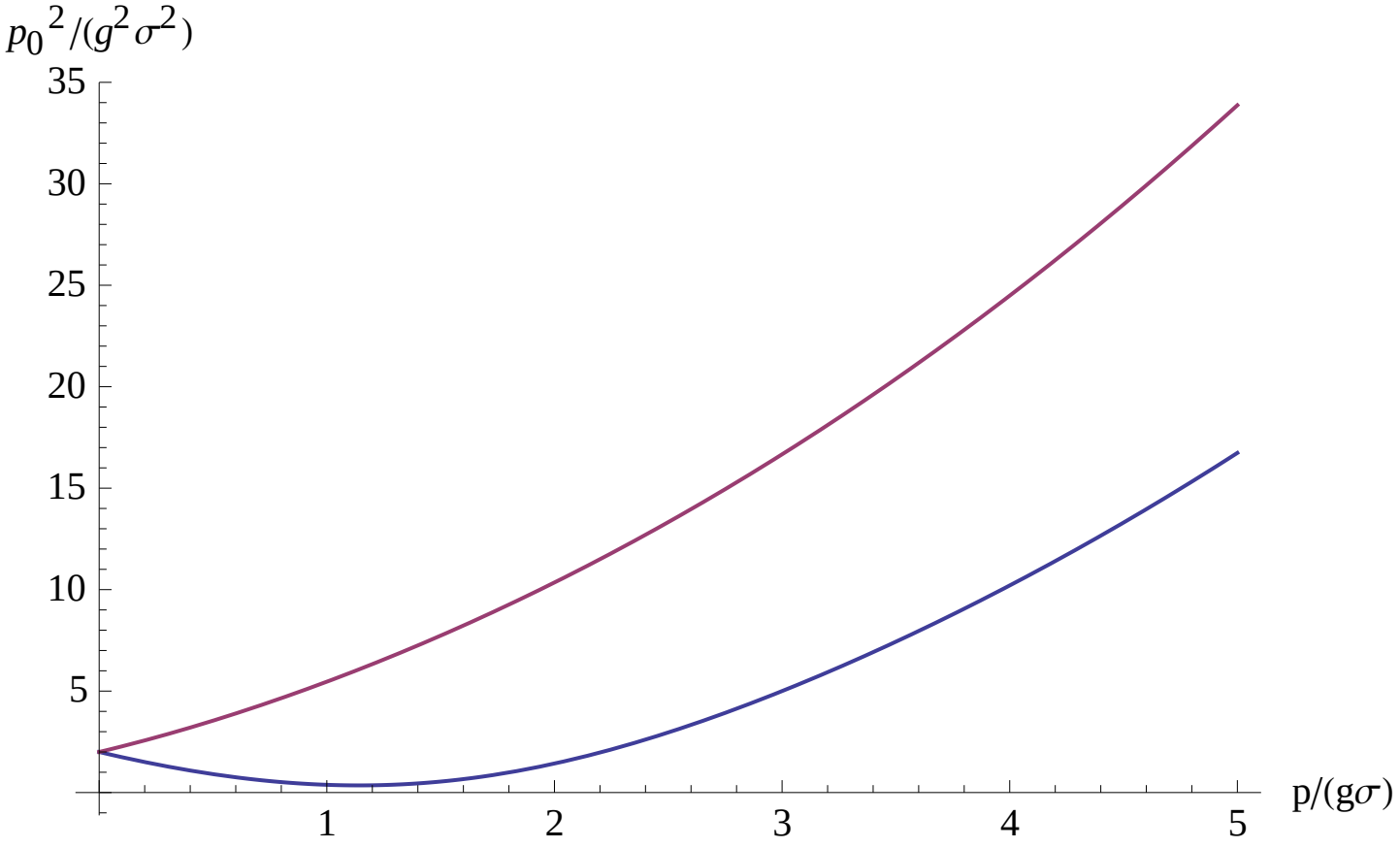

Dispersion relations 2

C-even tensors of rank two

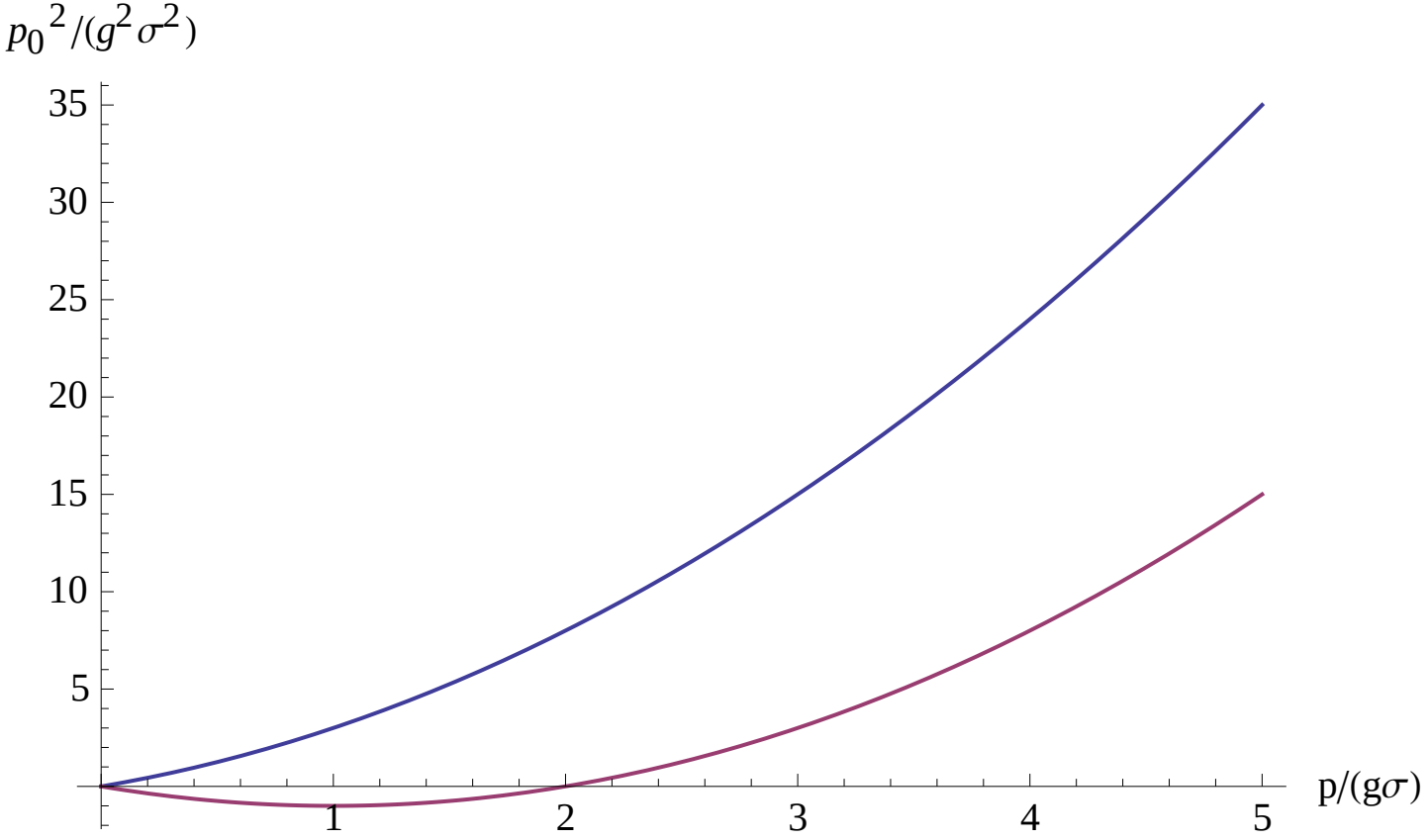

Dispersion relations 3

C-odd scalars

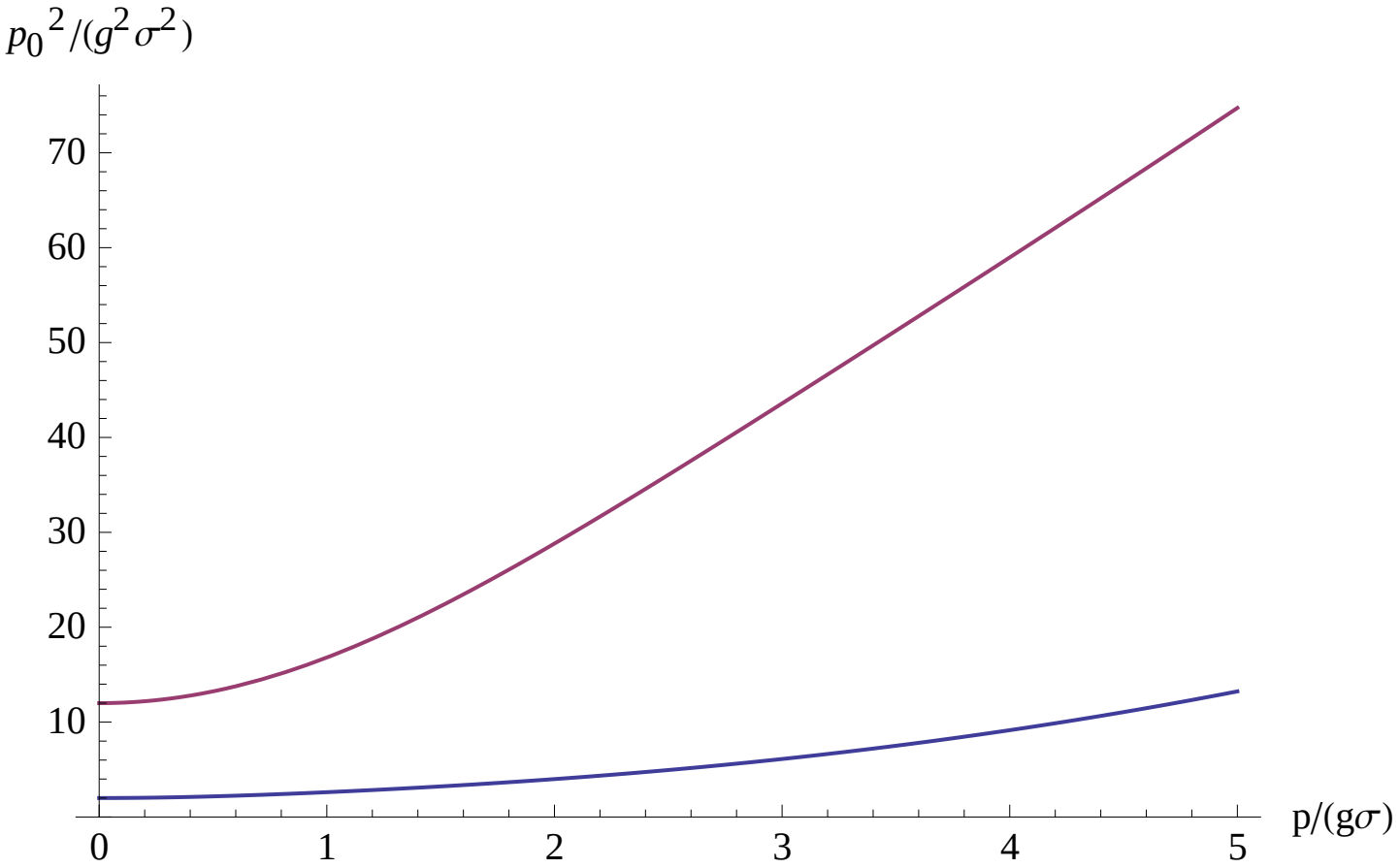

Dispersion relations 4

C-even scalars

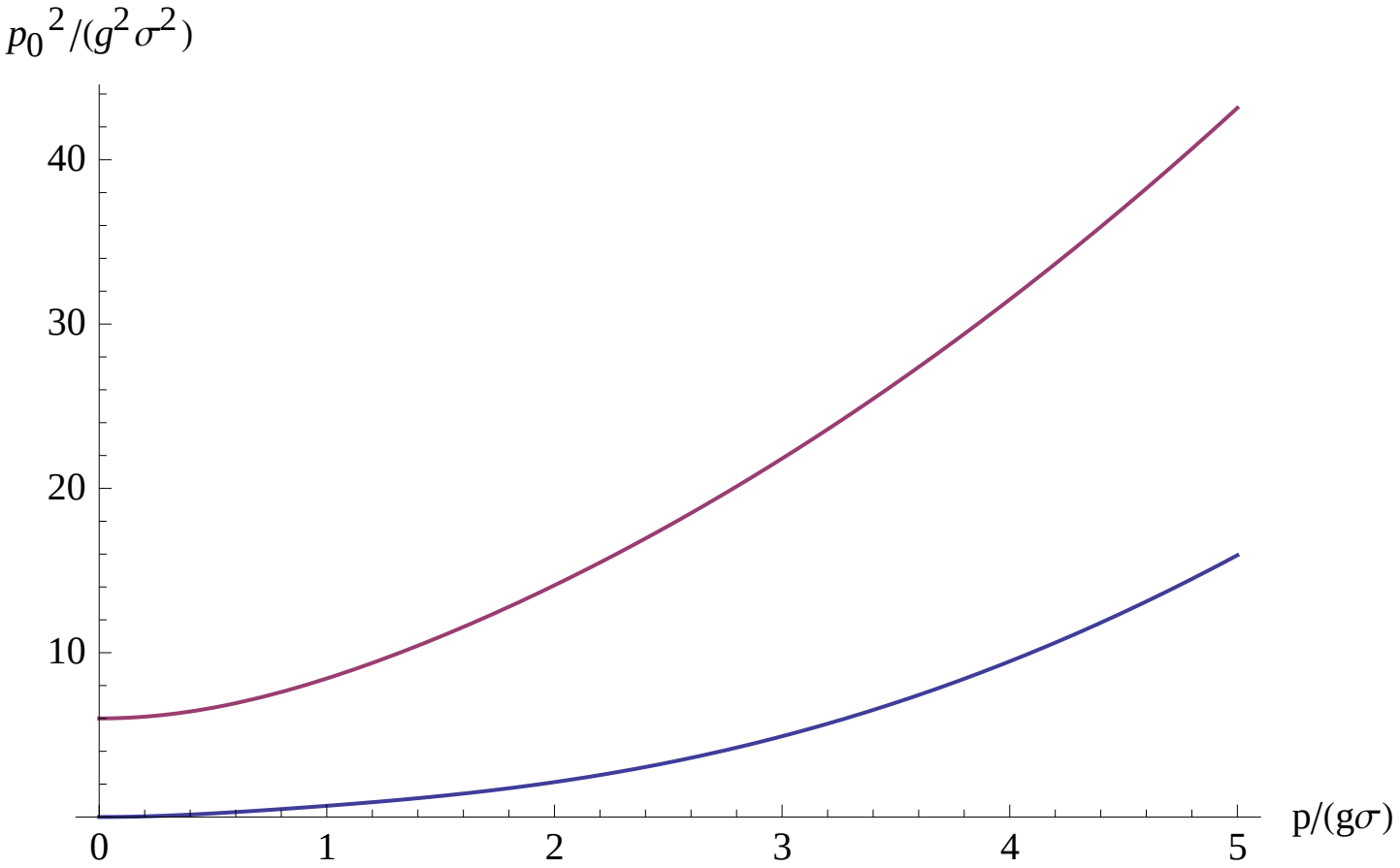

Conclusions

- Color field condensate may be simple qualitative description for state with high gluon occupation numbers.
- Modified rotation symmetry (involving a gauge transformation) provides powerful ordering principle.
- Collective dynamics provides efficient mechanism for approximate isotropization.
- Nielsen-Olesen type instabilities can trigger decay of color field condensate into quasi-particle excitations.
- Particle production from decay of isotropic condensate can be approximately isotropic, as well.

BACKUP

Alternative embedding of $SU(2) \in SU(3)$

- Lie algebra of $SU(2)$ spanned by Gell-Mann matrices $\lambda_1, \lambda_2, \lambda_3$.
- Contains singlets
  - in spatial part
$$(A_j)_{mn} = \sigma(\lambda_j)_{mn}.$$
  - in temporal part
$$(A_0)_{mn} = \sigma'(\lambda_8)_{mn}$$
- More general decomposition of gauge field according to
  - temporal part $\mathbf{8} = \mathbf{3} + 2 \times \mathbf{2} + \mathbf{1}$,
  - spatial part $\mathbf{24} = \mathbf{5} + 2 \times \mathbf{4} + 2 \times \mathbf{3} + 2 \times \mathbf{2} + \mathbf{1}$.

Parametric resonances

- Here we considered excitations around constant background σ.
- For oscillating condensate one has additional parametric resonance phenomenon leading to an additional instability band [Berges et al, PRD 85, 034507 (2012)].
- Parametric resonance instability subleading compared to Nielsen-Olesen instability.

Real-time Stochastic Quantization — Problems and Simulations —

Kenji Fukushima (U. of Tokyo)

In collaboration with
R. Anzaki, T. Oka (U. of Tokyo)
Y. Hidaka (RIKEN)

Physics Motivation

Isotropization / Thermalization in HIC?

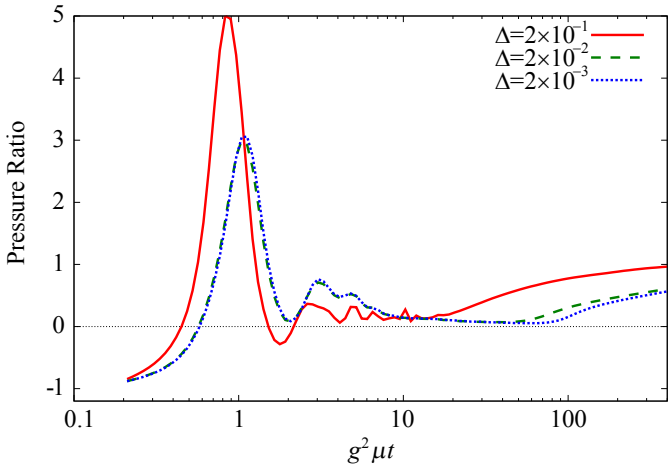

Check of isotropization
with CGC in a fixed box

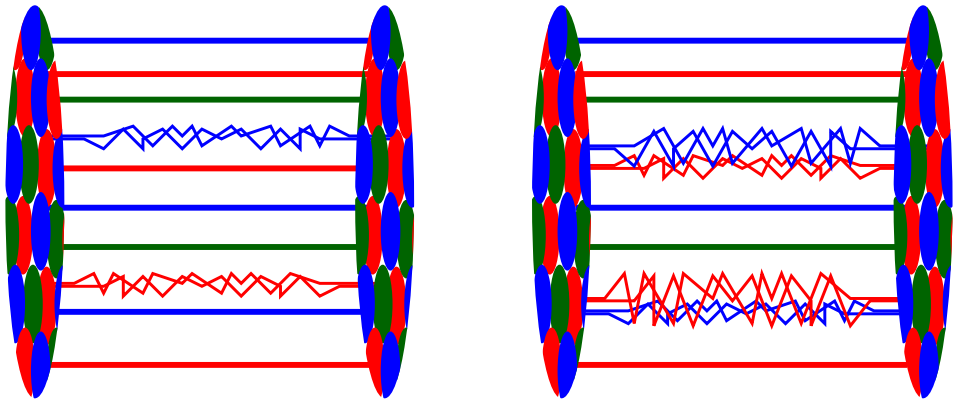

(a) Local Avalanche in Longitudinal

(b) Diffusion in Transverse

Fukushima (2013)

Transverse inhomogeneity at small *kz* is non-linearly amplified toward larger *kz* => Diffusion on the transverse plane

Physics Motivation

Isotropization / Thermalization in HIC?

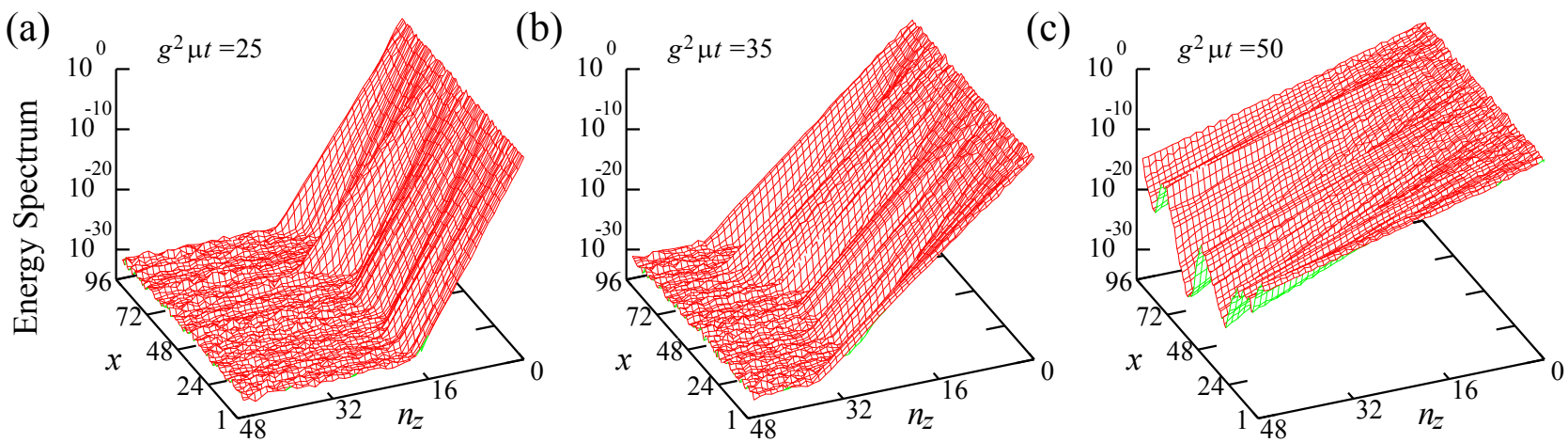

Fukushima (2013)

Isotropization / Thermalization understood in a fixed box?
If not, how can we for an expanding case?

Fixed-box Simulation

Transverse Coulomb gauge

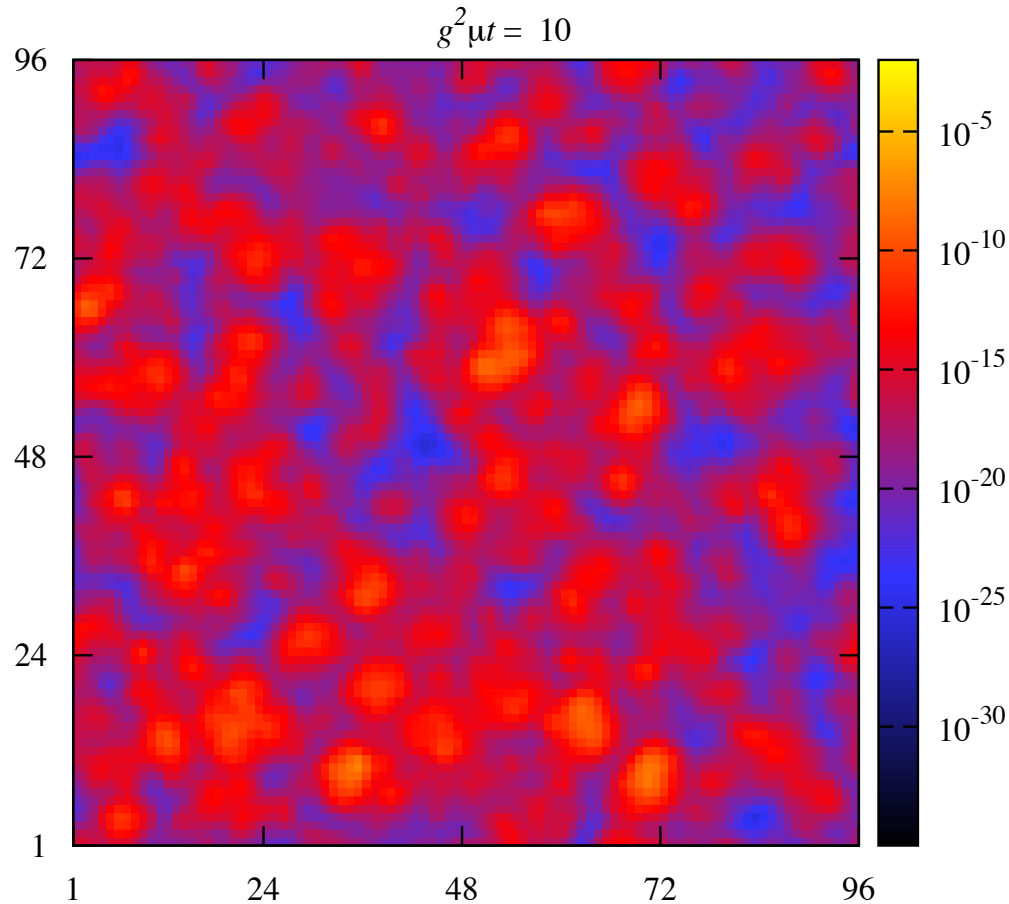

Brighter color
=> Longitudinally disturbed

Isotropization is incomplete
Thermal dist. (exponential)
is achieved fast

Anisotropic Thermalization

if the initial cond. is anisotropic
even in an isotropic box

cf. Attems, Strickland, etc…

Success of the CSA

Classical Statistical Approximation

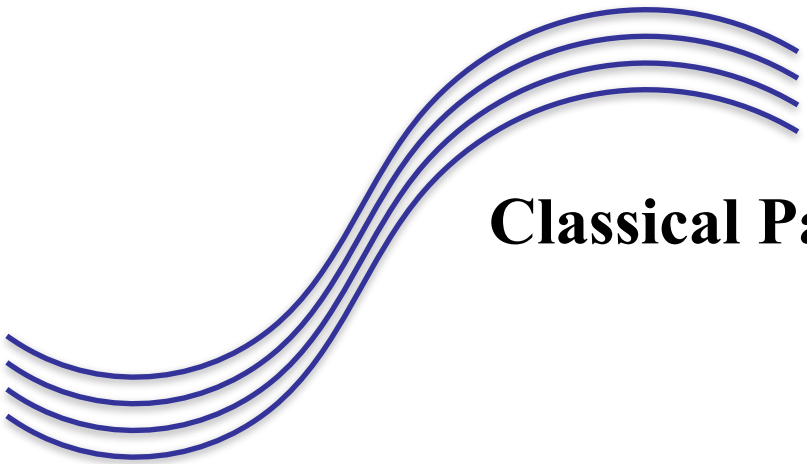

Berges, Epelbaum, Fukushima, Gelis, Kunihiro, Muller, Lappi, Ohnishi, Romatschke, Schaefer, Schlichting, Sexty, Tanji, Venugopalan, Wu

Foundation from the first-principle quantization scheme?

cf. von Neumann eq. for the Wigner func. (Gelis)

Quantization Methods

Canonical Quantization

- □ Creation/Annihilation Operators

~~Numerical Simulation~~

Functional Integral

- □ Classical Fields + Path Integral

~~Complex Weight~~

Functional Renormalization Group Equation

- □ Classical Fields + Differential Equation (**with *k***)

Holographic Correspondence

- □ Classical Fields + Equation of Motion (**with *z***)

Stochastic Quantization (Parisi-Wu, Klauder, …)

- □ Classical Fields + Complex Langevin Eq. (**with** θ)

Higher-dimensional Diff. Eq.

Stochastic Quantization

Step 1 (Solve a complex Langevin eq. — ϕ^4 theory)

$$\partial_\theta \, \phi(x,\theta) = i \, \frac{\delta S}{\delta \phi(x)} \bigg|_{\phi(x) \to \phi(x,\theta)} + \eta(x,\theta)$$

$$= -i(\Box + m^2 - i\epsilon) \, \phi(x,\theta) - i\lambda \, \phi^3(x,\theta) + \eta(x,\theta)$$

Step 2 (Take a noise average)

$$\langle \eta(x,\theta) \, \eta(x',\theta') \rangle_\eta = 2 \, \delta^{(4)}(x - x') \, \delta(\theta - \theta')$$

Step3 (Send θ to infinity)

$$\langle \mathcal{O}[\phi(x)] \rangle = \lim_{\theta \to \infty} \langle \mathcal{O}[\phi(x,\theta)] \rangle_\eta$$

Recovery of the Free Propagator

Explicit solution without interaction

$$\phi_k(\theta) = \frac{1}{\partial_\theta - i(\omega^2 - \xi_{\boldsymbol{k}}^2 + i\epsilon)}\,\eta_k(\theta)$$

Initial Condition

$$= \int_0^\theta d\theta'\, e^{i(\omega^2-\xi_{\boldsymbol{k}}^2+i\epsilon)(\theta-\theta')}\,\eta_k(\theta') + \cancel{e^{i(\omega^2-\xi_{\boldsymbol{k}}^2+i\epsilon)\theta}\,\phi_k(0)}$$

Two-point function

$$G_0(k,k') = \lim_{\theta\to\infty}\langle\phi_k(\theta)\,\phi_{k'}(\theta)\rangle_\eta$$

$$= (2\pi)^4\delta^{(4)}(k+k')\,\frac{i}{\omega^2-\xi_{\boldsymbol{k}}^2+i\epsilon}\,\lim_{\theta\to\infty}\left[1-e^{2i(\omega^2-\xi_{\boldsymbol{k}}^2+i\epsilon)\theta}\right]$$

$i\varepsilon$ prescription from the convergence factor

Recovery of the Feynman Diagrams

Integral equation with interaction

$$\phi_k(\theta) = \int_0^\theta d\theta' \, e^{i(\omega^2 - \xi_{\boldsymbol{k}}^2 + i\epsilon)(\theta - \theta')} \Big[\eta_k(\theta') - i\lambda \int \frac{d^4k_1 d^4k_2}{(2\pi)^8} \phi_{k-k_1-k_2}(\theta') \phi_{k_1}(\theta') \phi_{k_2}(\theta') \Big]$$

Iterative solutions

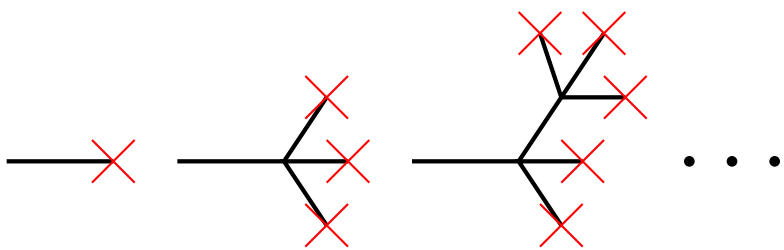

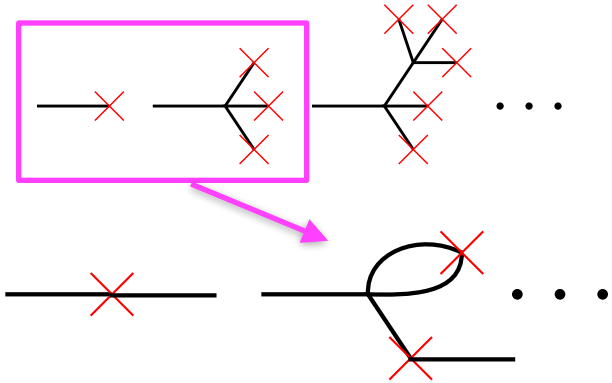

"Perturbatively" equivalent to conventional ones

Numerical Simulation

Berges-Stamatescu (2005)

- Temporal oscillation emerges in a scalar field theory
- With and without interactions

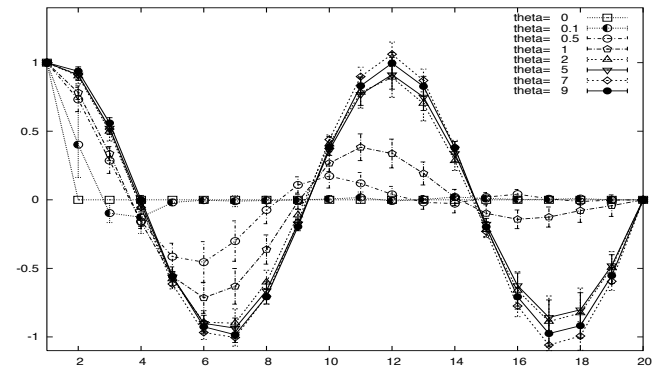

Berges-Borsanyi-Sexty-Stamatescu (2006)

- Scalar field theory and non-Abelian gauge theory
- Comparison with full results from other methods

Although the results were "promising", there is no major development since then… it is time to revisit this method and clarify the connection to the classical statistical approx.

Connection to the CSA

Averaging over η solves the classical eq. of motion

Out-going boundary condition fixed at the initial time

η(0) and η(1) "unintegrated"

$$\eta(0) \text{ and } \eta(1)$$

$$\Rightarrow \delta\phi(0) \text{ and } \delta\dot{\phi}(0)$$

Classical Statistical Approx.

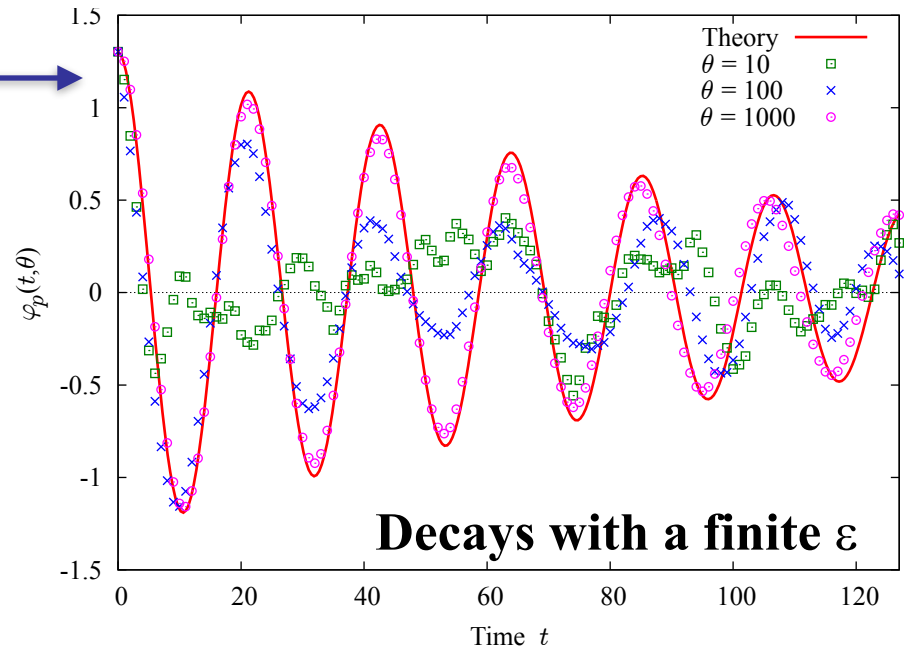

Fukushima-Hayata (2014)

Initial quantum spectrum is trivial for η(0) and η(1)

Correlation missed $\langle \mathcal{O}[\phi] \rangle_\eta \neq \mathcal{O}[\langle \phi \rangle_\eta]$

Particle Production

Mapping to the Schroedinger equation

$$\theta \to -t \qquad t \to x$$

Fixed point = Zero energy scattering

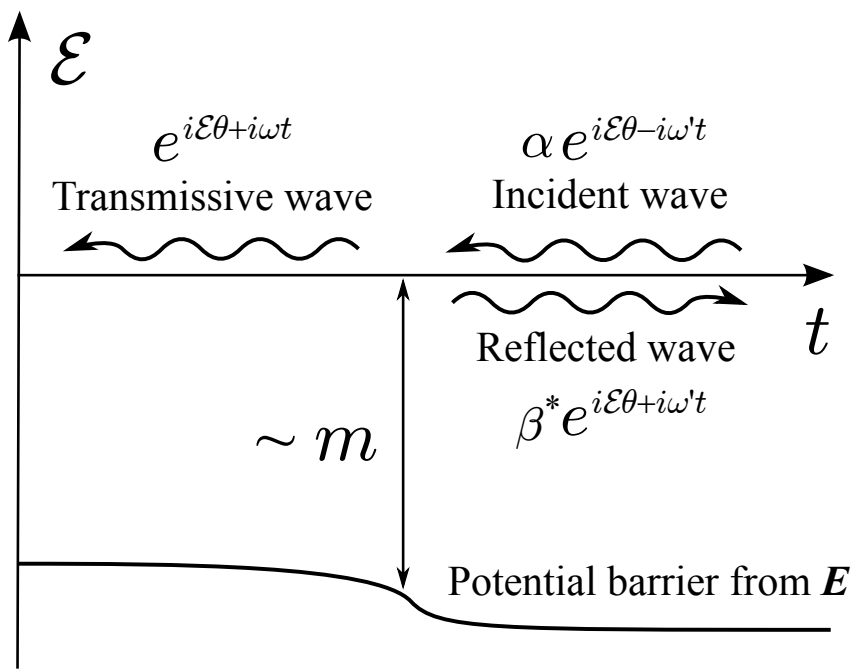

Problems in Numerics

Numerical Instability (controllable)

- □ Diffusion equation even without interaction may develop instability => Implicit method (Crank-Nicolson)

Wrong Answer (much more subtle…)

- □ Results may look like non-singular but may be different from the physical answer.
- □ Boundary condition, non-converging trajectory, etc…

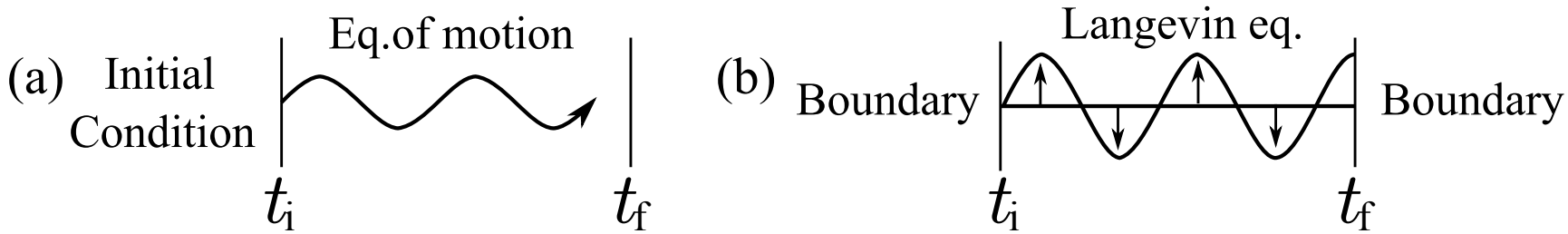

Improvement Needed

Berges-Borsanyi-Sexty-Stamatescu (2006)

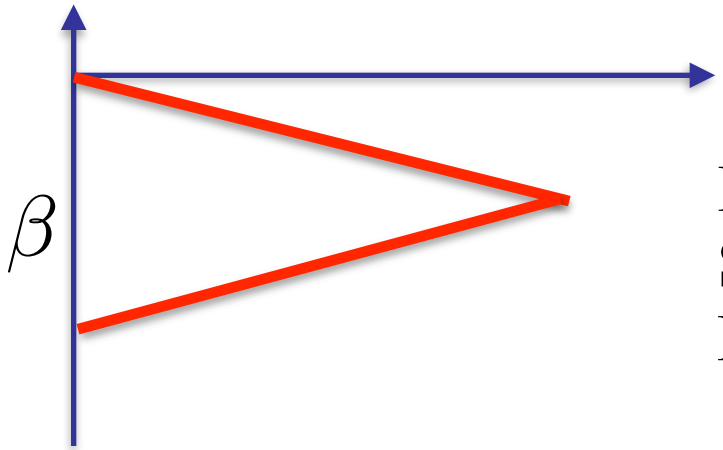

Initial density matrix ~ thermal
Stable simulation possible
How to put a CGC-type init. cond.?

Closed-time path formalism ?

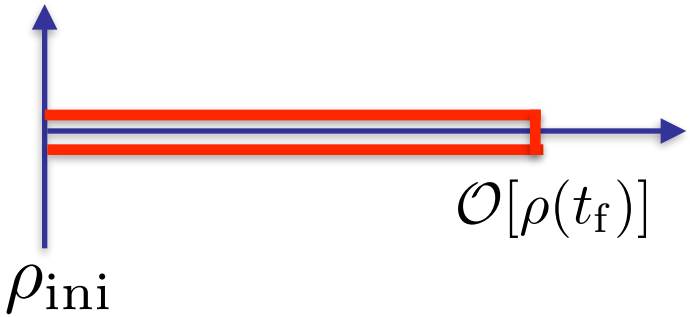

Test in the "vacuum"
Not very stable
Could hit a wrong answer

Simple Numerical Test

"Toy" model

$$\eta_\omega(\theta) = \cos(\omega_0 t)$$

Equation of motion

$$\partial_\theta \, \phi(t,\theta) = -i(\partial_t^2 + \xi^2 - i\epsilon)\, \phi(t,\theta) + \cos(\omega_0 t)$$

Analytical expectation

Unwanted oscillatory part

$$\phi(t,\theta) = \frac{i}{\omega_0^2 - \xi^2 + i\epsilon}\left[1 - \boxed{e^{i(\omega_0^2 - \xi^2 + i\epsilon)\theta}}\right] \cos(\omega_0 t)$$

Boundary condition in *t* is chosen by the *i*ε prescription
=> **"vacuum-to-vacuum" physics**

Test with Fixed B.C.

Dirichlet boundary cond. (very "wrong" choice)

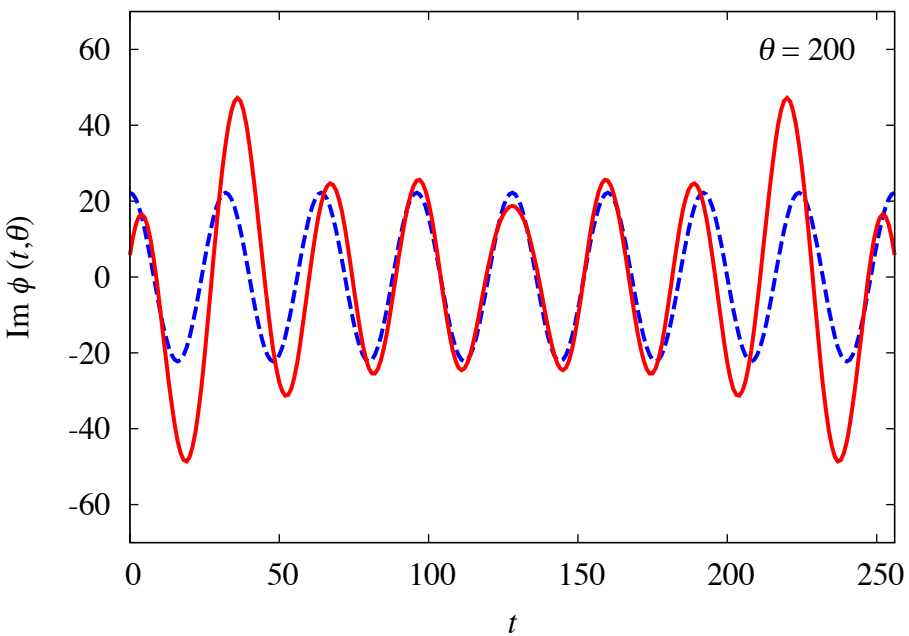

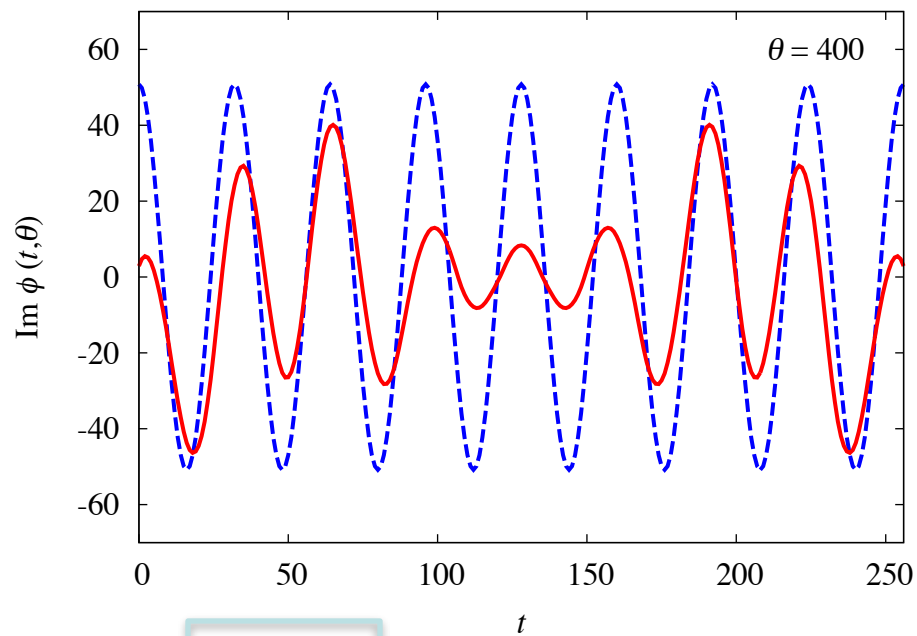

$\nu = 8$

Red curve — Numerical results

Blue curve — Analytical expectation

$$\omega_0 = \nu \times \frac{2\pi}{N_t}$$

Test with Free B.C.

Neumann (zero derivative) boundary condition

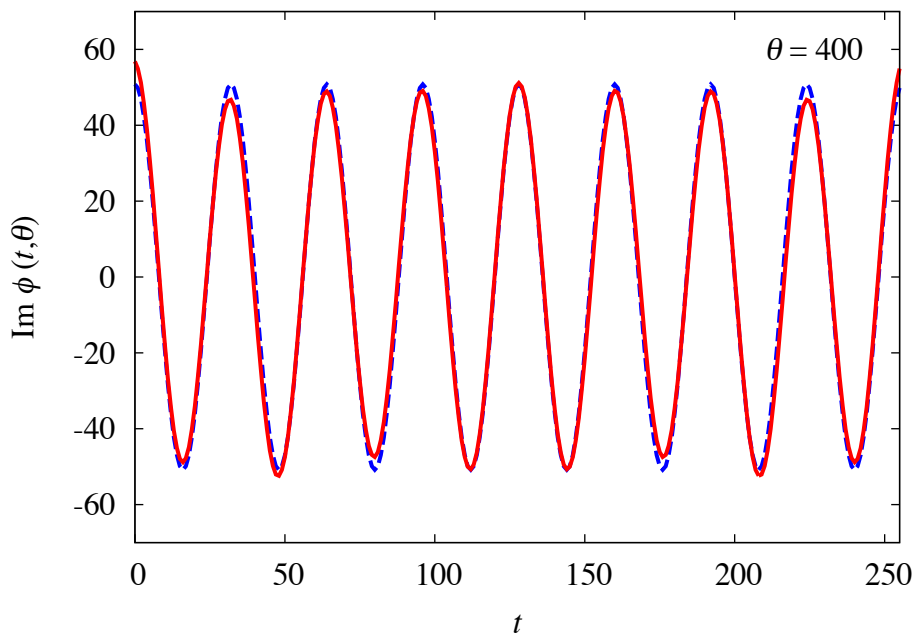

$\nu = 8$

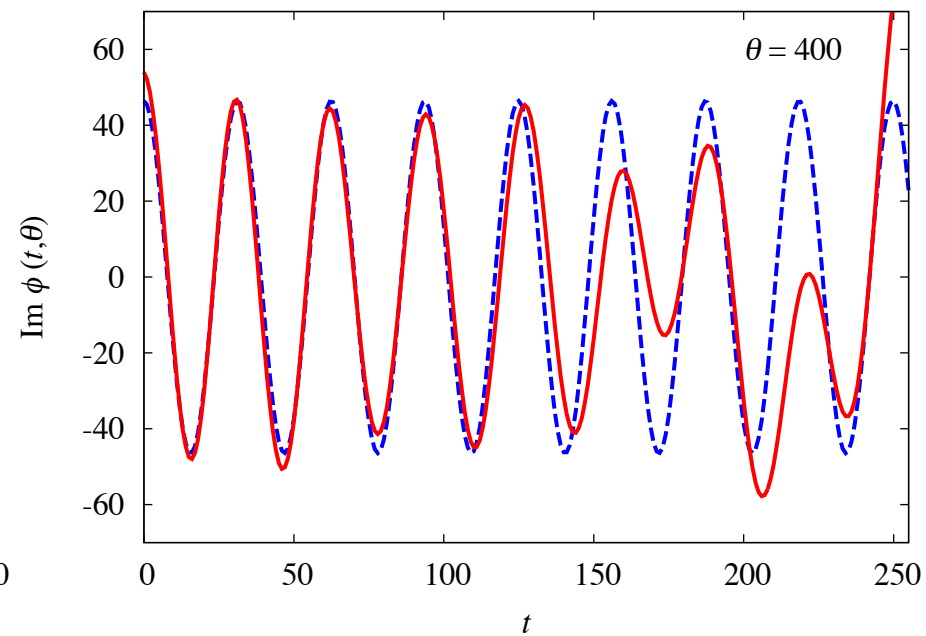

$\nu = 8.2$

No numerical instability
Blow-up solution (very harmful)

$$\omega_0 = \nu \times \frac{2\pi}{N_t}$$

Test with Periodic B.C.

Good for the "vacuum" physics

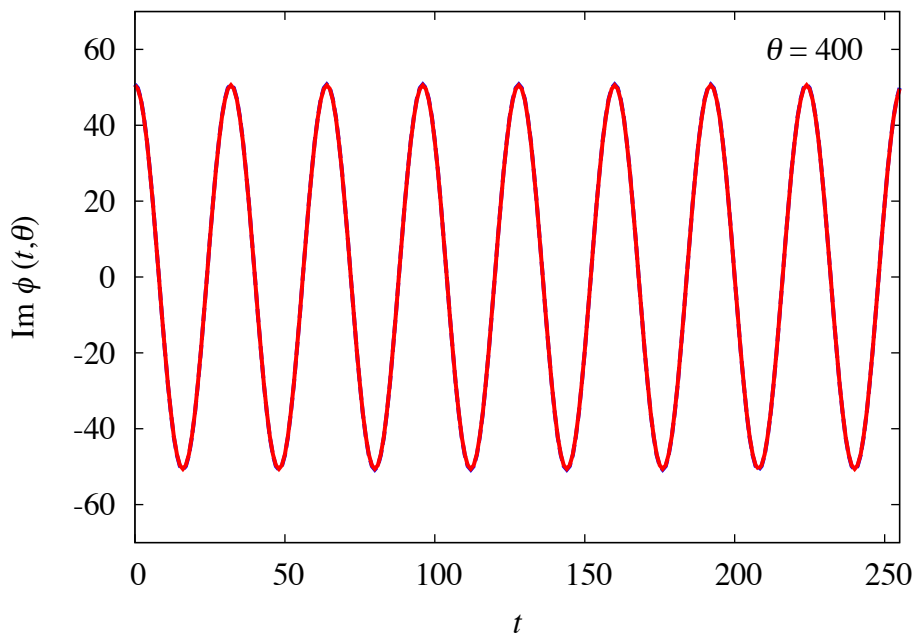

$\nu = 8$

Small deviation but no blow-up
Can be overcome with a small ε

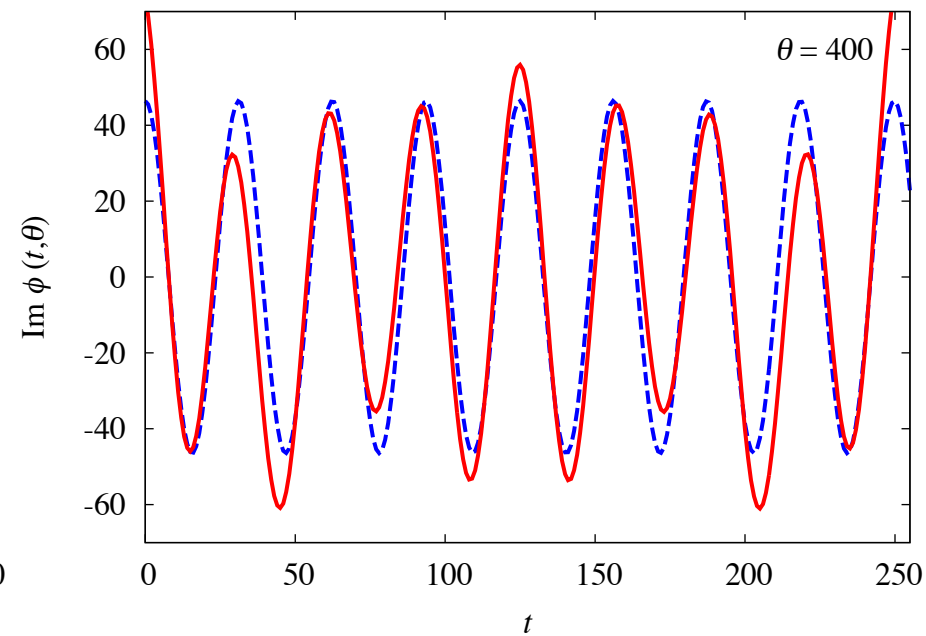

$\nu = 8.2$

Corresponds to high-T limit in the CTP

Test with Periodic B.C.

Picking up the vacuum part

$\nu = 8.2$

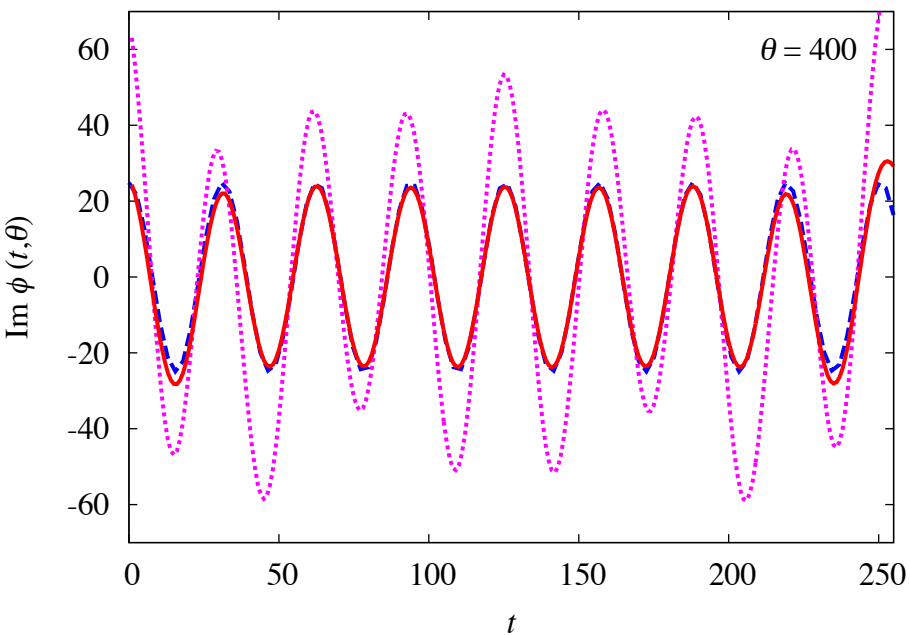

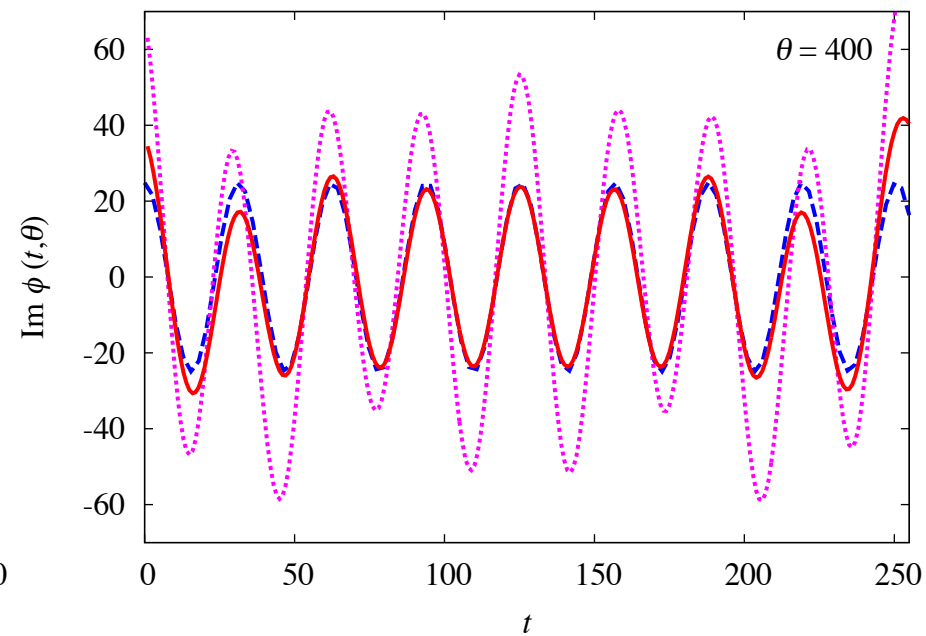

$\epsilon = 0.01$

$\epsilon\theta = 4$

θ-averaged $(\epsilon = 0)$

Our preferred prescription

$$\lim_{\theta\to\infty} \langle \mathcal{O}[\phi] \rangle_\eta = \lim_{\theta\to\infty} \overline{\langle \mathcal{O}[\phi] \rangle_{\eta,\epsilon=0}}$$ checked perturbatively

Free Propagator in Frequency Space

Expression (goal of the numerical simulation)

$$G(\omega,\theta) = N_t \frac{i}{\omega_{\min}^2(\nu^2-\mu^2)+i\epsilon}\left[1-e^{2i\omega_{\min}^2(\nu^2-\mu^2)\theta-2\epsilon\theta}\right]$$

Results with an ensemble of 1000 configurations

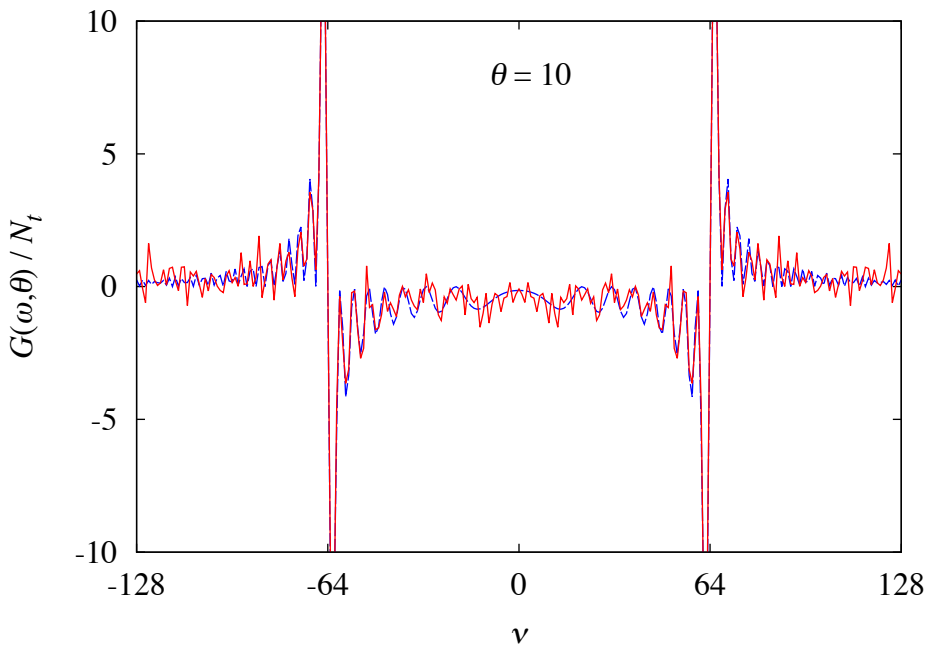

Stable simulation with very simple algorithm

Mass singularity appears soon but unphysical oscillations remain (with ε=0)

Averaged Free Propagator

- **Very fast convergence (might induce artificial contributions for composite operators)**

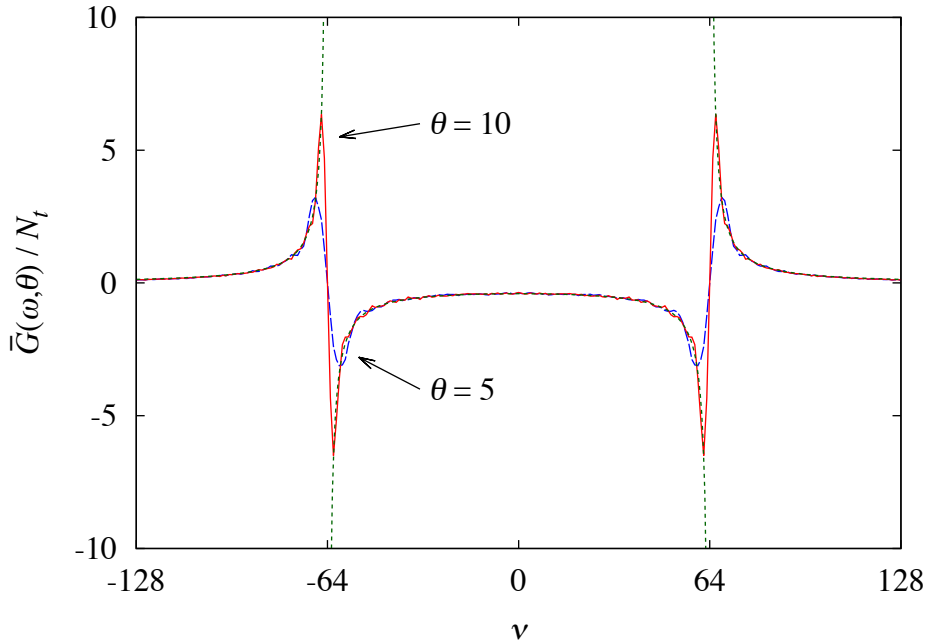

One may think that the inclusion of interaction is a piece of case once the free propagator is correctly reproduced… BUT!

So far…

- **Free propagator quickly emerges in a description in Fourier transformed bases.**

- **Inclusion of interaction => Numerical instability**
  - □ **Approximation**
    Introduce a simple truncation that is exact in the case with infinite components N.
  - □ **Implicit method**
    Change the interaction form that has the same continuum limit but leads to a better convergence.

Truncation Scheme (large N)

(Implicit method + Interaction) is often unstable
Truncation motivated from the Hartree approx.

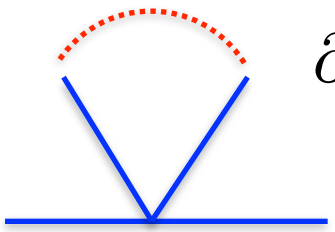

$$\partial_\theta \, \phi_\omega(\theta) = i(\omega^2 - \bar{\xi}^2 + i\epsilon) \, \phi_\omega(\theta) + \eta_\omega(\theta)$$

$$\bar{\xi}^2 = \xi^2 + \frac{3\lambda}{N_t^2} \sum_{\nu_1} \phi_{-\omega_1}(\theta) \, \phi_{\omega_1}(\theta)$$

cf. Hartree approximation

$$M^2 = \xi^2 + \frac{3\lambda}{2M}$$

Spatial momenta fixed
1D (time) integration

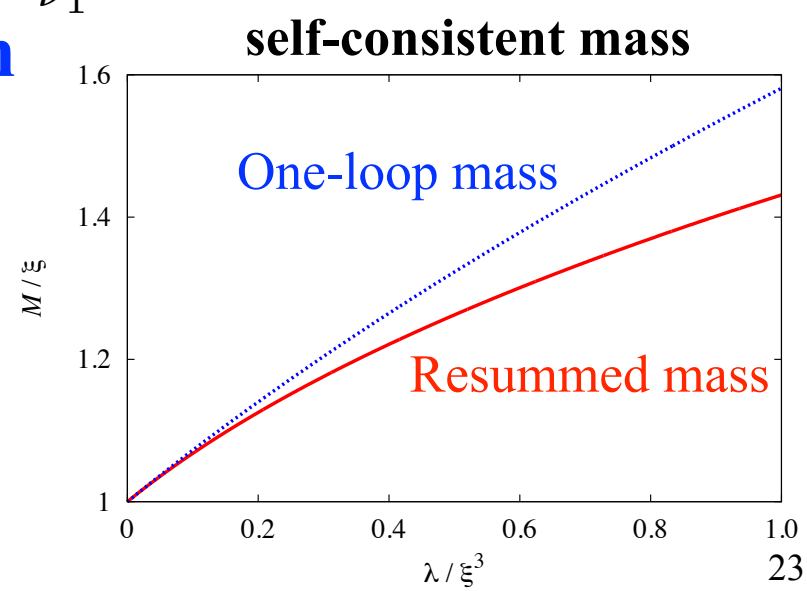

Results

Mass is replaced with the self-consistent mass that incorporates the interaction effects $\lambda = 0.5$

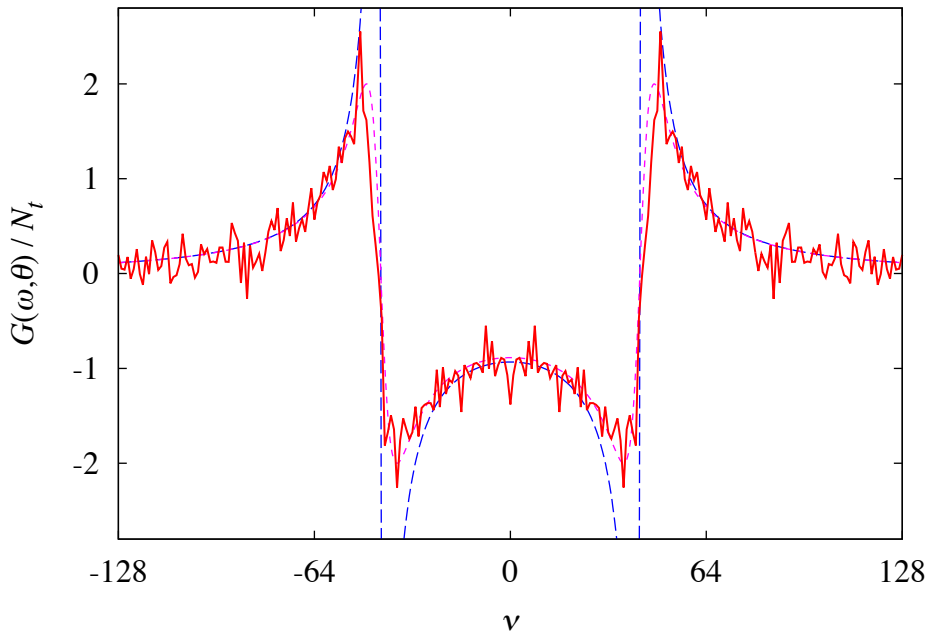

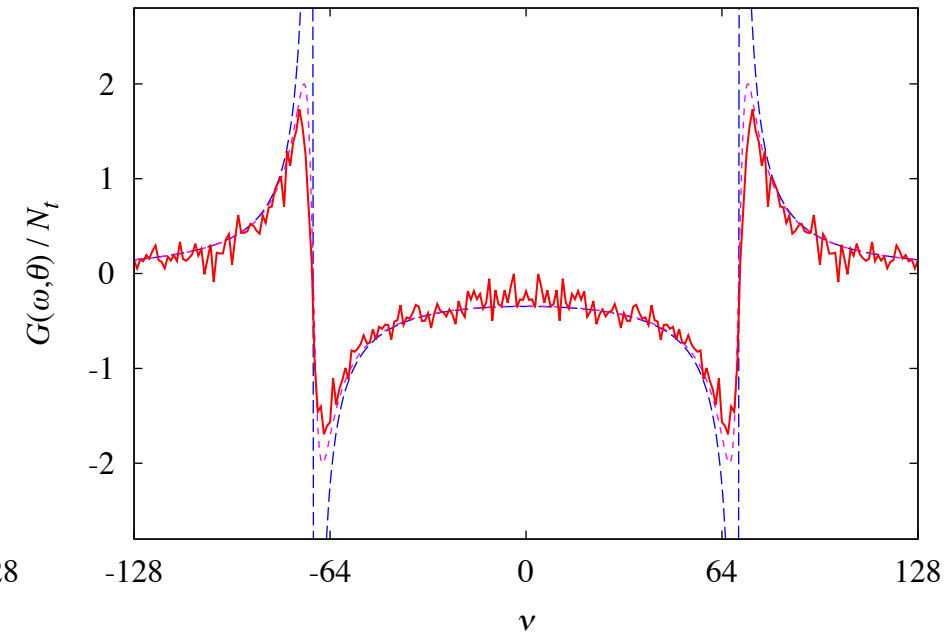

$\nu = 24 \;\rightarrow\; 42.3$ $\qquad$ $\nu = 64 \;\rightarrow\; 69.5$

Perfectly fits the resummed mass (with a width?)

Stabilizing the full interaction

Interaction part

$$\phi(\theta + \Delta\theta) \sim \phi(\theta) - i\lambda\phi(\theta)^3\Delta\theta$$

Could become large (harmful)

"Resummed" form

$$\frac{\phi(\theta)}{\sqrt{1 + 2i\lambda\phi(\theta)^2\Delta\theta}}$$

Very stable… but…

Stabilizing the full interaction

Interaction part

$$\phi(\theta + \Delta\theta) \sim \phi(\theta) - i\lambda\phi(\theta)^3\Delta\theta$$

Could become large (harmful)

"Resummed" form

$$\frac{\phi(\theta)}{\sqrt{1 + 2i\lambda\phi(\theta)^2\Delta\theta}}$$

Very stable… but…

Results turned out to be very unphysical
We can kill numerical instabilities but cannot exclude **unphysical trajectories**.

Summary

- **Direct real-time simulation** has become possible thanks to stochastic quantization… in principle!
- There are two obstacles:
  - □ **Numerical instability** (controllable but tough)
  - □ Convergence to **wrong results** (contaminated by b.c.)
- Periodic boundary condition or the frequency space description is useful. (cf. High-precision turbulence simulation is quite often done in momentum space.)
- Hartree-type truncation is proposed and consistency with the Hartree approximation is checked.

Outlook

- Full simulation (without truncation) is ongoing.
  Results are close to those in the Hartree approximation with artificial width (?)
- Extension from 1+0D to 1+3D is in progress.
  Spontaneous symmetry breaking and pattern formation would be very interesting. Bose-Einstein cond.
- Relation to the holographic quantization.
  The stochastic diagrams look like…
  A new view point to understand the holography and the renormalization group.
- Computation of transport coefficients etc…

Isotropization, Condensation and elliptic flow in a kinetic approach with a Q_s scale

V. Greco
UNIVERSITY of CATANIA & INFN-LNS

In collaboration with:
M. Ruggieri
F. Scardina
D. Perricone
S. Plumari

Outline

- Boltzmann Kinetic Approach :
  - Motivations
  - How to fix locally η/s
  - First developments including Bose (1+f) terms

- <u>Some results for HIC</u>:
  - Elliptic flow from Color Glass Condensate (fKLN)

    going beyond ε_x and implementing also the p-space with the Qs saturation scale

  - Isotropization & Bose-Enstein Condensation

Relativistic Boltzmann-Vlasov approach

$$\left\{ p^{*\mu}\partial_\mu + \left[p^*_\nu F^{\mu\nu} + m^*\partial^\mu m^* \right] \partial^{p^*}_\mu \right\} f(x,p^*) = C[f]$$

Free streaming Field Interaction (EoS) Collisions -> $\eta \neq 0$

f(x,p) is the one-body distribution function

$$\mathcal{C}_{22} = \frac{1}{2E_1}\int \frac{d^3p_2}{(2\pi)^3 2E_2}\frac{1}{\nu}\int \frac{d^3p_1'}{(2\pi)^3 2E_1'}\frac{d^3p_2'}{(2\pi)^3 2E_2'} f_1' f_2' |\mathcal{M}_{1'2'\to 12}|^2 (2\pi)^4 \delta^{(4)}(p_1' + p_2' - p_1 - p_2)$$
$$- \frac{1}{2E_1}\int \frac{d^3p_2}{(2\pi)^3 2E_2}\frac{1}{\nu}\int \frac{d^3p_1'}{(2\pi)^3 2E_1'}\frac{d^3p_2'}{(2\pi)^3 2E_2'} f_1 f_2 |\mathcal{M}_{12\to 1'2'}|^2 (2\pi)^4 \delta^{(4)}(p_1 + p_2 - p_1' - p_2')$$

- $C[f_{eq}+\delta f] \neq 0$ deviation from ideal hydro (finite λ or η/s)
- We map with C[f] the phase space evolution of a fluid at fixed η/s !

One can expand over microscopic details (2<->2 , 2<->3...), but in a hydro language this is irrelevant: *only the global dissipative effect of C[f] is important!*

Motivation for Transport approach

$$\left\{ p^{*\mu}\partial_\mu + \left[p^*_\nu F^{\mu\nu} + m^*\partial^\mu m^* \right] \partial^{p^*}_\mu \right\} f(x,p^*) = C_{2\leftrightarrow 2} + C_{2\leftrightarrow 3} + \ldots$$

Free streaming Field Interaction Collisions -> $\eta \neq 0$

- Starting from 1-body distribution function f(x,p) and not from $T_{\mu\nu}$:
  - Implement non-equilibrium implied by CGC-Qs scale (beyond ε_x)
  - Include off-equilibrium at high and intermediate p_T
  - Relevant at LHC due to large amount of minijet production
  - freeze-out self-consistently related with $\eta/s(T)$
- It's not a gradient expansion η/s:
  - valid also at high η/s -> LHC ($T \gg T_c$) or cross-over region ($T \approx T_c$)

Relativistic Boltzmann Equation

$$\left\{p^{\mu}\partial_{\mu} + m^{*}\partial^{\mu}m^{*}\partial^{p}_{\mu}\right\} f_g(x,p) = C_{2\leftrightarrow 2}$$

Free streaming Field Interaction Collisions

$f_g(x,p)$ is a one-body distribution function for fluons

$$\frac{(2\pi)^3 \Delta N_{coll}}{\Delta t \Delta^3 x \Delta^3 p} = g\frac{\Delta^3 q}{(2\pi)^3} f_g(p) f_g(q) v_{rel}\sigma_{p,q\to p-k,q+k}$$

Gain

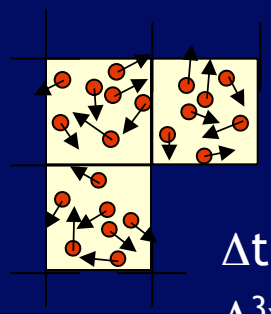

Solved discretizing the space in $(\eta, x, y)_\alpha$ cells

$\Delta t \to 0$

$\Delta^3 x \to 0$

exact solution

$$f_i = \frac{\Delta N_i}{\frac{1}{(2\pi)^3}\Delta^3 x\, \Delta^3 p_i},$$

$$P_{22} = \frac{\Delta N^{2\to 2}_{coll}}{\Delta N_1 \Delta N_2} = v_{rel}\sigma_{22}\frac{\Delta t}{\Delta^3 x}$$

$$R = \frac{1}{2} n_{tot}\langle \sigma v_{rel}\rangle = n_{tot}\frac{\beta}{8}\frac{\int_{\sqrt{s_0}}^{\infty} d\sqrt{s}\,\lambda(s)\sigma K_1(\beta\sqrt{s})}{M_a^2 M_b^2 K_2(\beta M_b)}$$

$$\lambda(s) = \left[s-(M_a+M_b)^2\right]\left[s-(M_a-M_b)^2\right]$$

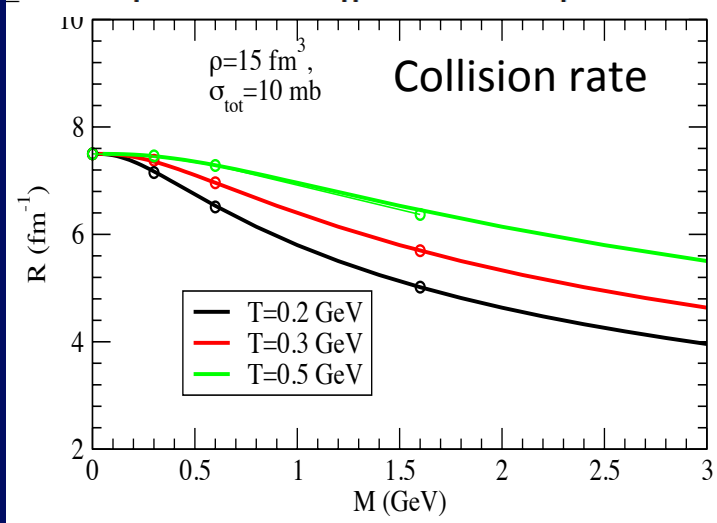

Part I – Kinetic Theory at fixed η/s

Instead of starting from *cross-sections and fields*,
we reverse the process starting from η/s

What is the relation η <-> σ, $d\sigma/d\Theta$, M, T, ρ?

- Check η with the Green-Kubo correlator

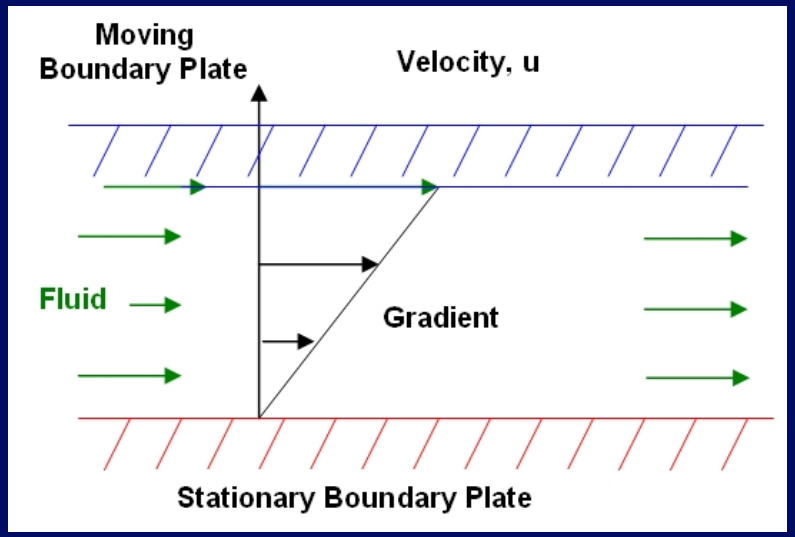

$$\frac{F}{A} = \eta \frac{\partial u}{\partial y}$$

Shear Viscosity in Box Calculation

Green-Kubo correlator

$$\eta = \frac{1}{T}\int_0^\infty dt \int_V d^3x \left\langle \Pi^{xy}(\vec{x},t)\,\Pi^{xy}(0,0)\right\rangle$$

$$\left\langle \Pi^{xy}(\vec{x},t)\Pi^{xy}(0,0)\right\rangle = \left\langle \Pi^{xy}(0,0)\Pi^{xy}(0,0)\right\rangle \cdot e^{-t/\tau}$$

microscopic details

$$\eta = \frac{V}{T}\underbrace{\left\langle \pi^{xy}(0)\,\pi^{xy}(0)\right\rangle}_{\text{macroscopic observables}} \tau$$

$$= \frac{4}{15}\frac{\varepsilon T}{V}$$

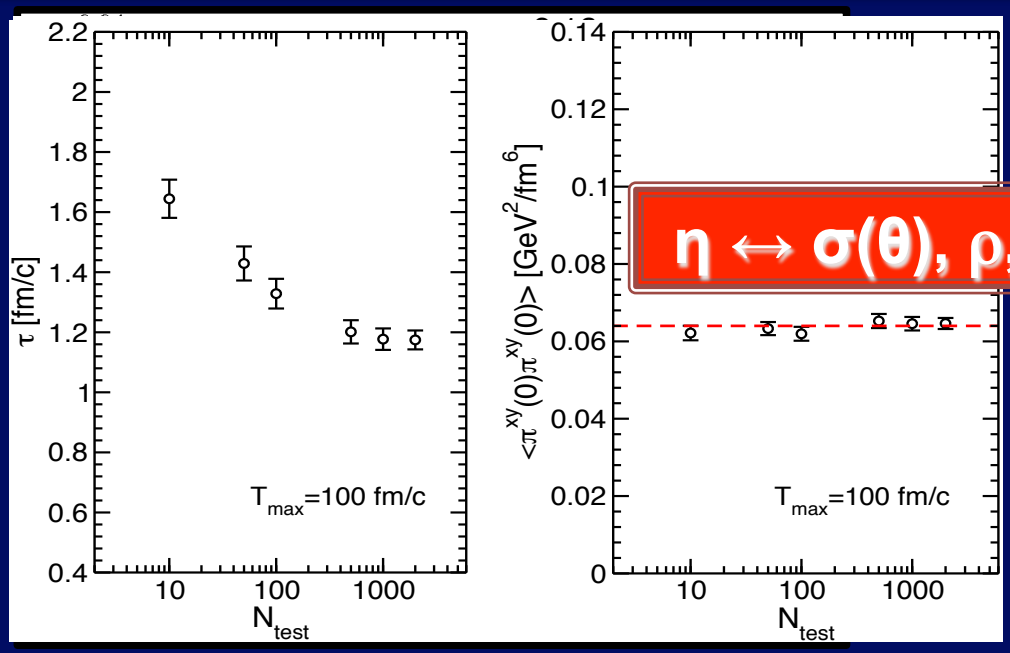

η ↔ σ(θ), ρ, M, T .... ?

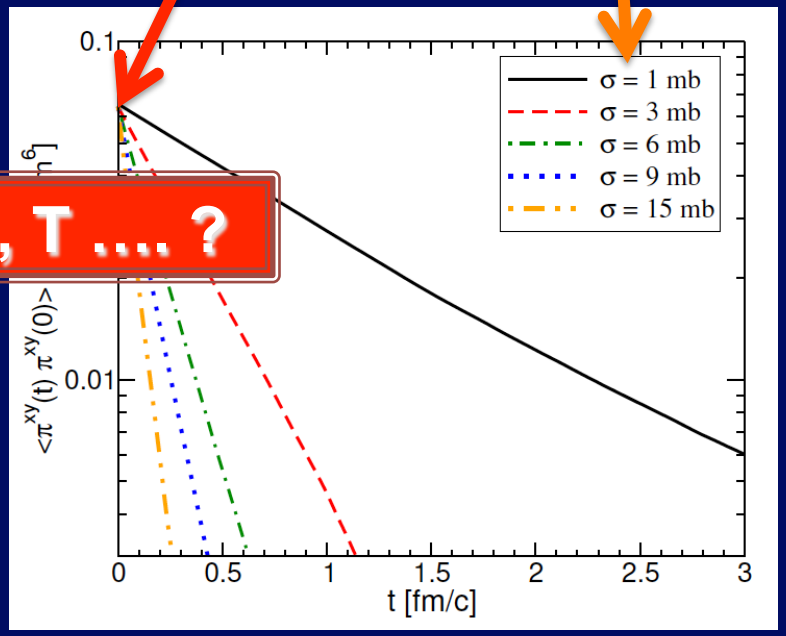

S. Plumari et al., arxiv:1208.0481;see also:
Wesp et al., Phys. Rev. C 84, 054911 (2011);
Fuini III et al. J. Phys. G38, 015004 (2011).

Needed very careful tests of convergency vs. N_{test}, Δx_{cell}, # time steps !

Simulate a fixed shear viscosity

Usually input of a transport approach are *cross-sections and fields*, but here we reverse it and start from η/s with aim of creating a more direct link to viscous hydrodynamics

Chapmann-Enskog

$$\frac{\eta}{s} = \frac{1}{15}\langle p\rangle \cdot \tau_\eta = \frac{1}{15}\frac{\langle p\rangle}{g(\frac{m_D}{T})\sigma_{TOT}\rho}$$

$$g(a) = \frac{1}{50}\int dy y^6 \left[(y^2+\frac{1}{3})K_3(2y) - yK_2(2y)\right] h\left(\frac{a^2}{y^2}\right)$$

g(a=m_D/2T) correct function that fix the relaxation time for the shear motion

$0 < g(m_D/2T) < 2/3$

forward peaked

Isotropic $m_D \to \infty$

Transport code

$$\sigma_{tot}(n(\vec{r}),T) = \frac{1}{15}\frac{\langle p_\alpha\rangle}{g(a)n_\alpha}\frac{1}{\eta/s}$$

Space-Time dependent cross section evaluated locally

G. Ferini et al., PLB670 (2009)

Chapman-Enskog agrees with Green-Kubo

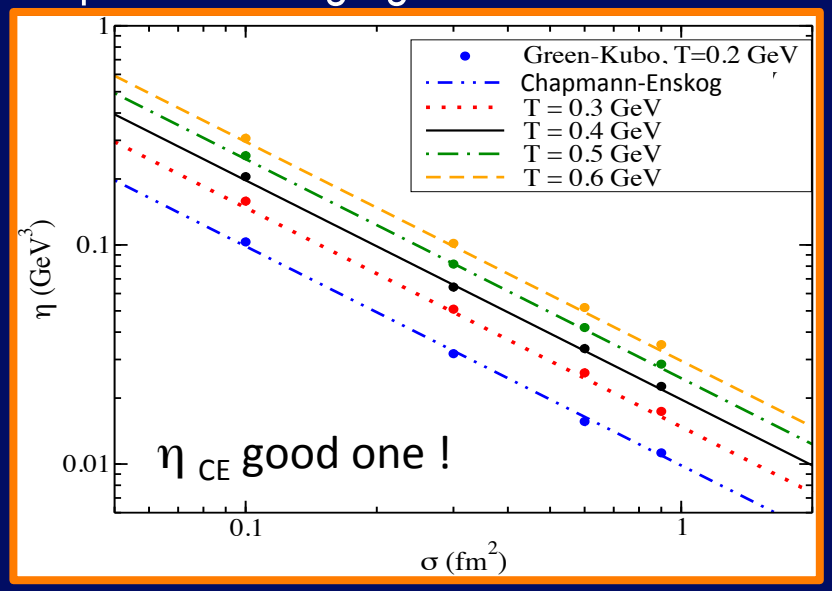

S.Plumari et al., PRC86(2012)

Transport at fixed η/s vs Viscous Hydro in 1+1D

Comparison for the relaxation of pressure anisotropy P_L/P_T

Huovinen and Molnar, PRC79(2009)

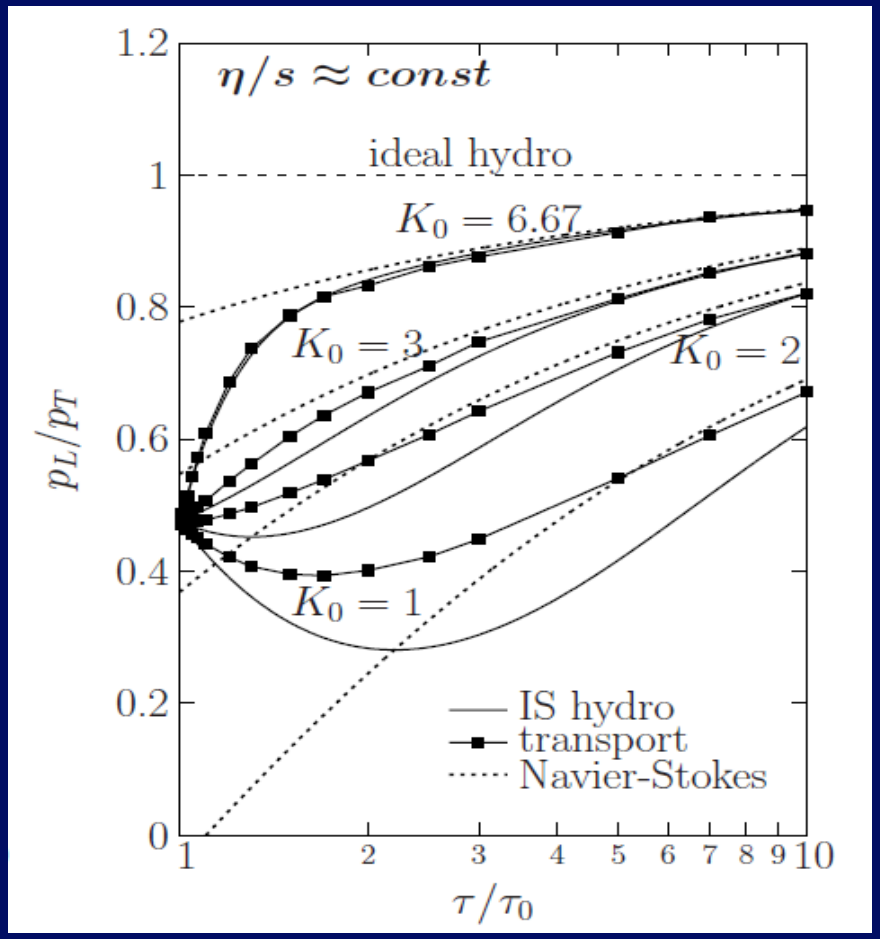

Knudsen number^{-1}

$$K = \frac{L}{\lambda} \rightarrow \frac{\tau}{\lambda}$$

Large K small η/s

$$K_0 = \frac{1}{5}\frac{T_0 \tau_0}{\eta / s}$$

$$\frac{\eta}{s} = \frac{1}{5} T \cdot \lambda$$

In the limit of small η/s (<0.16) transport converge to viscous hydro at least for the evolution p_L/p_T

Denicol et al. have studied derivation of viscous hydro from Boltzmann kinetic theory: PRD85 (2012) 114047

Similar results from BAMPS-Frankfurt

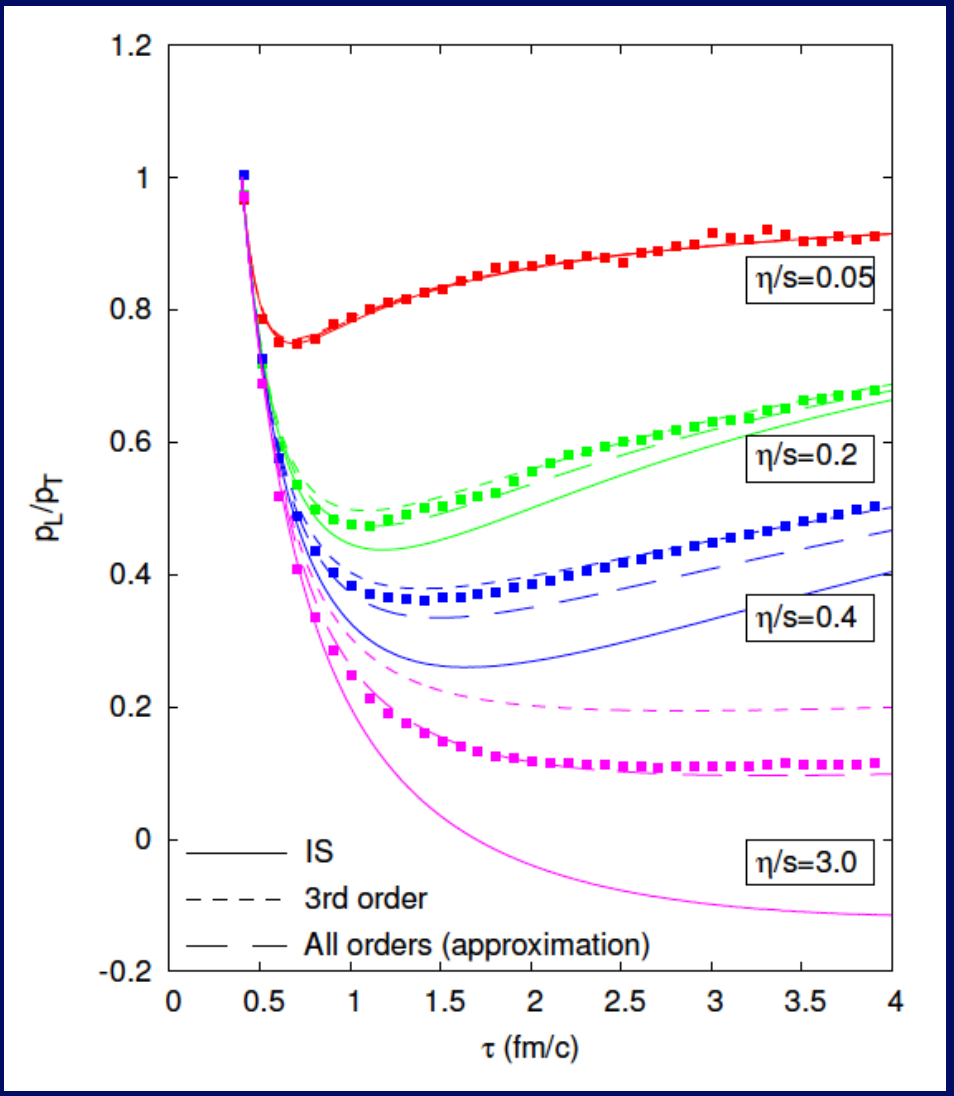

- Convergency for small η/s of Boltzmann transport at fixed η/s with viscous hydro

- Better agreement with 3rd order viscous hydro for large η/s

El, Xu, Greiner, Phys.Rev. C81 (2010) 041901

Test in 3+1D: v_2/ε response for almost ideal case

EoS $c_s^2=1/3$ (dN/dy tuned to RHIC)

Integrated v_2 vs time

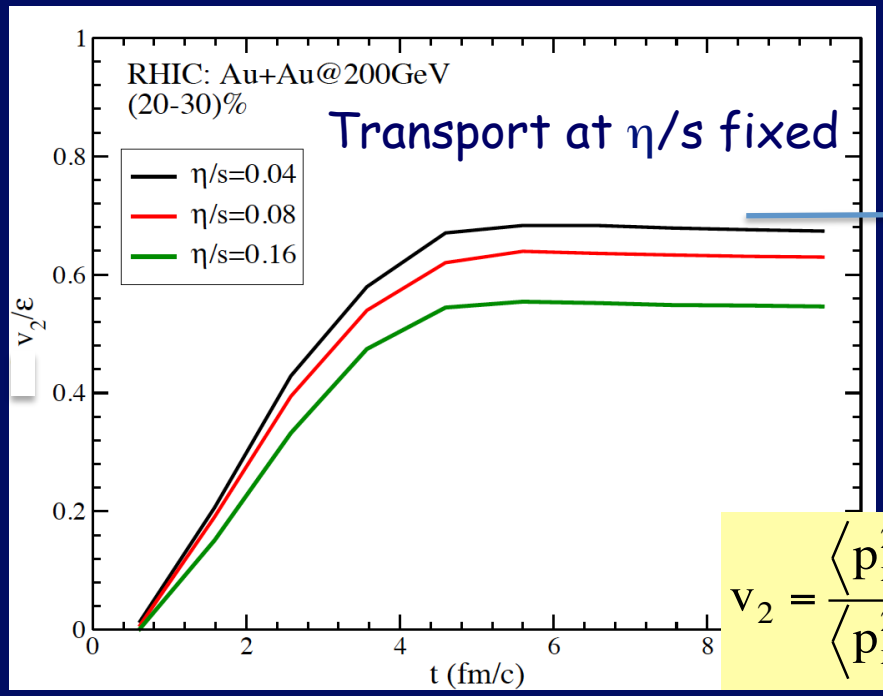

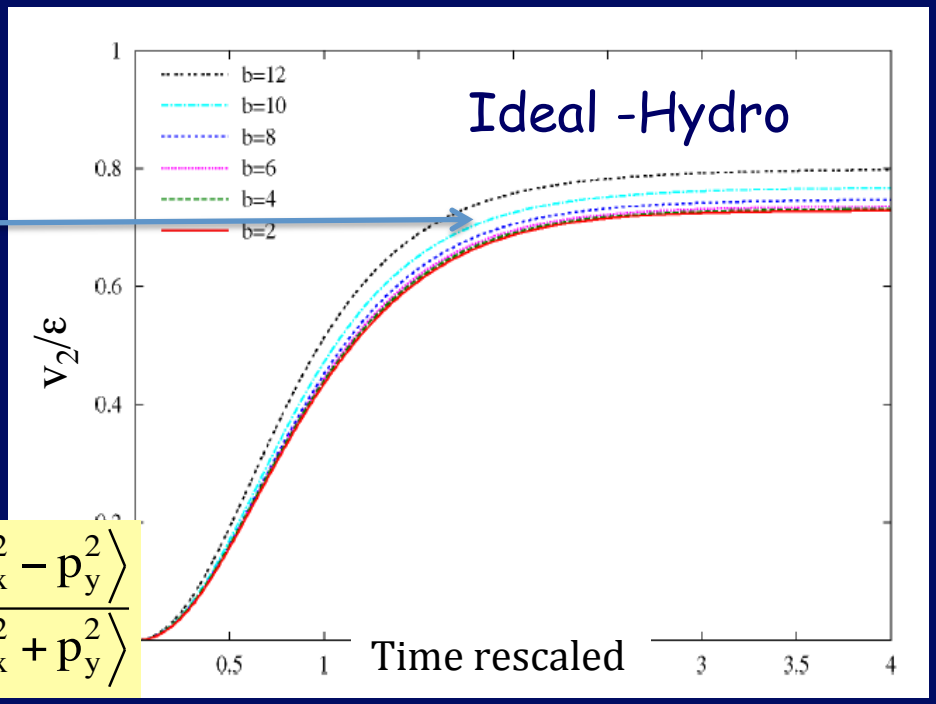

$$v_2 = \frac{\langle p_x^2 - p_y^2 \rangle}{\langle p_x^2 + p_y^2 \rangle}$$

Bhalerao et al., PLB627(2005)

In the bulk the transport has an hydro v_2/ε_2 response!

Part II - Transport at fixed η/s with Q_s saturation scale

What is the impact of non-equilibrium Color Glass condensate initial state?

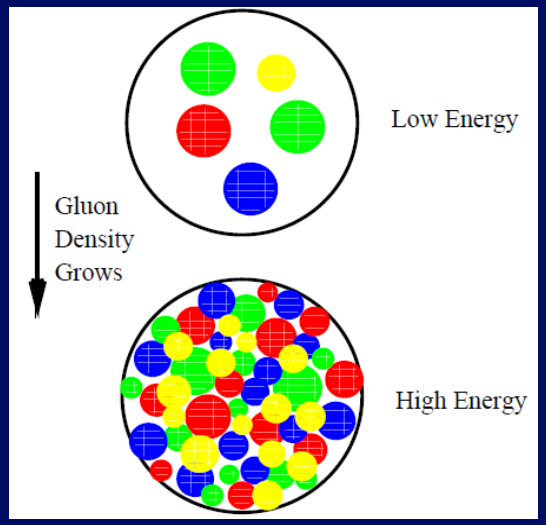

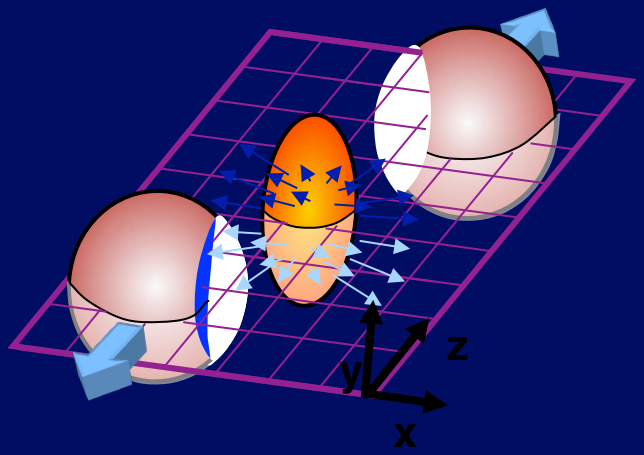

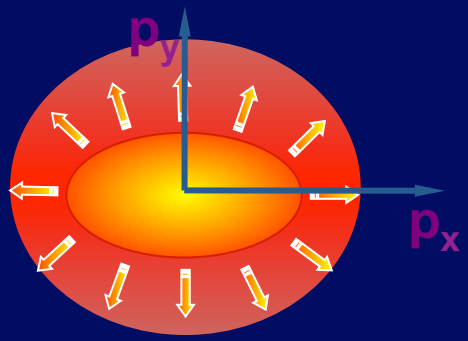

Cross section and freeze-out

Freeze-out is a smooth process: scattering rate < expansion rate

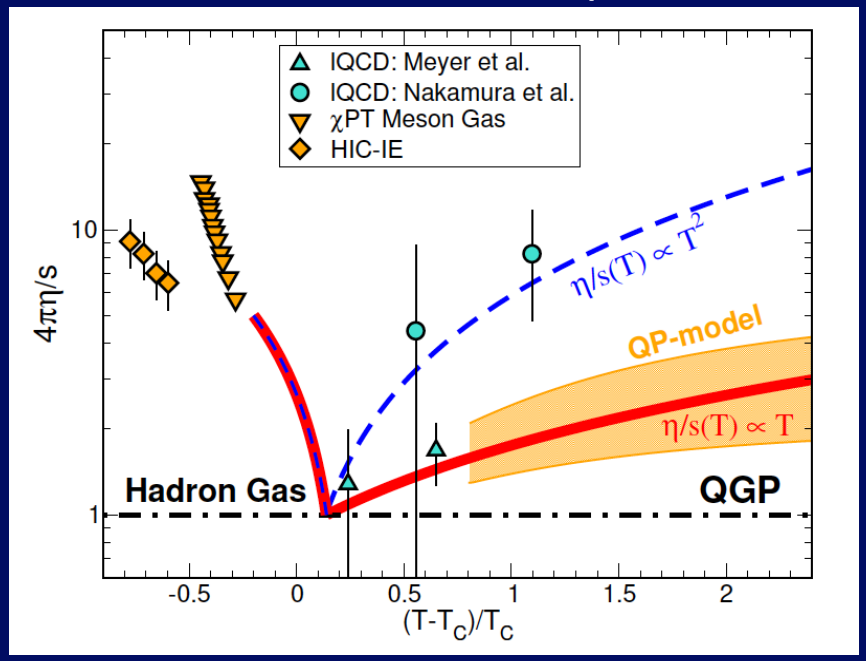

- ✓ η/s increases in the cross-over region, realizing a smooth f.o. self-consistently dependent on h/s:
- ✓ Different from hydro that is a sudden cut of expansion at some $T_{f.o.}$

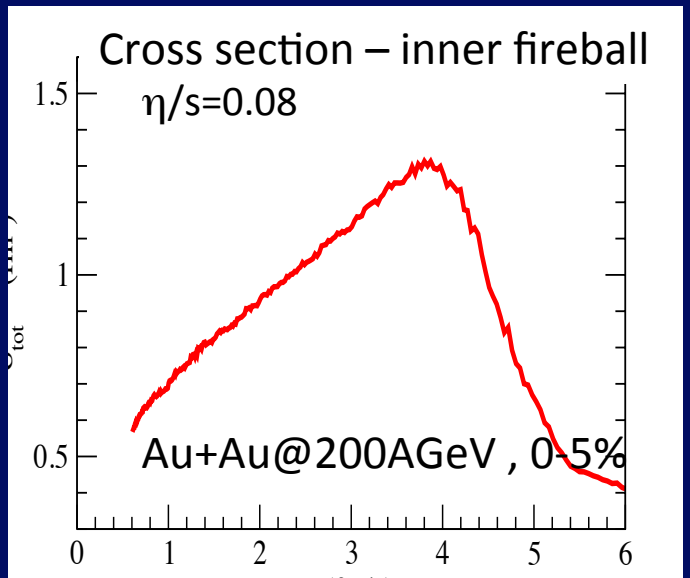

$$\sigma^* = g(a)\sigma_{tot} \approx \frac{1}{15}\frac{\bar{p}}{\rho}\frac{1}{\eta/s}$$

$\rho(\tau_0)$=23 fm^{-3}, η/s=0.08 → σ_{ToT}= 6 mb

$$\sigma_{pQCD} = \frac{9\pi\alpha_s^2}{m_D^2} \quad , \quad \alpha_s = \frac{4\pi}{11 ln\left(\frac{2\pi T}{\Lambda}\right)} \quad , \quad m_D^2 = 4\pi\alpha_s(T)T$$

T_0=340 MeV → σ_{pQCD}= 3.6 mb

fKLN realization of CGC

Factorization hypothesis: convolution of parton distribution functions in the parent nucleus.

Unintegrated distribution functions (uGDFs)

$$\frac{dN_g}{d^2x_\perp dy} \propto \int \frac{d^2p_T}{p_T^2} \int_0^{p_T} d^2k_T \alpha_s(Q^2) \times \phi_A\left(x_A, \frac{(p_T+k_T)^2}{4}; \boldsymbol{x}_\perp\right) \times \phi_B\left(x_B, \frac{(p_T-k_T)^2}{4}; \boldsymbol{x}_\perp\right)$$

$$\phi_A(x_1, k_T^2; \boldsymbol{x}_\perp) = \frac{\kappa Q_s^2}{\alpha_s(Q_s^2)}\left[\frac{\theta(Q_s-k_T)}{Q_s^2+\Lambda^2} + \frac{\theta(k_T-Q_s)}{k_T^2+\Lambda^2}\right]$$

Kharzeev et al., PLB561, 93 (2003)
Nardi et al., PLB507, 121 (2001)
Drescher et al, PRC75, 034905 (2007)
Hirano et al., PRC79, 064904 (2009)
Albacete and Dumitru, arXiv:1011.5161
...

p-space

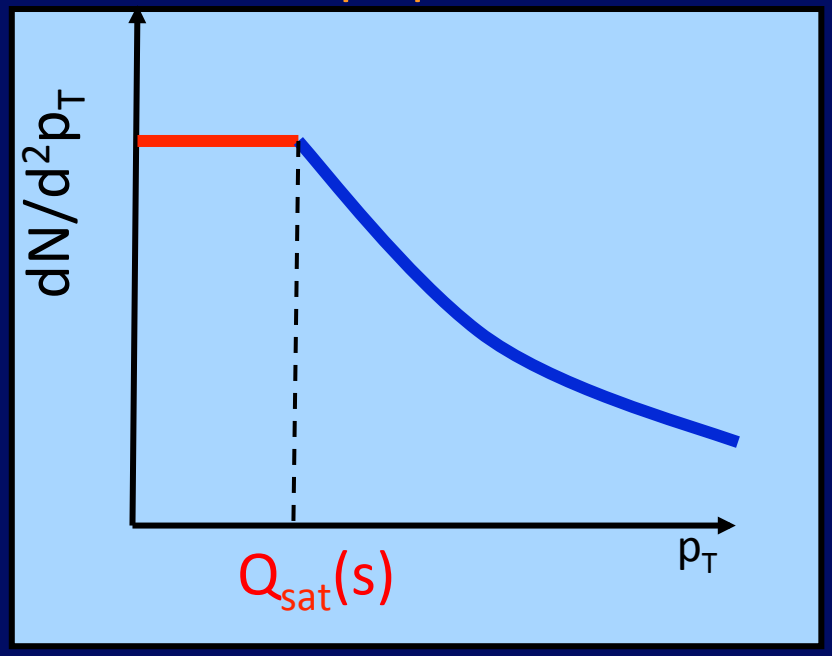

x-space

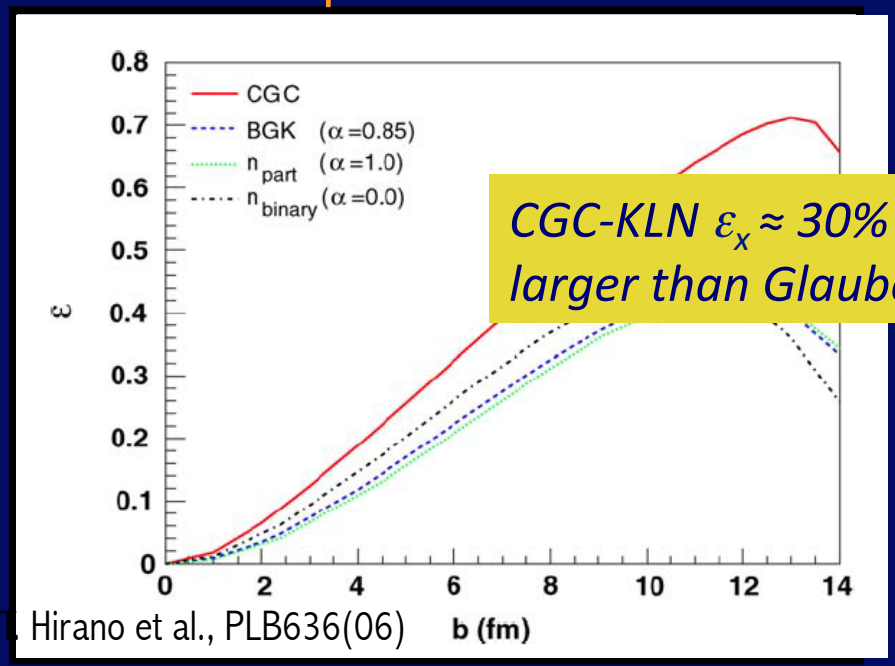

CGC-KLN $\varepsilon_x \approx 30\%$ larger than Glauber

Hirano et al., PLB636(06)

V_2 from KLN in Hydro

What does it KLN in hydro?

1) r-space from KLN (larger ε_x)

2) p-space thermal at $t_0 \approx 0.6$-0.9 fm/c - No Q_s scale , We'll call it **fKLN-Th**

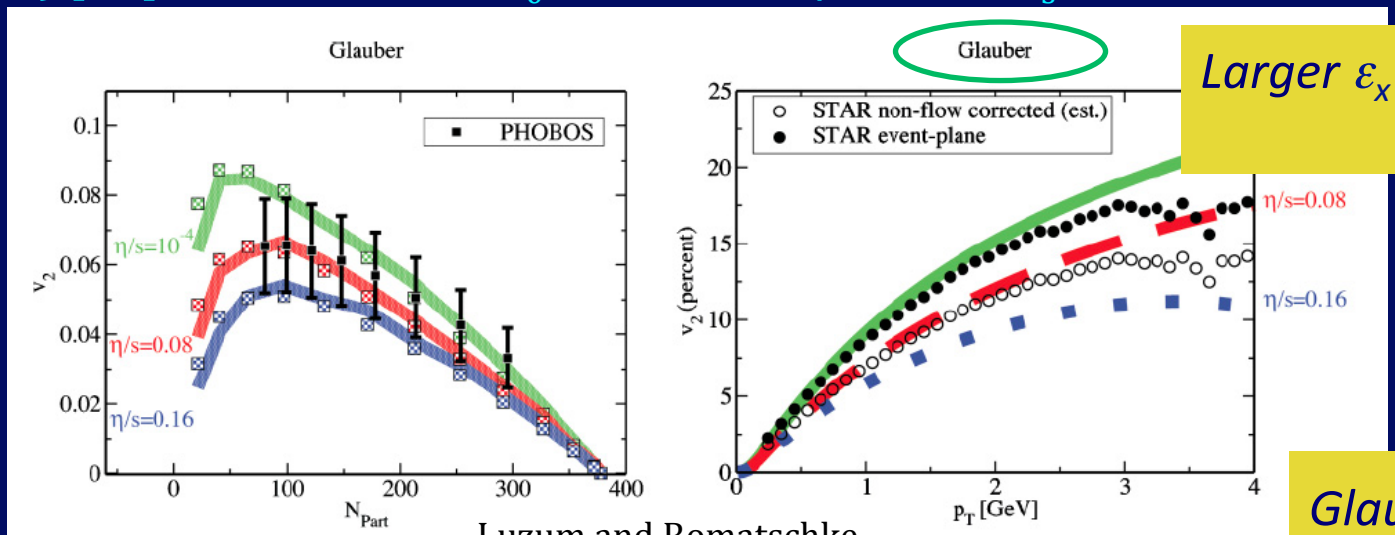

Larger ε_x - > higher η/s to get the same $v_2(p_T)$

Luzum and Romatschke
PRC78(2008) 034915

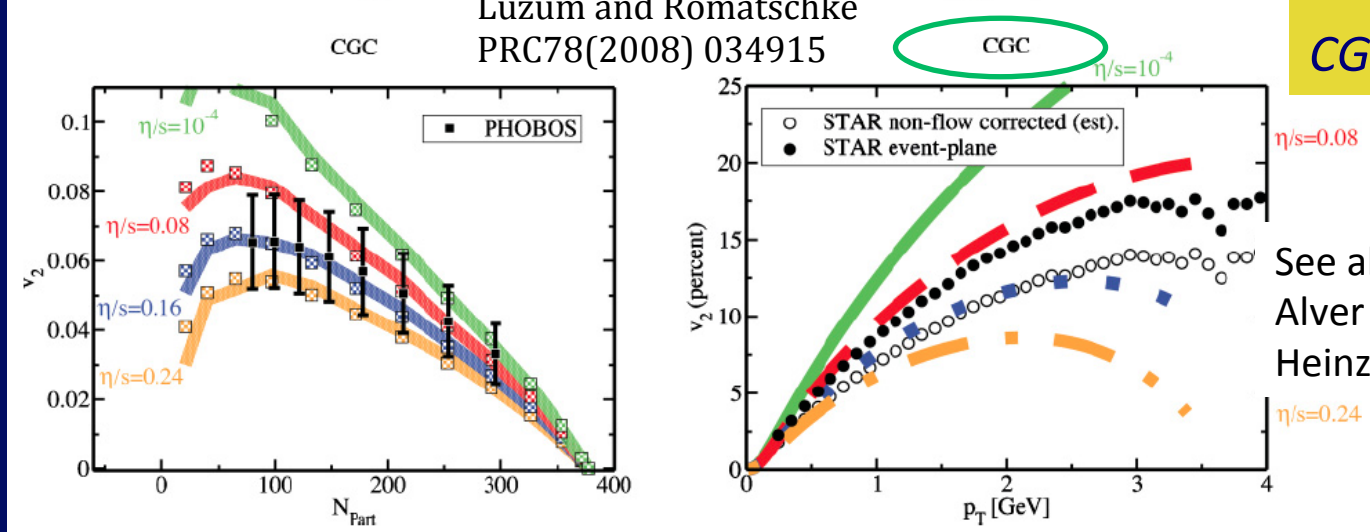

Glauber → $\eta/s = 0.08$

CGC-KLN → $\eta/s=0.16$

See also:
Alver et al., PRC 82, 034913 (2010)
Heinz *et al.*, PRC 83, 054910 (2011)

Implementing KLN p_T distribution

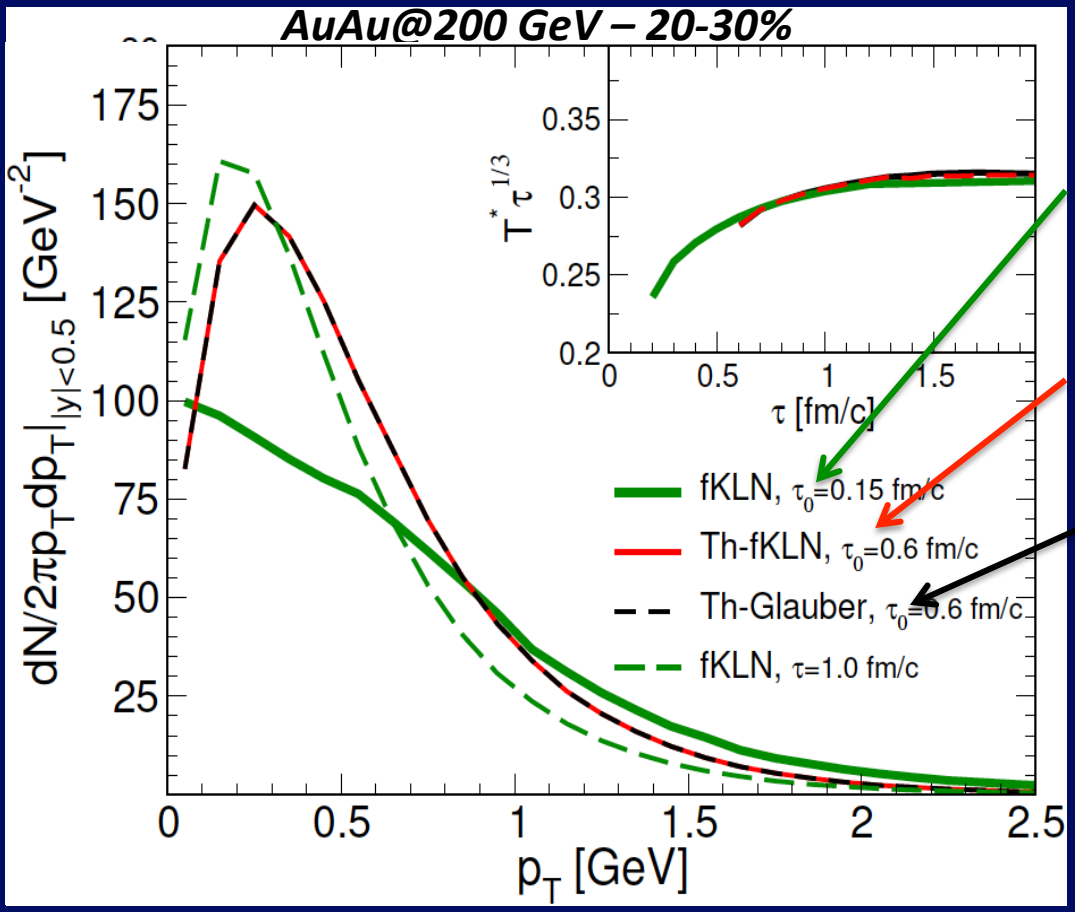

Using kinetic theory
we can implement full KLN
(x & p space) - ε_x=0.34, Qs =1.4 GeV

KLN only in x space (like in Hydro)
ε_x=0.341, Qs=0 -> Th-KLN

Glauber in x & thermal in p
ε_x=0.289 , Qs=0 -> Th-Glauber

M. Ruggieri *et al.*, Phys.Lett. B727 (2013) 177

Thermalization in less than 1 fm/c, in agreement with Greiner *et al.*, NPA**806**, 287 (2008).
Not so surprising: η/s is small -> large effective scattering rate -> fast thermalization.

$$\sigma_{tot} = \frac{\langle p \rangle}{\rho\, g(a)} \frac{1}{\eta/s}$$

Temperature evolution

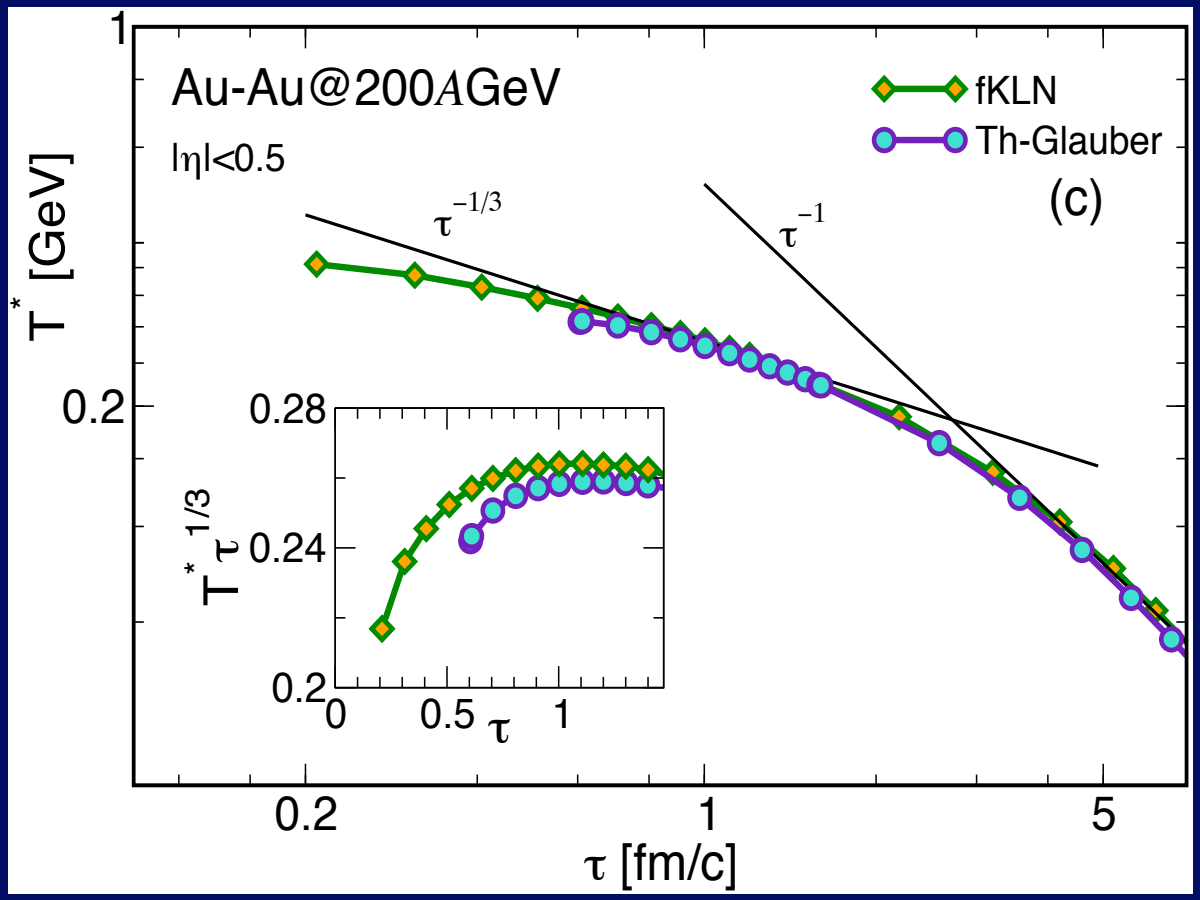

$$T \propto \tau^{-\delta}$$

$\delta = P_L/\varepsilon$ – 1D boost invariance

$\delta = 1/3$ - 1D ideal expansion

$\delta = 1$ - 3D expansion

$T^* = E/N$, in the local rest frame

Longitudinal and transverse pressure

t=1/Qs≈0.1-0.2 fm/c
-> $P_L/P_T > 0$
Gelis & Epelbaum
arXiV:1307.2214

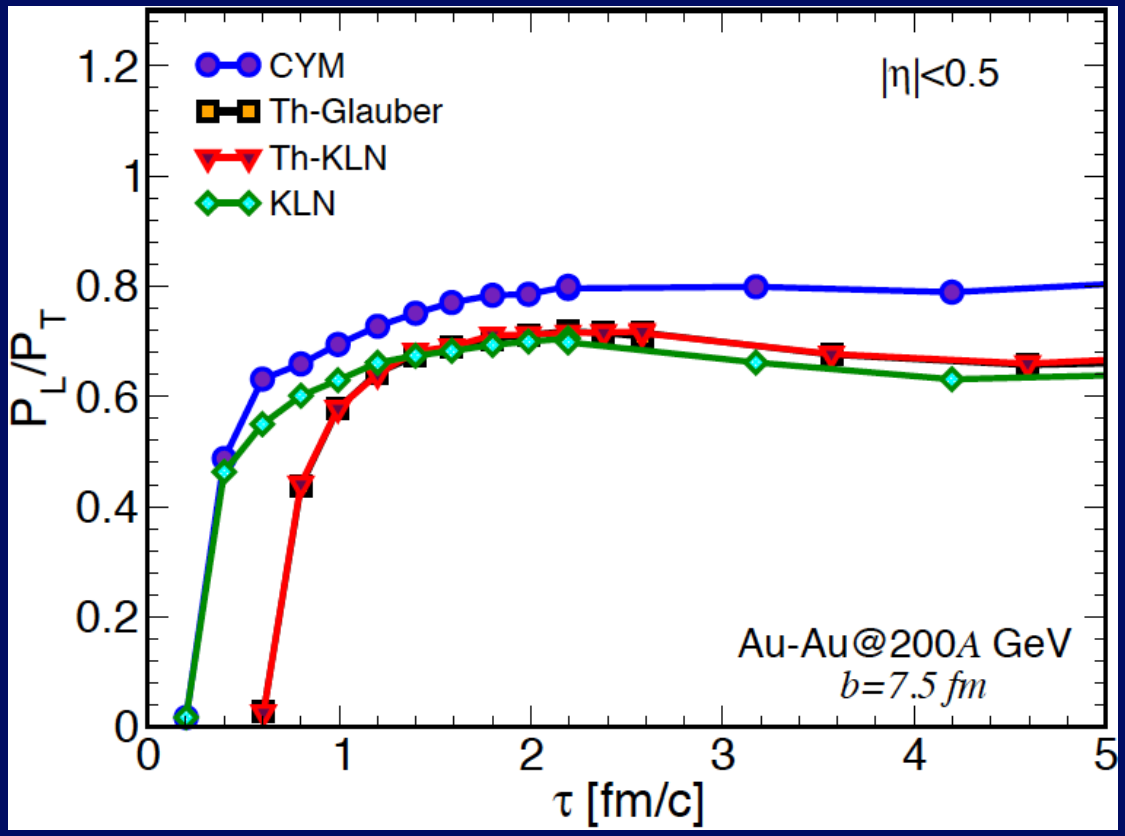

CYM (IP-Glasma)
Courtesy of B. Schenke
& R. Venugopalan

- ✧ P_L/P_T show also a very fast equilibration ($\Delta\tau_{isotr}$≈0.5 fm/c)!
- ✧ However it is not this that makes a difference for v_2:
  isotropization time quite similar for all the cases

Longitudinal and transverse pressure

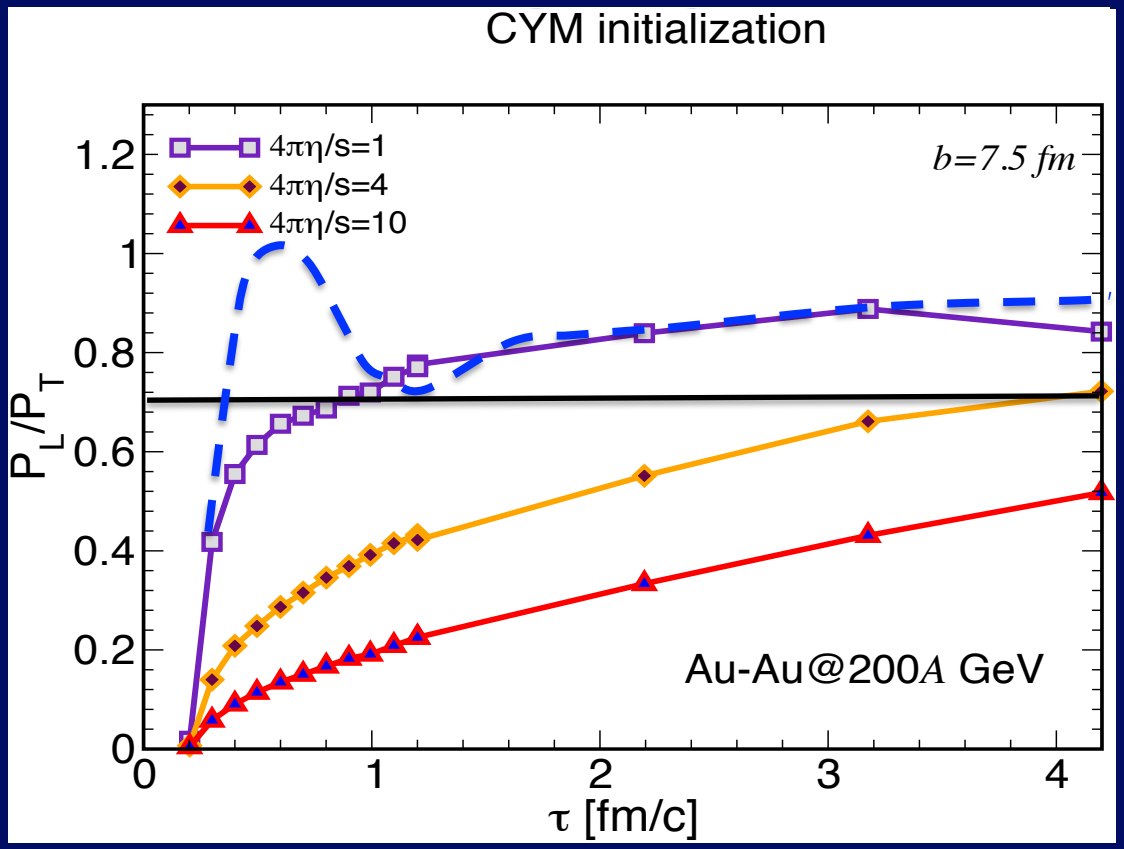

70% level of isotropization

- ✧ For $\eta/s > 0.3$ one misses fast isotropization in P_L/P_T ($\tau \geq$ 2-3 fm/c)
- ✧ For $\eta/s \approx$ pQCD no isotropization
- ✧ Semi-quantitative agreement with Florkowski et al., PRD88 (2013) 034028

  our is 3+1D not in relax.time but full integral but *no gauge field*

Results with kinetic theory

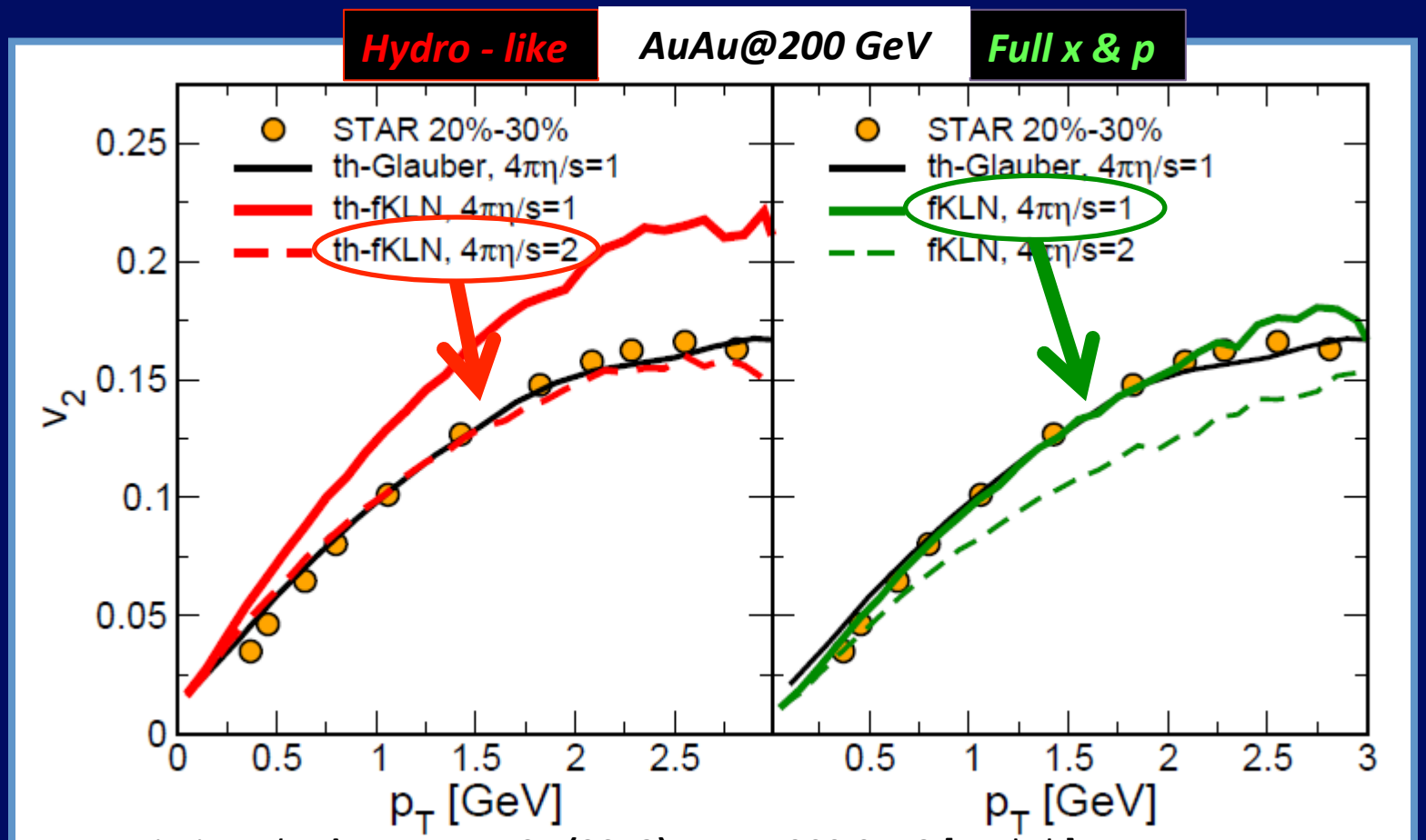

M. Ruggieri *et al.*, **Phys.Lett. B727 (2013) 177** - 1303.3178 [nucl-th]

- When implementing KLN and Glauber like in Hydro we get the same of Hydro
- When implementing full KLN we get close to the data with $4\pi\eta/s = 1$:
  larger ε_x compensated by Q_s saturation scale (non-equilibrium distribution)

What is going on?

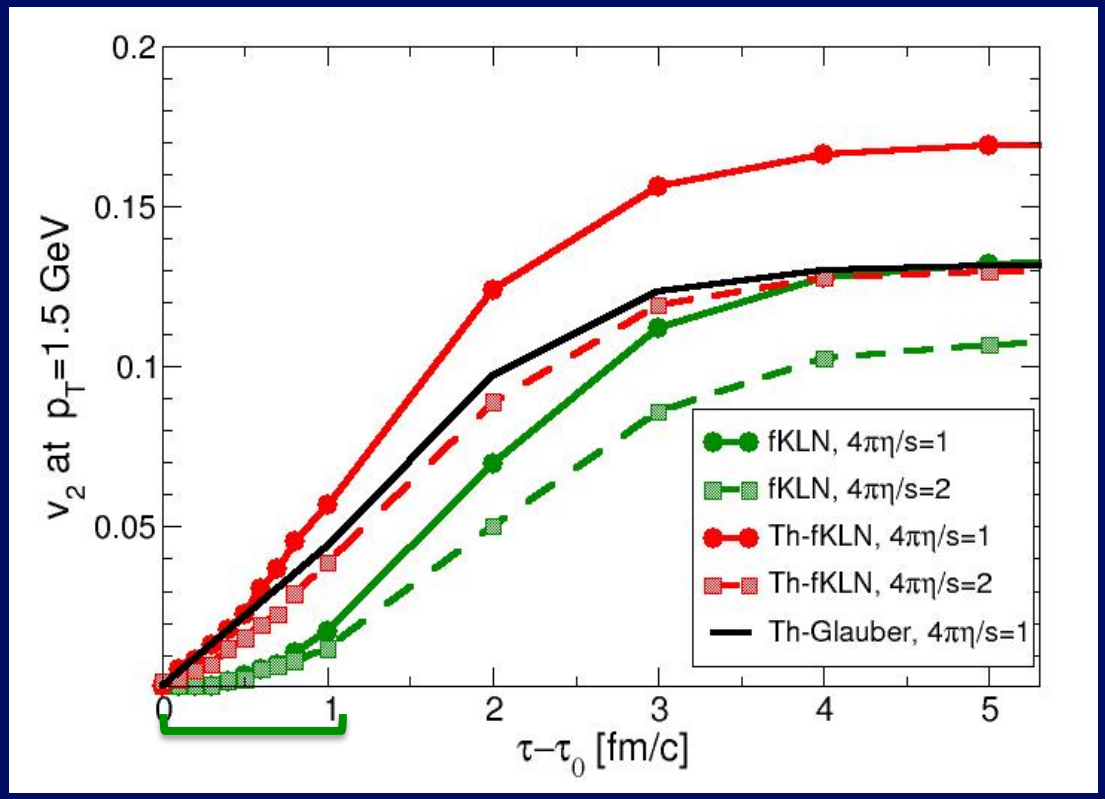

❖ We clearly see that when non-equilibrium distribution is implemented in the initial stage (≤ 1 fm/c) v_2 grows slowly respect to thermal one

❖ Deformation of p_T distribution -> affects $v_2(p_T)$

Evolution with Centrality

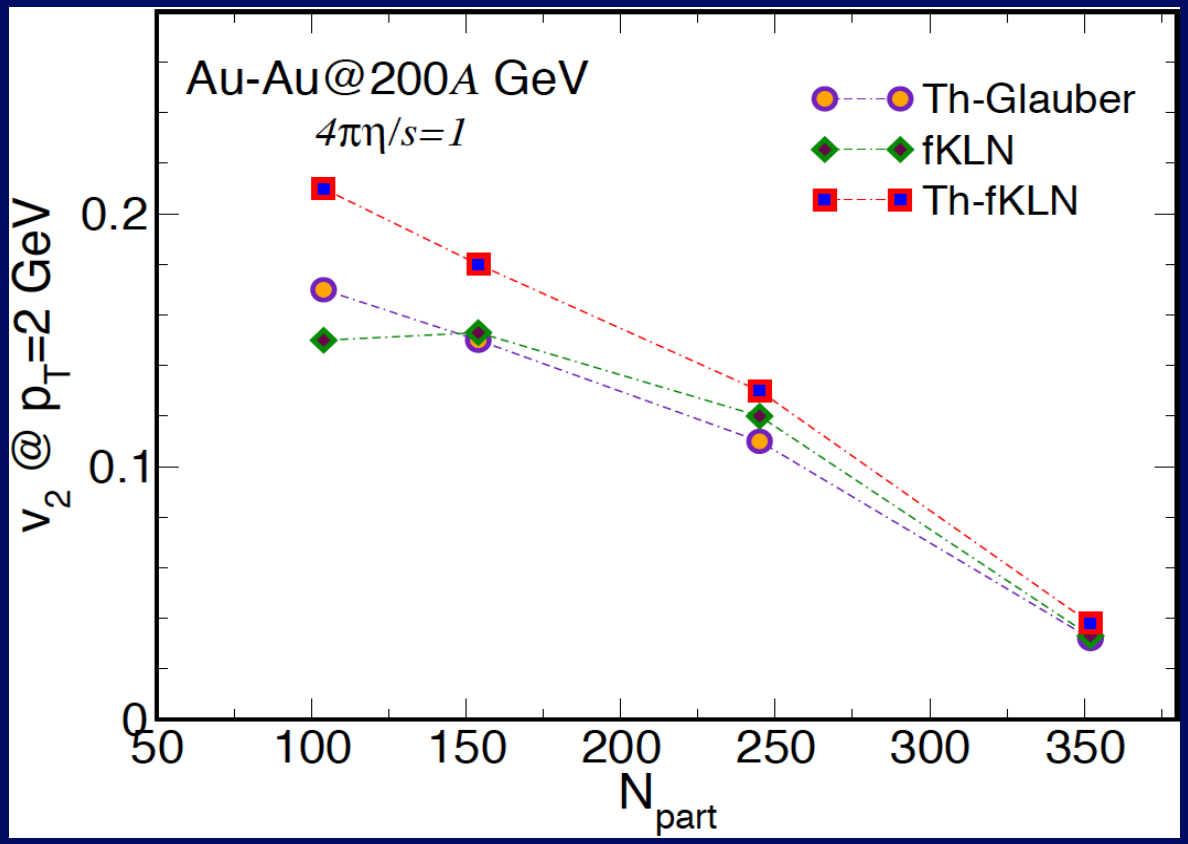

- The difference fKLN , Th-fKLN and Th-Glauber disappears at central collisions (like in hydro for Th-fKLN and Th-Glauber)
- In peripheral collisions fKLN would even be lower than Th-Glauber due to non-equilibrium impact

Higher η/s for Th-KLN leads to small v_3

Adare *et al.*, [PHENIX Collaboration], PRL **107**, 252301 (2011)

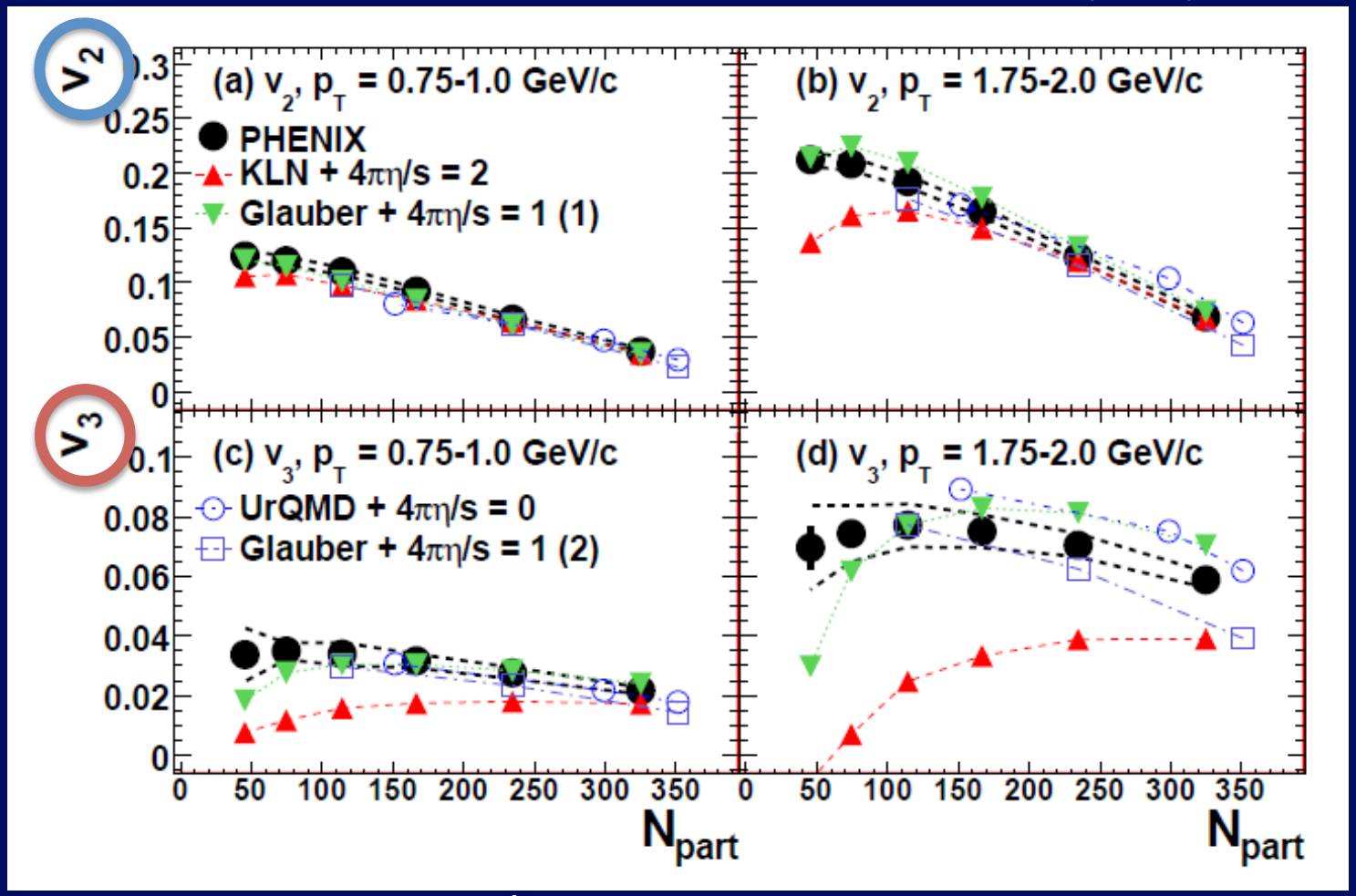

The value of η/s affects more higher harmonics!

Can we discard KLN or CGC?!

Well at least before one should implement <u>both x and p space</u>

Neglecting non-equilibrium in p-space

Classic Yang-Mills approach to gluon saturation

able to describe all v_n

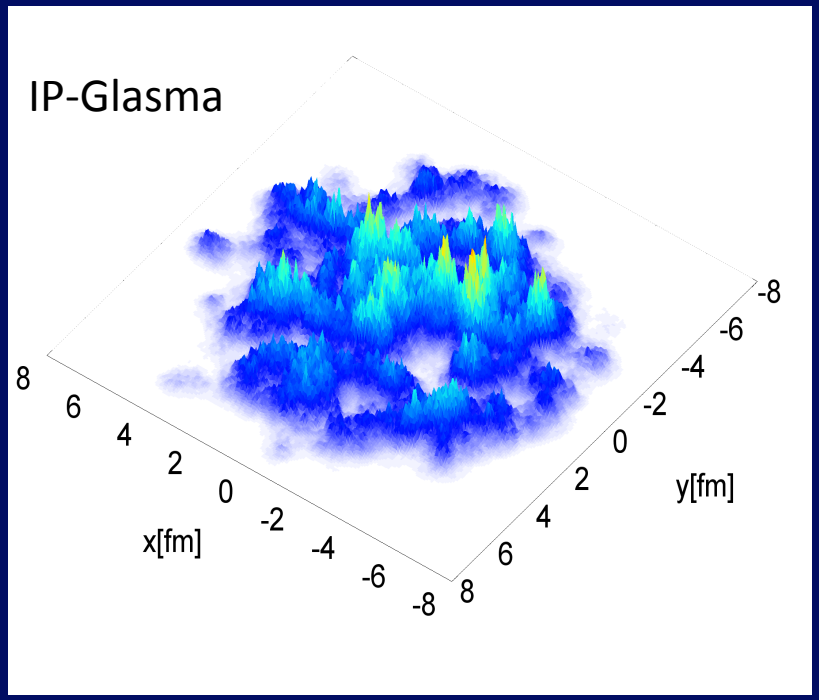

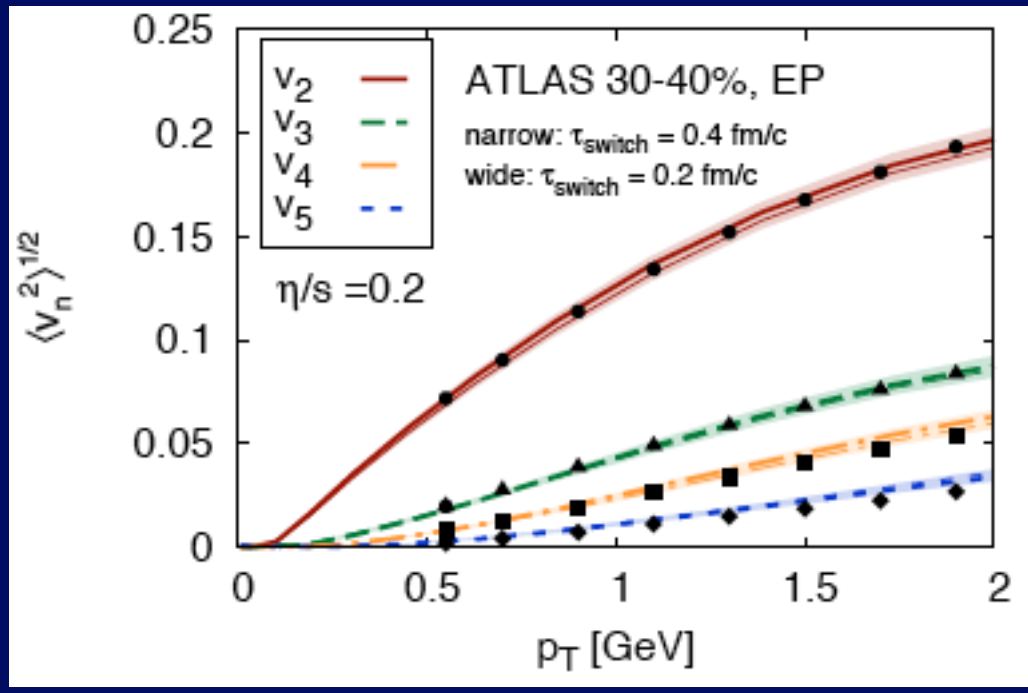

C. Gale et al., PRL111(2013)

KLN vs Classic Yang-Mills

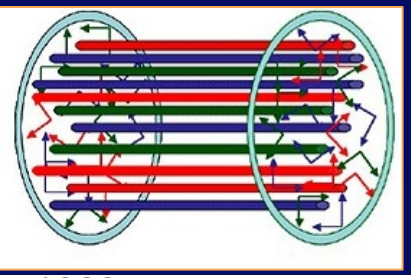

$$[D_\mu, F^{\mu\nu}] = J^\nu$$

Factorization of parton distr. funct not valid in AA -> Classic field approach

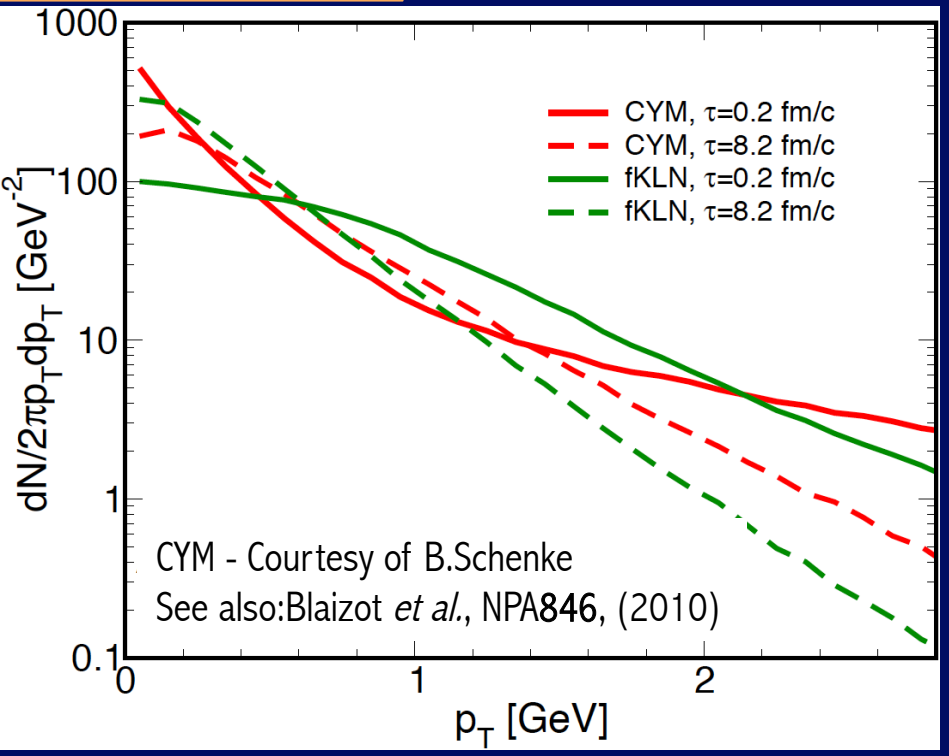

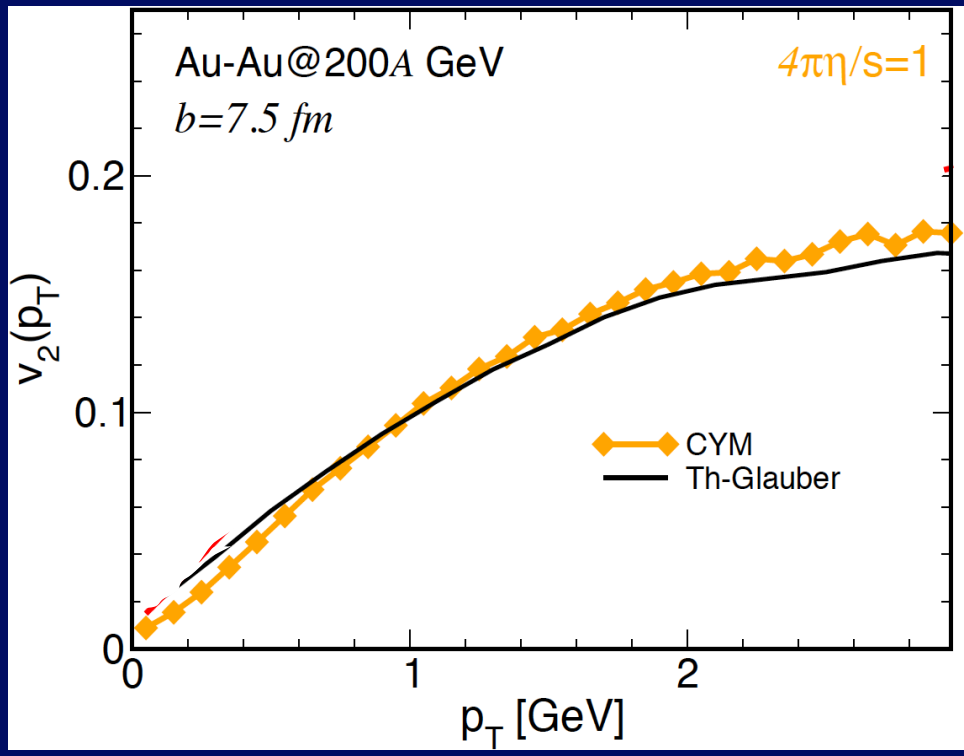

The effect nearly disappears but indeed there is <u>nearly No saturation!</u>

The slope is the opposite of KLN

Saturation -> Overpopulation -> Condensation?

In all of this the quantum nature of gluon has been ignored
In the regime of a Color Glass Condensate f ≈ $1/\alpha_s$ >1
The fixed point is not a Boltzmann distribution
but a Bose -Einstein

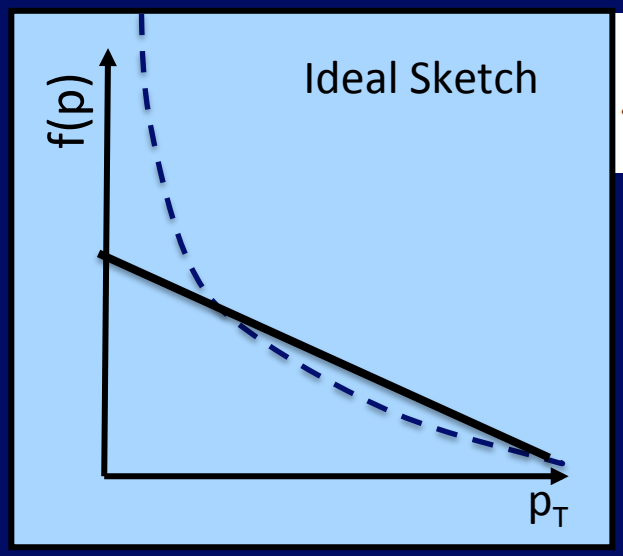

$$f_{eq}(p) = \frac{1}{e^{(p-\mu)/T} - 1},$$

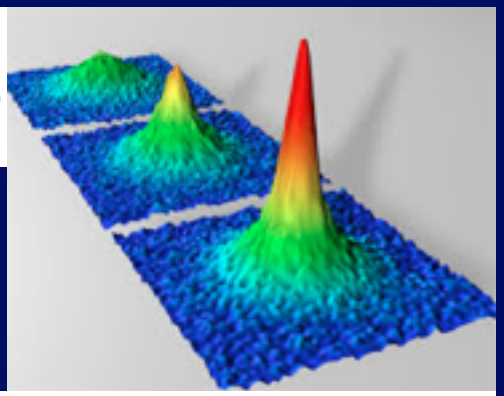

$$f_{\rm eq}(\boldsymbol{k}) = n_{\rm c}\delta(\boldsymbol{k}) + \frac{1}{e^{\beta(\omega_k - m_0)} - 1}$$

Treatment of the quantum statistics for gluons neglected till recently

Over population and onset of Bose –Einstein Condensation

Argument: *JP Blaizot, J. Liao, L. McLerran NPA920(2013) 58*

Blaizot, Gelis, Liao,McLerran, Venugopalan, NPA905 (2013) 829

Talks by Bin Wu, Xu-Guang Huang Yin Jiang

CGC-like distribution naively is

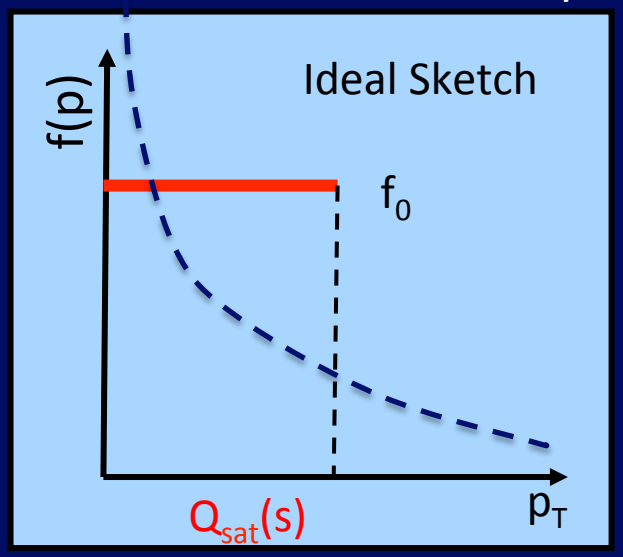

$$f(p) = f_0\,\theta(1 - p/Q_s)$$

Implies an energy density and density

$$\epsilon_0 = f_0\,\frac{Q_s^4}{8\pi^2}, \qquad n_0 = f_0\,\frac{Q_s^3}{6\pi^2}, \qquad n_0\,\epsilon_0^{-3/4} = f_0^{1/4}\,\frac{2^{5/4}}{3\,\pi^{1/2}},$$

The equilibrium value for a massless Bose Gas

$$n\,\epsilon^{-3/4}|_{SB} = \frac{30^{3/4}\,\zeta(3)}{\pi^{7/2}} \approx 0.28.$$

$$n_0\varepsilon_0^{-3/4} \geq 0.28$$

For a Theta distribution this happens for $f_0^c \approx 0.154$

For $f(p)=f_0 \exp(-p/T) \rightarrow f_c \approx 1.6$

Excess of particles accomodated by a Bose-Einstein Condensate?

Onset of Bose –Einstein Condensation

Boltzmann with Bose enhancement (1+f) -> Bose-Einstein distribution function

$$C_{22} = \frac{1}{2E_p}\int\frac{d^3q}{(2\pi)^3 2E_q}\int\frac{d^3p'}{(2\pi)^3 2E'_p}\frac{d^3q'}{(2\pi)^3 2E'_q}\left|M_{pq\to p'q'}\right|^2\Big[f(q')f(p')\big(1+f(p)\big)\big(1+f(q)\big)$$
$$-f(q)f(p)\big(1+f(p')\big)\big(1+f(q')\big)\Big](2\pi)^4\delta^4(p+q-p'-q')$$

In Small-angle Approximation → Fokker-Planck

$$\mathcal{D}_\tau f(\tau,\boldsymbol{p}) = \boldsymbol{\nabla}\cdot\left[I_a\boldsymbol{\nabla}f(\tau,\boldsymbol{p}) + \frac{\boldsymbol{p}}{p}I_b\, f(\tau,\boldsymbol{p})[1+f(\tau,\boldsymbol{p})]\right]$$

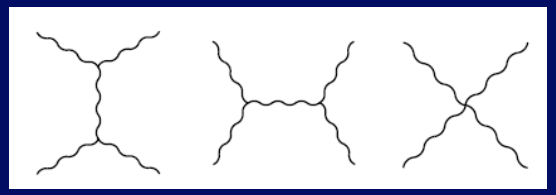

Evolution in a static Box

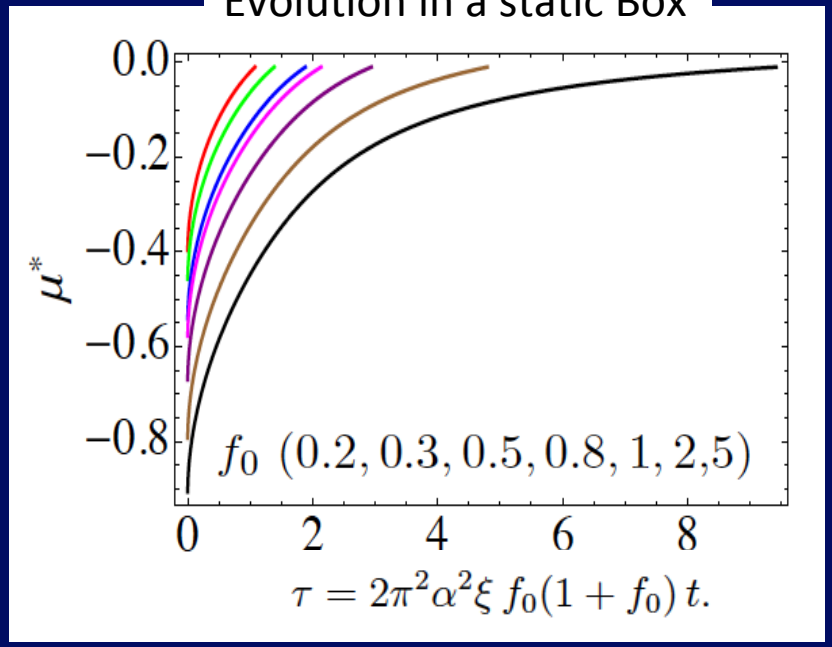

$$f_{eq}(p) = \frac{1}{e^{(p-\mu)/T}-1},$$

$$\mu^* = T^*\, ln\left(1+\frac{1}{f(0)}\right) \xrightarrow{\text{equilibrium}} \mu$$

Onset of BEC for $f_0 > 0.16$

JP Blaizot, J. Liao, L. McLerran NPA920(2013) 58

Solving Relativistic-Boltzmann with (1+f) factor

No small angle or mometum transfer pproximantion

$$C_{22} = \frac{1}{2E_p}\int\frac{d^3q}{(2\pi)^3 2E_q}\int\frac{d^3p'}{(2\pi)^3 2E'_p}\frac{d^3q'}{(2\pi)^3 2E'_q}\left|M_{pq\to p'q'}\right|^2\left[f(q')f(p')\left(1+f(p)\right)\left(1+f(q)\right)\right.$$
$$\left.-f(q)f(p)\left(1+f(p')\right)\left(1+f(q')\right)\right](2\pi)^4\delta^4(p+q-p'-q')$$

$$P_{22} = \frac{\Delta N_{coll}^{2\leftrightarrow 2}}{\Delta N_1 \Delta N_2} = \frac{\Delta t}{\Delta^3 x} v_{rel}\sigma_{p,q\to p',q'}\left[1+f(p')\right]\left[1+f(q')\right]$$

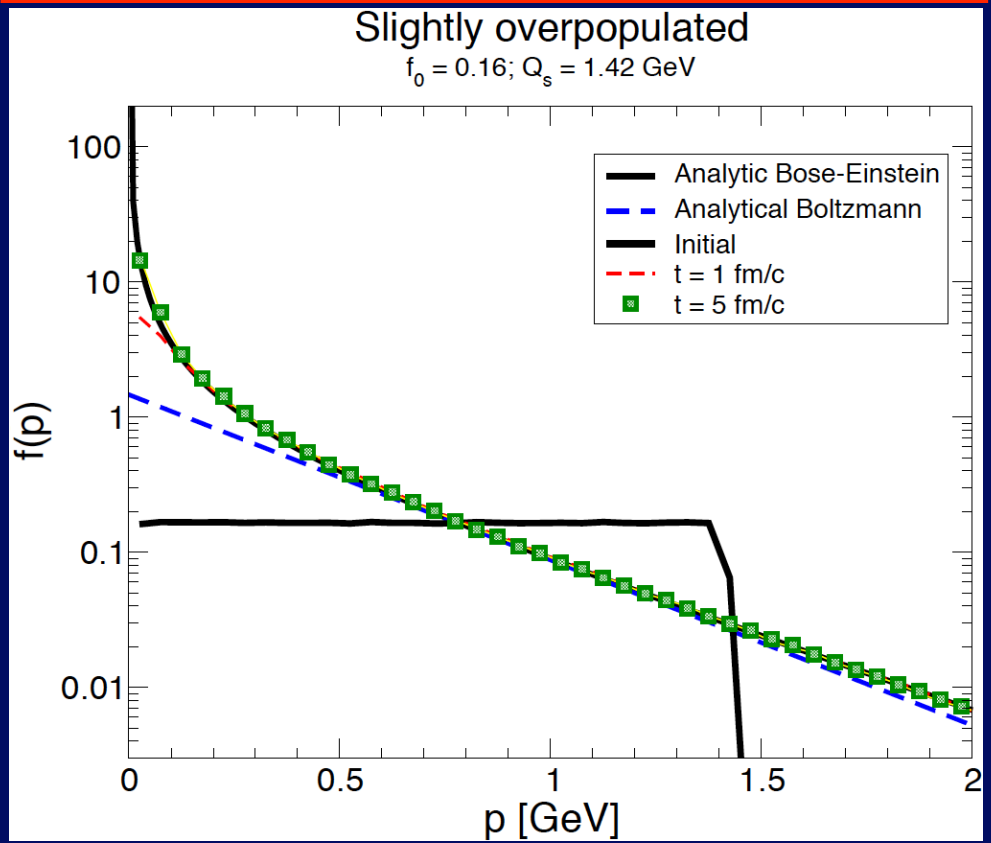

Using the gg<->gg cross section with m_D=0.1 GeV
[not exactly like in in Blaizot NPA920(2013)]

$$\frac{d\sigma^{gg\to gg}}{dt} = \frac{9\pi\alpha_s^2}{\left(m_D^2 - t\right)^2}$$

m_D=0.1 GeV

With an initial distribution function

$$f(p) = f_0\,\theta(1 - p/Q_s)$$

Relativistic-Boltzmann vs Fokker-Planck

$$\mu^* = T \ln\left(1 + \frac{1}{f(0)}\right) \xrightarrow{\text{equilibrium}} \mu$$

Boltzmann with (1+f)

Evolution in a static Box

Fokker-Planck

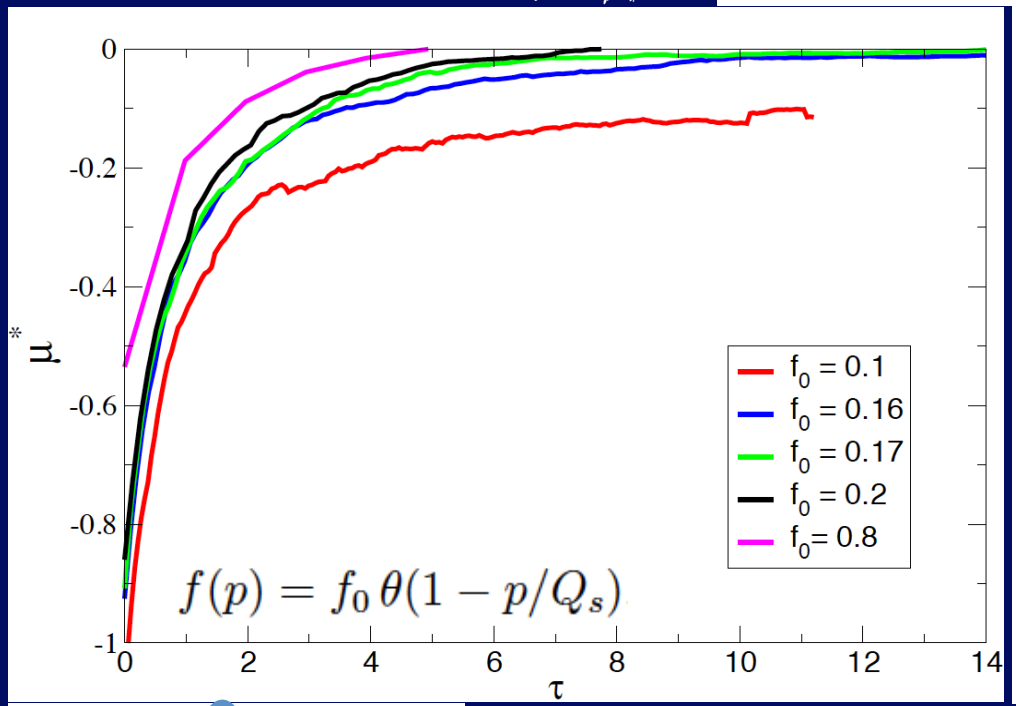

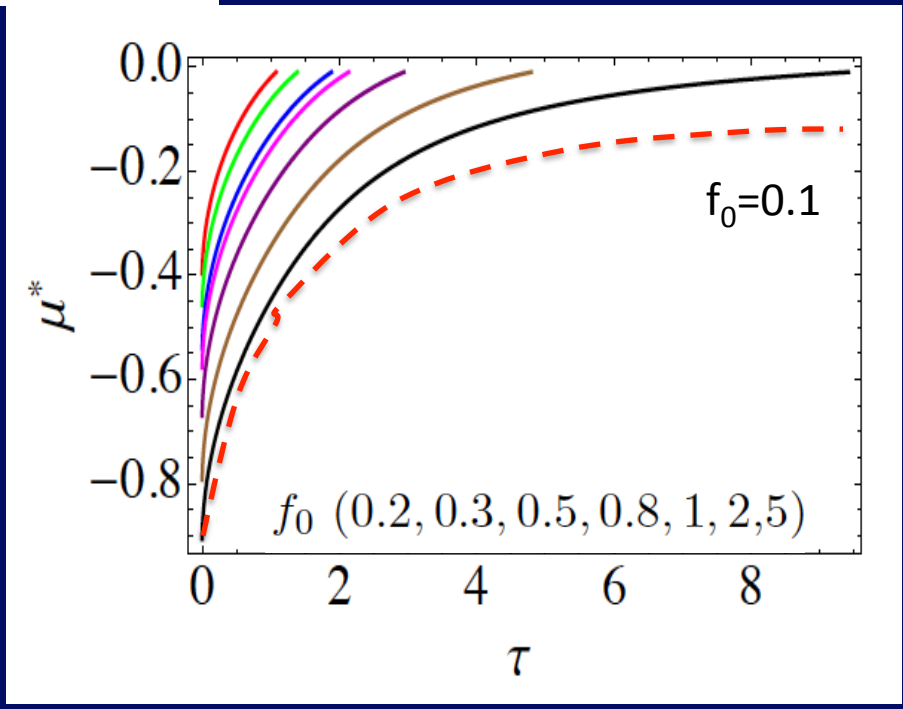

$$\tau = 2\pi^2\alpha^2\xi f_0(1+f_0)\,t.$$

Blaizot,Liao,McLerran NPA920(2013) 58

Quite good agreement, transition to BEC for $f_0 > 0.16$ in both cases!

Generally similar behavior FP or BM, but m_D is small

Upcoming and Possible developments

- *Finite mass screening m_D and finite gluon masses -> FP still good?*
- *1D Bjorken boost expansion (in a box) → what is the f_{0c}?*
- *Impact of q <-> g conversions (Blaizot, Wu, Yan arxiv.1402.5049)*
- Apply to 3+1D in AA collisions:

  - strong longitudinal expansion + q<->g (F. Scardina et al., PLB**724 (2013) 296)**
  - start from realistic KLN and/or CYM f(p)
  - impact on observable: v_2 and higher-lower harmonics v_n

- Inclusion of gauge field (in abelian approximation)
- Impact of 2 <-> 3 inelastic collisions

Effect of screening masses

If we keep fixed the total cross section (same scattering rate) and increase m_D:

- It does not modify the f_0 critical value
- It accelerates the time for BEC: m_D from 0.1 to 1 GeV makes t_{BEC} 3 times smaller

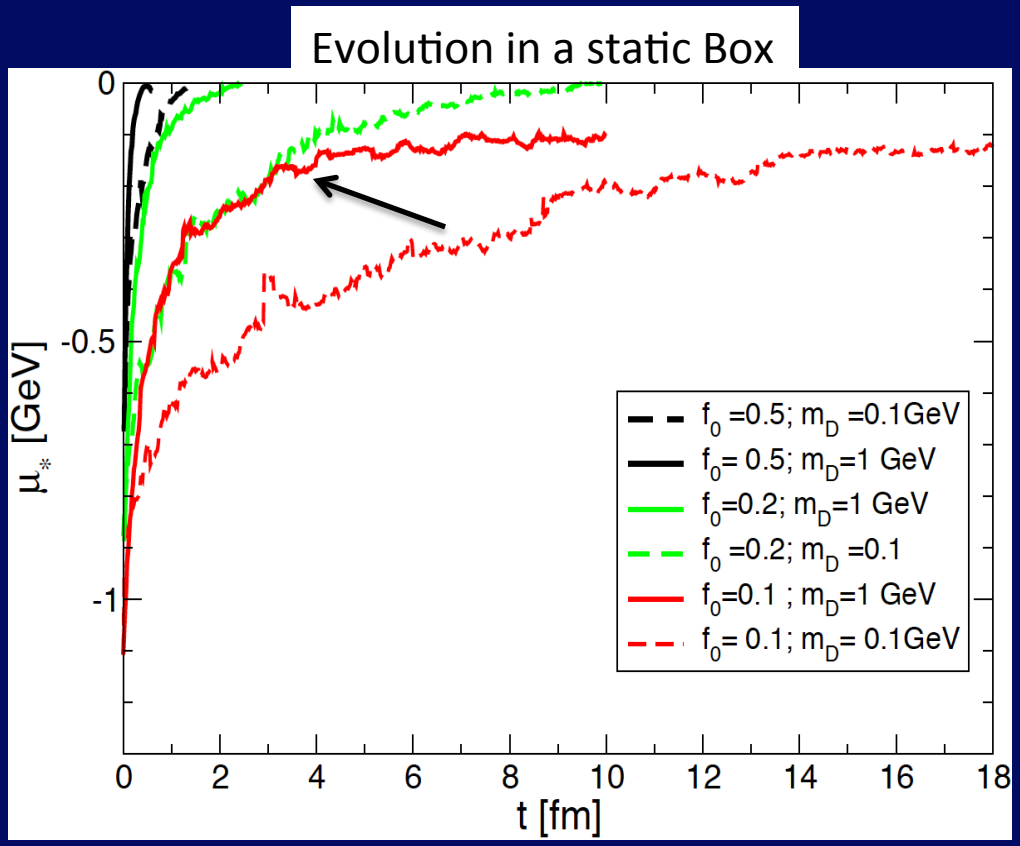

At large m_D = 2-3 T the Fokker-Planck may be not fully reliable, but …

Occupation number in AA collisions
w/o (1+f) terms

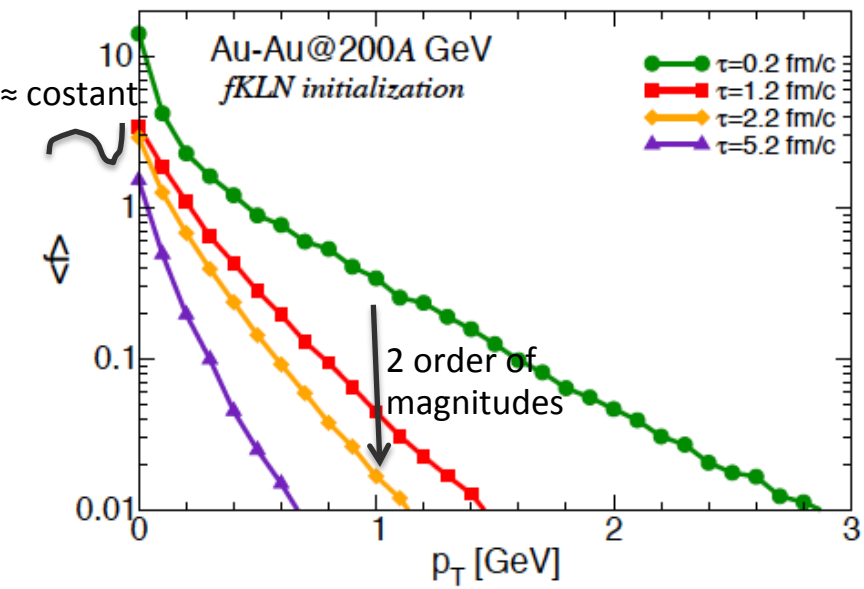

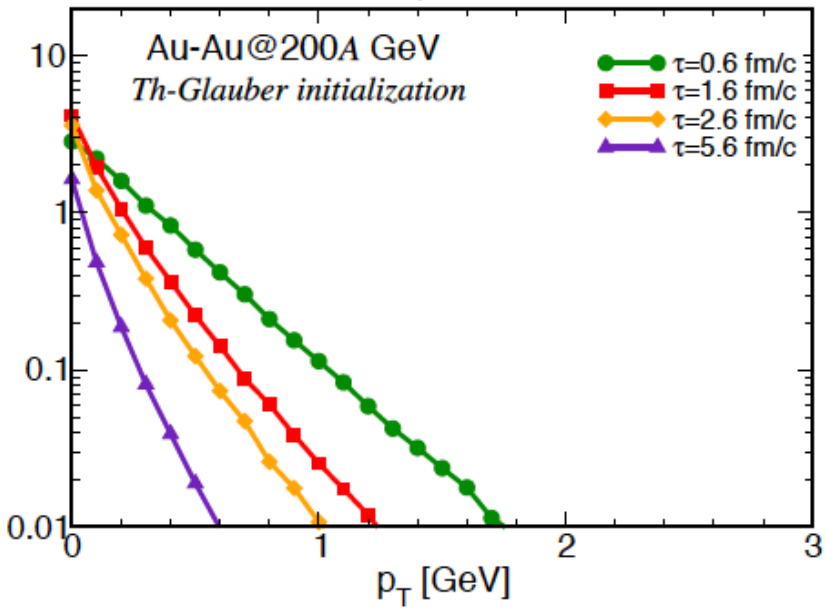

$$f = \frac{(2\pi)^3}{g}\frac{\Delta N}{\Delta^2 x_\perp \Delta^2 p_T}\frac{1}{\Delta z \Delta p_z}$$

$$\langle f \rangle = \frac{1}{2\pi}\int d\phi \int f dy$$

- f >1 need of Bose-Einstein statistics
  (1+f) terms needed in the collision integral
  -> possibility of Bose Condensate induced by CGC

  J. P. Blaizot et al., Nucl. Phys. A905, 829c (2013).

$f \approx 1/\tau$ + slope change

- ✓ Longitudinal expansion lowers average density by τ^{-1} but f(p->0) goes down slowly due to cooling
- ✓ f <<1 at p_T> 0.5 our effect on $v_2(p_T)$ manifest at larger p_T

M. Ruggieri et al.,arXiv:1312.6060 [nucl-th]

First very preliminary for AA collision with (1+f)

First result of Boltzmann + Bose factors for the 3+1D simulation

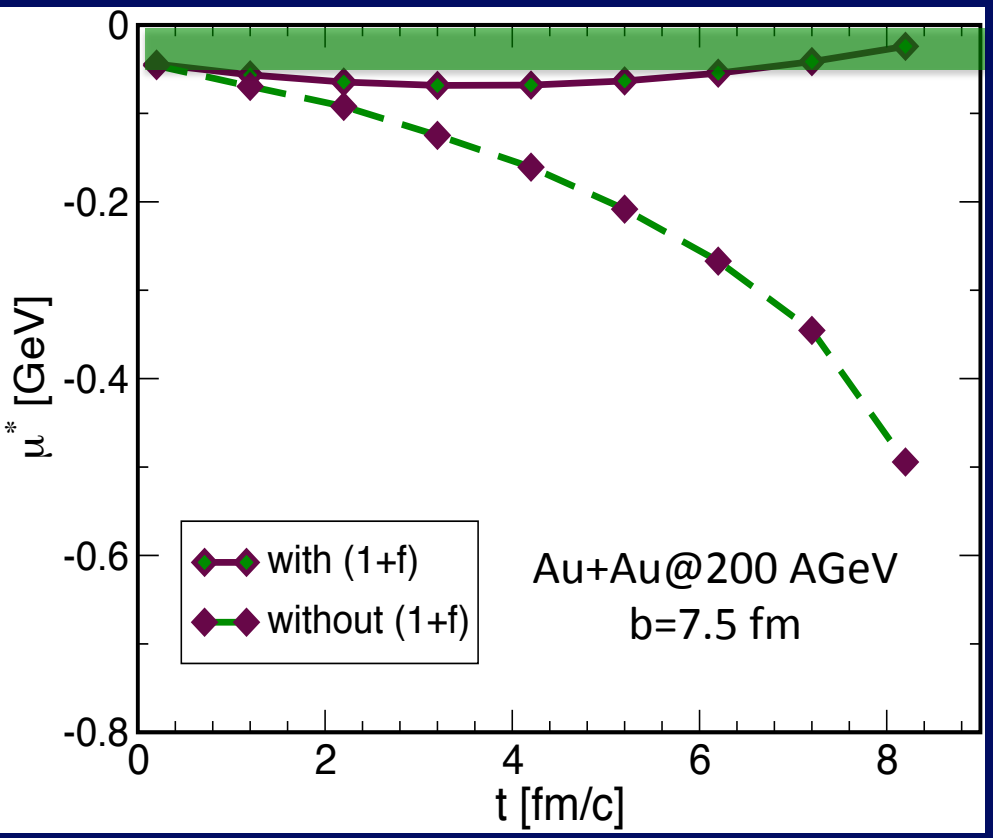

Very preliminary: not enough accurate

- Low statistics (small N_{test})
- not too small Δp grip

-> Systematic error in extracting f(p=0)

Strong Impact of the (1+f) terms kept also in 3D expansion -> (1+f) terms in the collision integral increase the IR cascade p->0

The fact that it stays nearly constant and then even decreases is promising!

Summary

Development of kinetic approach at fixed $\eta/s(T)$

- For η/s <0.1 -> P_L/P_T > 0.7 at $\Delta\tau_{isotr}$ <0.5 fm/c + $\Delta\tau_{therm}\approx$0.8 fm/c
  For $\eta/s \approx 1$ no pressure isotropization
- Boltzmann collision integral with (1+f) Bose terms in 3+1D:

  -> BEC in a box but possible also in AA collisions?!

  -> Larger m_D at fixed collision rate accelerate the process

Studying the CGC (fKLN):

- Non-equilibrium implied by Qs damps $v_2(p_T)$ compensating the larger ε_x -> $v_2(p_T)$ described with $4\pi\eta/s \approx 1$ also for KLN
- p_T spectra deformation can impact significantly v_2

Back-up

Outlook

for the kinetic theory approach

- Hadronization:
  - statistical model +Cooper-Frye vs. coalescence + fragm.
- Field Dynamics:
  - Realistic EoS: M(T) + Bag mean field dynamics [Done!]
- Include initial state fluctuations to study v_n:
  - more constraints on $\eta/s(T)$ and initial state?
  - something more or new at $p_T \approx 2\text{-}4$ GeV ?
  - pA ...

Endeavor already undertaken....

Viscosity of a pQCD gluon plasma

Agreement with AMY, JHEP 0305 (2003) 051

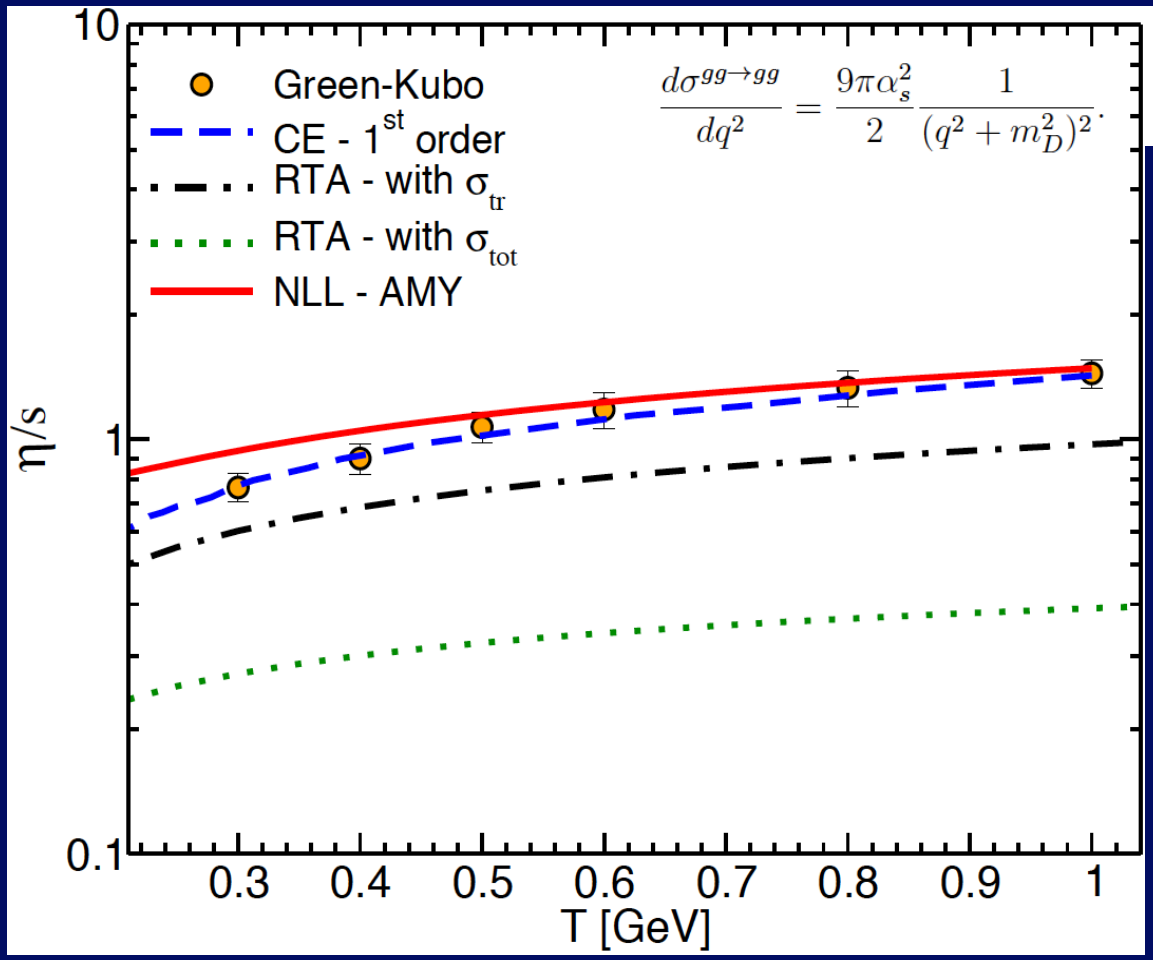

$$\alpha_s(T) = \frac{4\pi}{11\ln\left(\frac{2\pi T}{\Lambda}\right)^2}$$

$$m_D = T\sqrt{4\pi\alpha_s}$$

Relaxation Time Approximation

$$\eta_{RTA}/s = \frac{1}{15}\langle p\rangle\tau_{tr} = \frac{1}{15}\frac{\langle p\rangle}{\sigma_{tr}\rho}$$

Chapmann-Enskog (CE)

$$\eta/s = \frac{1}{15}\langle p\rangle\tau_\eta = \frac{1}{15}\frac{\langle p\rangle}{g(a)\sigma_{tot}\rho}$$

$g(a=m_D/2T)$ correct function that fix the momentum transfer for shear motion

$$0 < g(m_D/2T) < 2/3$$

∞ forward peaked

Isotropic $m_D \to \infty$

close to AMY result JHEP(2003),
but there is a significant simplification:
only direct u & t channels
with simplified HTL propagator

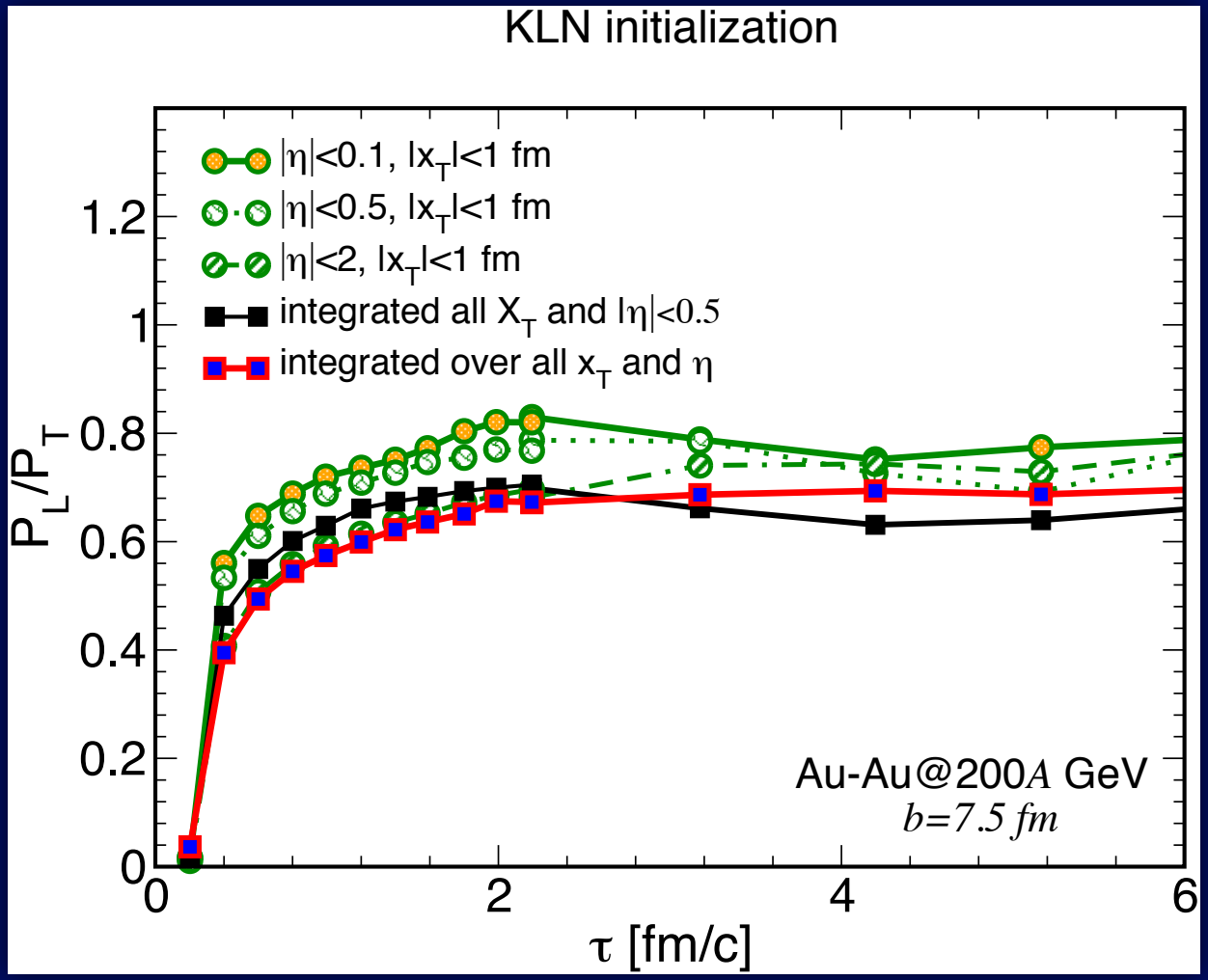
KLN initialization
|η|<0.1, |x_T|<1 fm
|η|<0.5, |x_T|<1 fm
|η|<2, |x_T|<1 fm
integrated all X_T and |η|<0.5
integrated over all x_T and η
Au-Au@200A GeV
b=7.5 fm
P_L/P_T
τ [fm/c]
0
0.2
0.4
0.6
0.8
1
1.2
0
2
4
6

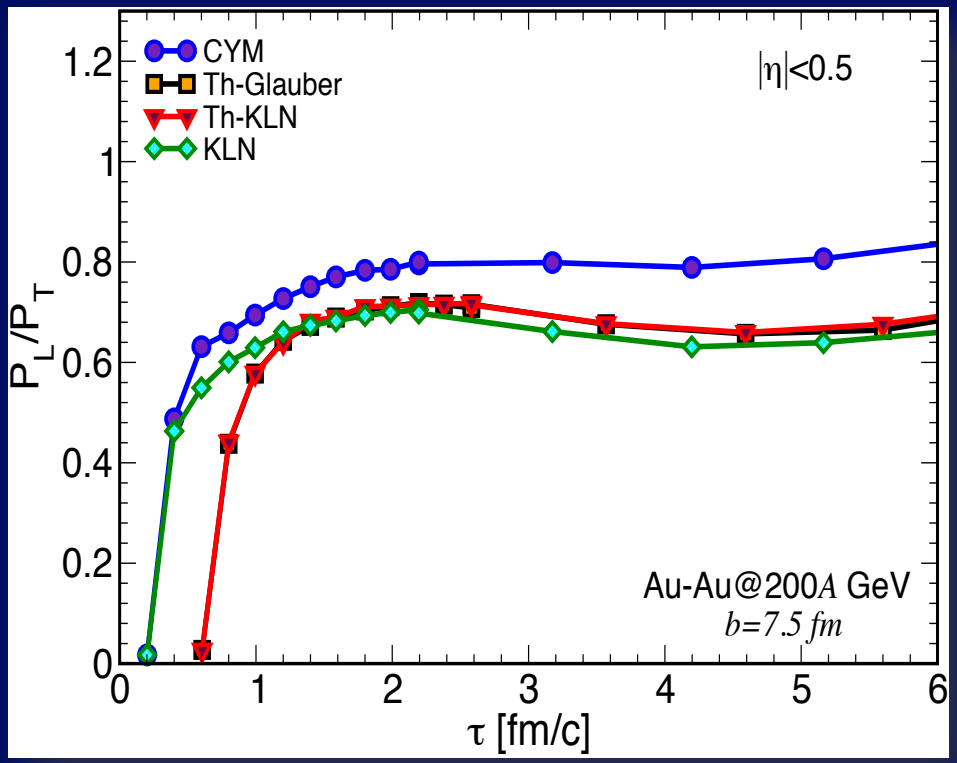
CYM
Th-Glauber
Th-KLN
KLN
|η|<0.5
Au-Au@200A GeV
b=7.5 fm
P_L/P_T
τ [fm/c]

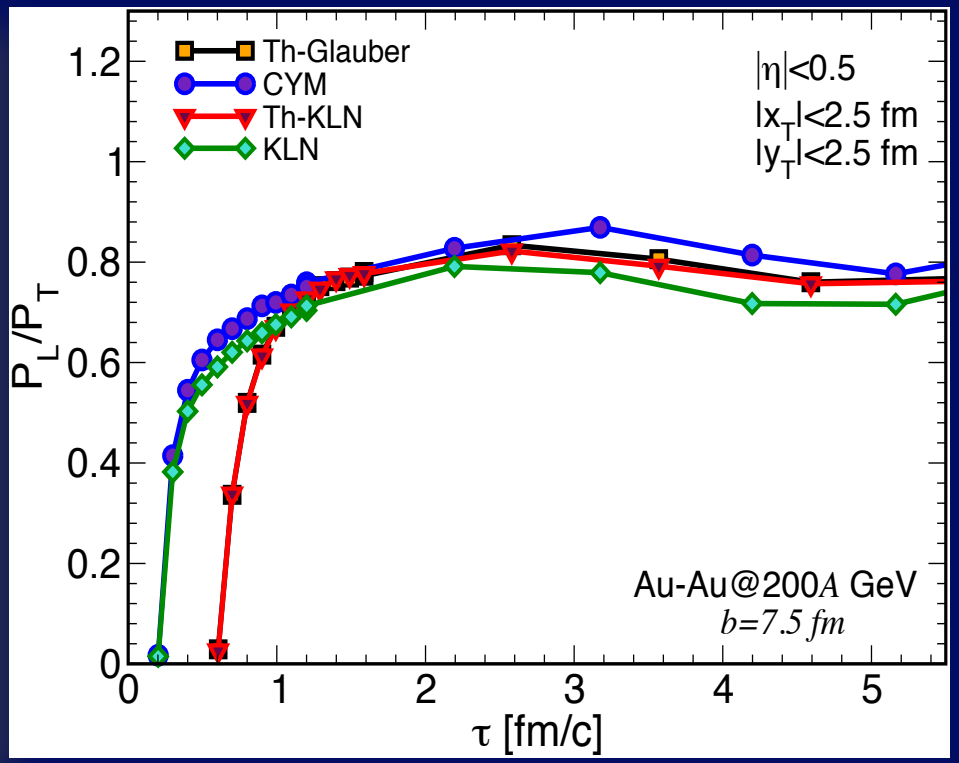
Th-Glauber
CYM
Th-KLN
KLN
|η|<0.5
|x_T|<2.5 fm
|y_T|<2.5 fm
Au-Au@200A GeV
b=7.5 fm
P_L/P_T
τ [fm/c]

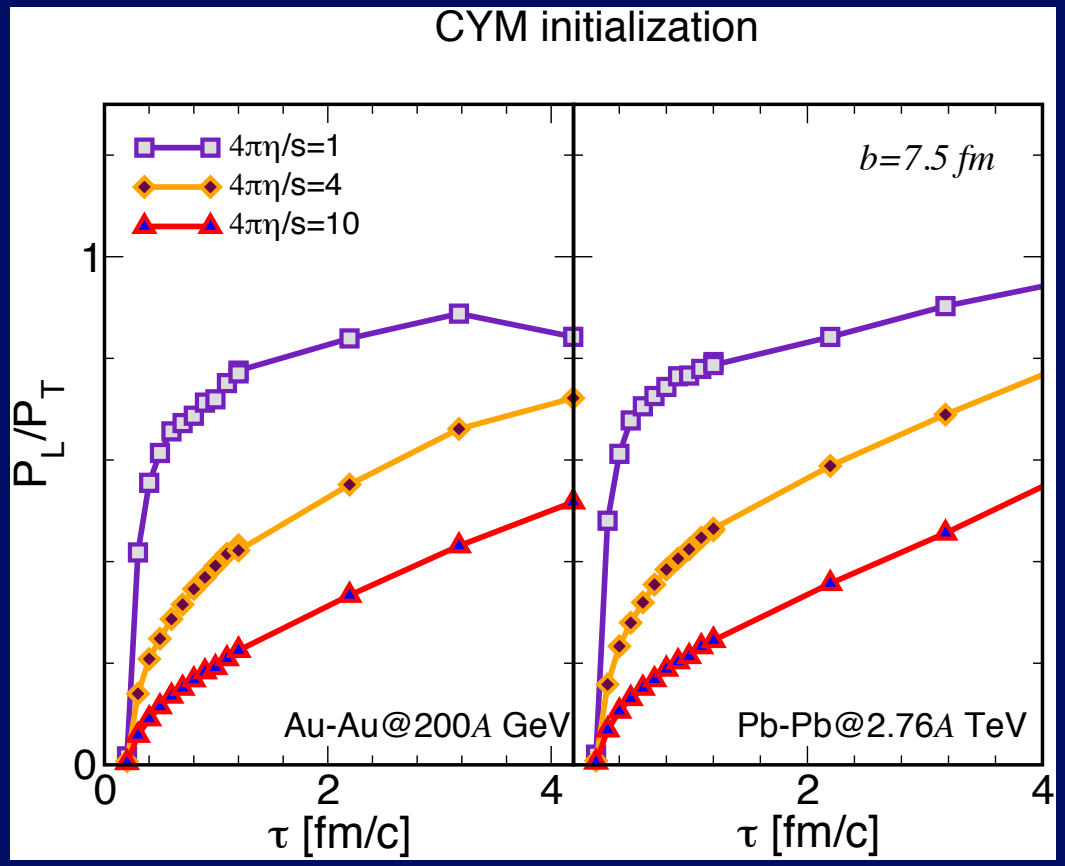
CYM initialization
4πη/s=1
4πη/s=4
4πη/s=10
b=7.5 fm
Au-Au@200A GeV
Pb-Pb@2.76A TeV
P_L/P_T
τ [fm/c]
τ [fm/c]
0
1
0
2
4
2
4

Longitudinal and transverse pressure

t=1/Qs≈0.1-0.2 fm/c
-> $P_L/P_T > 0$
Gelis & Epelbaum
arXiV:1307.2214

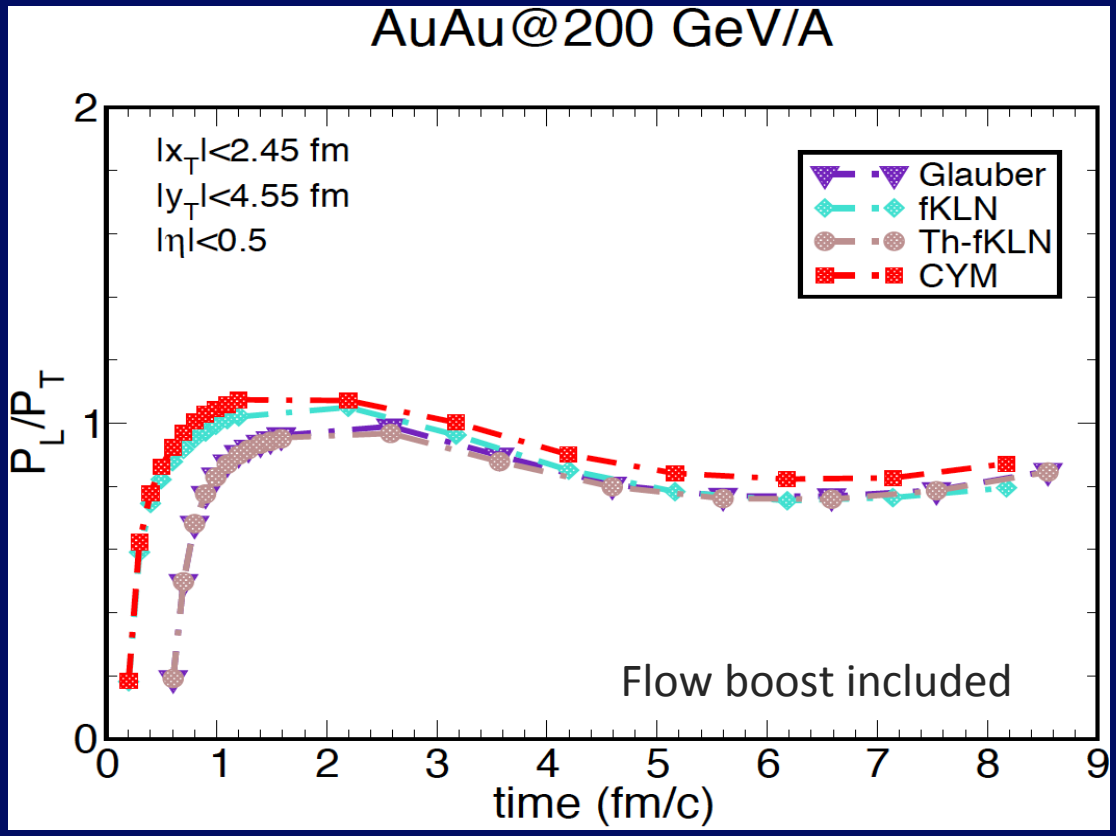

M. Ruggieri et al.,arXiv:1312.6060 [nucl-th]

- ✧ P_L/P_T show also a very fast equilibration ($\Delta\tau_{isotr}$≈0.4 fm/c)!
- ✧ However it is not this that makes a difference for v_2:
  isotropization time very similar for all the cases

Evolution with Energy

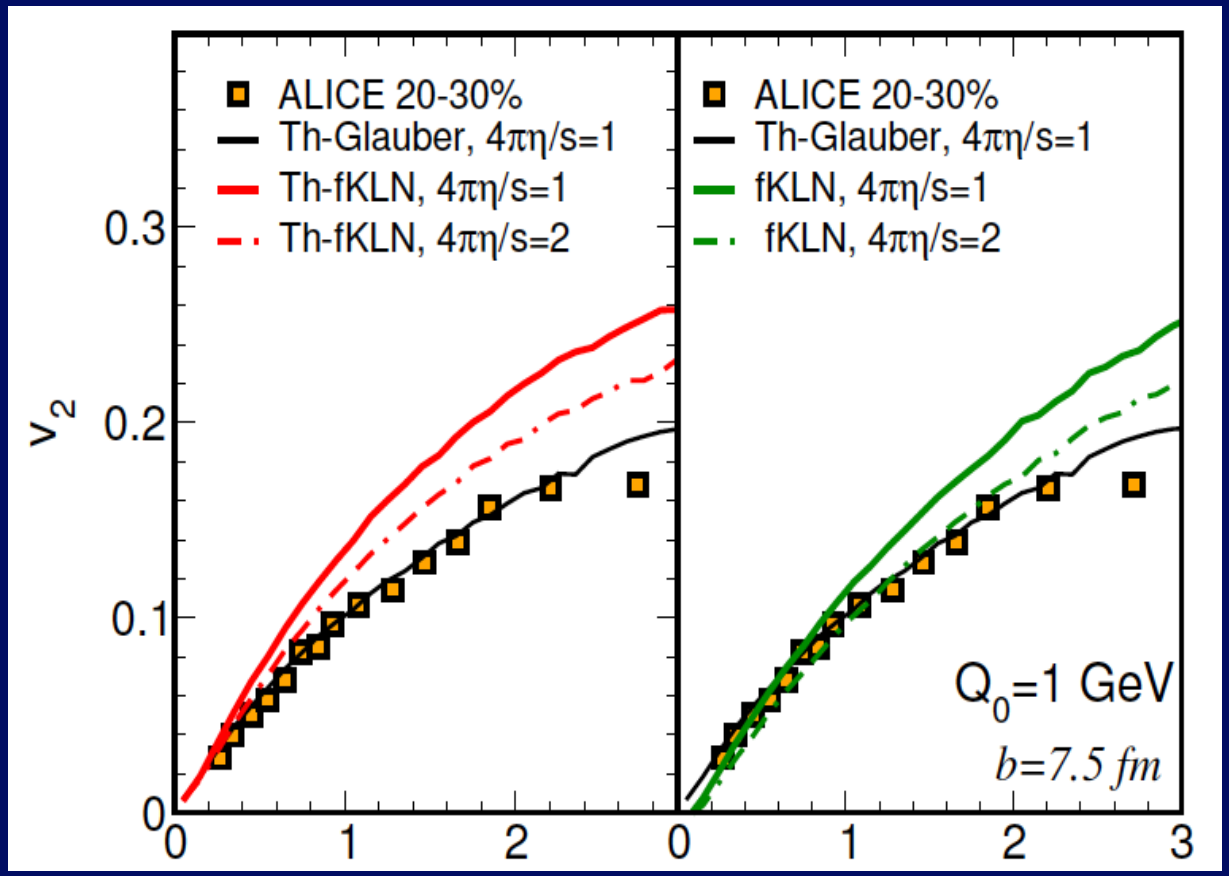

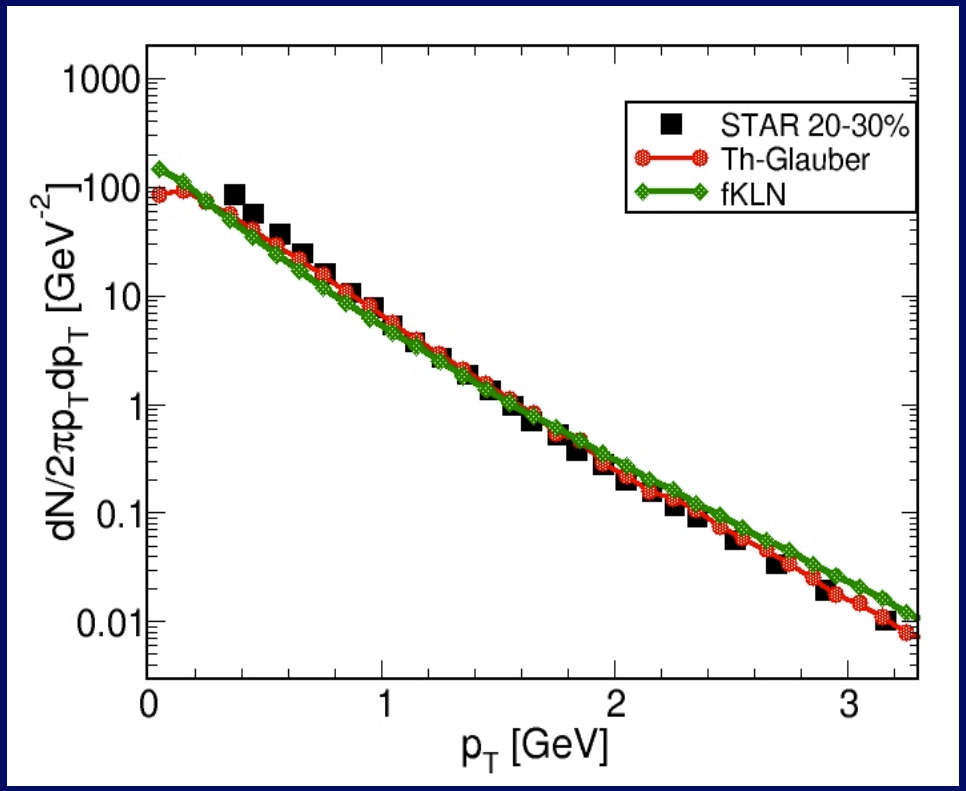
STAR 20-30%
Th-Glauber
fKLN
1000
100
10
1
0.1
0.01
0
1
2
3
$dN/2\pi p_T dp_T$ [GeV^{-2}]
p_T [GeV]

What is v_2?

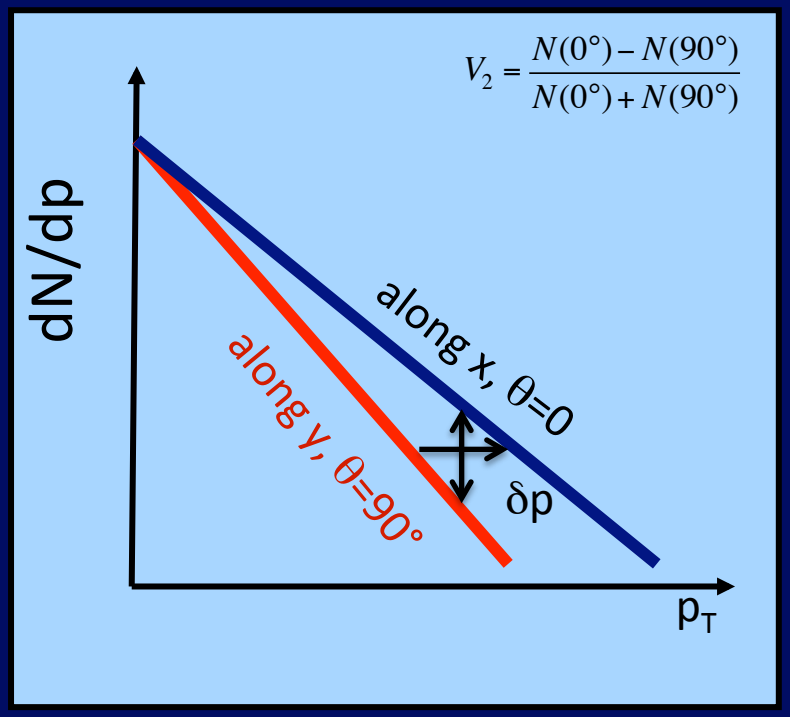

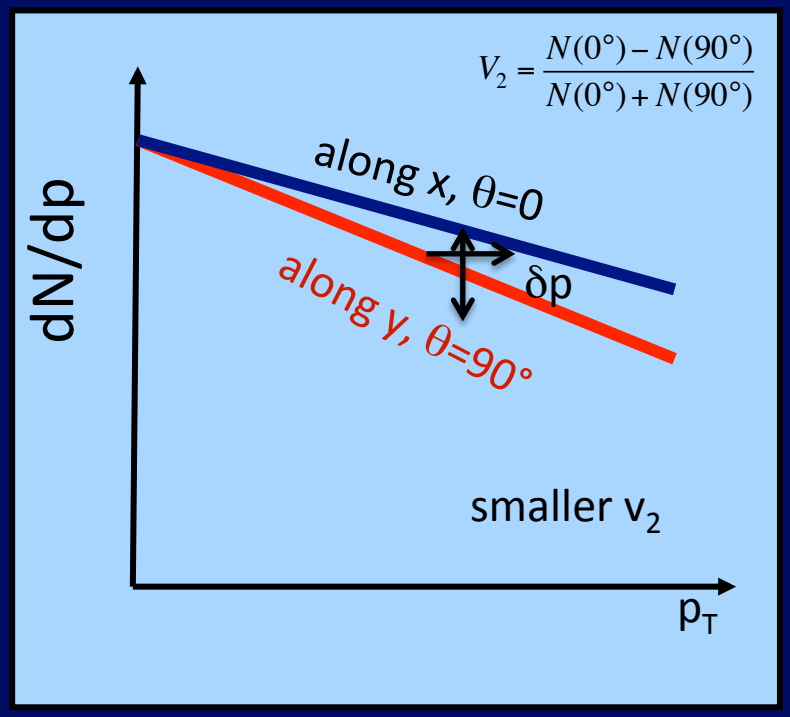

Put it very simplistic:

$$f(p_T, \phi) = e^{-\frac{p_T - \delta p \cos(2\phi)}{T^*}}$$

$$v_2(p_T, \phi) \cong \frac{\delta p}{4T^*}$$

If the momentum δp shift is the same we can expect flatter distribution are less efficient in build-up v2

Solving Relativistic-Boltzmann with (1+f) factor

No small angle or mometum transfer pproximantion

$$C_{22} = \frac{1}{2E_p}\int \frac{d^3q}{(2\pi)^3 2E_q}\int \frac{d^3p'}{(2\pi)^3 2E'_p}\frac{d^3q'}{(2\pi)^3 2E'_q}\left|M_{pq\to p'q'}\right|^2 \left[f(q')f(p')\left(1+f(p)\right)\left(1+f(q)\right) - f(q)f(p)\left(1+f(p')\right)\left(1+f(q')\right)\right](2\pi)^4\delta^4(p+q-p'-q')$$

$$\frac{(2\pi)^3 \Delta N_{coll}}{\Delta t \Delta^3 x \Delta^3 p} = g\frac{\Delta^3 q}{(2\pi)^3} f_g(p) f_g(q) v_{rel}\sigma_{p,q\to p',q'}\left[1+f(p')\right]\left[1+f(q')\right]$$

$$f_i = \frac{\Delta N_i}{\frac{1}{(2\pi)^3}\Delta^3 x\, \Delta^3 p_i},$$

$$P_{22} = \frac{\Delta N_{coll}^{2\leftrightarrow 2}}{\Delta N_1 \Delta N_2} = \frac{\Delta t}{\Delta^3 x} v_{rel}\sigma_{p,q\to p',q'}\left[1+f(p')\right]\left[1+f(q')\right]$$

$$\frac{d\sigma^{gg\to gg}}{dt} = \frac{9\pi\alpha_s^2}{\left(m_D^2 - t\right)^2}$$

Using the gg<->gg cross section
with m_D=0.1 GeV
[not exactly like in in Blaizot NPA920(2013)]

Technically quite more twisted
than simple Boltzmann integral

Ideally

Hydro $\xleftarrow[\eta/s<<1]{p_T \approx 3T}$ Transport

- Higher p_T (no Ansatz for df)
- Larger η/s, and local large stress tensor
- Initial off-equilibrium
- Higher $m_Q >> T, \Lambda_{qcd}$
- Microscopic level: Hadronization

η/s or details of the cross section?

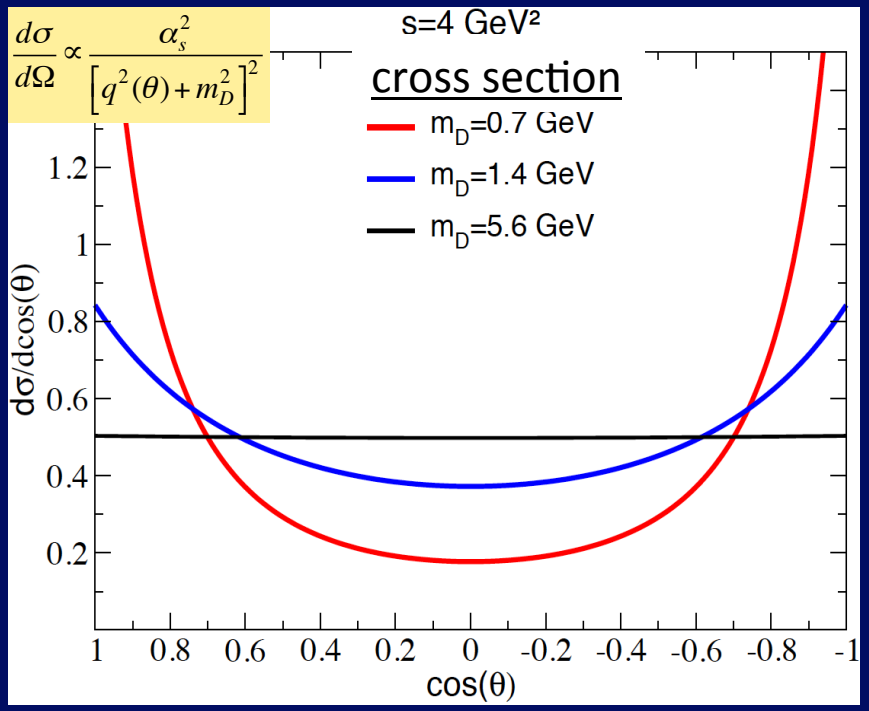

Keep same η/s means:

$$\frac{\eta}{s} = \frac{1}{15}\langle p \rangle \cdot \tau_\eta$$

$$\tau_\eta^{-1} = g\left(\frac{m_D}{T}\right)\sigma_{TOT}\rho$$

$$\frac{\sigma_{TOT}(m_{1D})}{\sigma_{TOT}(m_{2D})} = \frac{g(m_{2D})}{g(m_{1D})}$$

for m_D=0.7 GeV -> factor 2 larger σ_{tot} is needed respect to isotropic case

η/s or details of the cross section?

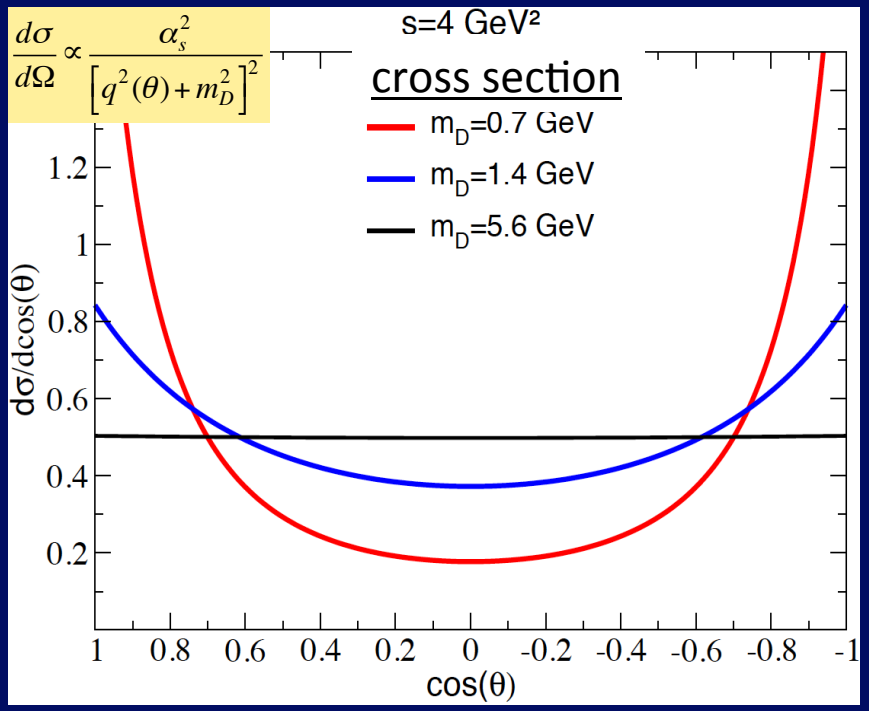

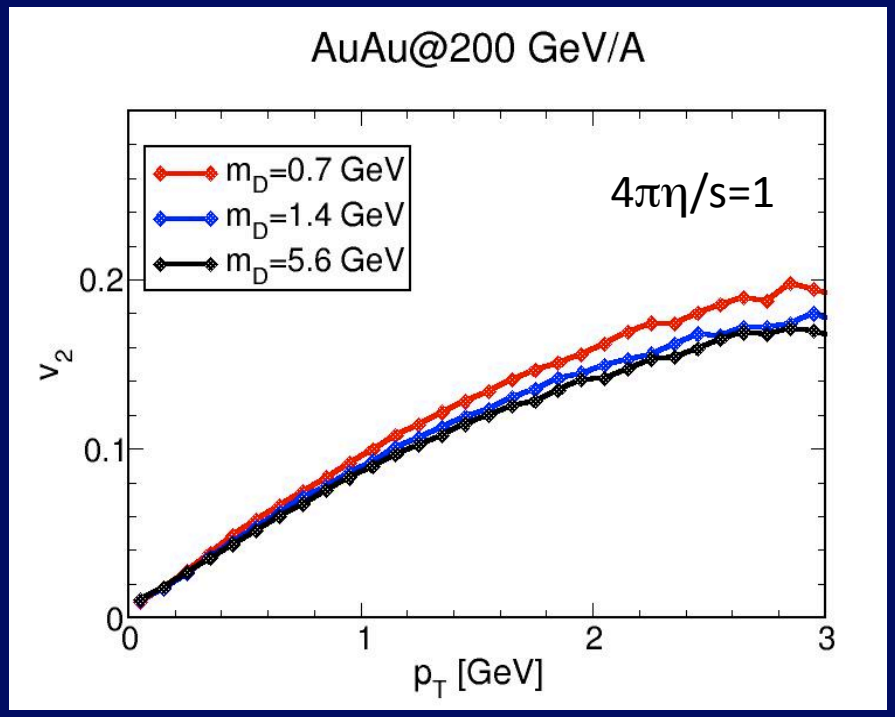

Keep same η/s means:

$$\frac{\eta}{s} = \frac{1}{15}\langle p \rangle \cdot \tau_\eta$$

$$\tau_\eta^{-1} =$$

$$\frac{\sigma_{TOT}(m_{1D})}{\sigma_{TOT}(m_{2D})} = \frac{g(m_{2D})}{g(m_{1D})}$$

- ✧ η/s is really the physical parameter determining v_2 at least up to 1.5-2 GeV
- ✧ microscopic details become relevant at higher p_T
- ✧ First time η/s<-> v_2 hypothesis is verified!

for m_D=0.7 GeV -> factor 2 larger σ_{tot} is needed respect to isotropic case

η/s or details of the cross section?

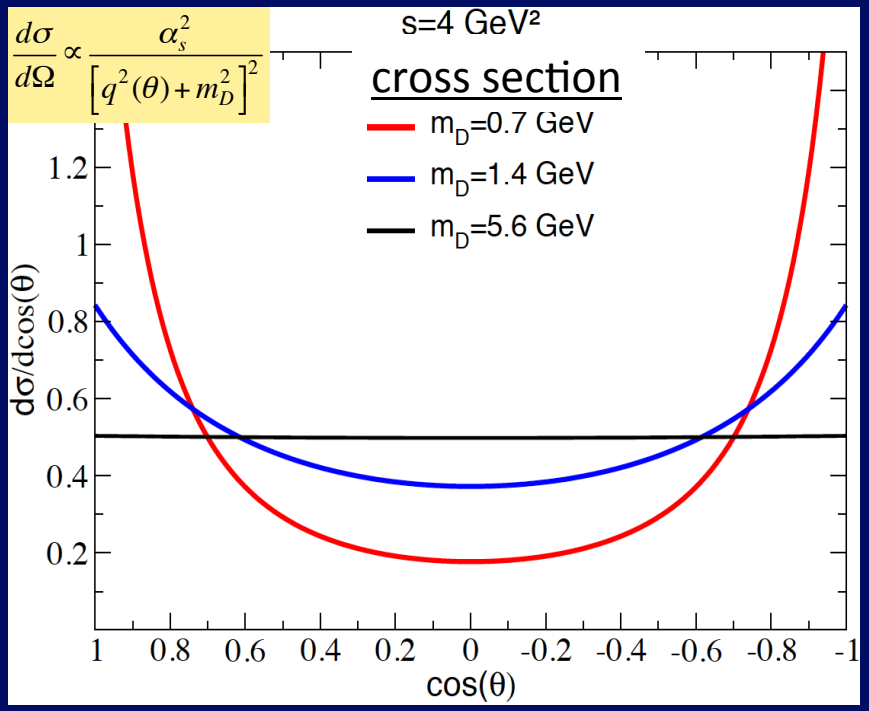

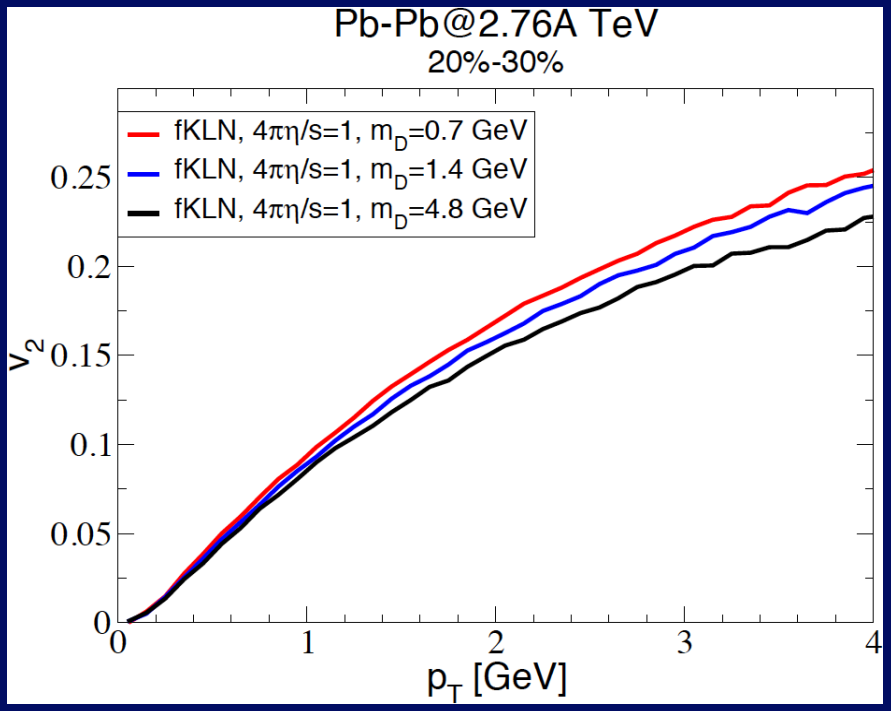

Keep same η/s means:

$$\frac{\eta}{s} = \frac{1}{15}\langle p \rangle \cdot \tau_\eta$$

$$\tau_\eta^{-1} =$$

$$\frac{\sigma_{TOT}(m_{1D})}{\sigma_{TOT}(m_{2D})} = \frac{g(m_{2D})}{g(m_{1D})}$$

- ✧ η/s is really the physical parameter determining v_2 at least up to 1.5-2 GeV
- ✧ microscopic details become relevant at higher p_T
- ✧ First time η/s<-> v_2 hypothesis is verified!

for m_D=1.4 GeV -> 25% smaller σ_{tot}

for m_D=5.6 GeV -> 40% smaller σ_{tot}

η/s or details of the cross section?

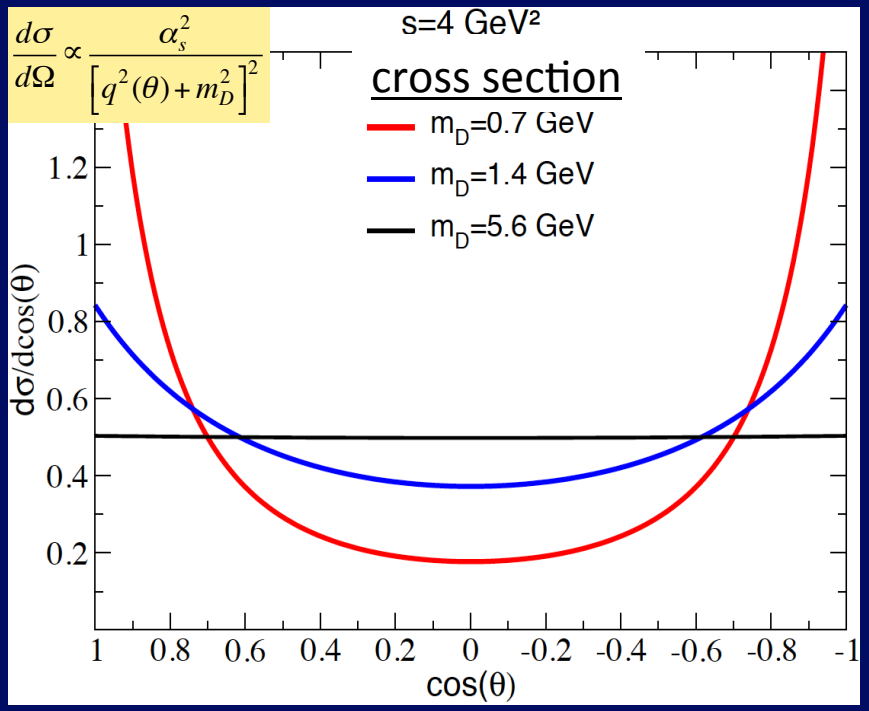

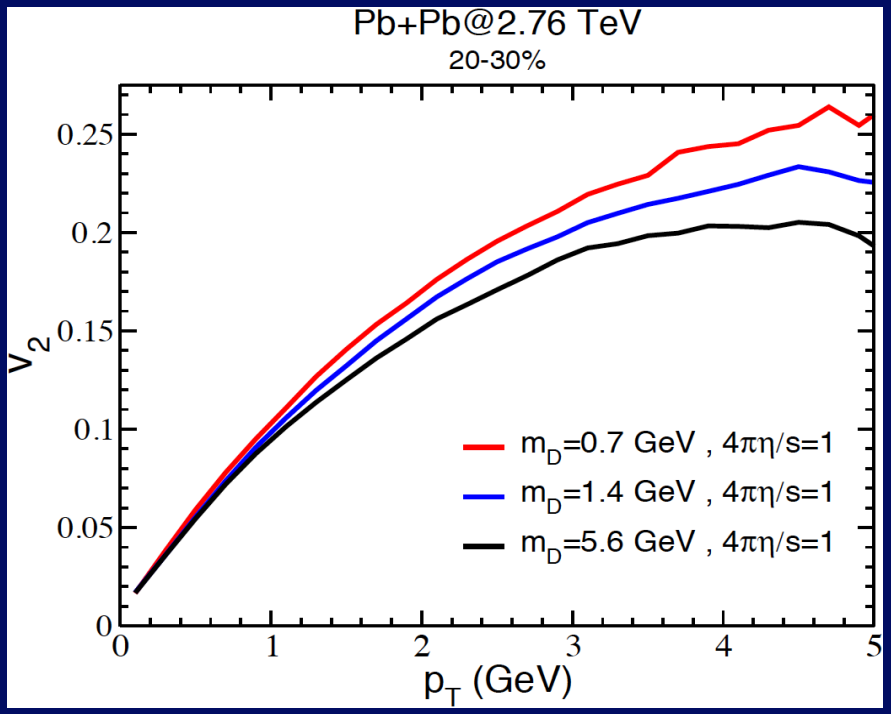

Keep same η/s means:

$$\frac{\eta}{s} = \frac{1}{15}\langle p \rangle \cdot \tau_\eta$$

$$\tau_\eta^{-1} =$$

$$\frac{\sigma_{TOT}(m_{1D})}{\sigma_{TOT}(m_{2D})} = \frac{g(m_{2D})}{g(m_{1D})}$$

- ✧ η/s is really the physical parameter determining v_2 at least up to 1.5-2 GeV
- ✧ microscopic details become relevant at higher p_T
- ✧ First time η/s<-> v_2 hypothesis is verified!

Differences arises just where in viscous hydro δf becomes relevant

$$\delta f = \frac{\pi^{\mu\nu}}{\varepsilon + P}\frac{p_\mu p_\nu}{T^2} f_{eq}$$

Viscous Hydrodynamics

Relativistic Navier-Stokes

$$T^{\mu\nu} = T^{\mu\nu}_{ideal} + \eta(\nabla^\mu u^\nu + \nabla^\nu u^\mu - \frac{2}{3}\Delta^{\mu\nu}\partial^\alpha u_\alpha)$$

but it violates causality,

II^0 order expansion needed -> Israel-Stewart tensor based on entropy increase $\partial_\mu s^\mu > 0$

$$\pi^{\mu\nu} = \eta\nabla^{<\mu}u^{\nu>} + \tau_\pi\left[\Delta^\mu_\alpha\Delta^\nu_\beta D\pi^{\alpha\beta}\ldots\right]$$

-Dissipative correction to u^μ, T, n

-Dissipative correction to f -> $f_{eq}+\delta f_{neq}$

There is no one to one correspondence!

$$T^{\mu\nu}_{eq} + \delta T^{\mu\nu} \Leftarrow f_{eq} + \delta f$$

An Asantz

$$\delta f = \frac{\pi^{\mu\nu}}{\varepsilon + P}\frac{p_\mu p_\nu}{T^2} f_{eq}$$

- this implies RTA and not CE
- $p_T \sim 3$ GeV -> $\delta f/f \approx 4$
- $\Pi^{\mu\nu}(t_0) = 0$ -> discard initial non-eq (ex. minijets)

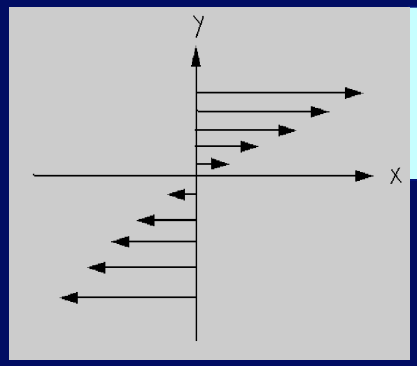

$$\frac{F_x}{A_{yz}} = -\eta\frac{\partial v_x}{\partial y}$$

τ_η, τ_ξ two parameters appears +

$\delta f \sim f_{eq}$ reduce the p_T validity range

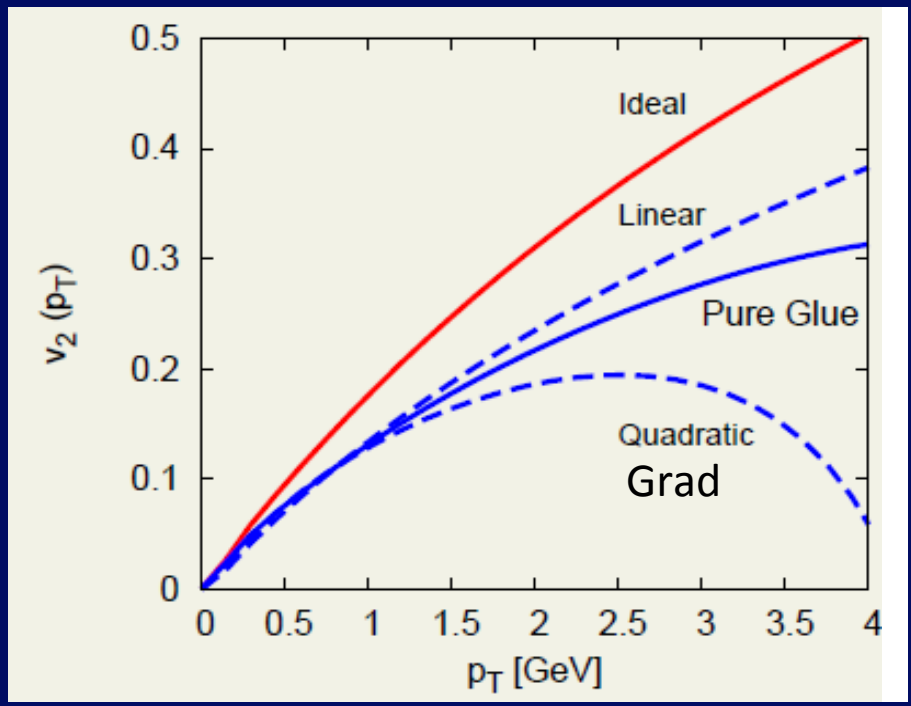

Non Isotropic Cross Section - $\sigma(\theta)$

Relaxation Time Approximation

$$\eta_{RTA}/s = \frac{1}{15} < p > \tau_{tr} = \frac{1}{15}\frac{< p >}{\langle h(a) \rangle \sigma_{TOT}\rho}$$

$$h(a) = 4a(1+a)\left[(2a+1)\ln(1+a^{-1}) - 2\right] \quad , a = m_D^2 / s$$

$h(a)=\sigma_{tr}/\sigma_{tot}$ weights cross section by q^2

RTA is the one usually emplyed to make theroethical estimates: Gavin NPA(1985); Kapusta, PRC82(10); Redlich and Sasaki, PRC79(10), NPA832(10); Khvorostukhin PRC (2010) …

for a generic cross section:

$$\frac{d\sigma}{d\Omega} \propto \left(q^2(\theta) + m_D^2\right)^{-2}$$

m_D regulates the angular dependence

Chapmann-Enskog (CE)

$$\eta/s = \frac{1}{15}\langle p \rangle \tau_\eta = \frac{1}{15}\frac{\langle p \rangle}{g(a)\sigma_{tot}\rho}$$

$$g(a) = \frac{1}{50}\int dy y^6 \left[(y^2 + \frac{1}{3})K_3(2y) - yK_2(2y)\right] h\left(\frac{a^2}{y^2}\right)$$

g(a) correct function that fix the momentum transfer for shear motion

- CE and RTA can differ by about a factor 2-3
- Green-Kubo agrees with CE

Green-Kubo in a box - $\sigma(\theta)$

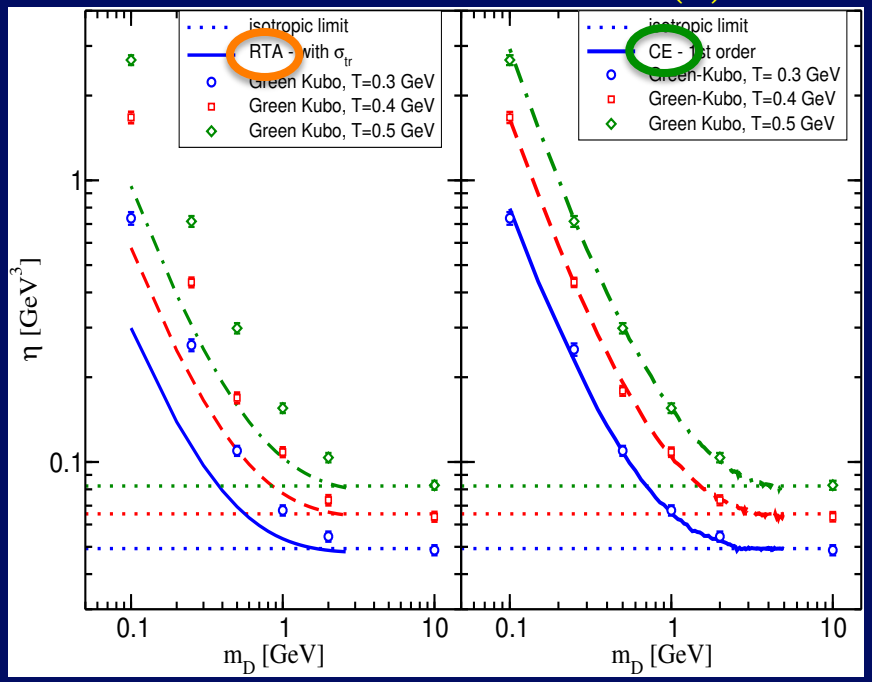

S. Plumari et al., PRC86(2012)054902

Next step –

Include Initial State Fluctuations

(Preliminary results)

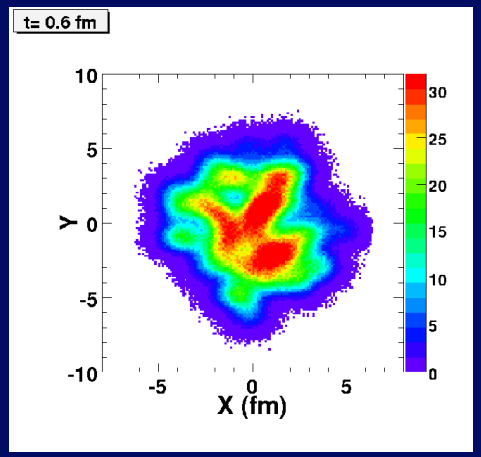

Monte Carlo Glauber

$$\rho_\perp \propto \sum_{i=1}^{N_{part}} \exp\left\{-\left[(x-x_i)^2+(y-y_i)^2\right]/2\sigma^2\right\}$$

σ = 0.5 fm

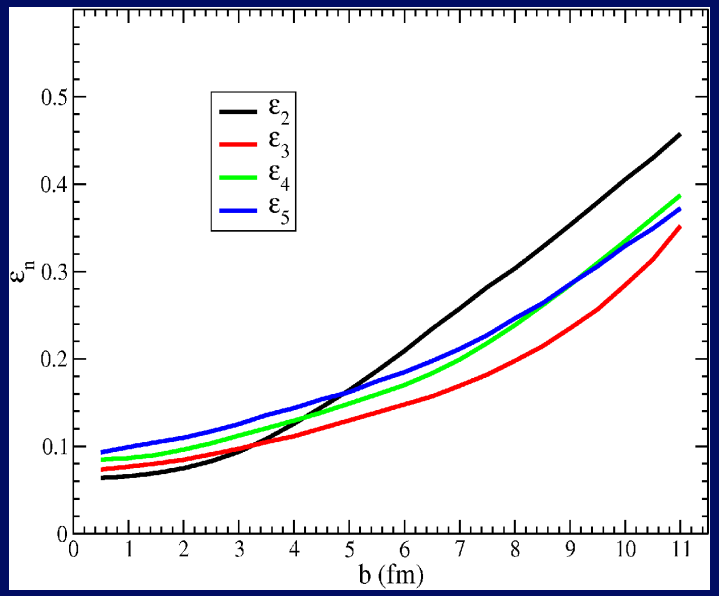

$$\varepsilon_n = \frac{\left\langle r_\perp^n \cos\left[n(\phi-\Phi_n)\right]\right\rangle}{\left\langle r_\perp^n \right\rangle}$$

$$\Phi_n = \frac{1}{n}\arctan\frac{\left\langle r_\perp^n sen\left[n(\phi-\Phi_n)\right]\right\rangle}{\left\langle r_\perp^n \cos\left[n(\phi-\Phi_n)\right]\right\rangle}$$

G-Y. Qin, H. Petersen, S.A. Bass and B. Muller, PRC82,064903 (2010)

H.Holopainen, H. Niemi and K.J. Eskola, PRC83, 034901 (2011)

Initial State Fluctuations: v_n vs ε_n (Preliminary)

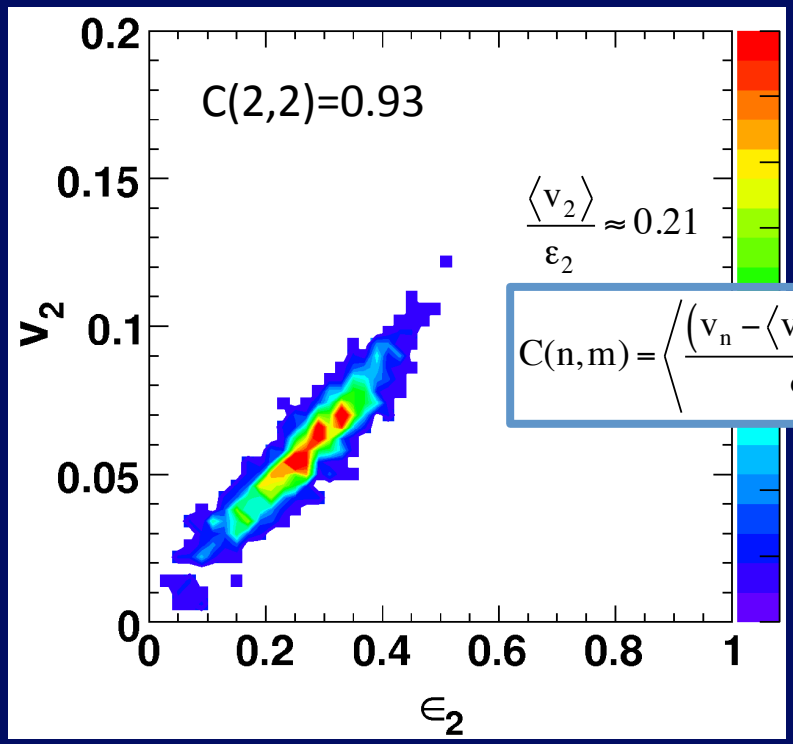

$4\pi\eta/s=1 \approx 5$

$$C(n,m) = \left\langle \frac{\left(v_n - \langle v_n \rangle\right)\left(\varepsilon_n - \langle \varepsilon_n \rangle\right)}{\sigma_{V_n}\sigma_{\varepsilon_n}} \right\rangle$$

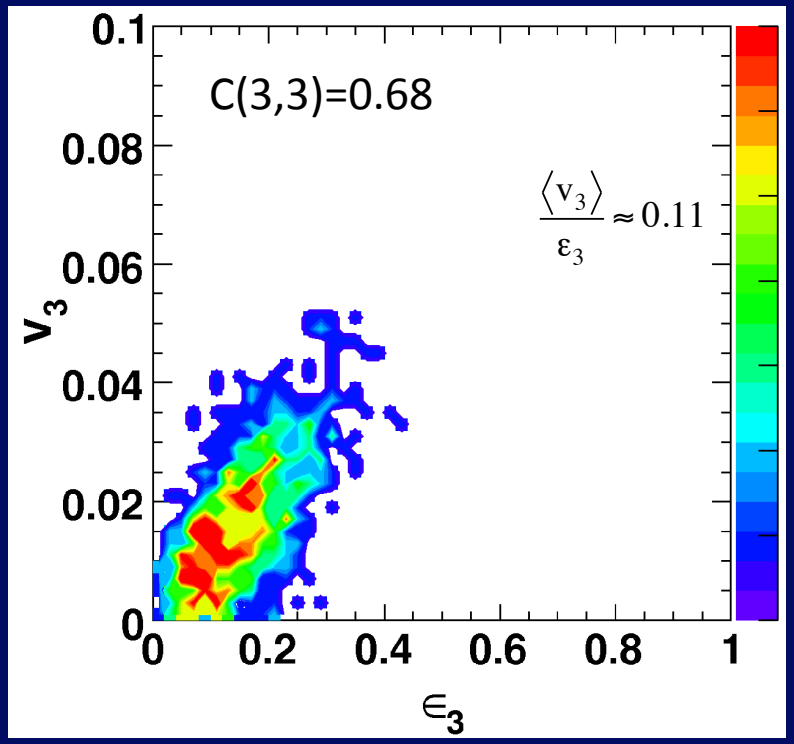

- v_2 and v_3 linearly correlated to the corresponding eccentricities ε_2 and ε_3

Initial State Fluctuations: v_n vs ε_n (Preliminary)

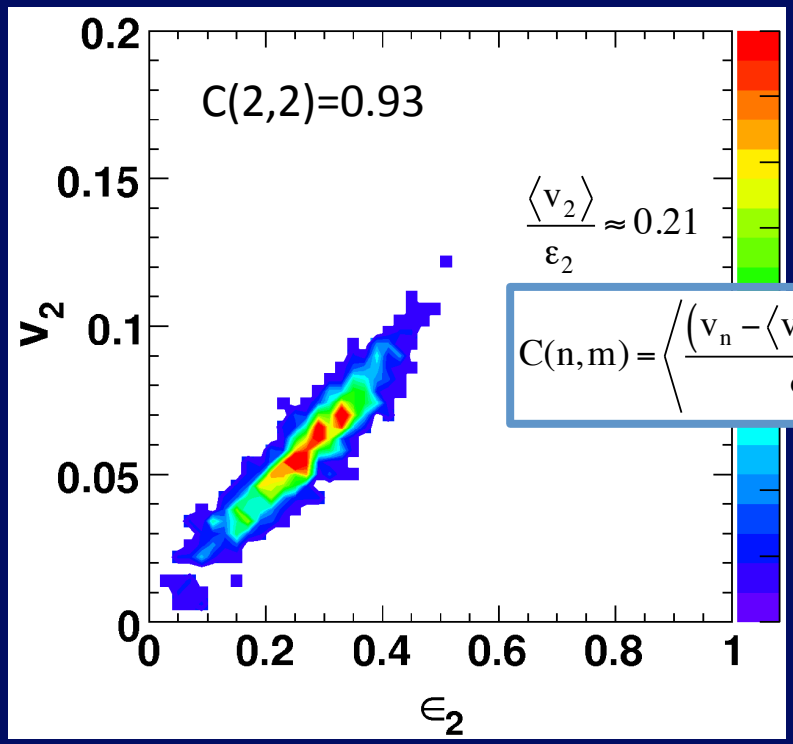

$$C(n,m) = \left\langle \frac{(v_n - \langle v_n \rangle)(\varepsilon_n - \langle \varepsilon_n \rangle)}{\sigma_{v_n} \sigma_{\varepsilon_n}} \right\rangle$$

$4\pi\eta/s=1 \approx 5$

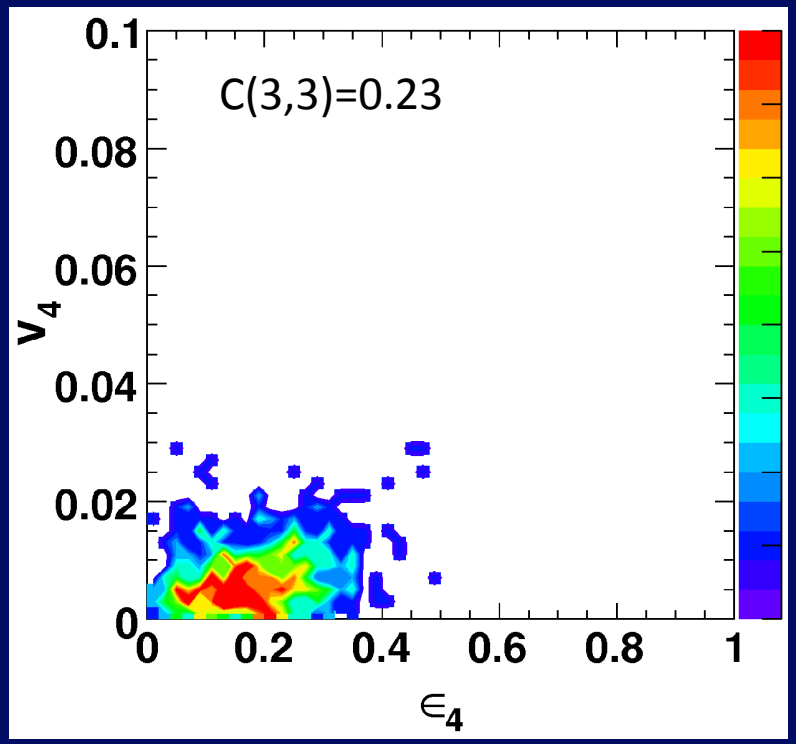

- v_4 and ε_4 weak correlated similar to hydro calculations:

  F.G.Gardim,F.Grassi,M.Luzum and J.Y.Ollitrault NPA904 (2013) 503.

  Niemi, Denicol, Holopainen and Huovinen PRC87(2013) 054901.

General agreement with hydro Niemi et al. PRC87(2013), but:

- η/s not constant (include cross-over increase)
- 3+1 D not 2+1D
- σ =0.5 fm not 0.8 fm (if relevant at all!)

What is v_2?

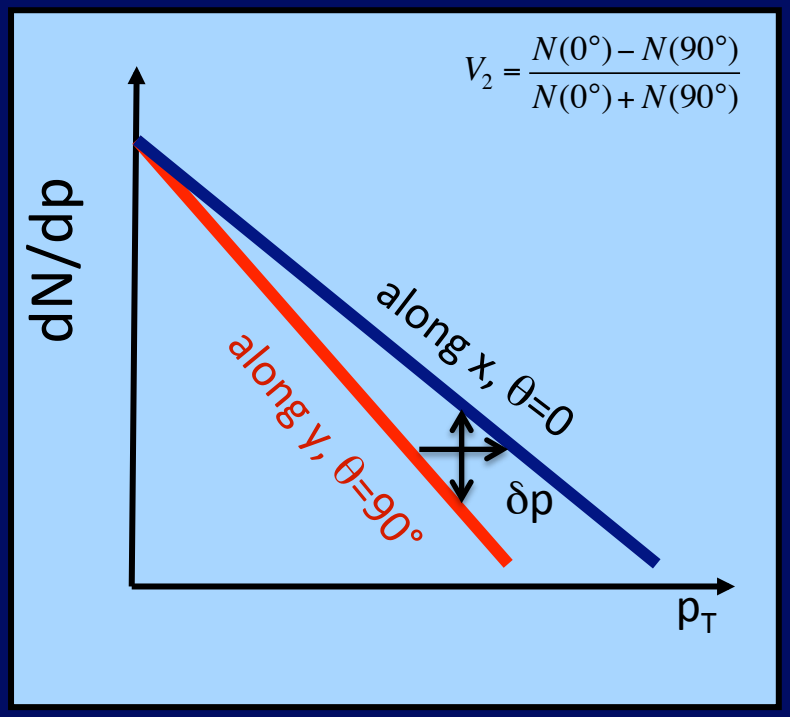

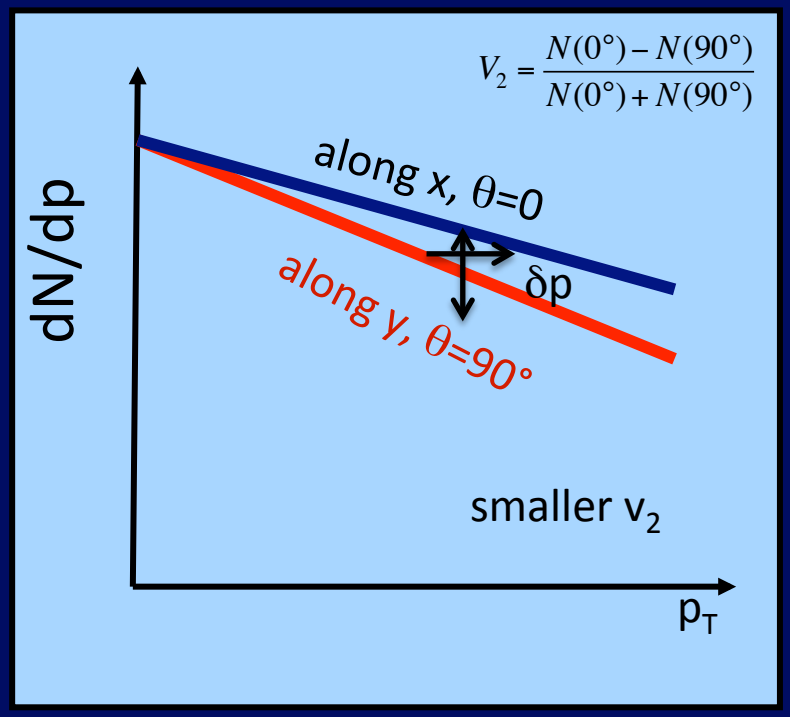

Put it very simplistic:

$$f(p_T, \phi) = e^{-\frac{p_T - \delta p \cos(2\phi)}{T^*}}$$

$$v_2(p_T, \phi) \cong \frac{\delta p}{4T^*}$$

If the momentum δp shift is the same we can expect flatter distribution are less efficient in build-up v2

pT-spectra versus h/s(T)

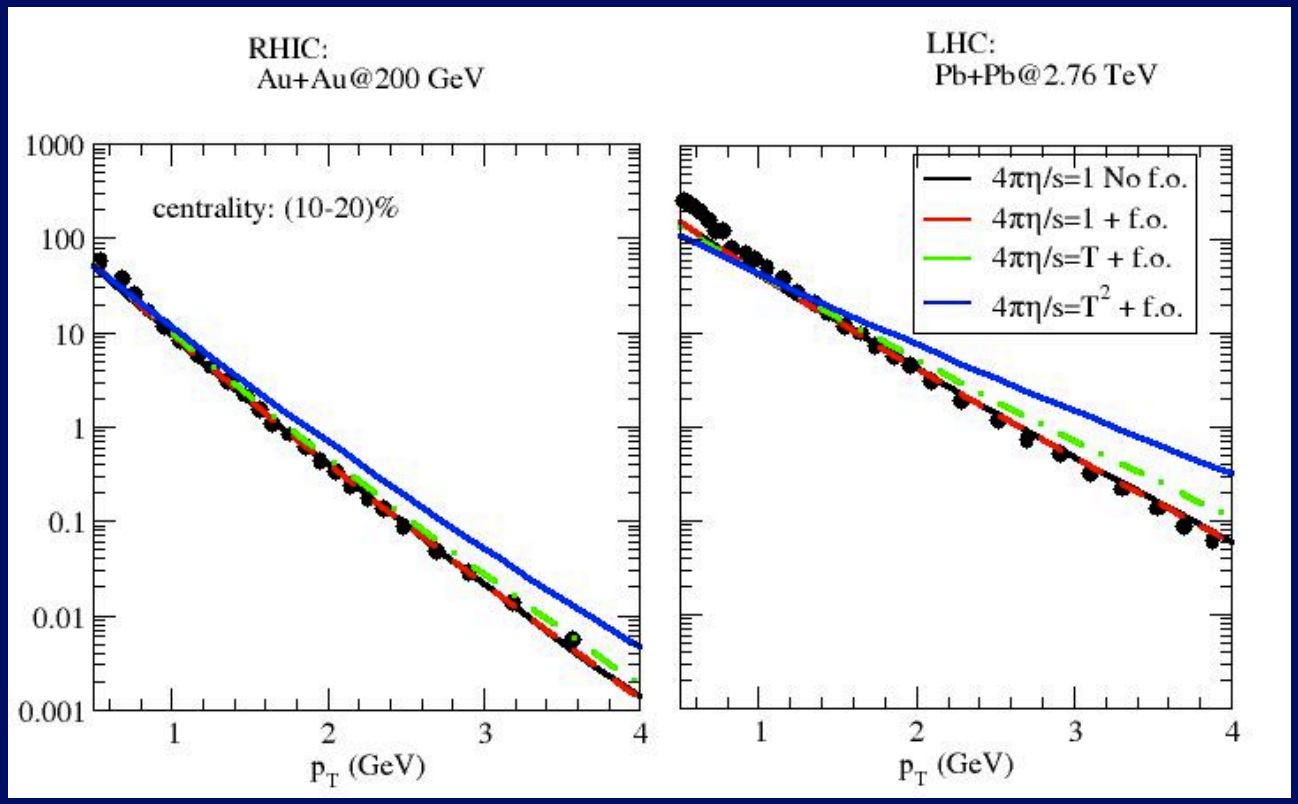

With h/s(T) T^2 we cannot reproduce the data:

- RHIC we can recover the spectra by lowering T_0 by a 30 MeV
- LHC impact of minijets too large one would need a $T_0 \approx 340$ MeV ≈ RHIC

Transport at fixed η/s vs Viscous Hydro a test in 3+1D

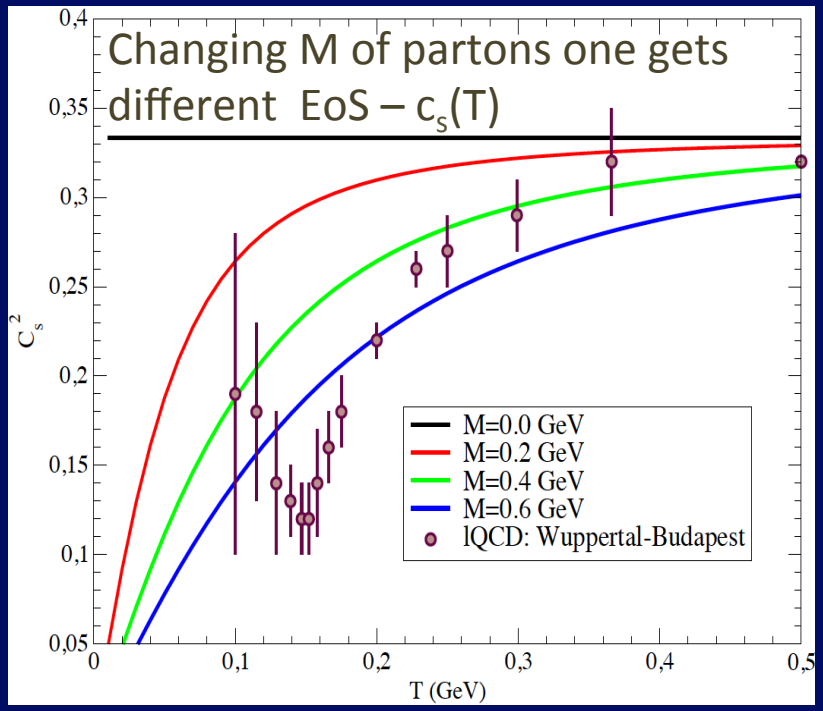

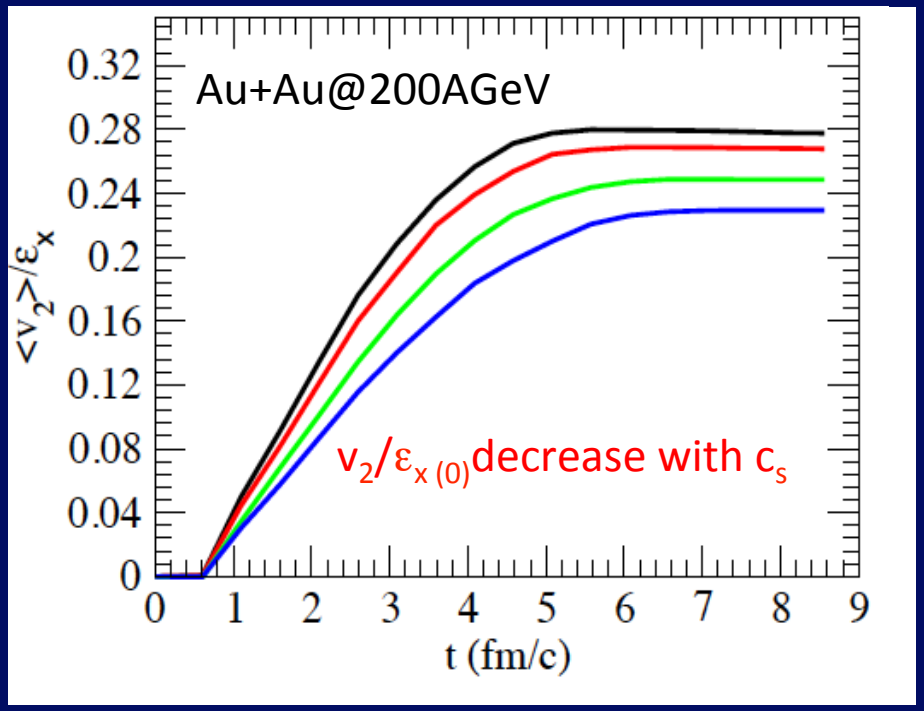

- Time scales, trends and value quite similar to hydro evolution
- An exact comparison under the same conditions has not been done

σ_{tot}=15 mb

Multiplicity & Spectra

- ✧ r-space: standard Glauber condition
- ✧ p-space: Boltzmann-Juttner T_{max}=2(3) T_c [p_T<2 GeV]+ minijet [p_T>2-3GeV]

No fine tuning

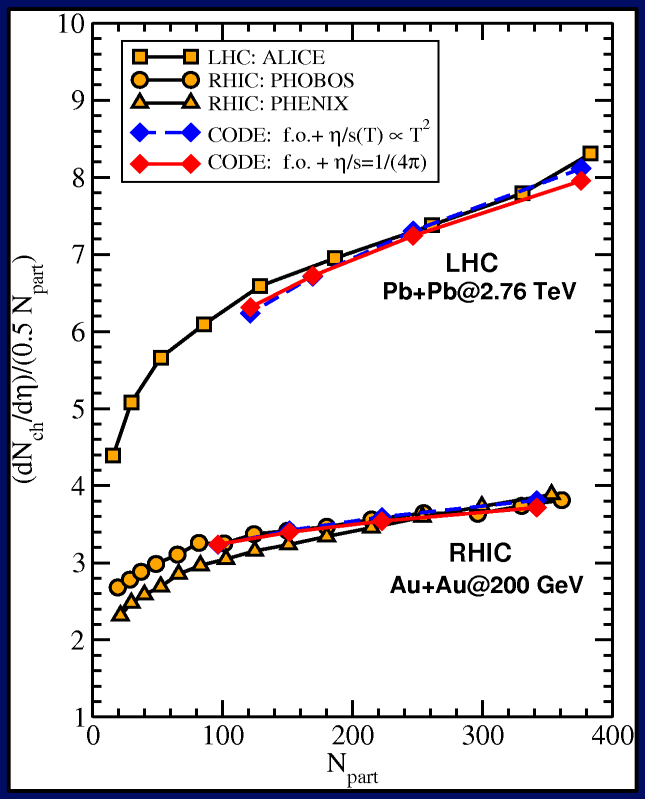

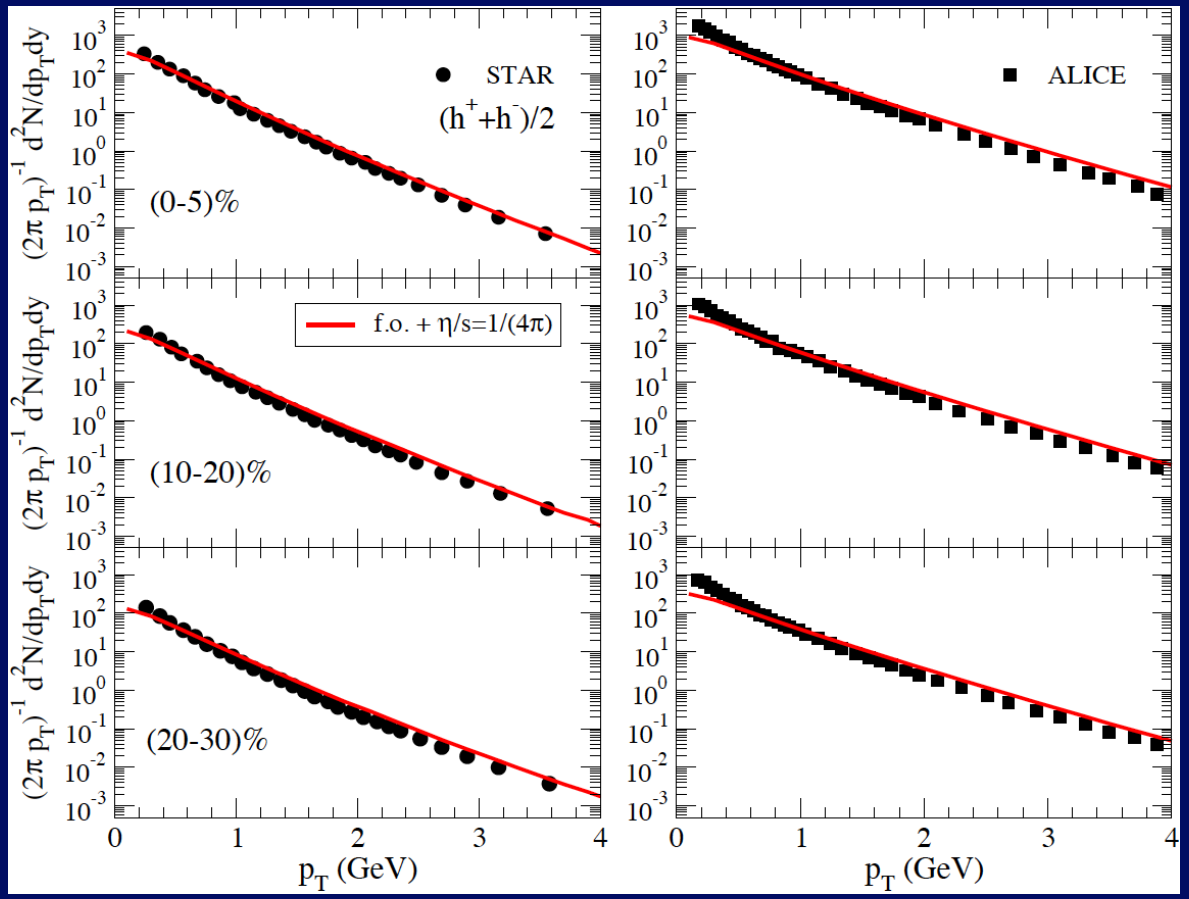

Viscous fluid dynamics for anisotropically expanding fireballs*

Ulrich Heinz
The Ohio State University

RBRC Workshop on
"The Approach to Equilibrium in Strongly Interacting Matter"
Brookhaven National Laboratory, 2-4 April 2014

THE OHIO STATE UNIVERSITY DEPARTMENT OF PHYSICS

*Supported by the U.S. Department of Energy

JET Collaboration

Reference: D. Bazow, U. Heinz, M. Strickland, arXiv:1311:6720 [nucl-th]

Motivation

- Large differences between the longitudinal and transverse expansion rates lead to large shear viscous effects (longitudinal/transverse pressure anisotropies) in the early stage of heavy-ion collisions.

- These cause Israel-Stewart theory to break down at early times.

- Anisotropic hydrodynamics (aHydro) deals with the large longitudinal/transverse pressure anisotropy "nonperturbatively"; this improves the performance of hydrodynamics at early times.

- But: aHydro accounts for only one of the 5 independent components of the shear stress tensor, ignoring the others $\Longrightarrow$ unreliable for the computation of elliptic flow which is sensitive to $\pi^{xx} - \pi^{yy}$, for example.

- On the other hand: these 4 remaining components of the viscous stress tensor become never as large as the longitudinal/transverse pressure difference (with smooth initial density profiles they start out as zero, with fluctuating initial conditions they are initially small).

- $\Longrightarrow$ Idea: treat large longitudinal/transverse pressure anisotropy "nonperturbatively" with aHydro, add remaining viscus corrections "perturbatively" à la Israel-Stewart $\Longrightarrow$ vaHydro.

- Expect better performance at all times compared to both aHydro and Israel-Stewart theory.

Kinetic theory vs. hydrodynamics

Both simultaneously valid if weakly coupled and pressure gradients are small

hydro equations remain structurally unchanged for strongly coupled systems

$$p^\mu \partial_\mu f(x,p) = C(x,p) = \frac{p\cdot u(x)}{\tau_{\rm rel}(x)}\Big(f_{\rm eq}(x,p) - f(x,p)\Big)$$

in relaxation time approximation (RTA)

For conformal systems $\tau_{\rm rel}(x) = c/T(x)$.

Macroscopic currents:

$$j^\mu(x) = \int_p p^\mu\, f(x,p) \equiv \langle p^\mu \rangle$$

$$T^{\mu\nu}(x) = \int_p p^\mu\, p^\nu\, f(x,p) \equiv \langle p^\mu p^\nu \rangle$$

where

$$\int_p \ldots \equiv \frac{g}{(2\pi)^3} \int \frac{d^3p}{E_p} \ldots \equiv \langle \ldots \rangle$$

Ideal fluid dynamics (I)

Ideal hydro $\Longleftrightarrow f(x,p) = f_{\rm iso}(x,p) \equiv f_{\rm iso}\left(\frac{p{\cdot}u(x) - \mu(x)}{T(x)}\right)$

(Locally isotropic momentum distribution, not necessarily exponential or in chemical equilibrium)

If not in chemical equilibrium, then $\partial_\mu j^\mu \neq 0$.

If not exponential in $(p{\cdot}u(x) - \mu(x))/T(x)$, then $C(x,p) \neq 0$, but still $\int_p p^\mu C = 0$ (energy-momentum conservation).

For ideal hydro

$$j^\mu_{\rm id}(x) = n(x)\, u^\mu(x)$$
$$T^{\mu\nu}_{\rm id} = e(x) u^\mu(x) u^\nu(x) - P\big(e(x)\big)\Delta^{\mu\nu}(x)$$

where $\Delta^{\mu\nu} \equiv g^{\mu\nu} - u^\mu u^\nu =$ spatial projector in l.r.f.

Write

$$p^\mu = E u^\mu + p^{\langle\mu\rangle}$$

where $E \equiv u{\cdot}p =$ energy in l.r.f., $p^{\langle\mu\rangle} \equiv \Delta^{\mu\nu} p_\nu =$ spatial momentum in l.r.f.

Ideal fluid dynamics (II)

Ideal hydro equations follow from

$$\partial_\mu j^\mu = \frac{n_{\rm eq} - n(x)}{\tau_{\rm rel}(x)}$$
$$\partial_\mu T^{\mu\nu} = 0$$

which one can solve for $n(x)$, $e(x)$, $u^\mu(x)$.

Then $T(x)$, $\mu(x)$, $P(x)$ follow from the EOS.

Note: if system is locally isotropic but not in chemical and thermal equilibrium, this can be accounted for by non-equilibrium chemical potentials and a non-equilibrium pressure in the EOS $P(e,n) = P(T,\mu)$. In this case one sees non-zero entropy production $\partial_\mu S^\mu \sim 1/\tau_{\rm rel} \neq 0$.

Israel-Stewart viscous fluid dynamics (I)

$$f(x,p) = f_{\rm iso}\left(\frac{p\cdot u(x) - \mu(x)}{T(x)}\right) + \delta f(x,p)$$

Separation made unique by Landau matching:
first define l.r.f. by $T^{\mu\nu}u_\nu = eu^\mu$ with $u^\nu u_\nu = 1 \Longrightarrow$ fixes flow vector u^μ

Next, require

$$e(x) = e_{\rm iso}(T,\mu) \Rightarrow \langle E^2\rangle = \langle E^2\rangle_{\rm iso}(T,\mu)$$
$$n(x) = n_{\rm iso}(T,\mu) \Rightarrow \langle E\rangle = \langle E\rangle_{\rm iso}(T,\mu)$$

$\Longrightarrow \quad \langle E\rangle_\delta = \langle E^2\rangle_\delta = 0 \Longrightarrow$ fixes $T(x)$, $\mu(x)$

Viscous decomposition of j^μ, $T^{\mu\nu}$:

$$j^\mu = j^\mu_{\rm id} + V^\mu \qquad V^\mu = \left\langle p^{\langle\mu\rangle}\right\rangle_\delta$$

$$T^{\mu\nu} = T^{\mu\nu}_{\rm id} - \Pi\Delta^{\mu\nu} + \pi^{\mu\nu} \qquad \Pi = -\tfrac{1}{3}\left\langle p^{\langle\alpha\rangle}p_{\langle\alpha\rangle}\right\rangle_\delta, \quad \pi^{\mu\nu} = \left\langle p^{\langle\mu}p^{\nu\rangle}\right\rangle_\delta .$$

Here $A^{\langle\mu\nu\rangle} \equiv \Delta^{\mu\nu}_{\alpha\beta}A^{\alpha\beta}$ with $\Delta^{\mu\nu}\alpha\beta = \frac{1}{2}\left(\Delta^\mu{}_\alpha\Delta^\nu{}_\beta + \Delta^\nu{}_\alpha\Delta^\mu{}_\beta\right) - \frac{1}{3}\Delta^{\mu\nu}\Delta_{\alpha\beta}$
$\Longrightarrow \pi^{\mu\nu} = T^{\langle\mu\nu\rangle}$ has 5 independent components (3 for (2+1)-d, 1 for (0+1)-d)

Altogether 9 viscous flow degrees of freedom.

Israel-Stewart viscous fluid dynamics (II)

Israel-Stewart equations of motion for viscous pressures (Israel&Stewart 1979, Muronga 2002):
Define $\dot{F} \equiv DF \equiv u^\mu \partial_\mu F,\ \theta \equiv \partial \cdot u, \sigma^{\mu\nu} = \partial^{\langle\mu} u^{\nu\rangle}$:

$$\dot{\Pi} = -\frac{1}{\tau_\Pi}\left[\Pi + \zeta\theta + \Pi\zeta T\partial_\mu\left(\frac{\tau_\Pi u^\mu}{2\zeta T}\right)\right] \equiv -\frac{1}{\tau'_\Pi}\left[\Pi + \zeta'\theta\right],$$

$$\dot{\pi}^{\langle\mu\nu\rangle} \equiv \Delta^{\mu\nu}_{\alpha\beta} D\pi^{\alpha\beta} = -\frac{1}{\tau_\pi}\left[\pi^{\mu\nu} - 2\eta\sigma^{\mu\nu} + \pi^{\mu\nu}\eta T\partial_\mu\left(\frac{\tau_\pi u^\mu}{2\eta T}\right)\right] \equiv -\frac{1}{\tau'_\pi}\left[\pi^{\mu\nu} - 2\eta'\sigma^{\mu\nu}\right],$$

where η, ζ are shear and bulk viscosity (first order transp. coeffs.), τ_Π, τ_π are shear and bulk pressure relaxation times (second order transp. coeffs.), and

$$\tau'_\Pi = \frac{\tau_\Pi}{1+\gamma_\Pi},\ \tau'_\pi = \frac{\tau_\pi}{1+\gamma_\pi},\ \zeta' = \frac{\zeta}{1+\gamma_\Pi},\ \eta' = \frac{\eta}{1+\gamma_\pi}$$

$$\gamma_\Pi = \frac{1}{2}\zeta T\partial_\mu\left(\frac{\tau_\Pi u^\mu}{2\zeta T}\right) \longrightarrow \frac{4}{3}\tau_\Pi\theta,$$

$$\gamma_\pi = \frac{1}{2}\eta T\partial_\mu\left(\frac{\tau_\pi u^\mu}{2\eta T}\right) \longrightarrow \frac{4}{3}\tau_\pi\theta,$$

where the arrow indicates the conformal limit.

Israel-Stewart viscous fluid dynamics (III)

The Israel-Stewart equations are not the most general form of second order equations of motion for the viscous pressures. For a complete set of second-order terms, together with the associated transport coefficients computed from Boltzmann theory, see Denicol, Molnar, Niemi, Rischke, EPJA 48 (2012) 170 (DMNR).

Problem with applying IS theory to heavy-ion collisions:
for early times, as $\tau \to 0$,

$$\tau^2 \sigma^{\eta\eta} = -(\sigma^{xx} + \sigma^{yy}) \to -\frac{2}{3\tau}$$

$\Longrightarrow$ very large viscous corrections! $\Longrightarrow$ δf no longer small.

This problem is caused by the rapid self-similar longitudinal expansion.

Anisotropic hydrodynamics (aHydro) (I)

Martinez and Strickland 2009

A non-perturbative method to account for large shear viscous effects stemming from large difference between longitudinal and transverse expansion rates.

$$f(x,p) = f_{\rm iso}\left(\frac{\sqrt{p_\mu \Xi^{\mu\nu}(x) p_\nu} - \tilde{\mu}(x)}{\Lambda(x)}\right) \equiv f_{\rm RS}(x,p)$$

where $\Xi^{\mu\nu}(x) = u^\mu(x)u^\nu(x) + \xi(x) z^\mu(x) z^\nu x$. (Romatschke&Strickland 2003)
3 flow and 3 "thermodynamic" parameters: $u^\mu(x)$; $\Lambda(x)$, $\tilde{\mu}(x)$, $\xi(x)$.

aHydro decomposition:

$$j^\mu_{\rm RS} = n_{\rm RS} u^\mu, \qquad T^{\mu\nu}_{\rm RS} = e_{\rm RS} u^\mu u^\nu - P_T \Delta^{\mu\nu} + (P_L - P_T) z^\mu z^\nu,$$

where, for massless partons ($m = 0$), the effects of local momentum anisotropy can be factored out:

$$\begin{aligned} n_{\rm RS} &= \langle E \rangle_{\rm RS} = \mathcal{R}_0(\xi) n_{\rm iso}(\Lambda, \tilde{\mu}), \\ e_{\rm RS} &= \langle E^2 \rangle_{\rm RS} = \mathcal{R}(\xi) e_{\rm iso}(\Lambda, \tilde{\mu}), \\ P_{T,L} &= \langle p^2_{T,L} \rangle_{\rm RS} = \mathcal{R}_{T,L}(\xi) P_{\rm iso}(\Lambda, \tilde{\mu}). \end{aligned}$$

(See Strickland's talk for $\mathcal{R}$-functions.) The isotropic pressure is obtained from a locally isotropic EOS,

$$P_{\rm iso}(\Lambda, \tilde{\mu}) = P_{\rm iso}(e_{\rm iso}(\Lambda, \tilde{\mu}), n_{\rm iso}(\Lambda, \tilde{\mu}))$$

For massless noninteracting partons, $P_{\rm iso}(\Lambda, \tilde{\mu}) = \frac{1}{3} e_{\rm iso}(\Lambda, \tilde{\mu})$ independent of chemical composition.

Anisotropic hydrodynamics (aHydro) (II)

Martinez and Strickland 2009

If we want to compare aHydro with ideal and IS viscous hydro, we need to assign the locally anisotropic system an appropriate temperature $T(x) = T\Big(\xi(x), \Lambda(x), \tilde{\mu}(x)\Big)$ and chemical potential $\mu(x) = \mu\Big(\xi(x), \Lambda(x), \tilde{\mu}(x)\Big)$, and think of $f_{\rm RS}(\xi, \Lambda)$ as an expansion around the locally isotropic distribution $f_{\rm iso}(T)$. This is done by "dynamical Landau matching": We demand that $e_{\rm RS}(\xi, \Lambda, \tilde{\mu}) = e_{\rm iso}(T, \mu)$ and $n_{\rm RS}(\xi, \Lambda, \tilde{\mu}) = \mathcal{R}_0(\xi) n_{\rm iso}(T, \mu)$.

For example, using a Boltzmann distribution for $f_{\rm iso}(x, p)$ with $\mu = \tilde{\mu} = 0$, one finds (Martinez & Strickland 2010)

$$T = \Lambda \mathcal{R}^{1/4}(\xi)$$

With this matching we can write

$$T^{\mu\nu}_{\rm RS} = T^{\mu\nu}_{\rm id} - (\Delta P + \Pi_{\rm RS})\Delta^{\mu\nu} + \pi^{\mu\nu}_{\rm RS}$$

where

$$\Delta P + \Pi_{\rm RS} = -\frac{1}{3}\int_p p_\alpha \Delta^{\alpha\beta} p_\beta (f_{\rm RS} - f_{\rm iso}) \qquad (= 0 \text{ for } m = 0),$$

$$\pi^{\mu\nu}_{\rm RS} = \int_p p^{\langle\mu} p^{\nu\rangle}(f_{\rm RS} - f_{\rm iso}) = (P_T - P_L)\,\frac{x^\mu x^\nu + y^\mu y^\nu - 2z^\mu z^\nu}{3}$$

We see that $\pi^{\mu\nu}_{\rm RS}$ has only one independent component, $P_T - P_L$, so aHydro leaves 4 of the 5 components of $\pi^{\mu\nu}$ unaccounted for.

Anisotropic hydrodynamics (aHydro) (III)

Martinez and Strickland 2009

For massless particles we have

$$\frac{P_T - P_L}{P_{\rm iso}(e)} = \mathcal{R}_T(\xi) - \mathcal{R}_L(\xi),$$

so the EOM for $\pi^{\mu\nu}_{\rm RS}$ can be replaced by an EOM for ξ.

For $m \neq 0$, to separate ΔP from the viscous pressure Π, we need an "anisotropic EOS" for

$$\frac{\Delta P}{P_{\rm iso}} \equiv \frac{2P_T + P_L}{3P_{\rm iso}} - 1.$$

Viscous anisotropic hydrodynamics (vaHydro) (I)

$$f(x,p) = f_{\rm RS}(x,p) + \delta\tilde{f}(x,p) = f_{\rm iso}\left(\frac{\sqrt{p_\mu \Xi^{\mu\nu}(x) p_\nu} - \tilde{\mu}(x)}{\Lambda(x)}\right) + \delta\tilde{f}(x,p)$$

Landau matching: $T^\mu{}_\nu u^\nu = e u^\mu$ with $u^\mu u_\mu = 1 \Longrightarrow$ fixes u^μ

no contribution to e, n from $\delta\tilde{f}$: $\langle E\rangle_{\tilde{\delta}} = \langle E\rangle_{\tilde{\delta}} = 0 \Longrightarrow$ fixes $\Lambda, \tilde{\mu}$.

no contribution to $P_T - P_L$ from $\delta\tilde{f}$: $\frac{x_\mu x_\nu + y_\mu y_\nu - 2 z_\mu z_\nu}{2}\langle p^{\langle\mu} p^{\nu\rangle}\rangle_{\tilde{\delta}} = 0 \Longrightarrow$ fixes ξ.

vaHydro decomposition:

$$j^\mu = j^\mu_{\rm RS} + \tilde{V}^\mu, \qquad \tilde{V}^\mu = \left\langle p^{\langle\mu\rangle}\right\rangle_{\tilde{\delta}},$$

$$T^{\mu\nu} = T^{\mu\nu}_{\rm RS} - \tilde{\Pi}\Delta^{\mu\nu} + \tilde{\pi}^{\mu\nu}, \qquad \tilde{\Pi} = -\frac{1}{3}\left\langle p^{\langle\alpha\rangle} p_{\langle\alpha\rangle}\right\rangle_{\tilde{\delta}}, \quad \tilde{\pi}^{\mu\nu} = \left\langle p^{\langle\mu} p^{\nu\rangle}\right\rangle_{\tilde{\delta}},$$

$u_\mu \tilde{\pi}^{\mu\nu} = \tilde{\pi}^{\mu\nu} u_\nu = (x_\mu x_\nu + y_\mu y_\nu - 2 z_\mu z_\nu)\tilde{\pi}^{\mu\nu} = \tilde{\pi}^\mu_\mu = 0 \Longrightarrow \tilde{\pi}^{\mu\nu}$ has 4 degrees of freedom.

Strategy: solve hydrodynamic equations for aHydro (which treat $P_T - P_L$ nonperturbatively) with added viscous flows from $\delta\tilde{f}$, together with IS-like "perturbative" equations of motion for $\tilde{\Pi}$, $\tilde{V}^\mu$, $\tilde{\pi}^{\mu\nu}$.

Viscous anisotropic hydrodynamics (vaHydro) (II)

Hydrodynamic equations of motion:

$\partial_\mu j^\mu = C \equiv \int_p C(x,p) \Longrightarrow \dot{n}_{\rm RS} = -n_{\rm RS}\theta - \partial_\mu \tilde{V}^\mu + \frac{n_{\rm RS}-n_{\rm iso}}{\tau_{\rm rel}}$ in RTA

$\partial_\mu T^{\mu\nu} = 0 \Longrightarrow$

$$\dot{e} = -(e+P_T)\theta_\perp - (e+P_L)\frac{u_0}{\tau} - \tilde{\Pi}\theta + \tilde{\pi}^{\mu\nu}\sigma_{\mu\nu},$$

$$(e+P_T+\tilde{\Pi})\dot{u}_\perp = -\partial_\perp(P_T+\tilde{\Pi}) - u_\perp(\dot{P}_T+\dot{\tilde{\Pi}}) - u_\perp(P_T-P_L)\frac{u_0}{\tau} + \left(\frac{u_x\Delta^1{}_\nu+u_y\Delta^2{}_\nu}{u_\perp}\right)\partial_\mu\tilde{\pi}^{\mu\nu},$$

$$(e+P_T+\tilde{\Pi})u_\perp\dot{\phi}_u = -D_\perp(P_T+\tilde{\Pi}) - \frac{u_y\partial_\mu\tilde{\pi}^{\mu 1}-u_x\partial_\mu\tilde{\pi}^{\mu 2}}{u_\perp},$$

where $\theta_\perp = \partial_\tau u_0 + \nabla_\perp\cdot\boldsymbol{u}_\perp$ and $D_\perp = (u_x\partial_y - u_y\partial_x)/u_\perp$.

To derive **equations of motion for $\tilde{\Pi}$, $\tilde{V}^\mu$, and $\tilde{\pi}^{\mu\nu}$**, we follow DMNR (2012). Ignoring heat conduction by setting $\tilde{\mu} = 0$ and taking $m = 0$ we find (Bazow, UH, Strickland, 1311.6720)

$$\dot{\tilde{\pi}}^{\mu\nu} = -2\dot{u}_\alpha\tilde{\pi}^{\alpha(\mu}u^{\nu)} - \frac{1}{\tau_{\rm rel}}\Big[(P-P_T)\Delta^{\mu\nu} + (P_L-P_T)z^\mu z^\nu + \tilde{\pi}^{\mu\nu}\Big] + \mathcal{K}_0^{\mu\nu} + \mathcal{L}_0^{\mu\nu} + \mathcal{H}_0^{\mu\nu\lambda}\dot{z}_\lambda$$
$$+\mathcal{Q}_0^{\mu\nu\lambda\alpha}\nabla_\lambda u_\alpha + \mathcal{X}_0^{\mu\nu\lambda}u^\alpha\nabla_\lambda z_\alpha - 2\lambda^0_{\pi\pi}\tilde{\pi}^{\lambda\langle\mu}\sigma^{\nu\rangle}_{\ \lambda} + 2\tilde{\pi}^{\lambda\langle\mu}\omega^{\nu\rangle}_{\ \lambda} - 2\delta^0_{\pi\pi}\tilde{\pi}^{\mu\nu}\theta,$$

Test of vaHydro: (0+1)-dimensional expansion (I)

As you heard in Mike Strickland's talk, for (0+1)-d (longitudinally boost-invariant) expansion, the BE can be solved exactly in RTA, and the solution can be used to test the various macroscopic hydrodynamic approximation schemes.

Setting homogeneous initial conditions in r and η_s and zero transverse flow, $\tilde{\pi}^{\mu\nu}$ reduces to a single non-vanishing component $\tilde{\pi}$: $\tilde{\pi}^{\mu\nu} = \mathrm{diag}(0, -\tilde{\pi}/2, -\tilde{\pi}/2, \tilde{\pi})$ at $z = 0$.

We use the factorization $n_{\mathrm{RS}}(\xi\Lambda) = \mathcal{R}_0(\xi) n_{\mathrm{iso}}(\Lambda)$ etc. to get EOMs for $\dot{\xi}$, $\dot{\Lambda}$, $\dot{\tilde{\pi}}$:

$$\frac{\dot{\xi}}{1+\xi} - 6\frac{\dot{\Lambda}}{\Lambda} = \frac{2}{\tau} + \frac{2}{\tau_{\mathrm{rel}}}\left(1 - \sqrt{1+\xi}\,\mathcal{R}^{3/4}(\xi)\right) \ ,$$

$$\mathcal{R}'(\xi)\dot{\xi} + 4\mathcal{R}(\xi)\frac{\dot{\Lambda}}{\Lambda} = -\left(\mathcal{R}(\xi) + \frac{1}{3}\mathcal{R}_L(\xi)\right)\frac{1}{\tau} + \frac{\tilde{\pi}}{e_{\mathrm{iso}}(\Lambda)\tau},$$

$$\dot{\tilde{\pi}} = -\frac{1}{\tau_{\mathrm{rel}}}\left[\left(\mathcal{R}(\xi) - \mathcal{R}_{\mathrm{L}}(\xi)\right)P_{\mathrm{iso}}(\Lambda) + \tilde{\pi}\right] - \frac{38}{21}\frac{\tilde{\pi}}{\tau}$$
$$+12\left[\frac{\dot{\Lambda}}{\Lambda}\left(\mathcal{R}_{\mathrm{L}}(\xi) - \frac{1}{3}\mathcal{R}(\xi)\right) + \left(\frac{1+\xi}{\tau} - \frac{\dot{\xi}}{2}\right)\left(\mathcal{R}^{zzzz}_{-1}(\xi) - \frac{1}{3}\mathcal{R}^{zz}_{1}(\xi)\right)\right]P_{\mathrm{iso}}(\Lambda),$$

τ_{del} and η/s are related by (Denicol, Koide, Rischke, PRL 105 (2010))

$$\tau_{\mathrm{rel}} = 5\frac{\eta/s}{T} = 5\frac{\eta/s}{\mathcal{R}^{1/4}(\xi)\Lambda}$$

We solve these equations and compare with the exact solution:

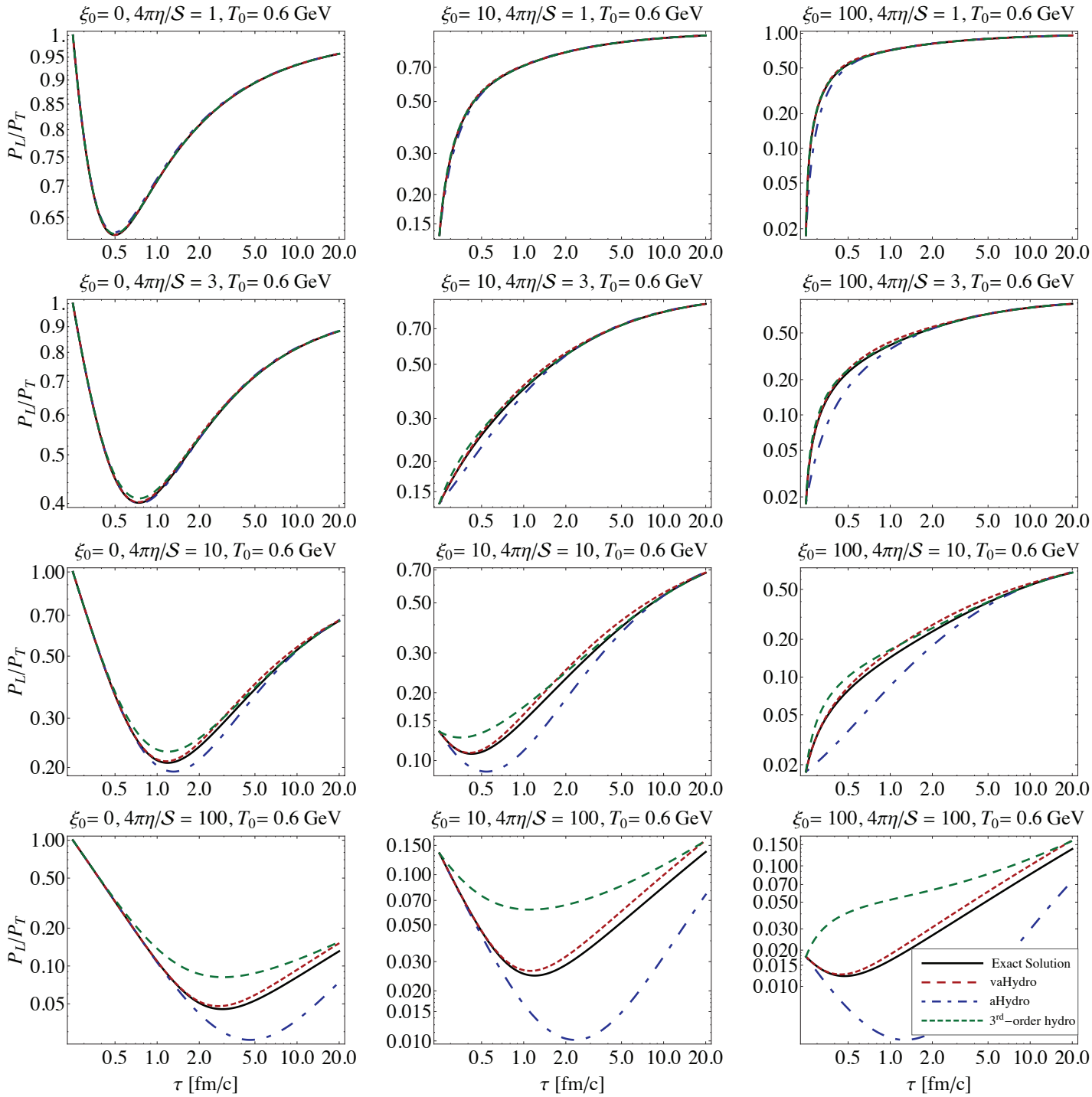
ξ_0= 0, $4\pi\eta/\mathcal{S}$ = 1, T_0= 0.6 GeV
ξ_0= 10, $4\pi\eta/\mathcal{S}$ = 1, T_0= 0.6 GeV
ξ_0= 100, $4\pi\eta/\mathcal{S}$ = 1, T_0= 0.6 GeV
ξ_0= 0, $4\pi\eta/\mathcal{S}$ = 3, T_0= 0.6 GeV
ξ_0= 10, $4\pi\eta/\mathcal{S}$ = 3, T_0= 0.6 GeV
ξ_0= 100, $4\pi\eta/\mathcal{S}$ = 3, T_0= 0.6 GeV
ξ_0= 0, $4\pi\eta/\mathcal{S}$ = 10, T_0= 0.6 GeV
ξ_0= 10, $4\pi\eta/\mathcal{S}$ = 10, T_0= 0.6 GeV
ξ_0= 100, $4\pi\eta/\mathcal{S}$ = 10, T_0= 0.6 GeV
ξ_0= 0, $4\pi\eta/\mathcal{S}$ = 100, T_0= 0.6 GeV
ξ_0= 10, $4\pi\eta/\mathcal{S}$ = 100, T_0= 0.6 GeV
ξ_0= 100, $4\pi\eta/\mathcal{S}$ = 100, T_0= 0.6 GeV
P_L/P_T
τ [fm/c]
Exact Solution
vaHydro
aHydro
3rd−order hydro

Test of vaHydro: (0+1)-dimensional expansion (II)

Pressure anisotropy P_L/P_T vs. τ:

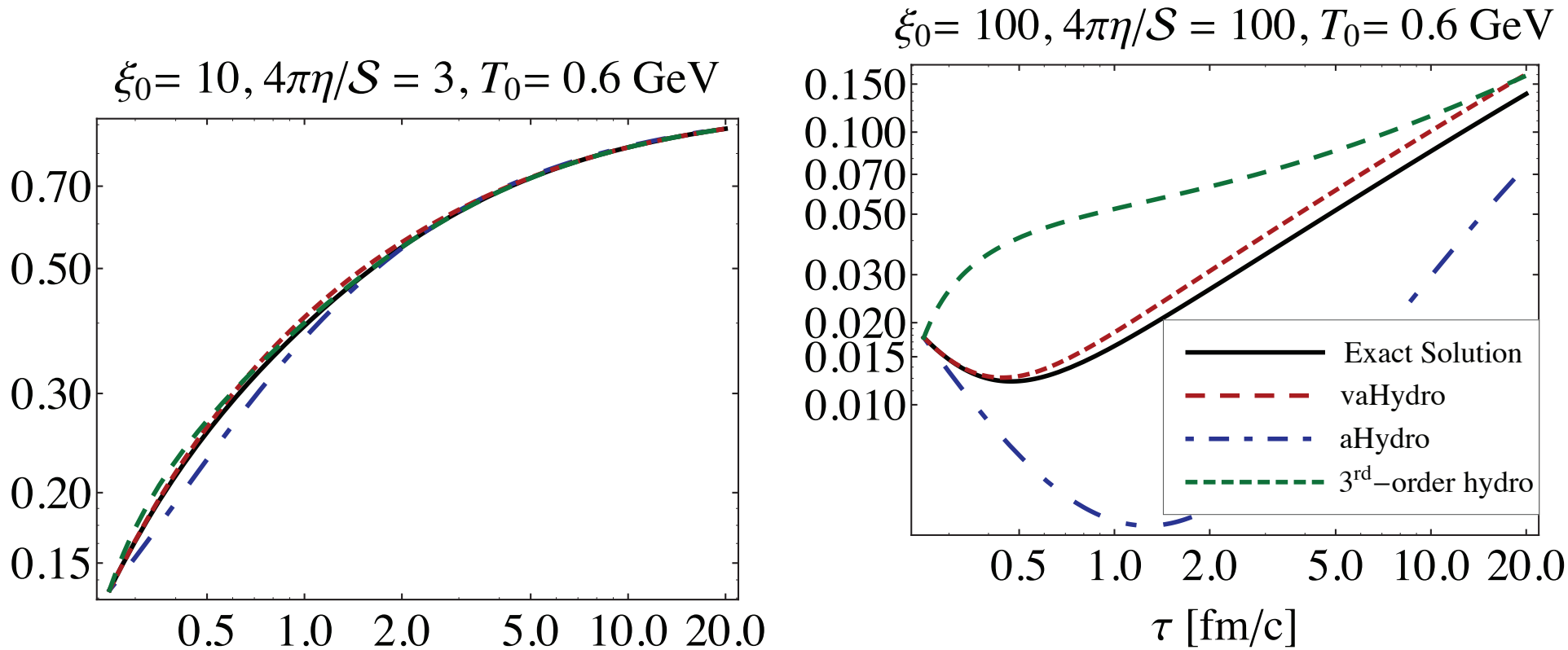

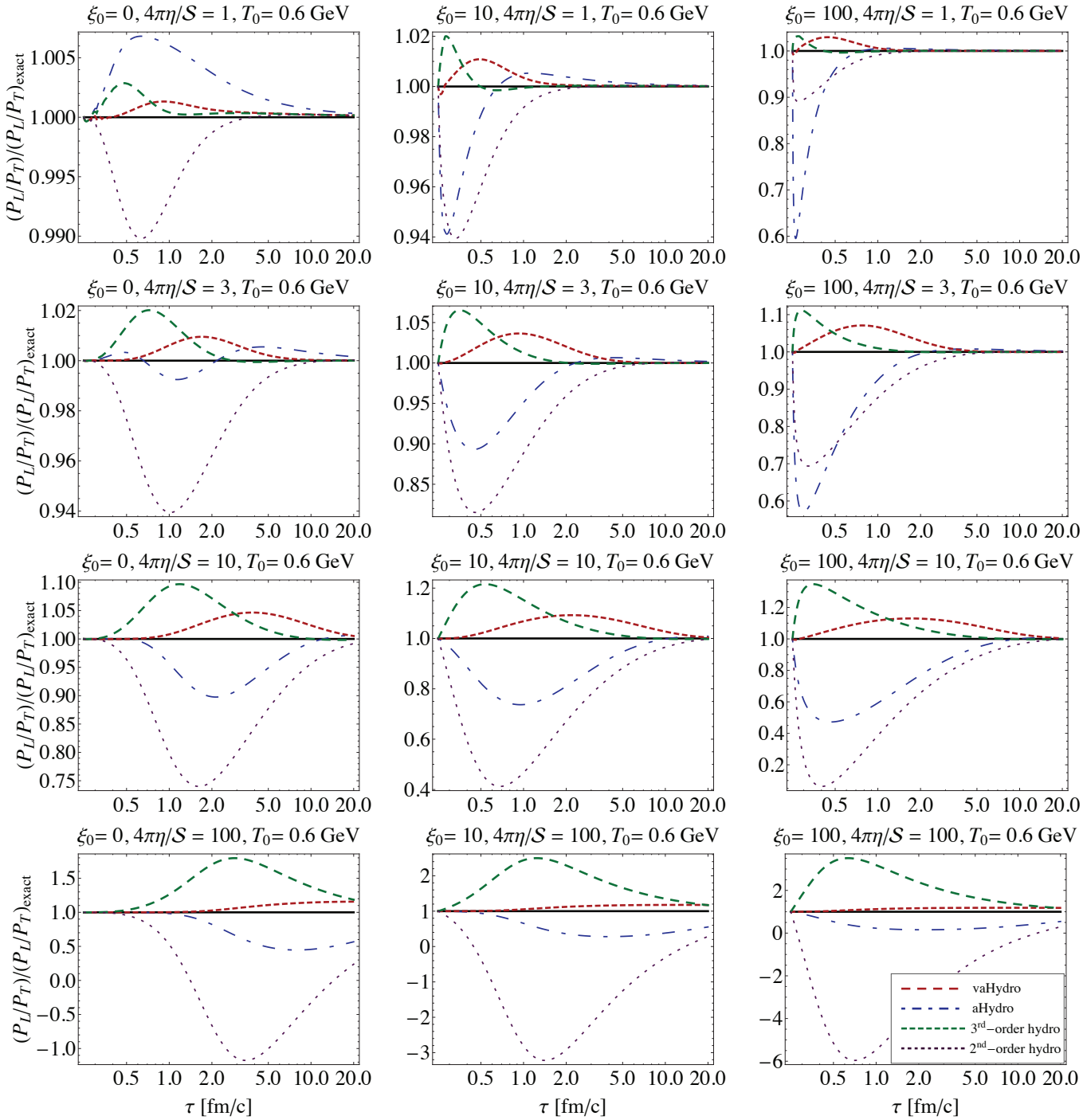
ξ_0= 0, $4\pi\eta/\mathcal{S}$ = 1, T_0= 0.6 GeV
ξ_0= 10, $4\pi\eta/\mathcal{S}$ = 1, T_0= 0.6 GeV
ξ_0= 100, $4\pi\eta/\mathcal{S}$ = 1, T_0= 0.6 GeV
ξ_0= 0, $4\pi\eta/\mathcal{S}$ = 3, T_0= 0.6 GeV
ξ_0= 10, $4\pi\eta/\mathcal{S}$ = 3, T_0= 0.6 GeV
ξ_0= 100, $4\pi\eta/\mathcal{S}$ = 3, T_0= 0.6 GeV
ξ_0= 0, $4\pi\eta/\mathcal{S}$ = 10, T_0= 0.6 GeV
ξ_0= 10, $4\pi\eta/\mathcal{S}$ = 10, T_0= 0.6 GeV
ξ_0= 100, $4\pi\eta/\mathcal{S}$ = 10, T_0= 0.6 GeV
ξ_0= 0, $4\pi\eta/\mathcal{S}$ = 100, T_0= 0.6 GeV
ξ_0= 10, $4\pi\eta/\mathcal{S}$ = 100, T_0= 0.6 GeV
ξ_0= 100, $4\pi\eta/\mathcal{S}$ = 100, T_0= 0.6 GeV
$(P_L/P_T)/(P_L/P_T)_{\rm exact}$
τ [fm/c]
0.5 1.0 2.0 5.0 10.0 20.0
vaHydro
aHydro
3rd−order hydro
2nd−order hydro

Test of vaHydro: (0+1)-dimensional expansion (III)

Total entropy (particle) production $\frac{n(\tau_f)\cdot\tau_f}{n(\tau_0)\cdot\tau_0} - 1$

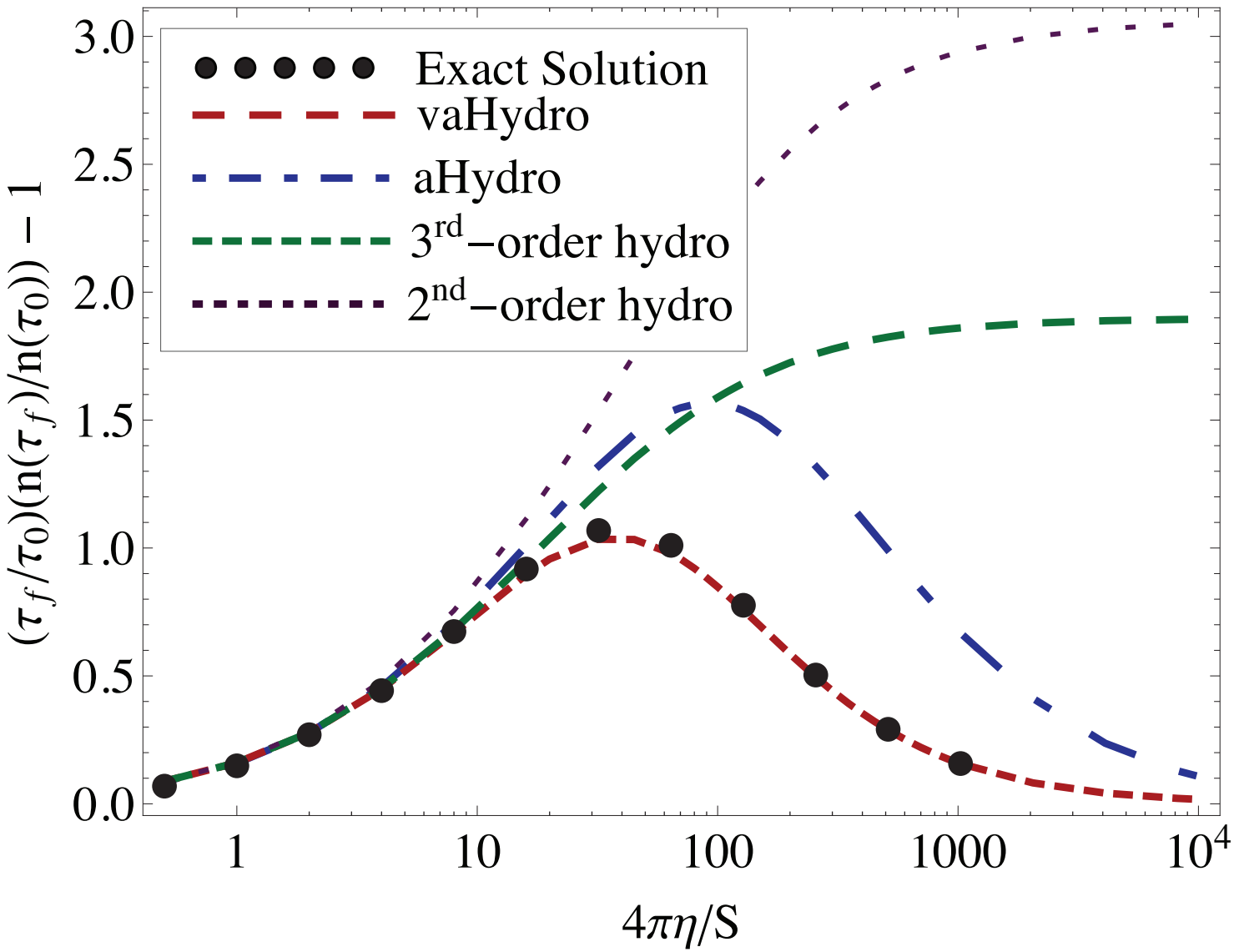

Conclusions

- For early times and/or near the transverse edge in heavy-ion collision fireballs, rapid longitudinal expansion generates large inverse Reynolds numbers for the shear pressure, $\mathrm{R}_\pi^{-1} = \sqrt{\pi^{\mu\nu}\pi_{\mu\nu}}/P_{\rm iso}$, causing Israel-Stewart second order viscous hydrodynamics to break down.
- The large local pressure anisotropies caused by a large difference in longitudinal and transverse expansion rates can be treated efficiently by using the non-perturbative aHydro approach which is based on an expanseion around a locally spheroidally deformed distribution $f_{\rm RS}$.
- This strongly reduces the shear inverse Reynolds numbers $\tilde{\mathrm{R}}_\pi^{-1} = \sqrt{\tilde{\pi}^{\mu\nu}\tilde{\pi}_{\mu\nu}}/\mathcal{P}_{\rm iso}$ associated with the remaining shear stress tensor $\tilde{\pi}^{\mu\nu}$ resulting from the much smaller deviation $\delta\tilde{f}$ of the local distribution function from $f_{\rm RS}$.
- vaHydro combines the advantages of aHydro with a complete (although perturbative) second-order treatment of all remaining viscous effects à la Israel-Stewart.
- In a test of (0+1)-d expansion, which maximizes the difference between longitudinal and transverse expansion rates, against an exact solution of the Boltzmann equation, vaHydro outperforms all other known hydrodynamic approximation schemes by a considerable margin.
- This should open the door in (3+1)-d systems to match microscopic pre-equilibrium theories to viscous hydrodynamics at earlier times than possible with IS-theory and its variants.

The approach to hydrodynamics in holographic gauge theories

Michał P. Heller
Universiteit van Amsterdam, the Netherlands
&
National Centre for Nuclear Research, Poland

NWO
Netherlands Organisation for Scientific Research
NATIONAL SCIENCE CENTRE
POLAND
stringtheory.pl
Teoria strun w Polsce

holography

$=_{\text{for us}}$

ab initio approach to certain YM theories*

* All that I am going to say applies directly to N=4 SYM at large N_c and strong 't Hooft coupling. This theory is conformal.

Hydrodynamics is an asymptotic series

1302.0697 [hep-th] PRL 110 (2013) 211602: MPH, R. A. Janik & P. Witaszczyk

$$\epsilon = \frac{3}{8} N_c^2 \pi^2 \frac{1}{\tau^{4/3}} \left(\epsilon_2 + \epsilon_3 \frac{1}{\tau^{2/3}} + \epsilon_4 \frac{1}{\tau^{4/3}} + \dots \right) \quad (T^{-1} \nabla_\mu u^\nu \sim \tau^{-2/3})$$

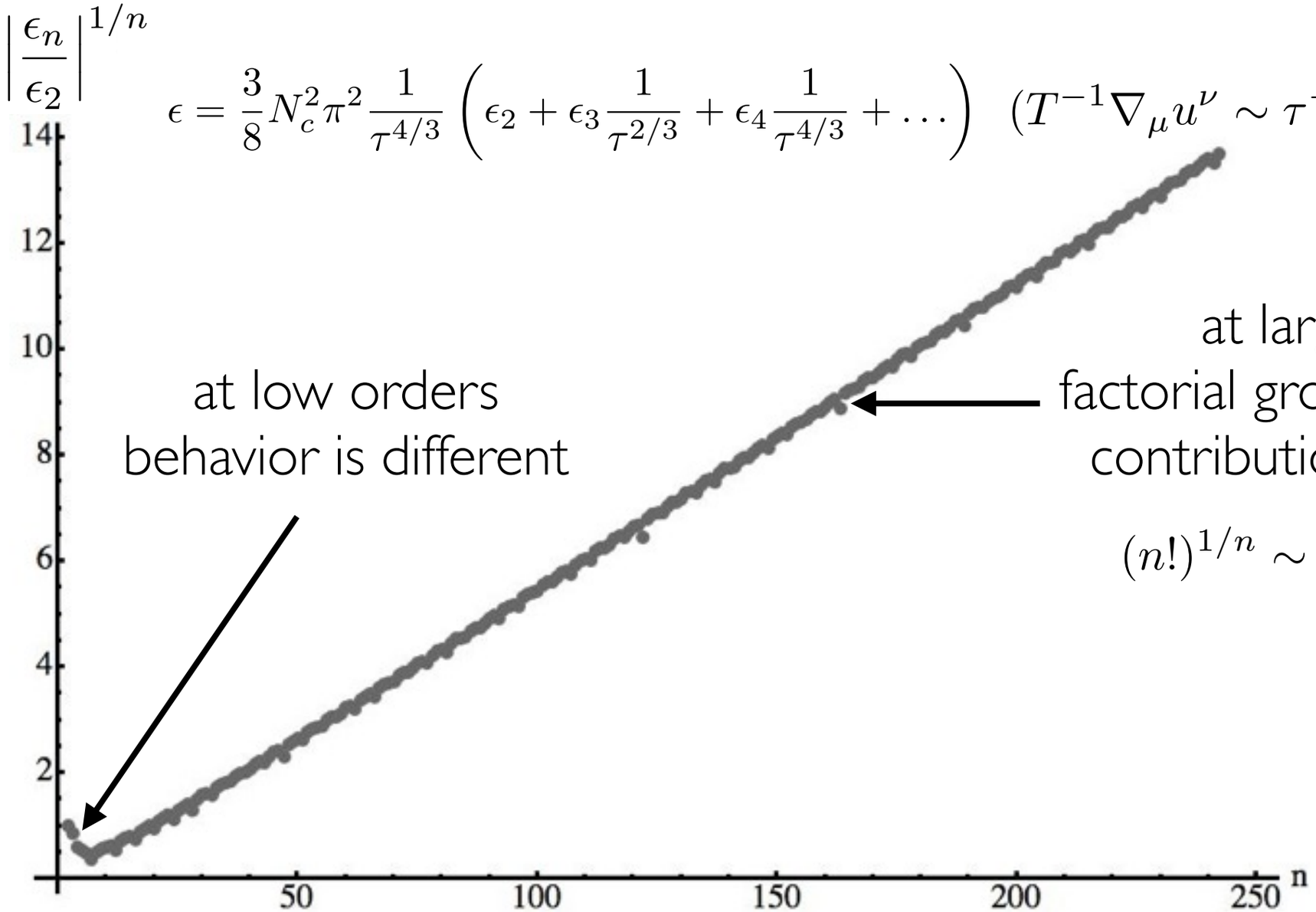

at low orders
behavior is different

at large orders
factorial growth of gradient
contributions with order

$$(n!)^{1/n} \sim \frac{(2\pi n)^{1/2n}}{e} \cdot n$$

First evidence that hydrodynamic expansion has a zero radius of convergence!

Fast hydrodynamization

1103.3452 [hep-th] PRL 108 (2012) 201602: MPH, R. A. Janik & P. Witaszczyk

similar findings in Chesler & Yaffe 0906.4426 & 1011.3562

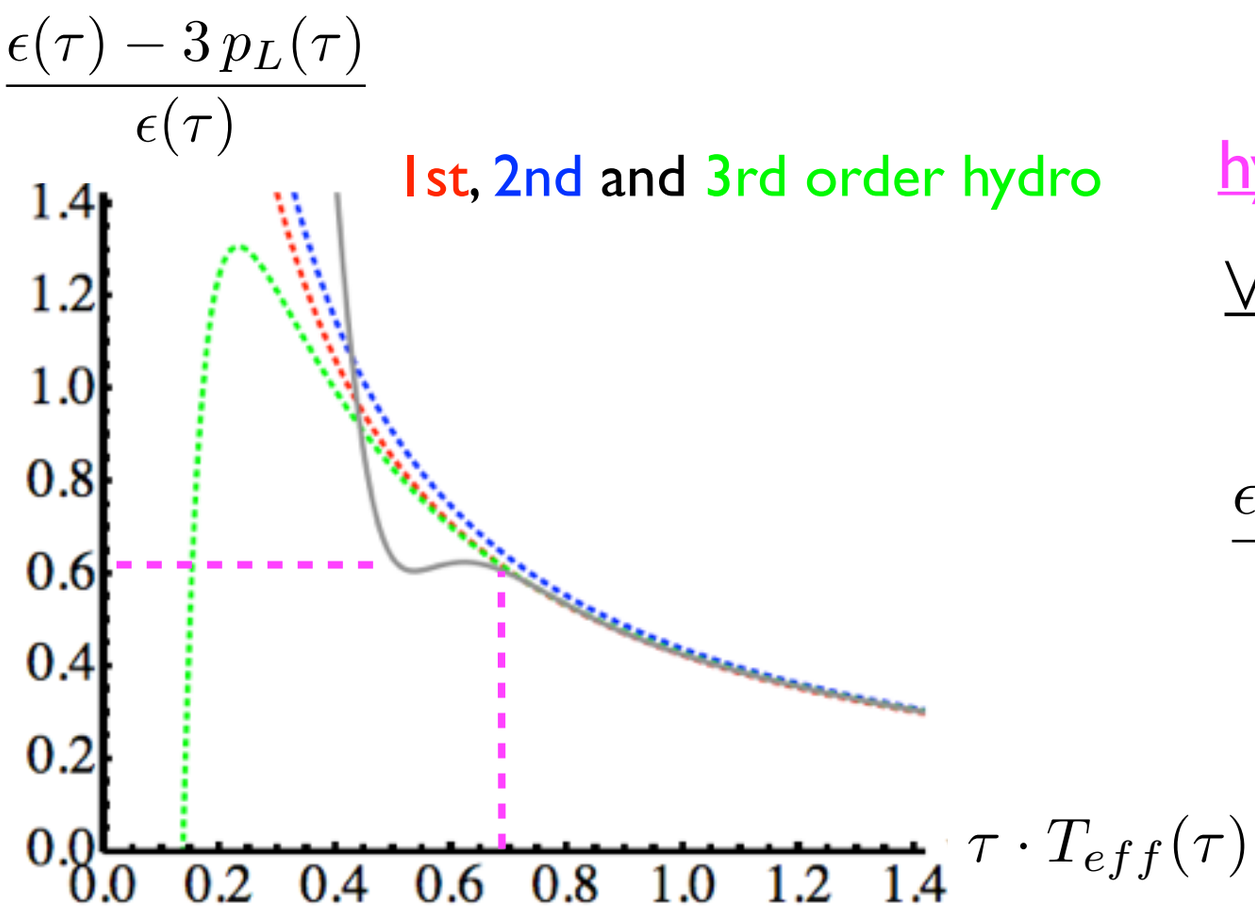

hydrodynamization $\neq$ thermalization:

Viscous hydro works remarkably well despite huge anisotropies due to (shear) gradients.

$$\frac{\epsilon(\tau) - 3p_L(\tau)}{\epsilon(\tau)} = 0.6 \longrightarrow \frac{p_T(\tau) - p_L(\tau)}{\frac{1}{3}\epsilon(\tau)} = 0.9$$

(RHIC c=0-5%: $0.25\,\mathrm{fm} \times 500\,\mathrm{MeV} = 0.63$)

0801.4361 [nucl-th] W. Broniowski et al.

Consequences of hydrodynamization

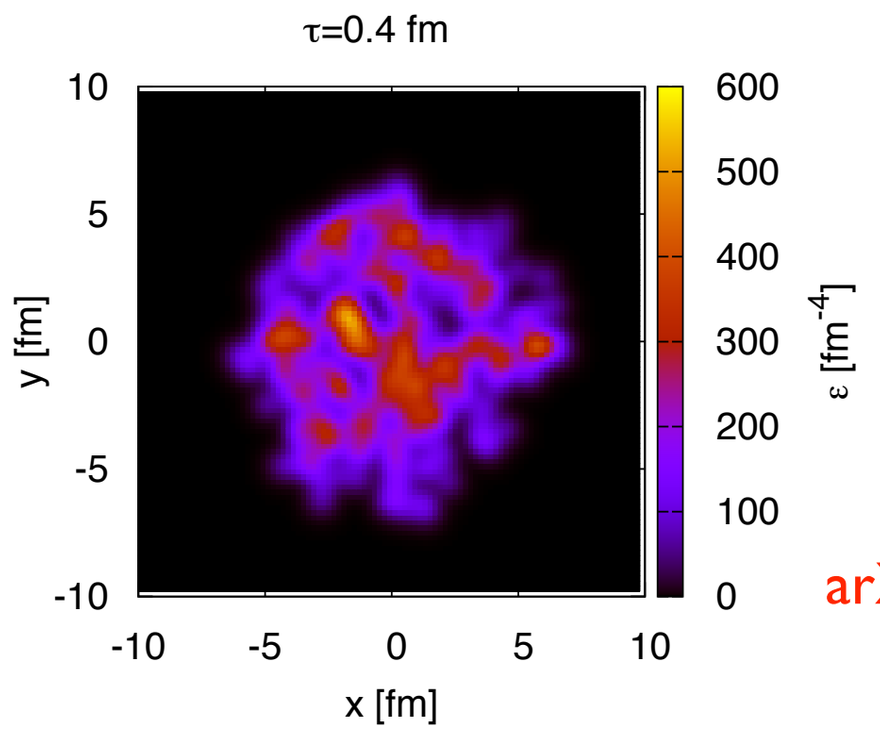

Using hydro under such circumstances might not be a totally outrageous idea.

arXiv:1009.3244 [hep-ph]
Schenke, Jeon & Gale

Possibility of significant entropy production during hydrodynamics expansion due to large shear

$$\frac{\Delta S_{hydro}}{\Delta S_{total}} \text{ can be } \sim 15\text{-}30\ \%$$

estimated using the data from

1103.3452 [hep-th] PRL 108 (2012) 201602:
MPH, R. A. Janik & P. Witaszczyk

A new look at the generalized Müller-Israel-Stewart theory

1404.xxxx [hep-th]: MPH, R. Janik, M. Spaliński, P. Witaszczyk

DOFs of strongly coupled plasmas

Kovtun & Starinets
[hep-th/0506184]

Consider small amplitude perturbations ($\delta T_{\mu\nu}/{N_c}^2 \ll T^4$) on top of a holographic plasma

$$T_{\mu\nu} = \frac{1}{8}\pi^2 N_c^2 T^4 \,\mathrm{diag}\,(3,1,1,1)_{\mu\nu} + \delta T_{\mu\nu} \quad (\sim e^{-i\,\omega(k)\,t + i\,\vec{k}\cdot\vec{x}})$$

Dissipation leads to modes with complex $\omega(k)$, which look like

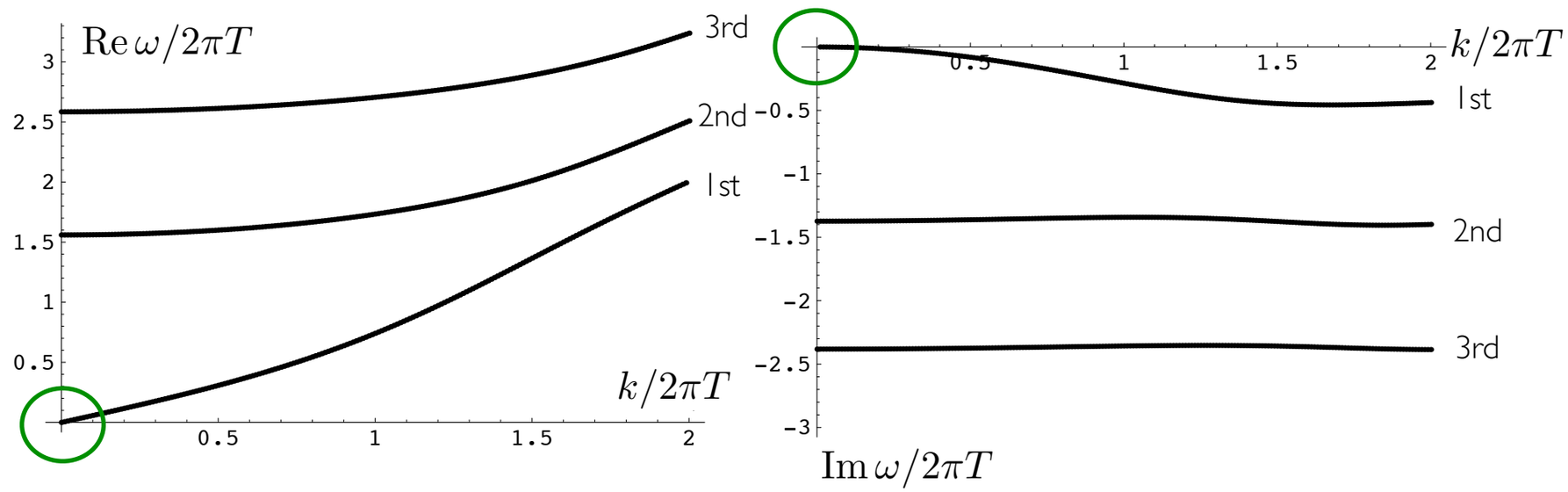

$$\left.\frac{\partial\omega}{\partial k}\right|_{k\to 0} = c_{sound}$$

$\omega(k) \to 0$ as $k \to 0$: slowly dissipating modes (hydrodynamic sound waves)

all the rest: far from equilibrium (QNM) modes dampened over $t_{therm} = \mathcal{O}(1)/T$

Generalized Müller-Israel-Stewart relativistic "hydro"

0712.2451 [hep-th] R. Baier et al.

$$\nabla_\mu\Big(\epsilon\, u^\mu u^\nu + P(\epsilon)\,\{g^{\mu\nu} + u^\mu u^\nu\} - \eta(\epsilon)\sigma^{\mu\nu}\Big) = 0 \longrightarrow \text{acausal modes: } \omega = -i\frac{\eta}{\epsilon + P}k^2$$

Idea: $\nabla_\mu\Big(\epsilon\, u^\mu u^\nu + P(\epsilon)\,\{g^{\mu\nu} + u^\mu u^\nu\} + \Pi^{\mu\nu}\Big) = 0$ + pheno EoM for $\Pi^{\mu\nu}$ such that:

1) the set reproduces low order hydro, 2) ~~acausal modes~~, 3) $\exists$ entropy current.

The following equation turns out to do the job:

$$\boxed{\Pi^{\mu\nu} = -\eta\sigma^{\mu\nu} - \tau_\Pi\Big[{}^{\langle}D\Pi^{\mu\nu\rangle}}\Big. + \frac{d}{d-1}\Pi^{\mu\nu}(\nabla\cdot u)\Big]$$
$$+\,\kappa\Big[R^{\langle\mu\nu\rangle} - (d-2)u_\alpha R^{\alpha\langle\mu\nu\rangle\beta}u_\beta\Big]$$
$$+\,\frac{\lambda_1}{\eta^2}\Pi^{\langle\mu}{}_\lambda\Pi^{\nu\rangle\lambda} - \frac{\lambda_2}{\eta}\Pi^{\langle\mu}{}_\lambda\Omega^{\nu\rangle\lambda} + \lambda_3\Omega^{\langle\mu}{}_\lambda\Omega^{\nu\rangle\lambda}$$

The generalized Müller-Israel-Stewart theory is a <u>UV-completion of hydro</u>.

Why? Because **its structure** leads to the nonhydro mode $\Pi^{\mu\nu} - (-\eta\sigma^{\mu\nu}) \sim e^{-\tau_\Pi^{-1}t}$.

EOMs for non-hydrodynamic DOFs

The lowest quasinormal mode controls the direct approach to hydrodynamics.

Idea: "improve" hydrodynamics in a <u>systematic way</u> by including this new DOF.

ideologically, similar to anisotropic hydro ⟶ M. Strickland's talk

MIS theory does sth similar, but with $\mathrm{Re}(\omega) = 0$! How to add these oscillations?

Basic idea: add the second derivative to MIS constitutive relation for $\Pi_{\mu\nu}$.

see also 1104.2415 [hep-th]: Noronha & Denicol

MIS (neglecting gradients of fluid variables' and nonlinearities):

$$\nabla_\mu \left\{ P(T)(\eta^{\mu\nu} + 4u^\mu u^\nu) + \Pi_{\mu\nu} \right\} = 0 \quad \text{and} \quad \boxed{\hat{\tau}_\Pi \frac{1}{T} \mathcal{D}\, \Pi_{\mu\nu} + \Pi_{\mu\nu} = 0} \quad \text{with} \quad \mathcal{D} = u^\mu \nabla_\mu$$

schematically

$$\boxed{\frac{1}{T}\mathcal{D}\frac{1}{T}\mathcal{D}\,\Pi_{\mu\nu} + 2\,\mathrm{Im}(\omega)\frac{1}{T}\mathcal{D}\,\Pi_{\mu\nu} + \left\{\mathrm{Re}(\omega)^2 + \mathrm{Im}(\omega)^2\right\}\Pi_{\mu\nu} = 0}$$

Test: the boost-invariant flow

$$\tau_{ini} = \frac{1}{3}\tau_{hydro}:$$

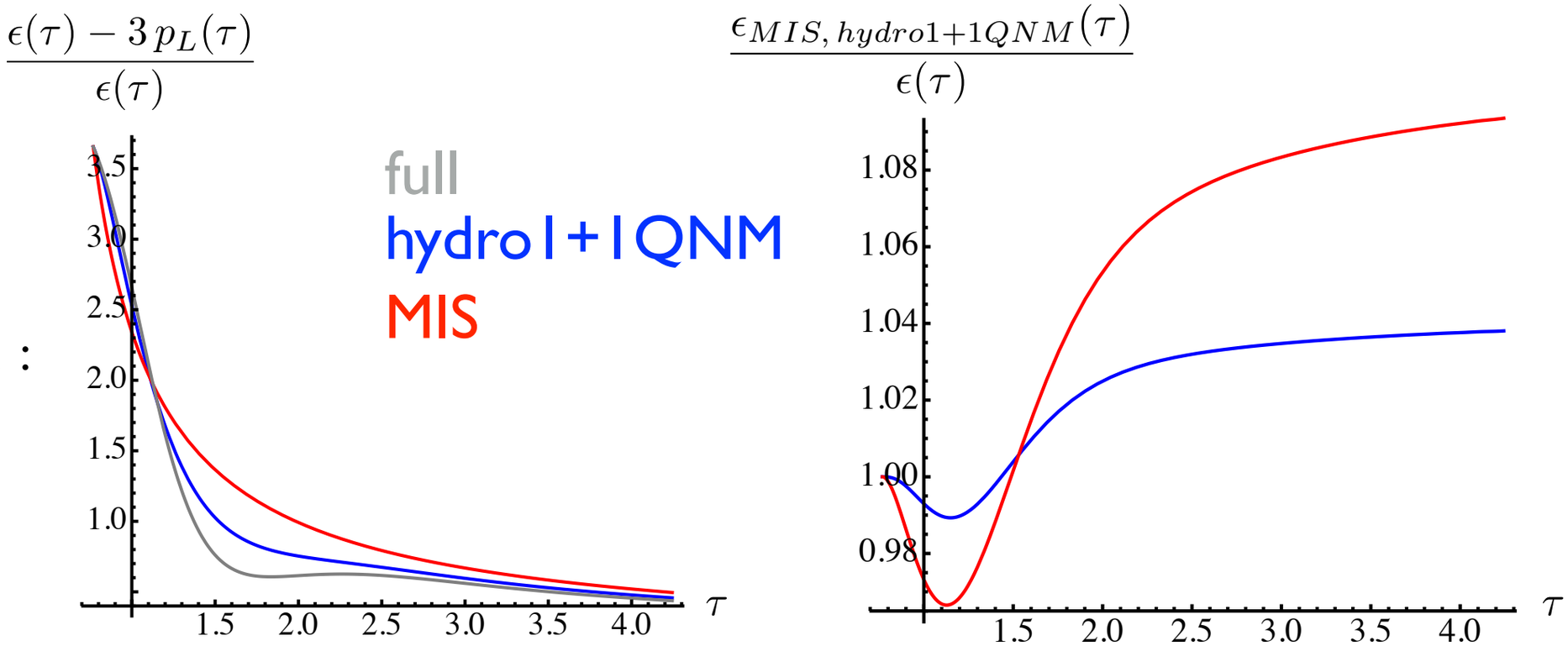

$$\tau_{ini} = \tau_{hydro}:$$

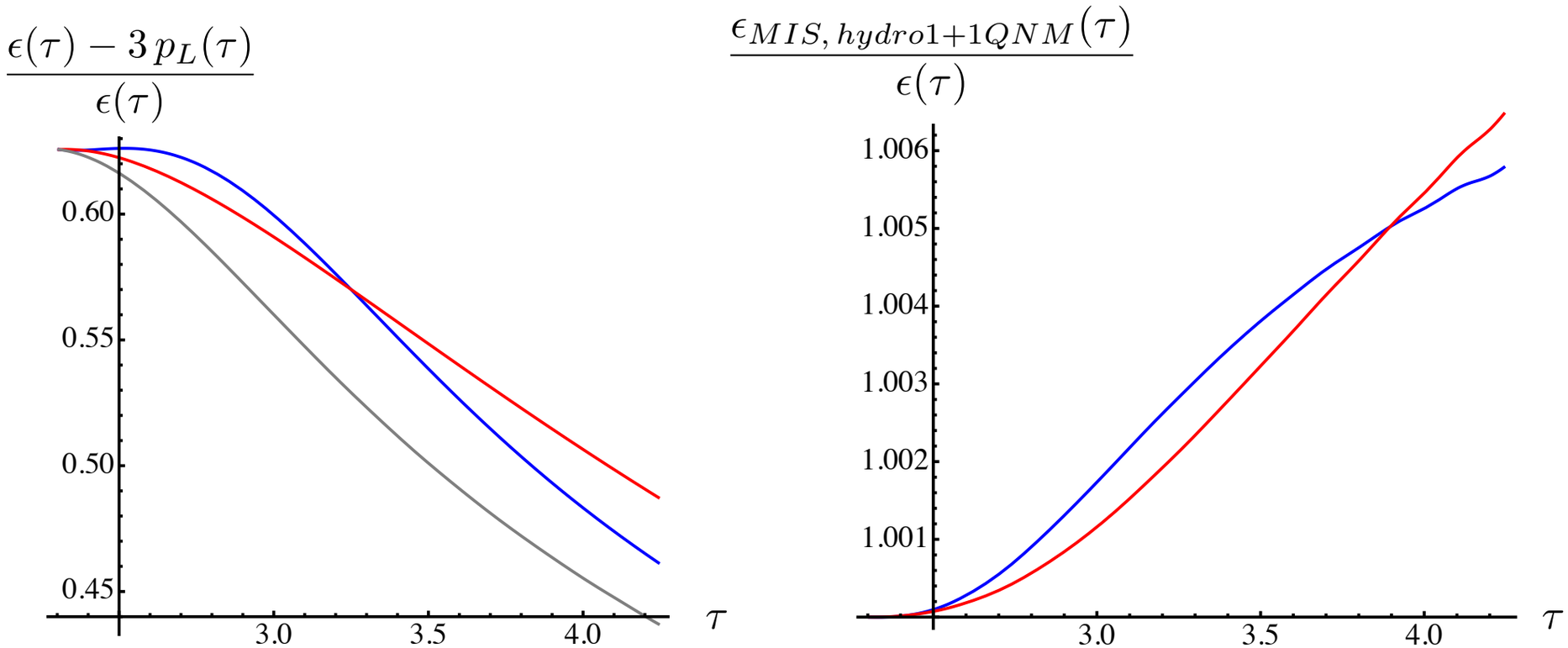

Holographic collisions

1305.4919 [hep-th] PRL 111 (2013) 181601: J. Casalderrey-Solana, MPH, D. Mateos & W. van der Schee

1312.2956 [hep-th] Casalderrey-Solana, MPH, Mateos, van der Schee

Towards holographic "HIC": the projectiles

Janik & Peschanski **[hep-th/0512162]** Chesler & Yaffe **1011.3562 [hep-th]**

practical viewpoint: collide two lumps of matter moving at relativistic speeds.

state of the art (Apr 2014): planar shock wave collisions

the shock wave: infinite sheet of matter moving at the speed of light with

$$\langle T^{tt}\rangle = \langle T^{zz}\rangle = \pm\langle T^{tz}\rangle = \frac{N_c^2}{2\pi^2} h(t \mp z)$$ and ***h*** "arbitrary"

Let's focus now on Gaussians $h(t \pm z) = \rho^4 \exp\left[-(t \pm z)^2/2\sigma^2\right]$. No scale (CFT!), so only $e = \rho\,\sigma$ matters. In HIC $e \sim \gamma^{-1/2}$ and $e_{CY} \approx 0.64$ corresponds to Pb at RHIC.

Confusion about the initial boost-invariance

discussion with F. Gelis & R. Janik

Boost-invariance: the system is invariant under the longitudinal boosts.

The collision needs to be a point-like event in the longitudinal direction $\longrightarrow$ $\delta(x^{\pm})$

The initial state needs to be boost-invariant. For the CGC we have

$$J_\mu dx^\mu \sim \delta(x^{\pm})dx^{\pm} \longrightarrow \delta(x'^{\pm})dx'^{\pm}$$

The initial state there is thus boost-invariant, but this symmetry gets broken.

How about the shock-waves?

$\langle T^{shock}_{\mu\nu}\rangle\, dx^\mu dx^\nu \sim \delta(x^{\pm})\,(dx^{\pm})^2$ changes its form under the longitudinal boosts.

We should not expect the boost-invariant outcome soon after the collision.

Problematic resolutions: $\langle T^{shock}_{\pm\pm}\rangle \sim \delta(x^{\pm})^2$ or $\langle T^{shock}_{\pm\pm}\rangle \sim \delta'(x^{\pm})$.

Dynamical crossover

1305.4919 [hep-th] PRL 111 (2013) 181601:
J. Casalderrey-Solana, MPH, D. Mateos & W. van der Schee

$$\langle T^{tt} \rangle = \frac{N_c^2}{2\pi^2}\mathcal{E}$$

$e_{left} = 2\, e_{CY}$ „low energy"

$e_{right} = 0.125\, e_{CY}$ „high energy"

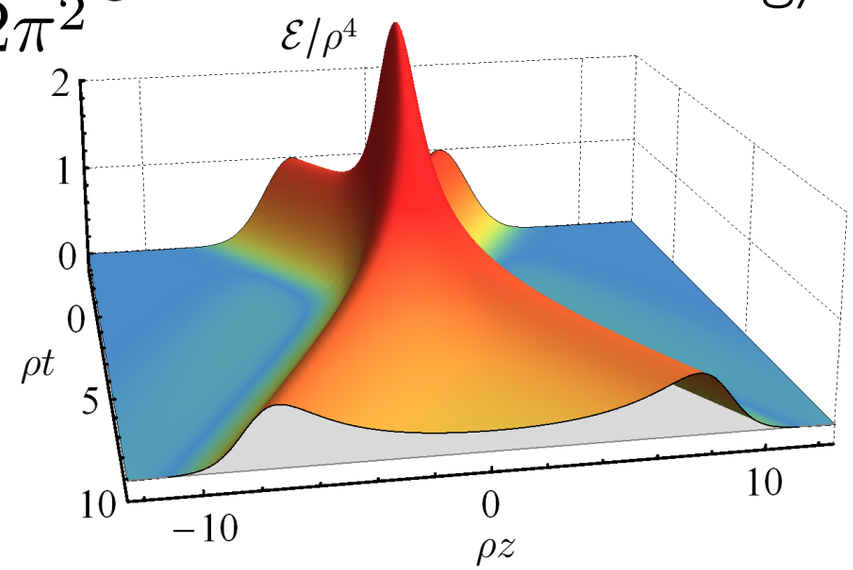

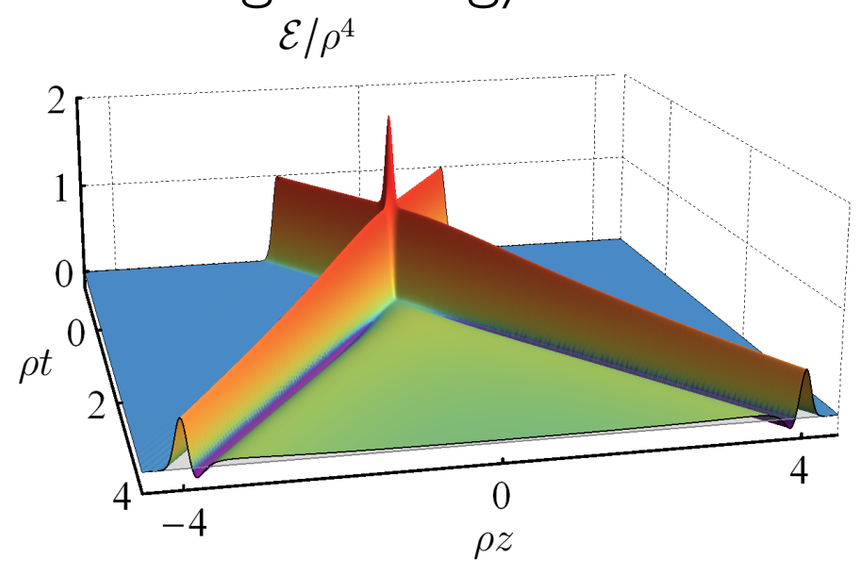

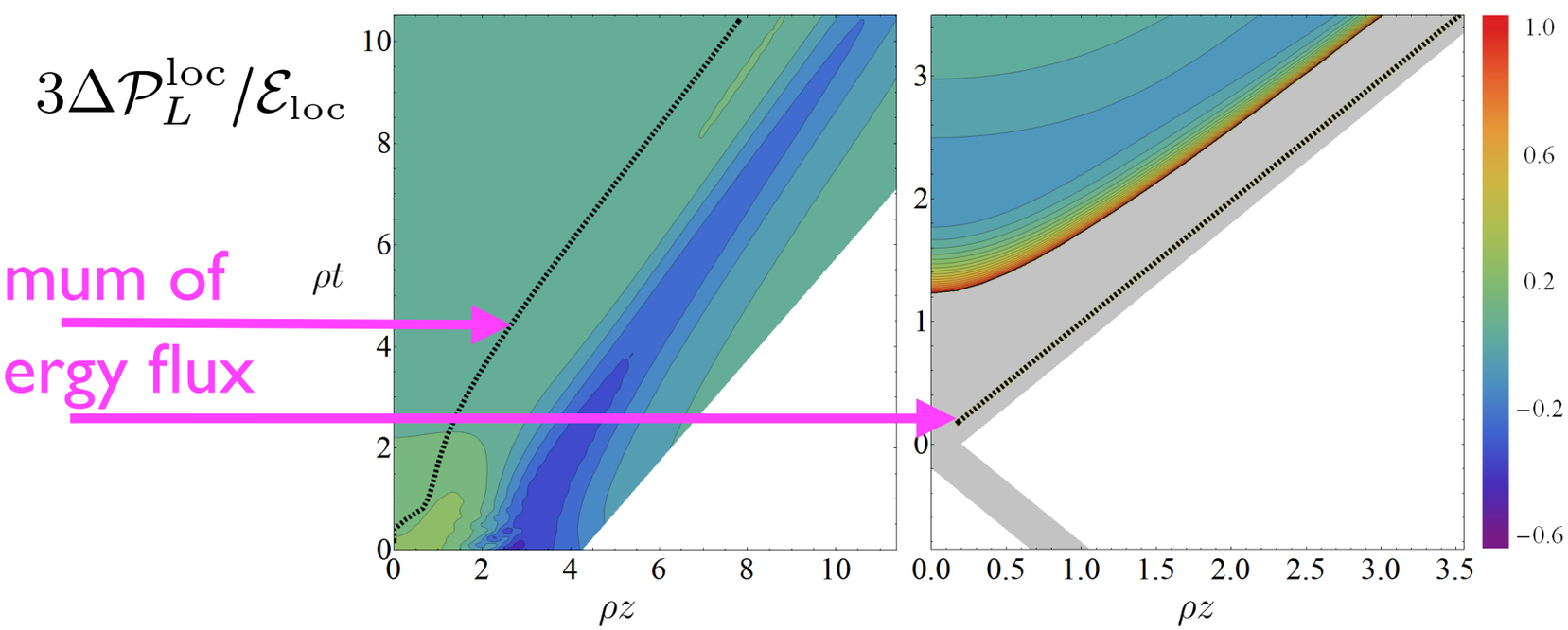

maximum of the energy flux

deviation from viscous hydro

shocks coalesce and explode hydro-dynamically (similar to the Landau picture)

hydro applicable only at mid-rapidities and late enough!!!

Dispels the myth that strong coupling necessarily leads to immediate stopping*

Plasma creation for thin shocks collision

1305.4919 [hep-th] PRL 111 (2013) 181601: J. Casalderrey-Solana, MPH, D. Mateos & W. van der Schee

$\frac{\mathcal{P}_L}{\mathcal{E}}$ & $\frac{\mathcal{P}_T}{\mathcal{E}}$

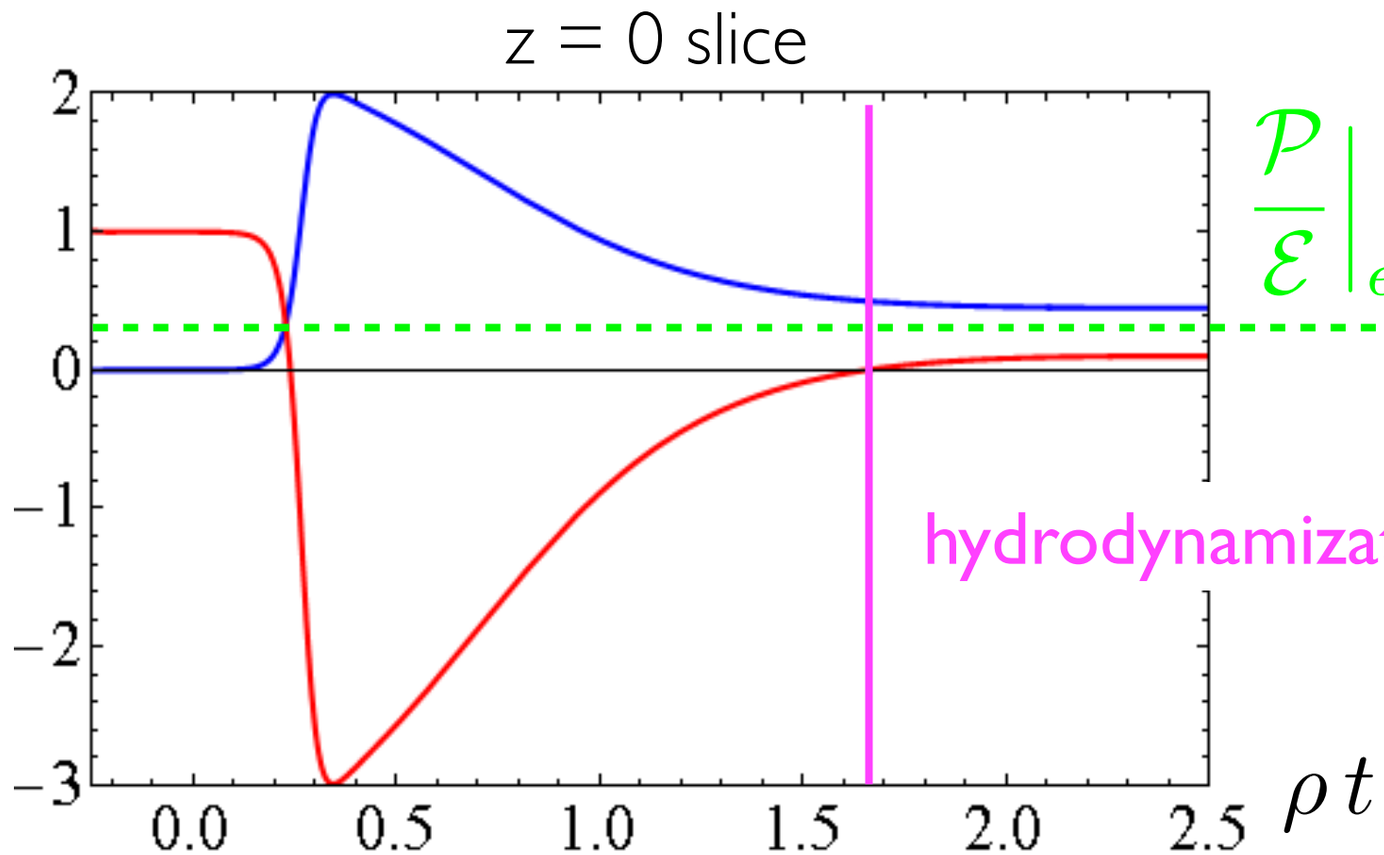

$$\left.\frac{\mathcal{P}}{\mathcal{E}}\right|_{equilibrium} = \frac{1}{3}$$

<u>Assume</u> boost-invariance: $\mathcal{P}_L = -\mathcal{E} - \tau\,\mathcal{E}'$ and $\mathcal{P}_T = \mathcal{E} + \frac{1}{2}\tau\,\mathcal{E}'$

$\mathcal{E}\Big|_{\tau=0} \sim 1$ leads to $\left.\frac{\mathcal{P}_L}{\mathcal{E}}\right|_{\tau=0} = -1$ and $\left.\frac{\mathcal{P}_T}{\mathcal{E}}\right|_{\tau=0} = 1$

what one gets in the CGC

$\mathcal{E}\Big|_{\tau=0} \sim \tau^2$ leads to $\left.\frac{\mathcal{P}_L}{\mathcal{E}}\right|_{\tau=0} = -3$ and $\left.\frac{\mathcal{P}_T}{\mathcal{E}}\right|_{\tau=0} = 2$

shock waves seem to be different!

$\mathcal{E}_{loc}$ at hydrodynamization

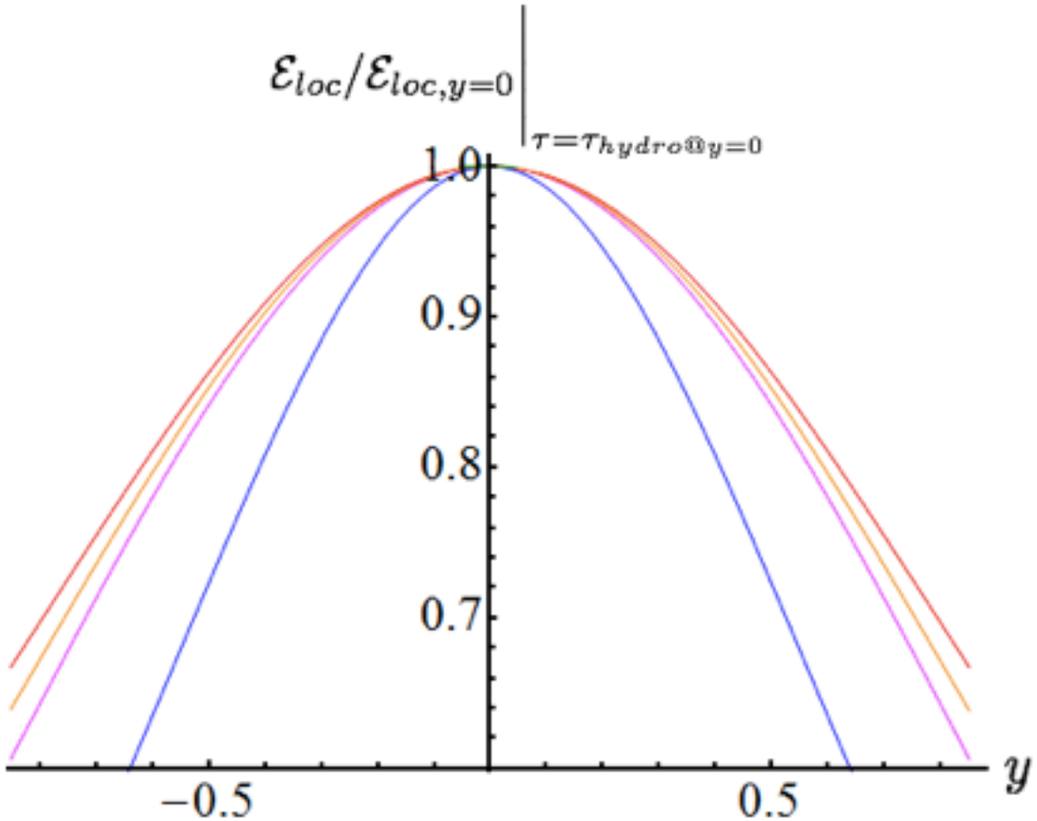

$e = \frac{1}{8} e_{CY}$

$e = \frac{1}{4} e_{CY}$

$e = \frac{1}{2} e_{CY}$

$e = e_{CY}$

The dynamics <u>is not</u> boost-invariant in the sense introduced by Bjorken.

1305.4919 [hep-th] PRL 111 (2013) 181601:
J. Casalderrey-Solana, MPH, D. Mateos & W. van der Schee

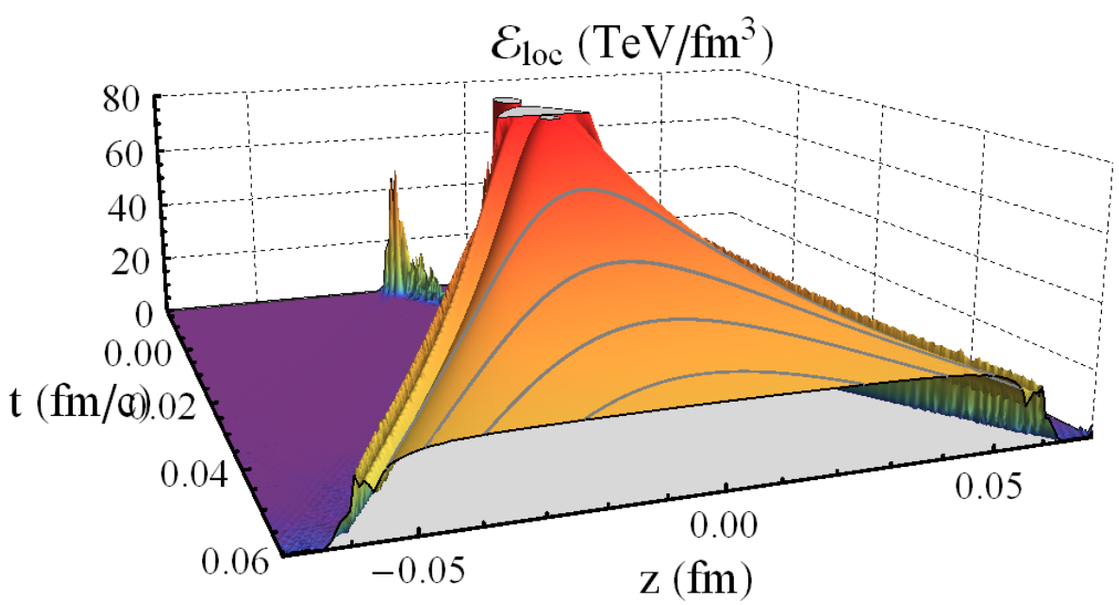

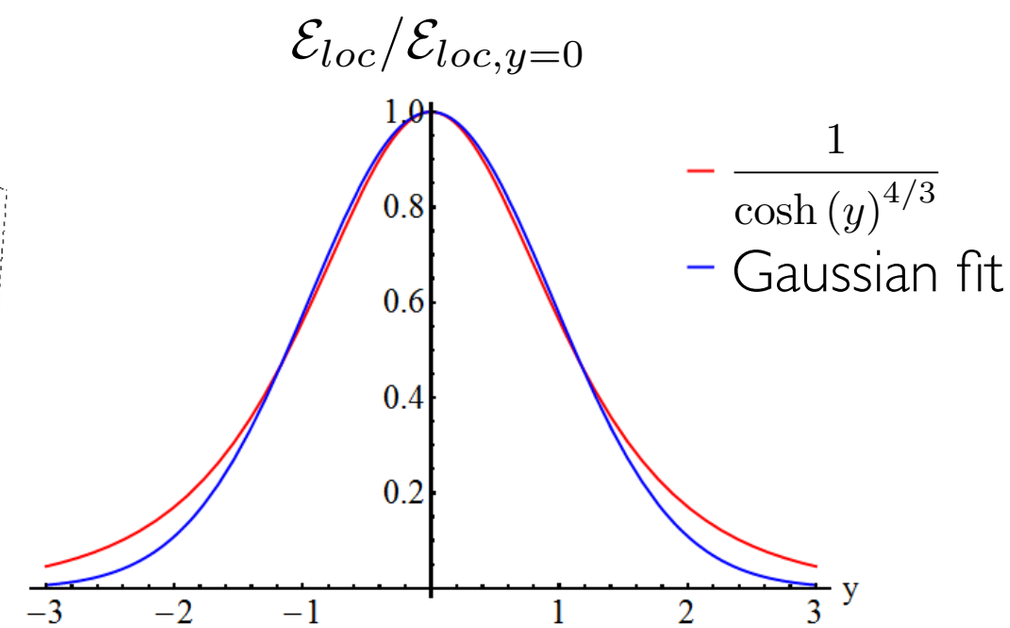

W. van der Schee's Ph.D. thesis

Coherence effects

1312.2956 [hep-th] Casalderrey-Solana, MPH, Mateos, van der Schee

(Asymmetric) collisions in the centre of mass frame, e.g.

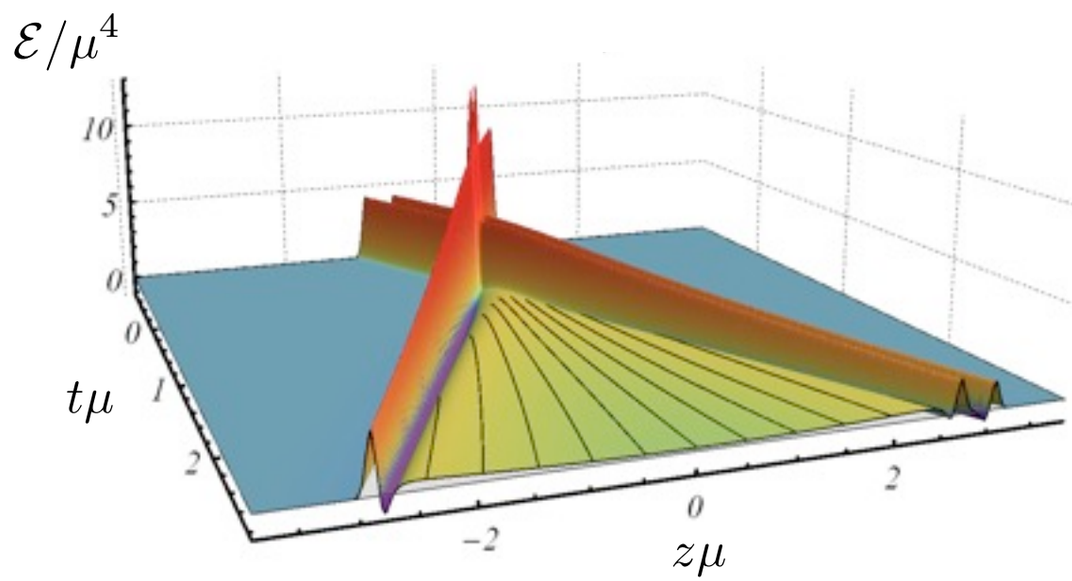

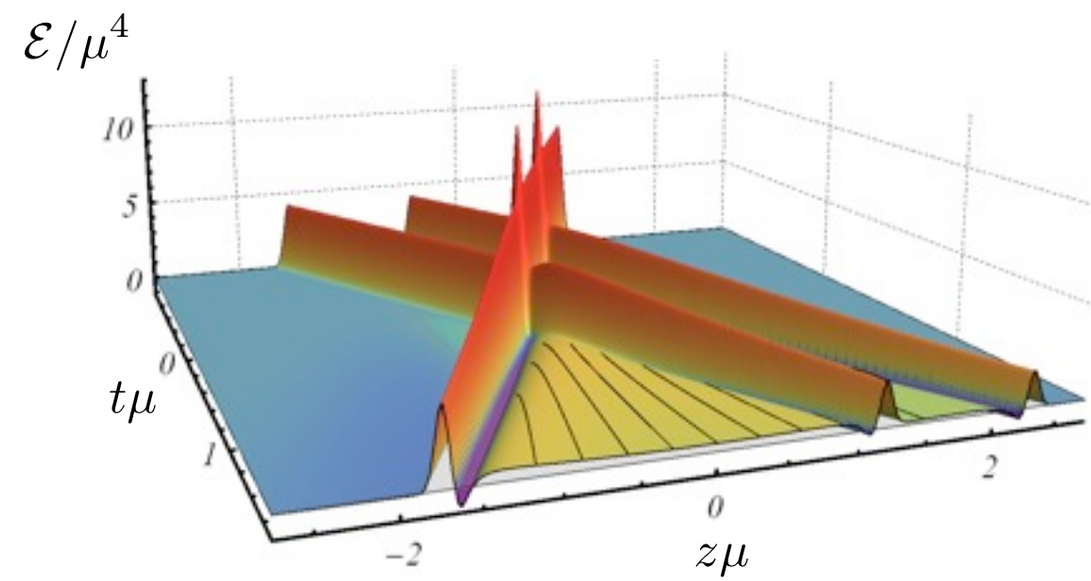

$\mu^3 \sim$ total energy per unit transversal area

longitudinal structure within

coherent $< \mathcal{O}(0.2/T_{hyd}) <$ not coherent

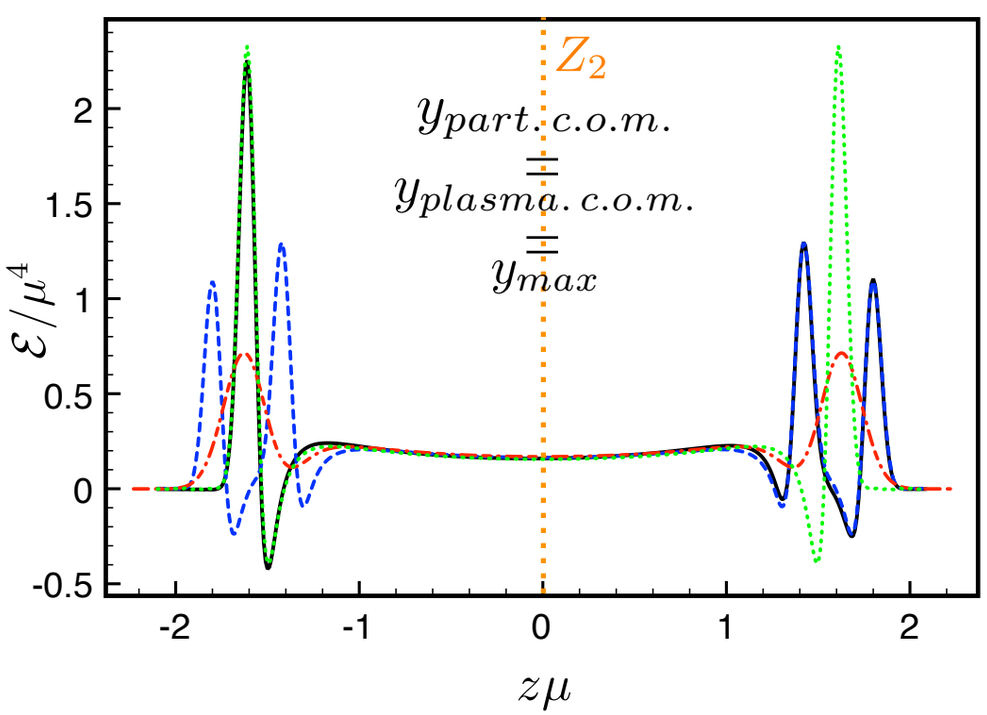

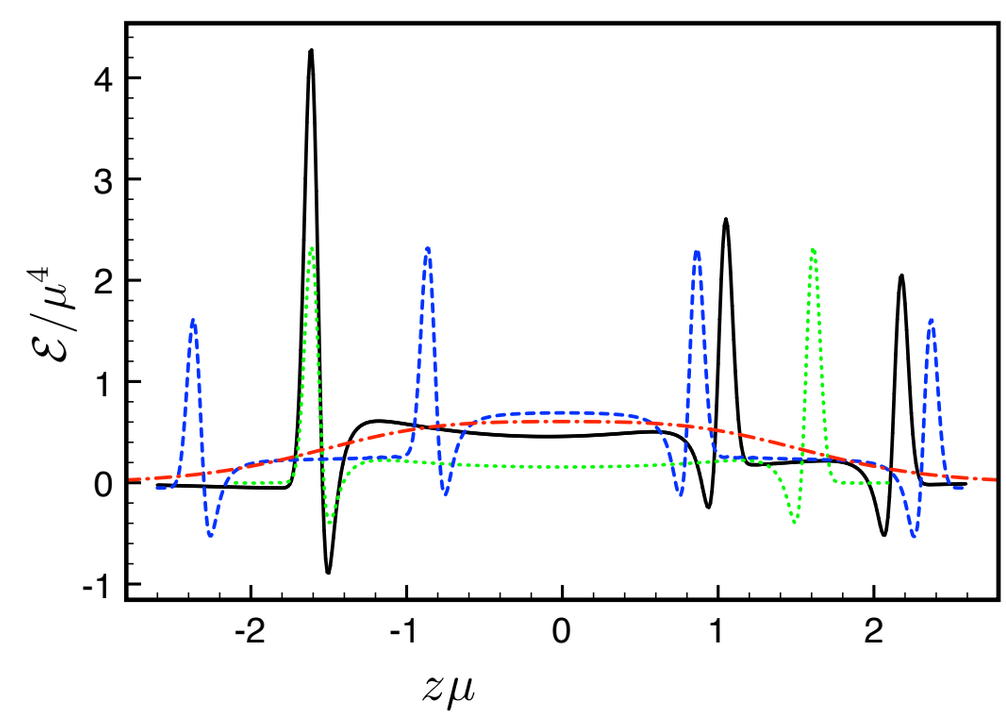

plotted at τ_{hyd}

Summary

Summary

New way of thinking about the transition to hydrodynamics, in particular

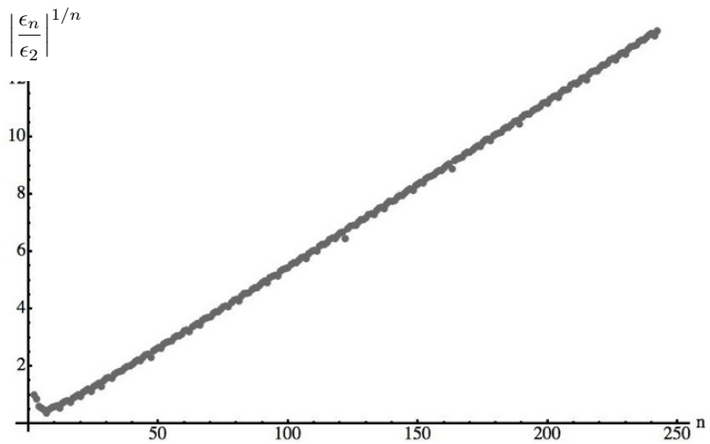

1302.0697 [hep-th] PRL 110 (2013) 211602:
MPH, R. A. Janik & P. Witaszczyk

$$\frac{1}{T}\mathcal{D}\frac{1}{T}\mathcal{D}\,\Pi_{\mu\nu} + 2\,\mathrm{Im}(\omega)\frac{1}{T}\mathcal{D}\,\Pi_{\mu\nu} + \left\{\mathrm{Re}(\omega)^2 + \mathrm{Im}(\omega)^2\right\}\Pi_{\mu\nu} = 0$$

1404.xxxx [hep-th]: MPH, R. Janik, M. Spaliński, P. Witaszczyk
see also 1104.2415 [hep-th]: Noronha & Denicol

"Landau hydro" vs. "transparency" ("coherence")

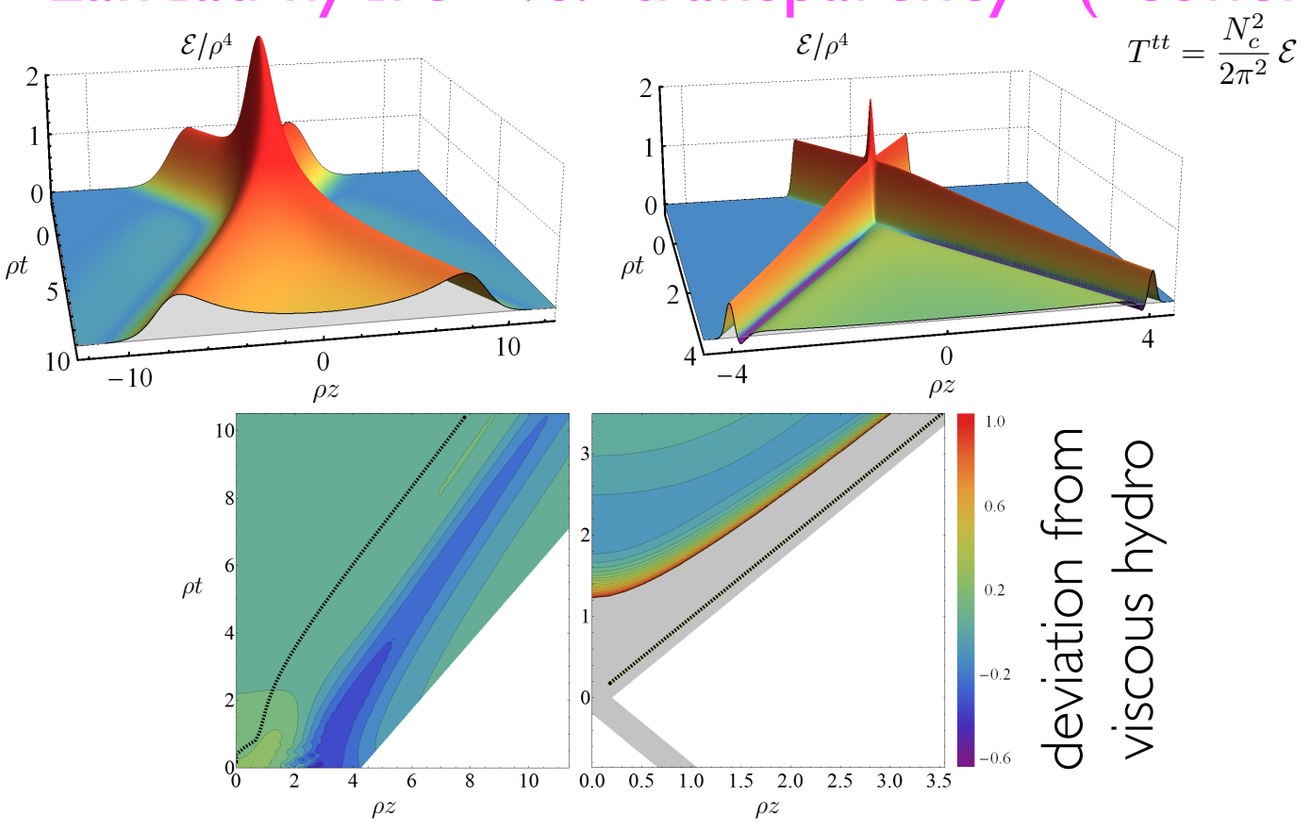

1305.4919 [hep-th] PRL 111 (2013) 181601:
J. Casalderrey-Solana, MPH, D. Mateos & W. van der Schee

1312.2956 [hep-th]
Casalderrey-Solana, MPH, Mateos, van der Schee

CERN-CKC TH Institute on Numerical Holography

8-18 December 2014
CERN
Europe/Zurich timezone

Search

- Overview
- Scientific Programme
- Timetable
- Contribution List
- Author List
- My Conference
- Registration
  - Registration Form

CERN TH-secretariat

th-unit-secretariat@c...

Gauge/gravity duality (or holographic duality) relates the dynamics of certain strongly interacting quantum field theories to the dynamics of classical gravity in one higher dimension. Over the last decade holographic duality has emerged as a powerful tool for studying strongly interacting systems. A significant part of these developments has been motivated by experimentally explored strongly coupled systems ranging from the quark-gluon plasma produced in ultra-relativistic heavy ion collisions at RHIC and at the LHC to various condensed matter systems including superfluidity, quantum phase transitions, and non-Fermi liquids. One of the assets of holography is that it can yield insight into the real-time dynamics of strongly coupled quantum field theories via classical partial differential equations in the gravity dual. To date, the vast majority of work in holographic duality is focused on problems which are either static, or sufficiently close to equilibrium that analytic methods can be used to solve the required differential equations. However, in recent years there has been increasing attention focused on challenging problems which require greater use of numerical techniques. These include the question of how strongly coupled systems far from equilibrium relax, how turbulent behavior can be studied in the gravity dual description of fluids or superfluids, and how ground states of strongly interacting matter with broken translational invariance can be found. This workshop aims at an in-depth exchange on the class of challenging problems that are now under study with numerical techniques in holography.

Starts 8 Dec 2014 08:00
Ends 18 Dec 2014 18:00
Europe/Zurich

CERN
TH Conference Room

Heller, Michal P.
Wiedemann, Urs
Chesler, Paul
Hong, Deog-Ki
Yaffe, Larry
Herzog, Christopher

No material yet

→ http://goo.gl/BBYh7J

extra

Thermalization and Transient Gluon BEC: Effect of the Inelastic Process

Xu-Guang Huang
Physics Department, Fudan University

Based on XGH and Jinfeng Liao, arXiv:1303.7214 and 1402.5578

April 03, 2014 @ "Approach to equilibrium"

Xu-Guang Huang

Glasma Evolution and Bose-Einstein Condensation with Elastic and Inelastic Collisions

Xu-Guang Huang[1,2], Jinfeng Liao[1,3]

arXiv:1303.7214

International Journal of Modern Physics E
Vol. 23, No. 3 (2014) 1430003 (40 pages)
© World Scientific Publishing Company
DOI: 10.1142/S0218301314300033

World Scientific
www.worldscientific.com

Kinetic evolution of the glasma and thermalization in heavy-ion collisions

arXiv:1402.5578

Jinfeng Liao
Indiana University, Physics Dept. & CEEM
RIKEN BNL Research Center

Contents

Introduction
- Thermalization
- Thermalization in Heavy-Ion Collisions

Kinetic description
- Elastic thermalization and BEC
- Inelastic procedures
- Small p analysis

Summary

Introduction

Thermalization

- A general question of non-equilibrium many-body system:

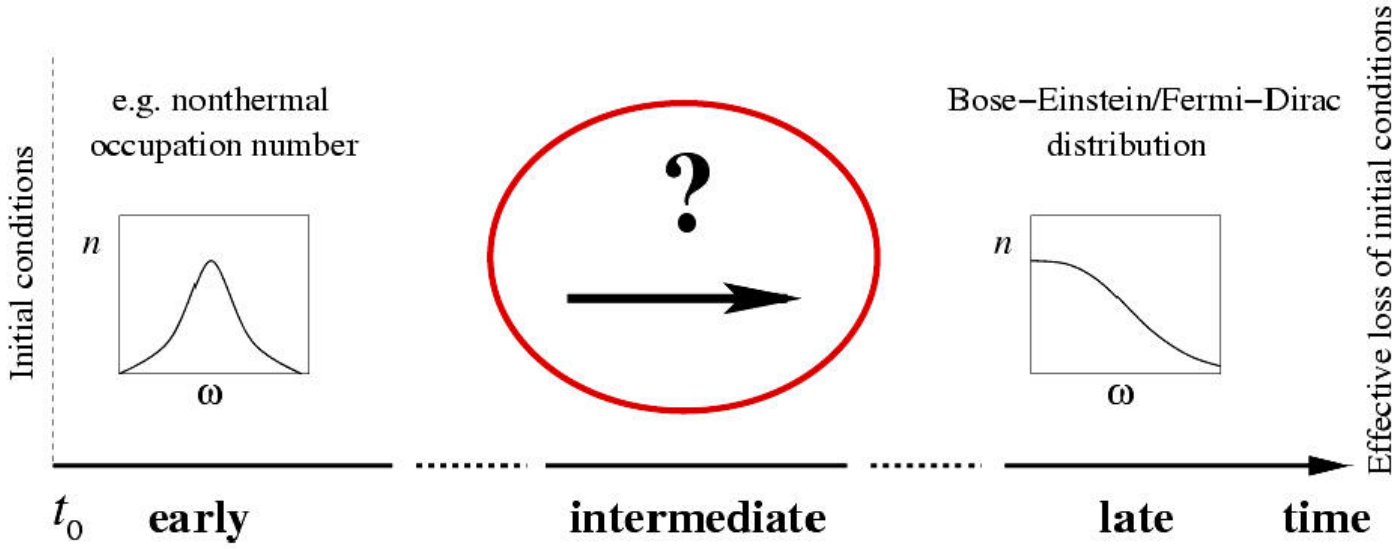

  - How the system gets thermalized?
  - How the initial states map to final states?
  - How long the thermalization takes?
  - What can the intermediate states be?
  - ... ...

Heavy-Ion Collisions

- We are interested in HIC.
- Time evolution of HIC:

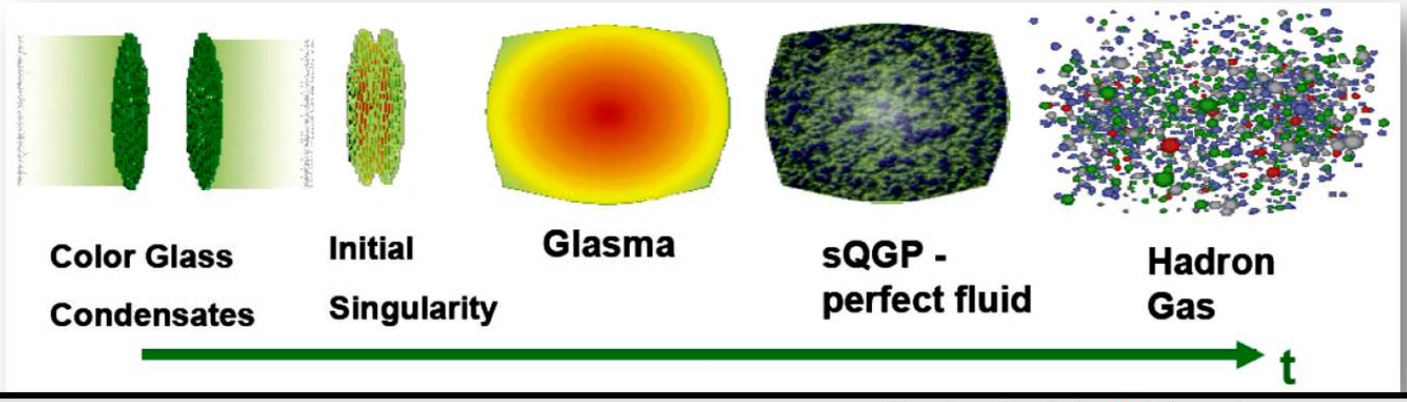

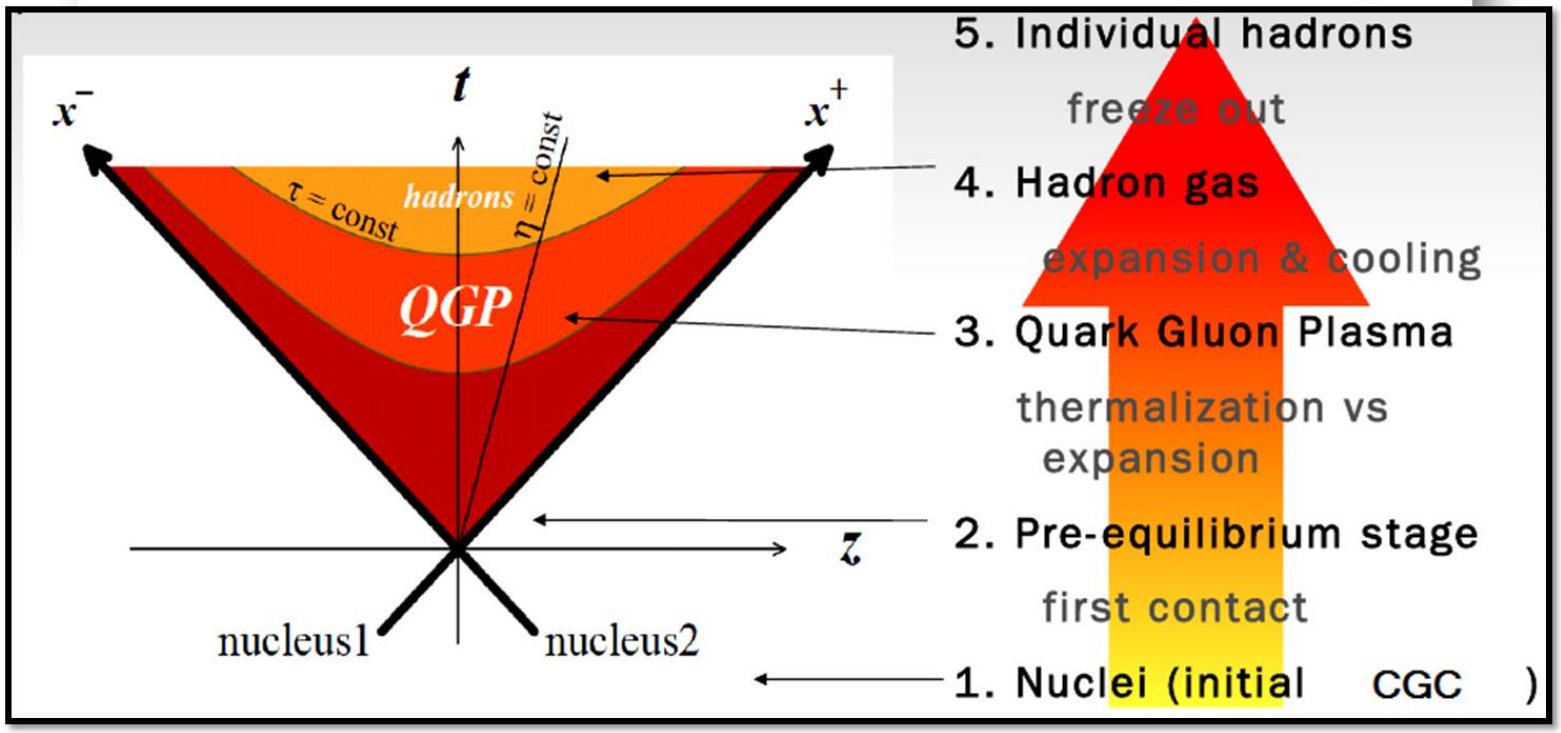

Heavy-Ion Collisions

- We are interested in HIC.
- Time evolution of HIC:

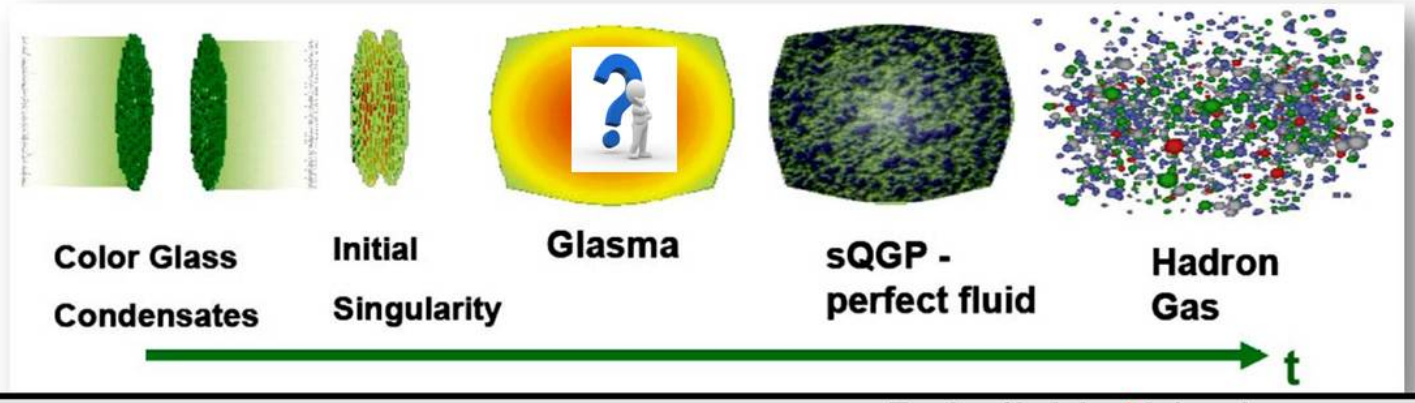

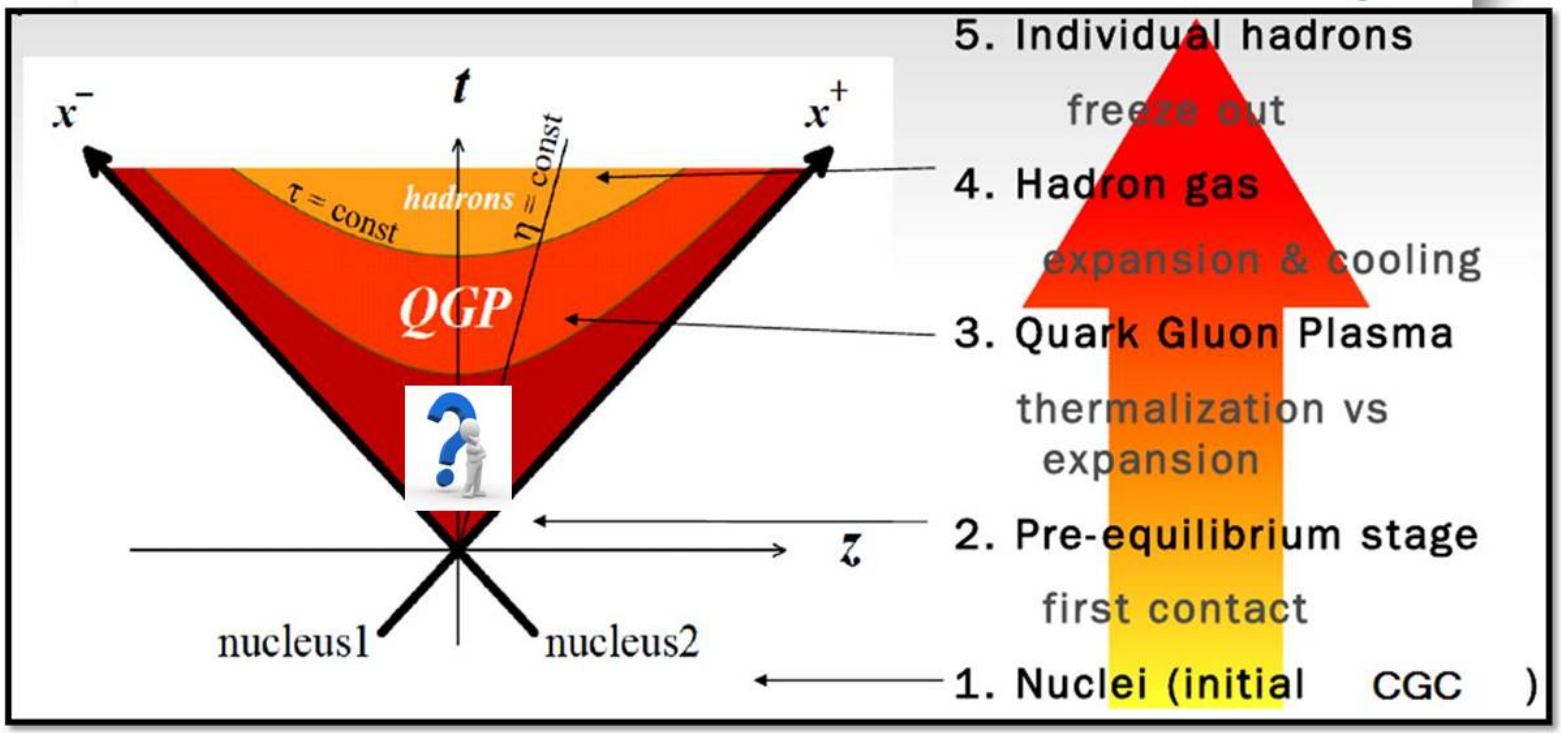

Fast thermalization of quark-gluon plasma

- Thermalization of QGP is not only a fundamental problem, but also a need to understand the effectiveness of hydrodynamical evolution.
- QGP: hydrodynamical evolution: collective flow, ...

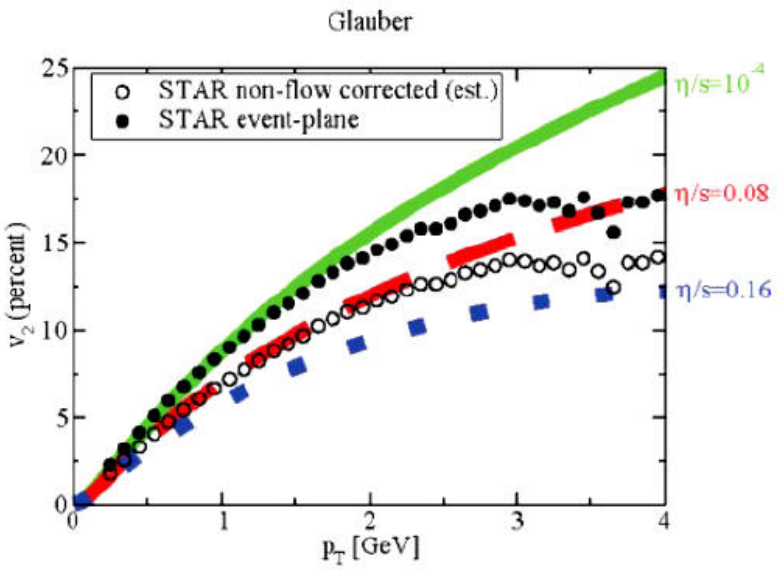

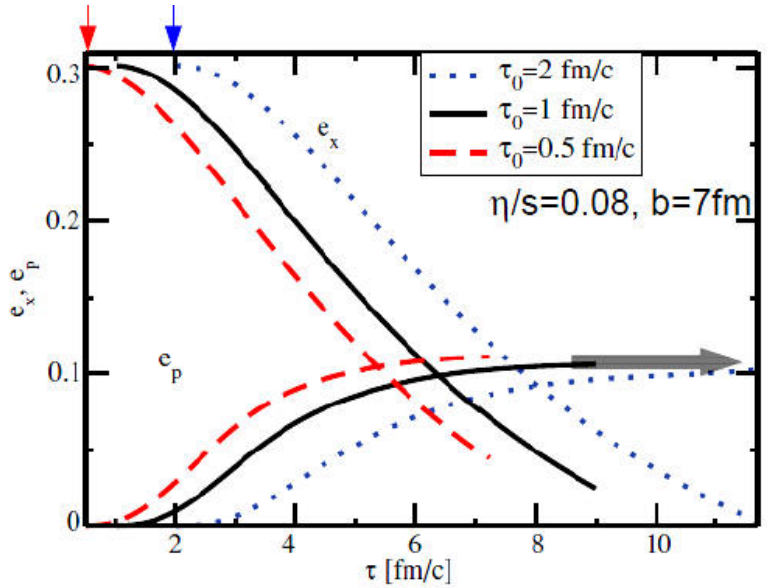

2nd order shear viscous hydro
Luzum-Romatschke (2008)

- Matching hydro. to data needs a very fast therm., $\tau_{\rm therm} \sim 1$ fm.
- Puzzle: Why and how a "weakly interacting" system thermalize fast?

Fast thermalization of quark-gluon plasma

- This puzzle is partially understood by the saturation physics: $xG(x, p < Q_s) \sim 1/\alpha_s$.

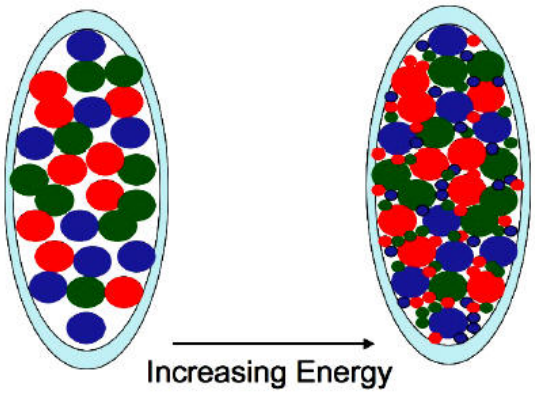

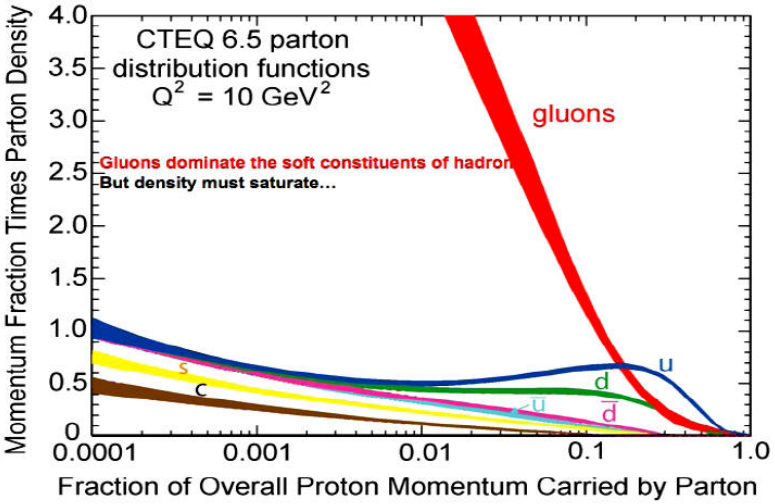

- After collision, in a short time scale $\tau_0 \sim 1/Q_s$, coherent chromo-EM fields decay to gluon quanta with the same order of density, $f \sim 1/\alpha_s$. Quarks can be neglected.
- High occupation of gluon make the system effectively "strongly interacting", with an effective coupling $f\alpha_s \sim 1$.
- It permits fast thermalization. Question is how? And what can occur during thermalization.

Kinetic description

A scenario for thermalization

Blaizot, Gelis, Liao, McLerran, and Venugopalan, Nucl. Phys. A 873, 68 (2012). [1]

- Initial distribution is $f_p \sim (1/\alpha_s)\Theta(Q_s - p)$ at $t_0 = 1/Q_s$, energy distribution is $\sim p f_0 \Theta(Q_s - p)$, peaks at $p \sim Q_s$.
- Thermalization needs entropy to grow:

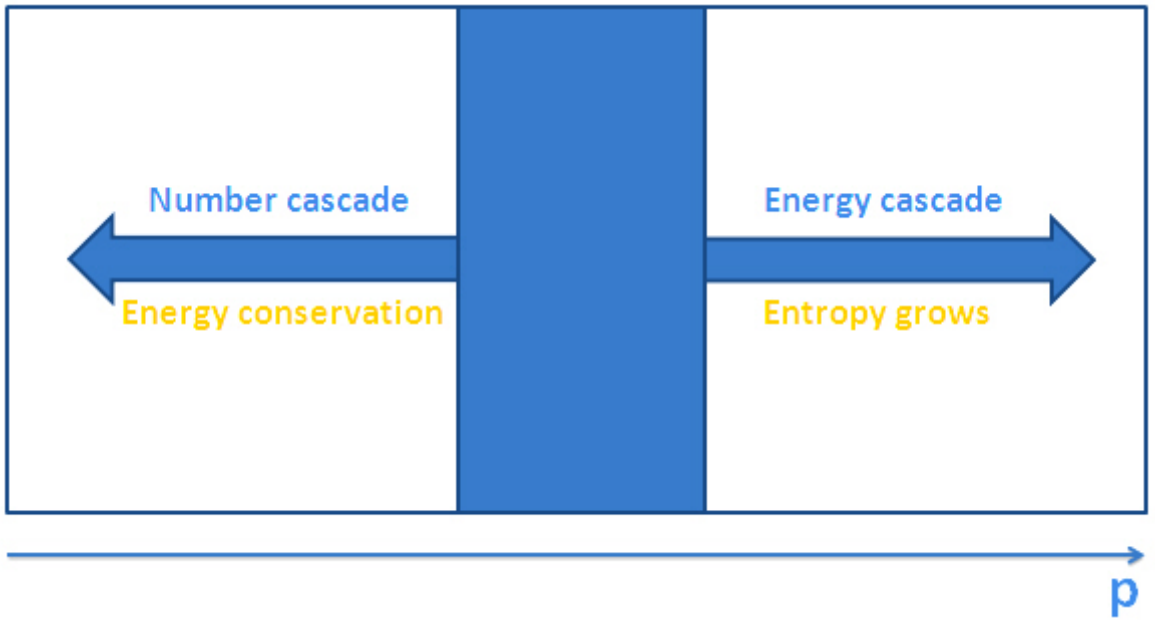

- Two scales emerge from Q_s, one hard Λ for energy cascade, one soft Λ_s for number cascade.
- Thermalized when they are naturally separated, $\Lambda_s \sim \alpha_s \Lambda$.

[1] See also: Berges and Sexty, Phys. Rev. Lett. 108, 161601 (2012); Kurkela and Moore, JHEP 12, 044 (2011).

Evaporative cooling of the cold Bose gases

- An example: BEC in equilibrium cold Bose gases.

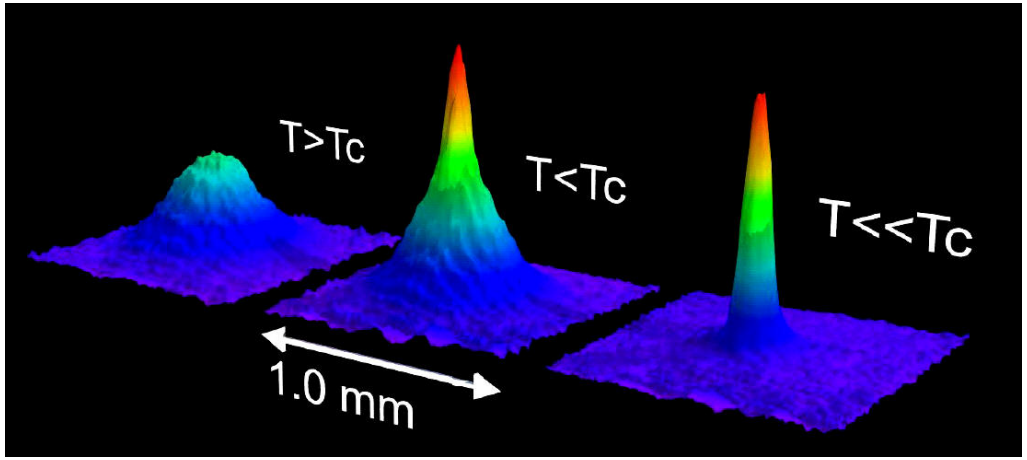

- Cooling procedure:
  Take out fast atoms and let the system relax to new equilibrium.

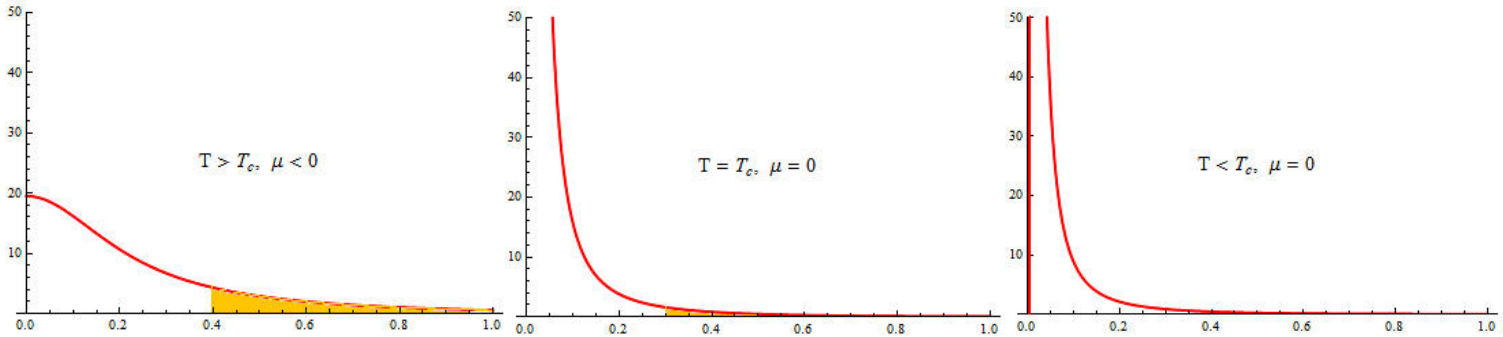

- Energy cascade towards UV region while particle cascade towards IR region, finally condensate emerges.

Boltzmann equation for "static box" gluons

- Quantitative study, from simplest case: gluons in a static, uniform, isotropic box, subject to $2 \to 2$ and $2 \to 3$ scattering.
- Gluon distribution function($N_g = 2(N_c^2 - 1)$):

$$f_p(t) \equiv \frac{(2\pi)^3}{N_g} \frac{dN(t)}{d^3\mathbf{x} d^3\mathbf{p}}.$$

- Boltzmann equation:

$$\partial_t f_p \quad = \quad \mathcal{C}_{2\to 2}[f_p] + \mathcal{C}_{2\to 3}[f_p].$$

- Elastic $2 \to 2$ collision kernel:

$$\begin{aligned} \mathcal{C}_{2\to 2}[f_p] \quad = \quad & \frac{1}{N_g}\frac{1}{2}\int_{123} \frac{1}{2E_p} |M_{12\to 3p}|^2 (2\pi)^4 \delta^4(p_1 + p_2 - p_3 - p) \\ & \times [(1+f_p)(1+f_3)f_1 f_2 - f_p f_3 (1+f_1)(1+f_2)]. \end{aligned}$$

  - $|M_{2\to 2}|^2$ has small angle singularity for $t, u \to 0$ (regularized by screening effects),

$$|M_{2\to 2}|^2 \quad \approx \quad -2 \times 8 g^4 N_c^2 N_g \frac{su}{t^2}.$$

Boltzmann equation for "static box" gluons

- Inelastic $2 \to 3$ collision kernel:

$$
\begin{aligned}
\mathcal{C}_{2\to 3}[f_p] &= \mathcal{C}^a_{2\to 3}[f_p] + \mathcal{C}^b_{2\to 3}[f_p], \\
\mathcal{C}^a_{2\to 3}[f_p] &= \frac{1}{N_g}\frac{1}{6}\int_{123k} \frac{1}{2E_p}|M_{1p\to 23k}|^2 (2\pi)^4 \delta^4(p+p_1-p_2-p_3-k) \\
&\quad \times [(1+f_p)(1+f_1)f_2 f_3 f_k - f_p f_1 (1+f_2)(1+f_3)(1+f_k)], \\
\mathcal{C}^b_{2\to 3}[f_p] &= \frac{1}{N_g}\frac{1}{4}\int_{123k} \frac{1}{2E_p}|M_{23\to 1kp}|^2 (2\pi)^4 \delta^4(p+p_1+k-p_2-p_3) \\
&\quad \times [(1+f_p)(1+f_1)(1+f_k)f_3 f_2 - f_p f_1 f_k (1+f_3)(1+f_2)].
\end{aligned}
$$

  - $|M_{1p\to 23k}|^2$ and $|M_{23\to 1kp}|^2$ have small angle singularity, collinear singularity, and soft singularity. Gunion-Bertsch:

$$
\begin{aligned}
|M^a_{1p\to 23k}|^2 &\approx 6 \times 64 g^6 N_c^3 N_g \frac{(p\cdot p_1)^3}{q^2(q-k)^2(p\cdot k)(p_1\cdot k)}, \\
|M^b_{23\to 1kp}|^2 &\approx 4 \times 64 g^6 N_c^3 N_g \frac{(p_2\cdot p_3)^3}{q^2(q+k)^2(p_2\cdot k)(p_3\cdot k)}.
\end{aligned}
$$

Boltzmann equation for "static box" gluons

- The very complicated Boltzmann equation can be simplified at small angle, collinear, and soft limit:

$$\partial_t f_p = \mathcal{C}^{\rm eff}_{2\to 2}[f_p] + \mathcal{C}^{\rm eff}_{1\to 2}[f_p],$$

where

$$\mathcal{C}^{\rm eff}_{2\to 2} = \alpha_s^2 \xi (1+D) \frac{1}{p^2} \partial_p \left\{ p^2 \left[I_a \frac{\partial f_p}{\partial p} + I_b f_p (1+f_p) \right] \right\},$$

with (Denote $A = \int_{-1}^{1} dx/(1-x)$ from collinear singularity)

$$\begin{aligned}
\xi &= \frac{2N_c^2}{\pi} \int \frac{dq}{q} \quad \text{from small angle singularity}, \\
D &= 2A \frac{g^2 N_c}{(2\pi)^2} \int_0^{m_D} dk \frac{1+2f_k}{k} \quad \text{from soft singularity}, \\
I_a &= \int_0^\infty dp p^2 f_p (1+f_p), \\
I_b &= \int_0^\infty dp p f_p.
\end{aligned}$$

Boltzmann Equation for "static box" gluons

- The expression for $\mathcal{C}^{\rm eff}_{1\to 2}$ is

$$\begin{aligned}
\mathcal{C}^{\rm eff}_{1\to 2} &= \alpha_s^2 R\xi \frac{I_a}{I_b}\left\{\int_0^{z_c}\frac{dz}{z}\left[g_p f_{(1-z)p} f_{zp} - f_p g_{(1-z)p} g_{zp}\right]\right. \\
&+ \left.\int_0^{z_c}\frac{dz}{(1-z)^4 z}\left[g_p g_{zp/(1-z)} f_{p/(1-z)} - f_p f_{zp/(1-z)} g_{p/(1-z)})\right]\right\}, \\
R &= \frac{12AN_c^3 I_b}{\pi^2\xi}\alpha_s\int\frac{dq}{q^3}\sim O(1),
\end{aligned}$$

  z_c is a cut that implements the phase space constraint $k < p$ under which $\mathcal{C}^{\rm eff}_{1\to 2}$ is derived.$\Rightarrow z_c < 1/2$, we take $z_c = 1/2$.
- We will rescale time by $\alpha_s^2\xi$, so that we can drop one parameter ξ.
- We have 2 parameters D, R in the equation, plus another parameter f_0 in the initial condition.
- Note $2\to 3$ inelastic process contribute at the same order as $2\to 2$ elastic process.

Elastic processes dominated thermalization

- First let us consider elastic dominated thermalization, $D = R = 0$ case[2].
- Well-defined the mathematical problem:
  - Evolution equation:

$$\begin{aligned}
\partial_t f_p &= \frac{1}{p^2}\partial_p\left[p^2\left(I_a f_p' + I_b f_p(1+f_p)\right)\right], \\
I_a &= \int_0^\infty dp p^2 f_p(1+f_p), \\
I_b &= \int_0^\infty dp p f_p.
\end{aligned}$$

  - Initial condition for static box at $t_0 = 1/Q_s$

$$f_p = f_0\Theta(Q_s - p).$$

  - Aim: solve for $f_p(t)$, get $t_{\rm therm}$ when $f_p(t)$ becomes BE distribution. Explore how this happens.
  - Universal evolution: independent of α_s.

[2] See also Blaizot, Gelis, Liao, McLerran, and Venugopalan, Nucl. Phys. A 873, 68 (2012), and Blaizot, Liao, and McLerran, Nucl. Phys. A 920, 58 (2013).

Elastic processes dominated thermalization

- Thermodynamical consideration
  - Initial energy density and number density

$$\varepsilon_0 = f_0 \frac{Q_s^4}{8\pi^2}, \quad n_0 = f_0 \frac{Q_s^3}{6\pi^2} \quad \Rightarrow n_0 \varepsilon_0^{-3/4} = f_0^{1/4} \frac{2^{5/4}}{3\pi^{1/2}}$$

  - In a saturated thermal equilibrium state (BE distribution with any temperature T and zero chemical potential)

$$\varepsilon_{eq} = \frac{\pi^2 T^4}{30}, \quad n_{eq} = \frac{\zeta(3) T^3}{\pi^2} \quad \Rightarrow n_{eq} \varepsilon_{eq}^{-3/4} \approx 0.28$$

  - If $f_0 < f_0^c \approx 0.154$, underpopulated, system smoothly evolves to BE distribution with a negative μ.
  - If $f_0 > f_0^c \approx 0.154$ (indeed for glasma initial condition), the initial state contains too many gluons than a smooth thermal state can permit! Overpopulated!
- Where the excess gluons accommodate? Bose-Einstain Condensate?

Elastic processes dominated thermalization

- Solution of the Boltzmann equation for $f_0 = 0.1 < f_0^c$: underpopulation
- Thermalize to BE distribution with $T = 0.34$ determined by energy conservation and $\mu = -0.103$ by number conservation

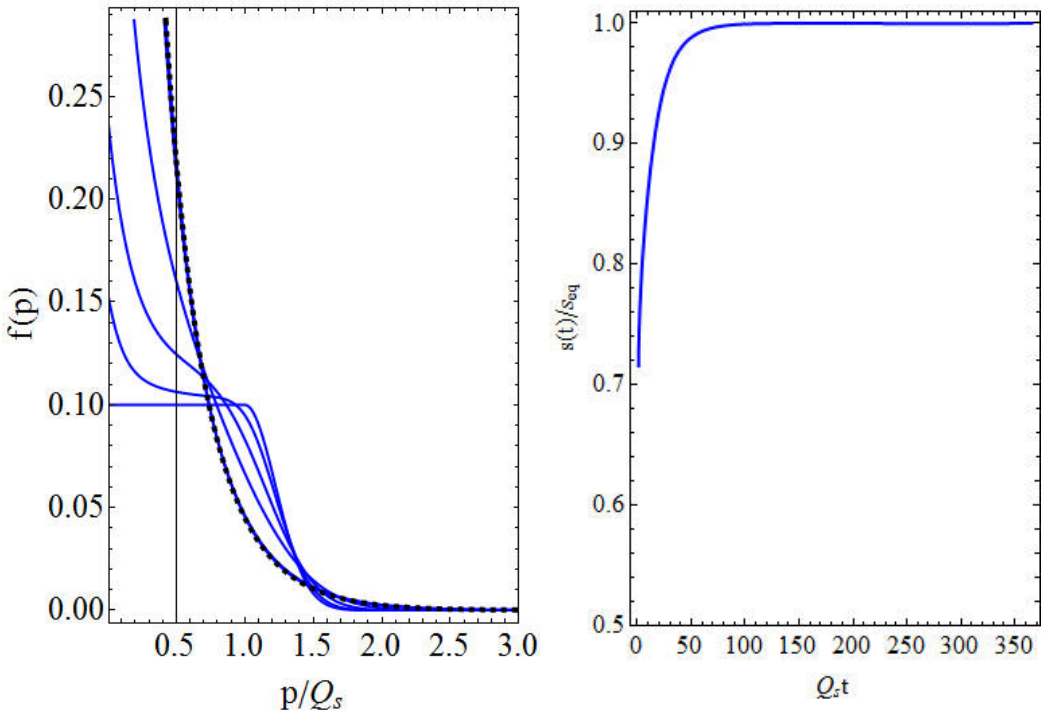

- $t = 1, 2.71, 7.38, 20.09, 163.8, 367$ in unit of $1/Q_s$. Black dots is BE distribution.
- The system is thermalized: entropy is maximized and stationary

Elastic processes dominated thermalization

- Solution of the Boltzmann equation for $f_0 = 1 > f_0^c$: overpopulation
- Hit BEC at $Q_s t \approx 2.0$! Singularity at $p \sim 0$

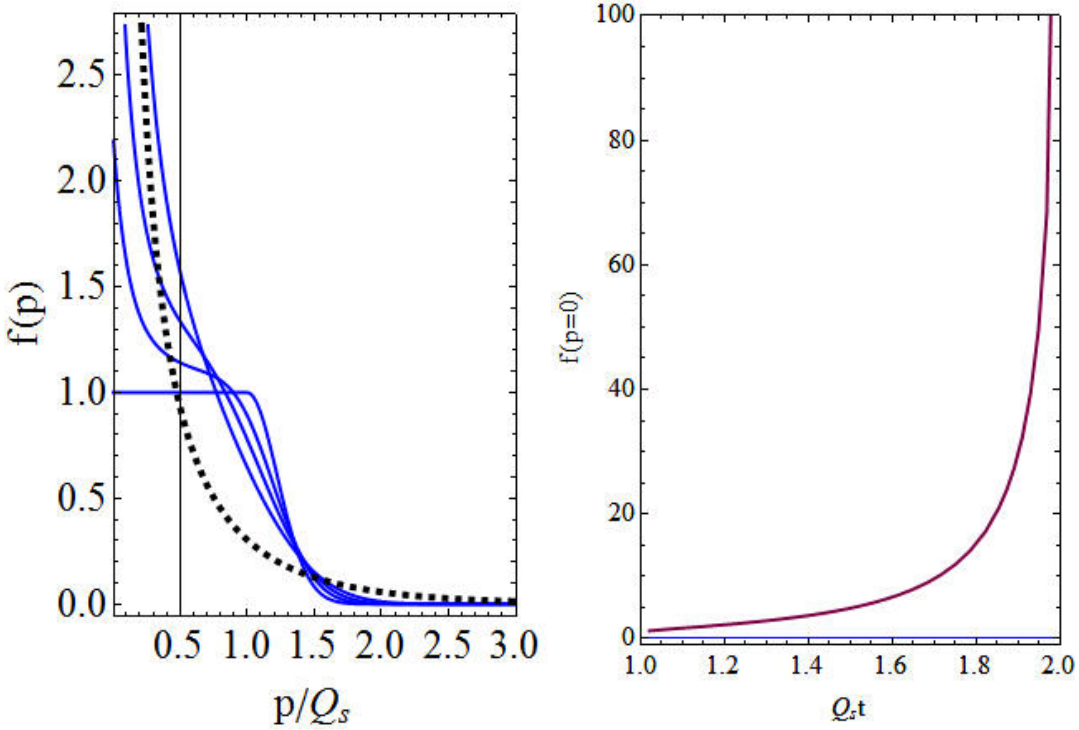

- Not thermalized!

Elastic processes dominated thermalization

- $f_0 = 1 > f_0^c$: overpopulation
- Entropy and chemical potential

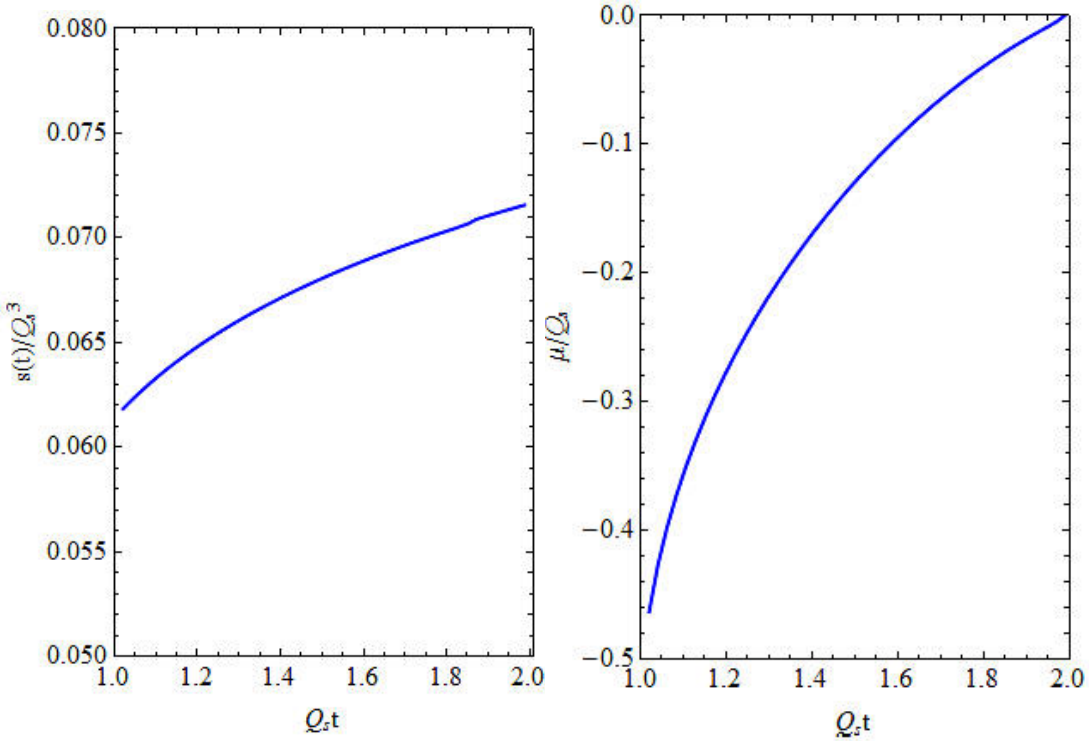

- Entropy does not reach its maximum, still in non-equilibrium. Chemical potential touch zero: a criterion of onset of BEC for massless boson
- A non-equilibrium BEC of gluons!

Inelastic effects

Inelastic processes dominated thermalization

- Natural question: can inelastic processes forbid BEC?
- Let us first explore the purely inelastic case.
- For $f_0 = 1$, we do not expect any singularity.

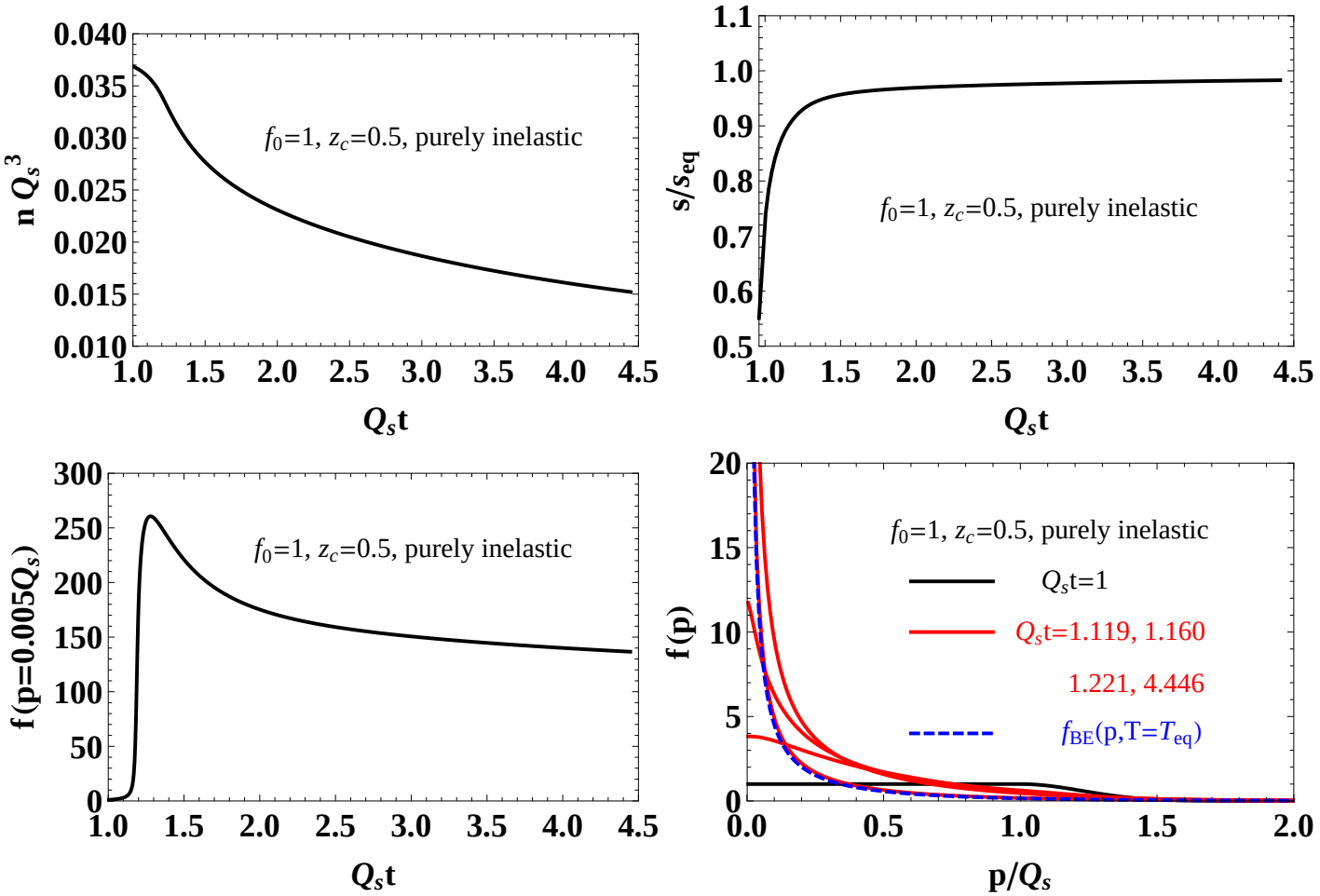

Elastic + inelastic

- $f_0 = 1$, R dependence: the importance of inelastic processes.
- Low p region get fast thermalized to a BE form, $\sim 1/(e^{(p-\mu^*)/T^*} - 1)$ (discuss it latter).

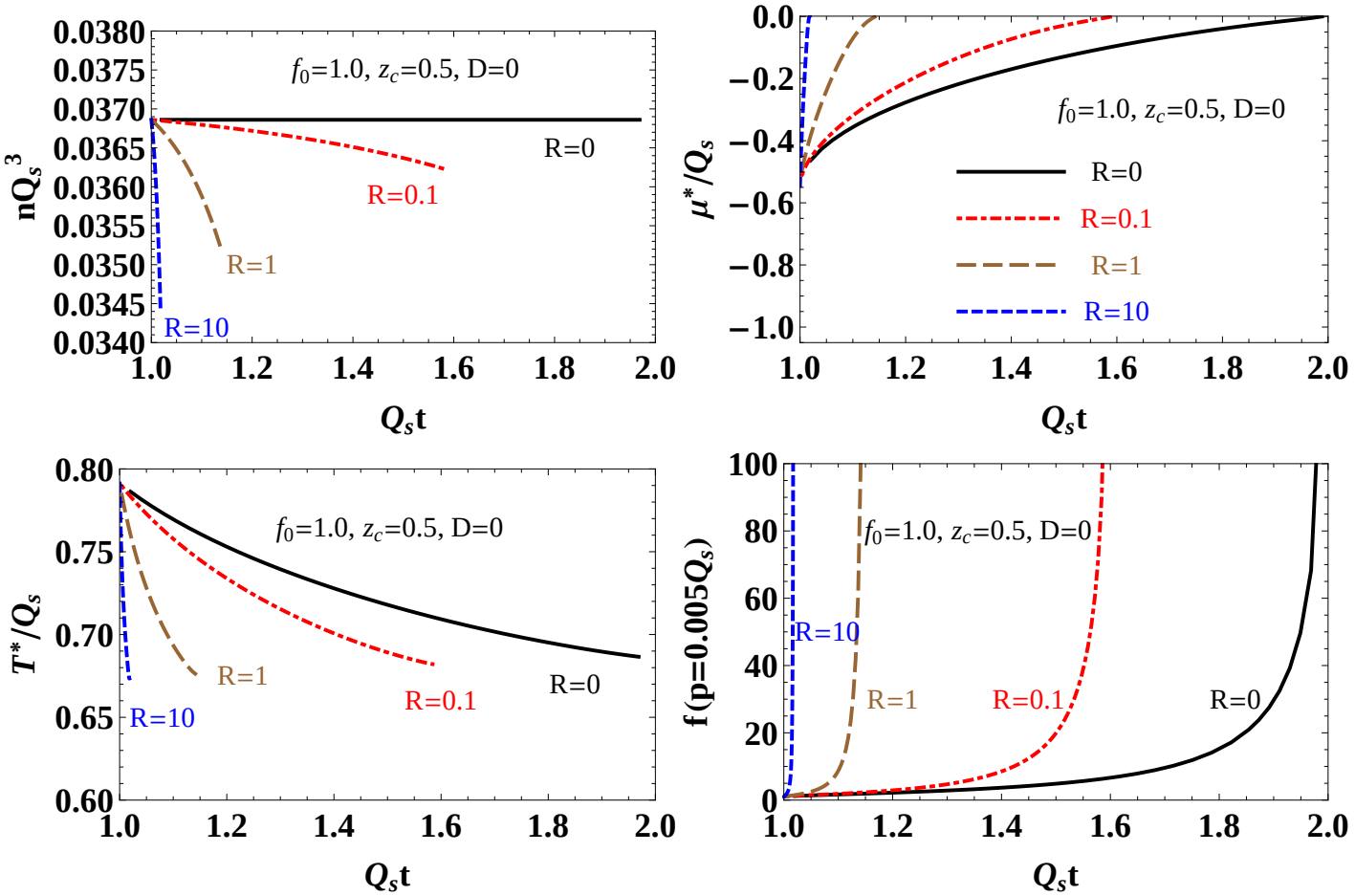

- BEC appears much earlier that pure elastic case!

Elastic + inelastic

- $f_0 = 1, R = 1$, entropy and distribution.

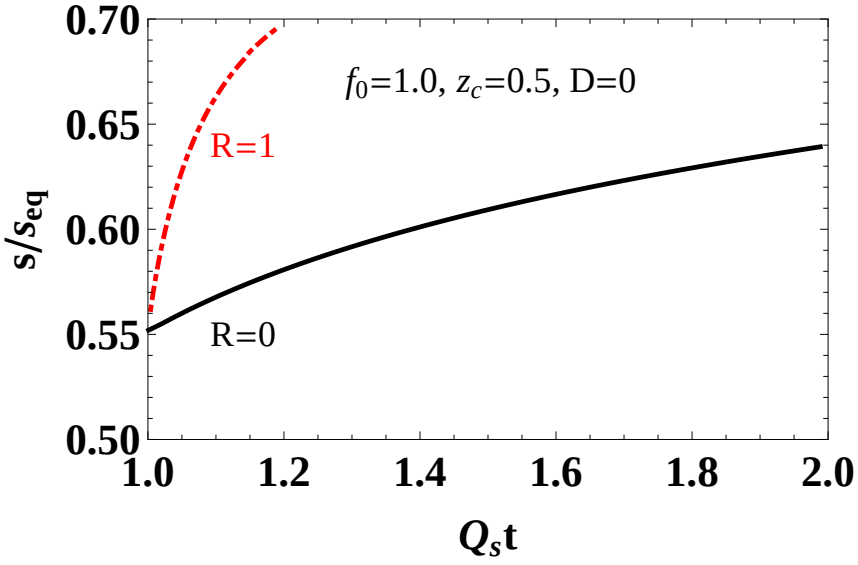

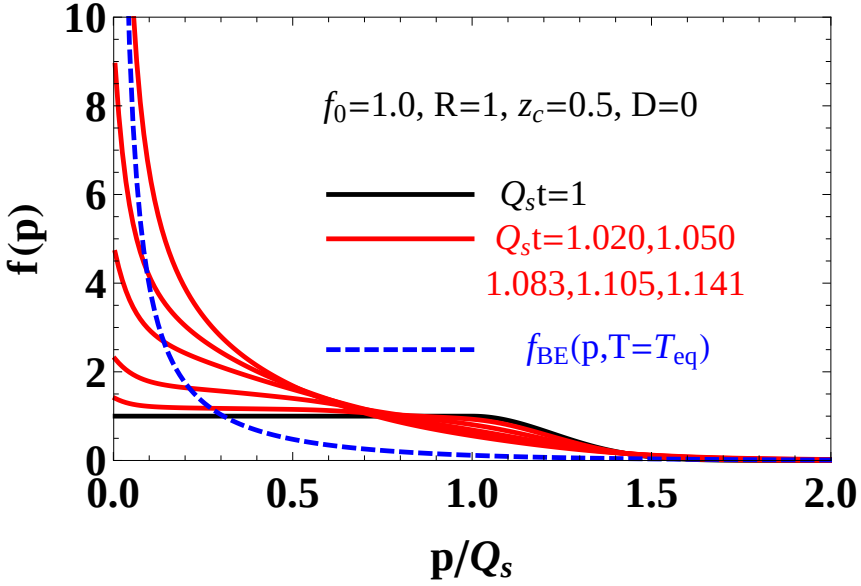

- BEC appears much earlier that pure elastic case! Inelastic kernel catalyze the onset of BEC!
- Question: how to understand it?

Small p analysis

- Inelastic effects: for long enough time, if $n\varepsilon^{-3/4} < 0.28$, it increases particle number; if $n\varepsilon^{-3/4} > 0.28$, it decreases particle number.
- In a short time scale, before any singularity appears. We can do small p expansion:

$$\mathcal{C}^{\text{eff}}_{1\to 2} \approx R\frac{I_a}{I_b}\left[A_0 h_0 + A_1 p f_0'(1+2f_0) + O(p)^2\right],$$

where $h_p = f_p(1+f_p)$ and

$$A_0 = \ln\frac{1}{1-z_c} + \frac{1}{6}\frac{z_c(11z_c^2 - 27z_c + 18)}{(1-z_c)^3},$$

$$A_1 = \ln\frac{1}{1-z_c} - \frac{1}{12}\frac{z_c(25z_c^3 - 88z_c^2 + 108z_c - 48)}{(1-z_c)^4}$$

All these A's are positive for $0 < z_c < 1$.

- Inelastic kernel always produces zero momentum gluon, thus can catalyze onset of BEC.

Small p analysis

- Elastic kernel has a $1/p$ IR structure:

$$\mathcal{C}^{\rm eff}_{2\to 2} \approx \frac{2(I_a f_0' + I_b h_0)}{p} + 3(I_a f_0' + I_b h_0)' + 2p(I_a f_0' + I_b h_0)'' + \frac{5p^2}{6}(I_a f_0' + I_b h_0)''' + O(p)^3.$$

- Quickly arranges IR gluons towards a local BE distribution:

$$f_p = \frac{1}{\exp\left(\frac{p-\mu^*}{T^*}\right) - 1} + \frac{K_2}{2}p^2 + O(p)^3,$$

with $T^* = I_a/I_b$.

- Small p distribution is always thermal form, indicating that "thermalization" happens first for soft gluon
- "Thermalization" grows toward higher momentum, bottom-up picture: $K_2 \to 0$, $K_3 \to 0$, $\cdots$

Small p analysis

- Something wrong. The assumption that there is no singularity is not always true, because inelastic term always try to kill $\mu^* \to 0$, then f_p becomes singular at $p = 0$.
- Small p expansion breaks, but because the elastic term contains

$$\mathcal{C}^{\text{eff}}_{2\to 2} \quad \ni \quad \frac{1}{p^2}\partial_p[p^2 f_p'] \sim \nabla^2 f_p.$$

- Substituting $f_p \sim T^*/p$, it develops a $\delta^{(3)}(\mathbf{p})$ function, that is the BEC.
- BEC is driven by elastic process, while inelastic processes catalyze the vanishing of μ^* and thus speed up the onset of BEC.

A possible evolution picture

- Stronger inelastic processes, earlier the appearance of the BEC.
- Stronger inelastic processes, faster the destroy of the BEC.
- Two time scales compete, a possible picture is:

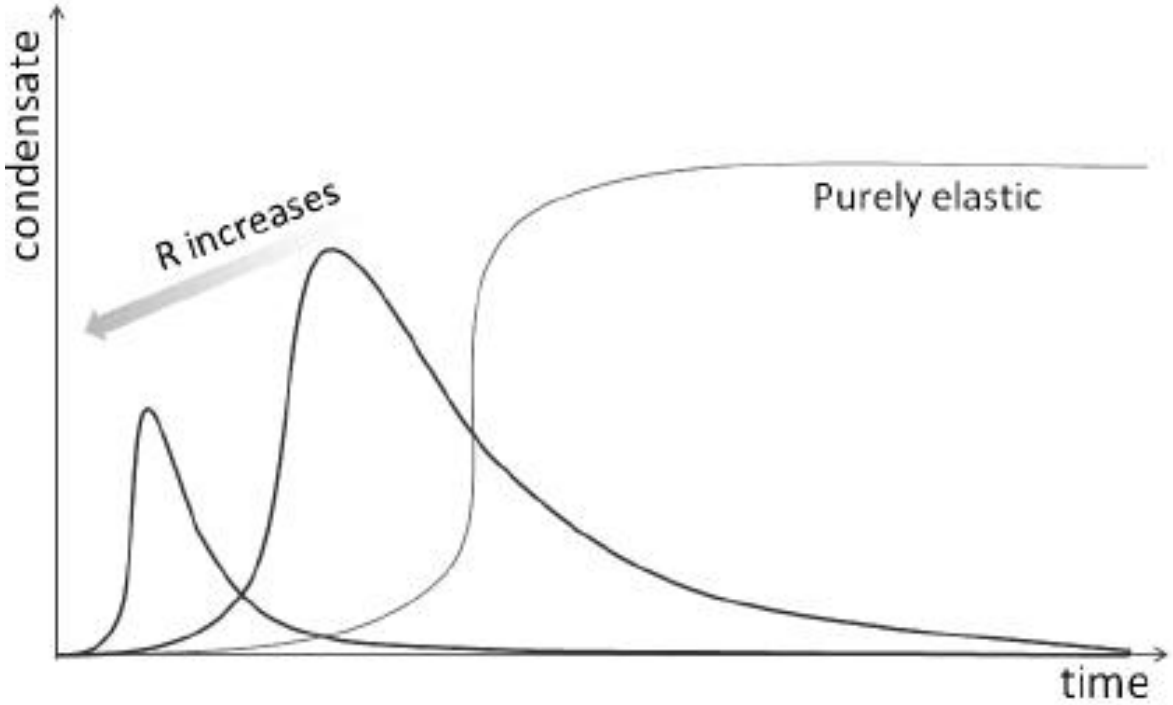

- Still an open problem of determination of the two scales.

Summary and outlook

- Fast thermalization is possible in weakly interacting, highly occupied, gluon system
- A new scenario for thermalization in gluon system by Blaizot, Gelis, Liao, McLerran, and Venugopalan, in which a non-equilibrium gluon BEC state is possible.
- Inelastic processes speed up the onset of BEC
- LPM effect will change quantitative results
- Effect of longitudinal expansion and anisotropic distribution
- How inelastic finally destroy BEC? Need kinetic equation within BEC.
- What is the nature of the condensation of gauge boson?
- Phenomenology of this non-equilibrium gluon BEC.
- Other intermediate state? Turbulence?
- ... ...

Thank you!

Thermalization: An experimentalist's view

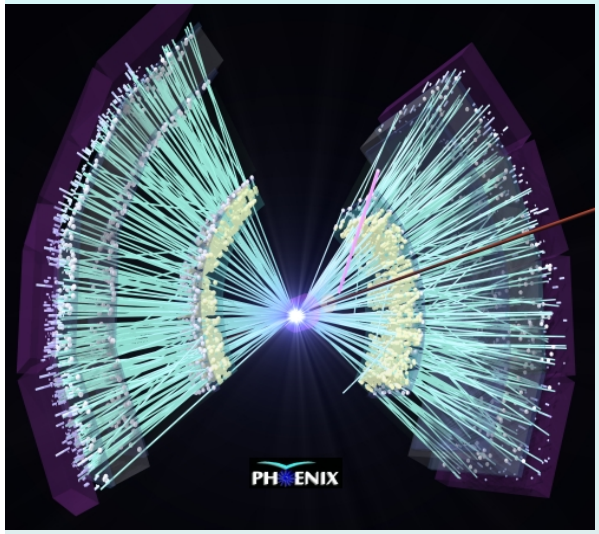

Barbara Jacak

Stony Brook

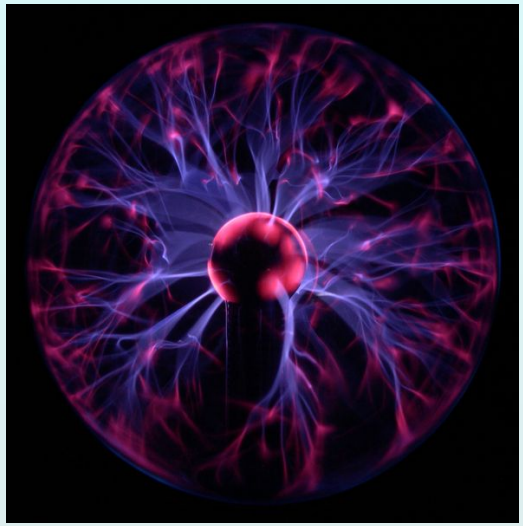

Workshop on the Approach to Equilibrium in Strongly Interacting Matter

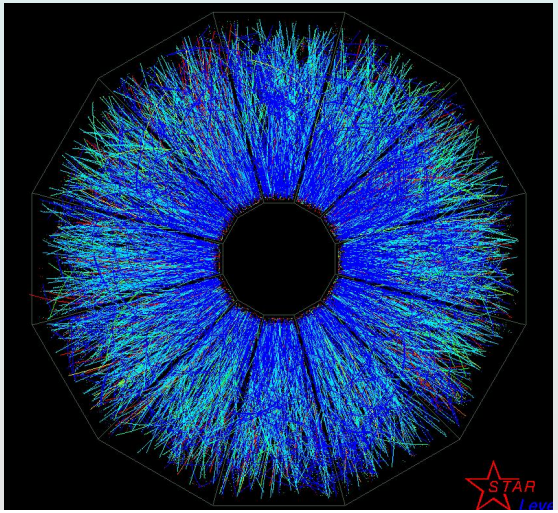

April 4, 2014

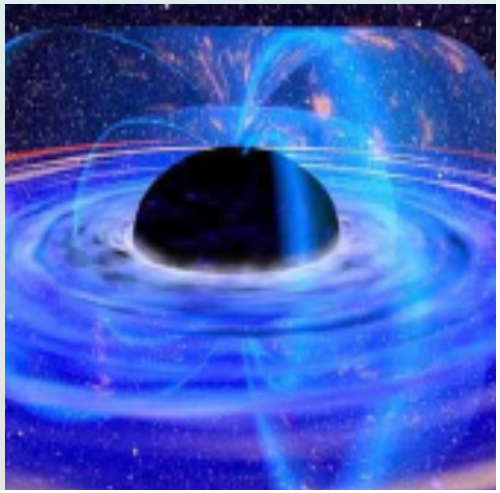

THIS experimentalist's view

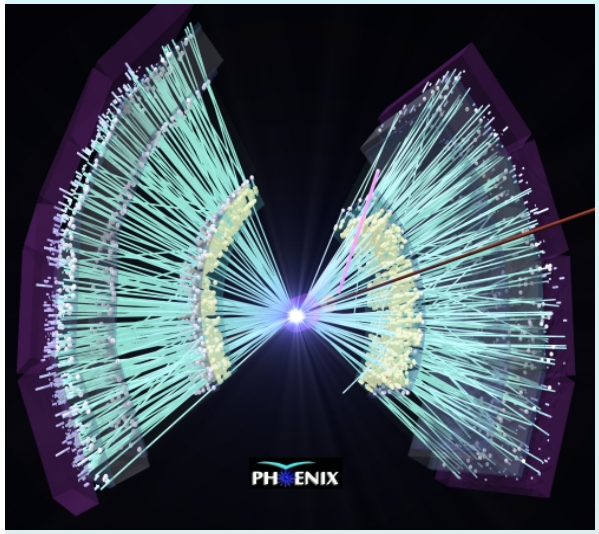

Barbara Jacak

Stony Brook

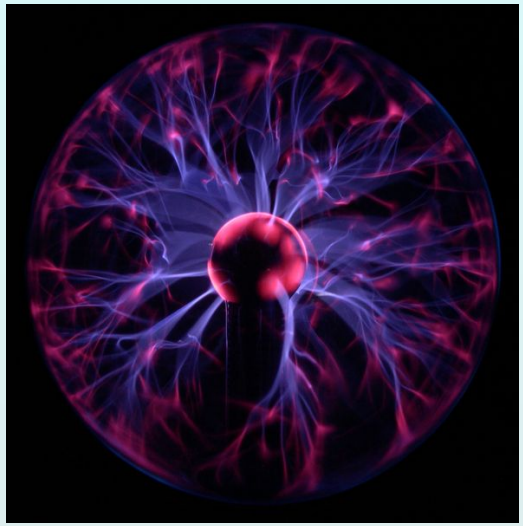

Workshop on the Approach to Equilibrium in Strongly Interacting Matter

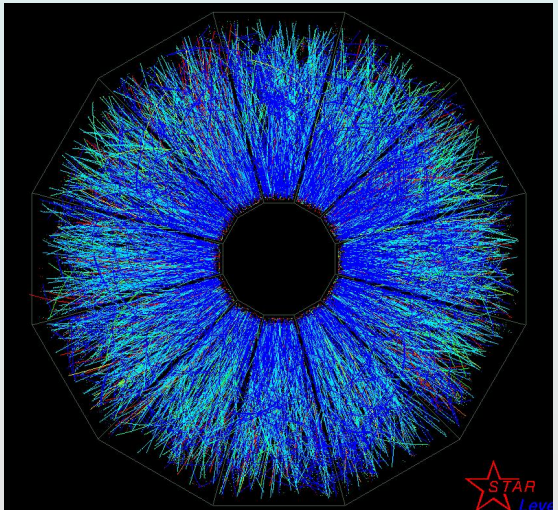

April 4, 2014

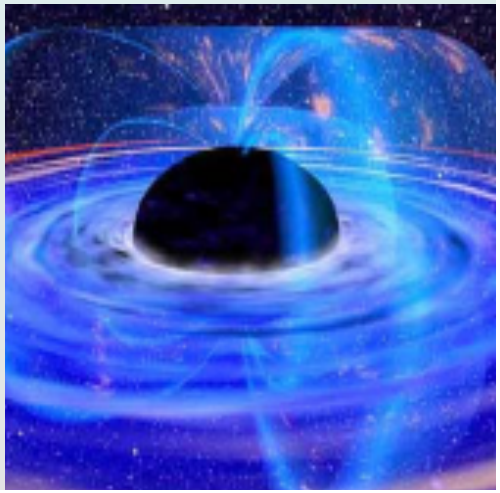

A big mystery: fast equilibration

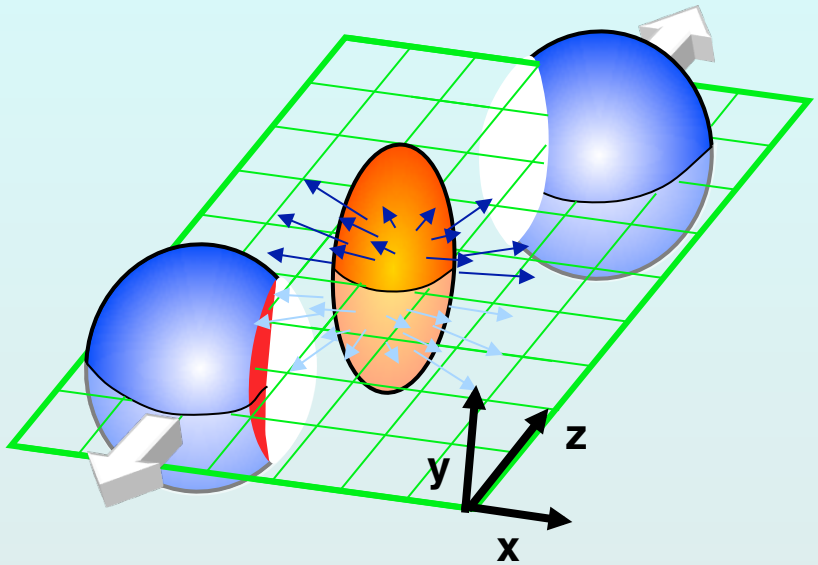

- **Build up pressure fast**
  - Else too little elliptic flow (v_2)
- **Hydrodynamics works!**
  - But only if you start it within 1 fm/c of collision
- **Hydro implies (local) equilibrium**
  - Cascade of q and g collisions can't get there in time!
- **So what gives?**
  - Fast equilibration due to tiny black hole?
  - Plasma instabilities?
  - Smart ideas discussed here?
  - Gluons start out closer to a thermal distribution?

An interesting question

- Just *WHAT* is inside the hot dense QCD plasma?

  Individual gluons?

  Pure fields?

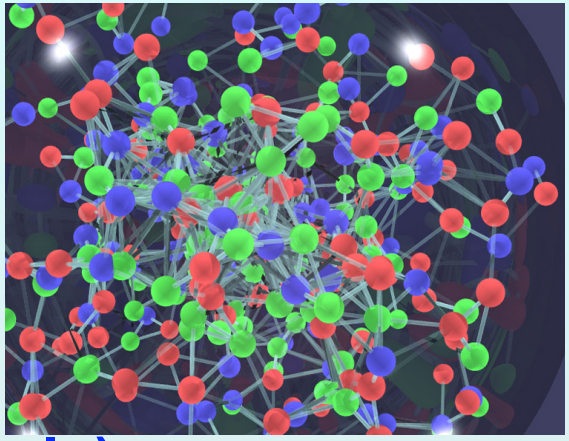

  Multi-gluons that continuously split & re-form?

  i.e. composite quasiparticles

  (in classical liquids voids fill this role)

- Energy loss: radiative? elastic?

  Excite collective modes in QGP?

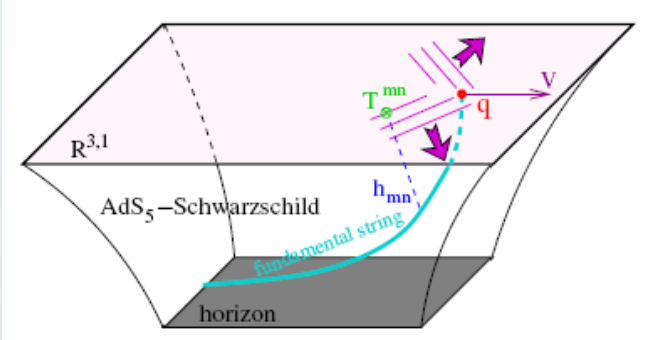

- Quantify dynamical properties of this new material:

  Viscosity, speed of sound, diffusion

- Properties ⟷ thermalization mechanism

What can an experimenter say?

- EM Observables in A+A
  Reflect early time (pre-equilibrium?)

- Teeny tiny drops of plasma?
  Collective behavior in p/d+A

- Structure vs. dynamics in cold nuclear matter
  Initial and final state parton energy loss

Can we *measure* thermalization in action?

Thermal radiation

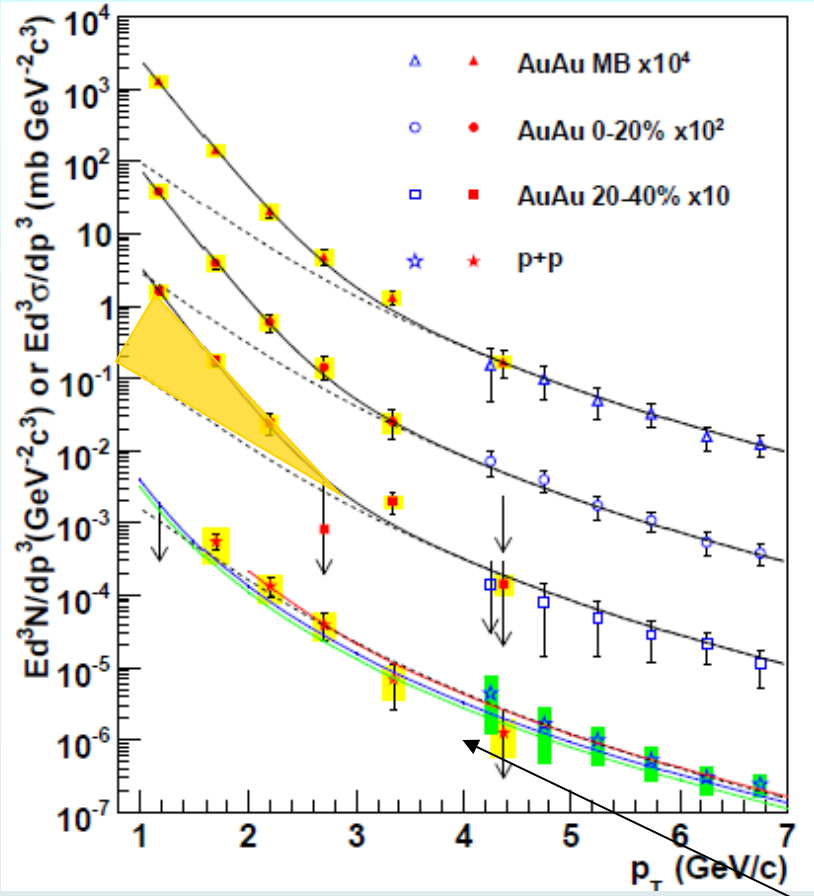

PRL 104, 132301 (2010)

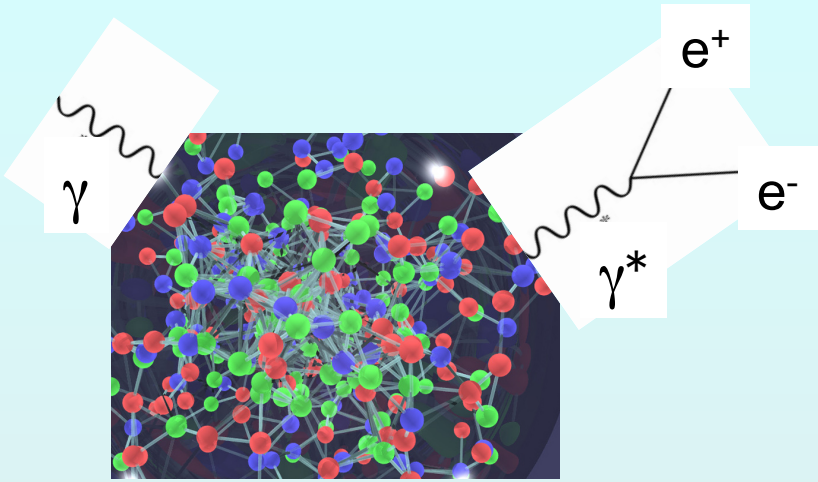

Low mass, high p_T e^+e^- → nearly real photons

Large enhancement above p+p in the thermal region

pQCD γ spectrum (Compton scattering @ NLO) agrees with p+p data

direct photons: $T_{init} > T_c$!

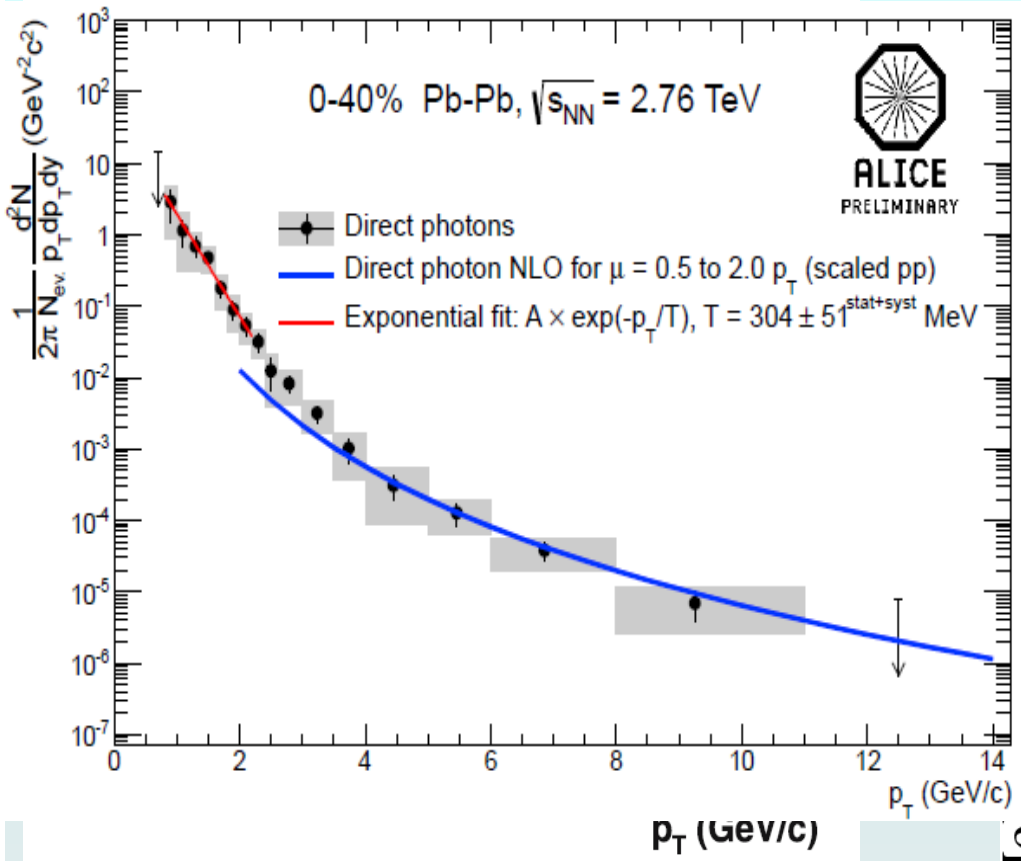

- **Exponential fit in p_T:**
  T_{avg} = 221 ±23 ±18 MeV

- **Multiple hydrodynamics models reproduce data**
  $T_{init} \geq 300$ MeV

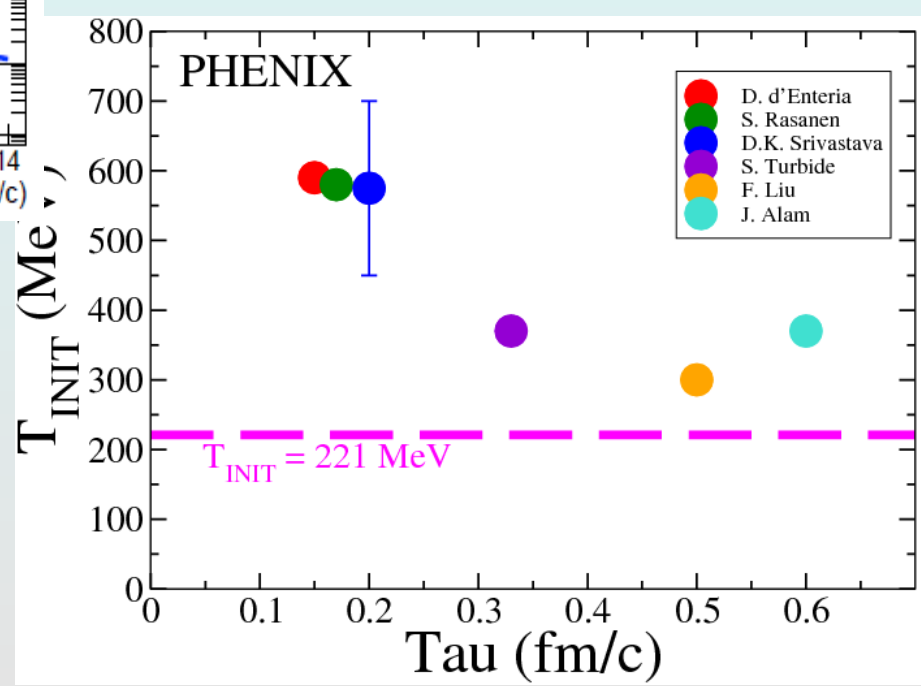

NB: T_c ~ 150 MeV
@ LHC T_{avg} = 304±51 MeV
hydrodynamic T_{init} ~ 30% higher than at RHIC

Di-electrons from thermal γ conversions in Au+Au

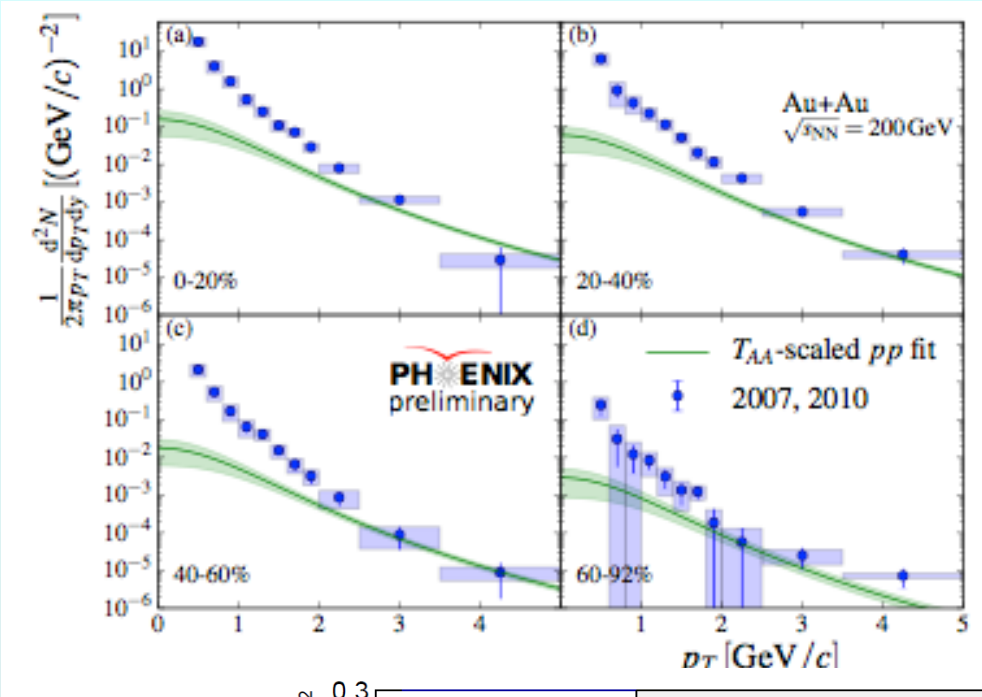

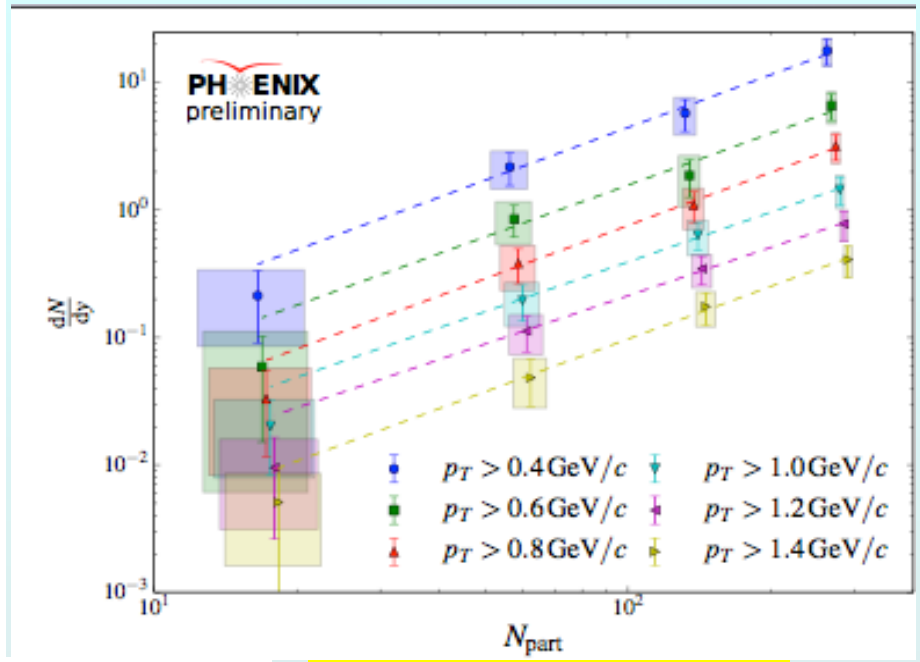

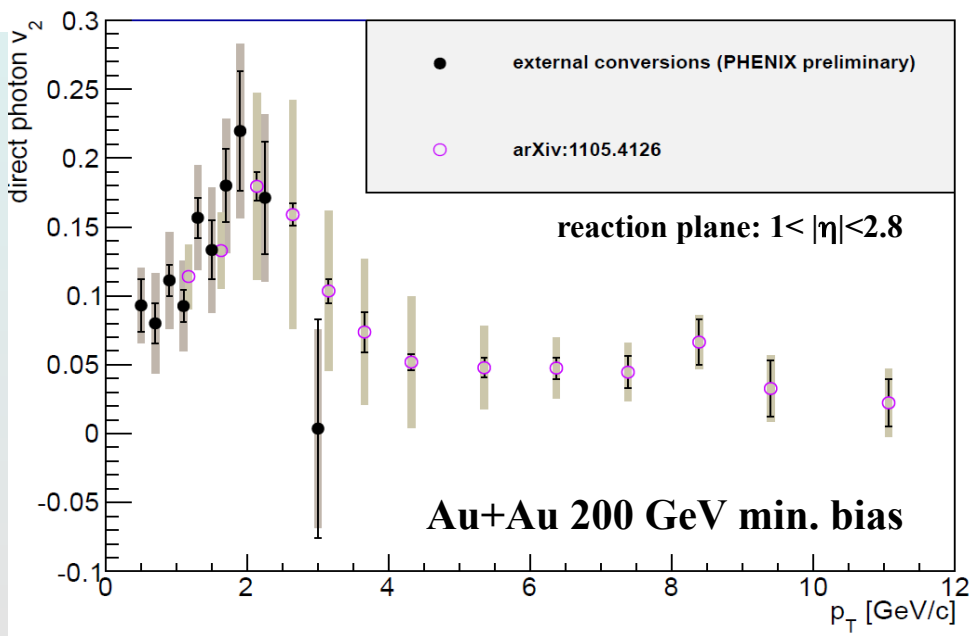

$dN_\gamma/dy \sim aN_{part}^{1.5}$
similar in hydro
(U. Heinz)

photons flow!
but more than in hydro

Larry told us: glasma emits photons

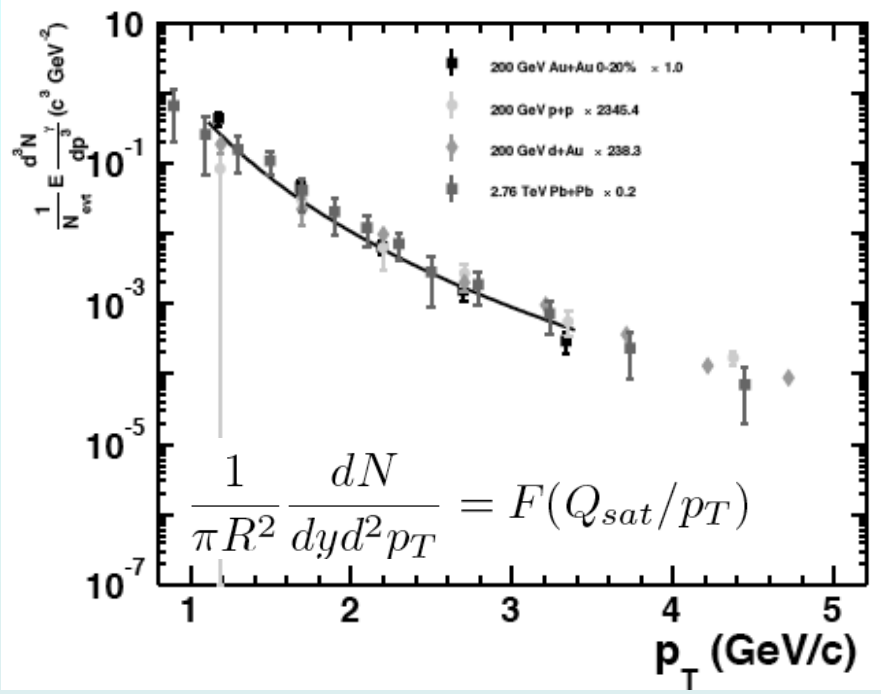

pp, dA and AA at all centralities at RHIC and PbPb

Data are on the same universal scaling curve!

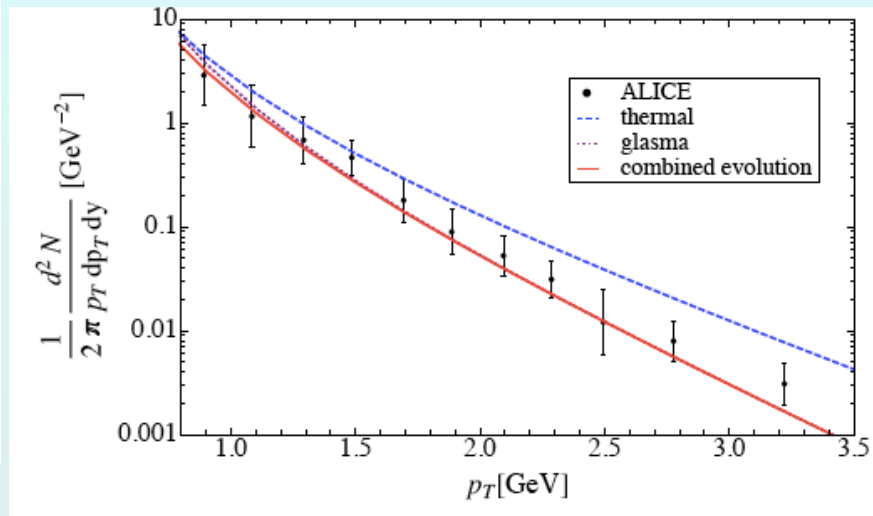

$\langle t \rangle$ [fm/c]	thermal	Glasma+th, $\delta = 1/3$	Glasma+th, $\delta = 1/5$
$p_T = 1$ GeV	12	16.5	13.7
$p_T = 2$ GeV	2	3.1	3.3
$p_T = 3$ GeV	1	1.4	1.8

Emission times much larger: Time for flow to develop?

Thermalization in tiny systems?

Two-particle angular correlations

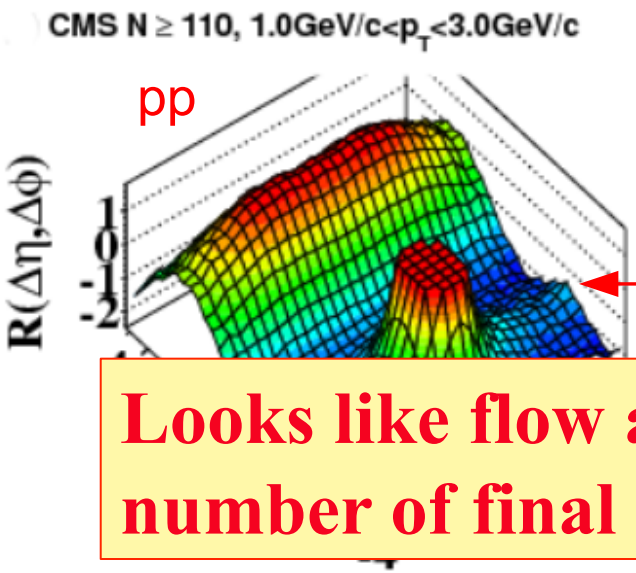

Near-side ridges apparent in high multiplicity events

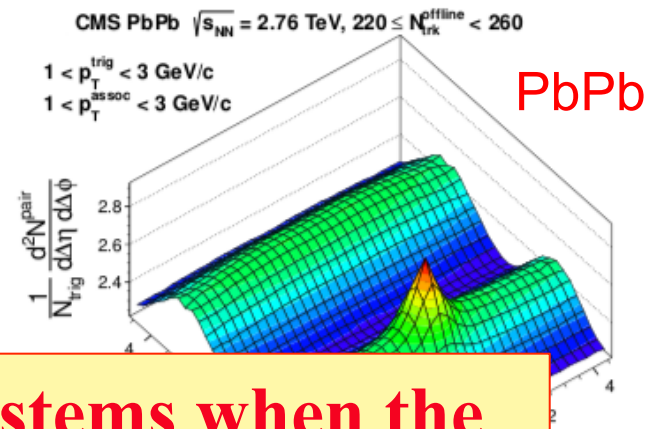

Looks like flow at LHC in small systems when the number of final particles > 100

CMS, JHEP 1009 (2010) 91

CMS, PLB 724 (2013) 213

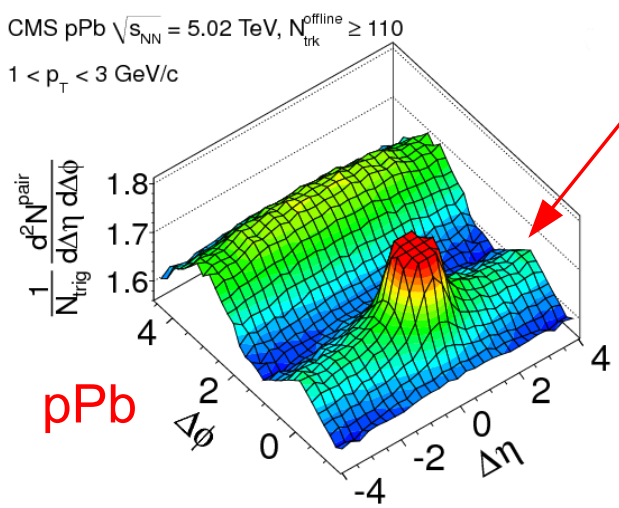

CMS, PLB 718 (2012) 795

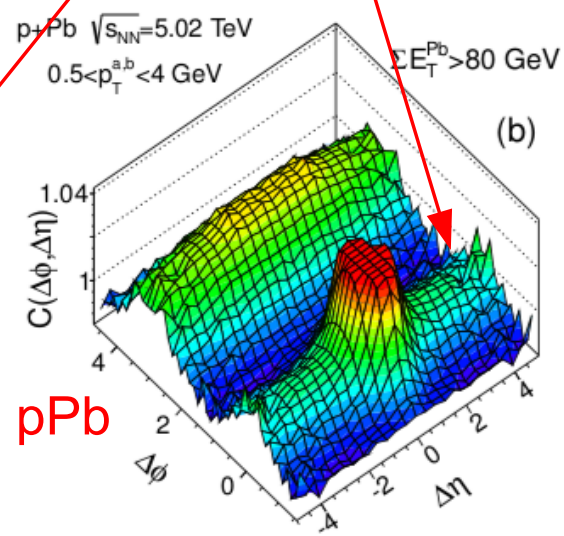

ATLAS, PRL 110 (2013) 182302

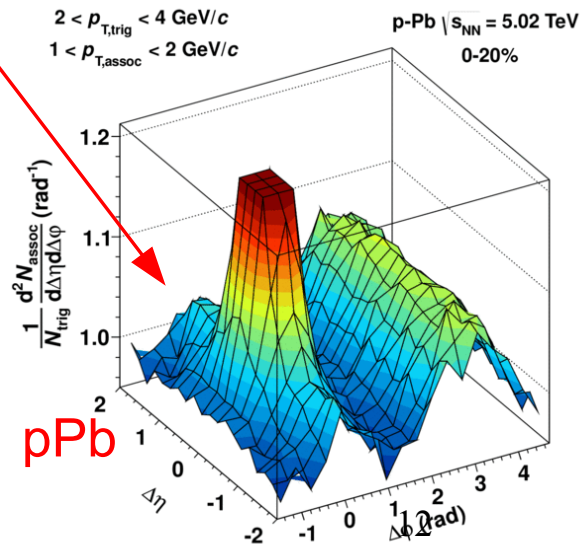

ALICE, PLB 719 (2013) 29

How about at RHIC?

- To quantify the Fourier expansion

must remove the jet

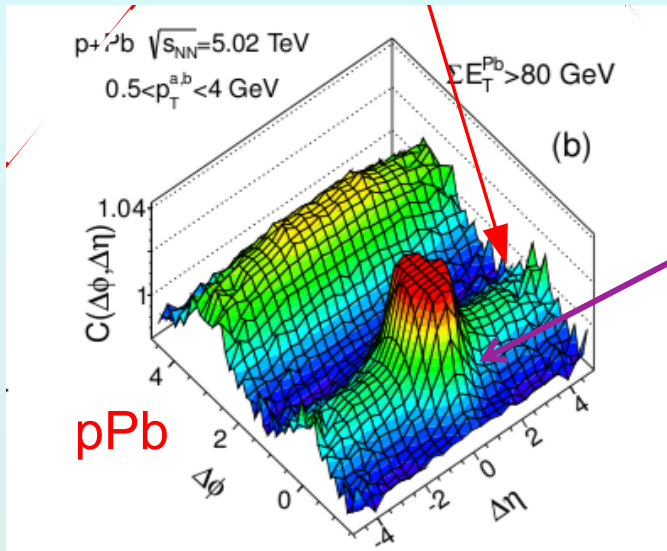

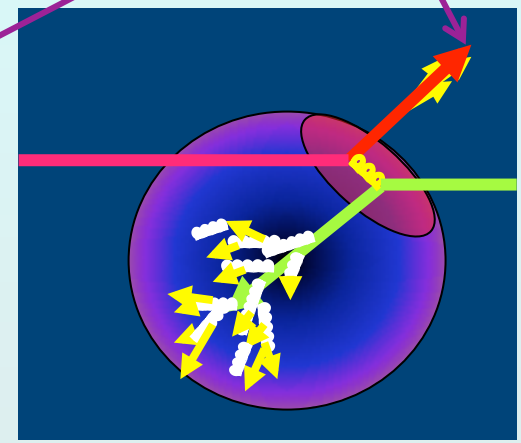

- Do by subtraction: (central d+Au – peripheral d+Au)

  i.e. high multiplicity – low multiplicity

Fourier coefficients & v_2 value

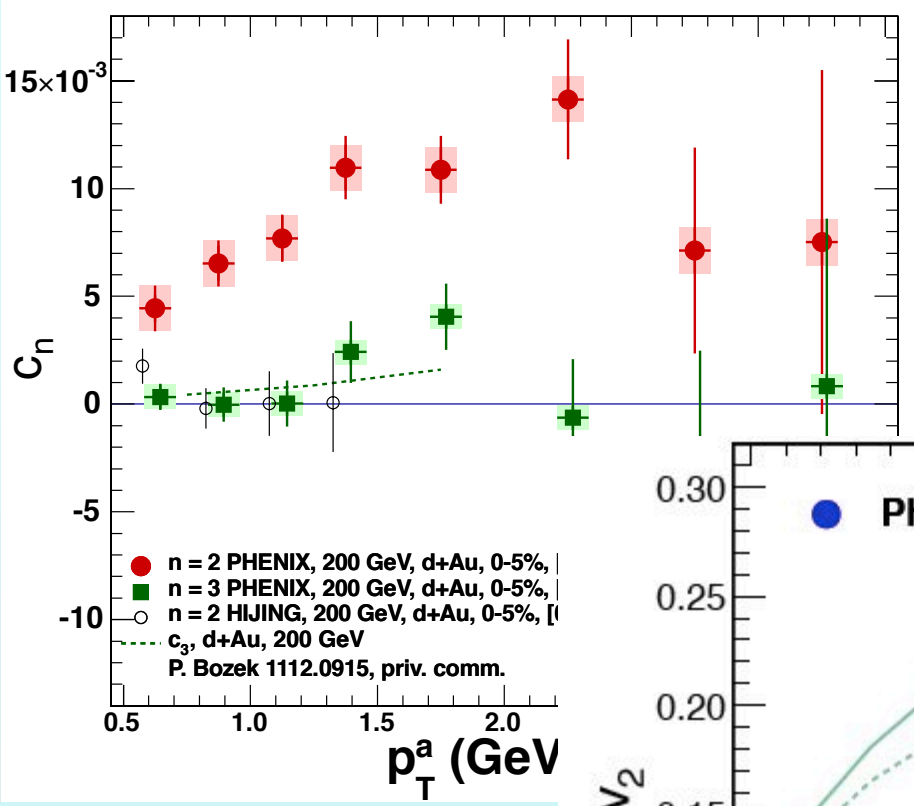

Extract v_2:

$$C_2(p_{Ta}, p_{Tb}) = v_2(p_{Ta})\, v_2(p_{Tb})$$

A. Sickles

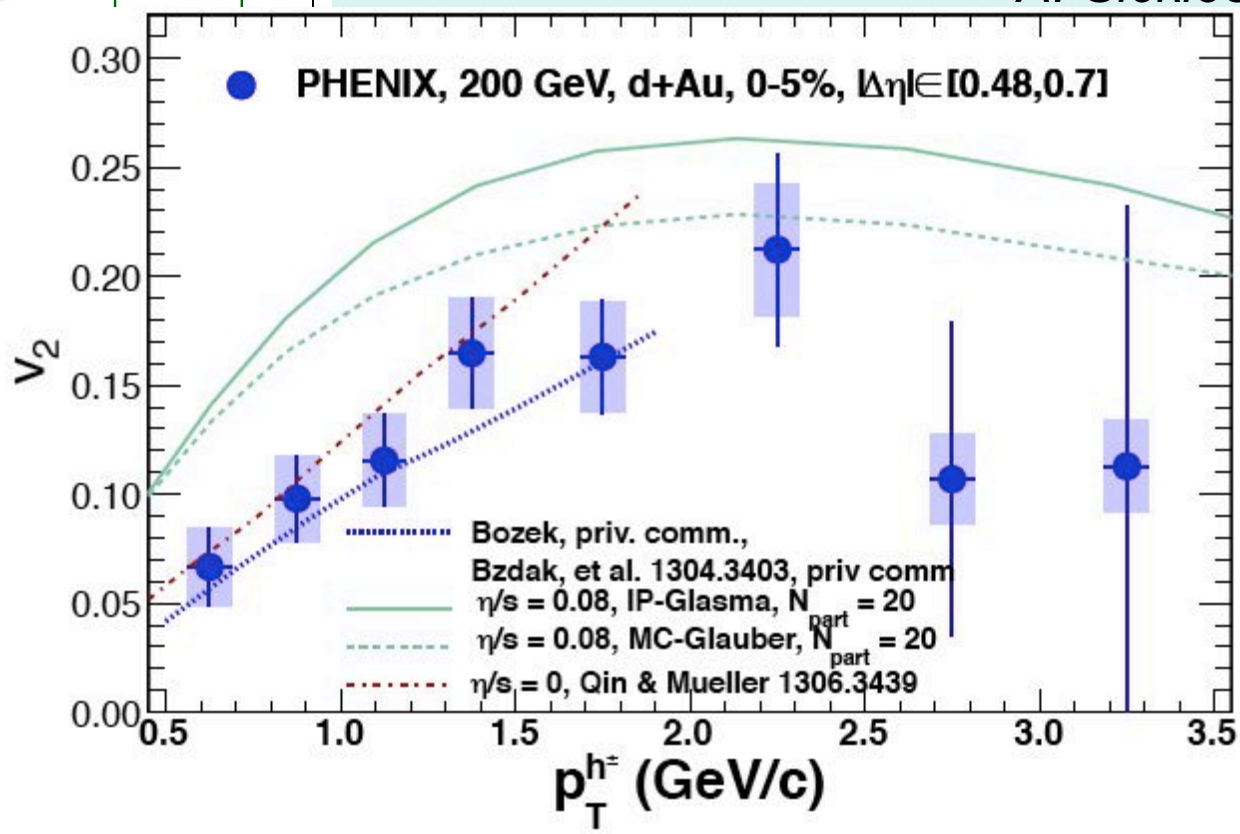

$v_2 > v_2$ at LHC

ε_2 d+Au > ε_2 p+Au

v_2 agrees w/hydro!

$\eta/s \leq 0.08$

$v_3 \sim 0$

Larger rapidity gap reduces jet contribution

Muon Piston Calorimeters

both d-going & Au-going directions

$3 < |\eta| < 4$

Look at $E_T \geq 300$ MeV/c clusters

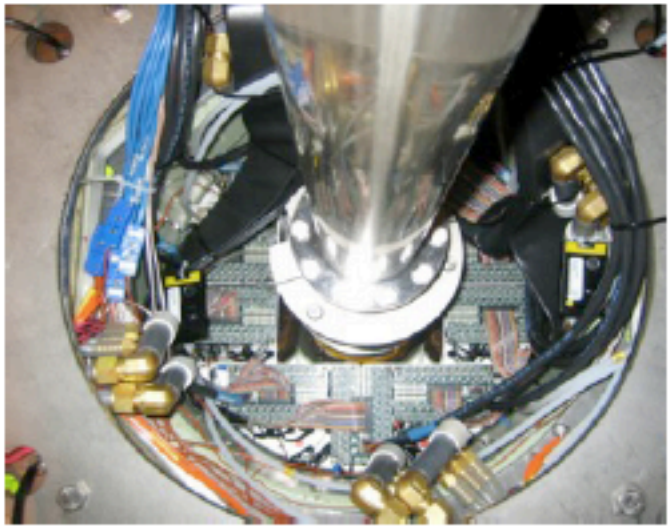

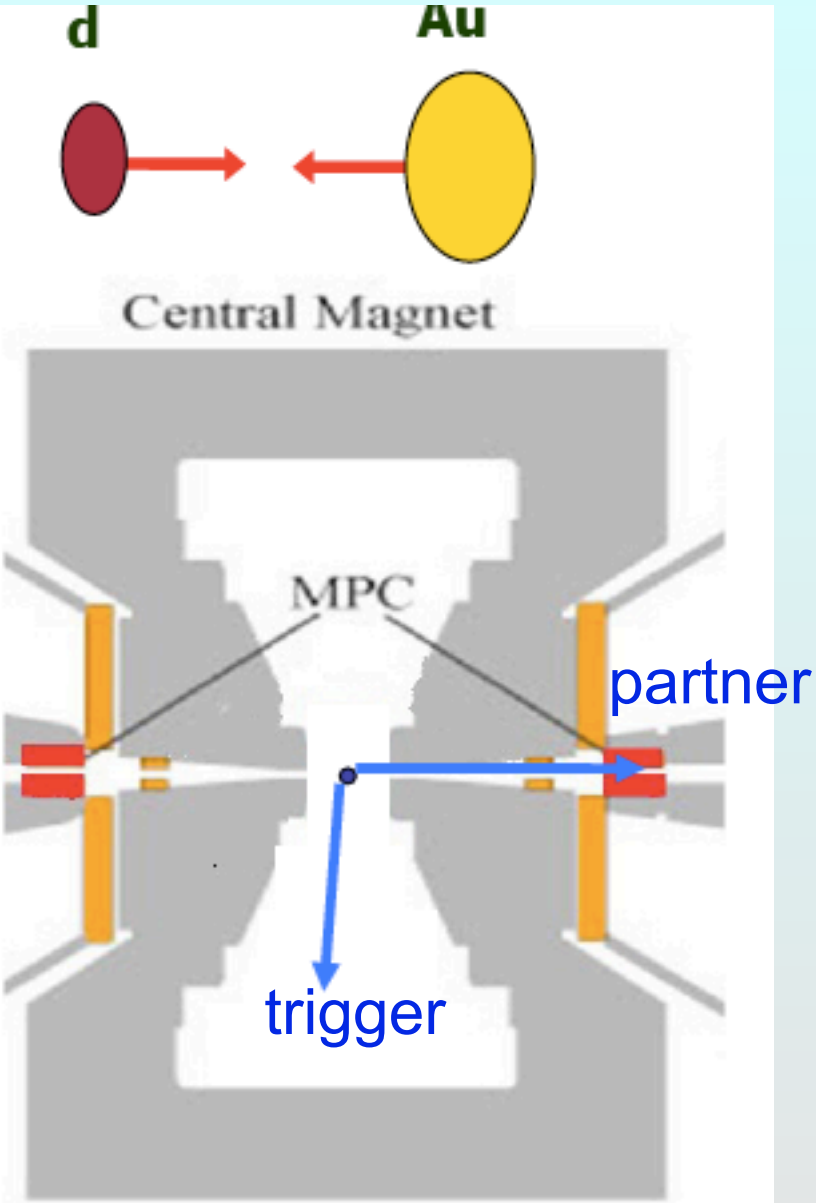

Long range correlations in d+Au at RHIC!

S. Huang

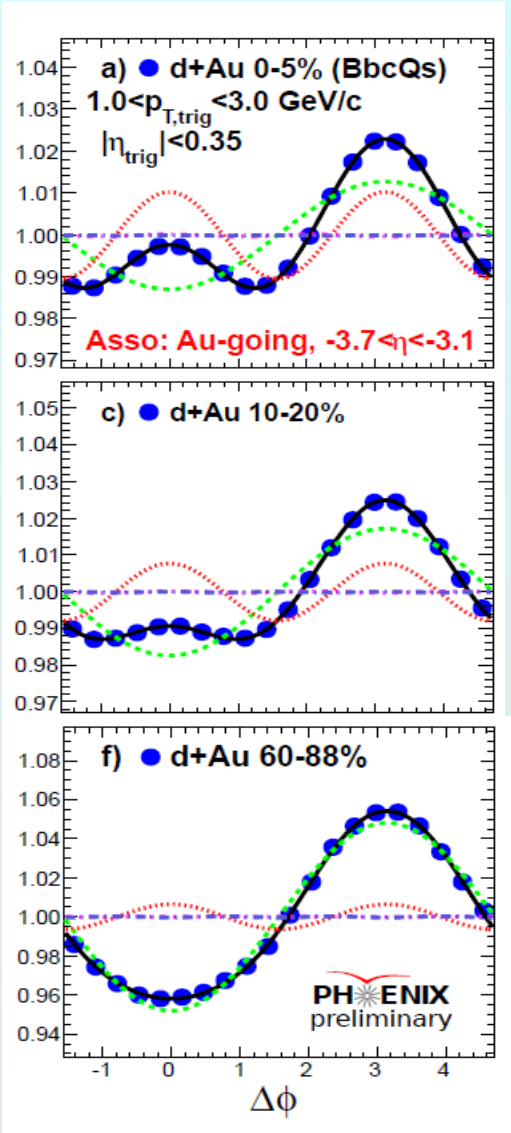

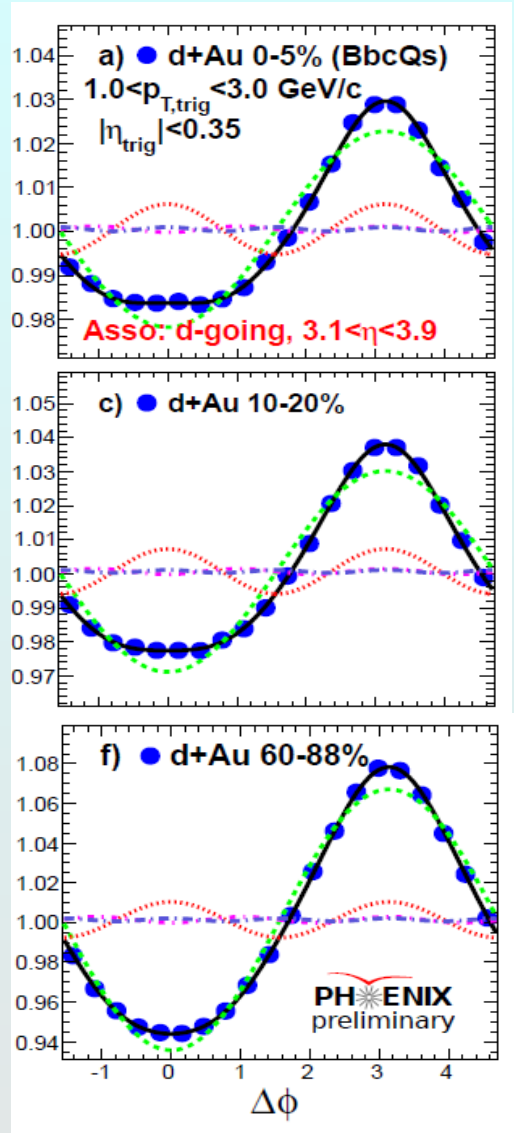

"ridge" @ large η *NB: jets not removed; v_3 ~0*

Even larger rapidity gap

S. Huang

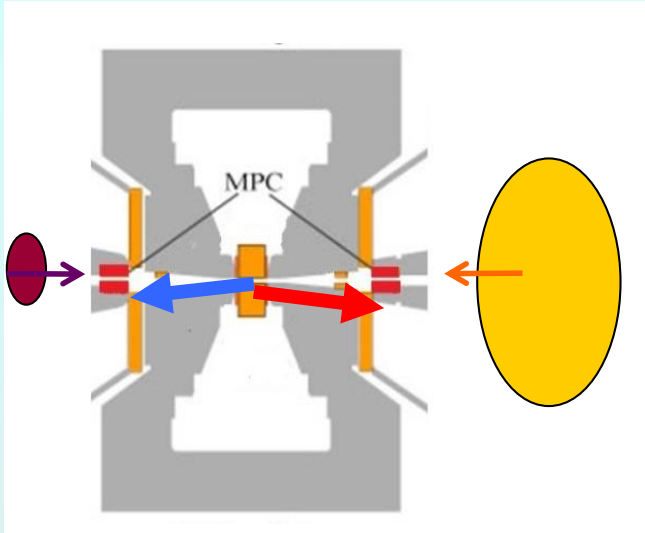

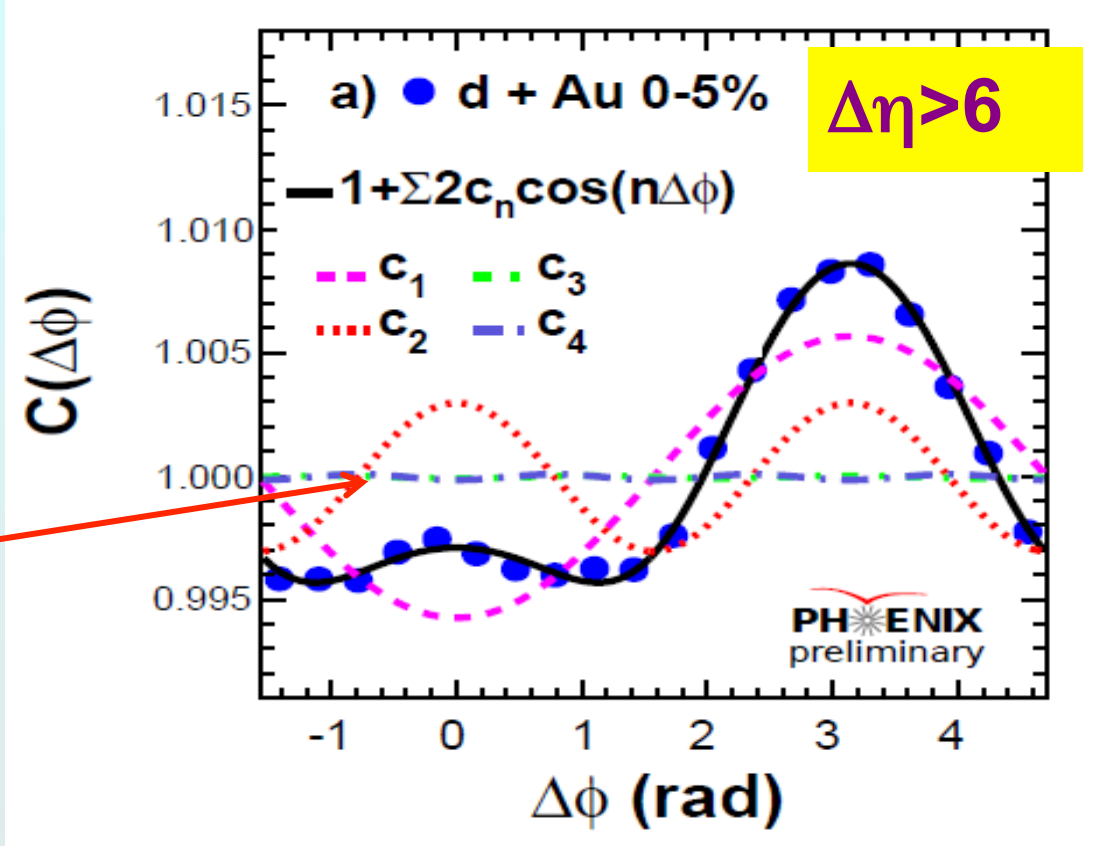

- v_2 is still non-zero!
- Looks like hydrodynamic flow…
- Other evidence?

Radial expansion, too

- Radial velocity boost -> mass dependent momentum boost
- Mass splitting seen; smaller than at LHC… less dense & less flow

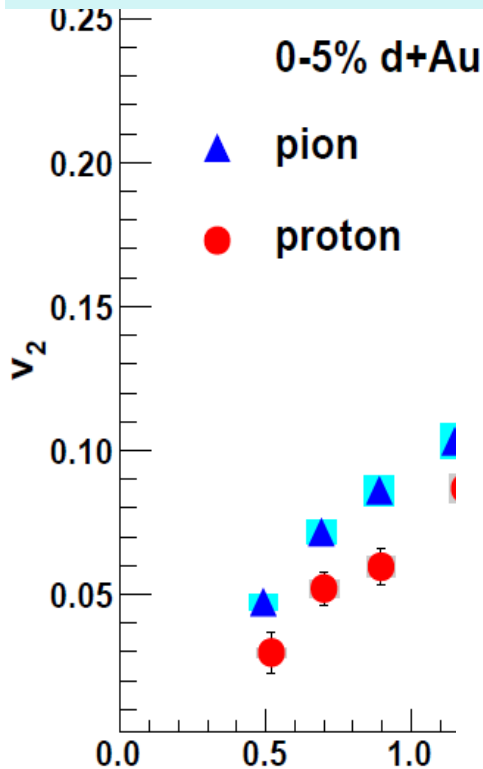

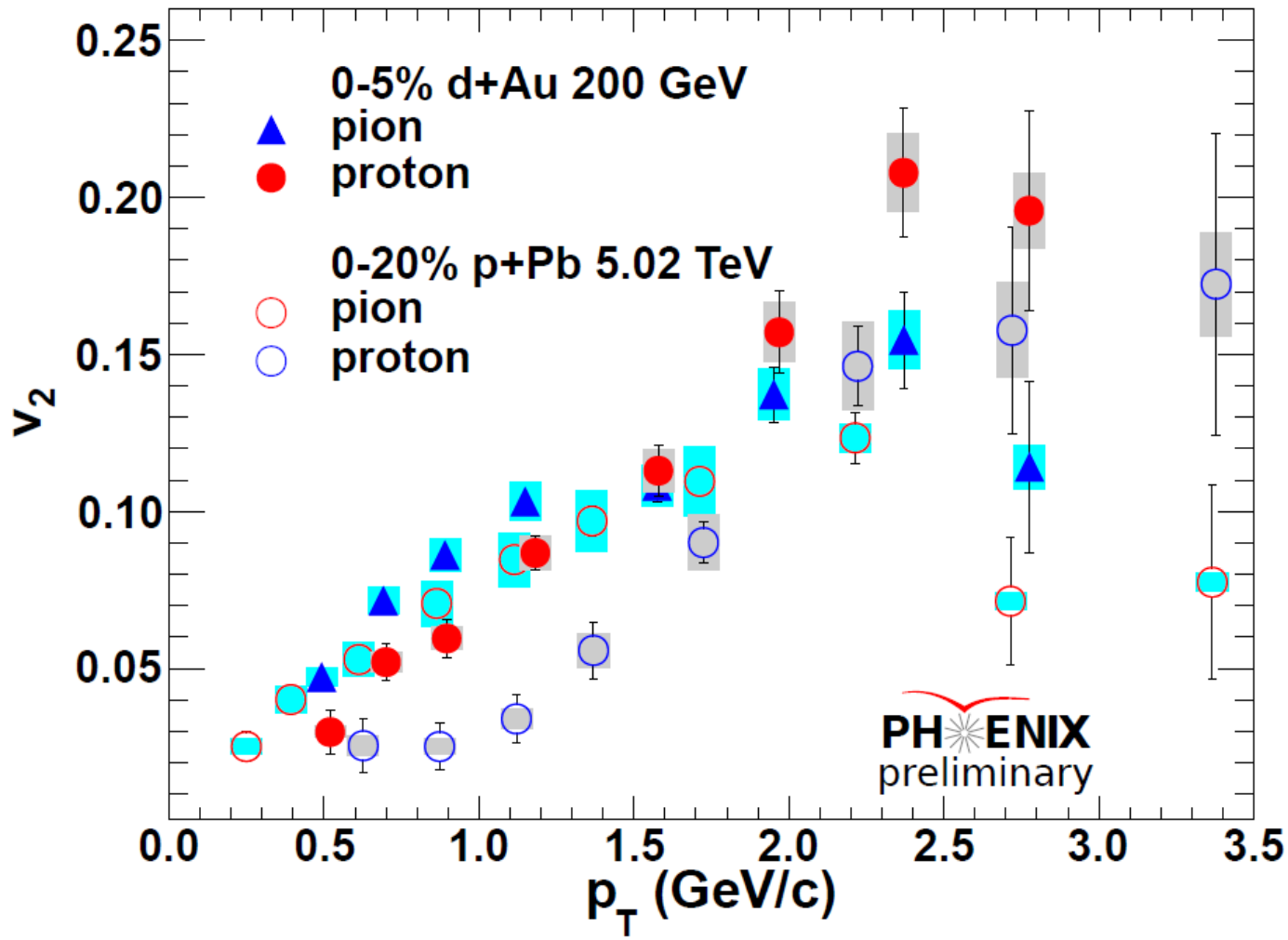

Position-momentum correlations? HBT!

N. Ajitanand

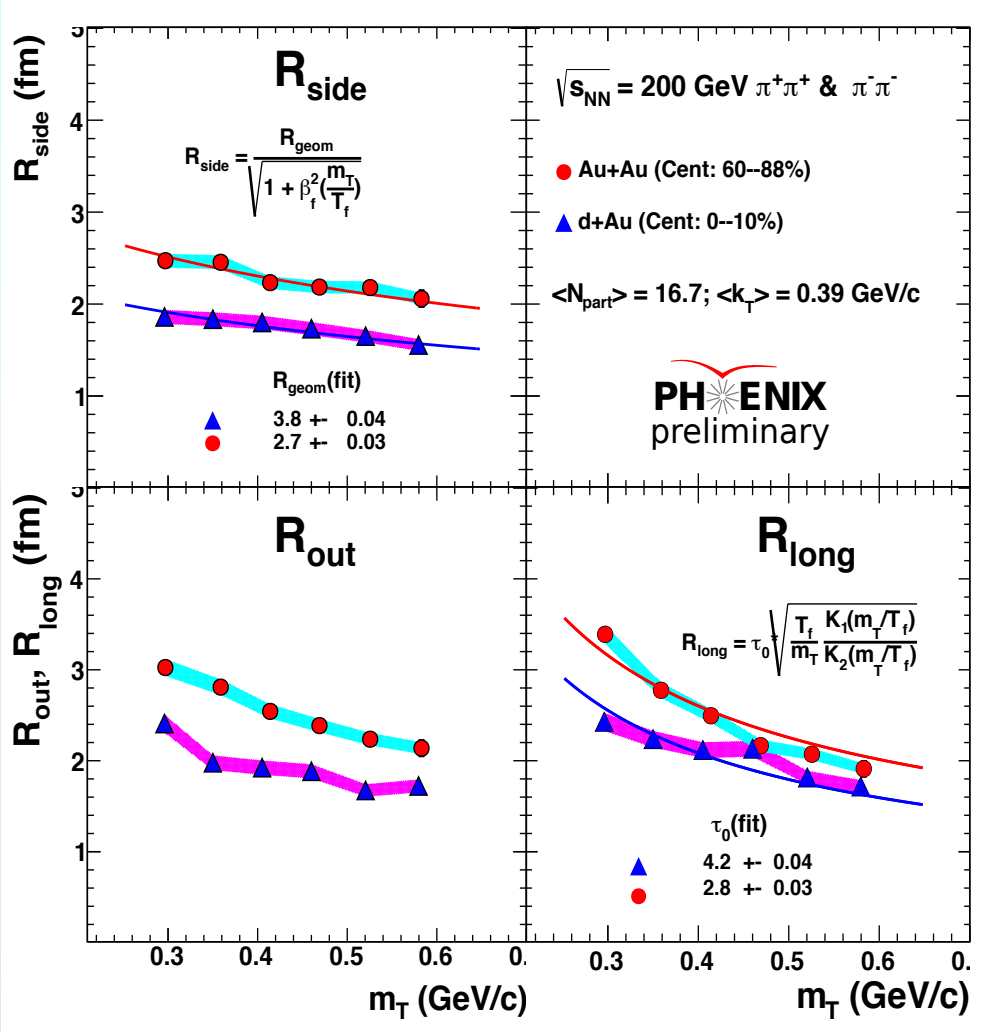

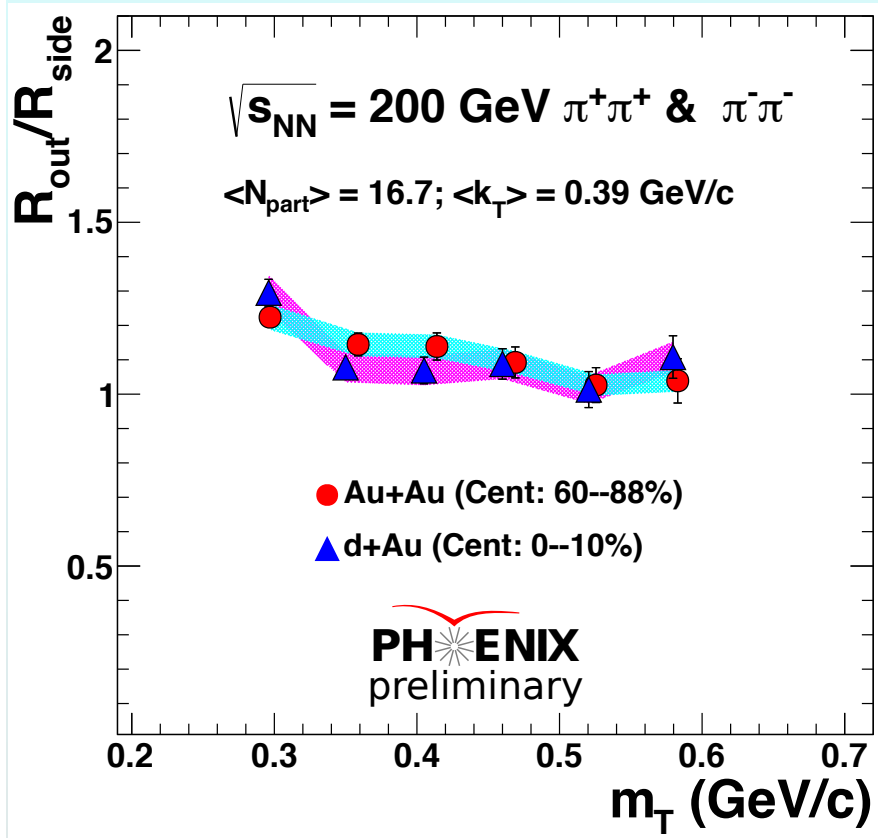

More evidence for hydro expansion, as in Au+Au!

same Npart = same emission duration (but smaller system)

A drop of QGP is made in p/d+Au?

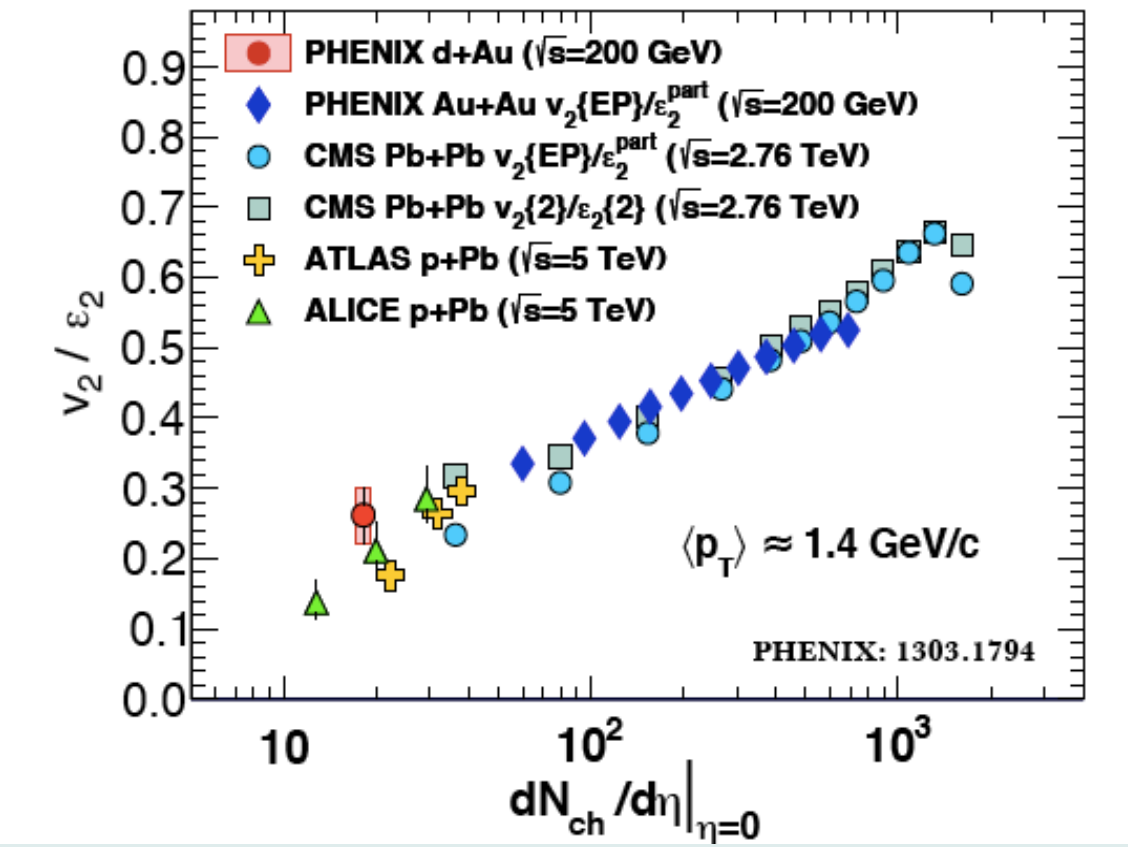

- *Hydrodynamics needs equipartition of particle momenta to be usable (~local equilibrium)*
  + sufficient volume to call it "matter"
- *Also in small systems?*
  Seem to evolve hydrodynamically!
  Plasma with R not > $r_{interparticle}$?
- *Until a few years ago, everyone thought "no"*

Deepens mystery: how can so little matter thermalize so fast?

Structure deep inside nuclei?

- High gluon density, small coupling at low x (p_g/p_N)
  More in nuclei than nucleons

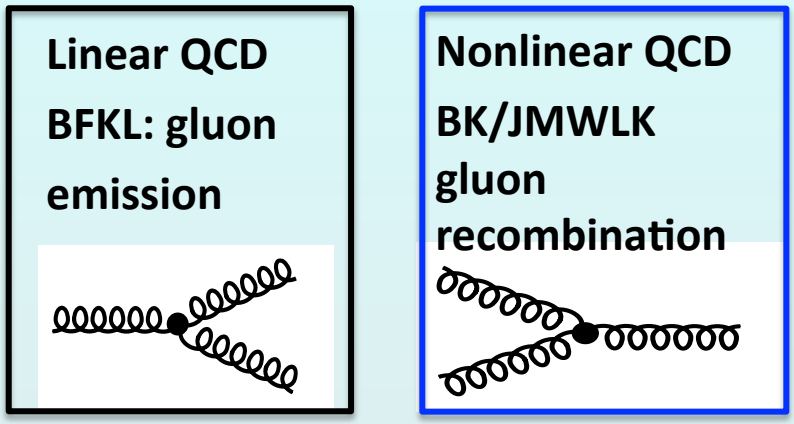

(McLerran, Venugopalan)

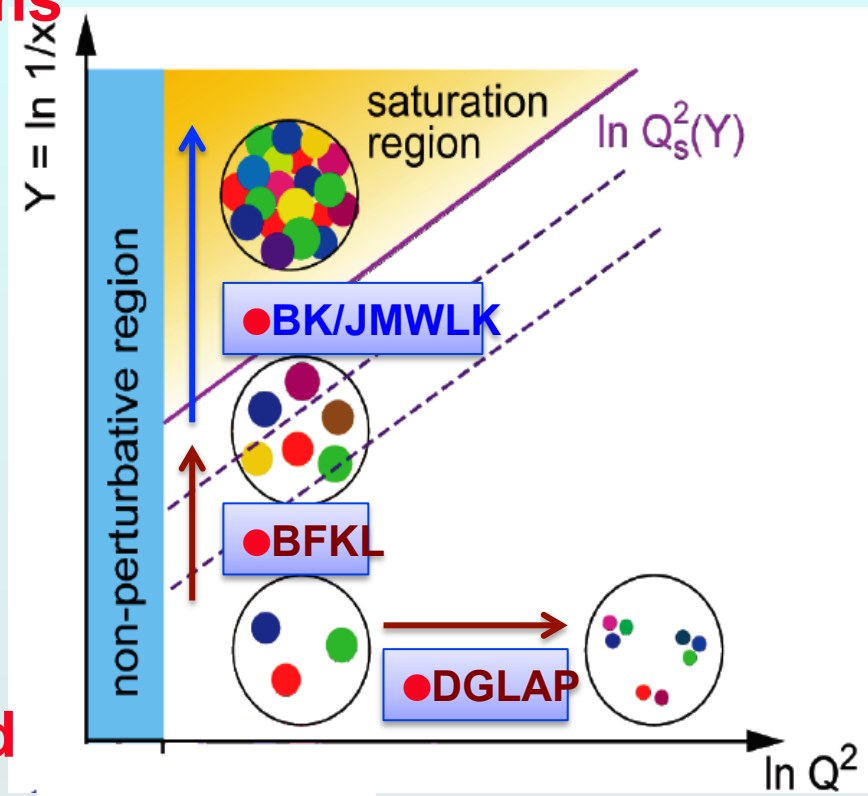

- Can describe saturated gluon distribution as a field
- Easier to equilibrate if we start from this?
- What effects of incoming parton dynamics?

See Ann. Rev. Nucl Part (60) 2010 F. Gelis et al., , arXiv:1002.0333)

First hints at RHIC for saturation of gluons

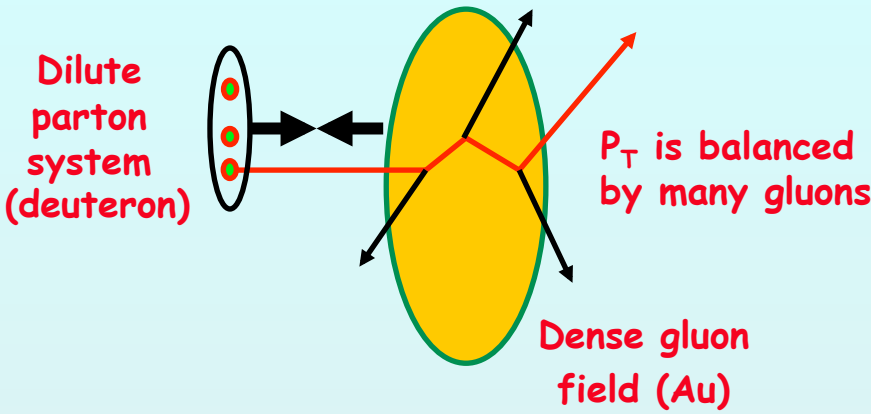

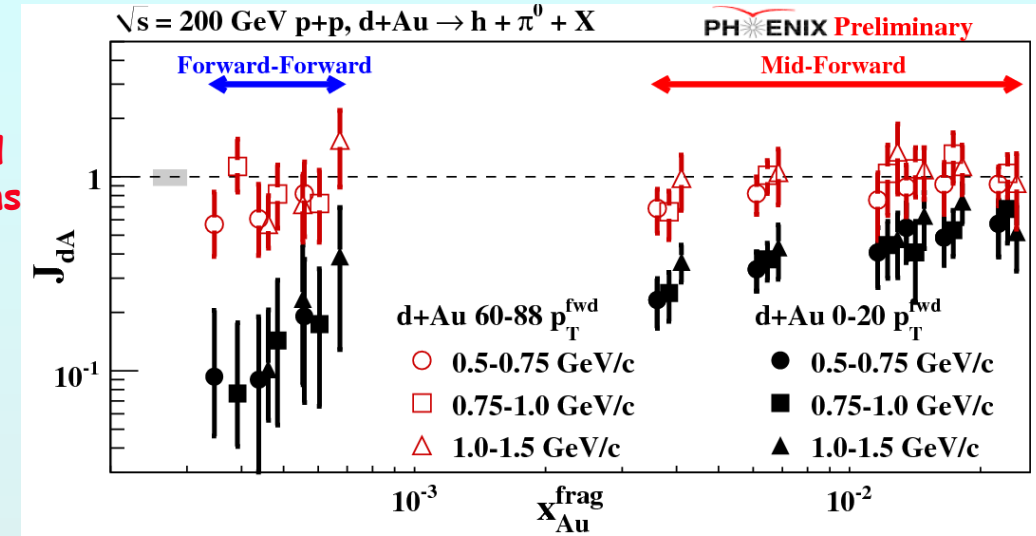

Saturation = dense gluon field

Easier to equilibrate???

QCD Compton scattering to find out (q+g -> q+γ):

no final state effects on γ!

Forward rapidity to reach small x & high g density

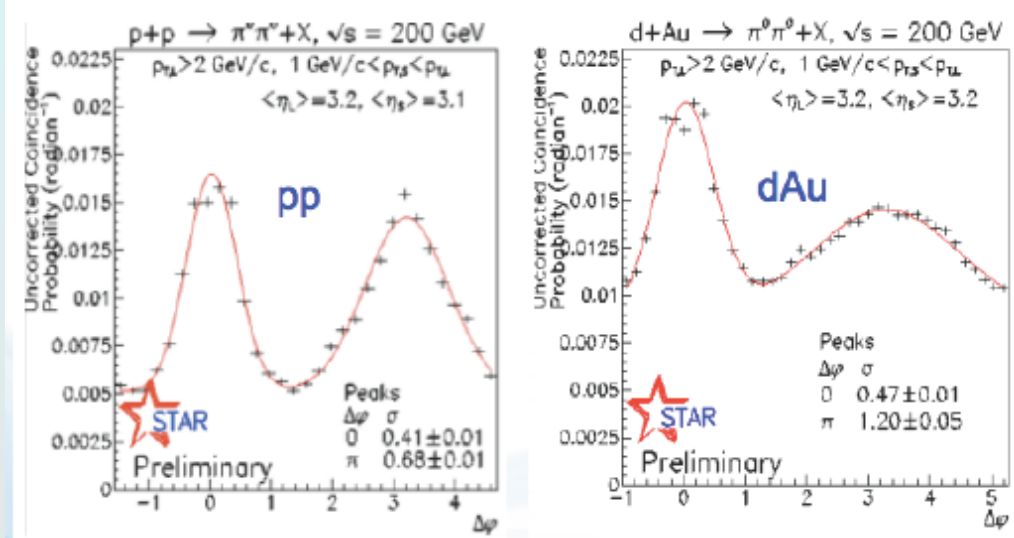

p+A in 2015 at RHIC

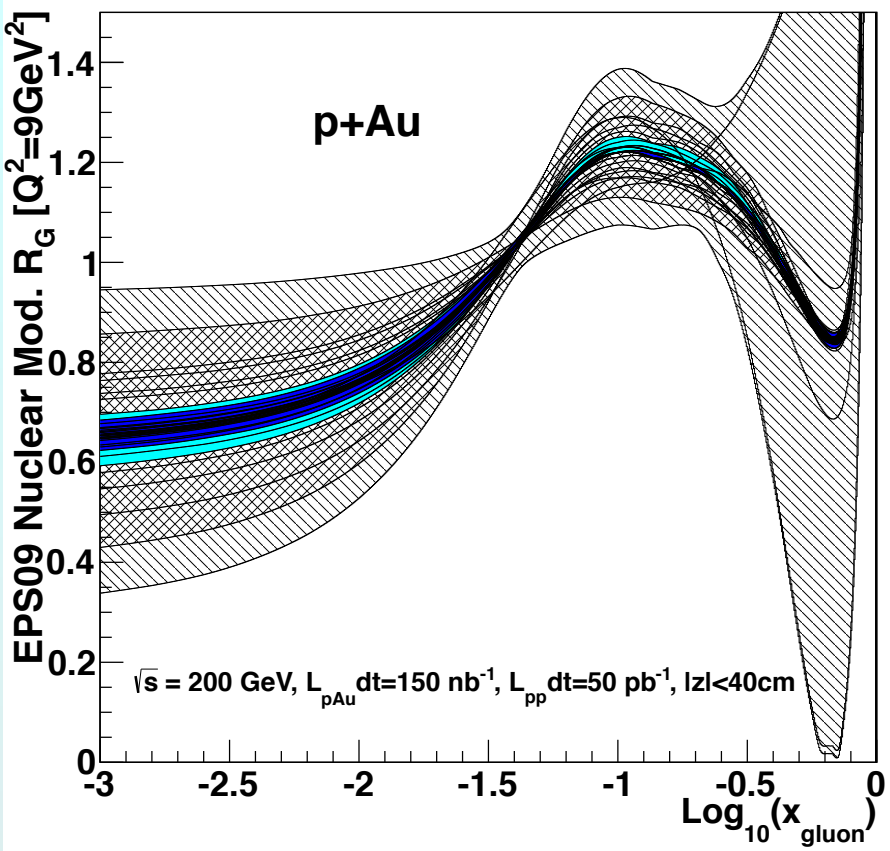

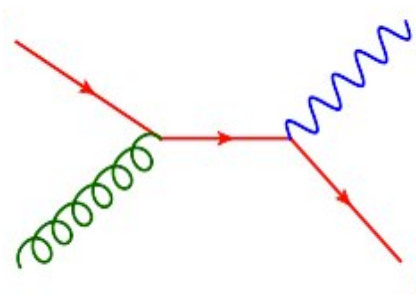

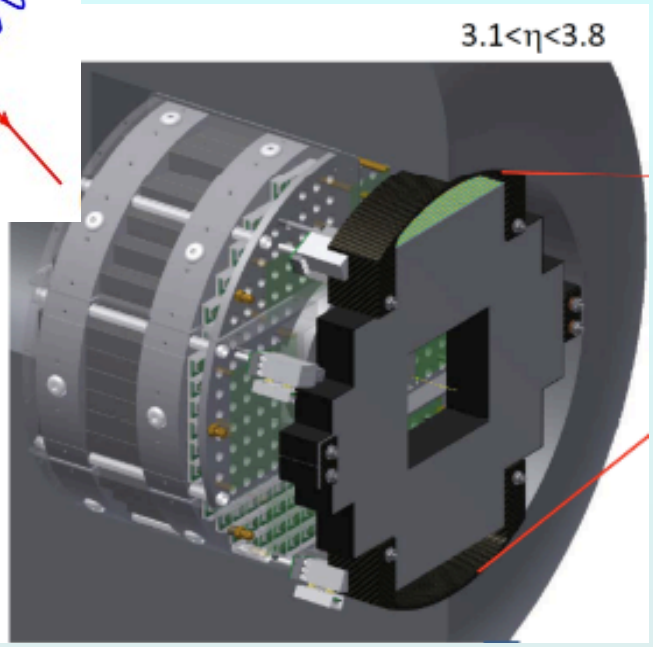

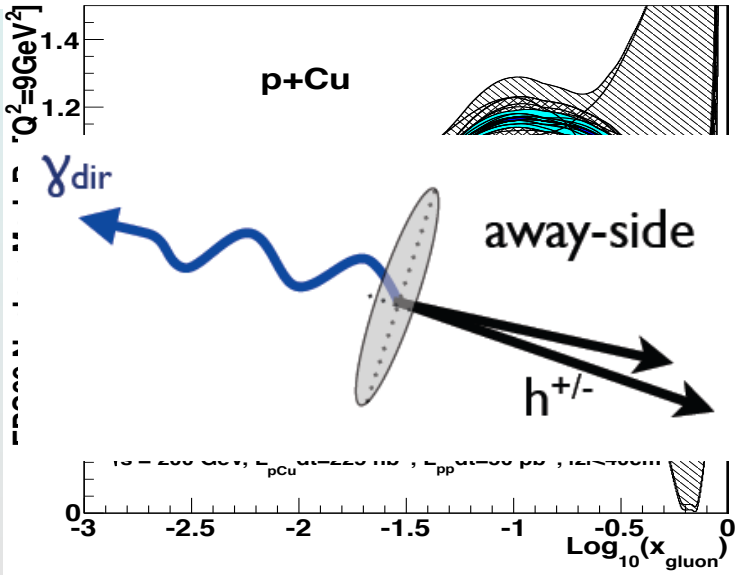

Si/W preshower + PbW cal.

γ vs. π^0 decay

Substantially improve nPDFs!

to x ~ 10^{-3} and at high x

γ + h for parton dynamics

Caution –
ignore parton dynamics
at your own peril!

Initial State structure

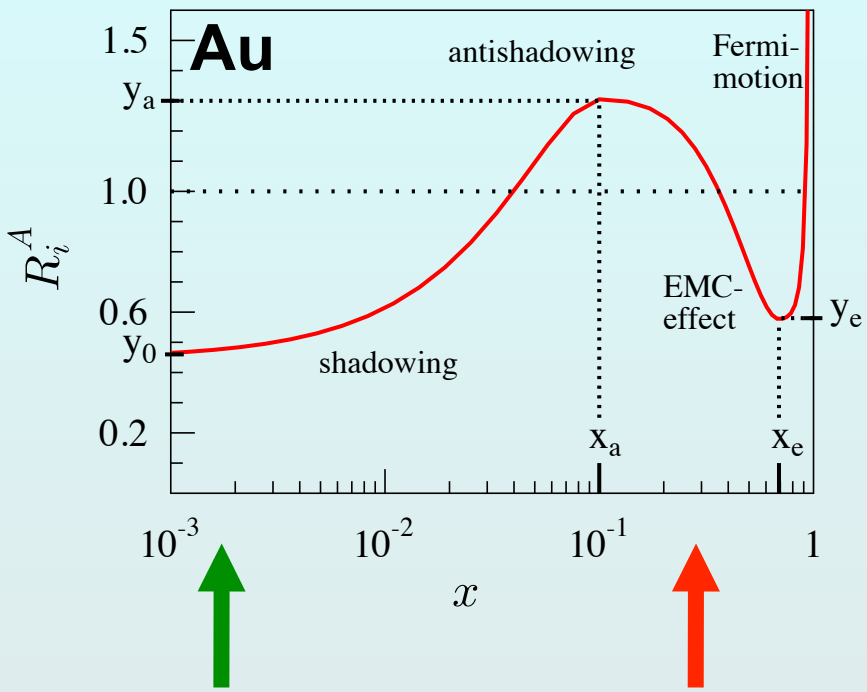

Forward
+ y
d-going

Backward
- y
Au-going

d+Au -> J/ψ from PHENIX

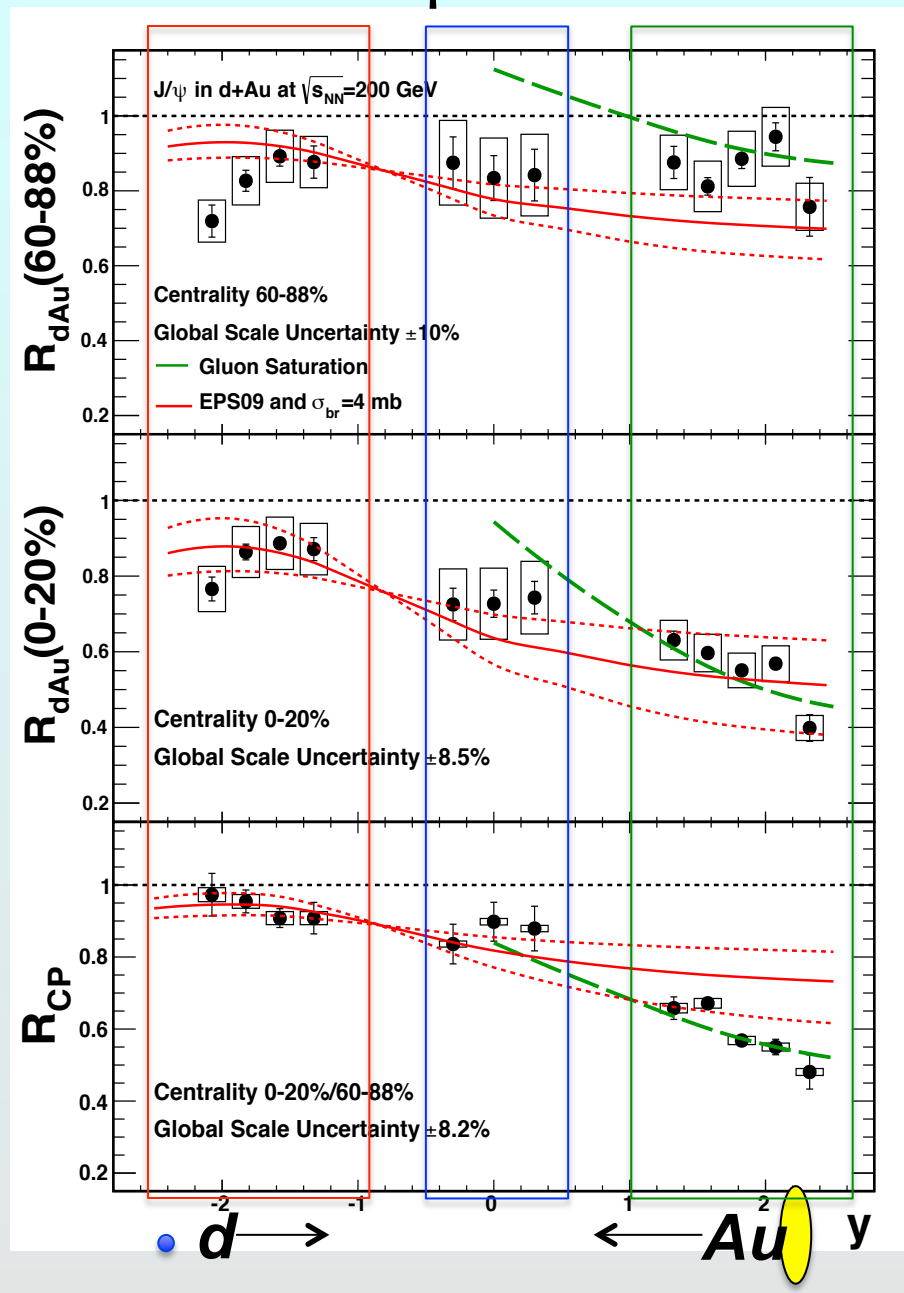

Shadowing, breakup & Cronin effect

PRC87, 034911 (2013)

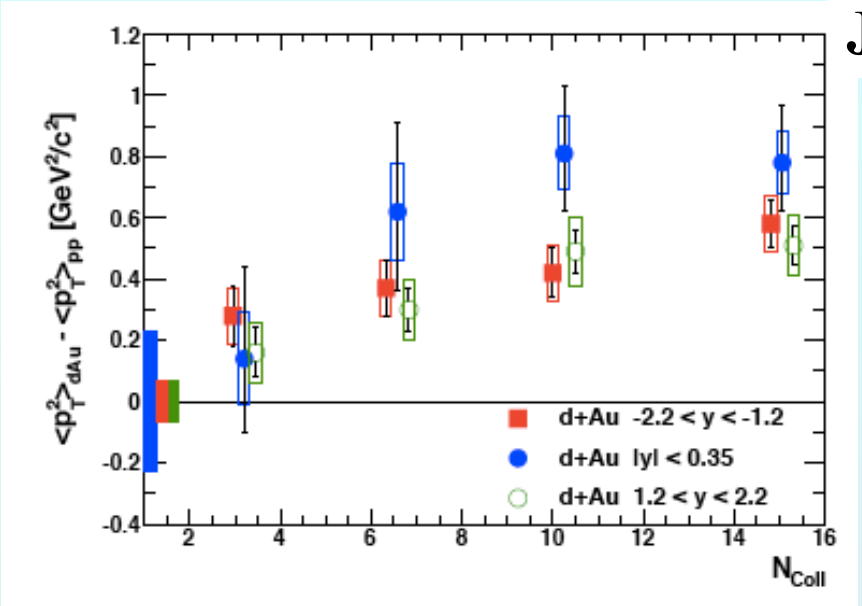

J/ψ

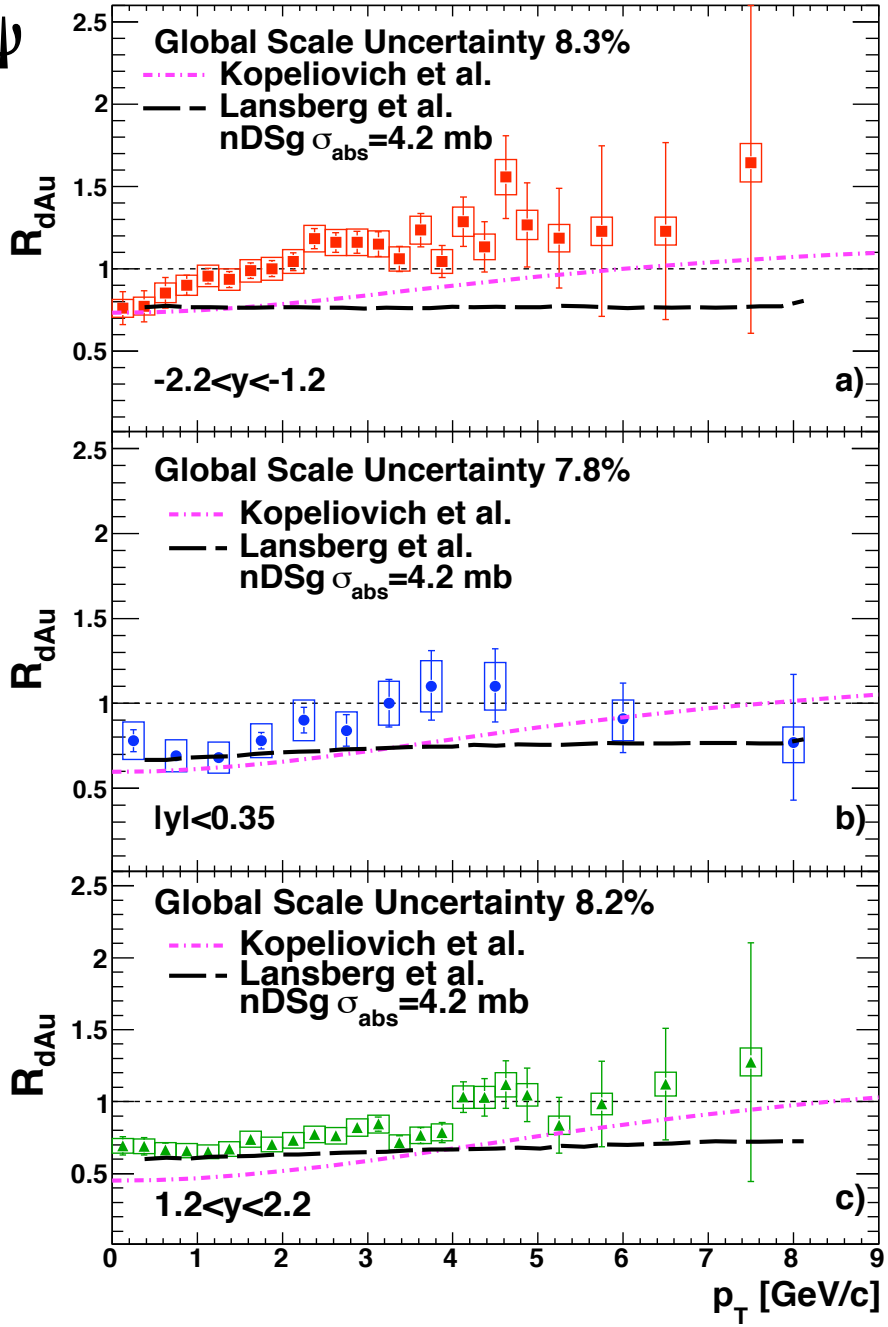

- ✦ p_T broadens (multiple scattering) w/N_{coll}; effect stronger at y=0
- ✦ J/ψ suppressed to higher p_T @ mid & forward y (lower x in Au);
- ✦ R_{dA}>1 at high p_T backward (Cronin effect in Au nucleus)
- ✦ p_T, y, centrality dependence was not reproduced by the models

but

Arleo, et al 1304.090

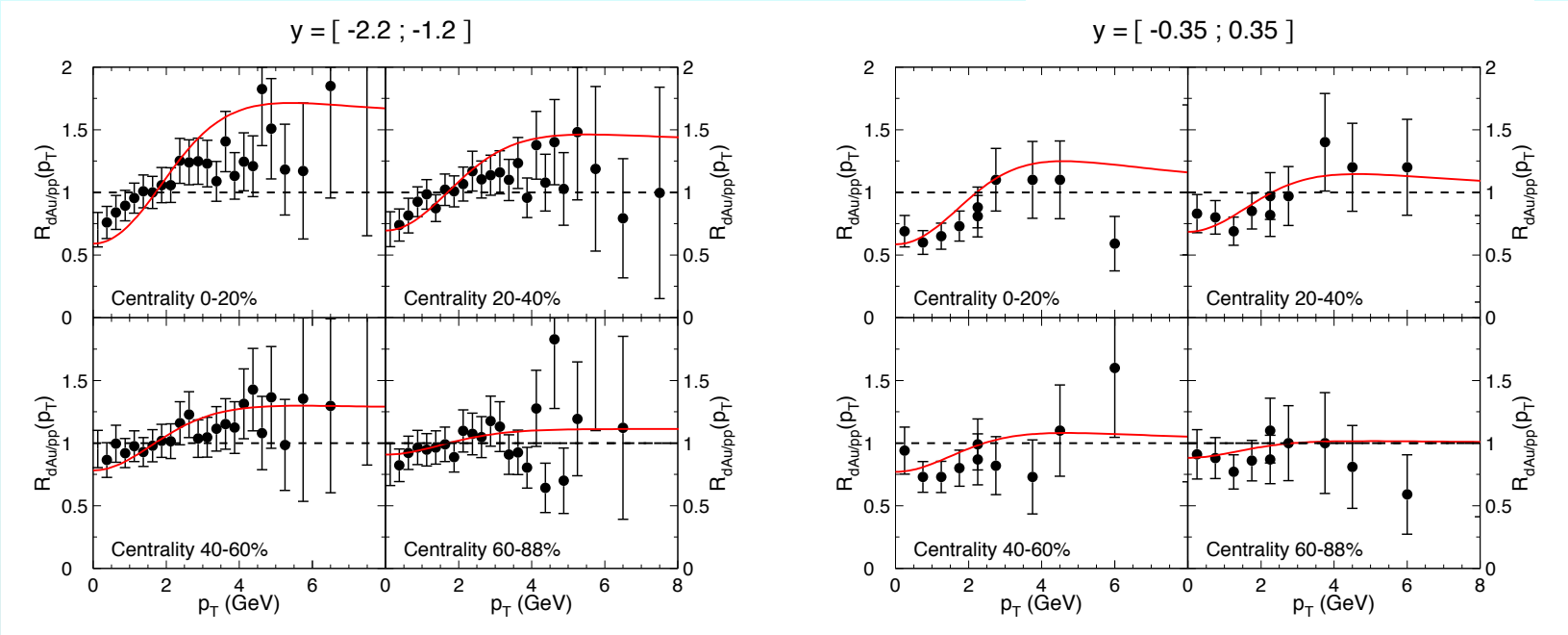

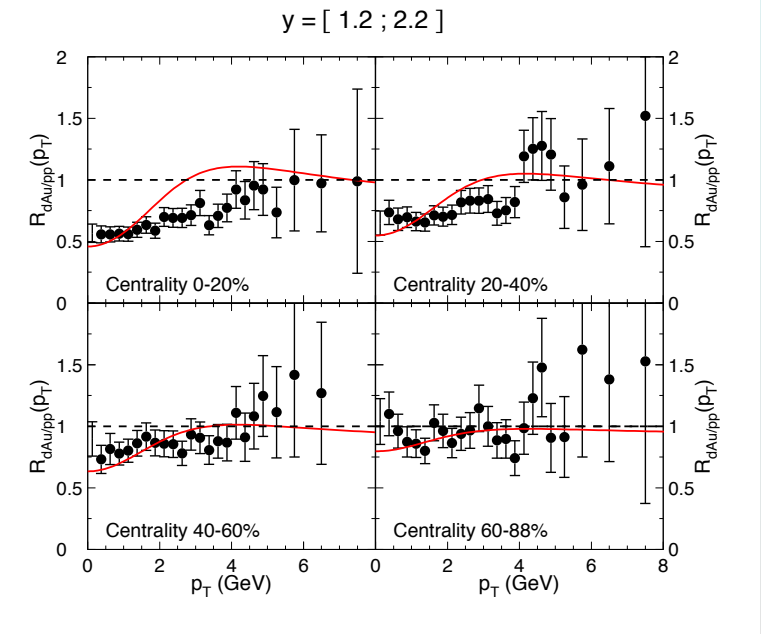

coherent parton energy loss and p_T broadening from multiple scattering in the nucleus is consistent with the data!

$\hat{q}_0 = 0.075$ GeV^2/fm

Larger, less tightly bound c-cbar: ψ'

arXiv: 1305.5516

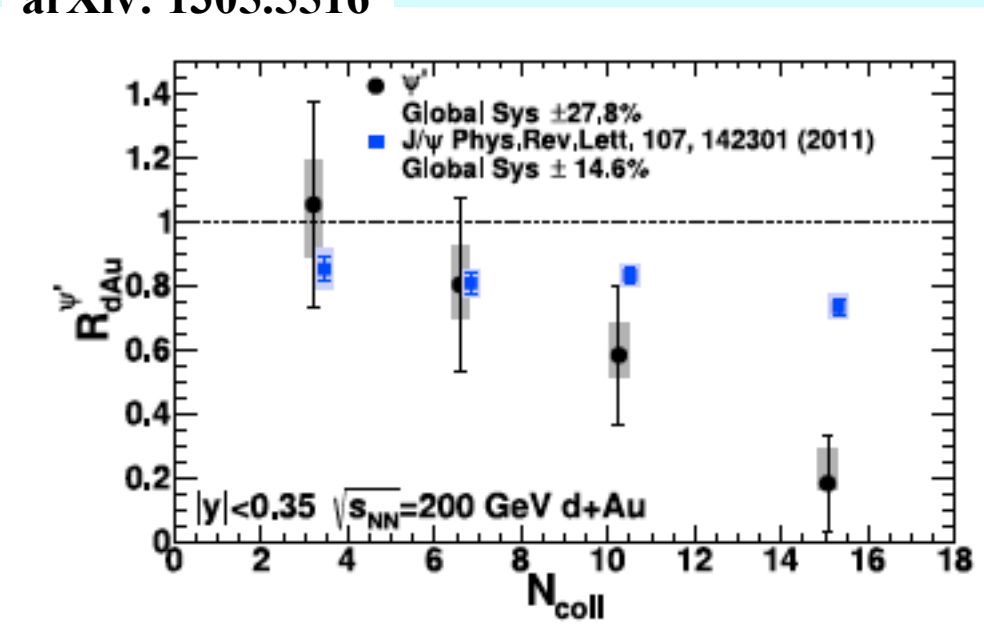

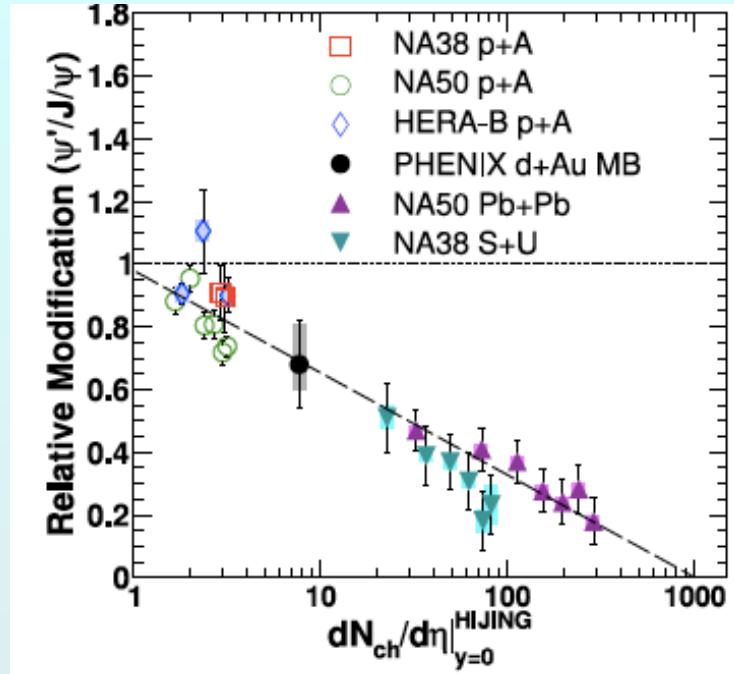

- Clearly more suppressed than J/ψ
- Cannot be shadowing or parton energy loss
  These are initial state effects
  & affect c-cbar precursor

- ψ'/ J/ψ decreases linearly with $dN_{ch}/d\eta$
- Break-up of some sort!
  early or late?

To sort out parton dynamics

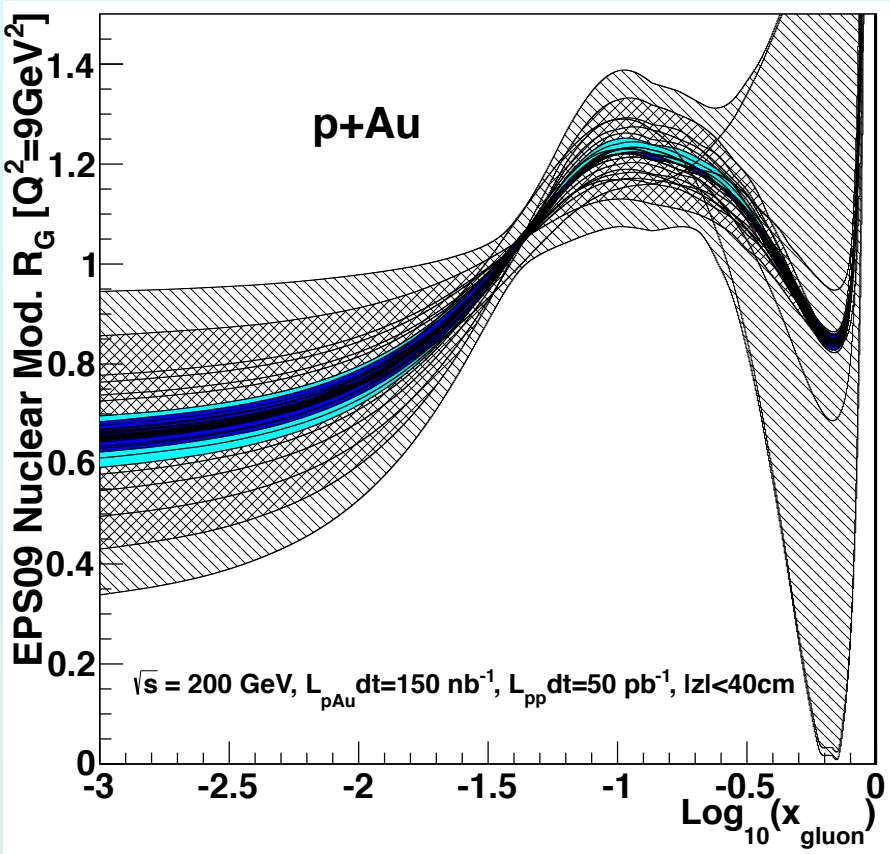

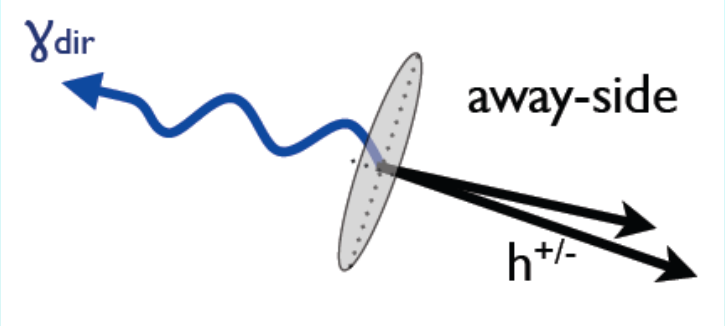

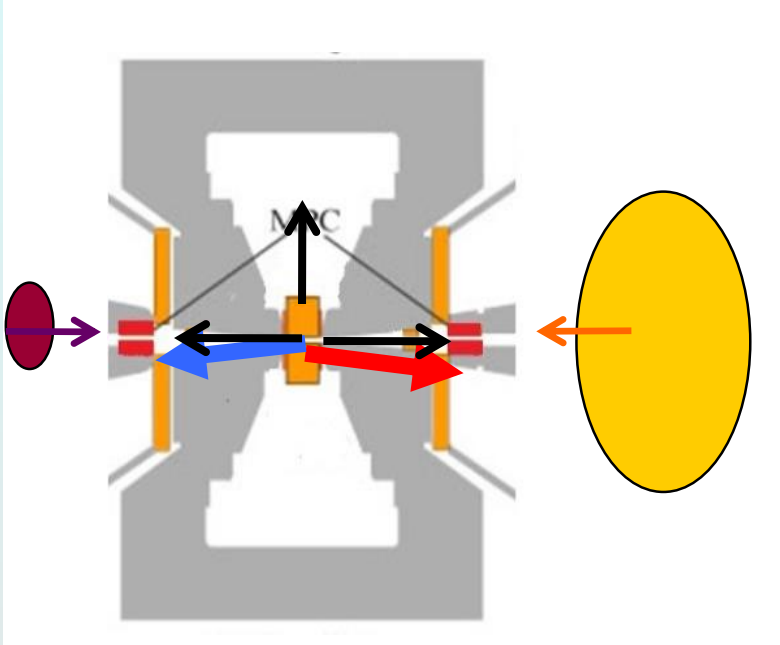

- Direct γ reflect structure + initial state energy loss
- Correlations: γ vs. h reflect final state parton dynamics probe as function of y

What gluon structure does the system thermalize *FROM*?

- Measure gluon distribution in p/d+A
  - pro: will do it next year!
  - con: incoming/outgoing parton dynamics (e.g. energy loss)
- Future electron-A collider to measure parton structure
  - pro: electron probe cleaner
  - BUT: must wait for EIC
    - need heavy nuclei
    - see gluons indirectly

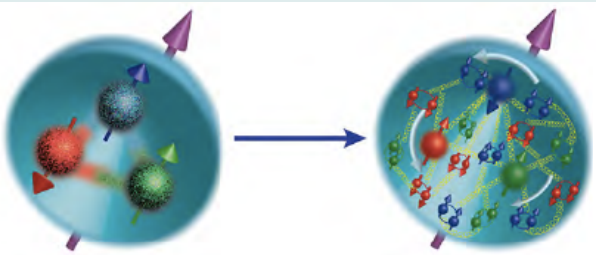

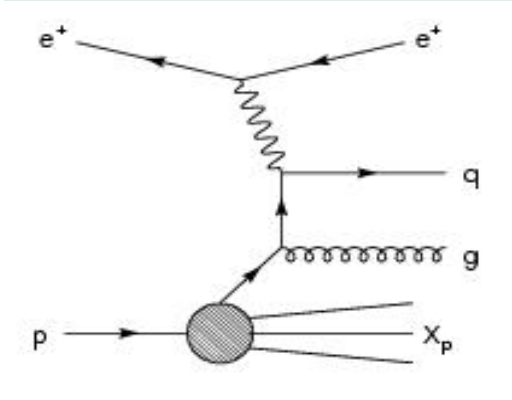

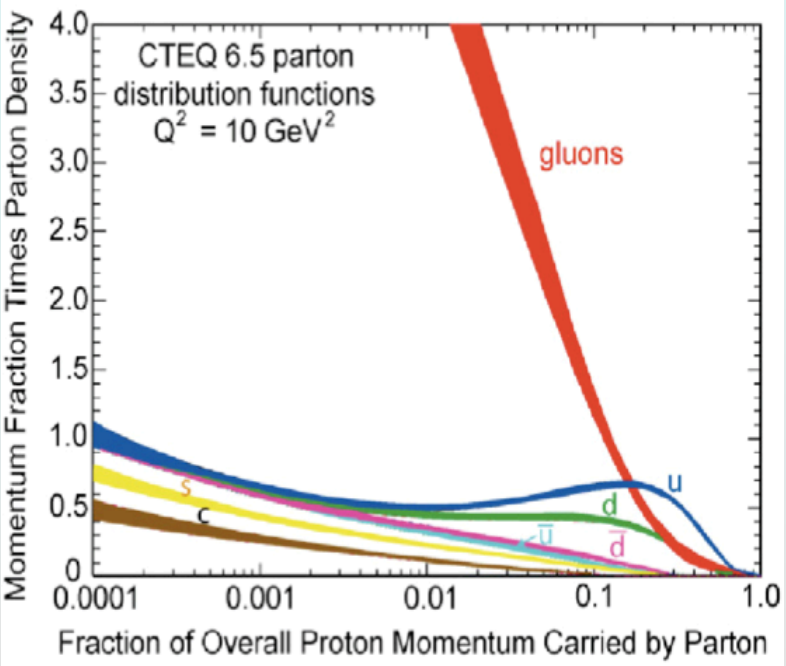

In the longer term

An electron-ion collider probe structure directly

Enhance Q_S with A, not energy

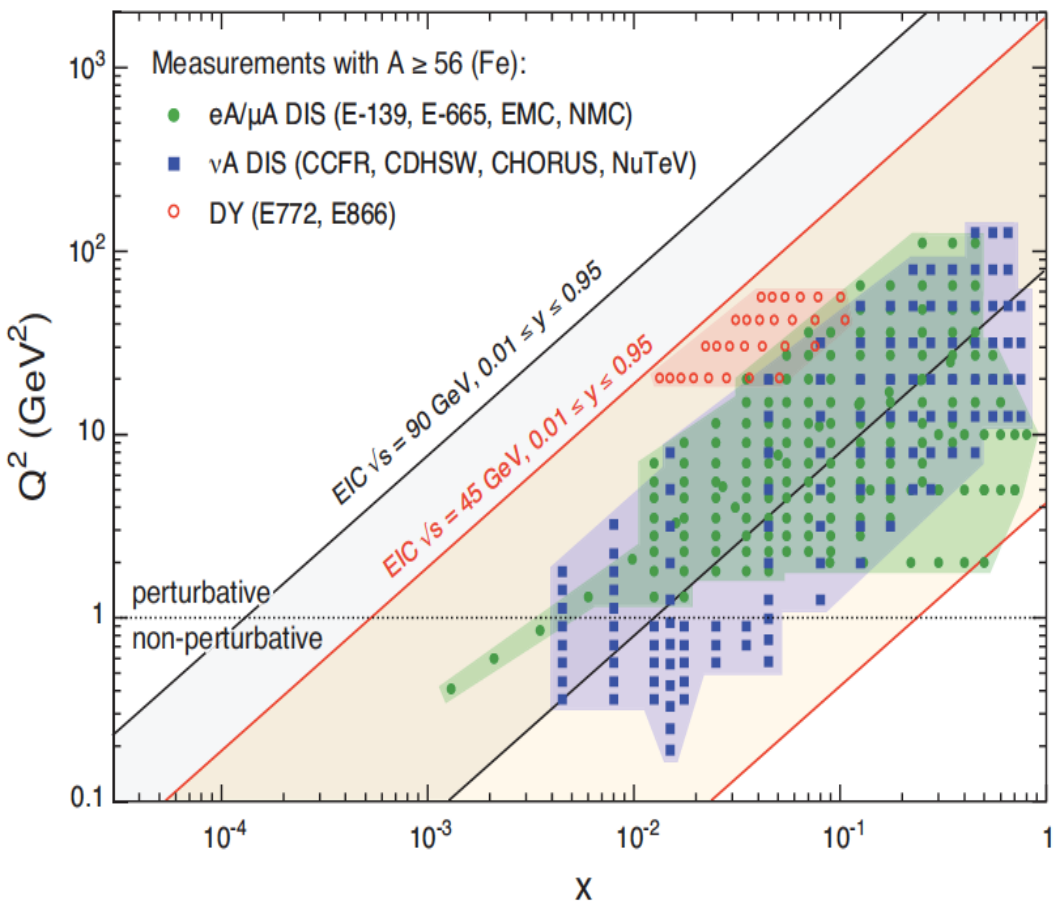

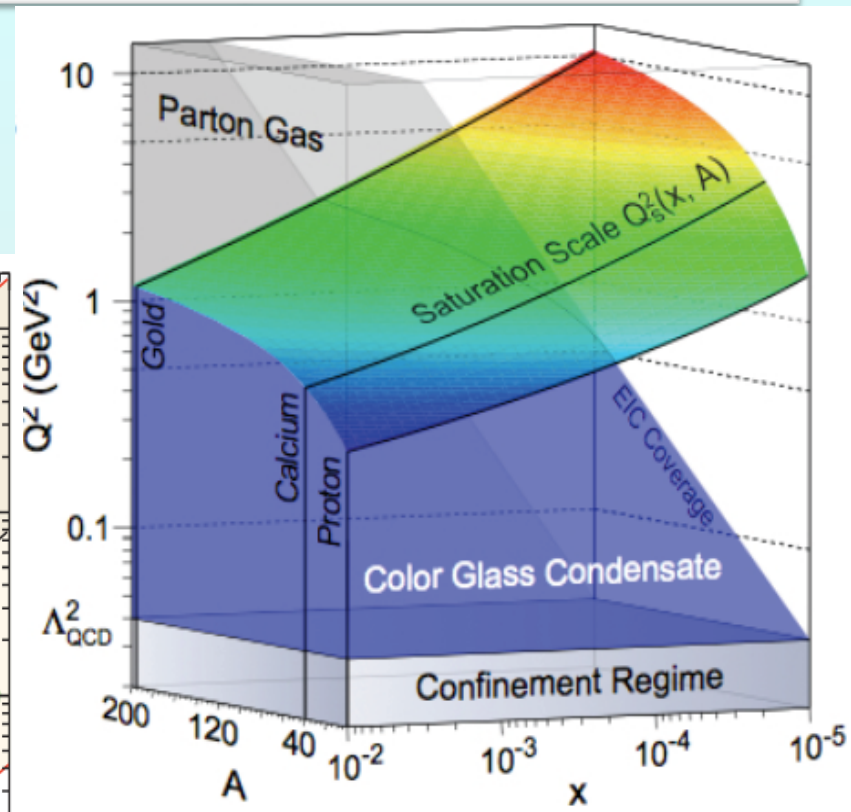

Detector concepts: spin AND e+A gluon studies

eRHIC @ BNL

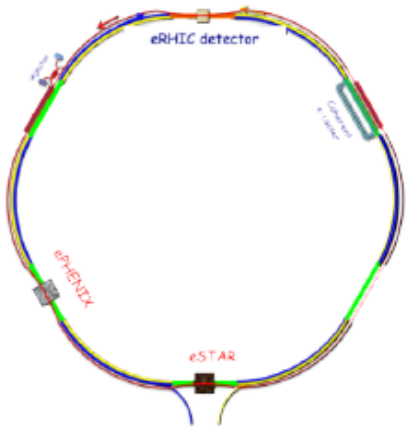

Stage I

Stage II

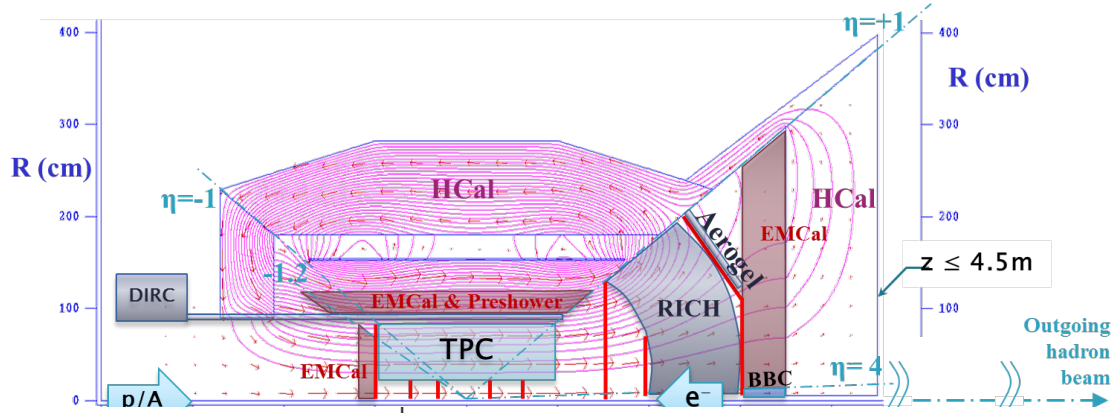

MEIC / EIC @ JLab

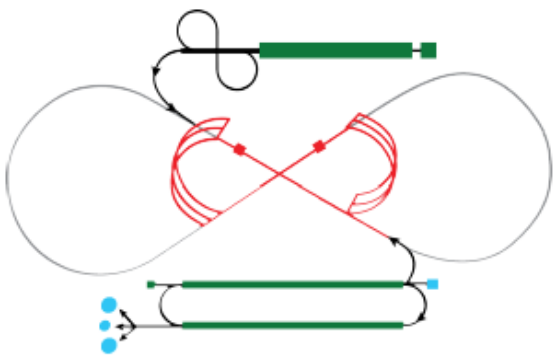

$\sqrt{s}$ = 13 – 70 GeV

E_e = 3 – 12 GeV

E_p = 15 – 100 GeV

E_{Pb} = up to 40 GeV/A

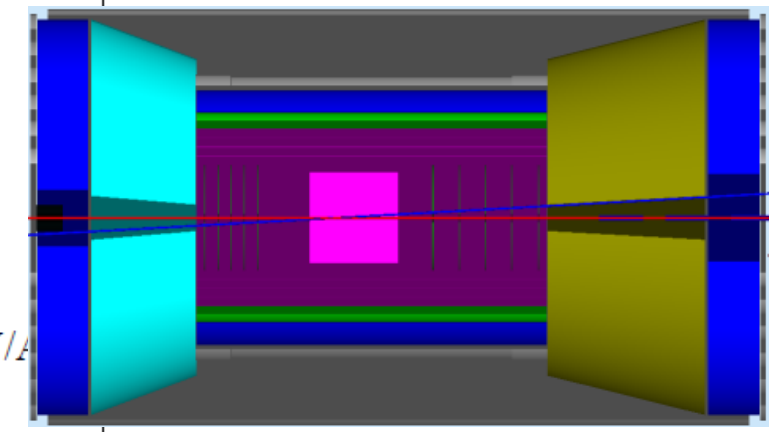

(MEIC) (EIC)

Conclusions

- **Perhaps we start off with a gluon system approaching an equilibrium distribution?**

- **Probe in near term with QCD Compton scattering in p+A collisions**
  Work hard to disentangle dynamics & structure

- **Probe structure directly with electrons at EIC**
  Work hard to ensure heavy nuclei beams!

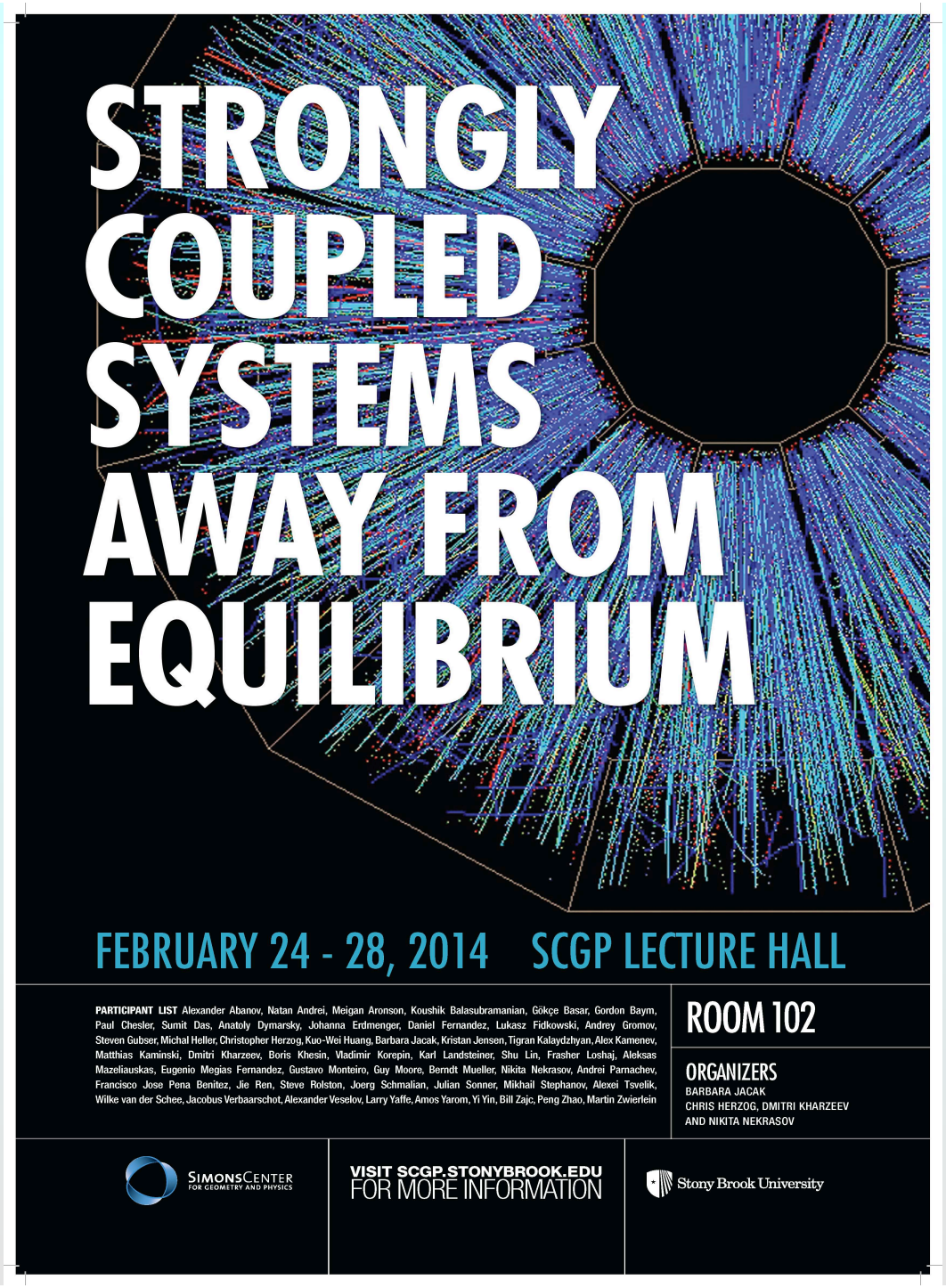
STRONGLY COUPLED SYSTEMS AWAY FROM EQUILIBRIUM
FEBRUARY 24 - 28, 2014 SCGP LECTURE HALL
PARTICIPANT LIST Alexander Abanov, Natan Andrei, Meigan Aronson, Koushik Balasubramanian, Gökçe Basar, Gordon Baym, Paul Chesler, Sumit Das, Anatoly Dymarsky, Johanna Erdmenger, Daniel Fernandez, Lukasz Fidkowski, Andrey Gromov, Steven Gubser, Michal Heller, Christopher Herzog, Kuo-Wei Huang, Barbara Jacak, Kristan Jensen, Tigran Kalaydzhyan, Alex Kamenev, Matthias Kaminski, Dmitri Kharzeev, Boris Khesin, Vladimir Korepin, Karl Landsteiner, Shu Lin, Frasher Loshaj, Aleksas Mazeliauskas, Eugenio Megias Fernandez, Gustavo Monteiro, Guy Moore, Berndt Mueller, Nikita Nekrasov, Andrei Parnachev, Francisco Jose Pena Benitez, Jie Ren, Steve Rolston, Joerg Schmalian, Julian Sonner, Mikhail Stephanov, Alexei Tsvelik, Wilke van der Schee, Jacobus Verbaarschot, Alexander Veselov, Larry Yaffe, Amos Yarom, Yi Yin, Bill Zajc, Peng Zhao, Martin Zwierlein
ROOM 102
ORGANIZERS
BARBARA JACAK
CHRIS HERZOG, DMITRI KHARZEEV
AND NIKITA NEKRASOV
SIMONS CENTER FOR GEOMETRY AND PHYSICS
VISIT SCGP.STONYBROOK.EDU FOR MORE INFORMATION
Stony Brook University

non-equilibrium QFT

Few d.o.f.
Brute force

Integrable systems
Open Bethe ansatz

Strongly coupled systems
holographic descriptions
numerical gravity
hydrodynamics

$$i\,\frac{\partial}{\partial t}\,\rho = [H,\rho]$$

$$\rho(t) = U(t)\,\rho(0)\,U(t)^\dagger$$

$$\langle \mathcal{O}(t)\rangle = \mathrm{Tr}\,(\rho(t)\,\mathcal{O})$$

Weakly coupled systems
Schwinger-Keldysh diagrammatics
kinetic theory
classical field theory
hydrodynamics

Not weakly coupled,
not holographic
"hope & pray"

Open problems to tackle

- Use data to extract transport coefficients using hydro, e.g. bulk viscosity
  - Measure vn's for systems of different sizes
  - Characterize the hadronic phase better
  - In cold atoms: study thermalization, scale invariant systems, how to understand steady state near quantum critical point?
  - Measure shear viscosity in highly correlated electron systems, graphene
- Holography
  - Apply to very low temperature systems
  - Establish connection to condensed matter
  - What bounds might exist near superconducting phase transition? How to use quantum critical points to gain a common language?

Page 2.

- Holography, continued

  Identify more cases amenable to holography

  What ground state solutions in holography?

  Figure out how to solve holographic results also in field theory

  How to evade eta/s lower bound? How strong would the experimental evidence need to be?

  Need a decent formulation of classical string theory on highly curved manifolds
- Is there an effective theory of QCD in the vicinity of Tc?
- Can we institute a classification system for non-equilibrium systems? E.g. an RG for time evolution?
- How does long thermalization look in holography?

Page 3

- **Can we separate problems by the nature of the initial state?**

  Is many-body localization useful as a more general concept? What is specific and what is general?

- **Backup**

Centrality dependence

Similar slope vs. N_{part} as in Au+Au

What do we learn from the fact that the system is smaller?

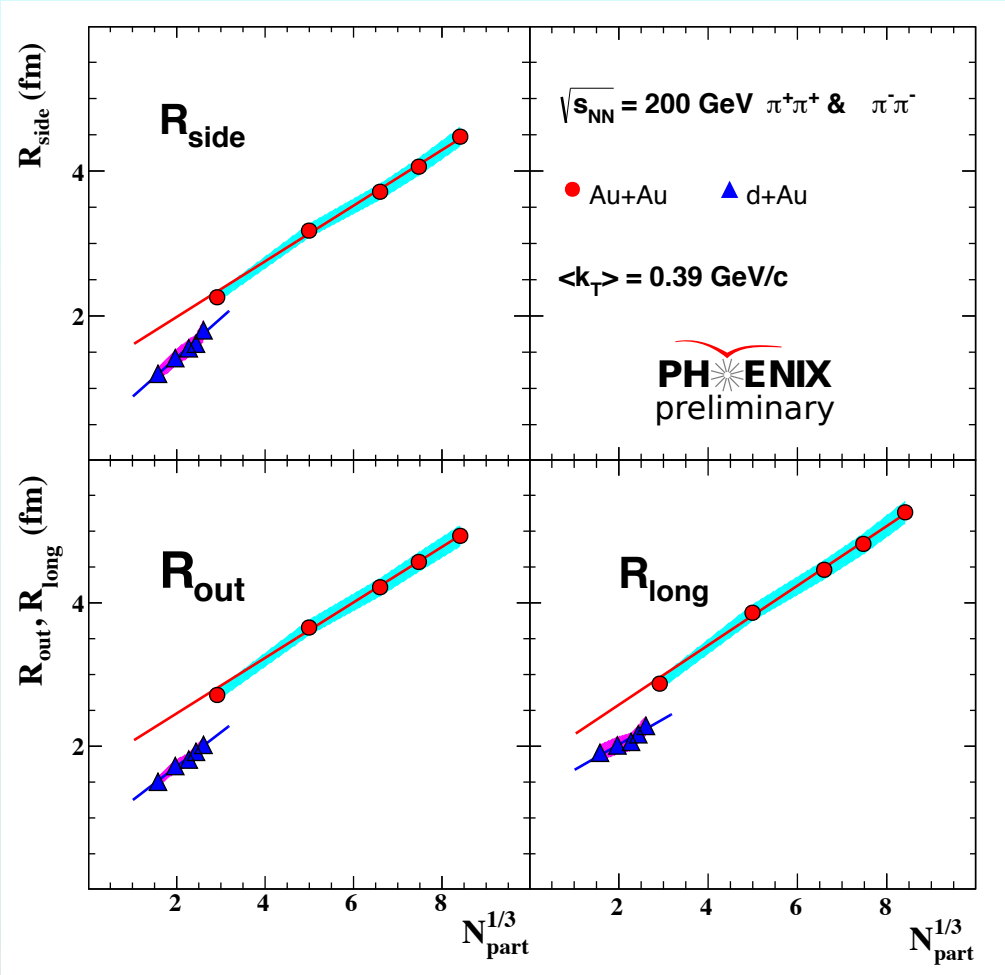

Many types of strongly coupled matter

Quark gluon plasma is like other systems with strong coupling - all flow and exhibit phase transitions

Cold atoms: coldest & hottest matter on earth are alike!

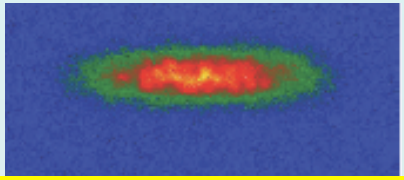

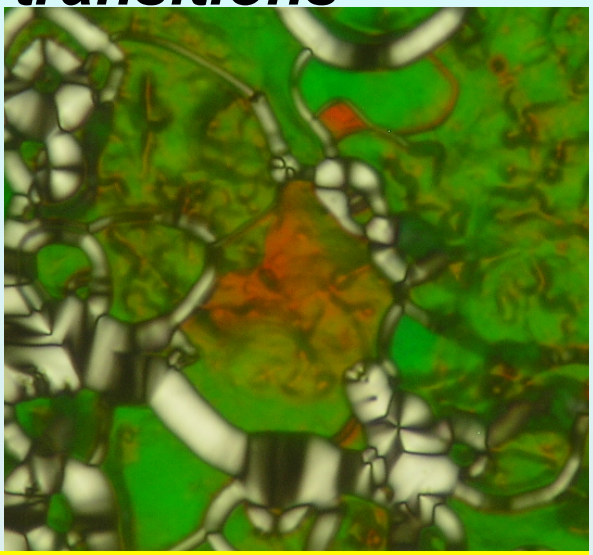

Dusty plasmas &

In all these cases have a competition:

Attractive forces ⇔ repulsive force or kinetic energy

High T_c superconductors: magnetic vs. potential energy

Result: many-body interactions, not pairwise!

QCD is a great test lab: we *know* the Lagrangian!

Upgrade PHENIX for jets at RHIC

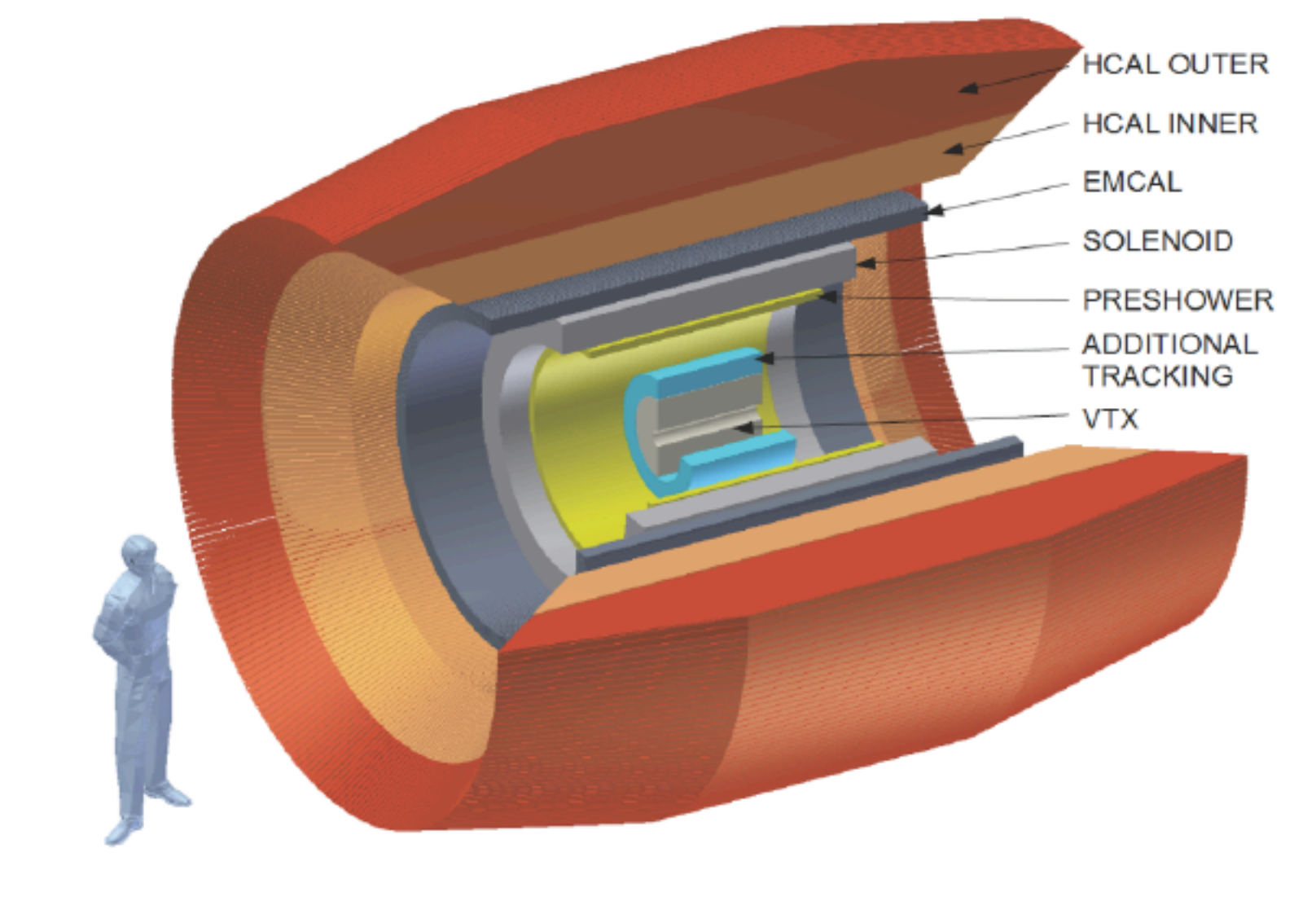

sPHENIX Proposal: arXiv:1207.6378

Compact, hermetic jet and quarkonium detector

Higher harmonics exist & are useful!

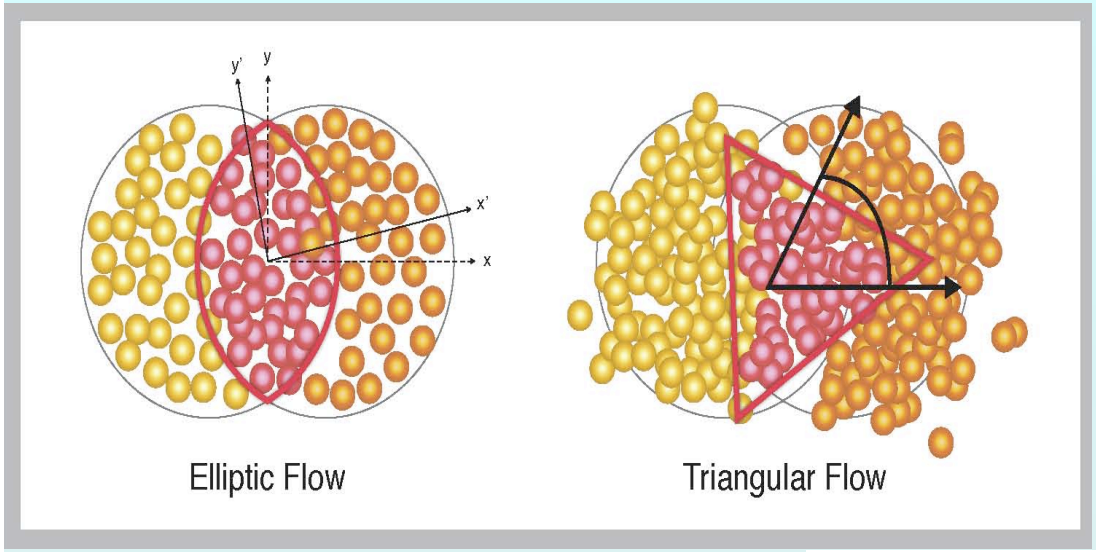

Nucleons move around inside the nucleus

-> locations of NN scattering fluctuate

- Hydro gets it right if initial conditions are allowed to fluctuate
- Better sensitivity to the viscosity/entropy ratio (viscosity increases dissipation)
- $\eta/s = 0.08$ works better!

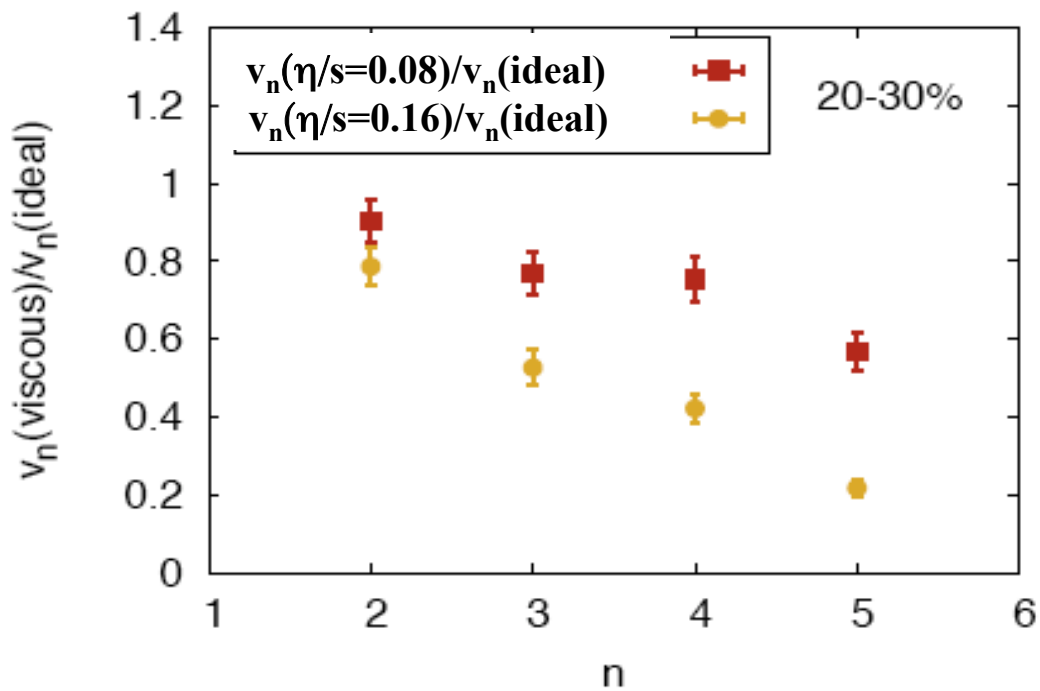

At the LHC

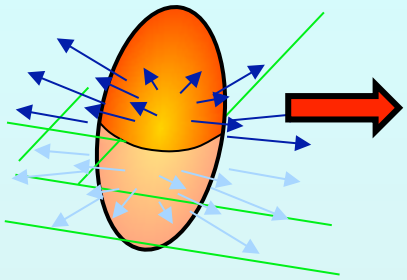

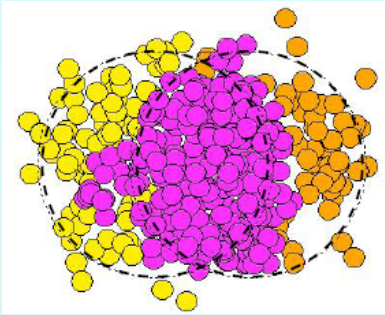

- **Hydro: T_{init} 30% higher than at RHIC**

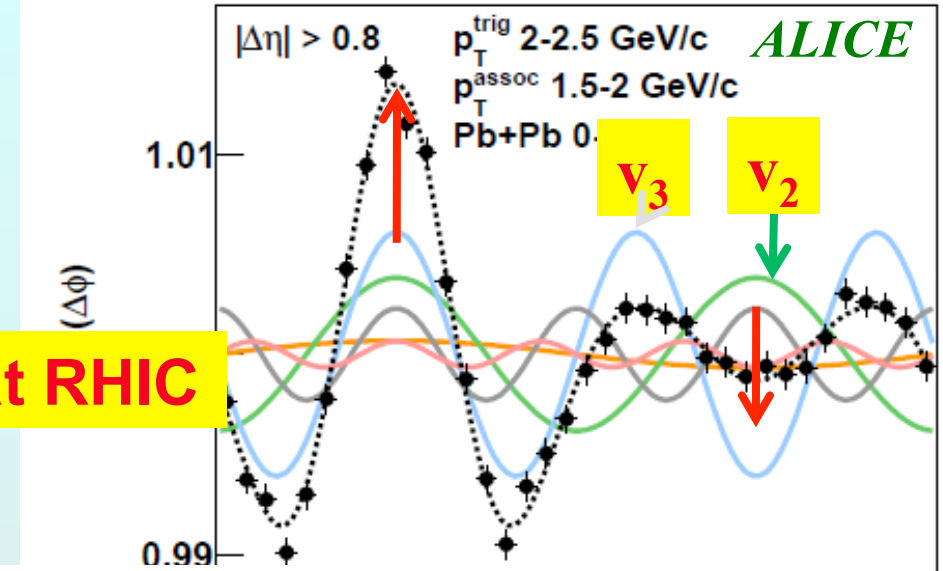

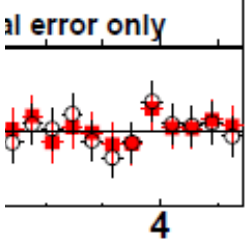

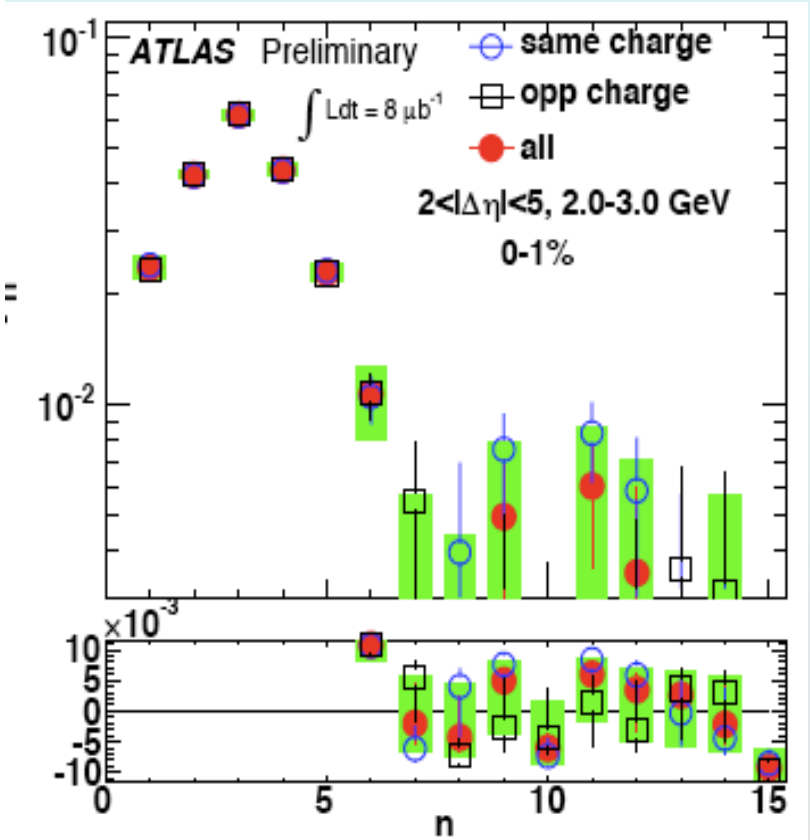

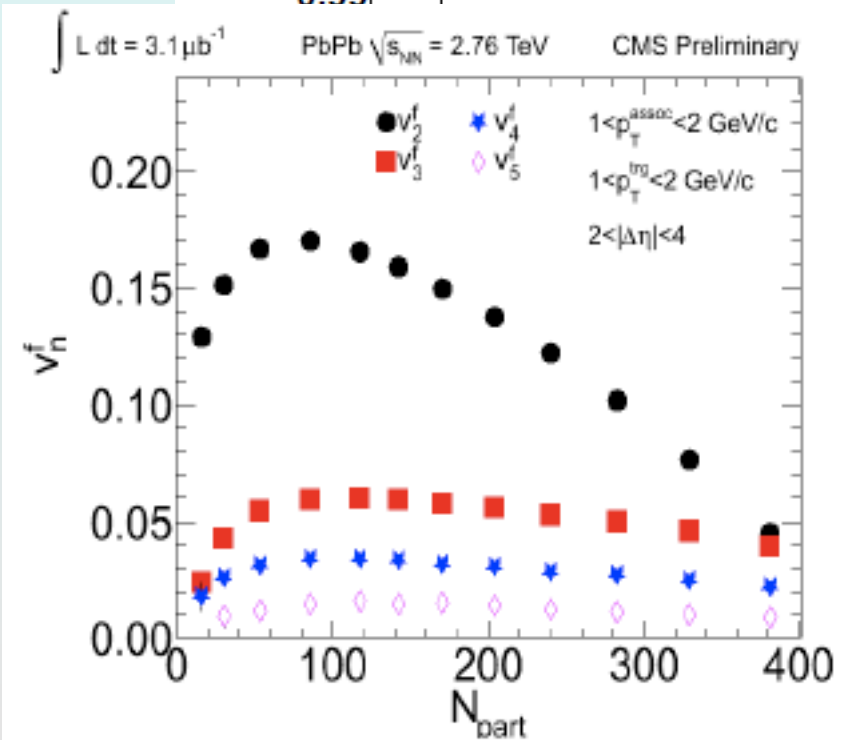

Same behavior in QGP at LHC

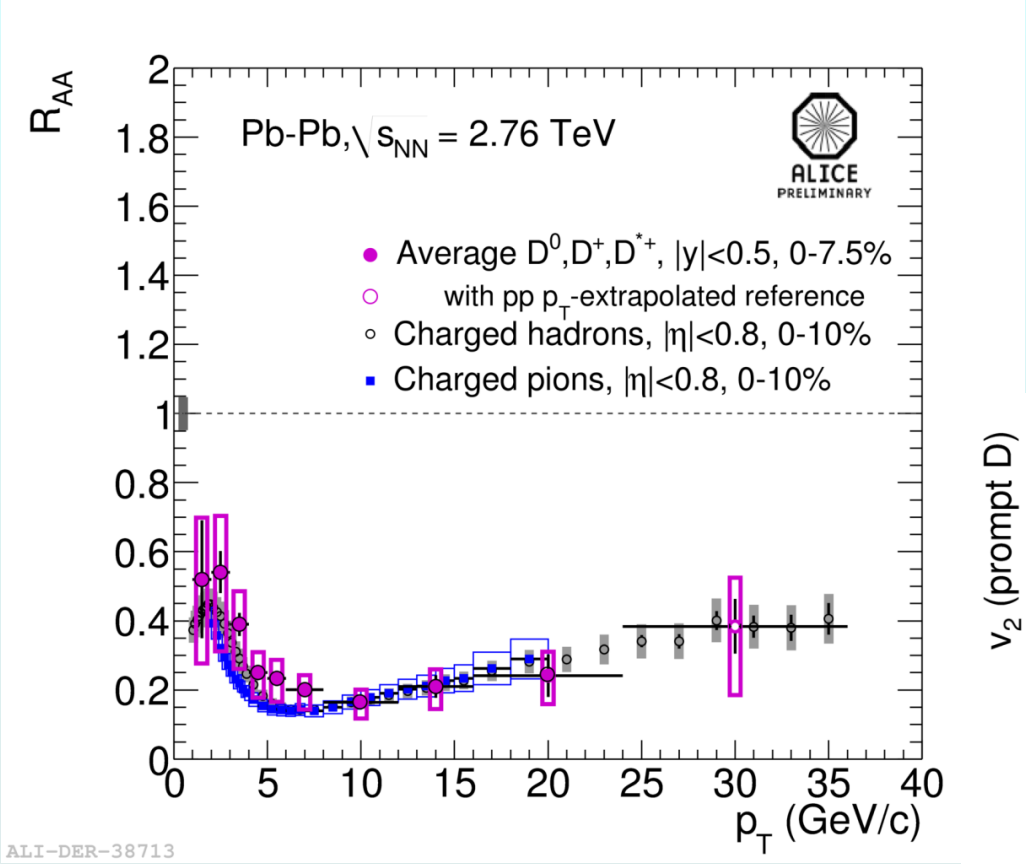

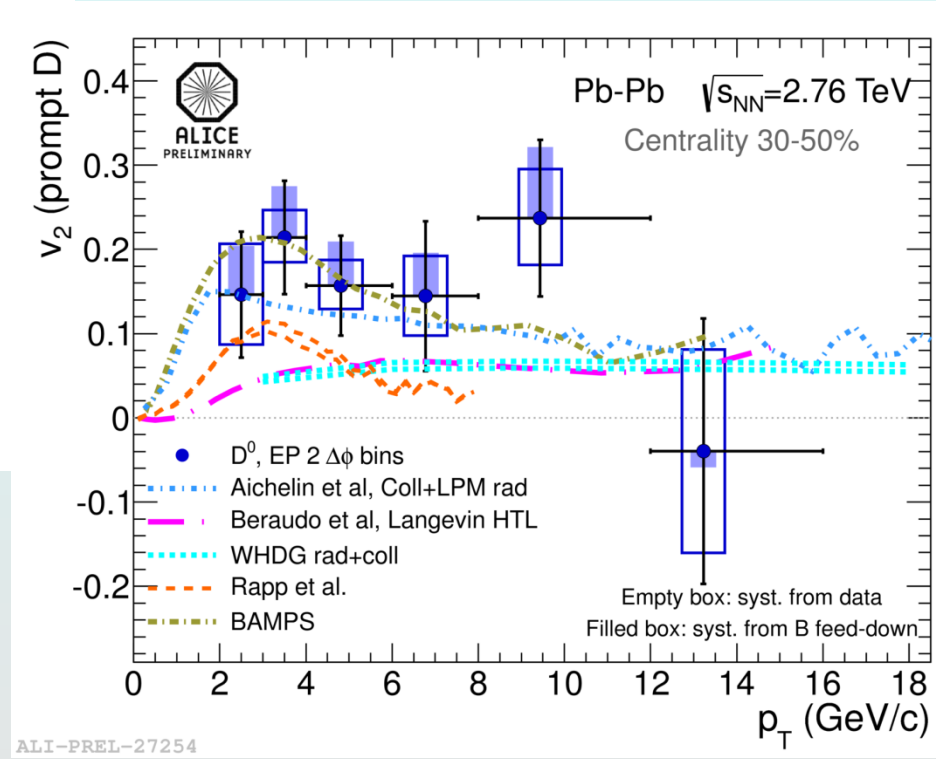

- **Can reproduce energy loss and flow at both energies**
- **Charm quarks diffusing thru strongly coupled QGP**

Jet Fragmentation function

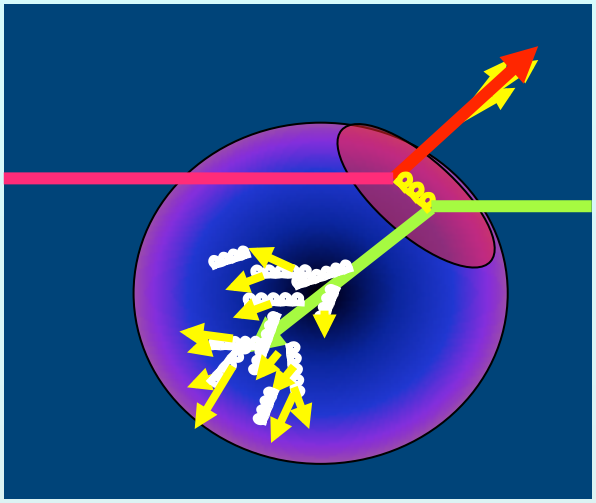

$$D(z) = 1/N_{jet}\, dN(z)/dz;\ z = p_{had}/p_{jet}$$

Measure: count partners per trigger as fraction of trigger momentum

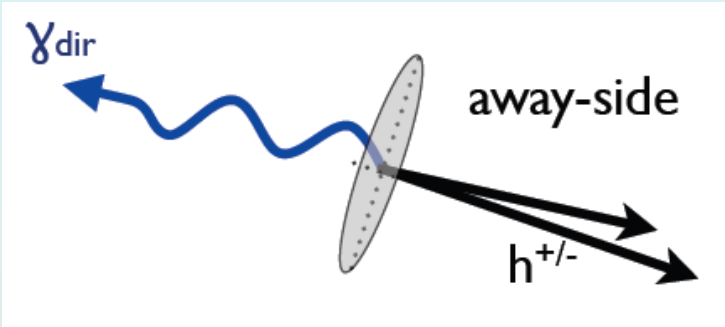

$z_T = p_{Ta}/p_{Tt} \sim z$ **for γ trigger**

$\xi = \ln(1/z_T)$

Modification factor similar to R_{AA}:

$$I_{AA} \equiv \frac{(1/N_{trig}dN/d\xi)_{AA}}{(1/N_{trig}dN/d\xi)_{pp}}$$

FFn experimental challenge:

measure the parton p

Use trigger γ or jet

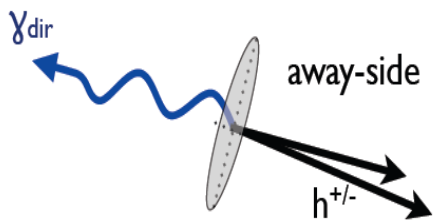

Frag. Function via γ-h correlation

γ: parton energy, h: fragmentation fn.

"Extra" soft particles at larger angles near the away side jet

Provide constraints on gluon splitting

Is it perturbative?

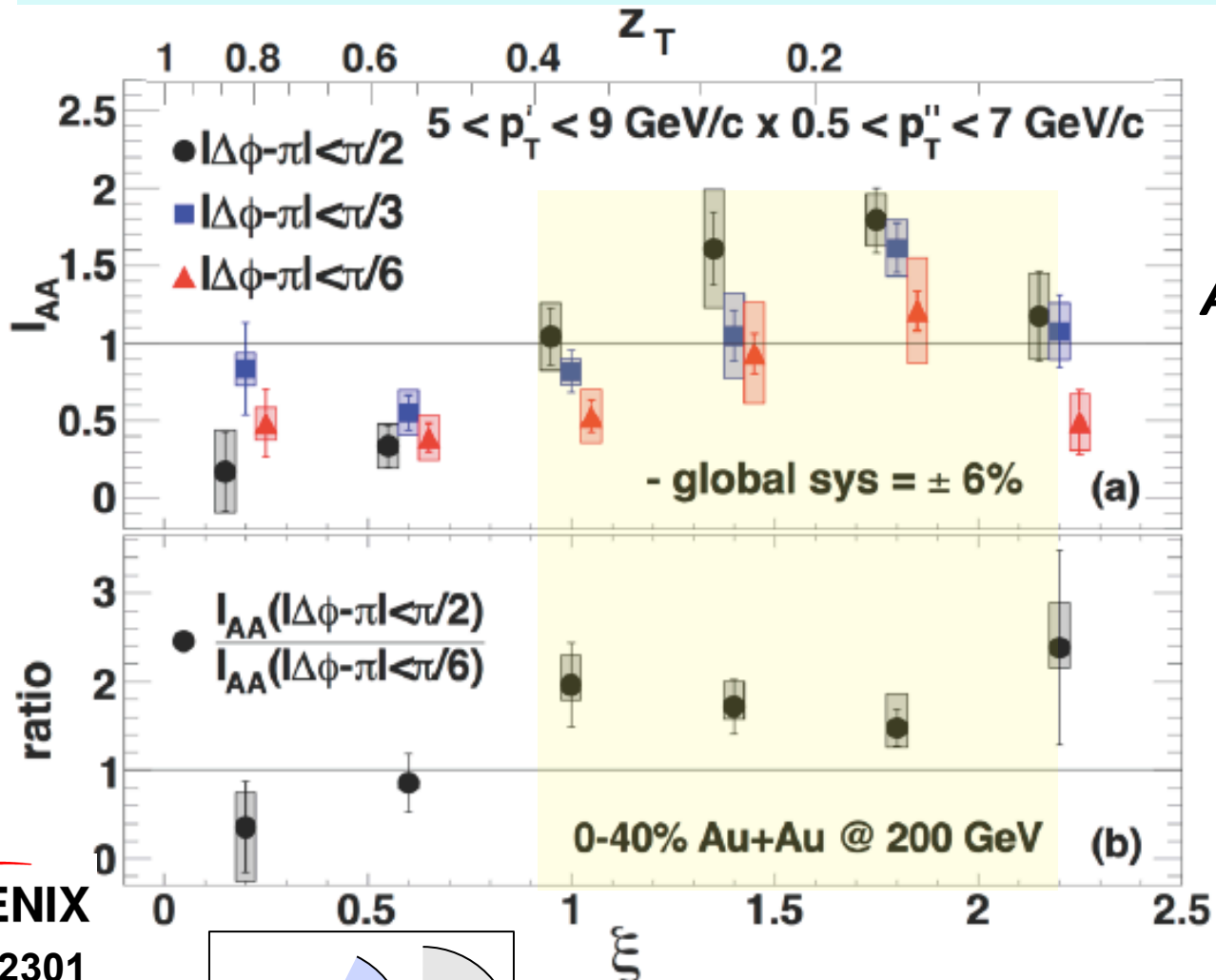

Au+Au/ p+p

PHENIX

PRL 111, 032301 (2013)

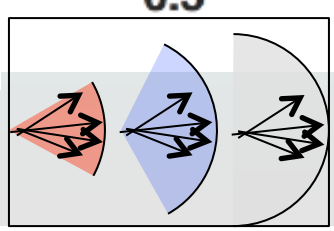

Heavy quark probe answers this year!

- Do even *b* quarks come to a screeching halt?
  $M_b \sim 4.2\ GeV/c^2$
  What does *b* fate tell us about interactions inside?
- Add silicon detector arrays around beam pipe to both PHENIX and STAR; ALICE already has one
  Tag displaced vertex
  to separate c,b
  Reconstruct D & B mesons

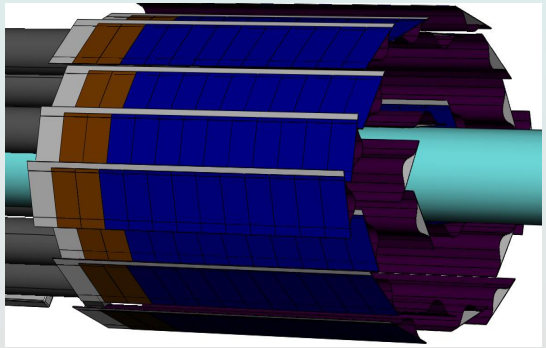

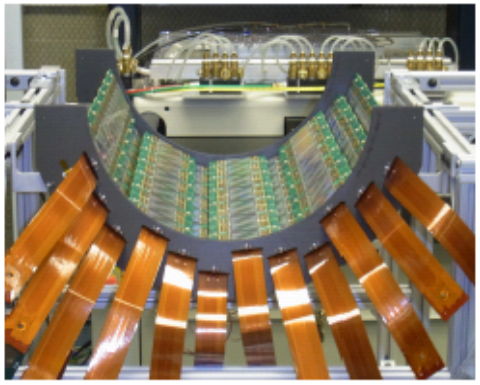

VTX Stripixel Layer 4

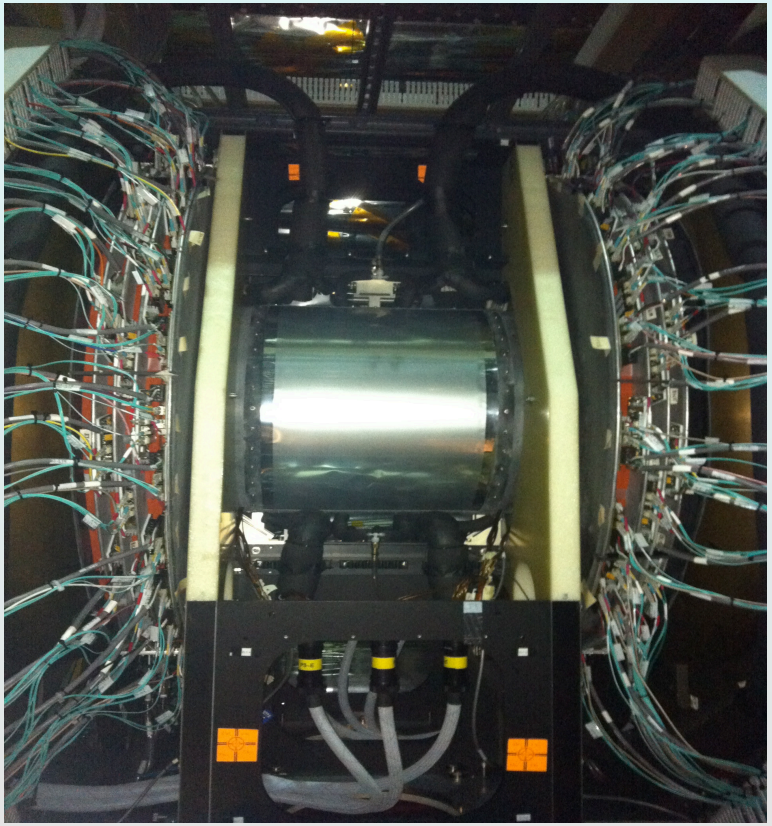

+ photons from expanding hadron gas

vanHees, Gale & Rapp, arXiv:1108.2131

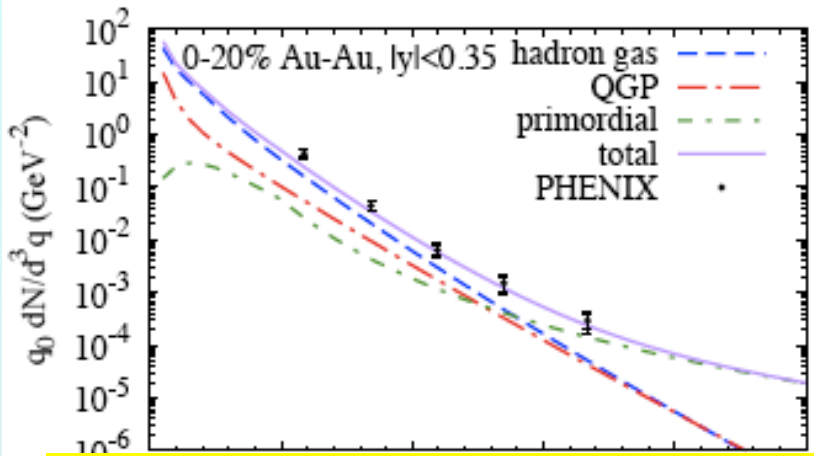

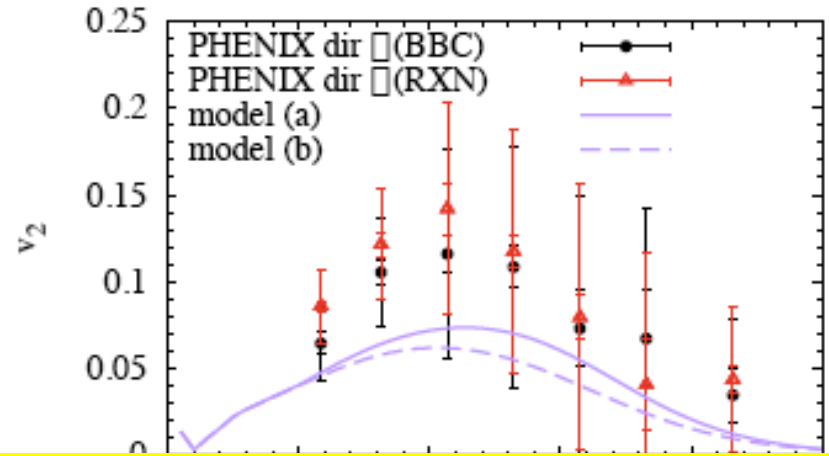

Answer = yes, if "extras" come from a very rapidly expanding hadron gas, that lives longer than initially expected

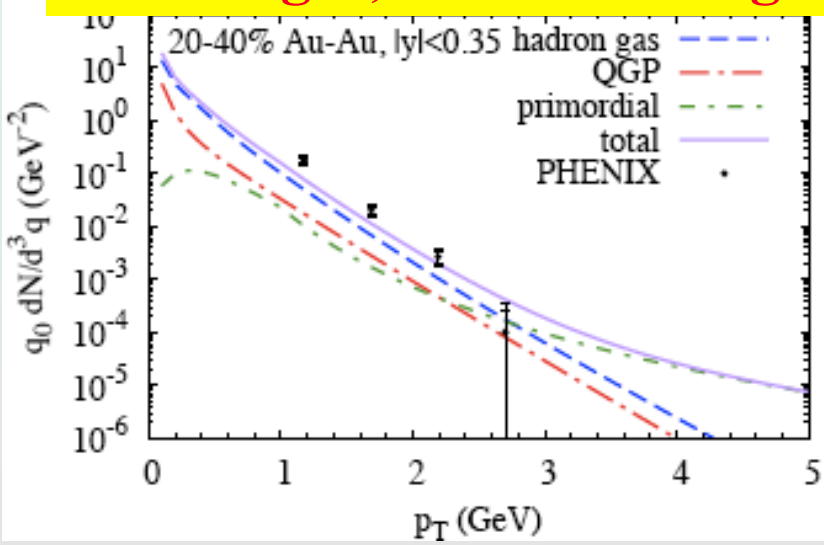

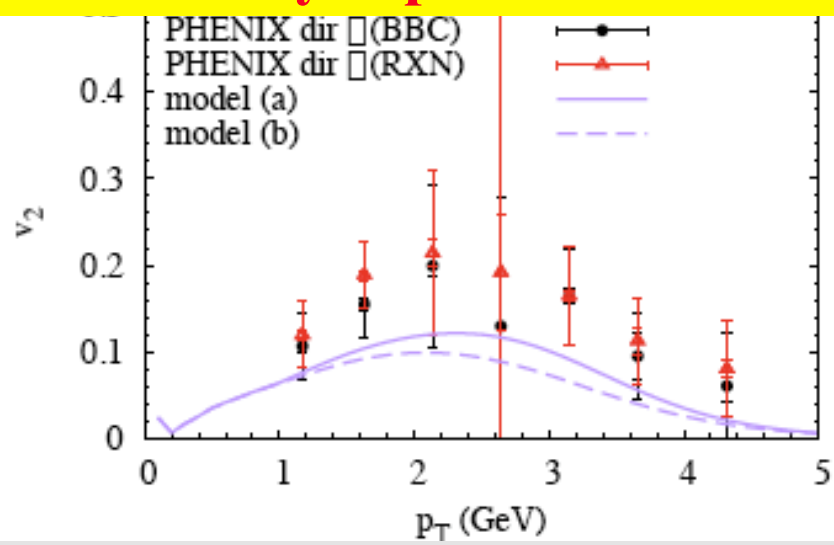

Lepton pair emission ↔ EM correlator

e.g. Rapp, Wambach Adv.Nucl.Phys 25 (2000)

Emission rate of dileptons per volume

$$\frac{dR_{ll}}{d^4q} = -\frac{\alpha^2}{3\pi^3}\frac{L(M)}{M^2}\mathrm{Im}\Pi^{\mu}_{em,\mu}(M,q;T)f^B(q_0,T)$$

$$f^B(q_0,T) = 1/(e^{q_0/T}-1)$$

$$L(M) = \sqrt{1-\frac{4m_l^2}{M^2}}(1+\frac{2m_l^2}{M^2})$$

γ*→ee decay

EM correlator
Medium property

Boltzmann factor
temperature

Hadronic contribution
Vector Meson Dominance

Medium modification of meson
Chiral restoration

$$\mathrm{Im}\Pi^{\mathrm{vac}}_{\mathrm{em}}(M) = \begin{cases} \sum_{V=\rho,\omega,\phi}\left(\frac{m_V^2}{g_V}\right)^2 \mathrm{Im}D_V(M) & , \\ -\frac{M^2}{12\pi}\left(1+\frac{\alpha_s(M)}{\pi}+\ldots\right)N_c\sum_{q=u,d,s}(e_q)^2 & , \end{cases}$$

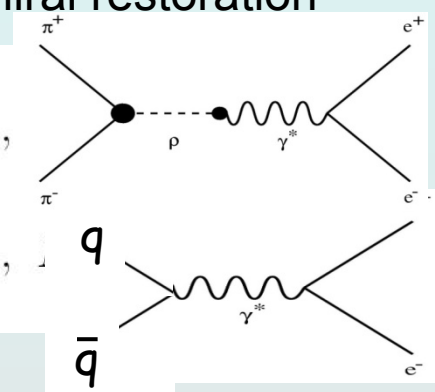

$q\bar{q}$ annihilation

Thermal radiation from
partonic phase (QGP)

From emission rate of dileptons, the medium effect on the EM correlator as well as temperature of the medium can be decoded.

e^+e^- looks intriguing

2004 data

arXiv: 0912.0244

PRC, in press

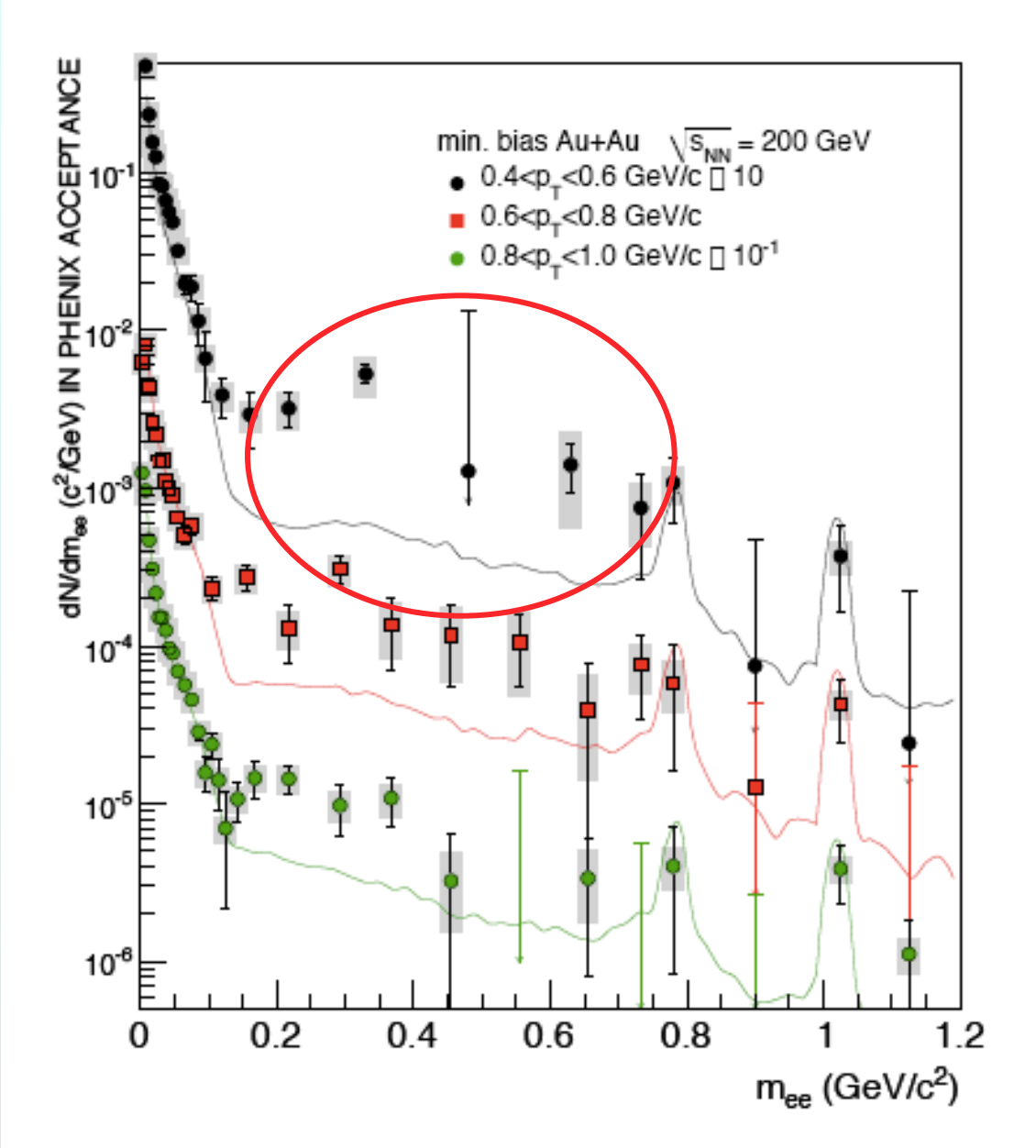

We're taking more, better data now

Fluctuations, flow and the quest for η/s

arXiv:1105.3928

v_2 described by both Glauber and CGC

but different values of η/s

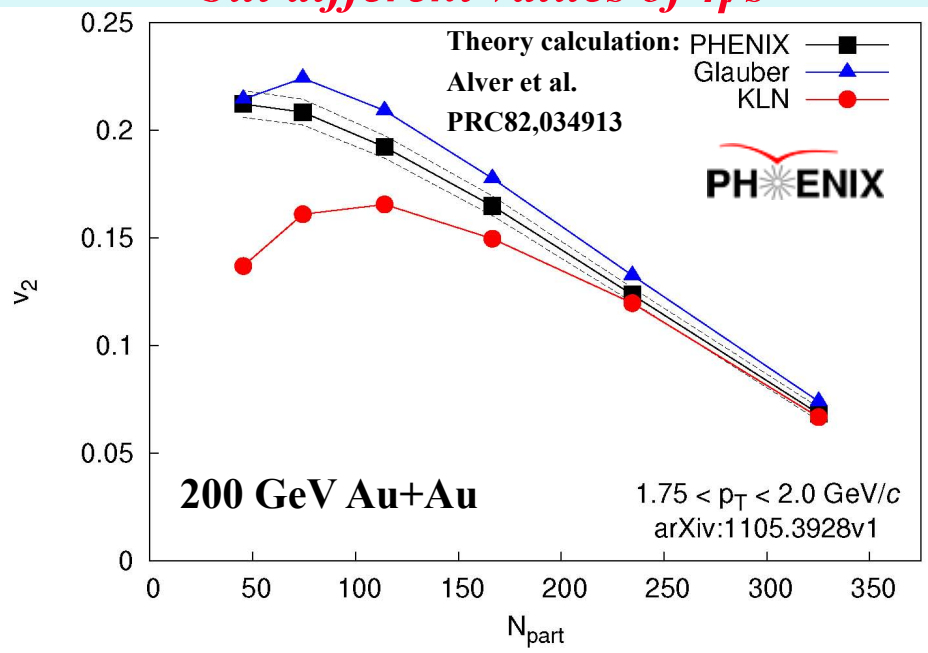

v_3 described only by Glauber

breaks degeneracy

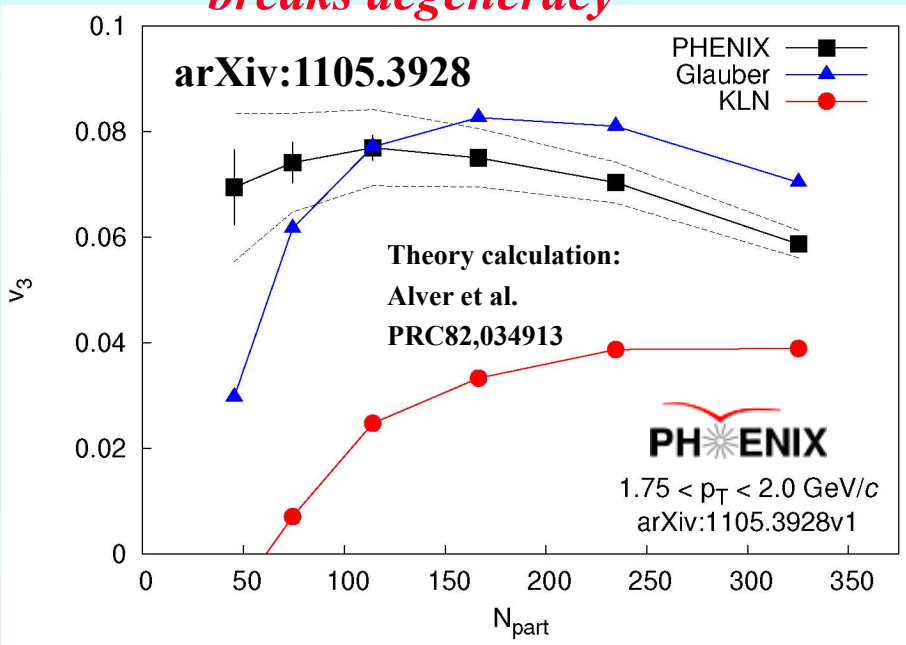

Lappi, Venugopalan, PRC74, 054905
Drescher, Nara, PRC76, 041903

- Glauber
  - Glauber initial state
  - $\eta/s = 1/4\pi$

2 models with
Different fluctuations,
Eccentricity, ρ distribution

- MC-KLN
  - CGC initial state
  - $\eta/s = 2/4\pi$

c,b decays via single electron spectrum

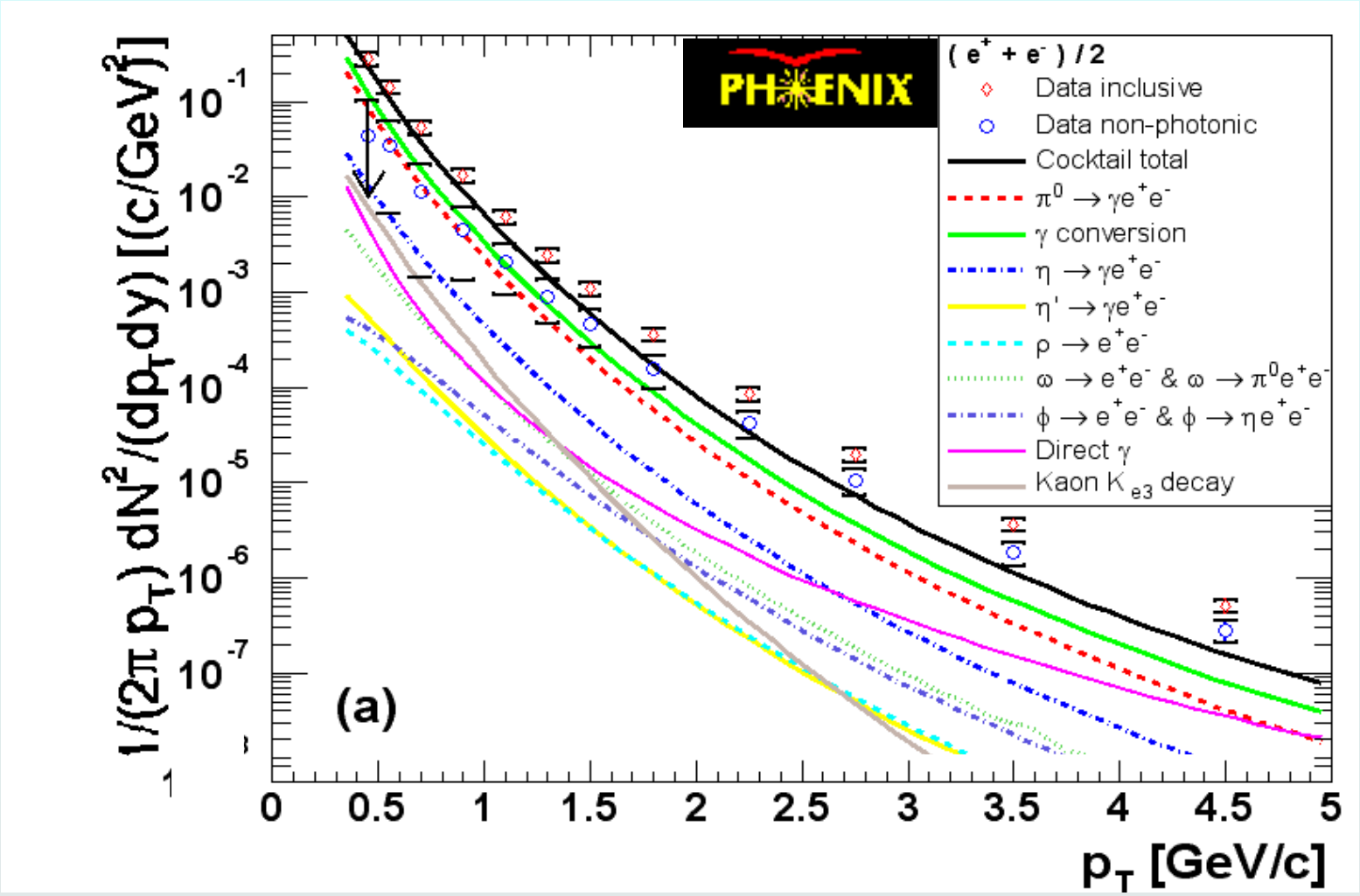

compare data to "cocktail" of (measured) hadronic decays

PRL 96, 032301 (2006)

Viscosity/Entropy (natural units)

Duke Physics
Atom Cooling and Trapping

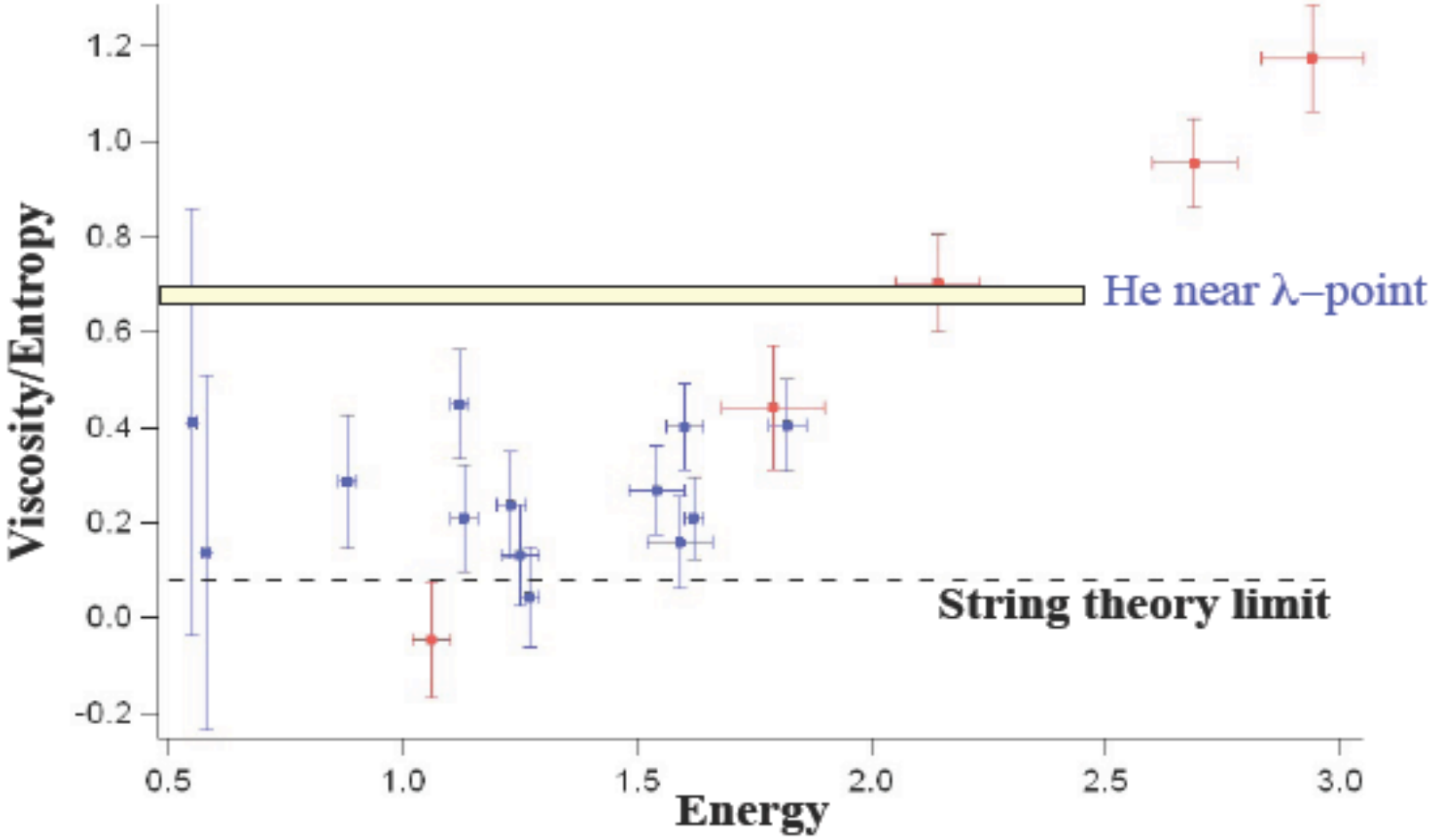

minimum η at phase boundary?

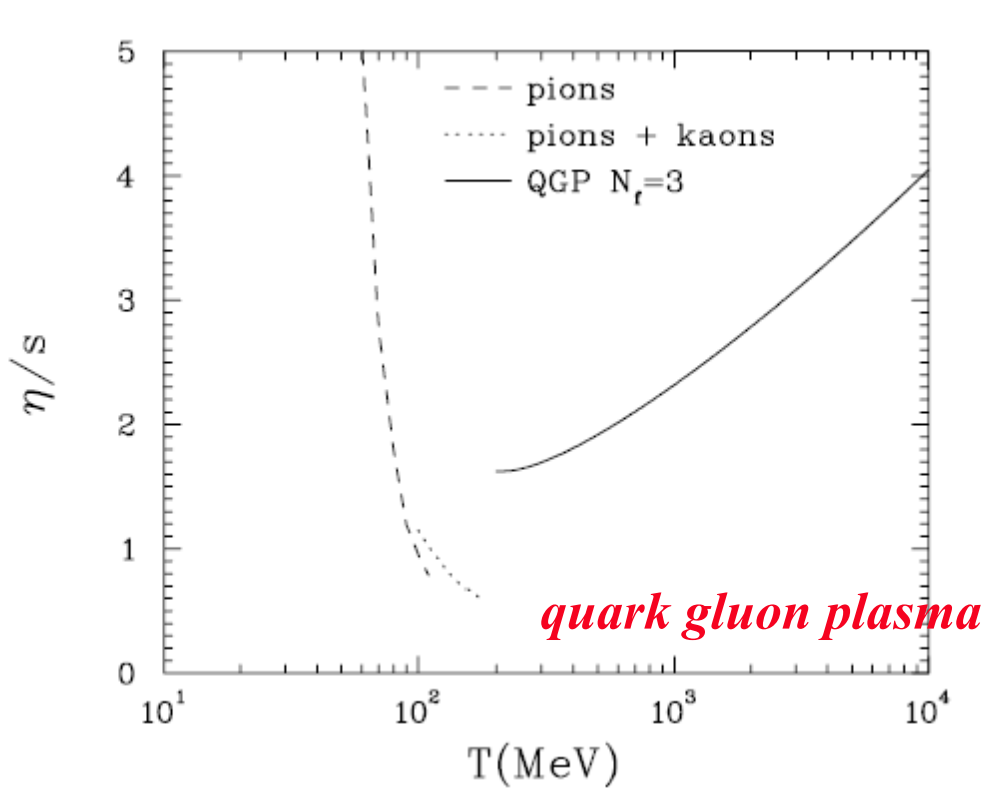

Csernai, Kapusta & McLerran
PRL97, 152303 (2006)

strongly coupled dusty plasma

B. Liu and J. Goree,

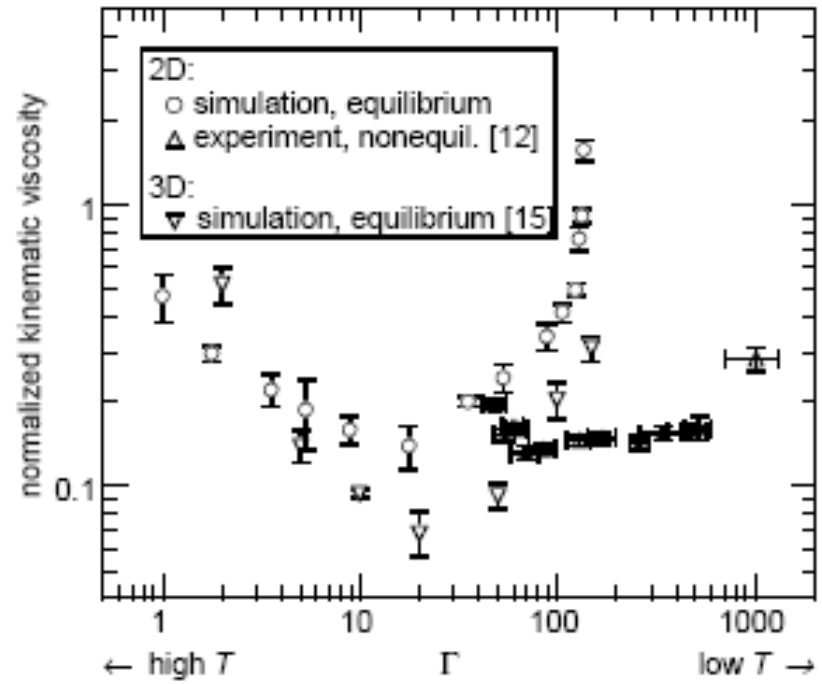

minimum observed in other strongly coupled systems – kinetic part of η decreases with Γ while potential part increases

Thermalization according to AdS/CFT

- Horizon of black hole in AdS at distance $1/\pi T$ from boundary
  - Sets light arrival time
  - Black holes form by gravity
  - Gravitons travel at c
- Timescale for black hole formation is $\tau = 1/\pi T$
  - For T=318 MeV, τ = hbar c /1 GeV = 0.2 fm
- Decay rate for non-hydro modes
  - $\tau_{e\text{-}fold} \sim 1/8.6T_{init}$ yielding $\tau \sim 0.3$ fm/c
- still need to separate τ and T_{init}

Gubser & Karch, Ann Rev. Nucl. Part. Sci. 59, 145 (2009)

Friess, Gubser, Michalogiorgakis, Pufu, JHEP 04, 80 (2008))

- Of course, the coupling is NOT ∞

Medium effect on Glasma evolution

Yin Jiang
Indiana University, Physics Dept. & CEEM

In collaboration with Jean-Paul Blaizot and Jinfeng Liao.

Particular thanks to Larry McLerran for discussions and the early stage of this work.

Outline

- Motivation
- Boltzmann equation with mass effect
- Evolution of under- and over-populated systems
- Scaling behavior
- Self- consistent mass
- Conclusions

Motivation

- In pre-equilibrium stage of heavy ion collision, high over-population gluon system is produced.
- Large occupation number($f \sim 1/\alpha_s$, $n_0 \varepsilon_0^{-3/4} \gg O(1)$) and weak coupling lead to a BEC of gluons.

1. Bose-Einstein Condensation and Thermalization of the Quark Gluon Plasma Jean-Paul Blaizot, Francois Gelis , Jin-Feng Liao, Larry McLerran, Raju Venugopalan. Nucl.Phys. A873 (2012) 68-80 .

2. Gluon Transport Equation in the Small Angle Approximation and the Onset of Bose-Einstein Condensation Jean-Paul Blaizot, Jinfeng Liao, Larry McLerran. Nucl.Phys. A920 (2013) 58-77 .

✓ Rapid IR "Local Thermalization".

✓ Onset of Dynamical BEC and scaling exponent.

✓ Massless gluons

Motivation

- Medium effect on evolution and scaling behavior.
- Screening mass as one of most important medium effects.

- ☐ What is the mass effect on both the IR thermalization and onset of BEC?
- ☐ Whether the critical scaling behavior will be changed by screening mass?

Boltzmann equation for gluons

- Only consider 2 to 2 interaction

- $\partial_t f_1 = \int_{2,3,4} \frac{1}{\varepsilon_1 \varepsilon_2 \varepsilon_3 \varepsilon_4} |M|^2 [(1+f_1)(1+f_2) f_3 f_4 - (1+f_1)(1+f_2) f_3 f_4]$

- Small angle approximation, including mass naively

$$|M|^2 = 72 g^4 \left(3 - \frac{tu}{s^2} - \frac{st}{u^2} - \frac{us}{t^2}\right) \to -144 g^4 \frac{s(4m^2 - s)}{t^2 - m_{int}^2}$$

and $\varepsilon = \sqrt{k^2 + m_{ext}^2}$

- In small angle approximation, collision term can be reduced to a diffusion in momentum space

$$\partial_t f = -\nabla_{\vec{p}} \cdot \vec{S}$$

Isotropic case

- In isotropic case $f(\vec{p}) = f(\varepsilon)$, flux reduced as
- $\vec{s} =$

$$\vec{e}_{\vec{p}_1} \frac{36\alpha^2}{\pi} \int \frac{dq}{q} \int dp_2 p_2^2 \frac{Z(q,v_1,v_2)}{v_1} (h_1 \dot{f}_2 - h_2 \dot{f}_1)$$

where $h_1 = f_1(1 + f_1)$.

- q can be analytically integrated out. No IR divergence.

Isotropic case

- Effective temperature

$$\vec{s} = \vec{e}_{\vec{p}_1} \frac{36\alpha^2}{\pi} \int \frac{dq}{q} \int dp_2 p_2^2 \frac{Z(q, v_1, v_2)}{v_1} (h_1 \dot{f}_2 - h_2 \dot{f}_1)$$

$$= \vec{e}_{\vec{p}_1} (h_1 I_b(p_1) - I_a(p_1) \dot{f}_1)$$

Near thermalization point $T_{eff} = I_a / I_b$ in small p limit.

- Solving the equation with implicit Gaussian method.

Redefining time as $\tau = \frac{36\alpha^2 t}{\pi}$. Two parameter f_0 and m.

Approach to thermalization

- Underpopulated case: $f_{\tau=0} = \frac{f_0}{e^{10(\varepsilon-1.5)}+1}$ with $f_0 = 0.1$ and $\mathrm{n} = 0.0056 < n_{max} = \int_{\vec{p}} f_{BE}(\mu = m, T(E)) = 0.0089.$
- Fit with $f = \frac{1}{e^{(\varepsilon-\mu)/T}-1}$ at $\tau = 6$.

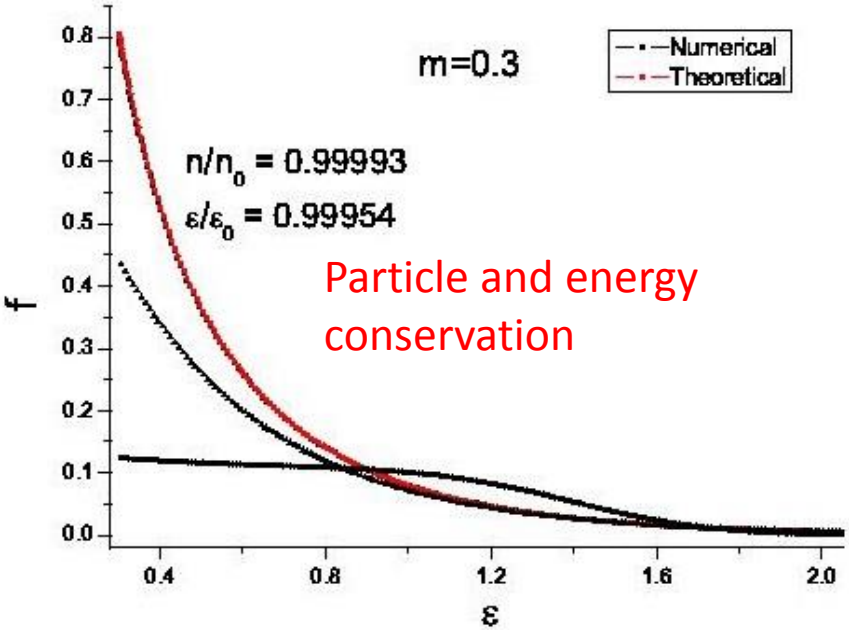

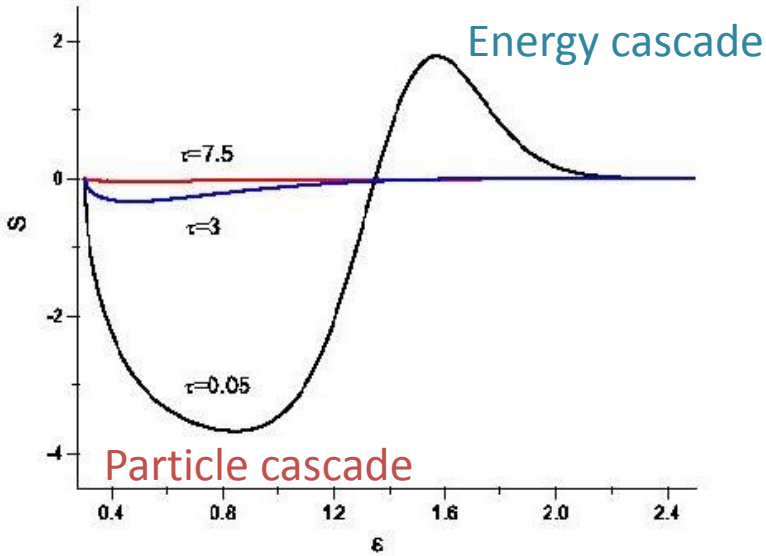

Approach to BEC onset

- Overpopulated case $f_{\tau=0} = \frac{f_0}{e^{10(\varepsilon-1.5)}+1}$ with $f_0 = 1.0$ and $\mathrm{n} = 0.056 > n_{max} = 0.051.$

- Fit with BE distribution(local IR $f^{-1} \approx \frac{\varepsilon-\mu}{T} = \frac{1}{T}(\frac{p^2}{2m} + \delta\mu))$ at $\tau = 0.1.$ $\mu \to m$

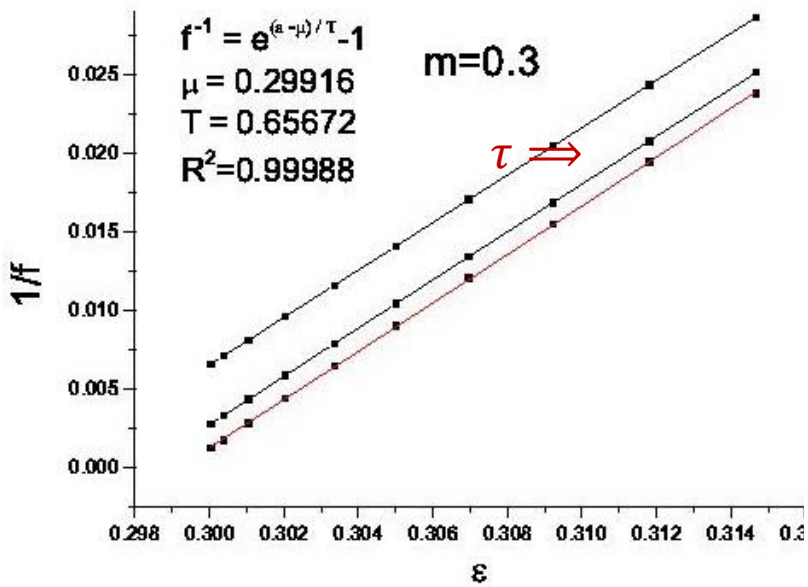

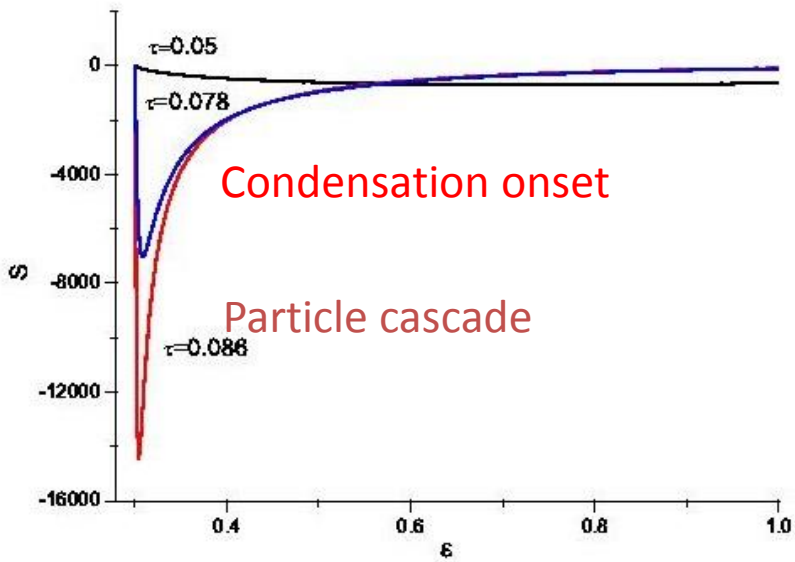

Approach to BEC onset

- Overpopulated case $f_{\tau=0} = \frac{f_0}{e^{10(\varepsilon-1.5)}+1}$, $f_0 = 1.0$ with different masses(0.1, 0.5 and 0.7).

$n > n_{max}$

$$f^{-1} \approx \frac{\varepsilon - \mu}{T}$$

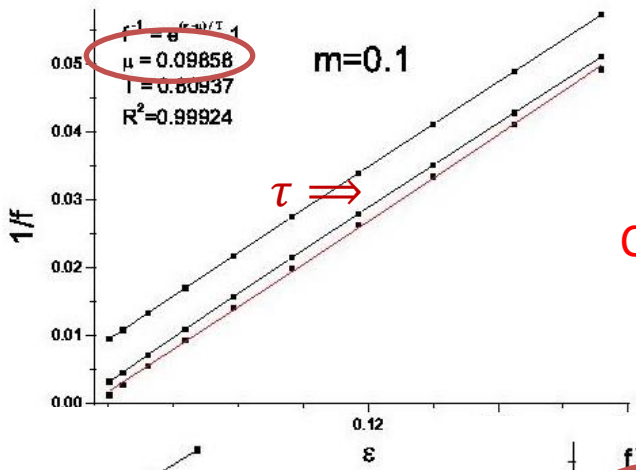

$\mu \to m$

Condensate onset

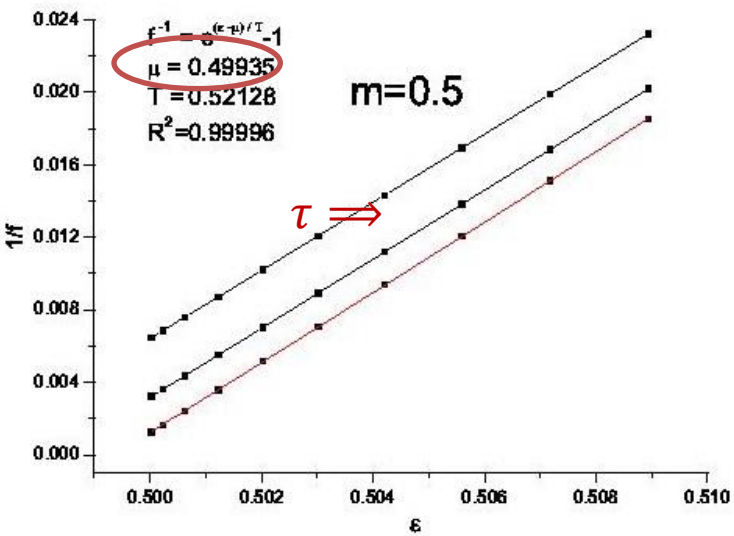

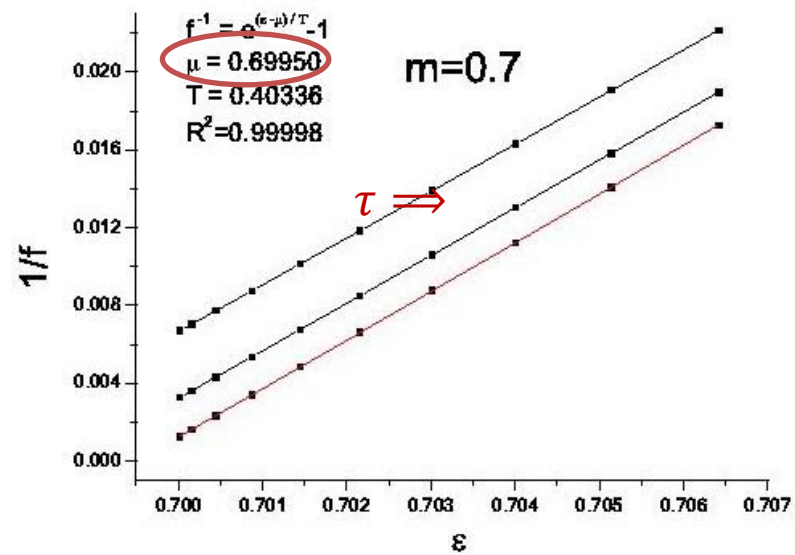

Approach to BEC onset

- Overpopulated case $f_{\tau=0} = \frac{f_0}{e^{10(\varepsilon-1.5)}+1}$, with different $f_0 = 1.0 \sim 2.0$ and $\mathrm{n} > n_{max}$.
- Chemical potential approaches the mass $\mu \to m$. Onset of BEC.
- How to obtain this critical scaling exponent analytically?

$$\mu \approx m - C(\tau_c - \tau)^{\eta}$$
$$= m - C \cdot \delta\tau^{\eta}$$

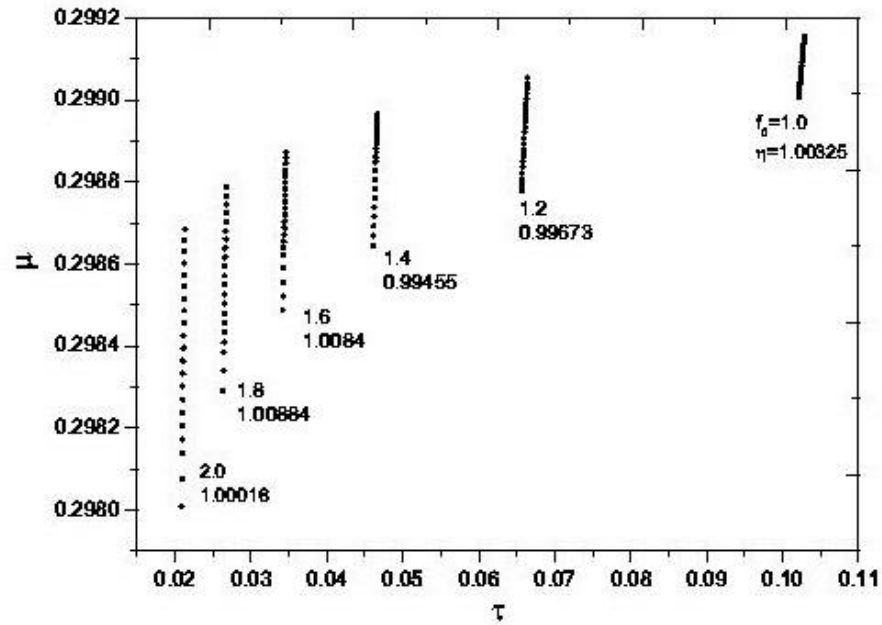

Scaling behavior

- Near thermal point $f \approx \frac{T(\tau)}{\frac{p^2}{2m} - \delta\mu(\tau)}$ at IR range, $\delta\mu = m - \mu$.
- Effective temperature almost invariant.
- Rescaling distribution with $\delta\mu(\tau)$

$$f \approx \frac{1}{\delta\mu(\tau)} \frac{T}{\tilde{p}^2/2m},$$

where $\tilde{p} = p/\sqrt{\delta\mu(\tau)}$.

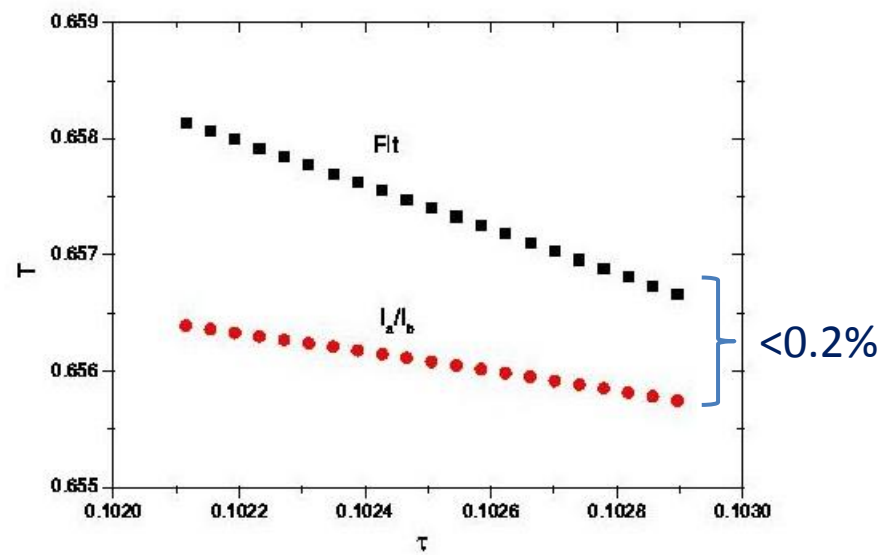

- Boltzmann equation gives $\delta\mu(\tau) \propto \delta\tau$.

Scaling behavior

Condensation of bosons in kinetic regime

D.V. Semikoz, I.I. Tkachev. Phys.Rev. D55 (1997) 489-502

- $\tilde{p} = p/A(\tau)$, and set $\tilde{I}_{a,b} = I_{a,b}(\tilde{p})$.
- Starting from self similarity solution $f(p) = A^n \tilde{p}^k$,

  Boltzmann equation gives

$$\partial_\tau A = const \cdot A^{2n+3}$$

$$(n-k)\tilde{p}^k = const \cdot [\tilde{I}_a(k^2+k)\tilde{p}^{k-2} + \tilde{I}_b/m(2k+3)\tilde{p}^{2k}]$$

- $n = k = -2$, $f(p) = A^{-2}\tilde{p}^{-2}$ is a solution.
- And $A(\tau) = \sqrt{m - \mu(\tau)} = \sqrt{\delta\mu}$.

$$\delta\mu = const \cdot \delta\tau$$

Scaling behavior

- Chemical potential approaches mass linearly.

m=0.3

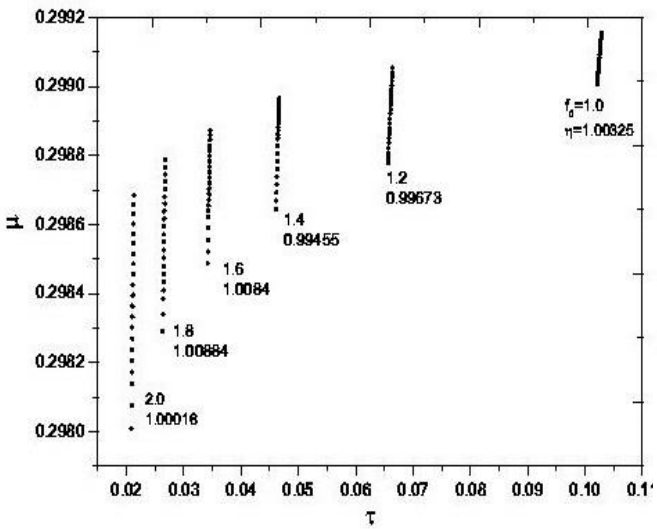

f_0=1.0

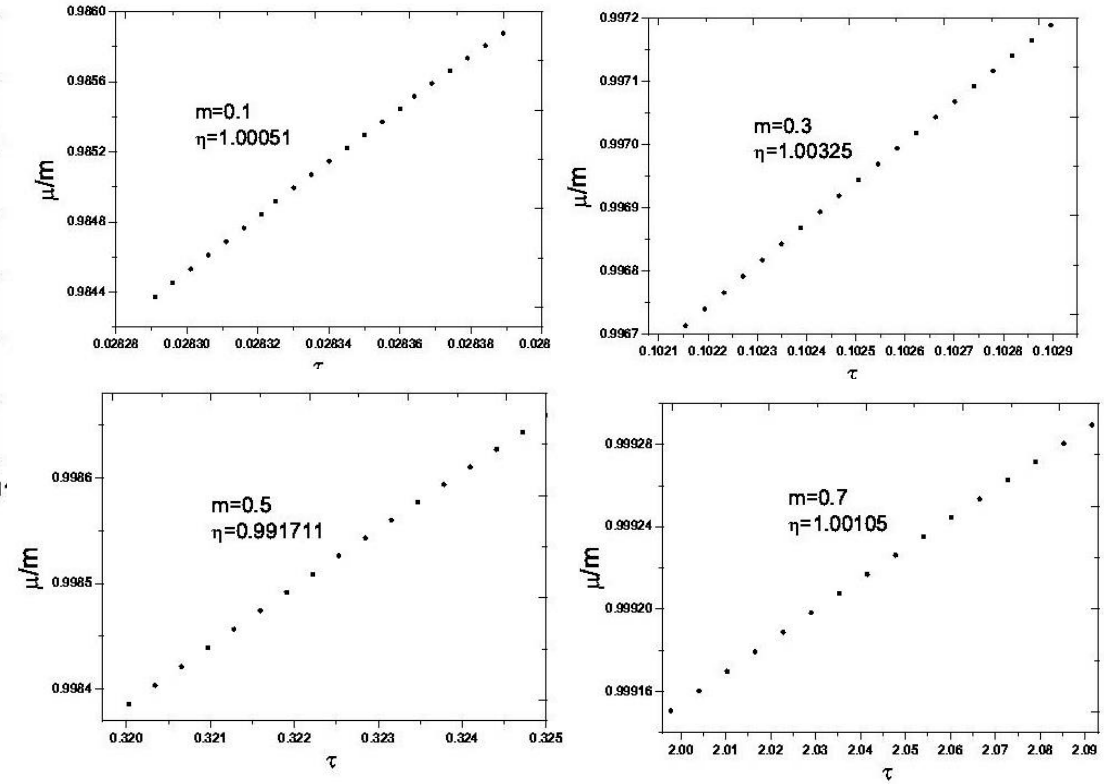

- Numerical results confirms our analysis,

$\mu \approx m - C(\tau_c - \tau)^\eta$ or $\delta\mu \propto \delta\tau^\eta, \eta = 1.$

Scaling behavior

- Fit the last 10(black) and 30(red) points with $\delta\tau^{\eta}$

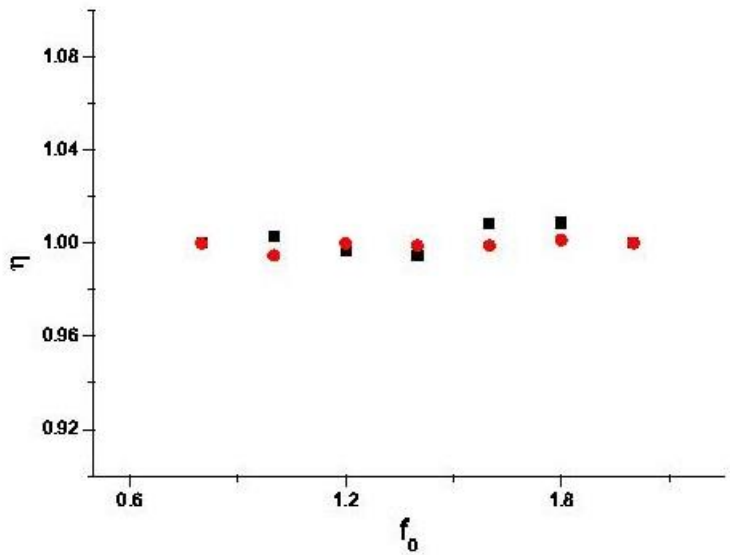

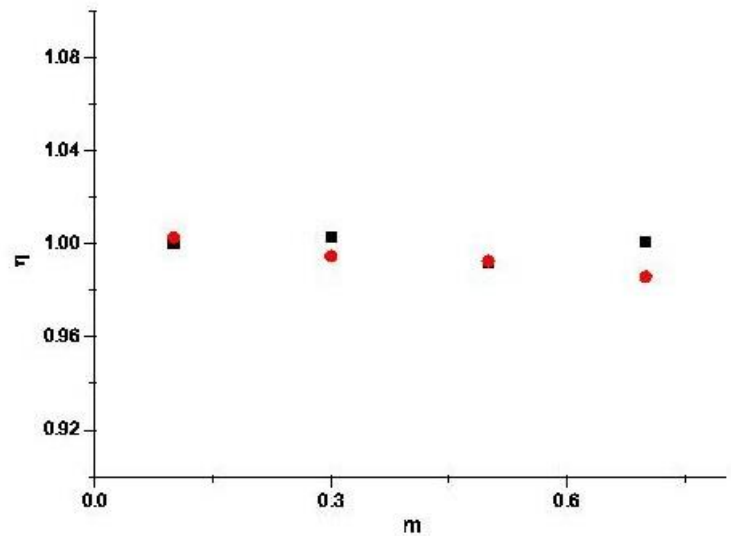

$$1 - R^2 = \sum_i \frac{(f_i - y_i)^2}{(\bar{y} - y_i)^2}$$

$R^2 = 1$, perfect fit

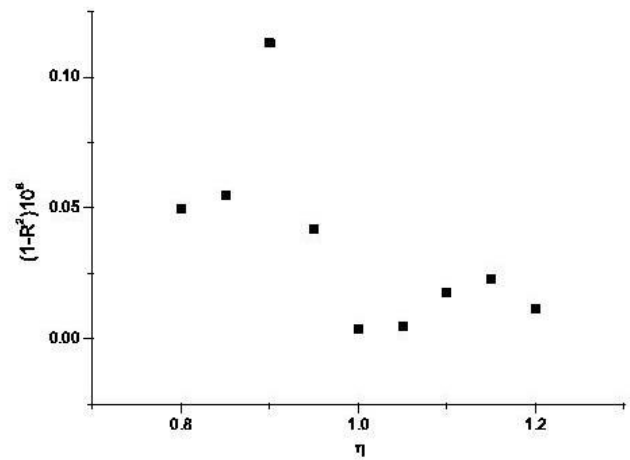

Self-consistent mass

- Using HTL result $m^2 = 2g^2 C_A \int f(\vec{p})/p$
- Time dependent mass will break energy conservation slightly.

$m_{initial} = 0.33$
$m = 0.468$

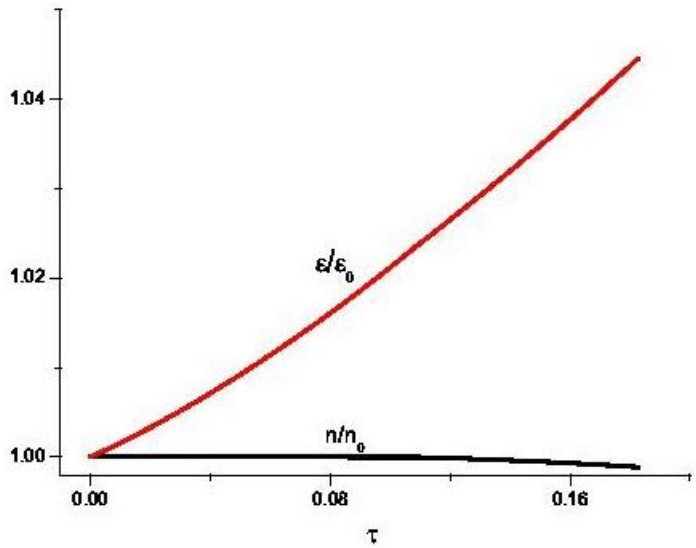

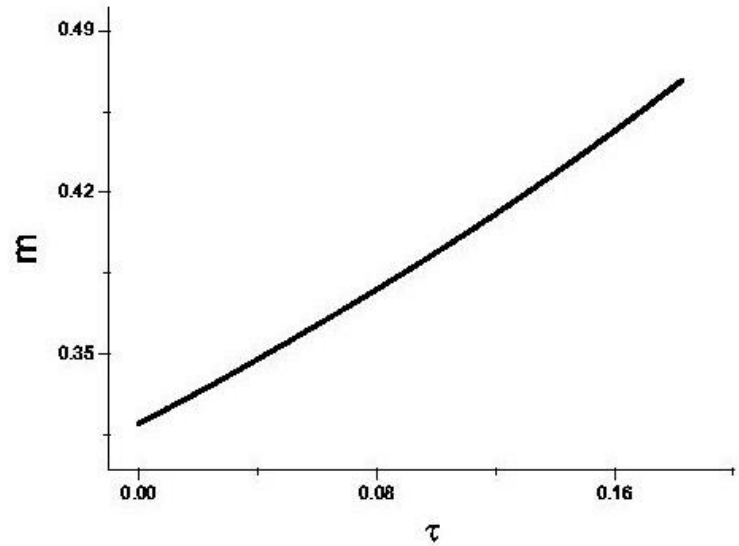

Self-consistent mass

- Using HTL result $m^2 = 2g^2 C_A \int f(\vec{p})/p$
- Overpopulated case $f_{\tau=0} = \frac{f_0}{e^{10(\varepsilon-1.5)}+1}$

$m_{initial} = 0.33$
$m = 0.468$

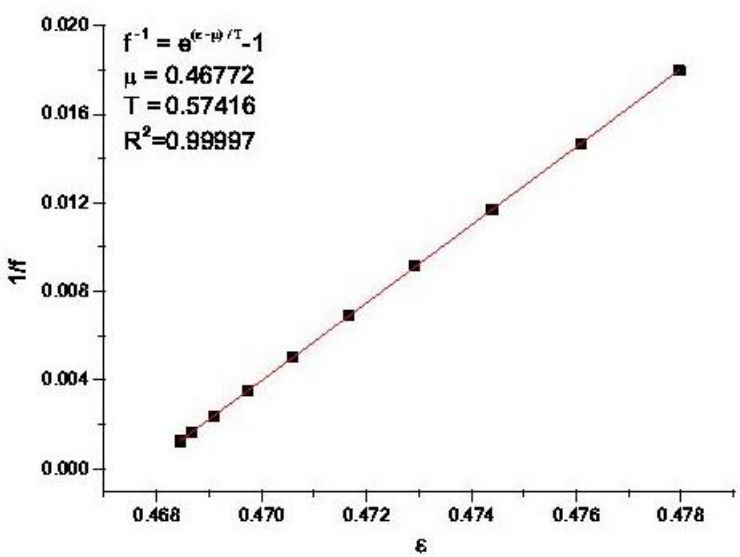

$m_{initial} = 3.45$
$m = 4.42$

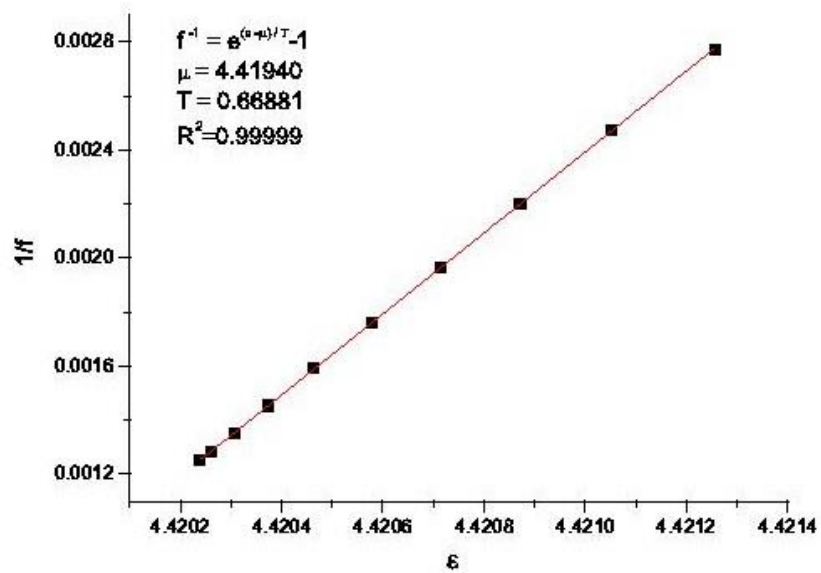

Self-consistent mass

- Mass $m^2 = 2g^2 C_A \int_{\vec{p}} f(\vec{p})/p$ does not change scaling behavior for $m^2(p) = m^2(\tilde{p})$.

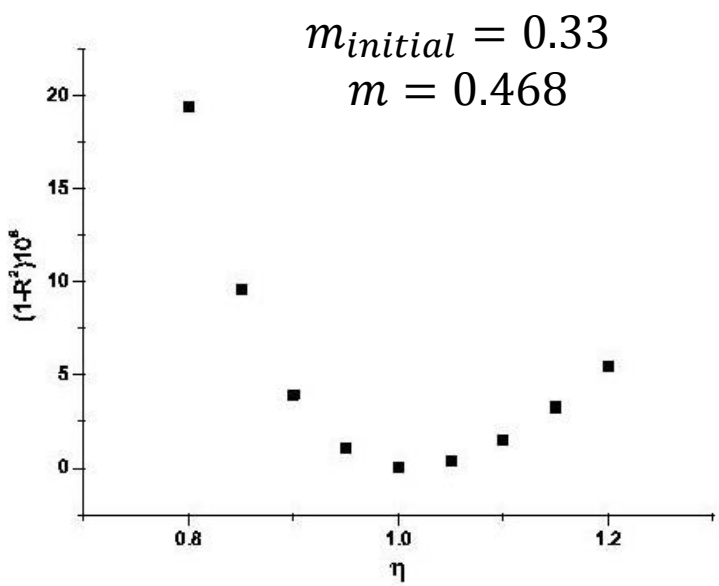

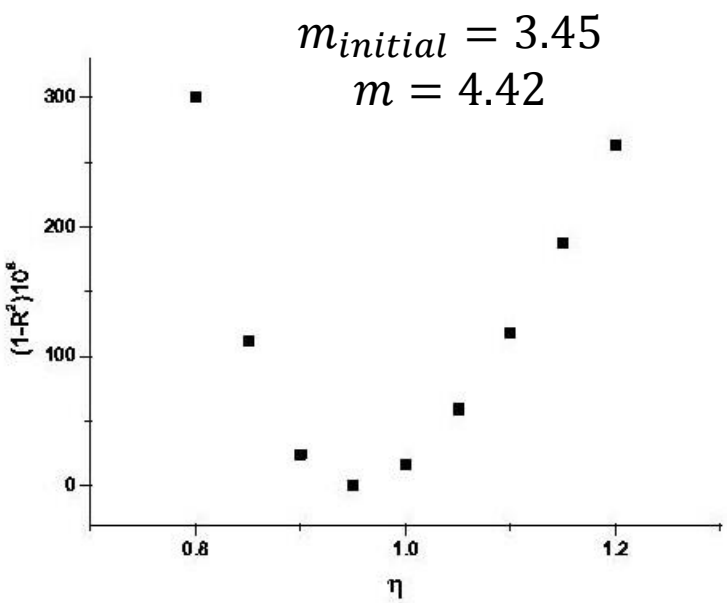

- $\delta\mu \propto \delta\tau^{\eta}, \ \ \eta = 1.$

Conclusion

- We have studied the dense gluon system with transport equation including the screening mass generated by medium.
- Numerically we have shown that the underpopulated system will thermalize while the overpopulated system will approach the BEC onset.
- Analytically and numerically we have found the critical scaling behavior of BEC onset, $\delta\mu \propto \delta\tau^{\eta}, \eta = 1$.
- The same behavior is also found in the case when screening mass is generated in a self-consistent way.

Thank you!

Energy and particle conservation

- Energy and particle conservation are respected during evolution.
- Both preserved at <0.1% level. The other cases are at the same order.

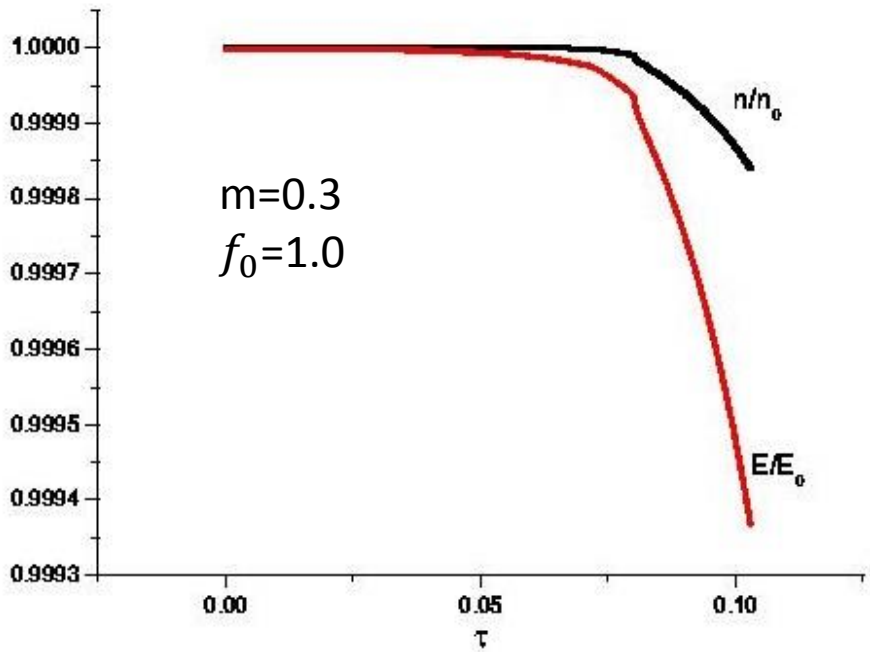

Rescaling behavior

- Power law distribution $f(p) = A^n \tilde{p}^k$
- Small p limit $h = f(1+f) \approx f^2$
- Rescaling

$$I_a = \int dp p^2 v h \rightarrow \tilde{I}_a = m^{-1} \int d\tilde{p} \tilde{p}^2 \tilde{p} \tilde{p}^{2k} \text{ and}$$

$$I_b = -\int dp p^2 v \dot{f} \rightarrow \tilde{I}_b = -\int d\tilde{p} \tilde{p}^2 \partial_{\tilde{p}} \tilde{p}^k$$

UV cascade of over-occupied gluons

Aleksi Kurkela, CERN
with Mark Abraao York, Egang Lu, and Guy Moore

What: Thermalization of overoccupied isotropic gauge fields

How: Using effective kinetic theory, $\alpha \ll 1$

New: Scaling solution $f \propto 1/p$

Over-occupied cascade

What happens if you have too many soft gluons, $f \sim 1/\alpha$

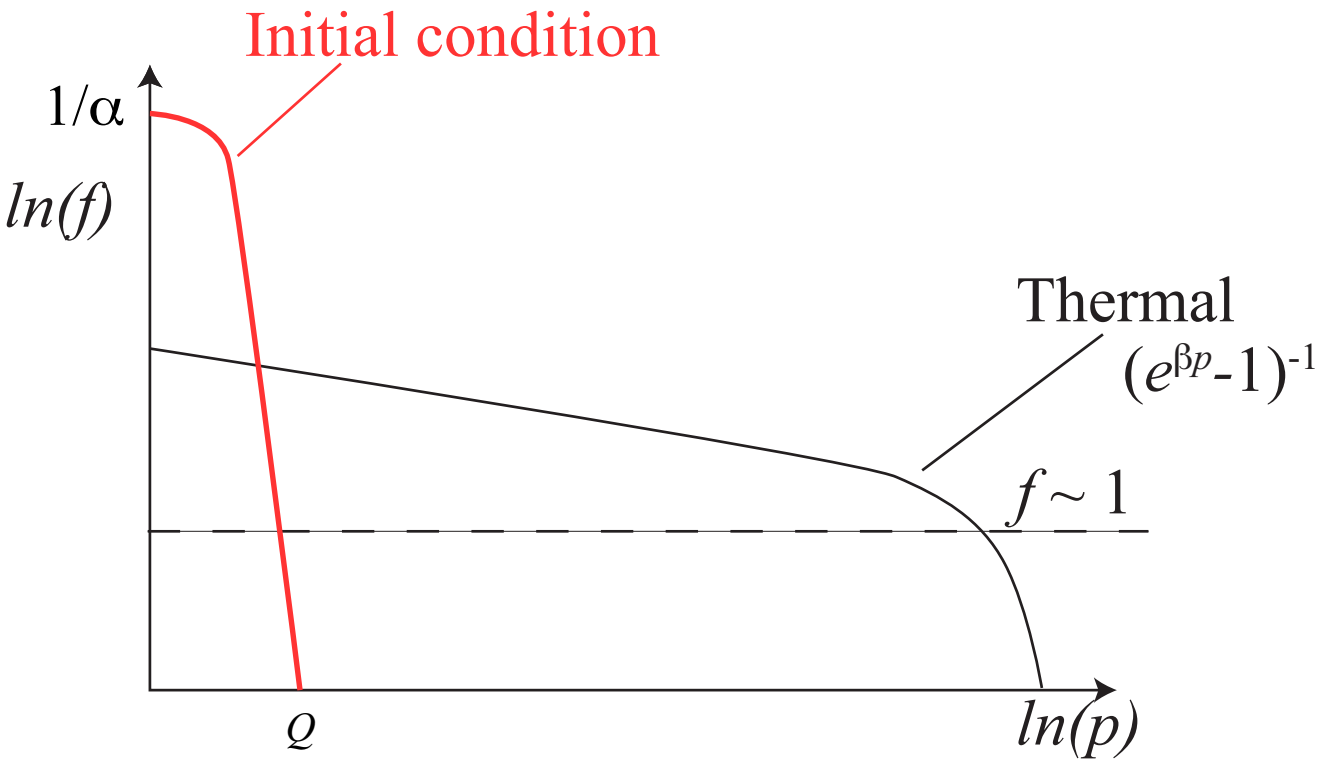

Over-occupied cascade

What happens if you have too many soft gluons, $f \sim 1/\alpha$

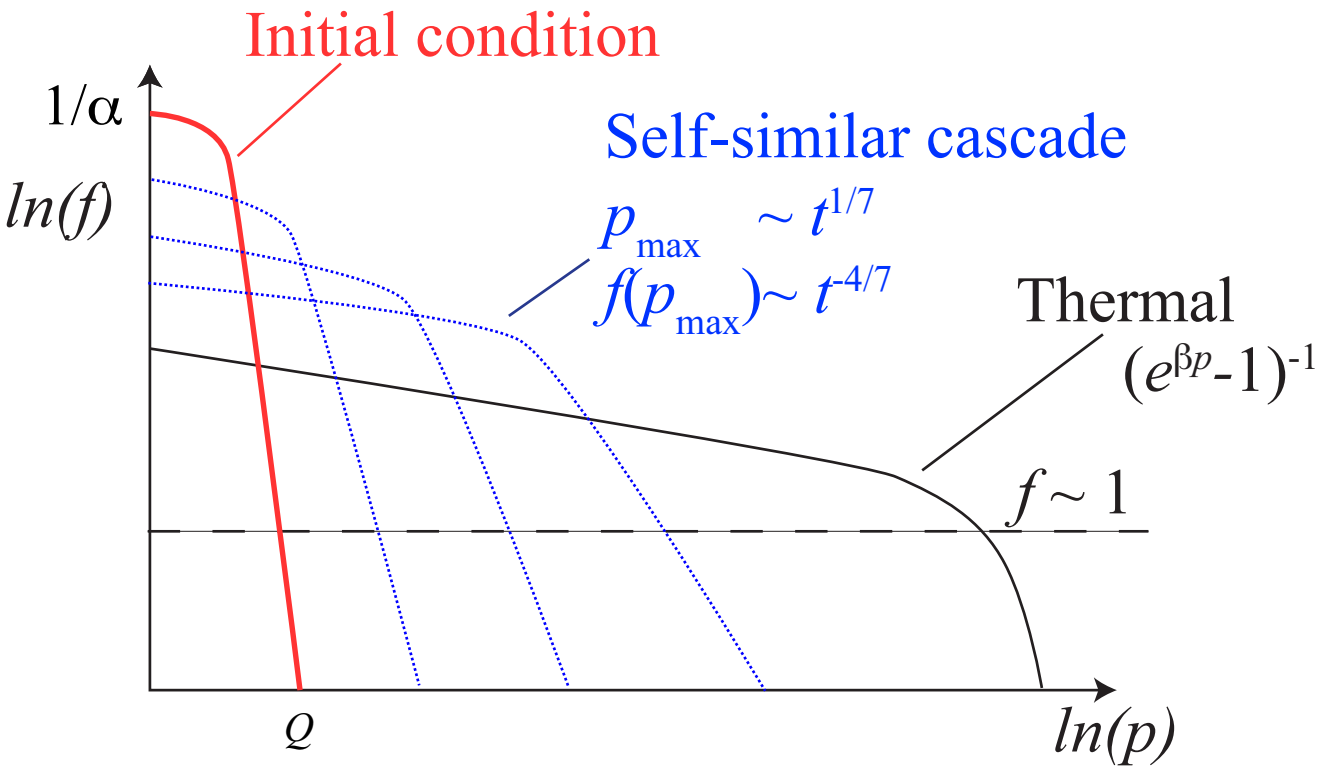

This talk: what are the details of the cascade

Motivation

Related to HIC:

Clean toy model with interesting physics

- BEC condensation, strong IR physics?
- Kolmogorov turbulence, $p^{-4/3}$?
- Vacuum fluctuations?

Theoretically very tractable, overlapping dual descriptions for $\alpha \ll 1$, $1 \ll f \ll 1/\alpha$

- Classical field theory
- Effective kinetic theory

Platform to develop and test technology.

- If BMSS is correct, this is exactly the technology we need.

Effective kinetic theory

Arnold et al. hep-ph/0209353

$$\frac{df}{dt} = -C_{2\leftrightarrow 2}[f] - C_{1\leftrightarrow 2}[f]$$

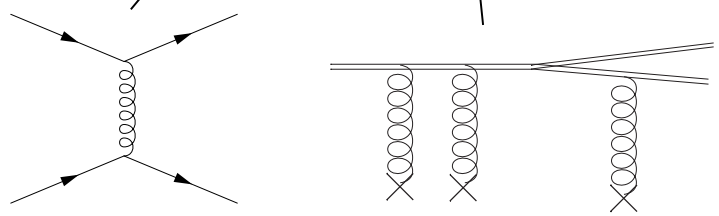

- Vacuum $2 \leftrightarrow 2$ term suffers from Coulomb divergence $q_\perp \to 0$

$$\Gamma_{q_\perp}[f] = \frac{d\Gamma_{\rm el}}{d\log q_\perp^2} \sim \frac{\alpha^2}{q_\perp^2}\int d^3p\, f_p\,(1+f_p)$$

  Regulated by physics of screening at scale

$$m^2 \sim \alpha \int d^3p \frac{f(p)}{p}$$

- Frequent soft scatterings induce soft and collinear radiation

$$\frac{d\Gamma_{\rm inelastic}}{d\log p\, d\log\theta} \sim \alpha\Gamma_m(1+f_p)$$

  Collinear divergence regulated by physics of LPM suppression.

- Based on massless spectral functions, fails at $p \lesssim m$ no BEC or Weibel

Loss of information, non-thermal fixed point

- Need only *few* (large-angle) collisions to lose information of initial state f_i:

$$\Gamma_Q[f_i] \sim (\alpha^2 Q^{-2})(Q^3 f_i) f_i \sim Q$$

- Need *many* collisions to go from $p \sim Q$ to T. For sure the system doesn't thermalize before $T^4 \sim \alpha^{-1} Q^4$

$$\Gamma_T[f_T] \sim \alpha^2 T \sim \alpha^{7/4} Q$$

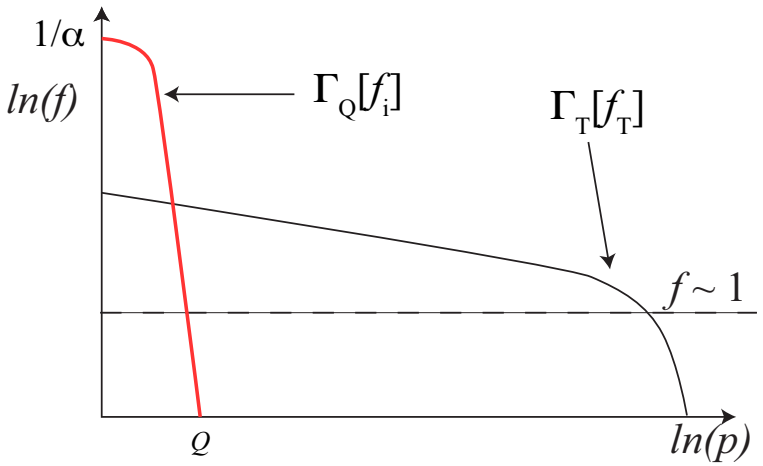

Parametrically long time during which the system is insensitive to initial conditions but not thermal.

Information on the initial condition lost quickly AK, Moore 1207.1663

6 very different initial conditions:

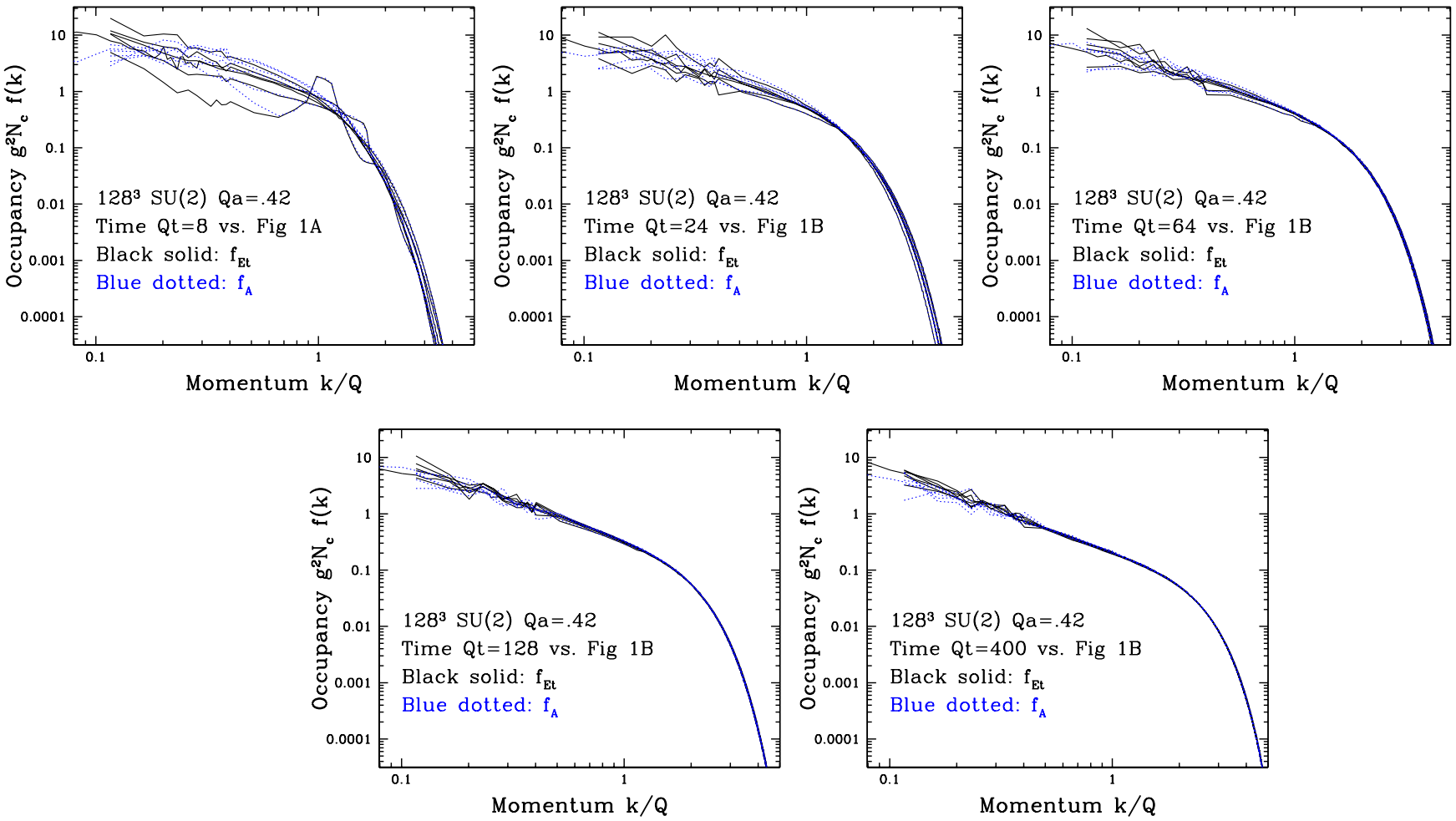

Differences vanish by $\Gamma_Q[f_i]t \sim Qt \sim 64$

See also Schlichting 1207.1450, Berges et al. 1312.5216

Evolution of the cascade

AK, Moore 1107.5050, 1207.1663

Dynamics: expect collision rate $\Gamma_{p_{\max}}[f]t \sim 1$:

$$t\alpha^2 p_{\max} f^2 \sim 1 \qquad p_{\max}^4 f \sim Q^4/\alpha$$

Solved by

$$p_{\max} \sim Q(Qt)^{1/7} \quad f \sim \alpha^{-1}(Qt)^{-4/7}$$

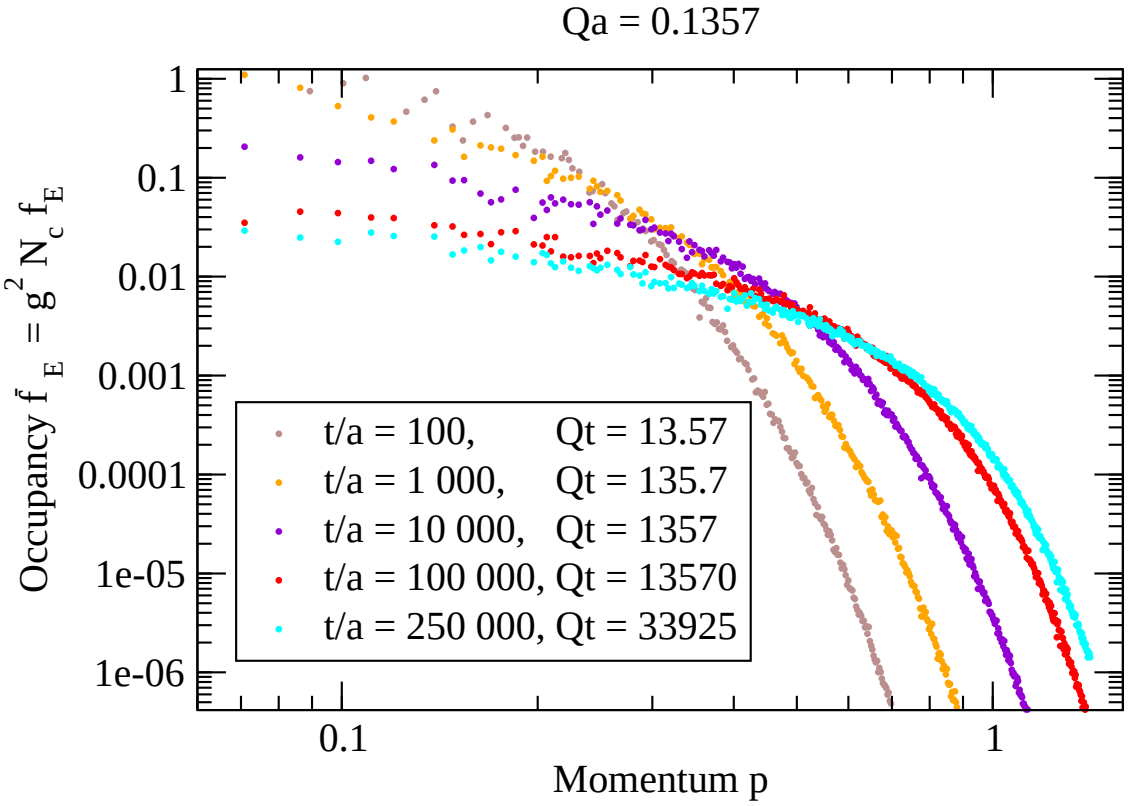

$V = 256^3$, SU(2), fixed lattice spacing, single initial condition

see also Blaizot et al. 1107.5296

Evolution of the cascade

AK, Moore 1107.5050, 1207.1663

Dynamics: expect collision rate $\Gamma_{p_{\max}}[f]t \sim 1$:

$$t\alpha^2 p_{\max} f^2 \sim 1 \qquad p_{\max}^4 f \sim Q^4/\alpha$$

Solved by

$$p_{\max} \sim Q(Qt)^{1/7} \quad f \sim \alpha^{-1}(Qt)^{-4/7}$$

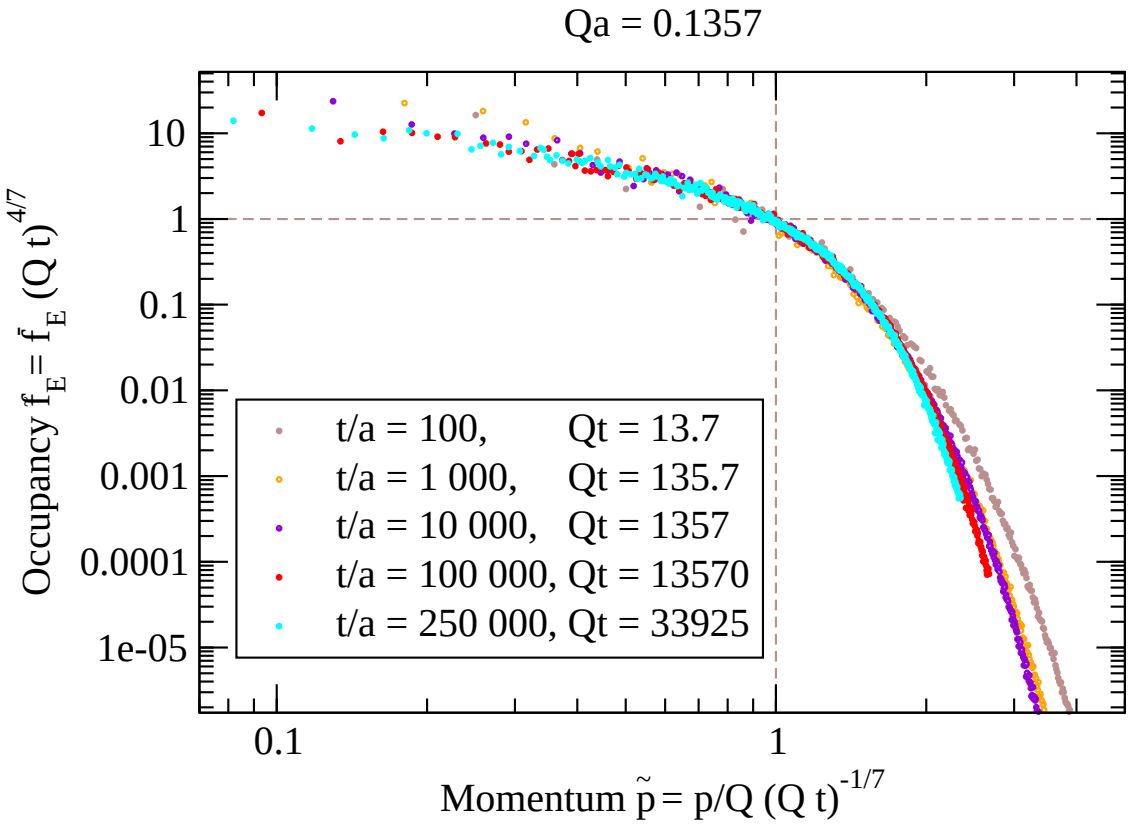

$V = 256^3$, SU(2), fixed lattice spacing, single initial condition

see also Blaizot et al. 1107.5296

Scaling solution

Self-similarity:

$$f(p,t) = (Qt)^{-4/7}\tilde{f}(\tilde{p},t) \qquad \tilde{p} = p/Q(Qt)^{1/7}$$

Claim: Scaling solution $\tilde{f}$ independent of time at late times

Scaling solution

Self-similarity:

$$f(p,t) = (Qt)^{-4/7}\tilde{f}(\tilde{p},t) \qquad \tilde{p} = p/Q(Qt)^{1/7}$$

Claim: Scaling solution $\tilde{f}$ independent of time at late times

$$t\frac{d\tilde{f}}{dt} = \frac{1}{7}\left(4\tilde{f} + \tilde{p}\frac{d\tilde{f}}{d\tilde{p}}\right) - \tilde{C}[\tilde{f}(\tilde{p})]_{1\leftrightarrow 2} - \tilde{C}[\tilde{f}(\tilde{p})]_{2\leftrightarrow 2} \longrightarrow 0$$

- Both sides scale homogenously $(Qt)^{-4/7}$ because of overoccupation.
- Rescaled collision terms depend only on $\tilde{p}$ and $\tilde{f}$ not on p.
- If there is an attractive solution, the system will quickly relax to it.

Scaling solution

Self-similarity:

$$f(p,t) = (Qt)^{-4/7}\tilde{f}(\tilde{p},t) \qquad \tilde{p} = p/Q(Qt)^{1/7}$$

Claim: Scaling solution $\tilde{f}$ independent of time at late times

$$t\frac{d\tilde{f}}{dt} = \frac{1}{7}\left(4\tilde{f} + \tilde{p}\frac{d\tilde{f}}{d\tilde{p}}\right) - \tilde{C}[\tilde{f}(\tilde{p})]_{1\leftrightarrow 2} - \tilde{C}[\tilde{f}(\tilde{p})]_{2\leftrightarrow 2} \longrightarrow 0$$

- Both sides scale homogenously $(Qt)^{-4/7}$ because of overoccupation.
- Rescaled collision terms depend only on $\tilde{p}$ and $\tilde{f}$ not on p.
- If there is an attractive solution, the system will quickly relax to it.

...Except that $|\mathcal{M}|^2$ contains the screening scale, and scales trivially only for $p \gg m$

Form of the scaling solution?

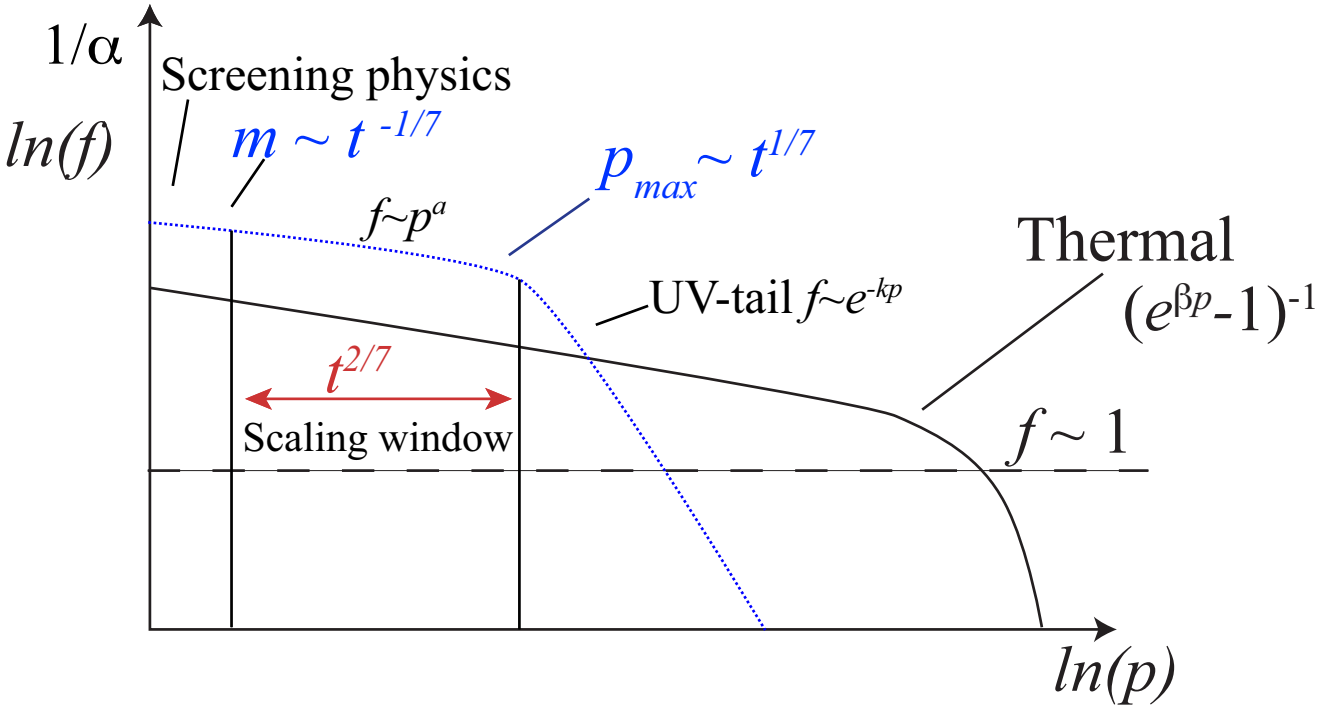

- All the scales below $p_{\max}$ have had time to undergo scattering and therefore have had time to reach thermal form $f(p) \propto p^{-1}$

AK, Moore 1107.5050 also Blaizot et al. arXiv:1107.5296

What does the data say?

Abraao York, AK, Lu, Moore 1401.3751.

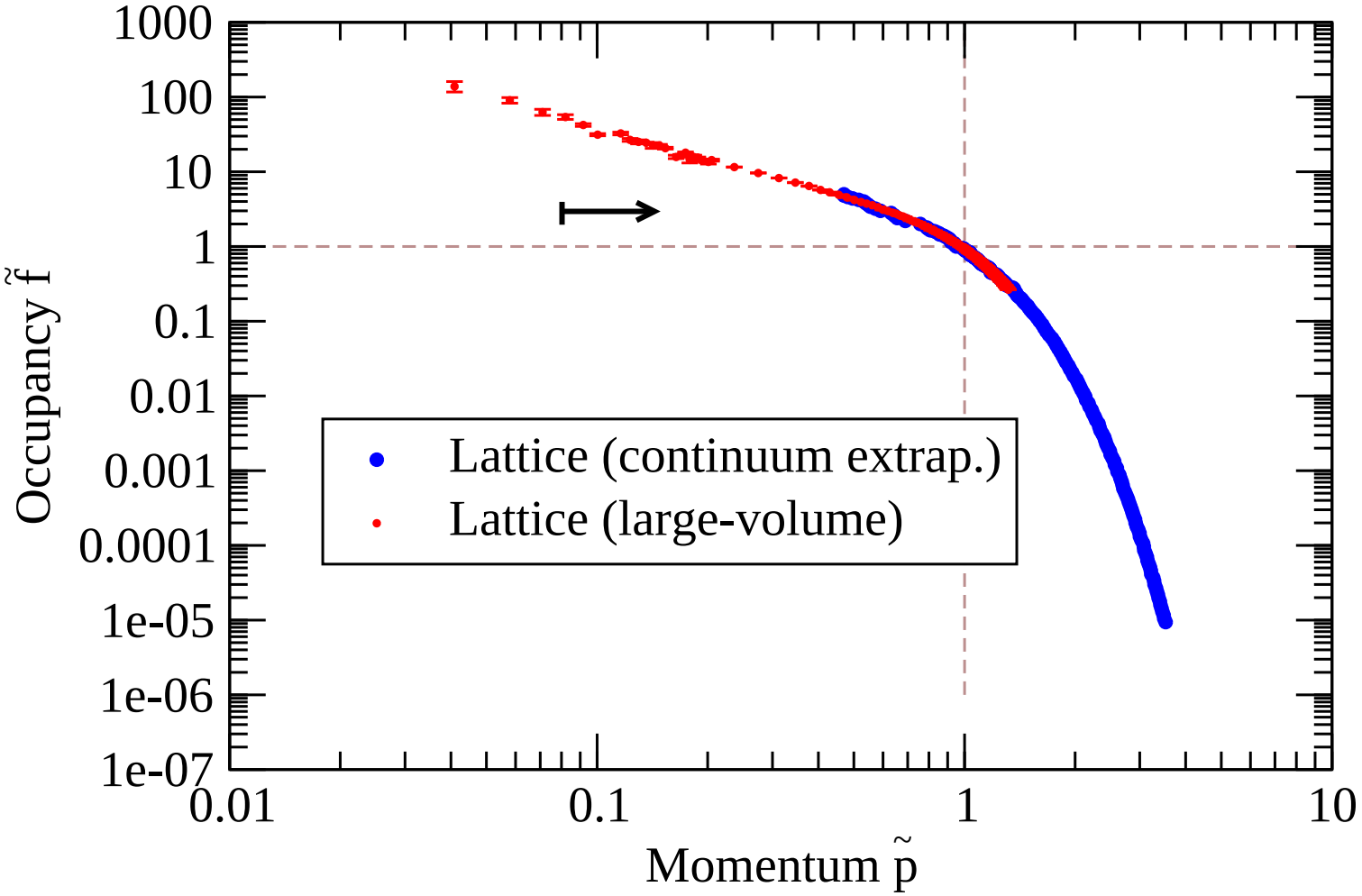

Large-volume: (Qa)=0.2, (QL)=51.2, Cont. extr.: down to (Qa)=0.1, (QL)=25.6 Qt=2000, $\tilde{m} = 0.08$

What does the data say?

Abraao York, AK, Lu, Moore 1401.3751.

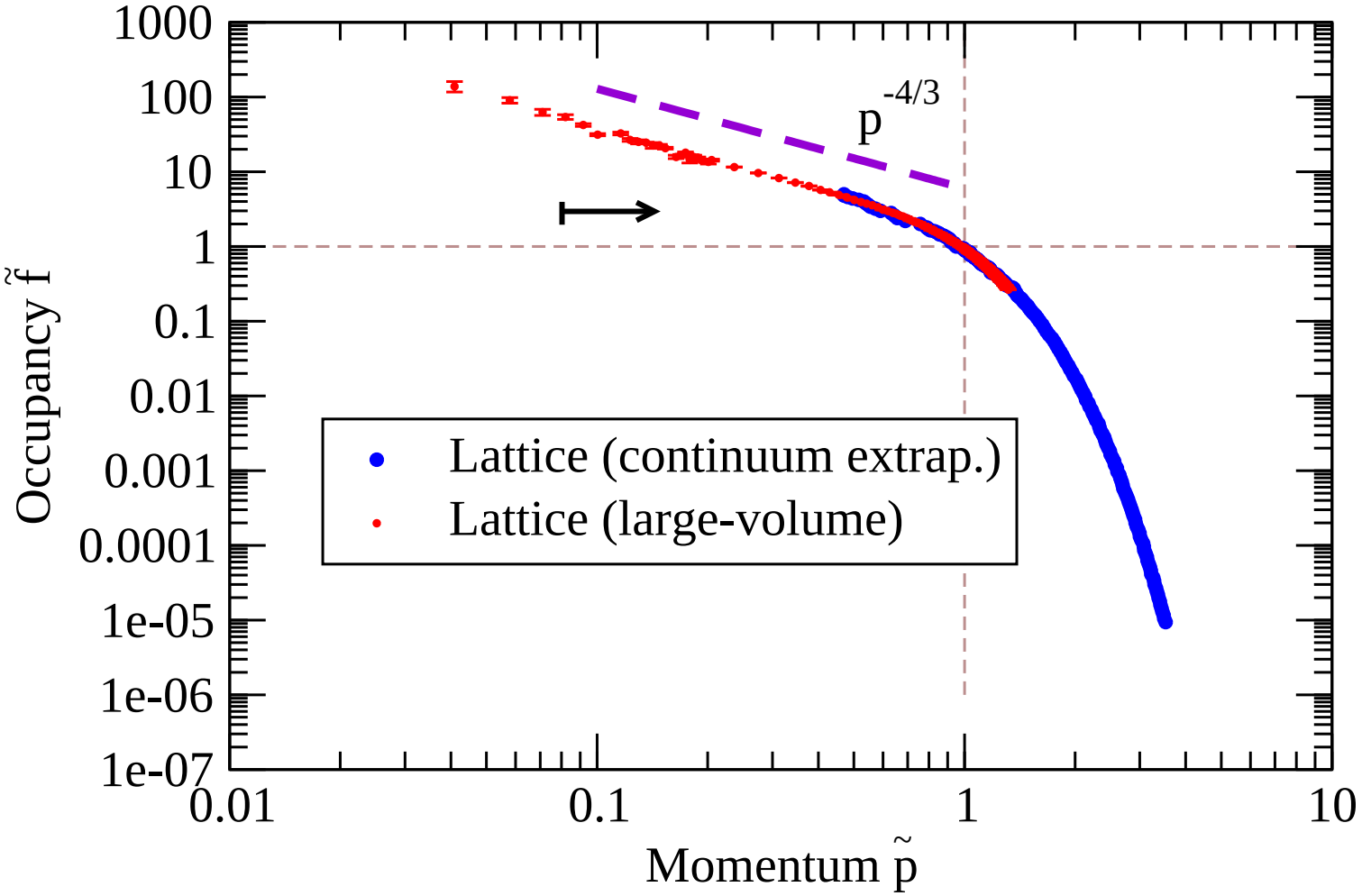

Large-volume: (Qa)=0.2, (QL)=51.2, Cont. extr.: down to (Qa)=0.1, (QL)=25.6 Qt=2000, $\tilde{m} = 0.08$

Turbulence in action?

Berges et al. 0811.4293

This empirical fact was actually observed already in 2008.

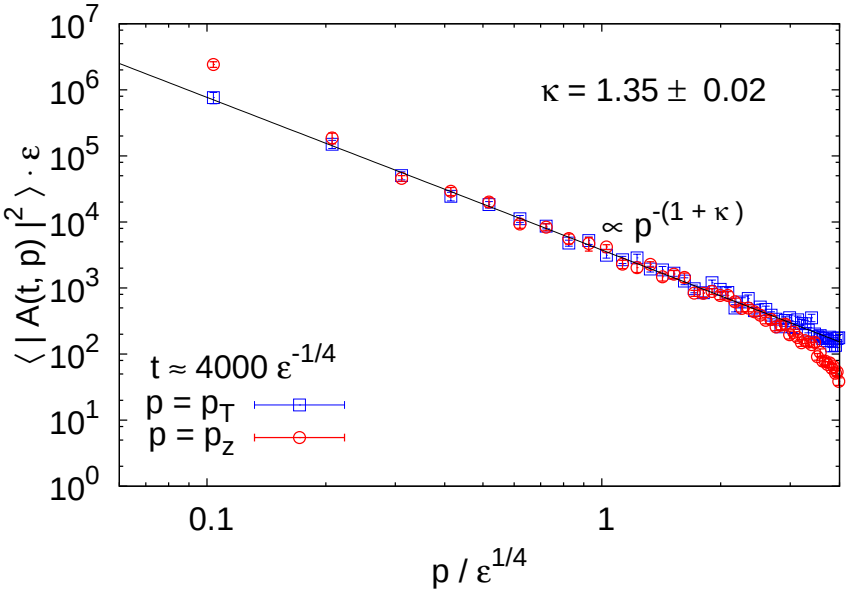

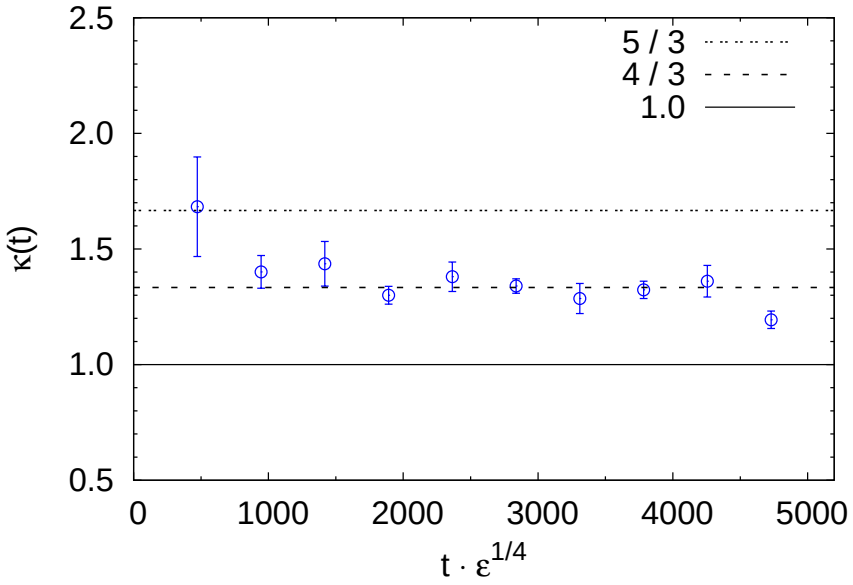

- Interpretation through Kolmogorov energy cascade towards UV with $p^{-4/3}$ or $p^{-3/2}$.

also Berges et al. 1203.4646

Can the data be trusted?

Abraao York, AK, Lu, Moore 1401.3751

$$0 = \int_{\tilde{p}} \left(\underbrace{\left[\frac{4}{7}\tilde{f} + \frac{\tilde{p}}{7}\frac{d\tilde{f}}{d\tilde{p}} \right]}_{\tilde{n}/7} - \tilde{C}_{1\leftrightarrow 2} - \underbrace{\tilde{C}_{2\leftrightarrow 2}}_{0} \right)$$

The contribution from inelastic scattering

$$\int_{\tilde{p}} \tilde{C}_{1\leftrightarrow 2} = 4\pi \int_{\tilde{p}>\tilde{k}} d\tilde{p} d\tilde{k}\, \tilde{\gamma}(\tilde{p}+\tilde{k};\tilde{p},\tilde{k}) \tilde{f}_{\tilde{p}+\tilde{k}} \tilde{f}_{\tilde{p}} \tilde{f}_{\tilde{k}} \left(\tilde{f}^{-1}_{\tilde{p}+\tilde{k}} - \tilde{f}^{-1}_{\tilde{p}} - \tilde{f}^{-1}_{\tilde{p}} \right)$$

with $\gamma \propto \frac{1}{\tilde{k}}$ at the Bethe-Heitler limit $k \ll p$

Can the data be trusted?

Abraao York, AK, Lu, Moore 1401.3751

$$0 = \int_{\tilde{p}} \left(\underbrace{\left[\frac{4}{7}\tilde{f} + \frac{\tilde{p}}{7}\frac{d\tilde{f}}{d\tilde{p}} \right]}_{\tilde{n}/7} - \tilde{C}_{1\leftrightarrow 2} - \underbrace{\tilde{C}_{2\leftrightarrow 2}}_{0} \right)$$

The contribution from inelastic scattering

$$\int_{\tilde{p}} \tilde{C}_{1\leftrightarrow 2} = 4\pi \int_{\tilde{p}>\tilde{k}} d\tilde{p} d\tilde{k}\, \tilde{\gamma}(\tilde{p}+\tilde{k};\tilde{p},\tilde{k}) \tilde{f}_{\tilde{p}+\tilde{k}} \tilde{f}_{\tilde{p}} \tilde{f}_{\tilde{k}} \left(\tilde{f}^{-1}_{\tilde{p}+\tilde{k}} - \tilde{f}^{-1}_{\tilde{p}} - \tilde{f}^{-1}_{\tilde{p}} \right)$$

with $\gamma \propto \frac{1}{\tilde{k}}$ at the Bethe-Heitler limit $k \ll p$

- $\widetilde{n}/7$ is finite, so must the integral for a scaling solution

Can the data be trusted?

Abraao York, AK, Lu, Moore 1401.3751

$$0 = \int_{\tilde{p}} \left(\underbrace{\left[\frac{4}{7}\tilde{f} + \frac{\tilde{p}}{7}\frac{d\tilde{f}}{d\tilde{p}} \right]}_{\tilde{n}/7} - \tilde{C}_{1\leftrightarrow 2} - \underbrace{\tilde{C}_{2\leftrightarrow 2}}_{0} \right)$$

The contribution from inelastic scattering

$$\int_{\tilde{p}} \tilde{C}_{1\leftrightarrow 2} = 4\pi \int_{\tilde{p}>\tilde{k}} d\tilde{p} d\tilde{k}\, \tilde{\gamma}(\tilde{p}+\tilde{k};\tilde{p},\tilde{k}) \tilde{f}_{\tilde{p}+\tilde{k}} \tilde{f}_{\tilde{p}} \tilde{f}_{\tilde{k}} \left(\tilde{f}^{-1}_{\tilde{p}+\tilde{k}} - \tilde{f}^{-1}_{\tilde{p}} - \tilde{f}^{-1}_{\tilde{p}} \right)$$

with $\gamma \propto \frac{1}{\tilde{k}}$ at the Bethe-Heitler limit $k \ll p$

- $\widetilde{n}/7$ is finite, so must the integral for a scaling solution
- $\tilde{\gamma}$ diverges, so product of f's must be finite.

Can the data be trusted?

Abraao York, AK, Lu, Moore 1401.3751

$$0 = \int_{\tilde{p}} \left(\underbrace{\left[\frac{4}{7}\tilde{f} + \frac{\tilde{p}}{7}\frac{d\tilde{f}}{d\tilde{p}} \right]}_{\tilde{n}/7} - \tilde{C}_{1\leftrightarrow 2} - \underbrace{\tilde{C}_{2\leftrightarrow 2}}_{0} \right)$$

The contribution from inelastic scattering

$$\int_{\tilde{p}} \tilde{C}_{1\leftrightarrow 2} = 4\pi \int_{\tilde{p}>\tilde{k}} d\tilde{p} d\tilde{k}\, \tilde{\gamma}(\tilde{p}+\tilde{k};\tilde{p},\tilde{k}) \tilde{f}_{\tilde{p}+\tilde{k}} \tilde{f}_{\tilde{p}} \tilde{f}_{\tilde{k}} \left(\tilde{f}^{-1}_{\tilde{p}+\tilde{k}} - \tilde{f}^{-1}_{\tilde{p}} - \tilde{f}^{-1}_{\tilde{p}} \right)$$

with $\gamma \propto \frac{1}{\tilde{k}}$ at the Bethe-Heitler limit $k \ll p$

- $\widetilde{n}/7$ is finite, so must the integral for a scaling solution
- $\tilde{\gamma}$ diverges, so product of f's must be finite.
- If $f_{\tilde{k}}$ falls faster than $1/\tilde{k}$ then

$$\tilde{f}^{-1}_{\tilde{p}+\tilde{k}} - \tilde{f}^{-1}_{\tilde{k}} - \tilde{f}^{-1}_{\tilde{p}} \approx \tilde{f}^{-1}_{\tilde{p}+\tilde{k}} - \tilde{f}^{-1}_{\tilde{p}} \approx \tilde{k}\frac{d\tilde{f}^{-1}_{\tilde{p}}}{d\tilde{p}}$$

Can the data be trusted?

Abraao York, AK, Lu, Moore 1401.3751

$$0 = \int_{\tilde{p}} \left(\underbrace{\left[\frac{4}{7}\tilde{f} + \frac{\tilde{p}}{7}\frac{d\tilde{f}}{d\tilde{p}} \right]}_{\tilde{n}/7} - \tilde{C}_{1\leftrightarrow 2} - \underbrace{\tilde{C}_{2\leftrightarrow 2}}_{0} \right)$$

The contribution from inelastic scattering

$$\int_{\tilde{p}} \tilde{C}_{1\leftrightarrow 2} = 4\pi \int_{\tilde{p}>\tilde{k}} d\tilde{p} d\tilde{k}\, \tilde{\gamma}(\tilde{p}+\tilde{k};\tilde{p},\tilde{k}) \tilde{f}_{\tilde{p}+\tilde{k}} \tilde{f}_{\tilde{p}} \tilde{f}_{\tilde{k}} \left(\tilde{f}^{-1}_{\tilde{p}+\tilde{k}} - \tilde{f}^{-1}_{\tilde{p}} - \tilde{f}^{-1}_{\tilde{p}} \right)$$

with $\gamma \propto \frac{1}{\tilde{k}}$ at the Bethe-Heitler limit $k \ll p$

- $\tilde{n}/7$ is finite, so must the integral for a scaling solution
- $\tilde{\gamma}$ diverges, so product of f's must be finite.
- If $f_{\tilde{k}}$ falls faster than $1/\tilde{k}$ then

$$\tilde{f}^{-1}_{\tilde{p}+\tilde{k}} - \tilde{f}^{-1}_{\tilde{k}} - \tilde{f}^{-1}_{\tilde{p}} \approx \tilde{f}^{-1}_{\tilde{p}+\tilde{k}} - \tilde{f}^{-1}_{\tilde{p}} \approx \tilde{k}\frac{d\tilde{f}^{-1}_{\tilde{p}}}{d\tilde{p}}$$

- $\tilde{k}$-Integral is then IR divergent: $\int d\tilde{k}\, \tilde{f}_{\tilde{k}}$

Can the data be trusted?

Abraao York, AK, Lu, Moore 1401.3751

$$0 = \int_{\tilde{p}} \left(\underbrace{\left[\frac{4}{7}\tilde{f} + \frac{\tilde{p}}{7}\frac{d\tilde{f}}{d\tilde{p}} \right]}_{\tilde{n}/7} - \tilde{C}_{1\leftrightarrow 2} - \underbrace{\tilde{C}_{2\leftrightarrow 2}}_{0} \right)$$

The contribution from inelastic scattering

$$\int_{\tilde{p}} \tilde{C}_{1\leftrightarrow 2} = 4\pi \int_{\tilde{p}>\tilde{k}} d\tilde{p} d\tilde{k}\, \tilde{\gamma}(\tilde{p}+\tilde{k};\tilde{p},\tilde{k}) \tilde{f}_{\tilde{p}+\tilde{k}} \tilde{f}_{\tilde{p}} \tilde{f}_{\tilde{k}} \left(\tilde{f}^{-1}_{\tilde{p}+\tilde{k}} - \tilde{f}^{-1}_{\tilde{p}} - \tilde{f}^{-1}_{\tilde{p}} \right)$$

with $\gamma \propto \frac{1}{\tilde{k}}$ at the Bethe-Heitler limit $k \ll p$

- $\widetilde{n}/7$ is finite, so must the integral for a scaling solution
- $\tilde{\gamma}$ diverges, so product of f's must be finite.
- If $f_{\tilde{k}}$ falls faster than $1/\tilde{k}$ then

$$\tilde{f}^{-1}_{\tilde{p}+\tilde{k}} - \tilde{f}^{-1}_{\tilde{k}} - \tilde{f}^{-1}_{\tilde{p}} \approx \tilde{f}^{-1}_{\tilde{p}+\tilde{k}} - \tilde{f}^{-1}_{\tilde{p}} \approx \tilde{k}\frac{d\tilde{f}^{-1}_{\tilde{p}}}{d\tilde{p}}$$

- $\tilde{k}$-Integral is then IR divergent: $\int d\tilde{k}\, \tilde{f}_{\tilde{k}}$
- Therefore, there is no scaling solution with steeper than $1/\widetilde{k}$ IR tail.

If data can't be trusted, need better data:

Abraao York, AK, Lu, Moore 1401.3751

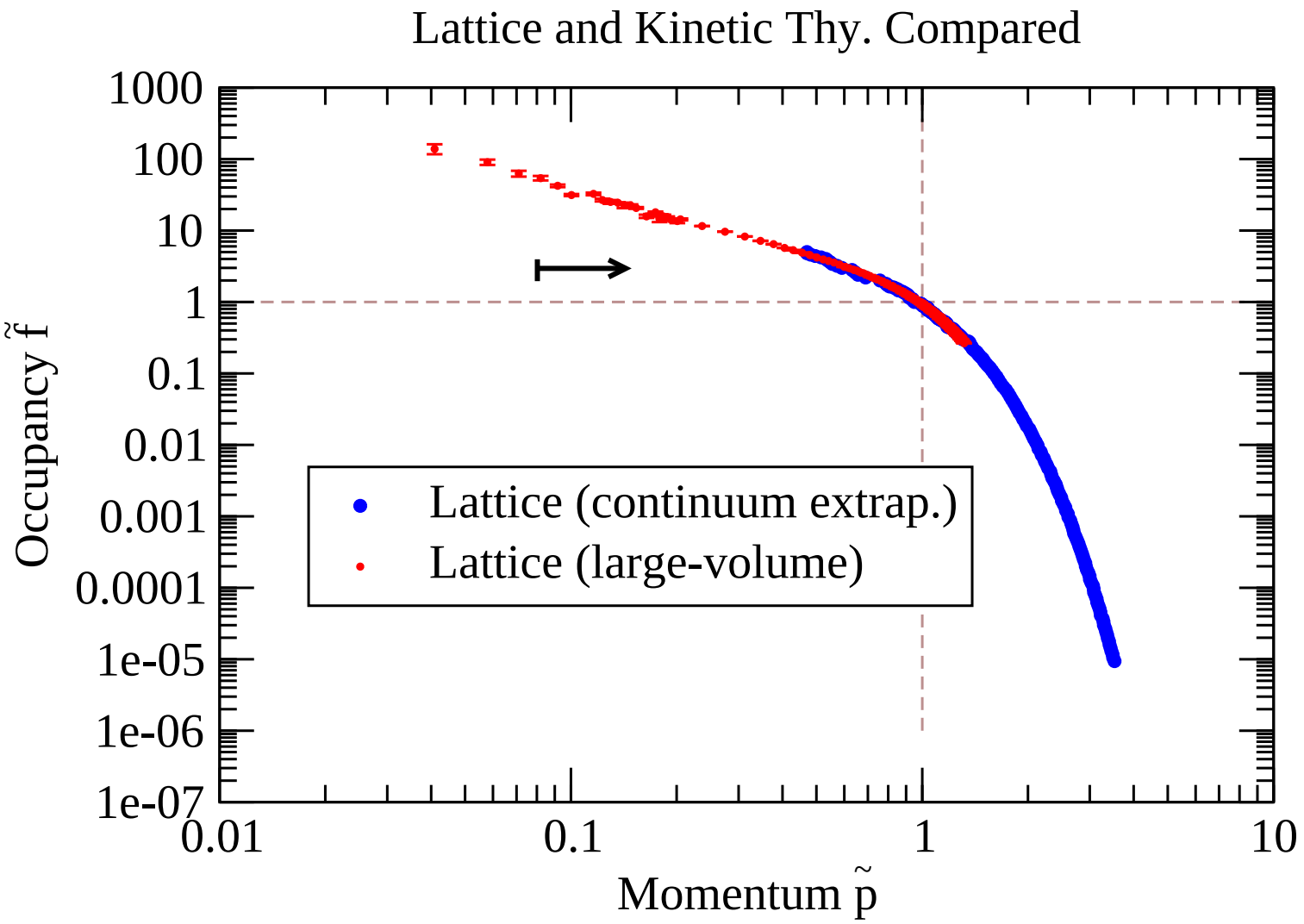

Large-volume: (Qa)=0.2, (QL)=51.2, Cont. extr.: down to (Qa)=0.1, (QL)=25.6 Qt=2000, $\tilde{m} = 0.08$

If data can't be trusted, need better data:

Abraao York, AK, Lu, Moore 1401.3751

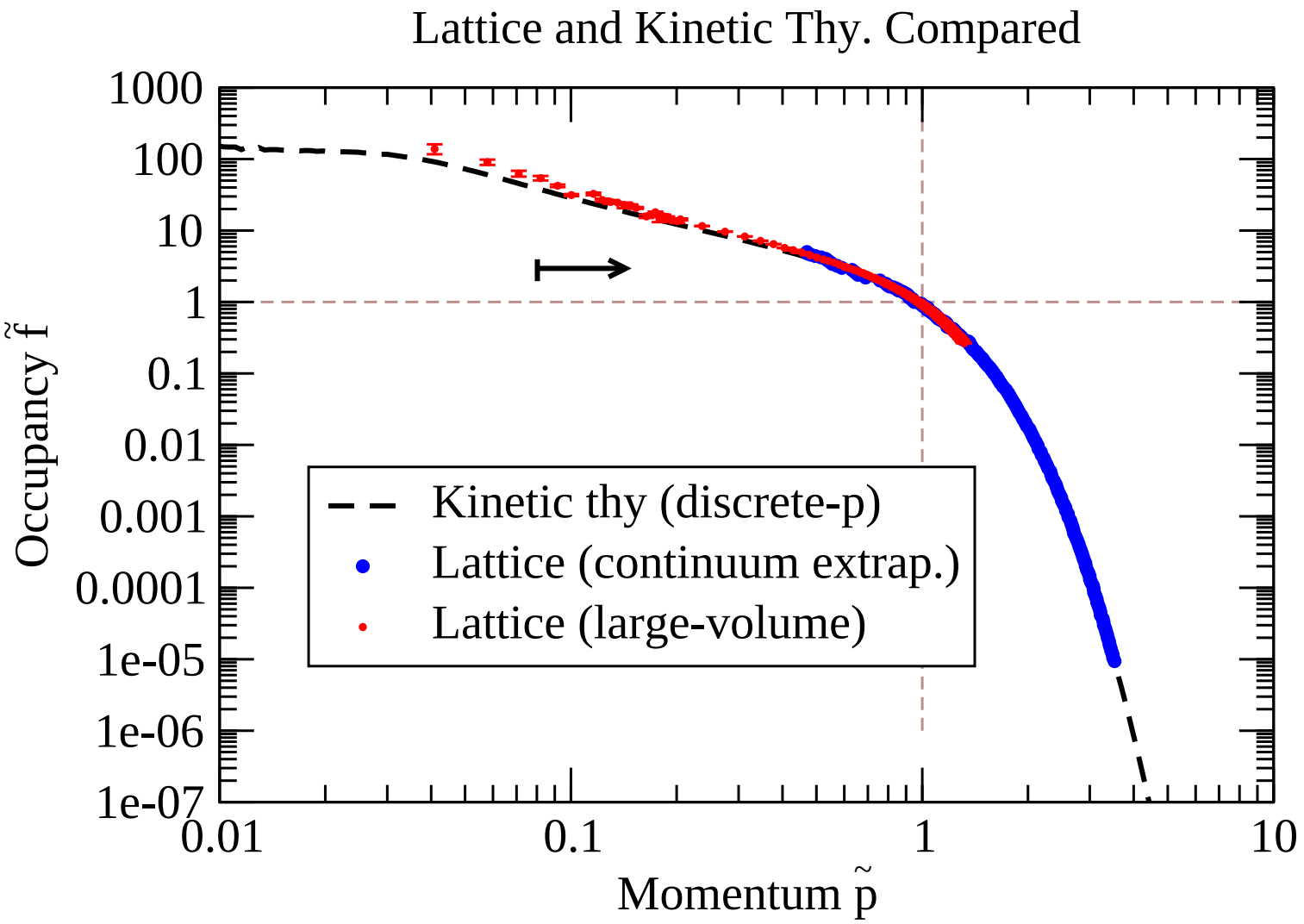

Explicit demonstration of particle-field duality!

Large-volume: (Qa)=0.2, (QL)=51.2, Cont. extr.: down to (Qa)=0.1, (QL)=25.6 Qt=2000, $\tilde{m} = 0.08$

The bump and the dip

Kinetic theory simulations $\sim$ 1000 times faster

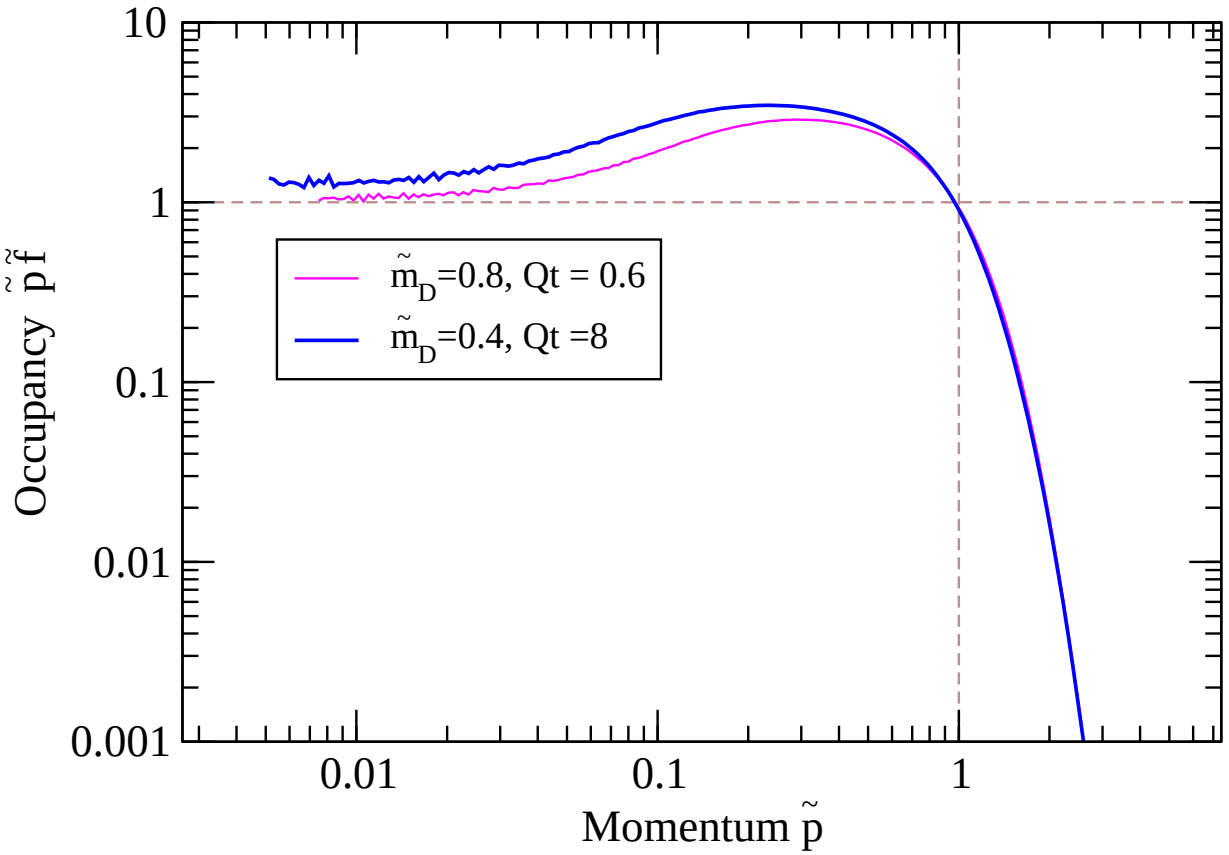

The bump and the dip

Kinetic theory simulations $\sim$ 1000 times faster

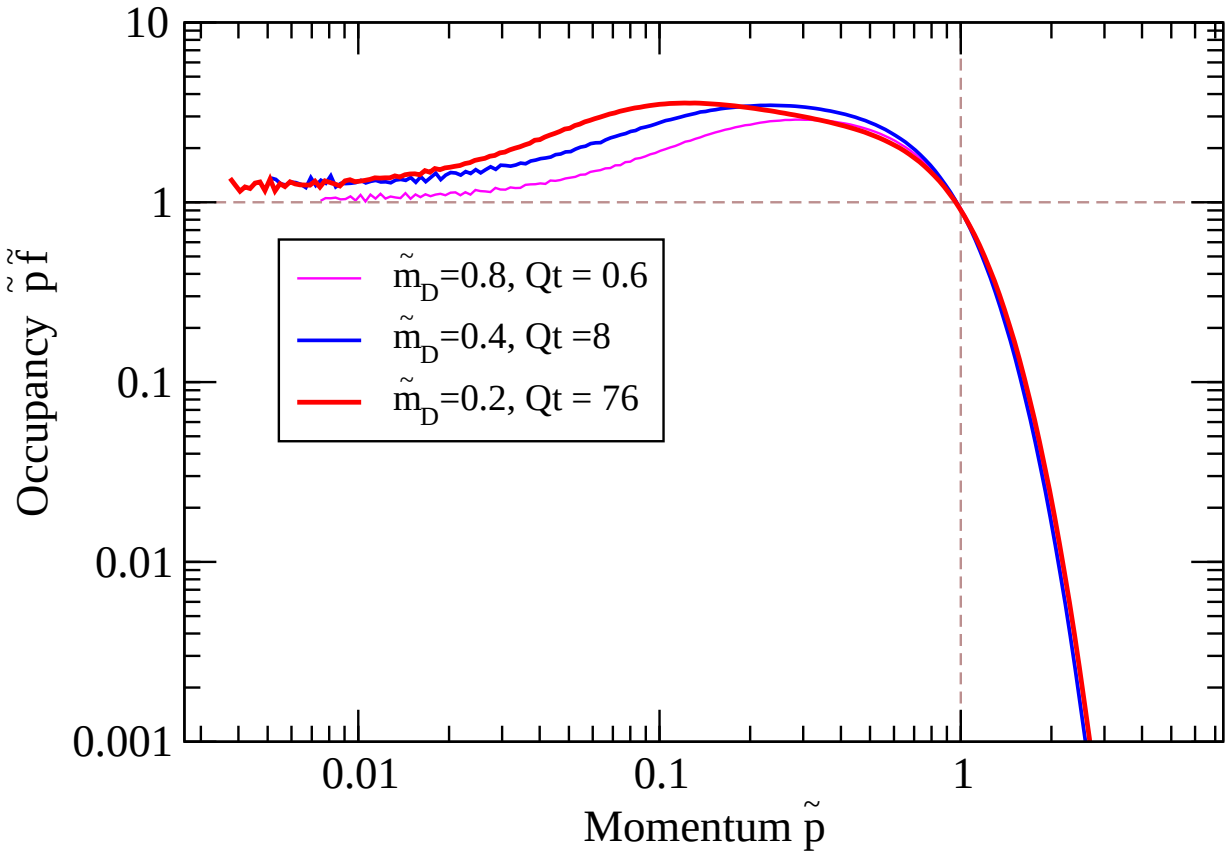

The bump and the dip

Kinetic theory simulations $\sim$ 1000 times faster

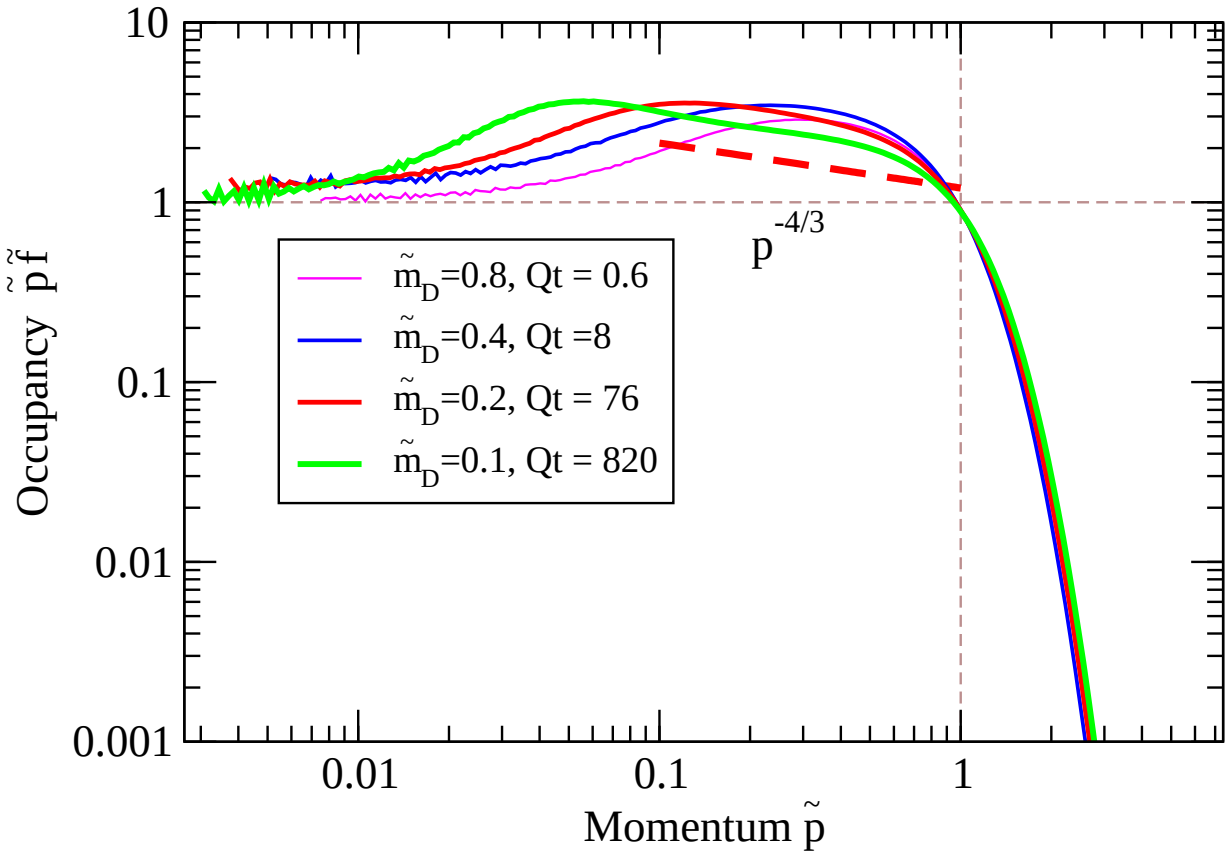

The bump and the dip

Kinetic theory simulations $\sim$ 1000 times faster

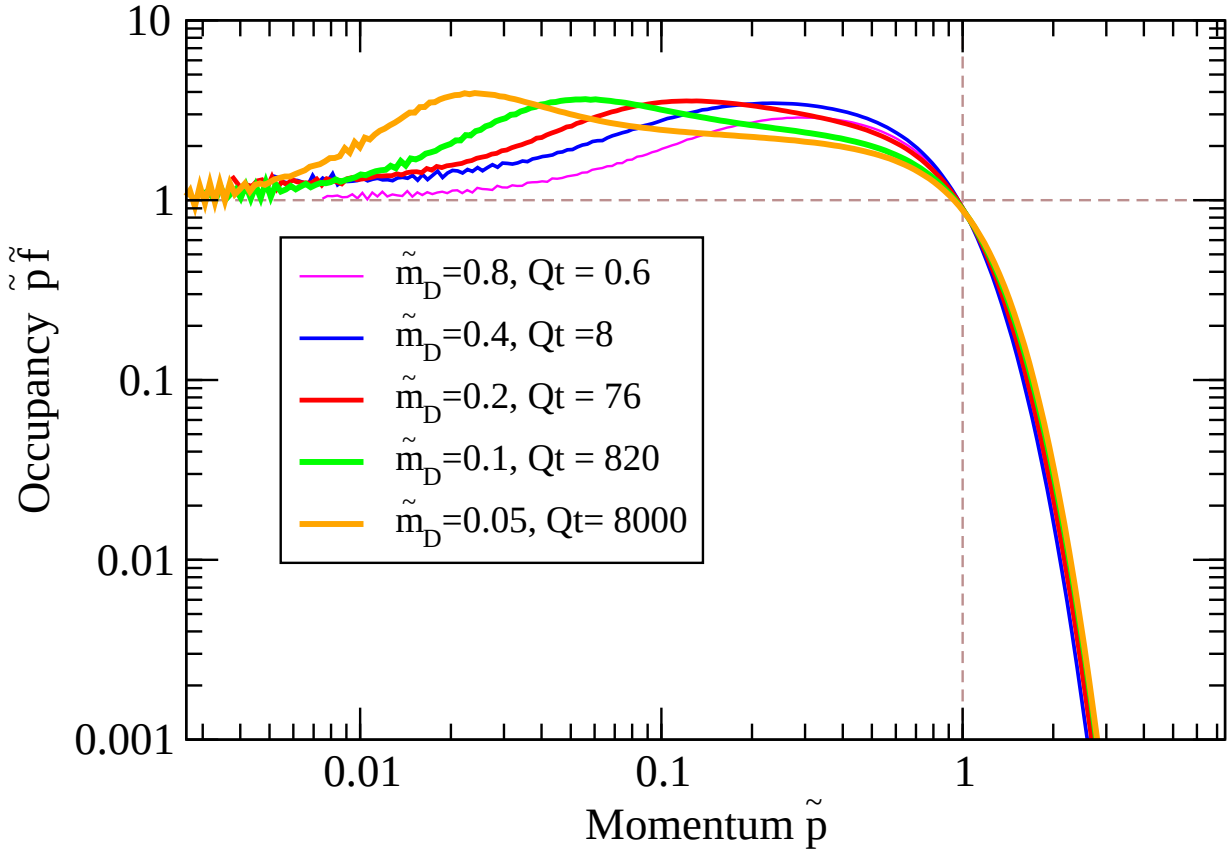

$Qt = 8000$ still feasible with lattice

The bump and the dip

Kinetic theory simulations $\sim$ 1000 times faster

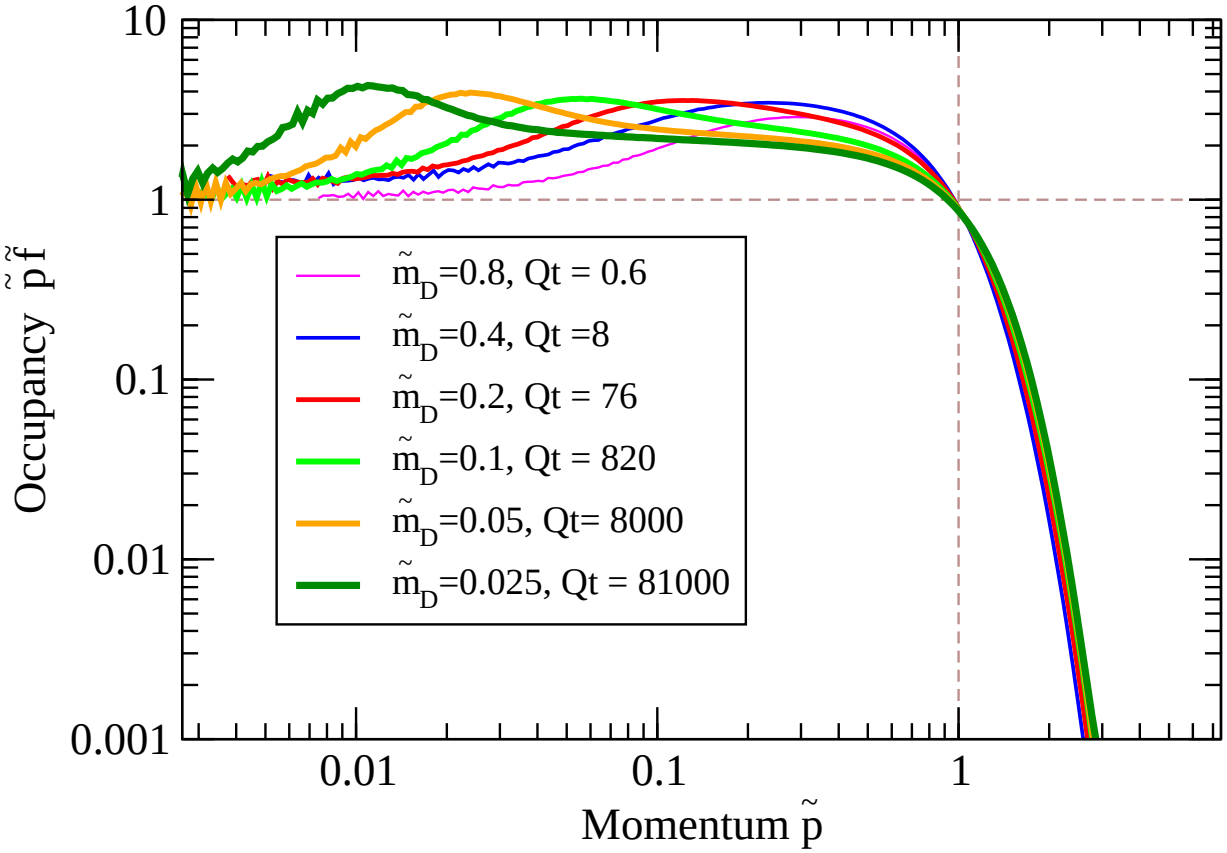

$Qt = 80000$ getting more difficult, separation of m and $p_{\max}$ starting to form

The bump and the dip

Kinetic theory simulations $\sim$ 1000 times faster

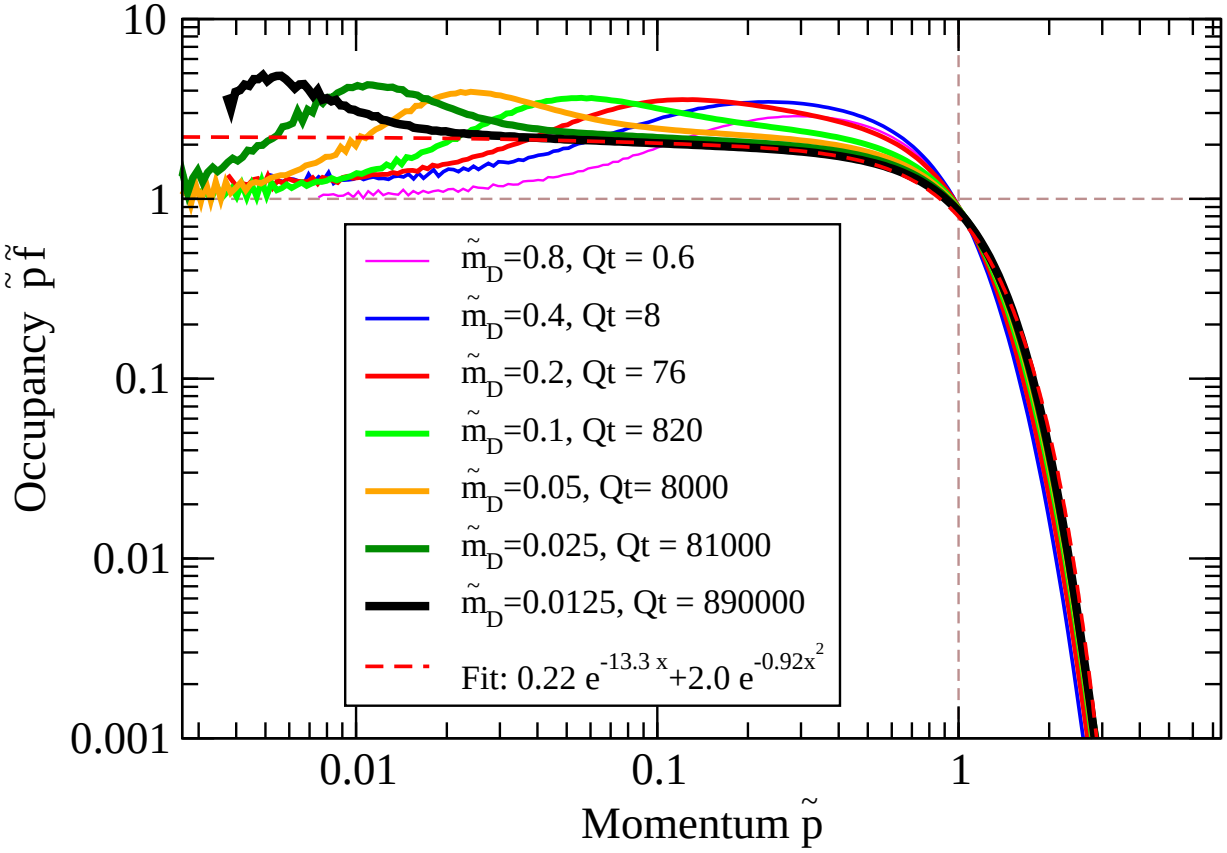

$Qt = 800000$ clear bump at m, dip at $p_{\max}$

The bump and the dip

Kinetic theory simulations $\sim$ 1000 times faster

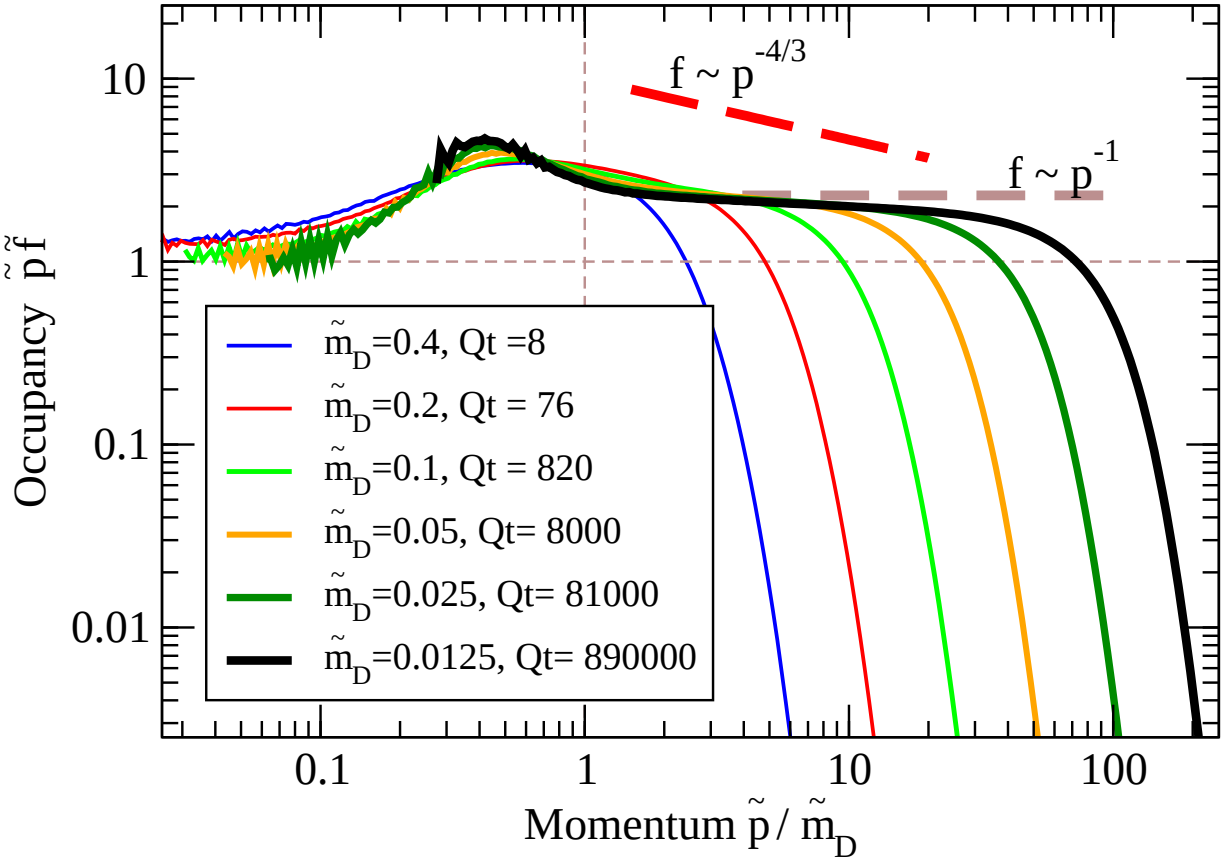

Solution to the mystery: No $p^{-4/3}$ scaling, rather large regions of special physics around m_{D} and p_{max}

Effect of elastic and inelastic scatterings:

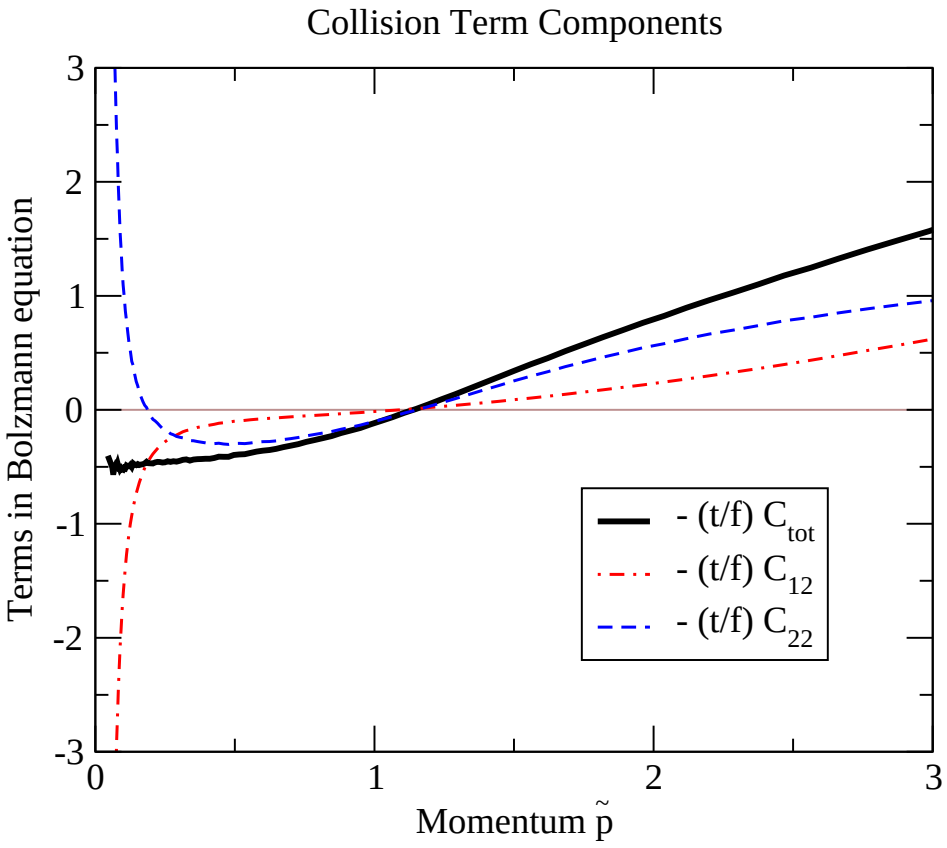

$$\frac{t}{f}\frac{df}{dt}$$

- Inelastic collisions destroy particles at IR and create at UV
- Elastic carry particle number to IR and to UV from $\tilde{p} \sim 1$

See also Liao, Hu 1303.7214, Blaizot et al. 1402.5049

Conclusions:

- Overoccupied gluons thermalize through a self-similar cascade.
- Mystery resolved, $1/p$ tail hidden by the bump and the dip.
- We have demonstrated the usefulness of the effective kinetic theory for quantitive considerations.
- The agreement of effective kinetic theory and lattice is a remarkable demonstration of particle-field duality.

Outlook:

- No need to take the overoccupied limit. Results are coming soon. Bottom-up thermalization.

And if there is still something to talk about after this workshop:

Equilibration mechanisms in Weakly
and
Strongly Coupled Quantum Field Theory

August 3, 2015 - August 28, 2015 (4 weeks)

Organizers: F. Gelis, A. Kurkela, J.C. Solana, A. Vuorinen

Dominance of scattering against hard particles:

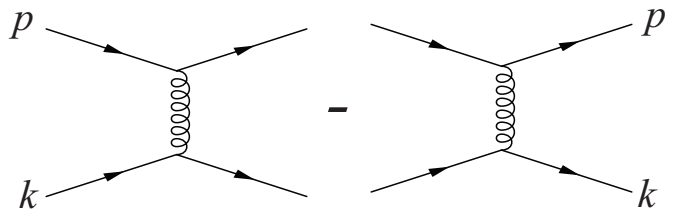

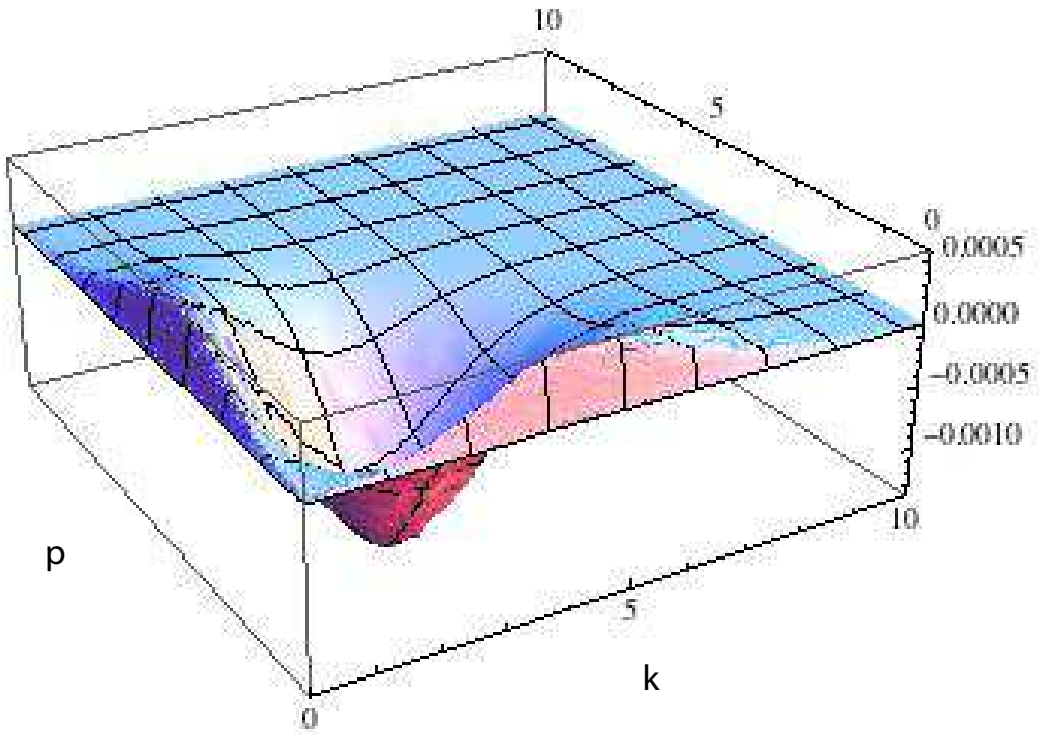

Spatial Wilson loops in the glasma

T. Lappi

University of Jyväskylä, Finland

RBRC approach to equilibrium workshop, April 2014

Outline

- CGC, Glasma, JIMWLK evolution
- JIMWLK as initial condition for CYM T.L., [arXiv:1105.5511], PLB 2011
- Wilson loop in glasma with MV or JIMWLK initial conditions
  Dumitru, T.L., Nara [arXiv:1401.4124]

Comments:

- This talk is purely 2+1d boost-invariant.
- Only $Q_s\tau \lesssim 10$
- Starting point for isotropization

Gluon saturation, Glass and Glasma

Small x: the hadron/nucleus wavefunction is characterized by **saturation scale** $Q_s \gg \Lambda_{QCD}$.

Gluon saturation, Glass and Glasma

Small x: the hadron/nucleus wavefunction is characterized by **saturation scale** $Q_s \gg \Lambda_{QCD}$.

$$\Downarrow$$

$\mathbf{p} \sim Q_s$: strong fields $A_\mu \sim 1/g$

- occupation numbers $\sim 1/\alpha_s$
- classical field approximation.
- small α_s, but nonperturbative

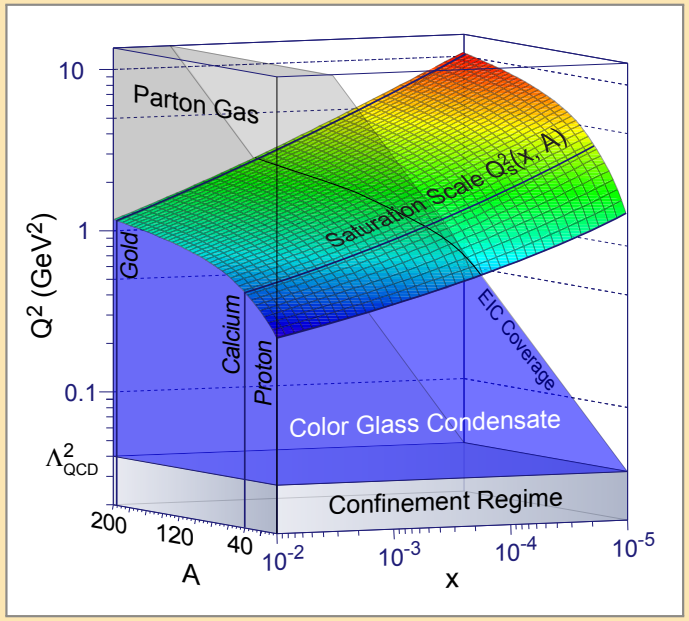

Gluon saturation, Glass and Glasma

Small x: the hadron/nucleus wavefunction is characterized by **saturation scale** $Q_s \gg \Lambda_{QCD}$.

$$\Downarrow$$

$\mathbf{p} \sim Q_s$: strong fields $A_\mu \sim 1/g$

- occupation numbers $\sim 1/\alpha_s$
- classical field approximation.
- small α_s, but nonperturbative

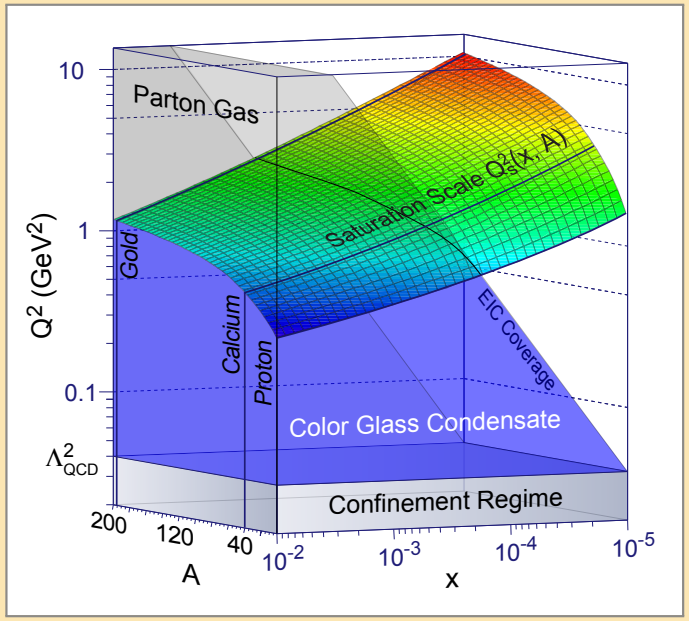

CGC: Effective theory for wavefunction of nucleus

- Large x = source ρ, **probability** distribution $W_y[\rho]$
- Small x = classical gluon field A_μ + quantum flucts.

Gluon saturation, Glass and Glasma

Small x: the hadron/nucleus wavefunction is characterized by **saturation scale** $Q_s \gg \Lambda_{QCD}$.

$$\Downarrow$$

$\mathbf{p} \sim Q_s$: strong fields $A_\mu \sim 1/g$

- occupation numbers $\sim 1/\alpha_s$
- classical field approximation.
- small α_s, but nonperturbative

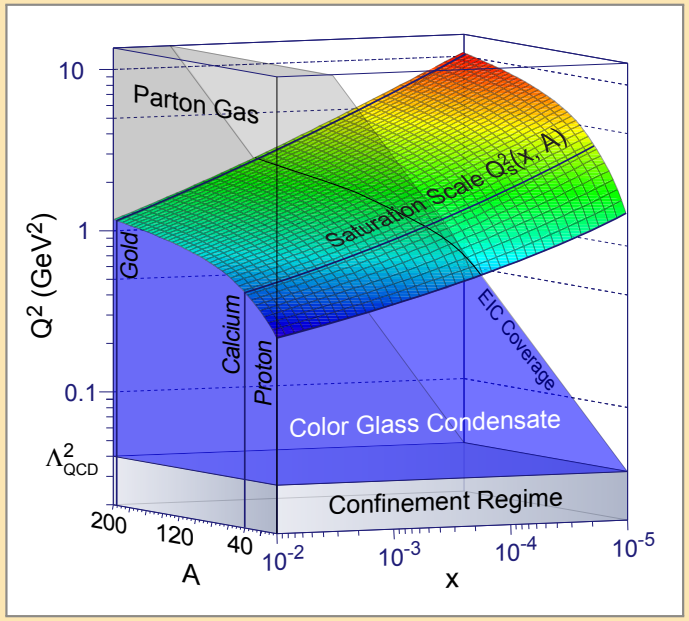

CGC: Effective theory for wavefunction of nucleus

- Large x = source ρ, **probability** distribution $W_y[\rho]$
- Small x = classical gluon field A_μ + quantum flucts.

Glasma: field configuration of two colliding sheets of CGC.
JIMWLK: y-dependence of $W_y[\rho]$; Langevin implementation

Wilson line

Classical color field described as Wilson line

$$U(\mathbf{x}) = P \exp\left\{ ig \int \mathrm{d}x^- A^+_{\mathrm{cov}}(\mathbf{x}, x^-) \right\} \quad \in \quad \mathrm{SU}(3)$$

Color charge ρ : $\quad \nabla^2 A^+_{\mathrm{cov}}(\mathbf{x}, x^-) = -g\rho(\mathbf{x}, x^-)$

($x^\pm = \frac{1}{\sqrt{2}}(t \pm z)$; $A^\pm = \frac{1}{\sqrt{2}}(A^0 \pm A^z)$; $\mathbf{x}$ 2d transverse)

Q_s is characteristic momentum/distance scale

Precise definition here is:

$$\frac{1}{N_c} \left\langle \mathrm{Tr}\, U^\dagger(\mathbf{0}) U(\mathbf{x}) \right\rangle = e^{-\frac{1}{2}}$$

$$\Longleftrightarrow \mathbf{x}^2 = \frac{2}{Q_s^2}$$

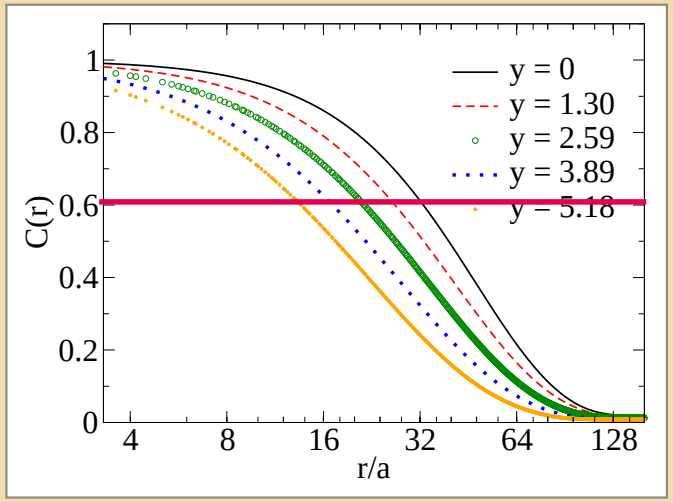

Gluon fields in AA collision

Classical **Y**ang-**M**ills

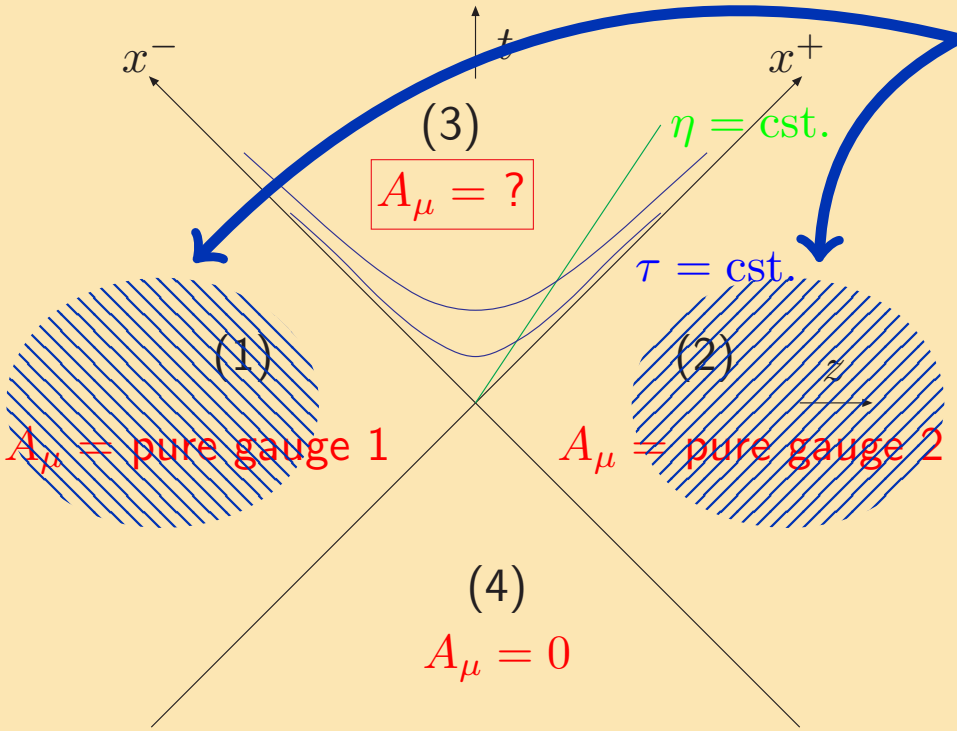

2 pure gauges

$$A^i_{(1,2)} = \frac{i}{g} U_{(1,2)}(\mathbf{x}) \partial_i U^\dagger_{(1,2)}(\mathbf{x})$$

$$U_{(1,2)}(\mathbf{x}) = P e^{ig \int \mathrm{d}x^- \frac{\rho(\mathbf{x}, x^-)}{\nabla^2}}$$

Gluon fields in AA collision

Classical **Y**ang-**M**ills

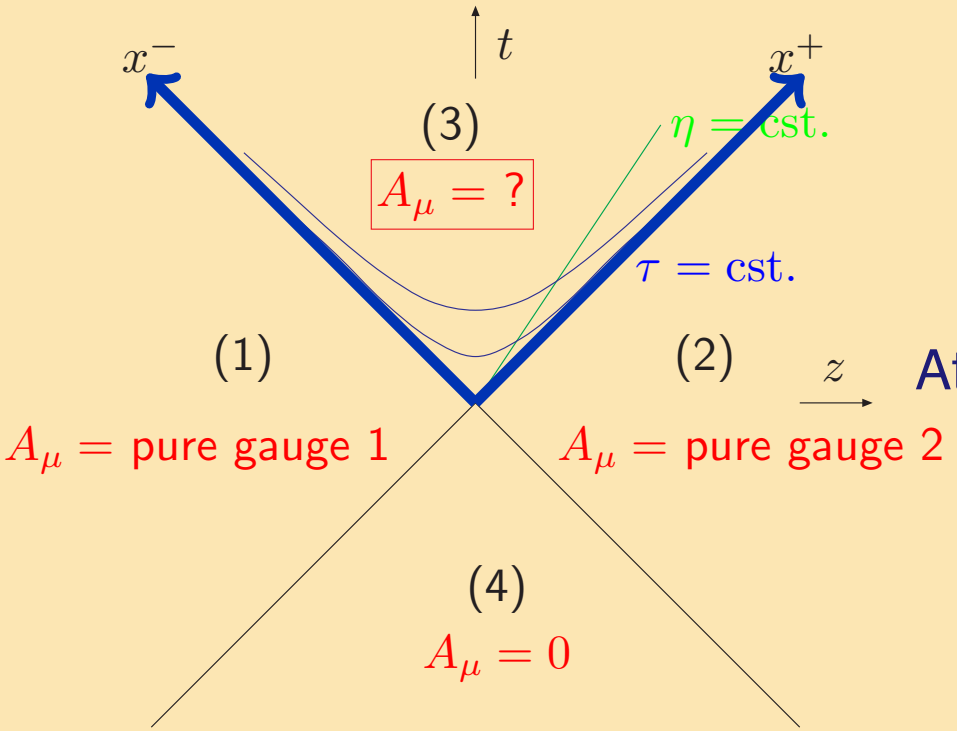

2 pure gauges

$$A^i_{(1,2)} = \frac{i}{g} U_{(1,2)}(\mathbf{x}) \partial_i U^\dagger_{(1,2)}(\mathbf{x})$$

$$U_{(1,2)}(\mathbf{x}) = P e^{ig \int \mathrm{d}x^- \frac{\rho(\mathbf{x}, x^-)}{\nabla^2}}$$

At $\boldsymbol{\tau = 0}$:

$$A^i\Big|_{\tau=0} = A^i_{(1)} + A^i_{(2)}$$

$$A^\eta\big|_{\tau=0} = \frac{ig}{2}[A^i_{(1)}, A^i_{(2)}]$$

Gluon fields in AA collision

Classical **Y**ang-**M**ills

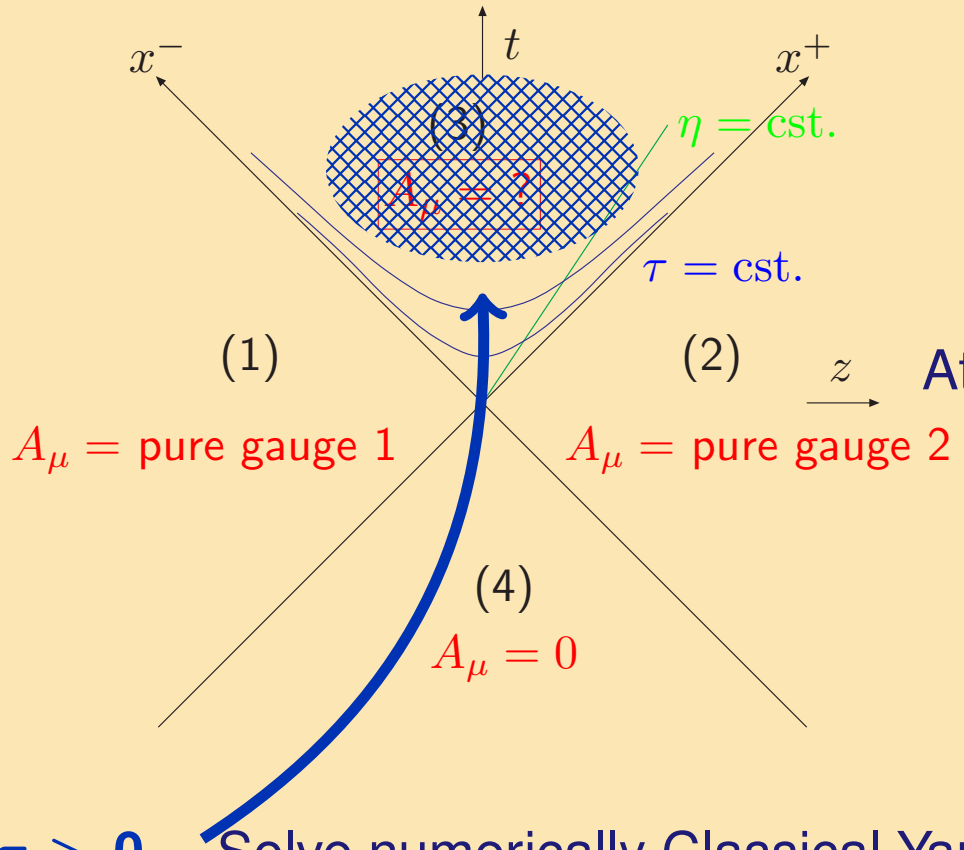

2 pure gauges

$$A^i_{(1,2)} = \frac{i}{g} U_{(1,2)}(\mathbf{x}) \partial_i U^\dagger_{(1,2)}(\mathbf{x})$$

$$U_{(1,2)}(\mathbf{x}) = P e^{ig \int \mathrm{d}x^- \frac{\rho(\mathbf{x}, x^-)}{\nabla^2}}$$

At $\tau = 0$:

$$A^i\Big|_{\tau=0} = A^i_{(1)} + A^i_{(2)}$$

$$A^\eta\big|_{\tau=0} = \frac{ig}{2}[A^i_{(1)}, A^i_{(2)}]$$

$\tau > 0$ Solve numerically Classical Yang-Mills **CYM** equations.
This is the **glasma** field $\Longrightarrow$ Then average over initial Wilson lines.

Gluons with $p \sim Q_s$ — strings of size $R \sim 1/Q_s$

Gluon spectrum in the glasma

T.L., *Phys.Lett.* **B703** (2011) 325

Q_s is only dominant scale

Parametrically gluon spectrum $$\frac{\mathrm{d}N_g}{\mathrm{d}y\,\mathrm{d}^2\mathbf{x}\,\mathrm{d}^2\mathbf{p}} = \frac{1}{\alpha_s} f\left(\frac{p}{Q_s}\right)$$

Gluon spectrum in the glasma

T.L., *Phys.Lett.* **B703** (2011) 325

Q_s is only dominant scale

Parametrically gluon spectrum $$\frac{dN_g}{dy\, d^2\mathbf{x}\, d^2\mathbf{p}} = \frac{1}{\alpha_s} f\left(\frac{p}{Q_s}\right)$$

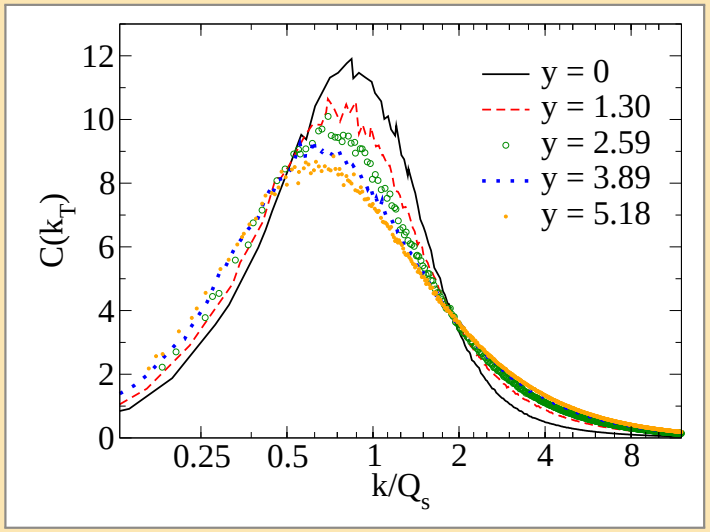

Unintegrated gluon distribution

$$C(\mathbf{k}) = \frac{k^2}{N_c} \mathrm{Tr}\, \langle U(\mathbf{k}) U^\dagger(\mathbf{k}) \rangle$$

becomes **harder** with evolution.

Gluon spectrum in the glasma

T.L., *Phys.Lett.* **B703** (2011) 325

Q_s is only dominant scale

Parametrically gluon spectrum $$\frac{dN_g}{dy\, d^2\mathbf{x}\, d^2\mathbf{p}} = \frac{1}{\alpha_s} f\left(\frac{p}{Q_s}\right)$$

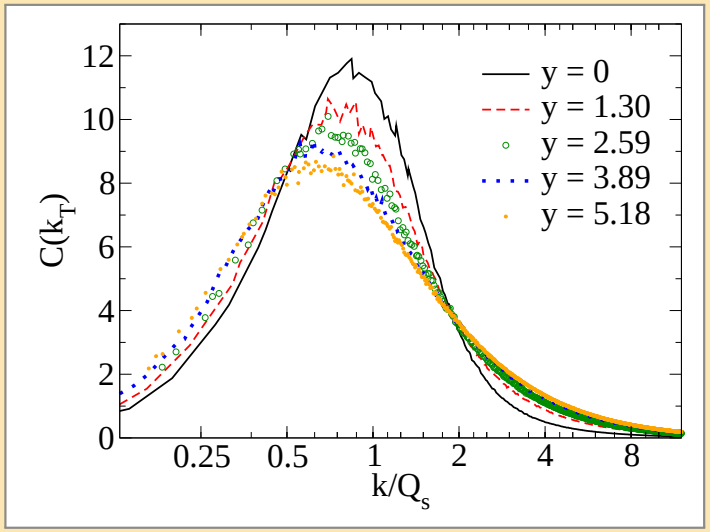

Unintegrated gluon distribution

$$C(\mathbf{k}) = \frac{k^2}{N_c} \mathrm{Tr}\,\langle U(\mathbf{k}) U^\dagger(\mathbf{k})\rangle$$

becomes **harder** with evolution.

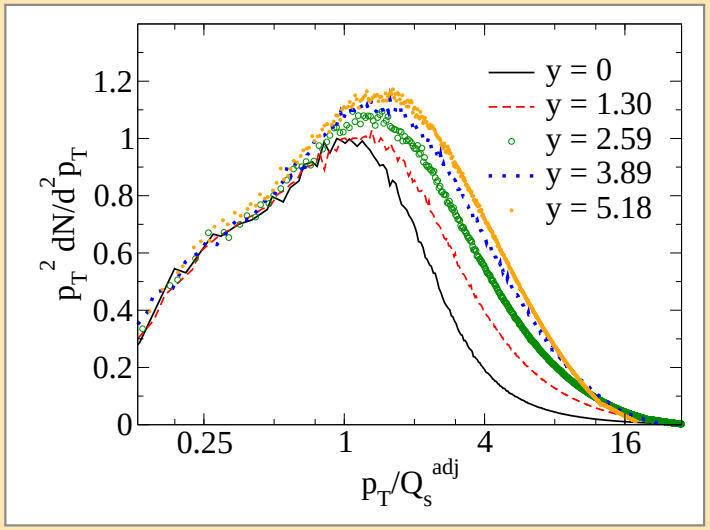

Produced gluon spectrum: harder at higher $\sqrt{s}$

(Here: midrapidity, $y \equiv \ln\sqrt{s/s_0}$)

Gluon multiplicity and mean p_T

Q_s is only dominant scale

Parametrically $$\frac{\mathrm{d}N_g}{\mathrm{d}y\,\mathrm{d}^2\mathbf{x}} = c_N \frac{C_F}{2\pi^2\alpha_s} Q_s^2 \qquad \langle p \rangle \sim Q_s$$

Note: in full CYM total gluon multiplicity is IR finite, no cutoff.

Gluon multiplicity and mean p_T

Q_s is only dominant scale

Parametrically $$\frac{dN_g}{dy\, d^2\mathbf{x}} = c_N \frac{C_F}{2\pi^2 \alpha_s} Q_s^2 \qquad \langle p \rangle \sim Q_s$$

Note: in full CYM total gluon multiplicity is IR finite, no cutoff.

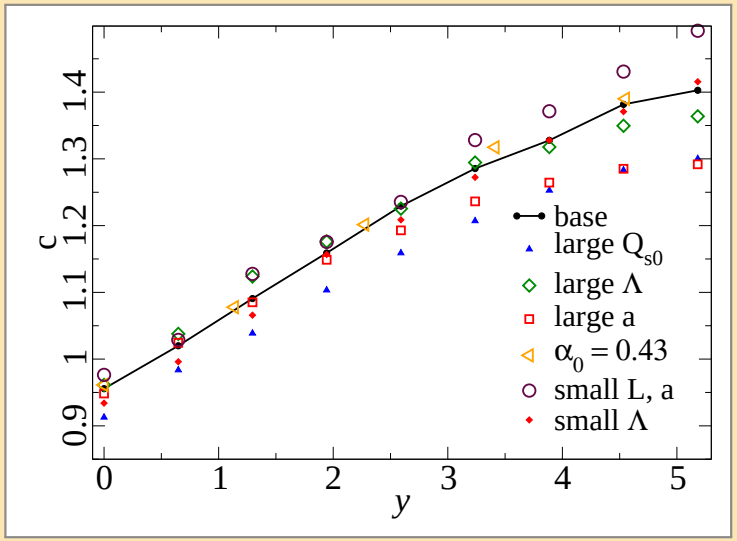

Scaled multiplicity increases with energy (Midrapidity, $y \equiv \ln \sqrt{s/s_0}$)

Gluon multiplicity and mean p_T

Q_s is only dominant scale

Parametrically $$\frac{\mathrm{d}N_g}{\mathrm{d}y\,\mathrm{d}^2\mathbf{x}} = c_N \frac{C_F}{2\pi^2\alpha_s} Q_s^2 \qquad \langle p \rangle \sim Q_s$$

Note: in full CYM total gluon multiplicity is IR finite, no cutoff.

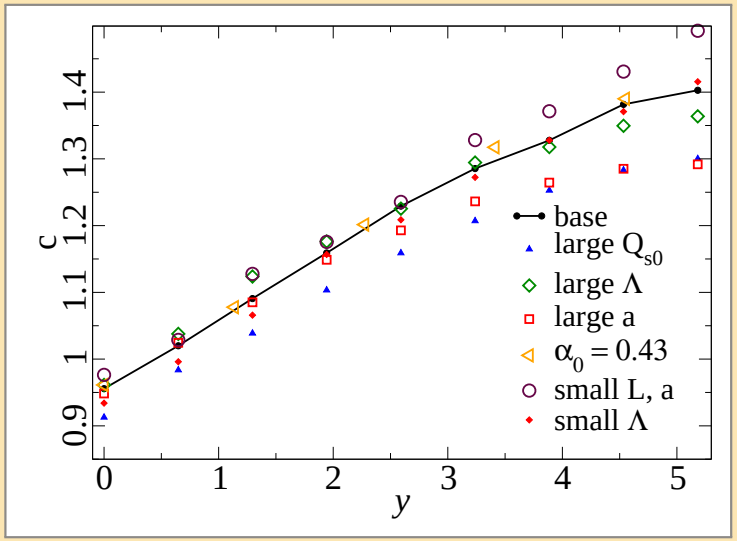

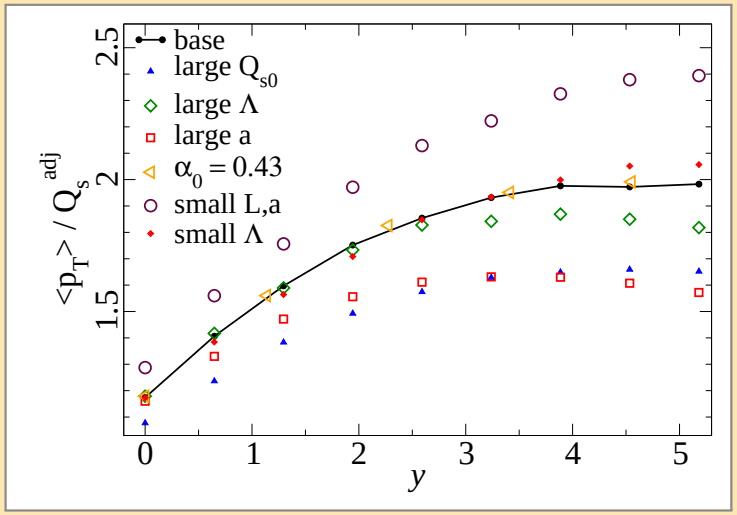

Scaled multiplicity increases with energy (Midrapidity, $y \equiv \ln\sqrt{s/s_0}$)

Harder gluon spectrum $\Longrightarrow$ higher $\langle p \rangle / Q_s$ as scaling regime sets in.

(Still very large lattice cutoff effects.)

Side note: CYM vs. k_T-factorization

Blaizot, T.L., Mehtar-Tani 2010 Compare to perturbative spectrum

$$\frac{dN}{d^2\mathbf{p}\,dy} = \frac{\#}{\alpha_s}\frac{1}{\mathbf{p}^2}\int_{\mathbf{k}}\Big[\theta(p-k)\Big]\phi_y(\mathbf{k})\phi_y(\mathbf{p}-\mathbf{k})$$

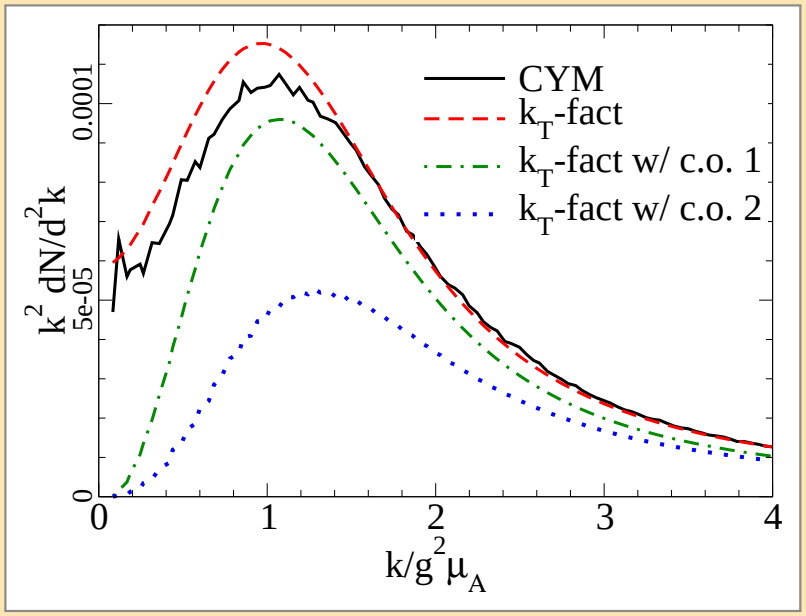

pA: k_T-factorization works

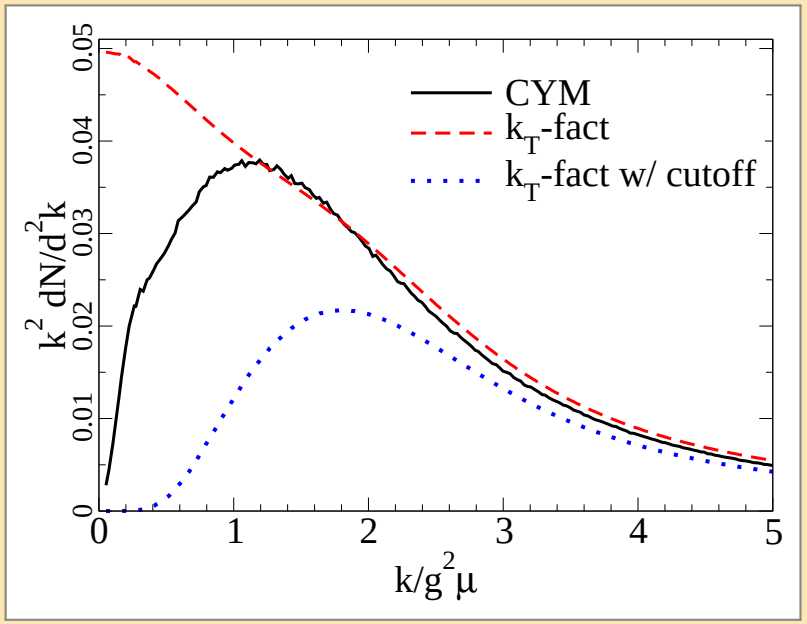

AA: only for hard modes

k_T-factorization works only for $p_T \gtrsim Q_s$

- OK for high-p_T spectra: freely streaming gluons
- Modes with $p_T \lesssim Q_s$: still dominated by nonlinear interactions

Universality in the IR spectrum?

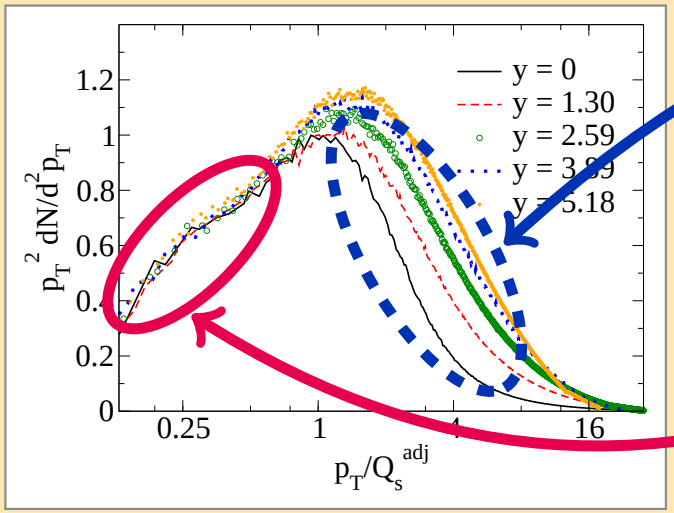

- Gluon spectrum in the UV depends on anomalous dimension $\Longrightarrow$ different for MV $(y = 0)$, JIMWLK $(y > 0)$
- IR seems to scale, close to

$$\frac{dN}{d^2\mathbf{p}} \sim \frac{1}{p_T}$$

Gauge inv. probe for $p \lesssim Q_s$?

Spatial Wilson loop

$$W(A) = \frac{1}{N_c} \mathrm{Tr}\, \mathbb{P} \exp\left\{ ig \oint_A d\mathbf{x} \cdot \mathbf{A} \right\}$$

2d lattice: transverse links:

$$\uparrow = U_i(\mathbf{x}) = \exp\{igaA_i\}$$

$$W(A) = \frac{1}{N_c} \mathrm{Tr}$$

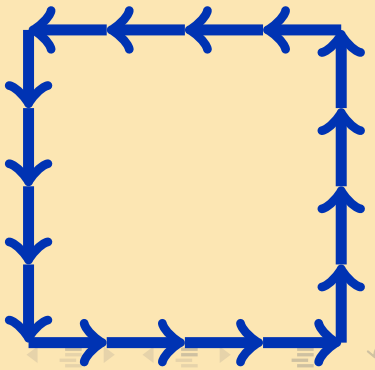

Measure Wilson loops

Dumitru, Nara, Petreska [arXiv:1302.2064], PRD 2013
& this work Dumitru, T.L., Nara [arXiv:1401.4124]

Calculation is simple:

- Construct initial glasma fields at $\tau = 0$ using e.g.
  - MV model
  - rcJIMWLK
  - fcJIMWLK

  (Try to have same $Q_s a$ to minimize lattice effects)
- Evolve forward in τ
- Measure $W(A)$

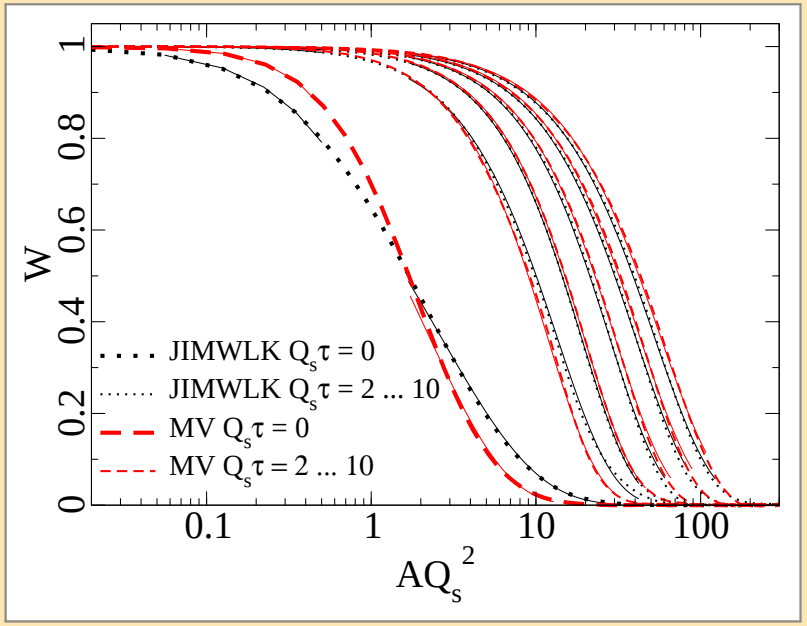

Behavior in both UV ($AQ_s^2 \lesssim 1$) and IR ($AQ_s^2 \gtrsim 1$) parametrized as

$$W = \exp\{-(\sigma A)^\gamma\}$$

Fit is quite good: solid lines in figure.

Fit to Wilson loop area dependence

$$W = \exp\{-(\sigma A)^\gamma\} \Longleftrightarrow \ln(-\ln W) = \gamma \ln(AQ_s) + \gamma \ln(\sigma/Q_s^2)$$

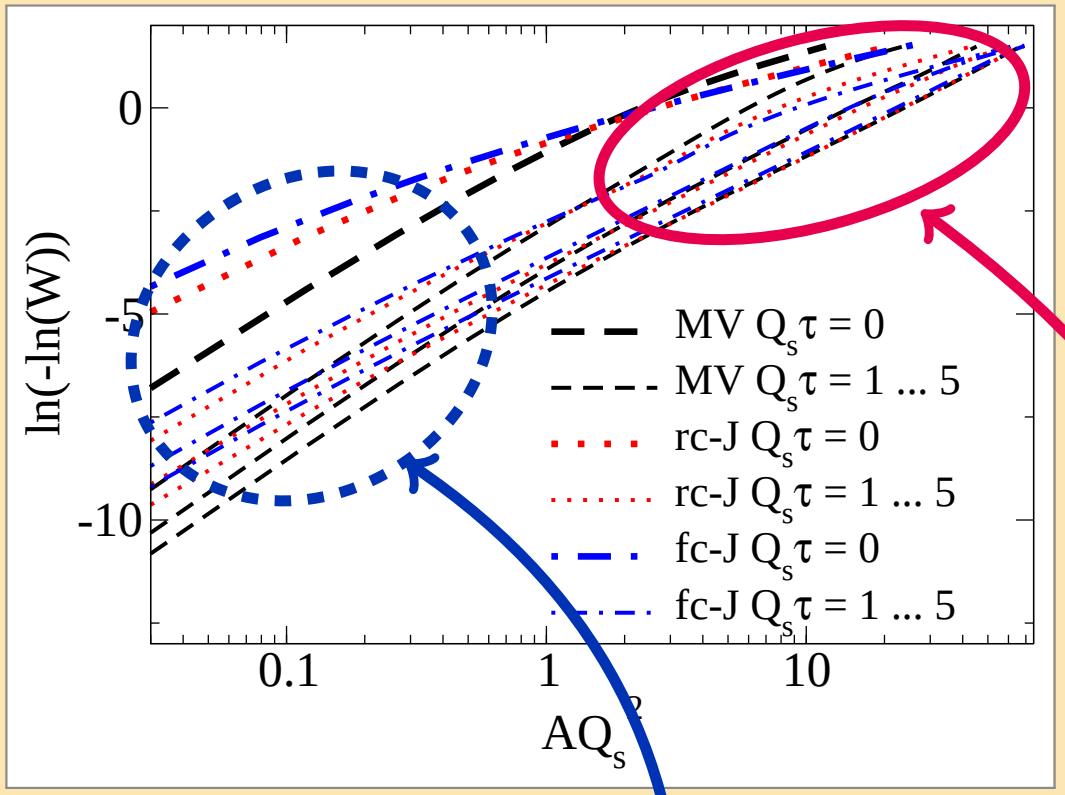

Main observations

- UV (small loop): initial slope γ stays
- IR (big loop): all init. conditions collapse to universal behavior

Wilson loop scaling exponents

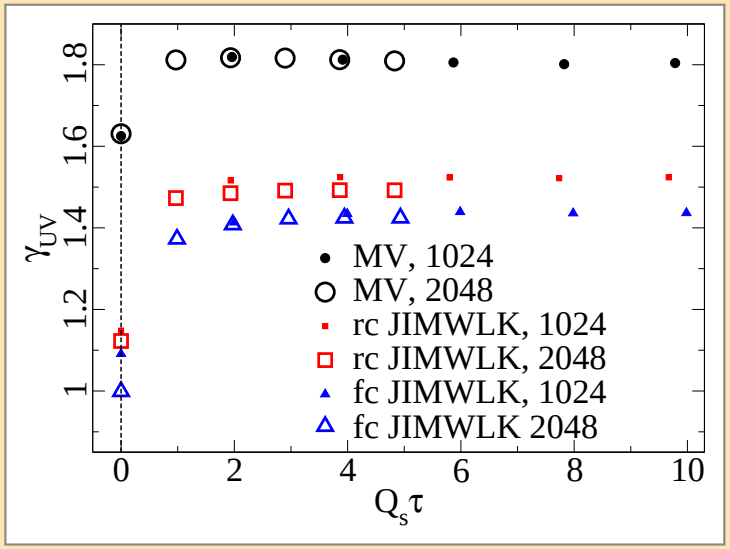

UV ($e^{-3.5} < AQ_s^2 < e^{-0.5}$)

Remembers initial condition

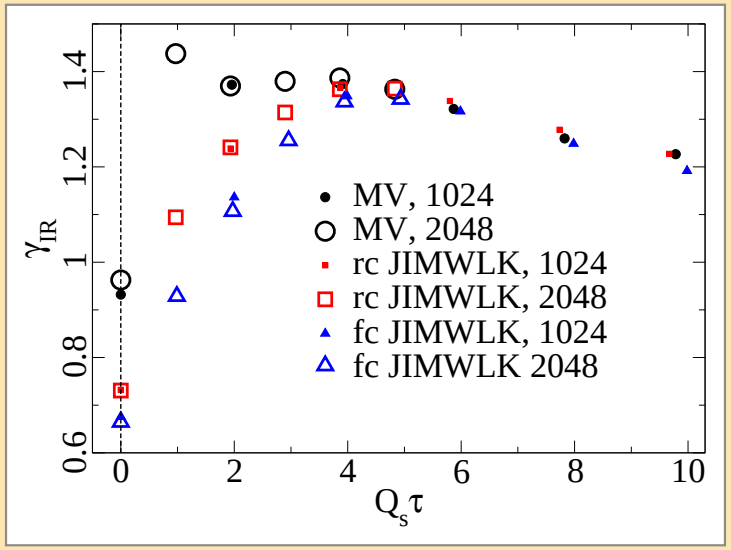

IR ($e^{0.5} < AQ_s^2 < e^{5}$)

Initial conditions collapse to

$\gamma_{IR} \approx 1.2$,

decreasing slowly with τ

“String tension” coefficients

In expanding system fields naturally decrease as

$$\tau \gg 1/Q_s \Longrightarrow A_\mu \sim 1/\sqrt{\tau} \Longrightarrow \sigma/Q_s^2 \sim 1/(Q_s\tau)$$

Plot “string tenstion” σ as scaling variable $\sigma\tau/Q_s$

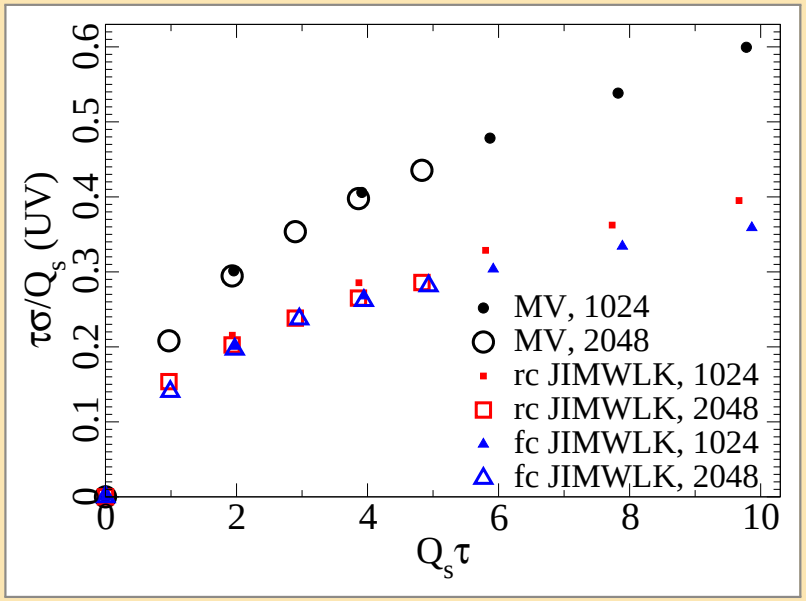

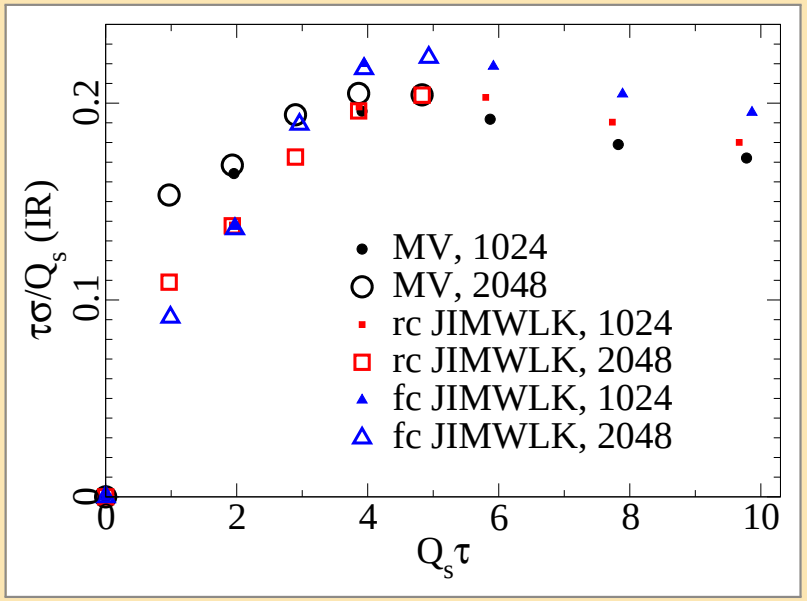

UV: initial conditions differ

IR: even σ universal within $\sim 10\%$

(Note: the numerical value of σ depends on the convention used to define Q_s)

At $\tau = 0$: $\sigma/Q_s^2 \approx 0.55 \ldots 0.6$ (UV) and $\sigma/Q_s^2 \approx 0.35 \ldots 0.45$ (IR)

Magnetic field correlator

Wilson loop measures magnetic flux:

$$W(A) = \frac{1}{N_c} \mathrm{Tr}\, \mathbb{P} \exp\left\{ ig \oint_A \mathrm{d}\mathbf{x} \cdot \mathbf{A} \right\} = \frac{1}{N_c} \mathrm{Tr}\, \exp\left\{ ig \int \mathrm{d}^2\mathbf{x} B_z(\mathbf{x}) \right\}$$

If magnetic field consists of **uncorrelated Gaussian domains**:

$$\langle W(A) \rangle = \exp\left\{ -\frac{1}{2} \frac{1}{N_c} \mathrm{Tr} \left\langle \left[\int \mathrm{d}^2\mathbf{x} g B_z(\mathbf{x}) \right]^2 \right\rangle \right\}$$

$\Longrightarrow$ $W(A)$ related to $\langle B(\mathbf{x}) B(\mathbf{y}) \rangle$

Here: no gauge fixing, connect $B(\mathbf{x})$ and $B(\mathbf{y})$ with gauge link

Check: compare

- Direct measurement of $W(A)$
- Reconstruction from BB-correlator

good agreement.

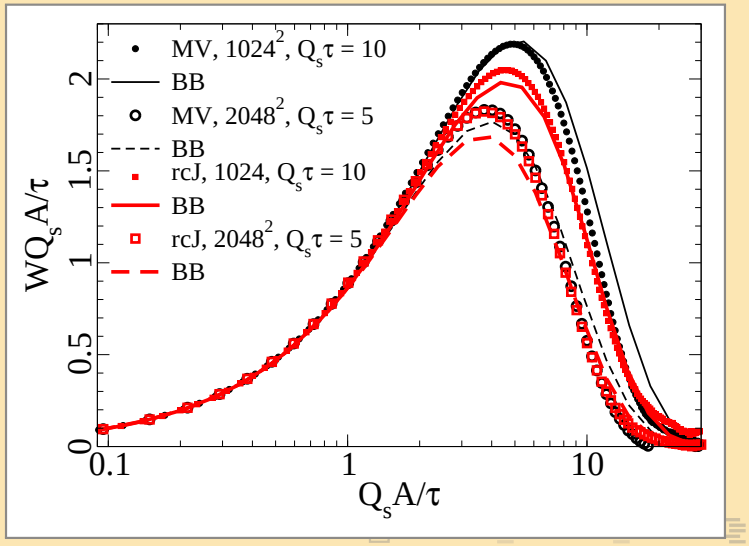

Magnetic field correlator

However: no obvious scaling seen in *BB*-correlator

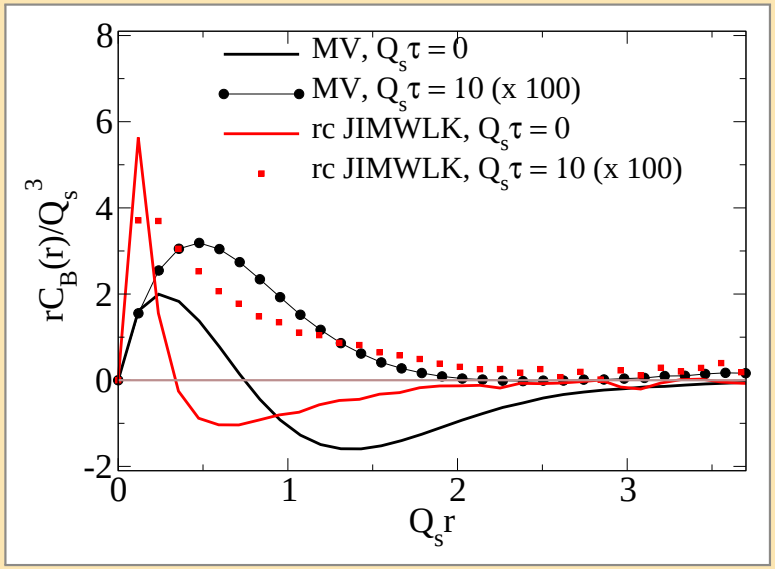

Same on log plot

$$C(|\mathbf{x}-\mathbf{y}|) \equiv \mathrm{Tr}\left\langle [B(\mathbf{x})B(\mathbf{y})]_{\text{gauge link}} \right\rangle$$

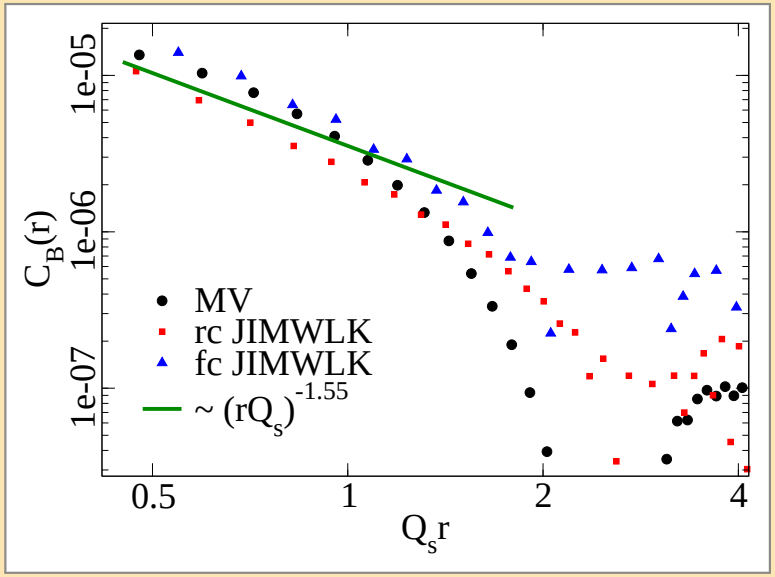

Straight line: $\sim (rQ_s)^{-1.55}$.

(For $C(r) \sim (rQ_s)^{-\alpha}$ one would get $\gamma = 2 - \alpha/2 \iff \alpha = 4 - 2\gamma$;
from $W(A)$ measured $\gamma = 1.22$)

Conclusions

- CYM initial state for AA collision
- Universal behavior in the for $p_T \ll Q_s$ seen in gluon spectrum
  - Nontrivial area dependence of the loop $W \sim \exp\{-A^{1.2}\}$
- New observation: same universality seen in spatial Wilson loop
- Note: this is still in the boost-invariant 2d theory.
  - Effect of instabilities, isotropization on the soft modes?

The Glasma and Thermalization: Ups and Downs

Glasma Initial Conditions: A Classical Field

One scale: Q_{sat}

Coupling: α_s

$$A^\mu \sim 1/g$$

$$< N > \sim < a^\dagger a > \sim 1/\alpha_s$$

Phase space density is very high:

$$\frac{dN}{d^3x d^3p} \sim 1/\alpha_s, \; p < Q_{sat}$$

$$\sim 0, \; p > Q_{sat}$$

Similar to a recently cooled Bosonic atomic gas

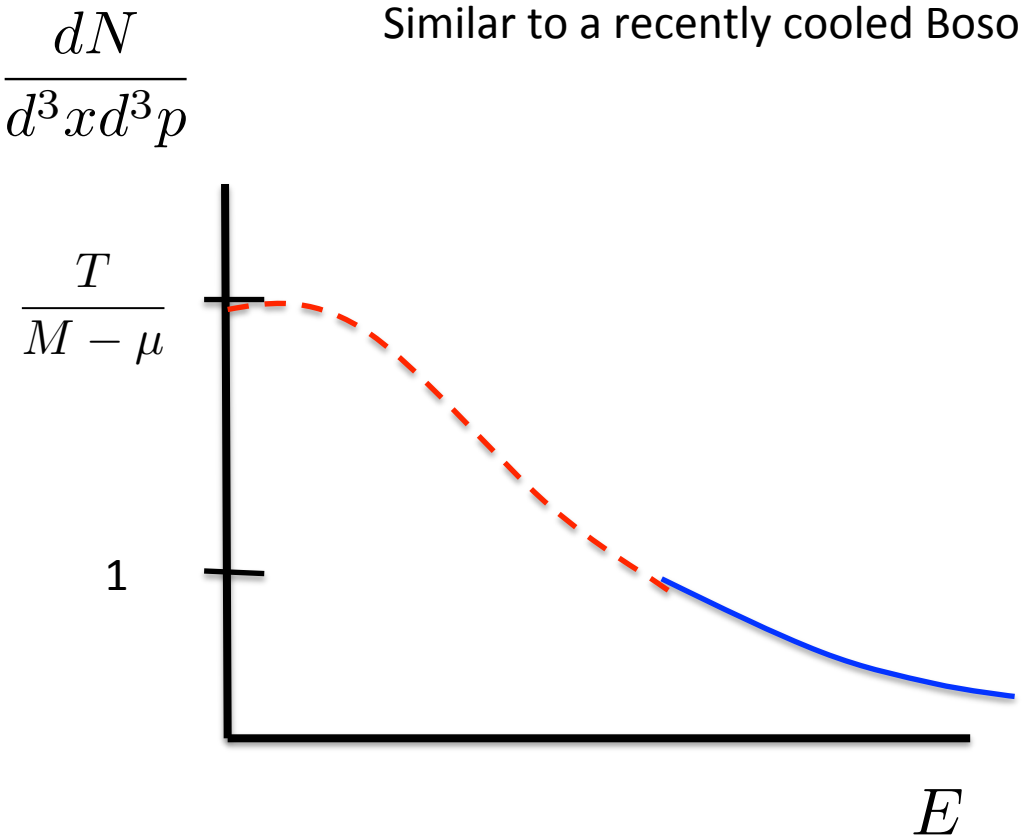

When high end of momentum distribution is blown away, system is cooled, but it is over occupied

$$\frac{dN}{d^3x d^3p} = \frac{1}{e^{(E-\mu)/T} - 1} \sim \frac{T}{E-\mu}$$

$$\mu < M$$

There is a maximum occupation for a thermalized Bosonic system

Easiest to understand for a massless system like gluons:

$$\rho \sim Q_{sat}^3/\alpha_s \qquad \epsilon \sim Q_{sat}^4/\alpha_s$$

$$\rho \sim \epsilon^{3/4}/\alpha_s^{1/4} \geq \epsilon^{3/4}$$

The Glasma is over occupied:
Perhaps particle number adjusts itself by inelastic processes
Perhaps one needs top include a condensation

$$\frac{dN}{d^3x d^3p} \sim \rho_c \; \delta^{(3)}(\vec{p})$$

How might a condensate form dynamically: The UV and IR cascades

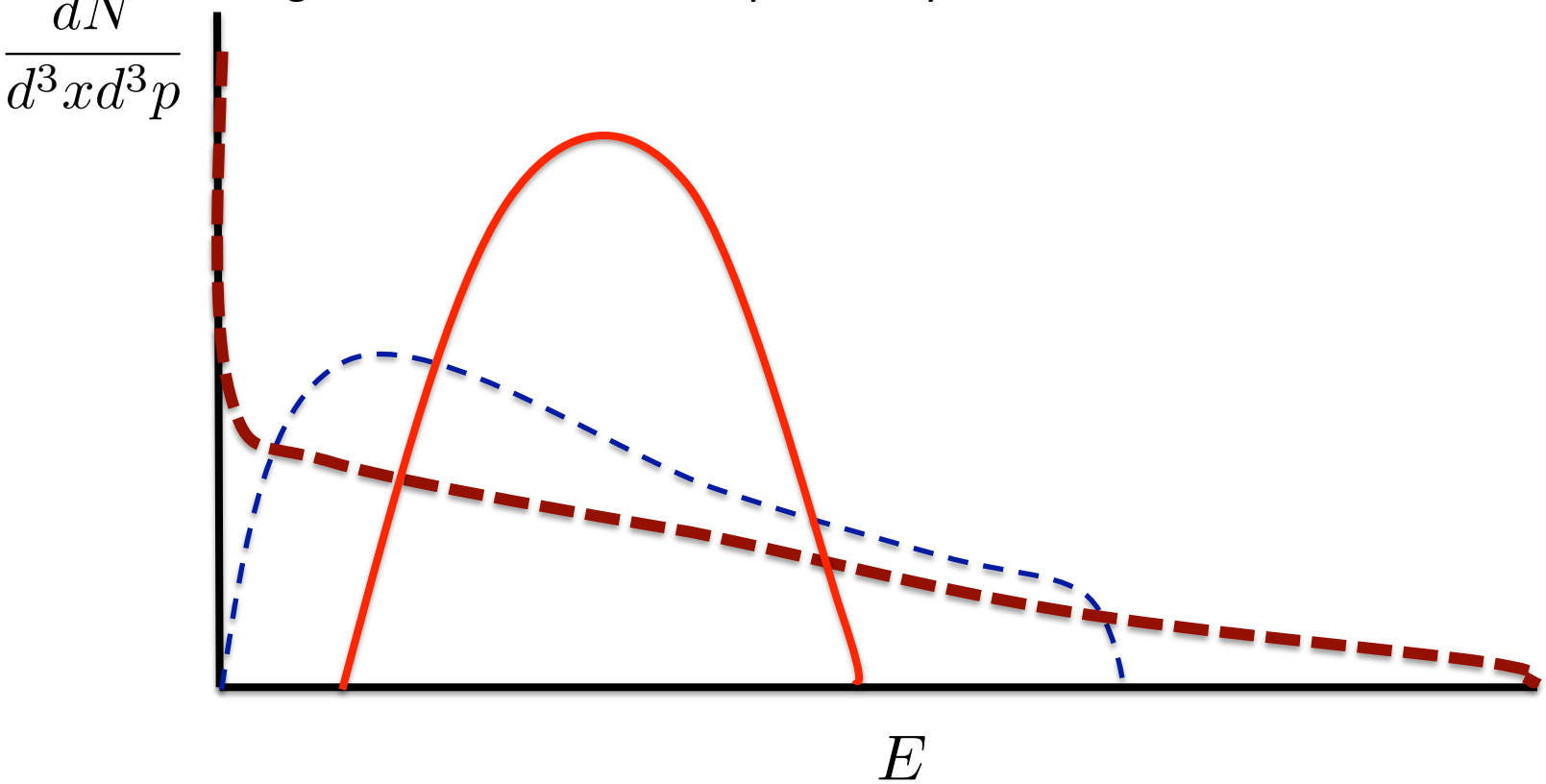

Diffusion into the UV and a Kolmogorov Spectrum

Diffusion into the infrared until a wall at p = 0

Talks by Huang, Jiang,Liao, Pawlowski, Sexty, Wu, Zhang

The Turbulent Cascade to Thermalization:

Let there be an infrared scale where the distribution has strength of order

$$1/\alpha_s$$

Let there be an ultraviolet scale where the distributions become of order 1

$$\Lambda_{IR}, \Lambda$$

Initially these scales are close together in the Glasma

For a thermalize Bosonic system, these scales must be separated by

$$\Lambda_{IR} \sim \alpha_s \Lambda$$

This separation of scales takes time and cannot be done by a few scatterings

The separation of scales occurs when the fields are multiply occupied so a classical approximation should be good

Need seed fluctuation fields of order g, that grow to order 1/g through turbulence
Typically exponential growth of seed fields: source is quantum fluctuations

A simple model for the Glasma

(LM & Schenke; Blaizot, Gelis, Liao, McLerran and Venugopalan; Kurkela, Moore)

$$n_g = \frac{\kappa \Lambda_{IR}}{\Lambda N_c \alpha_s} \frac{1}{e^{E/\Lambda} - 1} \qquad n_q = \frac{1}{e^{E/\Lambda} + 1}$$

$$n_g \sim T/E, \;\; E << \Lambda, T = \frac{\kappa \Lambda_{IR}}{N_c \alpha_s}$$

$$\Lambda(t_0) = \Lambda_{IR}(t_0) \qquad \Lambda_{IR}(t_{th}) \sim \frac{N_c \alpha_s}{\kappa} \Lambda(t_{th})$$

Energy density: $\epsilon_g \sim \frac{1}{\alpha_s} \Lambda_{IR} \Lambda^3$

Pressure
{allowing for possible momentum asymmetry): $P = \delta \epsilon$

Scattering time: $\tau \sim \tau_{scat} \sim \Lambda / \Lambda_{IR}^2$

Coupling constant disappears from estimate of scattering time

Find power law behaviour for the momentum scales

$$\Lambda_{IR} = \Lambda^0_{IR} \left(\frac{t_o}{t}\right)^{(4+\delta)/7} \qquad \Lambda = \Lambda^0 \left(\frac{t_o}{t}\right)^{(1+2\delta)/7}$$

Why a constant momentum asymmetry:

In hydrodynamics:

$$\frac{P_L}{P_T} = 1 - c\frac{\tau_{scat}}{\tau} \sim constant$$

Analysis is different if we are close to zero of the scattering kernal of the transport equation, ie close to thermalization

So what do we see by simulation:

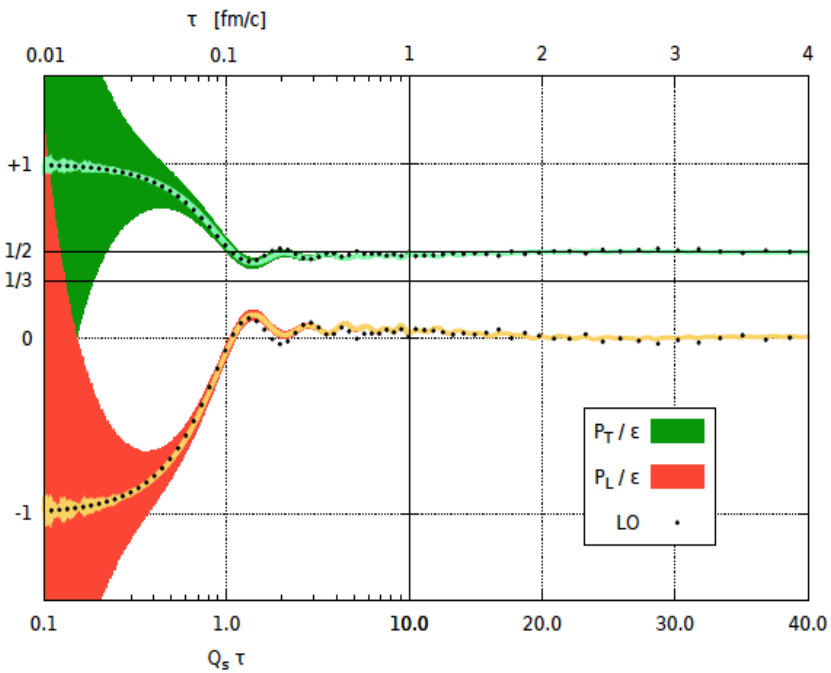

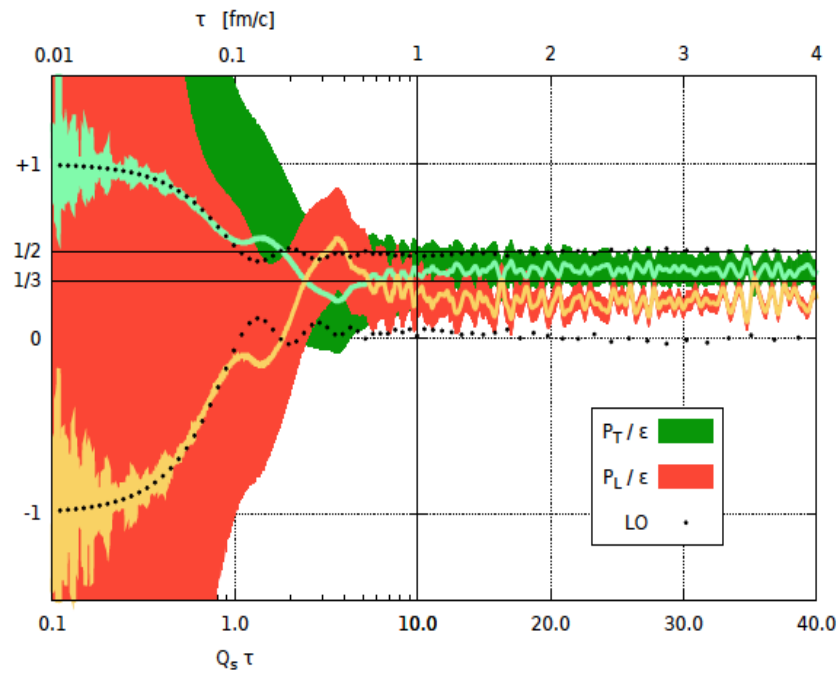

$$\alpha_s \sim 10^{-3}, P_L/P_T << 1$$

$$\alpha_s \sim 10^{-2}, P_L/P_T \sim 1$$

Behaviour in time looks like hydrodynamics

Epelbaum and Gelis:

On the other hand:
Computations at very weak coupling suggest a different story

Berges, Bugaslavsky, Schlichting and Venugopalan

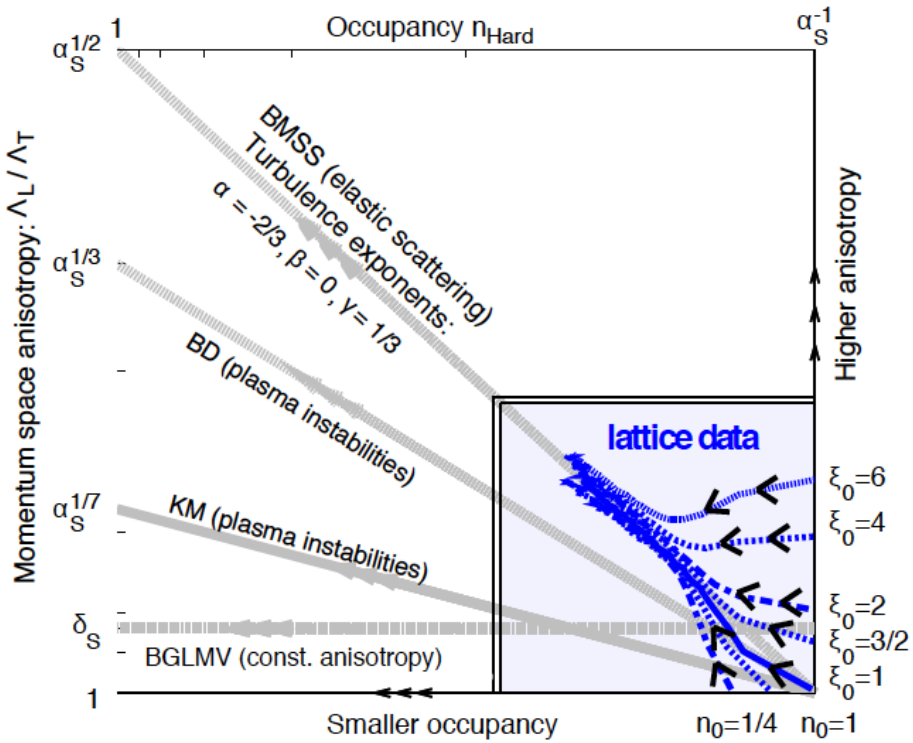

Becomes very anisotropic at late time

Different initial condition but claim there is a universal thermal fixed point
Results should be reliable at very weak coupling

Universal fixed point:

But can one approach a thermal fixed point before, above some small coupling?

The approach to fixed point depends upon initial conditions. Can one be outside the basin of attraction for the fixed point for some initial conditions?

Need to know the initial conditions?

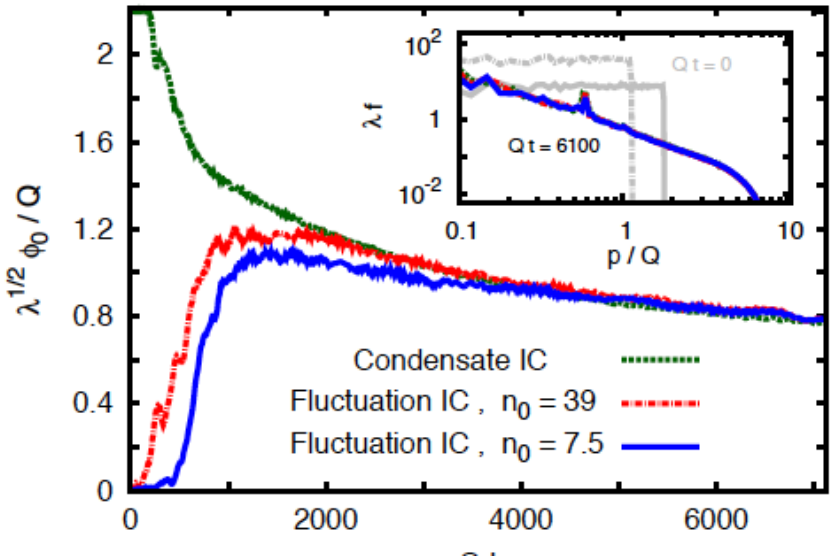

Universality of scalar case: but very long time scales

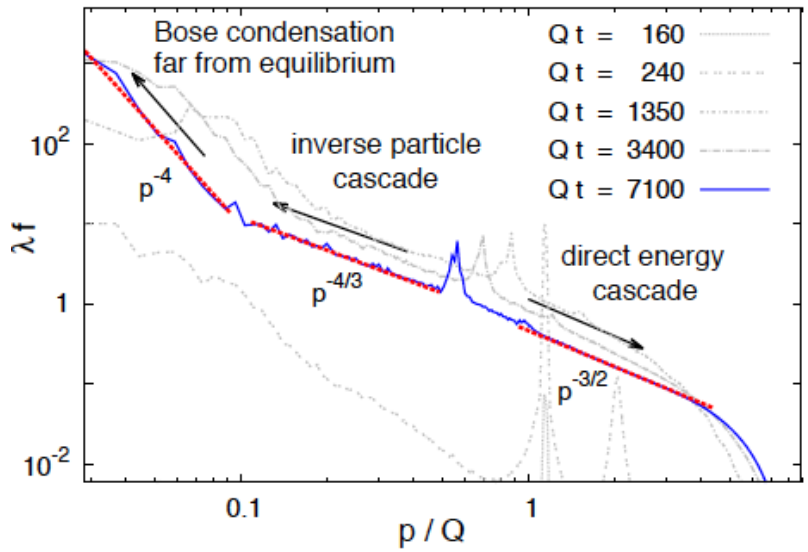

Power law behaviour:
But not similar to classical thermal distribution

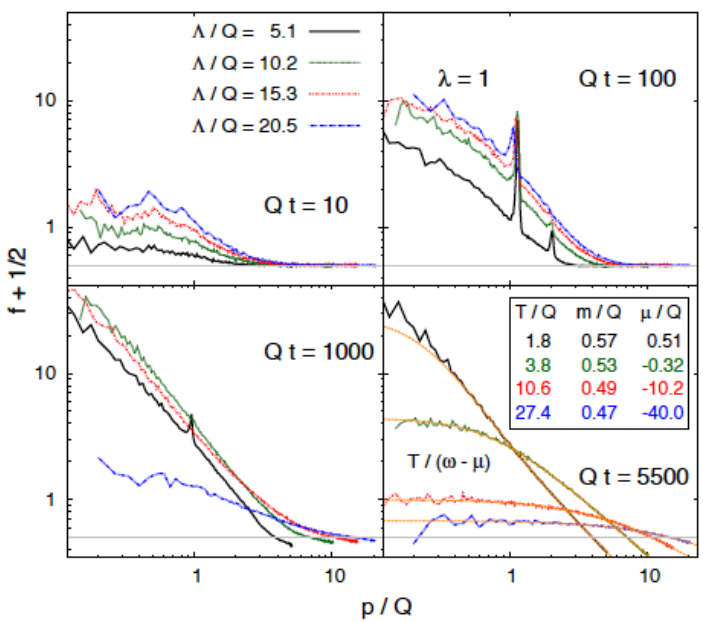

Results are cutoff dependent:
Found in case of coupling

$$\lambda = 1$$

But still weak interaction strength

$$\frac{\lambda}{16\pi^2} \sim 10^{-2}$$

Non-renormalizability of classical computation with small classical fluctuations added

Gelis, Epelbaum and Wu

Simulations involve smooth classical field of order 1/g plus quantum fluctuations added to the classical field of order g

There are some quantum fluctuations of order g which are ignored

This leads to a non-renormalizable approximation:
Mass and coupling constant redefinitions will not make the result finite

First non-renormalizable correction to classical equations occur in second order corrections to scalar self energy. There is a generated imaginary part of order

$$\lambda^2 \Lambda^2$$

This becomes of order the classical kinetic energy term, when

$$\Lambda_{IR} \sim \lambda \Lambda$$

Maybe these corrections are small so long as we are below the thermal fixed point?

Is there some window where one can do the computations, for a cutoff not to big for a fixed small coupling?

Can one fix the equations by adding in terms to cancel the non-renormalizable terms?

Is there an effective hard thermal loop theory where one can integrate out the UV modes to generate a well defined effective theory for the infrared?

Is it incurable and all of this is nonsense?

Some phenomenology of the Glasma: Photons

Chiu, Hemmick, Khachatryan, Leonidov ,Liao, Klein-Boesling, Schenke, LDM

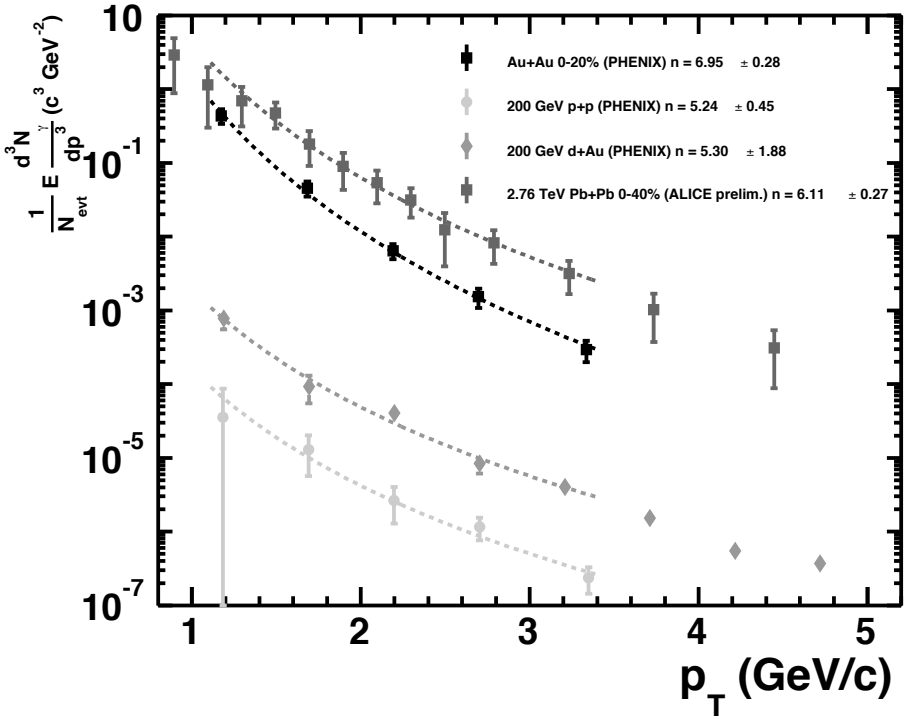

$$Q^2_{sat} = Q^2_0\ (1/x)^{.25} A^{1/3}$$

$$\frac{1}{\pi R^2}\frac{dN}{dyd^2p_T} = F(Q_{sat}/p_T)$$

pp, dA and AA at all centralities at RHIC and PbPb

Data are on the same universal scaling curve!

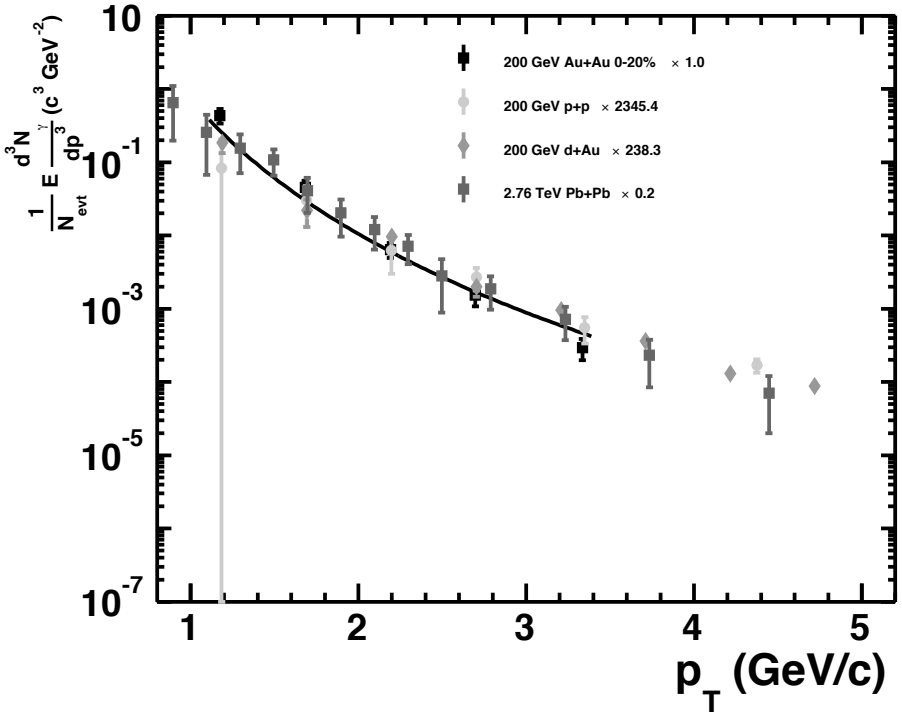

Suggest may be early time phenomena but what about flow?

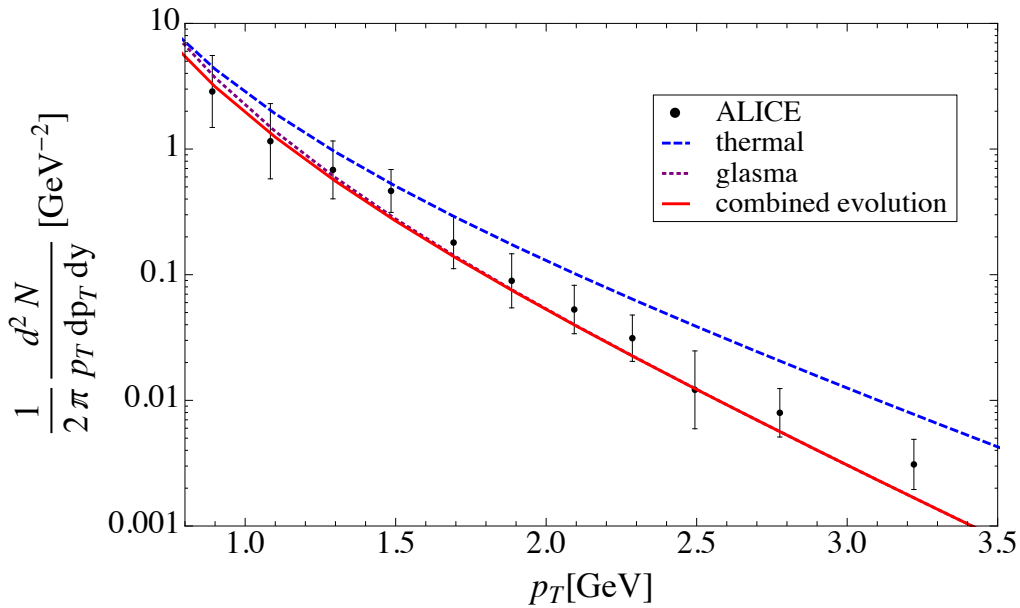

For an isotropic Glasma, get a good description of photon spectrum

$\langle t \rangle$ [fm/c]	thermal	Glasma+th, $\delta = 1/3$	Glasma+th, $\delta = 1/5$
$p_T = 1\,\mathrm{GeV}$	12	16.5	13.7
$p_T = 2\,\mathrm{GeV}$	2	3.1	3.3
$p_T = 3\,\mathrm{GeV}$	1	1.4	1.8

Emission times much larger: Time for flow to develop?

Summary:

Fundamental theoretical issue about how to make the theory of classical fields plus quantum corrections in real time renormalizable or an effective theory where the UV degrees of freedom have been integrated out.

Computational questions about the determination of the time evolution of the Glasma and its particle distributions .

Deep questions about universality, chaos and turbulence and thermalization

Phenomenological questions about how the Glasma and similar systems shows themselves in nature.

Relations to other fields such as cold atomic gasses and cosmology of inflation and axions

Entropy production in the classical Yang-Mills theory as the coherent state dynamics

Akira Ohnishi (YITP, Kyoto U.)
in collaboration with
H. Iida, T. Kunihiro (Kyoto), T.T.Takahashi (Gunma CT),
A. Schafer (Regensburg), B. Muller (Duke/BNL), A. Yamamoto (Tokyo)

The Approach to Equilibrium in Strongly Interacting Matter
April 2-4, 2014, BNL

Based on the works,

- ***Towards a Theory of Entropy Production in the Little and Big Bang*, T. Kunihiro, B. Müller, A. Ohnishi, A. Schäfer, Prog. Theor. Phys. 121 ('09), 555 [arXiv:0809.4831].**
- ***Chaotic behavior in classical Yang-Mills dynamics*, T. Kunihiro, B. Müller, A. Ohnishi, A. Schäfer, T. T. Takahashi, A. Yamamoto, Phys. Rev. D 82 (2010), 114015 [arXiv:1008.1156].**
- ***Entropy production in classical Yang-Mills theory from Glasma initial conditions*, H. Iida, T. Kunihiro, B. Müller, A. Ohnishi, A. Schäfer, T. T. Takahashi, Phys. Rev. D 88 (2013), 094006 [arXiv:1304.1807].**
- **H. Iida, T. Kunihiro, A. Ohnishi, T.T. Takahashi, arXiv:1404.xxxx**

Thermalization in High-Energy Heavy-Ion Collisions

- **Time Evolution at RHIC & LHC**

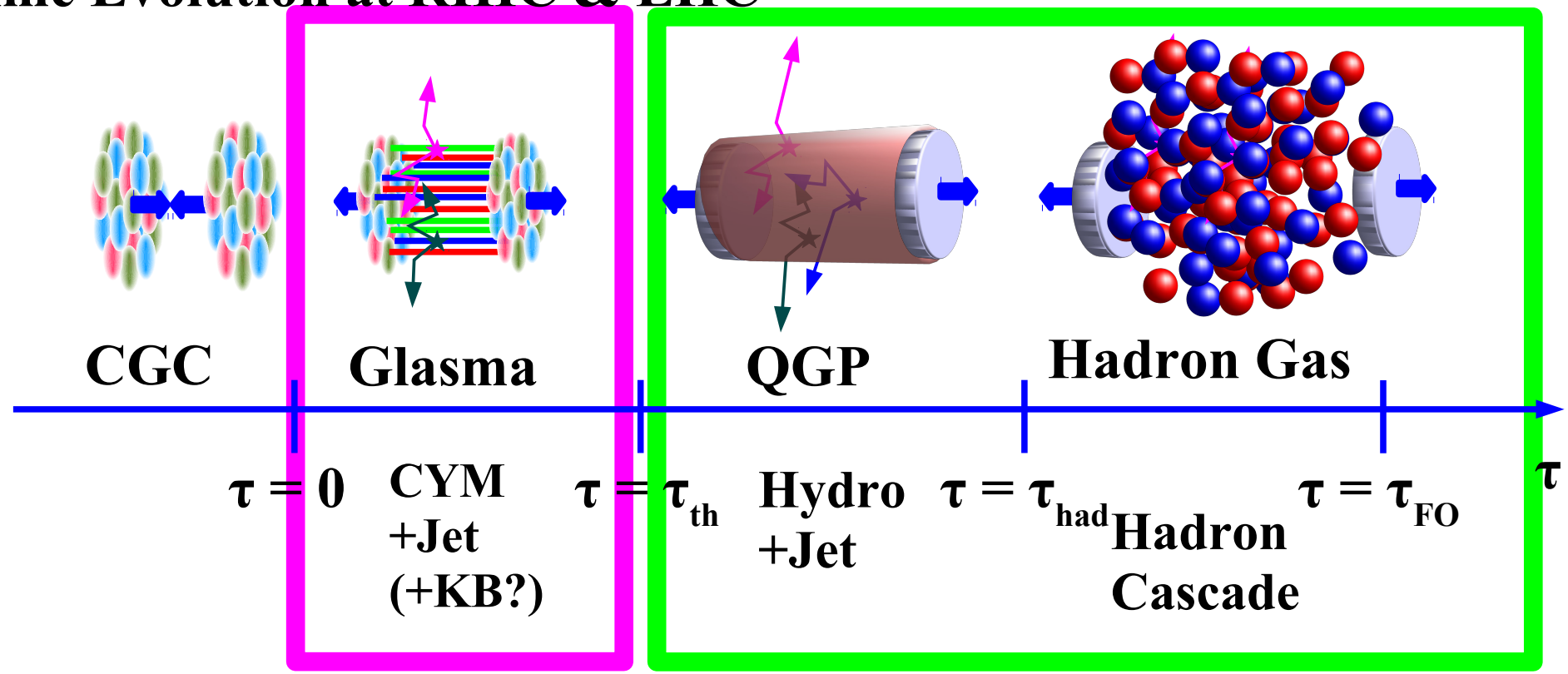

Theor. Challenges

- **Thermalization under dynamical classical field**
- **Theoretically interesting and Phenomenologically important. dN/ dη, init. cond. of hydro.**

Phen. Challenges

flow, jet, hard probes
→ hydro., transport coef., E-loss, hadron prop., phase diagram, ...

Entropy Production in Heavy-Ion Collisions

- **We have been working on entropy production in non-equilibrium stage, since the international Molecule-type workshop on "Entropy Production before QGP" (2008.08.01-28)**
  (A. Schafer, R. Fries, B. Mueller, M. Strickland, T. Schafer, M. Natsuume, Y. Nara, T. Hirano, K. Fukushima, T. Kunihiro, AO)

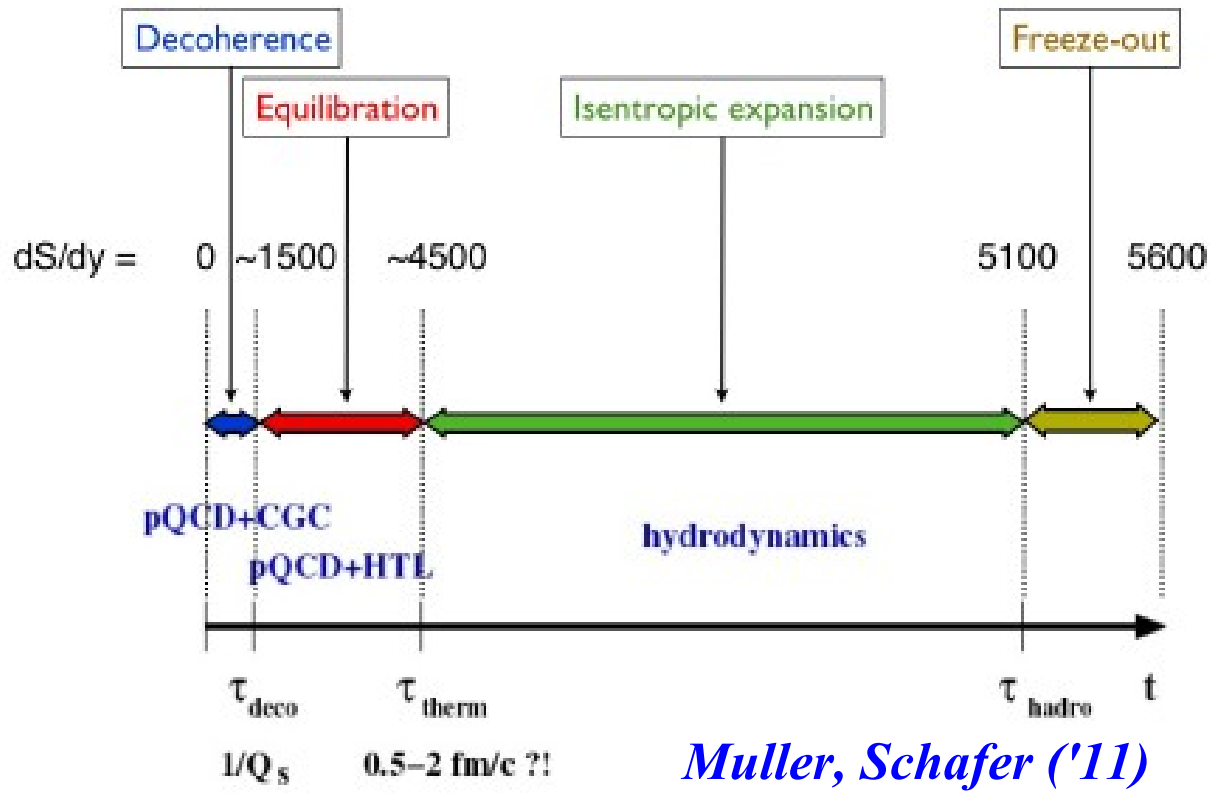

Muller, Schafer ('11)

Entropy production in Classical Yang-Mills dynamics

- **Perturbative estimate of thermalization time is longer than expected from hydrodynamics simulations.**
  → Classical Yang-Mills field is expected to play a role of entropy prod.
  Baier, A.Mueller, Schiff, Son ('01); Chatterjee, Srivastava ('09), Heinz, Kolb ('02)

- **How does CYM field have entropy ? Chaos & Decoherence !**
  - **Entropy from chaoticity**
    - **(Husimi-)Wehrl entropy** **Kunihiro, B. Müller, AO, Schäfer ('09)**

$$S_{Wehrl} = -\int \frac{d^n x\, d^n p}{(2\pi)^n} H \log H \quad (H = \text{phase space prob. fn.})$$

    - **Entropy production rate = Kolmogorov-Sinaii entropy**
      B. Muller, Trayanov ('92), Biro, Gong, B. Muller ('94), Bolte, B. Muller ('00). Kunihiro, B. Müller, AO, Schäfer, Takahashi, Yamamoto ('10), Iida, Kunihiro, B.Müller, AO, Schäfer, Takahashi ('13)
  - **Decoherence entropy**
    B.Muller, Schafer ('03, '06), Fries, B. Muller, Schafer ('09), Iida, Kunihiro, AO, Takahashi ('14)
  - **Classical Statistical simulation**
    Berges, Scheffler, Sexty ('08), Epelbaum, Gelis ('13)

Contents

We discuss the CYM entropy and its production rate with emphasis on the decoherence entropy

- **Introduction**
- **Entropy production from chaotic nature of CYM**
  - **Chaoticity, Lyapunov exponent, and Kolmogorov-Sinaii entropy**
  - **KS entropy from CYM**
    T. Kunihiro, B. Müller, AO, A. Schäfer, T.T. Takahashi, A. Yamamoto, PRD82('10),114015 [arXiv:1008.1156].
    H.Iida, T.Kunihiro, B.Müller, AO, A.Schäfer, T.T.Takahashi, PRD88('13),094006 [arXiv:1304.1807].
- **CYM as a coherent state and decoherence entropy**
  - **Decoherence entropy**
  - **CYM as a coherent state**
  - **Decoherence entropy from CYM dynamics**
    H.Iida, T.Kunihiro, AO, T.T.Takahashi, arXiv:1404.xxxx (to be submitted soon).
- **Summary**

Entropy production from chaotic nature of CYM

Chaoticity, Lyapunov exponent, and KS entropy

- **Entropy in classical dynamics = Wehrl entropy**

$$S = -\int d\Gamma\, H \log H$$

(dΓ= dx dp = phase space, H= phase space dist. fn., e.g. Husimi fn.)

- **Lyapunov exponent and Kolmogorov-Sinaii entropy**

$$\delta X_i(t) = \delta X_i(t_0) \exp[\lambda_i (t - t_0)] \quad (X = (x, p)),$$

$$dS/dt = S_{\mathrm{KS}} \equiv \sum_{i, \lambda_i > 0} \lambda_i$$

  - **δ X = difference of two trajectories from adjacent initial conditions**
    λ = initial state sensitivity (Lyapunov exponent, measure of chaoticity)
  - **When λ > 0, exponentially growing number of phase space cells are visited**
    → phase space dist. fn. becomes smooth after proper coarse graining
    → entropy production (Kolmogorov-Sinaii entropy)

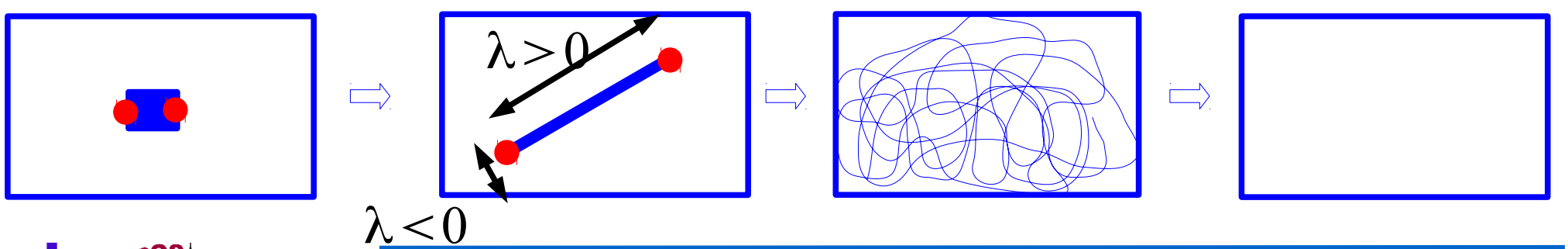

Evolution of the Wigner Function

- **Liouville theorem → conservation of the phase space volume**
  - **Exponential growth in (x+p/λ), Exponential narrowing in (x-p/λ)**

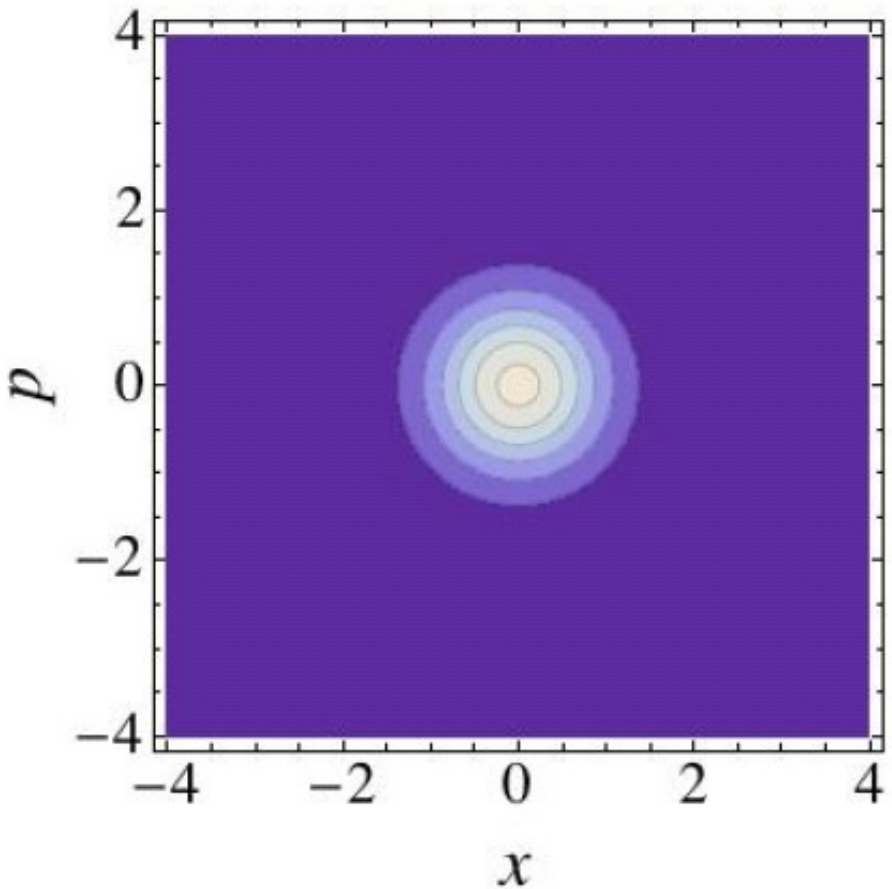

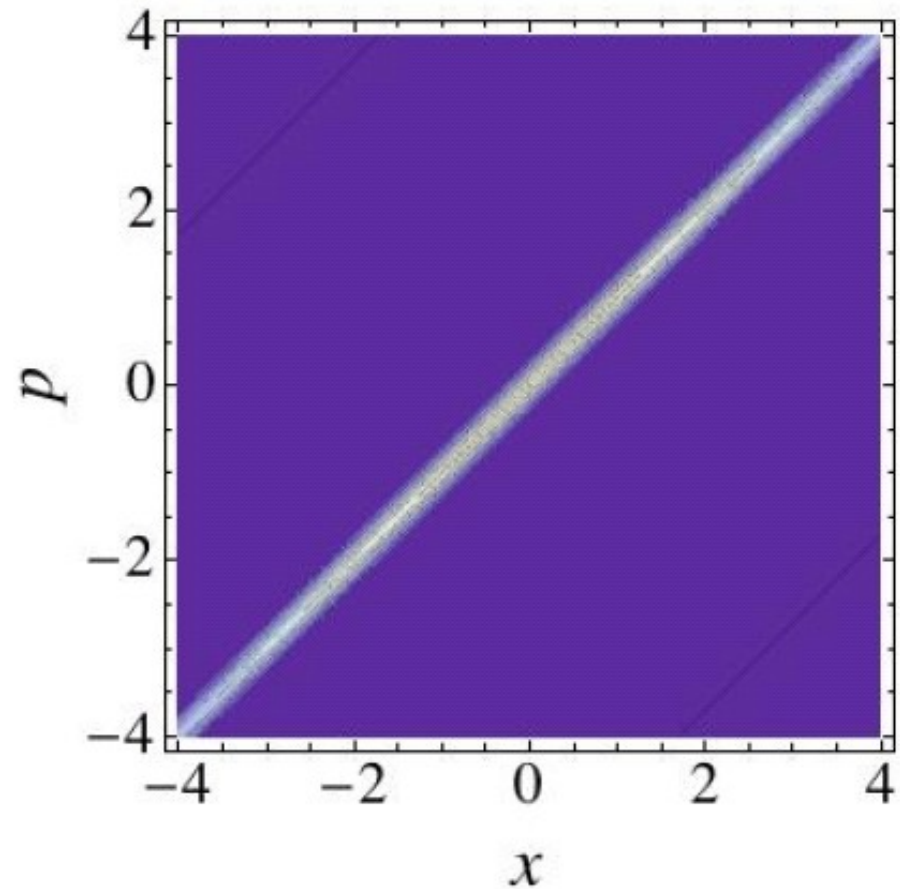

Kunihiro, Müller, AO, Schäfer ('09)

$$\hat{\mathcal{H}} = \frac{1}{2}\hat{p}^2 - \frac{1}{2}\lambda^2\hat{x}^2$$

λ=1, λt=0, 2

Evolution of the Husimi Function

- **Coherent state broadening of phase space**
  - **Minimum width in (x-p/λ) → phase space dist. func. is smeared !**

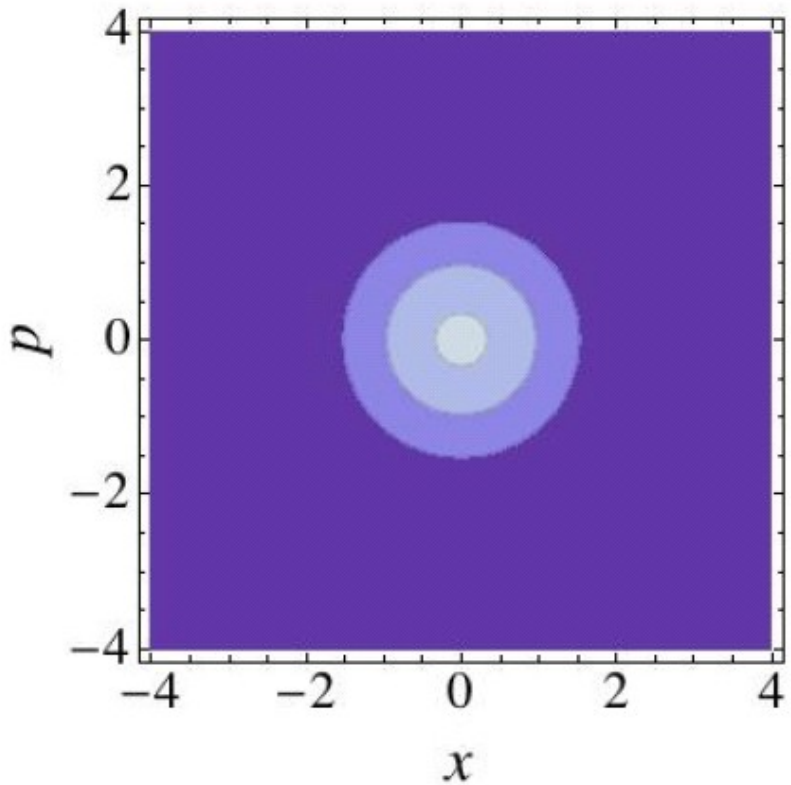

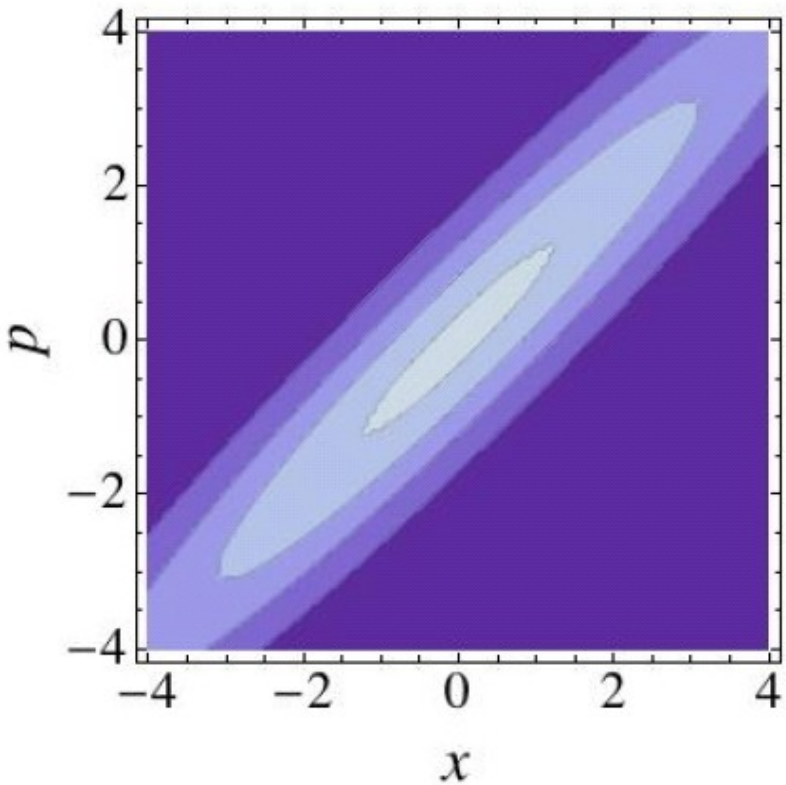

Kunihiro, Müller, AO, Schäfer ('09)

$$\hat{\mathcal{H}} = \frac{1}{2}\hat{p}^2 - \frac{1}{2}\lambda^2\hat{x}^2$$

λ=1, λt=0, 2

Classical Yang-Mills dynamics on the lattice

- **Lattice CYM Hamiltonian in temporal gauge (A_0=0) in the lattice unit**

$$H=\frac{1}{2}\sum_{x,a,i}\left[E_i^a(x)^2+B_i^a(x)^2\right]$$

$$F_{ij}^a(x)=\partial_i A_j^a(x)-\partial_j A_i^a(x)+\sum_{b,c} f^{abc}\boxed{A_i^b(x)A_j^c(x)}=\varepsilon_{ijk}B_k^a(x)$$

Non-linear & coupling

- **Non-compact (A, E) form !**
  - **Demerit: Gauge invariance is not fully satisfied at finite lattice spacing.**
  - **Merit: Easy to consider the coherent state, and conformality is manifest.**
- **Initial conditions ($E_i^a(x)$=0 is assumed here.)**
  - **Random initial condition: $A_i^a(x)$ = random in [-η, η],**
  - **Modulated init. cond.:** $A_i^a(\vec{r})=\delta_{i2}\left[\epsilon_1\sin\left(\frac{2x\pi}{N_x}\right)+\epsilon_2\sin\left(\frac{2nx\pi}{N_x}\right)\sin\left(\frac{2mz\pi}{N_z}\right)\right]$
  - **Constant-A init. cond.** $A_i^a(x)=\sqrt{B/g}\left(\delta_{i2}\delta^{a3}+\delta_{i3}\delta^{a2}\right)$ *Berges et al.('12)*

magnetic field ~ z direction (ε_1 >> ε_2), w and w/o fluc.

How to obtain Lyapunov exponents

- **EOM of δX → Integral**

$$\dot{X}=\begin{pmatrix}\dot{x}\\ \dot{p}\end{pmatrix}=\begin{pmatrix}H_p\\ -H_x\end{pmatrix}\ \rightarrow\ \delta\dot{X}=\begin{pmatrix}H_{px} & H_{pp}\\ -H_{xx} & -H_{xp}\end{pmatrix}\delta X\equiv\tilde{H}\,\delta X$$

$$\left(H_{px}\equiv\partial^2 H/\partial p\,\partial x\ \ \text{etc}\right)$$

$$\delta X(t)=T\exp\left(\int_0^t dt'\,\tilde{H}(t')\right)\delta X(t=0)\simeq T\prod_{k=1,N}\left(1+\tilde{H}\,\Delta t\right)\delta X(t=0)$$

$$=U(0,t)\,\delta X(t=0)$$

- **Diagonalizing U and the eigen value becomes λt.**
- **Matrix size = 3 (xyz) x (N_c^2-1) x L^3 x 2 (A,E)**

Typical Lyapunov spectrum

- **Sum of all Lyapunov exponent = 0 (Liouville theorem)**
- **1/3 Positive, 1/3 negative, and 1/3 zero (or pure imag.)**

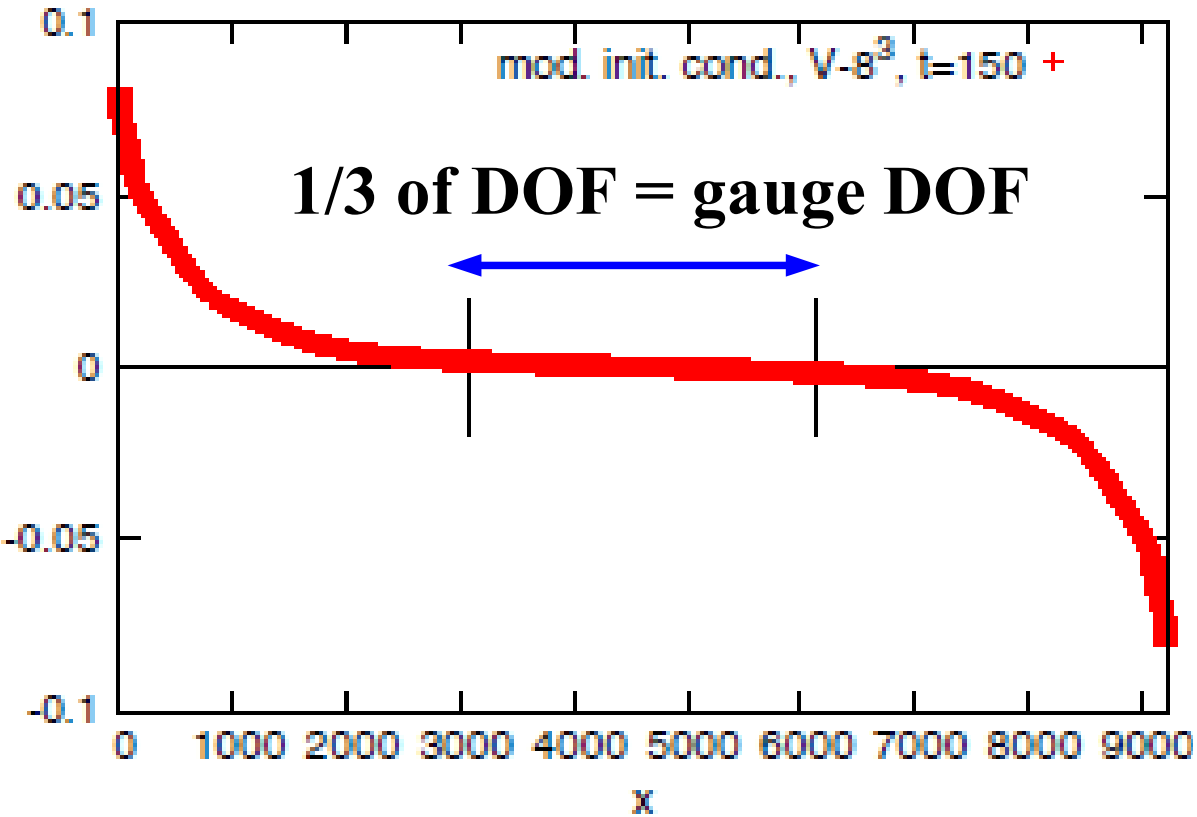

Iida, Kunihiro, B.Müller, AO, Schäfer, Takahashi ('13)

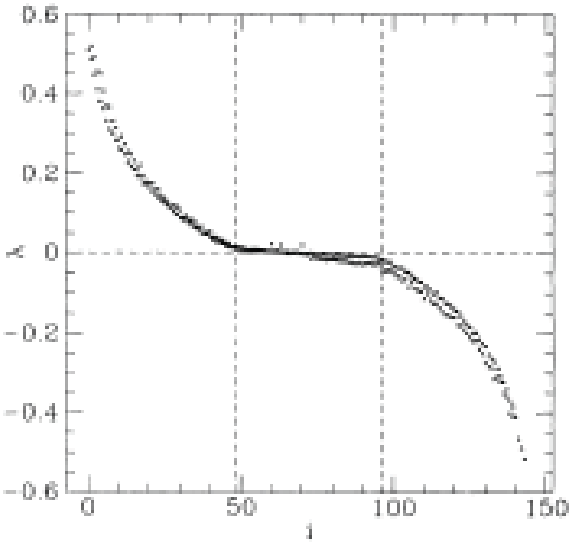

cf) Lyapunov spectrum (V=2^3)
Gong, Phys.Rev.D49, 2642 (1994).

KS entropy in CYM from random init. cond.

Kunihiro, Müller, AO, Schäfer, Takahashi, Yamamoto ('10)

- **Evolution of distance from adjacent init. cond.**
  - **Exponential growth of distance → Instability or Chaoticity**

$$D_{FF} = \sqrt{\sum_x \{\sum_{a,i,j} F^a_{ij}(x)^2 - \sum_{a,i,j} F'^a_{ij}(x)^2\}^2}$$

- **Lyapunov exponent distribution**
  - **Rapid spread of positive LEs and macroscopic # of positive LEs → Chaoticity**

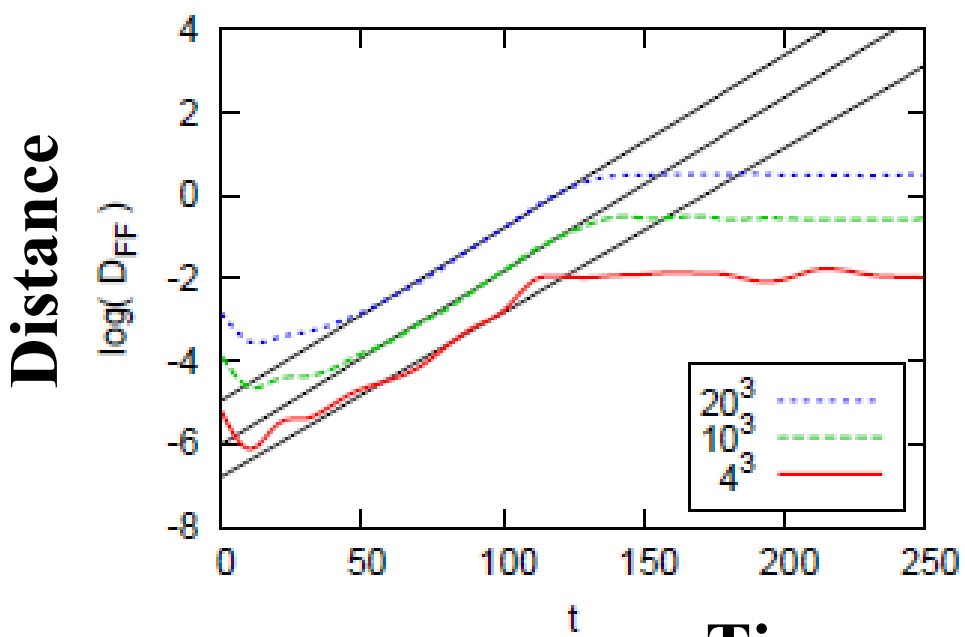

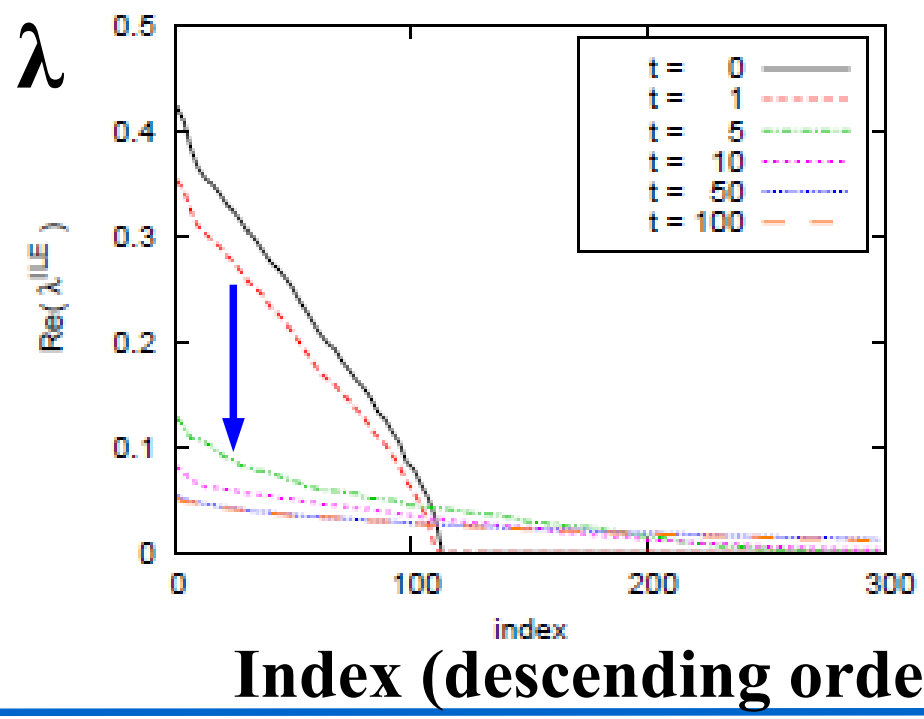

KS entropy in CYM from random init. cond.

Kunihiro, Müller, AO, Schäfer, Takahashi, Yamamoto ('10)

- **Energy density dependence**
  - **Larger energy → Larger Lyapunov exp.**
  - **CYM is conformal → $\lambda \propto \varepsilon^{1/4}$ (ε = E/V)**

$$\frac{dS}{dt} = S_{KS} \sim c_{KS}\,\varepsilon^{1/4} \quad , \quad c_{KS} \sim 2 \quad \text{(Lattice unit)}$$

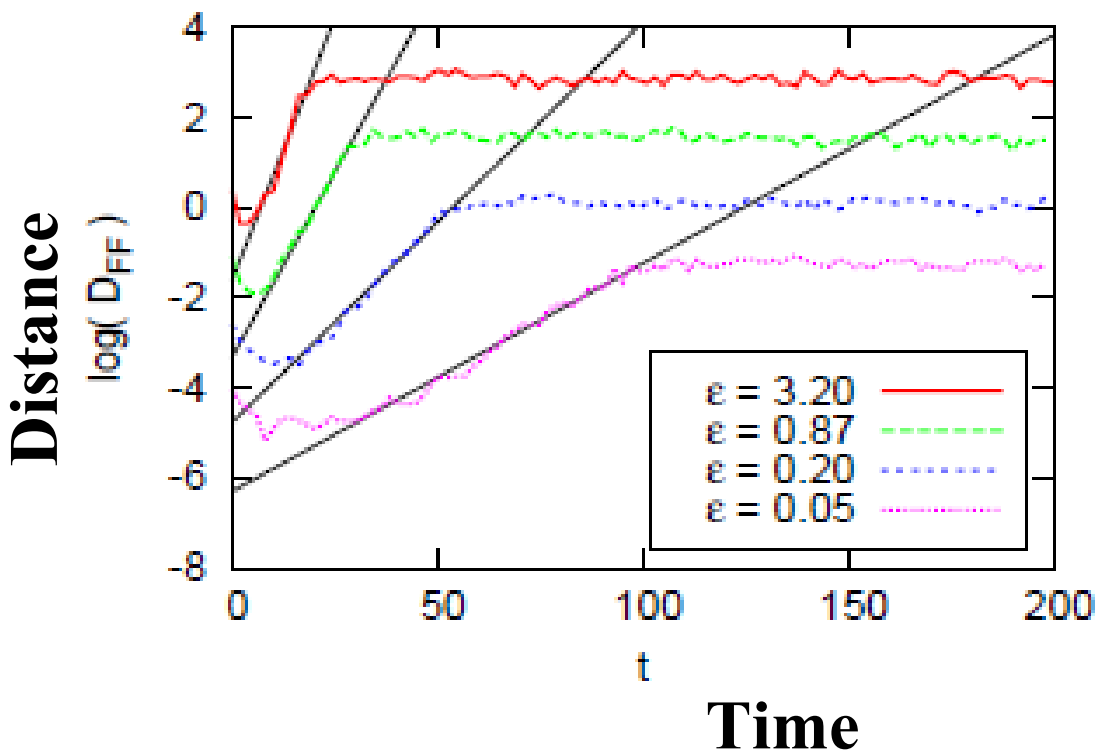

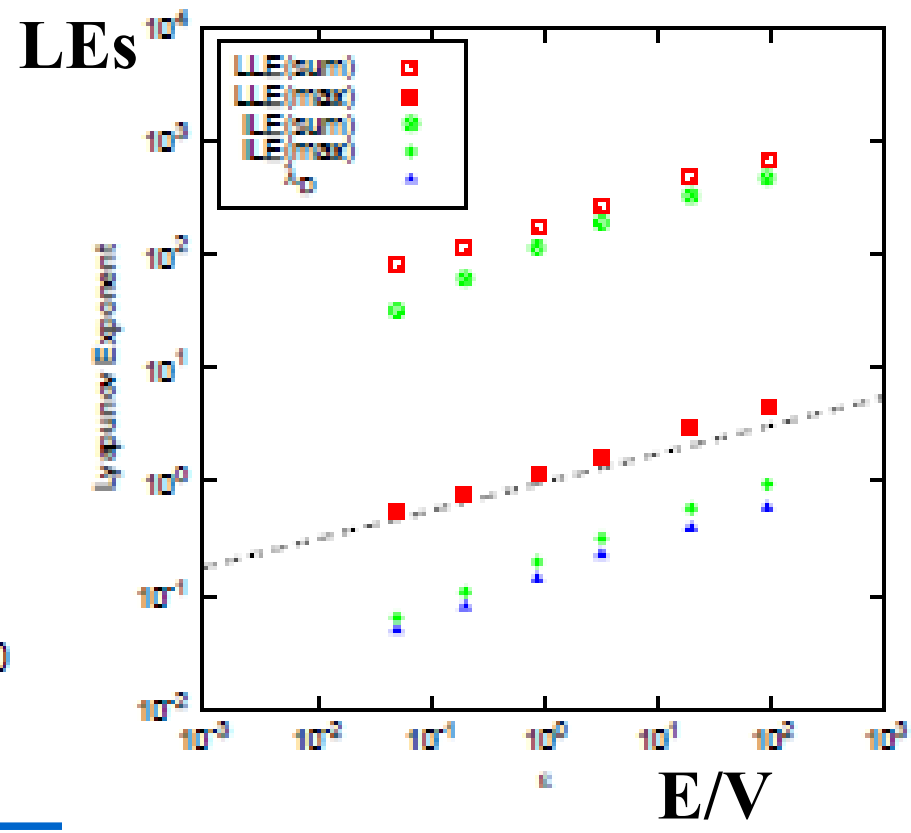

KS entropy in CYM from glasma-like init. cond.

- **Instability under strong color-magnetic field**
  Nielsen, Olesen ('78), Fujii, Itakura ('08), Berges, Scheffler, Schlichting, Sexty ('12)
  - **No chaotic behavior is observed with sine waves and constant-A w/o fluctuations.**
  - **Small fluctuations activate instability and chaoticity.**
  - **Chaoticity emerges after instability spreads to many modes.**

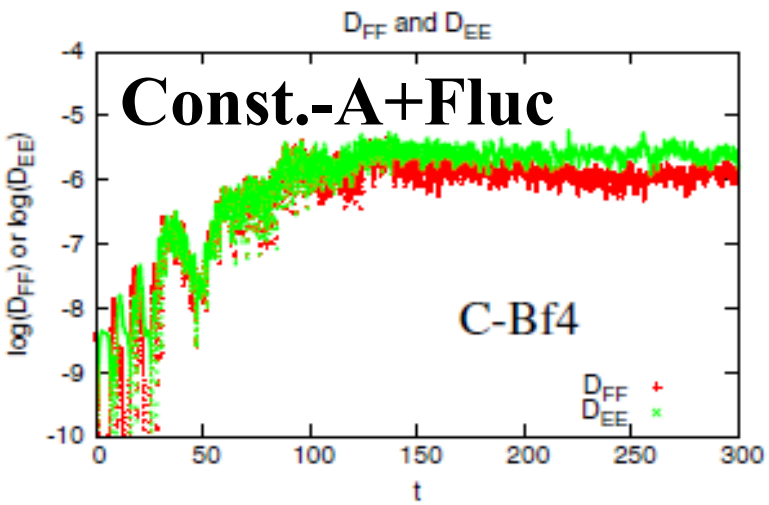

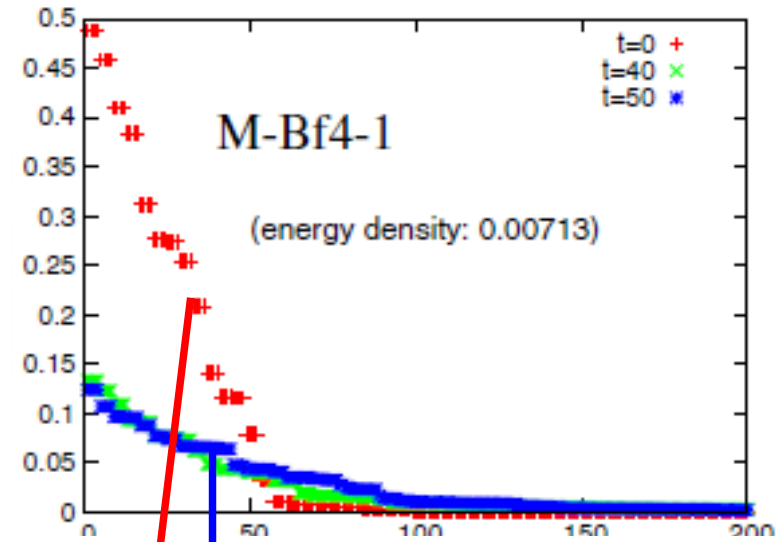

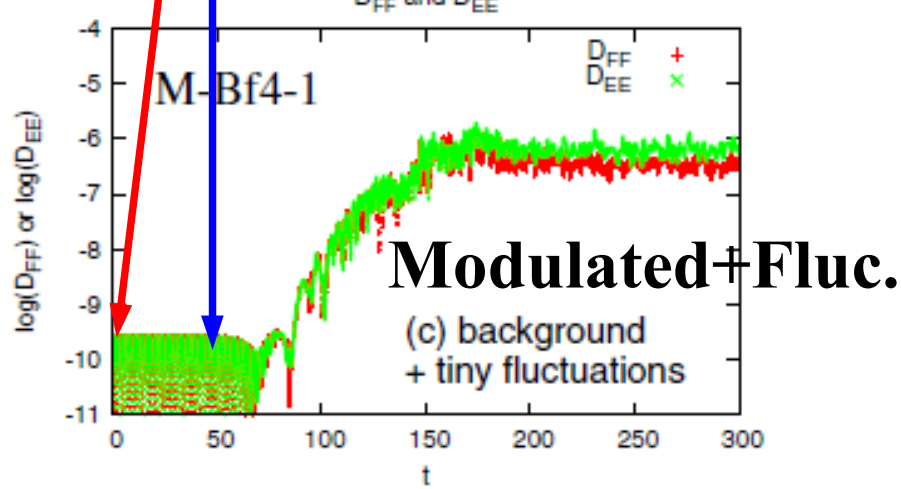

CYM as a coherent state and Decoherence entropy

Decoherence Entropy

Muller, Schafer ('03,'06), Fries, Muller, Schafer ('09), Iida, Kunihiro, AO, Takahashi ('14)

- **Coherent State**

$$\hat{a}|\alpha\rangle = \alpha|\alpha\rangle$$

$$|\alpha\rangle = N\exp(\alpha\hat{a}^{+})|0\rangle = \exp(-|\alpha|^2/2)\sum_n \frac{\alpha^n}{\sqrt{n!}}|n\rangle$$

  - **n-quanta states are coherently superposed in a coherent state.**
  - **When this coherence is broken, entropy is generated (decoherence entropy)**

$$P_n = \frac{|\alpha|^{2n}}{n!}\exp(-|\alpha|^2) \quad \text{(Poisson dist.)}$$

$$\rightarrow \quad S_{\text{dec}} = -\sum_{n=0}^{\infty} P_n \log P_n > 0$$

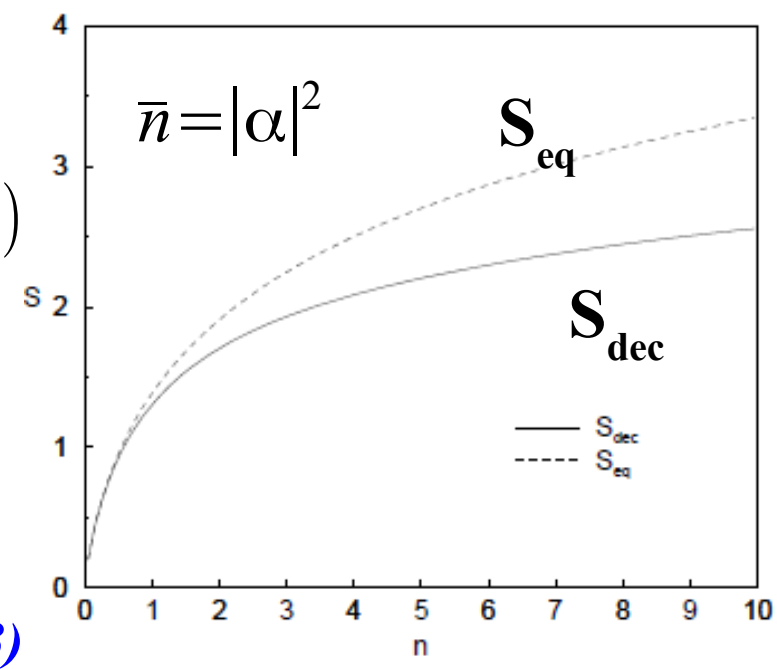

Muller, Schafer ('03)

CYM as a Coherent State

Muller, Schafer ('03,'06), Fries, Muller, Schafer ('09), Iida, Kunihiro, AO, Takahashi ('14)

- **What kind of state does the CYM correspond to ?**
  → Natural guess = Coherent State

$$|\,\mathrm{CYM}\,\rangle \simeq \prod_{\boldsymbol{k},a,i} |\alpha_{\boldsymbol{k}ai}\rangle$$

- **Decoherence entropy from CYM**

$$S_{\mathrm{dec}} = -\sum_{\boldsymbol{k},a,i}\sum_{n} P_n(\alpha_{\boldsymbol{k}ai}) \log P_n(\alpha_{\boldsymbol{k}ai})$$

$$\alpha_{\boldsymbol{k}ai} = \frac{1}{\sqrt{2\omega_{\boldsymbol{k}}}}\left[\omega_{\boldsymbol{k}} A_{ai}(\boldsymbol{k},t) + i E_{ai}(\boldsymbol{k},t)\right], \quad \omega_{\boldsymbol{k}} = \sqrt{\sin^2 k_x + \sin^2 k_y + \sin^2 k_z}$$

- **Is the above assignment unique ?**
  - **Coherent state in each "coherent domain"** *Fries, Muller, Schafer ('09)*
  - **Deviation from Poisson dist. with coupled oscillator**
    Glauber ('66), Gelis, Venugopalan ('06)

Initial Condition and Time Evolution

- **"Glasma-like" init. cond.**
  - **MV model (boost inv.)**
    + Longitudinal fluctuations

    → Bx,y, Ex,y, Bη, Eη
    McLerran, Venugopalan ('94), Romatschke, Venugopalan ('06), Fukushima, Gelis ('12)
  - **Non-expanding geometry is assumed, Substitute Bη and Eη in MV model into Bz and Ez at t=0.**
- **Time-evolution**
  - **Short time behavior of E^2 does not depend on the fluctuation strength. (and similar to expanding geo. results.)**
    E.g. Lappi, McLerran ('06)
  - **Long-time behavior:**
    Earlier "isotropization" in perp. and long. directions of E^2.

20^3 lattice

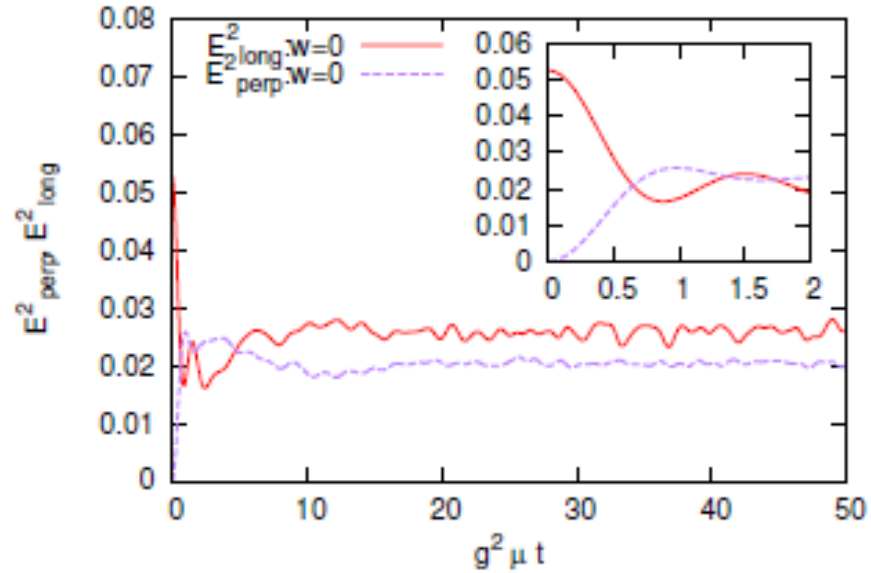

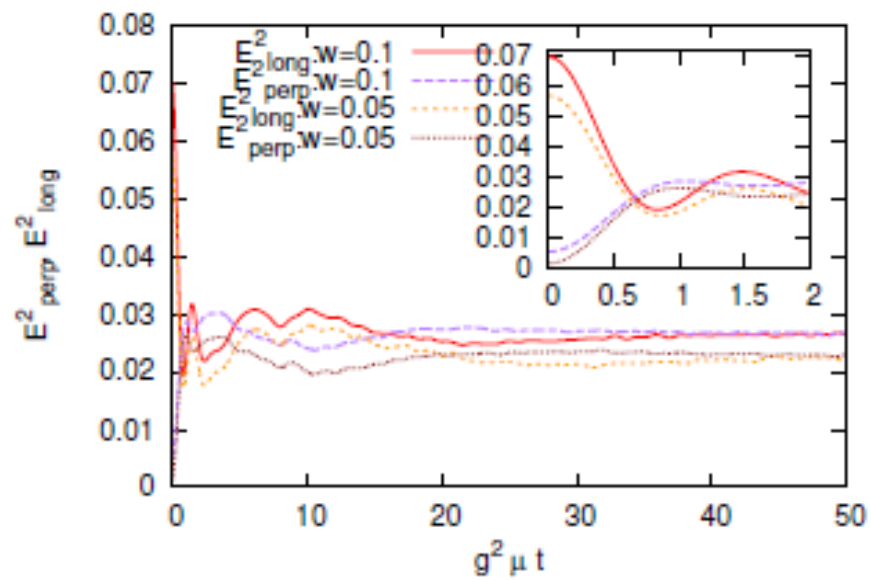

Iida, Kunihiro, AO, Takahashi ('14)

Initial Condition and Time Evolution

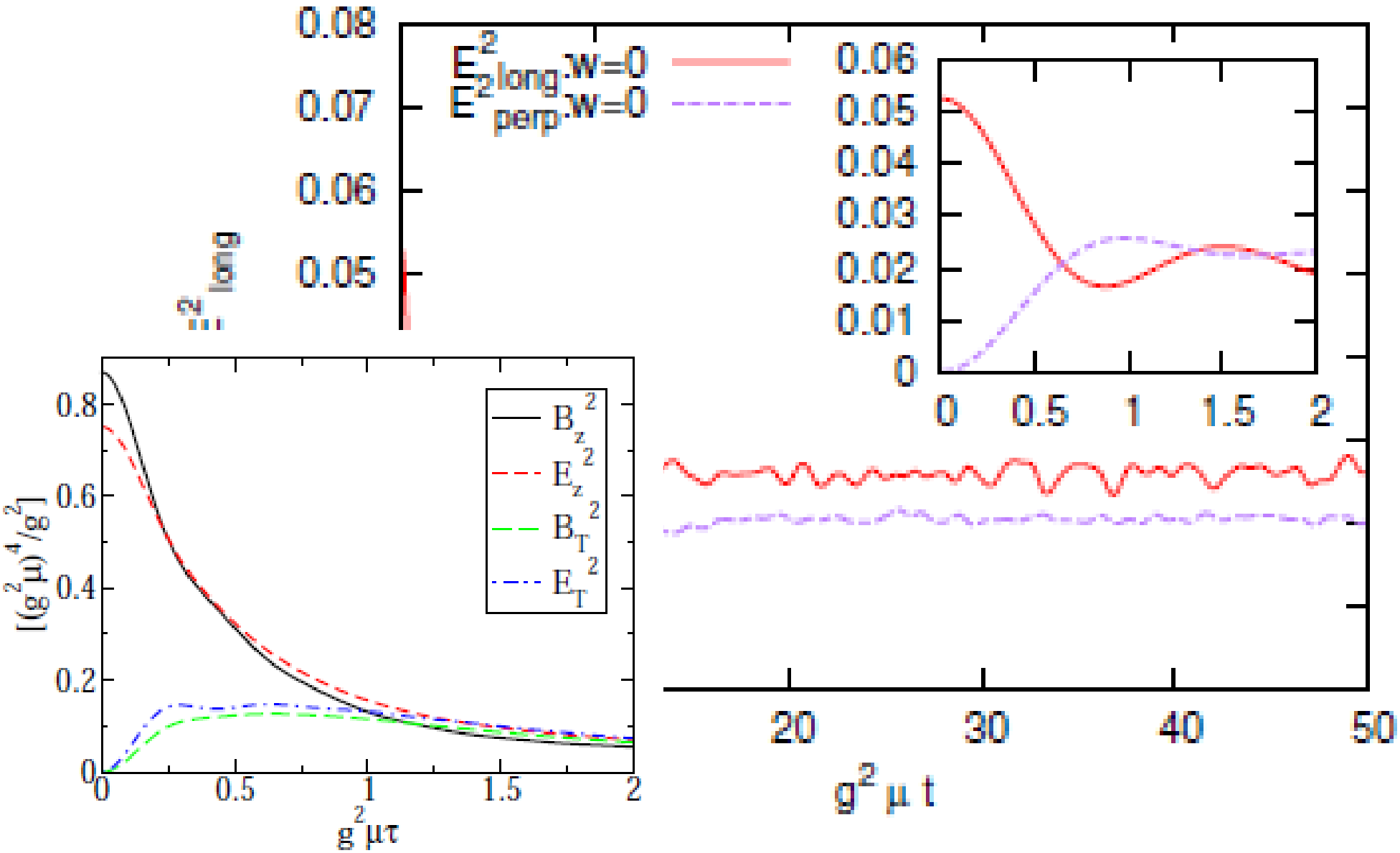

Lappi, McLerran ('06)

Iida, Kunihiro, AO, Takahashi ('14)

Physical Scale

- **Rough estimate: $L^2 \sim \pi R_{Au}^2 \rightarrow 1/a = g^2\mu \sim 0.32$ GeV ($a \sim 0.63$ fm)**
- **Thermal energy estimate** *Kunihiro et al.('10), Muller,Schafer('11)*

$$\varepsilon_{\mathrm{CYM}} = 2\left(N_c^2 - 1\right)\frac{T}{a^3}, \quad \varepsilon_{\mathrm{SB}} = 2\left(N_c^2 - 1\right)\frac{\pi^2}{30}T^4$$

  - **CYM energy density should not exceed Stefan-Boltzmann energy density in equilibrium.**

$$\varepsilon_{\mathrm{CYM}} < \varepsilon_{\mathrm{SB}}$$

$$\rightarrow \quad a > \frac{1}{T}\left(\frac{30}{\pi^2}\right)^{1/3} \sim \frac{1.4}{T}$$

This estimate gives
a > 0.8 fm (T=350 MeV),
a > 0.6 fm (T=500 MeV).

Decoherence Entropy of CYM

- **How about the decoherence entropy ?**
  - **$< \delta E^2 > / < E^2 > \sim 0.1$ (Δ=0.05) and 0.3 (Δ=0.1)**
  - **$S_{dec} \sim 2.3$ (Δ=0) and 33 (Δ=0.05, 0.1)**
  - **Entropy from initial state fluc. and chaoticity**
  - **No long. fluc. results in 2D (pz=0 mode) entropy, while 3D entropy is realized with finite long. fluc. (non-zero Δ).**

S_{dec}/site

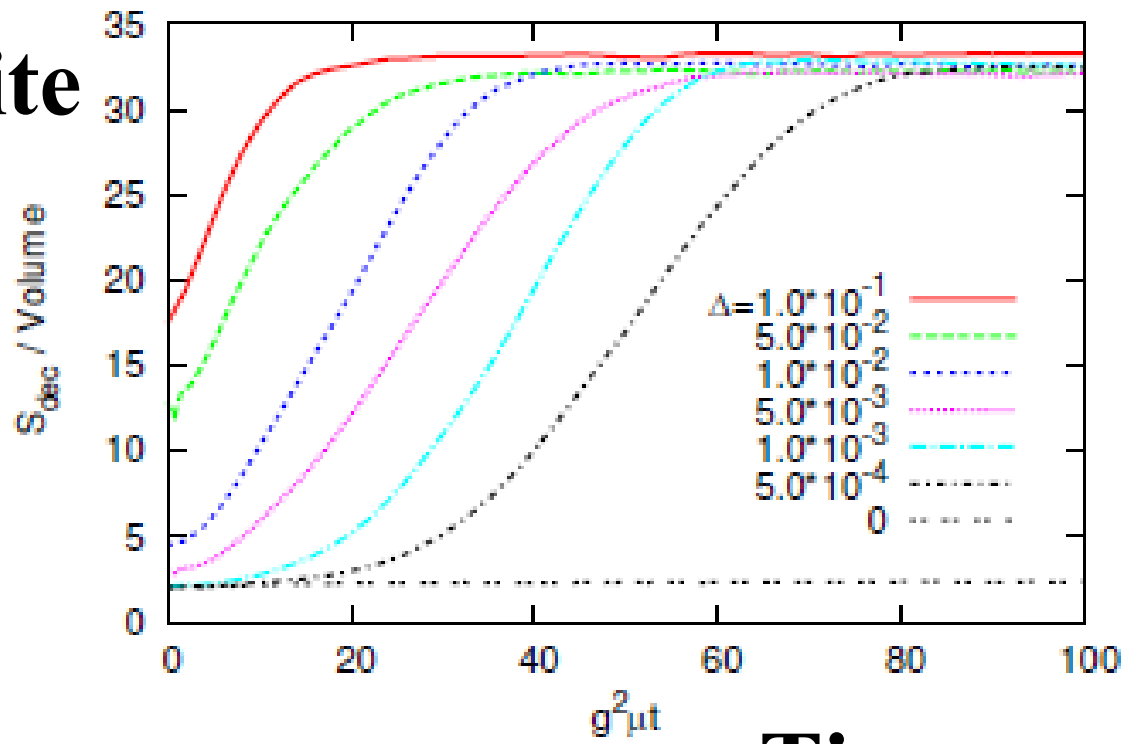

Time

Decoherence Entropy Production Rate

- **Decoherence entropy growth rate should be compared with KS entropy**
  - **$dS_{dec}/dt \sim 0.88$ (Δ=0.01), 1.05 (Δ=0.05), 1.36 (Δ=0.1)**
  - **KS entropy estimate: $S_{KS} \sim c_{KS}\, \varepsilon^{1/4}$, $c_{KS} \sim 2$ (conformal chaotic value)**
  - **Energy density: ε = 0.17 (Δ=0.01), 0.18 (Δ=0.05), 0.21 (Δ=0.1)**
    $\rightarrow c_{KS} = dS^{dec}/dt/\varepsilon^{1/4}$ = 1.4 (Δ=0.01), 1.6 (Δ=0.05), 2.0 (Δ=0.1)

$$\frac{1}{S_{\mathrm{KS}}}\frac{dS_{\mathrm{dec}}}{dt} \sim (0.7-1.0)$$

- **KS entropy**
  = Potentially realized growth rate

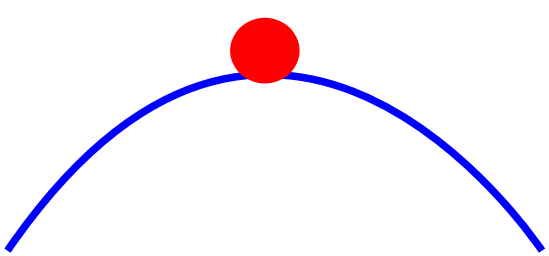

Δ=0: unstable but stationary

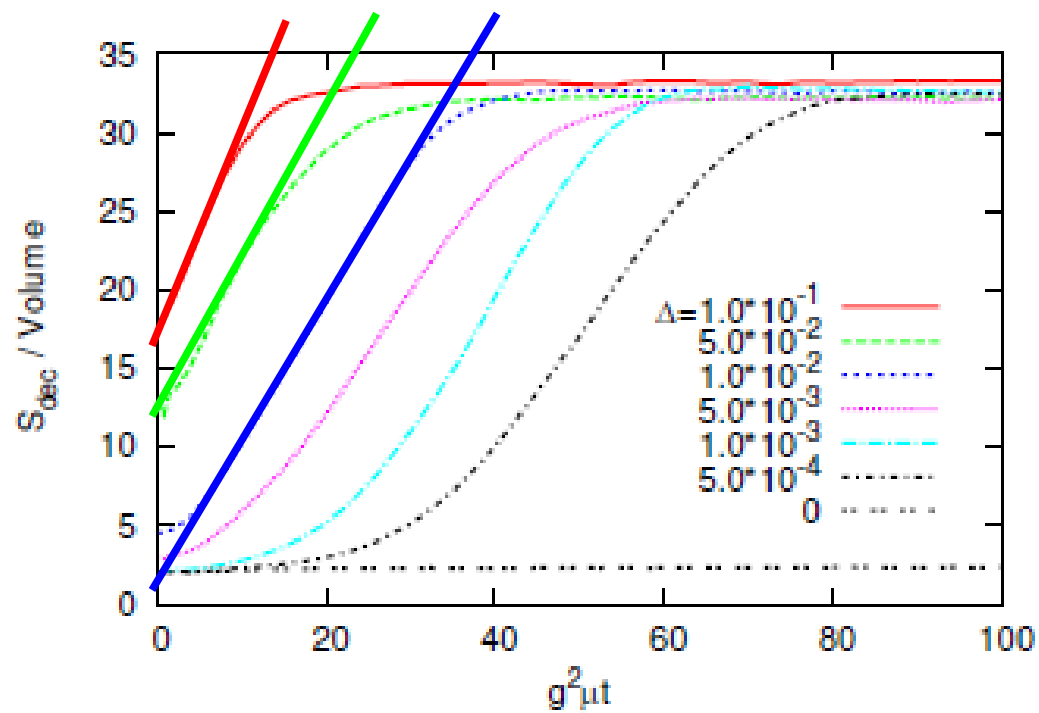

Physical Scale

- **Rough estimate: $L^2 \sim \pi R_{Au}^2 \rightarrow 1/a = g^2\mu \sim 0.32$ GeV ($a \sim 0.63$ fm)**
- **Thermal energy estimate** *Kunihiro et al.('10), Muller,Schafer('11)*

$$\varepsilon_{CYM} = 2\left(N_c^2 - 1\right)\frac{T}{a^3}, \quad \varepsilon_{SB} = 2\left(N_c^2 - 1\right)\frac{\pi^2}{30}T^4$$

  - **CYM energy density should not exceed Stefan-Boltzmann energy density in equilibrium.**

$$\varepsilon_{CYM} < \varepsilon_{SB}$$

$$\rightarrow \quad a > \frac{1}{T}\left(\frac{30}{\pi^2}\right)^{1/3} \sim \frac{1.4}{T}$$

This estimate gives
a > 0.8 fm (T=350 MeV),
a > 0.6 fm (T=500 MeV).

- **First 6 fm/c corresponds to lattice time $g^2\mu t < 10$!**

S_{dec}/site relevant to HIC

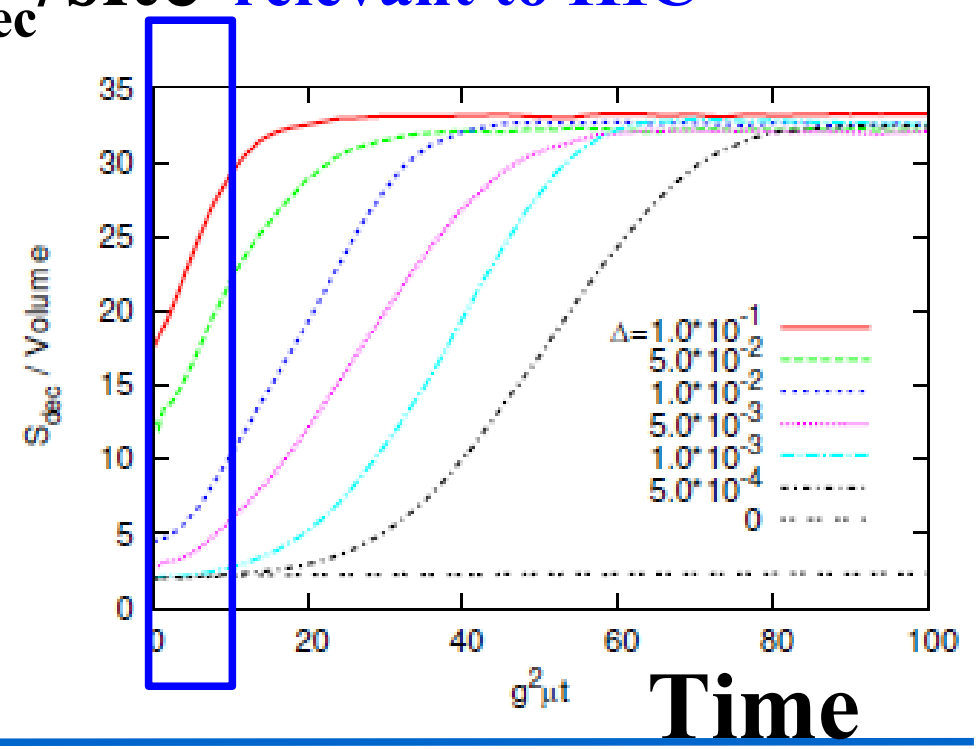

Time

Summary

- **We have evaluated the entropy from classical Yang-Mills field using**
  - **Kolmogorov-Sinai entropy (as a growth rate),**
  - **Decoherence entropy.**
- **Entropy could be produced even before classical Yang-Mills field decays into particles.**
  - **Suggested scenario: Fluctuation**
    → Realization of instability & Spread to many modes → Chaoticity
  - **Rough estimate of entropy production rate in non-expanding CYM**

$$\frac{dS}{dt} = S_{KS} \sim c_{KS}\,\varepsilon^{1/4} \quad , \quad c_{KS} \sim 2 \quad \text{(Lattice unit)}$$

  - **Decoherence entropy grows at about the c_{KS} = (1-2) rate, and saturates, and it is sensitive to longitudinal fluctuations.**
  - **For the initial stage entropy, both the time-evolution and the initial entropy value would be important.**

Future works

- **Decoherence entropy in expanding glasma with realistic fluctuation strength**
  E.g. Epelbaum, Gelis ('13)
- **Estimate of decoherence time during CYM evolution and Defining coherent domain in CYM**
  c.f. Fries, Muller, Schafer ('09)
- **Coupling to particle DOF**
  - **Fluctuation in classical statistical simulation ~ particles ?**
  - **CYM + gluon test particles**
    Dumitru, Nara, Strickland ('07)
  - **2PI formalism of CYM and gluon propagator**
    c.f. Nishiyama, AO ('10, w/o CYM), Hatta, Nishiyama ('11), Cassing ('09)

Thank you for your attention !

Non-equilibrium dynamics of gauge theories and transport coefficients

Jan M. Pawlowski

Universität Heidelberg & ExtreMe Matter Institute

BNL, April 3rd 2013

Outline

- **Gauge dynamics far from equilibrium**
- **Spectral functions and transport coefficients**
- **Summary and outlook**

Gauge dynamics far from equilibrium

Gasenzer, McLerran, JMP, Sexty ‘13

Gauge dynamics far from equilibrium

Abelian Higgs model in 2+1 dim

Gasenzer, McLerran, JMP, Sexty '13

Classical action:

$$S[A_\mu, \phi] = -\int_x \left[\frac{1}{4}F_{\mu\nu}F^{\mu\nu} + (D_\mu\phi)^* D^\mu\phi + V(\phi)\right]$$

ϕ **Higgs**

phase $\dfrac{\phi}{|\phi|} = e^{i\,\varphi}$

Gauge dynamics far from equilibrium

Abelian Higgs model in 2+1 dim

Gasenzer, McLerran, JMP, Sexty '13

Classical action:

$$S[A_\mu, \phi] = -\int_x \left[\frac{1}{4} F_{\mu\nu} F^{\mu\nu} + (D_\mu \phi)^* D^\mu \phi + V(\phi)\right]$$

ϕ **Higgs**

phase $\dfrac{\phi}{|\phi|} = e^{i\,\varphi}$

Classical action of Yang-Mills theory in diagonalisation gauges:

$$S_{\rm YM} \simeq \frac{1}{2}\int_x {\rm tr} F^2_{\bar\mu\bar\nu} + \frac{1}{2}\int_x {\rm tr}\,(D_{\bar\mu} A_2)^2$$

$A_2 = A_2^c(x_0, x_1)$

Wilson loop

$$\mathcal{W}_2 = \mathcal{P}\exp\left\{i\int_0^{L_2} dx_2\, A_2(x)\right\} = \exp\{i\,\phi\}$$

Vortex winding **phase**

$$n(\mathcal{S}) = \frac{1}{16\pi\, i}\oint_{\mathcal{S}} d^2x\, \epsilon_{ij} {\rm tr}\, \hat\phi\, \partial_i \hat\phi\, \partial_j \hat\phi \qquad \hat\phi = \frac{\phi}{\|\phi\|}$$

Quiz

Complex scalar vs Abelian Higgs

Gasenzer, McLerran, JMP, Sexty '13

phase φ of scalar field

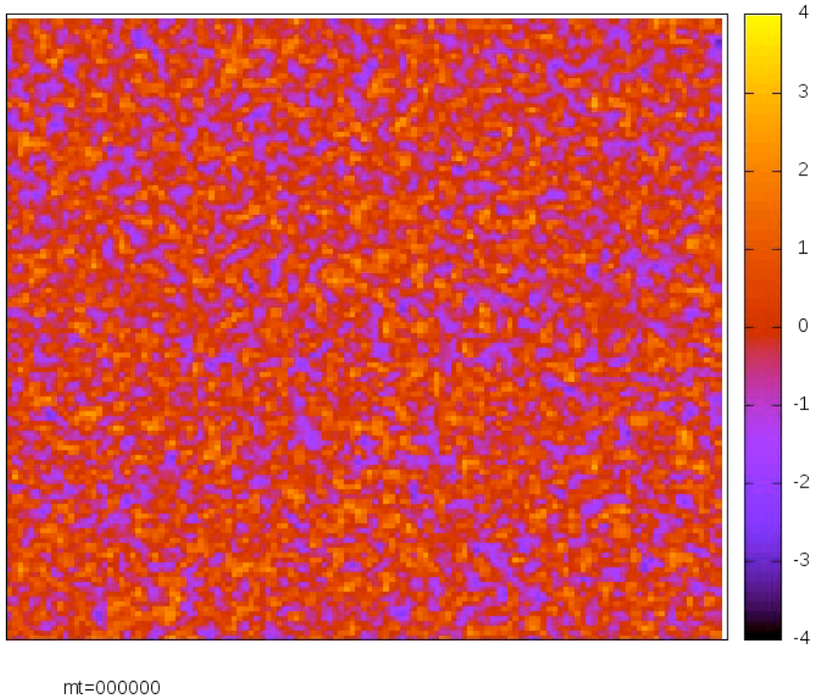

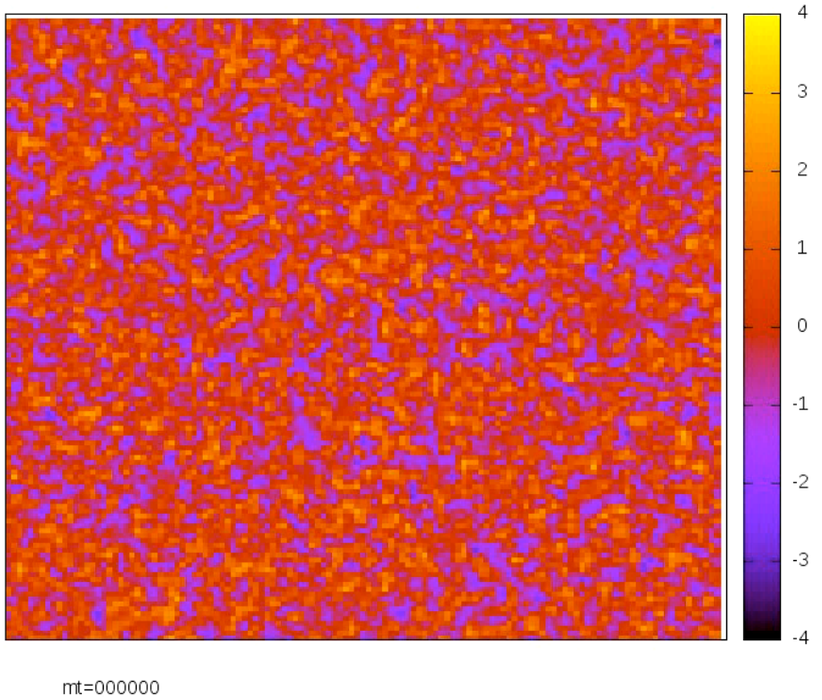

'tachyonic' initial conditions

classical statistical lattice simulations

Which is which?

Gauge dynamics far from equilibrium

Abelian Higgs model in 2+1 dim

Gasenzer, McLerran, JMP, Sexty '13

magnetic field

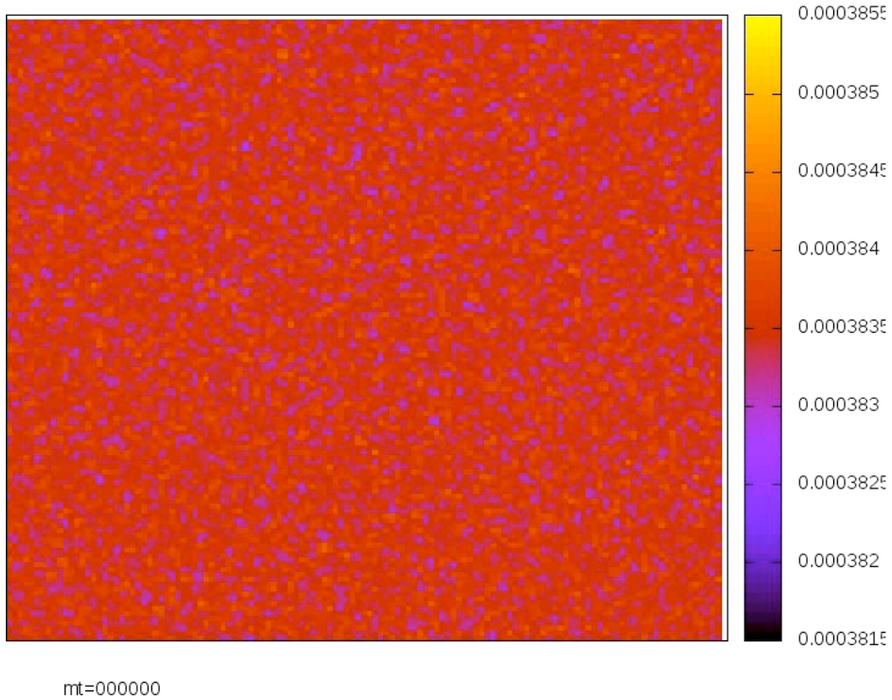

phase of Higgs

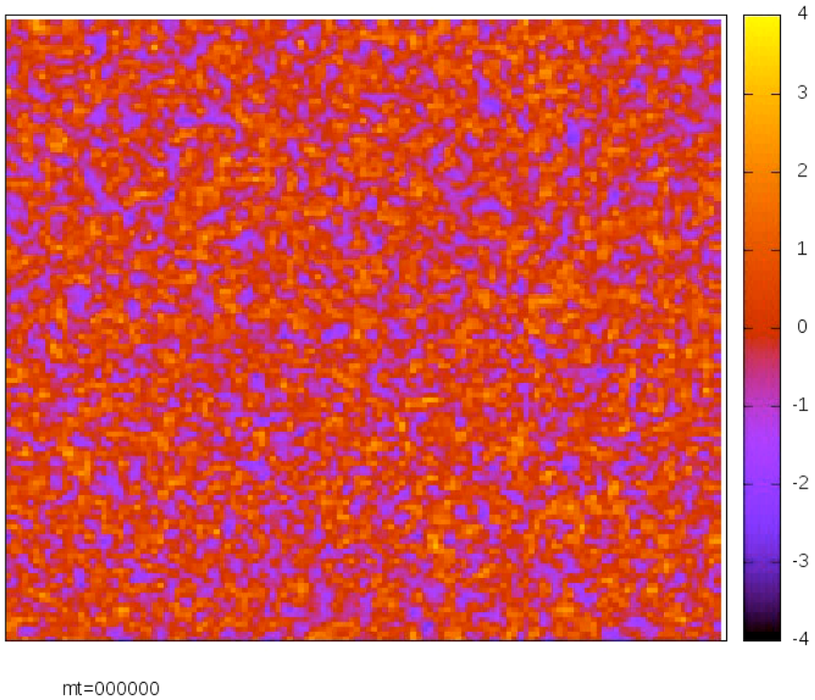

'tachyonic' initial conditions

classical statistical lattice simulations

Gauge dynamics far from equilibrium

Abelian Higgs model in 2+1 dim

'overpopulation' initial conditions

modulus of Higgs

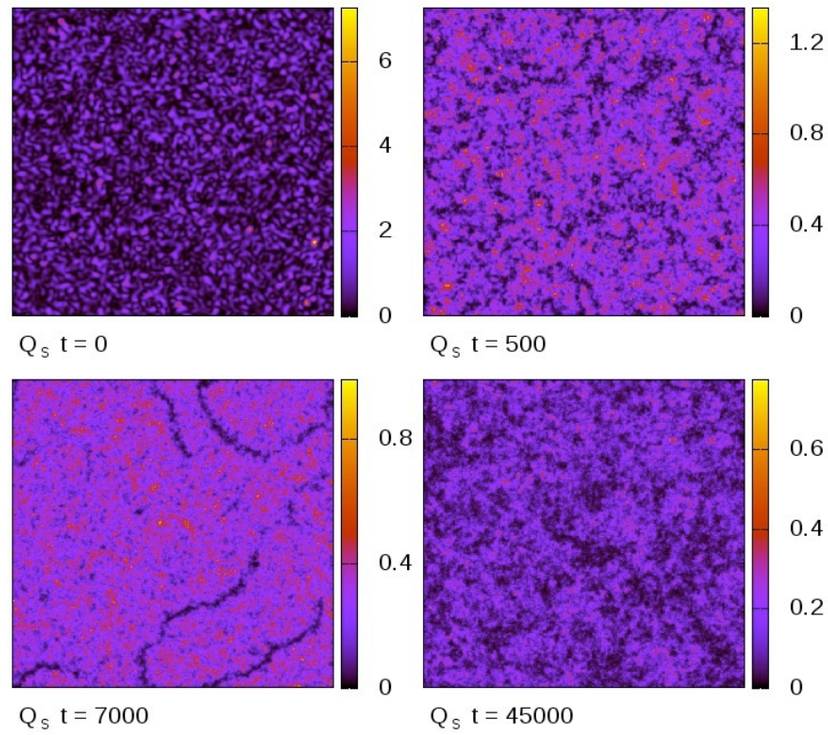

$$\xi = 0.025$$

coupling

$$\xi = \frac{6e^2}{\lambda}$$

relative phase

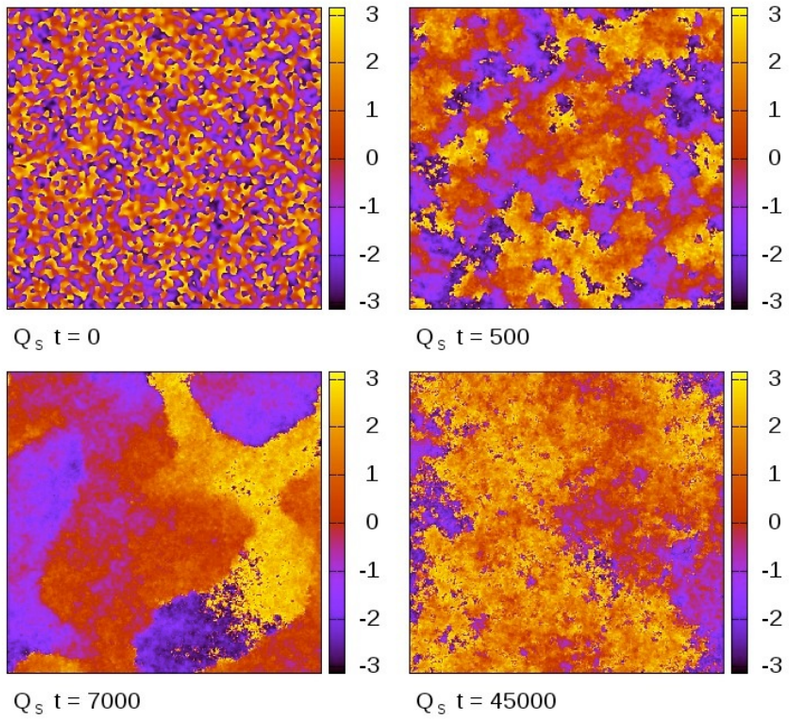

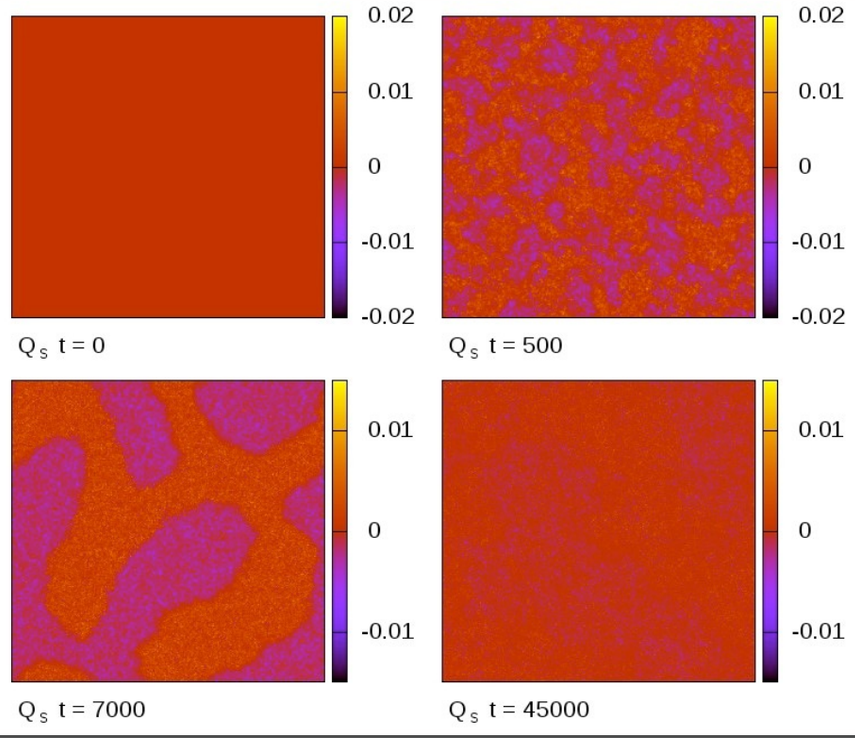

charge

$$\varphi^U(\vec{x},t) = \arg(G^U(\vec{0},\vec{x},t))$$

relative phase

$$G^U(\vec{x},\vec{y},t) = \langle \phi(\vec{x},t) U(\vec{x},\vec{y},t) \phi(\vec{y},t)^* \rangle_{\rm cl}$$

parallel transport U

Gasenzer, McLerran, JMP, Sexty '13

Gauge dynamics far from equilibrium

Abelian Higgs model in 2+1 dim

'overpopulation' initial conditions

Gasenzer, McLerran, JMP, Sexty '13

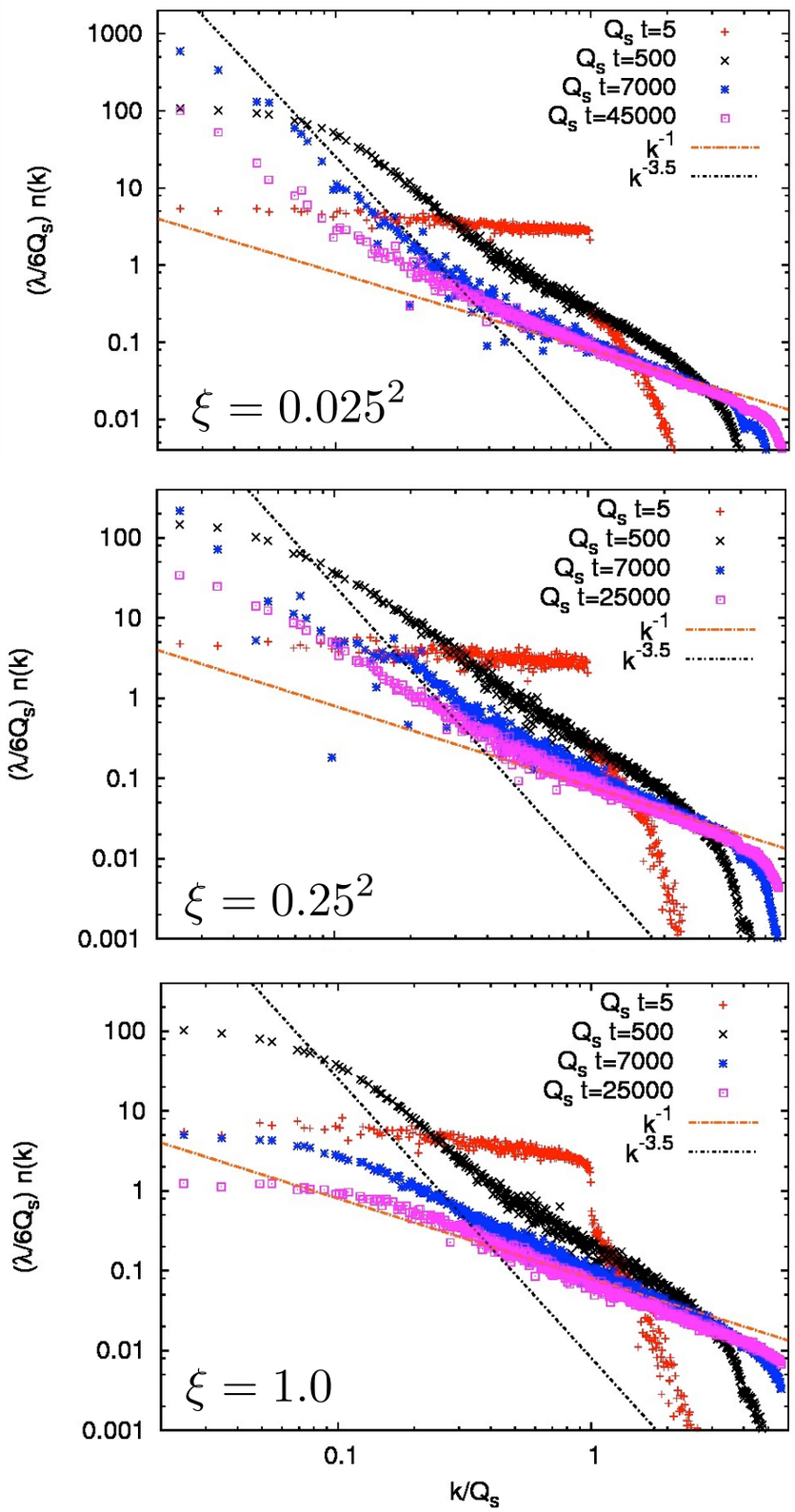

$$\frac{F_{\rm gi}(p=0)}{V} = \frac{1}{V^2}\int dxdy\phi^*(x)U(x,y)\phi(y)$$

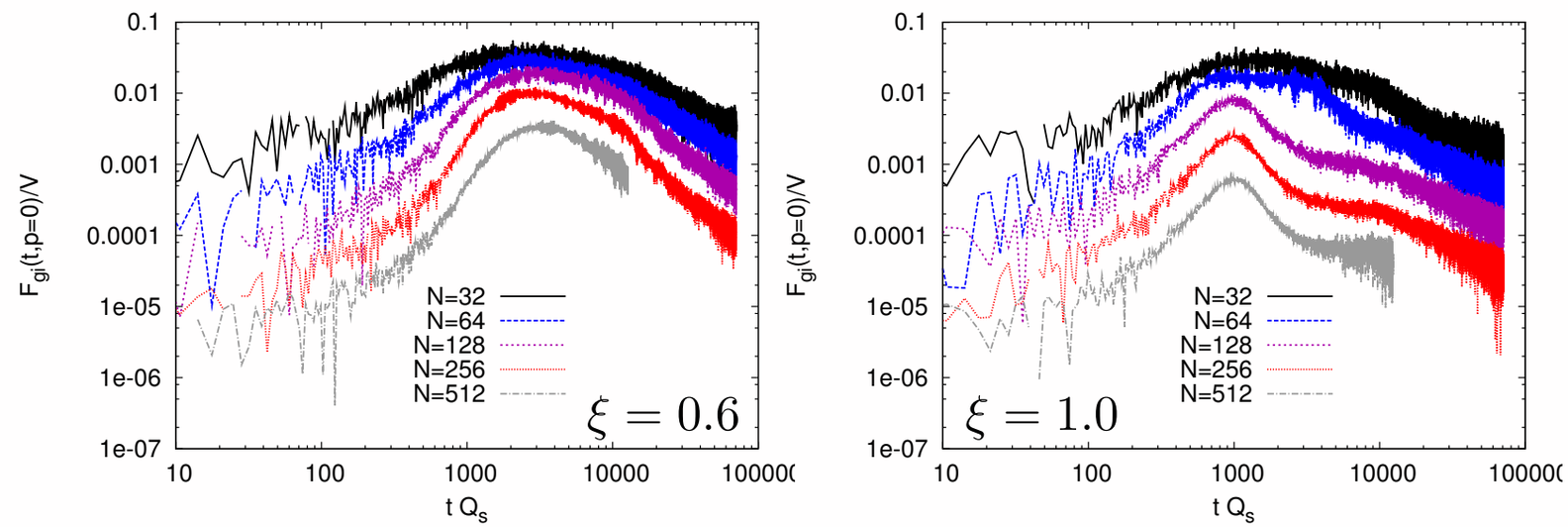

coupling

$$\xi = \frac{6e^2}{\lambda}$$

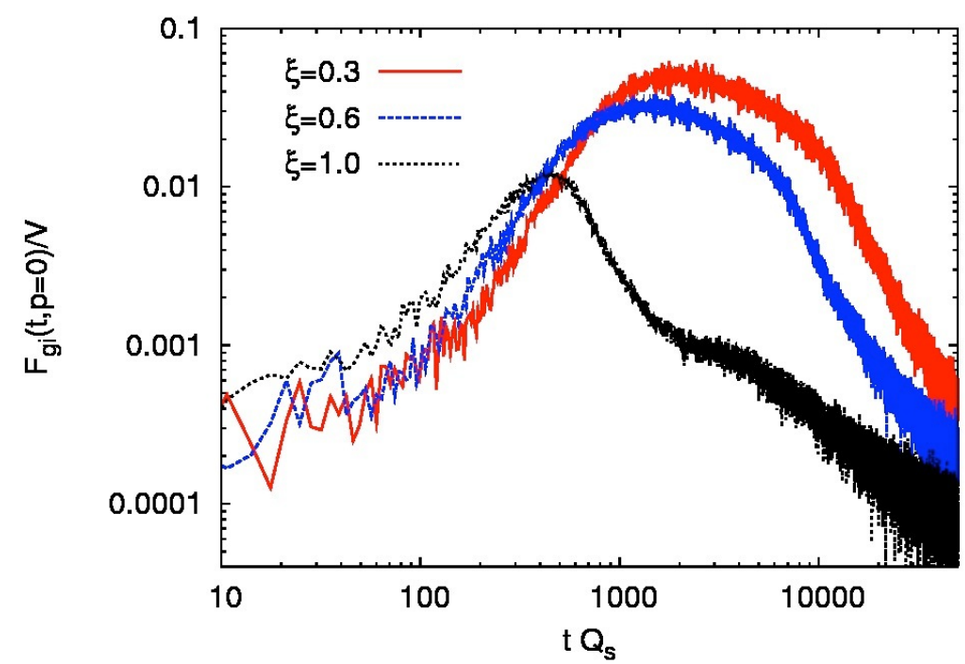

Spectral functions & transport coefficients

M. Haas, Fister, JMP ´13

Christiansen, M. Haas, JMP, Strodthoff, in prep.

Helmboldt, JMP, Strodthoff, in prep.

Heavy ion collisions

Shooting the elephant

Zhi Qiu and U. Heinz, to be published

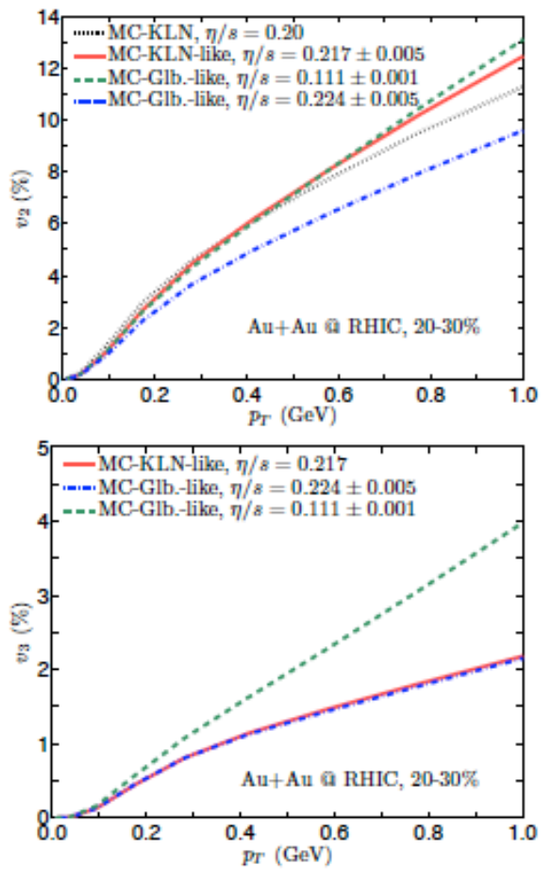

Proof of principle calculation:

- Take ensemble of sum of deformed Gaussian profiles, $s(\boldsymbol{r}_\perp) = s_2(\boldsymbol{r}_\perp; \tilde{\varepsilon}_2, \psi_2) + s_3(\boldsymbol{r}_\perp; \tilde{\varepsilon}_3, \psi_3)$, with
  1. equal Gaussian radii $R_2^2 = R_3^2 = 8\,\text{fm}^2$ to reproduce $\langle r_\perp^2 \rangle$ of MC-KLN source for 20-30% AuAu
  2. $\tilde{\varepsilon}_2$ and $\tilde{\varepsilon}_3$ adjusted such that
     - $\bar{\varepsilon}_{2,3} = \langle \varepsilon_{2,3} \rangle_{\text{KLN}}^{20-30\%}$ ("MC-KLN-like")
     - $\bar{\varepsilon}_{2,3} = \langle \varepsilon_{2,3} \rangle_{\text{Gl}}^{20-30\%}$ ("MC-Glauber-like")
  3. $\psi_2 = 0$, ψ_3 (direction of triangularity) distributed randomly
- Use $v_2^\pi(p_T)$ from VISH2+1 for $\eta/s = 0.20$ with MC-KLN initial conditions for 20-30% AuAu as "mock data"
- Fit mock $v_2^\pi(p_T)$ data with VISH2+1 for "MC-Glauber-like" or "MC-KLN-like" Gaussian initial conditions with both elliptic and triangular deformations by adjusting η/s
  $\Longrightarrow$ $(\eta/s)_{\text{KLN}} = 0.217 \pm 0.005$ for "MC-KLN-like",
  $(\eta/s)_{\text{Gl}} = 0.111 \pm 0.001$ for "MC-Glauber-like"
- Compute $v_3^\pi(p_T)$ for "MC-KLN-like" fit with $(\eta/s)_{\text{Gl}}$=0.217 and reproduce it with "MC-Glauber-like" initial condition by readjusting η/s
  $\Longrightarrow$ $(\eta/s)_{\text{Gl}}^{v_3} = 0.224 \pm 0.005$ for "MC-Glauber-like"
- Compute $v_2^\pi(p_T)$ for "MC-Glauber-like" initial profiles with readjusted $(\eta/s)_{\text{Gl}}^{v_3} = 0.224$ and compare with "MC-Glauber-like" fit to original mock data $\Longrightarrow$ clearly visible (and measurable) difference!

This exercise proves: (i) Fitting $v_3(p_T)$ data with MC-Glauber and MC-KLN initial conditions yields the same η/s (within narrow error band); (ii) The corresponding $v_2(p_T)$ fits are quite different, and only one (more precisely: at most one!) of the models will fit the corresponding $v_2(p_T)$ data.

U. Heinz, talk at RETUNE '12

Heavy ion collisions

Computing the elephant

Zhi Qiu and U. Heinz, to be published

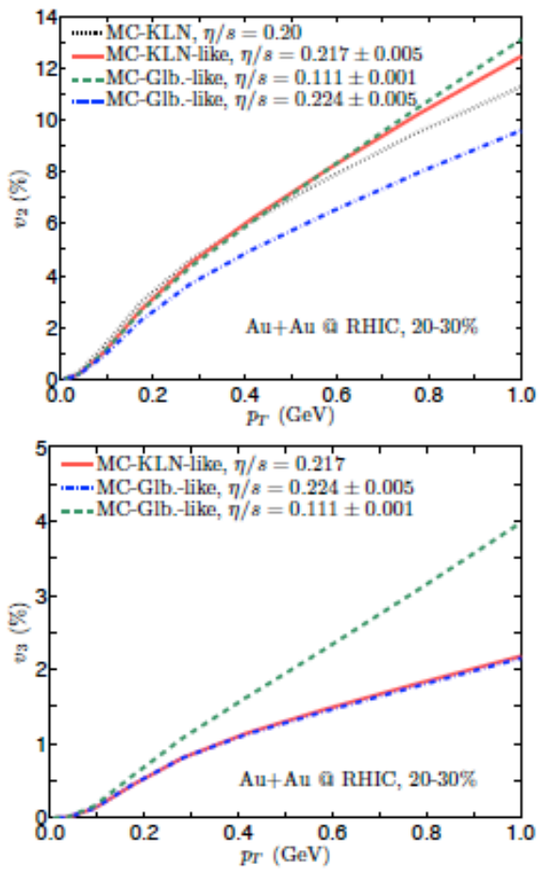

Proof of principle calculation:

- Take ensemble of sum of deformed Gaussian profiles, $s(\boldsymbol{r}_\perp) = s_2(\boldsymbol{r}_\perp; \tilde{\varepsilon}_2, \psi_2) + s_3(\boldsymbol{r}_\perp; \tilde{\varepsilon}_3, \psi_3)$, with
  1. equal Gaussian radii $R_2^2 = R_3^2 = 8\,\text{fm}^2$ to reproduce $\langle r_\perp^2 \rangle$ of MC-KLN source for 20-30% AuAu
  2. $\tilde{\varepsilon}_2$ and $\tilde{\varepsilon}_3$ adjusted such that
     - $\bar{\varepsilon}_{2,3} = \langle \varepsilon_{2,3} \rangle_{\text{KLN}}^{20-30\%}$ ("MC-KLN-like")
     - $\bar{\varepsilon}_{2,3} = \langle \varepsilon_{2,3} \rangle_{\text{Gl}}^{20-30\%}$ ("MC-Glauber-like")
  3. $\psi_2 = 0$, ψ_3 (direction of triangularity) distributed randomly
- Use $v_2^\pi(p_T)$ from VISH2+1 for $\eta/s = 0.20$ with MC-KLN initial conditions for 20-30% AuAu as "mock data"
- Fit mock $v_2^\pi(p_T)$ data with VISH2+1 for "MC-Glauber-like" or "MC-KLN-like" Gaussian initial conditions with both elliptic and triangular deformations by adjusting η/s
  $\Longrightarrow (\eta/s)_{\text{KLN}} = 0.217 \pm 0.005$ for "MC-KLN-like",
  $(\eta/s)_{\text{Gl}} = 0.111 \pm 0.001$ for "MC-Glauber-like"
- Compute $v_3^\pi(p_T)$ for "MC-KLN-like" fit with $(\eta/s)_{\text{Gl}}$=0.217 and reproduce it with "MC-Glauber-like" initial condition by readjusting η/s
  $\Longrightarrow (\eta/s)_{\text{Gl}}^{v_3} = 0.224 \pm 0.005$ for "MC-Glauber-like"
- Compute $v_2^\pi(p_T)$ for "MC-Glauber-like" initial profiles with readjusted $(\eta/s)_{\text{Gl}}^{v_3} = 0.224$ and compare with "MC-Glauber-like" fit to original mock data $\Longrightarrow$ clearly visible (and measurable) difference!

This exercise proves: (i) Fitting $v_3(p_T)$ data with MC-Glauber and MC-KLN initial conditions yields the same η/s (within narrow error band); (ii) The corresponding $v_2(p_T)$ fits are quite different, and only one (more precisely: at most one!) of the models will fit the corresponding $v_2(p_T)$ data.

Transport in QCD

correlations of energy-momentum tensor

M. Haas, Fister, JMP ´13

Flow

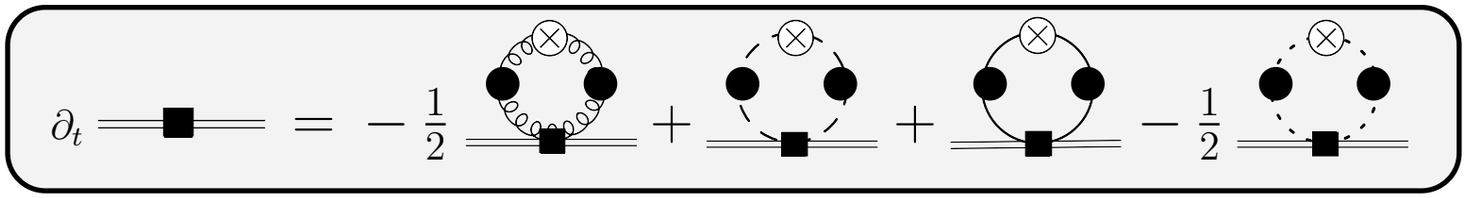

$\rho_{\pi\pi}$

Diagrammatic representation

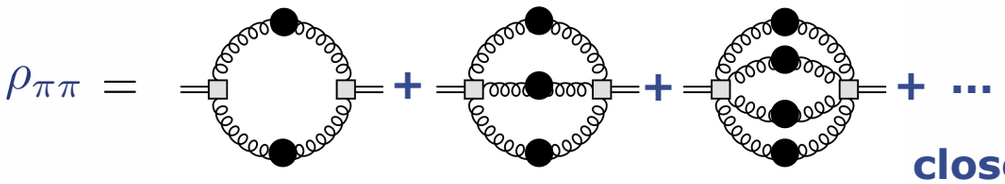

closed form

full computation Christiansen, Haas, JMP, Strodthoff, in prep.

Vertex corrections

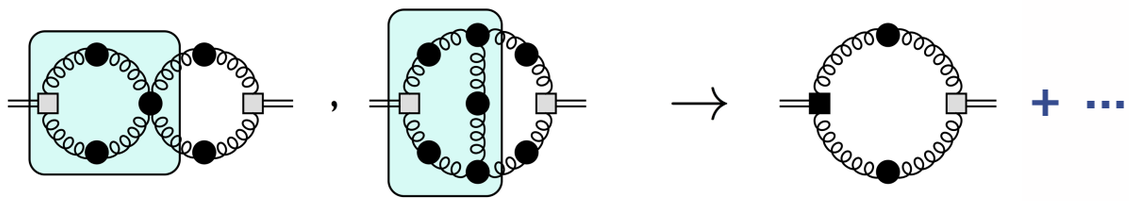

Transport in QCD

correlations of energy-momentum tensor

M. Haas, Fister, JMP ´13

Flow

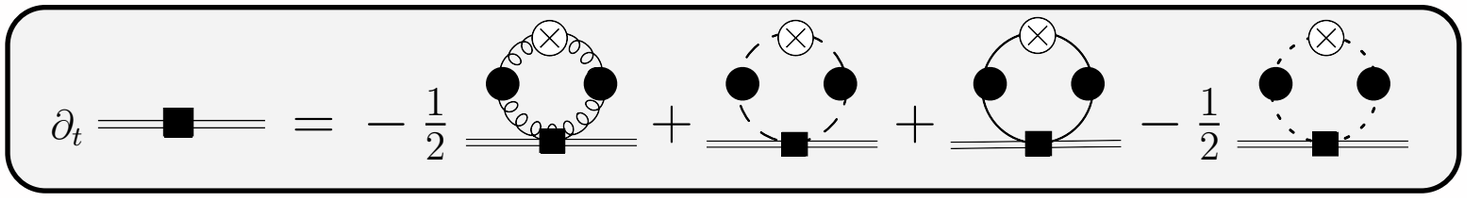

$\rho_{\pi\pi}$

Diagrammatic representation

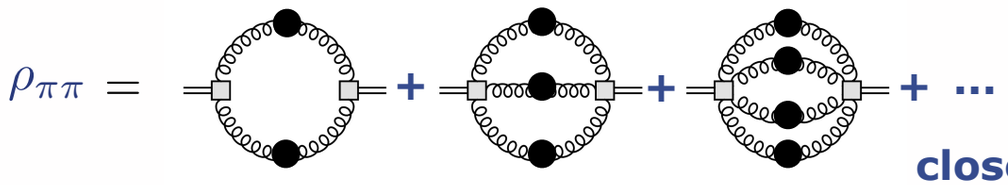

closed form

full computation Christiansen, Haas, JMP, Strodthoff, in prep.

Complete 2-loop corrections

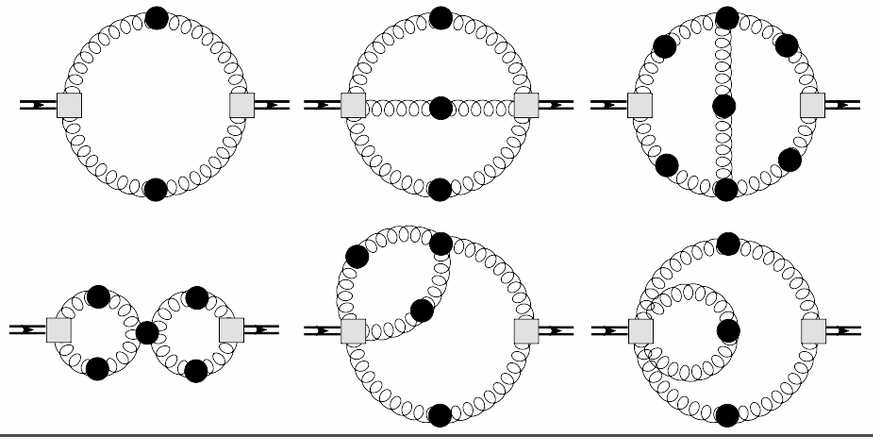

Transport in QCD

correlations of energy-momentum tensor

M. Haas, Fister, JMP ´13

Flow

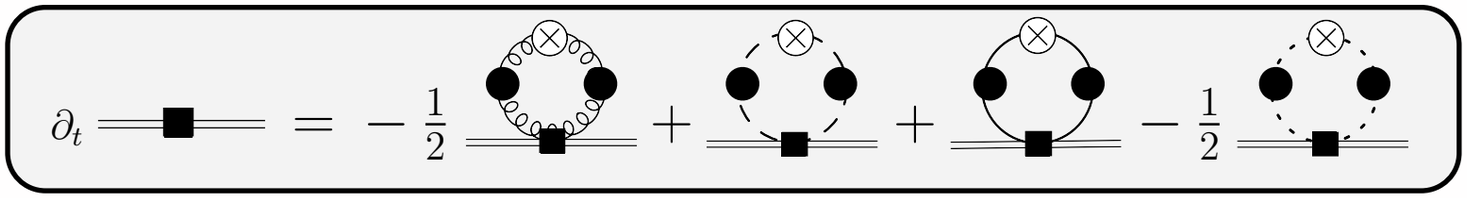

$\rho_{\pi\pi}$

Current approximation

$\rho_{\pi\pi} =$

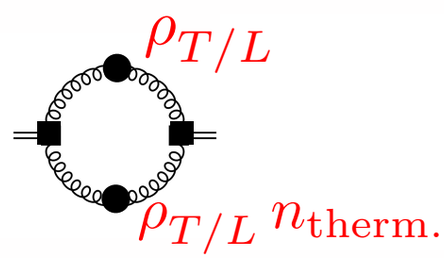

with optimised RG-scheme from Fister, JMP ’13

$\rho_{T/L}$ with MEM

$$\rho_{\pi\pi}(p) = \frac{2d_A}{3}\int \frac{d^4k}{(2\pi)^4}\left[n(k^0) - n(k^0+p_0)\right]\left(V_{TT}\rho_T(k)\rho_T(k+p) + V_{TL}\rho_T(k)\rho_L(k+p) + V_{LL}\rho_L(k)\rho_L(k+p)\right)$$

Transport in QCD

correlations of energy-momentum tensor

M. Haas, Fister, JMP ´13

Flow

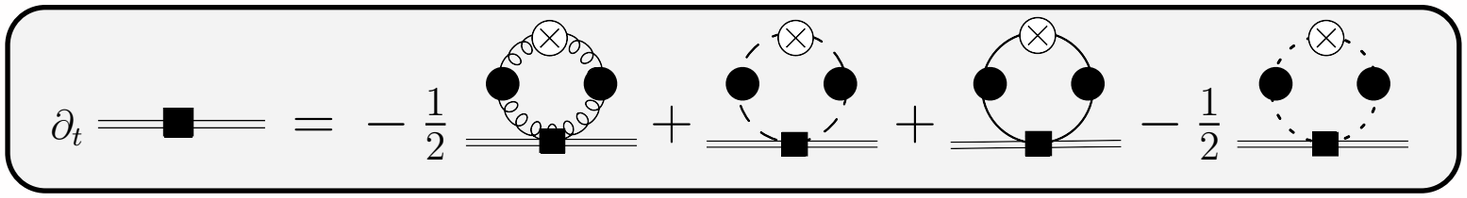

$\rho_{\pi\pi}$

Current approximation

$\rho_{\pi\pi} =$

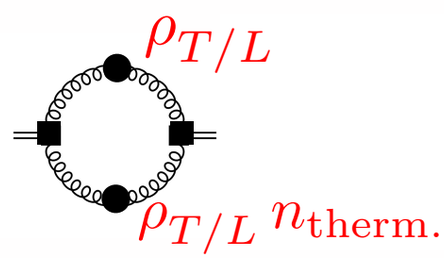

with optimised RG-scheme from **Fister, JMP '13**

$\rho_{T/L}$ **with MEM**

'Those are my methods (principles),
and if you don't like them...well, I have others'

direct computation **Groucho Marx**

$$\rho_{\pi\pi}(p) = \frac{2d_A}{3}\int \frac{d^4k}{(2\pi)^4}\left[n(k^0) - n(k^0+p_0)\right]\left(V_{TT}\rho_T(k)\rho_T(k+p) + V_{TL}\rho_T(k)\rho_L(k+p) + V_{LL}\rho_L(k)\rho_L(k+p)\right)$$

Transport in QCD

correlations of energy-momentum tensor

M. Haas, Fister, JMP ´13

Shear viscosity

$$\eta = \frac{1}{20} \left.\frac{d}{d\omega}\right|_{\omega=0} \rho_{\pi\pi}(\omega, 0)$$

Kubo relation

Current approximation

$\rho_{\pi\pi} =$

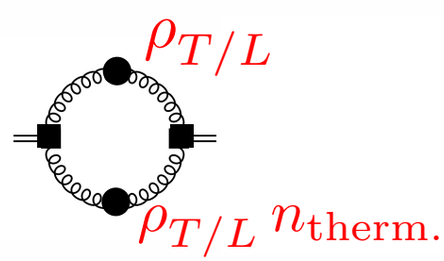

$\rho_{T/L}$ **with MEM**

$$\rho_{\pi\pi}(p) = \frac{2d_A}{3} \int \frac{d^4k}{(2\pi)^4} \left[n(k^0) - n(k^0 + p_0)\right] \left(V_{TT}\rho_T(k)\rho_T(k+p) + V_{TL}\rho_T(k)\rho_L(k+p) + V_{LL}\rho_L(k)\rho_L(k+p)\right)$$

Viscosity in pure glue

imaginary time correlations

M. Haas, Fister, JMP ´13

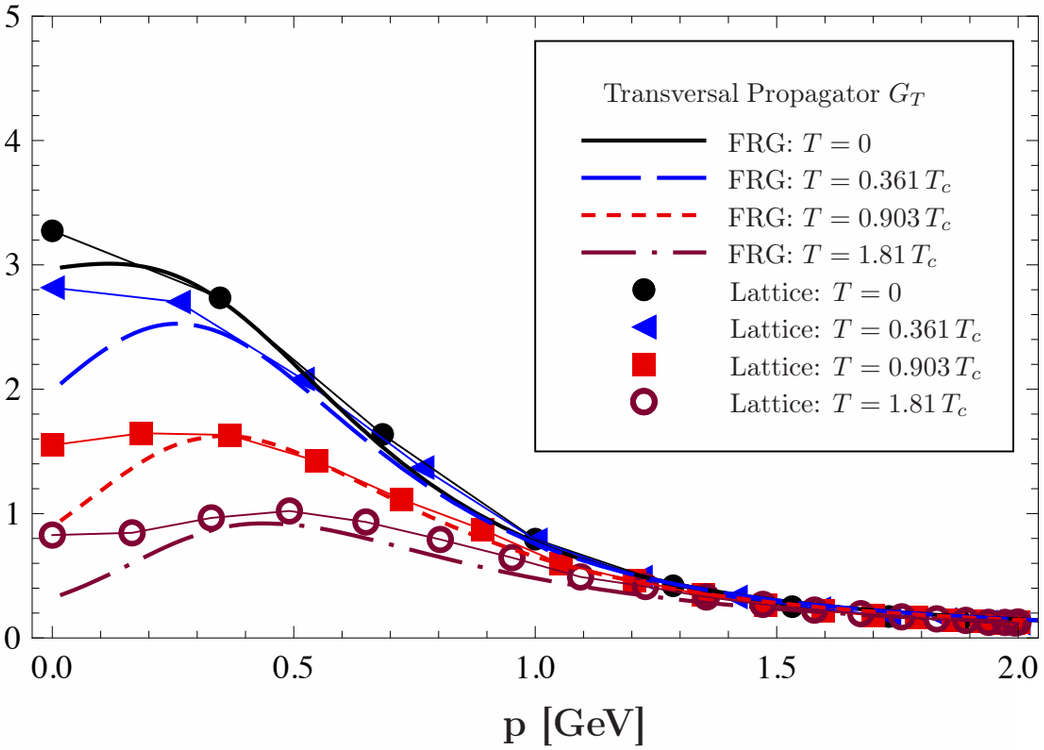

transversal gluon propagator

$G_T(\tau, \vec{p})$

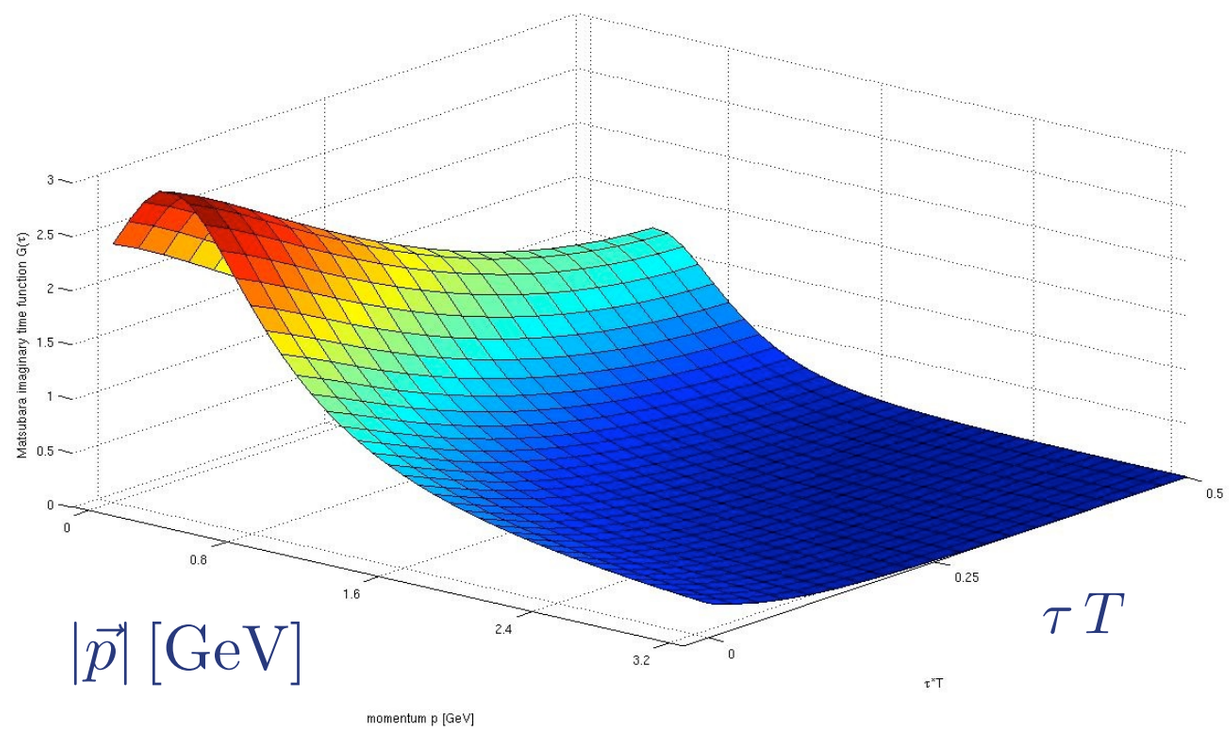

$|\vec{p}|$ [GeV]

$\tau\, T$

Viscosity in pure glue

gluon spectral functions

M. Haas, Fister, JMP ´13

transversal

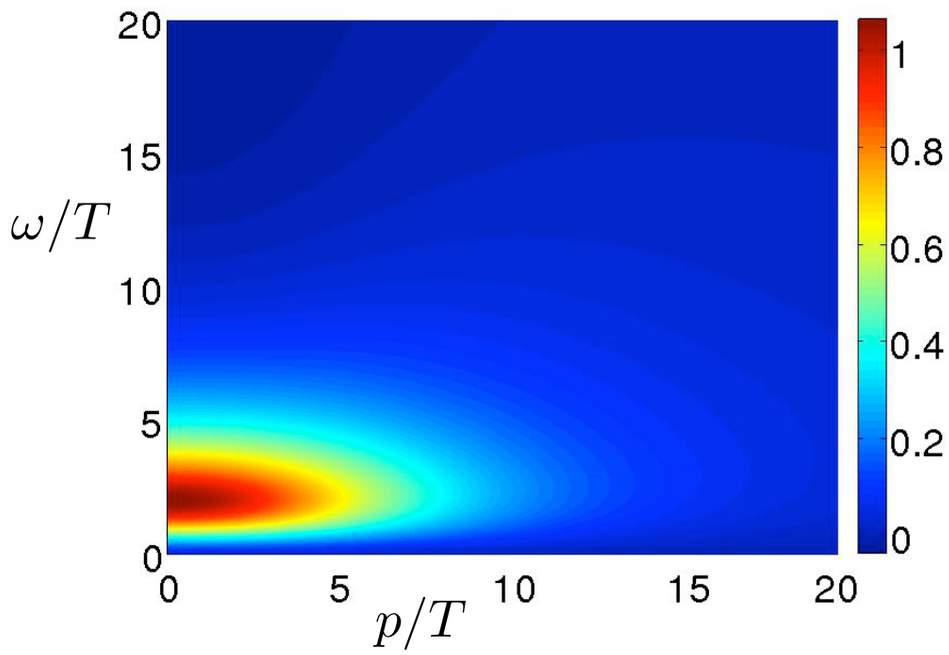

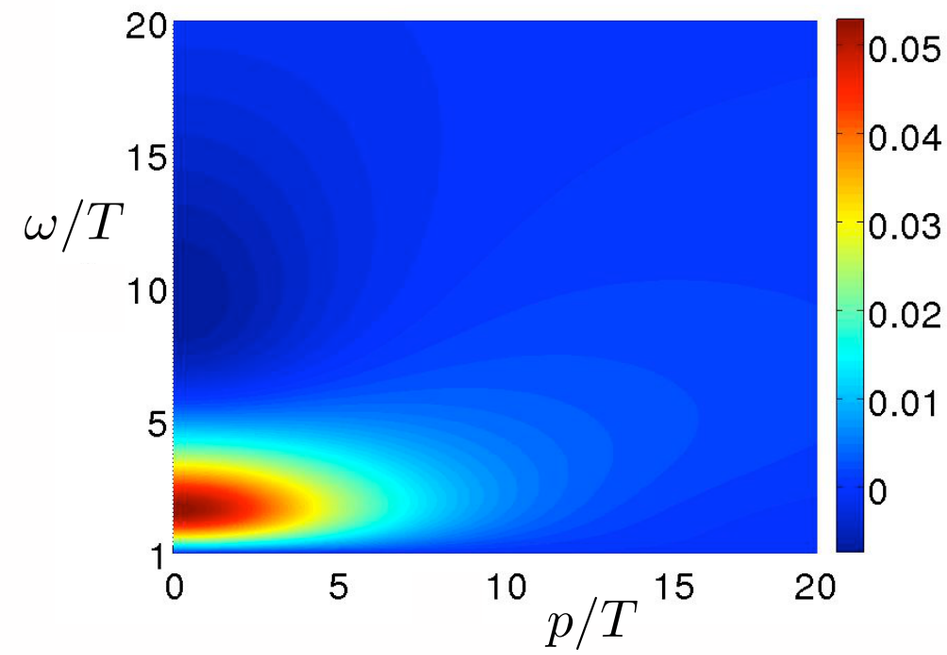

$\mathbf{T = 0.36T_c}$

longitudinal

$\mathbf{T = 1.8T_c}$

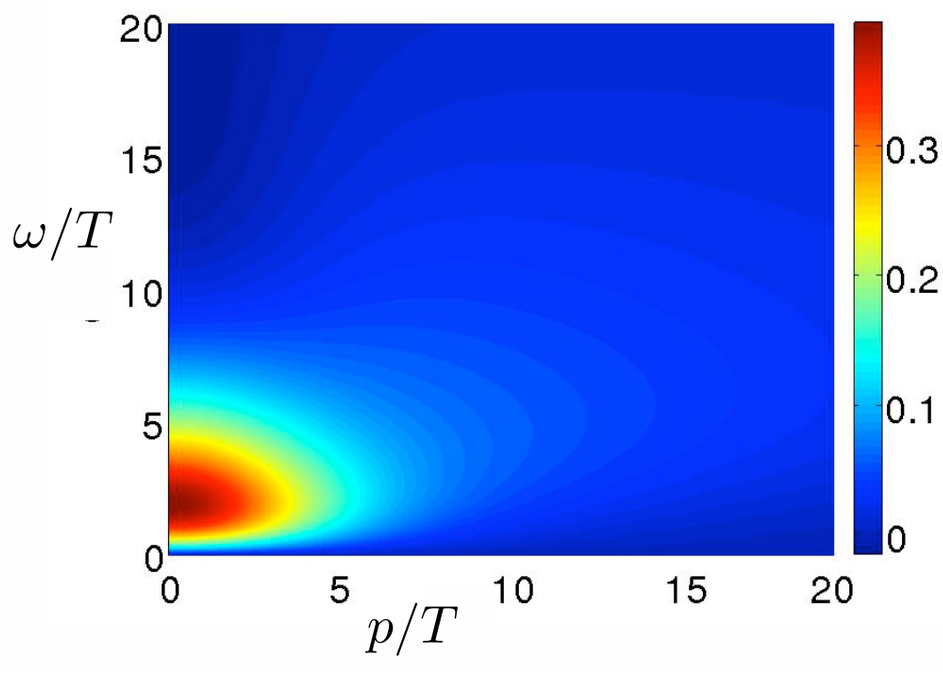

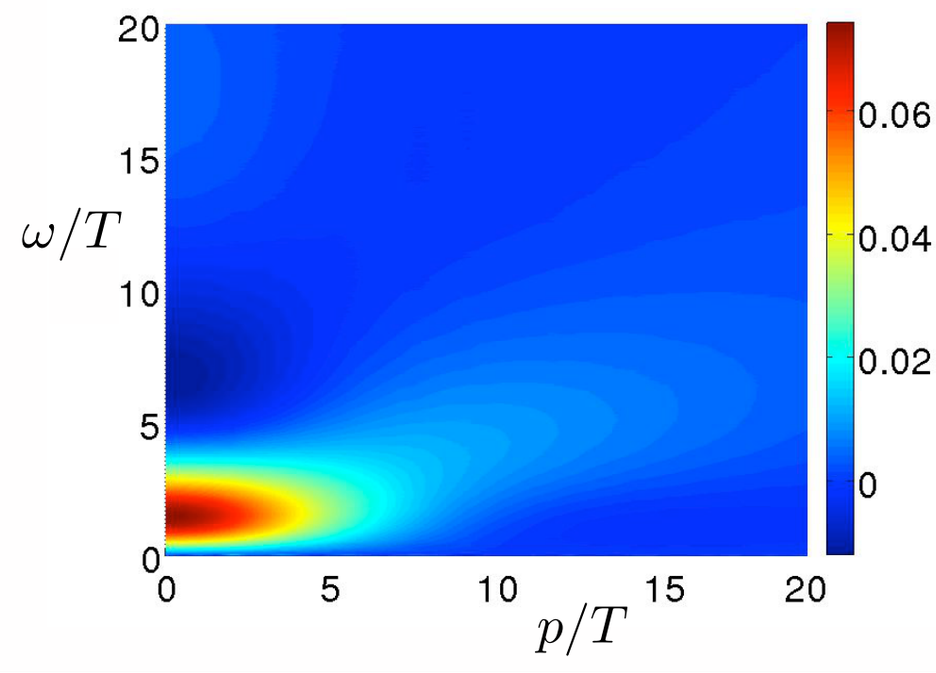

Viscosity in pure glue

spectral functions

transversal spectral function

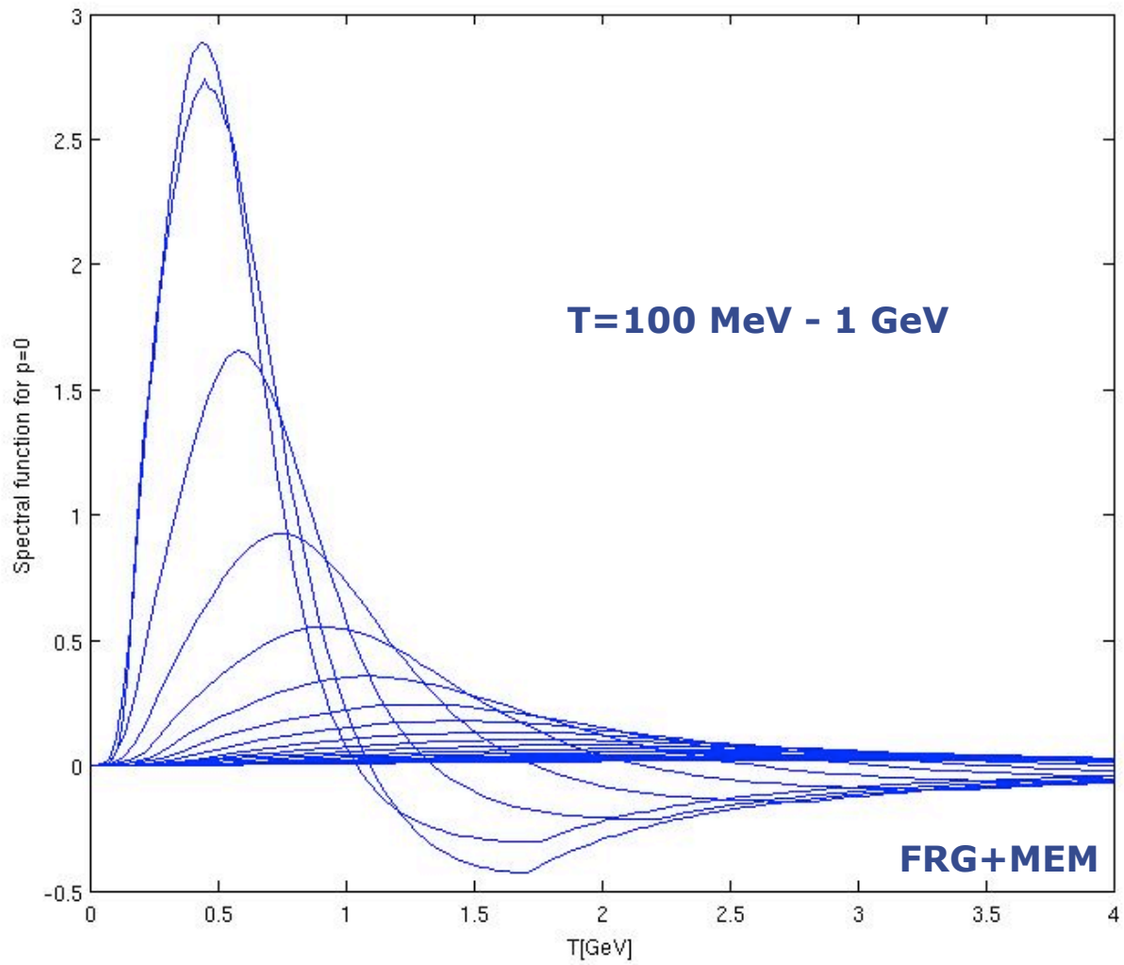

M. Haas, Fister, JMP ´13

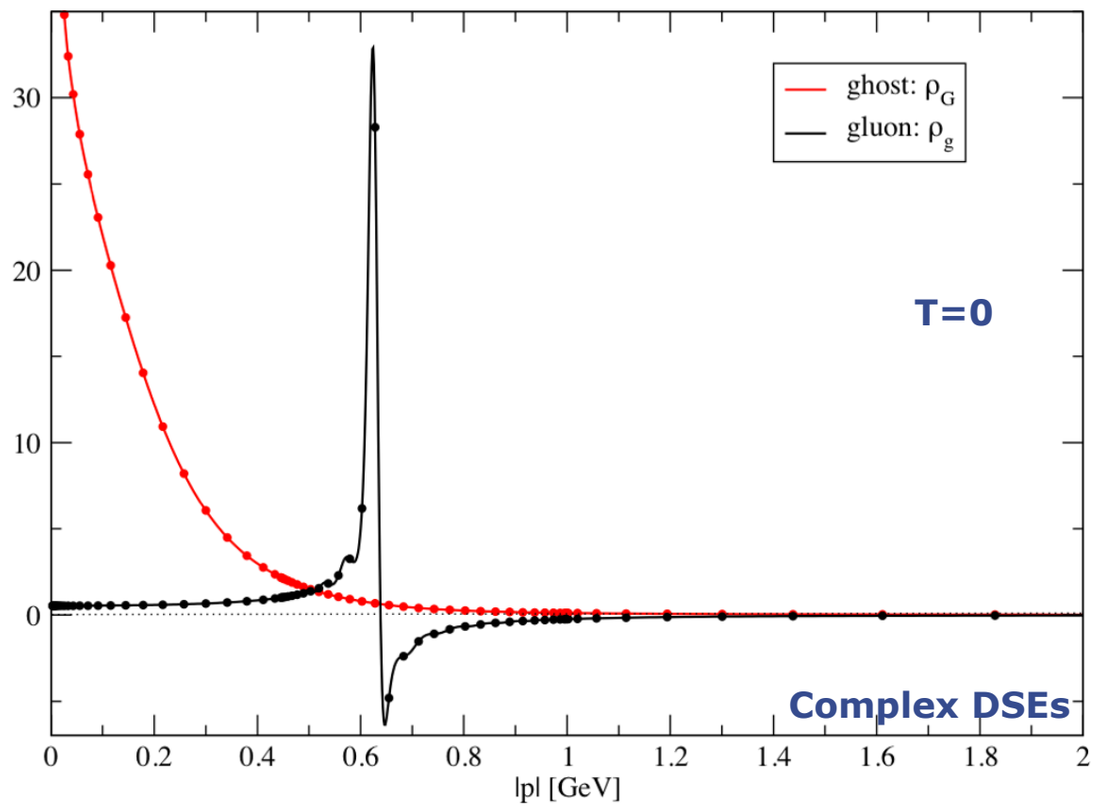

Strauss, Fischer, Kellermann ’12

pion and sigma spectral functions

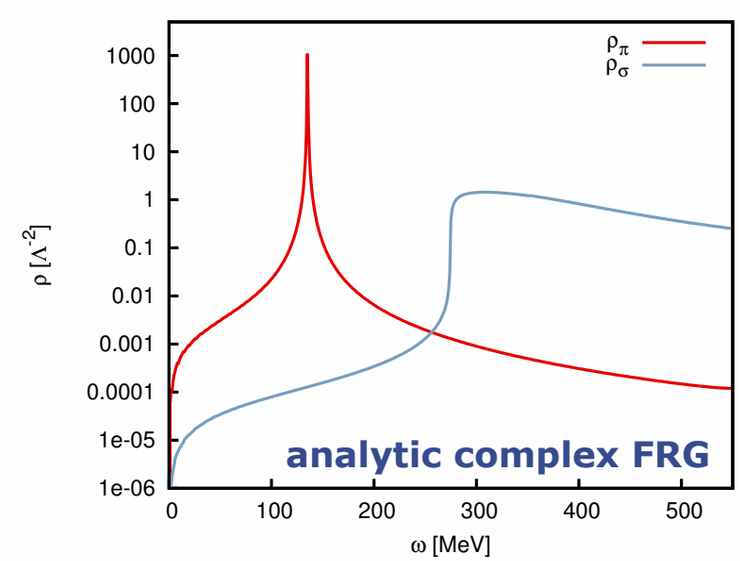

Kamikado, Strodthoff, von Smekal, Wambach ’13

Viscosity in pure glue

spectral functions

pion and sigma spectral functions

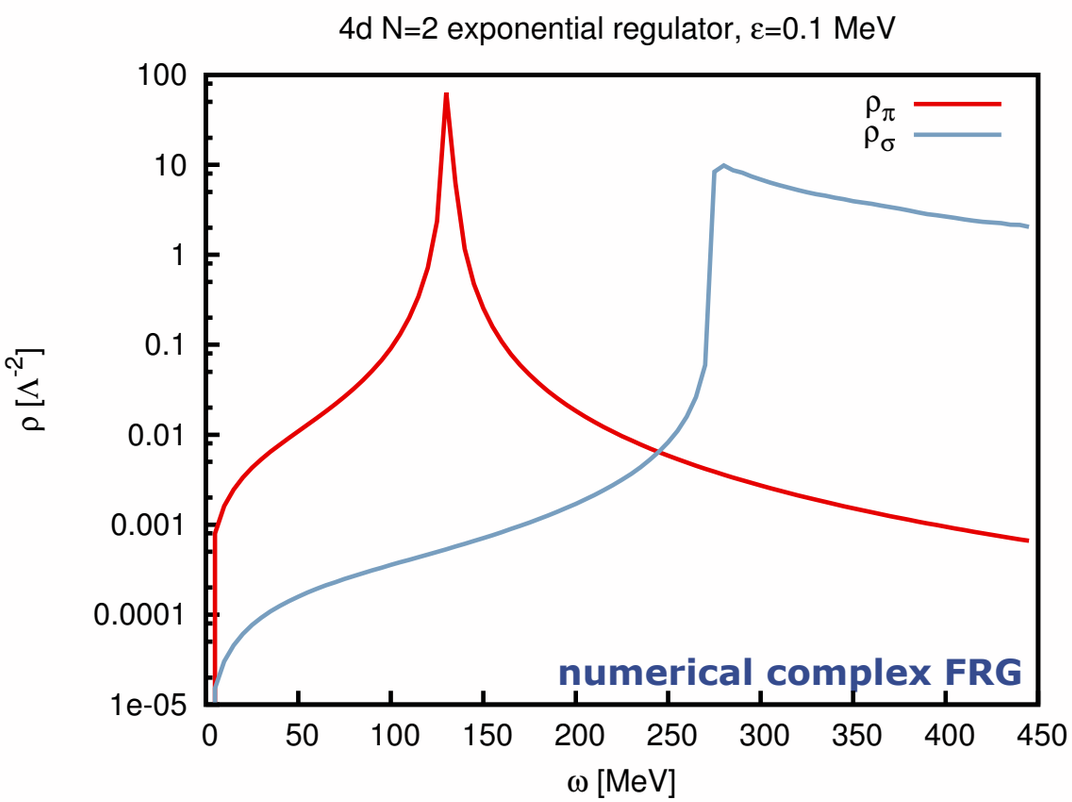

JMP, Strodthoff, in preparation

'Those are my methods (principles), and if you don't like them...well, I have others'

direct computation **Groucho Marx**

Viscosity in pure glue

spectral functions

pion and sigma spectral functions

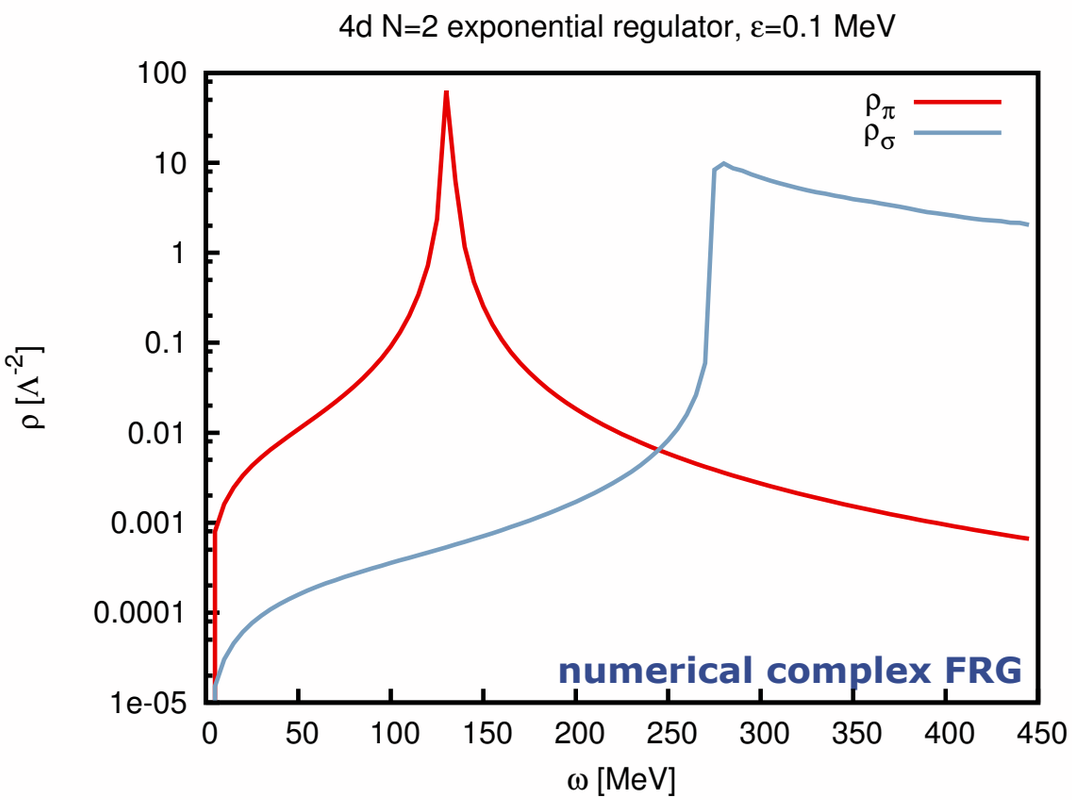

JMP, Strodthoff, in preparation

QM-model

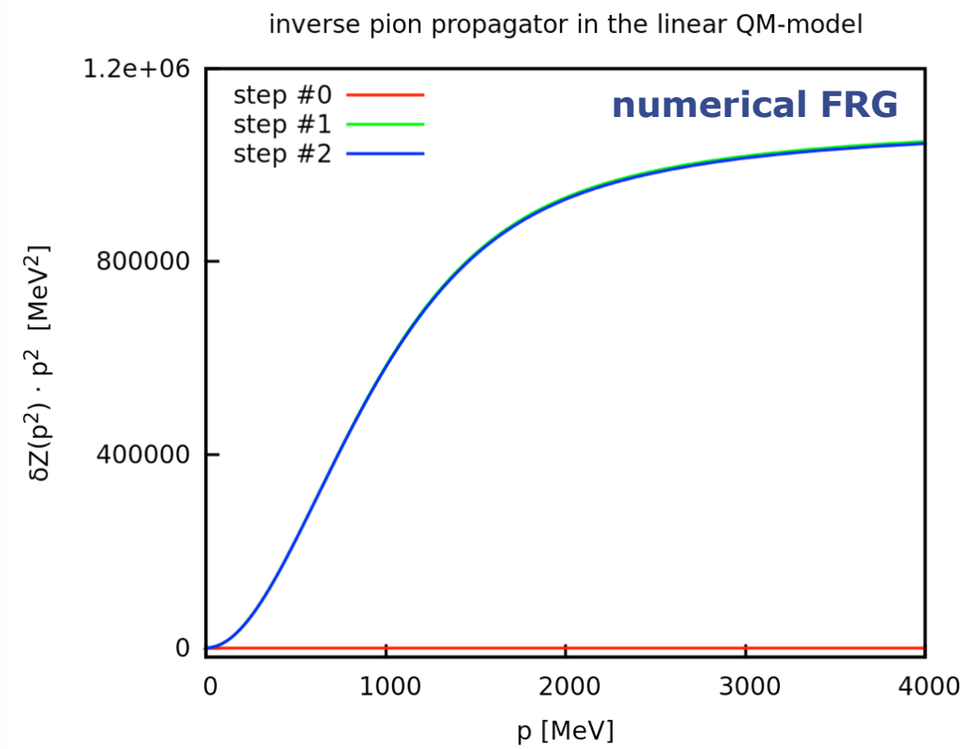

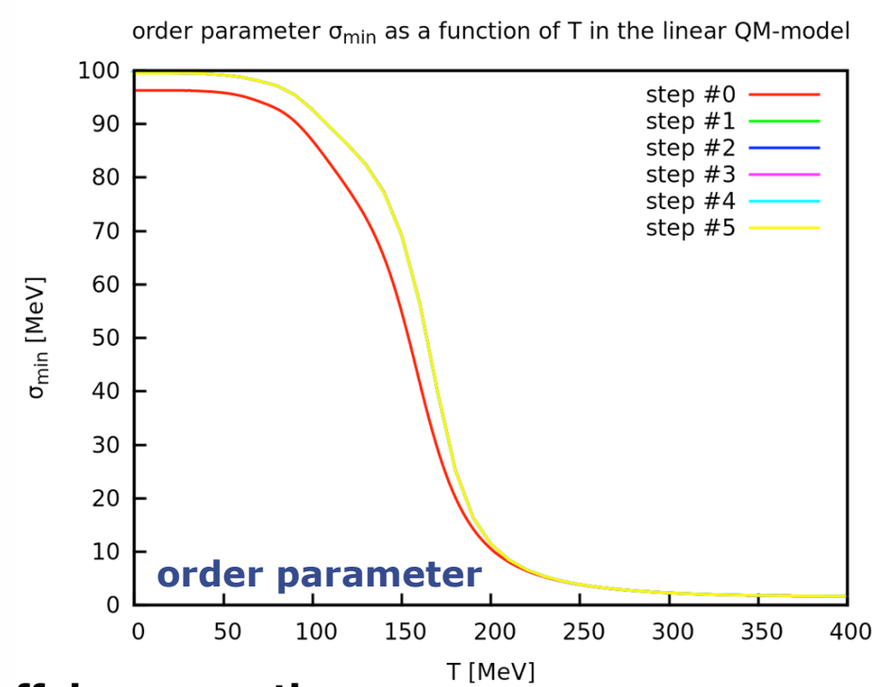

O(N)-model

iteration step	σ_0 [MeV]	δ_ρ [%]	m_{pole} [MeV]	m_{screen} [MeV]	δ_m [%]
0	93.55	0.0043	130.3113	136.7593	4.9
1	100.05	0.0028	126.6390	126.4590	0.14
5	99.38	0.0043	127.0347	127.0110	0.019

QM-model

iteration step	σ_0 [MeV]	δ_ρ [%]	m_{pole} [MeV]	m_{screen} [MeV]	δ_m [%]
0	96.25	0.0052	91.4911	134.8281	47
1	99.56	0.0044	90.8841	91.1611	0.30
5	99.56	0.0073	90.9244	91.1551	0.25

Helmboldt, JMP, Strodthoff, in preparation

Viscosity in pure glue

spectral functions

M. Haas, Fister, JMP ´13

transversal

T=1.44 T_c

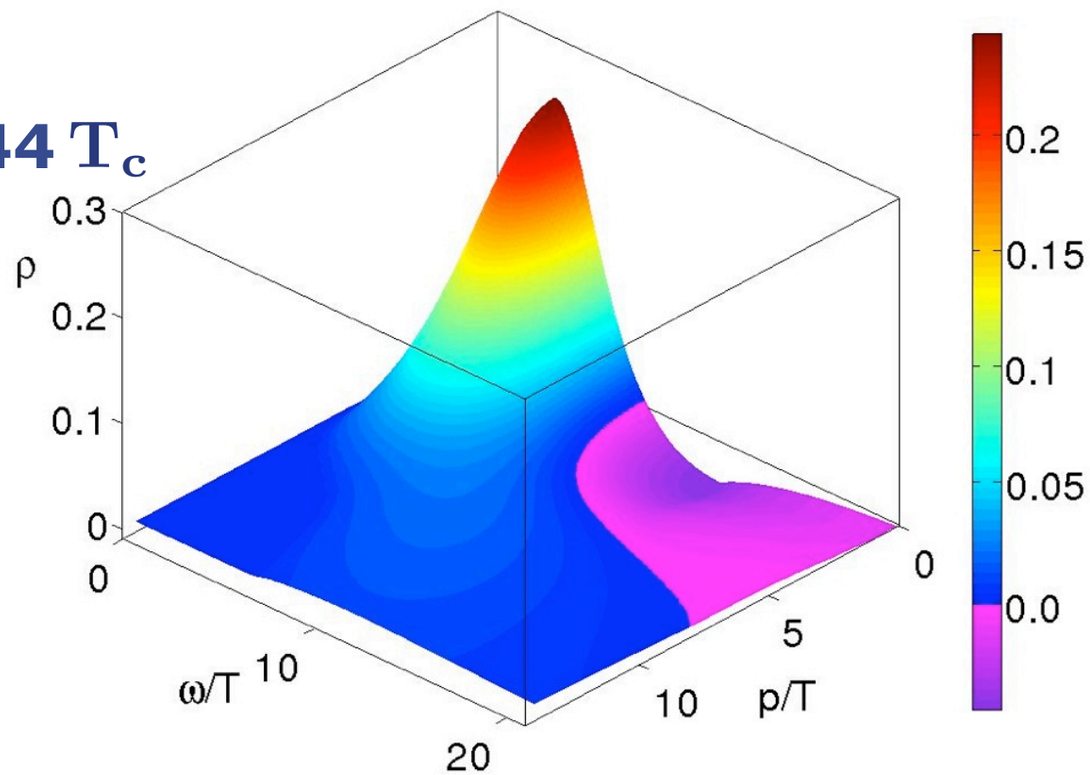

T=1.44 T_c

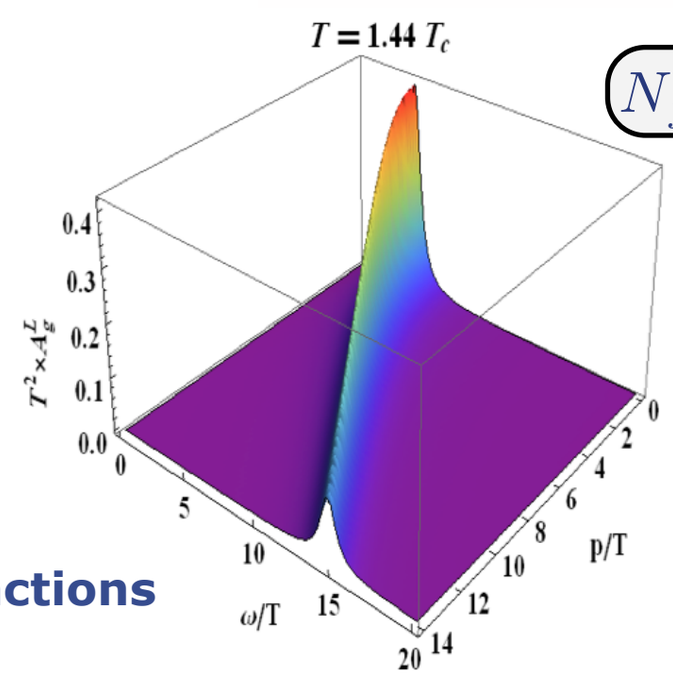

N_f=2+1

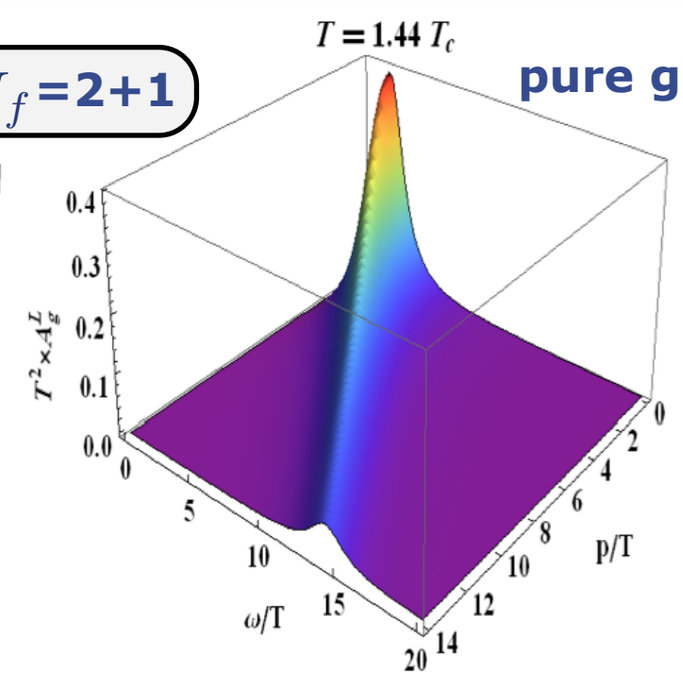

pure glue

PHSD spectral functions

Viscosity in pure glue

shear viscosity

M. Haas, Fister, JMP ´13

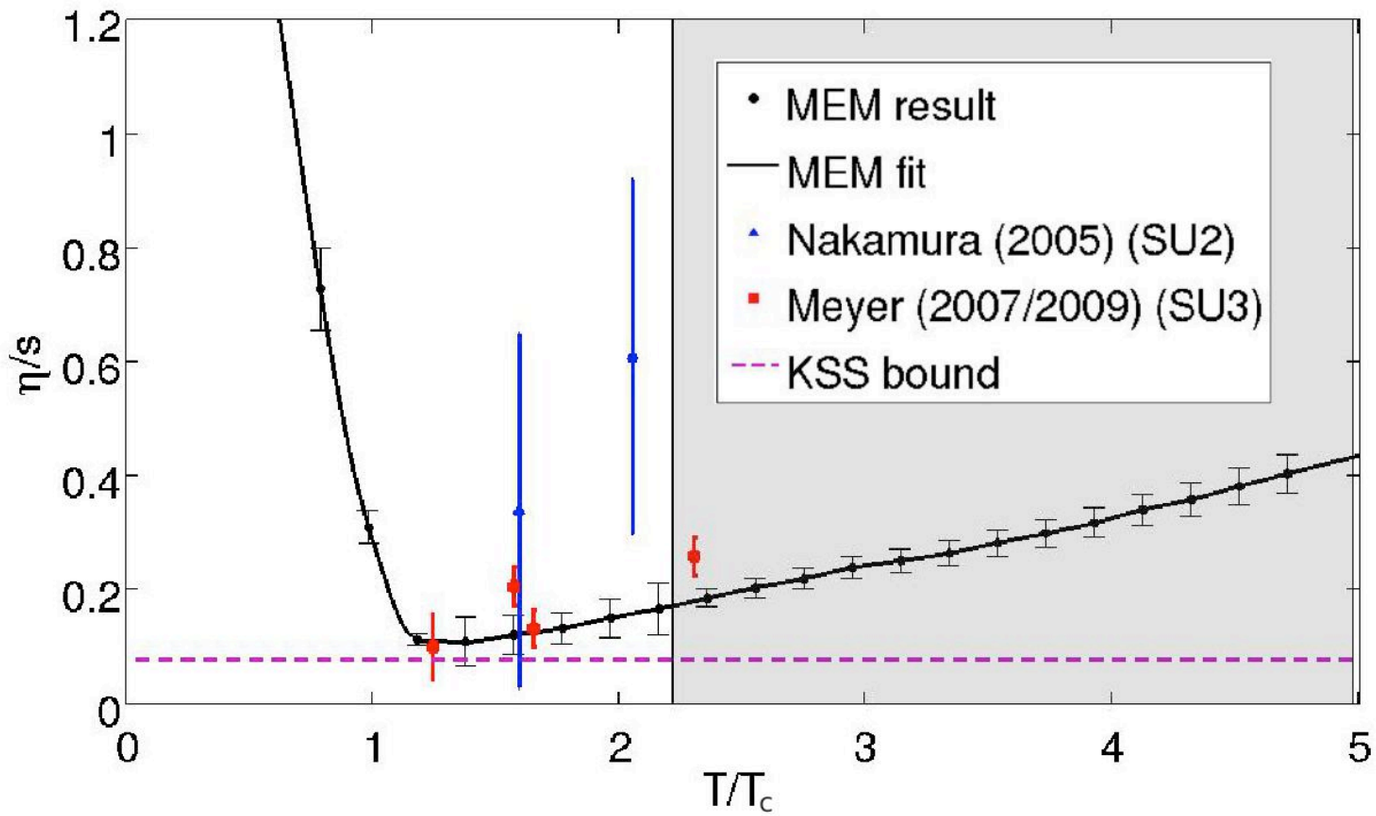

$T \lesssim 2T_c$: MEM+optimised RG-scheme systematic error estimates

Shaded area: MEM error estimates

Kubo relation

$$\eta = \frac{1}{20}\frac{d}{d\omega}\bigg|_{\omega=0}\rho_{\pi\pi}(\omega,0)$$

Diagrammatic representation

$\rho_{\pi\pi} =$ 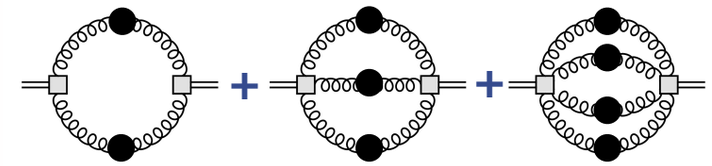

+ ··· closed form

minimum at T = 1.25$\mathrm{T_c}$: $\frac{\eta}{\mathrm{s}} = 1.45\frac{1}{4\pi}$

scale matching with QCD: $\frac{\eta}{\mathrm{s}} = 2.27\frac{1}{4\pi}$

H. Meyer ’09

Boyd, Engels, Karsch ’95

entropy lattice

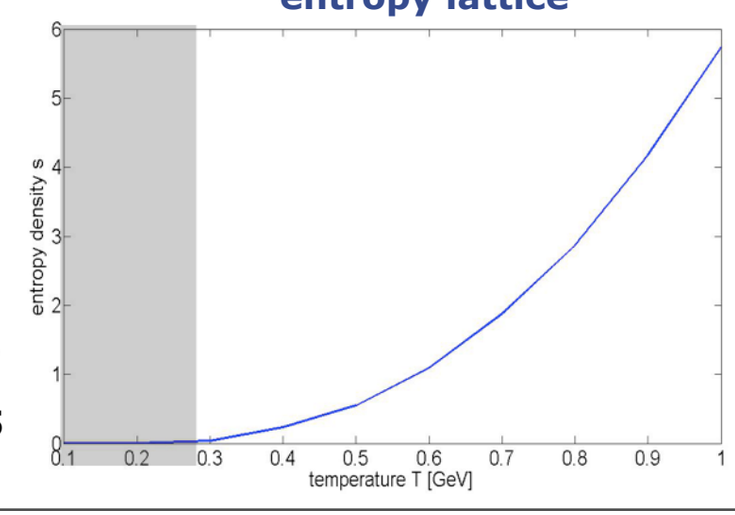

Viscosity in pure glue

shear viscosity

Christiansen, M. Haas, JMP, Strodthoff, in prep.

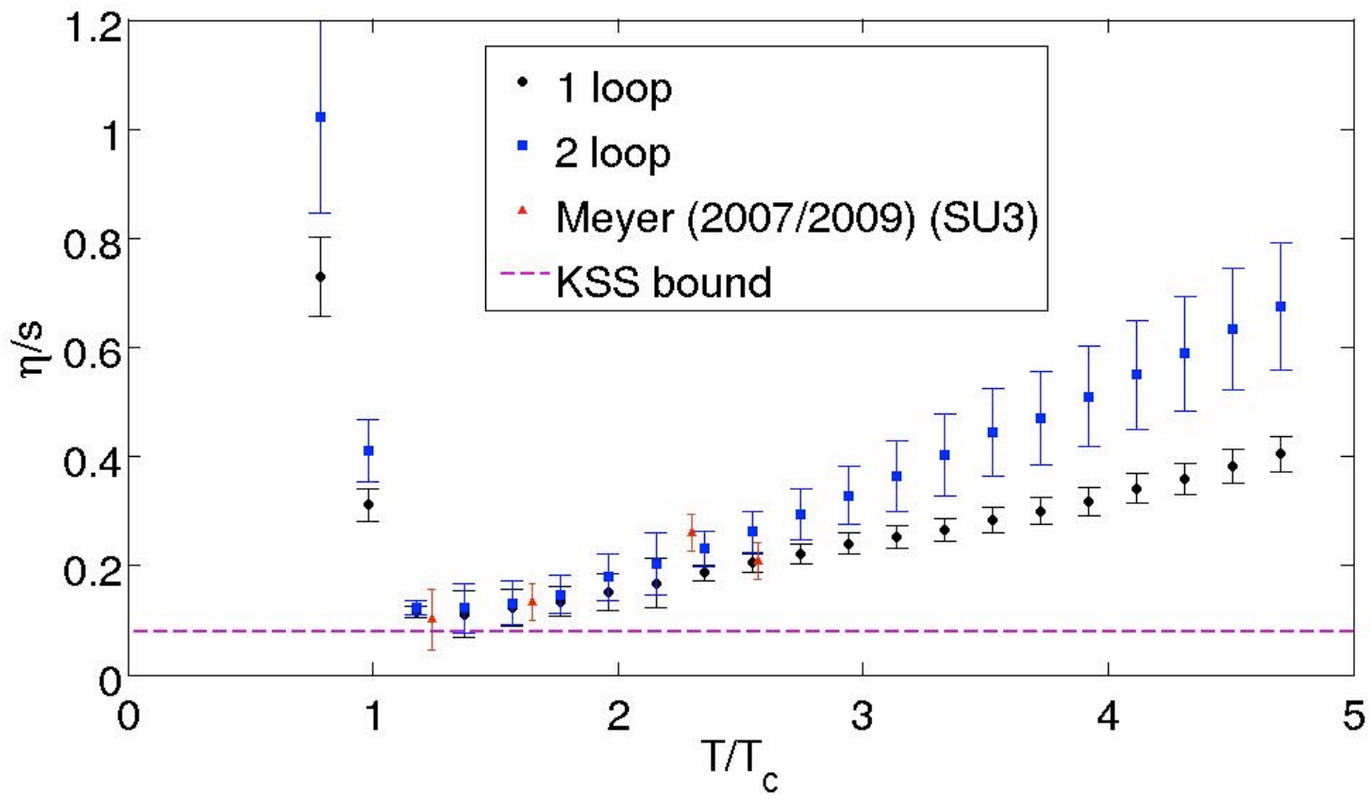

Kubo relation

$$\eta = \frac{1}{20}\frac{d}{d\omega}\bigg|_{\omega=0}\rho_{\pi\pi}(\omega,0)$$

Diagrammatic representation

$\rho_{\pi\pi} =$

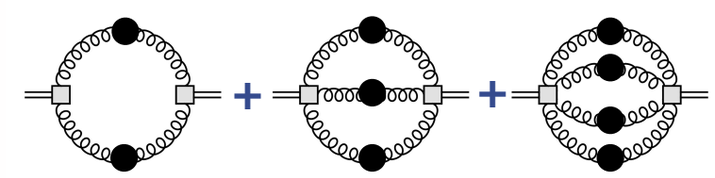

+ ··· closed form

minimum at T = 1.25T_c : $\frac{\eta}{s} = 1.45\frac{1}{4\pi}$

scale matching with QCD: $\frac{\eta}{s} = 2.27\frac{1}{4\pi}$

H. Meyer '09

Boyd, Engels, Karsch '95

entropy lattice

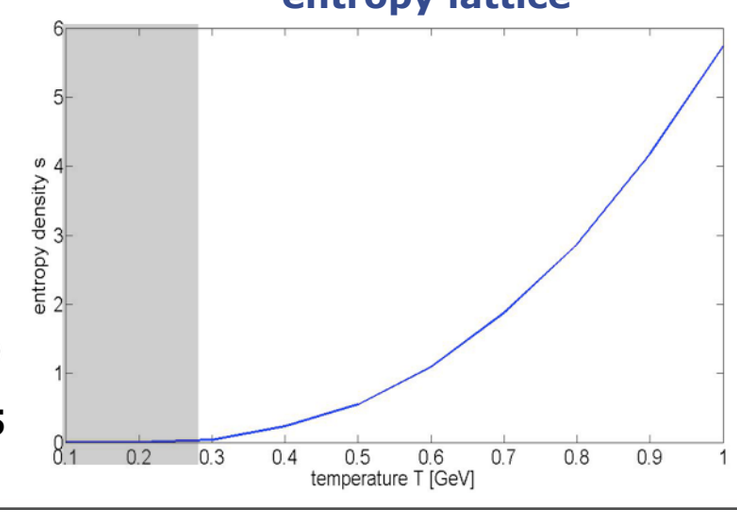

Viscosity in pure glue

shear viscosity

Christiansen, M. Haas, JMP, Strodthoff, in prep.

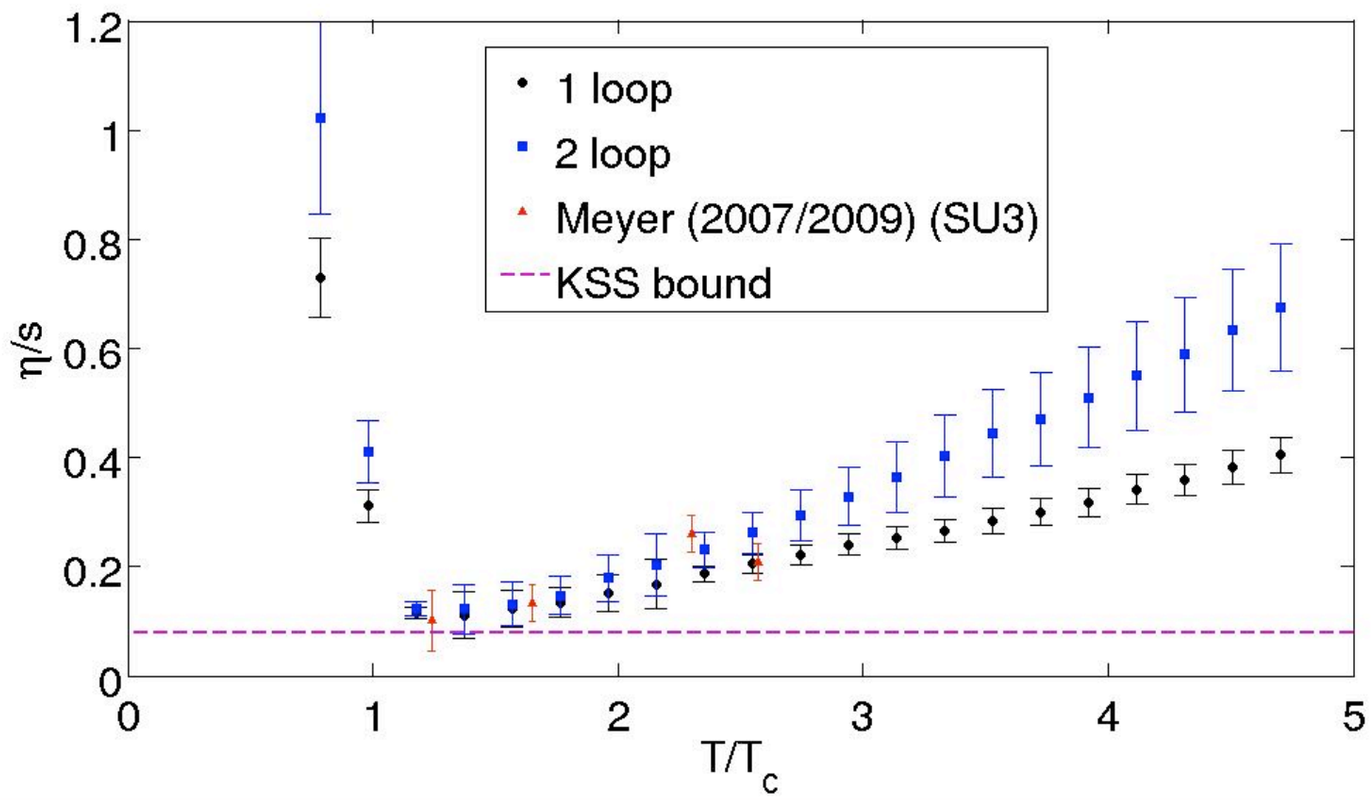

Kubo relation

$$\eta = \frac{1}{20}\frac{d}{d\omega}\bigg|_{\omega=0}\rho_{\pi\pi}(\omega,0)$$

Diagrammatic representation

$\rho_{\pi\pi} =$ 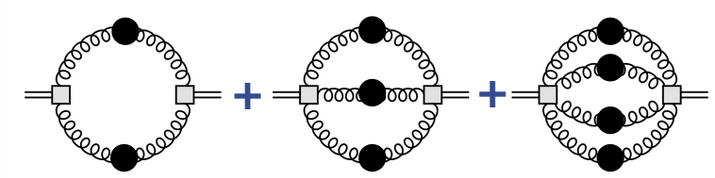

+ ··· closed form

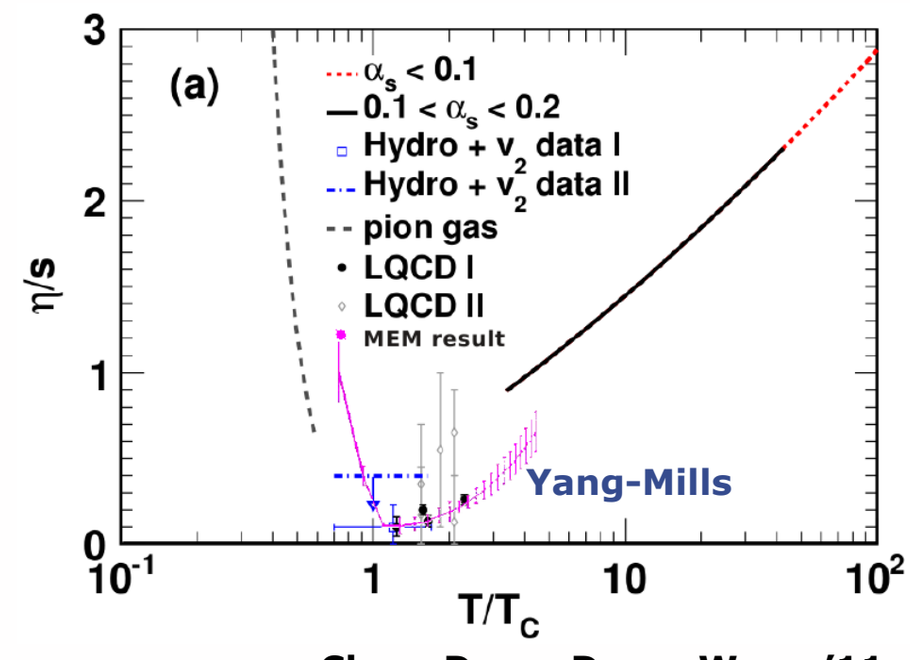

Chen, Deng, Dong, Wang '11

minimum at T = 1.25T_c : $\frac{\eta}{s} = 1.45\frac{1}{4\pi}$

scale matching with QCD: $\frac{\eta}{s} = 2.27\frac{1}{4\pi}$

Viscosity in pure glue

shear viscosity

Christiansen, M. Haas, JMP, Strodthoff, in prep.

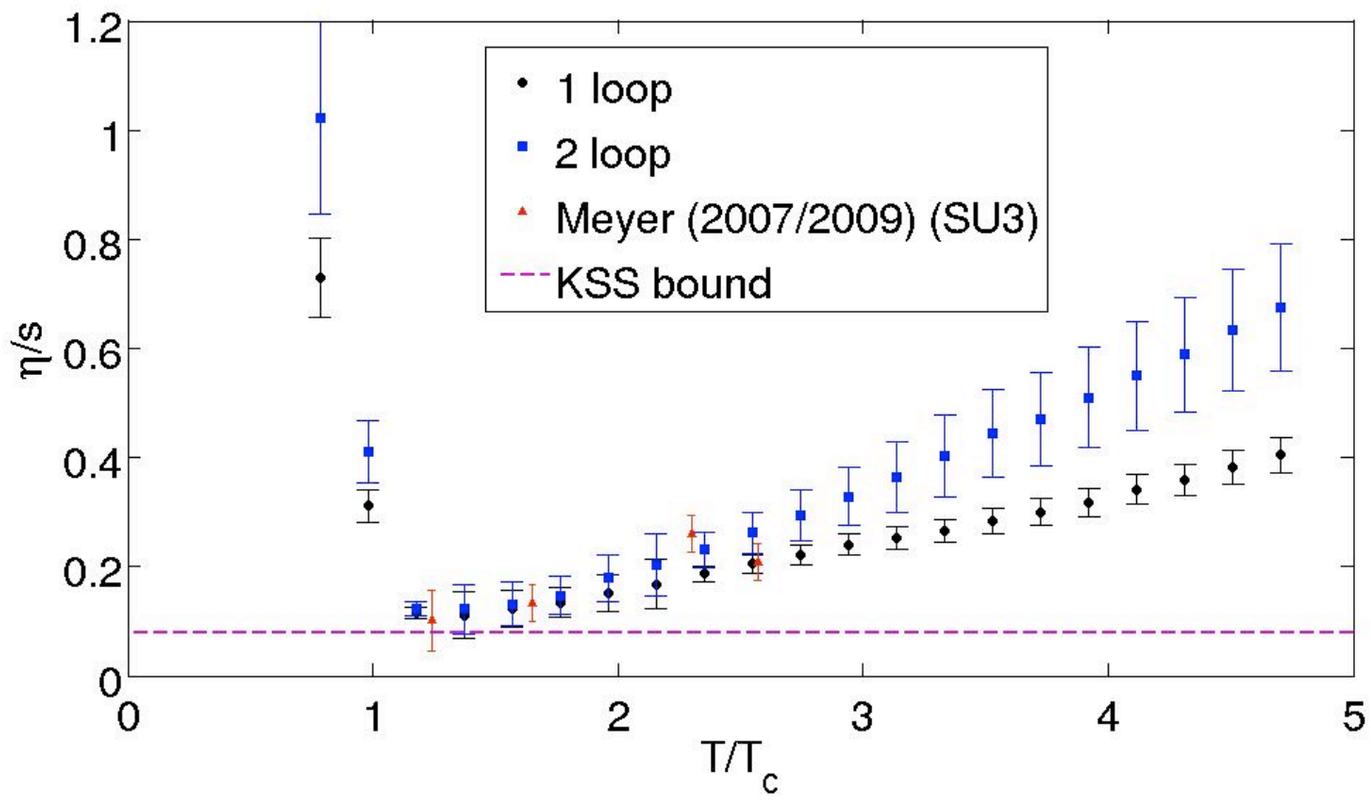

Kubo relation

$$\eta = \frac{1}{20}\frac{d}{d\omega}\bigg|_{\omega=0}\rho_{\pi\pi}(\omega,0)$$

Diagrammatic representation

$\rho_{\pi\pi} =$

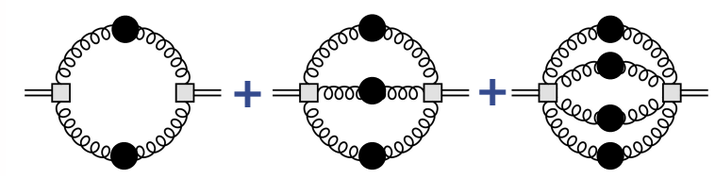

+ ··· closed form

minimum at T = 1.25T_c : $\frac{\eta}{s} = 1.45\frac{1}{4\pi}$

scale matching with QCD: $\frac{\eta}{s} = 2.27\frac{1}{4\pi}$

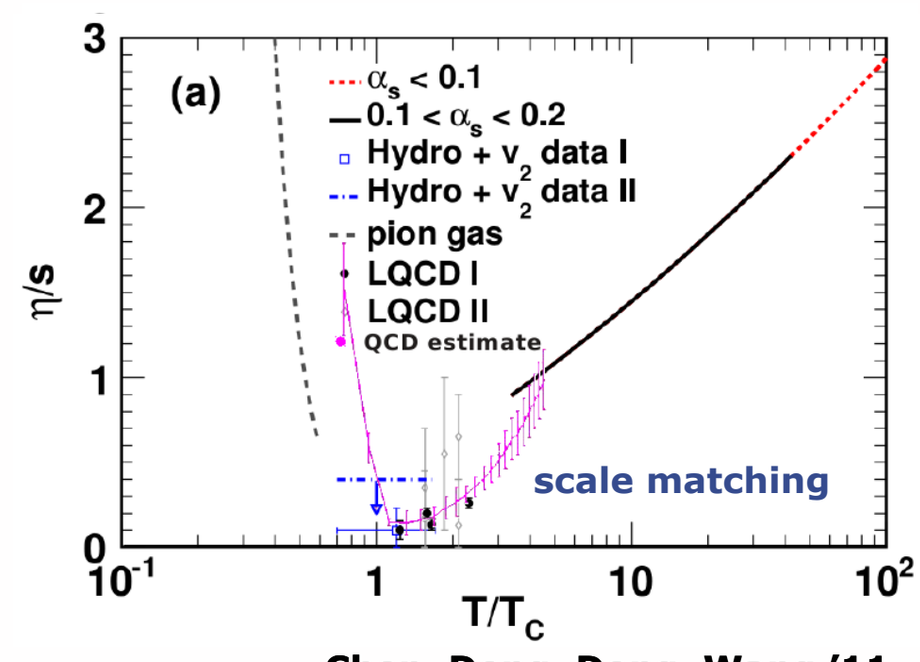

Chen, Deng, Dong, Wang '11

Summary & Outlook

Summary & outlook

- **Gauge dynamics far from equilibrium**

Abelian Higgs

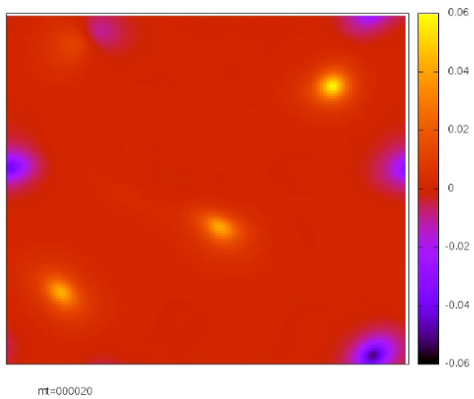

magnetic field

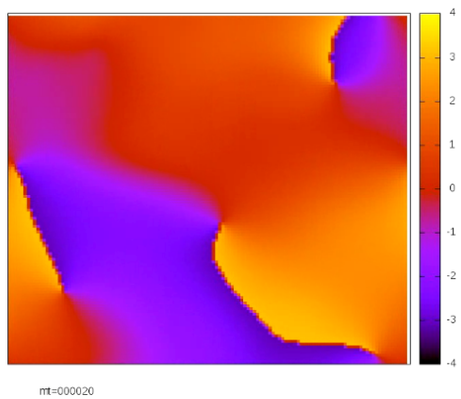

phase of Higgs

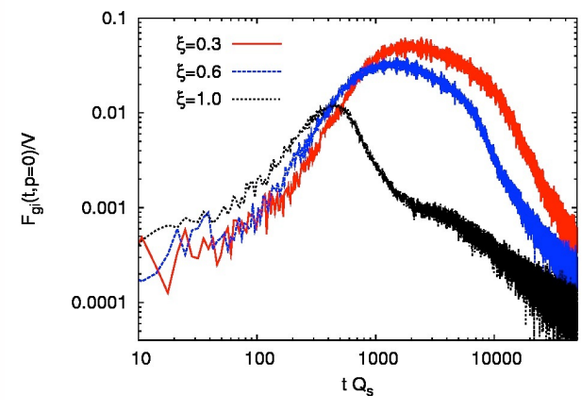

- **Spectral functions and transport coefficients**

spectral functions

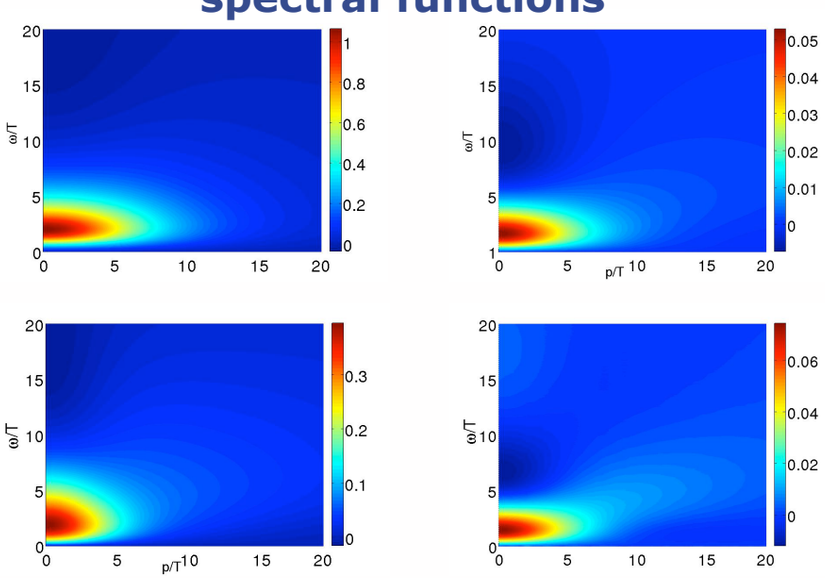

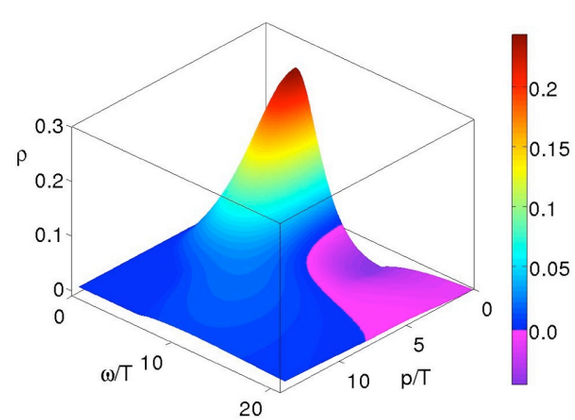

viscosity over entropy ratio

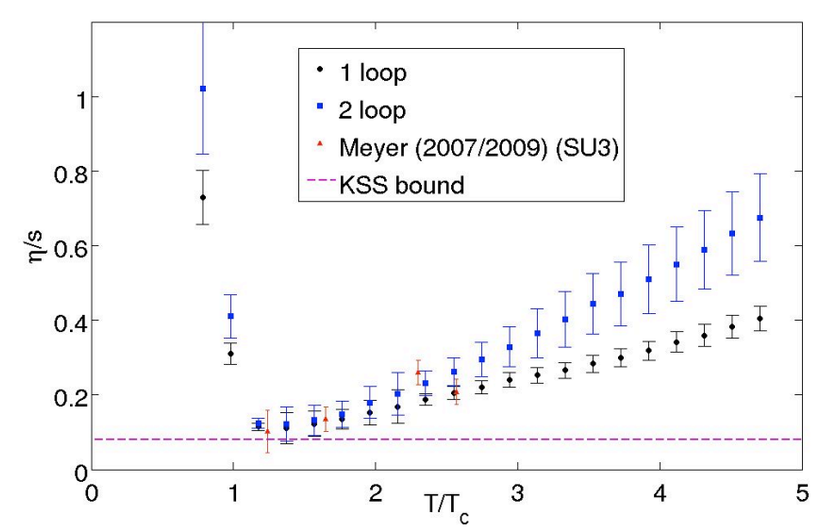

Lattice calculation of a second order transport coefficient for hydrodynamics

Owe Philipsen

and Christian Schäfer

HIC for FAIR
Helmholtz International Center

GOETHE UNIVERSITÄT FRANKFURT AM MAIN

- Introduction
- The first full lattice calculation of a real time quantity without MEM
- JHEP 1402 (2014) 003

Motivation + Introduction

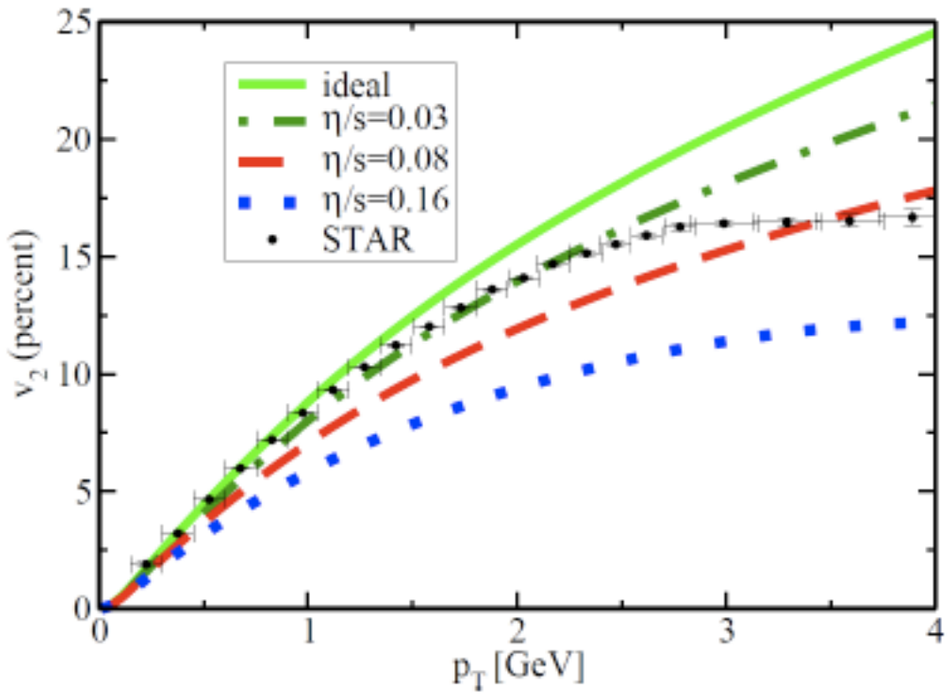

Romatschke: arXiv:0706.1522

- Measurement of elliptic flow v2 at RHIC and LHC
- Well described by viscous hydrodynamics with fitted transport coefficients
- Hydrodynamics = effective theory for long time evolution
- Transport coefficients predicted by underlying microscopic theory: QCD

Relativistic Hydrodynamics

- Central quantity: energy momentum tensor

$$T^{\mu\nu} = T^{\mu\nu}_{(0)} + \Pi^{\mu\nu}, \qquad \partial_\mu T^{\mu\nu} = 0$$

- Relativistic, ideal fluid

$$T^{\mu\nu}_{(0)} = \epsilon u^\mu u^\nu + p\,(g^{\mu\nu} + u^\mu u^\nu)$$

- Relativistic, viscous fluid

$$\Pi^{\mu\nu} = \pi^{\mu\nu} + (g^{\mu\nu} + u^\mu u^\nu)\,\Pi$$

- Represent Π and $\pi^{\mu\nu}$ by gradient expansion

- Second order gradient expansion in N=4 SYM

$$\pi^{\mu\nu} = -\eta\sigma^{\mu\nu} + \eta\tau_\pi \left(\langle D\sigma^{\mu\nu} \rangle + \frac{\nabla \cdot u}{3}\sigma^{\mu\nu} \right) \quad + \kappa \left(R^{\langle\mu\nu\rangle} - 2u_\alpha u_\beta R^{\alpha\langle\mu\nu\rangle\beta} \right) + \ldots$$

- Defines the transport coefficients such as the shear viscosity, η the relaxation time τ_π , 14 second order coefficients

Romatschke: arXiv:0902.3663

- "Thermodynamical" vs. "dynamical" coefficients

Moore, Kiyoumars, Sohrabi: arXiv:1210.3340

- Thermodynamical coefficients non-zero in complete equilibrium: 8

  Kubo relations to retarded correlators at zero frequency = euclidean correlators

- Only three independent ones: κ (two-point fcn.), λ_3 , λ_4 (three-point fcns.)

  known to LO in perturbation theory

AdS/CFT

- Anti-de Sitter/conformal field theory correspondence
- Strong-weak duality: Strongly interacting field theory corresponds to weakly interacting gravitational theory

- Minkowski space-time is given by boundary of Anti-de Sitter space
- Computation of 2nd order transport coefficient κ in strong coupling limit Baier, Romatschke, Son, Starinets & Stephanov: arXiv:0712.2451

For N=4 SYM

$$\kappa_{\mathrm{AdS/CFT}} = 1.125\, T^2$$

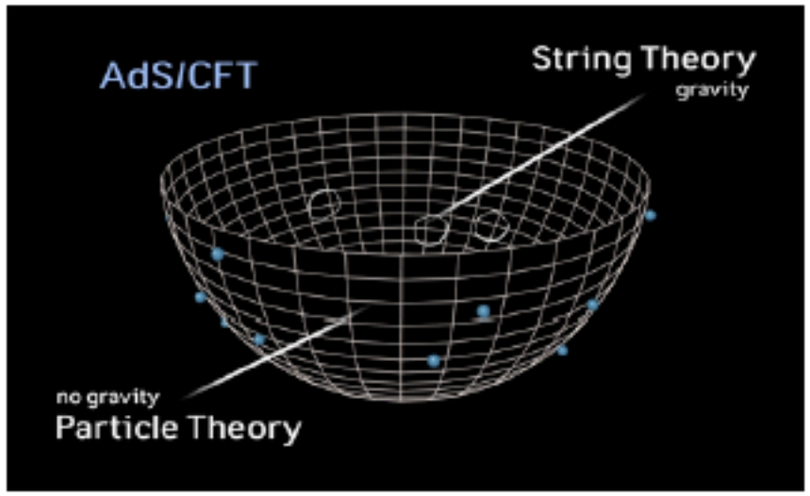

To compare with QCD, rescale with entropy:

$$\frac{\kappa}{T^2} = \frac{\eta}{s} \times \frac{s}{\pi T^3}$$

Shear viscosity from the lattice

- Extract shear viscosity η from Kubo formula (linear response theory)

$$\eta = \pi \lim_{\omega \to 0} \frac{\rho^{12,12}(\omega, \vec{q} = 0)}{\omega}$$

- Spectral function

$$\rho^{12,12}(q) = \int \frac{\mathrm{d}^4 q}{(2\pi)^3} \, \mathrm{e}^{\mathrm{i}qx} \left\langle \frac{1}{2} \left[T^{12}(x), T^{12}(0) \right] \right\rangle$$

- Lattice computation requires analytical continuation to retarded correlator Meyer: arXiv:0704.1801
- Only finite amount of data points to fit continuous function $\rho^{12,12}(\omega)$
- Usage of ansatz or maximum entropy method (MEM)
- No first principle calculation

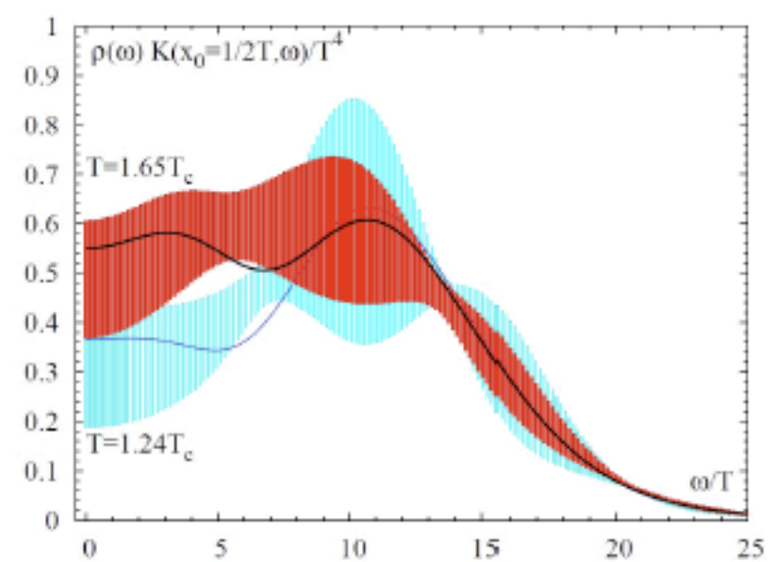

Thermal field theory, real time

- Retarded energy momentum correlator in the shear channel

$$G^{\mathrm{R}}(x,y) = \langle [T_{12}(x), T_{12}(y)]\, \theta(x_0 - y_0) \rangle$$

$$G^{\mathrm{R}}(\omega, \vec{q}) = \int_{-\infty}^{\infty} \mathrm{d}t\, \mathrm{d}x^3\ \mathrm{e}^{-\mathrm{i}(\omega t - q_i x_i)} G^{\mathrm{R}}(x,0)$$

- Describes linear response to metric perturbation, Romatschke, Son: arXiv:0903.3946
  gradient expansion $\longrightarrow$ momentum expansion

$$G^{\mathrm{R}}(\omega = 0, \vec{q}) = G(0) + \frac{\kappa}{2}|\vec{q}|^2 + \mathcal{O}(|\vec{q}|^4)$$

- Can be related to euclidean correlation function

$$G^{\mathrm{E}}(x,y) = \langle T_{12}(x) T_{12}(y) \rangle$$

$$G^{\mathrm{E}}(\mathrm{i}\omega_n, \vec{q}) = \int_0^{1/T} \mathrm{d}\tau \int_{-\infty}^{\infty} \mathrm{d}x^3\ \mathrm{e}^{-\mathrm{i}(\omega_n \tau + q_i x_i)} G^{\mathrm{E}}(x,0)$$

$$\omega_n = n 2\pi T$$

$$G^{\mathrm{R}}(\omega,\vec{q}) = \mathrm{i}\int_{-\infty}^{\infty}\frac{\mathrm{d}\omega'}{2\pi}\,\frac{\rho(\omega',\vec{q})}{\omega-\omega'+\mathrm{i}\eta} \qquad G^{\mathrm{E}}(\mathrm{i}\omega_n,\vec{q}) = \int_{-\infty}^{\infty}\frac{\mathrm{d}\omega}{2\pi}\,\frac{\rho(\omega,\vec{q})}{\omega-\mathrm{i}\omega_n}$$

- Relation by analytic continuation (unique with suitable b.c.)

$$G^{\mathrm{R}}(\omega,\vec{q}) = G^{\mathrm{E}}(\omega+i\eta,\vec{q})$$

- Trivial continuation at zero frequency, but correct for contact term

$$G^{\mathrm{R}}(\omega=0,\vec{q}) = G^{\mathrm{E}}(\omega=0,\vec{q}) + B$$

- OPE: B is momentum independent

- Altogether: low momentum euclidean correlator, allows lattice extraction

$$G^{\mathrm{E}}(\omega=0,\vec{q}) = G'(0) + \frac{\kappa}{2}|\vec{q}|^2 + \mathcal{O}(|\vec{q}|^4)$$

The lattice framework

- SU(3) Yang-Mills theory

$$T_{\mu\nu} = \theta_{\mu\nu} + \frac{1}{4}\delta_{\mu\nu}\theta,$$

$$\theta_{\mu\nu} = \frac{1}{4}\delta_{\mu\nu}F^a_{\alpha\beta}F^a_{\alpha\beta} - F^a_{\mu\alpha}F^a_{\nu\alpha}$$

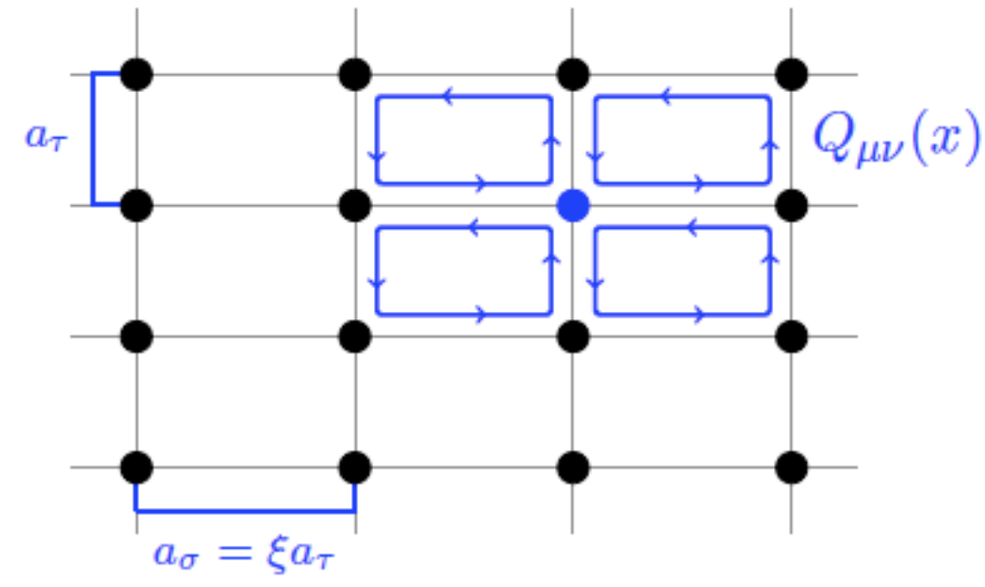

- Anisotropic, hypercubic lattice

$$\xi = a_\sigma / a_\tau \qquad N_\sigma^3 \times N_\tau$$

- Wilson action

$$S[U] = \frac{\beta}{N_c}\,\mathrm{Re}\,\mathrm{Tr}\left[\frac{1}{\xi_0}\sum_{x,i<j}(1 - U_{ij}(x)) + \xi_0 \sum_{x,i}(1 - U_{i0}(x))\right] \qquad \beta = 2N_c/g^2$$

- Field strength tensor represented by (clover) plaquettes (noise reduction)

$$Q_{\mu\nu}(x) \equiv \frac{1}{4}\left[U_{\mu\nu}(x) + U_{\nu-\mu}(x) + U_{-\mu-\nu}(x) + U_{-\nu\mu}(x)\right]$$

- Euclidean correlator of interest in momentum space

$$a_\sigma^3 a_\tau G^{\mathrm{E}}(q_3) = \frac{1}{V}\sum_{x,y} \mathrm{e}^{-\mathrm{i}q_3(x_3-y_3)} \langle T_{12}(x)T_{12}(y)\rangle$$

- Convenient for renormalisation purposes: express by diagonal elements

$$\langle T_{12}(x)T_{12}(y)\rangle = \frac{1}{2}\Big(\langle T_{11}(x)T_{11}(y)\rangle - \langle T_{22}(x)T_{22}(y)\rangle\Big)$$

- Requirements for small momentum regime $q_i/T < 1$

$$T = \frac{1}{a_\tau N_\tau}, \qquad q_i = \frac{2\pi}{a_\sigma N_\sigma} n_i, \qquad n_i = 0, 1, \ldots, N_\sigma - 1$$

$$\frac{q_i}{T} = \frac{2\pi N_\tau}{\xi N_\sigma} n_i < 1$$

- Need at least 3 momenta, N_τ fixed by T and lattice spacing

  Expensive! Need large N_σ , $\xi > 1$ helps: $\xi = 2, \quad N_\sigma = 120, \quad N_\tau = 6, \ldots, 72$

Perturbation theory

- Leading order = ideal gas: $F^a_{\mu\nu} = \partial^c_\mu A^a_\nu - \partial^c_\nu A^a_\mu$

- Requires 16 terms of the generalised form

$$C_{i_1 i_2 j_1 j_2 l_1 l_2 m_1 m_2}(x,y) = \left\langle \partial^c_{i_1} A^a_{i_2}(x) \partial^c_{j_1} A^a_{j_2}(x) \partial^c_{l_1} A^b_{l_2}(y) \partial^c_{m_1} A^b_{m_2}(y) \right\rangle$$

- Continuum result: $\kappa = \left(N_c^2 - 1\right) \dfrac{T^2}{18}$

- Lattice perturbation theory:

$$\sum\!\!\!\!\!\!\int_q \equiv \frac{1}{a_\tau N_\tau} \sum_{n=1}^{N_\tau} \int_{-\frac{\pi}{a_\sigma}}^{\frac{\pi}{a_\sigma}} \frac{\mathrm{d}^3 q}{(2\pi)^3} \qquad \tilde{q}_\mu = \frac{2}{a_\mu} \sin\left(\frac{a_\mu q_\mu}{2}\right)$$

- Correlator in momentum space for vanishing coupling

$$G^{\mathrm{E}}(q) = (N_{\mathrm{c}}^2 - 1) \sum\!\!\!\!\!\!\int_k \frac{1}{\widetilde{k}^2 \widetilde{(q+k)}^2} \Big\{ 4\widetilde{k}_x^2 \widetilde{k}_y^2 - 2\widetilde{k}\widetilde{(q+k)}(\widetilde{k}_x^2 + \widetilde{k}_y^2) + \widetilde{k}^2 \widetilde{k}_x^2 + \widetilde{(q+k)}^2 \widetilde{k}_y^2 + \Big[\widetilde{k}\widetilde{(q+k)}\Big]^2 \Big\}$$

- Matsubara sums, momentum integration

$$\frac{G^E(q)}{T^4} = (N_{\mathrm{c}}^2 - 1) \left\{ \frac{\pi^4}{N_\tau^2} \left(\frac{2\xi^2}{945} + \frac{4}{189} \right) + \frac{q^2}{T^2} \left[\frac{1}{36} + \frac{\pi^2}{N_\tau^2} \left(-\frac{\xi^2}{240} + \frac{49}{2160} \right) \right] \right\} + \mathcal{O}\left(q^4, N_\tau^{-4}\right)$$

$$\frac{\kappa}{T^2} = (N_c^2 - 1)\left[\frac{1}{18} + \frac{\pi^2}{N_\tau^2}\left(-\frac{\xi^2}{120} + \frac{49}{1080}\right)\right] + \mathcal{O}\left(q^4, N_\tau^{-4}\right)$$

- Continuum limit at fixed T:

  $a_\mu \to 0 \qquad N_\tau \to \infty$

- Cut-off effects depend on anisotropy, there is an optimal value, (known in perturbation theory only)

- <10% cut-off effect for $\xi = 2, N_\tau \geq 6$

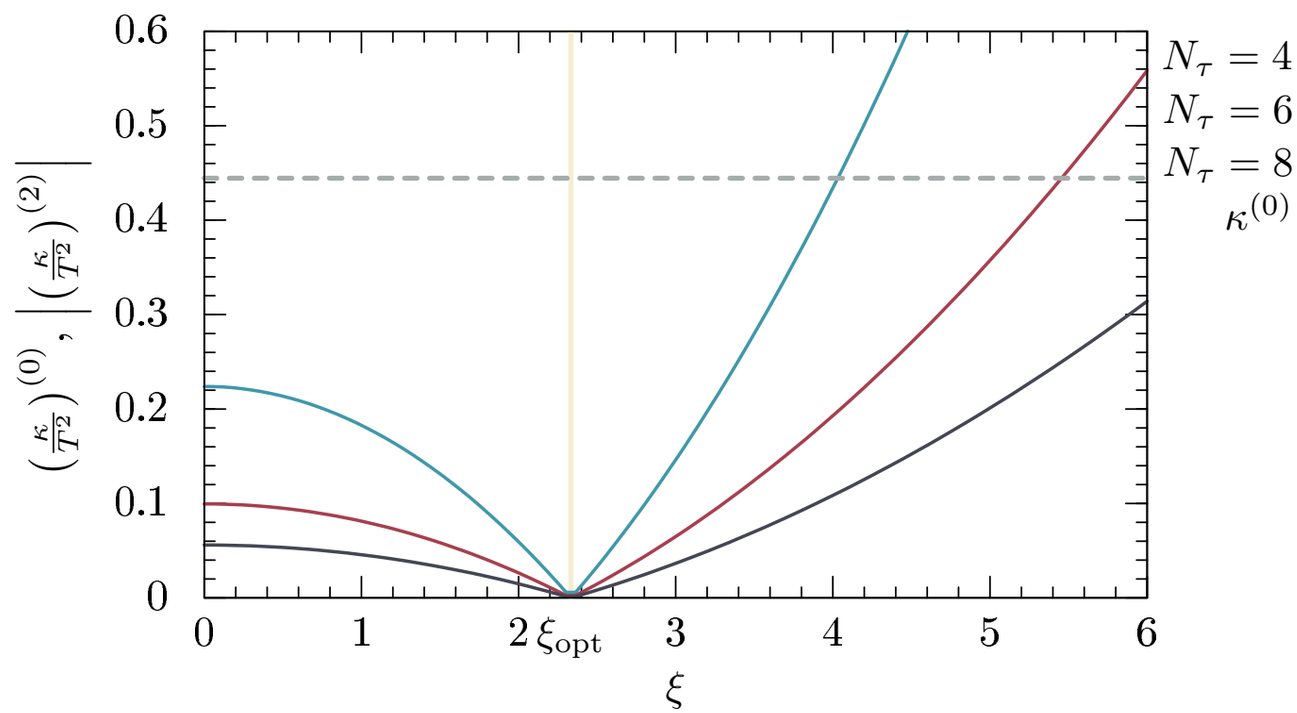

LPT result of κ for $N_\tau = 6$ and $\xi = 2$

$$\kappa_{\rm LPT} = 0.47\,T^2$$

Fully interacting: renormalisation

- Correlator UV divergent
- Additive renormalisation: subtract vacuum divergence $\langle \mathcal{O} \rangle = \langle \mathcal{O} \rangle_T - \langle \mathcal{O} \rangle_{T_{\rm vac}}$
- Requires two simulations per lattice spacing and temperature
- $T_{\rm vac} = 0 \Rightarrow N_\tau = \infty$; choose $T_{\rm vac} \approx 0.8 T_{\rm c}$, pressure still exponentially small
- Significant loss of accuracy (cf. equation of state) main weakness of the calculation!

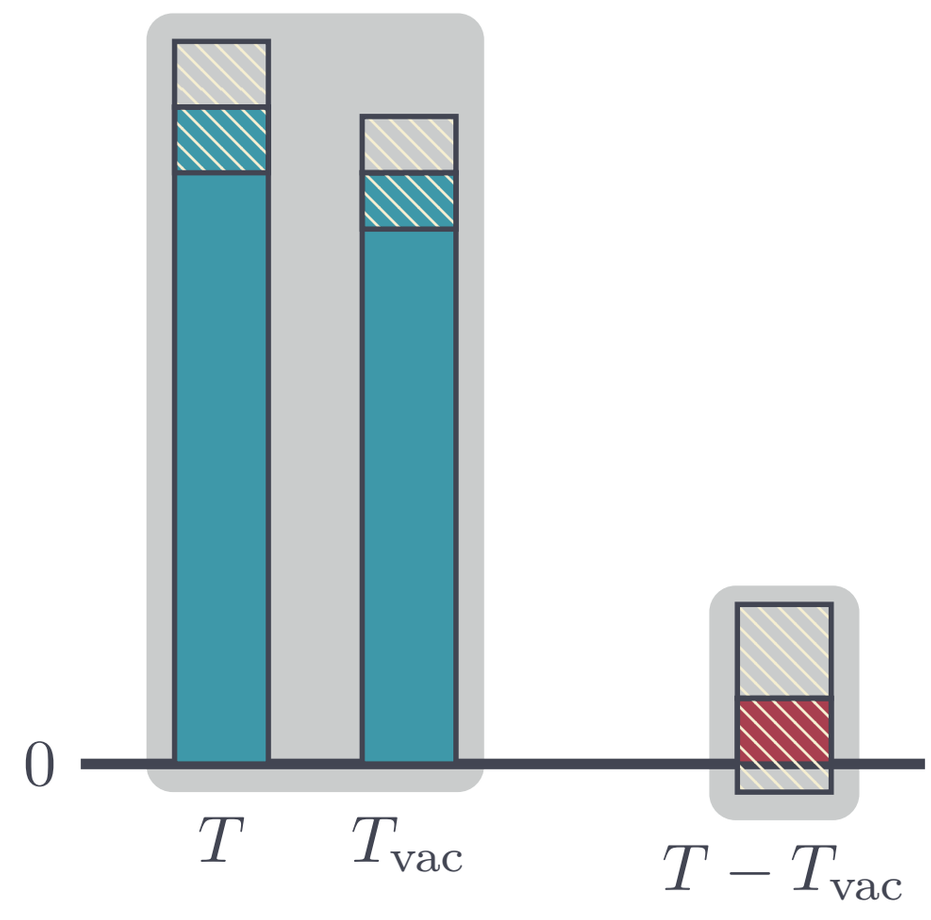

- Energy momentum tensor is Noether current of translation invariance
- Continuum: protected against renormalisation by symmetry
- Lattice: translation invariance broken to discrete sub group
- Multiplicative renormalisation necessary
- Anisotropic lattice requires two renormalisation factors:

$$T_{ii} = Z_\tau(\beta,\xi)\left[T^\tau_{ii} + \frac{Z_\sigma(\beta,\xi)}{Z_\tau(\beta,\xi)}T^\sigma_{ii}\right]$$

plaquettes in t-direction spatial plaquettes

- Ratio of renormalisation factors from RG-invariant quantities, e.g.

Meyer: arXiv:0809.5202

$$\frac{Z_\sigma(\beta,\xi)}{Z_\tau(\beta,\xi)} = \frac{\langle T^\tau_{00}\rangle_1 - \langle T^\tau_{11}\rangle_2}{\langle T^\sigma_{11}\rangle_2 - \langle T^\tau_{00}\rangle_1}$$

- Absolute renormalisation by matching to continuum pressure

$$\langle T_{ii}\rangle = Z_\tau(\beta,\xi)\left[\langle T^\tau_{ii}\rangle + \frac{Z_\sigma(\beta,\xi)}{Z_\tau(\beta,\xi)}\langle T^\sigma_{ii}\rangle\right] = p$$

Borsanyi, Endrodi, Fodor, Katz & Szabo: arXiv:1204.6184

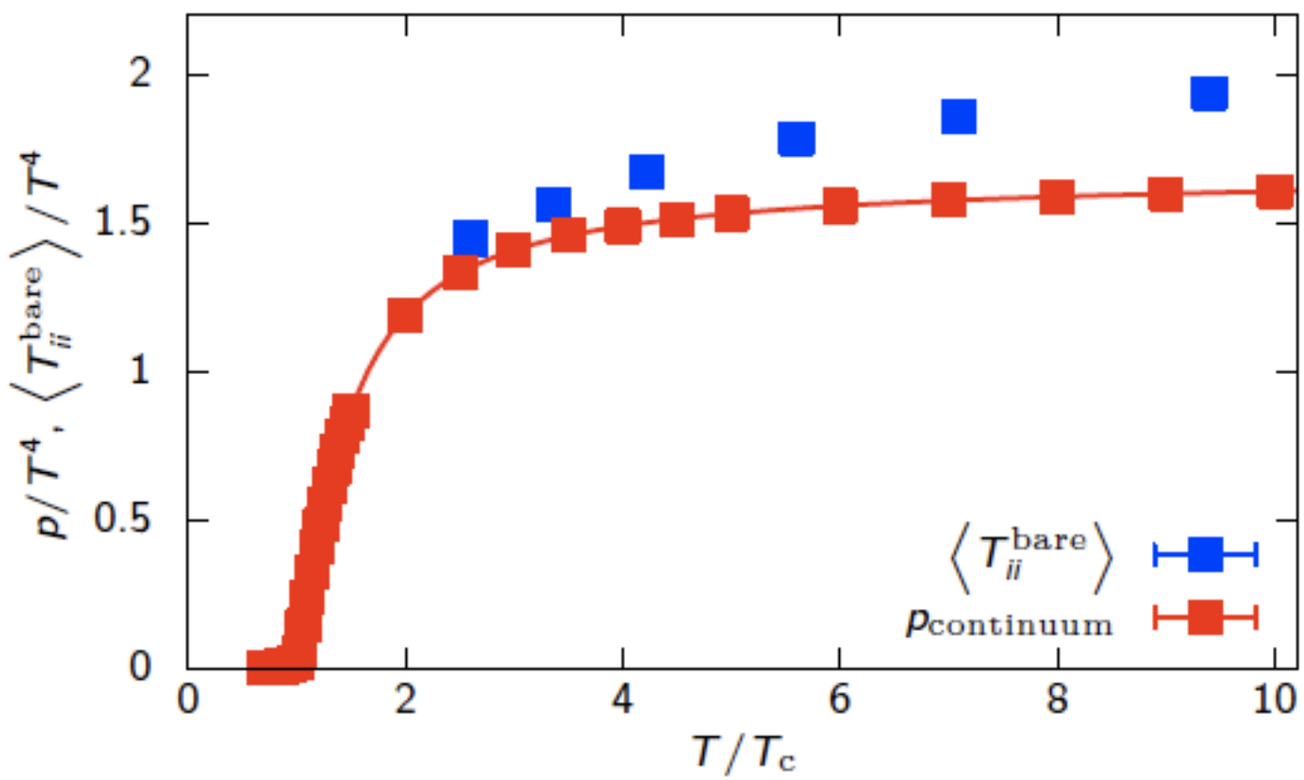

Full simulation vs. lattice perturbation theory

β	N_τ	N_σ	$N_\tau^{\rm vac}$	ξ	a_σ [fm]	T/T_c	$T_{\rm vac}/T_c$
7.1	6	120	72	2	0.026	9.4	0.8

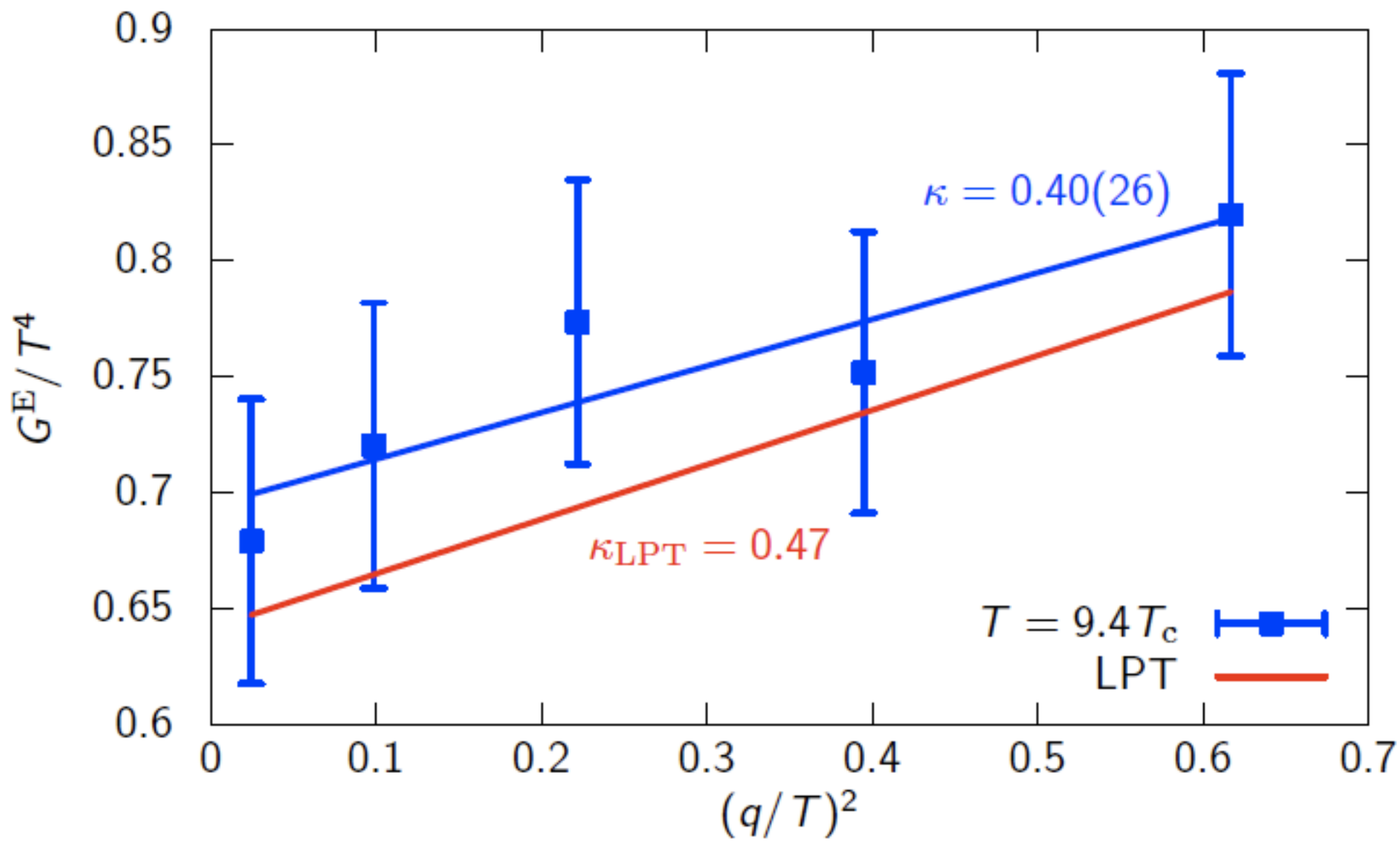

Temperature and cut-off dependence

$$T = \frac{1}{a_\tau(\beta) N_\tau}, \qquad a_\tau(\beta) = \text{const.}$$

- Due to low momentum expansion spatial lattice extent N_σ increases cubicly with temporal one N_τ

$$\frac{q_i}{T} = \frac{2\pi N_\tau}{\xi N_\sigma} n_i < 1$$

- Vary temperature and lattice spacing

Run	i	ii	iii	iv
β	7.1	7.1	6.68	6.14
N_τ	6	8	6	6
N_σ	120	120	120	120
N_τ^{vac}	72	72	42	24
ξ	2	2	2	2
a_σ [fm]	0.026	0.026	0.044	0.094
T/T_c	9.4	7.1	5.6	2.6
T_{vac}/T_c	0.8	0.8	0.8	0.7

The computing platform

LOEWE-CSC at GU Frankfurt

New AMD-based cluster with hybrid structure:

- approximately 800 nodes
- 2 AMD Opteron 12 Core ($\rightarrow$ 24 Cores total) per node
- 1 ATI Radeon 5870 (Cypress) per node

- Top500 rank 22 since 11/2010 (299 Tflops, rank 2 in Germany)
- Rank 10 of Green IT Machines (6/2011, 718 Mflops/W)

CSC

Temperature and cut-off dependence

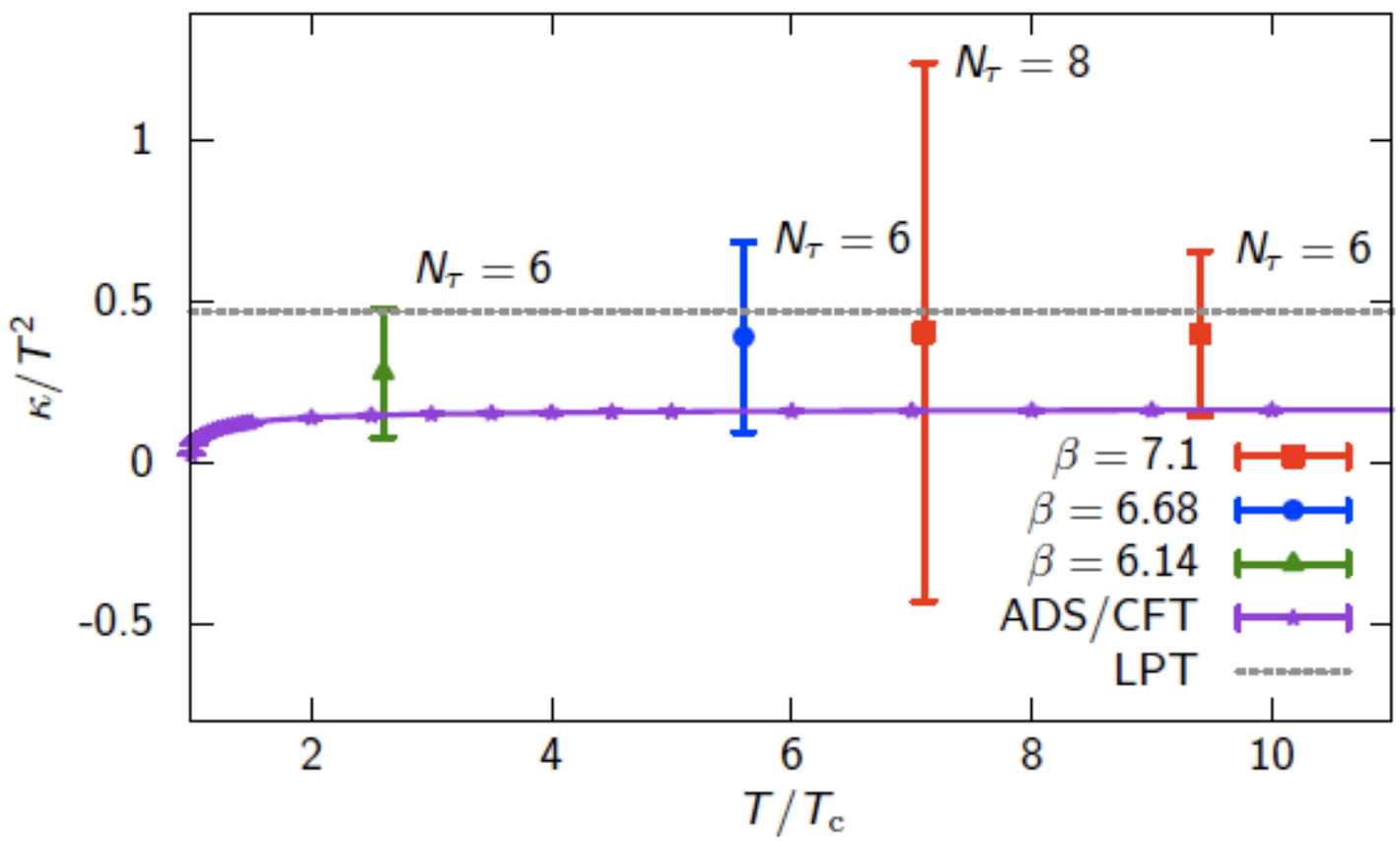

- Cut-off dependence smaller than statistical error
- Errors dominated by vacuum subtraction
- No T-dependence within current resolution

$$\kappa^{\mathrm{avr}} = 0.36(15)\, T^2$$

Conclusions

- First lattice computation of a transport coefficient without MEM

$$\kappa^{\mathrm{avr}} = 0.36(15)\,T^2$$

- Calculation in momentum space costly
- Large statistical error by vacuum subtraction, try methods without this step
- In principle: 8 coefficients doable; is it worth the effort?
- Result is not far from LO perturbative prediction, try NLO, HTL in the continuum!

Strong Coupling Far-From Equilibrium Thermalization for ‘nuclei’

Paul Romatschke
University of Colorado, Boulder

In collaboration with D. Grumiller, B. Wu, J.D. Hogg, W. van der Schee and S. Pratt

Motivation

Estimate for QCD coupling in HIC:

$\alpha_s \sim 0.3$, $g \sim 2$

For quantitative answers:

Weak coupling methods not applicable

Strong coupling methods not applicable

We probably need both

Motivation

- Strong Coupling Dynamics cannot be simulated in QCD
- Early Phase of Heavy-Ion Collisions probes QCD at 'sizeable' coupling
- Would like a model that naturally leads to hydrodynamics (thermalizes) and provides hydro initial conditions at τ_{hydro}
- Final results should be independent from τ_{hydro}

Why is this important at all?

- Hydro requires Initial Conditions
- These are chosen ‘ad-hoc’:

Author	Hydro Start Time	Flow velocity	Equili-brated?
Schenke et al. (2013)	0.2 fm/c	Non-zero (glasma)	no
Bozek & Broniowski (2013)	0.2/0.6 fm/c	zero	no
Heinz et al. (2013)	0.9 fm/c	zero	no
Niemi et al (2013)	0.05-0.2 fm/c	Non-zero (minijet)	no
[your name here]			

Hydro Initial Conditions Matter

- Different initial conditions for hydrodynamics lead to different particle spectra
- Unfortunately (some of) these differences can also be generated by changing ‘physical’ parameters such as transport coefficients (viscosities), EoS, …

This limits our ability to learn about QCD!

Hydro Initial Conditions Matter

We would like a model for how system equilibrates rather than guessing its state after hydrodynamics starts to apply

AdS/CFT may provide such a model

Heavy Ion Collisions as BH Collisions in AdS5

- Dynamical QCD not solvable exactly (e.g. sign problem in lattice QCD, strong coupling, many body system, …)
- Try changing the problem:

QCD -> N=4 SYM

N_c, α_s->∞

Voila, we can use AdS/CFT!

…but we have lost asymptotic freedom, confinement and have many more dofs..!

Want: QCD, $N_c=3$, $g=1$

Can do: N=4 SYM, $N_c=\infty$, $g=\infty$ via holography

So we propose to approximate what we want by

- a theory theory not realized in nature
- a wrong gauge group
- a wrong coupling value
- Using a method that is only conjectured to work

Why? Because we are desperate !

- At g=2, we don't trust weak coupling methods
- Lattice QCD doesn't work for dynamics
- AdS/CFT is the only generic strong coupling technique we have

Why not AdS/CFT

IMHO, there are many applications for which AdS/CFT is be a bad model…

Why AdS/CFT

… but I will argue that it is a robust model for thermalization in heavy-ion collisions in a universe where α_s is extremely large

Some ‘issues’ of N=4 SYM may not be so bad:

- While QCD is not conformal, we apply our model only at T>400 MeV where $c_s^2 \sim 0.3$
- QCD is confining but at T~170 MeV, much below the scale we stop applying our model
- $N_c = \infty$ may not be such a bad description of $N_c = 3$ in view of success of large N_c QCD

So if we’re interested in the bulk dynamics of a gauge theory at strong coupling, AdS/CFT may even be quantitatively close to sQCD

Heavy Ion Collisions as BH Collisions in AdS5

If we are willing to accept these 'approximations', then holographic renormalization lets us recast 'nuclear collisions' in 3+1d with

$$T_{++} \propto \rho(x_\perp)\delta(x^+)$$

as shock wave collisions in AdS5:

$$ds^2 = \frac{-2dx^+dx^- + dx_\perp^2 + dz^2 + dx^{+2}\Phi(x_\perp, z)\delta(x^+)}{z^2}$$

$$\boxed{\lim_{z\to 0} \frac{\Phi(x_\perp, z)}{z^4} = \frac{\rho(x_\perp)}{\kappa}}$$

Heavy Ion Collisions as BH Collisions in AdS5

- Two infinitely boosted ‘nuclei’ superimposed become two shock waves in gravity
- Extremely high-energy analogue of black-hole collisions (Aichelburg-Sexl shock waves)
- Hard to treat collision process via numerical relativity
- Some insight may be gained analytically

Shock Wave Collisions in AdS_5

- Coordinate Transformation turns delta-functions into C_2 functions in the metric:

$$x^+ = u\,, \quad x^- = v + \frac{1}{2}\Phi\theta(u) + \frac{u\theta^2(u)}{8}\partial_i\Phi\,\delta^{ij}\,\partial_j\Phi\,, \quad x^i = \tilde{x}^i + \frac{1}{2}u\theta(u)\delta^{ij}\partial_j\Phi$$

$$ds^2_{\rm pre} = \frac{-2dudv + d\tilde{x}^i d\tilde{x}^j\left(\delta^{kl}H^{(1)}_{ik}H^{(1)}_{jl} + \delta^{kl}H^{(2)}_{ik}H^{(2)}_{jl} - \delta_{ij}\right)}{\left[\tilde{z} + \frac{1}{2}\left(u\theta(u)\partial_z\Phi_{(1)} + v\theta(v)\partial_z\Phi_{(2)}\right)\right]^2}$$

Shock Wave Collisions in AdS_5: perturbative GR (pGR)

- Close to collision point u=0, v=0, may find line element after collision by solving Einstein Equations ('early time perturbation theory')
- Via AdS/CFT, can obtain information about QFT energy-momentum tensor

[Grumiller&PR 2008; PR & Hogg 2013]

Problem: Expansion uncontrolled close to horizon, would need to resum (see Bhattacharyya & Minwalla, JHEP 909])

pGR shock collisions

- Analytic results predicts non-equilibrium 'flow':

$$\epsilon = \frac{2}{\kappa}\rho^2(r)\tau^2\,, \quad u^r = -\frac{\rho'(r)}{3\rho(r)}\tau + \mathcal{O}(\tau^3)\,,$$ $u^\xi = 3\,\tau^2\,\rho(r)\,\xi$

[Grumiller&PR 2008; PR & Hogg 2013]

- Pre-equilibrium transverse flow is consistent with ideal hydro (with $s=\rho(r)$)
- Pre-equilibrium energy density evolution is NOT consistent with hydro

From pGR to full GR

- Use analytic post-collision line element to obtain (approximate) initial data & follow full evolution using numerical GR
- Simplest case: planar shocks --- we did this using a characteristic scheme (Chesler-Yaffe)

[Wu & PR, 2011]

- More realistic: shocks with transverse profile (corresponding to head-on 'nuclear' collisions)

[van der Schee, PR & Pratt, 2013]

From pGR to full GR

In all the cases we study, the analytic post-collision line element is not quite ‘good enough’ to serve as valid initial data. Reason: poor convergence of perturbative series close to horizon.

We resort to adding a regulator to the analytic data that smoothes the data in the bulk while leaving the near-boundary data unaffected.

Because of this, our results have to be taken with a grain of salt.

Planar Shock Collisions in AdS_5

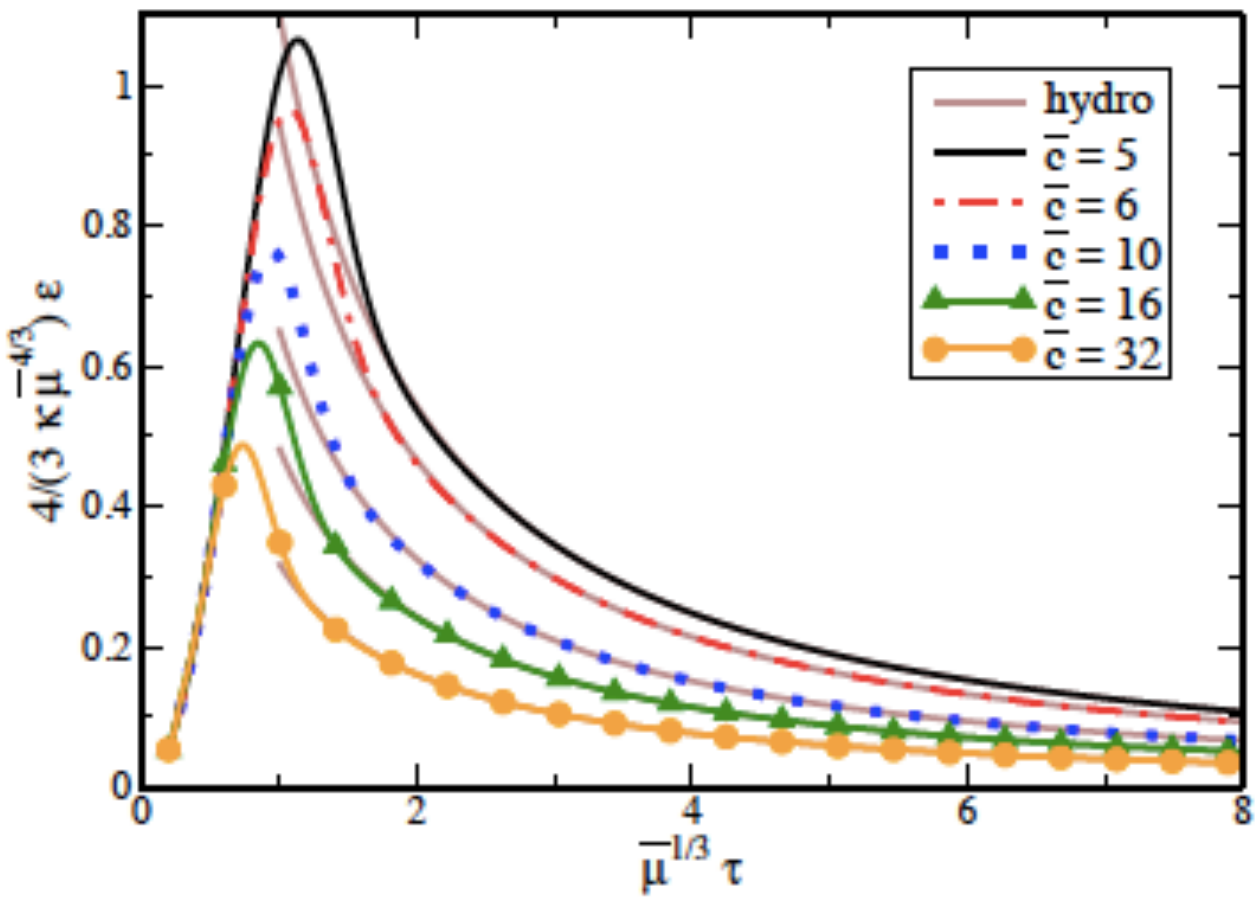

Consistent with numerical treatment of collision, Casalderrey-Solana et al., PRL 111

[Wu & PR, 2011]

Planar Shock Collisions in AdS_5

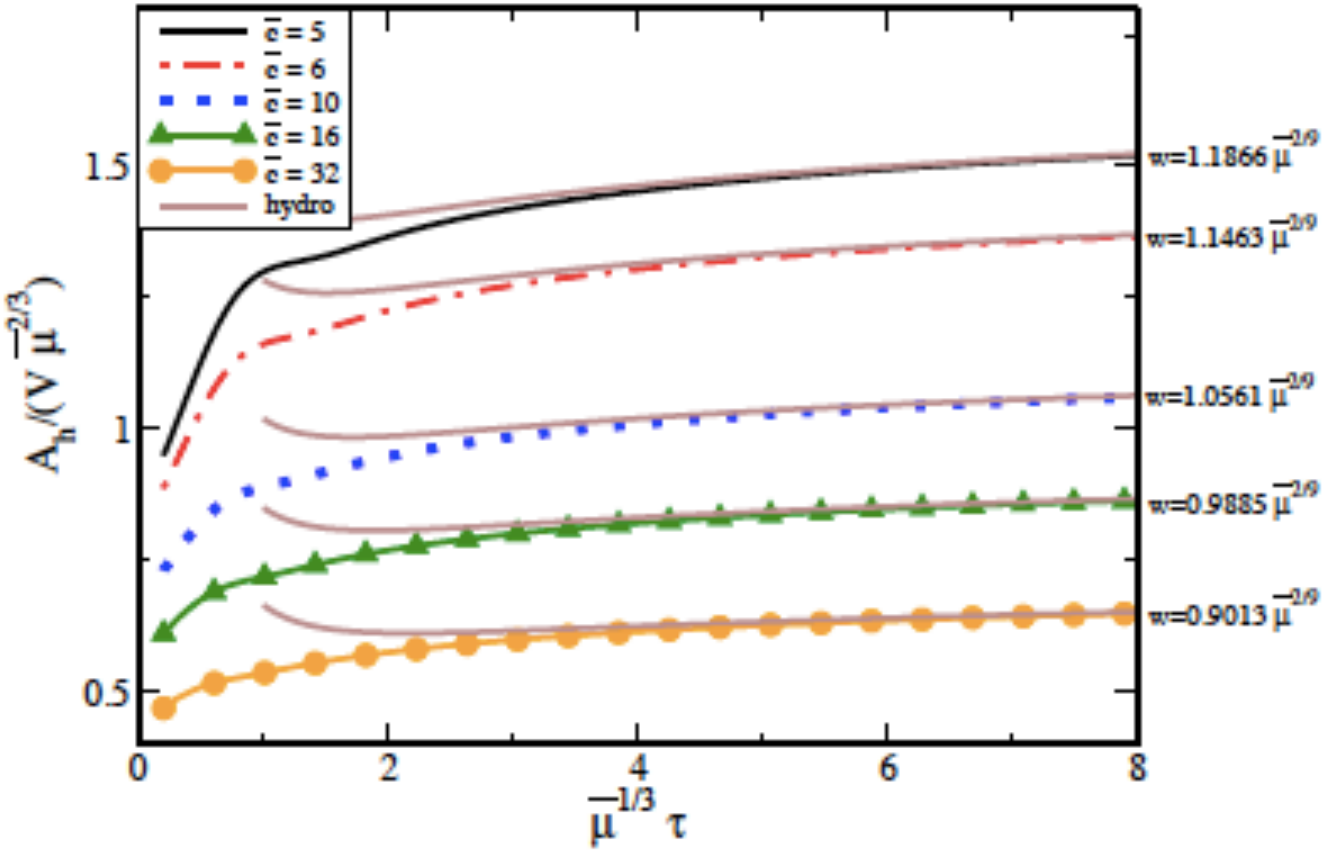

[Wu & PR, 2011]

Planar Collisions -- Summary

- We find that despite far from equilibrium initial state the system always equilibrates
- Details of the equilibration process depend on our regulator function, but local energy density tends to first rise and then fall according to late-time hydrodynamic behaviour

Shocks with Transverse Profiles

- We are able to generalize our methods to collide shock waves with arbitrary transverse profiles and thus have a model of pre-equilibrium radial flow
- Radius of Au/Pb ion sets transverse scale. This fixes scale conversion of model to physical units

AdS+hydro+cascade

- We are able to follow dynamics until (and beyond) equilibration
- Resulting Energy-Stress Tensor is used as initial data in subsequent hydrodynamic evolution code (matching) with QCD EoS
- Hydro evolution proceeds until system has cooled below QCD phase transition. Evolution is stopped and data is fed into a standard hadron cascade code
- Particle spectra from cascade are compared to experiment

AdS+hydro+cascade

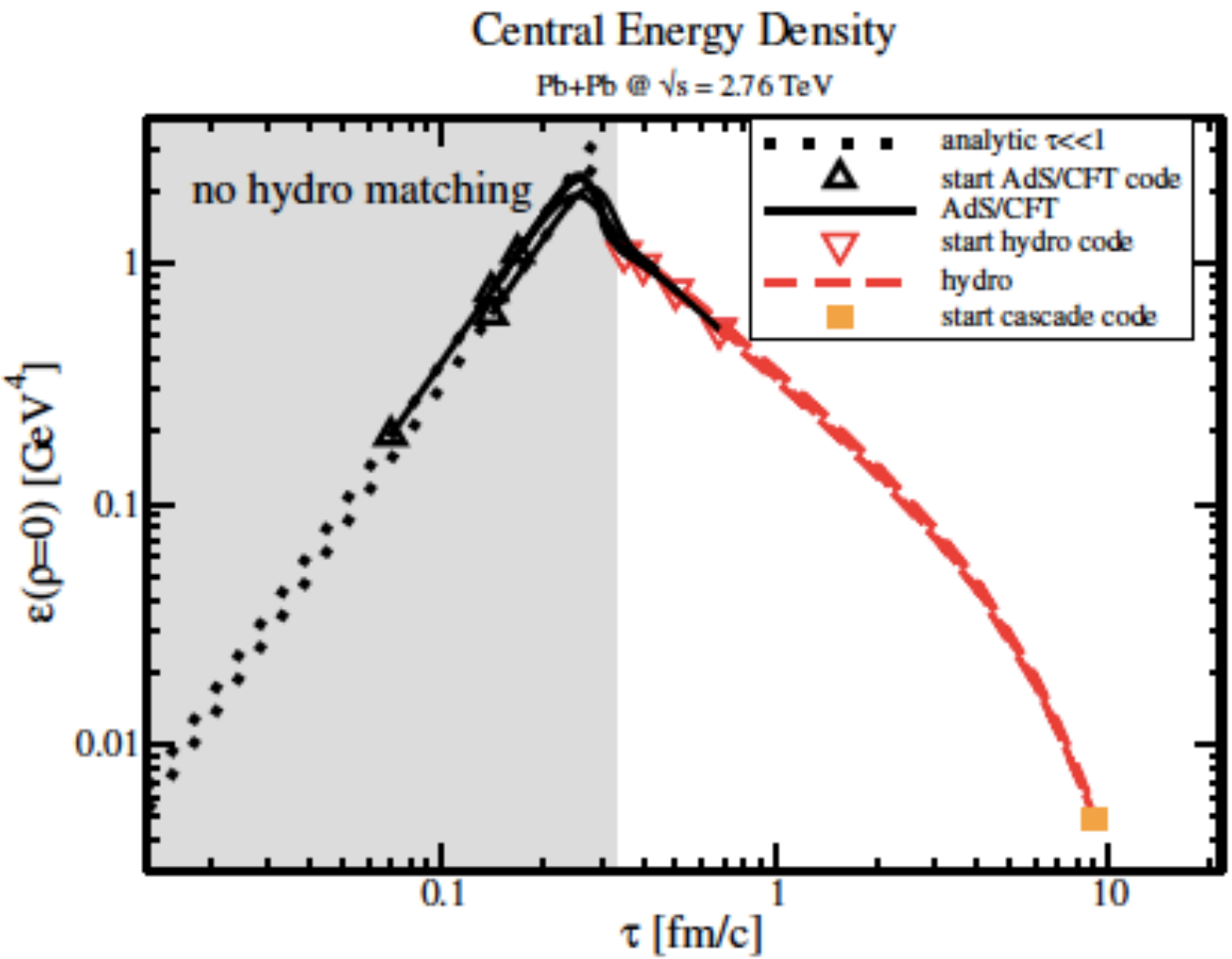

[van der Schee, PR & Pratt, 2013]

AdS+hydro+cascade

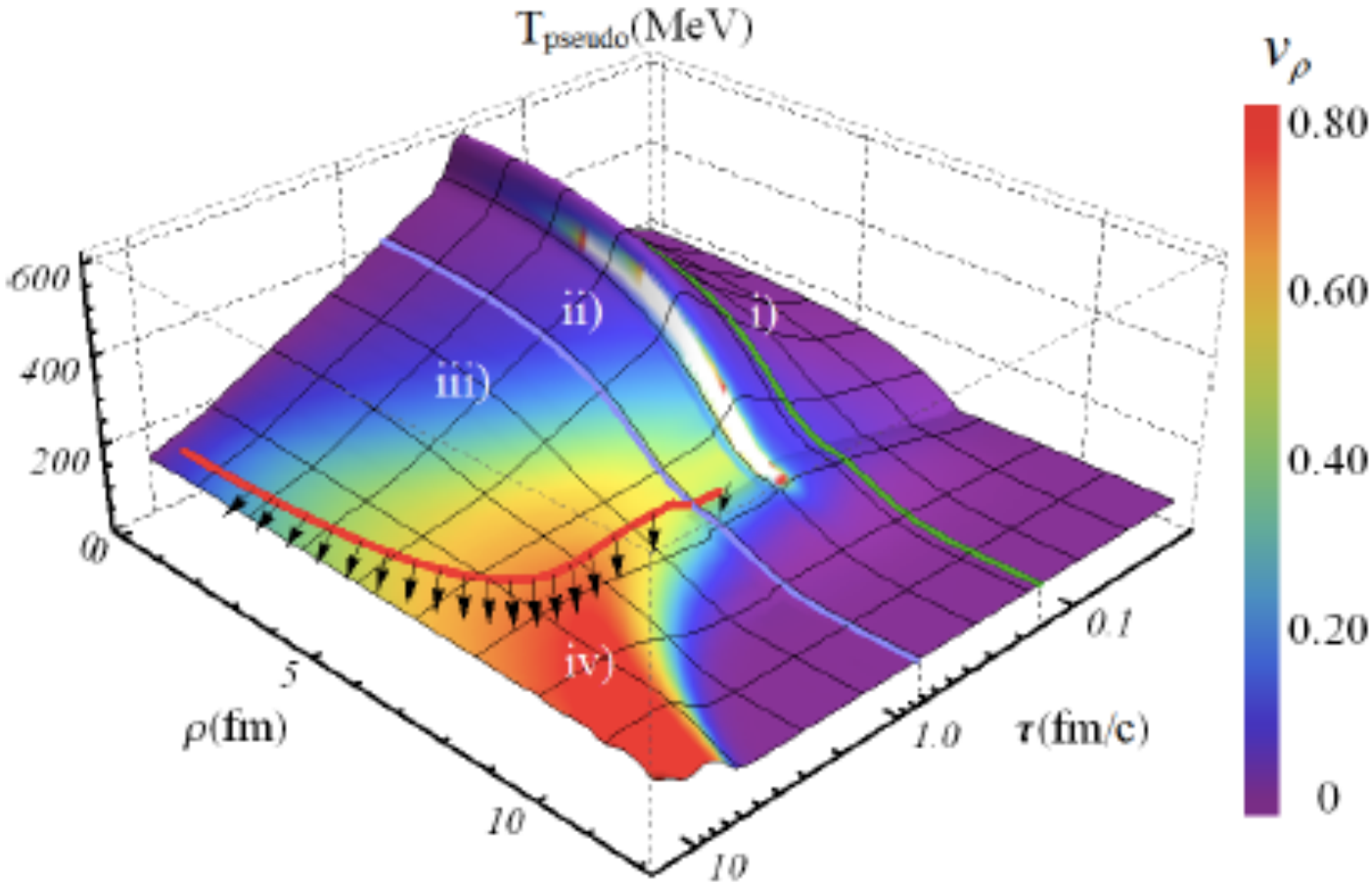

[van der Schee, PR & Pratt, 2013]

AdS+hydro+cascade

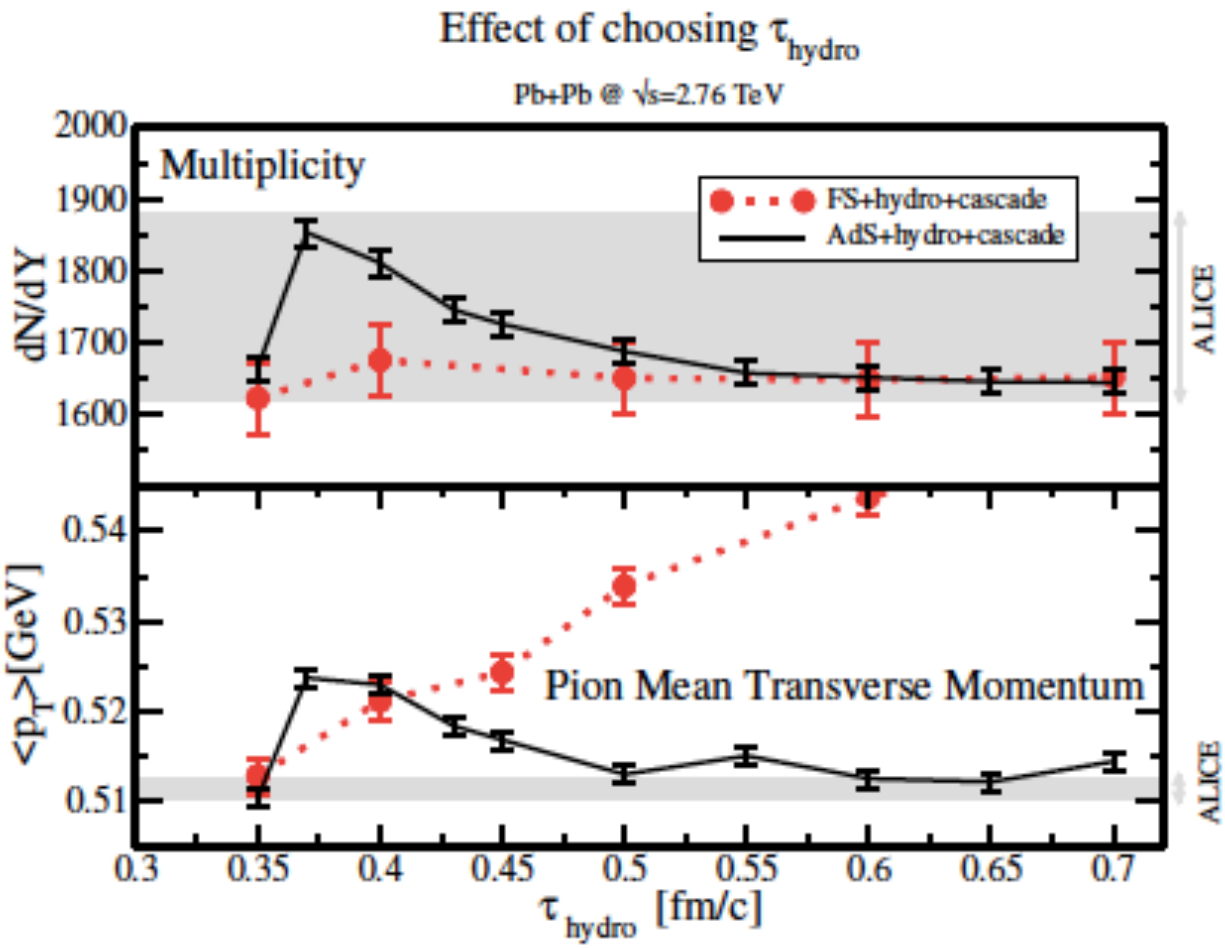

[van der Schee, PR & Pratt, 2013]

AdS+hydro+cascade

AdS/CFT+hydro results are independent of choice of switching time

You get what you get.
No ‘tuning’

Why AdS/CFT if hydro works anyway?

- Hydro requires Initial Conditions

Author	Hydro Start Time	Flow velocity	Equili-brated?
Schenke et al. (2013)	0.2 fm/c	Non-zero (glasma)	no
Bozek & Broniowski (2013)	0.2/0.6 fm/c	zero	no
Heinz et al. (2013)	0.9 fm/c	zero	no
Niemi et al (2013)	0.05-0.2 fm/c	Non-zero (minijet)	no
Van der Schee et al (2013)	Arbitrary, >0.5 fm/c	Non-zero (AdS/CFT)	yes

Shocks with Transverse Profiles

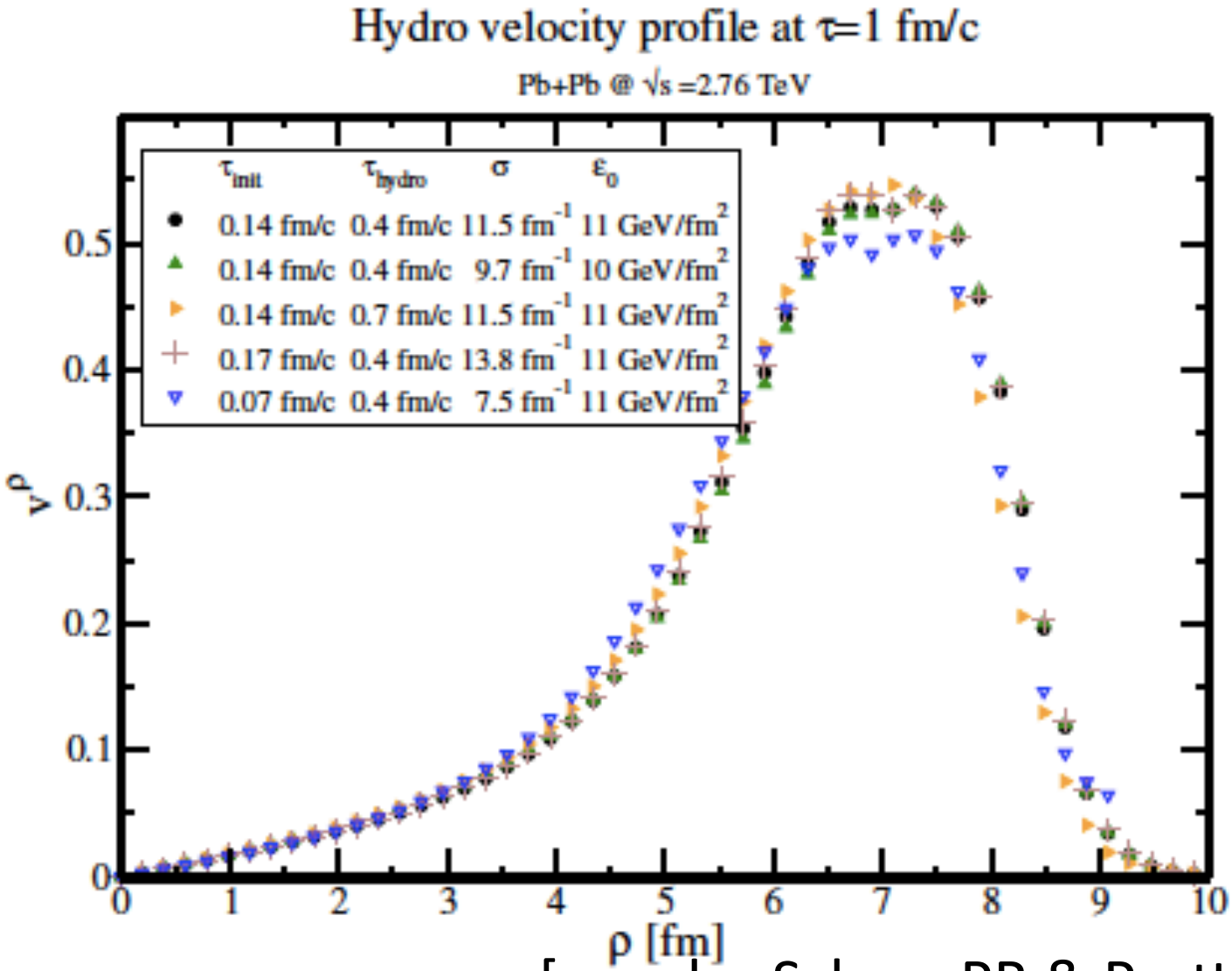

[van der Schee, PR & Pratt, 2013]

Shocks with Transverse Profiles

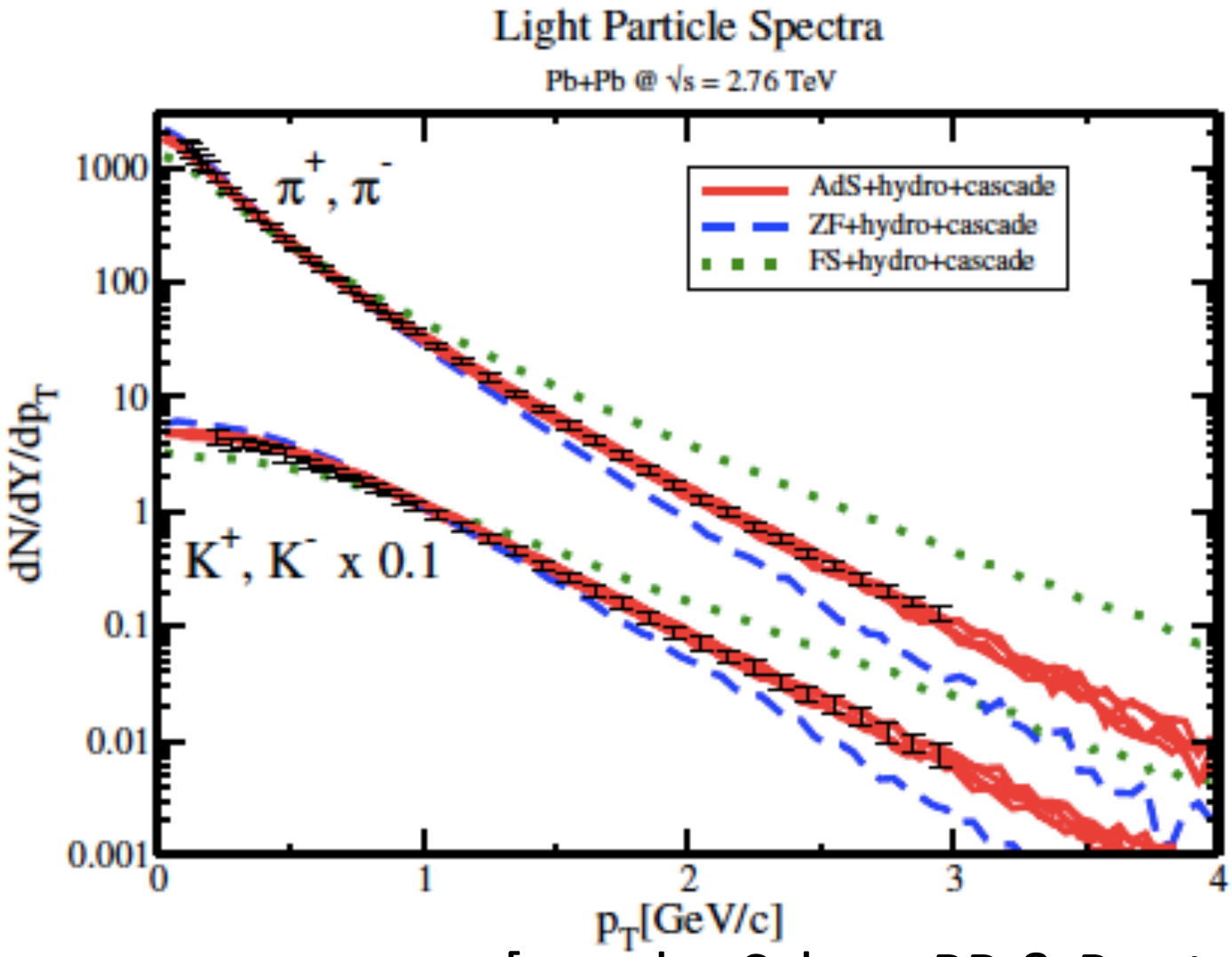

[van der Schee, PR & Pratt, 2013]

Strong vs. Weak Coupling

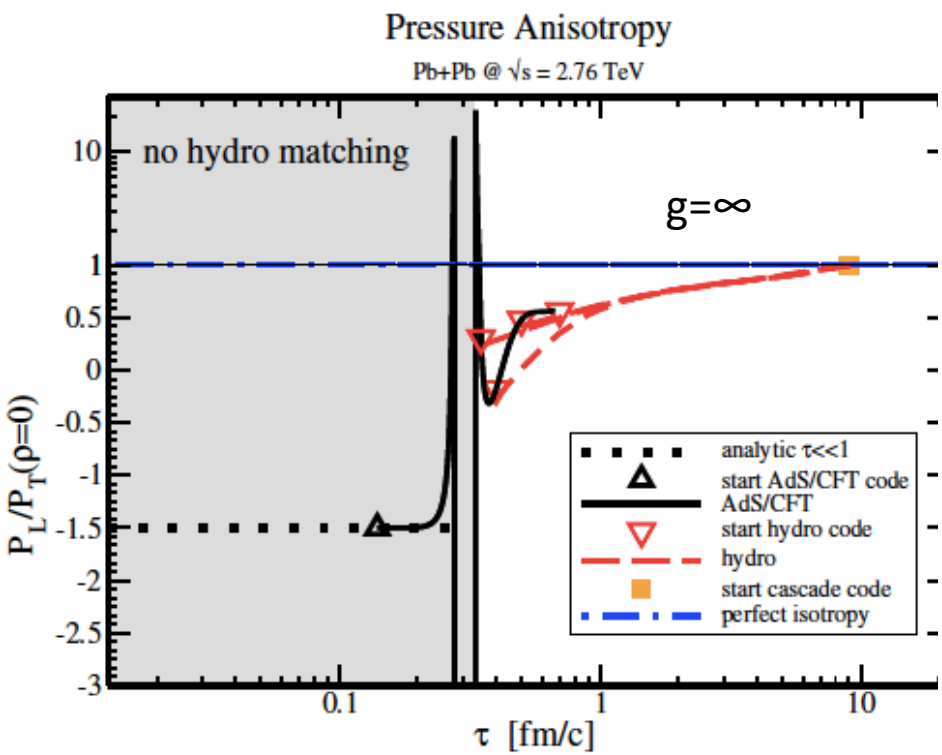

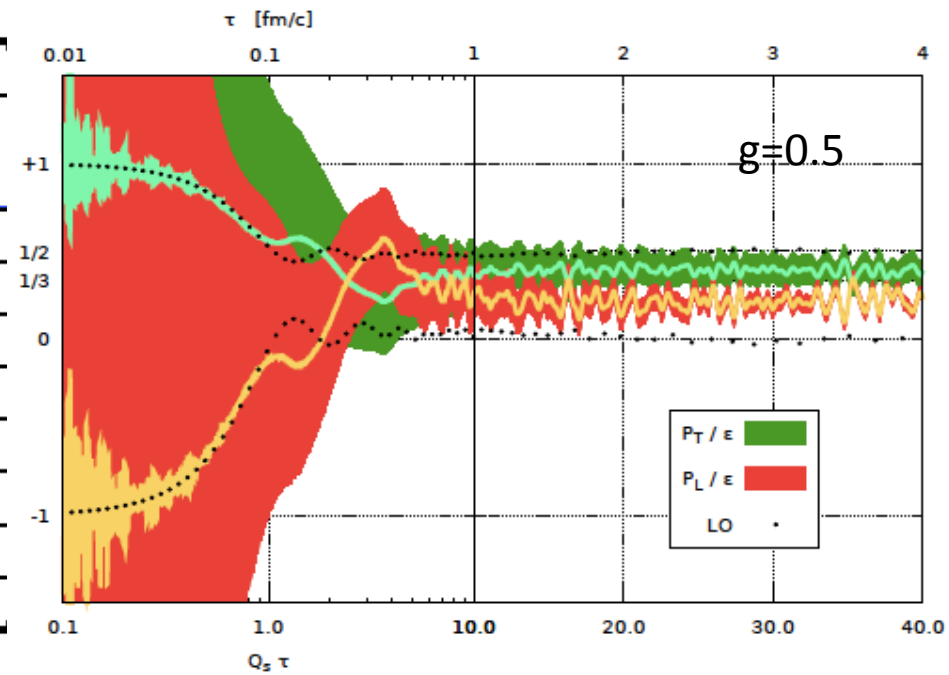

[van der Schee, PR & Pratt, 2013] [Epelbaum, Gelis, 2013]

How about making more comparisons like these???

Summary and Conclusion

- AdS/CFT is robust tool to model early-time heavy-ion collisions at very large coupling
- Leads natural to thermalization for $\tau > 0.5$ fm/c
- Results have fewer parameters than standard hydro models, but still depend on regulator

Wish list:

- Simulate non-central and 'lumpy hotspot' shocks
- Finite Coupling Corrections (match $dN/dY_{experiment}$?)
- Perform boosted BH collisions in AdS_5
- Weak coupling thermalization results to compare to

My message

It’s not Weak Coupling vs. AdS/CFT. We may need both to describe nature at g~2.

Backup

Towards real BH collisions in AdS

- Results so far use analytic approximate metric as initial data for GR evolution
- Advantages: ‘easy’ for numerical GR, promises quick contact with experiment
- Disadvantage: require (unphysical?) regulator
- Alternative: collide black holes in global AdS_5 (ongoing work with Hans Bantilan)

BH ‘collisions’ in global AdS_5

- Coordinates $x^\mu = (t, r, \chi, \theta, \phi)$
- Line element:

$ds^2 = g_{tt} dt^2 + g_{t\chi} dt d\chi + g_{tr} dt dr + g_{r\chi} dr d\chi$
$+ g_{\chi\chi} d\chi^2 + g_{rr} dr^2 + g_{\psi}(d\vartheta^2 + \sin^2\vartheta d\phi^2)$

- Gauge Condition: Generalized Harmonic (H^μ is lengthy!)

BH ‘collisions’ in global AdS_5

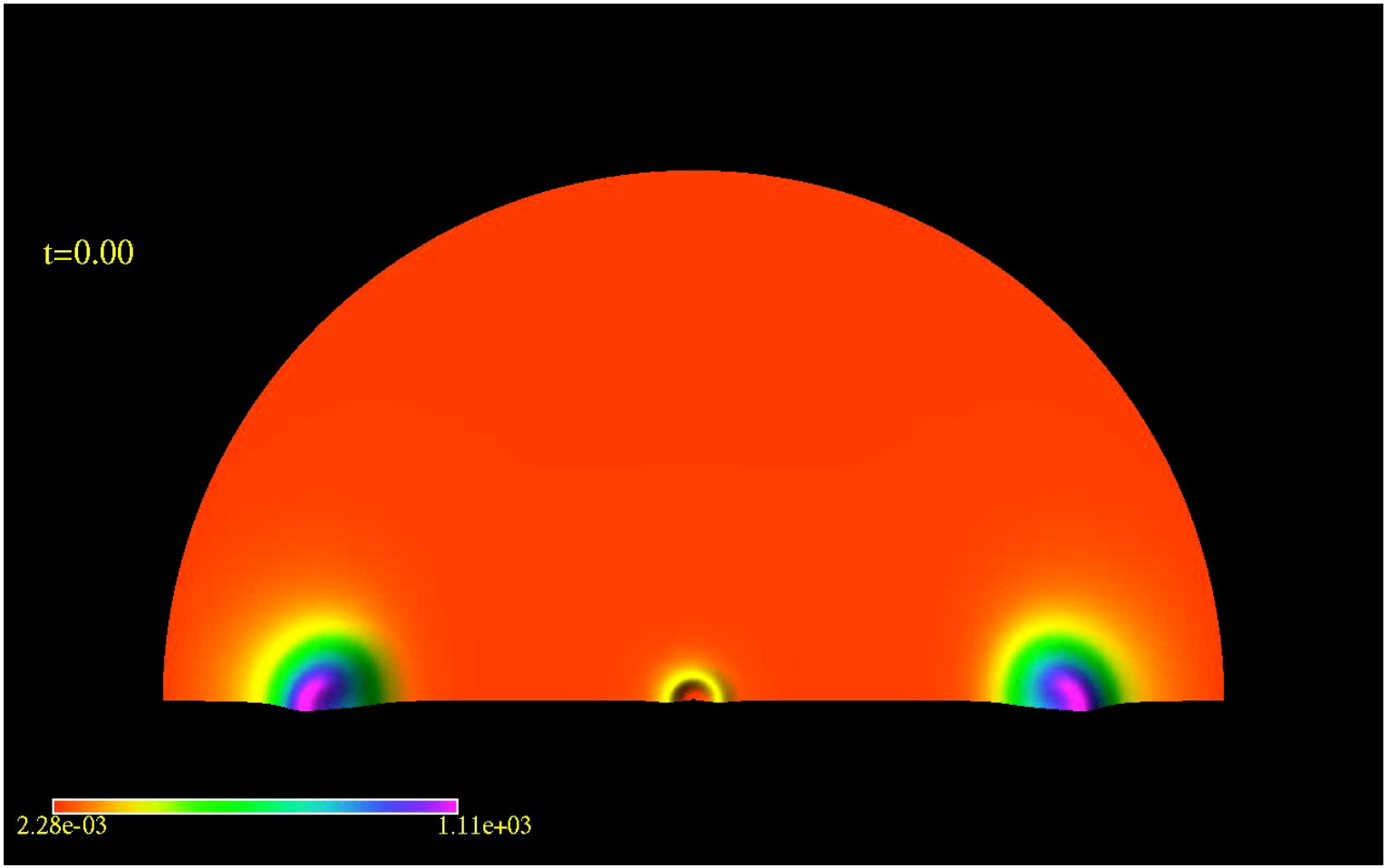

BH ‘collisions’ in global AdS_5

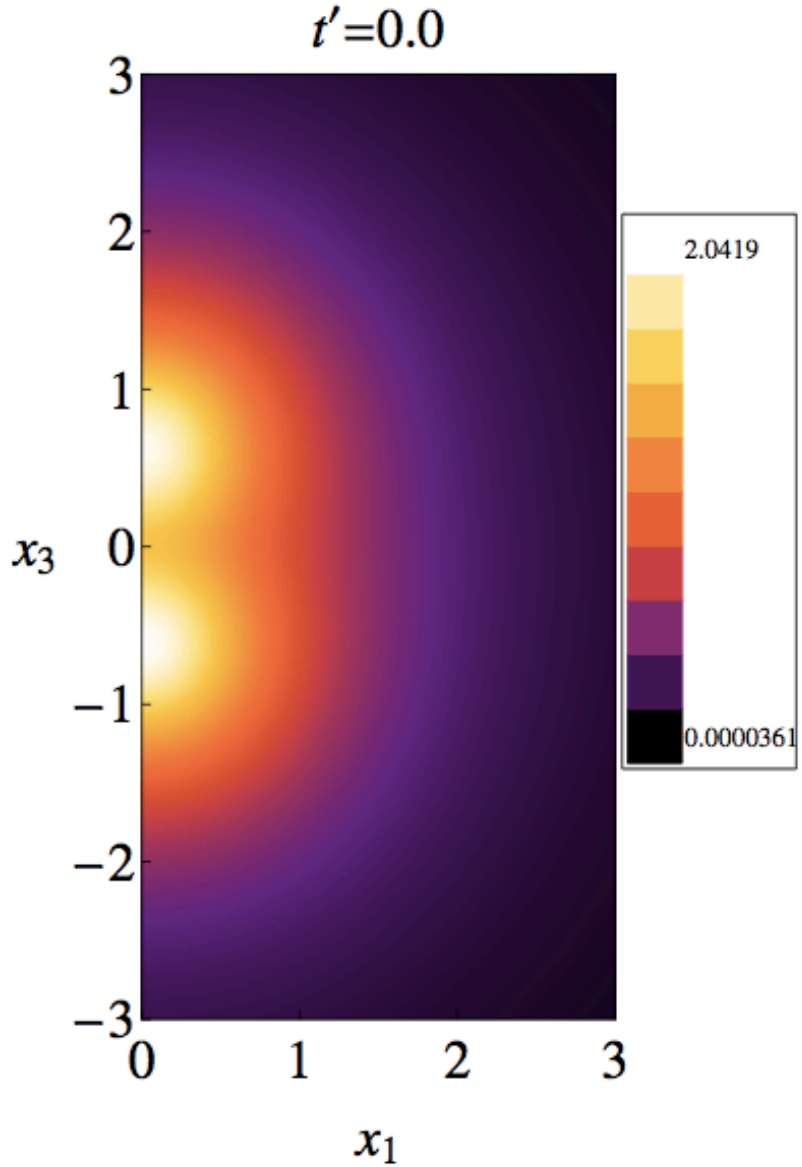

BH ‘collisions’ in global AdS_5

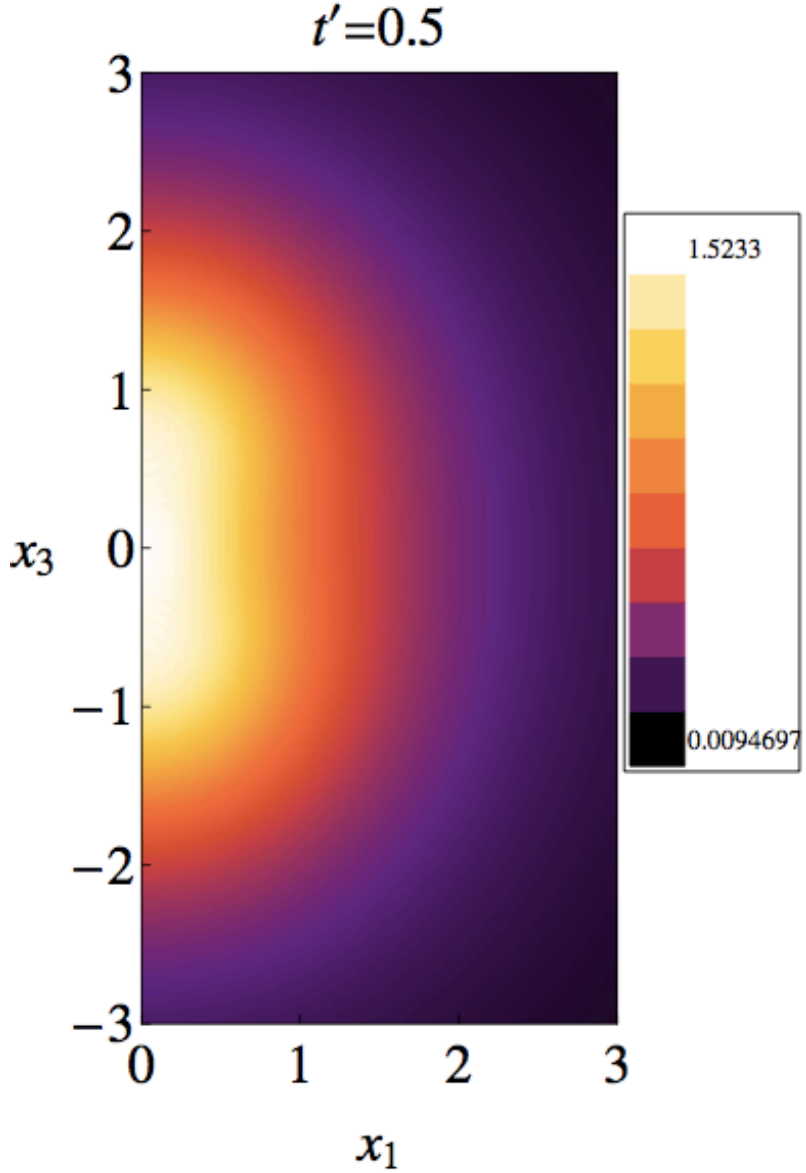

BH ‘collisions’ in global AdS_5

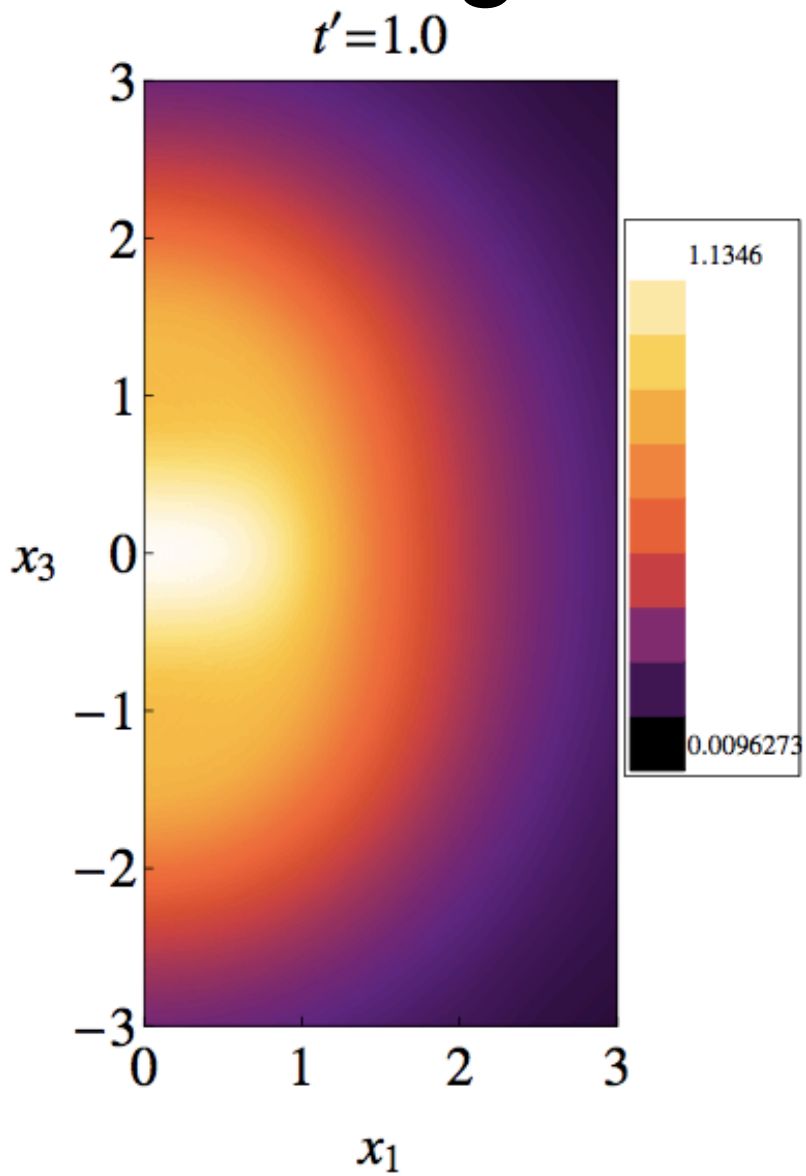

BH ‘collisions’ in global AdS_5

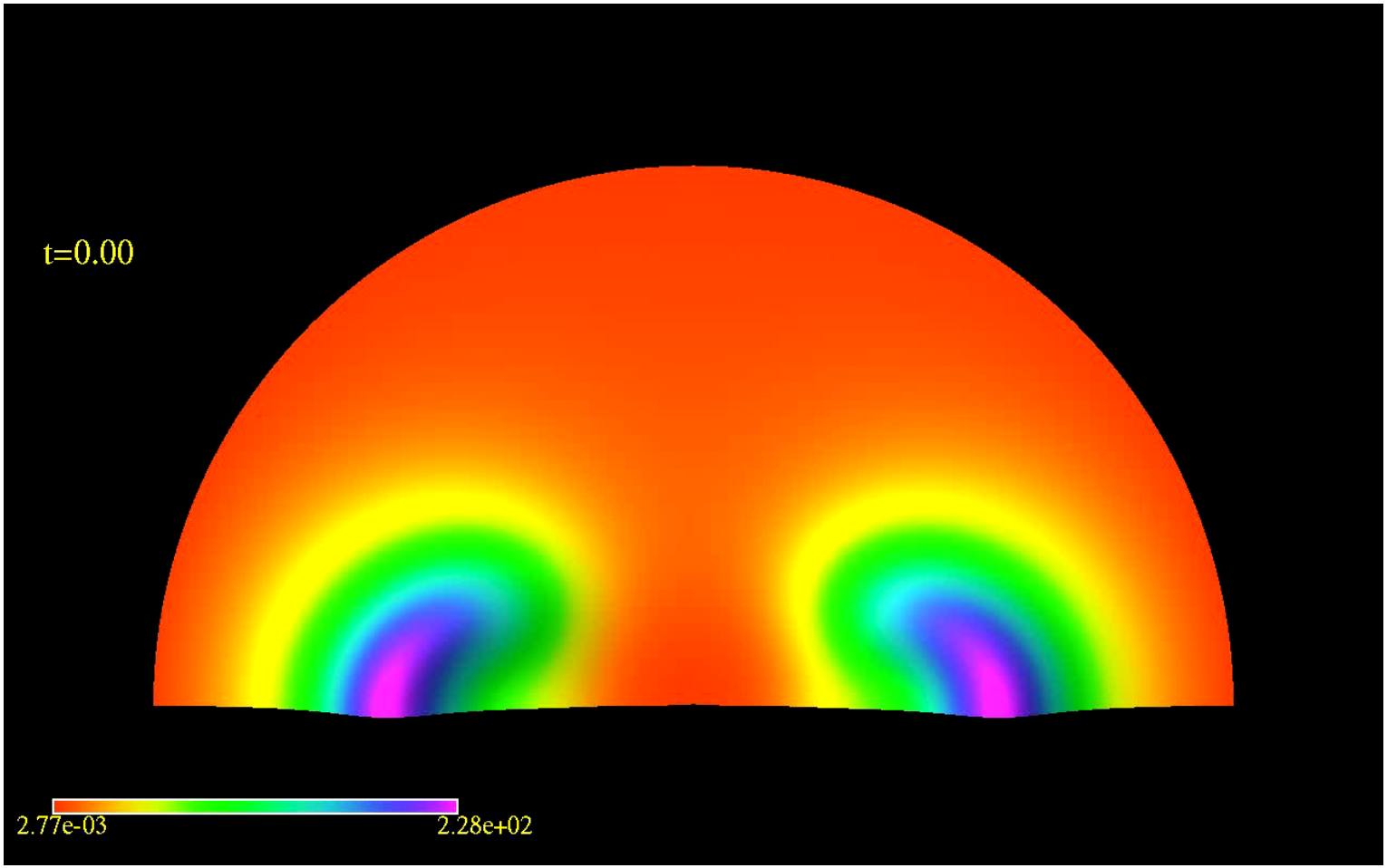

GEOMETRY AND FLUCTUATIONS IN LARGE AND SMALL NUCLEAR COLLISION SYSTEMS

BJÖRN SCHENKE, BROOKHAVEN NATIONAL LABORATORY

THE APPROACH TO EQUILIBRIUM
IN STRONGLY INTERACTING MATTER
APRIL 4 2014

BROOKHAVEN
NATIONAL LABORATORY

INTRODUCTION

- Heavy Ion Collisions:
  Initial state fluctuations and collective flow can describe lots of experimental data

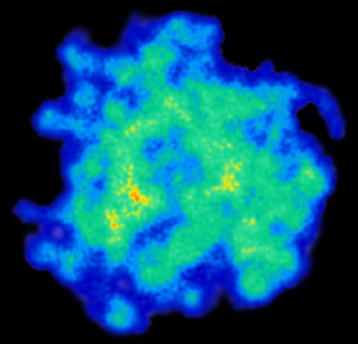

- Details of the fluctuations are important
- How to distinguish between different models of multi-particle production

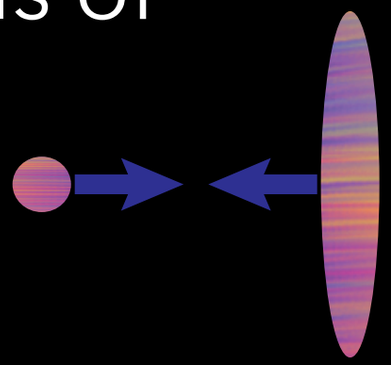

- Are the physics the same in small systems?

COMPUTING THE INITIAL STATE

B.SCHENKE, P.TRIBEDY, R.VENUGOPALAN, PRL108, 252301 (2012), PRC86, 034908 (2012)

- Gluon saturation at $p_T \lesssim Q_s(x, \mathbf{b})$

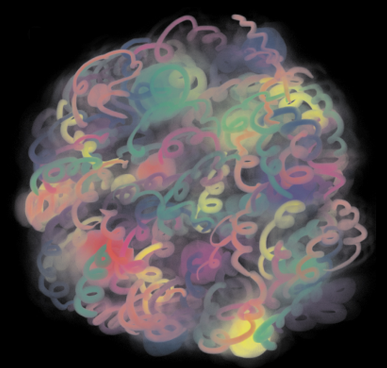

- Strong fields with occupation $\sim 1/\alpha_s$
  Classical description possible

- IP-Sat model parametrizes $Q_s(x, \mathbf{b})$
  (simple way to include impact parameter dependence)
  KOWALSKI, TEANEY, PHYS.REV. D68 (2003) 114005

- Fit parameters to HERA diffractive data

COMPUTING THE INITIAL STATE

B.SCHENKE, P.TRIBEDY, R.VENUGOPALAN, PRL108, 252301 (2012), PRC86, 034908 (2012)

- Sample nucleon positions from Woods-Saxon distribution
- Add all (Gaussian) thickness functions
- Extract $Q_s(x, \mathbf{x}_T)$ and get color charge density distribution

$$\frac{d\sigma^{p}_{dip}}{d^2\mathbf{x}_T}(\mathbf{r}_T, x, \mathbf{x}_T) = 2\mathcal{N}(\mathbf{r}_T, x, \mathbf{x}_T) = 2\left[1 - \exp\left(-\frac{\pi^2}{2N_c}\mathbf{r}_T^2\alpha_s(Q^2)xg(x, Q^2)\sum_{i=1}^{A} T_p(\mathbf{x}_T - \mathbf{x}_T^i)\right)\right]$$

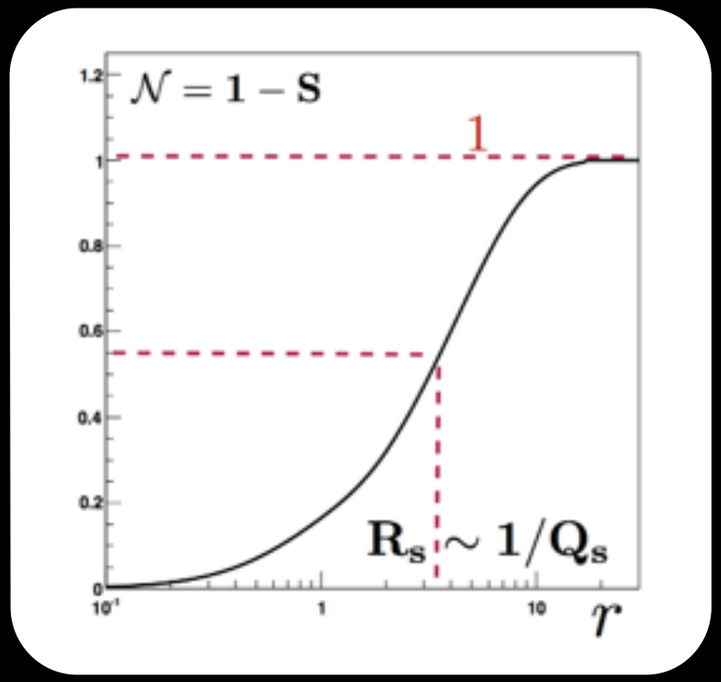

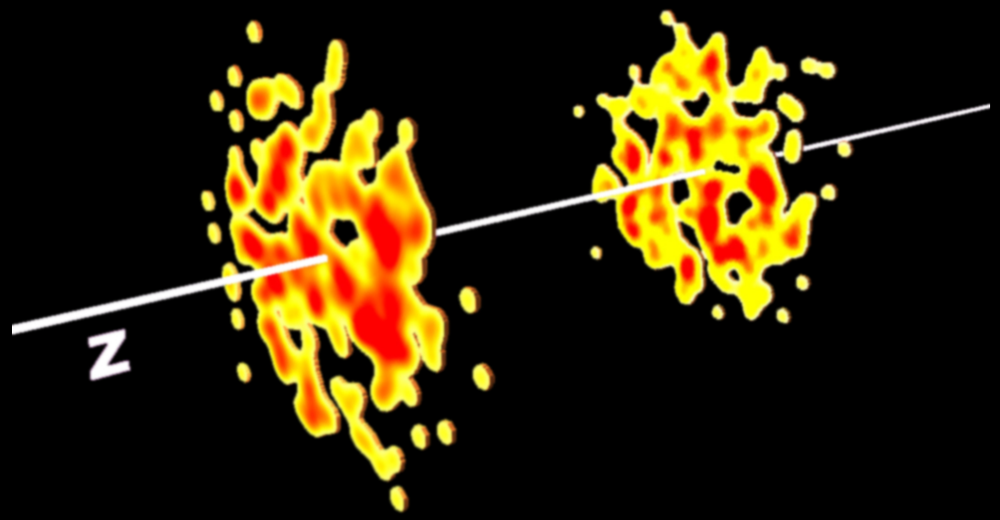

COMPUTING THE INITIAL STATE

B.SCHENKE, P.TRIBEDY, R.VENUGOPALAN, PRL108, 252301 (2012), PRC86, 034908 (2012)

- Sample color charge density $\rho^{A/B}(\mathbf{x}_T)$
- For nucleus A and B compute the path-ordered exponential over its longitudinal extend

$$V_{A/B}(\mathbf{x}_T) = \prod_{k=1}^{N_y} \exp\left(- ig \frac{\rho_k^{A/B}(\mathbf{x}_T)}{\nabla_T^2 + m^2} \right)$$

- m is an infrared cutoff of order Λ_{QCD}
- Wilson lines after the collision are then obtained from V_A and V_B via the Yang-Mills equations

COMPUTING THE INITIAL STATE

B.SCHENKE, P.TRIBEDY, R.VENUGOPALAN, PRL108, 252301 (2012), PRC86, 034908 (2012)

- Yang-Mills equations determine:
  KRASNITZ, VENUGOPALAN, NUCL.PHYS. B557 (1999) 237
  - Initial gluon fields from color charges
  - Energy density after the collision
  - Early non-equilibrium time evolution

INITIAL STATE AND FLUID DYNAMICS

C.GALE, S.JEON, B.SCHENKE, P.TRIBEDY, R.VENUGOPALAN, PHYS.REV.LETT. 110, 012302 (2013)

- Compute energy-momentum tensor $T^{\mu\nu}$ of the classical fields
- Extract energy density and flow vector via $u_\mu T^{\mu\nu} = \varepsilon u^\nu$
- This provides the initial conditions for fluid dynamic simulations
- At the moment set initial $\Pi^{\mu\nu} = 0$

INITIAL STATE AND FLUID DYNAMICS

C.GALE, S.JEON, B.SCHENKE, P.TRIBEDY, R.VENUGOPALAN, PHYS.REV.LETT. 110, 012302 (2013)

$\eta/s = 0$ $\eta/s = 0.1$ $\eta/s = 0.2$

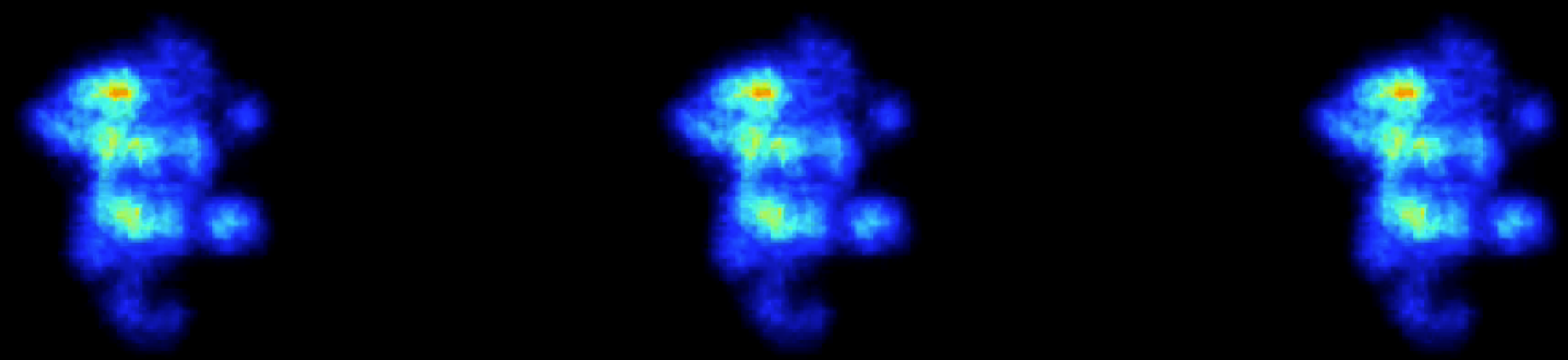

t = 0.40 fm

EVENT-BY-EVENT FLUID DYNAMICS

C.GALE, S.JEON, B.SCHENKE, P.TRIBEDY, R.VENUGOPALAN, PHYS.REV.LETT. 110, 012302 (2013)

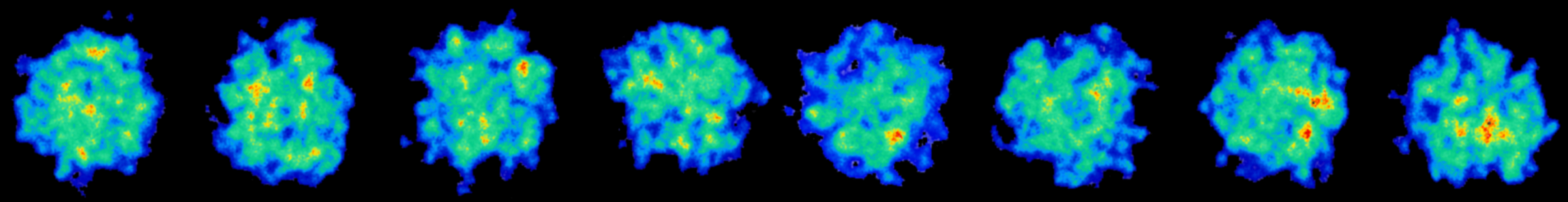

- Evolve many initial shapes using fluid dynamics
- Convert energy density to particles ("freeze-out")
- Determine v_n coefficients of particle distributions
- Average and compare to experimental data

AVERAGE AND RMS v_n

ATLAS COLLABORATION, JHEP 1311 (2013) 183
CMS COLLABORATION, PRC 87(2013) 014902, ARXIV:1310.8651

ATLAS

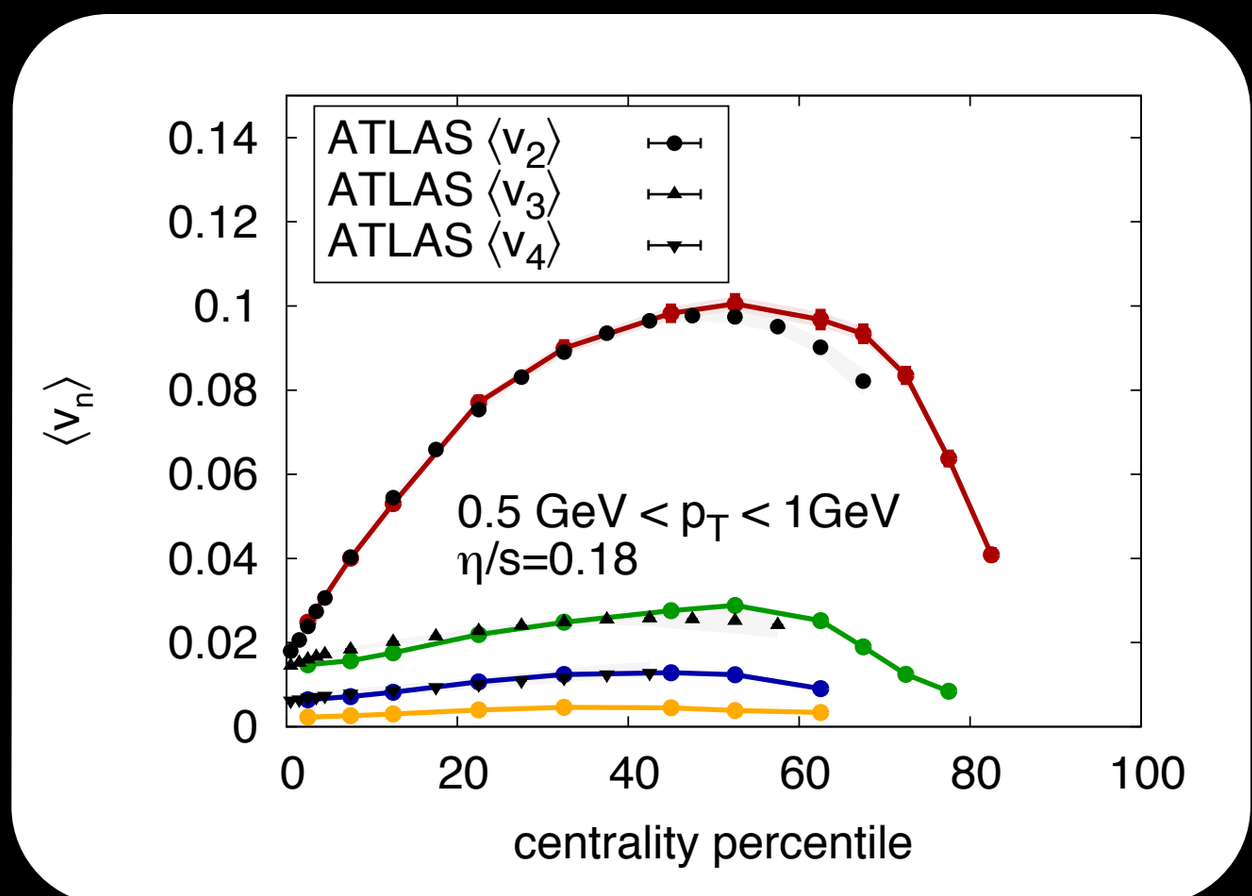

Mean from distributions

CMS

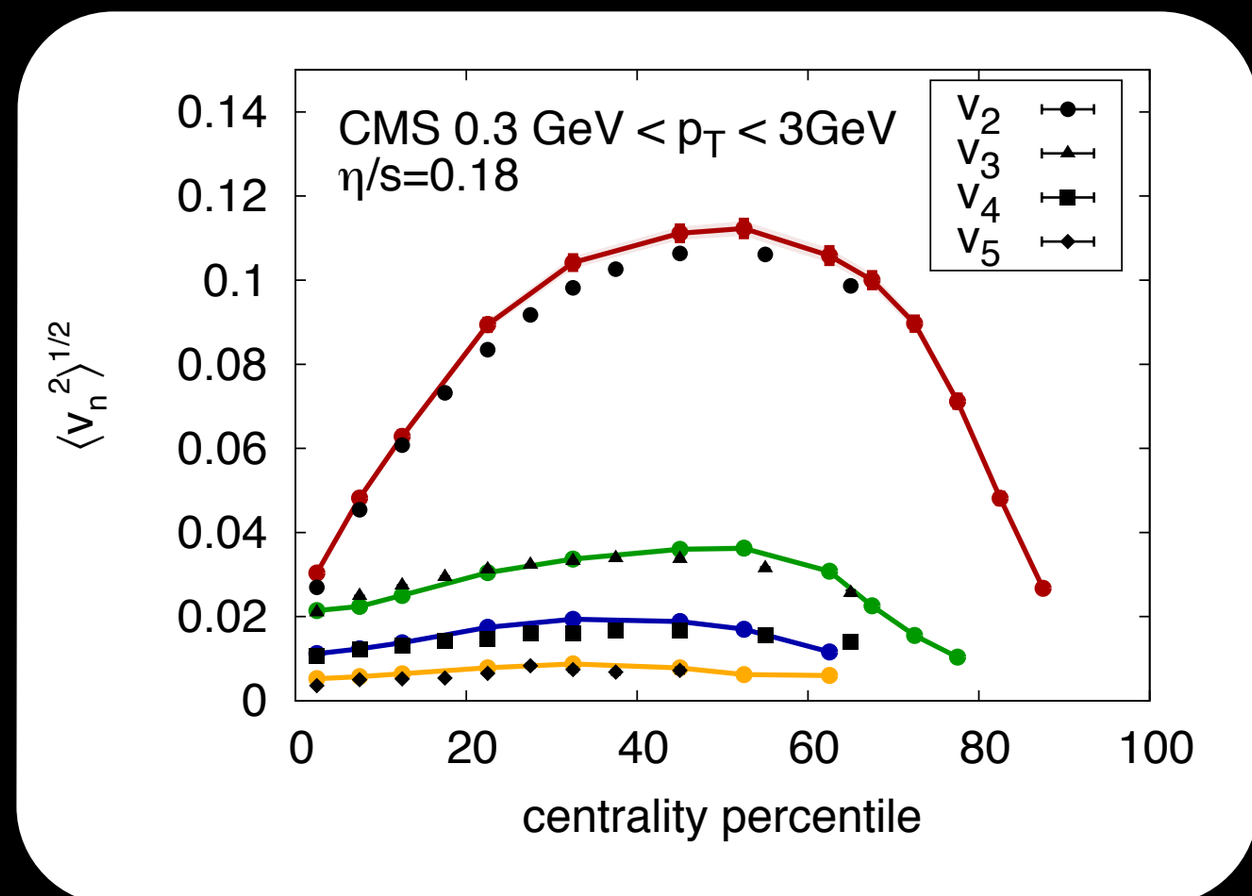

Event-plane method

EVENT-BY-EVENT FLOW

ATLAS COLLABORATION, JHEP 1311 (2013) 183

C. GALE, S. JEON, B.SCHENKE, P.TRIBEDY, R.VENUGOPALAN, PRL110, 012302 (2013)

$0-5\%$ $\qquad$ $20-25\%$

v_2

v_3

v_4

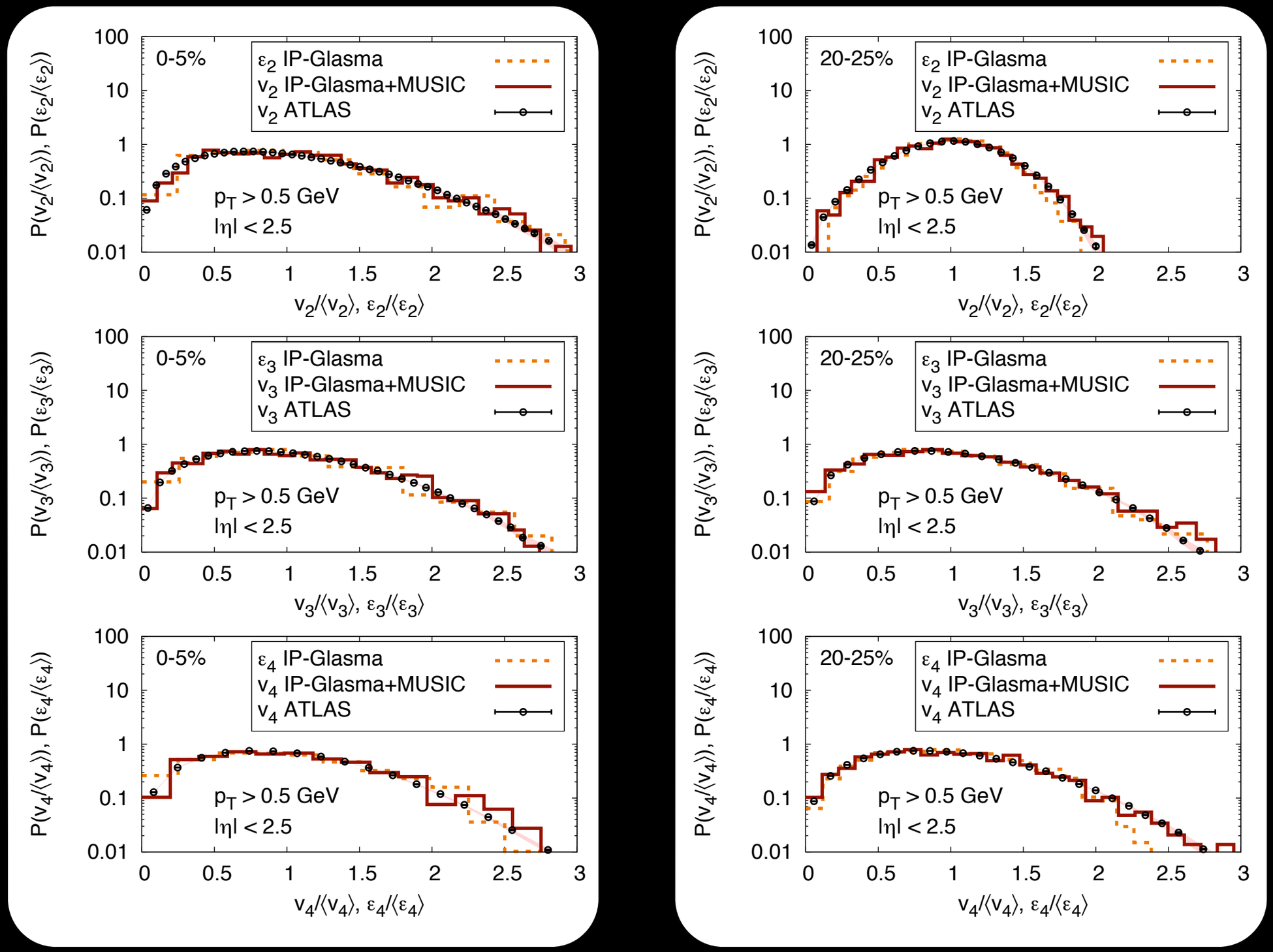

EVENT-BY-EVENT FLOW

ATLAS COLLABORATION, JHEP 1311 (2013) 183

v_2

v_3

v_4

45 – 50%

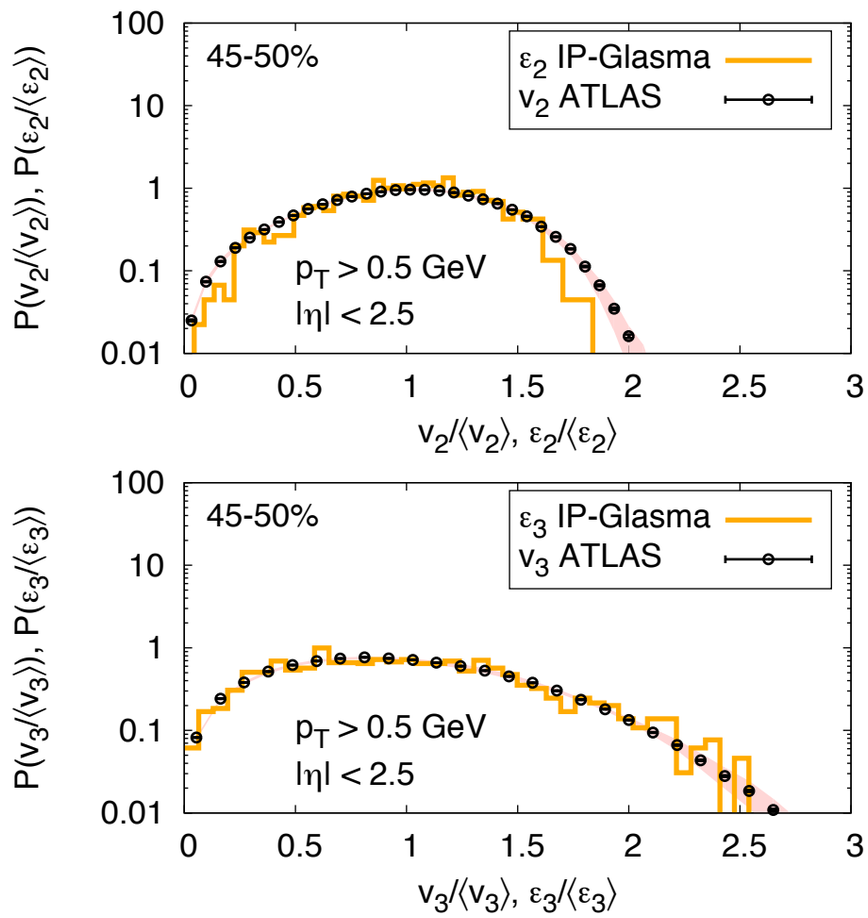

65 – 70%

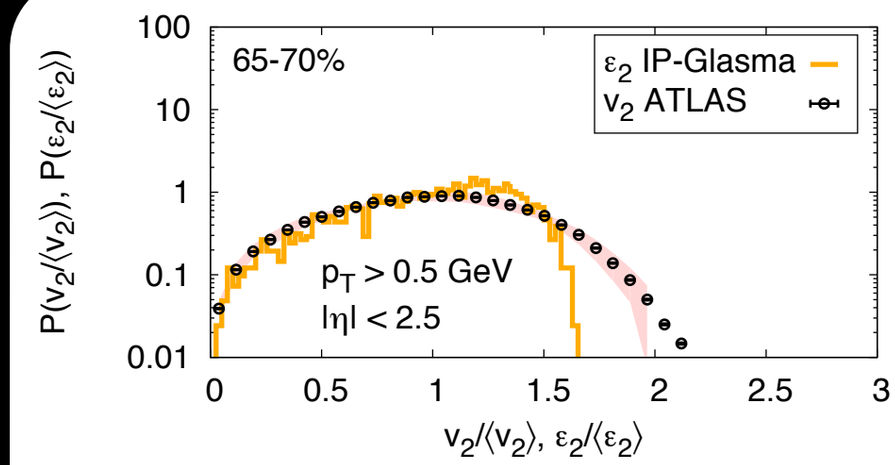

EVENT-BY-EVENT FLOW

ATLAS COLLABORATION, JHEP 1311 (2013) 183

v_2

v_3

v_4

45 – 50%

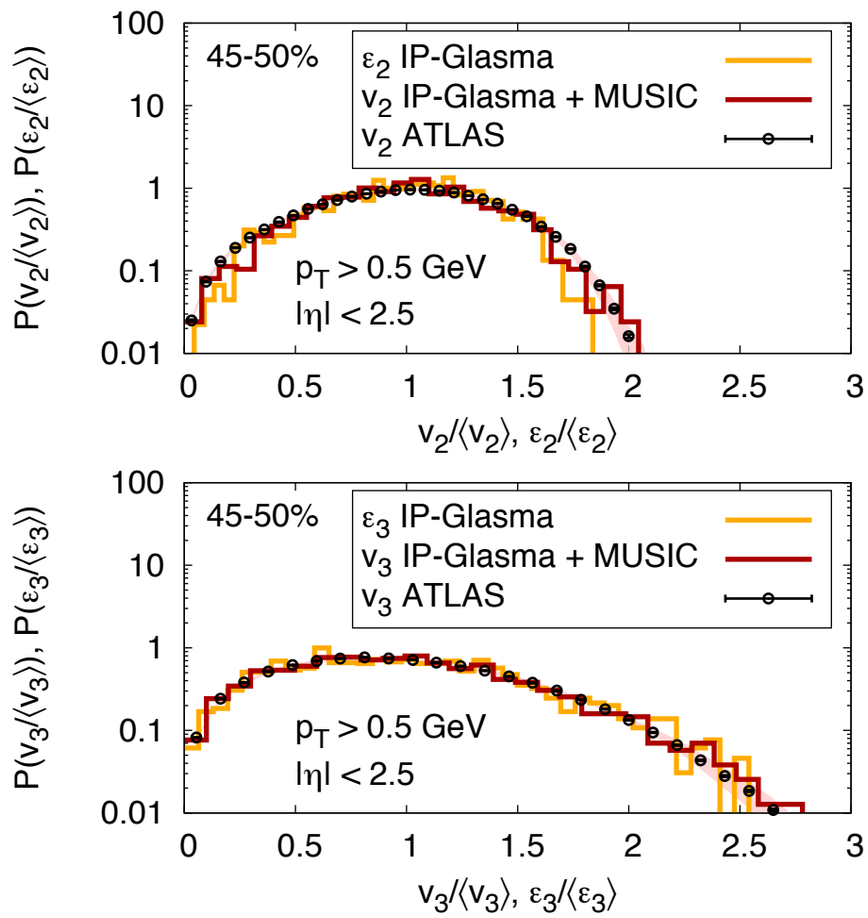

65 – 70%

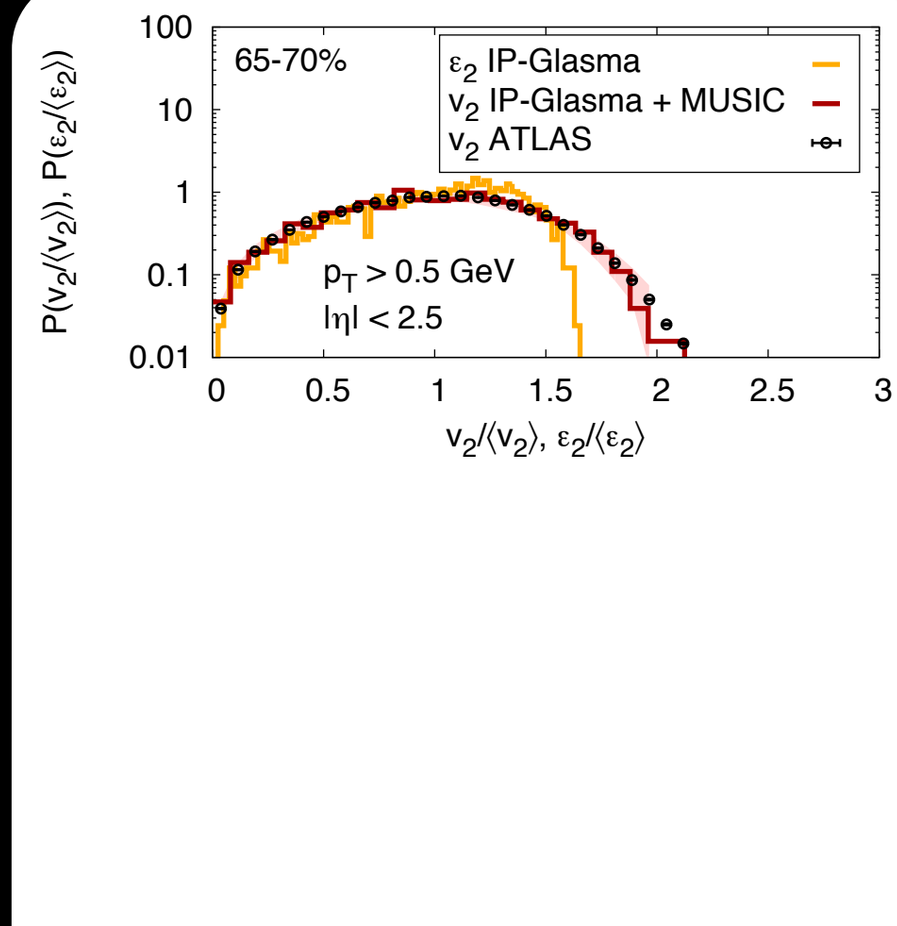

EVENT-BY-EVENT FLOW

ATLAS COLLABORATION, JHEP 1311 (2013) 183

45 – 50%

65 – 70% IDEAL

v_2

v_3

v_4

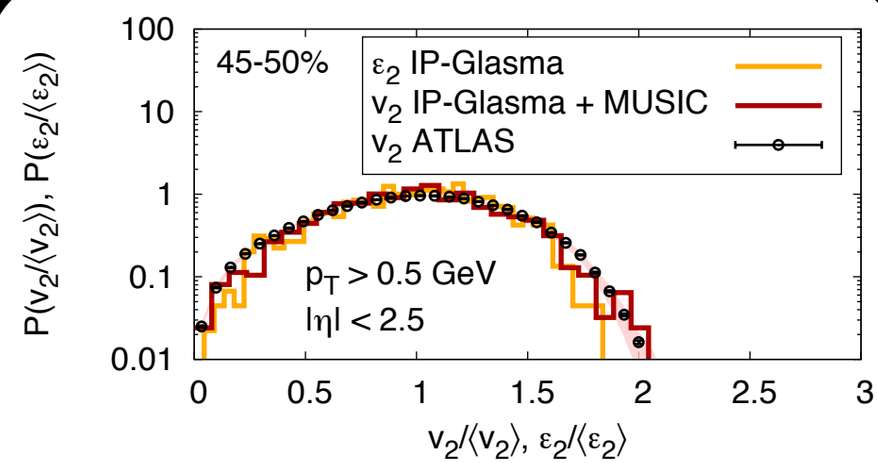

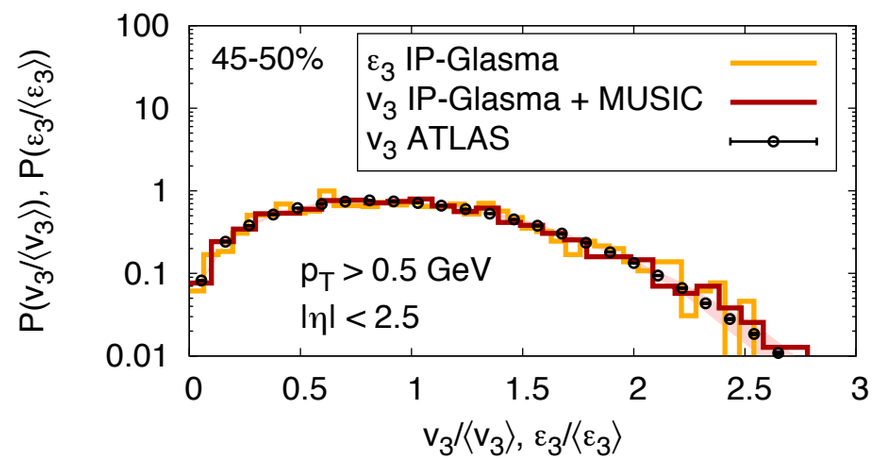

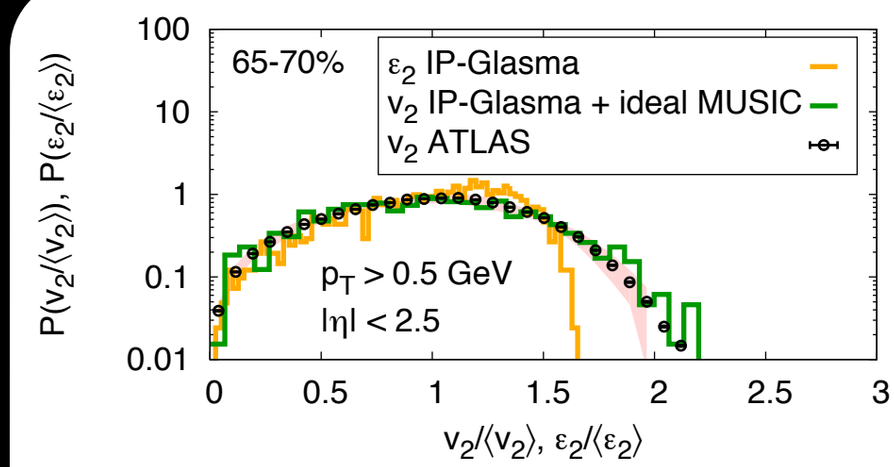

IDENTIFIED PARTICLE FLOW

ALICE COLLABORATION, J.PHYS. G38 (2011) 124047

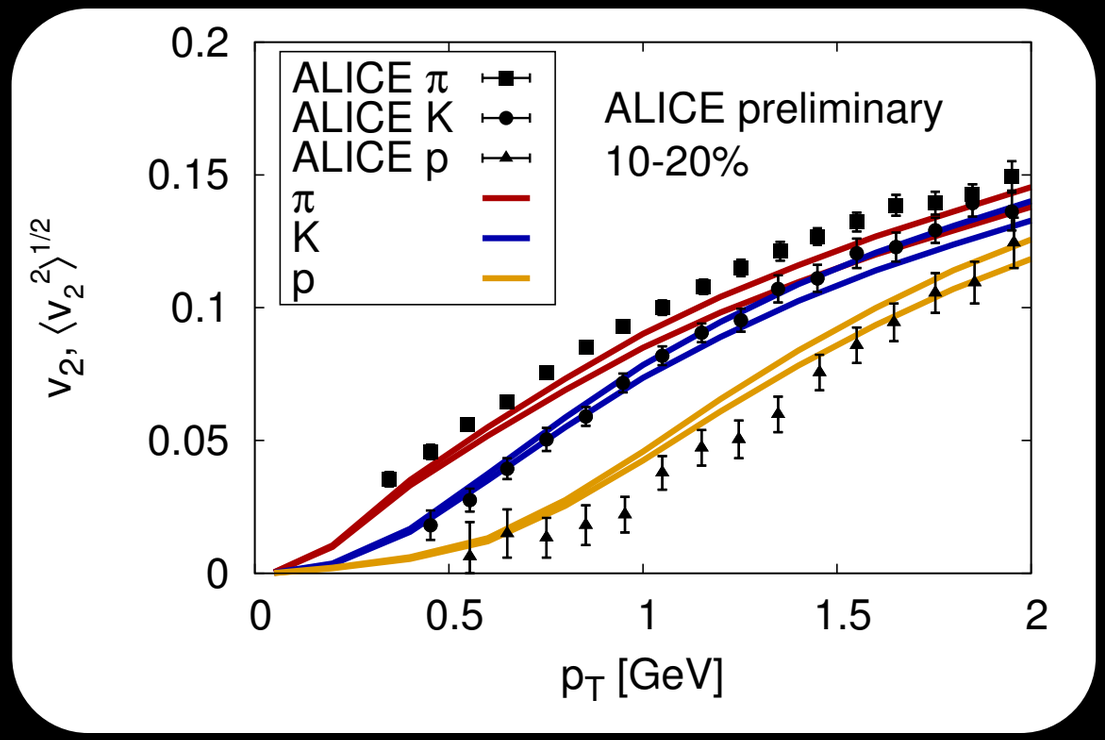

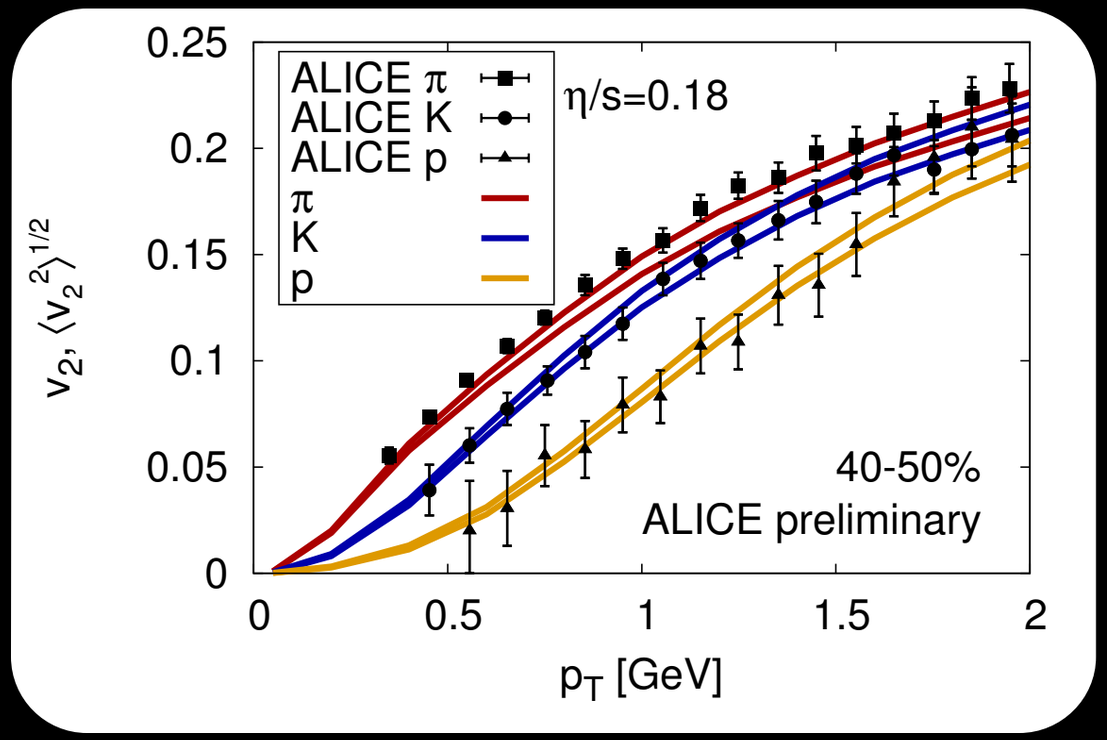

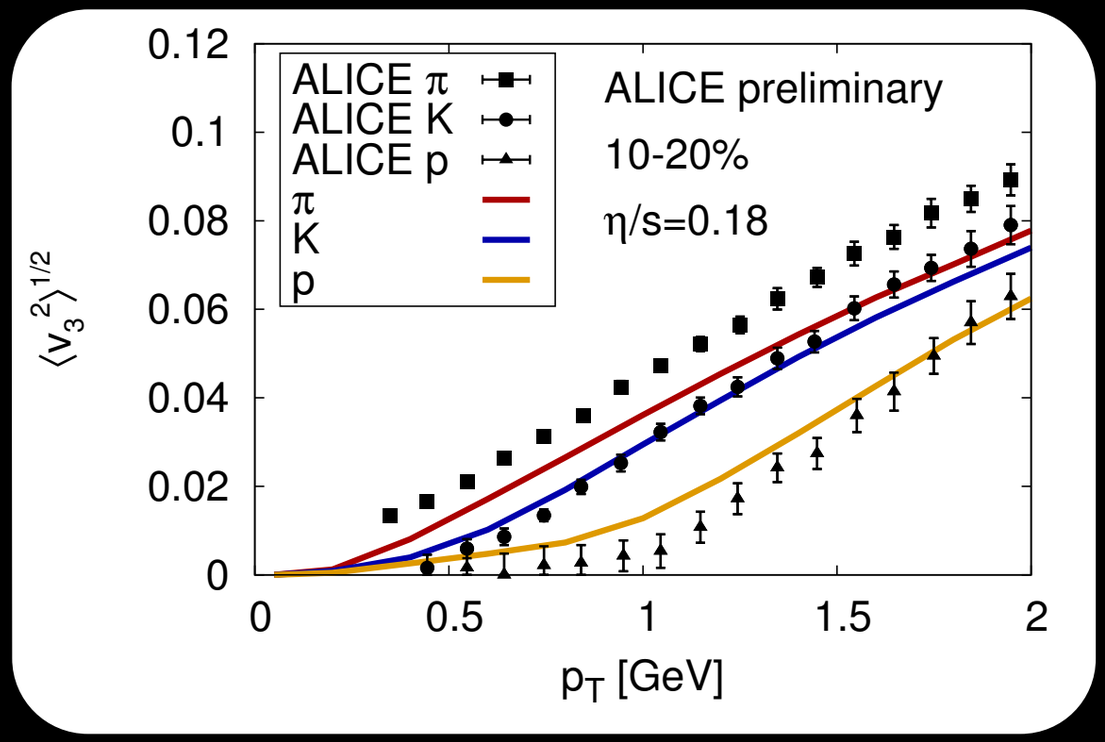

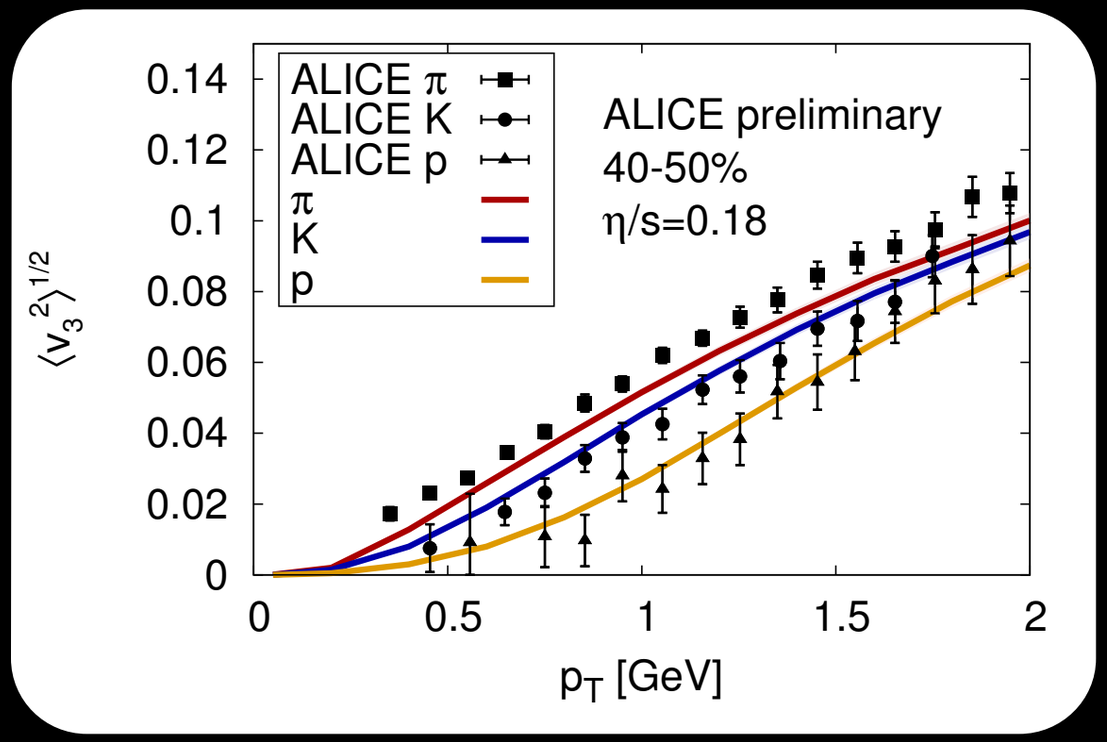

DEFORMED NUCLEI

B. SCHENKE, P. TRIBEDY, R. VENUGOPALAN, ARXIV:1403.2232

- Select ultra-central events based on neutrons in the ZDC
- Study correlation between v_2 and multiplicity
- MC-Glauber gets (anti-)correlation because of N_{coll} in

$$\frac{dN}{d\eta} = n_{\mathrm{pp}}\left(xN_{\mathrm{coll}} + (1-x)\frac{N_{\mathrm{part}}}{2}\right)$$

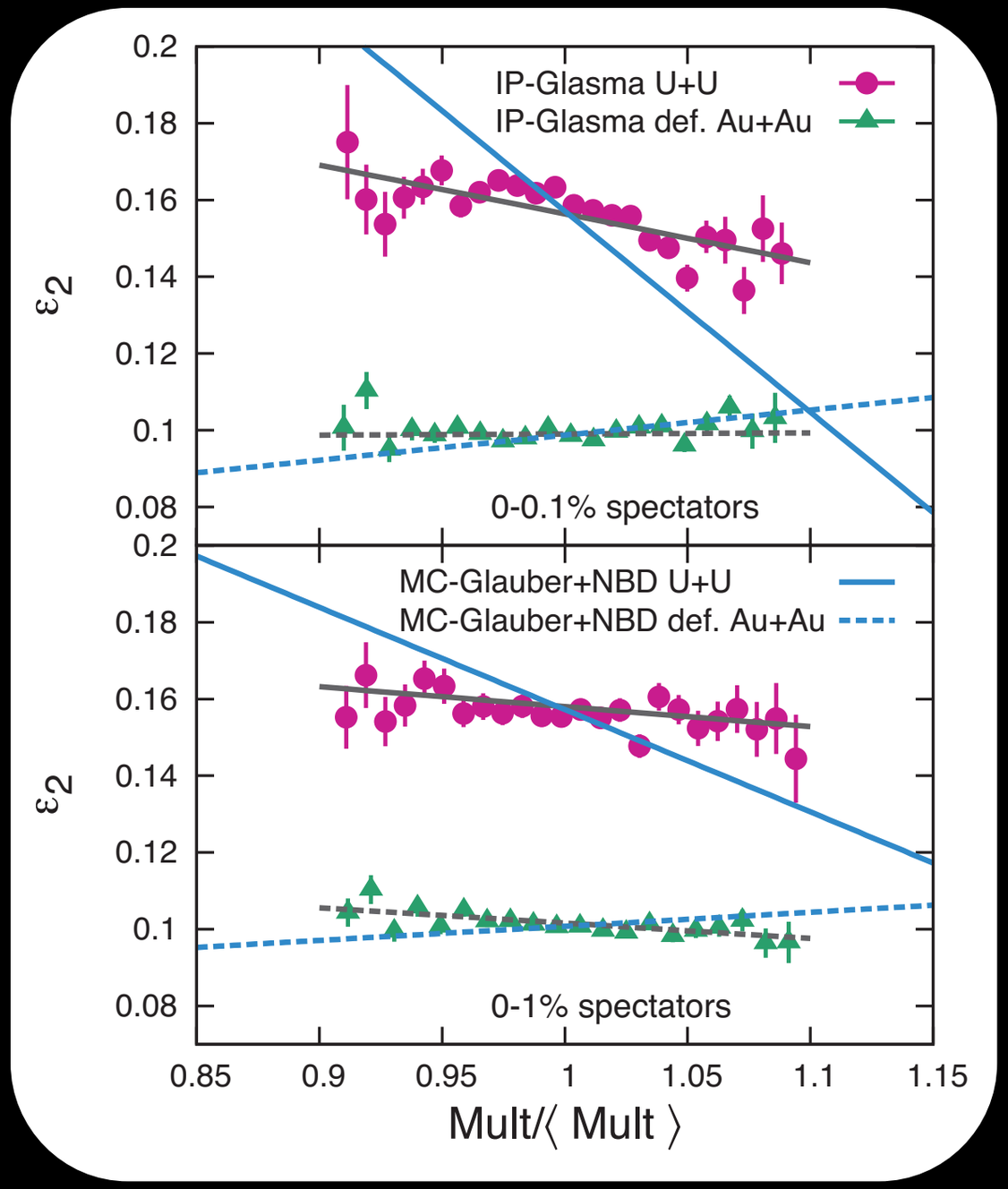

- IP-Glasma finds weaker anti-correlation

DEFORMED NUCLEI

B. SCHENKE, P. TRIBEDY, R. VENUGOPALAN, ARXIV:1403.2232

- Uranium: prolate
- Gold: oblate

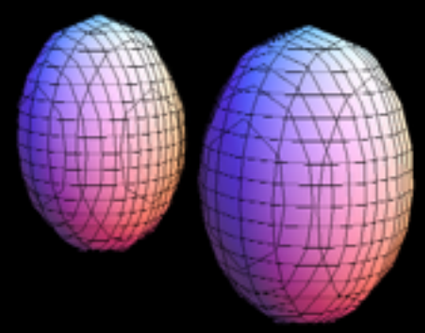

U+U, side-side

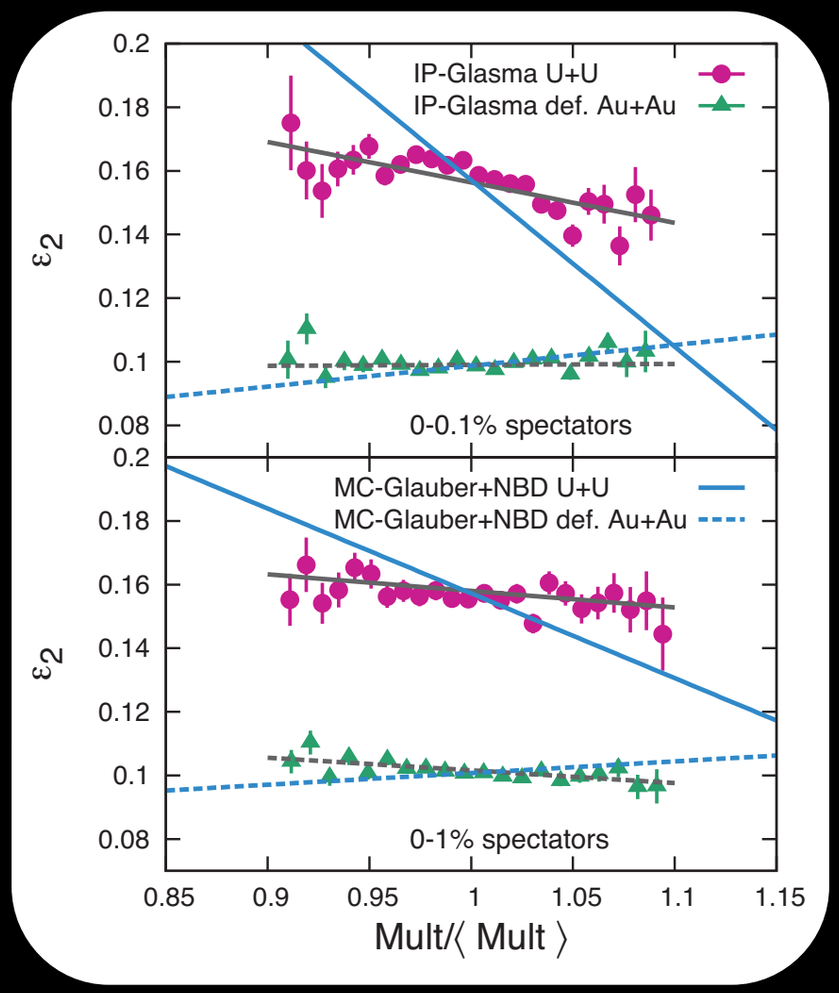

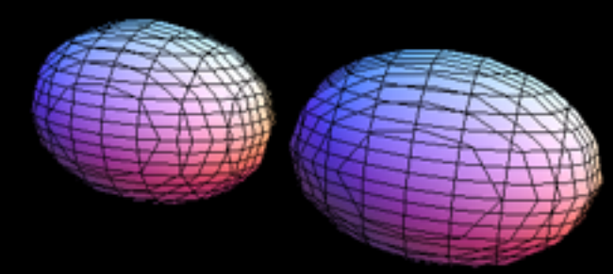

U+U, tip-tip

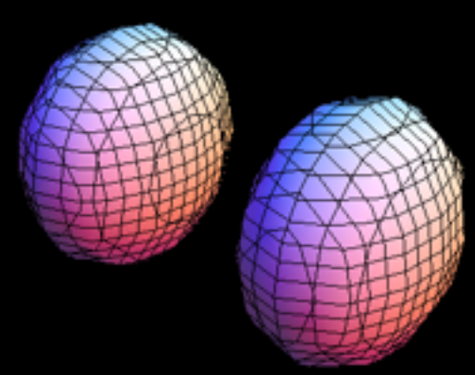

Au+Au, side-side

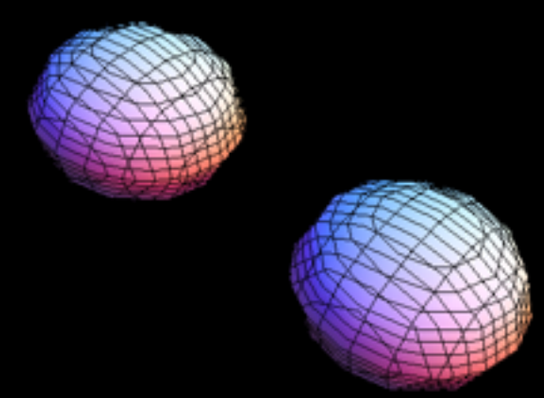

Au+Au, “tip-tip”

SMALL SYSTEMS

A. BZDAK, B. SCHENKE, P. TRIBEDY, R. VENUGOPALAN, PRC87, 064906 (2013)

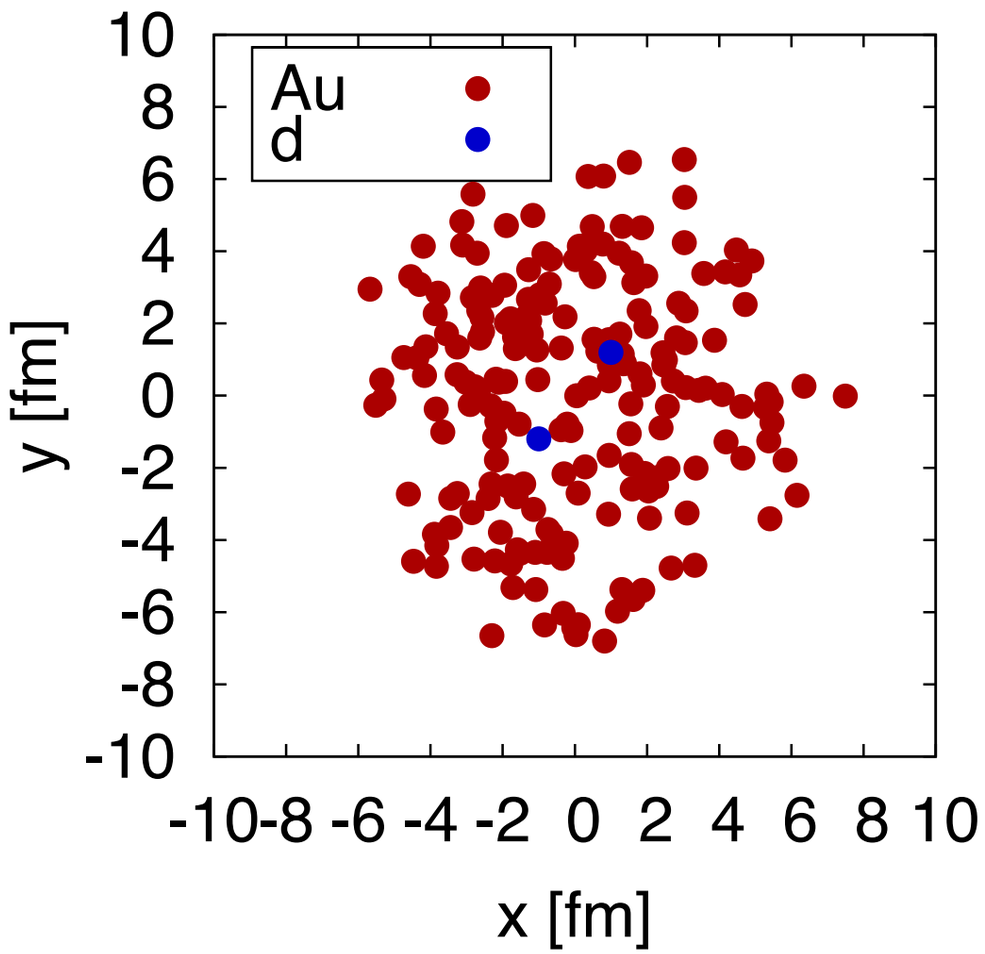

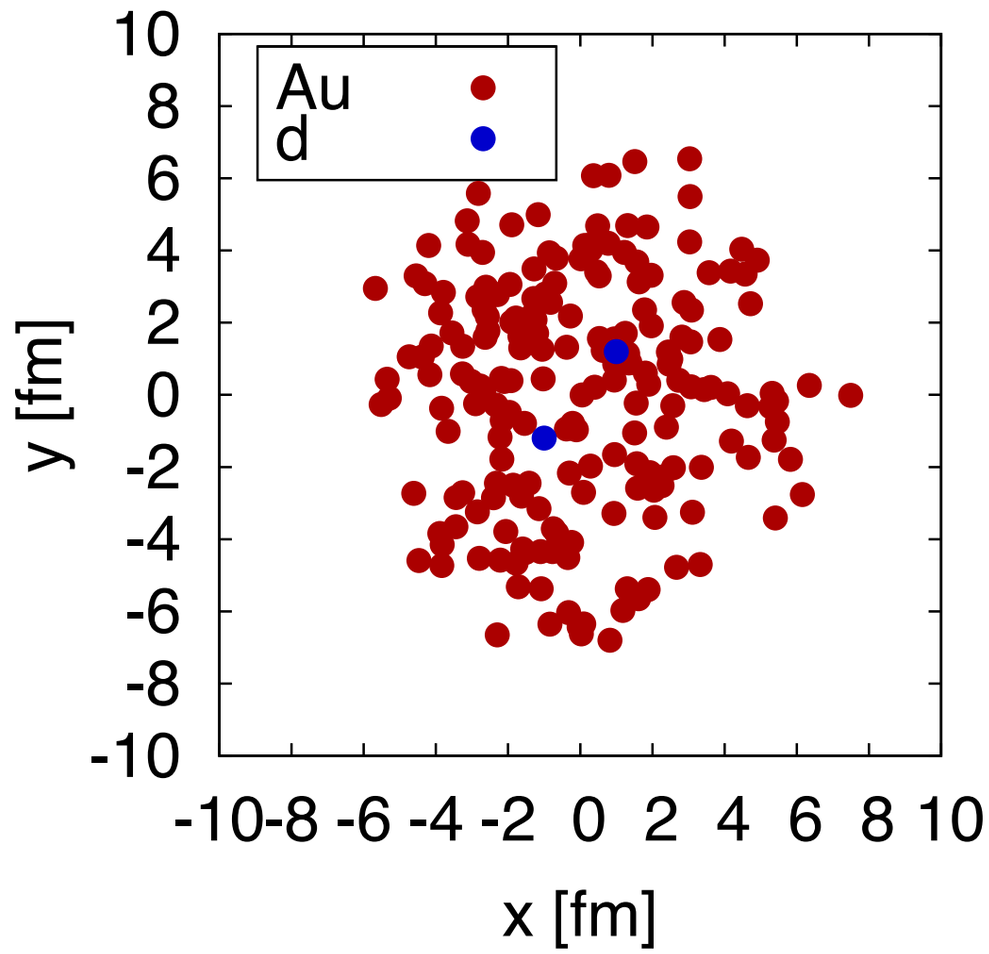

SMALL SYSTEMS

A. BZDAK, B. SCHENKE, P. TRIBEDY, R. VENUGOPALAN, PRC87, 064906 (2013)

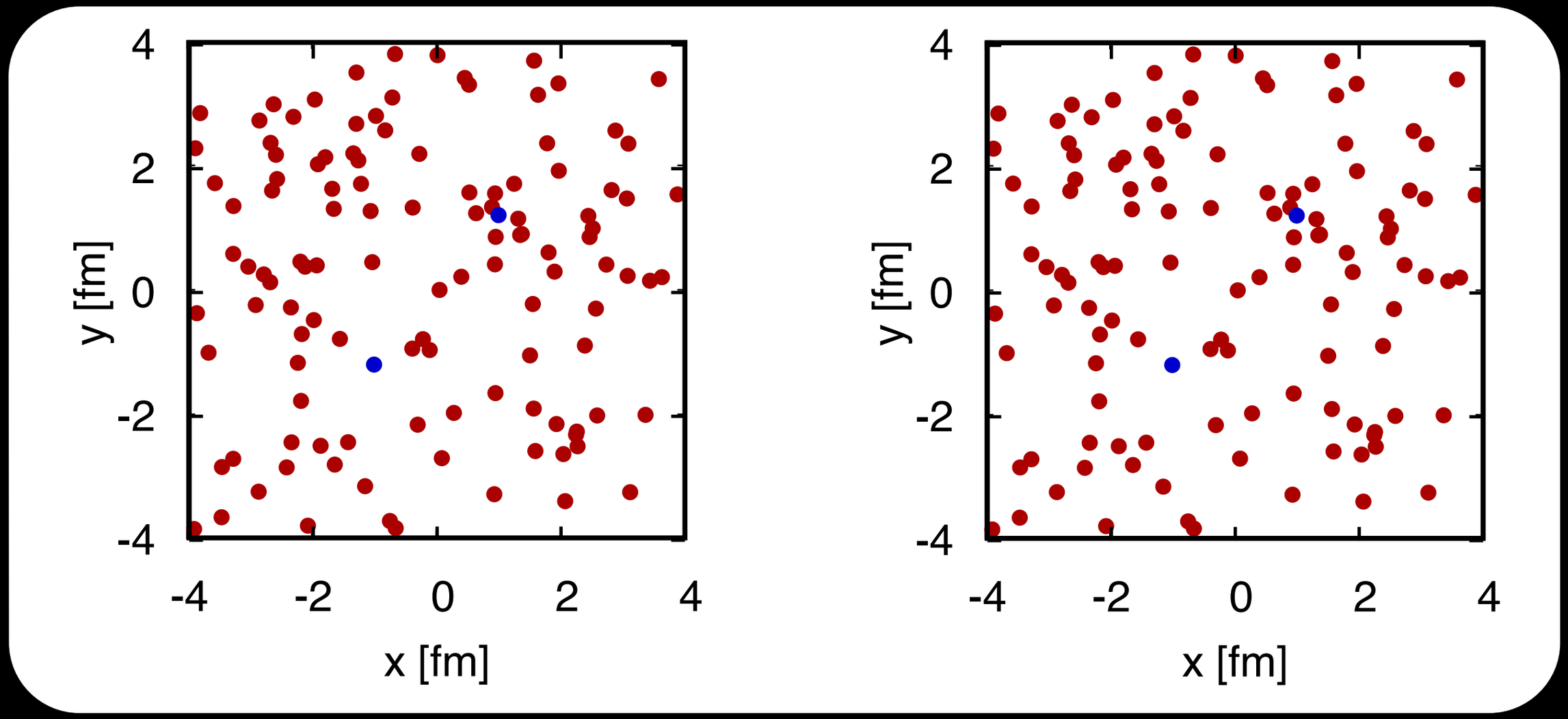

SMALL SYSTEMS

A. BZDAK, B. SCHENKE, P. TRIBEDY, R. VENUGOPALAN, PRC87, 064906 (2013)

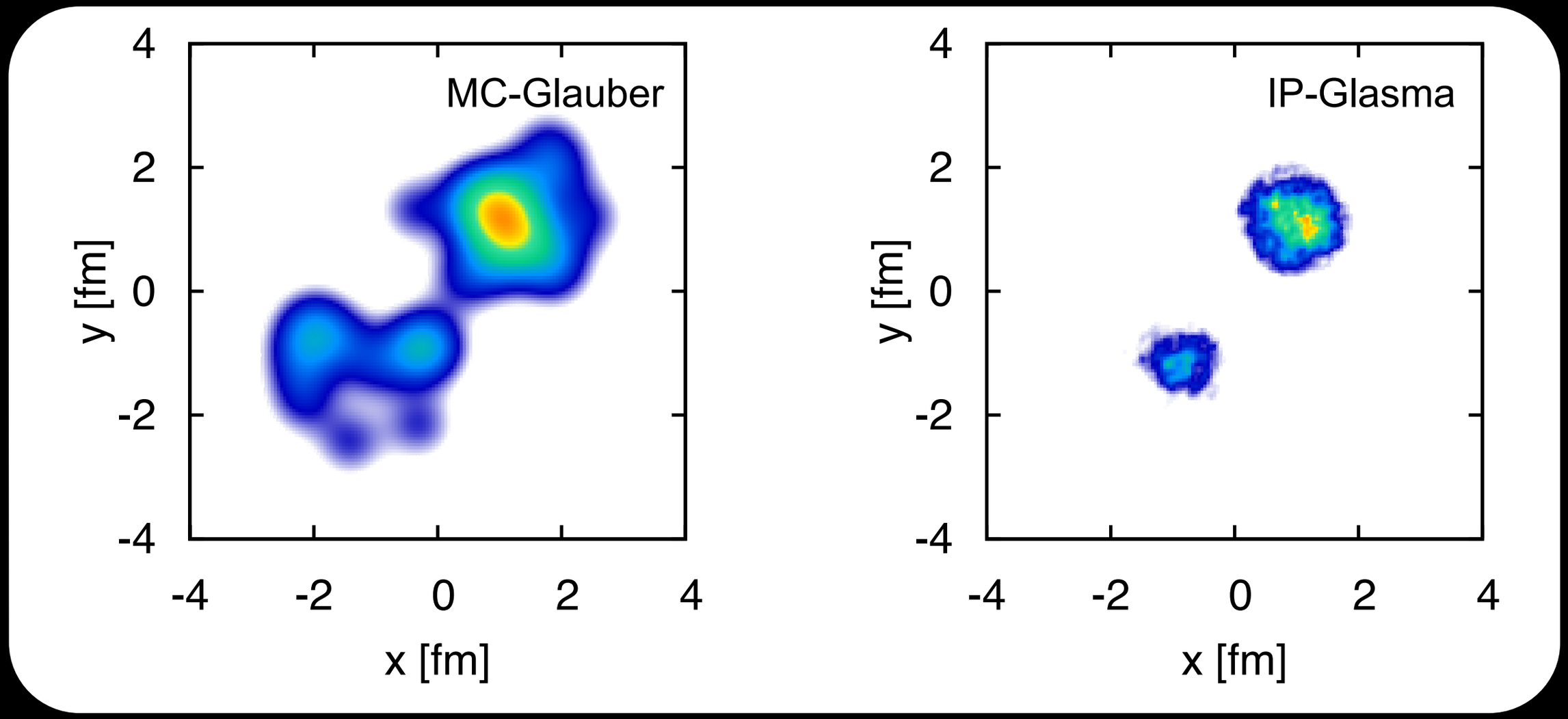

SMALL SYSTEMS

A. BZDAK, B. SCHENKE, P. TRIBEDY, R. VENUGOPALAN, PRC87, 064906 (2013)

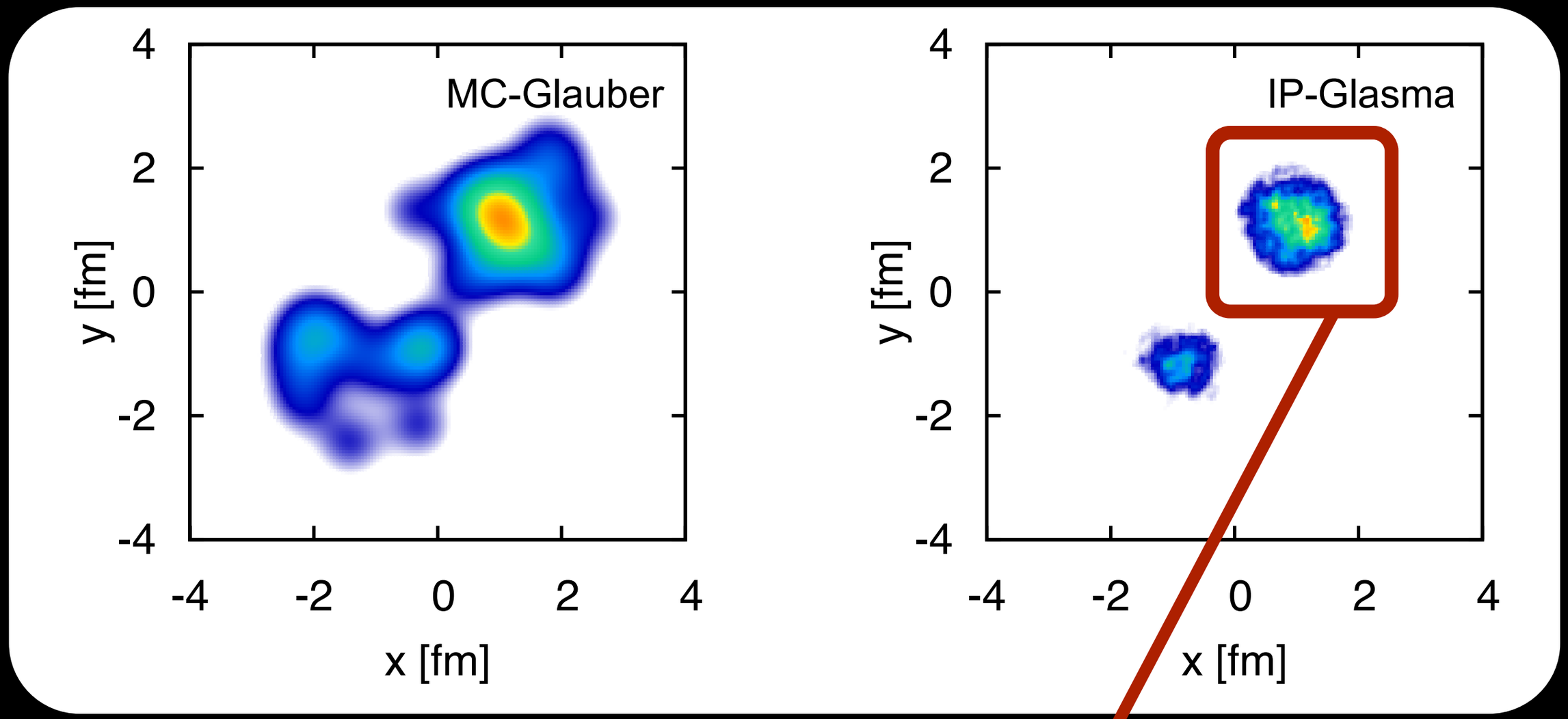

p+A will look like this

SMALL SYSTEMS

A. BZDAK, B. SCHENKE, P. TRIBEDY, R. VENUGOPALAN, PRC87, 064906 (2013)

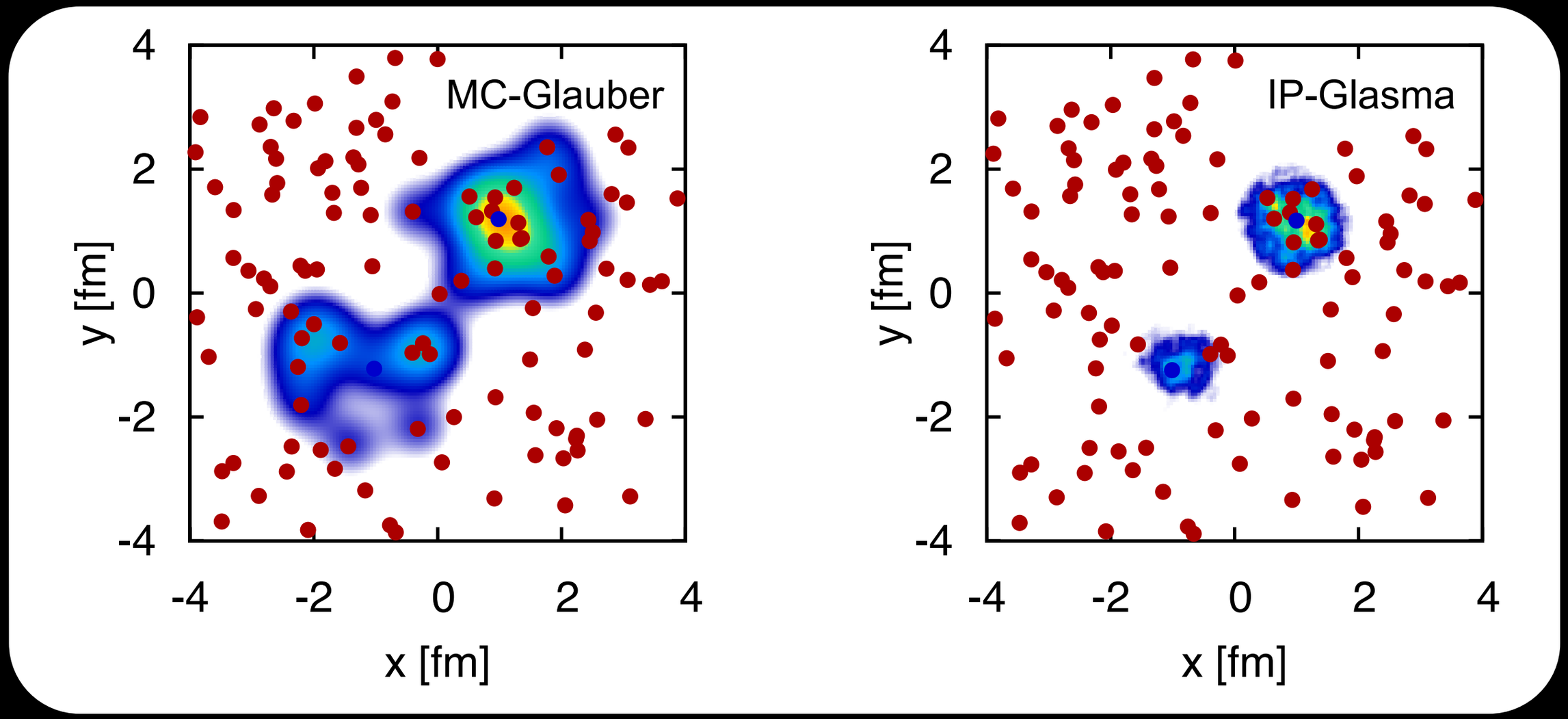

SYSTEM SIZE

A. BZDAK, B. SCHENKE, P. TRIBEDY, R. VENUGOPALAN, PRC87, 064906 (2013)

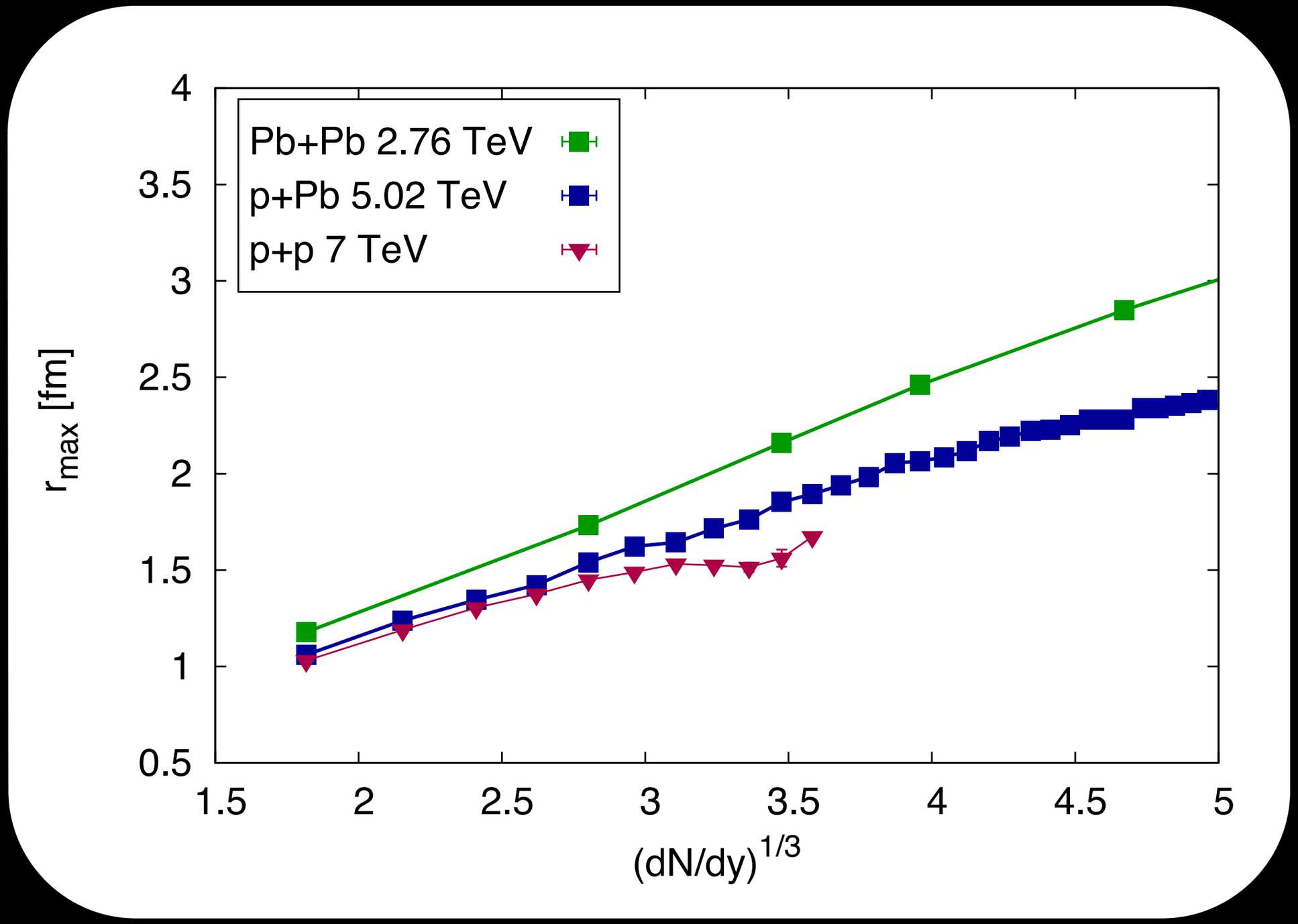

see talk by B. Jacak: HBT d+Au vs. Au+Au

MULTIPLICITY DISTRIBUTIONS

B. SCHENKE, P. TRIBEDY, R. VENUGOPALAN, PHYS. REV. C89, 024901 (2014)
CMS COLLABORATION, JHEP 1101, 079 (2011)

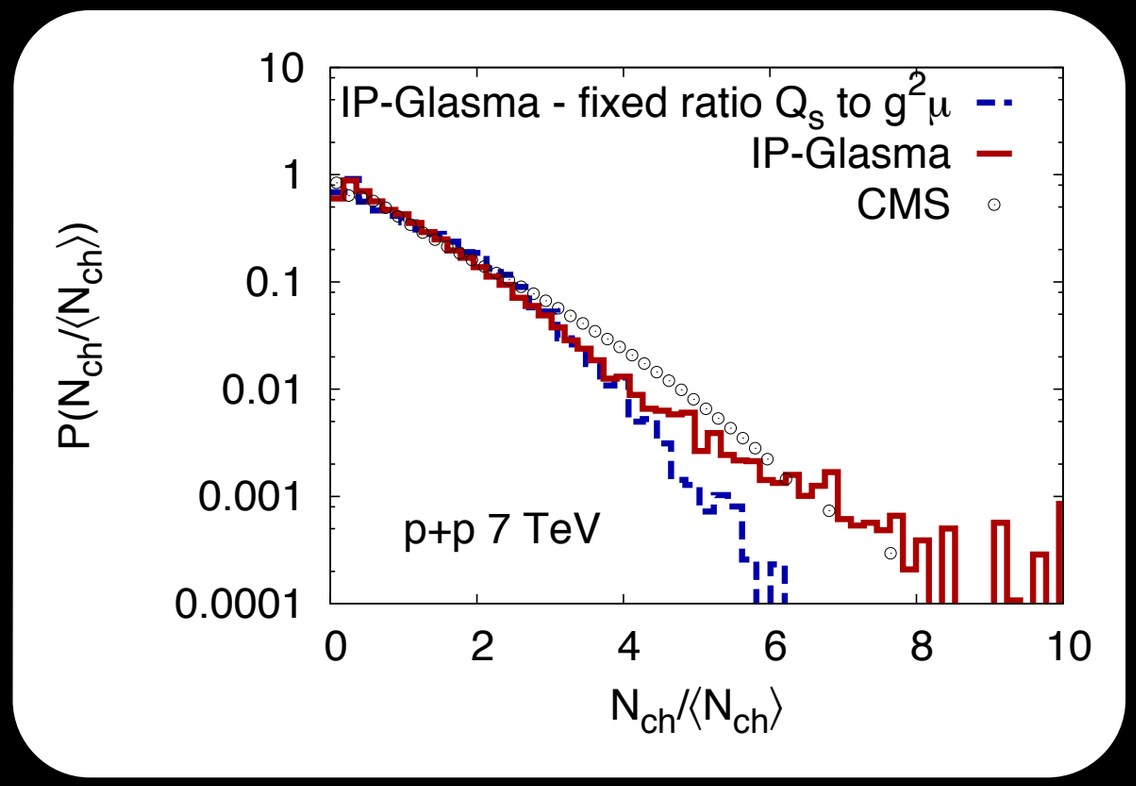

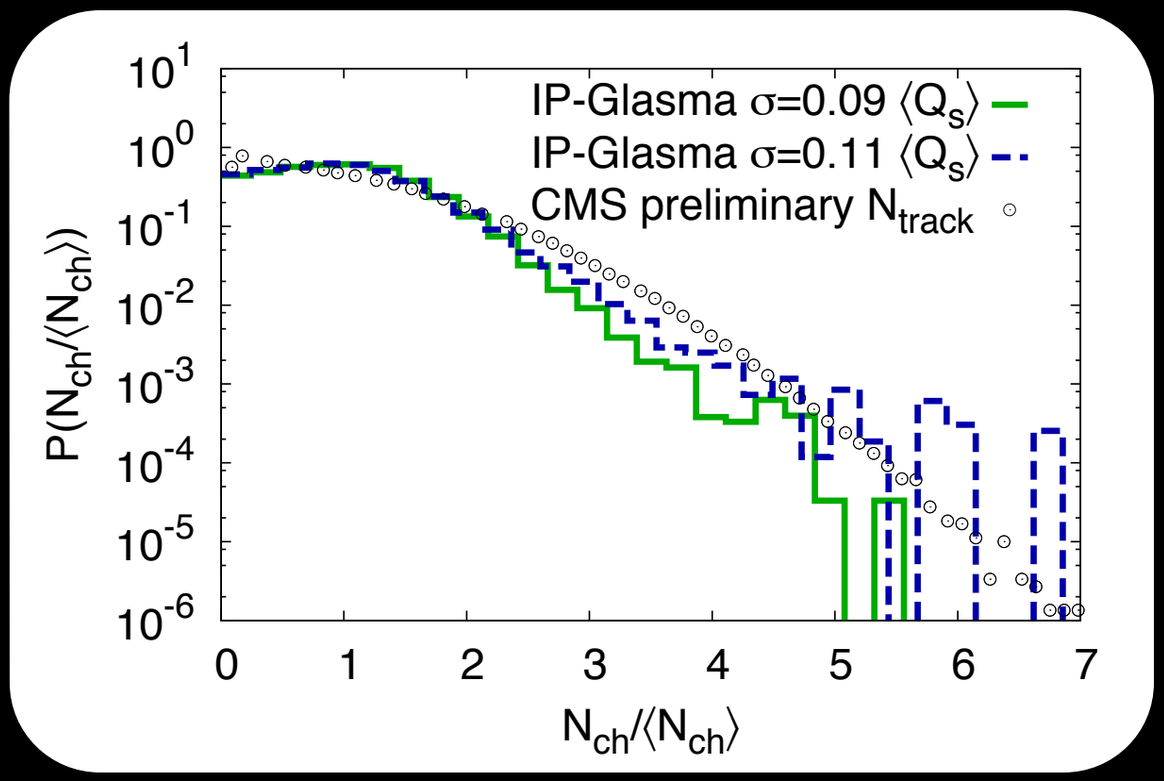

Multiplicity distributions in p+p and p+Pb collisions are not as wide as the experimental data

Introduce fluctuation of color charge density

Hadronization can also widen the distribution

FOURIER HARMONICS IN p+A

CMS COLLABORATION, PHYS.LETT. B724 (2013) 213-240

v_2

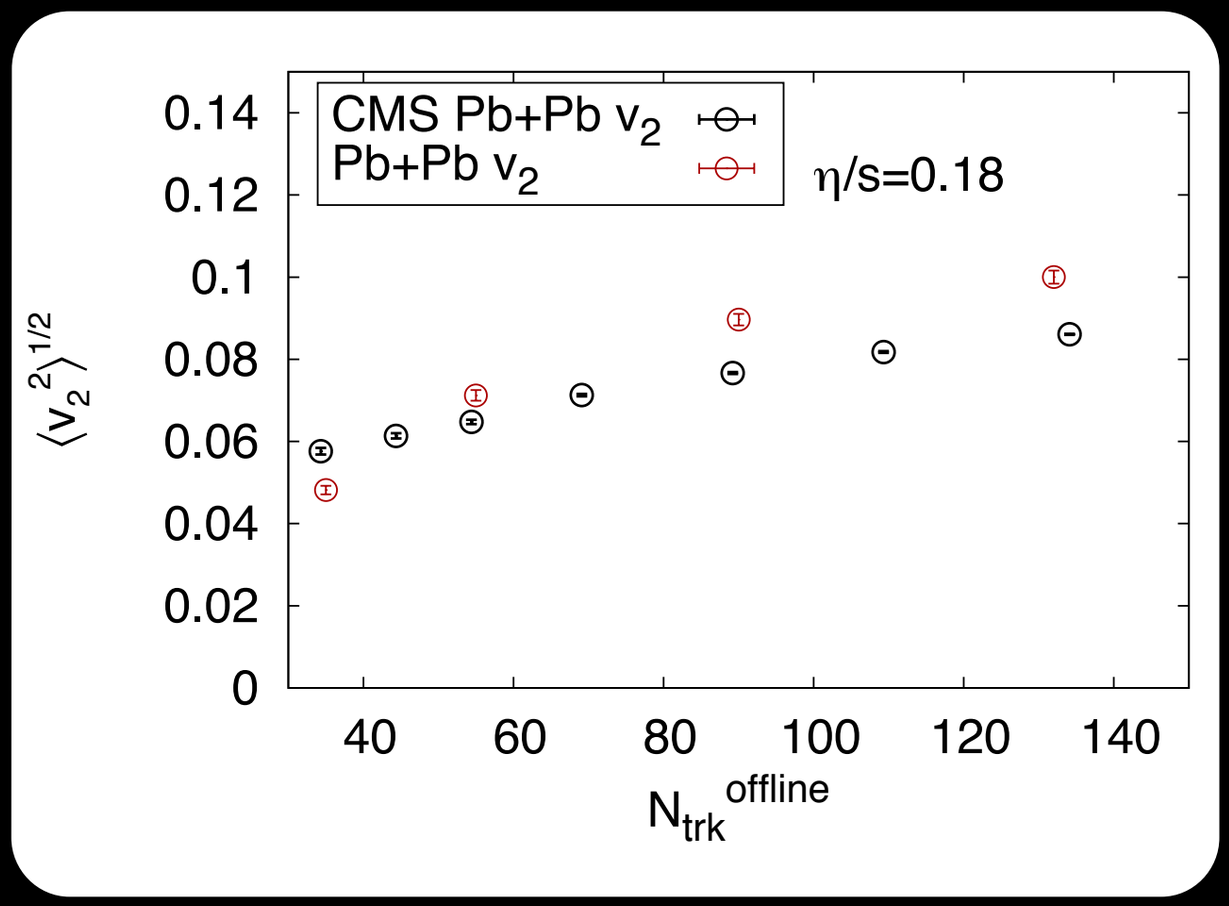

v_3

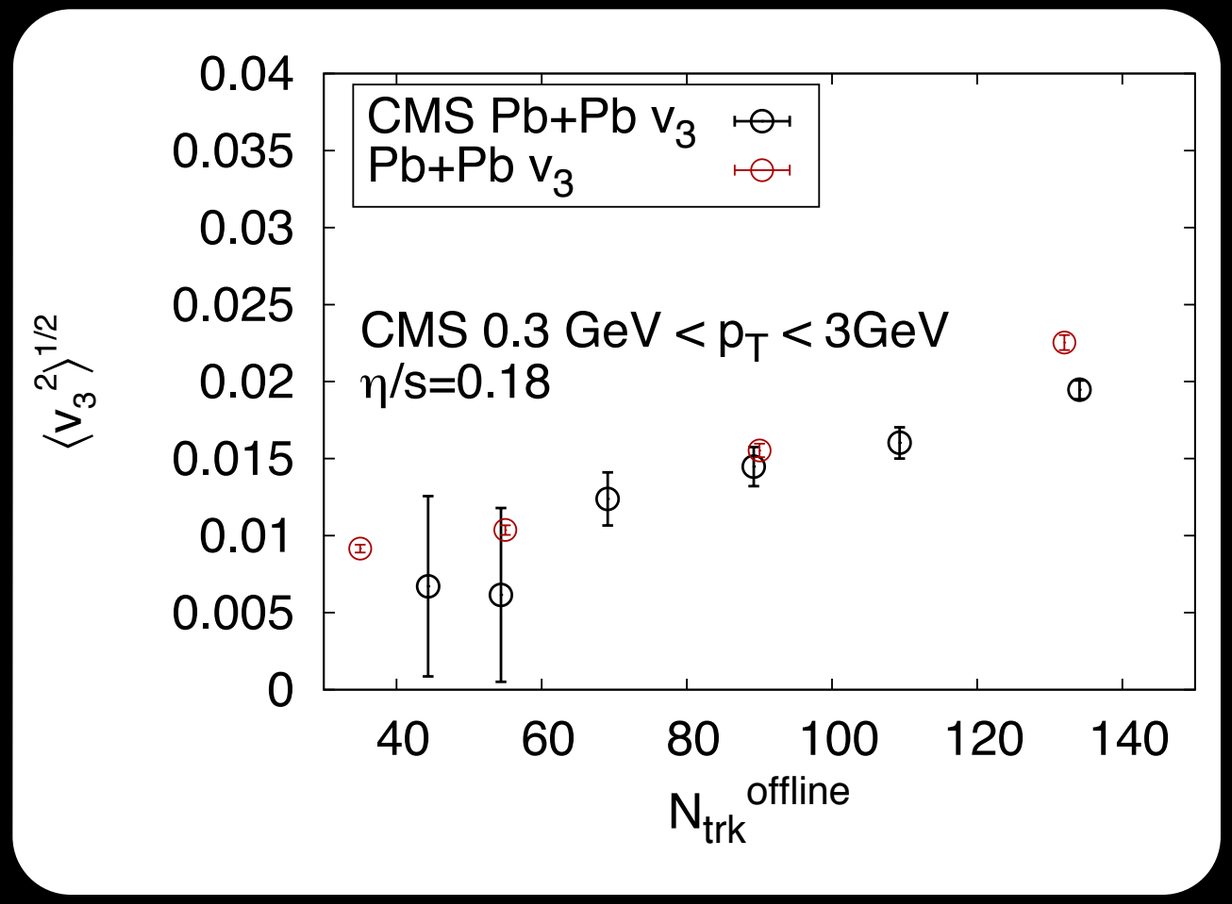

Open symbols: Pb+Pb

Filled symbols: p+Pb

Red points: IP-Glasma + MUSIC

FOURIER HARMONICS IN p+A

CMS COLLABORATION, PHYS.LETT. B724 (2013) 213-240

v_2

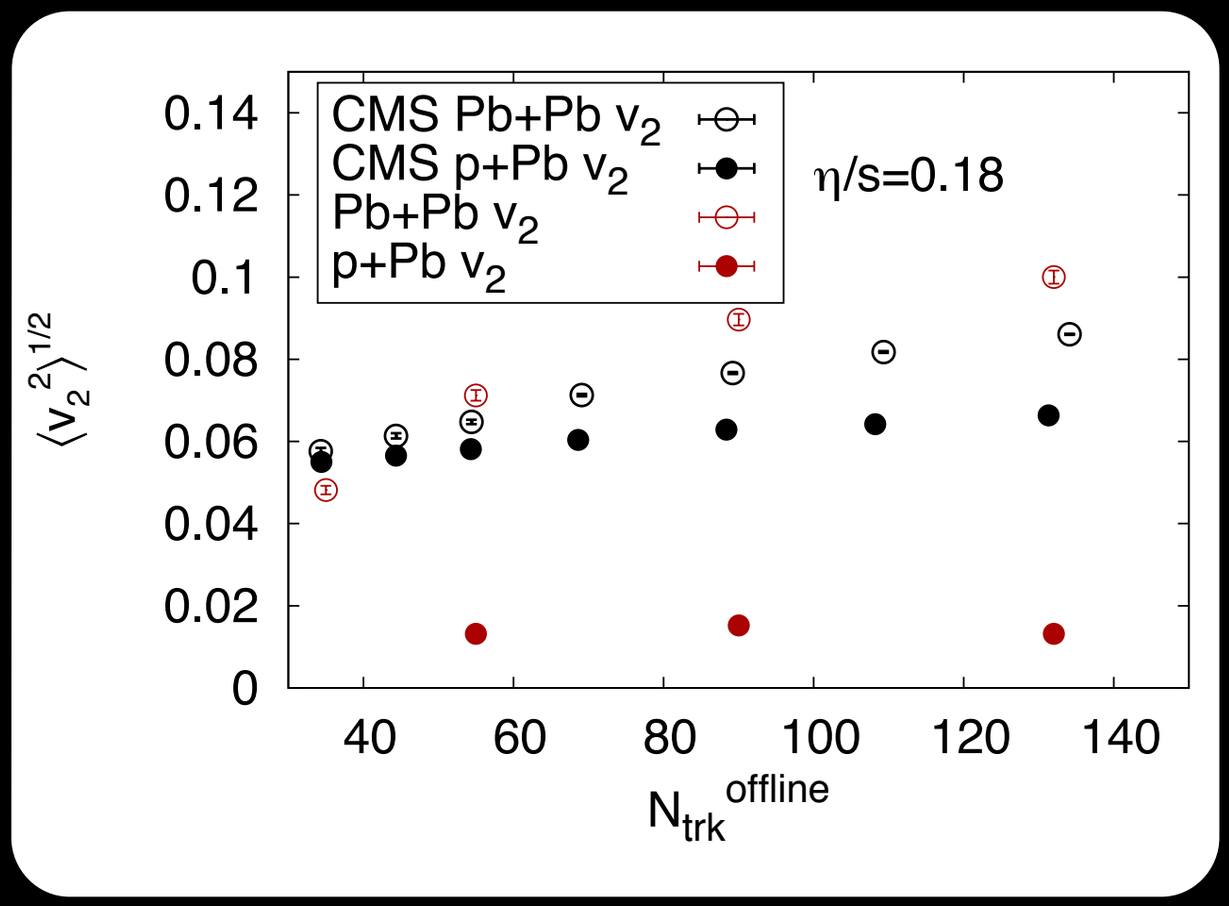

v_3

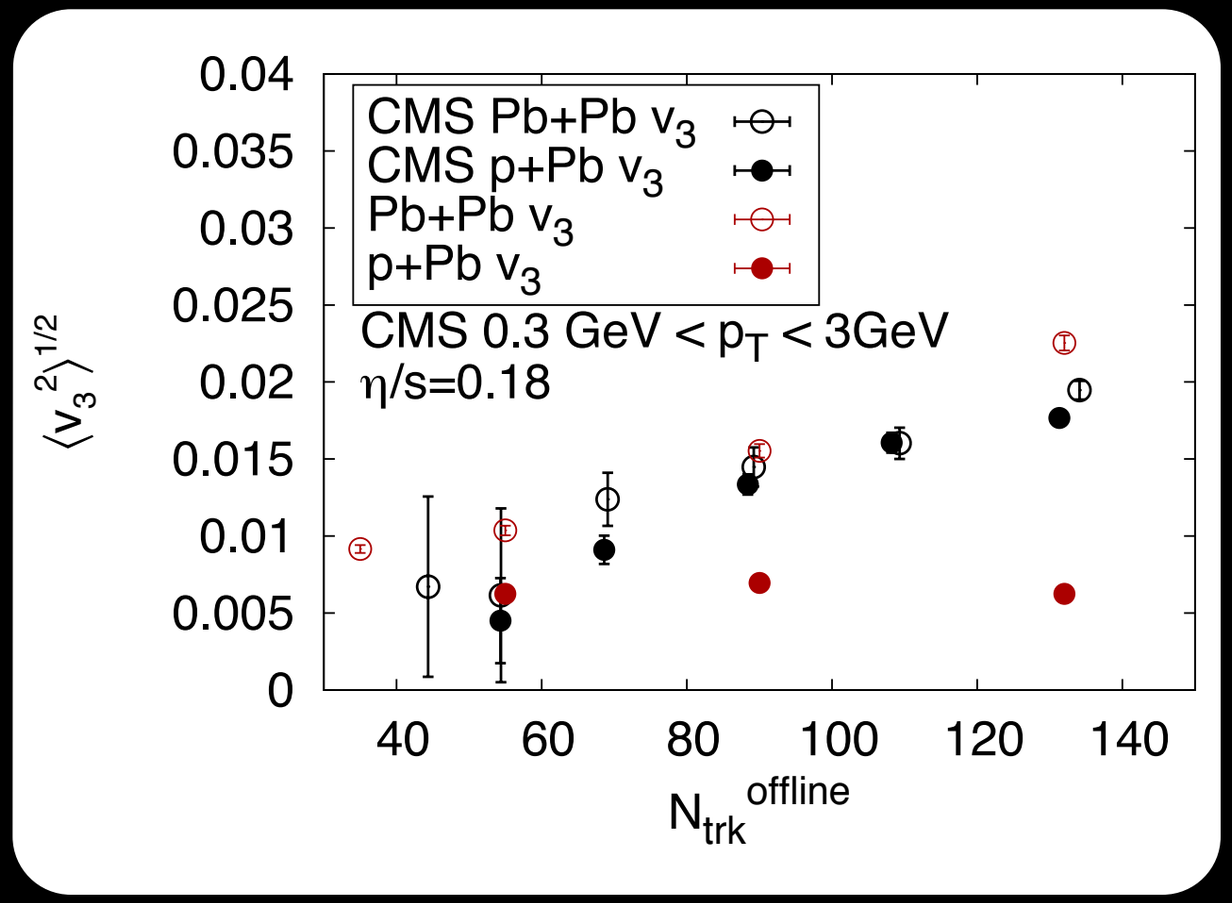

Open symbols: Pb+Pb

Filled symbols: p+Pb

Red points: IP-Glasma + MUSIC

FOURIER HARMONICS IN p+A

CMS COLLABORATION, PHYS.LETT. B724 (2013) 213-240

v_2

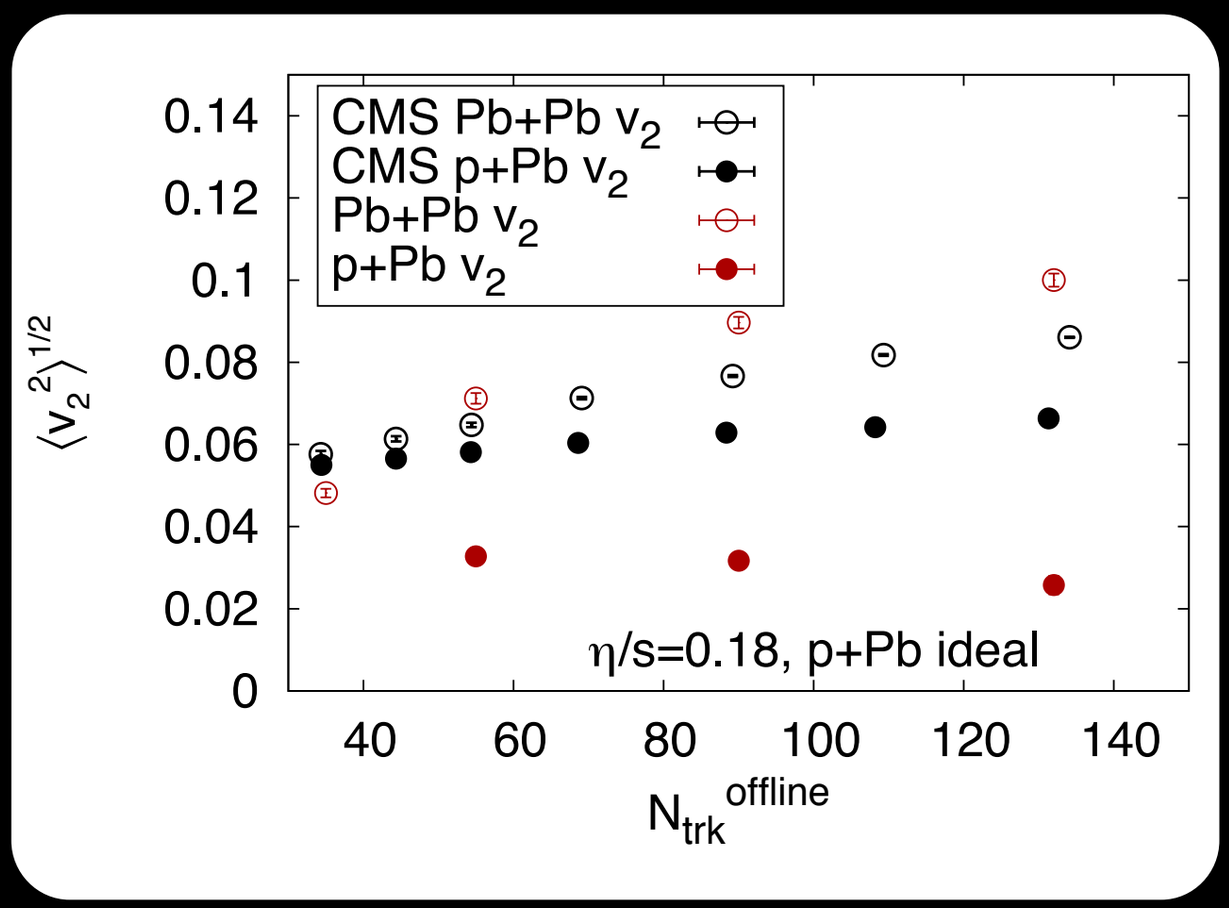

v_3

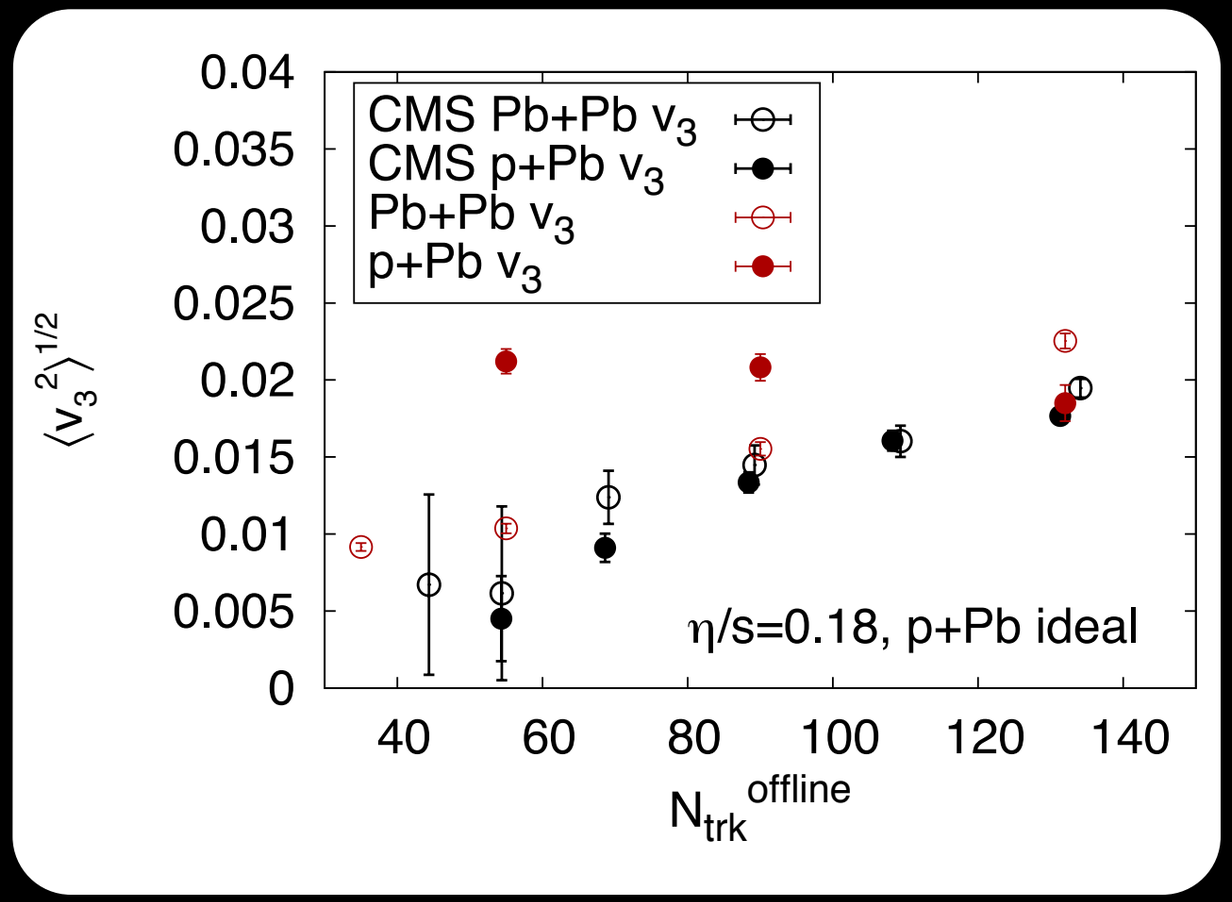

Open symbols: Pb+Pb

Filled symbols: p+Pb

Red points: IP-Glasma + MUSIC

FOURIER HARMONICS IN p+A

Why doesn't it work?
Two possibilities:

a) We neglected correlations from the initial state

K. DUSLING, R. VENUGOPALAN, PHYS.REV. D87 054014 (2013)

They are there in IP-Glasma - just need to keep them

b) The proton is not spherical and its shape fluctuates

Will this give the right centrality dependence?

SUMMARY

- IP-Glasma + fluid dynamics does very good job in describing experimental data in A+A collisions
- v_n distributions in peripheral events are well described when nonlinear effects from the evolution are included
- Ultra-central collisions of deformed nuclei can give information on particle production mechanism
- Within IP-Glasma+MUSIC model and ignoring initial state correlations, v_n in p+Pb are not well described

BACKUP

SYSTEM SIZE

A. BZDAK, B. SCHENKE, P. TRIBEDY, R. VENUGOPALAN, PRC87, 064906 (2013)

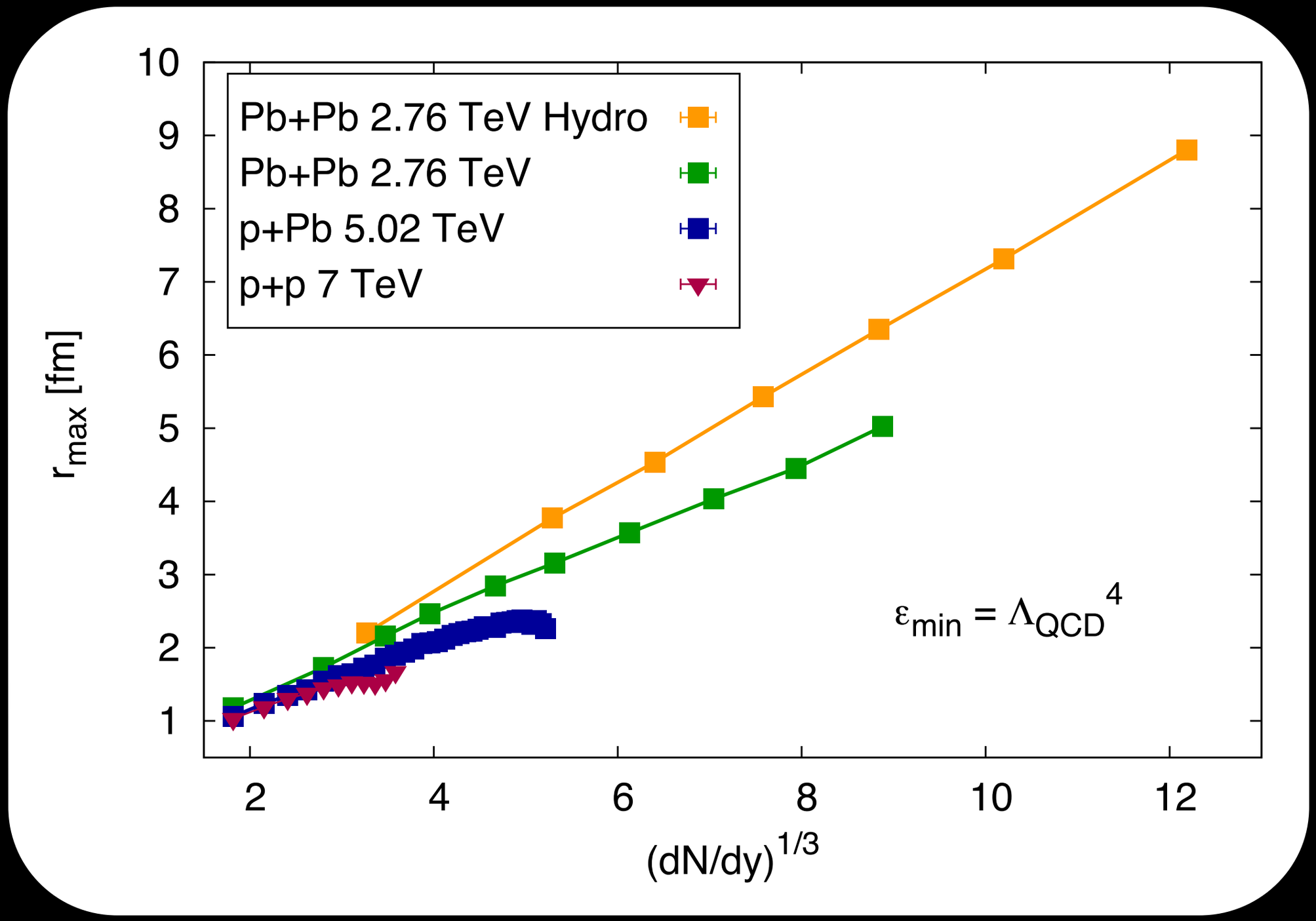

SYSTEM SIZE

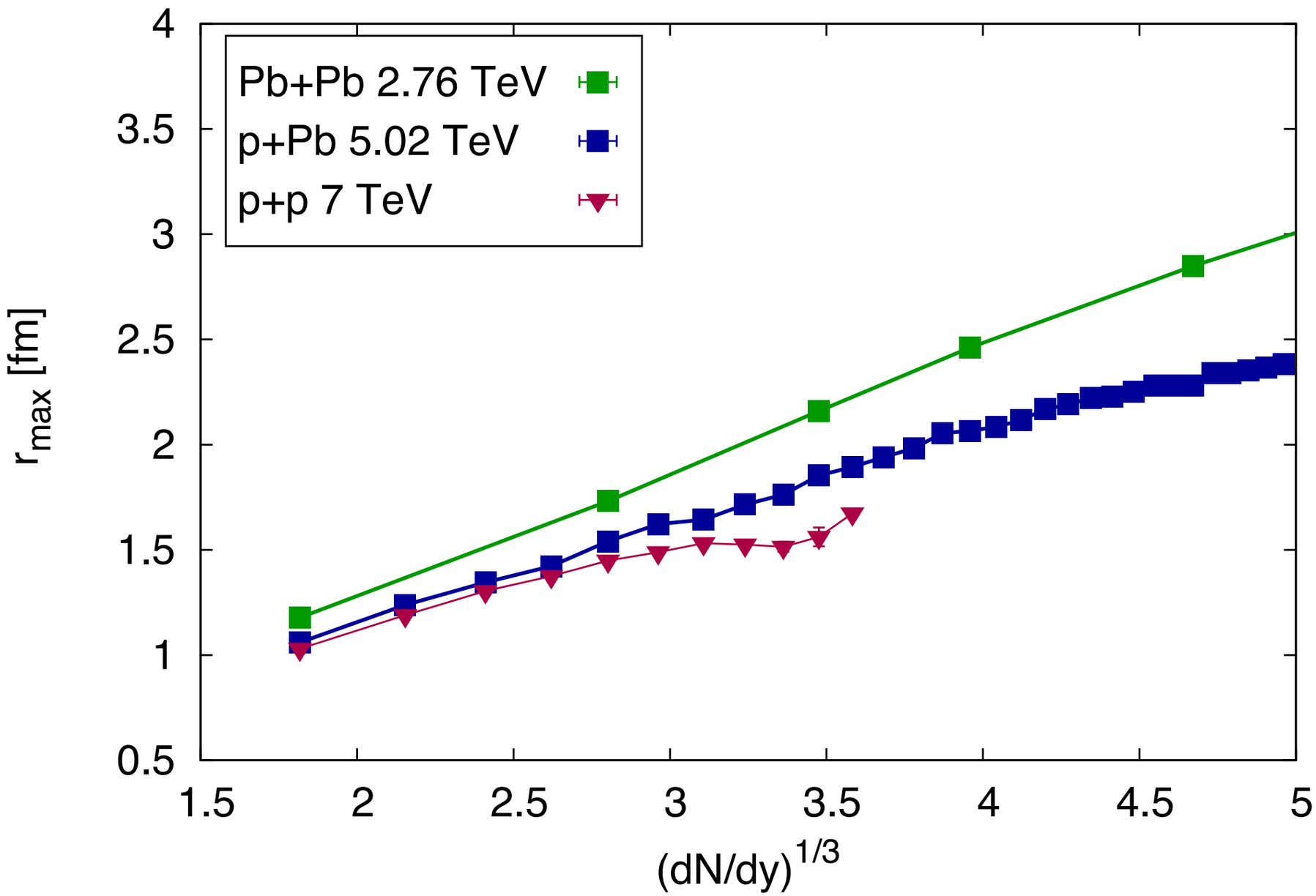
Pb+Pb 2.76 TeV
p+Pb 5.02 TeV
p+p 7 TeV
r_{max} [fm]
$(dN/dy)^{1/3}$
4
3.5
3
2.5
2
1.5
1
0.5
1.5
2
2.5
3
3.5
4
4.5
5

VISCOUS CORRECTION

Fraction of cells with viscous correction larger than 25% (50%) of the ideal term

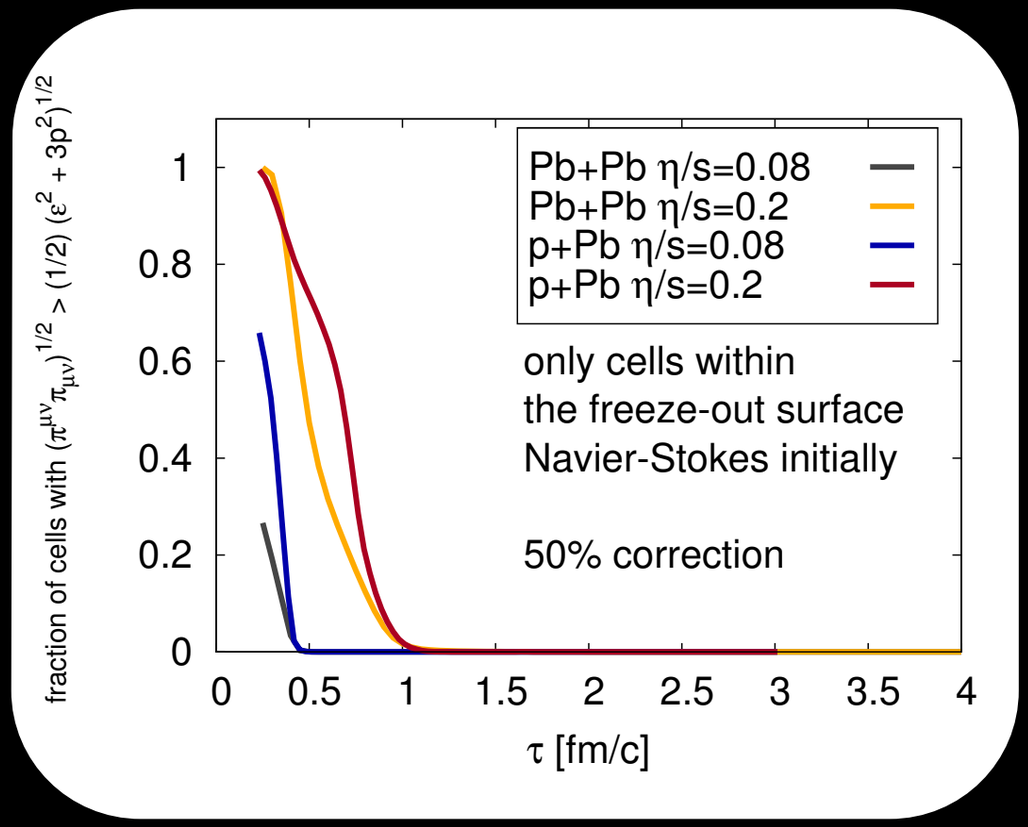

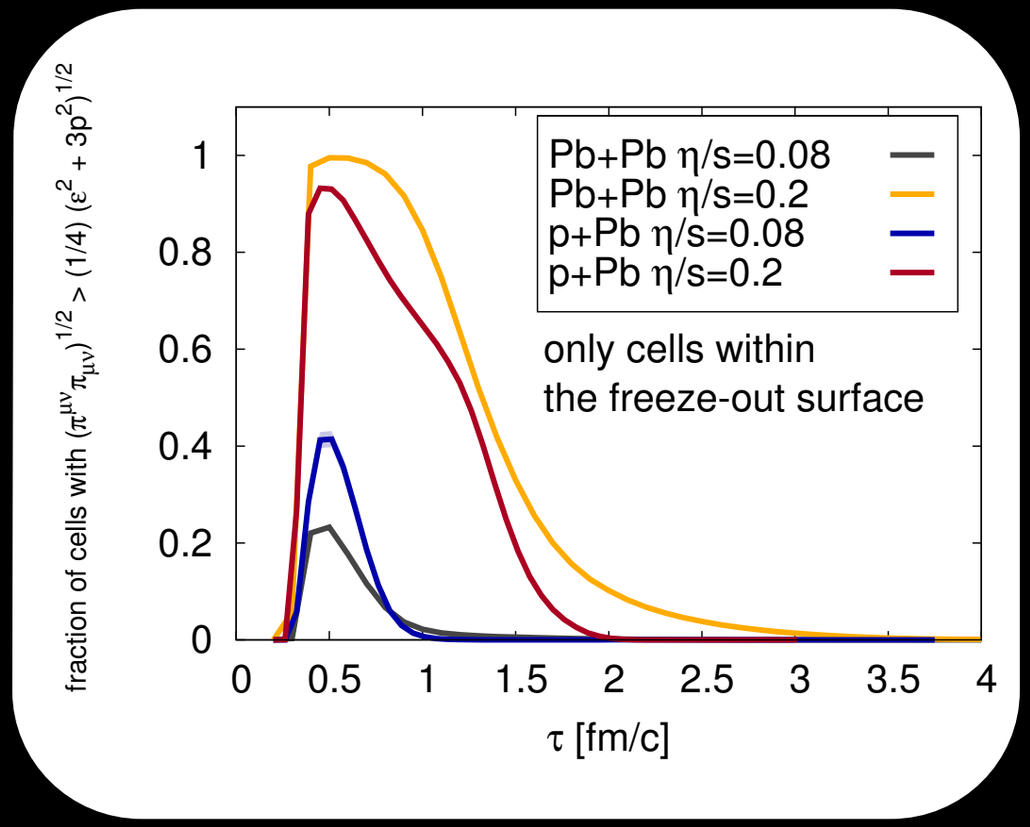

IDENTIFIED PARTICLE SPECTRA

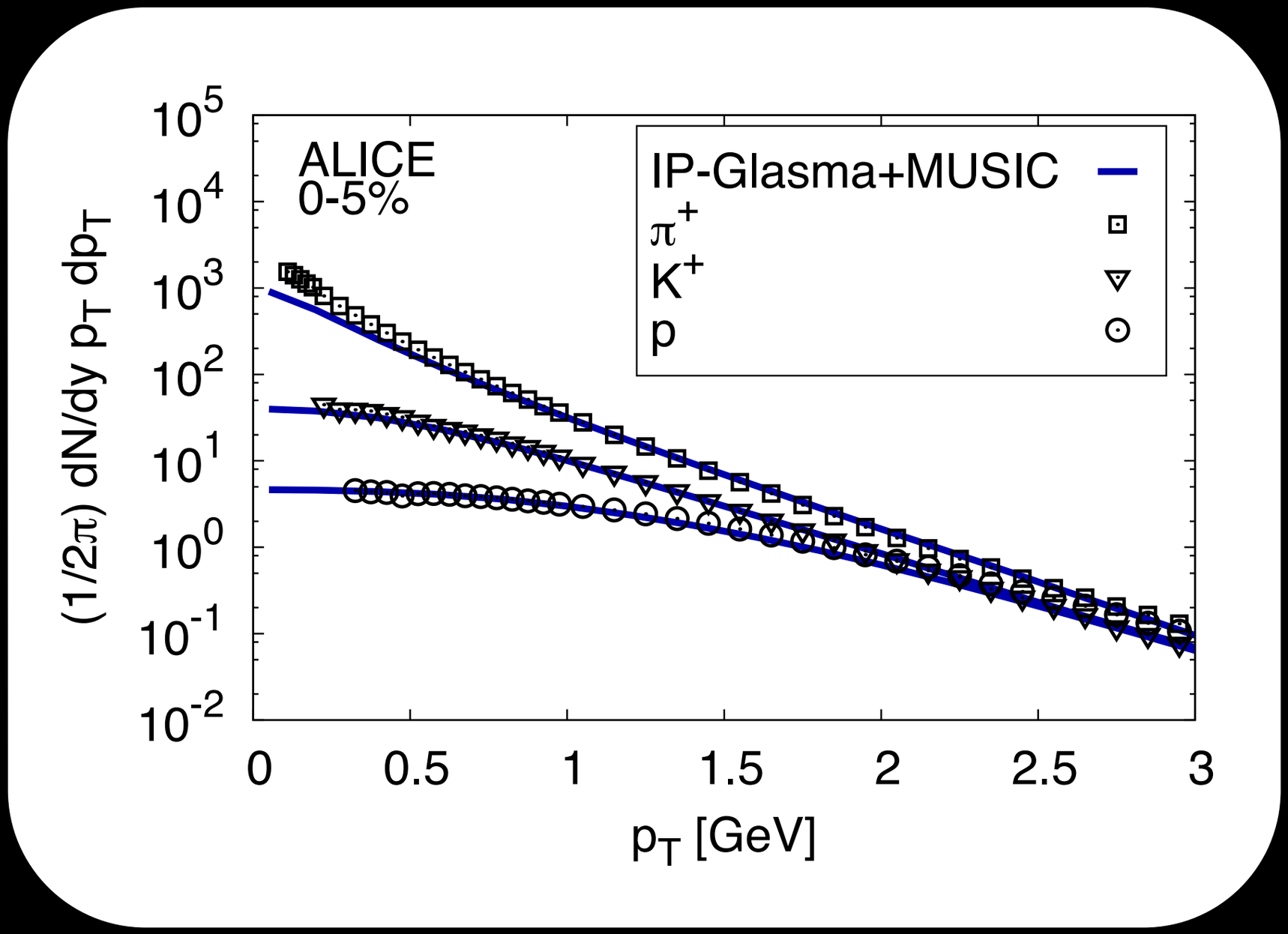

PARAMETER DEPENDENCIES

B. SCHENKE, P. TRIBEDY, R. VENUGOPALAN, PHYS. REV. C89, 024901 (2014)

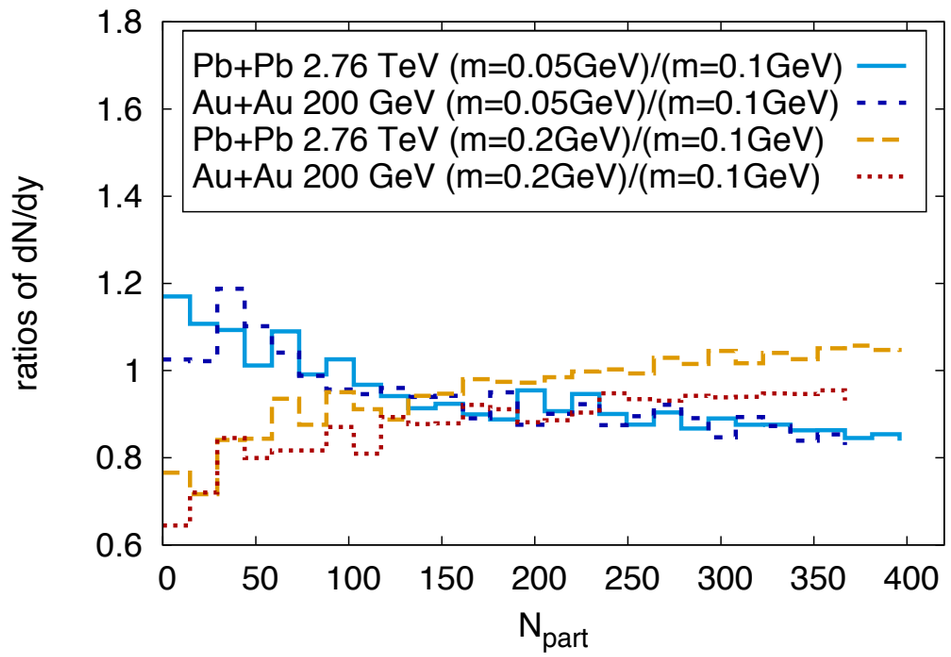

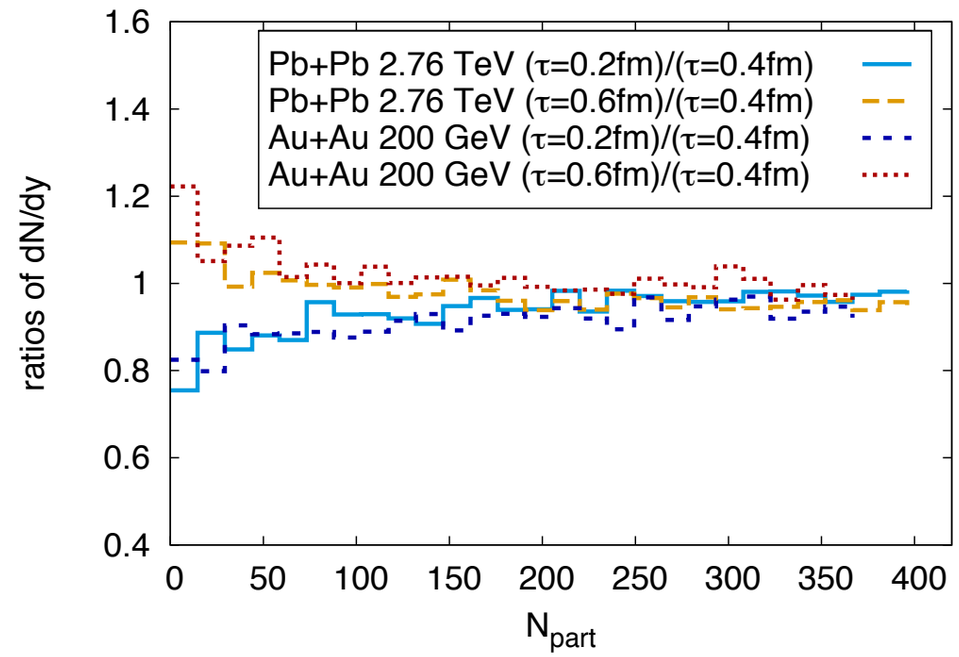

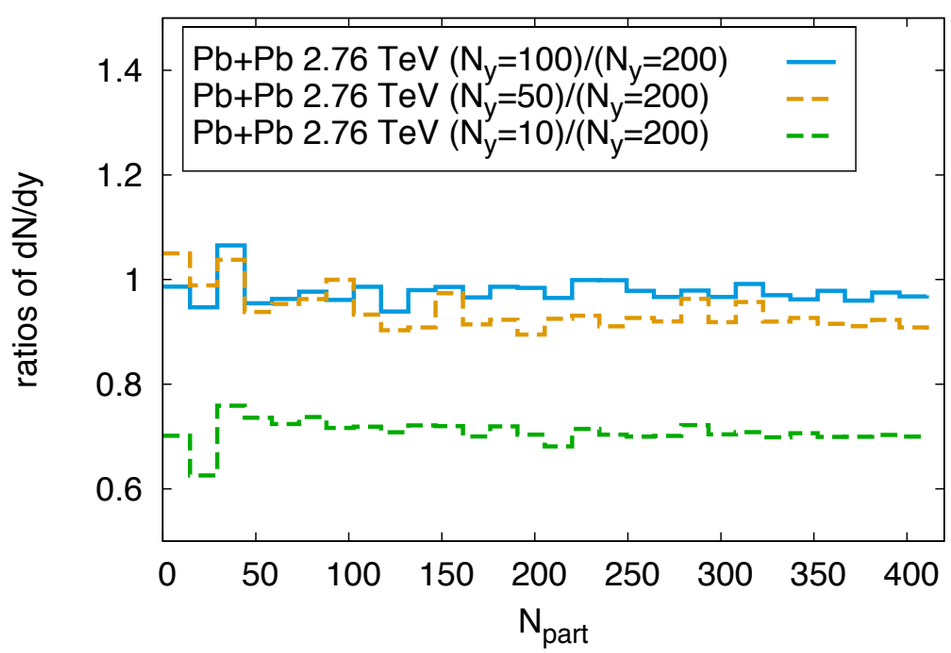

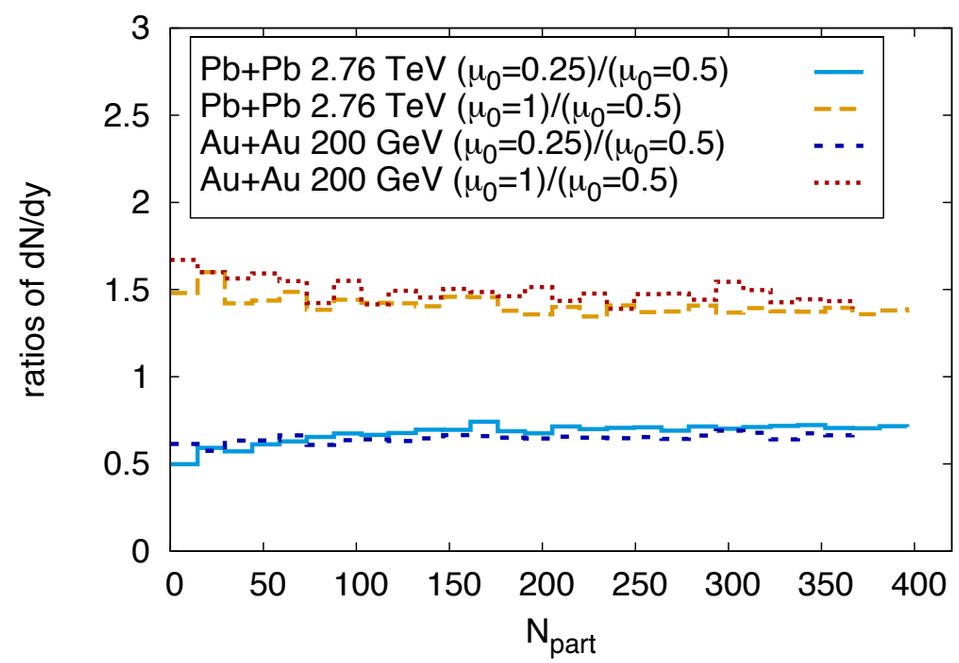

PARAMETER DEPENDENCIES

B. SCHENKE, P. TRIBEDY, R. VENUGOPALAN, PHYS. REV. C89, 024901 (2014)

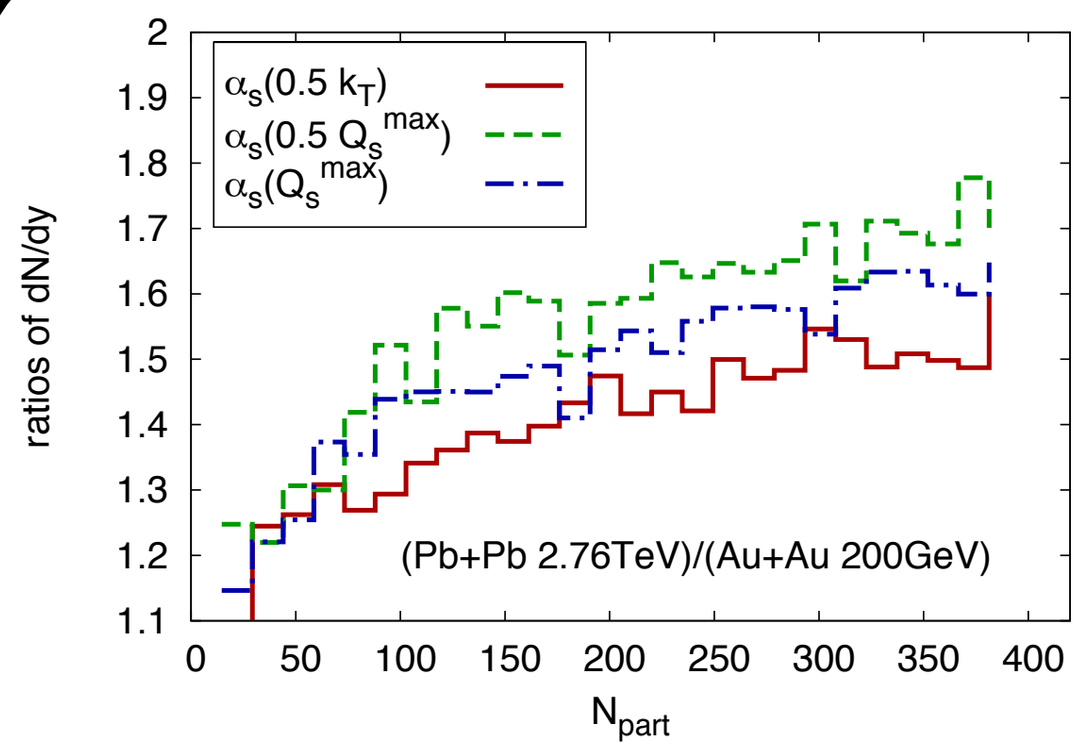

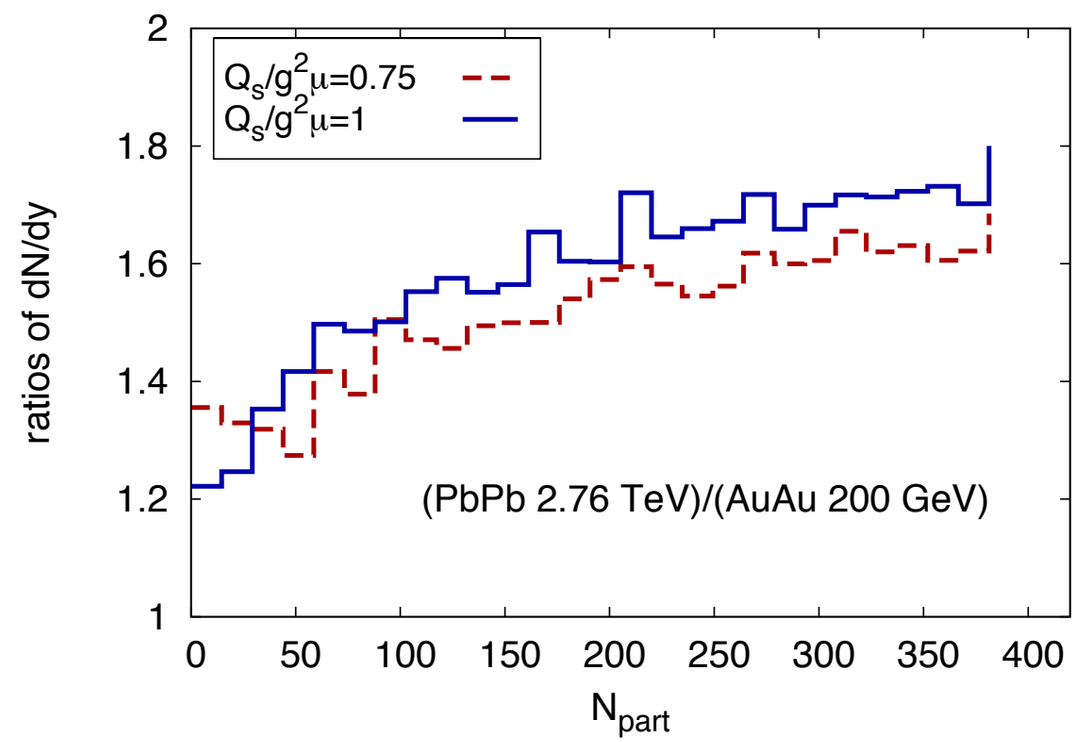

SENSITIVITY OF v_n TO VISCOSITY AND FLUCTUATIONS

B. Schenke, S. Jeon, C. Gale, Phys.Rev.C85, 024901 (2012)

viscous to ideal results

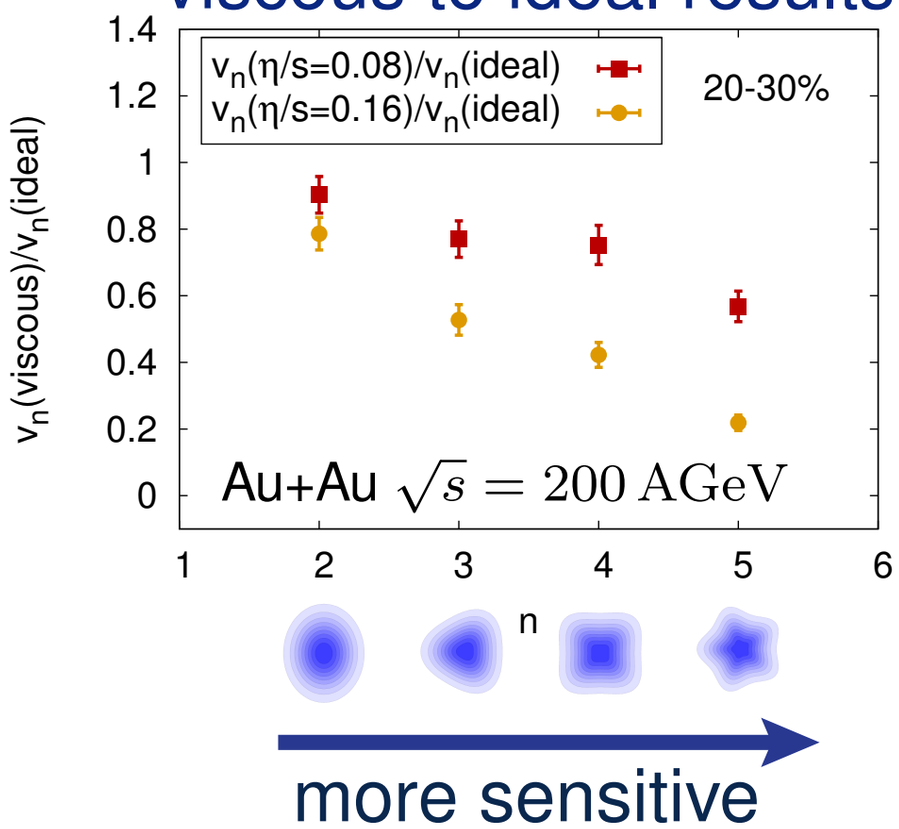

smoother to more granular results

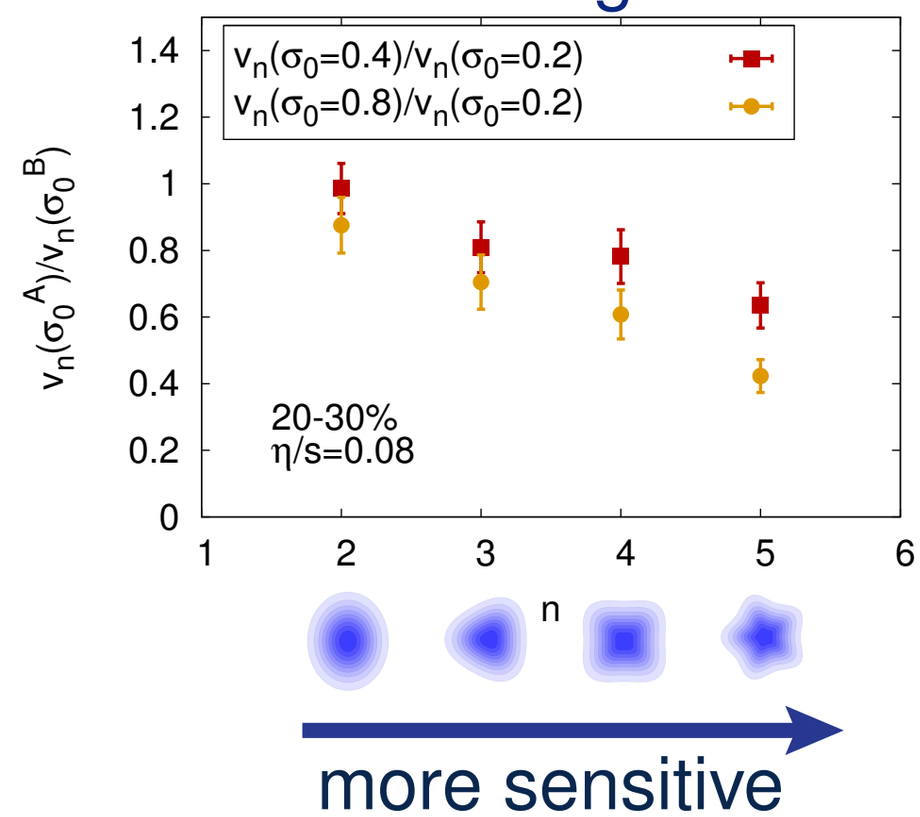

Viscosity decreases anisotropic flow (it's friction)
Smoother initial conditions decrease anisotropic flow

Sensitivity to viscosity and initial state structure increases with n

TEMPERATURE DEPENDENT η/s

Use $\eta/s(T)$ as in Niemi et al., Phys.Rev.Lett. 106 (2011) 212302

Experimental data: A. Adare et al. (PHENIX), Phys.Rev.Lett. 107, 252301 (2011)
Y. Pandit (STAR), Quark Matter 2012, (2012)
ATLAS collaboration, Phys. Rev. C 86, 014907 (2012)

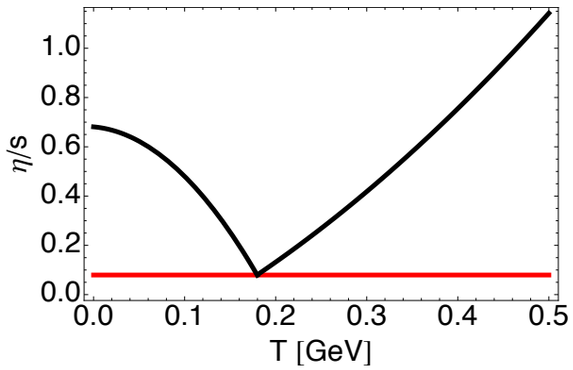

RHIC

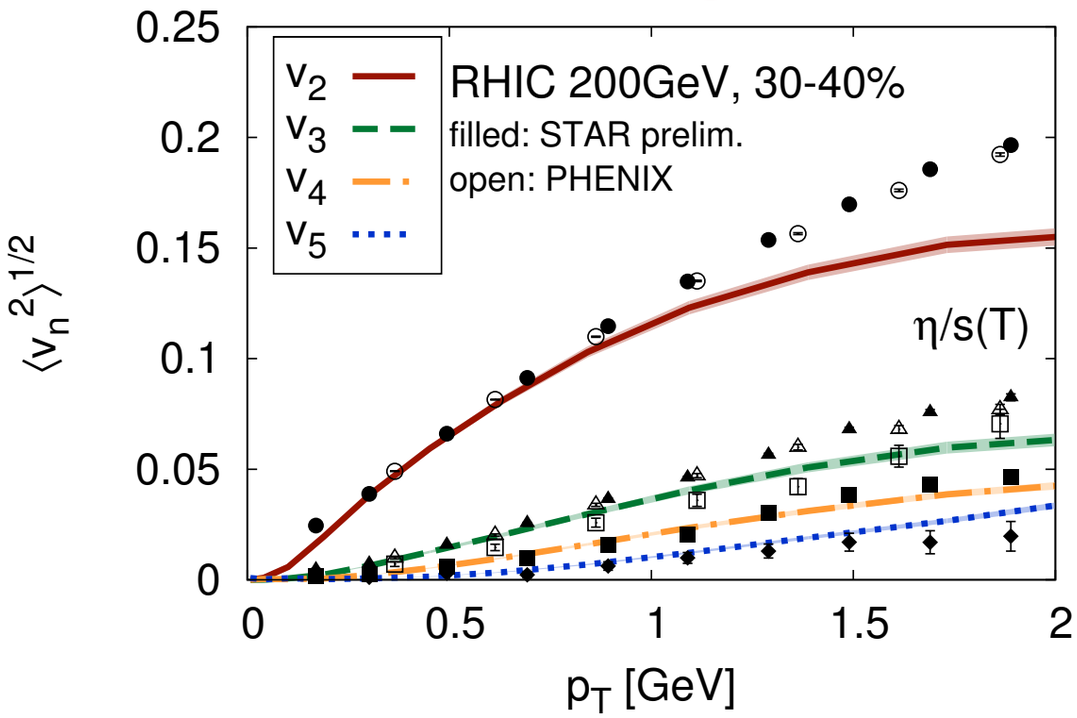

LHC

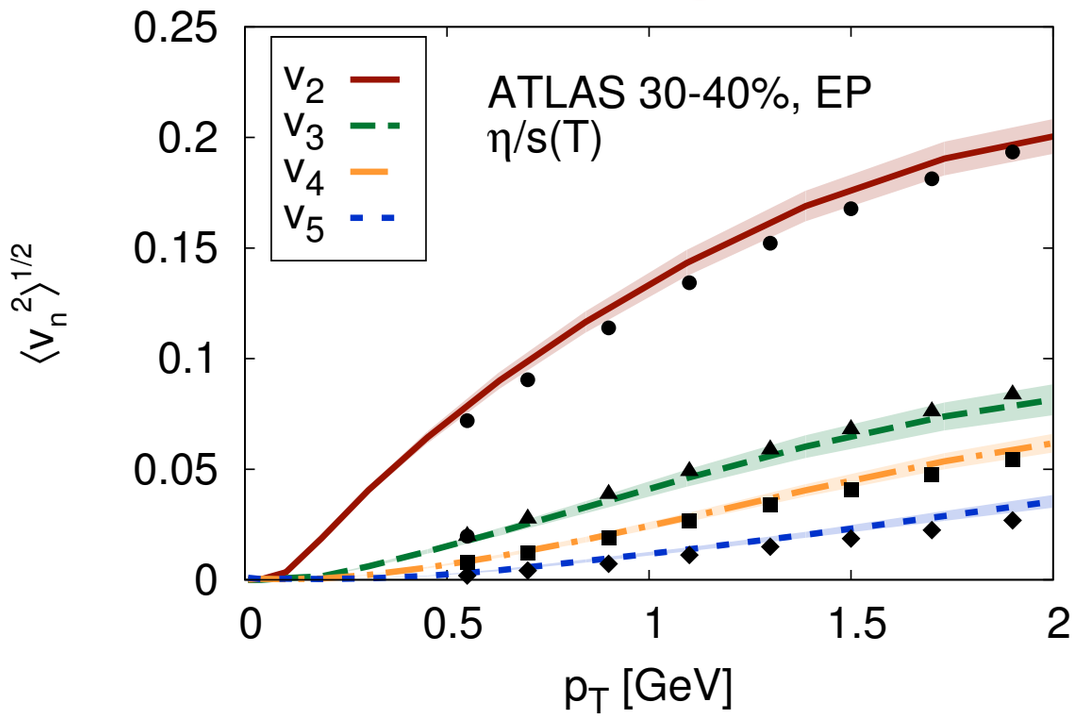

One $(\eta/s)(T)$ will be able to describe both RHIC and LHC data
Used parametrization not yet perfect: no surprise
More detailed study needed - include different RHIC energies and LHC

GEOMETRY AND FLUCTUATIONS DRIVE FLOW

C.GALE, S.JEON, B.SCHENKE, P.TRIBEDY, R.VENUGOPALAN, PHYS.REV.LETT.110, 012302 (2013)

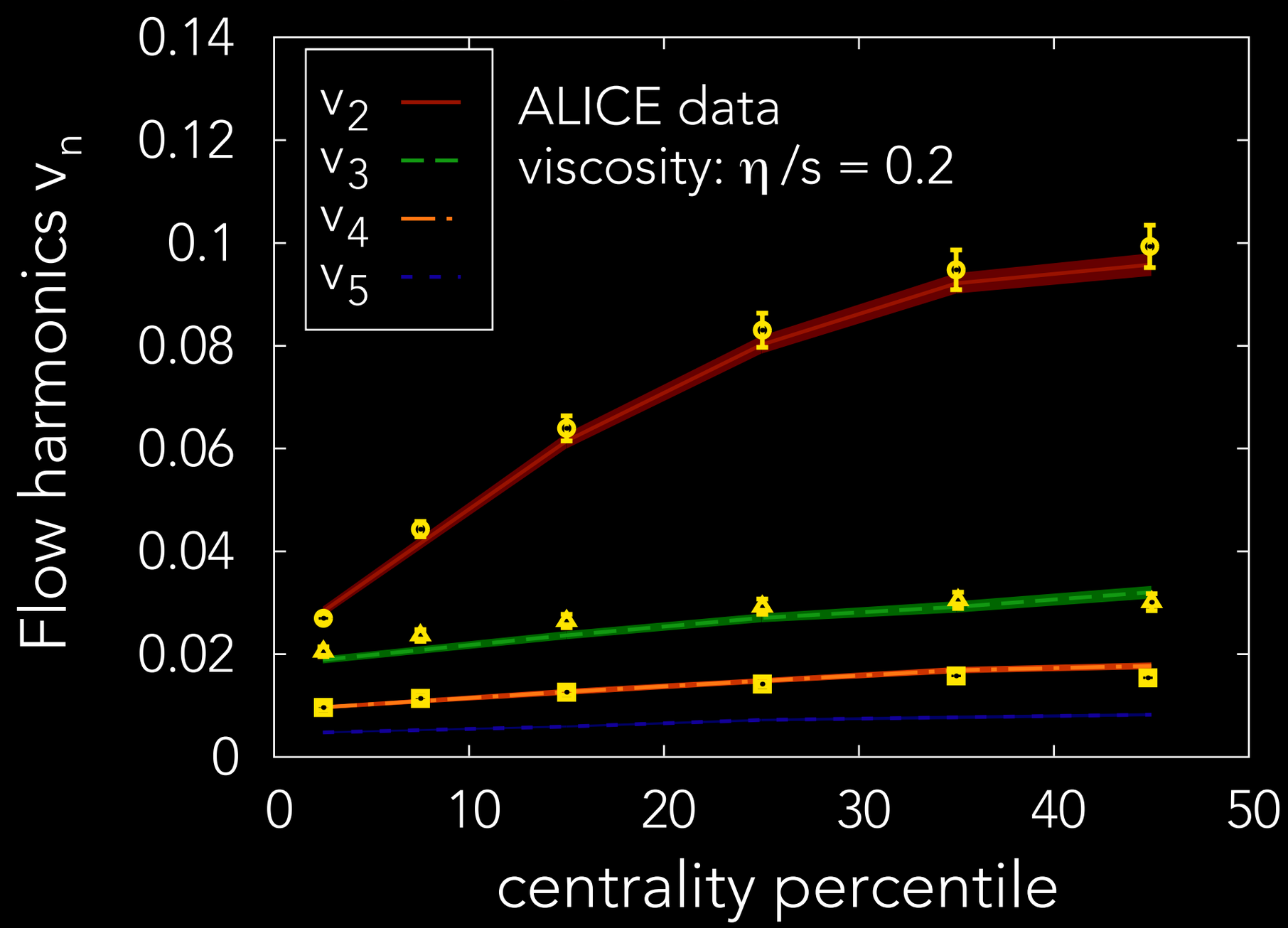

EXPERIMENTAL DATA: ALICE COLLABORATION, PHYS. REV. LETT. 107, 032301 (2011)

VISCOUS FLOW AT LHC

C.GALE, S.JEON, B.SCHENKE, P.TRIBEDY, R.VENUGOPALAN, PHYS.REV.LETT.110, 012302 (2013)

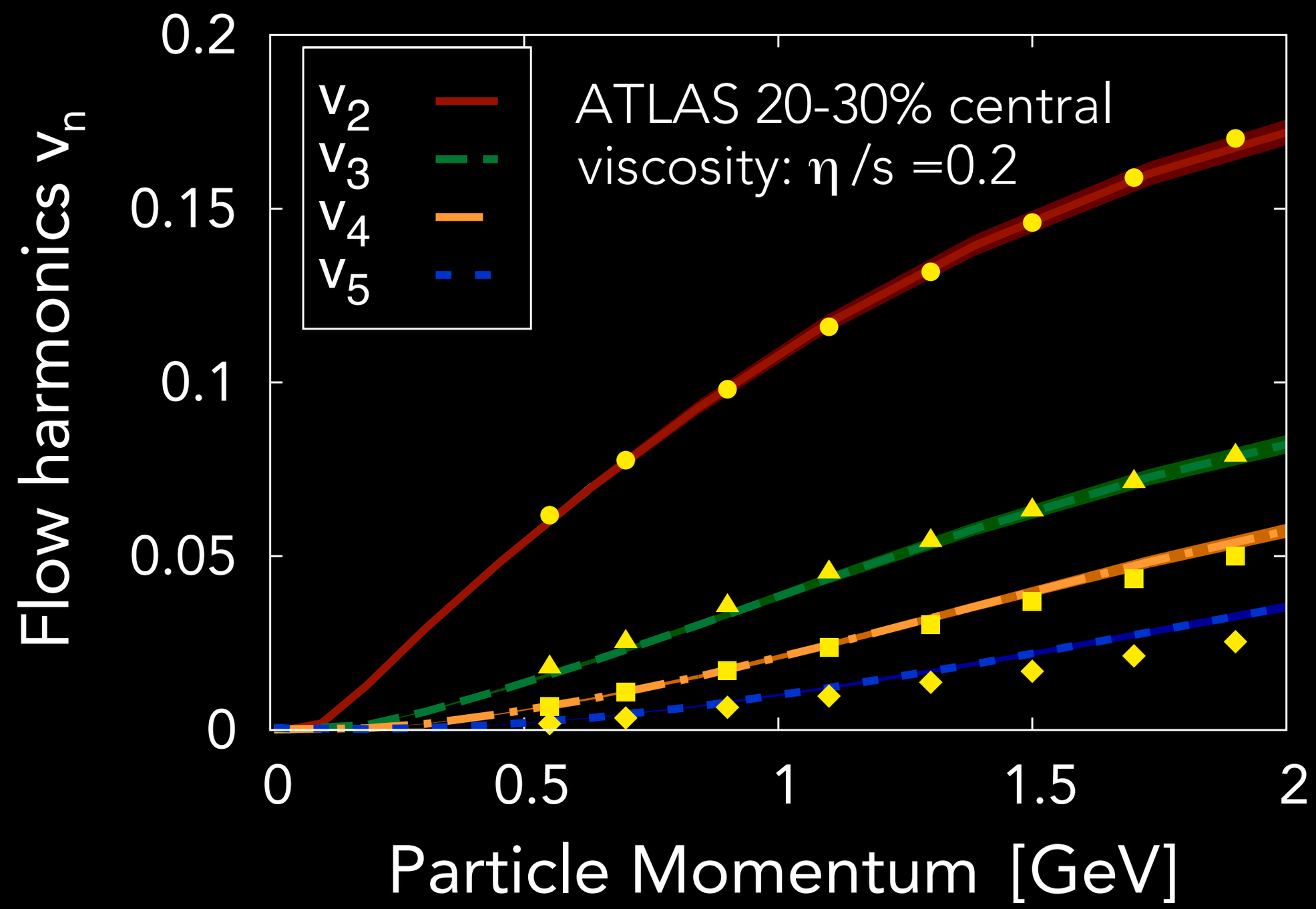

EXPERIMENTAL DATA: ATLAS COLLABORATION, PHYS. REV. C86, 014907 (2012)

VISCOSITY AT RHIC AND LHC

RHIC

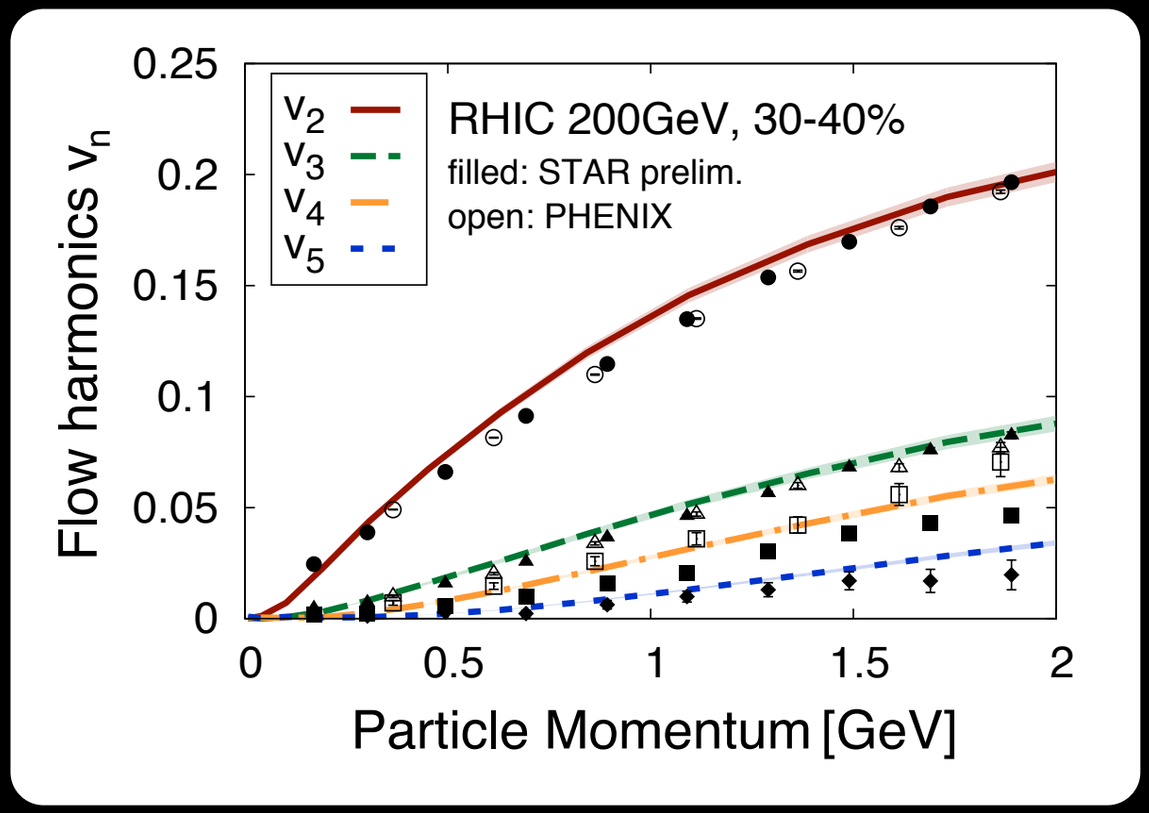

LHC ~14 x higher energy

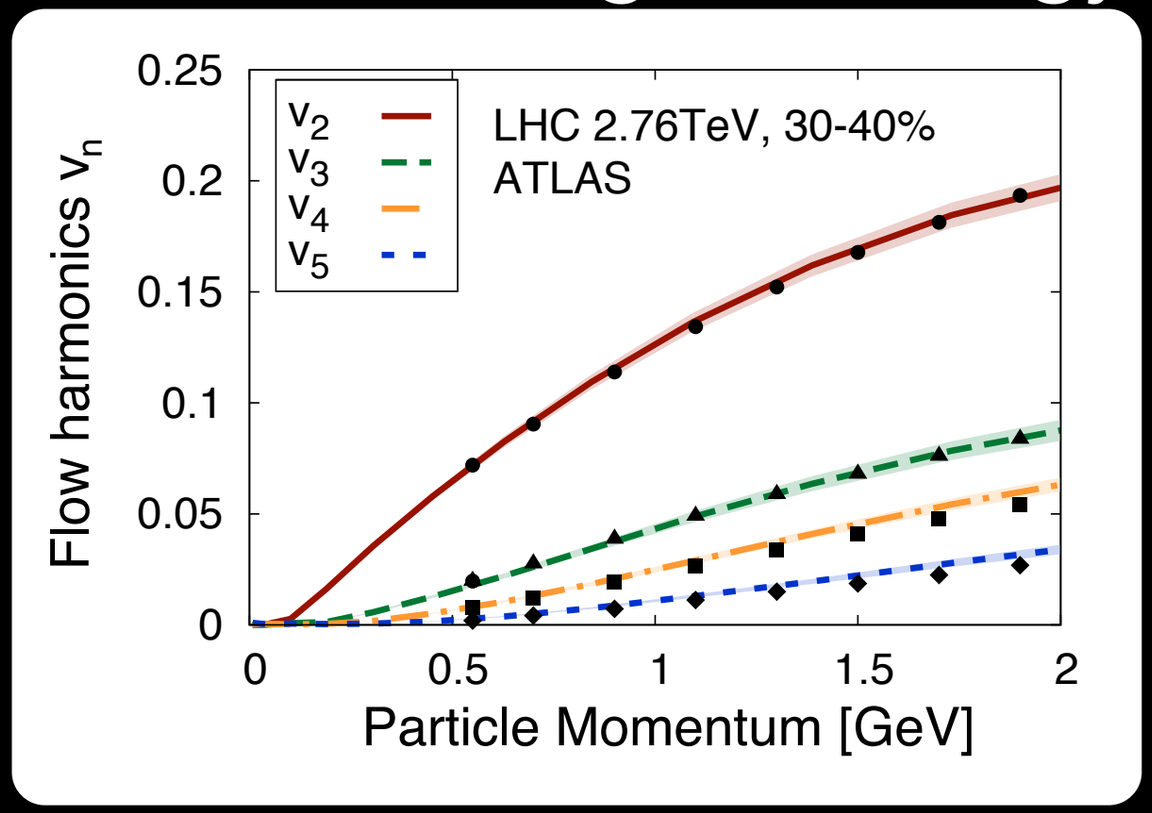

RHIC viscosity $\eta/s = 0.12$

LHC viscosity $\eta/s = 0.2$

Hints at increasing viscosity η/s with increasing temperature

EXPERIMENTAL DATA:
A. ADARE ET AL. (PHENIX COLLABORATION), PHYS.REV.LETT. 107, 252301 (2011)
Y. PANDIT (STAR COLLABORATION), QUARK MATTER 2012, (2012)
ATLAS COLLABORATION, PHYS. REV. C 86, 014907 (2012)

Turbulent thermalization process in high-energy heavy-ion collisions

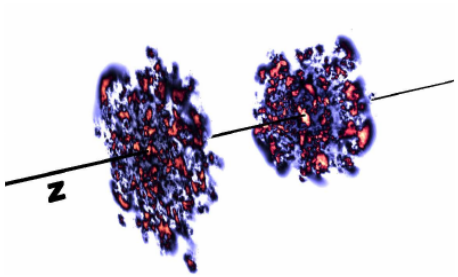

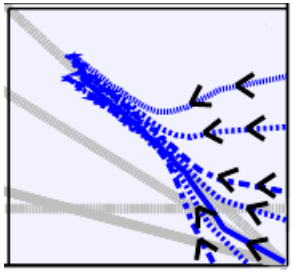

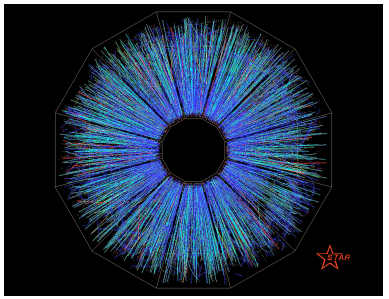

Soeren Schlichting

In collaboration with

Juergen Berges, Kirill Boguslavski (Heidelberg)

Raju Venugopalan (Brookhaven)

RBRC Workshop, BNL, 04/04/2014

BROOKHAVEN NATIONAL LABORATORY

Heavy Ion physics
& the thermalization problem

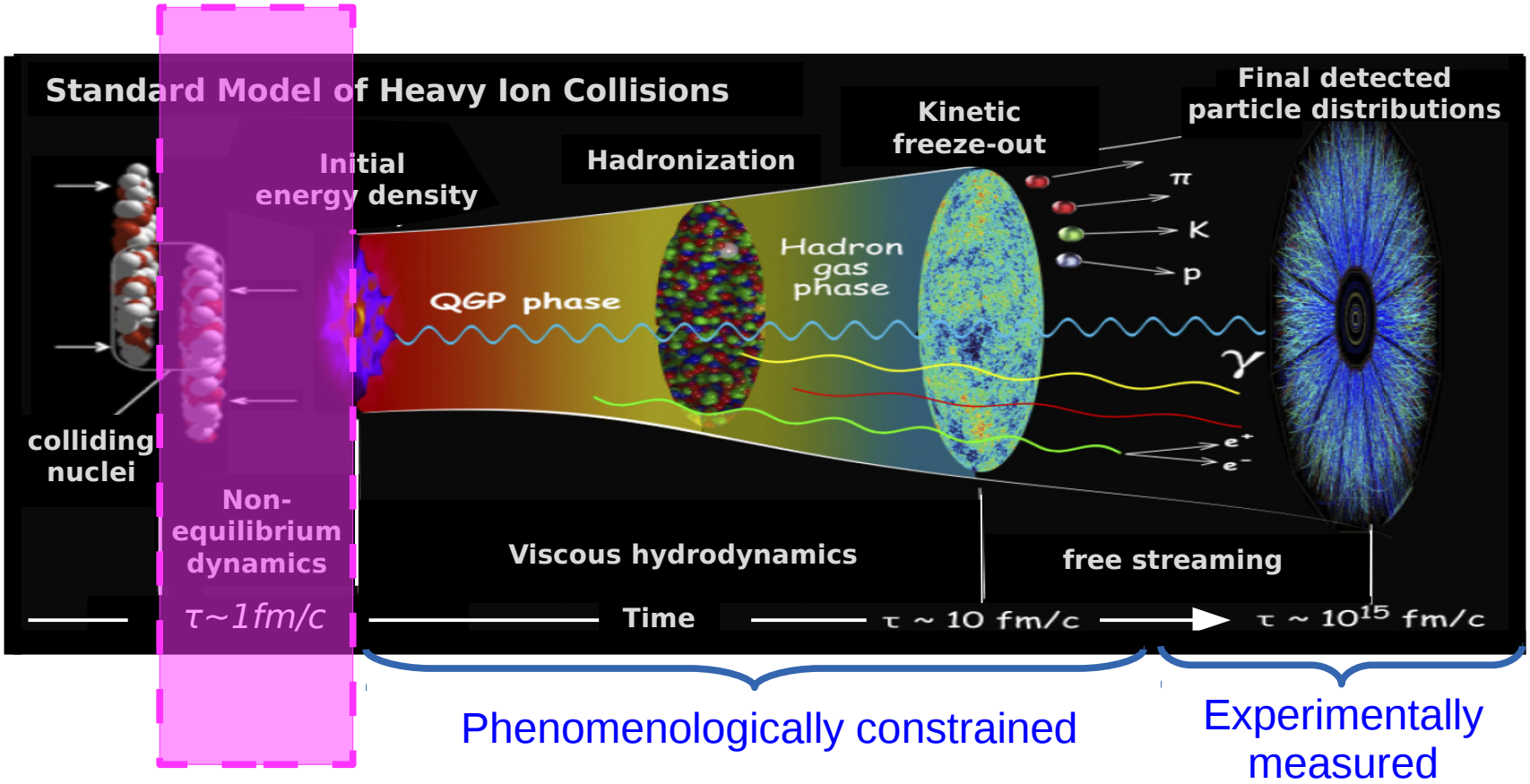

Phenomenologically constrained

Experimentally measured

When and to what extent is a thermalized QGP achieved? How does this happen?

First principles description in two limiting cases

- Strong coupling in related theories ($g^2 N_c \gg 1$) (e.g. $N=4$ SYM)

  Gauge gravity duality – Collision of gravitational shock waves

  → c.f. talks by Romatschke,Heller, Balasubramanian

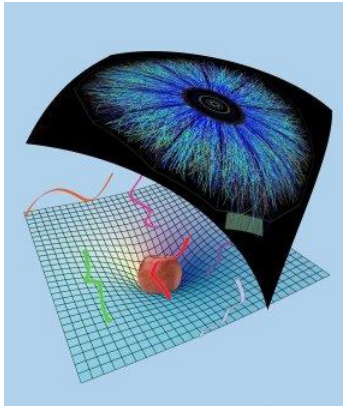

http://strings.net.technion.ac.il

- QCD at weak coupling ($g^2 \ll 1$) and high occupancy ($g^2 f \sim 1$)

  Effective field theory description (CGC) of the primary collision leads to a state where the energy density is dominated by a large number of gluons with typical momenta Q_s *at times* $\tau \sim 1/Q_s$ *after the collision*

  Initial energy density: $\epsilon \sim Q_s^4/\alpha_s$ *i.e. 'occupancy'* $f(p \sim Q_s) \sim 1/\alpha_s$

  Thermal equilibrium: $\epsilon \sim T^4$ *i.e. 'occupancy'* $f(p \sim T) \sim 1$

  → Strongly correlated & far from equilibrium

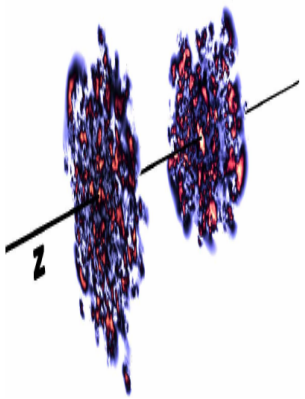

Schenke,Tribedy, Venugopalan Phys.Rev. C86 (2012) 034908Â

Theoretical methods

- There are two complementary methods to study non-equilibrium dynamics at weak coupling ($\alpha_s \ll 1$) and high occupancy ($1/\alpha_s > f > 1$)

$f(t,p) \sim 1/\alpha_s$
('overoccupied plasma')

$1/\alpha_s > f(t,p) > 1$
('classical particles')

$f(t,p) \sim 1$
('quantum')

Classical-statistical lattice gauge theory

Description in terms of classical field equations of motion

$$D_\mu F^{\mu\nu} = J^\nu$$

→ Solved numerically on a space-time lattice using lattice gauge theory techniques

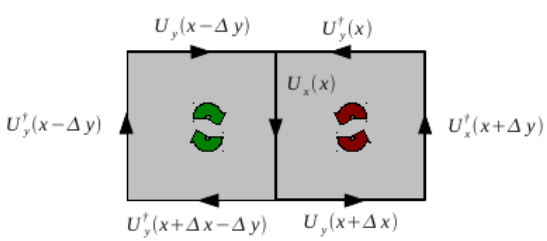

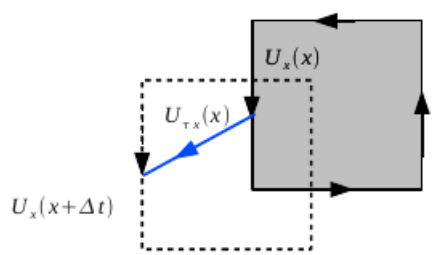

Kinetic theory

Description in terms of quasi particle excitations.

$$\partial_t f(t,p) = C[f](t,p)$$

→ Study the effect of different scattering processes (e.g. 2 ↔2; 2↔3) analytically

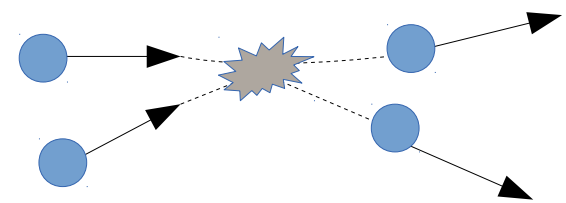

From the violence of the collision ...to the calm of the quark-gluon fluid

Initial state:
Far from equilibrium

Non-equilibrium dynamics

Final state:
Thermal equilibrium

How is thermal equilibrium achieved?

Thermalization process

The thermalization process at weak coupling proceeds in a similar way for a large class of strongly correlated many-body systems

- Thermalization in scalar field theories – Cosmology
  (Micha, Tkachev PRD 70 (2004) 043538)
  (Berges, Boguslavski, SS, Venezuelan arXiv:1312.5216)
  → *c.f. talk by Kirill Boguslavski*

- Thermalization in non-Abelian gauge theories in a 'static box'
  (Berges,SS,Sexty PRD 86 (2012) 074006; SS PRD 86 (2012) 065008)
  (Kurkela, Moore PRD 86, (2012) 056008)
  (York, Kurkela, Lu, Moore, arXiv:1401.3751)
  → c.f. talk by Aleksi Kurkela

- Thermalization in heavy-ion collisions at very high energies
  (Berges,Boguslavski,SS,Venugopalan arXiv:1303.5650, arXiv:1311.3005)

Non-Abelian plasma in a 'static box'

- Consider homegenous and ***isotropic systems*** which are initially ***highly occupied*** and initially characterized by a single momentum scale Q

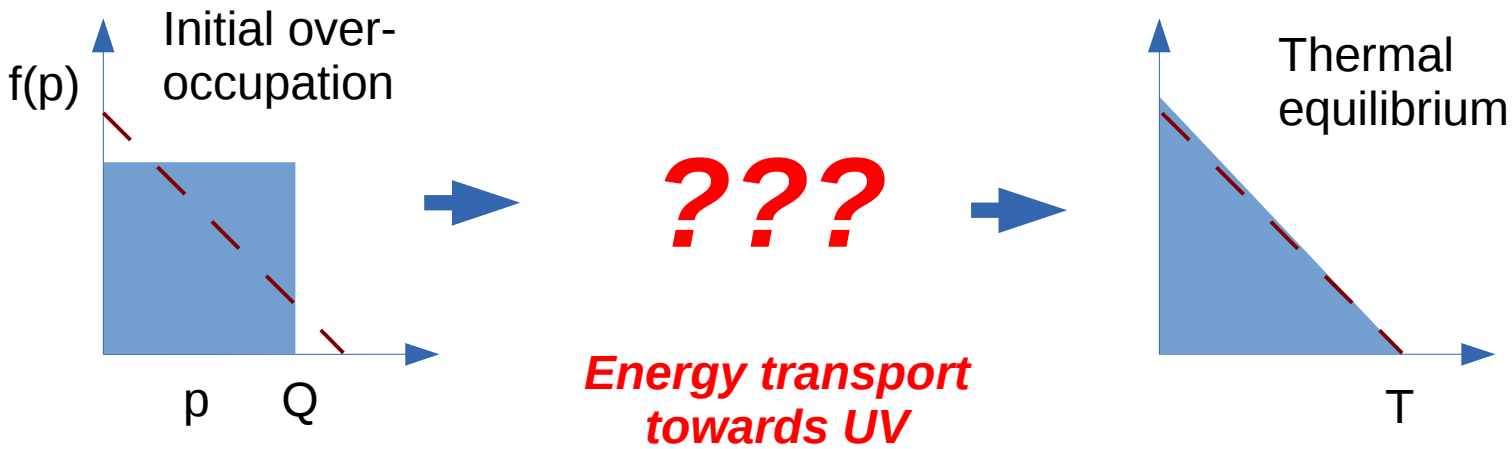

How does thermalization proceed?
What are the relevant (kinetic) processes?

→ Since classical-statistical lattice gauge theory and kinetic theory have an overlap in the range of validity they can be combined to obtain a detailed understanding of the thermalization process

Classical-statistical lattice simulations

- ***Initial conditions*** chosen to mimic quasi-particle picture

$$A^a_\mu(t_0, x) = \int \frac{d^3k}{(2\pi)^3} \sqrt{f(k, t_0)} \times [c^k_{\lambda,a} \xi^{(\lambda)k}_\mu(t_0) e^{ikx} + c.c]$$

- Define ***single particle distribution*** to facilitate comparison with kinetic theory

$$f(p,t) = \langle \left| \xi^{(\lambda)k}_\mu(t) \bar{\partial}_t A^\mu_a(t,p) \right|^2 \rangle$$

(Coulomb gauge)

(see e.g. Kurkela, Moore PRD 86, (2012) 056008; Berges,Boguslavski,SS, Venugopalan arXiv:1311.3005)

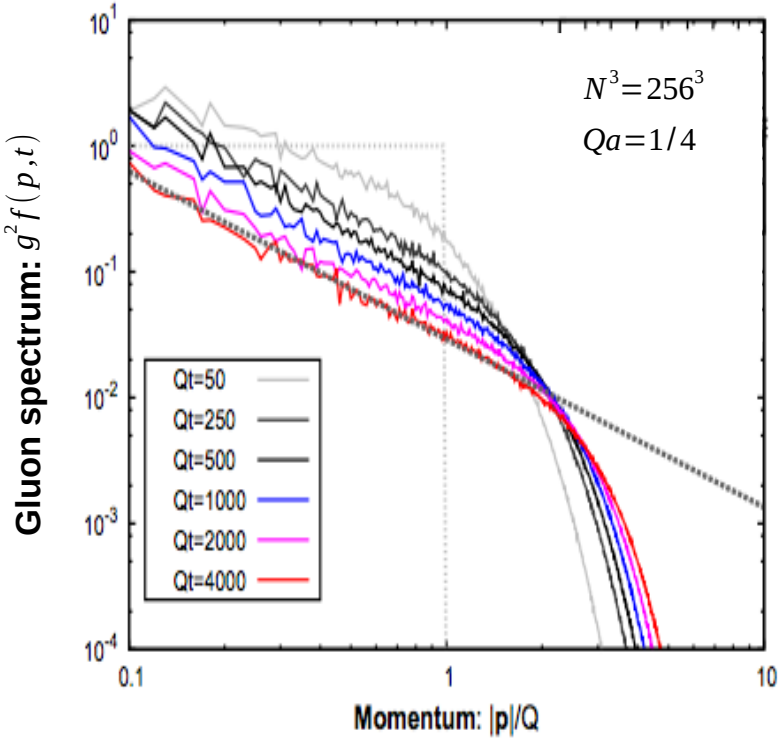

Self-similarity

- Evolution at late times shows a ***self-similar*** behavior

$$f(p,t) = (Qt)^{\alpha} f_S((Qt)^{\beta} p)$$

with dynamical scaling exponents

α = -4/7

β = -1/7

consistent with ***elastic & inelastic scattering*** processes

(c.f. Kurkela, Moore JHEP 1112 (2011) 044; Blaizot et al. Nucl.Phys. A873 (2012) 68-80)

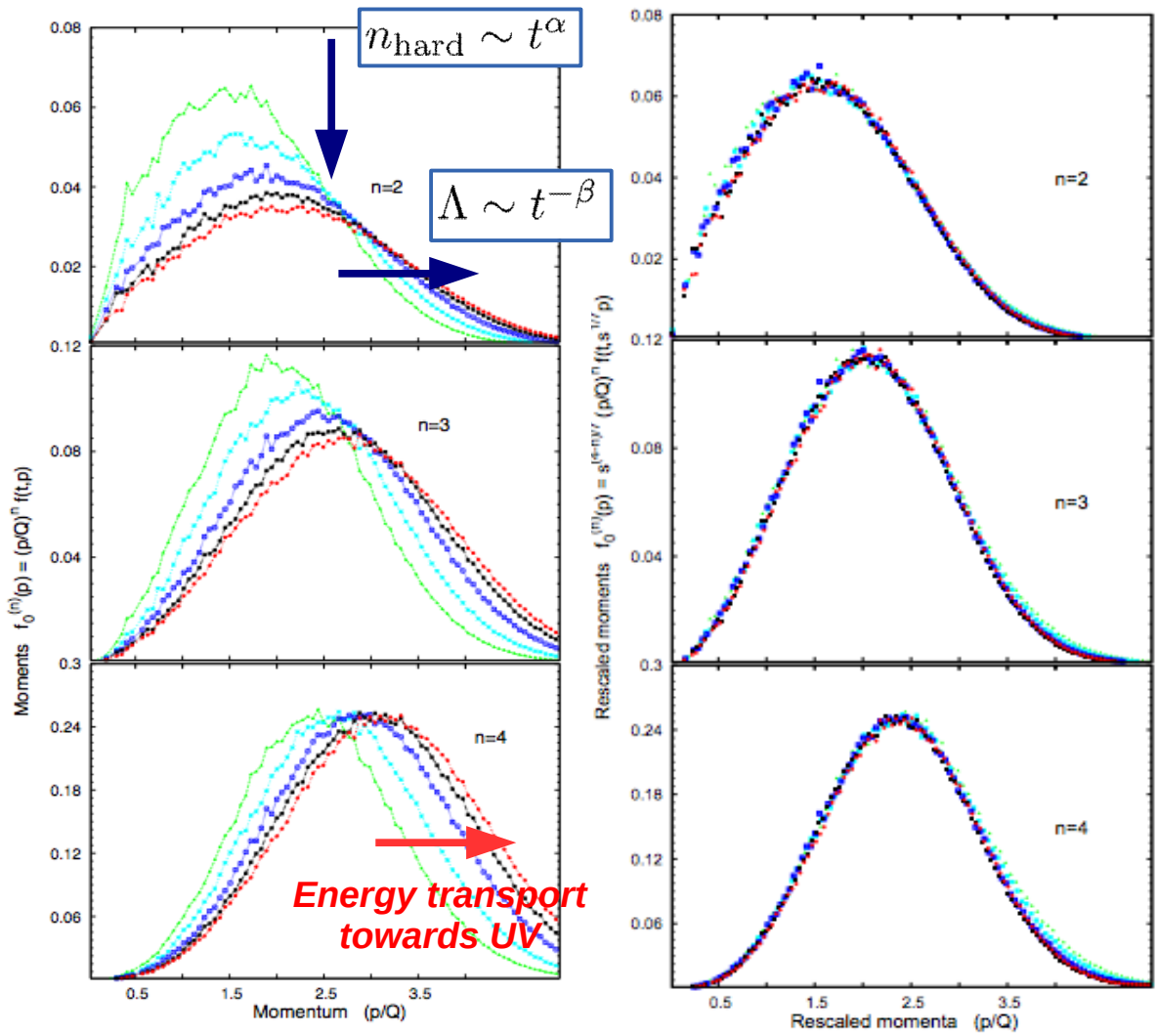

(SS PRD 86 (2012) 065008; Kurkela, Moore PRD 86, (2012) 056008)

Turbulent thermalization process

Thermalization for a system far from equilibrium proceeds as a ***self-similar evolution*** associated to the presence of a ***non-thermal fixed point***

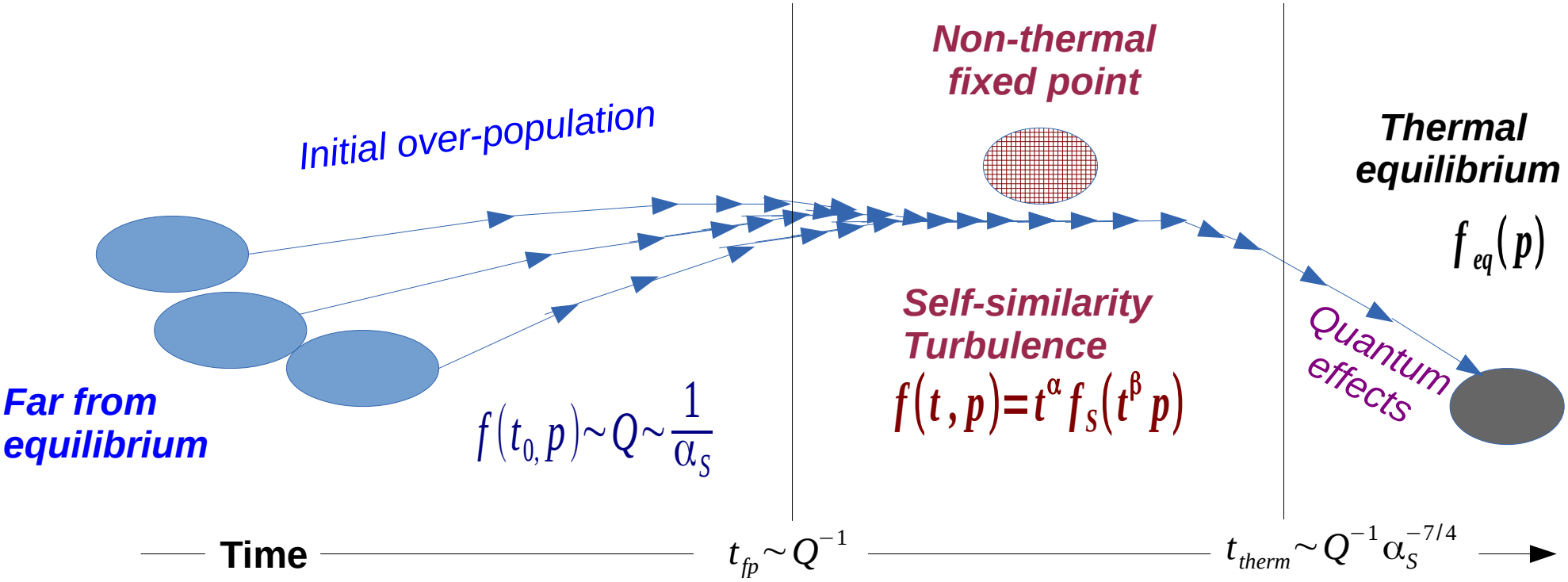

How does this picture apply to relativistic heavy-ion collisions in the weak coupling limit?

The 'Glasma' and the over-occupied QGP

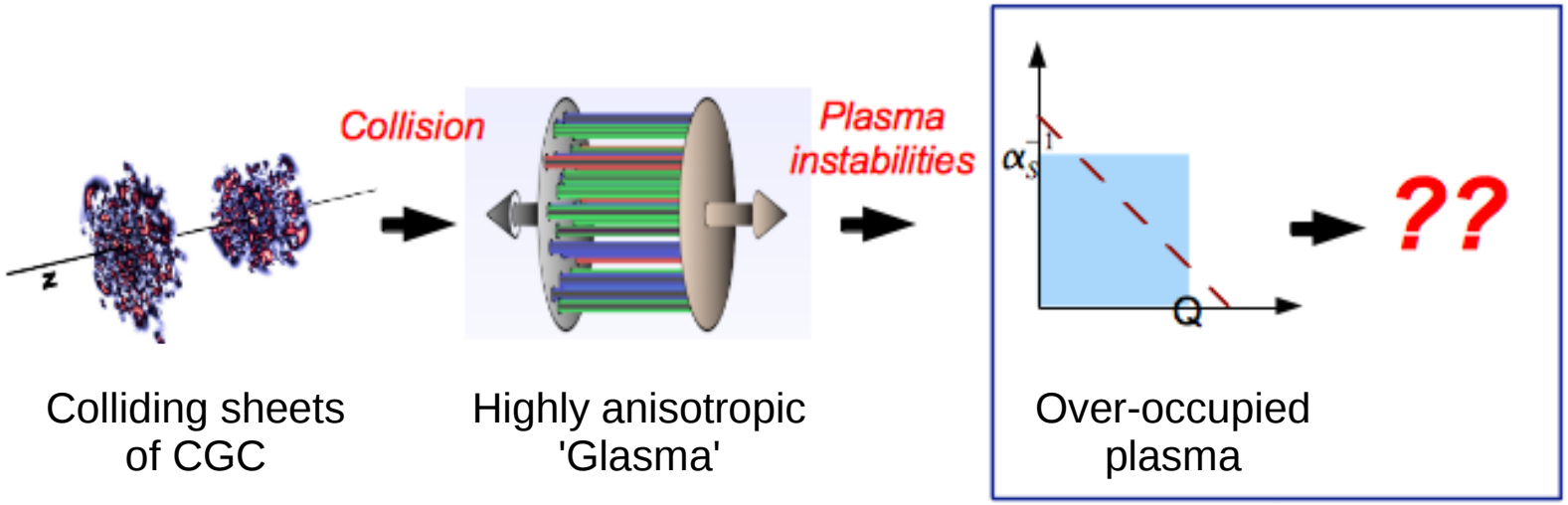

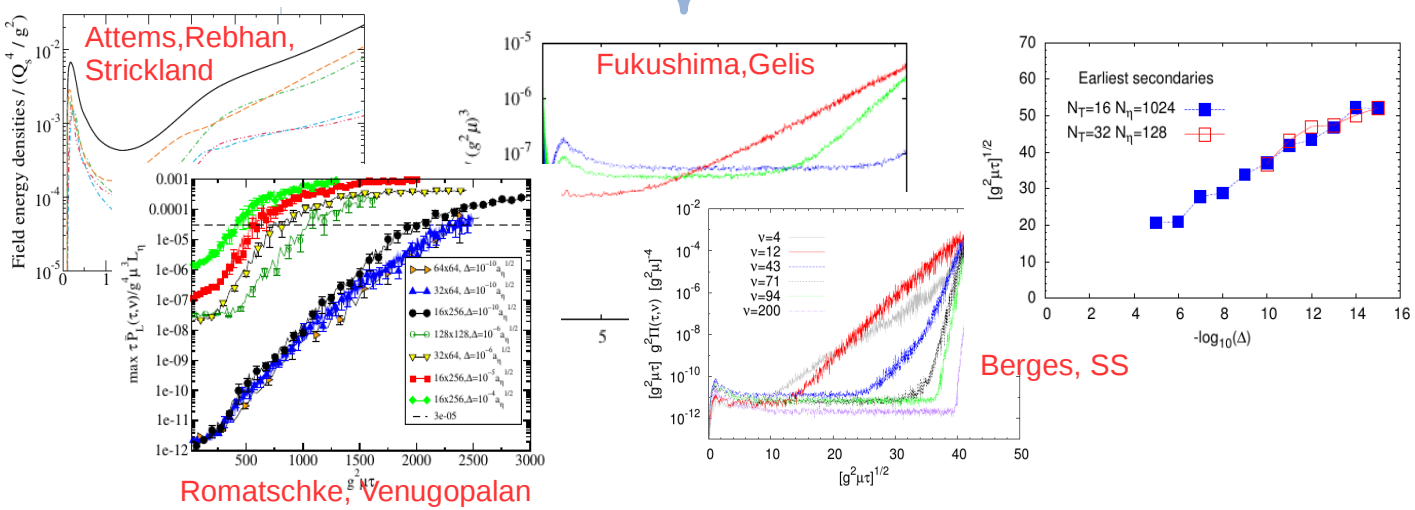

Thermalization of the over-occupied QGP

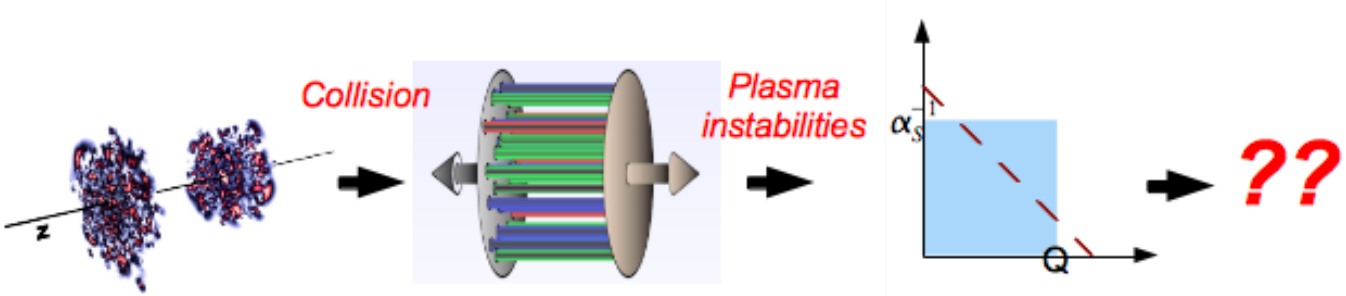

- There is always a ***competition between interactions*** and the ***longitudinal expansion***, which may render the system ***anisotropic on large time scales.***

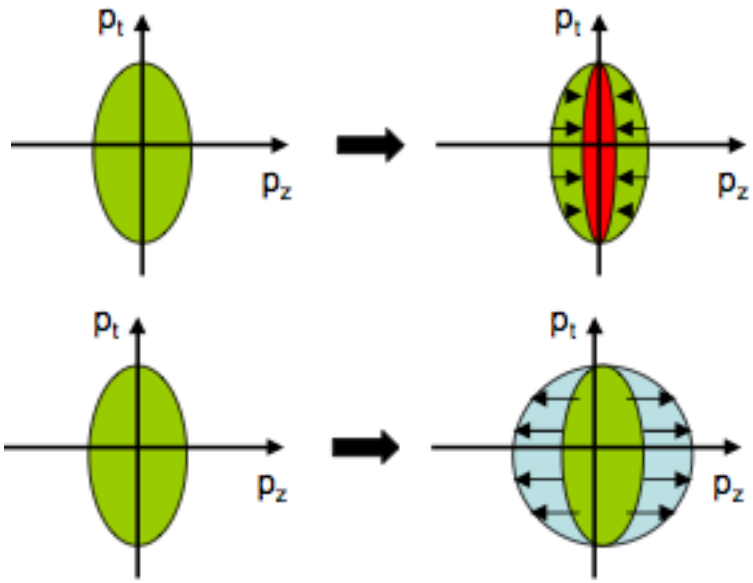

Longitudinal Expansion:
- red-shift of longitudinal momenta p
  → increase of anisotropy
- dilution of the system

Interactions:
- isotropize the system

Kinetic theory description

- Different scenarios of how thermalization proceeds have been proposed in the literature

Baier et al. (BMSS),
PLB 502 (2001) 51-58

Kurkela, Moore (KM),
JHEP 1111 (2011) 120

Blaizot et al. (BGLMV),
Nucl. Phys. A 873 (2012) 68-80

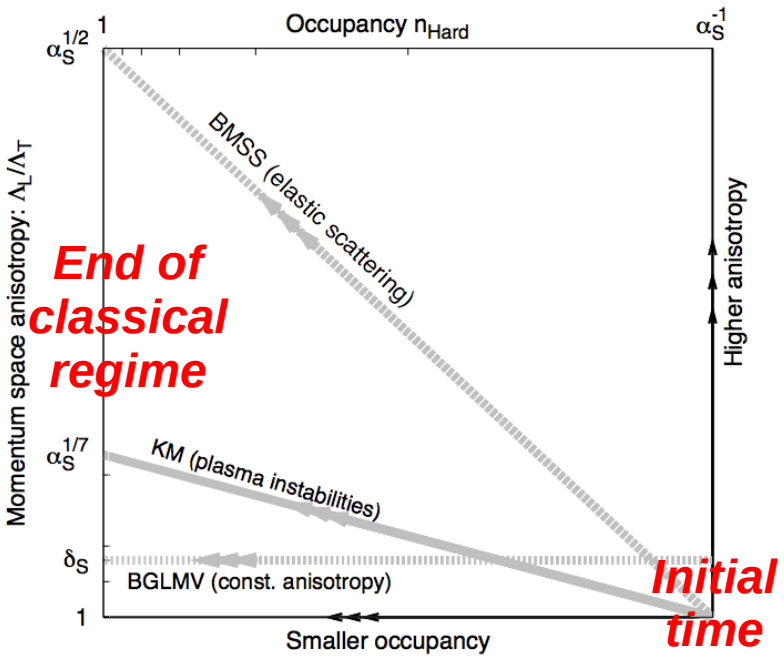

- Difference arises from the treatment of soft (non-perturbative) physics of modes below the Debye scale.

→ ***Since the classical-statistical theory and kinetic theory have an overlap in the range of validity, non-perturbative lattice simulations can be used to determine which scenario is realized***

Classical-statistical simulations

Choose a large range of different initial conditions to describe the properties of the system at the initial time $\tau_0 = 1/Q_s \ln^2(1/\alpha_s)$ very shortly after the collision

Controls initial overoccupation

$$f(p_T, p_Z, \tau_0) = \frac{n_0}{\alpha_s}\theta\left(Q_s - \sqrt{p_T^2 + \xi_0^2 p_Z^2}\right)$$

(Coulomb gauge)

Controls initial momentum space anisotropy

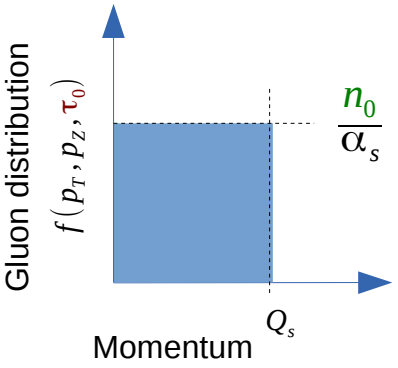

Computations performed at very weak coupling $\alpha_s \sim 10^{-2} - 10^{-5}$ to ensure accurate description of the dynamics at all times in simulation.

Corresponds to $Q_s \tau_0 \approx 20 - 100$, i.e. much smaller than expected thermalization time at weak coupling $Q_s \tau_{therm} \approx 10^5 - 10^{13}$

Bulk anisotropy

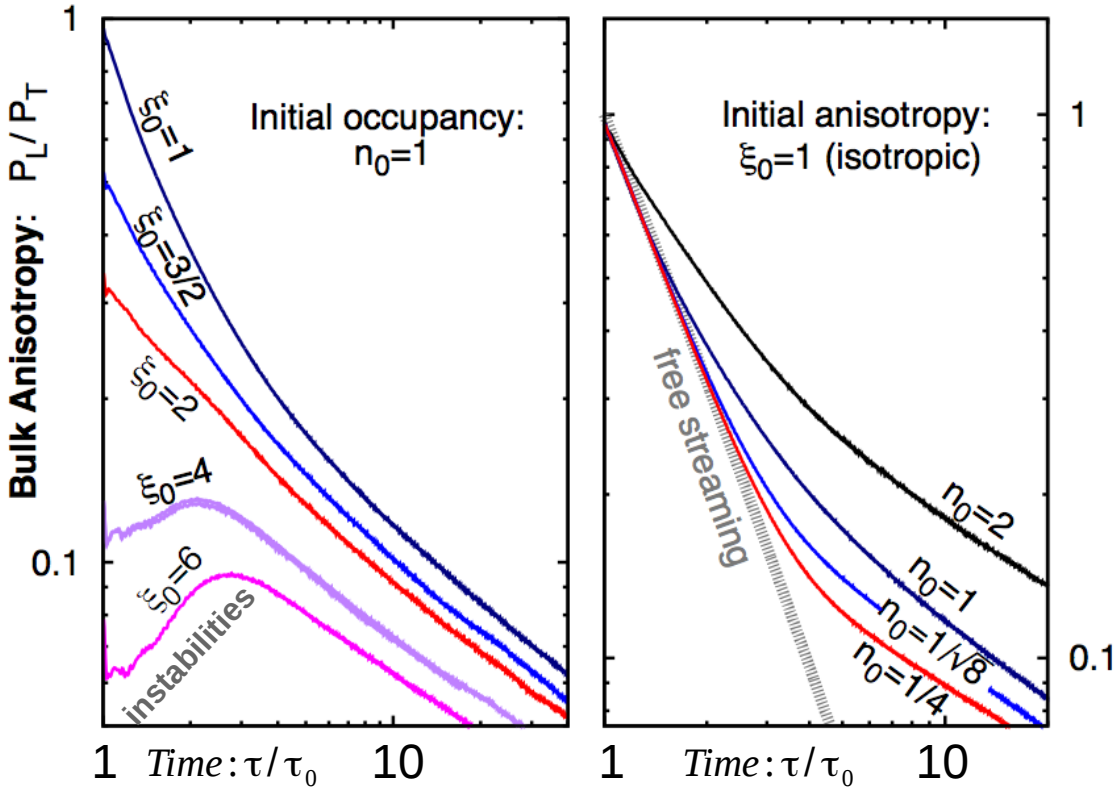

Initial distribution: $f(p_T, p_Z, \tau_0) = \frac{n_0}{\alpha_s} \theta\left(Q_s - \sqrt{p_T^2 + \xi_0^2 p_Z^2}\right)$

- Small occupancy leads to initial free streaming behavior.
- Large initial anisotropy leads to transient increase of isotropy via plasma instabilities
- The system remains ***strongly interacting*** throughout the entire evolution.
- At late times, the evolution becomes ***insensitive to the details of the initial conditions*** and the anisotropy increases.

Universal scaling

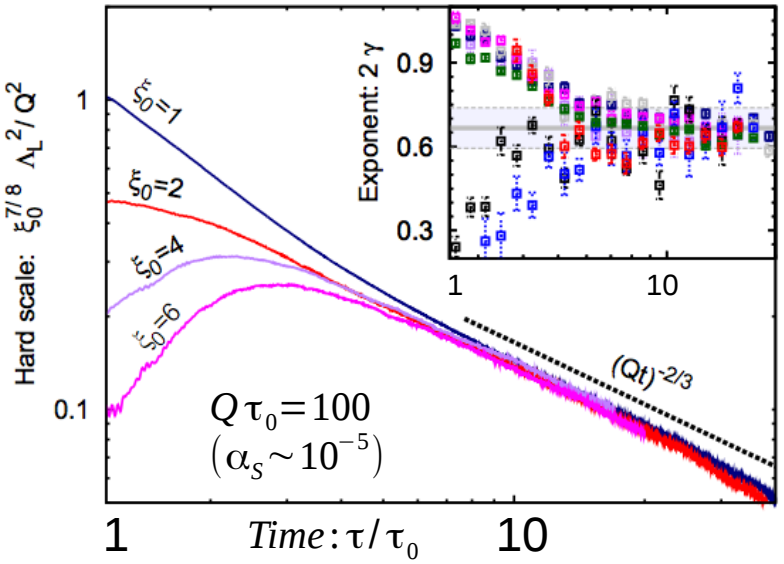

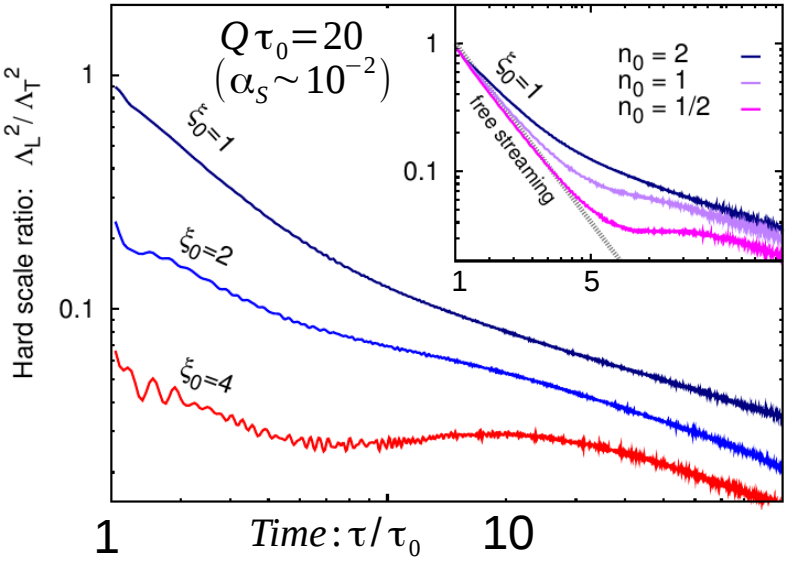

- The typical ***longitudinal momentum*** of hard excitations exhibits a ***universal scaling*** behavior

$$\Lambda_L^2/Q^2 \sim (Qt)^{-2\gamma}$$

$$2\gamma = 0.67 \pm 0.07$$

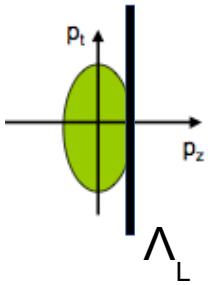

- The typical ***transverse momentum*** of hard excitations remains approximately ***constant***

$$\Lambda_T^2/Q^2 \sim (Qt)^{-2\beta}$$

$$2\beta \simeq 0$$

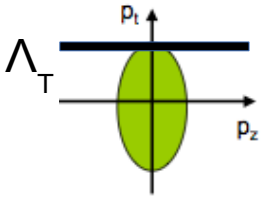

Discretization errors

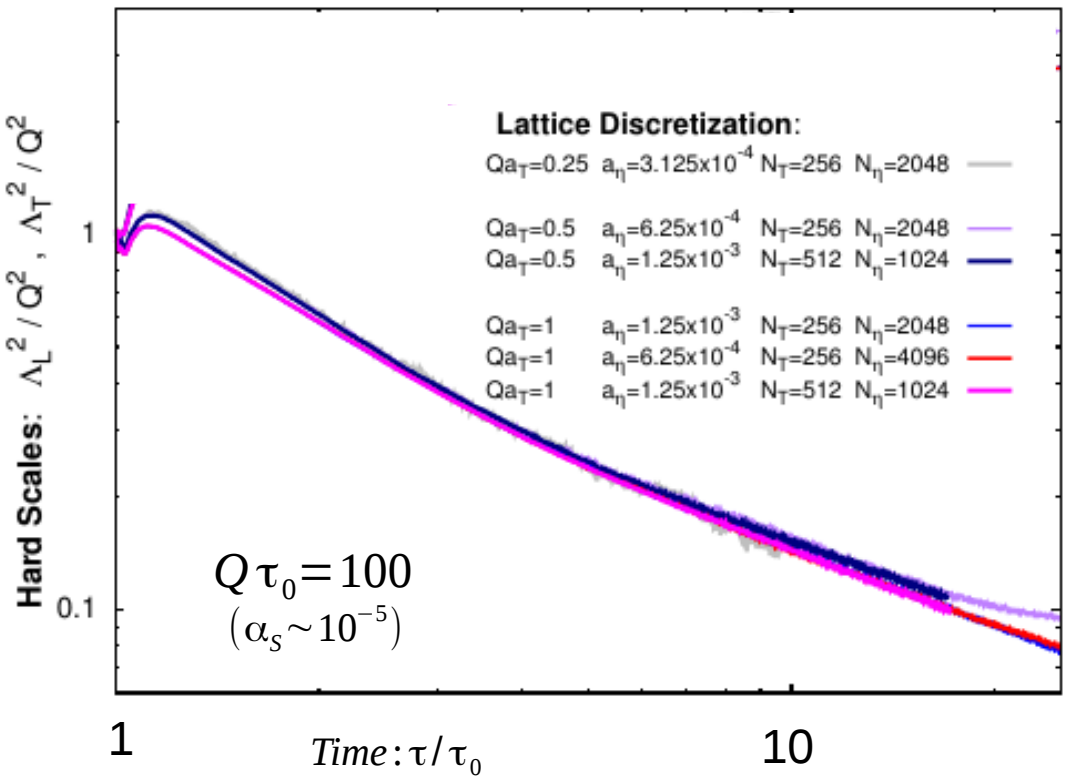

- ***Universal scaling independent of the lattice discretization***
- Need very large lattices up to

  256x256x4096

  to properly resolve all the relevant scales

Gluon spectra

Transverse spectrum

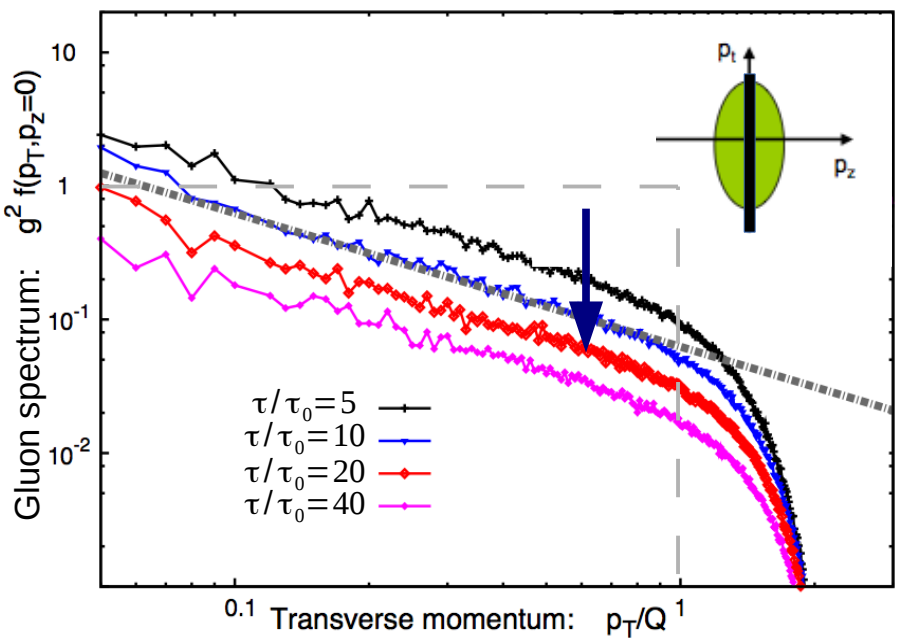

Longitudinal spectrum

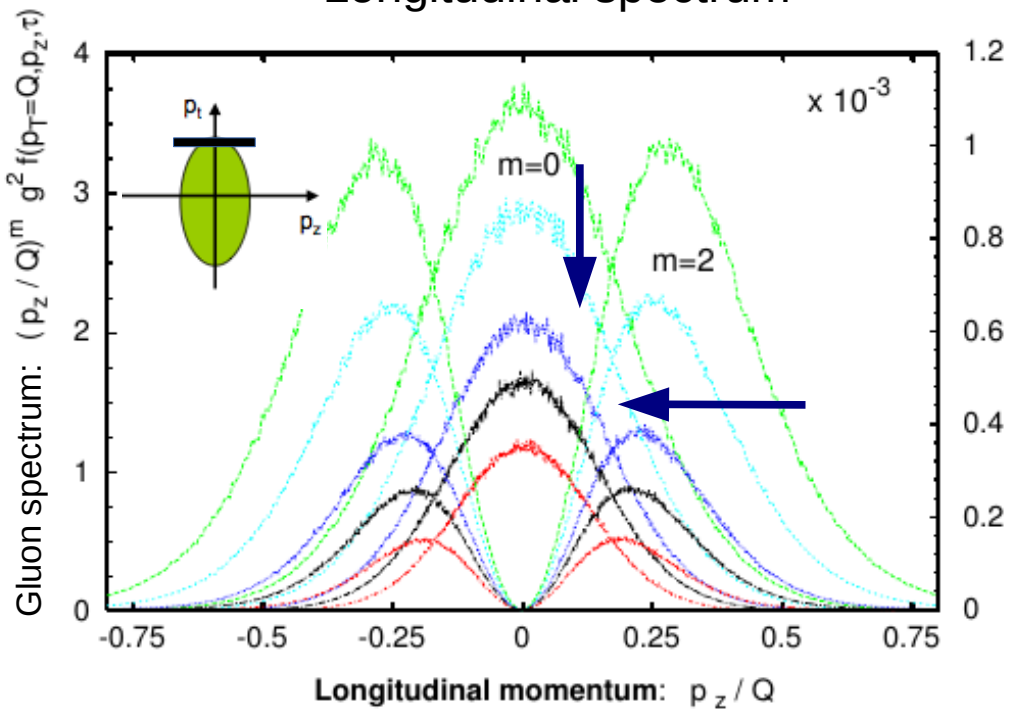

Transverse spectrum quickly approaches 'thermal' like T/p_T shape, with decreasing amplitude

Significant momentum (p_Z) broadening observed. However not strong enough to compensate for the red shift.

Self-similarity

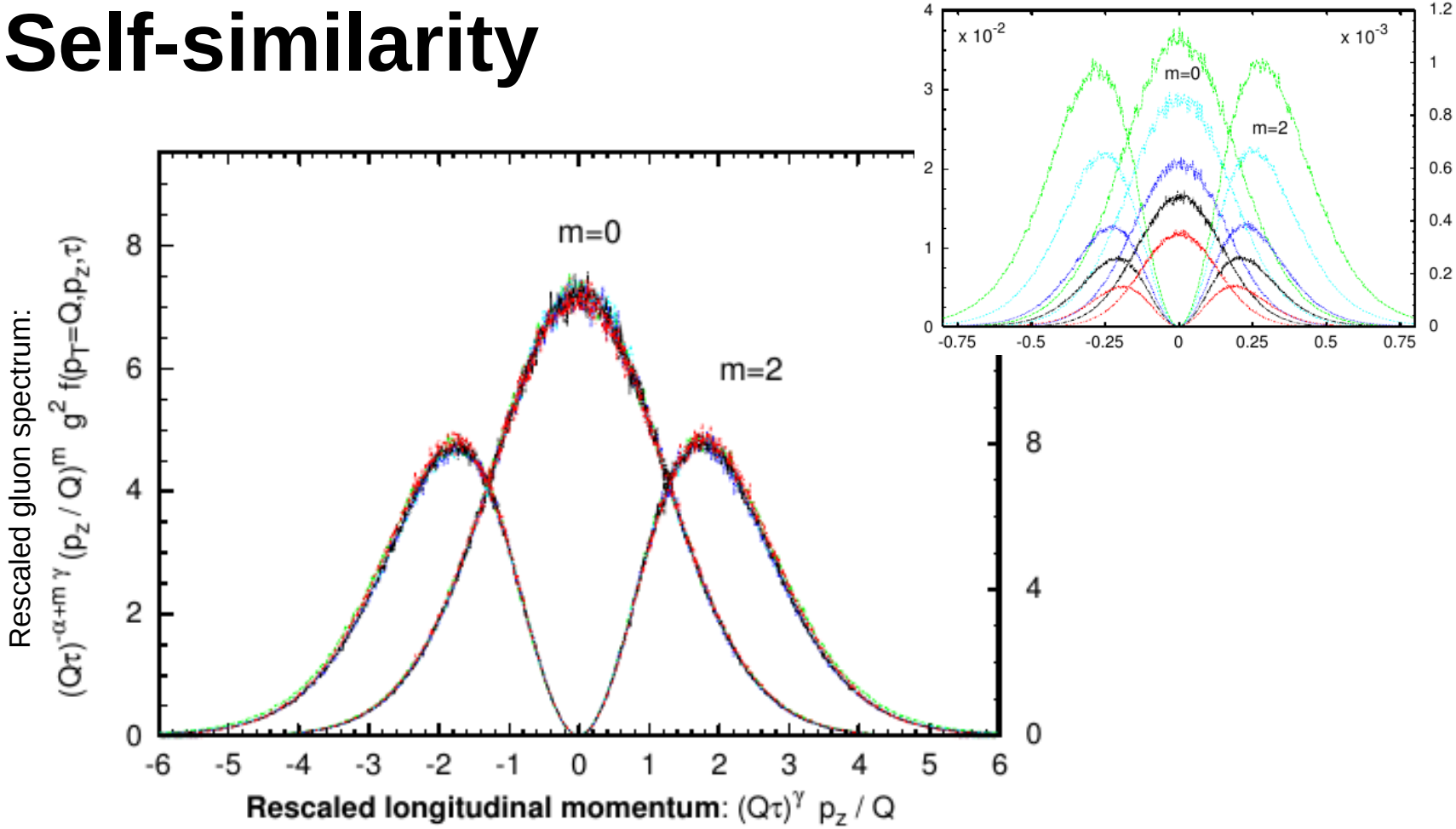

The system reaches a non-thermal fixed point, where the space-time evolution becomes self-similar, i.e. $f(p_T, p_Z, \tau) = (Q\tau)^{\alpha} f_S((Q\tau)^{\beta} p_T, (Q\tau)^{\gamma} p_Z)$

with a ***stationary distribution*** f_S and scaling exponents $\alpha = -2/3, \beta = 0, \gamma = 1/3$

Kinetic interpretation

Consider the Boltzmann equation

$$[\partial_\tau - \frac{p_Z}{\tau}\partial_{p_Z}] f(p_T, p_Z, \tau) = C[f](p_T, p_Z, \tau)$$

with a self-similar evolution

$$f(p_T, p_Z, \tau) = (Q\tau)^\alpha f_S((Q\tau)^\beta p_T, (Q\tau)^\gamma p_Z)$$

→ ***Non-thermal fixed point solution*** $(f \gg 1)$

$$[\alpha + \beta p_T \partial_{p_T} + (\gamma - 1) p_Z \partial_{p_Z}] f_S(p_T, p_Z) = Q^{-1} C[f_S](p_T, p_Z)$$

→ ***Scaling exponents determined by scaling relations for***

- Small angle elastic scattering $(2\alpha - 2\beta + \gamma = -1)$
- Energy conservation $(\alpha - 3\beta - \gamma = -1)$
- Particle number conservation $(\alpha - 2\beta - \gamma = -1)$

→ $\alpha = -2/3, \beta = 0, \gamma = 1/3$ ***in excellent agreement with lattice data!***

Comparison with weak-coupling thermalization scenarios

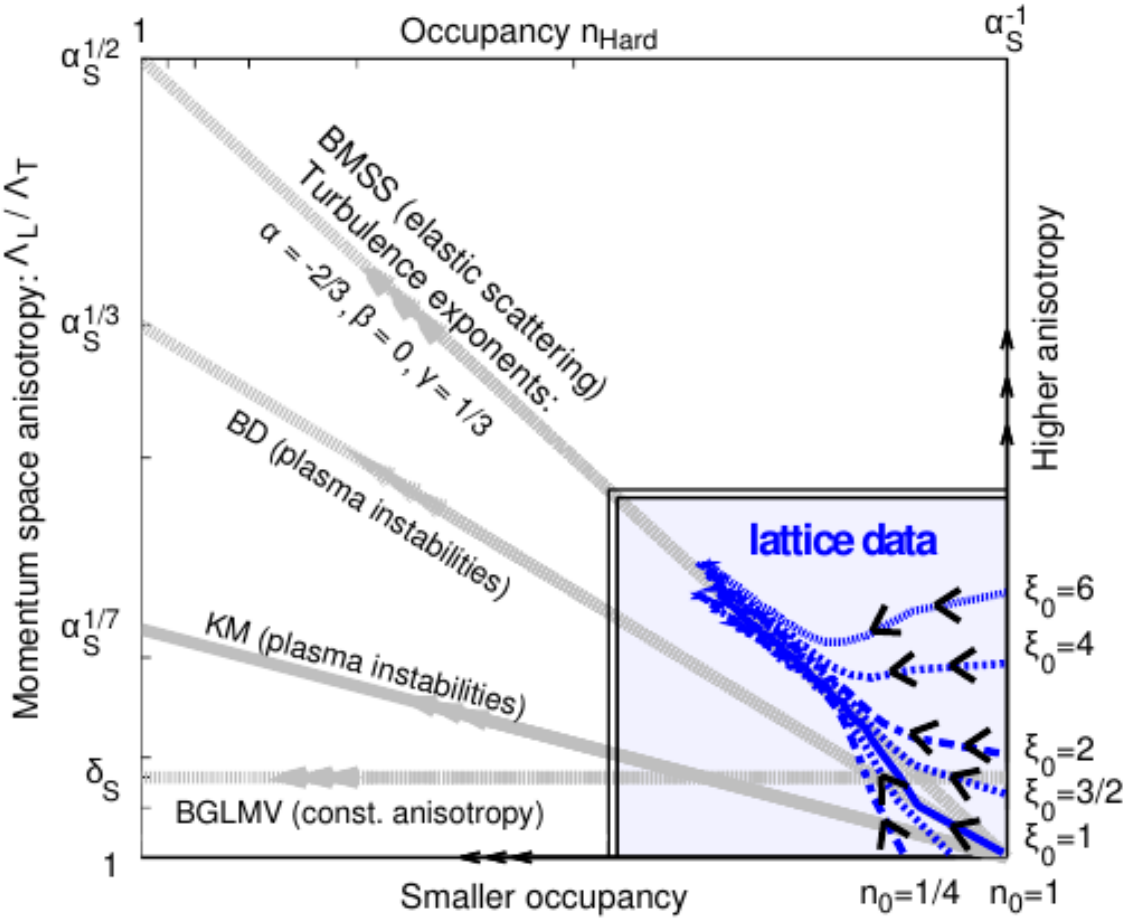

'Bottum up' scenario* emerges as a non-thermal fixed point of the evolution!

**Baier,Mueller,Schiff and Son, Phys. Lett. B 502, 51 (2001)*

Turbulent thermalization process

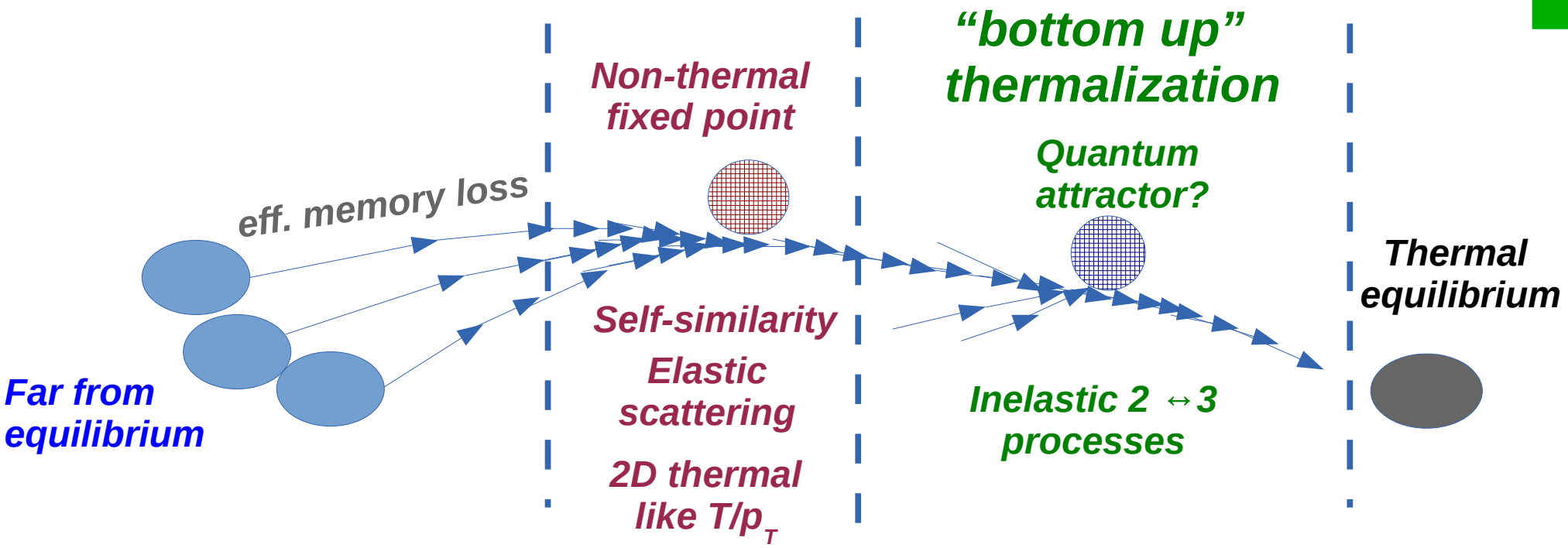

Time $\tau_{inst} \sim Q^{-1} \ln^2(\alpha_S^{-1})$ $\tau_{quant} \sim Q^{-1} \alpha_S^{-3/2}$ $\tau_{therm} \sim Q^{-1} \alpha_S^{-13/5}$

Classical regime | Quantum regime

Extrapolation to realistic coupling $\alpha_S \sim 0.3$ for $Q \sim 2\,GeV$

$\tau_{inst} \sim 0.1\,fm/c$ $\tau_{quant} \sim 0.6\,fm/c$ $\tau_{inst} \sim 2\,fm/c$

Summary & Conclusions

- The thermalization process at weak coupling ($g^2 \ll 1$, $g^2 f \sim 1$) is governed by non-thermal fixed points, where the system exhibits the self-similar dynamics characteristic of wave turbulence.

- Generic feature of strongly correlated many-body systems across different energy scales ('big bang', 'little bang', 'ultracold bang')

- We have established the connection between non-perturbative classical statistical lattice simulations and kinetic theory for the expanding non-Abelian plasma.

- Extrapolation to realistic values of the coupling yields reasonable results, consistent with heavy-ion phenomenology.

Open questions

- *How does the approach to the weak coupling attractor occur for more realistic initial conditions and values of the coupling constant?*

- *How exactly is thermalization completed in the quantum regime?*

Backup Slides

Thermalization process

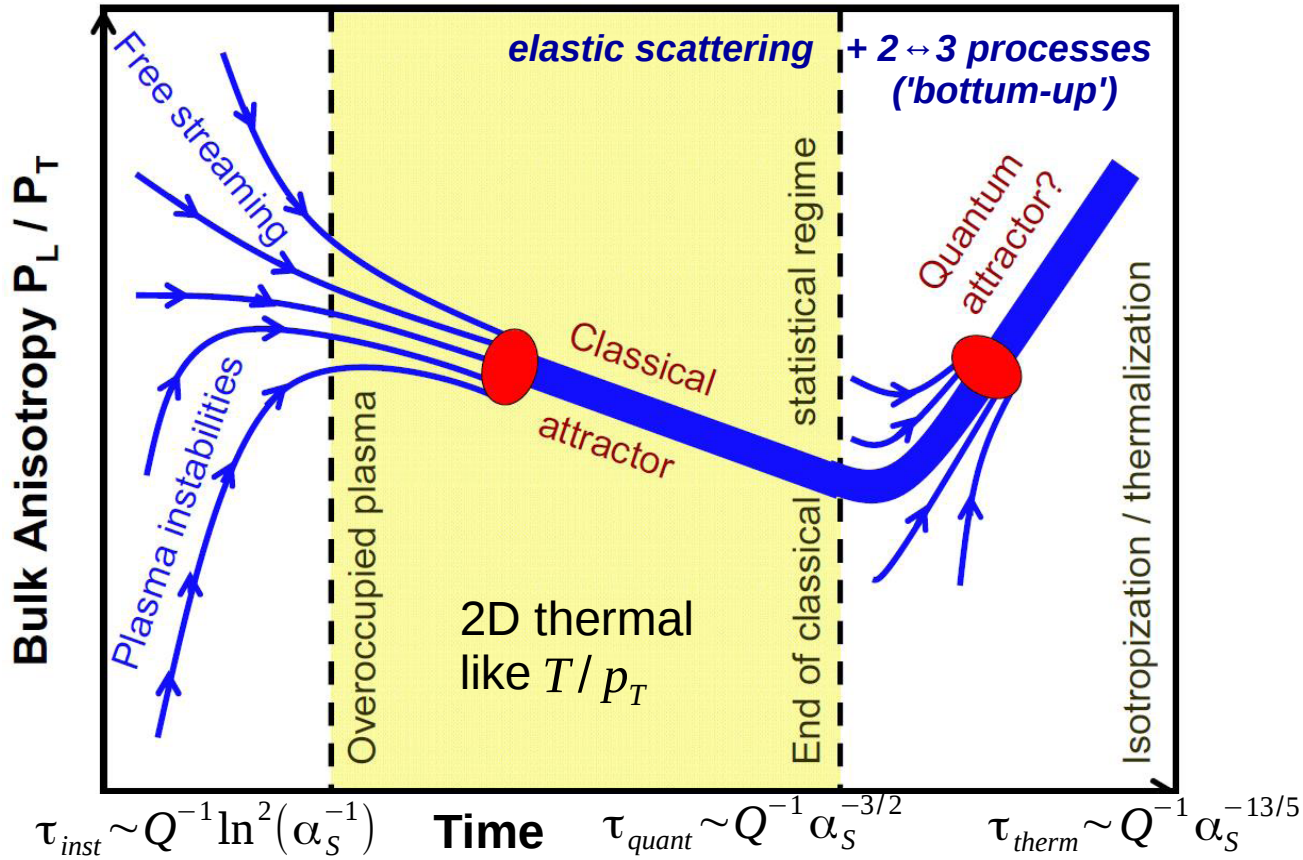

Extrapolation to realistic coupling $\alpha_S \sim 0.3$ for $Q \sim 2\,GeV$

$\tau_{inst} \sim 0.1\,fm/c$ $\tau_{quant} \sim 0.6\,fm/c$ $\tau_{inst} \sim 2\,fm/c$

Comparison with Epelbaum & Gelis

I) Time scales are very different

Epelbaum, Gelis
PRL 111 (2013) 232301

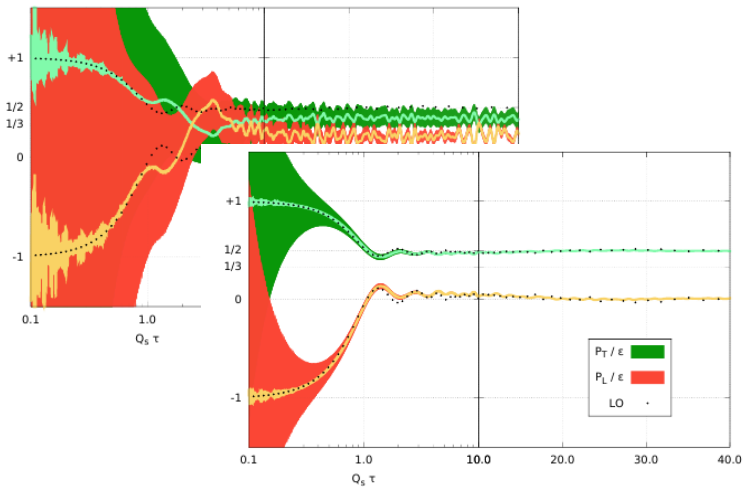

Berges, Boguslavski, SS, Venugopalan
arXiv:1303.5650; arXiv:1311.3005;

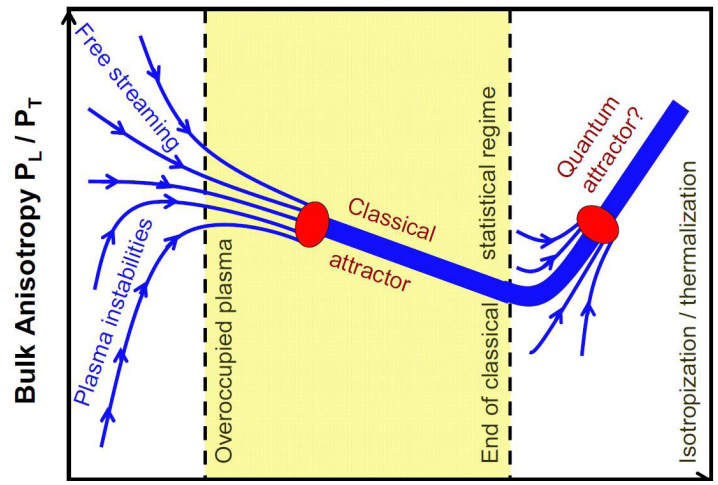

Time —— $\tau = 0$ —— $\tau_{inst} \sim Q^{-1} \ln^2(\alpha_S^{-1})$ —— $\tau_{quant} \sim Q^{-1} \alpha_S^{-3/2}$ —— $\tau_{therm} \sim Q^{-1} \alpha_S^{-13/5}$ ——►

II) Different range of couplings → *classical-statistical method still reliable?*

→ Need more detailed comparison to establish how the weak coupling attractor is approached & whether there may be a change of behavior at larger values of the coupling (work in progress)

Thermalization process - Cosmology

Model for thermalization of the early universe:

Scalar field theory ($\lambda\Phi^4$); Small coupling $\lambda = 10^{-8}$

$$S[\varphi] = \int d^4x \left(\frac{1}{2}\partial_\mu\varphi\partial^\mu\varphi - \frac{\lambda}{24}\varphi^4 \right)$$

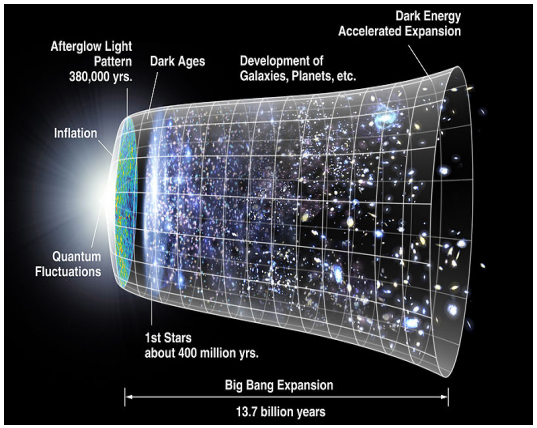

At the end of inflation: Background field $\Phi_0 \sim 1/\sqrt{\lambda}$ + vacuum fluctuations

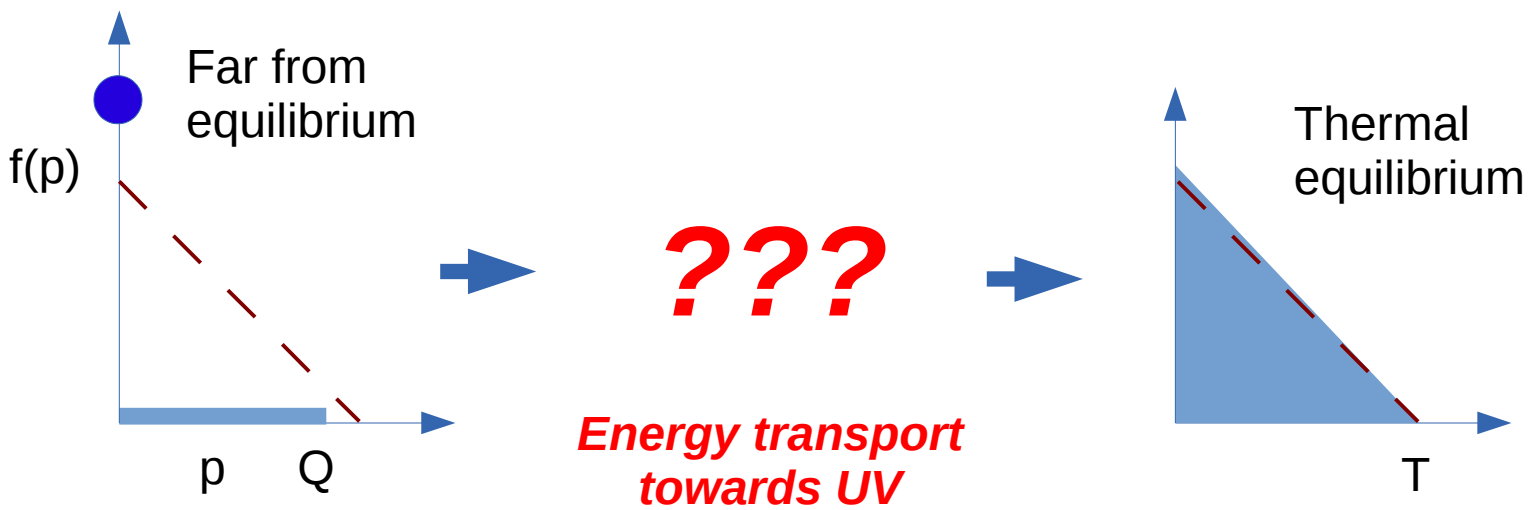

Thermalization process - Cosmology

Non-thermal fixed point

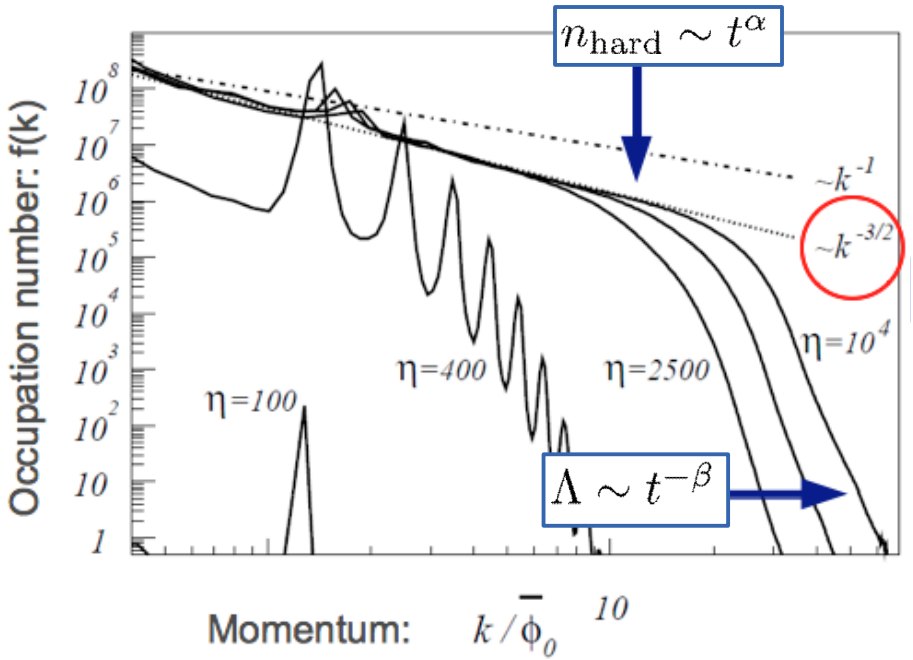

Self-similar evolution

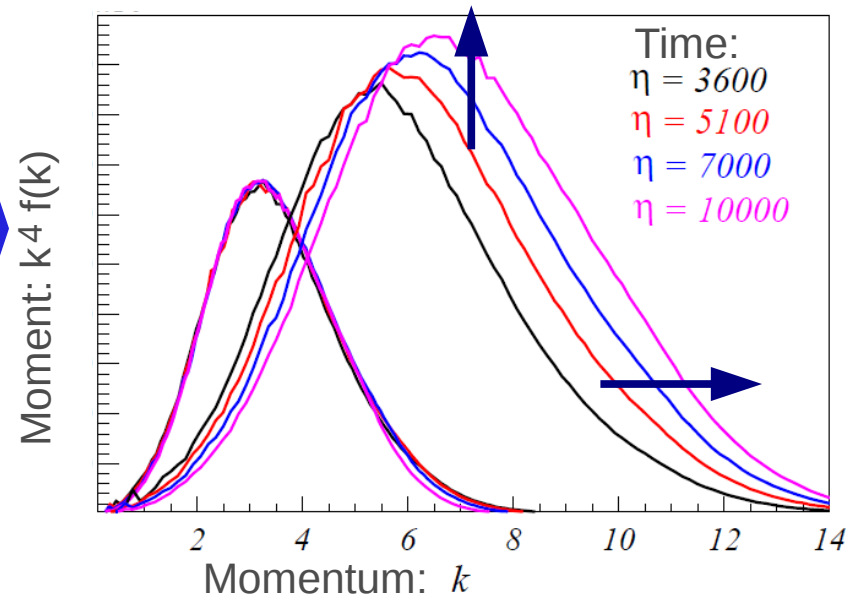

- The evolution becomes ***self-similar*** $f(p,t) = t^{\alpha}\ f_S(t^{\beta} p)$

- The thermalization process is described by a ***quasi-stationary evolution*** with ***scaling exponents*** Dynamic: α=-4/5 β=-1/5 Spectral: κ=-3/2

(Micha, Tkachev PRD 70 (2004) 043538)

Independence of Initial conditions

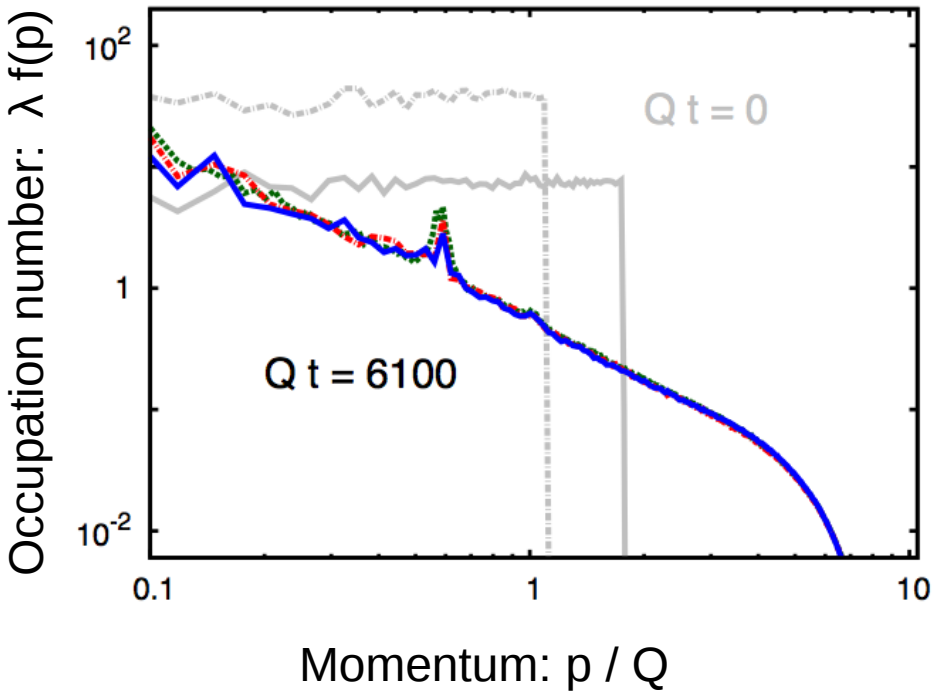

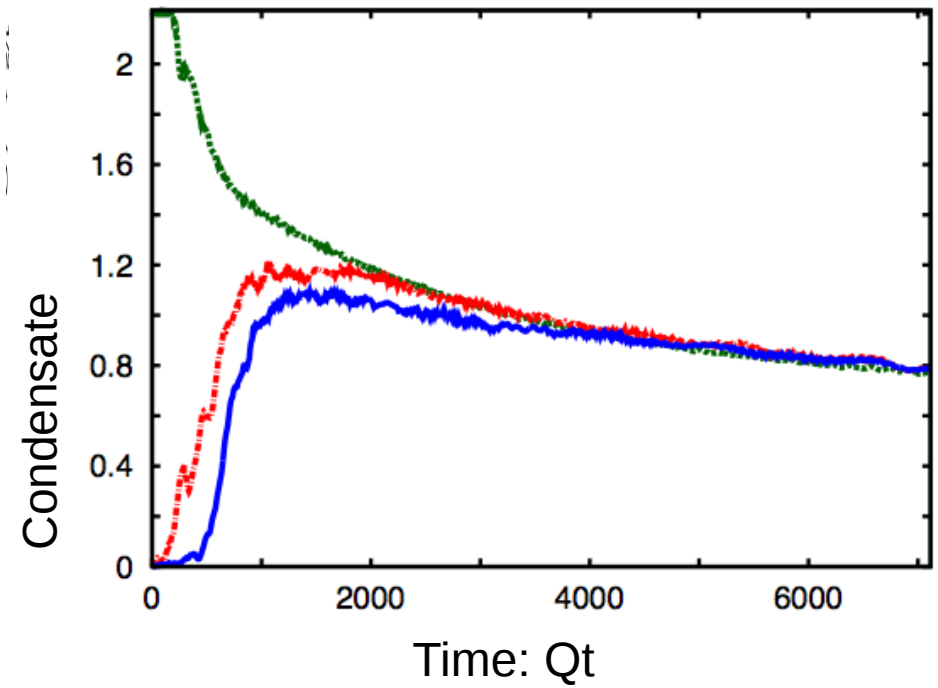

- The turbulent scaling behavior is really a property of the thermalization process – ***independent of the underlying initial conditions***

- An ***effective memory loss*** occurs ***already at the early stages*** of the thermalization process

(Berges,Boguslavski,SS,Venugopalan arXiv:1312.5216)

Manifestation of turbulence

"Driven" Turbulence – Kolmogorov wave turbulence

vs.

"Free" Turbulence – Turbulent Thermalization

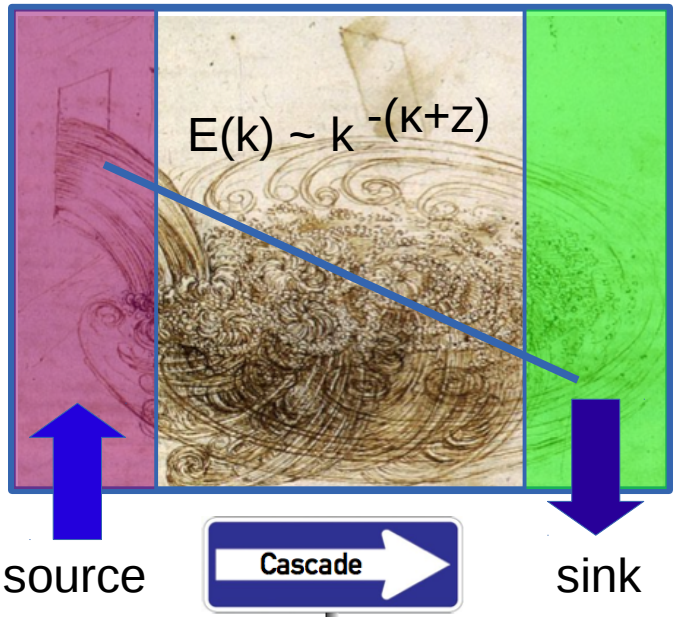

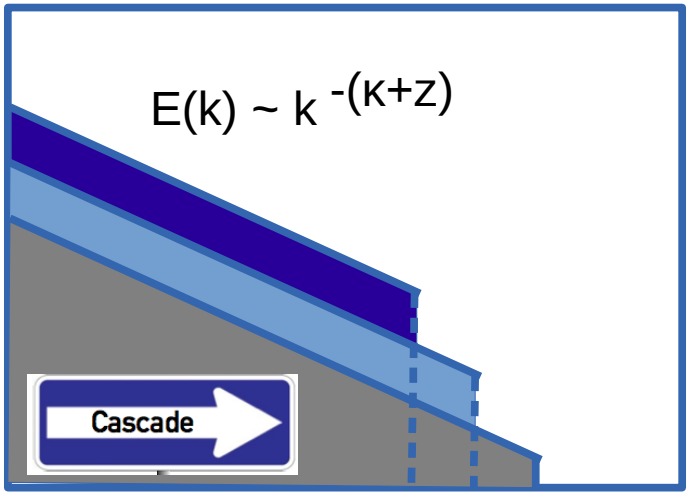

closed system

- ***Stationary scaling solution*** associated to scale invariant energy flux

- ***quasi-stationary solution*** with universal ***non-thermal spectral exponents***

- ***Self-similar evolution*** with universal ***dynamical scaling exponents***

Uriel Frisch, "*Turbulence. The Legacy of A. N. Kolmogorov.*"

Zakharov, V. E.; L'vov, V. S.; Falkovich, G, "*Kolmogorov spectra of turbulence 1. Wave turbulence.*"

Turbulent thermalization process

Thermalization process is controlled by the ***transport of conserved quantities*** (energy and particle number) over a large separation of scales

→ ***Wave turbulence***

Similar manifestations across far from equilibrium systems at all energy scales

Cosmology

WMAP Science Team

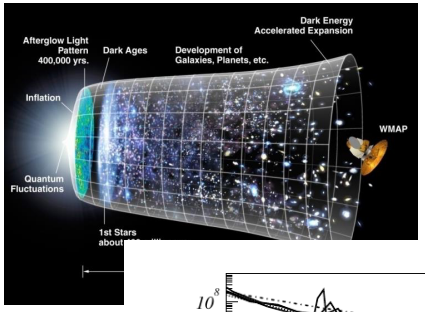

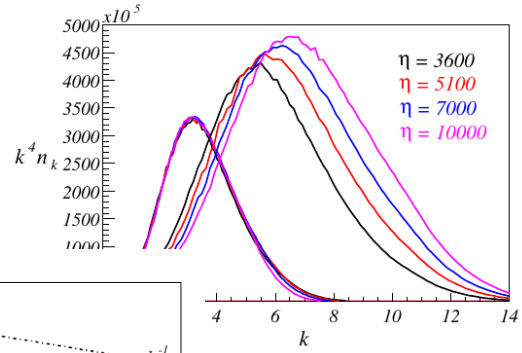

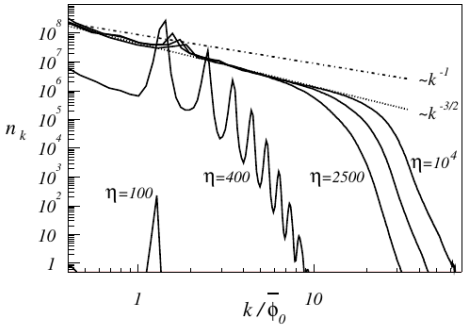

Micha, Tkachev PRD 70 (2004) 043538

→ ***Universality far from equilibrium***

Cold quantum gases

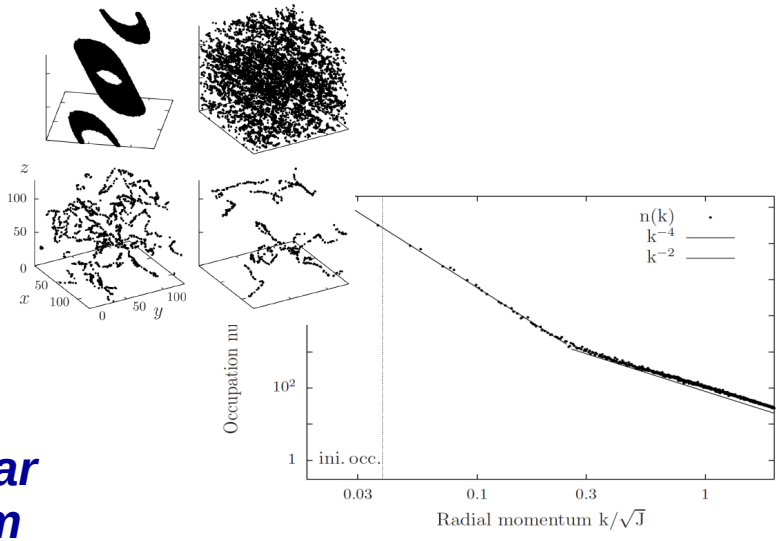

Nowak, Sexty, Gasenzer, PRB 84 (2011) 020506(R)

Non-equilibrium Bose-Einstein condensation in scalar and gauge systems

Dénes Sexty

Uni Heidelberg

Approach to Equilibrium in Strongly Interacting Matter
April 3, 2014 , BNL

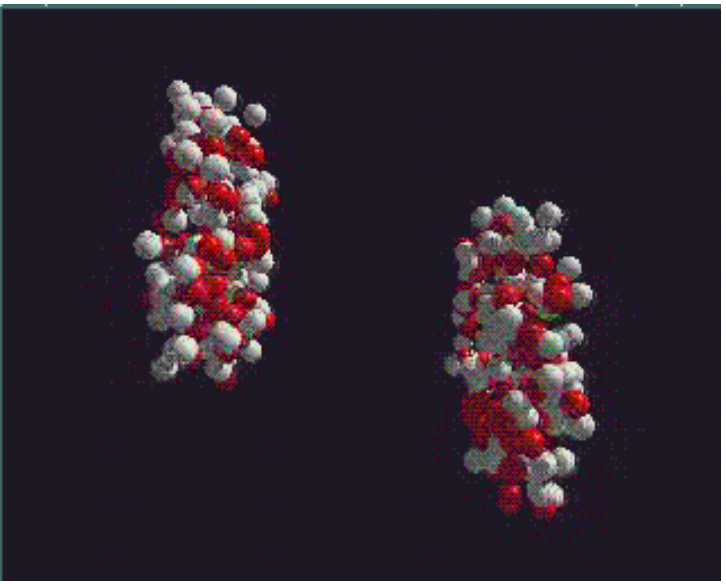

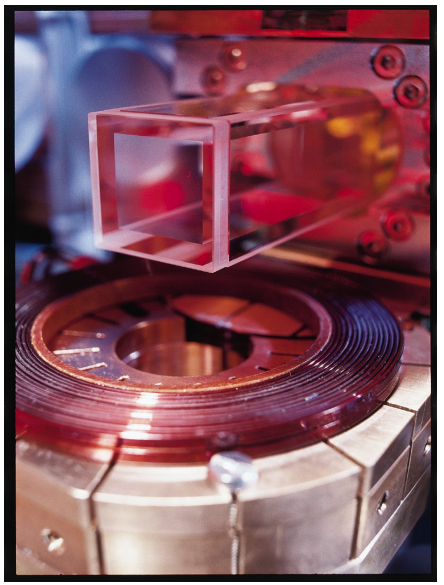

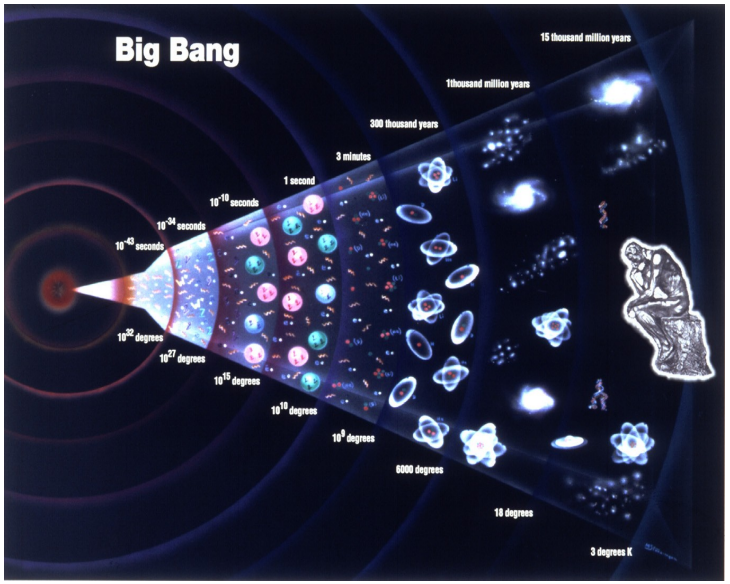

Non-equilibrium initial state

Turbulent flow

Thermal equilibrium

Kolmogorov turbulence

"local" interactions in momentum space

Constant flux in momentum space

Scale invariant transport

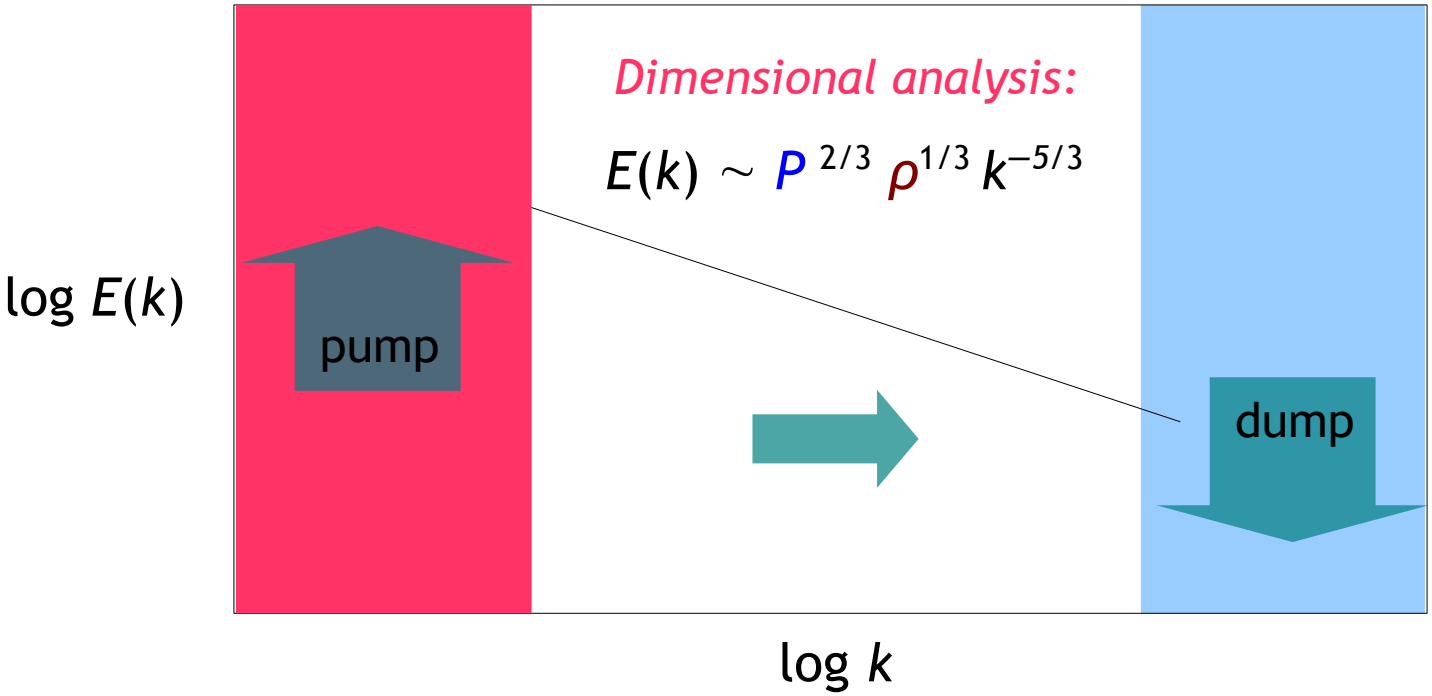

Turbulence in an incompressible fluid

3D:	Radial energy density	E	[kg s^{-2}]
	Radial energy flux	P	[kg m^{-1} s^{-3}]
	Density	ρ	[kg m^{-3}]

Turbulence = scale invariance = universality

Weak wave turbulence

[Micha, Tkachev (2004)]

Power law distributions $n(k) \sim k^{-\kappa}$

Self similar evolution: $n(k,t) \sim t^{-\gamma p} n_0(k t^{-p})$

Fluctuation decay $\langle \varphi^2 \rangle_{conn} \sim t^{-\nu}$

$\dot{n}(k) = I[n(k)]$

Interaction through m-vertex

k-independent stationary flow

Particle cascade
Energy cascade

$$\mu = d(m-2) - 1 - m \qquad \kappa = \frac{d+\mu}{m-1} \qquad \gamma = d \qquad p = \frac{1}{2m+1} \qquad \nu = \frac{2}{2m-1}$$

Universality far from equilibrium

“Natural” nonequilibrium initial conditions

Instability for some momentum band

Amplitude grows

$n \sim \lambda^{-2/3}$

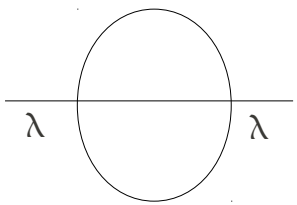

Secondary modes

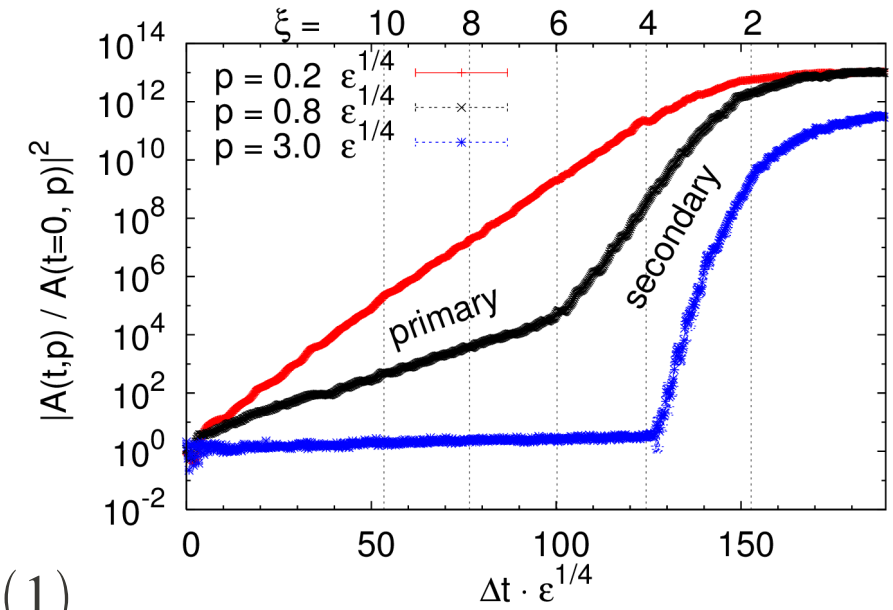

At $n \sim 1/\lambda$ all diagrams become $\sim O(1)$

Non-linear physics; instability saturates

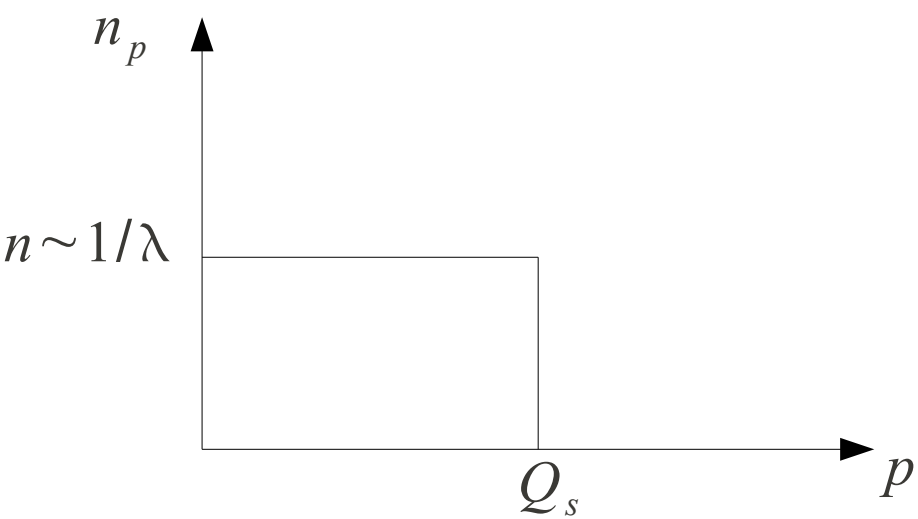

Overoccupation

Tachyonic reheating
Parametric reheating
Weibel instability
CGC

Turbulence and condensation in scalar field theories

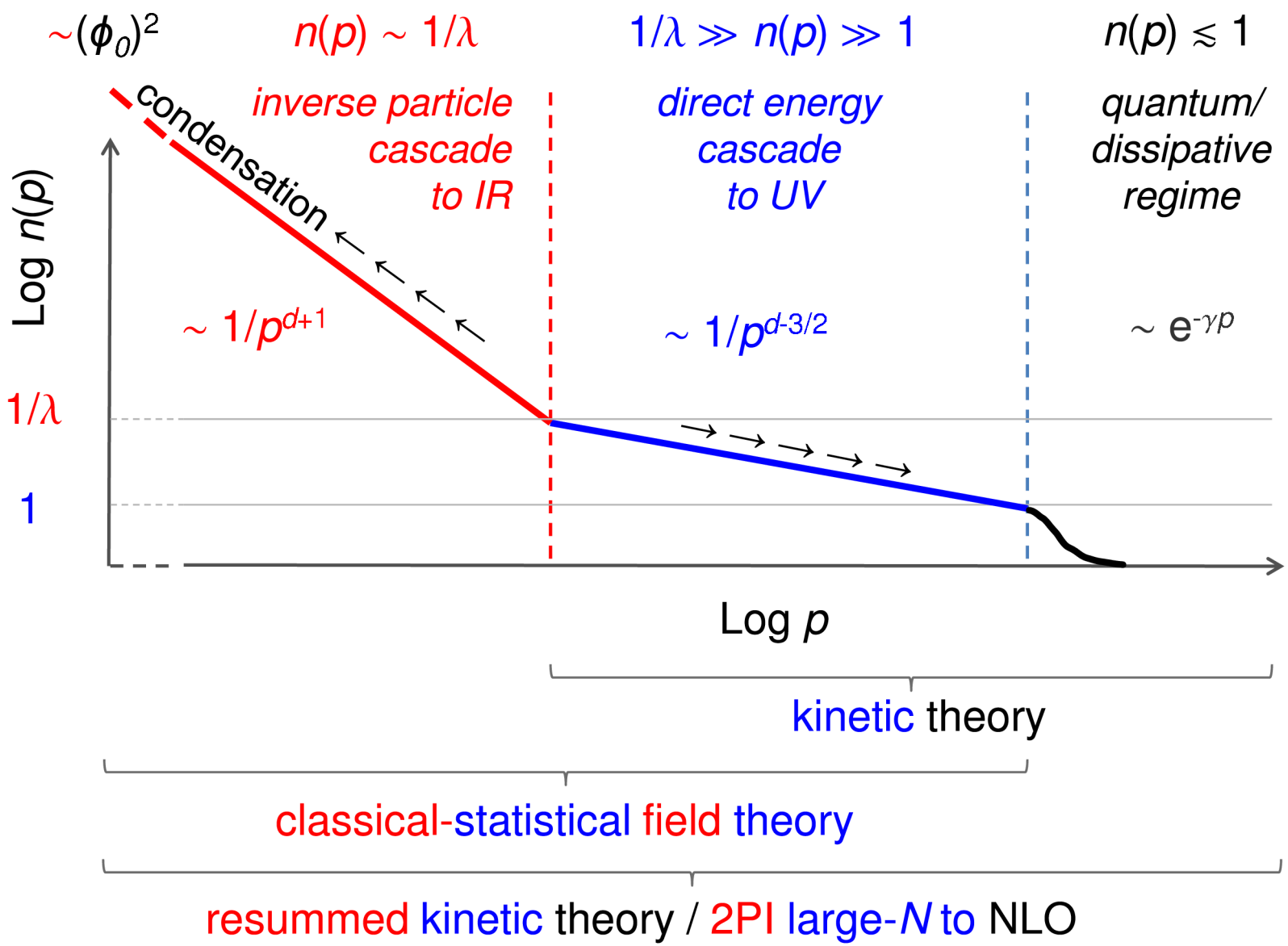

Bose-Einstein Condensation and Thermalization of the Quark Gluon Plasma

[Blaziot et al, 2011]

Initial CGC: $\epsilon_0 \sim \frac{Q_s^4}{\alpha_s}$ $\quad n_0 \sim \frac{Q_s^3}{\alpha_s}$ $\quad \rightarrow \quad n_0 e_0^{-3/4} \sim \alpha_s^{-1/4}$

Thermal eq: $\epsilon_{eq} \sim T^4$ $\quad n_{eq} \sim T^3$ $\quad \rightarrow \quad n_0 e_0^{-3/4} \sim 1$

Elastic processes dominate

Particles pile up in the IR

Overpopulation leads to emergence of condensate

What is a condensate?

In equilibrium: $$N = V \int \frac{d^3 k}{2\pi^3} \frac{1}{e^{\beta(\epsilon_k - \mu)} - 1}$$ Maximum at $\mu = \epsilon_0$

Condensation: $N > N_{max}$

Macroscopic occupation of the zero mode

Condensate fraction $\frac{N_0}{N}$

Particle distribution: $n_k = \delta^3(k) n_0 + n'_k$

In terms of 2point function $F(x, y) = \{\phi(x), \phi(y)\}$

$$n_k = F(k)\omega_k \Rightarrow \quad F(k=0) \sim V$$

condensate $$= \left(\frac{\int d^3 x \phi(x)}{V} \right)^2 = \frac{F(k=0)}{V}$$ Independent of the volume

Non-equilibrium Bose condensation

[Berges, Sexty (2012)]

O(4) massless relativistic scalars

Initial conditions: overpopulation

condensate $= \left\langle \left(\frac{\int d^3x \, \phi_a(x)}{V} \right)^2 \right\rangle_{ens}$

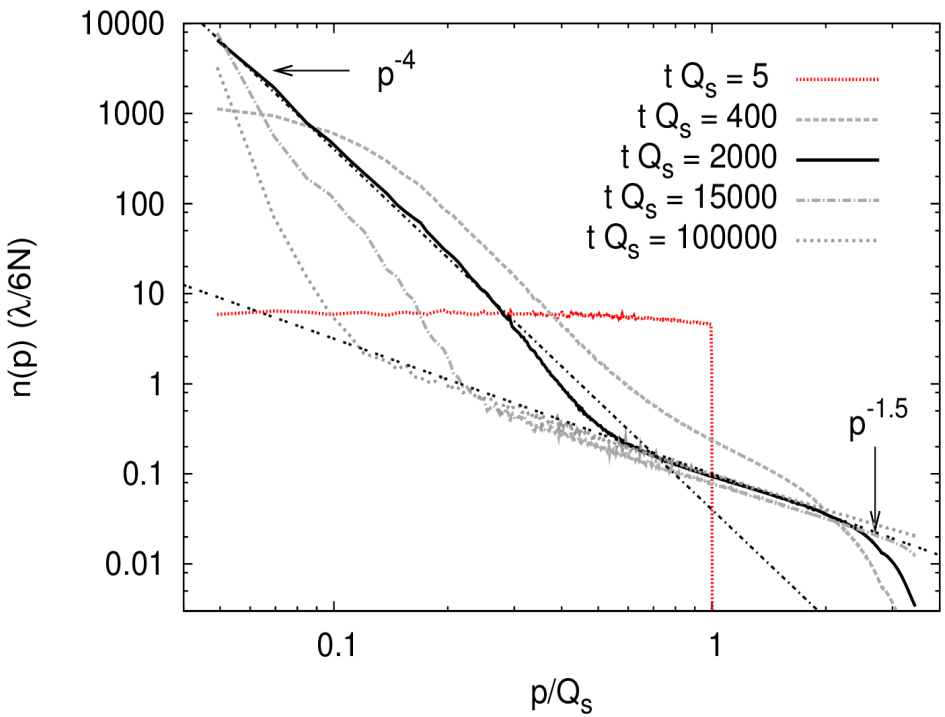

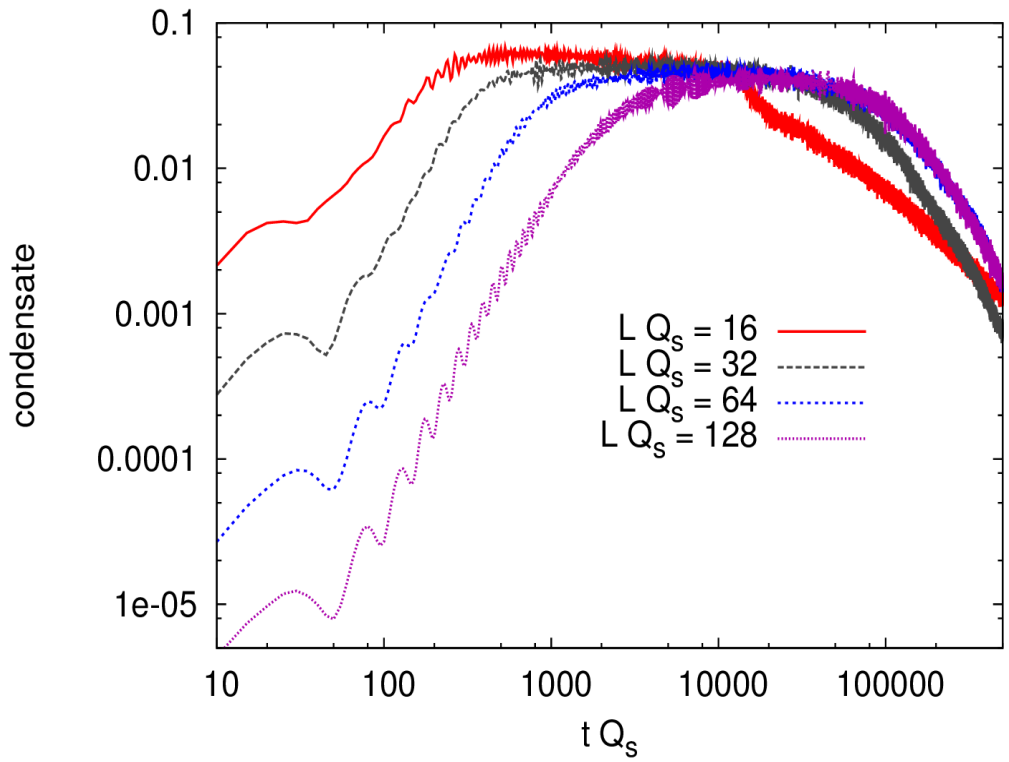

Decay of the condensate

Particle number changing processes suppressed → condensation

↓

decay of condensate

Suppression compared to 2->2 $\sim \frac{1}{N}$

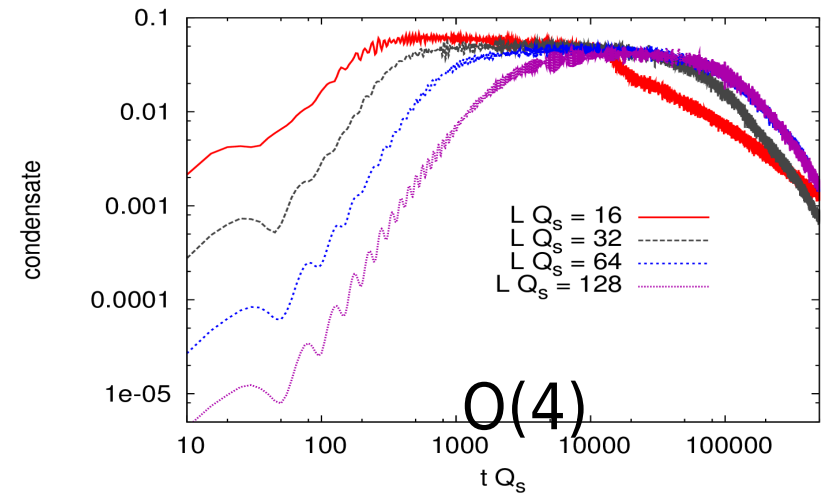

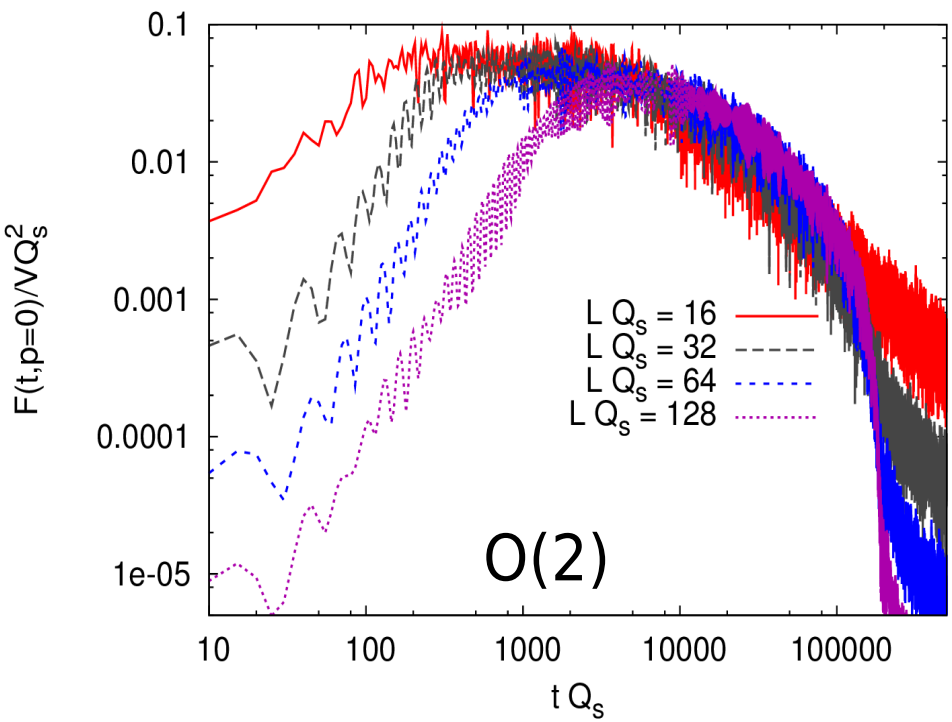

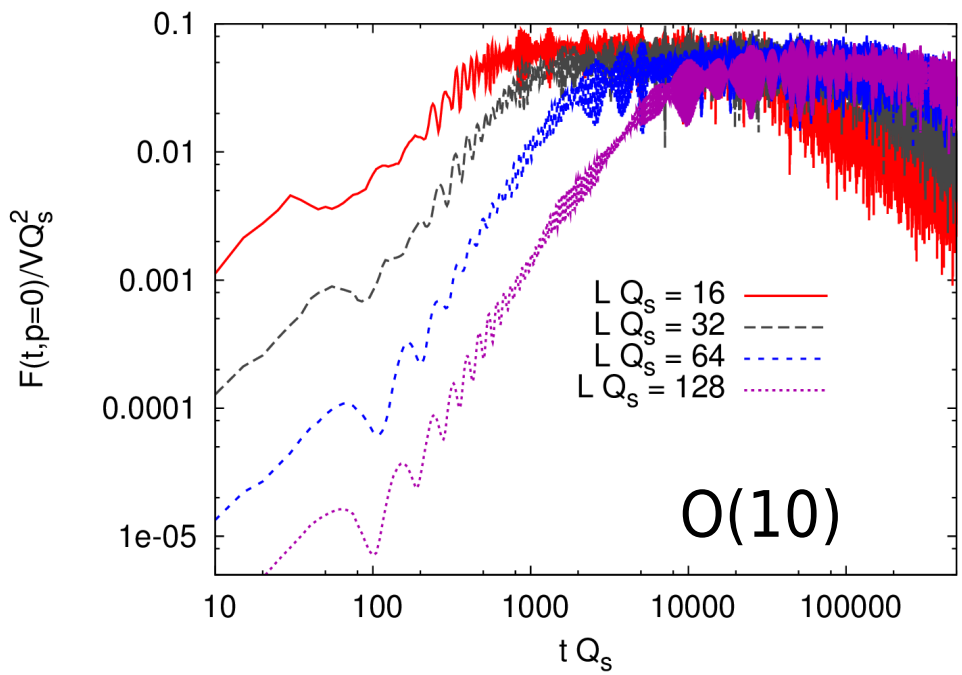

IR resummation – Strong turbulence

1/N resummation: effective vertex

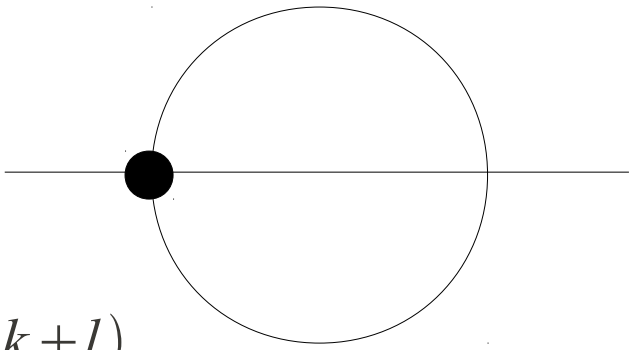

$$\Sigma(p)=\int_{kql}\lambda_{eff}(p+q)G(q)G(k)G(l)\delta^{(4)}(p+q+k+l)$$

$$\lambda_{eff}(p)=\frac{\lambda}{(1+\Pi^R(p))(1+\Pi^A(p))}$$

With one loop bubble:

$$\Pi(p)=\int_q G(p)G(p-q)$$

In the IR: $\Pi(p)\gg 1$

The vertex scales:

$$\lambda_{eff}(s\,p)=s^{2r}\lambda_{eff}(p) \text{ with } r=3+\kappa-d$$

In the UV: $\lambda_{eff}=\lambda$

$$\lambda(sp)=\lambda(p)$$

Strong turbulence in the IR: $\kappa=4$ or 5 (in d=3)

From 2PI to kinetic equations

Using Wigner coordinates

$$F_p(X)=\int d^4 s \exp(-ip_\mu s^\mu) F(X+s/2, X-s/2)$$

Gradient expansion, spatially homogeneous ensemble:

$$\partial_t \rho_p(X)=0$$

$$2 p_0 \partial_t F_p(X)=\Sigma_p^\rho(X) F_p(X)-\Sigma_p^F(X)\rho_p(X)$$

Define:

$$F_p(X)=(n_p(X)+1/2)\rho_p(X)$$

$$n_{eff}(t, \boldsymbol{p})=\int_0^\infty \frac{dp_0}{2\pi} 2 p_0 \rho_p(X) n_p(X)$$

On-shell limit, only 2->2 contributes

$$\partial_t n_{eff}(t, \boldsymbol{p})=\int d\Omega_{2\to 2}\left[(1+n_p)(1+n_l)n_q n_r - n_p n_l (1+n_q)(1+n_r)\right]\lambda_{eff}(p+l)$$

Effective kinetic description also valid at $\lambda n \gtrsim 1$

[Berges, Sexty (2011)]

UV cascade in gauge theories

SU(2) gauge theory
after Weibel instability and isotropisation

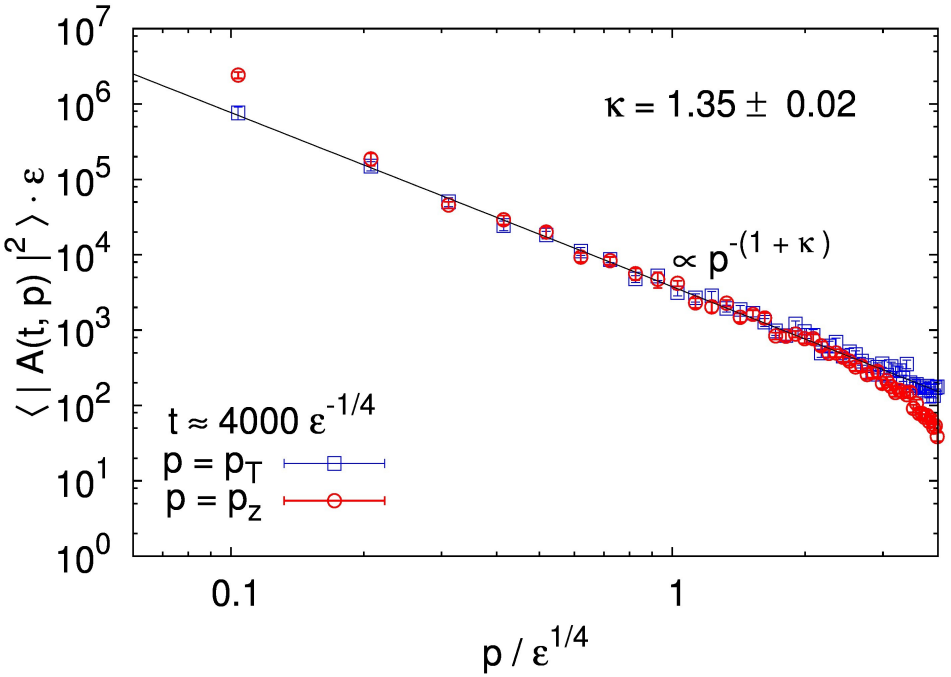

[Berges, Scheffler, Sexty (2009)]

Overpopulation

For short times $\kappa = 3/2$

Indication of condensation?

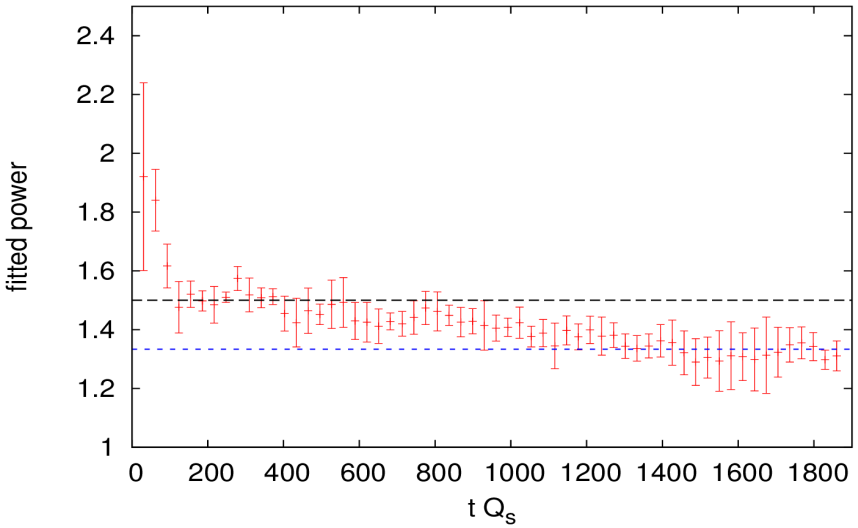

[Berges, Schlichting, Sexty (2012)]

Scalar electrodynamics in 2+1d

[Gasenzer, McLerran, Pawlowski, Sexty(2013)]

Action, couplings, vortices, initial cond

$$S[A_\mu,\phi]=-\int\left[\frac{1}{4}F_{\mu\nu}F^{\mu\nu}+(D_\mu\phi)^*D^\mu\phi+V(\phi)\right]$$

$$D^\mu=\partial^\mu+ieA_\mu \qquad V(\phi)=\frac{1}{2}m^2|\phi|^2+\frac{\lambda}{24}|\phi|^4$$

$$\xi=\frac{6e^2}{\lambda}$$

Ginzburg-Landau parameter

Initial conditions, parameters

1. Tachyonic instability

$$m^2<0,\ \ \phi(t=0)=0,\ \ n_k(t=0)=0 \quad \text{Late times} \rightarrow \text{Higgs phase}$$

2. Overpopulation

$$m^2=0,\quad n_k(t=0)=\frac{C}{\lambda}\Theta(Q-k) \quad \text{Late times} \rightarrow \text{Coulomb phase}$$

How to measure gauge invariant condensate?

Gauge invariant two point function
Screening properties

Condensate in a gauge theory

overpopulation initial cond.

$$\frac{F(p=0)}{V}=\frac{1}{V^2}\int dx\,dy\,G(x,y,t)$$

$$G(x,y,t)=\langle\phi(x,t)\phi^*(y,t)\rangle$$

Naive observable shows no condensation

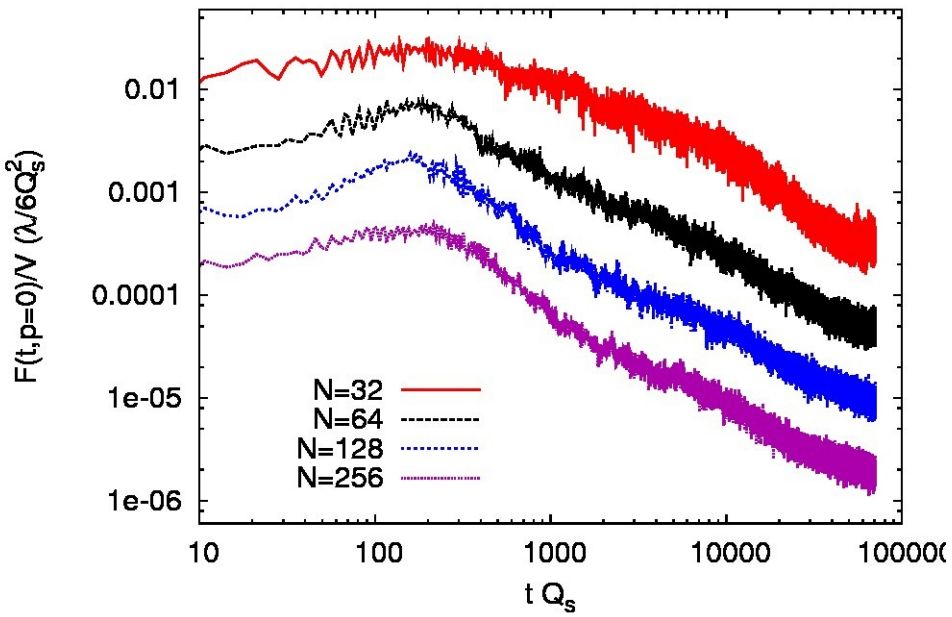

$$\xi=0.09$$

$$\frac{F(p=0)}{V}=\frac{1}{V^2}\int dx\,dy\,G^U(x,y,t)$$

$$G(x,y,t)=\langle\phi(x,t)U(x,y,t)\phi^*(y,t)\rangle$$

$$U(x,y,t)=\exp\left(ie\int_{\gamma(x,y)}dx^\mu A_\mu\right)$$

Condensation is present

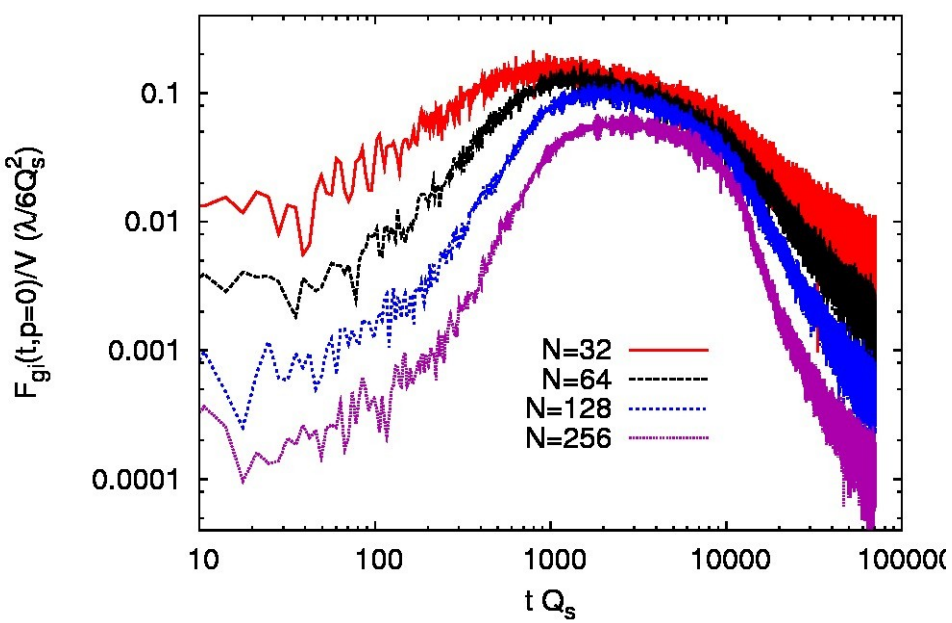

Large gauge coupling

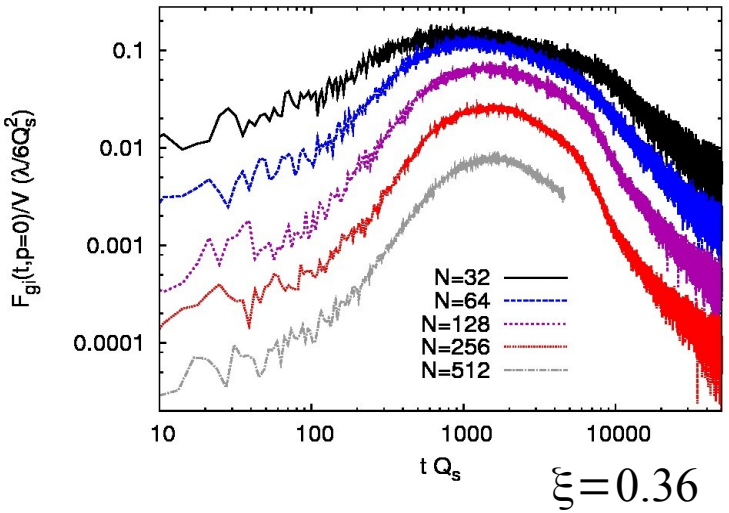

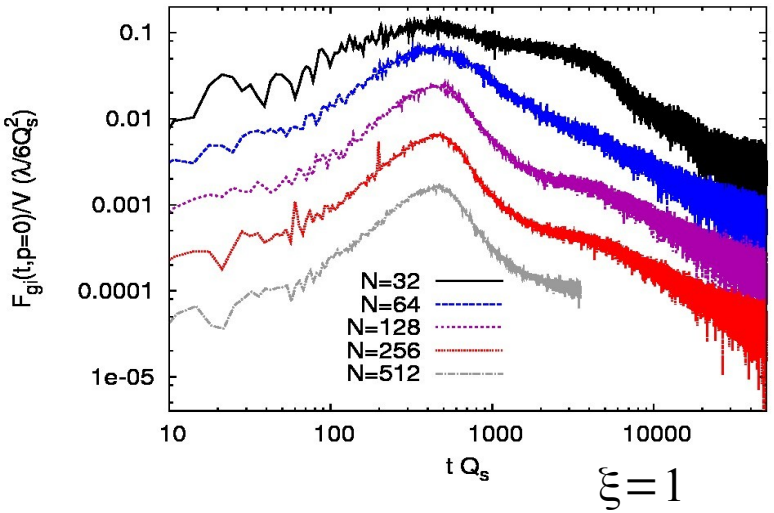

large $\xi \rightarrow$ condensation does not happen

Strong initial grow,
but decay starts earlier

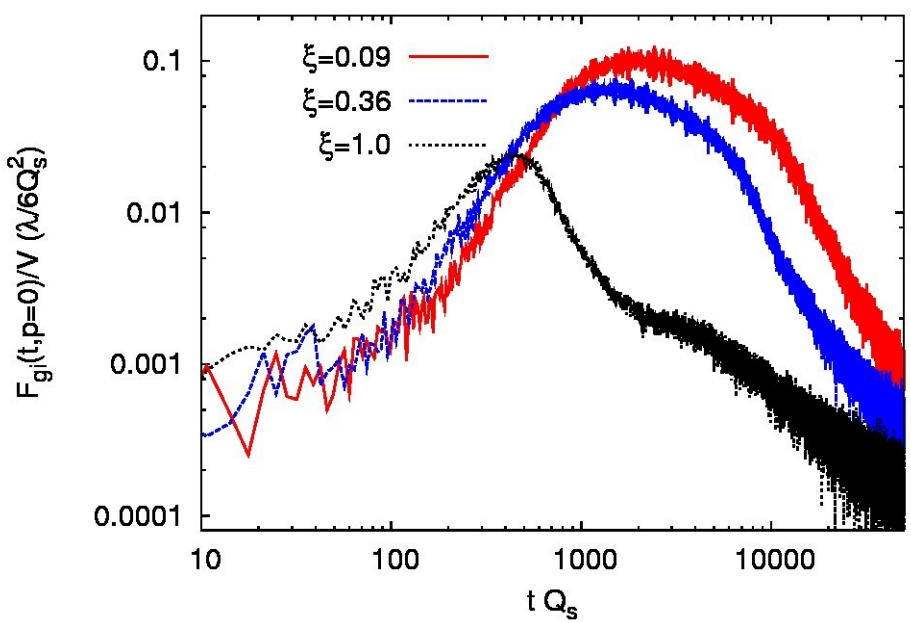

Turbulent behavior

Small gauge coupling:

IR cascade nicely visible
feeds condensation

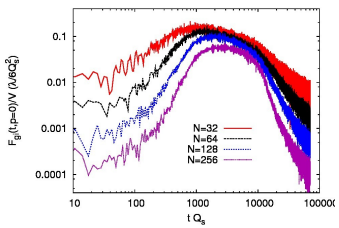

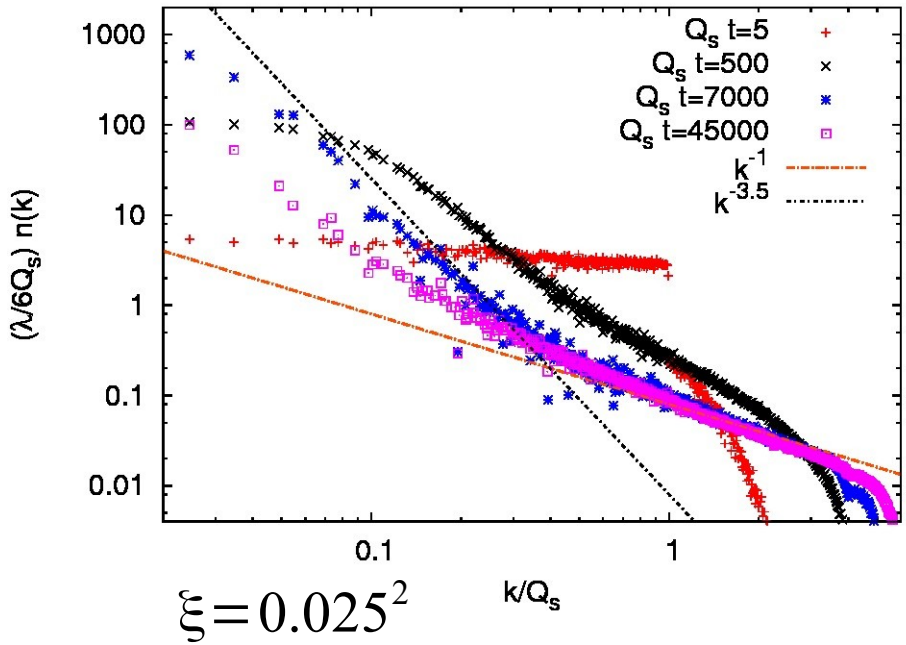

$\xi = 0.025^2$

Large gauge coupling:

IR cascade not present
no condensation

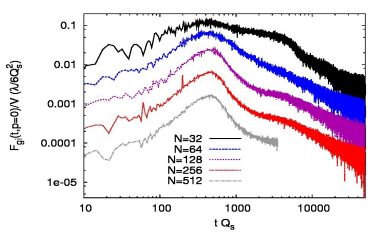

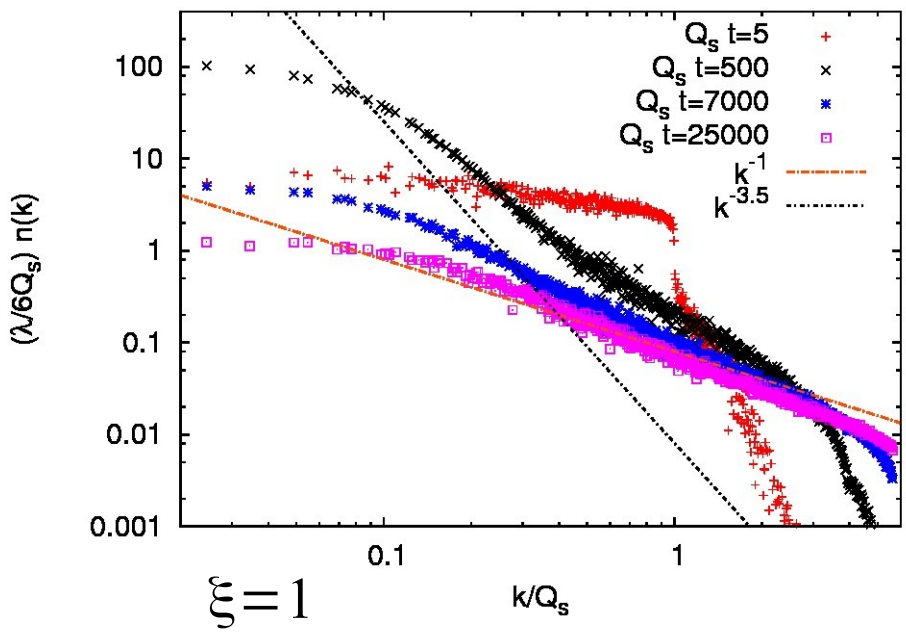

$\xi = 1$

Charge screening

Electric charges inserted into plasma

$$\rho_{ex} = c\,\delta(x - x_1) - c\,\delta(x - x_2)$$

$$t = 0 : E_x(x) \sim 1/x^2 \text{ unscreened}$$

$$t > 0 : E_x(x) \sim \exp(-x/x_0) \text{ screened}$$

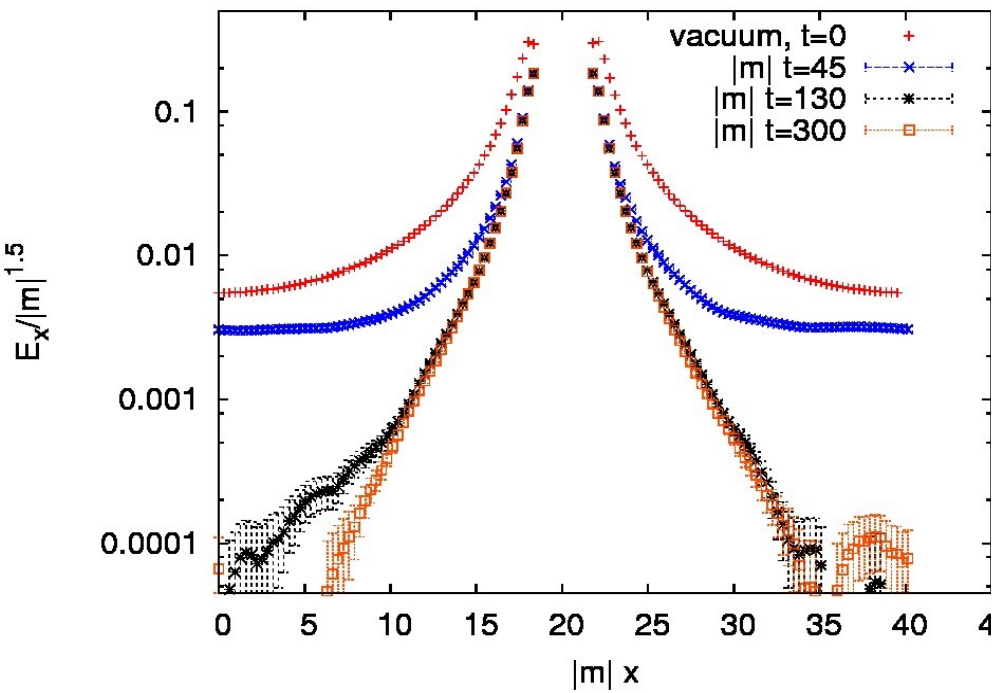

$m^2 < 0, \xi = 1$ Higgs phase

Screening is present

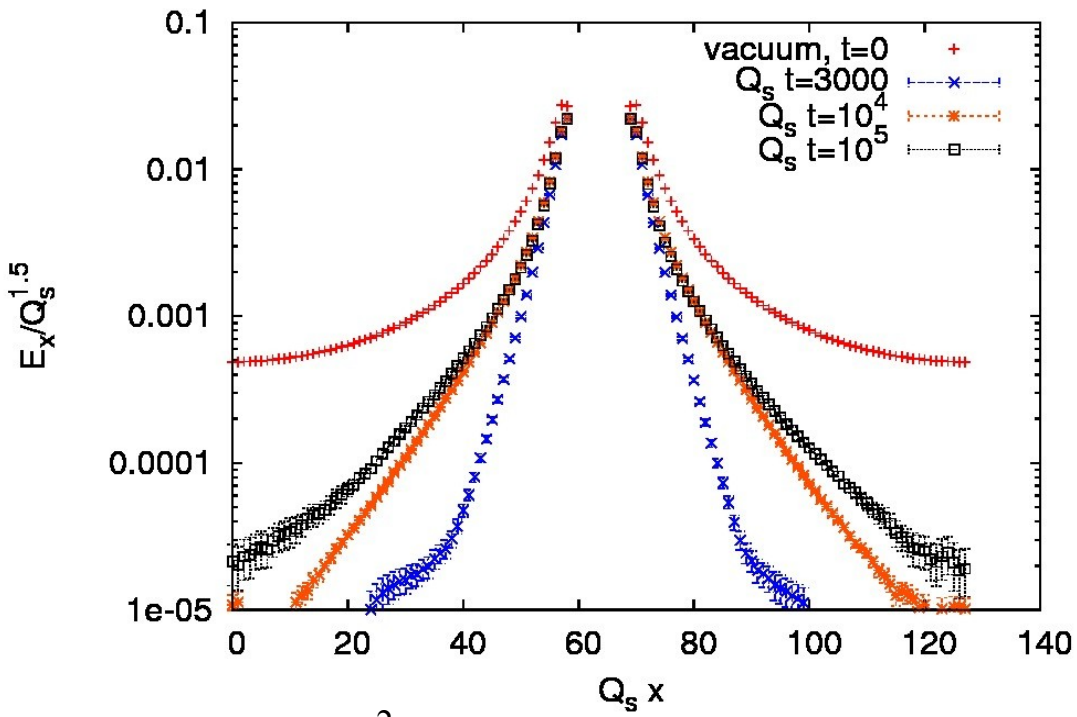

$m^2 = 0, \xi = 1$ overpopulation

Screeining behaviour for intermediate times

Strong scaling and topological defects

[Nowak, Sexty, Gasenzer (2011)]
[Nowak, Schole, Sexty, Gasenzer(2012)]

Non relativistic scalars described by complex field $\Psi(x,t)$

Gross-Pitaevski equation: $$i\partial_t \Psi(x,t) = \left(-\frac{\partial_i^2}{2m} + g|\Psi(x,t)|^2\right)\Psi(x,t)$$

Particle number density: $|\Psi(x)^2|$ nonzero almost everywhere

Topological defects

Zero density

Going around: phase changes by 2π

in 2D: positive and negative vortices
in 3D: vortex lines

Corresponds to discretized vortices (quantum turbulence) In hydrodynamics

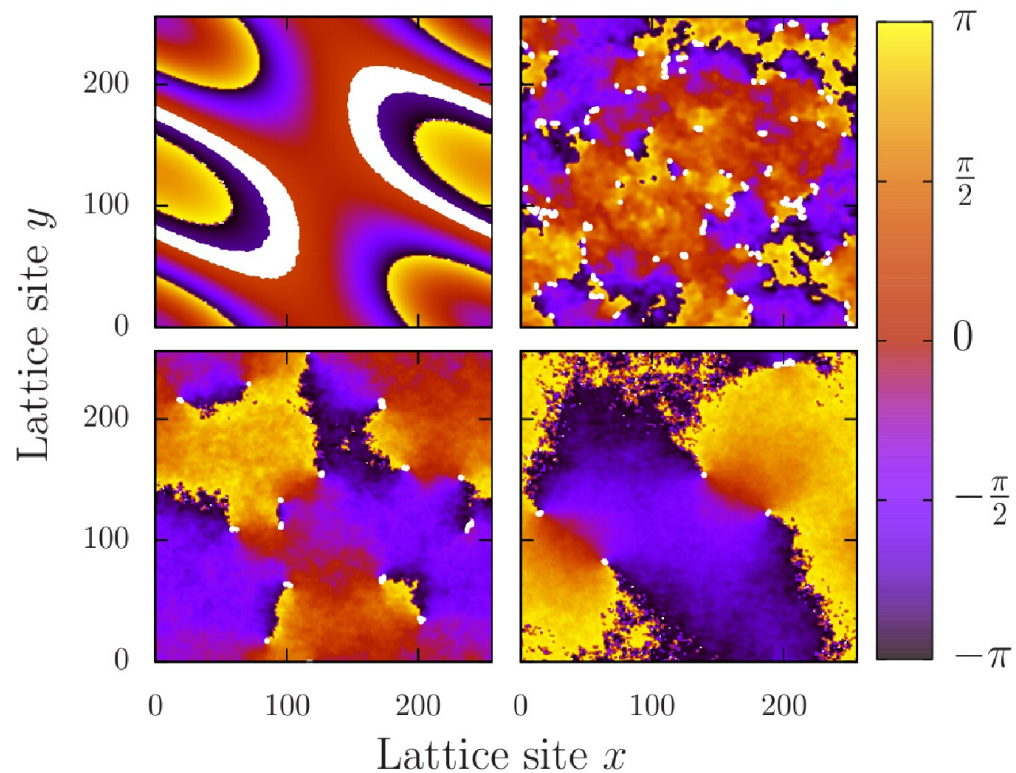

2D

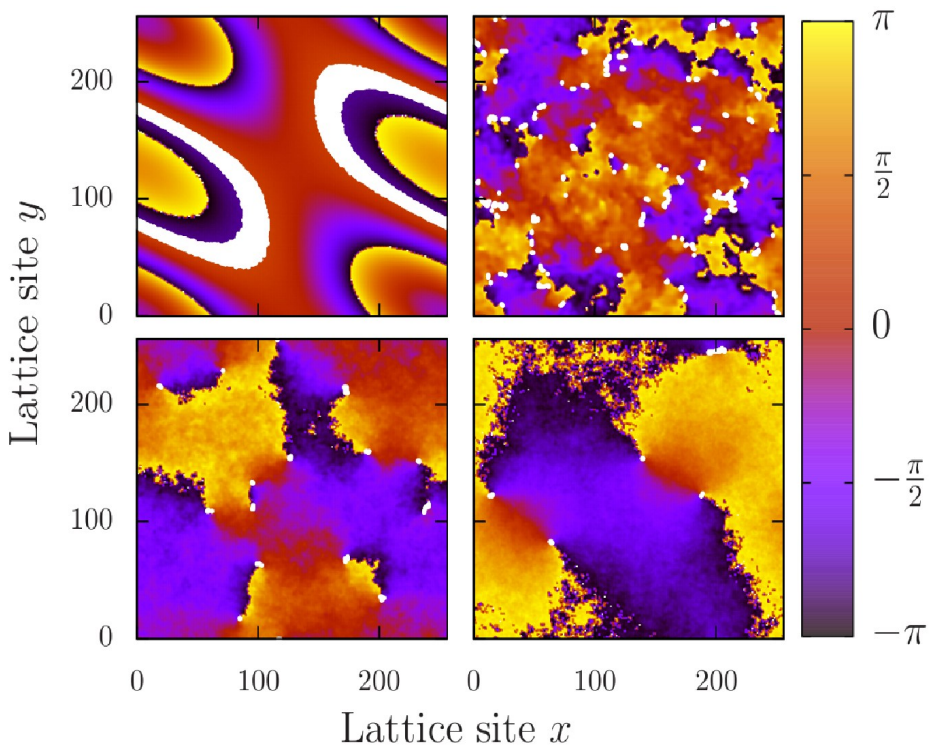

Phase distribution

3D

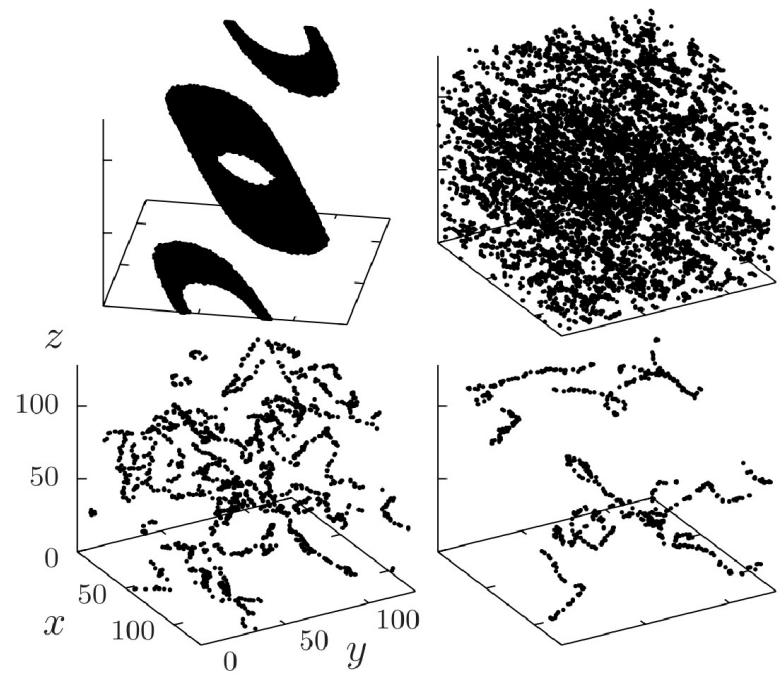

Points with $|\Psi(x)^2| < 0.05\rho$

In the ensemble average

Homogeneous state

Two point function

strong power law exponent

In typical configurations

topological defects present

Physics of strong turbulence ⟷ topological defects

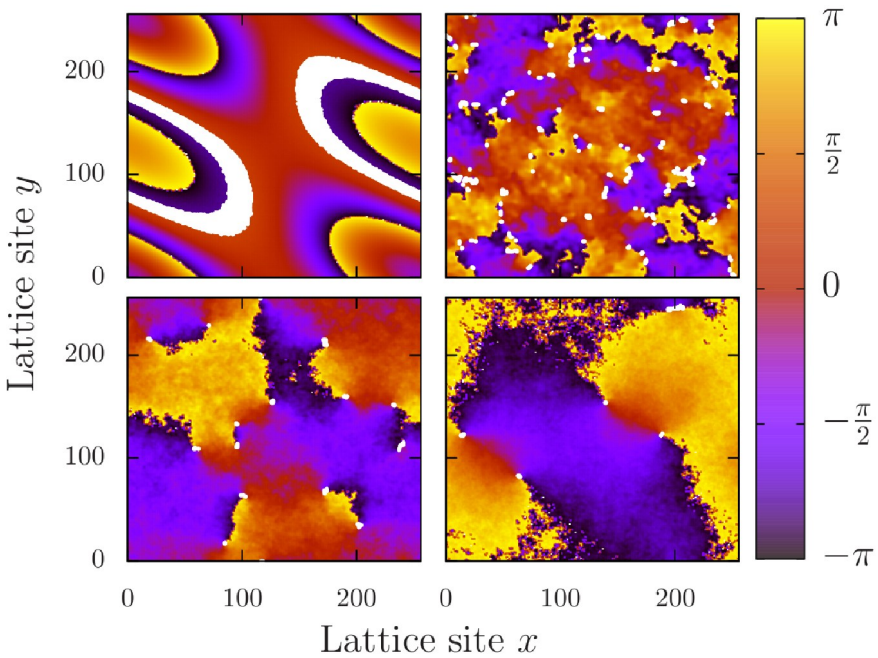

Particle spectrum

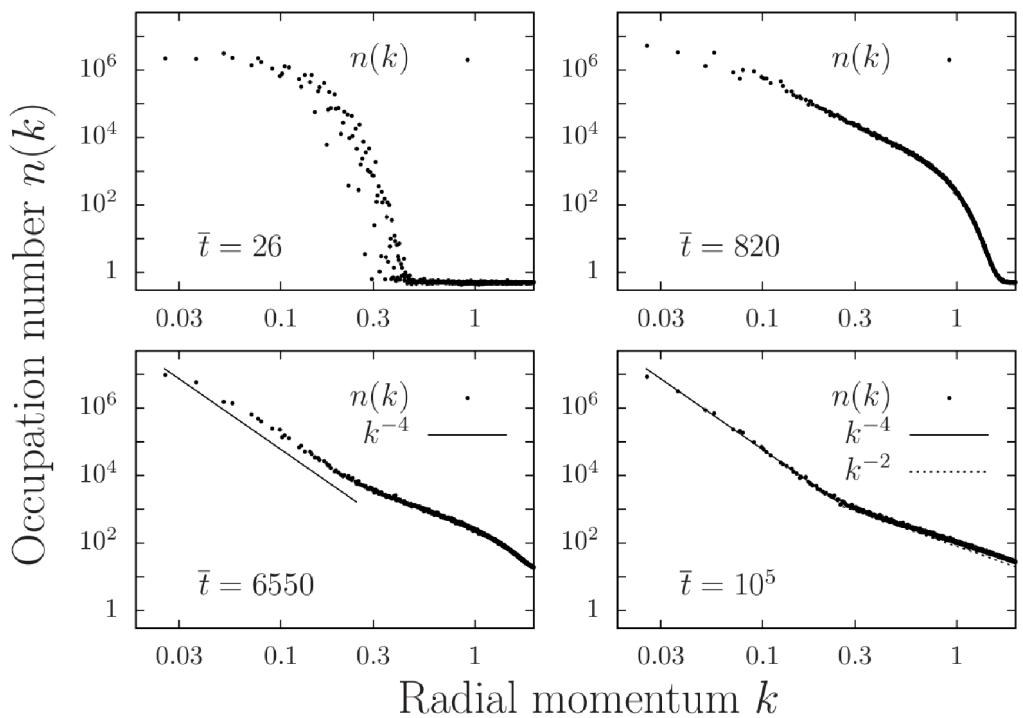

Charge Separation in Reheating

[Gasenzer, Nowak, Sexty (2012)]

Parametric reheating scenario for O(2) scalars

Using conformal time, rescalings, zero bare mass : $\left(\partial_t^2 - \Delta + \Phi^2\right)\Phi_a = 0$

Affleck-Dine scenario of baryogenesis

First in 2D for better visualization

Spatial dependence of field length

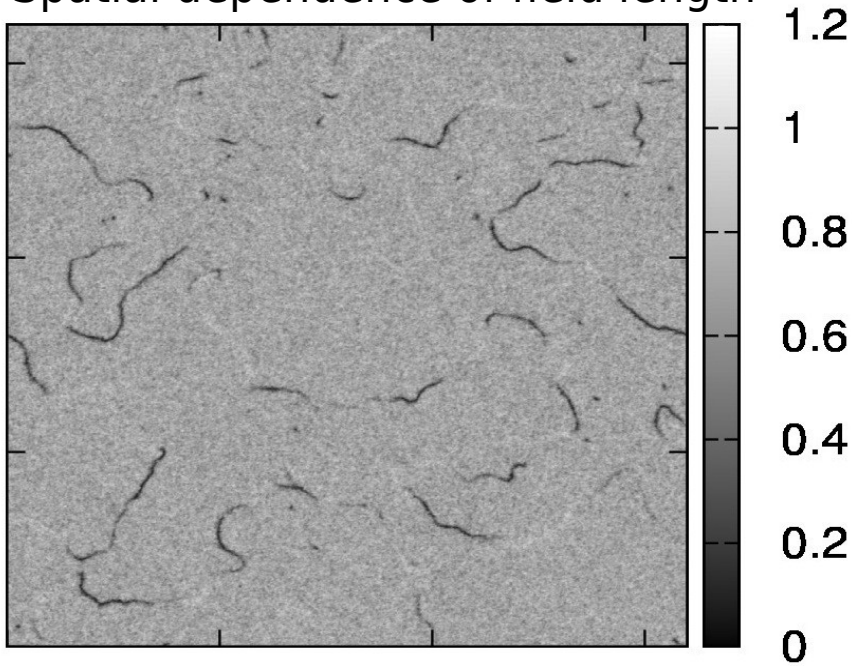

t=9000

Particle spectrum

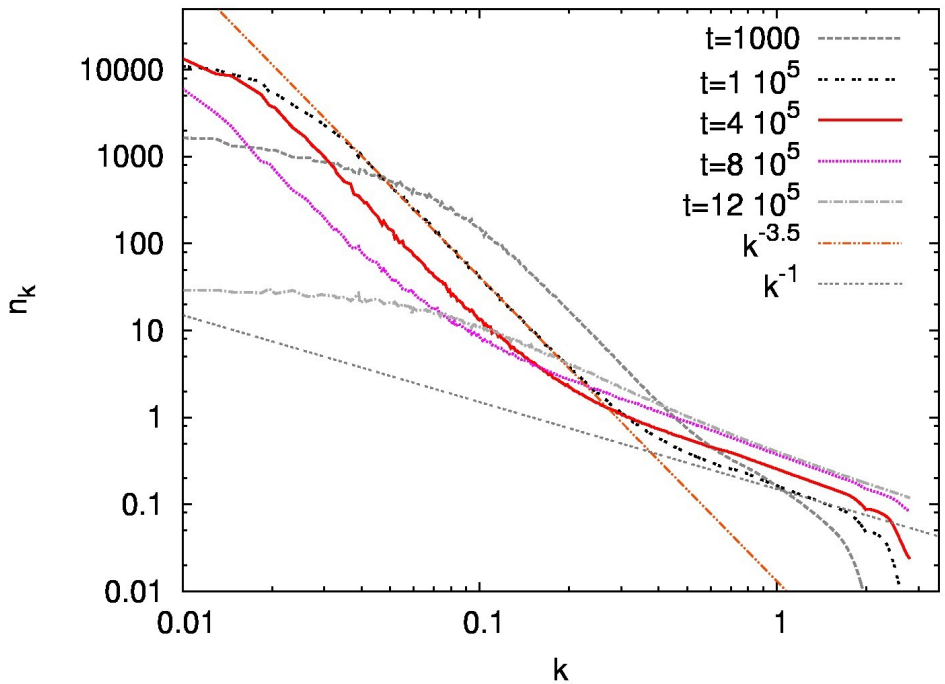

“Worms” are at the boundary of differently charged regions

No charge
field oscillates through zero
boundary is lit up periodically

Field length

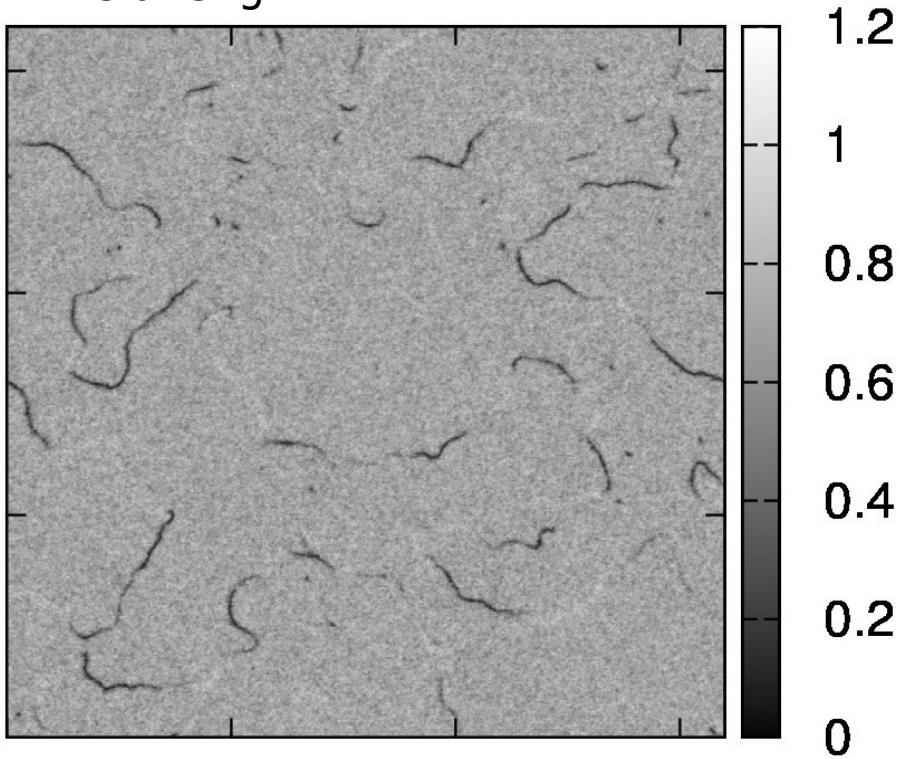

Charge density

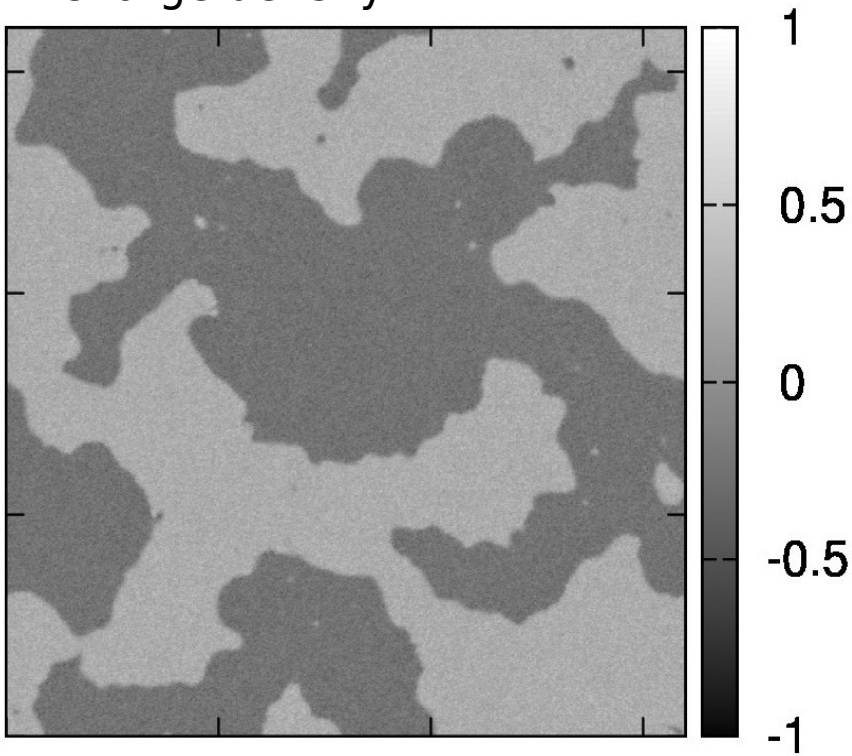

Charge separation appears without symmetry breaking

Symmetry breaking might induce net charge creation before equilibration

$m^2 > 0$ No phase transition

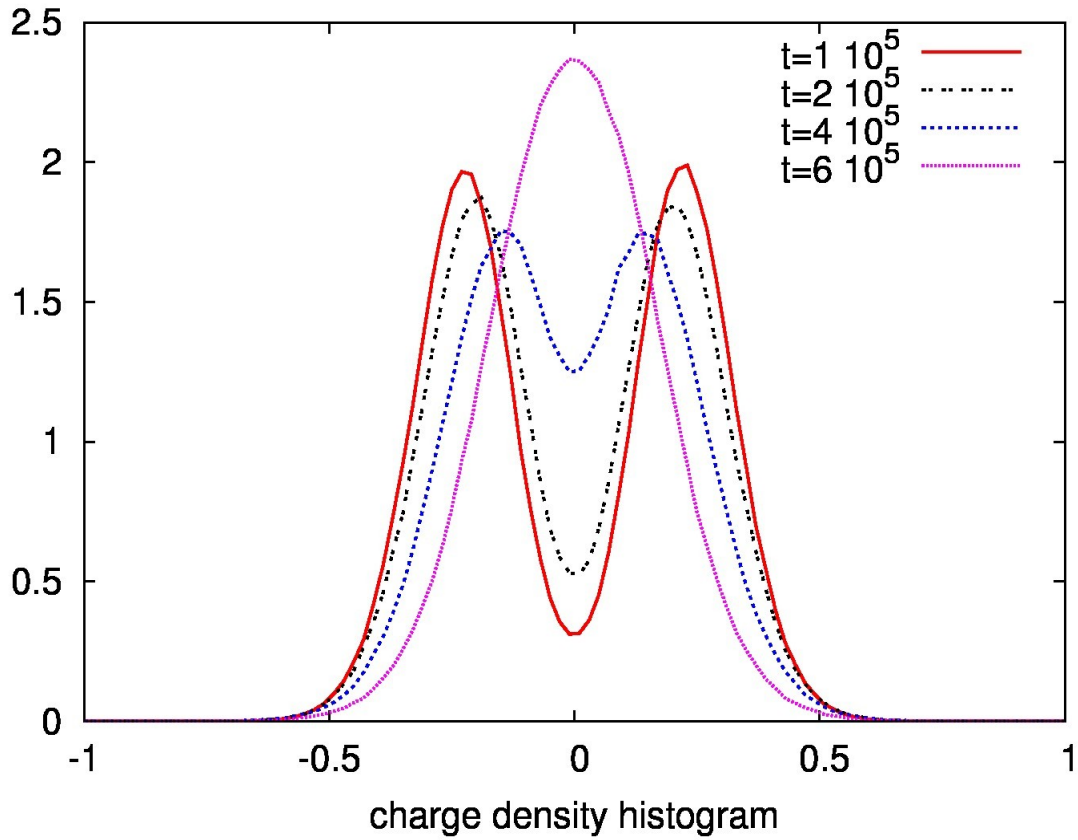

Gauged U(1) Higgs

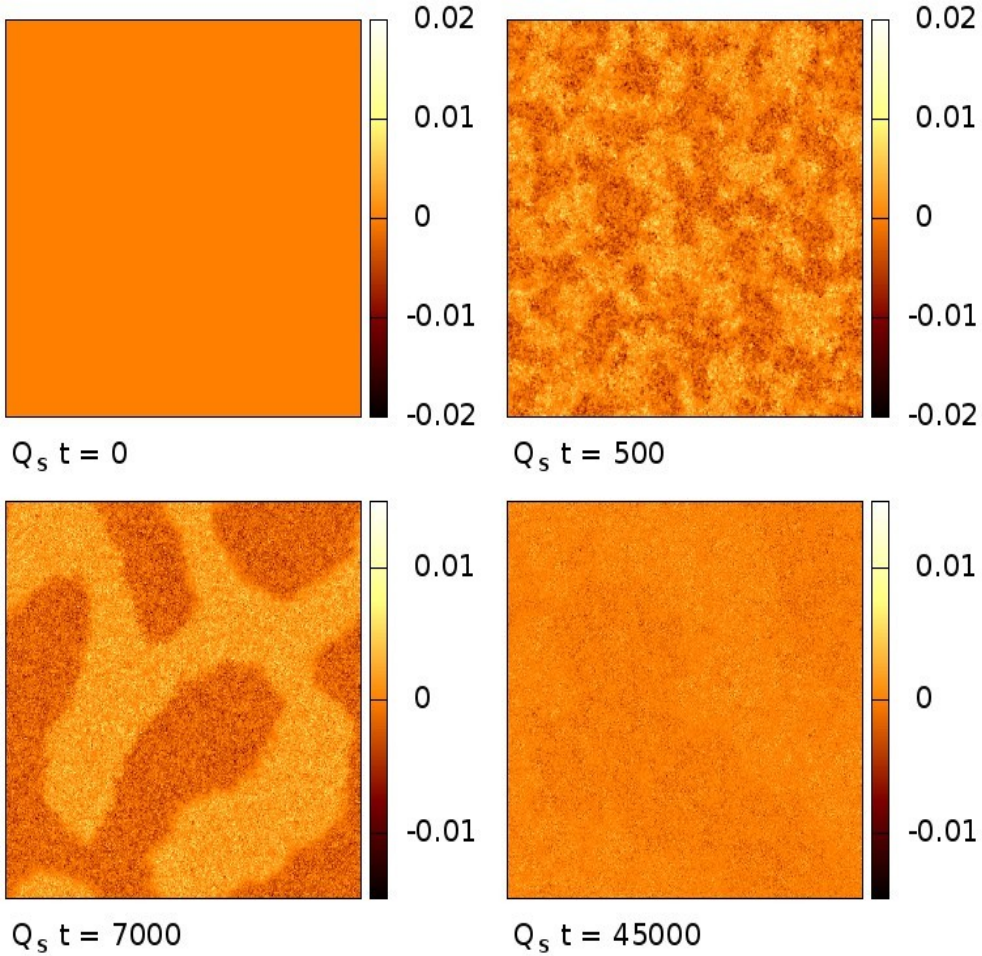

Charge density

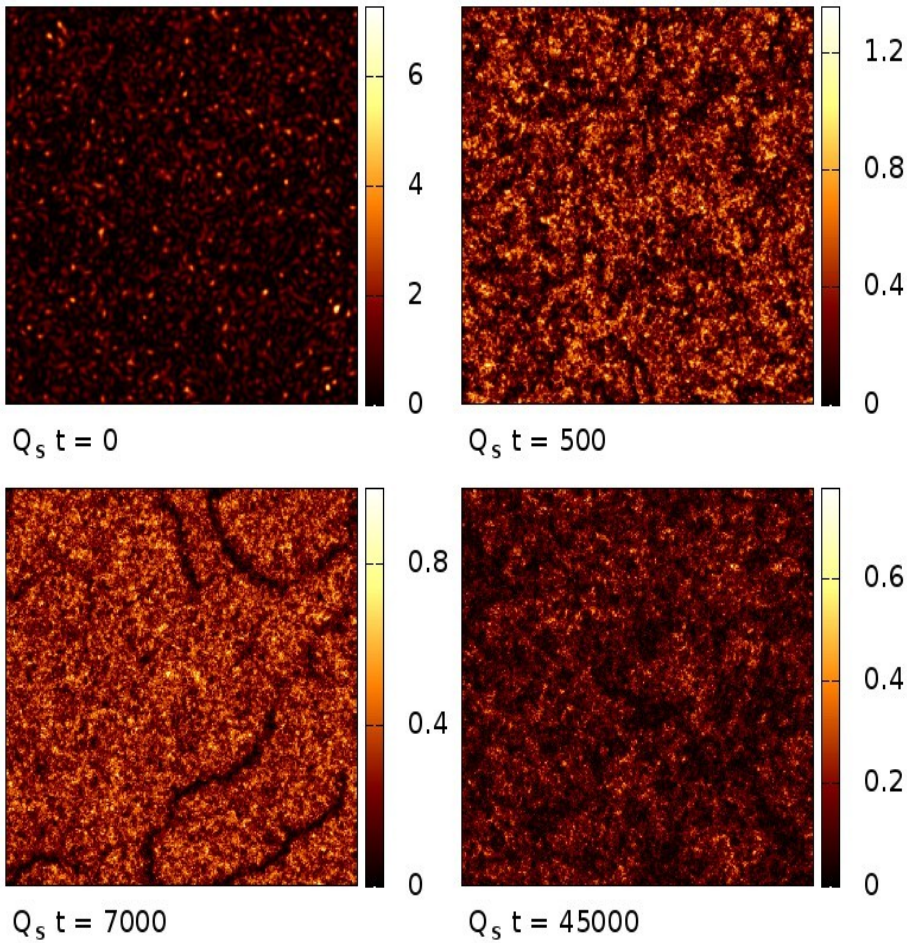

Field modulus

Conclusions

Scalar case well understood

Turbulence, Universal behavoiur

Dual cascade

Condensation

Weak and strong wave exponents
from kinetic theory (with resummation)

Gauge theory

U(1) Gauge-Higgs model: condensation for small ξ

Gauge invariant condensate, screening behaviour

Connection with topological excitations

QCD strings and equilibration in high multiplicity pA,pp collisions

Edward Shuryak
Stony Brook

3. Early stages of high multiplicity pA collisions

Tigran Kalaydzhyan and Edward Shuryak

2. Self-interacting QCD strings and String Balls
Tigran Kalaydzhyan, Edward Shuryak. Feb 28, 2014.
e-Print: **arXiv:1402.7363**

New Regimes of Stringy (Holographic) Pomeron and High Multiplicity pp and pA Collisions
Edward Shuryak, Ismail Zahed Nov 4, 2013. 24 pp.
e-Print: **arXiv:1311.0836**

why strings?

- using pQCD (quarks and gluons) it is very hard to explain the QCD phase transition to confinement
- using strings it is very easy: it is due to their exponentially growing density of states => the Hagedorn phenomenon near T_H:
- condensation of ``thermal scalar" mode => deconfined phase
- string balls prepare small size and large entropy of black holes

outline

- min.bias pp, pA: Pomerons, strings, spaghetti, Lund model
- QCD strings and their interaction
- spaghetti collapse
- (fundamental) string balls
- QCD string balls
- holographic Pomeron and its phases
- stringballs in high multiplicity pp

short history of QCD strings

- **1960's: Regge phenomenology, Veneziano amplitude. Strings have exponentially growing density of states N(E)**
- **1970's Polyakov,Susskind => Hagedorn phenomenon near deconfinement**
- **1980's: Lund model (now Pythia,Hijing): string stretching and breaking**
- **1990-now lattice studies. Dual Abrikosov flux tubes. (Very few) papers on string interaction**
- **2013 Zahed et al: holoraphic Pomeron and its regimes**

the simplest multi-string state: the spaghetti

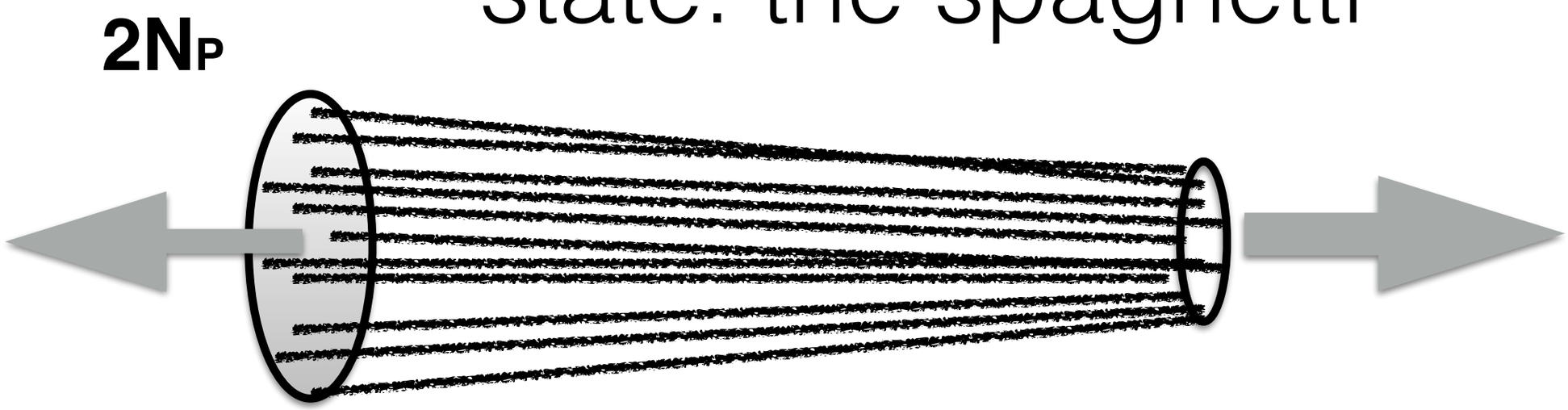

N(strings)=2N(Pomerons)

in small multiplicity bins strings are broken independently (the Lund model),

but one should obviously think about their interaction if their number grows

intro into pA collisions

Multiplicity distribution from CMS, pPb

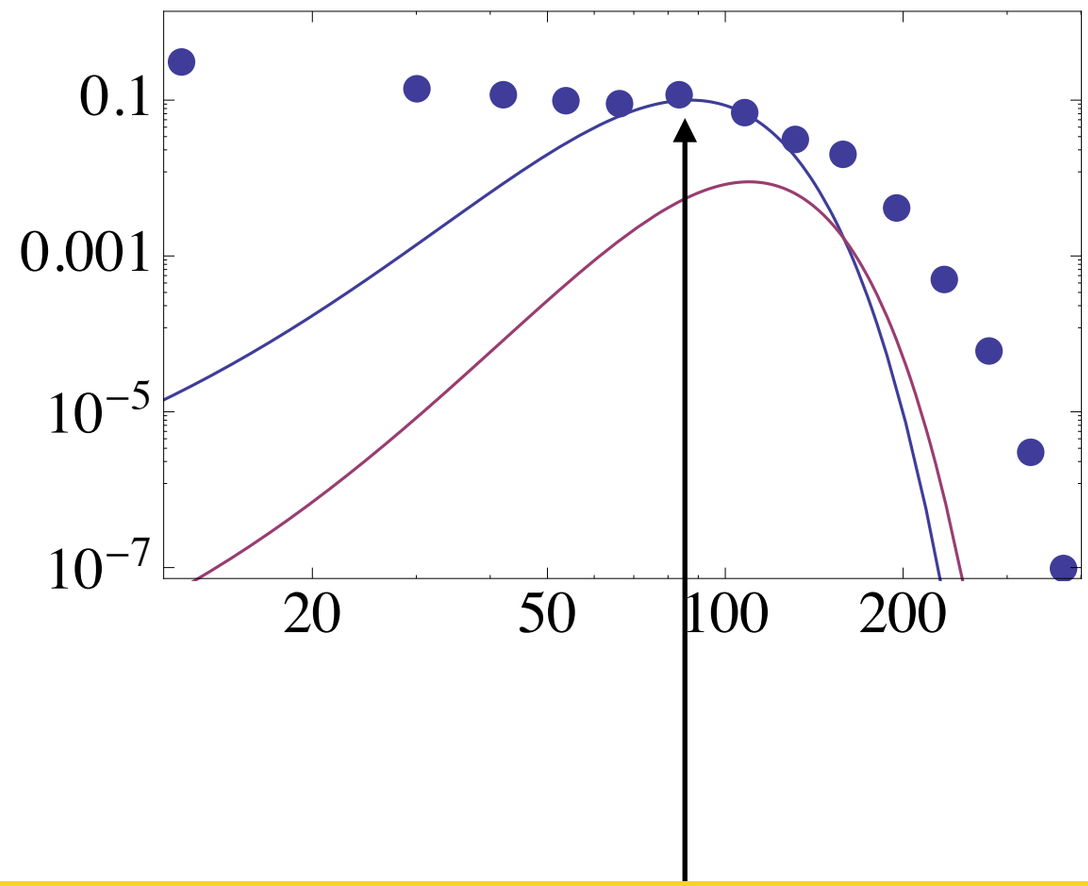

maximal mean number of participants is along the Pb diameter, about 16

blue line is Poisson with <Np>=16
red with <Np>=20
geometry — columns with smaller Np - explains well the left side (Bozek 2011)

what explains the large tail to the right?
not the "wounded nuclei model" in w
Nch/Np=const (= independent string fragmentation, Lund model)

are the two sides any different?

one needs to explain extra multiplicity, and — more importantly — appearance of radial, elliptic and triangular flows

CMS pPb: v2 from 2 and 4-particles

v_2 in pPb and PbPb

PbPb **pPb**

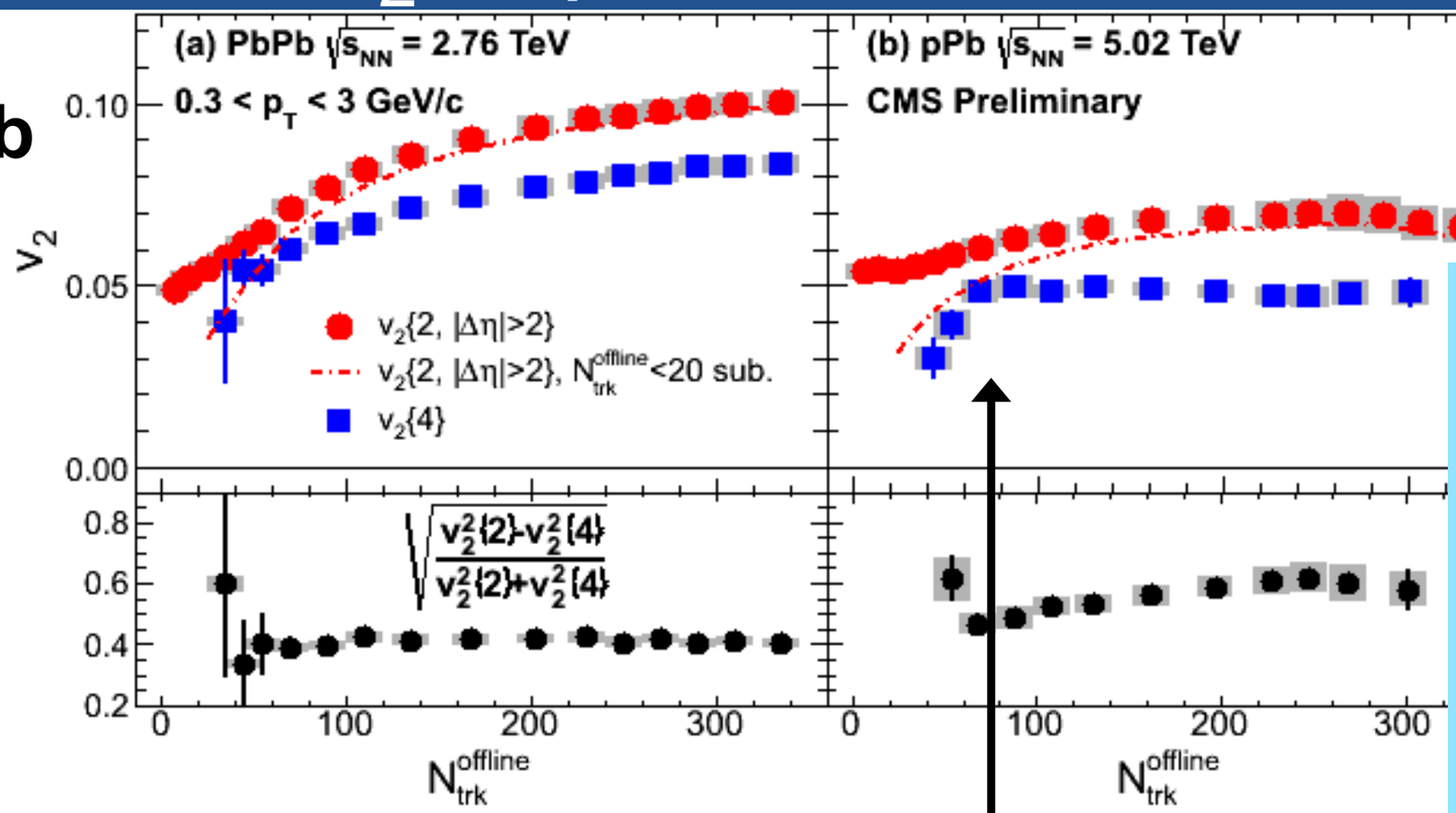

v_2 smaller in pPb than PbPb

$v_2\{4\}$ drops at low multiplicity

$$v_2\{2\} = \sqrt{< v_2 >^2 + \sigma_{v_2}^2}$$

$$v_2\{4\} = \sqrt{< v_2 >^2 - \sigma_{v_2}^2}$$

Which is the real end of hydro!

4 particle one is a clear sign of collectivity

it has clear onset at multiplcity of around 80

in AA fluctuations are too large

PHYSICAL REVIEW C **88**, 044915 (2013)

High-multiplicity *pp* and *pA* collisions: Hydrodynamics at its edge

Edward Shuryak and Ismail Zahed

We predicted the radial flow in pp/pA to be even stronger than in central AA

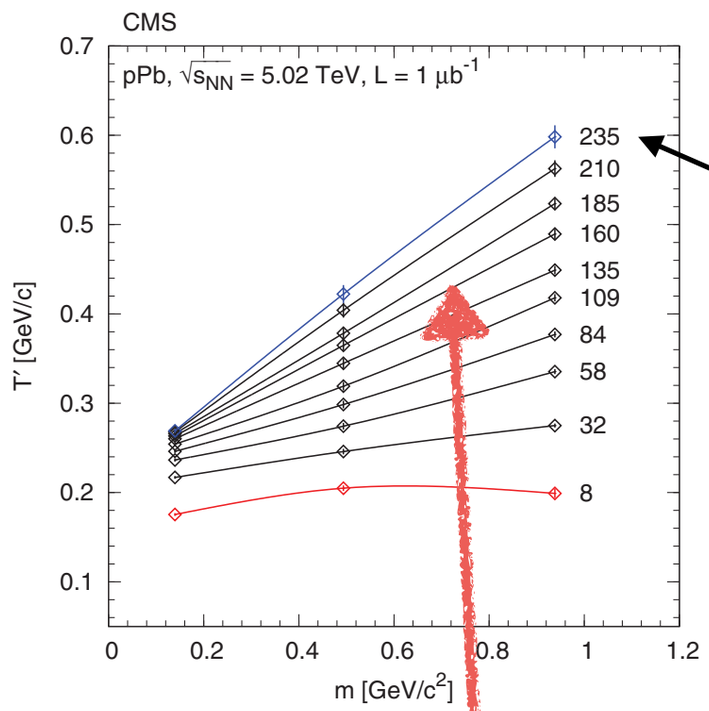

FIG. 8. (Color online) The slopes of the $m_\perp$ distribution T' (GeV) as a function of the particle mass, from [13]. The numbers on the right

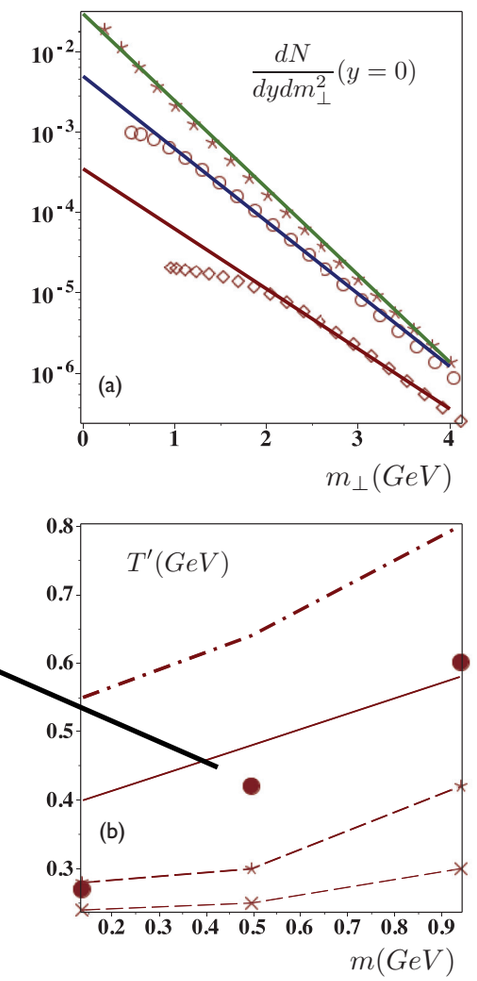

FIG. 9. (Color online) (a) A sample of spectra calculated for π, K, p, top-to-bottom, versus $m_\perp$ (GeV), together with fitted exponents.(b) Comparison of the experimental slopes $T'(m)$ versus the particle mass m (GeV). The solid circles are from the highest multiplicity bin data of Fig. 8, compared to the theoretical predictions. The solid and dash-dotted lines are our calculations for freeze-out temperatures $T_f = 0.17, 0.12$ GeV, respectively. The asterisk-marked dashed lines are for Epos LHC model, diagonal crosses on the dashed line are for AMTP model.

Not the Mt scaling at large Ntr => not a large Qs but a collective flow: p=m v

1 flux tube on the lattice

The dual superconductor: Higgs=monopole condesate

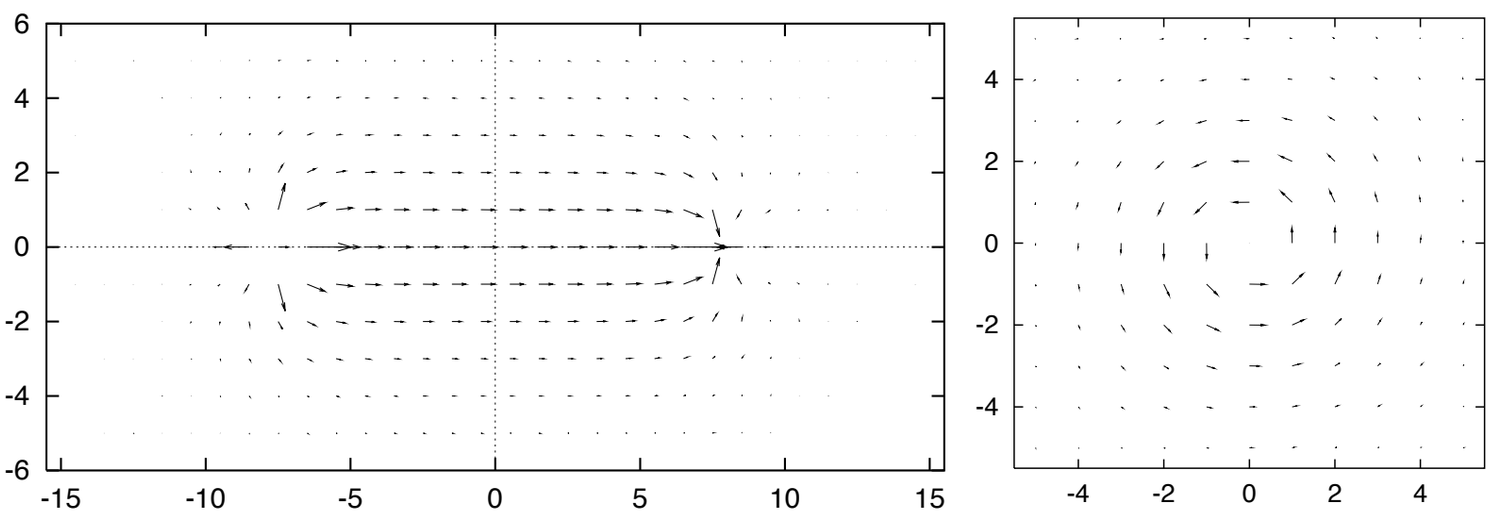

Fig. 7. Electric field **E** and magnetic super current **k** between two static sources.

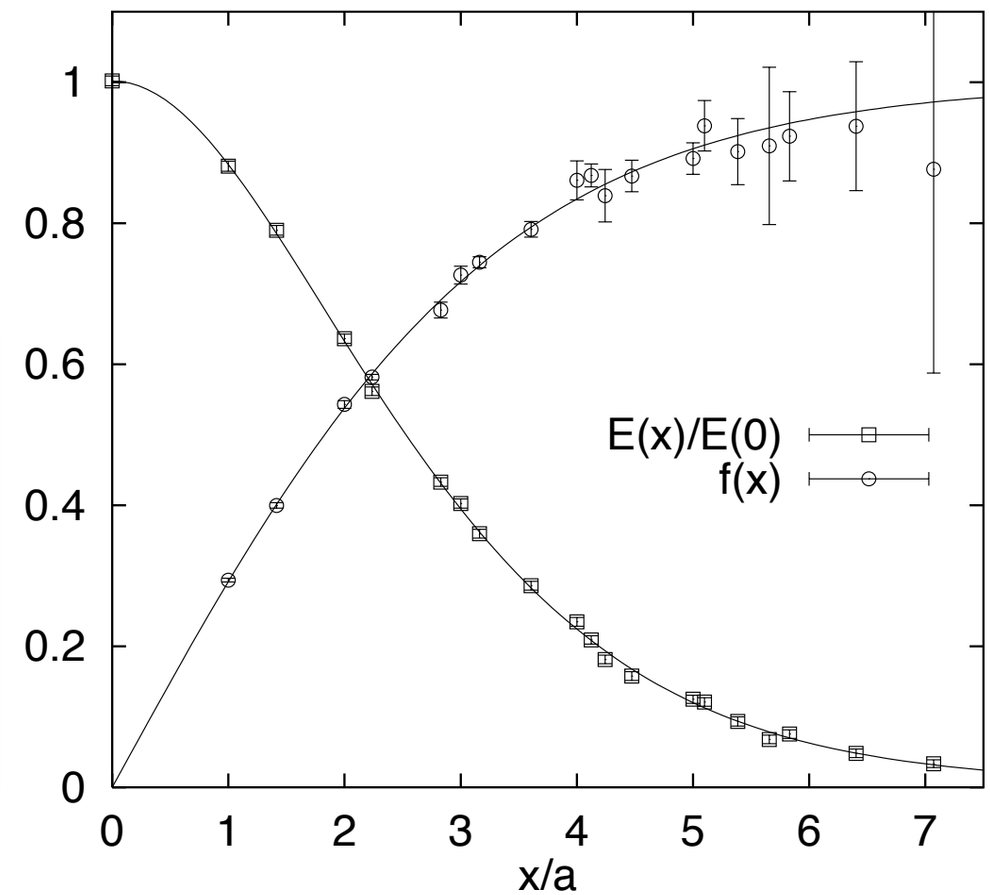

G. S. Bali, hep-ph/9809351.

Interaction strongly grows near Tc

2 flux tubes on the lattice

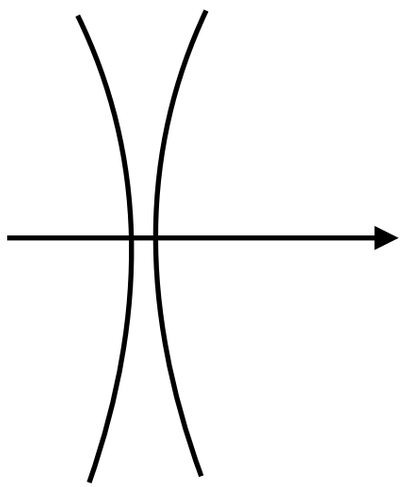

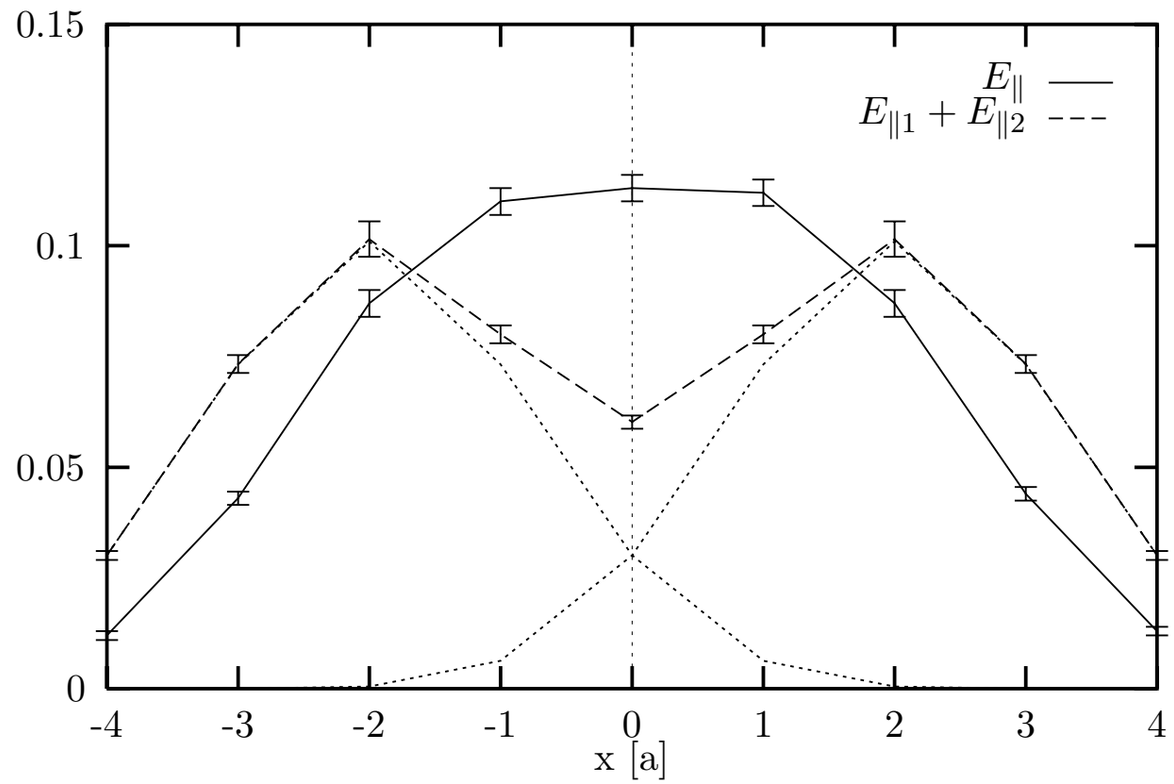

Figure 12: Longitudinal electric field profile of two interacting flux tubes in the symmetry plane ($E_{\|}$, solid line). The length of flux tubes is $d = 22a$, the transverse distance of equal charges is $4a$. For comparison, the dotted lines show the results for single flux tubes at $x = -2a$ and $x = +2a$, and the dashed line corresponds to the superposition $E_{\|1} + E_{\|2}$ of these two non-interacting flux tubes.

M. Zach, M. Faber and P. Skala, Nucl. Phys. B 529, 505 (1998) [hep-lat/9709017].

SELF-INTERACTING STRINGS

The lightest $J^{PC} = 0^{++}$ σ meson, or $f_0(500)$ in the PDG13 listings. Its mass $m_\sigma = 0.4 - 0.55$ GeV is comparable to its width $\Gamma_\sigma = 0.4 - 0.7$ GeV:

Sigma mass is expected to decrease near Tc as it meets its chiral partner, the pion

It is basically responsible for binding nuclei

$$V_{NN}(r) = \frac{g^2_{\sigma NN}}{4\pi} \frac{\exp(-m_\sigma r)}{r}$$

$$g_N^{max} = \frac{g^2_{\sigma NN}}{4\pi m_N^2} \approx \frac{357}{4\pi} \frac{m_\sigma^2}{m_N^4} \approx 13\,\mathrm{GeV}^{-2}$$

For non-nuclear physicists it may be worth reminding at this point that in NN case it is nearly completely cancelled by the repulsive vector ω exchanges, coupled to the nucleon baryon number. We also remind that this sigma term can be found in phenomenological potentials such as Paris and Bonn ones, or the so-called Walecka model of nuclear forces. More recent treatment uses a more accurate "correlated $\pi\pi$" exchange to account for it.

For non-string theorists it may be worth reminding that the fundamental strings and D-branes have also certain charges and repulsive vector forces, canceling attractive ones and making them "BPS-protected". Our QCD string is not like that, it is just a bosonic string without charges, there are no traces of supersymmetry or BPS protection.

string interaction via sigma meson exchange

our fit uses
the sigma mass
600 MeV

$$\frac{\langle \sigma(r_\perp) W \rangle}{\langle W \rangle \langle \sigma \rangle} = 1 - C K_0(m_\sigma \tilde{r}_\perp)$$

$$\tilde{r}_\perp = \sqrt{r_\perp^2 + s_{string}^2}$$

T. Iritani, G. Cossu and S. Hashimoto, arXiv:1311.0218

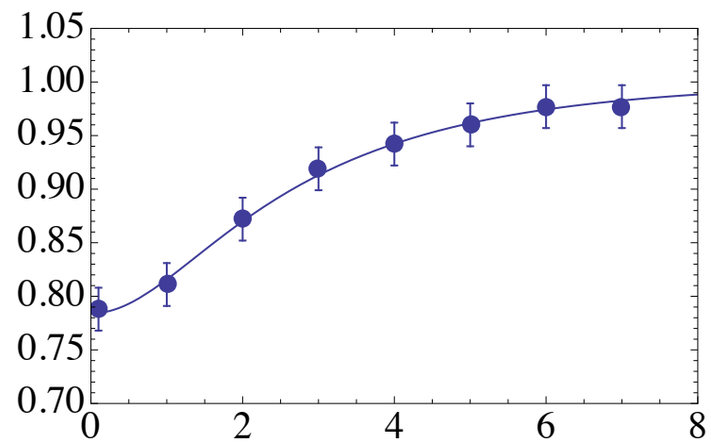

FIG. 2. (Color online). Points are lattice data from [12], the curve is expression (8) with $C = 0.26, s_{string} = 0.176\,\text{fm}$.

So the sigma cloud around a string is there!

2d spaghetti collapse

Basically strings can be viewed as a 2-d gas of particles with unit mass and forces between them are given by the derivative of the energy (8) , and so

$$\ddot{\vec{r}}_i = \vec{f}_{ij} = \frac{\vec{r}_{ij}}{\tilde{r}_{ij}}(g_N\sigma_T)m_\sigma 2K_1(m_\sigma\tilde{r}_{ij}) \qquad (19)$$

with $\vec{r}_{ij} = \vec{r}_i - \vec{r}_j$ and "regularized" $\tilde{r}$ (9).

$$E_{tot} = \sum_i \frac{v_i^2}{2} - 2g_N\sigma_T \sum_{i>j} K_0(m_\sigma r_{ij})$$

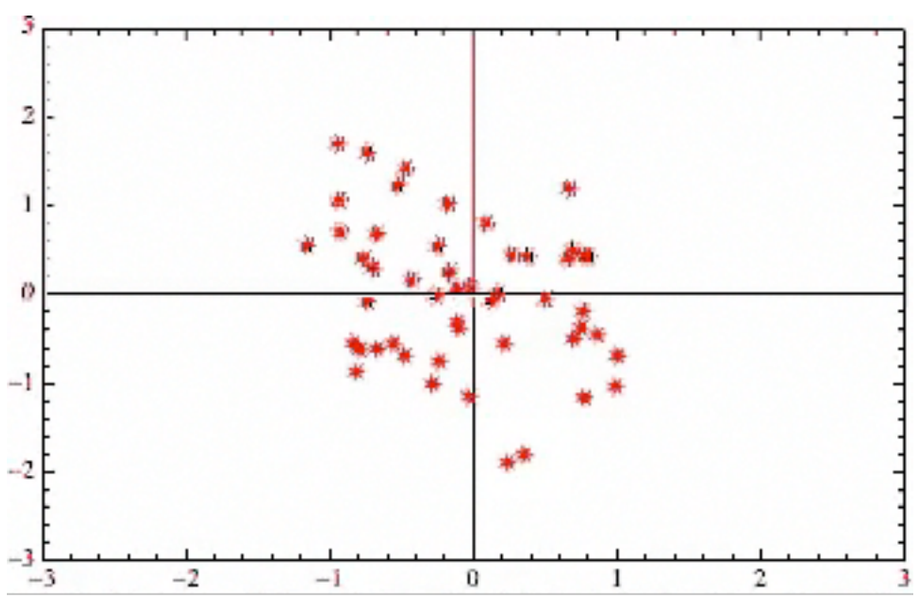

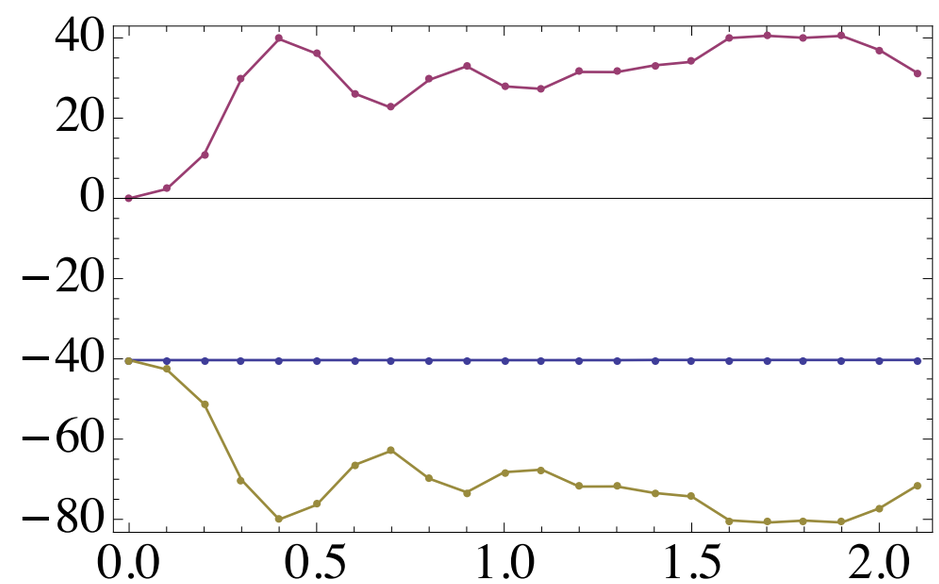

FIG. 4. (Color online) The (dimensionless) kinetic and potential energy of the system (upper and lower curves) for the same example as shown in Fig. 6, as a function of time t(fm). The horizontal line with dots is their sum, namely E_{tot}, which is conserved.

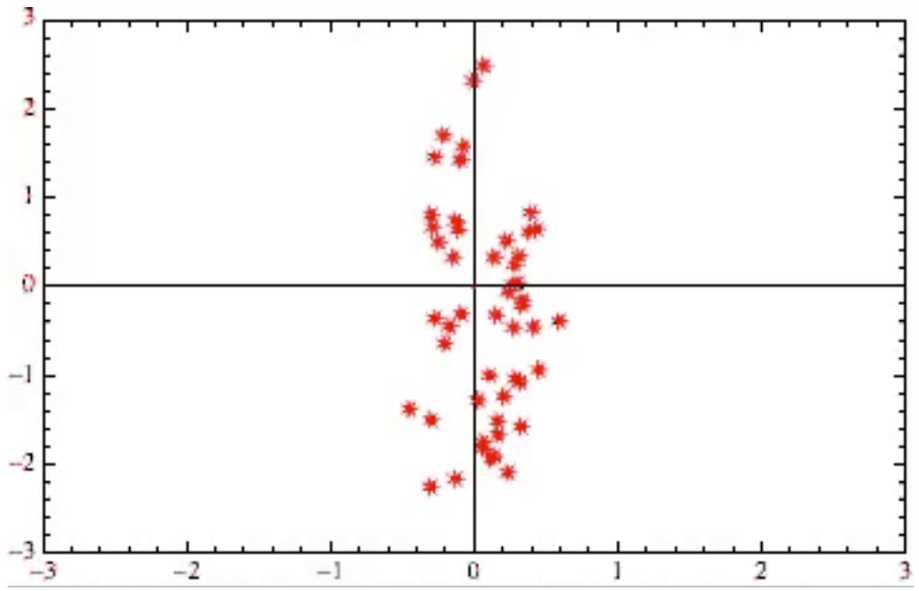

peripheral AA
contraction in x first
(and only: limited
time scale)

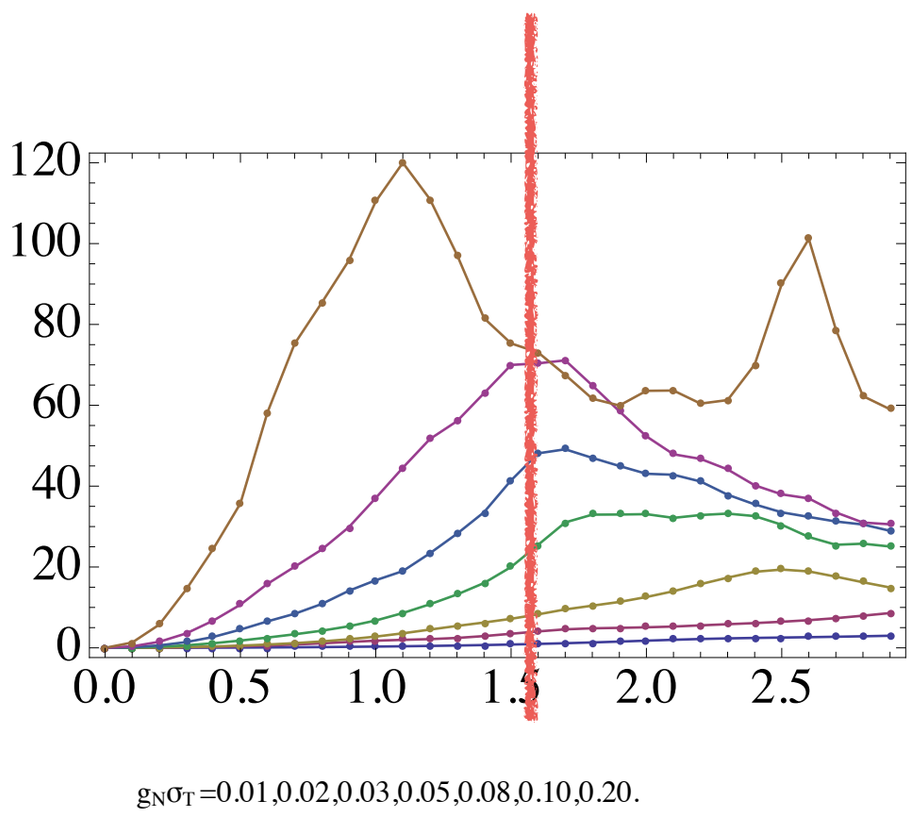

string stretching - about 1fm/c

1/4 period of yo-yo - another 0.5

so too small coupling does not work

fundamental string balls

A string ball can be naively generated by a "random walk" process, of M/M_s steps, where $M_s \sim 1/\sqrt{\alpha'}$ is the typical mass of a straight string segment. If so, the string entropy scales as the number of segments

$$S_{ball} \sim M/M_s \tag{1}$$

$$\frac{R_{ball,r.w.}}{l_s} \sim \sqrt{M}$$

The Schwarzschild radius of a black hole in d spatial dimensions is

$$R_{BH} \sim (M)^{\frac{1}{(d-2)}} \tag{2}$$

and the Bekenstein entropy

$$S_{BH} \sim Area \sim M^{\frac{d-1}{d-2}} \tag{3}$$

Can be matched for one M only => critical string ball its Hawking T is the Hagedorn T_H

Damour and Veneziano

entropy of a self-interacting string ball of radius R and mass M,

$$S(M,R) \sim M\left(1-\frac{1}{R^2}\right)\left(1-\frac{R^2}{M^2}\right)\left(1+\frac{g^2M}{R^{d-2}}\right) \tag{5}$$

where all numerical constants are for brevity suppressed and all dimensional quantities are in string units given

even for a very small g,

the importance of the last term depends not on g but on g^2M. So, very massive balls can be influenced by a very weak gravity (what, indeed, happens with planets and stars)

Our lattice model for string balls

$$Z \sim \int \mathrm{d}L \exp\left[\frac{L}{a}\ln(2d-1) - \frac{\sigma_T L}{T}\right], \qquad (18)$$

and hence the Hagedorn divergence happens at

$$T_H = \frac{\sigma_T a}{\ln(2d-1)}. \qquad (19)$$

Setting $T_H = 0.30\,\mathrm{GeV}$, according to the lattice data mentioned above and the string tension, we fix the 3-dimensional spacing to be

$$a_3 = 2.73\,\mathrm{GeV}^{-1} \approx 0.54\,\mathrm{fm}. \qquad (20)$$

$$E_{plaquette} = 4\sigma_T a \approx 1.9\,\mathrm{GeV}\,, \qquad (21)$$

is amusingly in the ballpark of the lowest glueball masses of QCD. (For completeness: the lowest "meson" is one link or mass 0.5 GeV, and the lowest "baryon" is three links – 1.5 GeV of string energy – plus that of the "baryon junction".)

The most compact (volume-filling or Hamiltonian) string wrapping visits each site of the lattice. If the string is closed, then the number of occupied links is the same as the number of occupied sites. Since in $d = 3$ each site is shared among 8 neighboring cubes, there is effectively only one occupied link per unit cube, and this wrapping produces the maximal energy density,

$$\frac{\epsilon_{max}}{T_c^4} = \frac{\sigma_T a}{a^3 T_c^4} \approx 4.4 \qquad (22)$$

(we normalized it to a power of T_c, the highest temperature of the hadronic phase). It is instructive to compare it to the energy density of the gluonic plasma, for which we use the free Stefan-Boltzmann value

$$\frac{\epsilon_{gluons}}{T^4} = (N_c^2 - 1)\frac{\pi^2}{15} \approx 5.26 \qquad (23)$$

Example of non-interacting strings

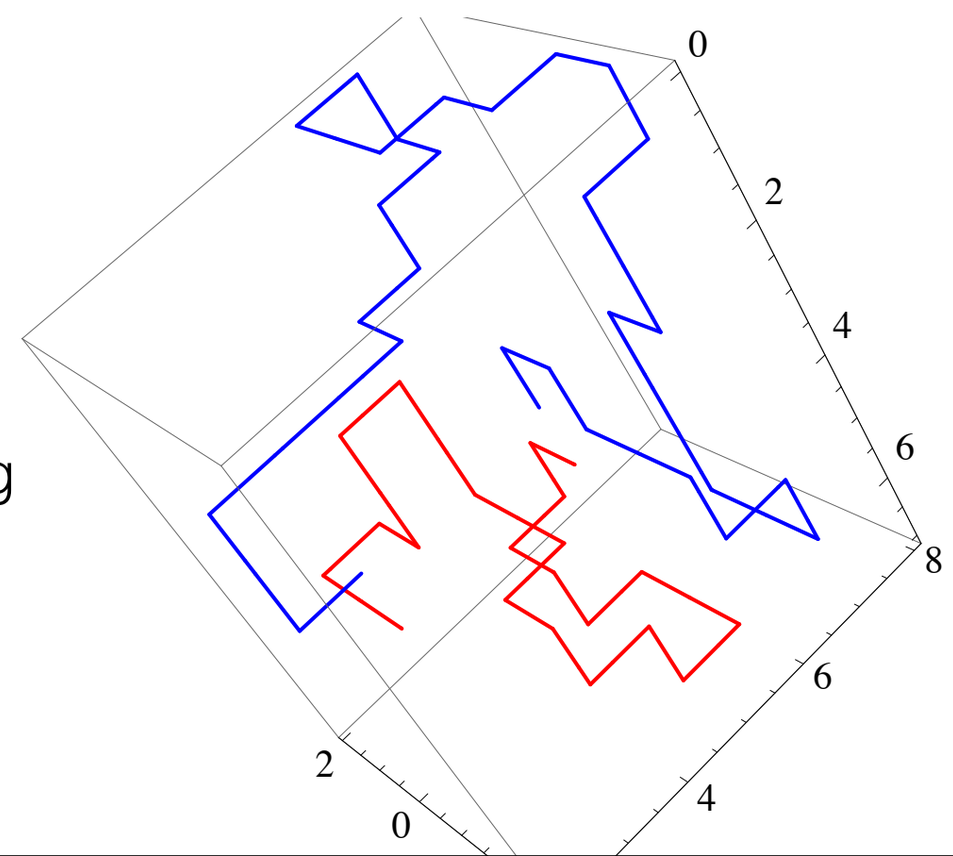

Self-interacting string balls

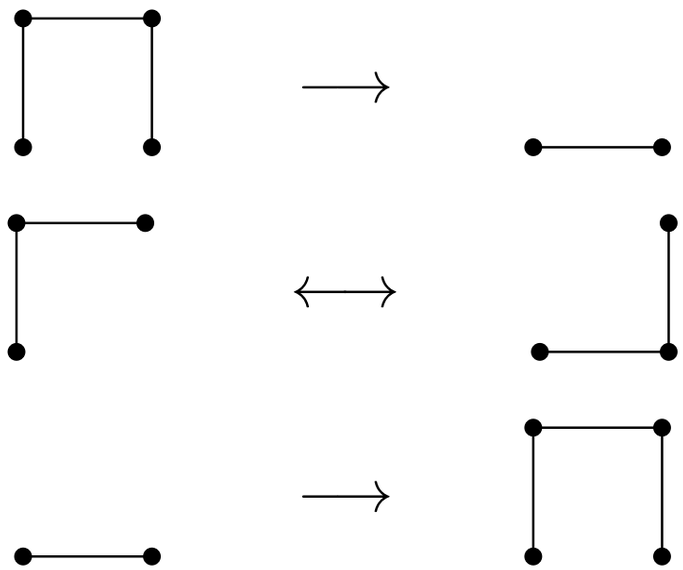

Metropolis algorithm, updates,
T(x) instead of a box
Yukawa self-interaction

we observe a new regime: the
entropy-rich self-balanced string balls

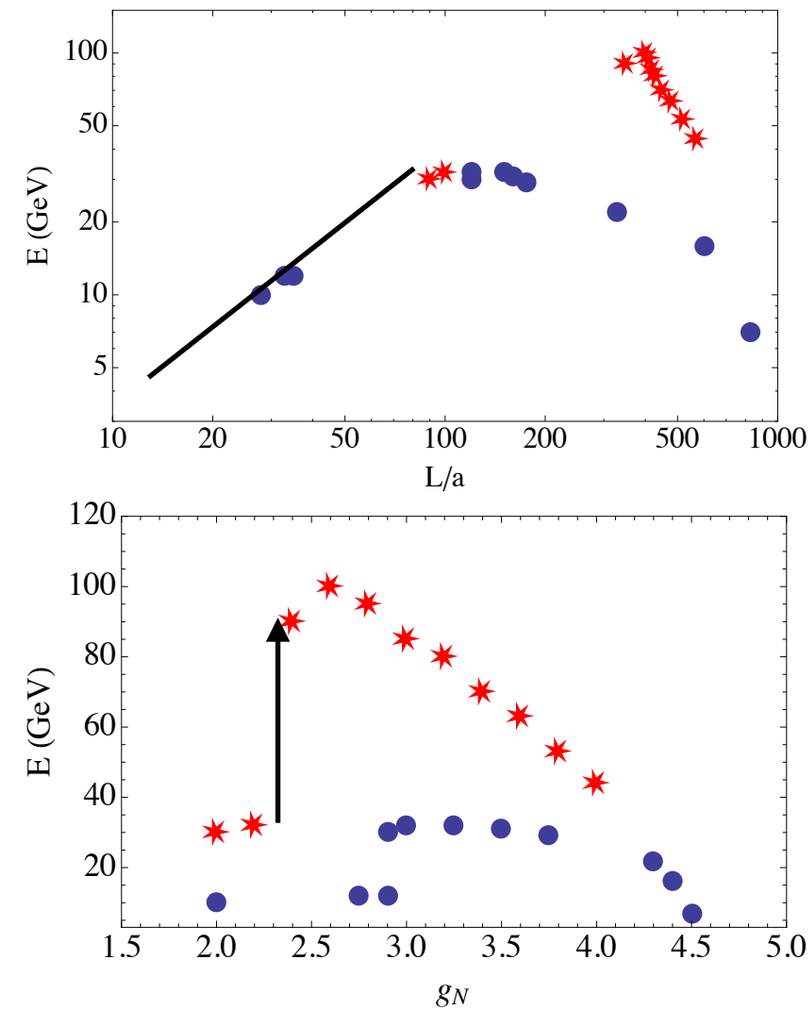

FIG. 7: Upper plot: The energy of the cluster $E\,(\mathrm{GeV})$ versus the length of the string L/a. Lower plot: The energy of the cluster $E\,(\mathrm{GeV})$ versus the "Newton coupling" $g_N\,(\mathrm{GeV}^{-2})$. Points show the results of the simulations in setting $T_0 = 1\,\mathrm{GeV}$ and size of the ball $s_T = 1.5a, 2a$, for circles and stars, respectively.

extreme example

in spite of a very large string length

L/a ~ 700, the total energy is only E ≈ 17GeV,

as a result of the balancing between

the string tension and self- interaction.

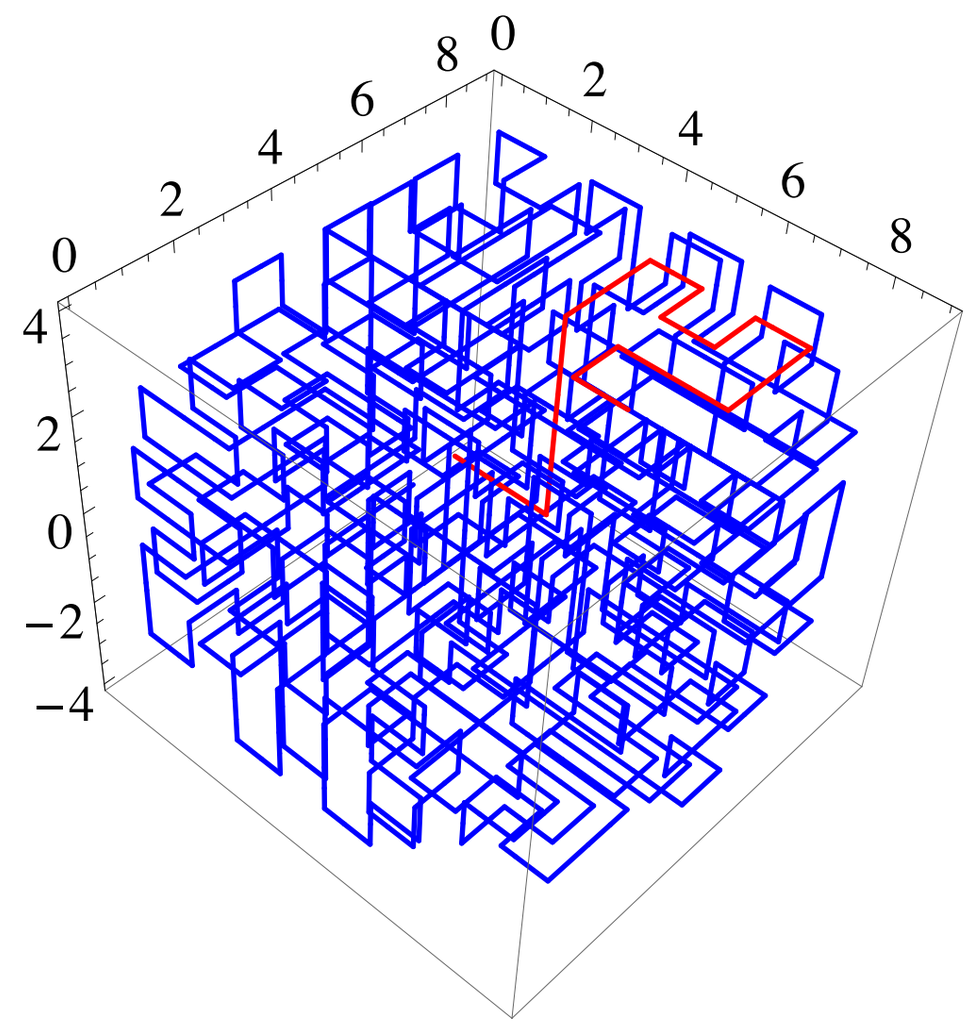

very strong dependence on the value of the sigma mass

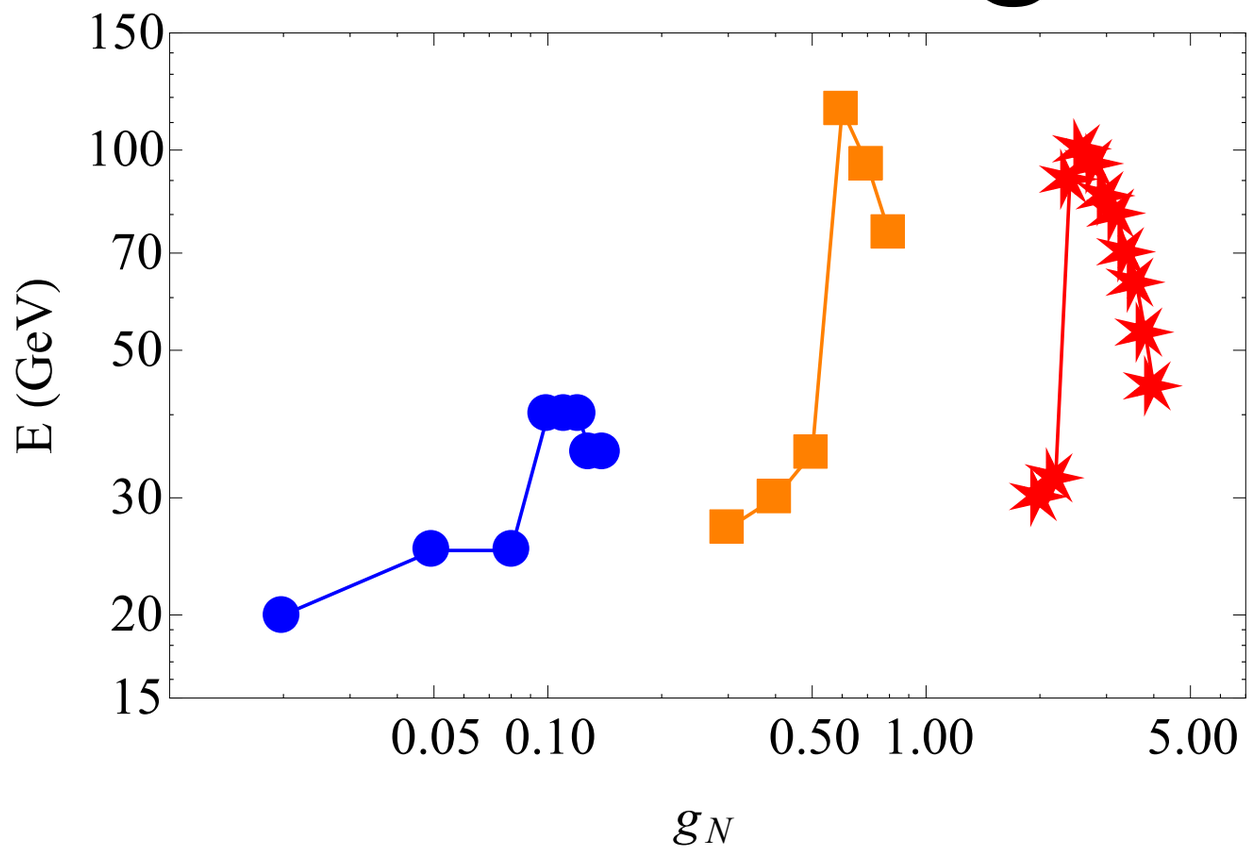

FIG. 9: (Color online) Blue circles, yellow squares and red stars show the dependence of the string ball energy E(GeV) on the coupling g_N (GeV^{-2}) for $m_\sigma = 0.1, 0.3, 0.6$ GeV, respectively. These simulations are performed in the setting $T_0 = 1$ GeV, $s_T = 2a$.

$\frac{\hat{q}}{s} \approx const$? Jet quenching during the mixed phase

It has however been pointed out long ago [24] that large experimental values of v_2 are difficult to explain by any simple model of quenching, in particular, they were in a strong contradiction with the simplest assumption (30). One possible solution to this puzzle has been suggested few years ago in Ref. [6]: the v_2 data can be reproduced, if $\hat{q}$ is significantly enhanced in the mixed phase. More

Here we want to point out that a natural explanation for the enhanced $\hat{q}$ in the mixed phase can be provided by the strings. As far as we know, the "kicks" induced by the color electric field inside the QCD strings has been ignored in all jet quenching phenomenology: only the fields of "charges" (quarks and gluons in QGP, hadrons alternatively) were included, in the spherical Debye approxima-

$$\hat{q} = \frac{\mathrm{d}\langle p_\perp^2 \rangle}{\mathrm{d}l}\,, \qquad \langle p_\perp^2 \rangle \approx (gEr_s)^2\,, \qquad E(x) = \frac{\Phi_e}{2\pi r_s^2} K_0(x/r_s)$$

the string radius $r_s = 1/(1.3\mathrm{GeV}) = 0.15\,\mathrm{fm}$.

string length inside 1 fm^3

$$\hat{q} \approx \frac{16}{3}\alpha_s \sigma_T \frac{\bar{L} r_s}{\mathrm{fm}^3}\,.$$

$$\hat{q}_{min} = 0.028, \qquad \hat{q}_{max} = 0.10 \left(\frac{\mathrm{GeV}^2}{\mathrm{fm}}\right).$$

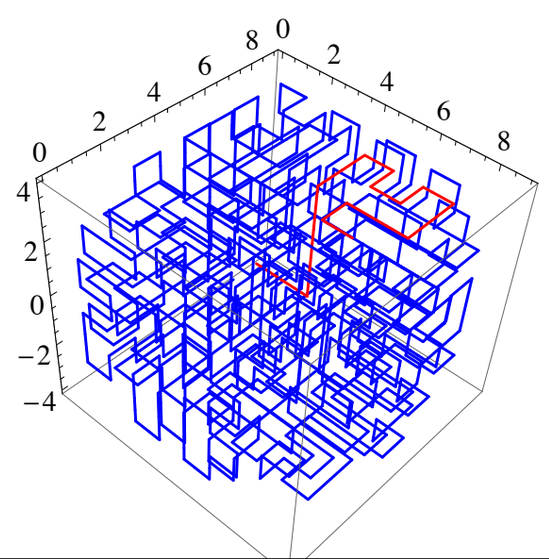

across the mixed phase, to be compared with values by the Jet coll. at Tc $\hat{q}_{min} = 0.025, \quad \hat{q}_{max} = 0.15 \left(\frac{\mathrm{GeV}^2}{\mathrm{fm}}\right)$

But in high entropy self-supporting balls it can be up to one order of magnitude larger!

Two historic views on the Pomeron

$$\frac{d\sigma}{dt} \sim s^{\alpha(t)}$$

Prehistoric: Regge, Pomeranchuk, Gribov

$$\alpha(t) = \alpha(0) + \alpha' t + \ldots$$

intercept +string scale

1960's: Veneziano

dual resonance amplitude => appearance of strings

1970's QCD

Gribov,Lipatov => gluon ladders => BFKL

So, do we have two different Pomerons, soft (strongly coupled) and hard (weakly coupled)?

Holographic Pomeron based on AdS/QCD

- the answer to the question is No:
- **Only one Pomeron** because the gauge description on the boundary is **dual to** string description in the bulk. Weak and strong coupling are its limits
- Concrete model of this type has been worked out by Zahed et al (Stoffers,Basar, Kharzeev): I will call it **Z+**
- **Our main statement: as a function of b there are three distinct regimes: subcritical, near-critical and supercritical!**

the “tube”

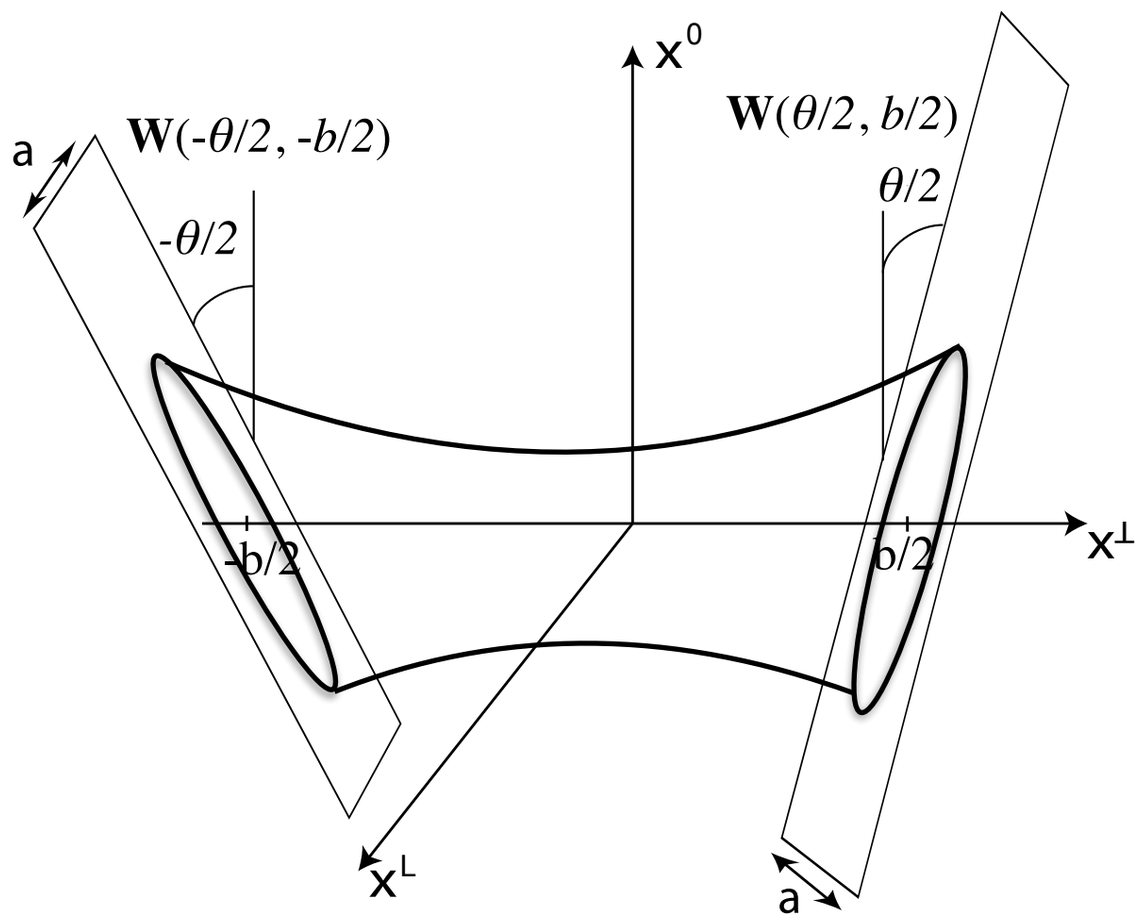

FIG. 1: Dipole-dipole scattering configuration in Euclidean space. The dipoles have size a and are b apart. The dipoles are tilted by $\pm\theta/2$ (Euclidean rapidity) in the longitudinal $x_0 x_L$ plane.

- **If cut horizontally, it describes production of a pair of open strings**
- **If cut vertically, it describes an exchange by a closed string**
- **string fluctuations are includ mode-by-mode**

$$\frac{1}{-2is}\mathcal{T}(s,t) \approx \frac{\pi^2 g_s^2 a^2}{2} \sum_{k=1}^{k_{\max}} \sum_{n=0}^{\infty} \frac{(-1)^k}{k} \left(\frac{k\pi}{\ln s}\right)^{D_\perp/2-1} \times d(n)\, s^{-2n/k+D_\perp/12k+\alpha' t/2k}\,, \qquad (70)$$

k=1 in SU(3), n is excitation

The previous literature focuses on what we call the "cold" regime of the string

$$\mathbf{b} \gg \beta \gg \tilde{\beta}_H \tag{17}$$

where the former inequality follows from large collision energy (14) and the latter implies that the string is nearly straight, with small effective excitations (small effective T). The meaning of

$$\beta = \frac{1}{T} = \frac{2\pi \mathbf{b}}{\chi}$$

$$\chi = log(s)$$

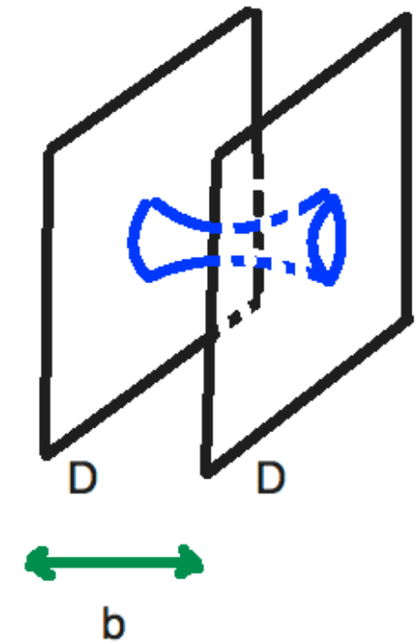

We will now review the Pomeron results in this setting. The amplitude of the elastic dipole-dipole scattering reads [2–4]

$$\frac{1}{-2is}\mathcal{T}(s,t;k) \approx g_s^2 \int d^2\mathbf{b}\, e^{iq\cdot\mathbf{b}}\, \mathbf{K}_T(\beta,\mathbf{b};k) \tag{15}$$

$$\mathbf{K}_T(\beta,\mathbf{b};1) = \left(\frac{\beta}{4\pi^2\mathbf{b}}\right)^{D_\perp/2}$$

classical action b^2
vibrations b-independent

$$\times e^{-\sigma\beta\mathbf{b}\left(1-(\tilde{\beta}_H/\beta)^2/2\right)}$$

$$\times \sum_{n=0..\infty} d(n) exp(-2\chi n)$$

Linear Regge trajectories, daughters shifted by 2 down

As we mentioned, the expression (18) has been derived in [4] from the semiclassical approach to a Polyakov string, but (to leading order in $1/\lambda$) it can alternatively be derived from a diffusion equation

$$\left(\partial_\chi + \mathbf{D}_k\left(\mathbf{M}_0^2 - \nabla_{\mathbf{b}}^2\right)\right)\mathbf{K}_T = 0 \tag{20}$$

where the rapidity χ interval is the time and the diffusion happens in the (curved) transverse space with the diffusion constant $\mathbf{D}_k = \alpha'/2k = l_s^2/k$. This diffusion (20) is nothing else but the Gribov diffusion of the Pomeron, leading on average to an impact parameter $\langle \mathbf{b}^2 \rangle = \mathbf{D}_k\chi$ for close Pomeron strings. If the "mother dipoles"

connection to Gribov diffusion

fluctuations of flat membrane and a tube are different

- The (T=0) potential <W>
  is linear at large b and Coulombic (pQCD)
  at small b : yet **transition is smooth**

- **The tube has a periodic variable => quantization formally the same as the (Matsubara) thermal formalism => thus we expect thermal-like behavior with a nontrivial transition to pQCD regime**

New Regimes of Stringy (Holographic) Pomeron

1. A "cold" regime, with low string excitations;

2. A "near-critical" or "HPS regime", in which strings indefinitely increase their energy and entropy, but not their free energy / pressure;

3. An "explosive regime", in which the string occupies large portion of space and generates sufficient pressure for hydrodynamical explosion.

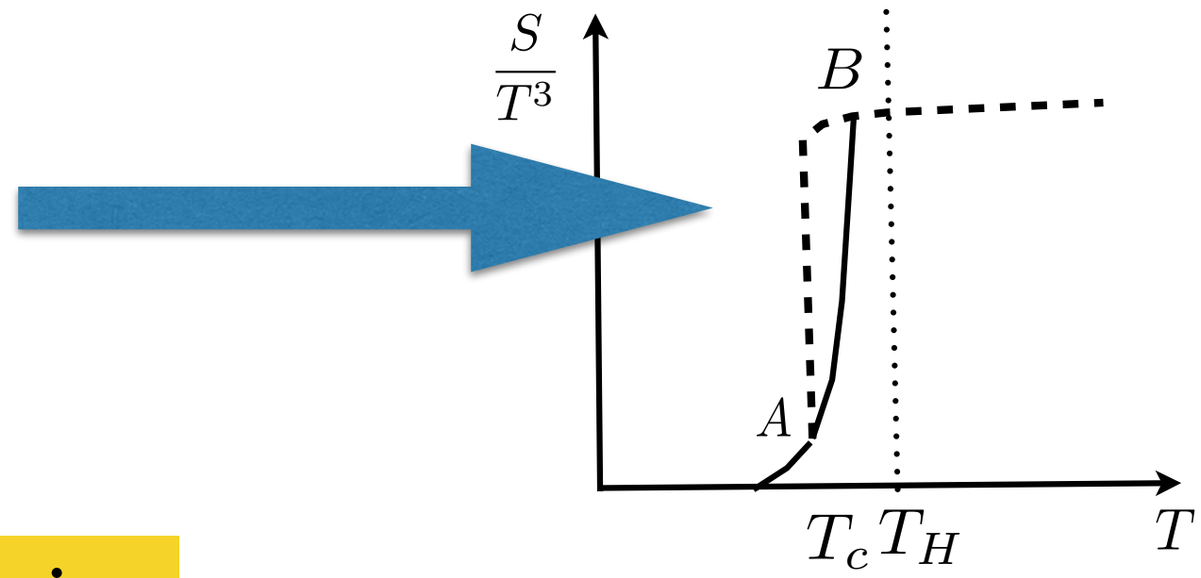

FIG. 3: (Color on-line) Schematic temperature dependence of the entropy density. The dashed line represents equilibrium gluodynamics with a first order transition at $T = T_c$. The solid line between points A and B represents the expected behavior of a single string approaching its Hagedorn temperature T_H.

Hagedorn-Polyakov-Susskind regime

stringy excitations grows with an excitation energy *exponentially*. To see this, imagine a d-dimensional lattice with spacing a and draw all possible strings of length L/a making all possible turns (except going backward) at each site, that is

$$N(E) \approx (2d-1)^{L/a} = e^{E(L)/T_H} \qquad (5)$$

where in the last term we changed length into energy using the string tension $E(L) = \sigma_T L$ and defined

$$T_H = \frac{\sigma_T a}{\ln(2d-1)} \qquad (6)$$

As T=>T_H the entropy and energy grow, but not free energy (pressure) as F=E-TS and two terms cance

Can new regimes be seen in the elastic amplitude?

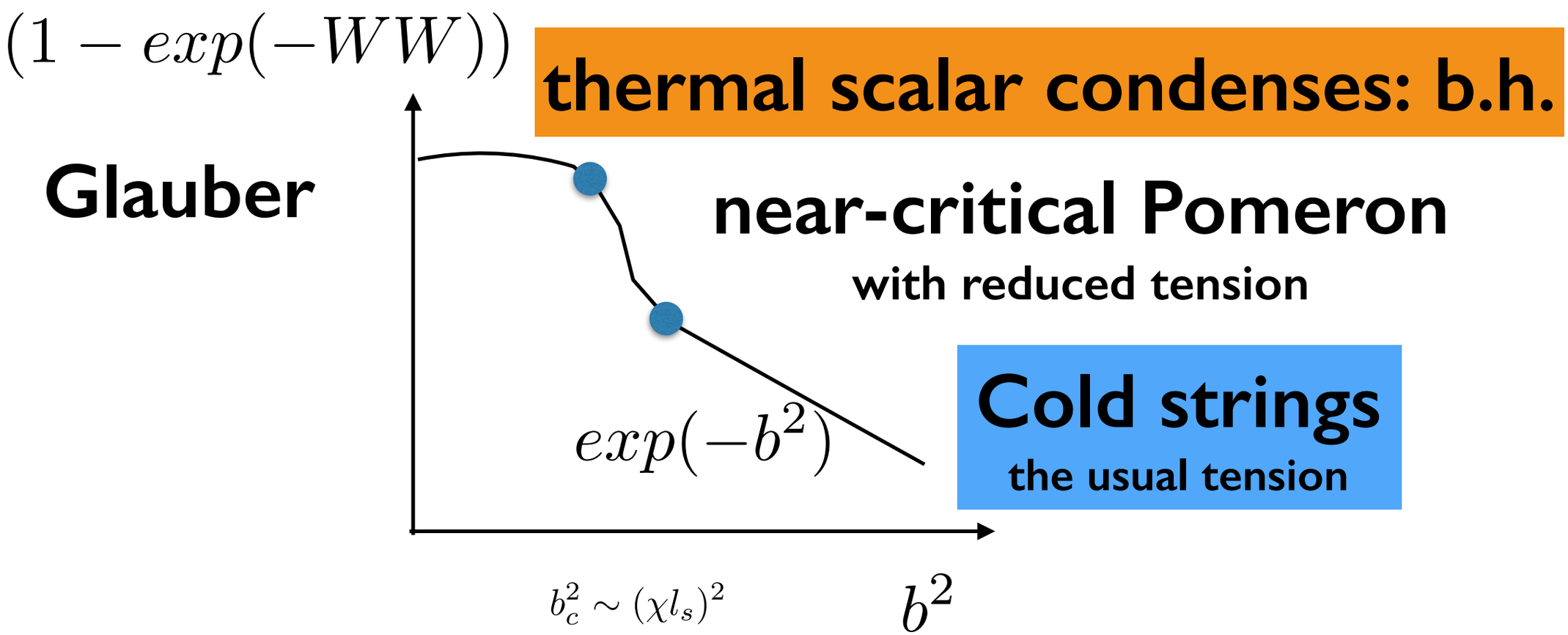

After integration over b and dipole sizes, can one still be able to see it in T(t) ?

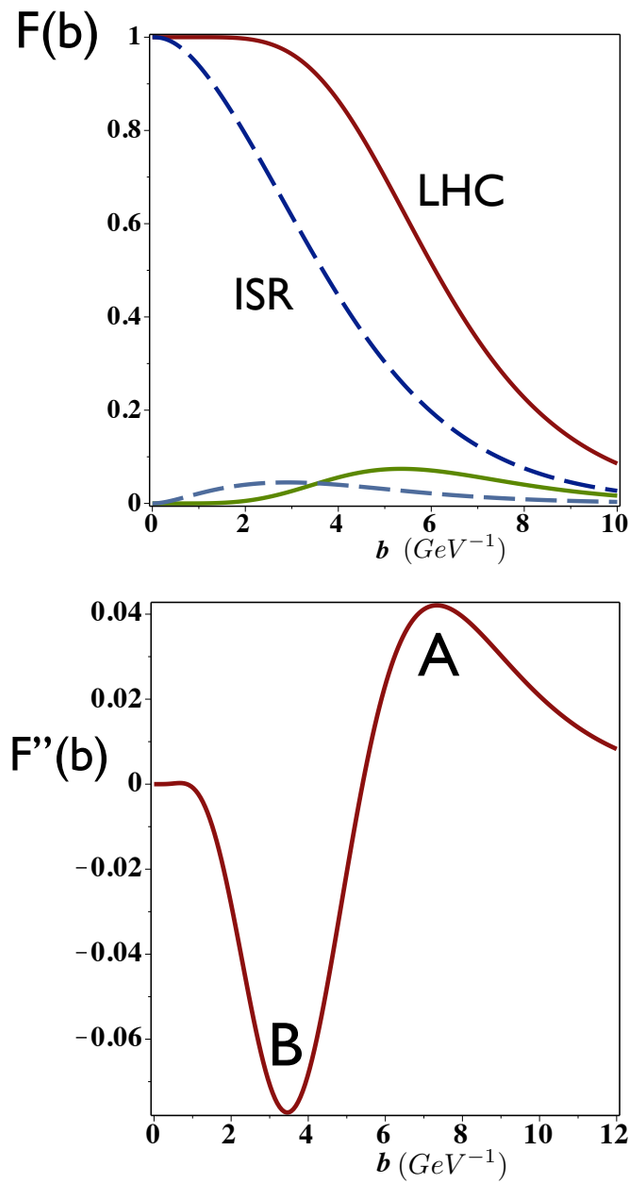

FIG. 4: (Color online) The upper figure shows the imaginary (upper) and real (down) parts of the profile function $F(s,b)$ versus $\mathbf{b}(\mathrm{GeV}^{-1})$ for $\sqrt{s} = 7\,\mathrm{TeV}$ (solid) and $\sqrt{s} = 63\,\mathrm{GeV}$ (dashed). The lower plot shows the second derivative over b for $\sqrt{s} = 7\,\mathrm{TeV}$. Two maxima correspond to the same points A, B as in the sketch in Fig. 1.

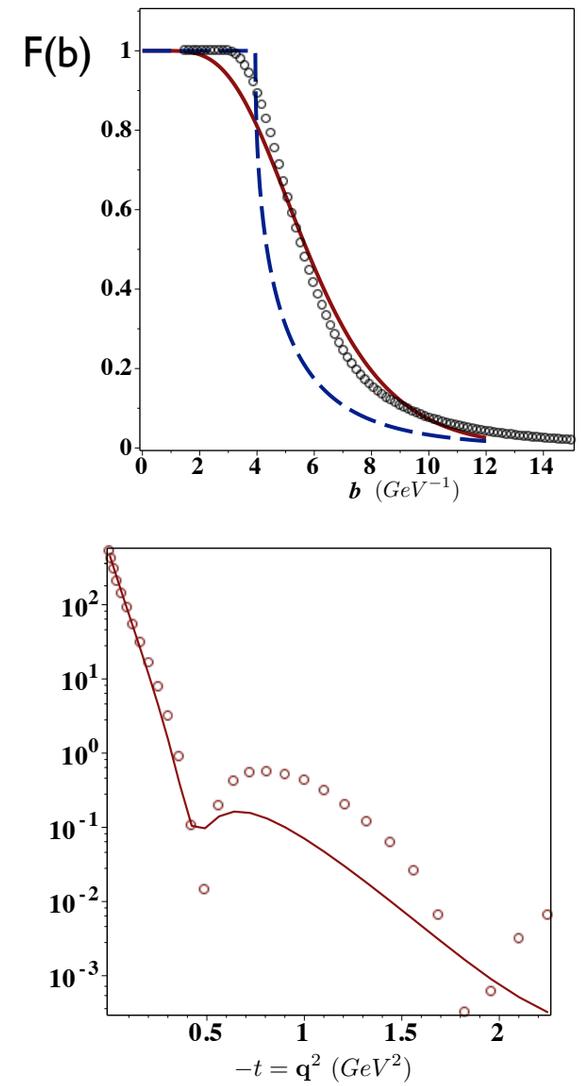

FIG. 12: (Color on-line) The profile function $F(\mathbf{b})$ versus the impact parameter $\mathbf{b}$ is shown in the upper plot for LHC $\sqrt{s} = 7\,\mathrm{TeV}$ energy. The solid line is the same curve as in Fig.4 corresponding to the BSW data parametrization. The dashed line is the shape corresponding to the approximation (59) for fixed sizes of the dipoles $u_1 = u_2$, while the circles correspond to the profile with the fluctuating dipoles. The lower plot shows the corresponding absolute value squared of its Bessel transform as a function of momentum transfer.

summary

- in ``central" pA and partly in peripheral AA "spaghetti" state **implodes** before **exploding**
- in **the mixed phase** (near Tc) **entropy-rich self-bound string balls** can exist: QCD analog of holographic string balls
- (QGP and deconfinement => black holes)
- stringy Pomeron has Euclidean tube derivation => thus thermal description => thus analogy to phase transition and 3 regimes,
- seen in elastic scattering profile

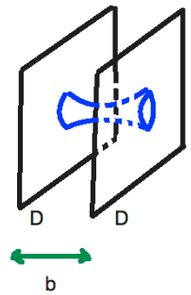

QUANTUM FLUCTUATIONS OF QCD STRINGS

The temperature and the entropy

Although the scattering amplitudes involve string dynamics at zero temperature, the ensuing formula resemble those of a thermodynamical string. The reason stems from the string membrane exchanged as shown in Fig. 1 which is quantized on a circle making it formally identical to the thermal Matsubara formalism. Furthermore, the effective string temperature depends on the world-sheet coordinate $0 \leq \sigma_W \leq 1$ [4]

$$T(\sigma_W) = \frac{\chi}{2\pi \mathbf{b}} \frac{1}{\cosh(\chi(\sigma_W - 1/2))} \qquad (33)$$

with its highest value at the center or $T(1/2) \equiv T = \chi/2\pi\mathbf{b}$. It is instructive to focus on the actual effective temperature values, corresponding to LHC collisions. For that we define a typical impact parameter $\mathbf{b}_{\rm eff}$ for pp collisions at energy s as

$$\mathbf{b}_{\rm eff}(s) = \sqrt{\frac{\sigma_P(s)}{\pi F_{\rm gray}}} \qquad (34)$$

where $\sigma_P(s)$ is the average of the total pp and $\bar{\rm p}$p cross section [50], and $F_{\rm gray} < 1$ is

We think the value to compare is

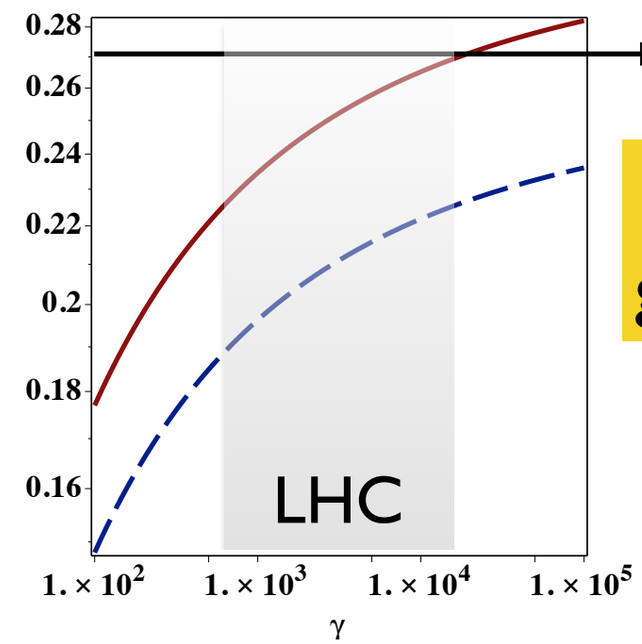

$T_c \approx 0.27\,\mathrm{GeV}$.

of SU(3) gluodynamics

FIG. 4: (Color on-line) The effective string temperature $T_{\rm eff}$ (GeV) versus the c.m. beam gamma factor γ, solid for black disc estimate $F_{\rm gray} = 1$ and dashed for gray factor $F_{\rm gray} = 0.7$. As argued in the text, its value is to be compared to the effective Hagedorn temperature $\tilde{T}_H$.

$$D_\perp \to \tilde{D}_\perp = D_\perp \left(1 - \frac{3(D_\perp - 1)^2}{2kD_\perp\sqrt{\lambda}}\right)$$

This translates to a higher effective Hagedorn temperature $\tilde{T}_H > T_H$ through (10) with

$$T_H^2 \to \tilde{T}_H^2 = \frac{3}{\tilde{D}_\perp}\frac{\sigma_T}{2\pi} \approx 1.8\, T_H^2 \qquad (36)$$

the near-critical Pomeron

One can re-sum "Luscher terms" in the potential

$$V(R) = \sqrt{\sigma_T^2 R^2 - const}$$

The re-summed result follows the paper of Arvis [38], which obtained the potential induced by the Nambu-Goto string. The result obtains the square root (which will play an important role in what follows)

$$\mathbf{K}_T(\beta, \mathbf{b}; 1) \approx \left(\frac{\beta}{4\pi^2 \mathbf{b}}\right)^{D_\perp/2} e^{-\sigma\beta\mathbf{b}\left(1-\tilde{\beta}_H^2/\beta^2\right)^{1/2}}$$

but the results get clearly inapplicable as root argument changes sign

Compare to "cold" one, in which it is a small correction

$$\mathbf{K}_T(\beta, \mathbf{b}; 1) \approx \left(\frac{\beta}{4\pi^2 \mathbf{b}}\right)^{D_\perp/2} e^{-\sigma\beta\mathbf{b}\left(1-\tilde{\beta}_H^2/2\beta^2\right)}$$

Can one figure out what to do when T>TH and argument of the sqrt <0?

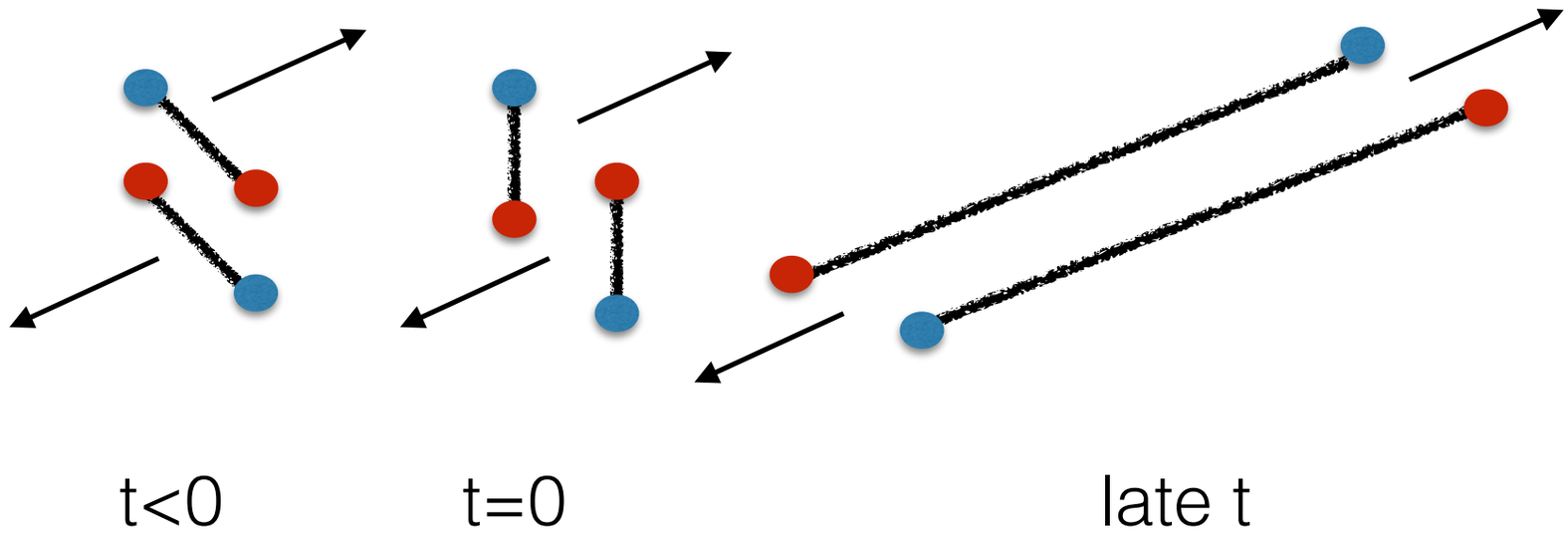
t<0
t=0
late t

“supernova” (implosion before explosion)

string mass and force are both “per length”,
so one can think of just 2d gas of points with
the 2d interaction: potential $K_0(mr)$
($\log(r)$ in the massless limit)

Molecular dynamics shows collapse
appears, very quick if the string number is large

in AdS/QCD strings are in 5d
their interaction is due to dilation and gravity
the result is a **bulk black hole**

Anisotropic Hydrodynamics: Recent Progress

Michael Strickland
Kent State University

The Approach to Equilibrium in Strongly Interacting Matter
Brookhaven National Laboratory - April 5, 2014

Collaborators: D. Bazow, U. Heinz, W. Florkowski, R. Maj, M. Martinez, R. Ryblewski, E. Maksymiuk, L. Tinti

Motivation

- Relativistic viscous hydrodynamical modeling for heavy ion collisions at RHIC and LHC is ubiquitous
- Application is justified a priori by the (relative) smallness of the shear viscosity of the plasma
- The canonical way to derive viscous hydrodynamics relies on a linearization around an isotropic equilibrium state (local rest frame = LRF)
- However, the **QGP is not isotropic in LRF** → there are large corrections to ideal hydrodynamics primarily due to strong longitudinal expansion
- Alternative approach: Anisotropic hydrodynamics builds in momentum-space anisotropies in the local rest frame from the beginning
- The goal is to create a quantitatively reliable viscous-hydro-like code that more accurately describes:
    - Early time dynamics
    - Dynamics near the transverse edges of the overlap region
    - Temperature-dependent (and potentially large) η/S

Estimating Early-time Pressure Anisotropy

- CGC @ leading order predicts negative → approximately zero longitudinal pressure
- QGP scattering + plasma instabilities work to drive the system <u>towards</u> isotropy on the fm/c timescale, but don't seem to fully restore it
- Viscous hydrodynamics predicts early-time anisotropies $P_L/P_T \leq 0.35 \rightarrow 0.5$ (see next slide)
- AdS-CFT dynamical calculations in the strong coupling limit predict anisotropies of $P_L/P_T \leq 0.3$ (see talks by Heller and Romatschke)

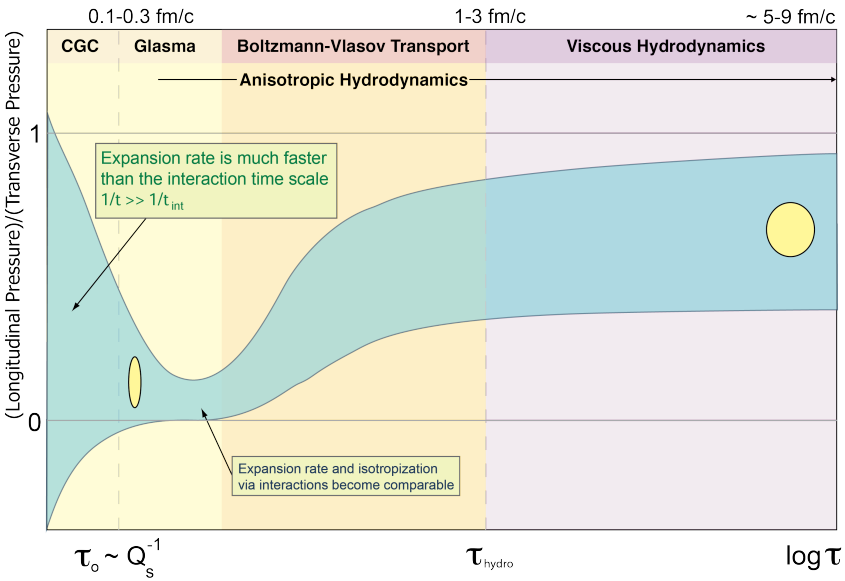

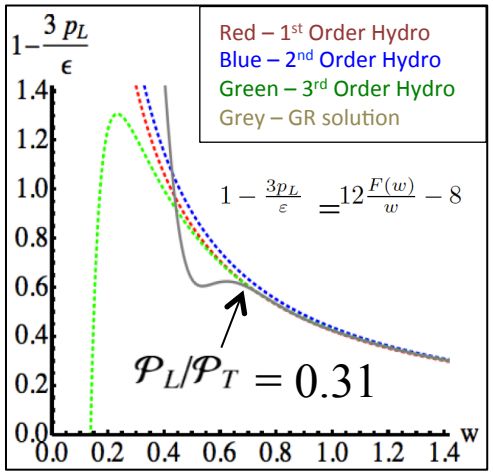

Estimating Anisotropy – Viscous hydro

- To get a feel for the magnitude of pressure anisotropies to expect let's consider the Navier-Stokes limit

$$\left(\frac{\mathcal{P}_L}{\mathcal{P}_T}\right)_{\rm NS} = \frac{P_{\rm eq} + \pi^{zz}_{\rm NS}}{P_{\rm eq} + \pi^{xx}_{\rm NS}} = \frac{3\tau T - 16\bar{\eta}}{3\tau T + 8\bar{\eta}}$$

$$\bar{\eta} = \frac{\eta}{\mathcal{S}}$$

$$\pi^{zz}_{\rm NS} = -2\pi^{xx}_{\rm NS} = -2\pi^{yy}_{\rm NS} = -4\eta/3\tau$$

- P_L/P_T decreases with increasing η/S.
- Assume $\eta/S = 1/4\pi$ in order to get an upper bound on the anisotropy
- Using RHIC initial conditions (T_0 = 400 MeV @ τ_0 = 0.5 fm/c) we obtain $P_L/P_T \leq 0.5$
- Using LHC initial conditions (T_0 = 600 MeV @ τ_0 = 0.25 fm/c) we obtain $P_L/P_T \leq 0.35$
- Negative P_L at large η/S or low temperatures!

Estimating Anisotropy – Viscous hydro

- Navier-Stokes solution is an "attractor" for the 2nd order solution
- τ_π sets timescale to approach Navier-Stokes evolution
- $\tau_\pi \sim 5\eta/(TS) \sim 0.1$ fm/c at LHC temperatures
- Assume isotropic LHC initial conditions T_0= 600 MeV @ τ_0 = 0.25 fm/c and solve for the 0+1d viscous hydrodynamics

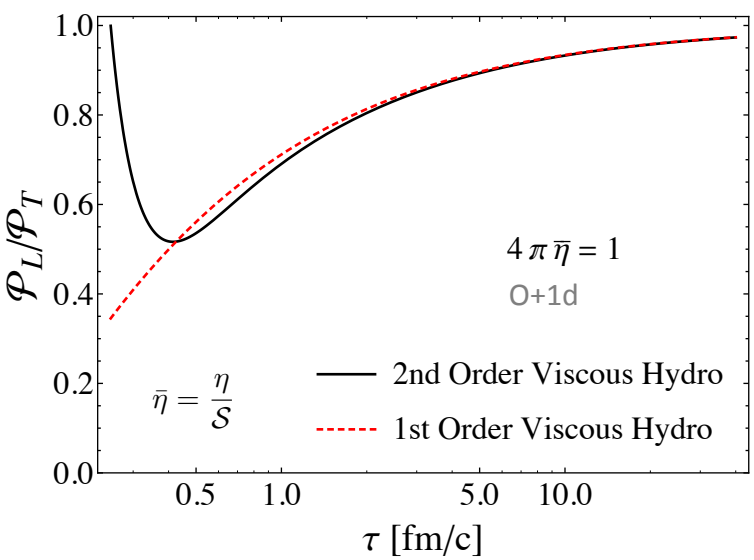

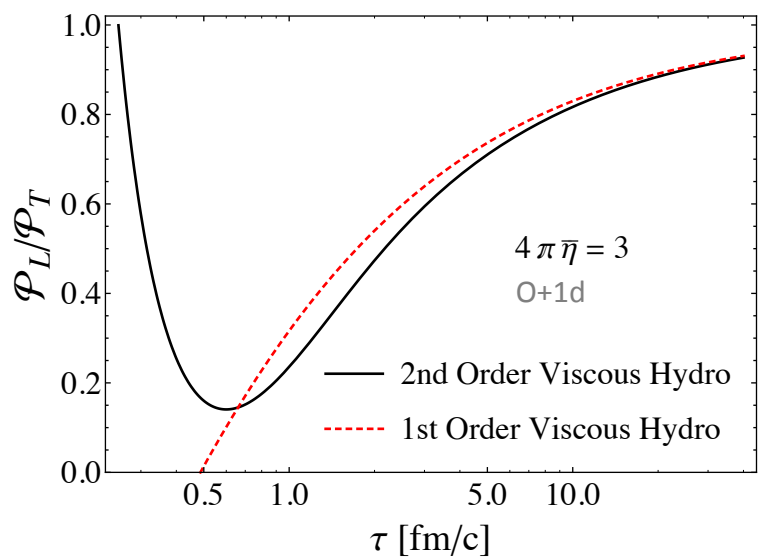

Anisotropic Hydrodynamics Basics

M. Martinez and MS, 1007.0889

Viscous Hydrodynamics Expansion

$$f(\tau,\mathbf{x},\mathbf{p}) = \underline{f_{\rm eq}(\mathbf{p},T(\tau,\mathbf{x}))} + \delta f$$

Isotropic in momentum space

Anisotropic Hydrodynamics Expansion

$$f(\tau,\mathbf{x},\mathbf{p}) = f_{\rm aniso}(\mathbf{p},\underbrace{\Lambda(\tau,\mathbf{x})}_{T_\perp},\underbrace{\xi(\tau,\mathbf{x})}_{\text{anisotropy}}) + \delta\tilde{f}$$

→ Assume spheroidal form in LRF

$$f^{LRF}_{\rm aniso} = f_{\rm iso}\left(\frac{\sqrt{\mathbf{p}^2+\xi(\mathbf{x},\tau)p_z^2}}{\Lambda(\mathbf{x},\tau)}\right)$$

$$\xi = \frac{\langle p_T^2\rangle}{2\langle p_L^2\rangle} - 1$$

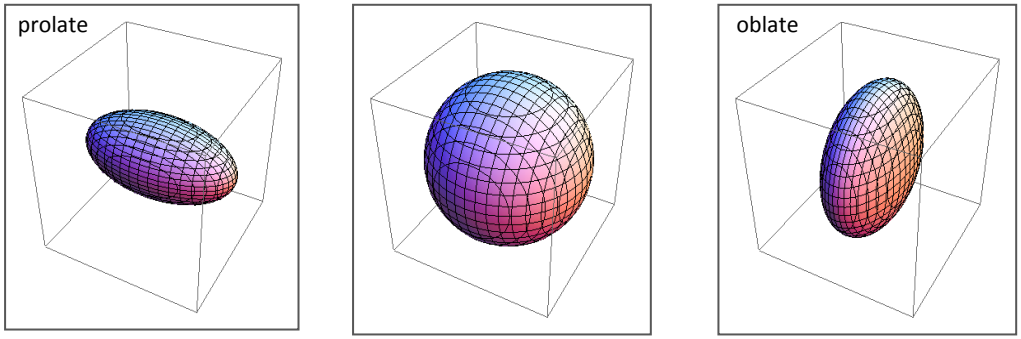

$-1 < \xi < 0$ $\quad$ $\xi = 0$ $\quad$ $\xi > 0$

Why spheroidal form at LO?

- What is special about this form at leading order? Can I choose any background distribution I like as the expansion point?

$$f_{\rm aniso}^{LRF} = f_{\rm iso}\left(\frac{\sqrt{\mathbf{p}^2 + \xi(\mathbf{x},\tau)p_z^2}}{\Lambda(\mathbf{x},\tau)}\right)$$

- Obviously can describe the ideal hydro limit when ξ=0 (Λ → T)
- For longitudinal (0+1d) free streaming, the Boltzmann equation can be solved analytically → LRF distribution function is of spheroidal form with

$$\xi_{\rm FS}(\tau) = (1+\xi_0)\left(\frac{\tau}{\tau_0}\right)^2 - 1$$

- Could also use ellipsoidal form etc (more discussion on this point later), but the spheroidal form is the simplest form that captures the largest components (see next slide) of the energy-momentum tensor
- Since $f_{iso} \geq 0$, the one-particle distribution function and bulk pressures are guaranteed to be ≥ 0 (not true in viscous hydro)

Hints from Viscous Hydro

H. Song, PhD Dissertation, 0908.3656

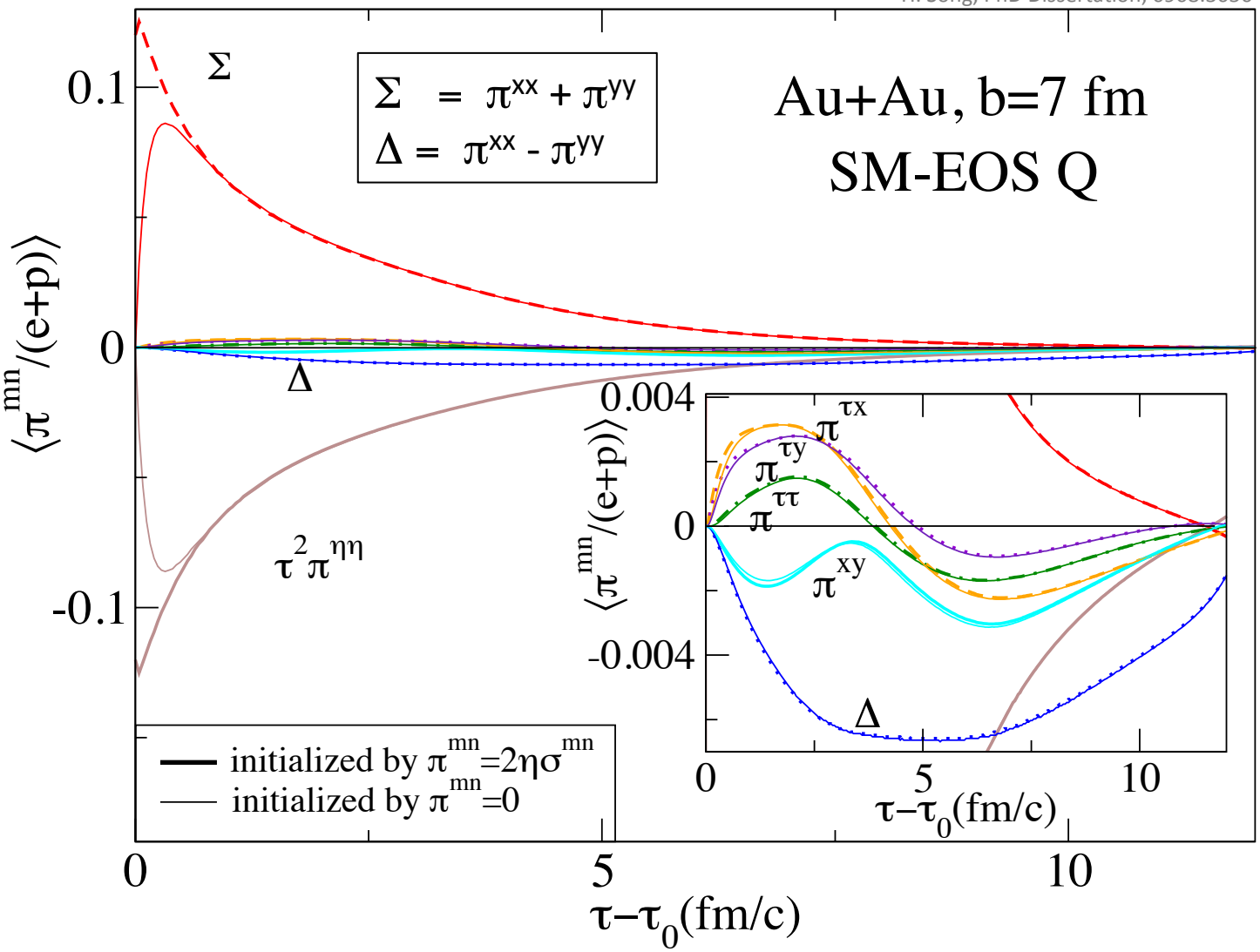

Anisotropic Hydrodynamics Basics

M. Martinez and MS, 1007.0889

Viscous Hydrodynamics Expansion

$$f(\tau,\mathbf{x},\mathbf{p}) = \underline{f_{\rm eq}(\mathbf{p},T(\tau,\mathbf{x}))} + \delta f$$

Isotropic in momentum space

Anisotropic Hydrodynamics Expansion

$$f(\tau,\mathbf{x},\mathbf{p}) = f_{\rm aniso}(\mathbf{p},\underbrace{\Lambda(\tau,\mathbf{x})}_{T_\perp},\underbrace{\xi(\tau,\mathbf{x})}_{\text{anisotropy}}) + \cancel{\delta\tilde{f}}$$

First, let's consider what happens when we ignore this term → "LO aHydro"

→ Assume spheroidal form in LRF

$$f^{LRF}_{\rm aniso} = f_{\rm iso}\left(\frac{\sqrt{\mathbf{p}^2+\xi(\mathbf{x},\tau)p_z^2}}{\Lambda(\mathbf{x},\tau)}\right)$$

$$\xi = \frac{\langle p_T^2\rangle}{2\langle p_L^2\rangle} - 1$$

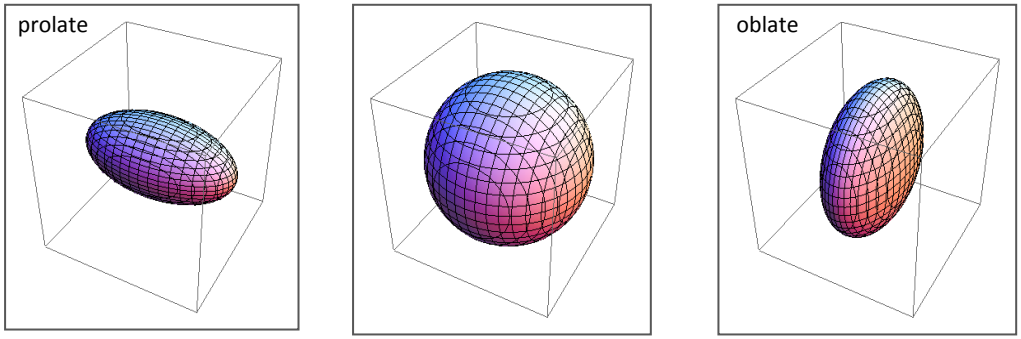

$-1 < \xi < 0$ $\quad$ $\xi = 0$ $\quad$ $\xi > 0$

Spheroidal Distribution Function

- Consider conformal system to start with
- In the conformal (massless) limit all bulk observables factorize into a product of two functions
- Note that, in the general case, it is also possible to define an anisotropic EOS

$$n(\Lambda,\xi) = \int \frac{d^3\mathbf{p}}{(2\pi)^3} f_{\rm aniso} = \frac{n_{\rm iso}(\Lambda)}{\sqrt{1+\xi}}$$

$$\mathcal{E}(\Lambda,\xi) = T^{\tau\tau} = \mathcal{R}(\xi)\,\mathcal{E}_{\rm iso}(\Lambda)$$

$$\mathcal{P}_\perp(\Lambda,\xi) = \frac{1}{2}\left(T^{xx}+T^{yy}\right) = \mathcal{R}_\perp(\xi)\mathcal{P}_{\rm iso}(\Lambda)$$

$$\mathcal{P}_L(\Lambda,\xi) = -T^{\varsigma}_{\varsigma} = \mathcal{R}_{\rm L}(\xi)\mathcal{P}_{\rm iso}(\Lambda)$$

$$\mathcal{R}(\xi) \equiv \frac{1}{2}\left(\frac{1}{1+\xi} + \frac{\arctan\sqrt{\xi}}{\sqrt{\xi}}\right)$$

$$\mathcal{R}_\perp(\xi) \equiv \frac{3}{2\xi}\left(\frac{1+(\xi^2-1)\mathcal{R}(\xi)}{\xi+1}\right)$$

$$\mathcal{R}_L(\xi) \equiv \frac{3}{\xi}\left(\frac{(\xi+1)\mathcal{R}(\xi)-1}{\xi+1}\right)$$

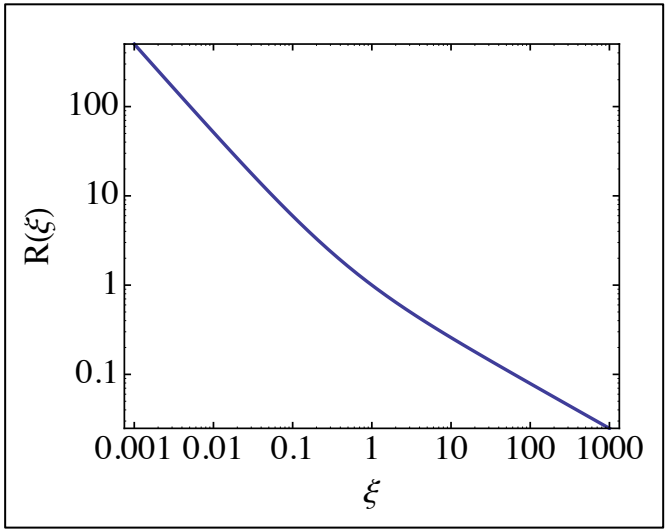

0+1d case – new Bjorken eqs

0th Moment of Boltzmann EQ

$$\partial_\alpha N^\alpha \neq 0$$

$$\frac{1}{1+\xi}\partial_\tau \xi - \frac{2}{\tau} - 6\,\partial_\tau \log\Lambda = 2\Gamma\left[1 - \mathcal{R}^{3/4}(\xi)\sqrt{1+\xi}\right]$$

1st Moment of Boltzmann EQ

$$\partial_\alpha T^{\alpha\beta} = 0$$

$$\frac{\mathcal{R}'(\xi)}{\mathcal{R}(\xi)}\partial_\tau \xi + 4\,\partial_\tau \log\Lambda = \frac{1}{\tau}\left[\frac{1}{\xi(1+\xi)\mathcal{R}(\xi)} - \frac{1}{\xi} - 1\right]$$

Where

$$\Gamma = \frac{2T(\tau)}{5\bar{\eta}} = \frac{2\mathcal{R}^{1/4}(\xi)\Lambda}{5\bar{\eta}}$$

$$\mathcal{R}(\xi) \equiv \frac{1}{2}\left(\frac{1}{1+\xi} + \frac{\arctan\sqrt{\xi}}{\sqrt{\xi}}\right)$$

$$\mathcal{E}(\Lambda,\xi) = \mathcal{R}(\xi)\mathcal{E}_{\rm iso}(\Lambda)$$

M. Martinez and MS, 1007.0889

Linearized Equations

If we expand the energy-momentum tensor to linear order in the anisotropy parameter and match to 2nd-order viscous hydro, we find

$$\frac{\Pi}{\mathcal{E}_{\rm eq}} = \frac{8}{45}\xi + \mathcal{O}(\xi^2)$$

If we similarly expand the coupled nonlinear differential equations to lowest order in the anisotropy parameter and rewrite in terms of the shear using the relation above, we obtain

$$\boxed{\begin{aligned} \partial_\tau \mathcal{E} &= -\frac{\mathcal{E}+\mathcal{P}}{\tau} + \frac{\Pi}{\tau} \\ \partial_\tau \Pi &= -\frac{\Pi}{\tau_\pi} + \frac{4}{3}\frac{\eta}{\tau_\pi \tau} - \frac{4}{3}\frac{\Pi}{\tau} \end{aligned}} \qquad \boxed{\begin{aligned} \Gamma &= \frac{2}{\tau_\pi} \\ \tau_\pi &= \frac{5}{4}\frac{\eta}{\mathcal{P}} \end{aligned}}$$

- Reproduces 2nd-order viscous hydro in the small anisotropy limit!
- Also correctly describes the free streaming limit!

Pressure Anisotropy

$$\frac{1}{1+\xi}\partial_\tau \xi - \frac{2}{\tau} - 6\,\partial_\tau \log\Lambda = 2\Gamma\left[1 - \mathcal{R}^{3/4}(\xi)\sqrt{1+\xi}\right]$$

$$\frac{\mathcal{R}'(\xi)}{\mathcal{R}(\xi)}\partial_\tau \xi + 4\,\partial_\tau \log\Lambda = \frac{1}{\tau}\left[\frac{1}{\xi(1+\xi)\mathcal{R}(\xi)} - \frac{1}{\xi} - 1\right]$$

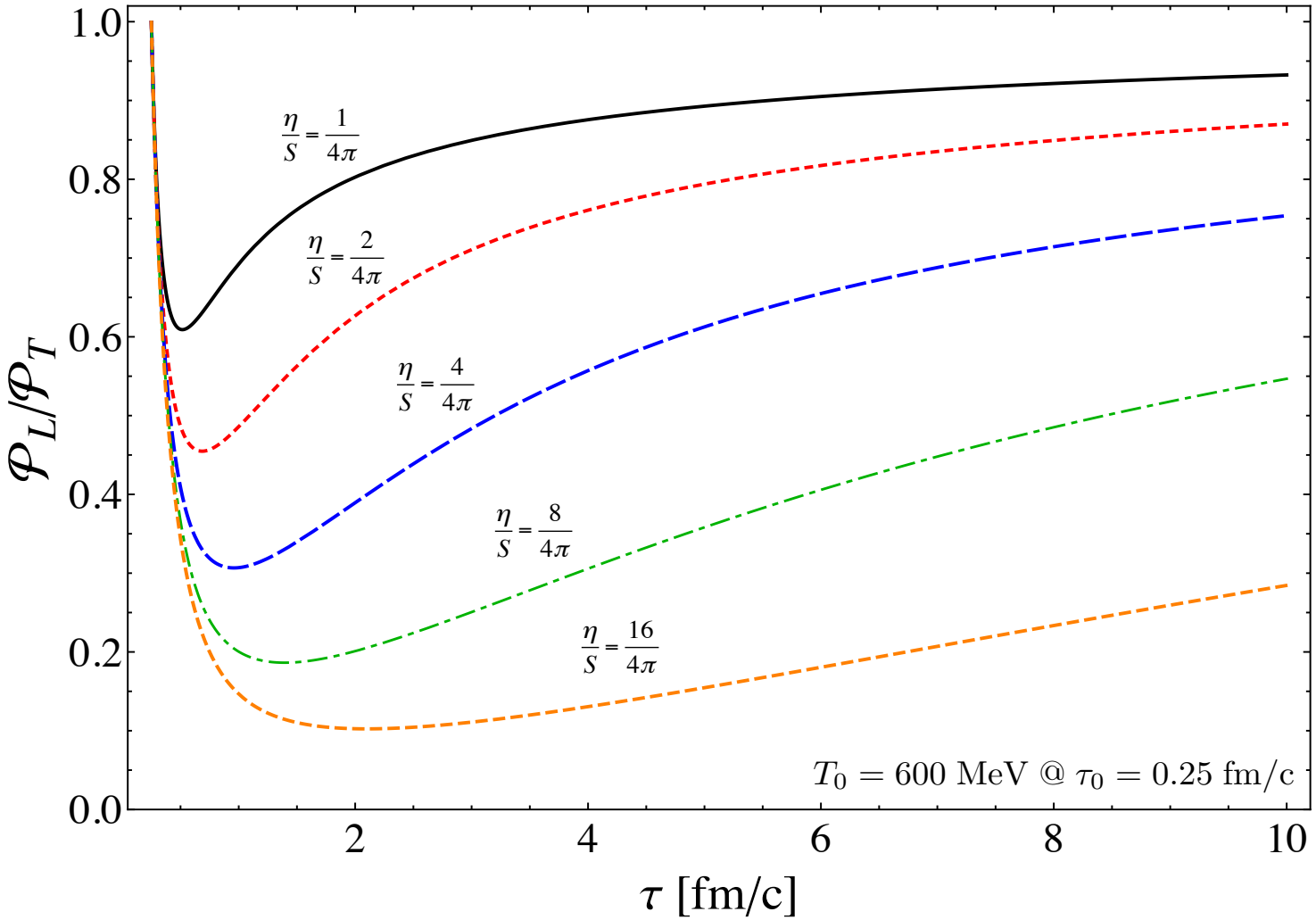

M. Strickland

Viscous Hydro vs LO aHydro

M. Martinez and MS, 1007.0889

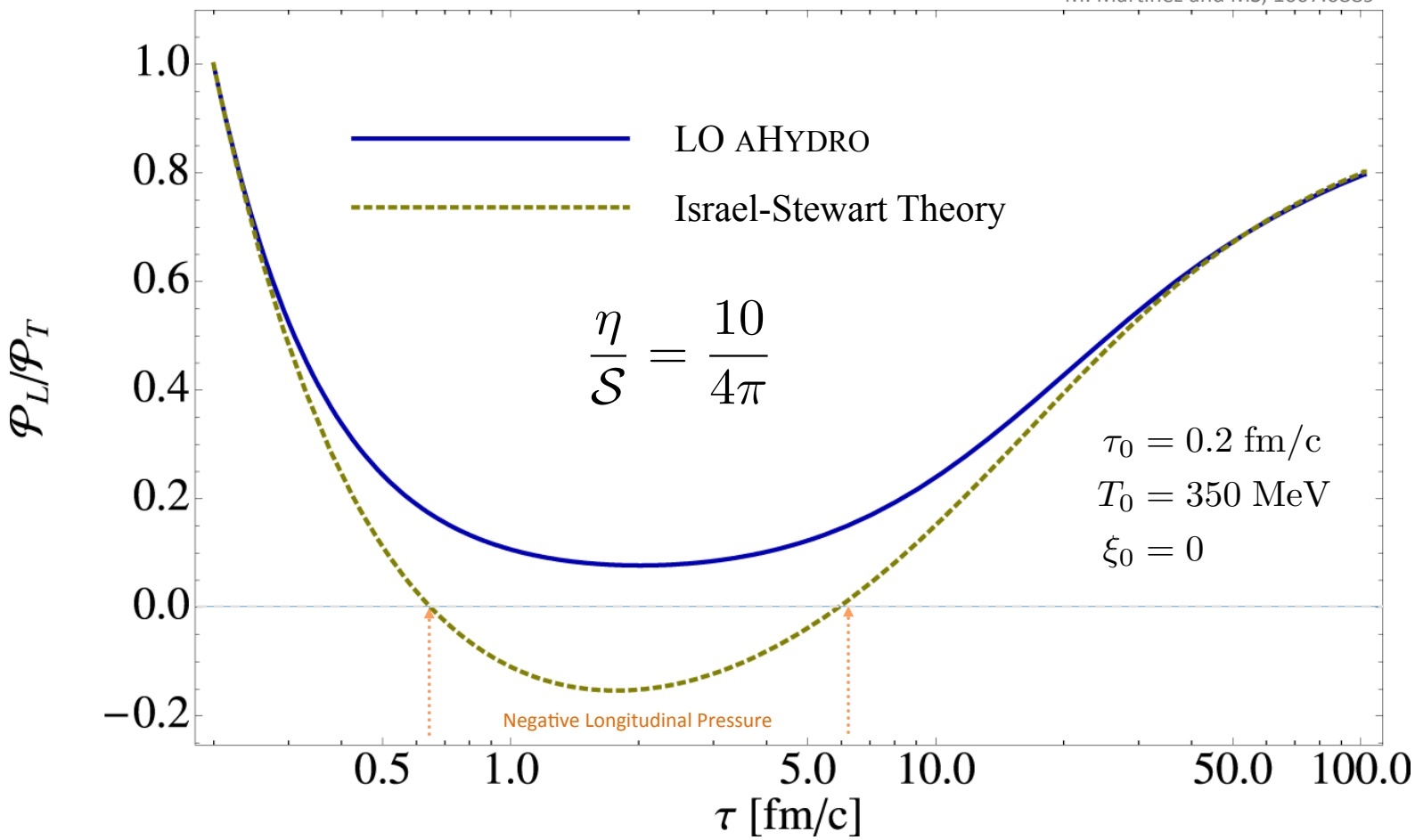

Transverse Dynamics

M. Martinez, R. Ryblewski, and MS, 1204.1473.

Pb-Pb @ 2.76 TeV
T_0 = 600 MeV
τ_0 = 0.25 fm/c
b = 7 fm

$$\frac{\eta}{\mathcal{S}} = \frac{1}{4\pi}$$

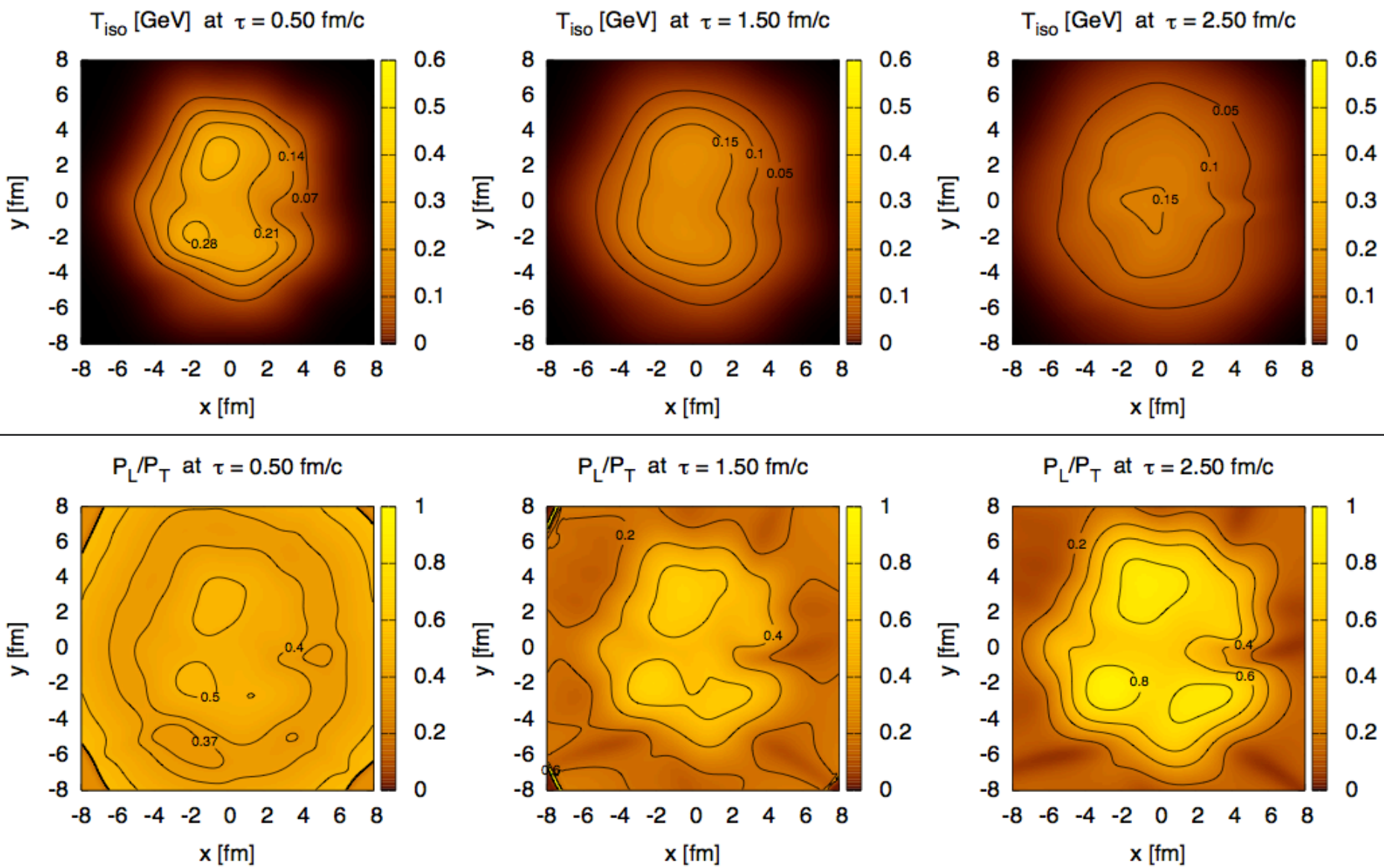

Anisotropic Hydrodynamics Basics

M. Martinez and MS, 1007.0889

Viscous Hydrodynamics Expansion

$$f(\tau, \mathbf{x}, \mathbf{p}) = \underline{f_{\rm eq}(\mathbf{p}, T(\tau, \mathbf{x}))} + \delta f$$

Isotropic in momentum space

Anisotropic Hydrodynamics Expansion

$$f(\tau, \mathbf{x}, \mathbf{p}) = f_{\rm aniso}(\mathbf{p}, \underbrace{\Lambda(\tau, \mathbf{x})}_{T_\perp}, \underbrace{\xi(\tau, \mathbf{x})}_{\text{anisotropy}}) + \delta \tilde{f}$$

Now try to treat this term "perturbatively"

See the next talk by U. Heinz

→ Assume spheroidal form in LRF

$$f^{LRF}_{\rm aniso} = f_{\rm iso}\left(\frac{\sqrt{\mathbf{p}^2 + \xi(\mathbf{x}, \tau) p_z^2}}{\Lambda(\mathbf{x}, \tau)}\right)$$

$$\xi = \frac{\langle p_T^2 \rangle}{2\langle p_L^2 \rangle} - 1$$

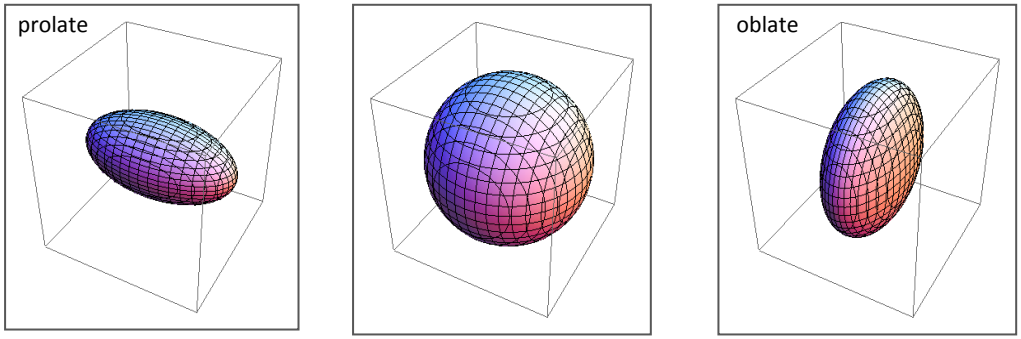

$-1 < \xi < 0$ $\quad$ $\xi = 0$ $\quad$ $\xi > 0$

Exact Solutions

- Simple model: Boost-invariant transversally homogeneous Boltzmann equation in relaxation time approximation (RTA)
- Many results in this model, so we can compare with the literature
- Can use this simple case to test the efficacy of different approximation schemes

Massless Particles
W. Florkowski, R. Ryblewski, and MS, arXiv:1304.0665 and arXiv:1305.7234

Massive Particles
W. Florkowski, E. Maksymiuk, R. Ryblewski, and MS, arXiv:1402.7348

Boltzmann EQ $$p^\mu \partial_\mu f(x,p) = C[f(x,p)]$$

RTA $$C[f] = \frac{p_\mu u^\mu}{\tau_{\rm eq}} \left[f_{\rm eq}\Big(p_\mu u^\mu, T(x)\Big) - f(x,p) \right]$$

Solution for the energy density (massless particle case)

$$\bar{\mathcal{E}}(\tau) = D(\tau,\tau_0)\,\frac{\mathcal{R}\big(\xi_{\rm FS}(\tau)\big)}{\mathcal{R}\left(\xi_0\right)} + \int_{\tau_0}^{\tau} \frac{d\tau'}{\tau_{\rm eq}(\tau')}\, D(\tau,\tau')\,\bar{\mathcal{E}}(\tau')\,\mathcal{R}\left(\left(\frac{\tau}{\tau'}\right)^2 - 1\right)$$

Time-dependent relaxtion time $\tau_{\rm eq}(\tau) = \dfrac{5\bar{\eta}}{T(\tau)}$	Damping Function $D(\tau_2,\tau_1) = \exp\left[-\int_{\tau_1}^{\tau_2} d\tau\, \tau_{\rm eq}^{-1}(\tau)\right]$

Exact Solutions

W. Florkowski, R. Ryblewski, and MS,
arXiv:1304.0665 and arXiv:1305.7234

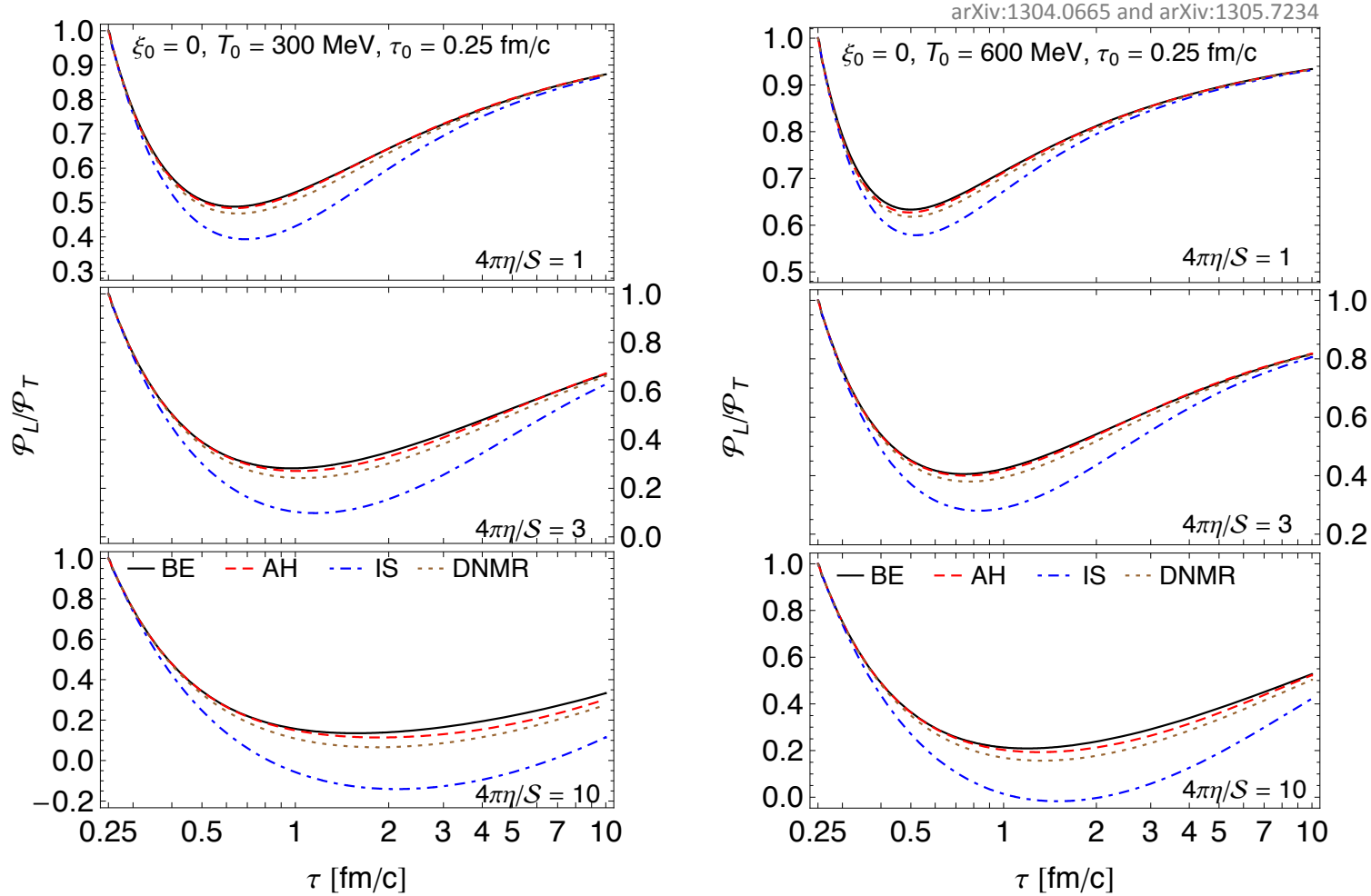

BE = Exact Solution AH = aHydro IS = Israel Stewart DNMR = Denicol et al, Phys. Rev. D 85, 114047 (2012)

Exact Solutions

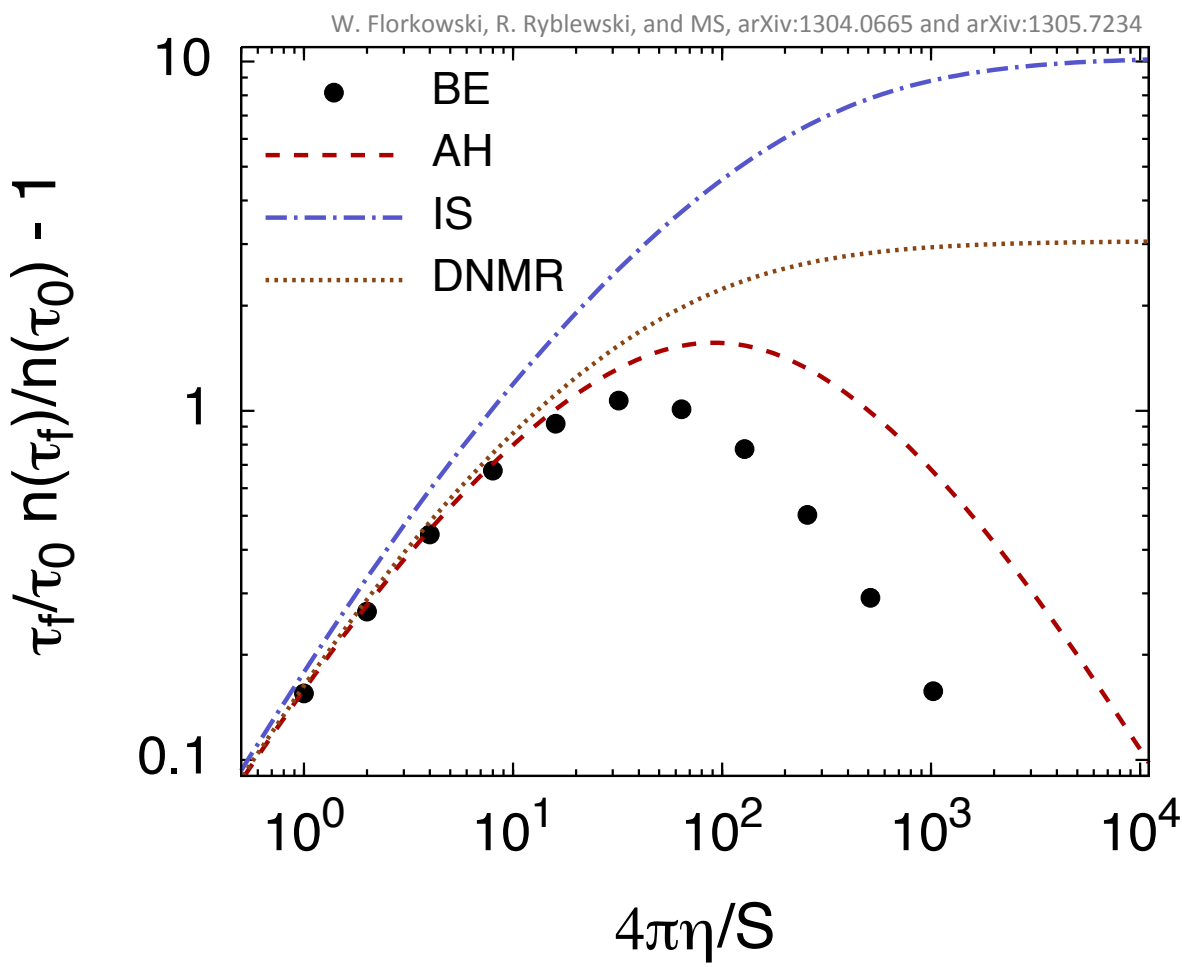

- Particle (entropy) production vanishes in two limits: ideal hydro and free streaming limits
- For conformal (massless) systems, the number density is proportional to entropy density
- **NLO spheroidal aHydro does even better! (see the next talk)**

Other recent developments

- Generalization of LO aHydro from spheroidal to ellipsoidal form + use of second moment of Boltzmann equation [Florkowski and Tinti, arXiv:1312.6614]

- Massive LO spheroidal and ellipsoidal formalisms
  [W. Florkowski, R. Ryblewski, MS, L. Tinti, arXiv:1403.1223]

- Finite mass only very weakly affects the pressure anisotropy

- Dynamical equations obtained from the second moment of the Boltzmann equation better reproduce the exact massive solution

- Work under way to include the off-diagonal anisotropies at LO and bulk pressure

$$f(x,p) = f_{\rm iso}\left(\frac{\sqrt{p^\mu \Xi_{\mu\nu}(x) p^\nu}}{\Lambda(x)}, \frac{\mu(x)}{\Lambda(x)}\right) \qquad \Xi^{\mu\nu} = u^\mu u^\nu + \xi^{\mu\nu} - \Delta^{\mu\nu}\Phi$$

Conclusions and Outlook

- Anisotropic hydrodynamics builds upon prior advances in relativistic hydrodynamics in an attempt to create an even more quantitatively reliable tool

- It incorporates some "facts of life" specific to the conditions generated in relativistic heavy ion collisions and, in doing so, optimizes the non-ideal hydrodynamics approach

- Having second-order anisotropic hydrodynamics (VAHYDRO) allows us to proceed to numerical modeling of heavy ion collisions

- The evolution of the matter (particularly at early times, near the transverse edges, or with large temperature-dependent η/S) should now be more reliably described

Quark production in classical statistical field theory

Naoto Tanji
RIKEN (-> BNL in May 2014)
collaboration with F. Gelis

RBRC Workshop
04/03/2014

Introduction

The time-evolution of Glasma toward isotropization and thermalization

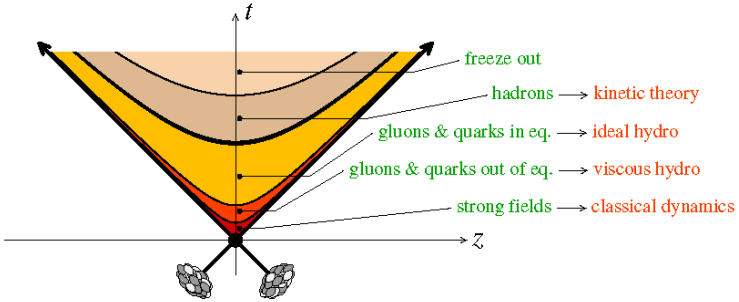

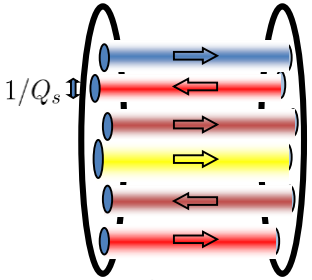

Glasma

large occupation number → classical dynamics

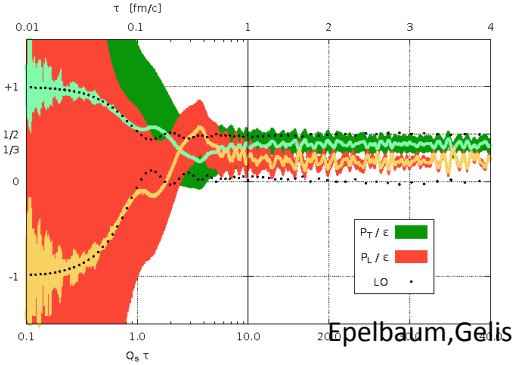

Epelbaum,Gelis (2013)

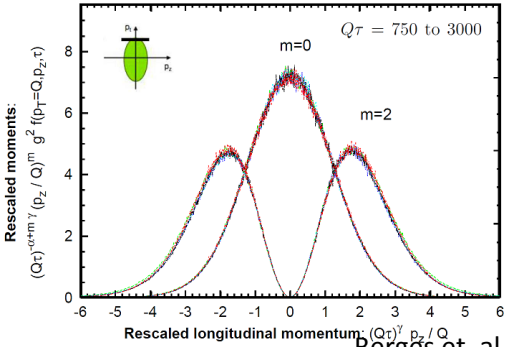

Berges et. al. (2013)

Classical statistical simulations of gluodynamics

How about quark production?

Quark production

CGC and glasma are almost purely gluonic matter.

How does the system reaches chemical equilibrium between light quarks and gluons?

Earlier works by F. Gelis, K. Kajantie and T. Lappi

PRC71, 024904(2005)
PRL96, 032304(2006)

- Limitation from numerical costs
- Treatment of the boost-invariance

There have been theoretical and technical advances on

- classical statistical method for over-occupied bosonic fields
- real-time lattice simulations of fermionic fields
- treatment of a boost-invariant system

Derivation of the classical statistical method

S. Jeon, PRC72, 014907 (2005); arXiv:1308.0263.

Compute $\langle 0_{\rm in}|\mathcal{O}|0_{\rm in}\rangle$ → the Schwinger-Keldysh (CTP) formalism

- gauge part
  - Generating functional

$$Z[J_+, J_-] = \int [dA^{i+} dA^{i-}]\, \rho[A^{i+}, A^{i-}] \int \mathcal{D}A^+ \mathcal{D}A^- e^{i\int d^4x [\mathcal{L}_{\rm SK} + J_+ A^+ - J_- A^-]}$$

  - SK Lagrangian

$$\mathcal{L}^{\rm SK}_{\rm gauge} = \mathcal{L}_{\rm gauge}[A^+] - \mathcal{L}_{\rm gauge}[A^-]$$

Derivation of the classical statistical method

S. Jeon, PRC72, 014907 (2005); arXiv:1308.0263.

Compute $\langle 0_{\rm in}|\mathcal{O}|0_{\rm in}\rangle$ → the Schwinger-Keldysh (CTP) formalism

- gauge part
  - Generating functional

$$Z[J_+,J_-]=\int\left[dA^{i+}dA^{i-}\right]\rho[A^{i+},A^{i-}]\int\mathcal{D}A^+\mathcal{D}A^-e^{i\int d^4x\left[\mathcal{L}_{\rm SK}+J_+A^+-J_-A^-\right]}$$

  - SK Lagrangian

$$\mathcal{L}^{\rm SK}_{\rm gauge}=\mathcal{L}_{\rm gauge}[A^+]-\mathcal{L}_{\rm gauge}[A^-]$$
$$=\left([D_\mu,F^{\mu\nu}]-J^\nu_{\rm ext}\right)^a\eta^a_\nu+\frac{ig}{4}[D_\mu,\eta_\mu]^a[\eta^\mu,\eta^\nu]^a$$

Change of variables

$$A^\mu=\frac{A^\mu_++A^\mu_-}{2}\qquad \eta^\mu=A^\mu_+-A^\mu_-$$

Derivation of the classical statistical method

S. Jeon, PRC72, 014907 (2005); arXiv:1308.0263.

Compute $\langle 0_{\rm in}|\mathcal{O}|0_{\rm in}\rangle$ → the Schwinger-Keldysh (CTP) formalism

☐ gauge part

- Generating functional

$$Z[J_+,J_-]=\int\left[dA^{i+}dA^{i-}\right]\rho[A^{i+},A^{i-}]\int\mathcal{D}A^+\mathcal{D}A^-e^{i\int d^4x\left[\mathcal{L}_{\rm SK}+J_+A^+-J_-A^-\right]}$$

- SK Lagrangian

$$\mathcal{L}^{\rm SK}_{\rm gauge}=\mathcal{L}_{\rm gauge}[A^+]-\mathcal{L}_{\rm gauge}[A^-]$$
$$=\boxed{\left([D_\mu,F^{\mu\nu}]-J^\nu_{\rm ext}\right)}^a\eta^a_\nu+\frac{ig}{4}[D_\mu,\eta_\mu]^a[\eta^\mu,\eta^\nu]^a$$

classical field equation

Change of variables

$$A^\mu=\frac{A^\mu_++A^\mu_-}{2}\qquad \eta^\mu=A^\mu_+-A^\mu_-$$

Derivation of the classical statistical method

- Classical approximation

Strong field → $A \gg \eta$

→ Neglect higher order terms in $\eta^\mu = A^\mu_+ - A^\mu_-$

$$\mathcal{L}^{\mathrm{SK}}_{\mathrm{gauge}} = \boxed{\left([D_\mu, F^{\mu\nu}] - J^\nu_{\mathrm{ext}}\right)}^a \eta^a_\nu + \frac{ig}{4}\cancel{[D_\mu, \eta_\mu]^a}\cancel{[\eta^\mu, \eta^\nu]^a}$$

classical field equation

Derivation of the classical statistical method

- Classical approximation

  Strong field → $A \gg \eta$

  → Neglect higher order terms in $\eta^\mu = A^\mu_+ - A^\mu_-$

$$\mathcal{L}^{\rm SK}_{\rm gauge} = \boxed{\left([D_\mu, F^{\mu\nu}] - J^\nu_{\rm ext}\right)}^a \eta^a_\nu + \frac{ig}{4}\cancel{[D_\mu, \eta_\mu]^a}\cancel{[\eta^\mu, \eta^\nu]^a}$$

classical field equation

- The path integration over η gives

$$\delta\left([D_\mu, F^{\mu\nu}] - J^\nu_{\rm ext}\right)$$

which constraints the field trajectory to the classical path.

- The integrations over initial fields contain some quantum effects (vacuum fluctuations)

Fermions and the classical statistical method

- quark part

Fermion's occupation number ≤ 1 → Fermions are always quantum.

$$\mathcal{L}_{\text{matter}} = \bar{\psi}\left(i\gamma^{\mu}D_{\mu} - m\right)\psi$$

$$\boxed{D_{\mu} = \partial_{\mu} + igA_{\mu}}$$

Fermions and the classical statistical method

☐ quark part

Fermion's occupation number ≤ 1 ➡ Fermions are always quantum.

$$\mathcal{L}_{\rm matter} = \bar{\psi}\left(i\gamma^\mu D_\mu - m\right)\psi$$

Quadratic fields can be integrated out.

$$D_\mu = \partial_\mu + igA_\mu$$

$$\int \mathcal{D}[\bar{\psi}_+, \bar{\psi}_-, \psi_+, \psi_-] e^{i\int d^4x \mathcal{L}^{SK}_{\rm matter}} = {\rm Det}\left[i(S_{\rm F}^+)^{-1}\right] {\rm Det}\left[i(S_{\rm F*}^-)^{-1}\right]]$$

$S_{\rm F}^+(x,y)$: time-ordered propagator dressed by the gauge field A_+

$S_{\rm F*}^-(x,y)$: anti-time-ordered propagator dressed by the gauge field A_-

- Expand the Dirac determinants w.r.t. η^μ

$$\mathrm{Det}\left[i(S_{\mathrm{F}}^{+})^{-1}\right]\mathrm{Det}\left[i(S_{\mathrm{F}*}^{-})^{-1}\right]$$
$$= \mathrm{Det}\left[i(S_{\mathrm{F}})^{-1}\right]\mathrm{Det}\left[i(S_{\mathrm{F}*})^{-1}\right] e^{-i\frac{g}{2}\mathrm{Tr}[(S_{\mathrm{F}}+S_{\mathrm{F}*})\gamma_\mu]\eta^\mu + \cancel{\mathcal{O}(\eta^2)}}$$

Propagator dressed by the averaged gauge field A^μ

- Expand the Dirac determinants w.r.t. η^μ

$$\mathrm{Det}\left[i(S_{\mathrm{F}}^{+})^{-1}\right]\mathrm{Det}\left[i(S_{\mathrm{F}*}^{-})^{-1}\right]$$
$$= \mathrm{Det}\left[i(S_{\mathrm{F}})^{-1}\right]\mathrm{Det}\left[i(S_{\mathrm{F}*})^{-1}\right] e^{\boxed{-i\frac{g}{2}\mathrm{Tr}[(S_{\mathrm{F}}+S_{\mathrm{F}*})\gamma_\mu]}\eta^\mu + \cancel{\mathcal{O}(\eta^2)}}$$

Propagator dressed by the averaged gauge field A^μ

- Integrate over η^μ

Classical Yang-Mills equation which couples to the quark current

$$\boxed{[D_\mu, F^{\mu\nu}] = J^\nu_{\mathrm{ext}} + J^\nu_{\mathrm{quark}}}$$

$$J^\nu_{\mathrm{quark}}(x) = i\frac{g}{2}\mathrm{Tr}[(S_{\mathrm{F}} + S_{\mathrm{F}*})\gamma^\nu]$$

- Expand the Dirac determinants w.r.t. η^μ

$$\mathrm{Det}\left[i(S_{\mathrm{F}}^{+})^{-1}\right]\mathrm{Det}\left[i(S_{\mathrm{F}*}^{-})^{-1}\right]$$
$$= \mathrm{Det}\left[i(S_{\mathrm{F}})^{-1}\right]\mathrm{Det}\left[i(S_{\mathrm{F}*})^{-1}\right] e^{\boxed{-i\frac{g}{2}\mathrm{Tr}[(S_{\mathrm{F}}+S_{\mathrm{F}*})\gamma_\mu]}\eta^\mu + \cancel{\mathcal{O}(\eta^2)}}$$

Propagator dressed by the averaged gauge field A^μ

- Integrate over η^μ

Classical Yang-Mills equation which couples to the quark current

$$\boxed{[D_\mu, F^{\mu\nu}] = J^\nu_{\mathrm{ext}} + J^\nu_{\mathrm{quark}}}$$

$$J^\nu_{\mathrm{quark}}(x) = i\frac{g}{2}\mathrm{Tr}[(S_{\mathrm{F}} + S_{\mathrm{F}*})\gamma^\nu]$$
$$= \frac{g}{2}\langle\Omega_{\mathrm{in}}|\left[\hat{\bar{\psi}}(x), \gamma^\nu\hat{\psi}(x)\right]|\Omega_{\mathrm{in}}\rangle$$

$\hat{\psi}(x)$ is a field operator satisfying the Dirac equation under the gauge field:

$$\boxed{[i\gamma^\mu(\partial_\mu + igA_\mu) - m]\,\hat{\psi}(x) = 0}$$

1. **Generate an ensemble of the initial gauge fields according to the Wigner function**

$$A^\mu(t_0, \mathbf{x}) = A^\mu_{\text{coherent}}(t_0, \mathbf{x}) + \sum_n \left[a^\mu_n(t_0, \mathbf{x}) c_n + a^{\mu\,*}_n(t_0, \mathbf{x}) c^*_n\right]$$

Gaussian random number $\langle c_n c^*_{n'} \rangle_{\text{ens}} = \frac{1}{2}\delta_{n,n'}$

2. **For each gauge configuration, solve the CYM equation and the Dirac equation as associated equations**

$$[D_\mu, F^{\mu\nu}] = J^\nu_{\text{ext}} + J^\nu_{\text{quark}}$$

$$[i\gamma^\mu(\partial_\mu + igA_\mu) - m]\,\hat{\psi}(x) = 0$$

3. **Take the ensemble average and the expectation values**

$$\langle \mathcal{O}(A) \rangle_{\text{ens}} \qquad \langle \Omega_{\text{in}} | \hat{\mathcal{O}}(\psi) | \Omega_{\text{in}} \rangle$$

1. **Generate an ensemble of the initial gauge fields according to the Wigner function**

$$A^\mu(t_0, \mathbf{x}) = A^\mu_{\text{coherent}}(t_0, \mathbf{x}) + \sum_n \left[\cancel{a^\mu_n(t_0, \mathbf{x}) c_n + a^{\mu *}_n(t_0, \mathbf{x}) c^*_n} \right]$$

pure classical approximation for gauge fields as a first step

2. **For each gauge configuration, solve the CYM equation and the Dirac equation as associated equations**

$$[D_\mu, F^{\mu\nu}] = J^\nu_{\text{ext}} + \cancel{J^\nu_{\text{quark}}}$$

Neglecting the back-reaction

$$[i\gamma^\mu(\partial_\mu + igA_\mu) - m]\,\hat{\psi}(x) = 0$$

3. **Take the ensemble average and the expectation values**

$$\mathcal{O}(A) \qquad \langle \Omega_{\text{in}} | \hat{\mathcal{O}}(\psi) | \Omega_{\text{in}} \rangle$$

Setup

☐ gauge fields

- SU(2)
- boost-invariant classical fields without fluctuations
- generated by colliding CGCs with the McLerran-Venugopalan model
- in the forward light cone, solve the classical YM eq. numerically
- no back reaction

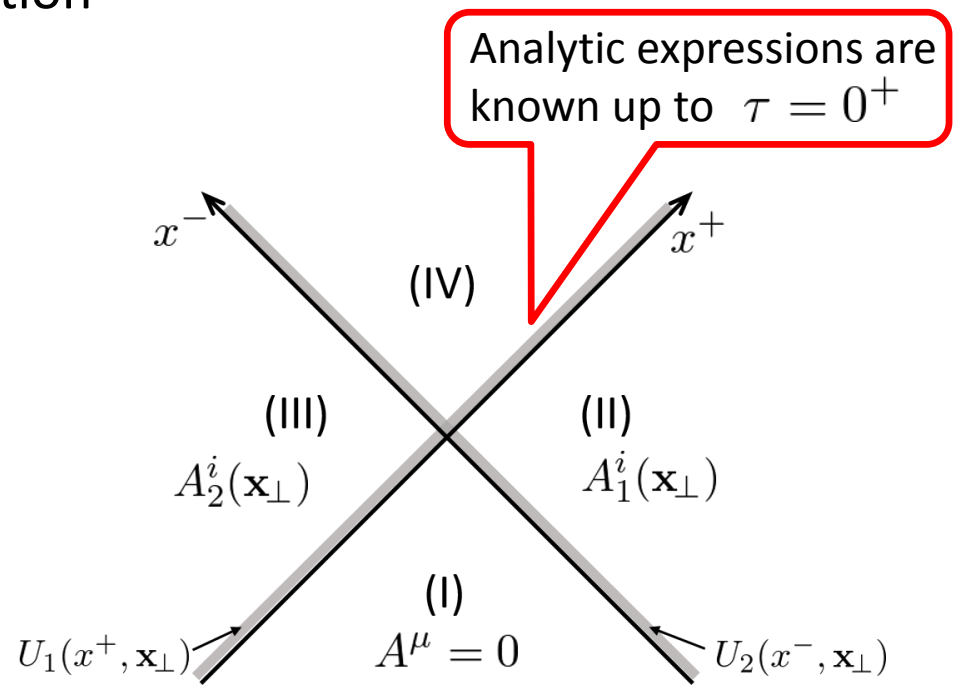

Setup

☐ quark fields

- obey the Dirac equation

$$[i\gamma^\mu(\partial_\mu + igA_\mu) - m]\,\hat{\psi}(x) = 0$$

- free fields in the region (I)
- in the forward light cone, solve the Dirac eq. numerically

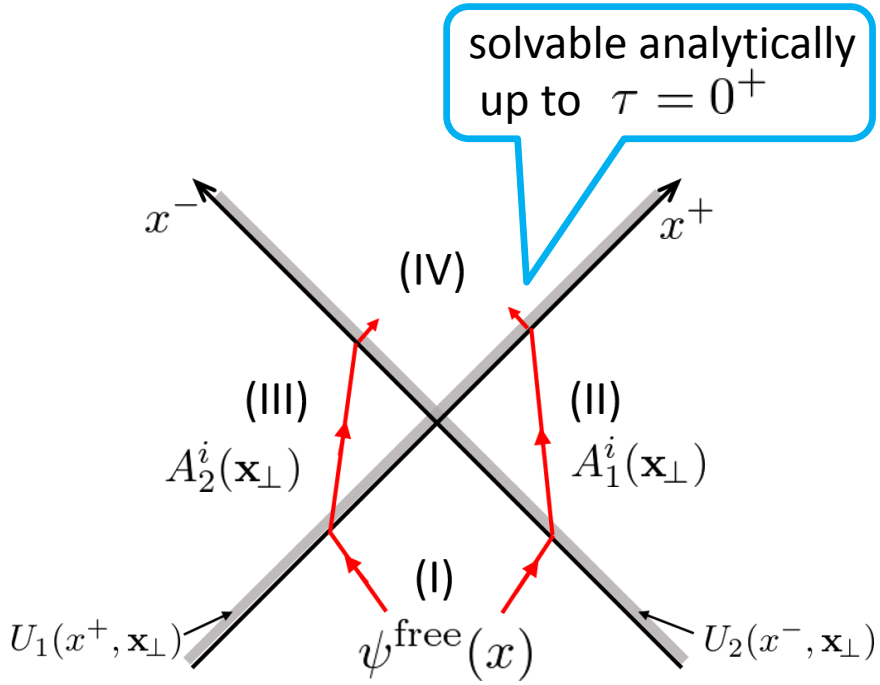

Computing fermion contributions

- Mode functions approach Aarts, Smit 1998

$$[i\gamma^\mu(\partial_\mu + igA_\mu) - m]\,\hat{\psi}(x) = 0$$

linear in the Dirac field

$$\hat{\psi}(x) = \sum_s \int d^3p\,[\psi^+_{\mathbf{p},s}(x)a_{\mathbf{p},s} + \psi^-_{\mathbf{p},s}(x)b^\dagger_{\mathbf{p},s}]$$

$\psi^\pm_{\mathbf{p},s}(x)$: mode functions, c-number solutions of the Dirac eq.

$$[i\gamma^\mu(\partial_\mu + igA_\mu) - m]\,\psi^\pm_{\mathbf{p},s}(x) = 0 \qquad \lim_{t\to-\infty}\psi^\pm_{\mathbf{p},s}(x) = \psi^{\mathrm{free},\pm}_{\mathbf{p},s}(x)$$

$$J^\mu_{\mathrm{quark}} = \frac{g}{2}\langle 0|\left[\hat{\bar{\psi}}(x), \gamma^\mu\hat{\psi}(x)\right]|0\rangle$$

$$= -\frac{g}{2}\sum_s \int d^3p\,\{\bar{\psi}^+_{\mathbf{p},s}(x)\gamma^\mu\psi^+_{\mathbf{p},s}(x) - \bar{\psi}^-_{\mathbf{p},s}(x)\gamma^\mu\psi^-_{\mathbf{p},s}(x)\}$$

With the c-number mode functions, expectation values can be computed.

Computing fermion contributions

- Mode functions approach Aarts, Smit 1998

$$[i\gamma^\mu(\partial_\mu + igA_\mu) - m]\,\hat{\psi}(x) = 0$$

linear in the Dirac field

$$\hat{\psi}(x) = \sum_s \int d^3p\,[\psi^+_{\mathbf{p},s}(x)a_{\mathbf{p},s} + \psi^-_{\mathbf{p},s}(x)b^\dagger_{\mathbf{p},s}]$$

$\psi^\pm_{\mathbf{p},s}(x)$: mode functions, c-number solutions of the Dirac eq.

$$[i\gamma^\mu(\partial_\mu + igA_\mu) - m]\,\psi^\pm_{\mathbf{p},s}(x) = 0 \qquad \lim_{t\to-\infty}\psi^\pm_{\mathbf{p},s}(x) = \psi^{\mathrm{free},\pm}_{\mathbf{p},s}(x)$$

$$J^\mu_{\mathrm{quark}} = \frac{g}{2}\langle 0|\left[\hat{\bar{\psi}}(x), \gamma^\mu\hat{\psi}(x)\right]$$

$$= -\frac{g}{2}\sum_s \int d^3p\,\{\bar{\psi}^+_{\mathbf{p},s}(x \qquad \psi^-_{\mathbf{p},s}(x)\}$$

Numerical cost

$$N_t \times N^2_{\mathrm{latt}}$$

expensive in 3+1dim.

With the c-number mode functions, expectation values can be computed.

Monte Carlo method with male and female stochastic fields

Borsanyi, Hindmarsh 2009

- Male and female fields
  - initial condition

$$\psi_{\mathrm{M}}(t_0, \mathbf{x}) = \sum_s \int d^3p \left[\psi^+_{\mathbf{p},s}(t_0, \mathbf{x}) c_{\mathbf{p},s} + \psi^-_{\mathbf{p},s}(t_0, \mathbf{x}) d_{\mathbf{p},s}\right]$$

$$\psi_{\mathrm{F}}(t_0, \mathbf{x}) = \sum_s \int d^3p \left[\psi^+_{\mathbf{p},s}(t_0, \mathbf{x}) c_{\mathbf{p},s} - \psi^-_{\mathbf{p},s}(t_0, \mathbf{x}) d_{\mathbf{p},s}\right]$$

  - evolution equation

$$\left[i\gamma^\mu(\partial_\mu + igA_\mu) - m\right]\psi_{\mathrm{M,F}}(x) = 0$$

- Gaussian random numbers

$$\langle c_{\mathbf{p},s} c^*_{\mathbf{p}',s'}\rangle = \langle d_{\mathbf{p},s} d^*_{\mathbf{p}',s'}\rangle = \frac{1}{2}\delta_{s,s'}\delta^3(\mathbf{p} - \mathbf{p}')$$

☐ Monte Carlo method with male and female stochastic fields

Borsanyi, Hindmarsh 2009

- ➢ Male and female fields
  - initial condition

$$\psi_{\mathrm{M}}(t_0,\mathbf{x}) = \sum_s \int d^3p \left[\psi^+_{\mathbf{p},s}(t_0,\mathbf{x})c_{\mathbf{p},s} + \psi^-_{\mathbf{p},s}(t_0,\mathbf{x})d_{\mathbf{p},s}\right]$$

$$\psi_{\mathrm{F}}(t_0,\mathbf{x}) = \sum_s \int d^3p \left[\psi^+_{\mathbf{p},s}(t_0,\mathbf{x})c_{\mathbf{p},s} - \psi^-_{\mathbf{p},s}(t_0,\mathbf{x})d_{\mathbf{p},s}\right]$$

  - evolution equation

$$\left[i\gamma^\mu(\partial_\mu + igA_\mu) - m\right]\psi_{\mathrm{M,F}}(x) = 0$$

- ➢ Gaussian random numbers

$$\langle c_{\mathbf{p},s}c^*_{\mathbf{p}',s'}\rangle = \langle d_{\mathbf{p},s}d^*_{\mathbf{p}',s'}\rangle = \frac{1}{2}\delta_{s,s'}\delta^3(\mathbf{p}-\mathbf{p}')$$

The expectation value can be reproduced by male-female ensemble average.

$$-g\langle\bar\psi_{\mathrm{M}}(x)\gamma^\mu\psi_{\mathrm{F}}\rangle = -\frac{g}{2}\sum_s\int d^3p\left\{\bar\psi^+_{\mathbf{p},s}(x)\gamma^\mu\psi^+_{\mathbf{p},s}(x) - \bar\psi^-_{\mathbf{p},s}(x)\gamma^\mu\psi^-_{\mathbf{p},s}(x)\right\}$$

$$= J^\mu_{\mathrm{quark}}$$

☐ Monte Carlo method with male and female stochastic fields

Borsanyi, Hindmarsh 2009

- Male and female fields
  - initial condition

$$\psi_{\mathrm{M}}(t_0,\mathbf{x}) = \sum_s \int d^3p \left[\psi^+_{\mathbf{p},s}(t_0,\mathbf{x})c_{\mathbf{p},s} + \psi^-_{\mathbf{p},s}(t_0,\mathbf{x})d_{\mathbf{p},s}\right]$$

$$\psi_{\mathrm{F}}(t_0,\mathbf{x}) = \sum_s \int d^3p \left[\psi^+_{\mathbf{p},s}(t_0,\mathbf{x})c_{\mathbf{p},s} - \psi^-_{\mathbf{p},s}(t_0,\mathbf{x})d_{\mathbf{p},s}\right]$$

  - evolution equation

$$\left[i\gamma^\mu(\partial_\mu + igA_\mu) - m\right]\psi_{\mathrm{M,F}}(x) = 0$$

- Gaussian random numbers

$$\langle c_{\mathbf{p},s}c^*_{\mathbf{p}',s'}\rangle = \langle d_{\mathbf{p},s}d^*_{\mathbf{p}',s'}\rangle = \frac{1}{2}\delta_{s,s'}\delta^3(\mathbf{p}-\mathbf{p}')$$

The expectation value can be reproduced by male-female ensemble average.

$$-g\langle\bar\psi_{\mathrm{M}}(x)\gamma^\mu\psi_{\mathrm{F}}\rangle = -\frac{g}{2}\sum_s\int d^3p\left\{\bar\psi^+_{\mathbf{p},s}(x)\gamma^\mu\psi^+_{\mathbf{p},s}(x) - \bar\psi^-_{\mathbf{p},s}(x)\gamma^\mu\psi^-_{\mathbf{p},s}(x)\right\}$$

$$= J^\mu_{\mathrm{quark}}$$

The male-female combination is necessary to get this minus sign which originates in anti-commutativity.

☐ Monte Carlo method with male and female stochastic fields

Borsanyi, Hindmarsh 2009

- ➢ Male and female fields
  - initial condition

$$\psi_{\mathrm{M}}(t_0,\mathbf{x}) = \sum_s \int d^3p \left[\psi^+_{\mathbf{p},s}(t_0,\mathbf{x})c_{\mathbf{p},s} + \psi^-_{\mathbf{p},s}(t_0,\mathbf{x})d_{\mathbf{p},s}\right]$$

$$\psi_{\mathrm{F}}(t_0,\mathbf{x}) = \sum_s \int d^3p \left[\psi^+_{\mathbf{p},s}(t_0,\mathbf{x})c_{\mathbf{p},s} - \psi^-_{\mathbf{p},s}\right.$$

Numerical cost

$$N_{\mathrm{config}} \times N_{\mathrm{latt}}^2$$

  - evolution equation

$$\left[i\gamma^\mu(\partial_\mu + igA_\mu) - m\right]\psi_{\mathrm{M,F}}(x) = 0$$

- ➢ Gaussian random numbers

$$\langle c_{\mathbf{p},s}c^*_{\mathbf{p}',s'}\rangle = \langle d_{\mathbf{p},s}d^*_{\mathbf{p}',s'}\rangle = \frac{1}{2}\delta_{s,s'}\delta^3(\mathbf{p}-\mathbf{p}')$$

$$N_{\mathrm{config}} \times N_t \times N_{\mathrm{latt}}$$

The expectation value can be reproduced by male-female ensemble average.

$$-g\langle\bar\psi_{\mathrm{M}}($$

$$^\mu\psi^-_{\mathbf{p},s}(x)\}$$

Total cost

$$N_{\mathrm{config}} \times N_{\mathrm{latt}} \times (N_{\mathrm{latt}} + N_t) \ll N_t \times N_{\mathrm{latt}}^2$$

if $N_{\mathrm{config}} \ll N_{\mathrm{latt}}$ and $N_{\mathrm{config}} \ll N_t$

necessary to get this minus sign which originates in anti-commutativity.

Benchmark --- QED uniform and constant electric field

Schwinger mechanism particle pair production

$$m = 0.1$$
$$N_x = N_y = 32$$
$$N_z = 128$$
$$N_{\text{config}} = 256$$
$$L_x = L_y = L_z = 10.$$

scaled by eE

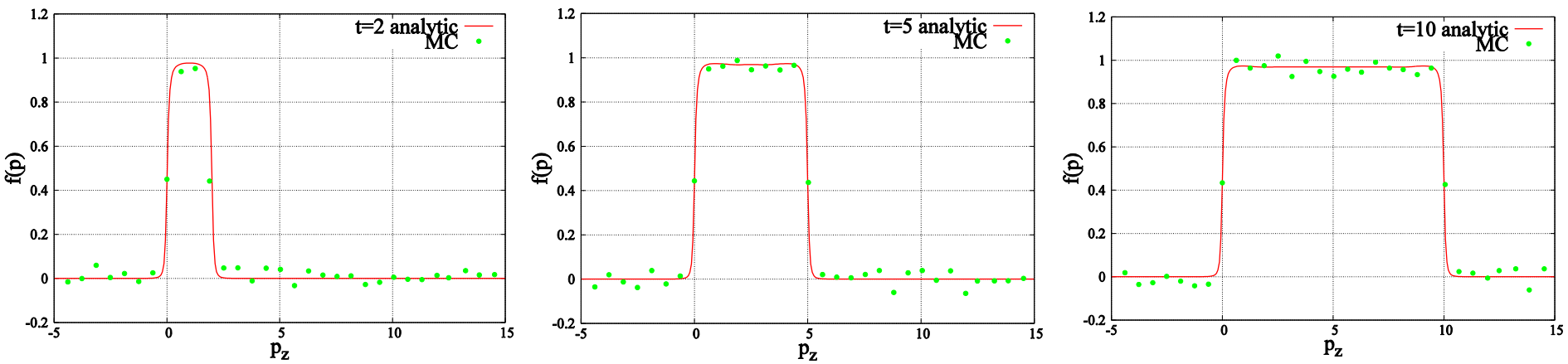

Comparison between the analytic and MC results

The MC method well reproduces the analytic results.

McLerran-Venugopalan initial condition

Random color sources

$$\langle \rho^{(n)}(x_\perp)\rho^{(m)}(x'_\perp)\rangle = g^2\mu^2\delta^{nm}\delta(x_\perp - x'_\perp)$$

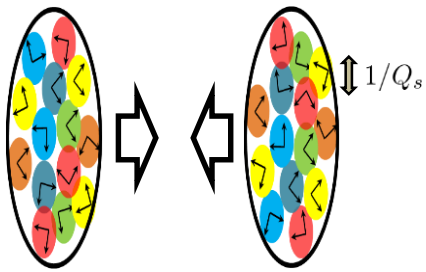

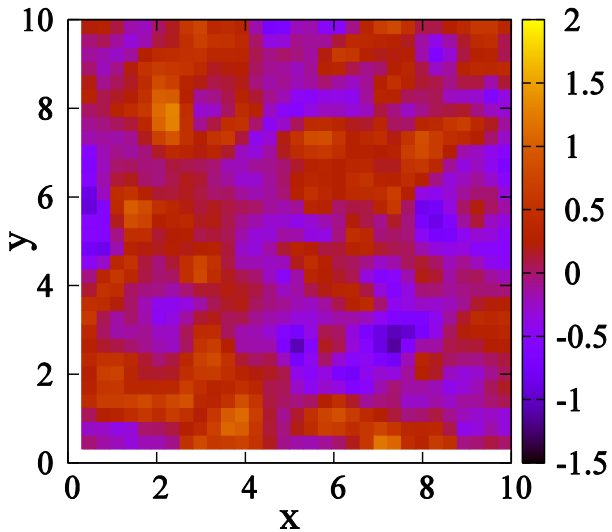

Initial electric field configuration

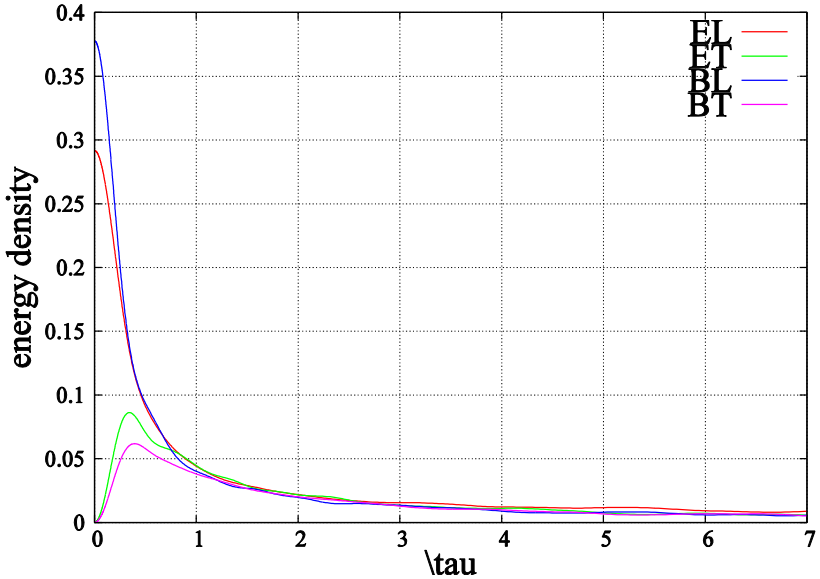

The time-evolution of energy density

All dimensionful quantities are scaled by $g^2\mu$.

Transverse spectra of produced quarks

$$N_x = N_y = 32$$
$$N_\eta = 128$$
$$N_{\rm config} = 256$$
$$L_x = L_y = 10.$$
$$L_\eta = 20.$$

scaled by $g^2\mu$

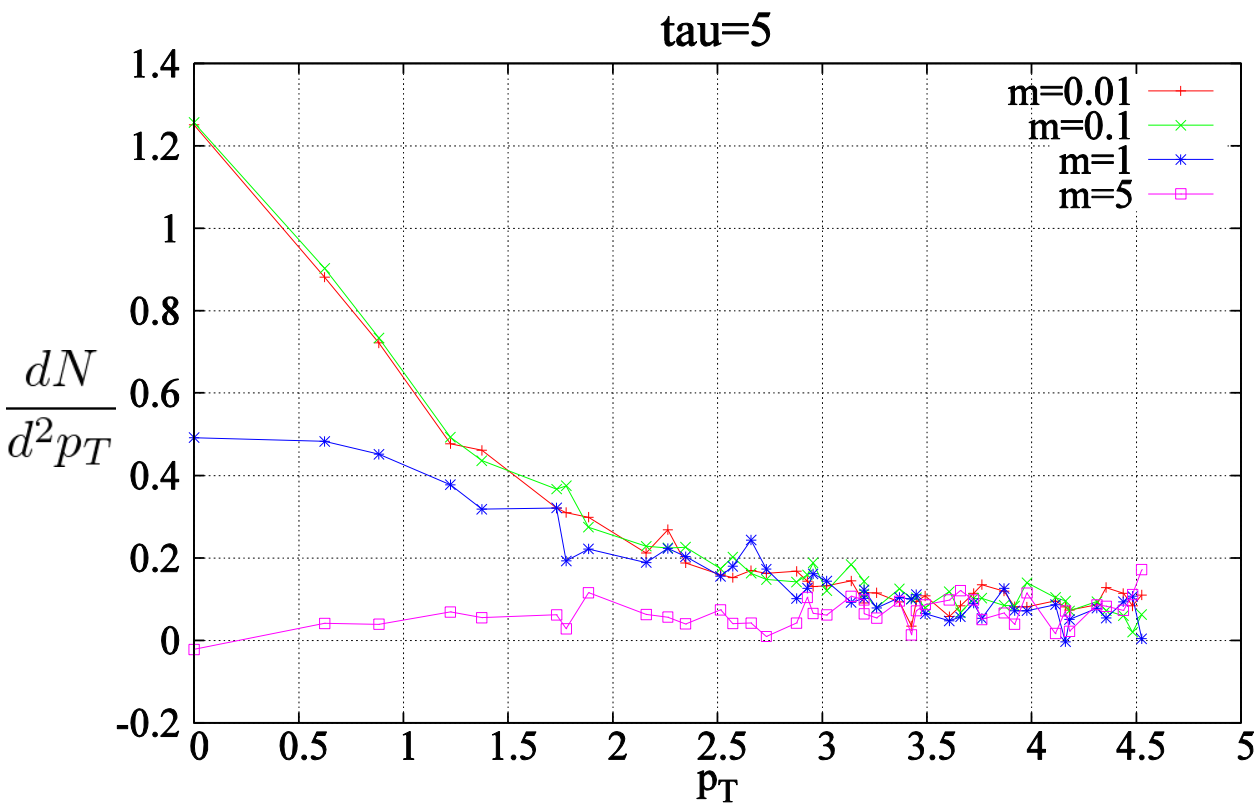

mass dependence of the transverse spectra

Transverse spectra of produced quarks

$N_x = N_y = 32$
$N_\eta = 128$
$N_{\rm config} = 256$
$L_x = L_y = 10.$
$L_\eta = 20.$
scaled by $g^2\mu$

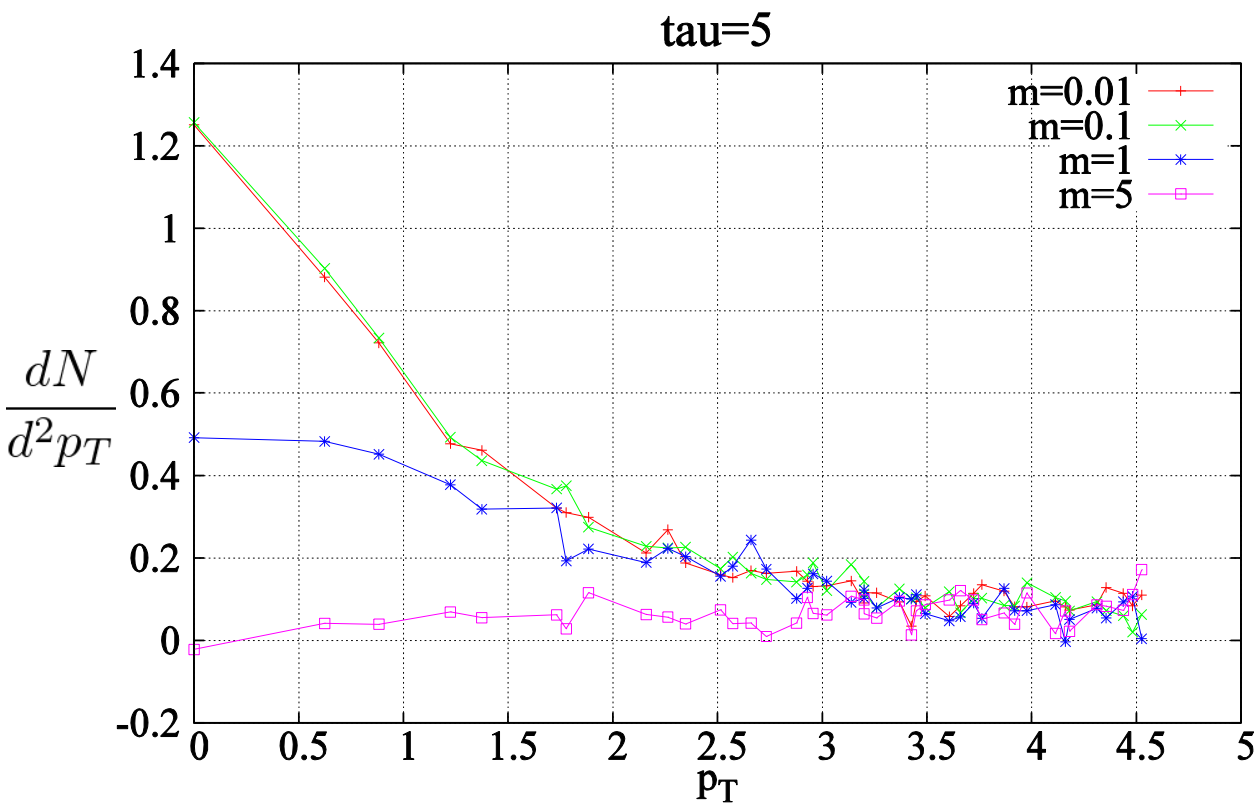

$1/p_{\rm T}^4$ spectra?

mass dependence of the transverse spectra

Energy density

$$N_x = N_y = 32$$
$$N_\eta = 128$$
$$N_{\text{config}} = 256$$
$$L_x = L_y = 10.$$
$$L_\eta = 20.$$

scaled by $g^2\mu$

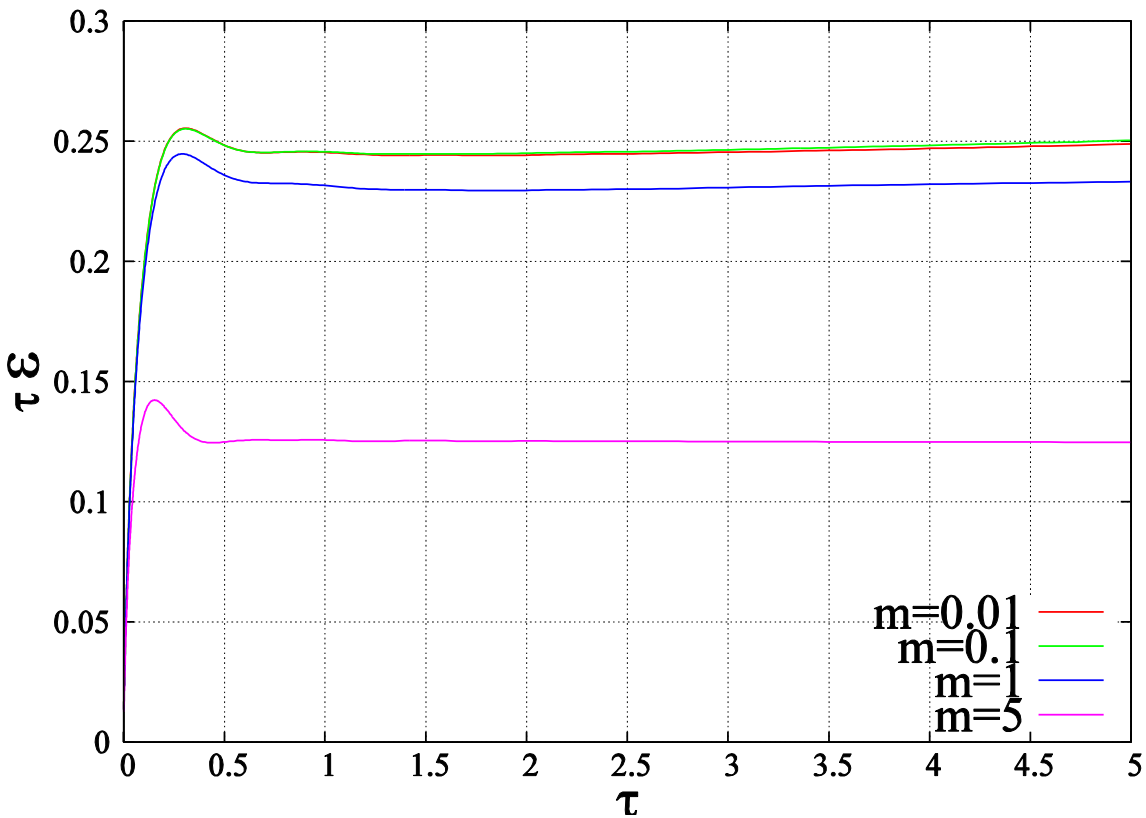

time evolution of $\tau\mathcal{E}$

Energy density

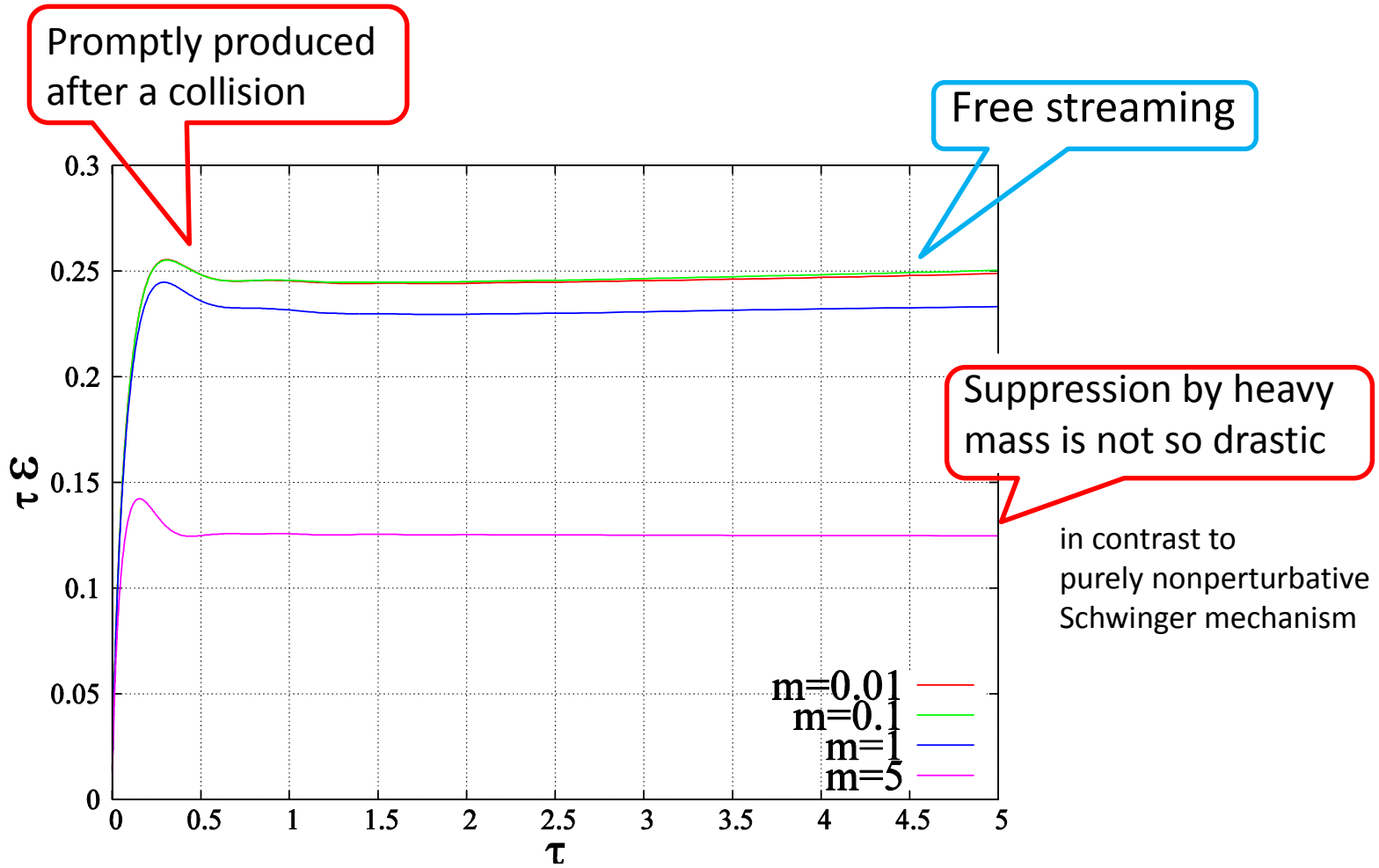

time evolution of $\tau\mathcal{E}$

Summary

- Fermion dynamics can be embedded in classical statistical simulations for gluons.
- The MC method enables us to simulate fermion dynamics in inhomogeneous classical gauge fields.
- The quark production in expanding gauge fields with the MV initial condition is computed.
- Quarks are promptly produced after a collision of color glass condensates.

Fluctuation-dissipation in equilibrating SYM plasma

Derek Teaney

Stony Brook University

- Simon Caron-Huot, DT, Paul Chesler; PRD, arXiv:1102.1073
- Paul Chesler and DT; arXiv:1112.6196
- Paul Chesler and DT; arXiv:1211.0343

Fluctuation-dissipation: problem setup

Non-equilibrium setup in 4D: (Chesler-Yaffe)

1. Chesler and Yaffe turn on a strong gravitational pulse in “our” world

$$ds^2 = -dt^2 + e^{B_o(t)} d\mathbf{x}_\perp^2 + e^{-2B_o(t)} dx_\parallel^2$$

where

$$B_o(t) \propto e^{-t^2/\Delta t^2}$$

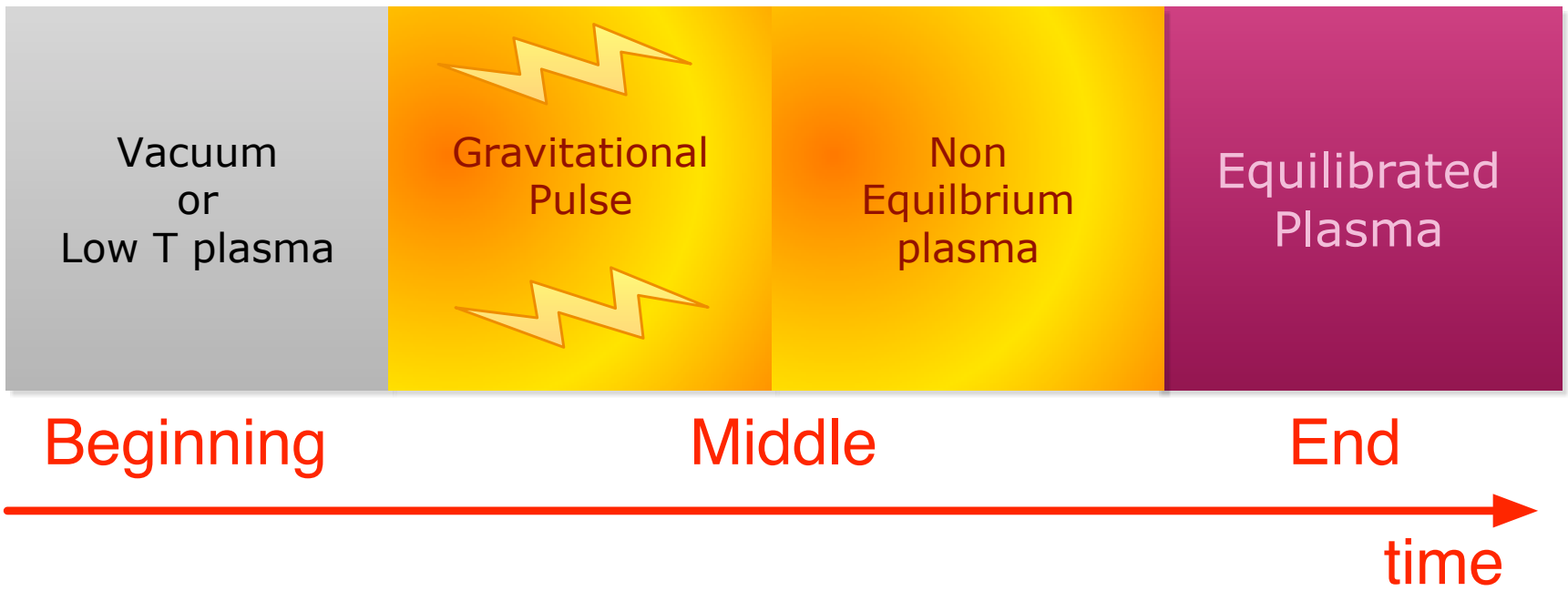

The boundary stress tensor

- The energy density increases by 50 times for a gaussian pulse with $\Delta t = 1/\pi T_{\rm f}$

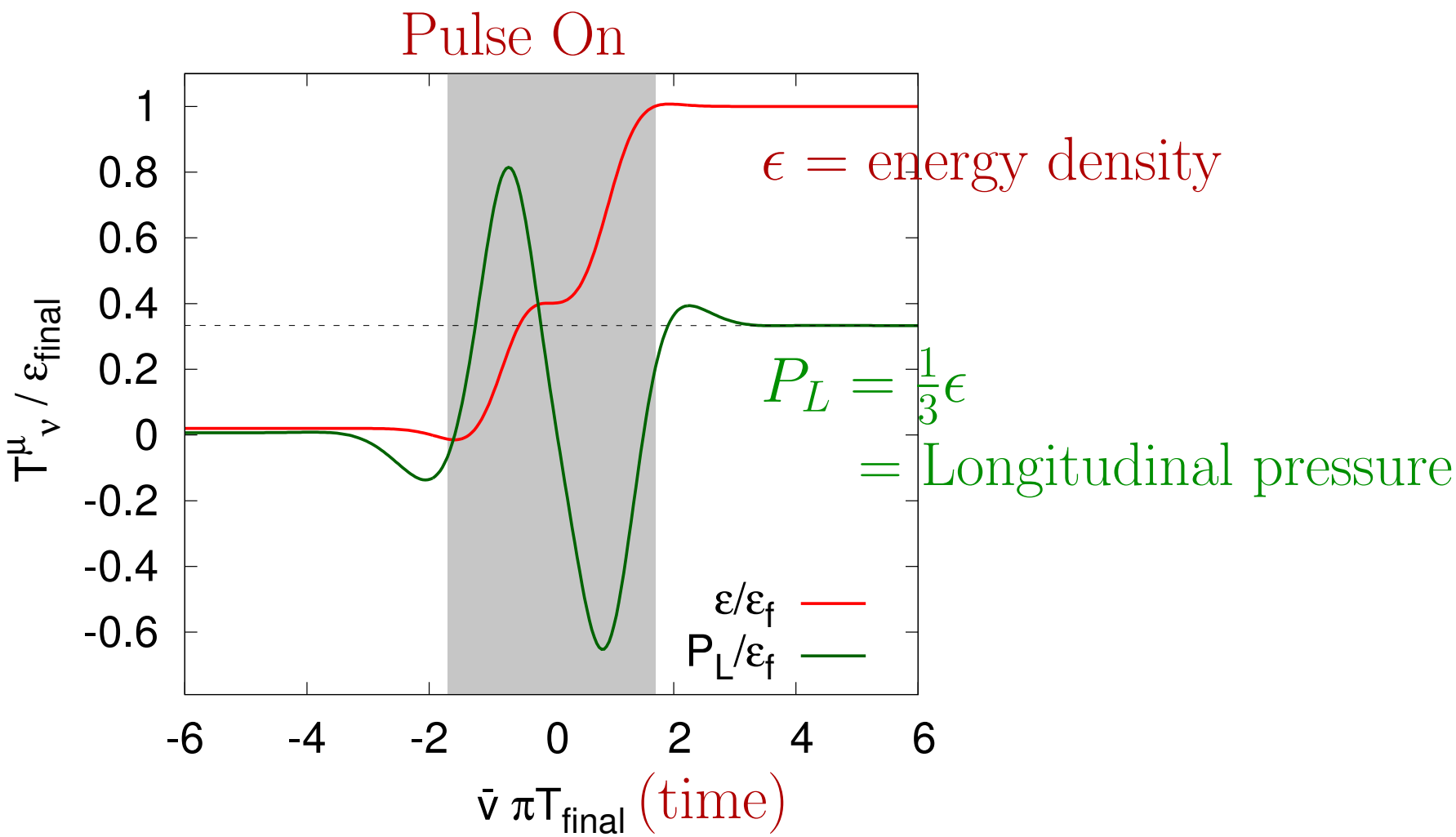

$T^\mu_\nu = \mathrm{diag}(\mathcal{E}, \mathcal{P}_T, \mathcal{P}_T, \mathcal{P}_L)$ (Effect. temperature)$^{-1} = \beta_{\rm eff}(v) \propto \mathcal{E}^{-1/4}$

My Goal and Motivation:

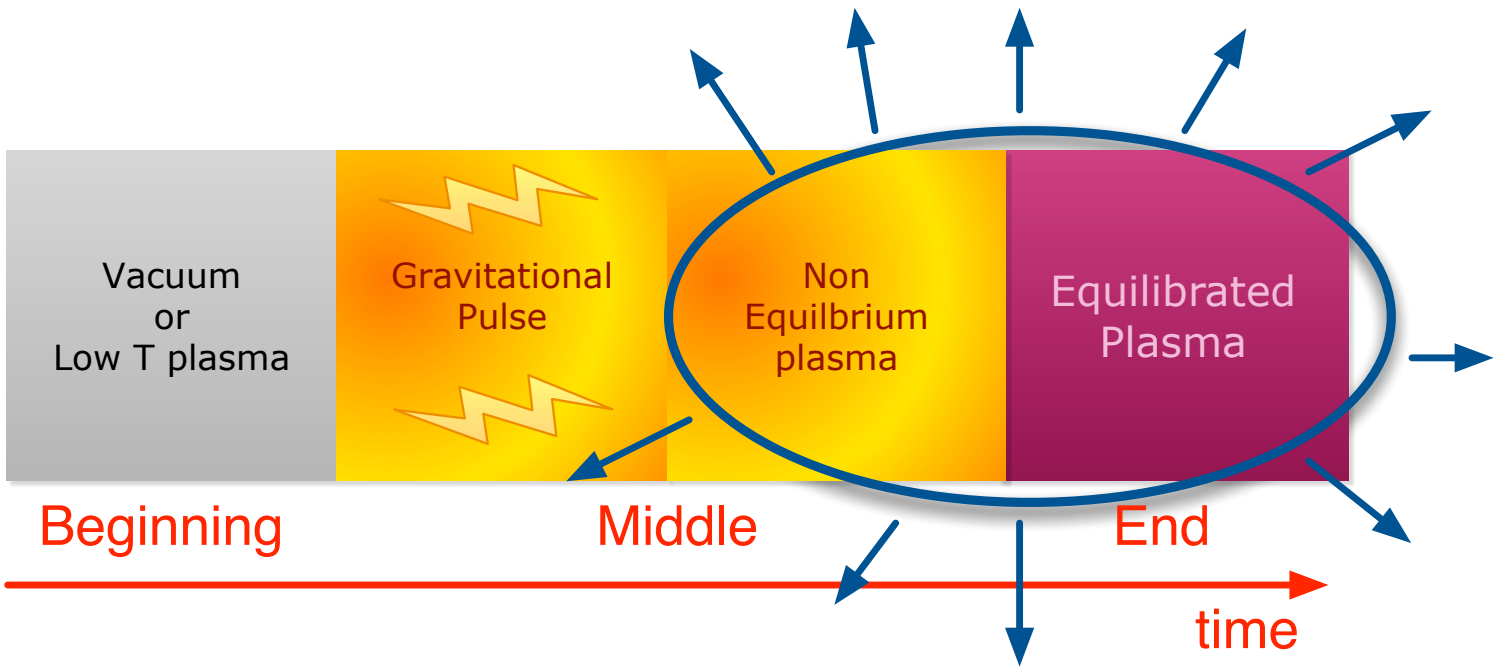

I want to compute the "photon" emission rate in the non-equilibrium plasma.

1. Study the equilibration of different modes in the plasma.

2. Study the non-equilibrium *emission* of quanta from the black brane

   - *Emission* is dual to *emission*

Emission of dilatons weakly interacting with equilibrium strongly coupled SYM plasma

$$iS_{\rm int} = i\int {\rm d}^4x\,\phi(x)J(x)$$

- Emission:

$$(2\pi)^3 2k\frac{d\Gamma^<}{d^3k} = G^<(K) \qquad\qquad G^<(K) = \left\langle \hat{J}(0)\hat{J}(K)\right\rangle$$

- Absorption: The absorption rate of Dilatons is

$$(2\pi)^3 2k\frac{d\Gamma^>}{d^3k} = G^>(K) \qquad\qquad G^>(K) = \left\langle \hat{J}(K)\hat{J}(0)\right\rangle$$

- FDT: The Fluctuation Dissipation Relation reads

$$\Big[\underbrace{G^<(K)}_{\text{emission}}\Big] / \Big[\underbrace{G^>(K)}_{\text{absorption}}\Big] = e^{-\omega/T}$$

We will compute the emission and absorption rates and check for detailed balance

What the classical AdS/CFT usually computes

$n_{\mathbf{k}} =$ Dilaton occupation number

$$\partial_t n_{\mathbf{k}} = -n_{\mathbf{k}} \underbrace{\Gamma^{>}}_{\text{absorb}} + (1 + n_{\mathbf{k}}) \underbrace{\Gamma^{<}}_{\text{emit}}$$

- For a classical dilaton field $n_{\mathbf{k}} \gg 1$ the damping is

$$\partial_t n_{\mathbf{k}} = -n_{\mathbf{k}} \times \underbrace{(\Gamma^{>} - \Gamma^{<})}_{\text{classical absorption rate}}$$

- The classical absorption rate

$$G^{>}(K) - G^{<}(K) = -2\,\mathrm{Im} G_R(K)$$

Without assuming FDT, only the classical absorption rate is computable with the classical black brane response.

Nonequilibrium definitions – spectral density and statistical fluctuations

- Spectral Density records classical dissipation (commutator or $G^{>} - G^{<}$)

$$\rho_{ra-ar}(t_1|t_2) = \underbrace{\langle[\phi(t_1), \phi(t_2)]\rangle}_{\text{classical dissipation}}$$

- Statistical fluctuations (anti-commutator or $\frac{1}{2}(G^{>} + G^{<})$)

$$G_{rr}(t_1|t_2) = \underbrace{\frac{1}{2}\langle\{\phi(t_1), \phi(t_2)\}\rangle}_{\text{fluctuations}}$$

  - Invariably suppressed at large N and only due to Hawking radiation.

What do you want to know about these things?

A non-equilibrium definition of the Emission and Absorption Rates

Want to know the rate to emit and absorb in a frequency band ω at time t

1. Wigner Transforms – perfect frequency resolution, but no time resolution

$$G^{<}(\bar{t},\omega) = \int_{-\infty}^{\infty} \mathrm{d}\Delta t e^{+i\omega\Delta t} \langle J(\bar{t}-\Delta t) J(\bar{t}+\Delta t)\rangle$$

2. Gabor Transform – Wigner smeared with a minimum uncertainty wave packet

$$\underbrace{\bar{G}^{<}(\bar{t}_o,\bar{\omega}_o)}_{\text{Gabor}} = \int \frac{dt d\omega}{2\pi} \underbrace{2e^{-(\omega-\omega_o)^2\sigma^2} e^{-(\bar{t}-\bar{t}_o)^2/\sigma^2}}_{\text{minimum wave packet}} \underbrace{G^{<}(\bar{t},\omega)}_{\text{Wigner Trans}}$$

3. The total number of dilatons emitted (in the band)

$$n(t,\omega_o,\sigma_\omega) = \int^{t} d\bar{t}_o \, \bar{G}^{<}(\bar{t}_o,\omega_o)$$

This is a good estimate for the local emission rate for a given temporal resolution

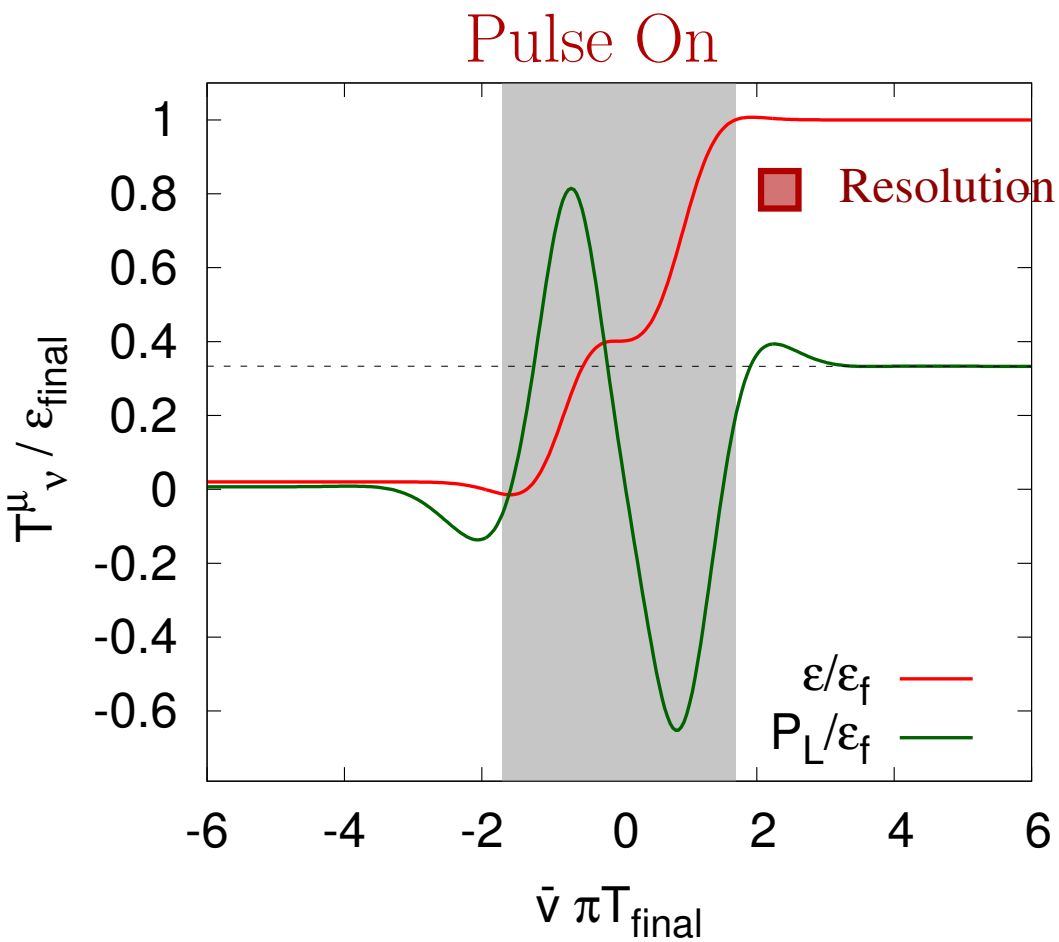

- High average frequency

$$\omega_o = 8\pi T_{\rm f}$$

- Temporal Resolution

$$\sigma_v \pi T_{\rm f} = \frac{1}{\sqrt{2}} \simeq 0.7$$

- Frequency Resolution

$$\frac{\sigma_\omega}{\omega} \simeq \frac{1/\sqrt{2}}{8} \simeq 10\%$$

Equilibration and the coarse-grained FDT

1. If the FDT is satisfied

$$G^{<}(K) = e^{-\omega/T} G^{>}(K)$$

then, the coarse-grained quantities satisfy

$$\underbrace{\bar{G}^{<}(\bar{t}_o, \bar{\omega}_o, \boldsymbol{q})}_{\text{emission}} = e^{-\omega_o \beta_{\text{eff}}} \underbrace{\left[e^{\beta_{\text{eff}}^2/4\sigma^2} \bar{G}^{>}(\bar{t}_o, \bar{\omega}_o - \beta_{\text{eff}}/2\sigma^2, \boldsymbol{q}) \right]}_{\text{absorption}}$$

We will monitor the FDT as a function of time to quantify equilibrium

Results

Emission&Absorption rates and the FDT:

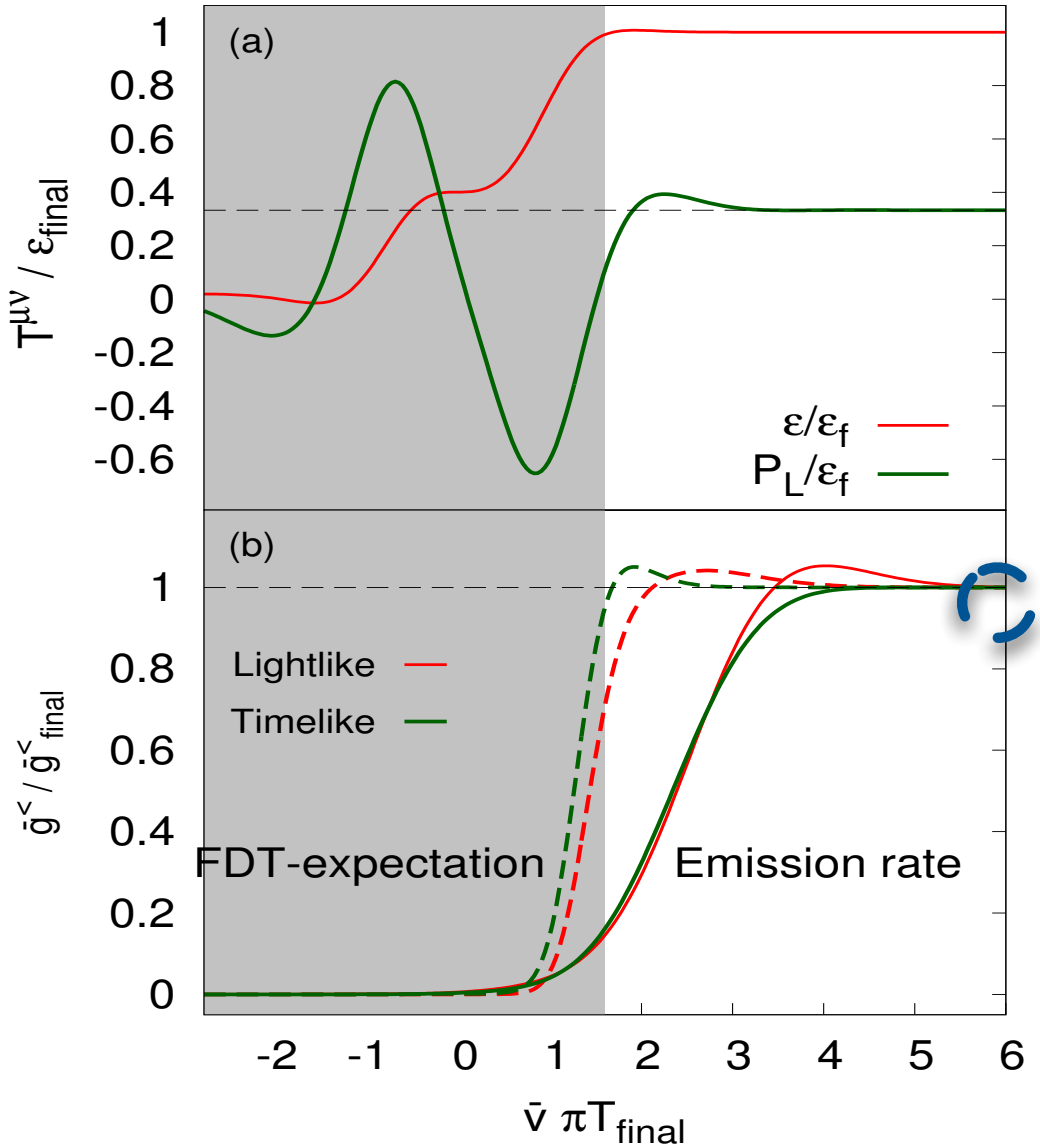

Stress Tensor

FDT satisfied

Emission & Absorption

Lightlike: $\omega \simeq 8\pi T_{\rm f}$ and $q_T = q_L = \omega/\sqrt{2}$

Pattern of equilibration:

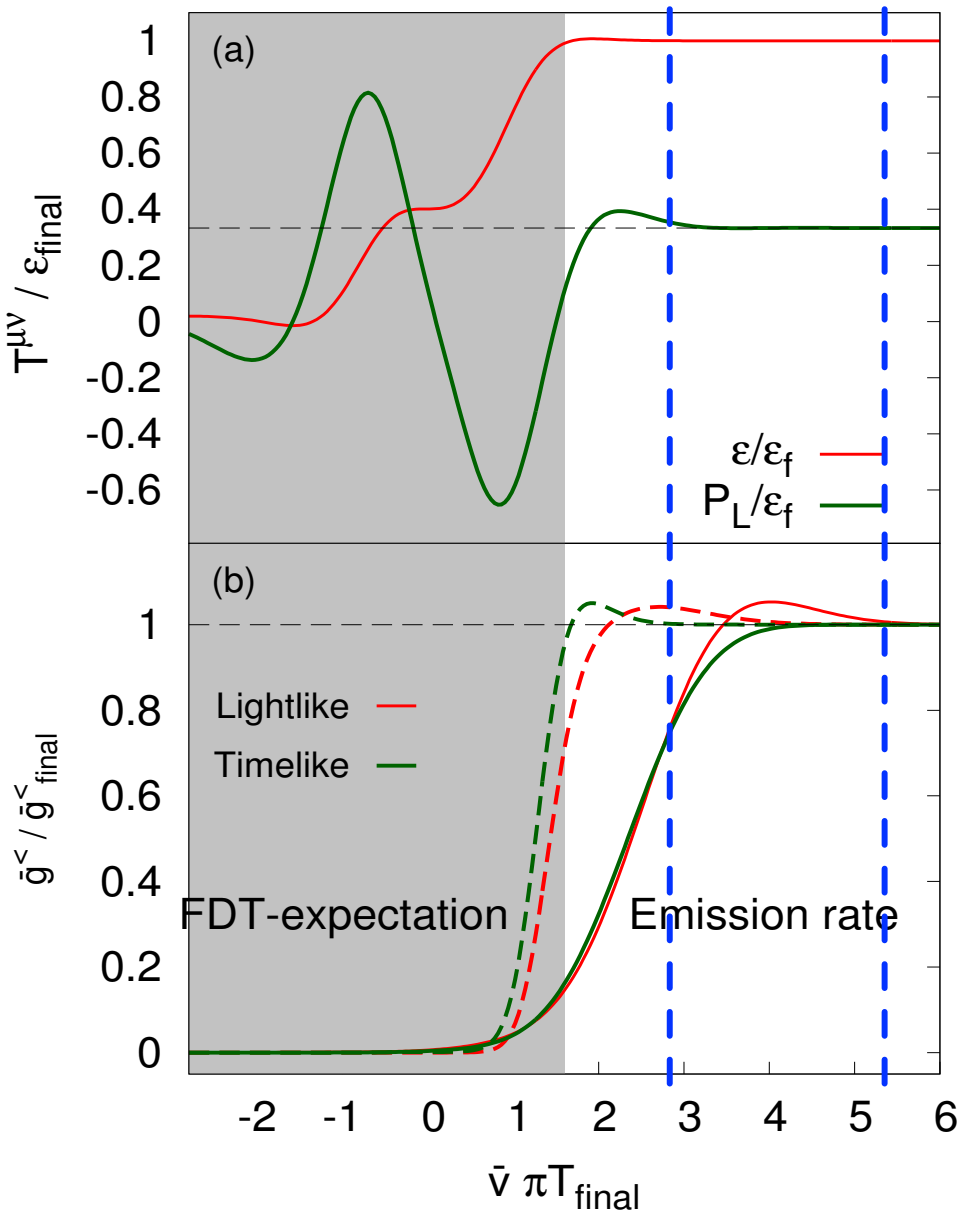

First the stress/geometry equilibrates

then

the emission rate equilibrates

Thermalization of Timelike Modes (units $\pi T_{\rm final}$): $\boldsymbol{q} = 0$ and $\omega =$ finite

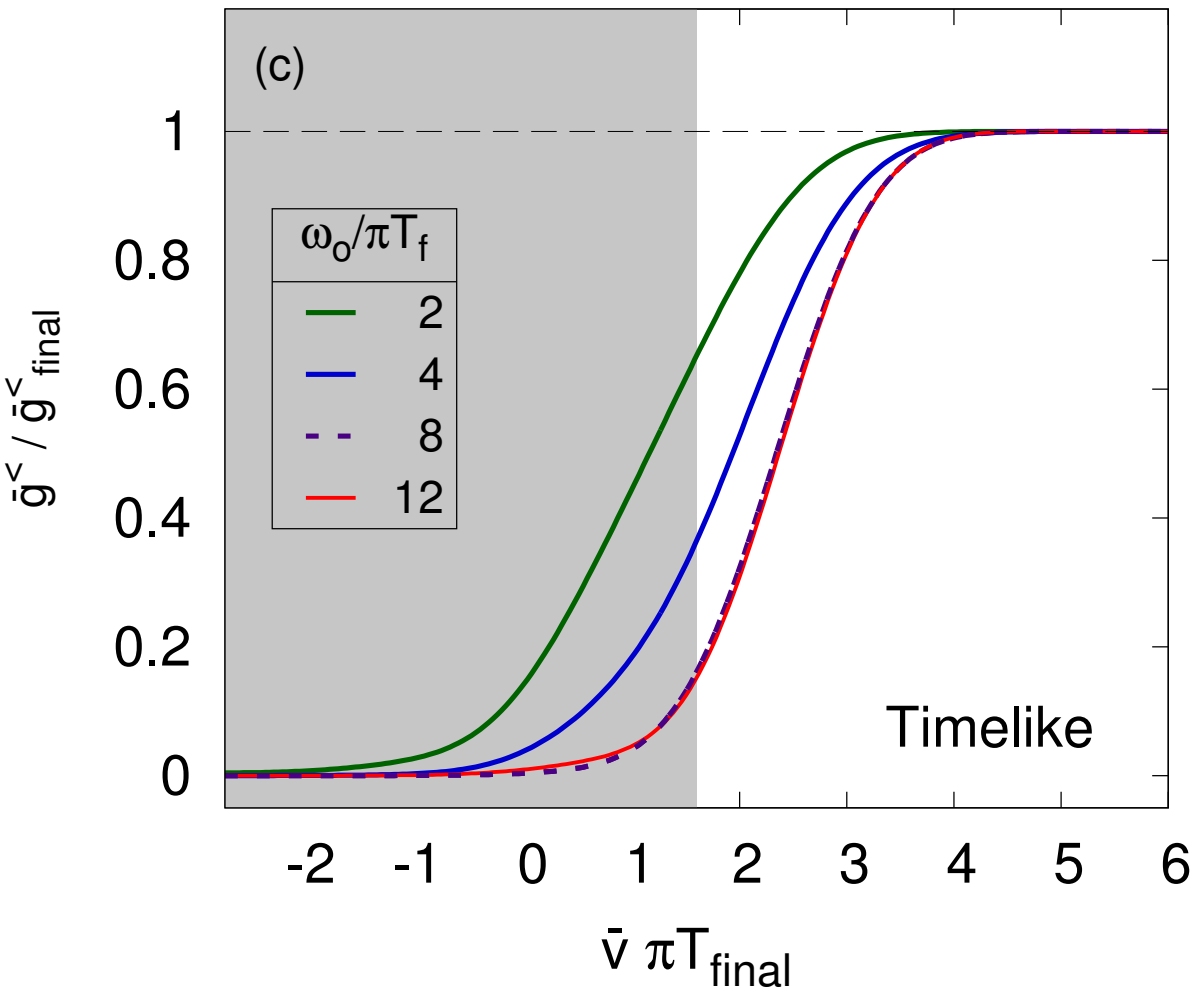

Find that massive timkelike modes thermalize in a finite time. . . will intuit that

$$\tau_{\rm thermalize} \sim {\rm const} \qquad \omega \to \infty$$

Thermalization of Lightlike Modes Chesler et al, Arnold&Vaman

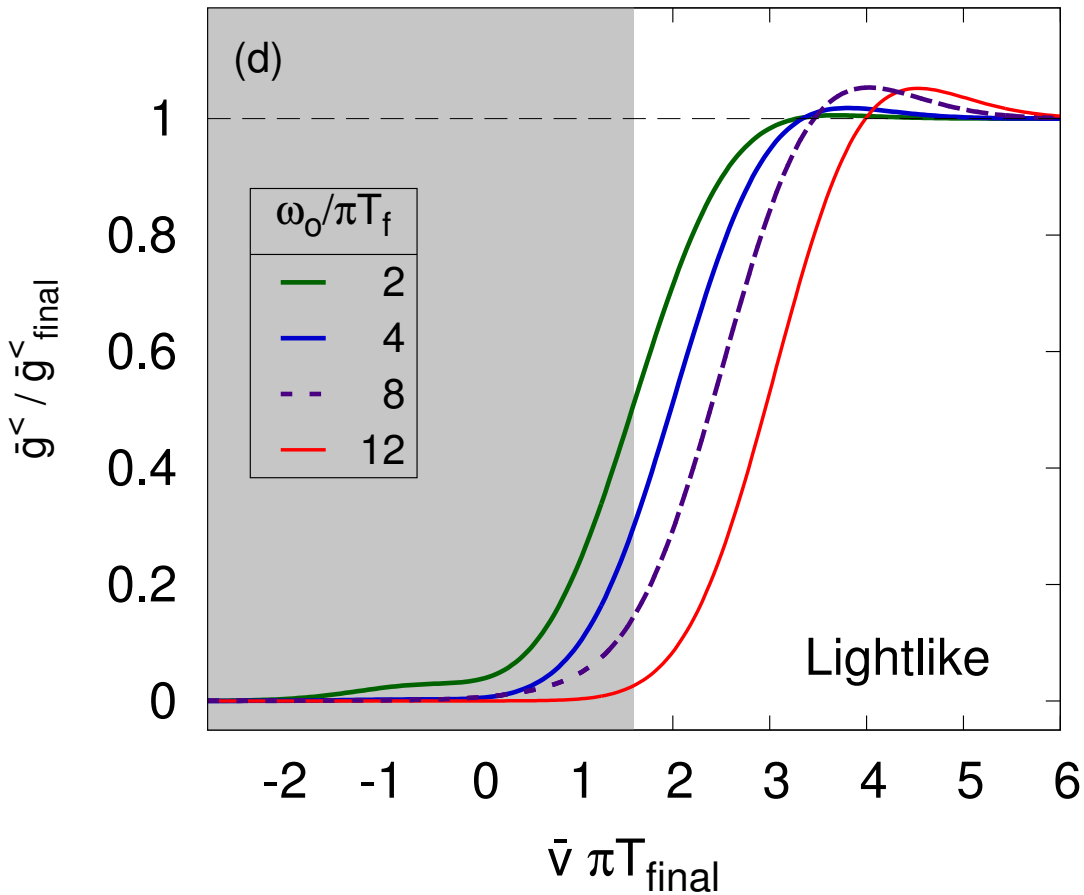

The harder the lightlike mode, the longer it takes to equilibrate. . . will intuit that

$$\tau_{\rm thermalize} \sim (\omega\sigma_v)^{1/4} \quad \text{for} \quad \omega \to \infty \quad \text{where} \quad Q^2 = (\omega^2 - q^2) \sim \underbrace{\omega\sigma_v^{-1}}_{\text{virtuality}}$$

Summary:

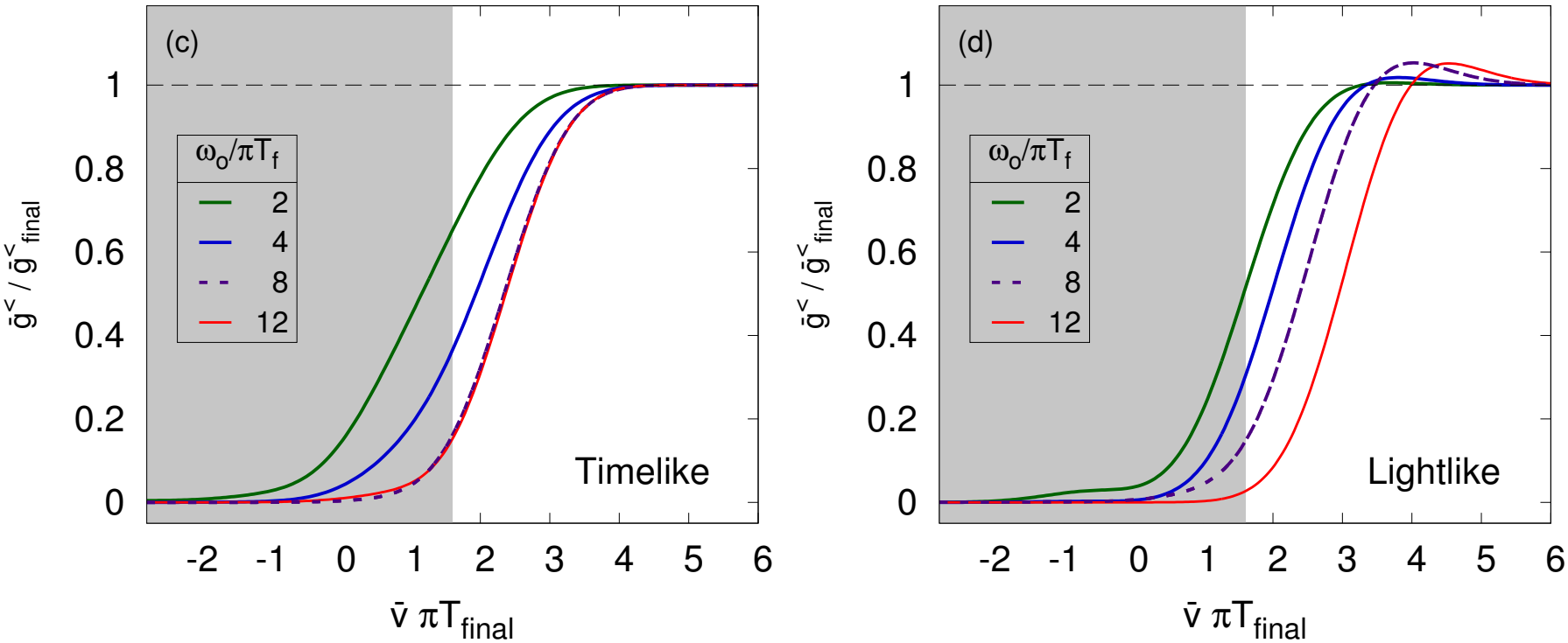

1. Find that massive timkelike modes thermalize in a finite time. . . will intuit that

$$\tau_{\rm thermalize} \sim {\rm const} \qquad \omega \to \infty$$

2. The harder the lightlike mode, the longer it takes to equilibrate. . . will intuit that

$$\tau_{\rm thermalize} \sim (\omega\sigma_v)^{1/4} \qquad \text{for} \qquad \omega \to \infty$$

Non-Equilibrium AdS/CFT and Hawking Radiation

Non-equilibrium: (Chesler-Yaffe)

- Paul and Larry Play God:

$$ds^2 = -dt^2 + e^{B_o(t)} d\mathbf{x}_\perp^2 + e^{-2B_o(t)} dx_\parallel^2$$

1. Corresponds to non-equilibrium geometry with BH formation in AdS_5

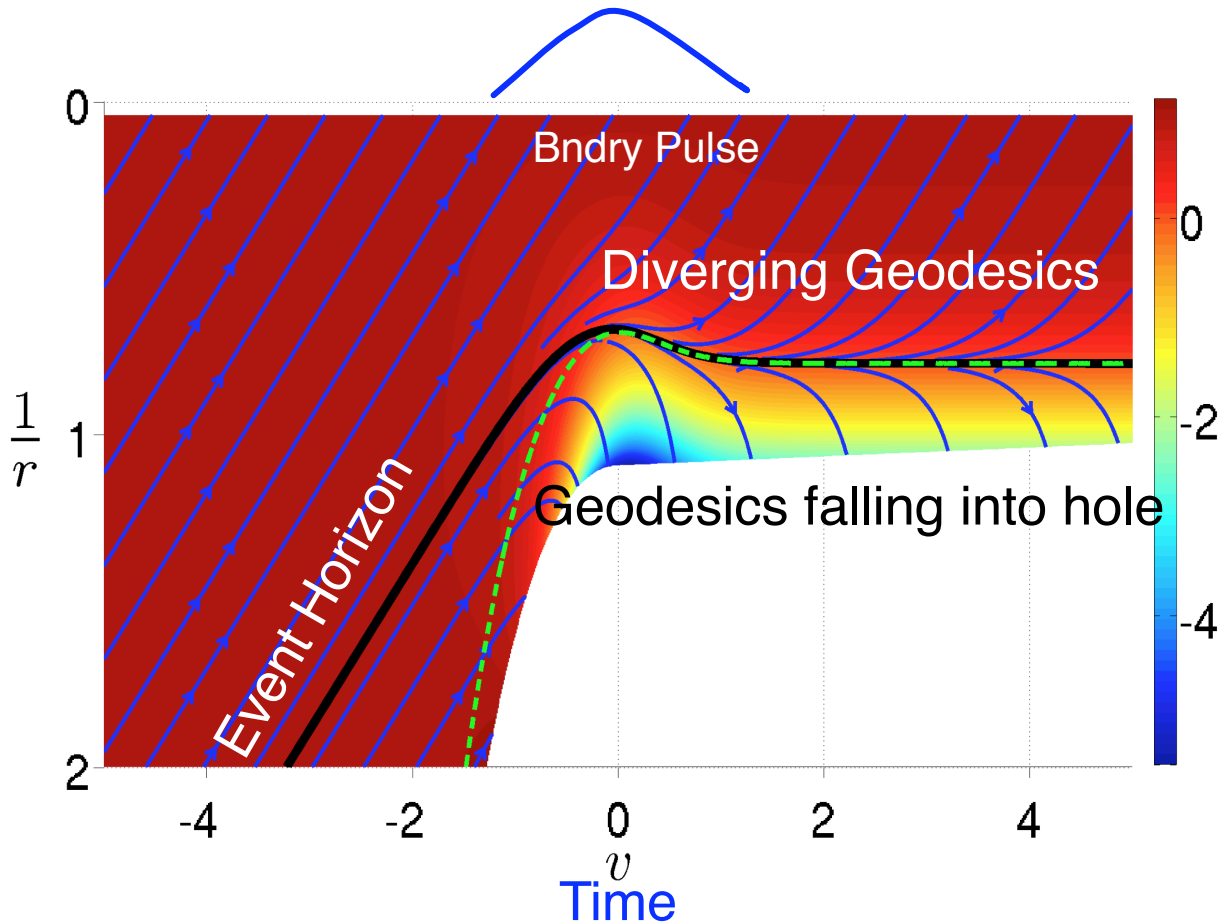

$$ds^2 = -A\,dv^2 + \Sigma^2\left[e^B d\boldsymbol{x}_\perp^2 + e^{-2B} dx_{||}^2\right] + 2dr\,dv\,,$$

What we want to compute in the gravitational theory:

1. We want to compute the *five* dimensional spectral weight

$$\rho_{ra-ar}(v_1 r_1 | v_2 r_2) = \underbrace{\langle [\phi(1), \phi(2)] \rangle}_{\text{computable with classical BH dissipation}}$$

2. And the *five* dimensional fluctuations (anti-commutator)

$$G_{rr}(v_1 r_1 | v_2 r_2) = \underbrace{\frac{1}{2} \langle \{\phi(1), \phi(2)\} \rangle}_{\text{Fluctuations due to Hawking}}$$

These correlators can be lifted to the boundary determining the boundary quantities

Hawking radiation in non-equilibrium geometries

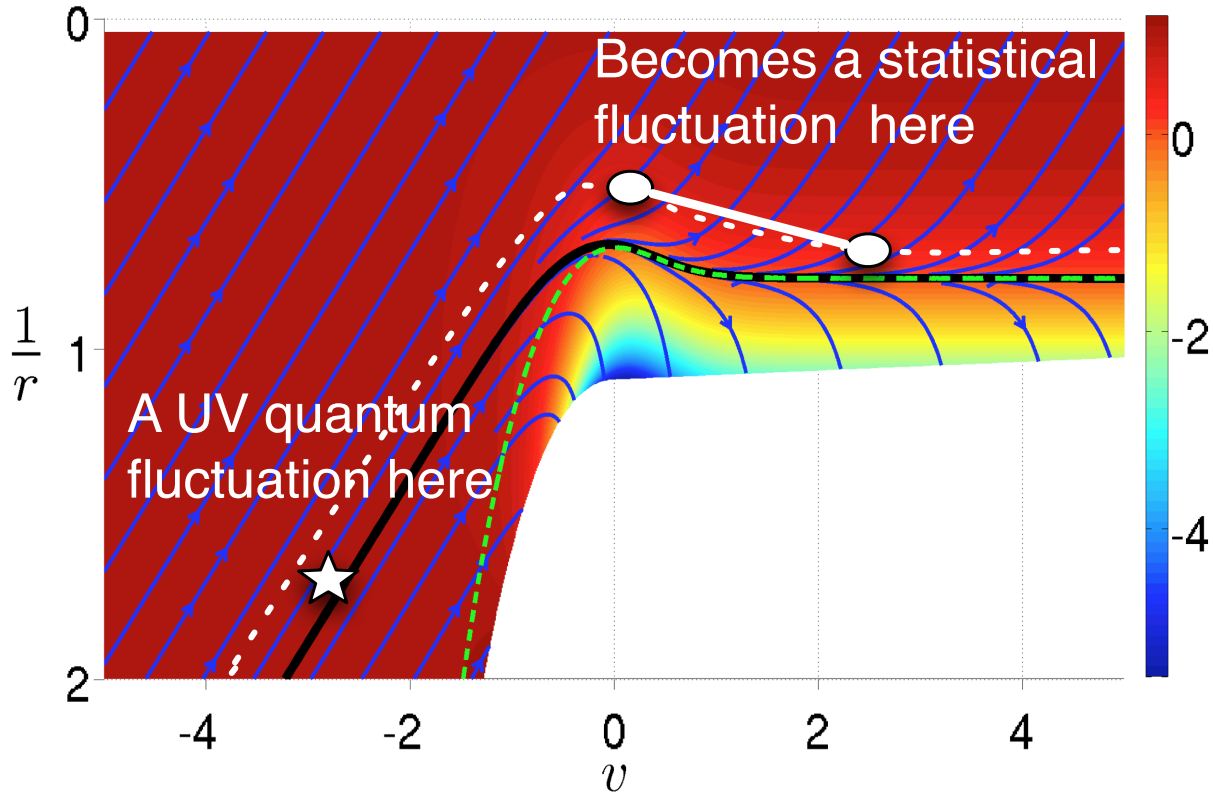

- Surface Properties – characterizes diverging geodesics near event horizon

$$\underbrace{\kappa(v)}_{\text{Lyapunov exponent}} \equiv \overbrace{\frac{1}{2}\frac{\partial A(r,v)}{\partial r}}^{\text{Metric}-\text{coeff}}\Bigg|_{r=r_h(v)}$$

Then propagate the horizon fluctuations up to the boundary

- General form of near horizon fluctuations in non-equilibrium

$$G^h_{rr}(v_1|v_2) = -\frac{\sqrt[4]{g(v_1)g(v_2)}}{\pi}\partial_{v_1}\partial_{v_2}\log|e^{\int^{v_1}\kappa(v')dv'} - e^{\int^{v_2}\kappa(v')dv'}|$$

- Can map the near horizon fluctuations up to boundary

$$G_{rr}(1|2) = \int \mathrm{d}v_{1h}\mathrm{d}v_{2h}\ \underbrace{G_R(1|1_h)\ G_R(2|2_h)}_{\text{outgoing Green Fcns}}\ \underbrace{G^h_{rr}(1_h|2_h)}_{\text{horizon flucts}}\ .$$

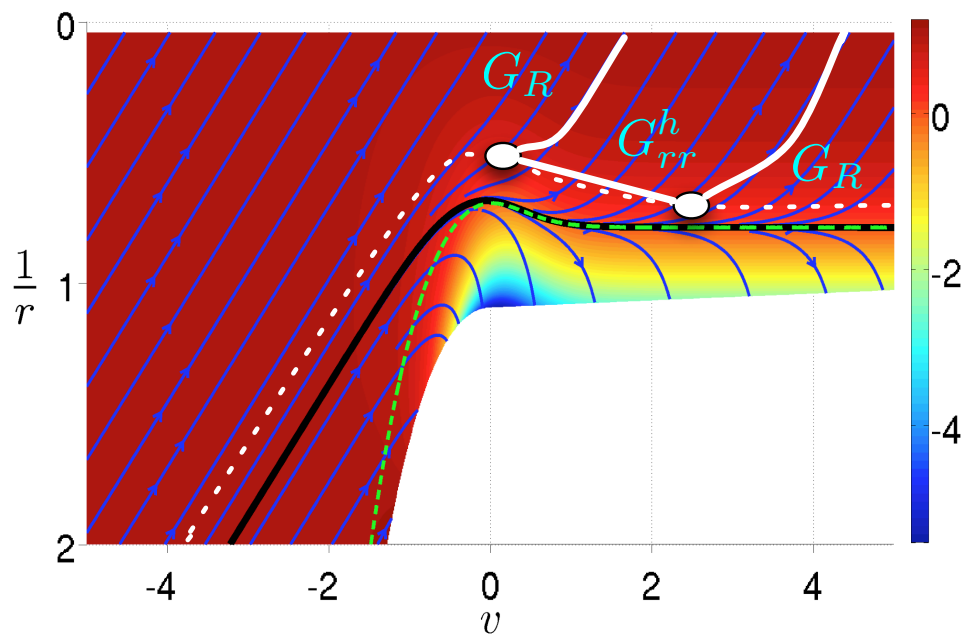

Qualitative explanation of our numerical results

- At large frequencies use a geometric approximation for Green fcns

$$G_{rr}(1|2) = \int \mathrm{d}v_{1h}\mathrm{d}v_{2h}\, \underbrace{G_R(1|1_h)\, G_R(2|2_h)}_{\text{outgoing Green Fcns}}\, \underbrace{G^h_{rr}(1_h|2_h)}_{\text{horizon flucts}} \,.$$

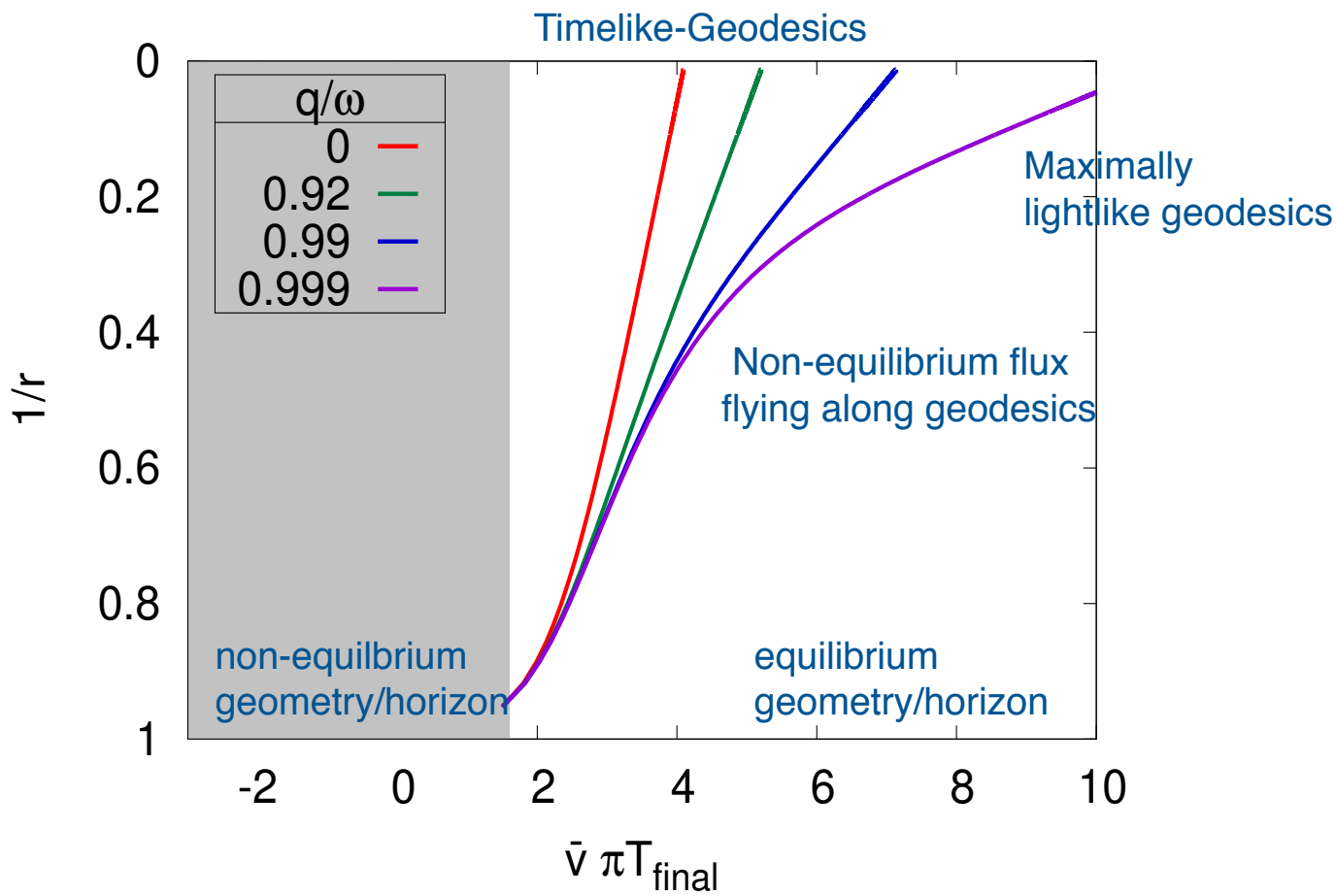

Qualitative Picture

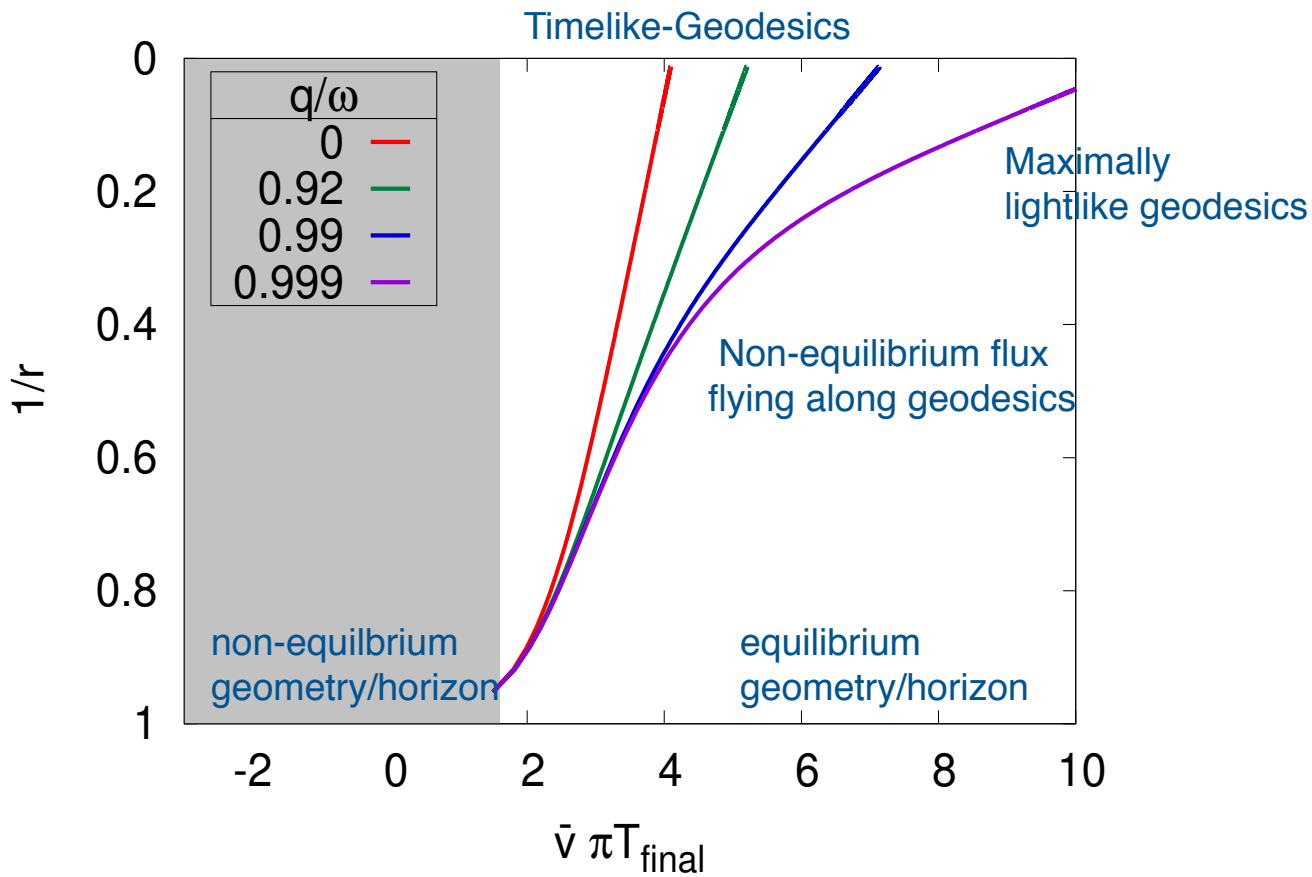

1. Time delay (fly-time) $\sim 2/\pi T_f$ between the equilibration of 1-pnt and 2-pnt fcns.

   - Timelike geodesics, $\omega \to \infty$, fly directly to the bndry and equilibrate (fall in)

Qualitative Picture

(see also Chesler et al, Arnold&Vaman)

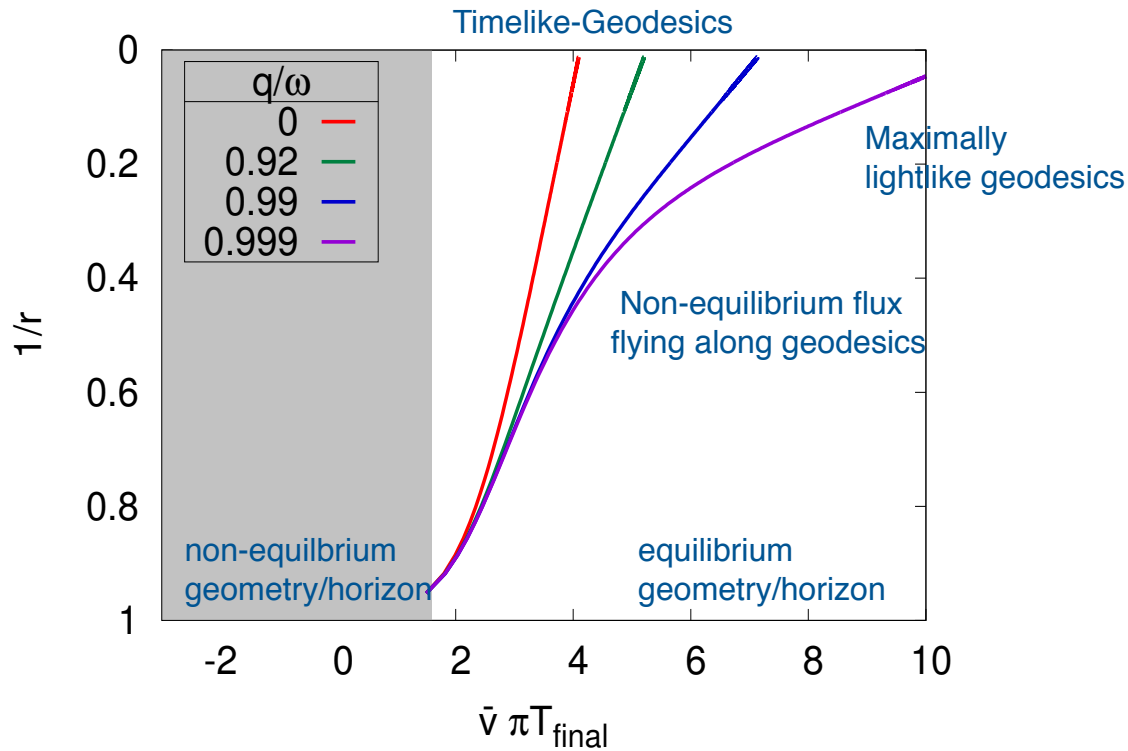

2. For large light like modes it takes a long time to reach the boundary.

   - For us, the virtuality is of order $Q^2 = \omega^2 - q^2 \sim \omega\sigma_v^{-1}$
   - For a lightlike geodesic with small virtuality Q^2

$$\tau_{\rm fly} \sim \left(\frac{\omega^2}{Q^2}\right)^{1/4} \sim (\omega\sigma_v)^{1/4}$$

Conclusions

1. Thermalization of emission rates in non-equilibrium plasmas corresponds to Hawking emission from non-equilibrium black holes.

2. General pattern of thermalization:

   (a) First the one point functions $\langle J(t) \rangle$ equilibrate

   (b) Then the two pnt functions $\langle J(t)\, J(0) \rangle$ equilibrate

   (c) Modes with large invariant mass (large Q^2) thermalize first

   (d) Hard onshell modes (small Q^2) take a long time to equilibrate

$$\tau \sim (\omega \sigma_v)^{1/4}$$

This picture of thermalization is not too different from weak-coupling

Quark production, Bose-Einstein condensates and thermalization of the quark-gluon plasma

Bin Wu

IPhT, CEA/Saclay

Workshop on the Approach to Equilibrium in Strongly Interacting Matter, BNL, USA
April 3, 2014

J. -P. Blaizot, B. Wu and L. Yan, arXiv:1402.5049 [hep-ph].

Outline

1. Introduction
2. The transport equations of partons in diffusion approximation
3. Quark production, BEC and thermalization
4. Discussions

Introduction

- **Motivations: Thermalization**
  - **In the relativistic heavy ion collisions**

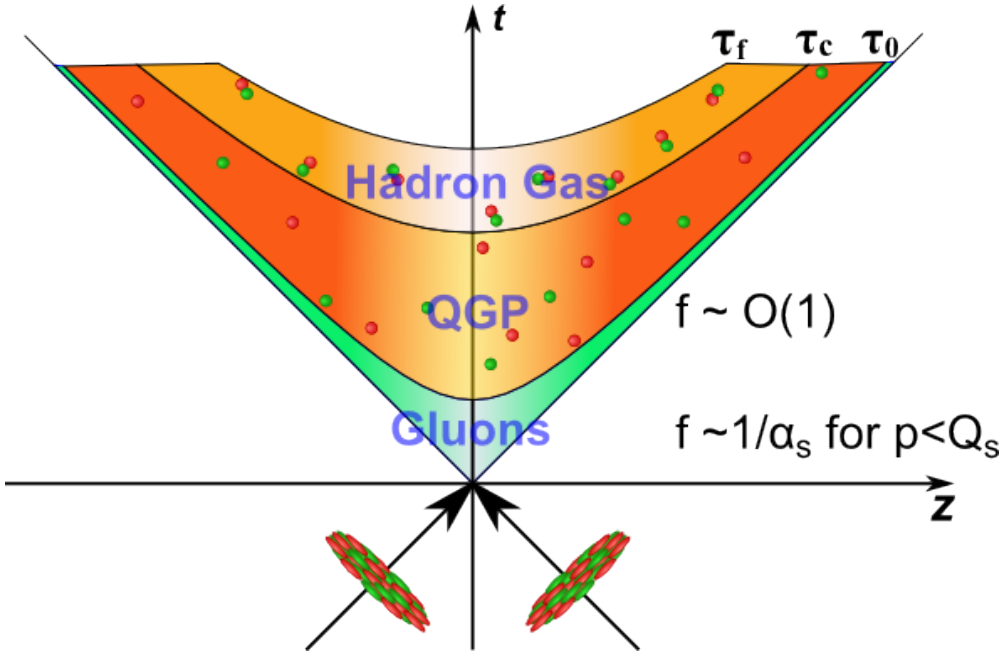

A. H. Mueller, Nucl. Phys. B **572**, *227 (2000) [hep-ph/9906322].*

  - **Cosmology: reheating, baryogenesis** $\cdots$

For example, A. Tranberg and B. Wu, JHEP **1301**, *046 (2013) [arXiv:1210.1779 [hep-ph]].*

Introduction

- **Theoretical tools: Schwinger-Keldysh formalism**

Take $\lambda\phi^4$ for example below!

$$\langle \hat{O}(t)\rangle = \mathrm{Tr}\left[\hat{O}(t)\rho(0)\right]$$

$$= \int d\phi_t d\phi_{+0} d\phi_{-0} \hat{O}[\phi_t]\langle\phi_{+0}|\hat{\rho}(0)|\phi_{-0}\rangle\langle\phi|U(t)|\phi_{+0}\rangle\langle\phi_{-0}|U(t)^\dagger|\phi_t\rangle$$

$$= \int D\phi_+ D\phi_- \langle\phi_{+0}|\hat{\rho}(0)|\phi_{-0}\rangle \hat{O}[\phi(t)] e^{\frac{i}{\hbar}\left\{S[\phi_+]-S[\phi_-]\right\}}$$

$$= \int d\phi_t d\sigma_0 d\phi_0 e^{-\frac{i}{\hbar}\sigma_0\pi_0}\langle\phi_0 + \frac{\sigma_0}{2}|\hat{\rho}(t_0)|\phi_0 - \frac{\sigma_0}{2}\rangle \hat{O}[\phi_t]$$

$$\times \int_{\substack{\sigma(0)=\sigma_0,\ \sigma(t)=0 \\ \phi(0)=\phi_0,\ \phi(t)=\phi_t}} D\phi D\sigma e^{-\frac{i}{\hbar}\int_0^t\left[\sigma\left(\Box\phi+\frac{g^2}{6}\phi^3-j\right)+\frac{g^2}{24}\sigma^3\phi\right]}$$

with $\phi_2 = \phi \equiv \frac{1}{2}(\phi_+ + \phi_-)$ and $\phi_1 = \sigma \equiv \phi_+ - \phi_-$.

Too complicated, approximations are needed!

For a review: K. -c. Chou, Z. -b. Su, B. -l. Hao and L. Yu, Phys. Rept. **118**, *1 (1985).*

Introduction

- **The quantum vacuum**

$$\rho_W[\phi_0,\pi_0] \equiv \int d\phi_0 e^{-\frac{i}{\hbar}\sigma_0\pi_0}\langle\phi_0+\frac{\sigma_0}{2}|\hat{\rho}(t_0)|\phi_0-\frac{\sigma_0}{2}\rangle$$
$$= \mathcal{N}e^{-\int\frac{d^3p}{(2\pi)^3}\left(p|\phi_0(p)|^2+\frac{1}{p}|\pi_0(p)|^2\right)}$$

- **Any coherent state**

$$\rho_W[\phi_0,\pi_0] = \mathcal{N}e^{-\int\frac{d^3p}{(2\pi)^3}\left(p|\phi_0(p)-\phi_{cl0}(p)|^2+\frac{1}{p}|\pi_0(p)-\pi_{cl0}(p)|^2\right)},$$

where ϕ_{cl0} and π_{cl0} are any field configuration.

All the high momentum modes are included!!

- **The classical statistical approximation**
  - **The formalism: drop** $\frac{g^2}{24}\sigma^3\phi$

$$\langle\hat{O}(t)\rangle = \int d\phi_t d\sigma_0 d\phi_0 e^{-\frac{i}{\hbar}\sigma_0\pi_0}\langle\phi_0+\frac{\sigma_0}{2}|\hat{\rho}(t_0)|\phi_0-\frac{\sigma_0}{2}\rangle\hat{O}[\phi_t]$$

$$\times \int_{\substack{\sigma(0)=\sigma_0,\,\sigma(t_\infty)=0\\ \phi(0)=\phi_0,\,\phi(t_\infty)=\phi_t}} D\phi \underbrace{D\sigma e^{-\frac{i}{\hbar}\int_{t_0}^{t_\infty}\left[\sigma\left(\Box\phi+\frac{g^2}{6}\phi^3-j\right)\right]}}_{\delta\left[\Box\phi+\frac{g^2}{6}\phi^3-j\right]}$$

$$= \int d\phi_0 d\pi_0 \rho_W[\phi_0,\pi_0]\hat{O}[\phi_{cl}(t)],$$

where

$$\Box\phi_{cl}+\frac{g^2}{6}\phi_{cl}^3 = j \text{ with } \phi_{cl}(0)=\phi_0, \dot{\phi}_{cl}(0)=\pi_0.$$

A. H. Mueller and D. T. Son, Phys. Lett. B **582**, *279 (2004) [hep-ph/0212198].*

Introduction

- **The classical statistical approximation**

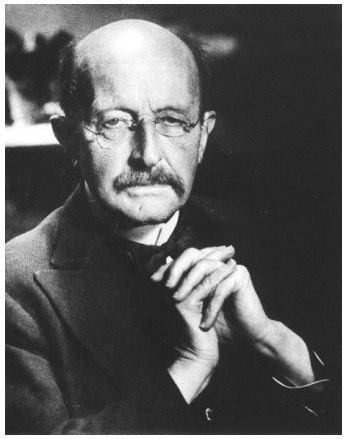

  - **Purely classical limit:** **neglect all the quanta with $p > Q_s$**
  - **Thermal equilibrium distribution:** $f_p = \underbrace{\frac{T}{\omega_p - \mu}}_{O(\hbar^0)}$
  - **Ultraviolet catastrophe**

Introduction

- **The classical statistical approximation**
  - **Including all the quanta in the vacuum**
  - **Thermal equilibrium distribution:** $f_p = \underbrace{\frac{T}{\omega_p - \mu}}_{O(\hbar^0)} \underbrace{-\frac{1}{2}}_{O(\hbar)}$
  - **Non-renormalizablity**

    For example,

$$-i\left[\Sigma_{11}(P)\right]^{2\text{ loop}}_{\text{CSA}} =$$

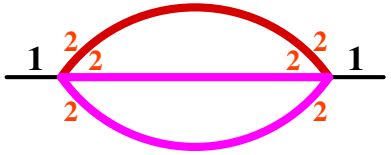

$$= -\frac{g^4}{1024\pi^3}\left(\Lambda^2_{\text{UV}} - \frac{2}{3}p^2\right),$$

$$\text{Im}\left[\Sigma_{12}(P)\right]^{2\text{ loop}}_{\text{CSA}} =$$

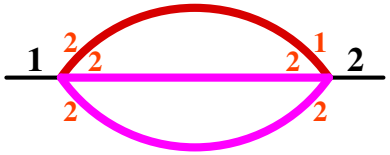

$$= -\frac{g^4}{1024\pi^3}\left(\Lambda^2_{\text{UV}} - \frac{2}{3}p^2\right)$$

with "1" $= \sigma$, "2" $= \phi$.

T. Epelbaum, F. Gelis and B. Wu, arXiv:1402.0115 [hep-ph].

Invalid for the late-time behavior!

- **The Boltzmann equation**

  - **The quasiparticle approximation:**

    With the assumption $X^\mu \equiv x^\mu + y^\mu/2$ is a slowly varying variable in $G_{ab}(x,y)$

$$G_{22}(X,p) = \left(f_p(X) + \underbrace{\frac{1}{2}}_{vacuum\ quanta} \right) 2\pi\delta(p^2 - m^2), \qquad G_{11}(X,p) = 0,$$

$$G_{12}(X,p) = \frac{i}{p^2 - m^2 + ip^0\epsilon}, \qquad G_{21}(X,p) = \frac{i}{p^2 - m^2 - ip^0\epsilon}.$$

  - **The Dyson-Schwinger equation**

$$D_t f_p \equiv \left(\frac{\partial}{\partial t} + \mathbf{v} \cdot \nabla_{\mathbf{x}} \right) f_p = -\frac{i}{2\omega_p} \left[(\Sigma_{12} - \Sigma_{21}) \left(f_p + \frac{1}{2} \right) - \Sigma_{11} \right].$$

A. H. Mueller and D. T. Son, Phys. Lett. B **582**, *279 (2004) [hep-ph/0212198].*

- **The Boltzmann equation**
  - **Valid for all** $f < O(\alpha_s^{-1}) \sim g^{-2}$

$$-i\Sigma_{11}(P) \quad = \quad$$

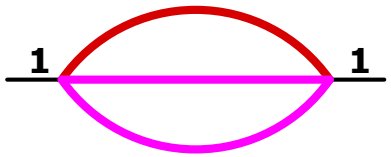

$$+ O(g^8),$$

$$-i\Sigma_{12}(P) \quad = \quad$$

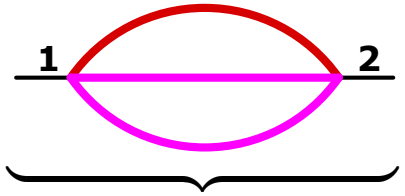

$$+O(g^8)$$

  - **Phase transition: may not be accurate** since the coherent length $\sim \infty$

E. Calzetta and B. L. Hu, Phys. Rev. D **37**, *2878 (1988).*

But the Boltzmann equation does KNOW something about it!

Go back to pQCD from next page!

Introduction

- **The Bose-Einstein condensate (BEC)**
  - **May exist before it disappears due to number changing processes!**

    J. -P. Blaizot, F. Gelis, J. -F. Liao, L. McLerran and R. Venugopalan, Nucl. Phys. A **873**, *68 (2012) [arXiv:1107.5296 [hep-ph]].*
  - **Classical statistical approximation (scalar field)**

    T. Epelbaum and F. Gelis, Nucl. Phys. A **872**, *210 (2011) [arXiv:1107.0668 [hep-ph]].*

    J. Berges and D. Sexty, Phys. Rev. Lett. **108**, *161601 (2012) [arXiv:1201.0687 [hep-ph]].*
  - **Kinetic theory (in pQCD)**

    In thermal equilibrium,

$$f = \frac{1}{e^{\frac{\omega_p}{T}} - 1} + (2\pi)^3 n_c \delta(\mathbf{p})$$

J. -P. Blaizot, J. Liao and L. McLerran, Nucl. Phys. A **920**, *58 (2013) [arXiv:1305.2119 [hep-ph]].*

X. -G. Huang and J. Liao, arXiv:1303.7214 [nucl-th].

- **Quark production**
  - **In a thermal bath of weakly couple QGP**

$$\epsilon = 3P = \left[16 + \frac{21}{2} N_f\right] \frac{\pi^2}{30} T^4$$

Quarks (and antiquark) carry 66% of ϵ for $N_f = 3$.

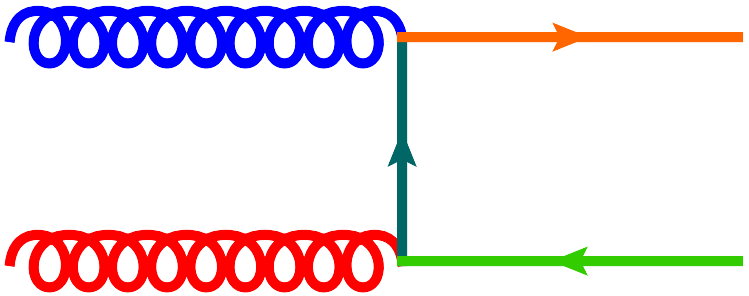

  - **The quark production process:** $gg \leftrightarrow q\bar{q}$

The transport equation

- **Assumptions**
  1. **Baryon number density = 0 anywhere**
  2. **No external fields (forces)**
  3. **Partons are massless**

     $2N_c \times 2N_f$ **quarks (and antiquarks) and** $2(N_c^2 - 1)$ **gluons!**
- **Symmetries**
  - ①+② $\Rightarrow$ **Charge conjugation symmetry + Spin and color to be averaged**
  - ③ $\Rightarrow$ $SU(N_f)$ **flavor symmetry**
- **Consequences**
  - **Two coupled transport equations for**

    The quark distribution F and the gluon distribution f

The transport equation

- **Diffusion approximation**

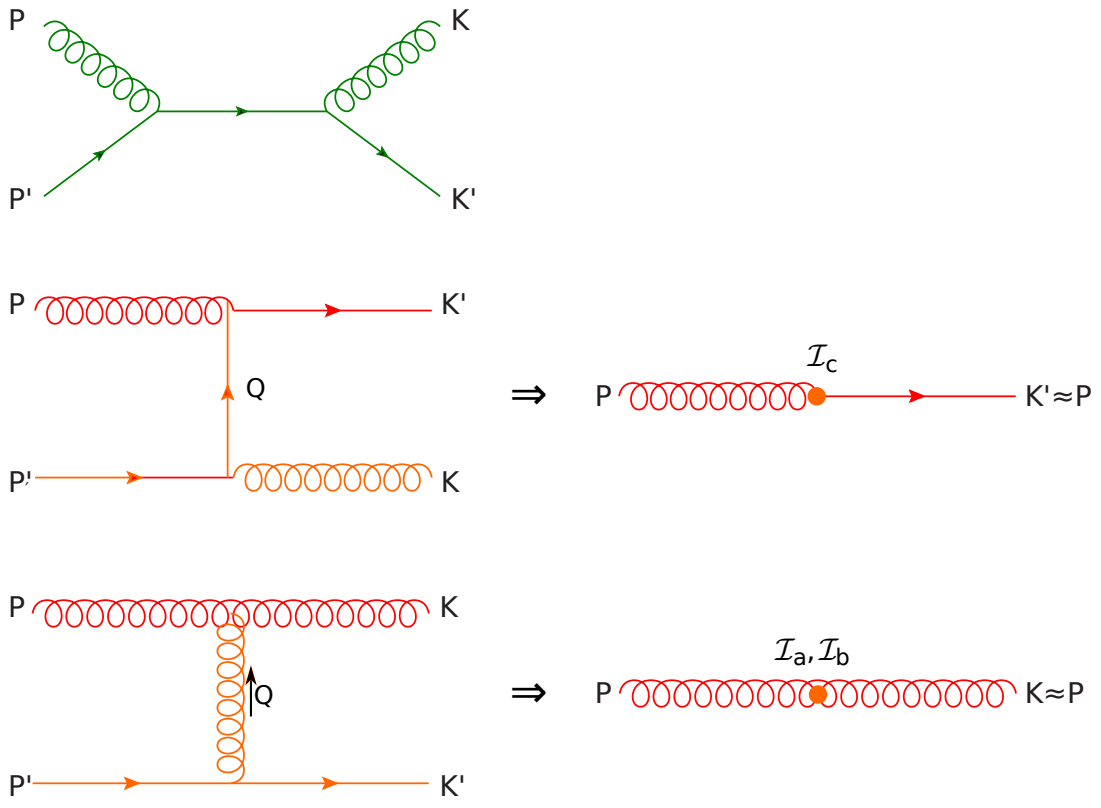

The transport equation

- **Diffusion approximation**

$ab \leftrightarrow cd$	$\lvert\mathcal{M}^{ab}_{cd}\rvert^2/g^4$	In diffusion approximation
$q_1 q_2 \leftrightarrow q_1 q_2$ $q_1 \bar{q}_2 \leftrightarrow q_1 \bar{q}_2$ $\bar{q}_1 q_2 \leftrightarrow \bar{q}_1 q_2$ $\bar{q}_1 \bar{q}_2 \leftrightarrow \bar{q}_1 \bar{q}_2$	$4N_c C_F \left(\frac{s^2+u^2}{t^2}\right)$	$8N_c C_F \frac{s^2}{t^2}$
$q_1 q_1 \leftrightarrow q_1 q_1$ $\bar{q}_1 \bar{q}_1 \leftrightarrow \bar{q}_1 \bar{q}_1$	$4N_c C_F \left(\frac{s^2+u^2}{t^2} + \frac{s^2+t^2}{u^2}\right) - 8C_F \frac{s^2}{tu}$	$8N_c C_F \left(\frac{s^2}{t^2} + \frac{s^2}{u^2}\right)$
$q_1 \bar{q}_1 \leftrightarrow q_1 \bar{q}_1$	$4N_c C_F \left(\frac{s^2+u^2}{t^2} + \frac{t^2+u^2}{s^2}\right) - 8C_F \frac{u^2}{st}$	$8N_c C_F \frac{s^2}{t^2}$
$q_1 \bar{q}_1 \leftrightarrow q_2 \bar{q}_2$	$4N_c C_F \left(\frac{t^2+u^2}{s^2}\right)$	0
$q_1 \bar{q}_1 \leftrightarrow gg$	$8N_c C_F^2 \left(\frac{u}{t} + \frac{t}{u}\right) - 8N_c^2 C_F \frac{t^2+u^2}{s^2}$	$-8N_c C_F^2 \left(\frac{s}{t} + \frac{s}{u}\right)$
$q_1 g \leftrightarrow q_1 g$ $\bar{q}_1 g \leftrightarrow \bar{q}_1 g$	$-8N_c C_F^2 \left(\frac{u}{s} + \frac{s}{u}\right) + 8N_c^2 C_F \frac{u^2+s^2}{t^2}$	$-8N_c C_F^2 \frac{s}{u} + 16N_c^2 C_F \frac{s^2}{t^2}$
$gg \leftrightarrow gg$	$16N_c^2(N_c^2-1)\left(3 - \frac{su}{t^2} - \frac{st}{u^2} - \frac{tu}{s^2}\right)$	$16N_c^2(N_c^2-1)\left(\frac{s^2}{t^2} + \frac{s^2}{u^2}\right)$

Table : Squares of the $2 \leftrightarrow 2$ scattering amplitudes in QCD, with spins and colors of all four partons summed over.

The transport equation

- **The Fokker-Planck equation**

$$D_t f = -\nabla_{\mathbf{p}} \cdot \mathcal{J}_g + \mathcal{S}_g, \qquad D_t F = -\nabla_{\mathbf{p}} \cdot \mathcal{J}_q + \mathcal{S}_q,$$

where the currents and sources are given by

$$\begin{aligned}
\mathcal{J}_g &= -4\pi\alpha_s^2 N_c \mathcal{L} \left[\mathcal{I}_a \nabla_{\mathbf{p}} f + \mathcal{I}_b \frac{\mathbf{p}}{p} f(1+f) \right], \\
\mathcal{J}_q &= -4\pi\alpha_s^2 C_F \mathcal{L} \left[\underbrace{\mathcal{I}_a \nabla_{\mathbf{p}} F}_{diffusion} + \underbrace{\mathcal{I}_b \frac{\mathbf{p}}{p} F(1-F)}_{drag} \right], \\
\mathcal{S}_g &= -\frac{N_f}{C_F} \mathcal{S}_q = \frac{4\pi\alpha_s^2 C_F N_f \mathcal{L} \mathcal{I}_c}{p} \left[F(1+f) - f(1-F) \right],
\end{aligned}$$

with

$$\begin{aligned}
\mathcal{I}_a &= \int \frac{d^3p}{(2\pi)^3} \left[N_c f(1+f) + N_f F(1-F) \right] \propto \hat{q}, \\
\mathcal{I}_b &= 2 \int \frac{d^3p}{(2\pi)^3} \frac{1}{p} \left(N_c f + N_f F \right), \mathcal{I}_c = \int \frac{d^3p}{(2\pi)^3} \frac{1}{p} (f + F).
\end{aligned}$$

The transport equation

- **For a spatially homogeneous system**

$$\dot{f} = -\frac{1}{p^2}\left(p^2 J_g\right)' + \frac{C_F N_f}{N_c} S_g = -\frac{1}{4\pi p^2}\mathcal{F}_g' - \frac{C_F N_f}{N_c} S_q,$$

$$\dot{F} = -\frac{C_F}{N_c}\frac{1}{p^2}\left(p^2 J_q\right)' + \frac{C_F^2}{N_c} S_q = -\frac{C_F}{N_c}\frac{1}{4\pi p^2}\mathcal{F}_q' + \frac{C_F^2}{N_c} S_q,$$

where

$$S_g = -S_q = \frac{I_c}{p}\left[F(1+f) - f(1-F)\right],$$

$$\frac{\mathcal{F}_g}{4\pi p^2} \equiv J_g \equiv -I_a f' - I_b f(1+f), \frac{\mathcal{F}_q}{4\pi p^2} \equiv J_q \equiv -I_a F' - I_b F(1-F),$$

with

$$I_a = 2\pi^2 \mathcal{I}_a, I_b = 2\pi^2 \mathcal{I}_b, I_c = 2\pi^2 \mathcal{I}_c.$$

The transport equation

- **Redefined time**

$$\tau = \frac{2\alpha_s^2 N_c \mathcal{L}}{\pi} t$$

with

$$\mathcal{L} \simeq \int_{q_{min}}^{q_{max}} \frac{dq}{q}$$

being taken as a constant.

J. -P. Blaizot, J. Liao and L. McLerran, Nucl. Phys. A **920**, *58 (2013) [arXiv:1305.2119 [hep-ph]].*

- **(Naive) scaling symmetry**

$$Q_s \to cQ_s, \quad \tau \to \frac{\tau}{c}, \quad \mathbf{p} \to c\mathbf{p}$$

with $c > 0$. As a result, one can express all momenta in units of Q_s and times in units of $1/Q_s$.

Quark production, BEC and thermalization

- **Thermodynamics**
  - **Underlying assumptions for $2 \leftrightarrow 2$ process:**

    The total parton number is conserved $\Rightarrow$ the same μ for all the partons.
  - **The fixed points of collision terms**

$$\mathbf{f_{eq} = \frac{1}{e^{(p-\mu)/T} - 1}, \qquad F_{eq} = \frac{1}{e^{(p-\mu)/T} + 1}.}$$

    where T and μ may be fixed by

$$\epsilon_{eq} = \epsilon_0, \qquad n_{eq} = n_0.$$

  - **Under- and over-populated systems**
    - **Under-polpulation: $\mu \leq 0$ exists.**
    - **Over-polpulation: $\mu = 0$ with BEC and**

$$T = \sqrt{\frac{2}{\pi}} \frac{(15\epsilon_0)^{1/4}}{(8N_c C_F + 7N_c N_f)^{1/4}}.$$

J. -P. Blaizot, J. Liao and L. McLerran, Nucl. Phys. A **920**, *58 (2013) [arXiv:1305.2119 [hep-ph]].*

Quark production, BEC and thermalization

- **Thermodynamics**
  - **Initial distributions**

$$\mathbf{f(0,p) = f_0\ \theta\left(1 - \frac{p}{Q_s}\right), \qquad F(0,p) = 0.}$$

with

$$\epsilon_0 = \frac{f_0}{2\pi^2} N_c C_F Q_s^4, \qquad n_0 = \frac{f_0}{3\pi^2} 2 N_c C_F Q_s^3.$$

  - **The transition from under- to over-population happens at**

$$f_{0c} = \frac{273375(4C_F + 3N_f)^4 \zeta(3)^4}{2C_F(8C_F + 7N_f)^3 \pi^{12}} \simeq \frac{0.309(4C_F + 3N_f)^4}{C_F(8C_F + 7N_f)^3},$$

$$T_c = \frac{45\zeta(3)\,(4C_F + 3N_f)}{\pi^4\,(8C_F + 7N_f)} Q_s \simeq \frac{0.555\,(4C_F + 3N_f)}{(8C_F + 7N_f)} Q_s.$$

  - **Examples**
    - $N_f = 0$: $f_{0c} = 0.154$, $N_f = 3$: $f_{0c} = 0.308$

Quark production, BEC and thermalization

- **Only two types of solutions to the transport equation**
  - **f is analytic at $p = 0$**

$$f = f(\tau, 0) + O(p), \qquad F = F(\tau, 0) + O(p).$$

with the flux

$$\mathcal{F}_g|_{p=0} = 0, \quad \mathcal{F}_q|_{p=0} = 0.$$

  - **f is singular at $p = 0$**

$$f = \frac{c_{-1}}{p} - \frac{1}{2} + O(p), \qquad F = \frac{1}{2} + O(p),$$

with

$$\mathcal{F}_g|_{p=0} = 4\pi c_{-1}\left(I_a - I_b c_{-1}\right), \qquad \mathcal{F}_q|_{p=0} = 0.$$

Indicates the formation of BEC!

  - **Boundary conditions for the formation of condensates**

$$\mathcal{F}_g|_{p=\infty} = 0, \mathcal{F}_g|_{p=0} = 4\pi c_{-1}\left(I_a - I_b c_{-1}\right), \mathcal{F}_q|_{p=\infty} = 0, \mathcal{F}_q|_{p=0} = 0.$$

Quark production, BEC and thermalization

- **Thermalization with BEC:** $f_0 > f_{0c} = 0.308$

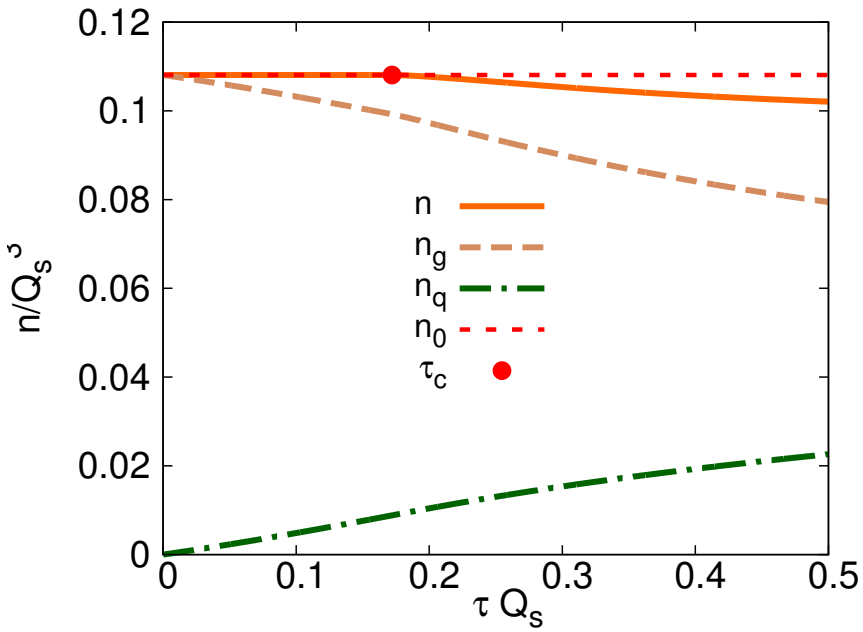

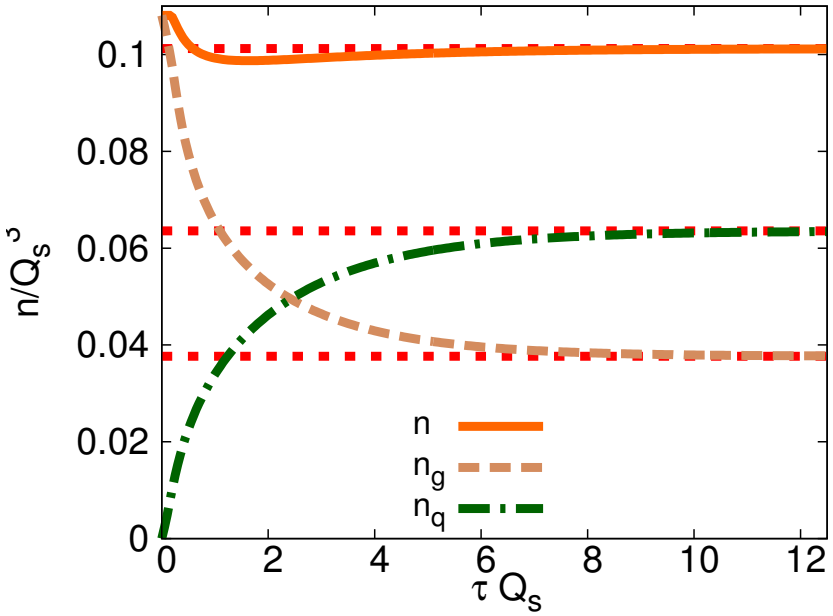

Quark production, BEC and thermalization

- τ_c: **time for the onset of BEC**
  - **Definition: time for f to build up the $1/p$ tail at small p**

    J. -P. Blaizot, J. Liao and L. McLerran, Nucl. Phys. A **920**, *58 (2013) [arXiv:1305.2119 [hep-ph]].*

  - **Parametric estimate**

    At early time for $f_0 > 1$

$$f \sim \frac{2}{p}\left[\underbrace{I_a(0)f'(0,p)}_{diffusion} + \underbrace{I_b(0)f(0,p)^2}_{drag} - I_c(0)N_f\frac{f_0^2}{p}\right]\tau \sim f_0^3\frac{Q_s^2}{p}\tau.$$

    τ_c given by

$$pf(p)|_{p\to 0} \sim Q_s f(Q_s) \sim Q_s f_0.$$

    That is

$$\boxed{\tau_c \sim \frac{1}{f_0^2}\frac{1}{Q_s}, \quad \textbf{or} \quad t_c \sim \frac{1}{(\alpha_s f_0)^2}\frac{1}{Q_s}.}$$

Quark production, BEC and thermalization

- τ_c: **time for the onset of BEC**

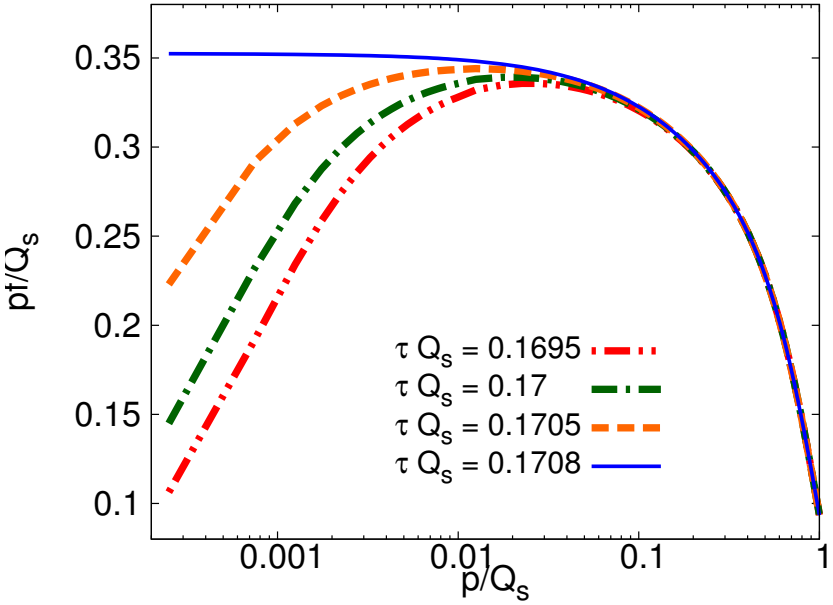

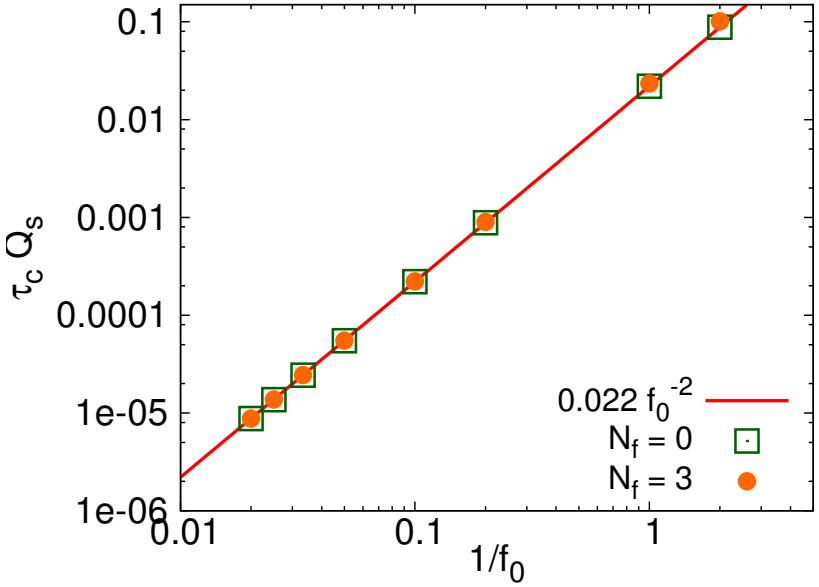

Quark production, BEC and thermalization

- **Thermalization with transient BEC:** $0.308 = f_{0c} > f_0 > f_{0t} = 0.25$

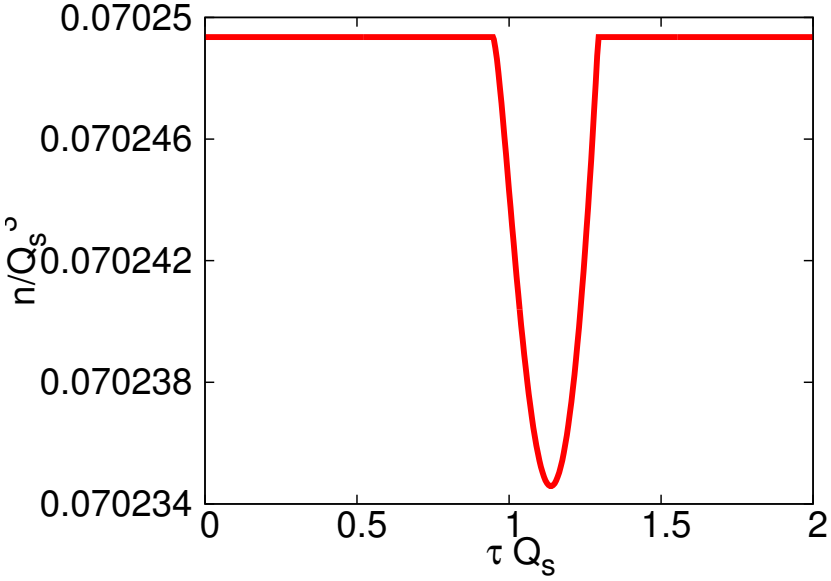

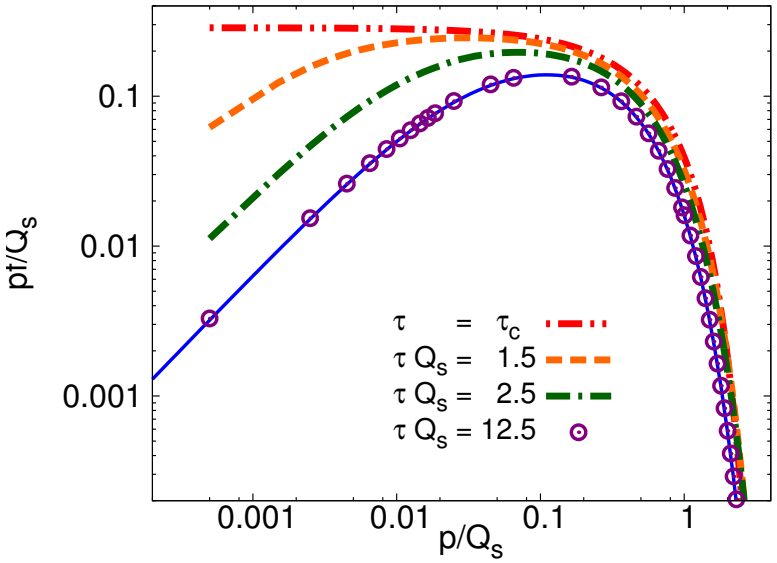

with $f_0 = 0.26$ and $N_f = 3$.

Quark production, BEC and thermalization

- **Quark production: produced mostly at low p**

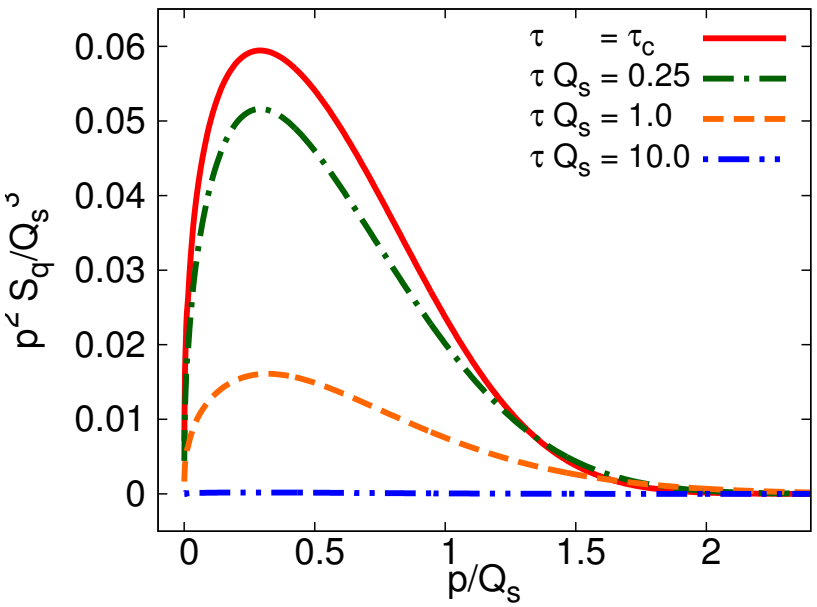

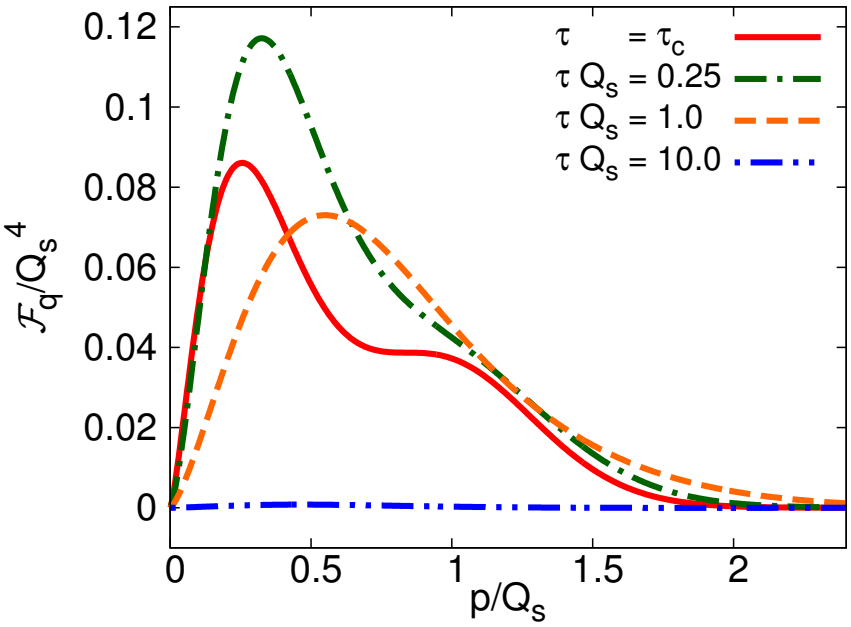

with $f_0 = 0.4$ and $N_f = 3$. **Quarks pick up a large momentum mainly by multiple scattering.**

Quark production, BEC and thermalization

- **Quark production slows down thermalization**

  For the same Q_s and f_0

  t_{eq} **for** $N_f = 3 \sim$ **5 to 6 times longer than** $N_f = 0$

  with the equilibration time t_{eq}

$$\left|\frac{T^*(\tau_{eq})}{T} - 1\right| \leq 0.05, \quad \left|\frac{n_g(\tau_{eq})}{n_{geq}} - 1\right| \leq 0.05, \quad \left|\frac{n_q(\tau_{eq})}{n_{qeq}} - 1\right| \leq 0.05,$$

  and

$$\left|\frac{s_g(\tau_{eq})}{s_{geq}} - 1\right| \leq 0.05, \quad \left|\frac{s_q(\tau_{eq})}{s_{qeq}} - 1\right| \leq 0.05.$$

  with $T^* \equiv I_a/I_b$.

Discussions

1. **What is BEC, quasi-particles or classical fields?**

   - **In kinetic theory**

     BEC is obviously quasi-particles with

     $$f_{tot}(t,p) = f_p + (2\pi)^3 n_c(t)\delta(\mathbf{p})$$

     For example, D. V. Semikoz and I. I. Tkachev, Phys. Rev. D **55**, *489 (1997) [hep-ph/9507306].*

   - **In classical statistical approximation**

     It does not look like condensate in the sense of the Higgs mechanism since

     $$\langle\phi\rangle = 0,$$

     but described by

     $$\bar{\phi}^2(t) \equiv \int d^3x dy^3 \langle\phi(x)\phi(y)\rangle\Big|_{x^0=y^0=t} = 2\int d^3x dy^3 G_{22}(x,y)\Big|_{x^0=y^0=X^0}$$

     which also has a nice quasi-particle interpretation

     $$\begin{aligned}\bar{\phi}^2 &= 2\int \frac{d^4p}{(2\pi)^4} e^{-i\mathbf{p}\cdot(\mathbf{x}-\mathbf{y})}(2\pi)\delta(p^2-m^2)(f_p+\frac{1}{2}) \\ &= V\int d^3p \frac{1}{\omega_p}\left(f_p+\frac{1}{2}\right)\delta(\mathbf{p}) \simeq V^2 n_c/m.\end{aligned}$$

Dénes Sexty's talk!

T. Epelbaum, F. Gelis, N. Tanji, B. Wu, In preparation.

The roles of elastic vs. inelastic scatterings in thermalization

Bin Zhang
Arkansas State University

The Approach to Equilibrium in Strongly Interacting Matter workshop
April 2– 4, 2014, Brookhaven National Laboratory, USA

- Introduction
- Pressure isotropization and parton equilibration
- gg <-> ggg with the exact matrix element
- Summary and discussions

Work supported by the U.S. National Science Foundation under Grant No. PHY-0970104

Introduction to Parton Cascade

- The Boltzmann equation

$$\left(\frac{\partial}{\partial t}+\frac{\boldsymbol{p}}{E}\frac{\partial}{\partial \boldsymbol{x}}\right)f(\boldsymbol{x},\boldsymbol{p},t)=S(\boldsymbol{x},\boldsymbol{p},t)+C_{22}+C_{23}+C_{32}+\mathrm{L}$$

C_{mn} are collision terms (each is an integral of (*m*+*n*-1)x3-4 dimensions with *m* phase space distributions)

Interactions with color field Color degrees of freedom

- Test particle method

$$f(\boldsymbol{x},\boldsymbol{p},t)=\sum_i w_i\,\delta^{(3)}(\boldsymbol{x}-(\boldsymbol{x}_i-\frac{\boldsymbol{p}_i}{E_i}(t-t_i)))\,\delta^{(3)}(\boldsymbol{p}-\boldsymbol{p}_i)$$

$(\boldsymbol{x}_i,\boldsymbol{p}_i,t_i)$ formation and collisions (geometric, stochastic)

Introduction: radiative transport

- The reaction rates

$$\sigma_{22} = \frac{9\pi\alpha_S^2}{2\mu^2}$$

$$\mu^2 = \frac{3\pi\alpha_S}{V}\sum_i \frac{1}{p_i}$$

$$\sigma_{23} = 0.5\,\sigma_{22}$$

$$I_{32} = 12\pi^2\sigma_{23}$$

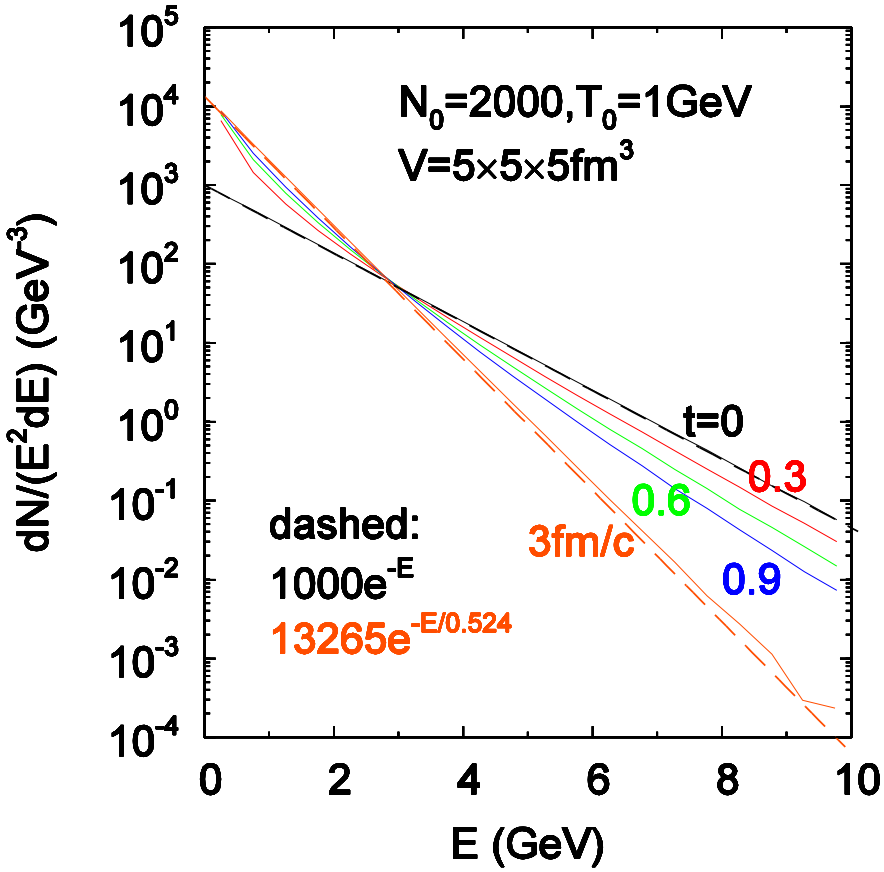

Longitudinal to transverse pressure ratio

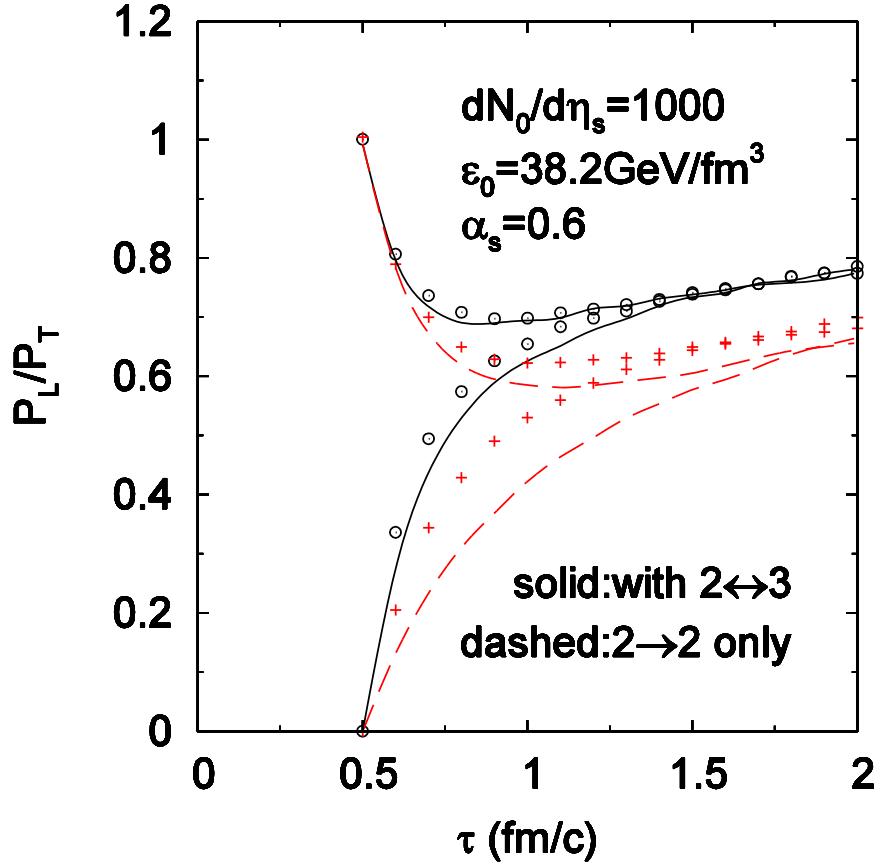

Lines (points): exponential (condensate) initial conditions

- competition between expansion and equilibration
- common asymptotic evolution
- more isotropization with inelastic processes
- not sensitive to initial momentum distribution with inelastic processes

Longitudinal to transverse pressure ratio

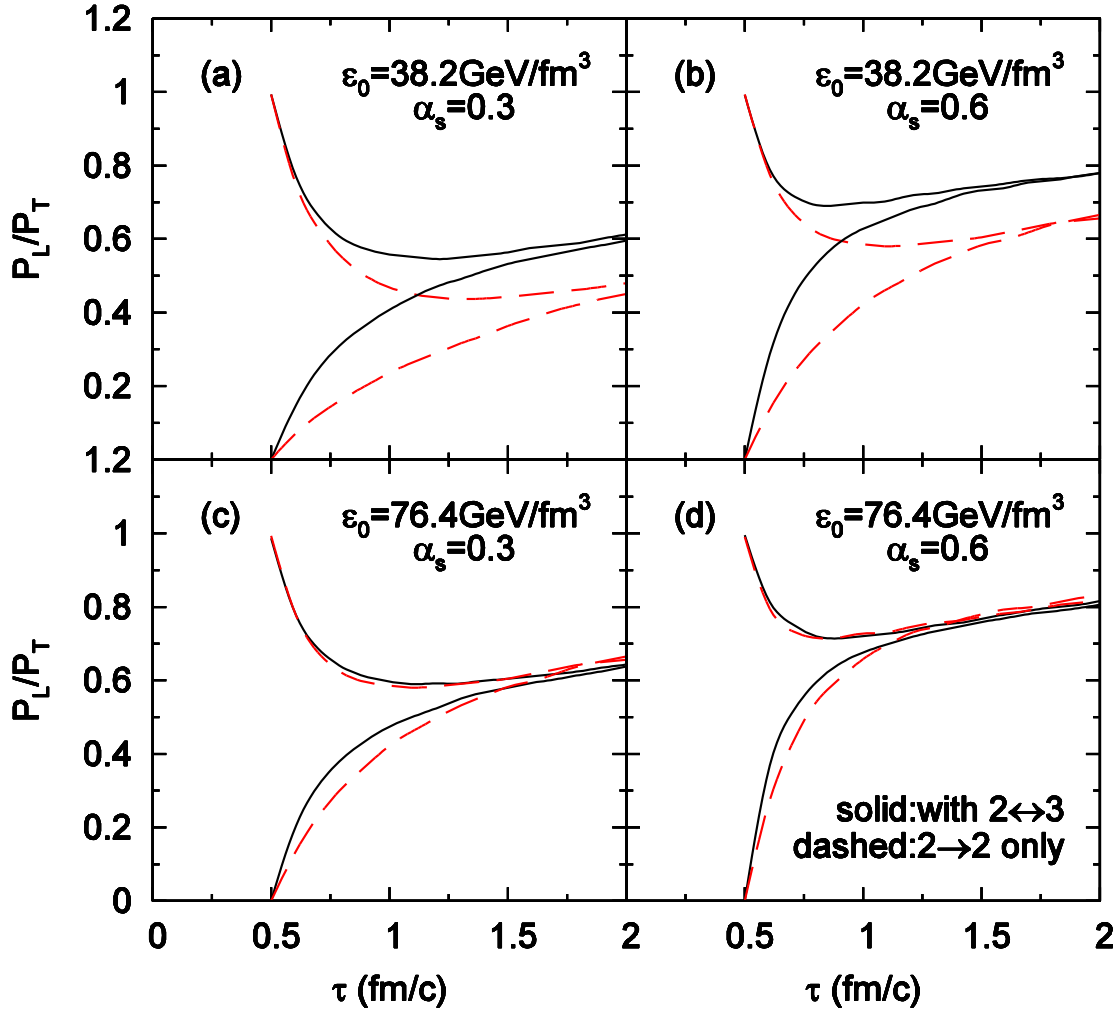

$\alpha_s\varepsilon_0$ scaling for elastic only. Approximate α_s scaling with inelastic.

Longitudinal to transverse pressure ratio

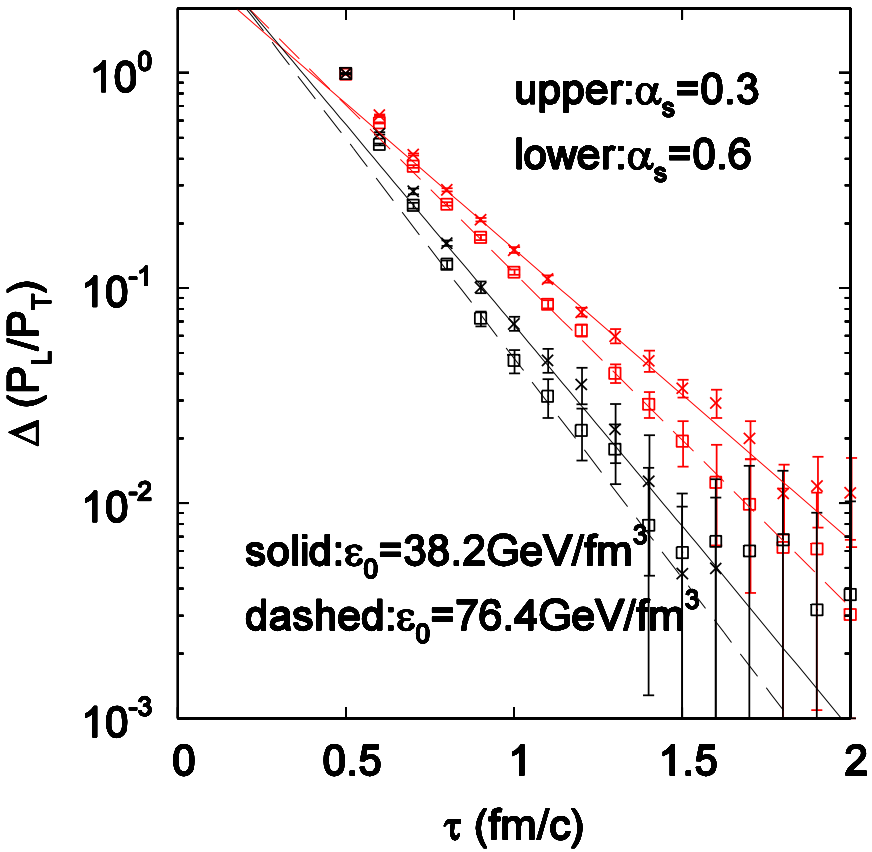

Inelastic included

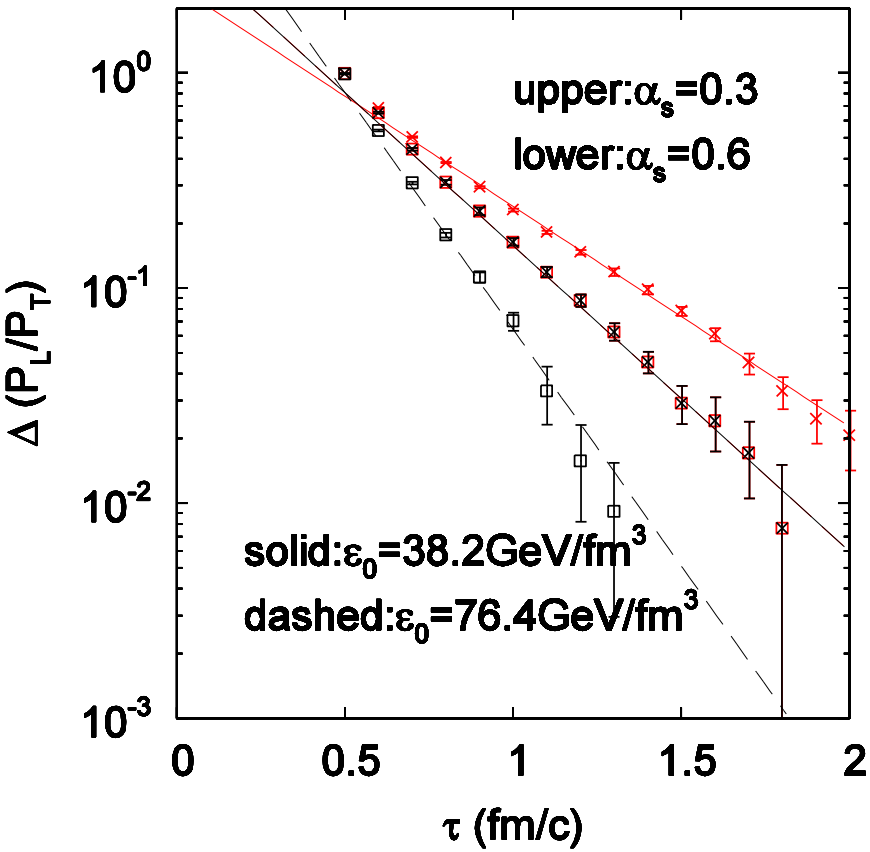

Elastic only

Fugacity evolution

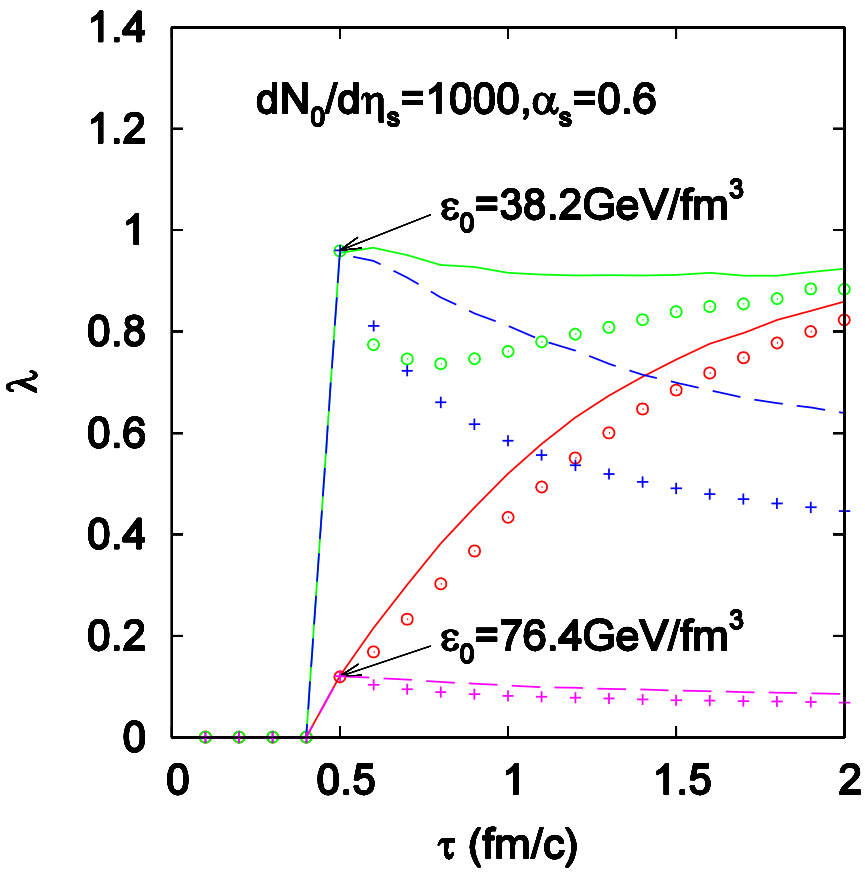

Lines (points): isotropic (transverse) initial conditions

- interplay between chemical and kinetic equilibrations
- inelastic more effective for kinetic equilibration at (or above) $\lambda=1$
- elastic deviates from chemical equilibrium
- isotropic initial more effective in chemical equilibration

Exact matrix element for gg↔ggg

$$\left|M_{gg\to ggg}\right|^2 = \frac{g^6 N_c^3}{2(N_c^2-1)} \frac{\sum (ij)^4 \sum (ijklm)}{\prod (ij)}$$

$$(ij) = p_i \cdot p_j$$

$$(ijklm) = (ij)(jk)(kl)(lm)(mi)$$

Propagators regulated by μ^2

When α_s=0.47, μ^2=10 fm^{-2}, s=4 GeV^2, σ_{22}=0.312 fm^2, and σ_{23}=0.0523 fm^2.

σ_{23}/σ_{22} ~ 0.168 < 0.5

When α_s=0.4, T=0.524 GeV, (preliminary) $\langle\sigma_{23}\rangle_{23}/\langle\sigma_{22}\rangle_{22}$~57%, $\langle\sigma_{23}\rangle/\langle\sigma_{22}\rangle$~17%, w_{23}/w_{22}~12%.

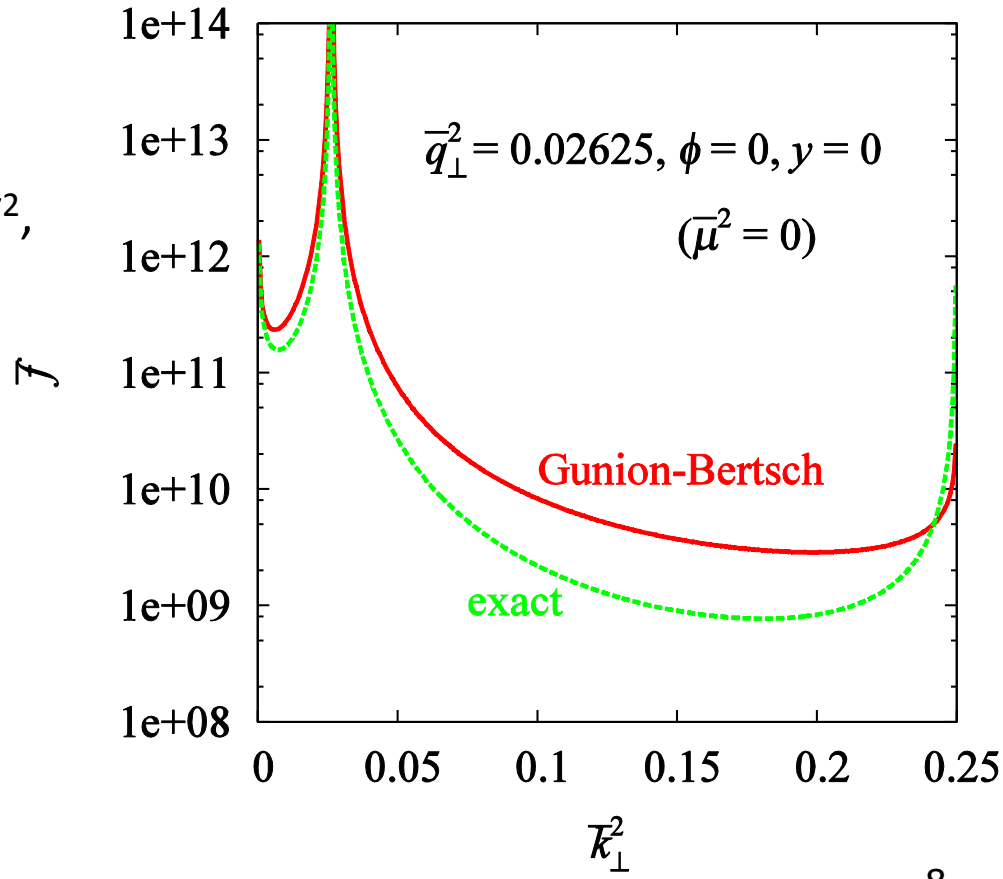

Summary and discussions

- Elastic collisions may be more important in thermalization than expected.

- Specific shear viscosity may be larger than the quantum limit.

- Formation time regularization can be approximated by screening mass regularization (replacement of the theta function by a Lorentzian).

- Exact and Gunion-Bertsch can have big differences.

- Bethe-Heitler limit may be important for bulk matter thermalization (formation time vs. mean free path).

- Elastic collisions can also be important for heavy quark equilibration (meson dissociation).

Energy density evolution

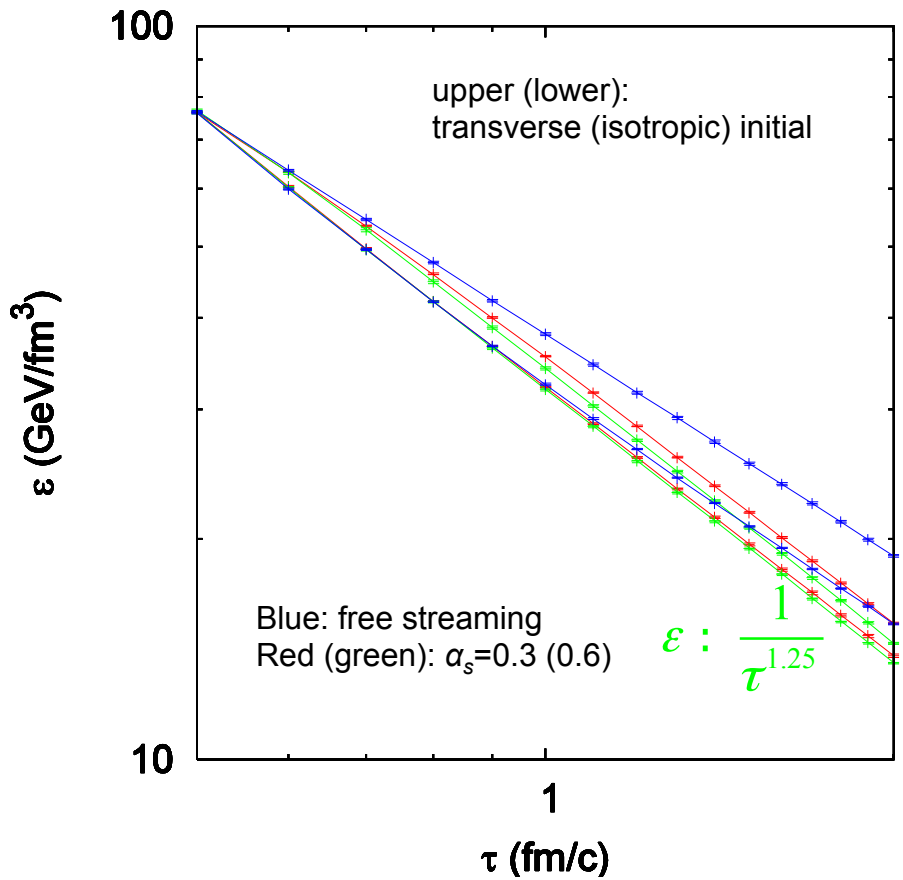

- early time power law behavior reflects initial isotropy
- asymptotic power law behavior reflects interactions
- behavior not sensitive to initial energy density

Viscous corrections can not be neglected

Exact matrix element for gg↔ggg

$$\left|M_{gg\to ggg}\right|^2 = \frac{g^6 N_c^3}{2(N_c^2-1)} \frac{\sum (ij)^4 \sum (ijklm)}{\prod (ij)}$$

$$(ij) = p_i \cdot p_j$$

$$(ijklm) = (ij)(jk)(kl)(lm)(mi)$$

Propagators regulated by μ^2

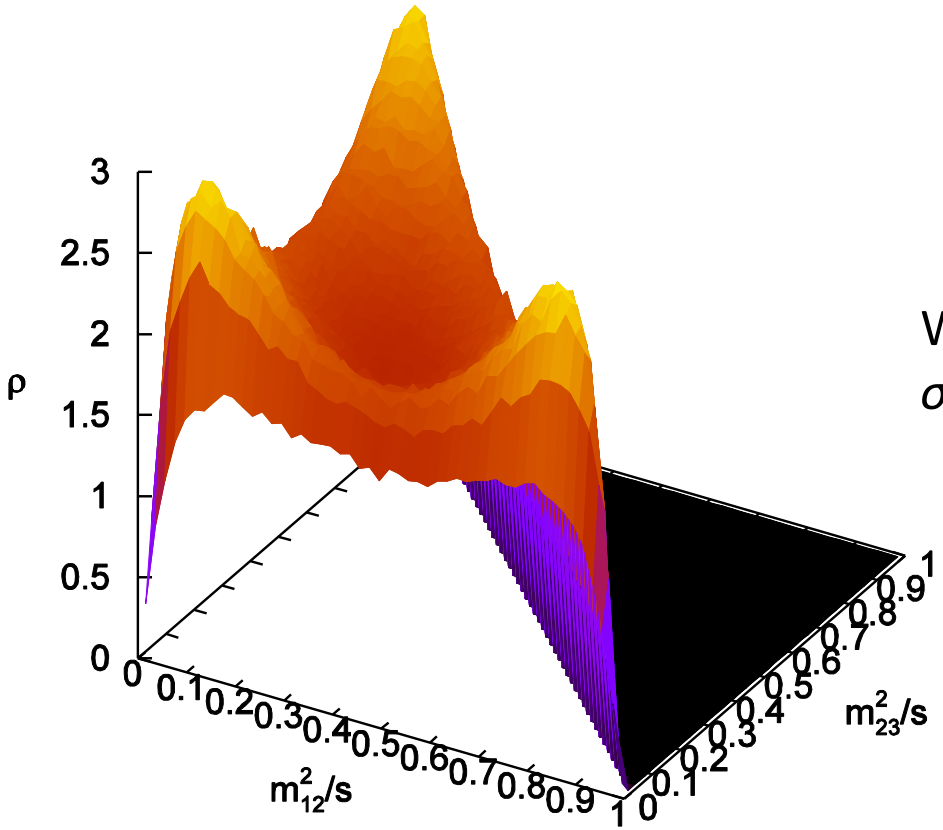

When α_s=0.47, μ^2=10 fm^{-2}, s=4 GeV^2, σ_{22}=0.312 fm^2, and σ_{23}=0.0523 fm^2.

σ_{23}/σ_{22} ~ 0.168 < 0.5

(When α_s=0.3, μ^2=6.38 fm^{-2}, s=4 GeV^2, σ_{22}=0.199 fm^2, and σ_{23}=0.0504 fm^2.)

Exact matrix element vs. Gunion-Bertsch

$$\left|M^{GB}_{gg\to ggg}\right|^2 = \frac{9g^4 s^2}{2(q_\perp^2+\mu^2)^2}\,\frac{12 g^2 q_\perp^2}{k_\perp^2((k_\perp - q_\perp)^2+\mu^2)}$$

singularity regulated by μ^2

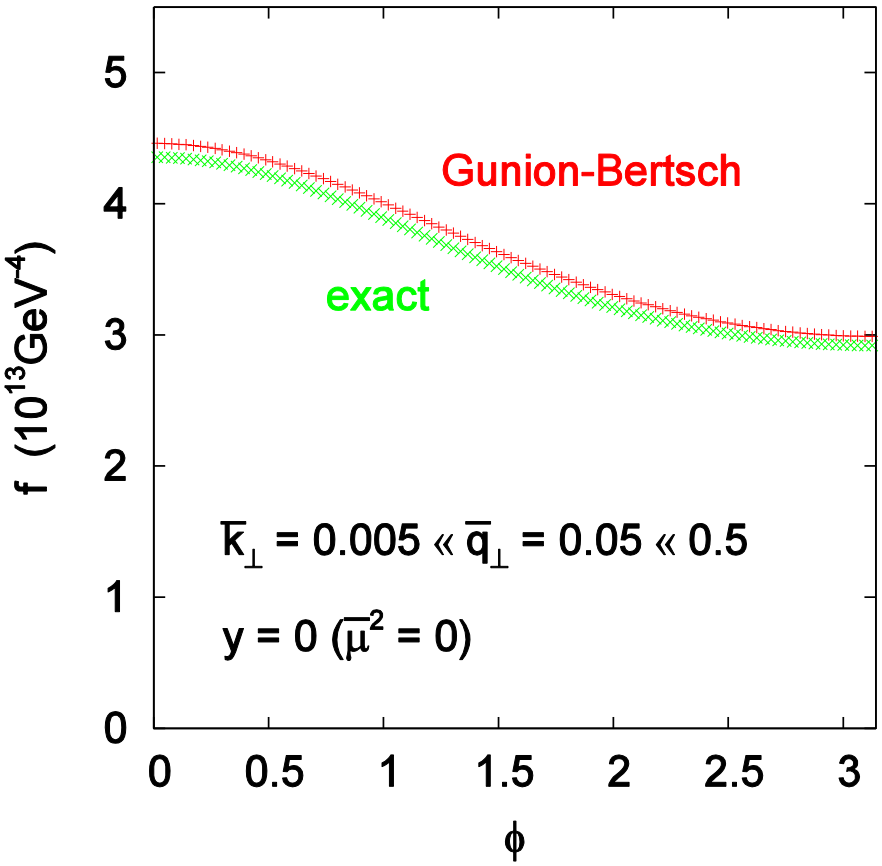

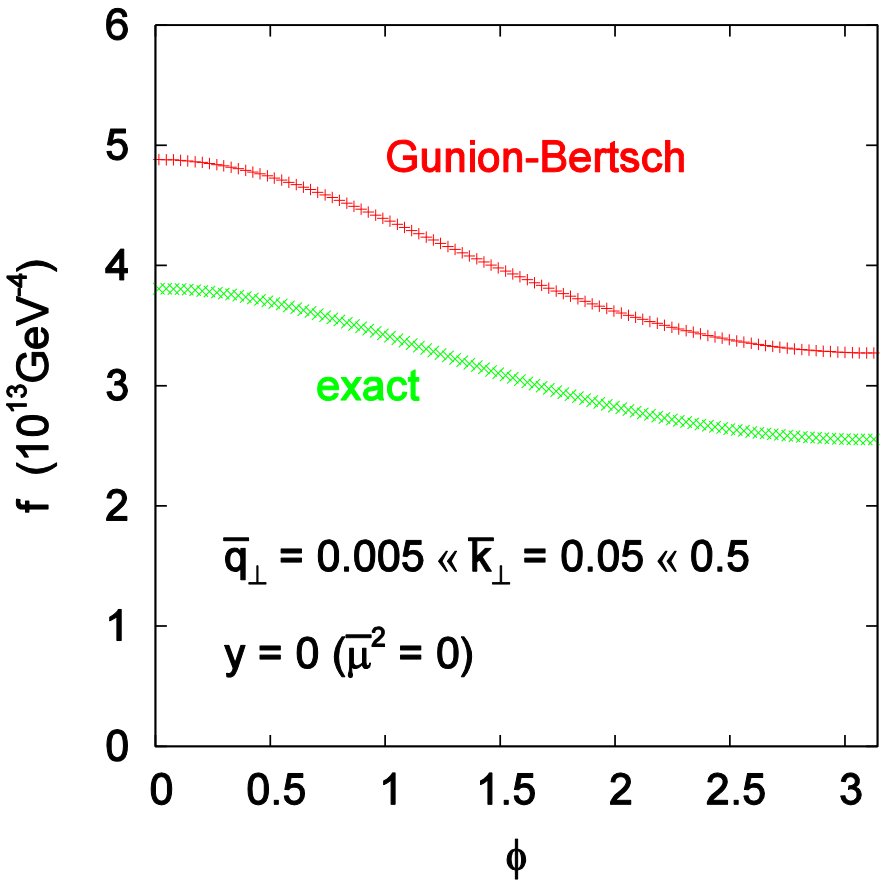

Exact matrix element vs. Gunion-Bertsch

$$\left|M^{GB}_{gg\to ggg}\right|^2 = \frac{9g^4s^2}{2(q_\perp^2+\mu^2)^2}\,\frac{12g^2q_\perp^2}{k_\perp^2((k_\perp-q_\perp)^2+\mu^2)}$$

singularity regulated by μ^2

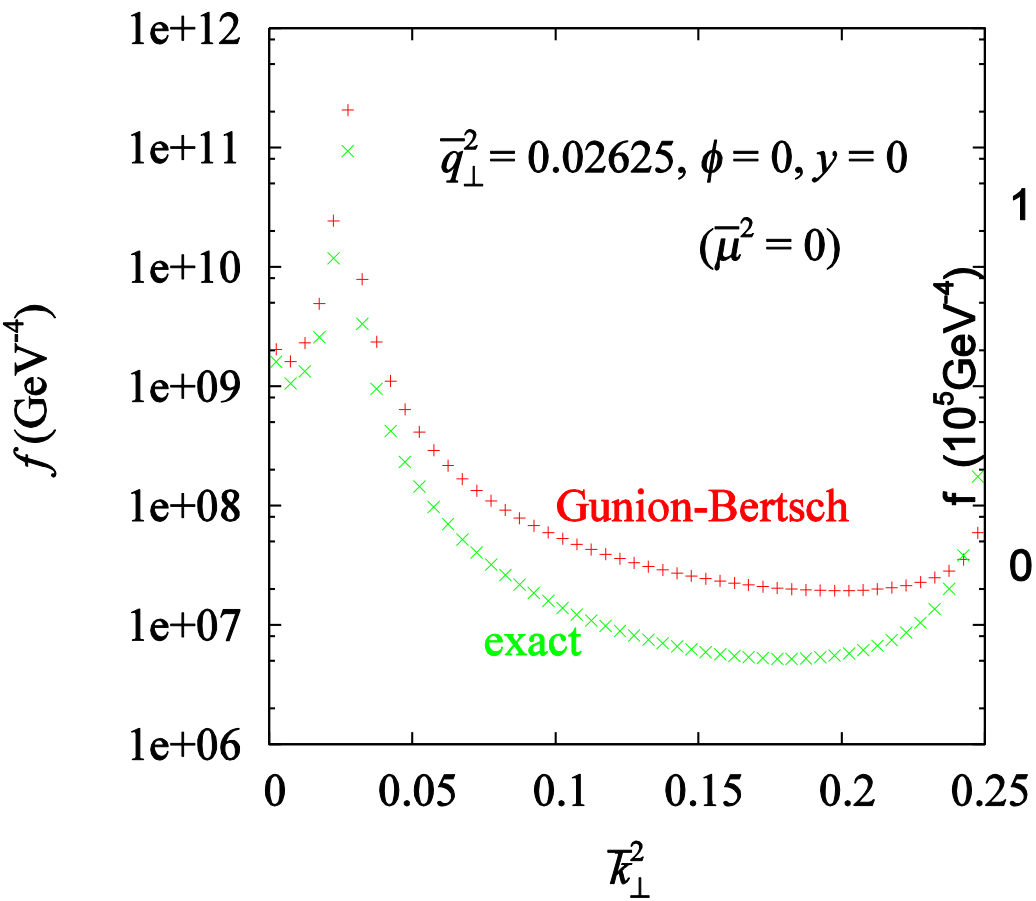

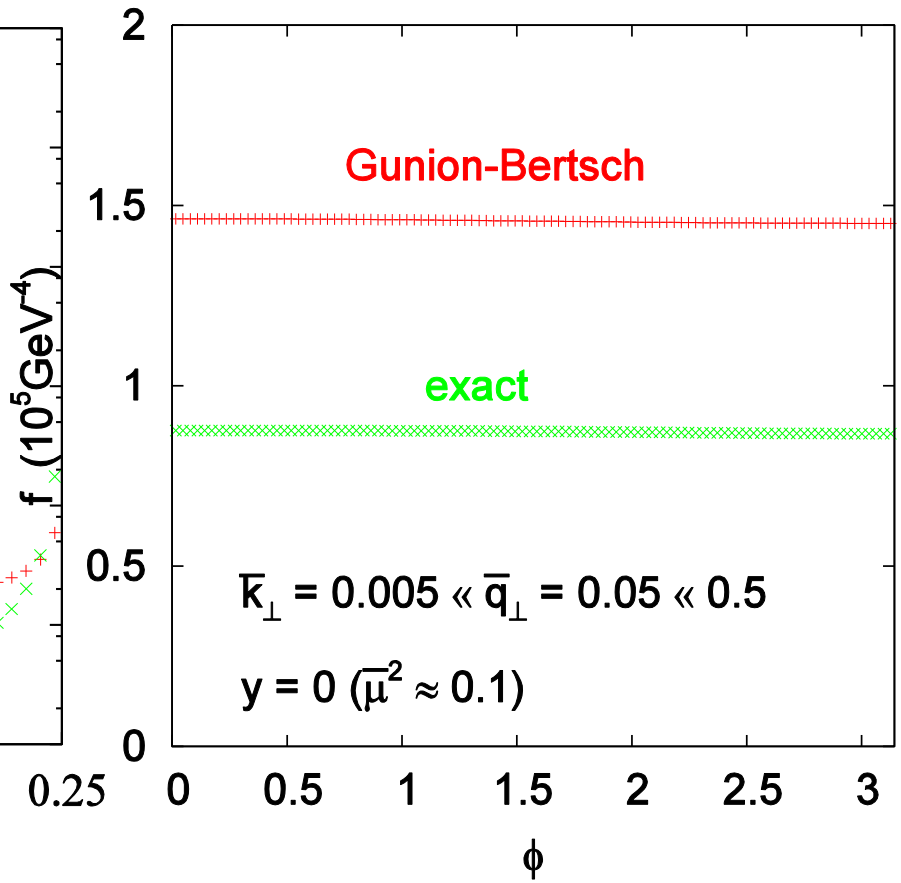

Exact matrix element for gg↔ggg

When α_s=0.47, μ^2=10 fm^{-2}, I_{32}=6.84 fm^2. Estimate with isotropic matrix element gives I_{32}=6.19 fm^2.

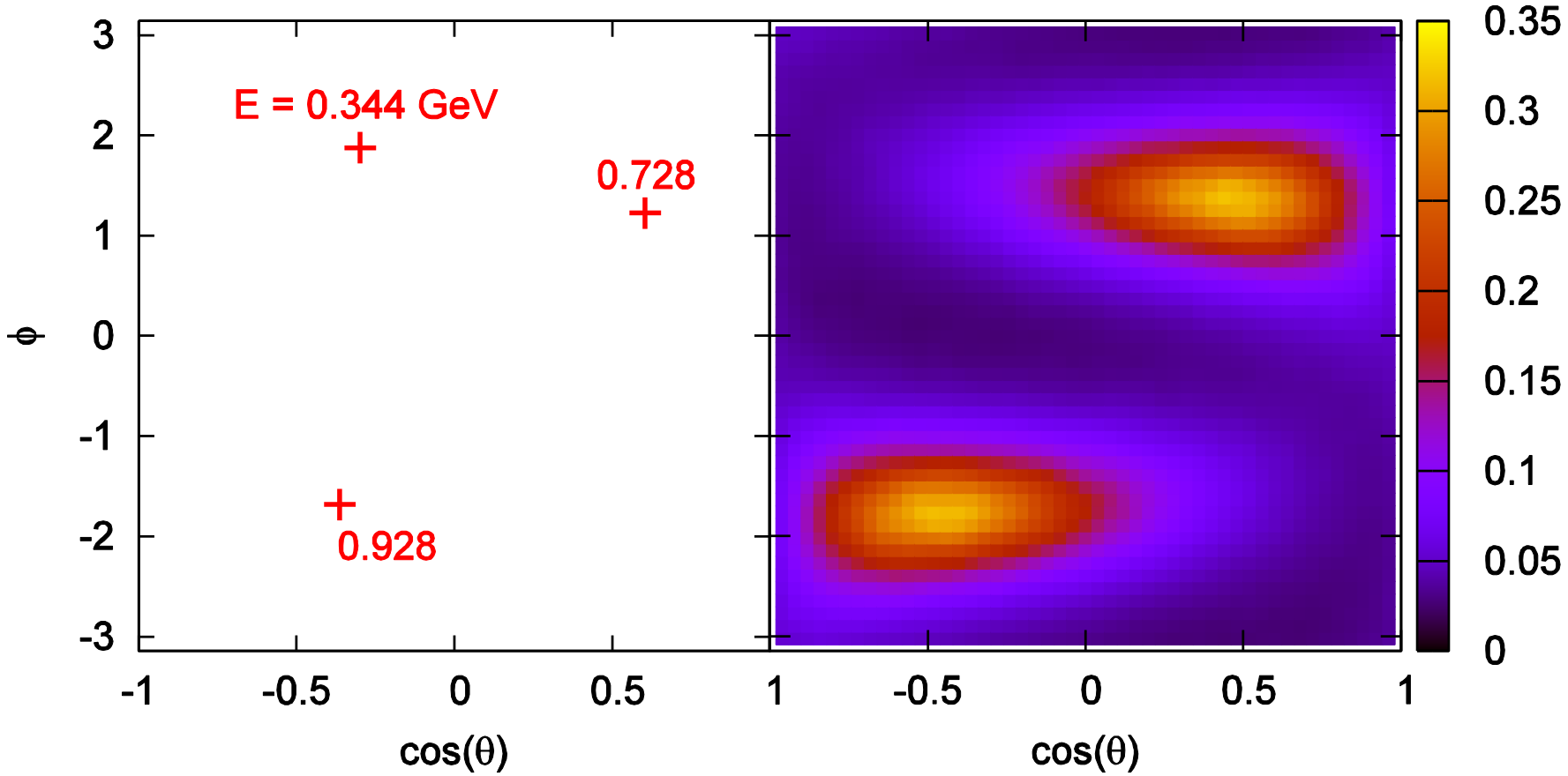

Exact matrix element for gg↔ggg

When α_s=0.47, μ^2=10 fm^{-2}, I_{32}=4.85 fm^2. Estimate with isotropic matrix element gives I_{32}=6.19 fm^2.

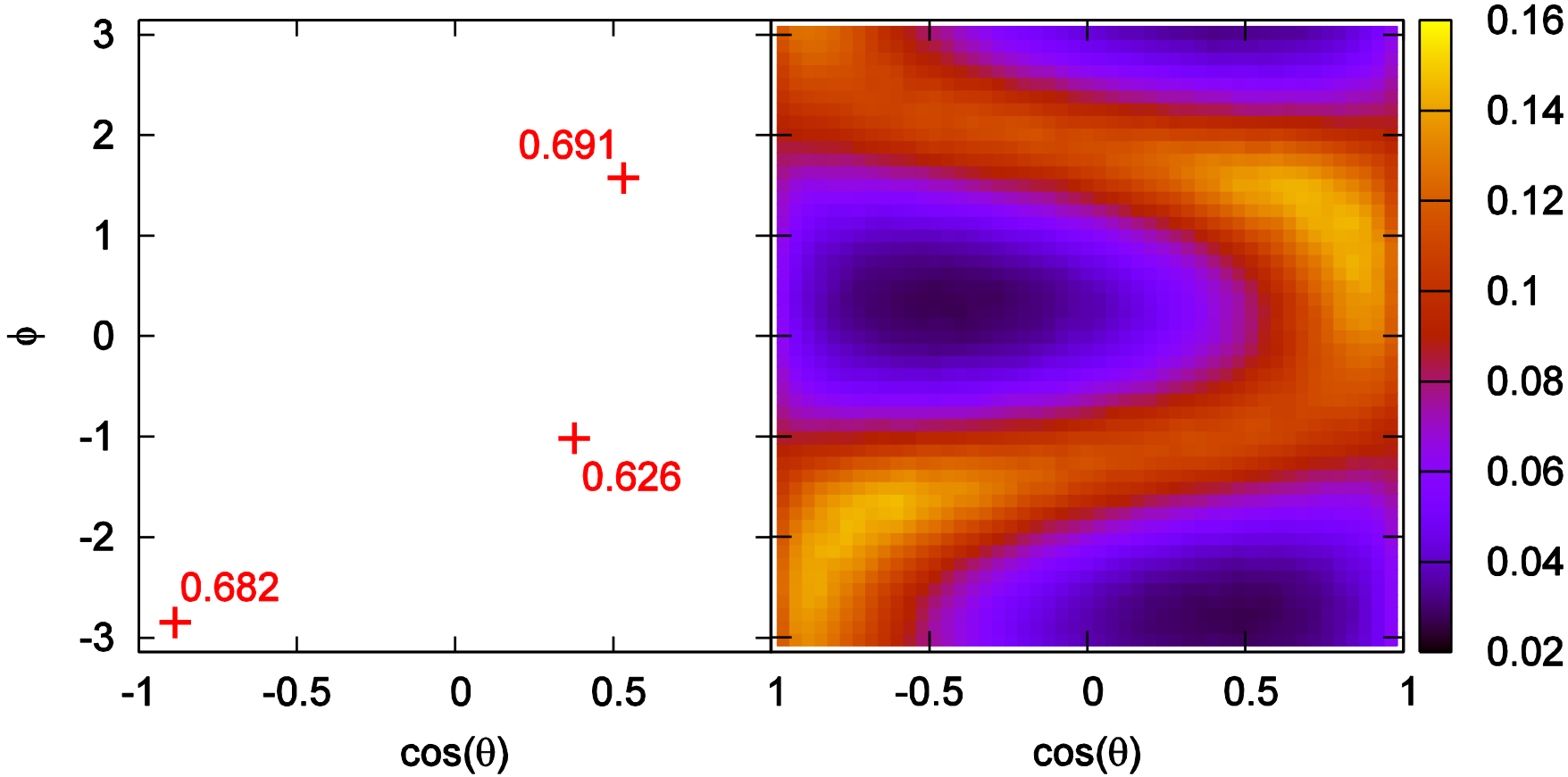

Equilibrium in a box with gg↔ggg

When α_s=0.4, T=0.524 GeV, $\langle\sigma_{23}\rangle_{23}/\langle\sigma_{22}\rangle_{22}$~57%, $\langle\sigma_{23}\rangle/\langle\sigma_{22}\rangle$~17%, w_{23}/w_{22}~12% (preliminary).

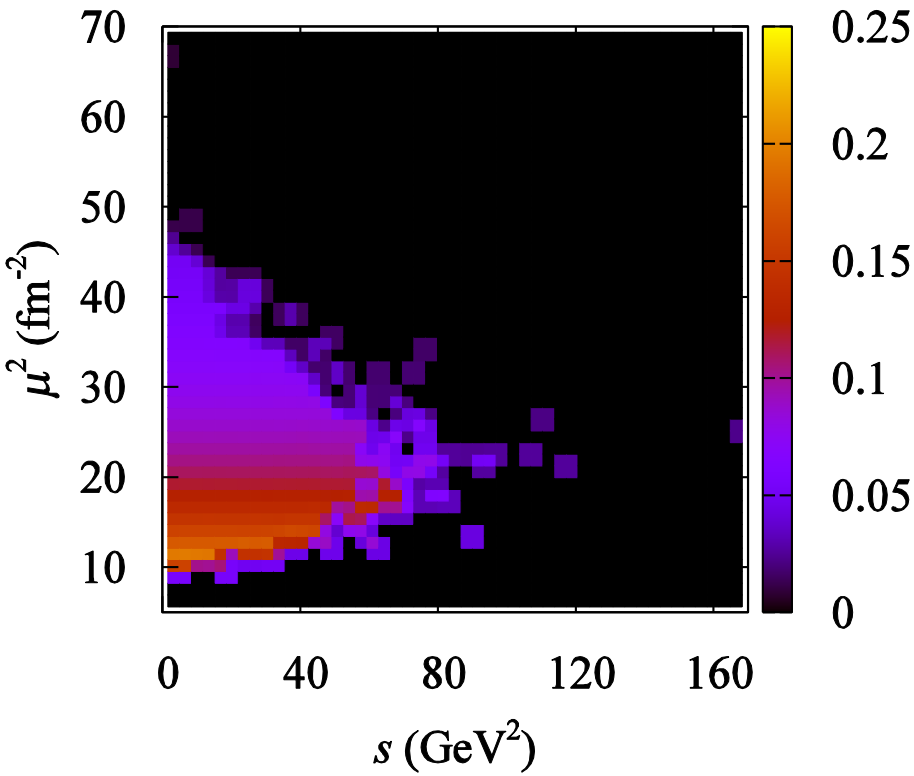

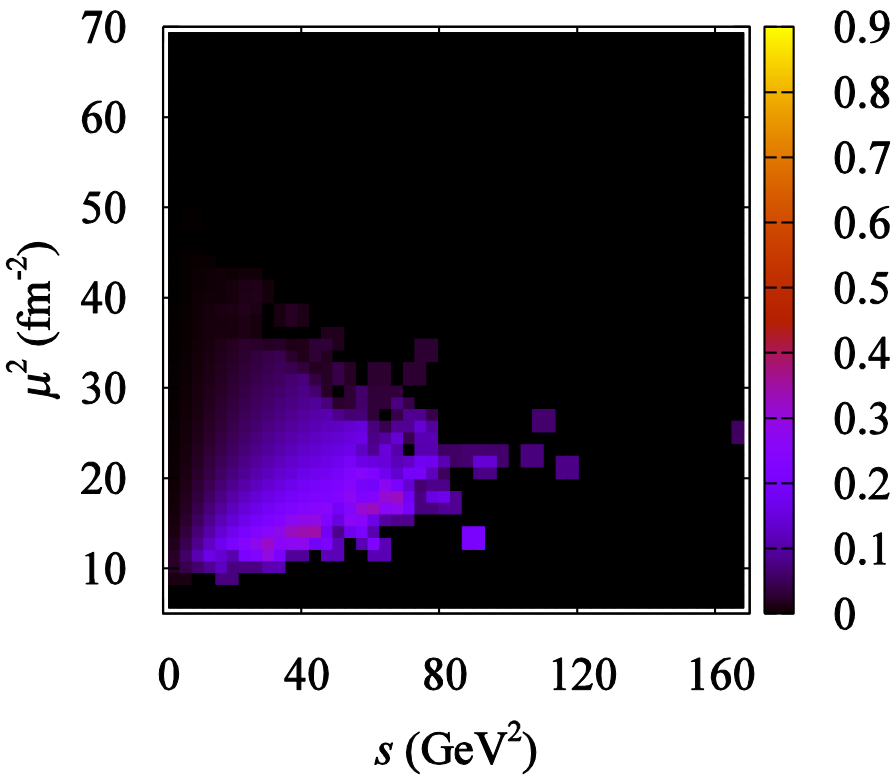

The Approach to Equilibrium in Strongly Interacting Matter

April 2-4, 2014
Large Seminar Room, Physics, Bldg. 510

WEDNESDAY, APRIL 2

08:30-09:15 **REGISTRATION**

09:15-12:15 Session I. Chair: Raju Venugopalan

09:15-09:30 Rob Pisarski ..... *Welcome*
09:30-10:15 Larry McLerran ..... *The glasma and thermalization: Ups and downs*
10:15-10:45 Aleksi Kurkela ..... *UV cascade of over-occupied gluons*

10:45-11:15 **COFFEE BREAK**

11:15-11:45 Thomas Epelbaum ..... *Early isotropization of the quark gluon plasma*
11:45-12:15 Soeren Schlichting ..... *Turbulent thermalization process in heavy-ion collisions at ultra-relativistic energies*

12:15-14:00 **LUNCH**

14:00-17:30 Session II. Chair: Francois Gelis

14:00-14:30 Maximilian Attems..... *Instabilities in non-Abelian expanding plasmas*
14:30-15:00 Stefan Floerchinger ..... *Isotropization from color field condensate in heavy ion collisions*
15:00-15:30 Akira Ohnishi ..... *Entropy production in the classical Yang-Mills theory as the coherent-state dynamics*
15:30-16:00 Tuomas Lappi..... *Spatial Wilson loops in the glasma*

16:00-16:30 **COFFEE BREAK**

16:30-17:00 Kirill Boguslavski ..... *Universality far from equilibrium and the range of validity of classical-statistical simulations*
17:00-17:30 Jean-Paul Blaizot..... *Medium induced QCD cascade and turbulence*

THURSDAY, APRIL 3

09:00-12:30 Session III. Chair: Jinfeng Liao

09:00-09:30 Bin Wu..... *Quark production, Bose-Einstein condensates and thermalization of the quark-gluon plasma*
09:30-10:00 Denes Sexty ..... *Non-equilibrium Bose-Einstein condensation in scalar and gauge systems*
10:00-10:30 Jan Pawlowski..... *Non-equilibrium dynamics of gauge theories, and transport coefficients*

10:30-11:00 **COFFEE BREAK**

11:00-11:30 Xu-Guang Huang ..... *Thermalization and transient BEC in glasma: Effects of inelastic processes*
11:30-12:00 Yin Jiang..... *Kinetic evolution with effective mass and dynamical onset of BEC in the glasma*
12:00-12:30 Bin Zhang ..... *The roles of elastic versus inelastic scatterings in thermalization*

12:30-14:00 **LUNCH**

Back to Contents

14:00-17:45 Session IV. Chair: Juergen Berges

14:00-14:30 Derek Teaney ..... *TBA*
14:30-15:00 Paul Romatschke..... *Strong coupling far-from-equilibrium thermalization for 'nuclei'*
15:00-15:30 Naoto Tanji..... *Quark production in classical statistical field theory*

15:30-16:00 **COFFEE BREAK**

16:00-16:30 Kenji Fukushima..... *Real-time stochastic quantization: Problems and simulations*
16:30-17:00 Vicenze Greco..... *Thermalization, isotropization and elliptic flow from nonequilibrium initial conditions with a saturation scale*
17:00-17:45 Moderated Discussions..... *(Juergen Berges and Francois Gelis)*

18:30-20:00 **WORKSHOP DINNER** @ Brookhaven Center, South Room

---

FRIDAY, APRIL 4

09:00-12:15 Session V. Chair: Larry McLerran

09:00-09:45 Barbara Jacak ..... *Thermalization: An experimentalist's view*
09:45-10:15 Michael Strickland..... *Anisotropic hydrodynamics: Recent progress*
10:15-10:45 Ulrich Heinz ..... *Viscous fluid dynamics for anisotropically expanding fireballs*

10:45-11:15 **COFFEE BREAK**

11:15-11:45 Bjoern Schenke ..... *Geometry and fluctuations in large and small nuclear collision systems*
11:45-12:15 Owe Philipsen ..... *Lattice calculation of a second order transport coefficient of hydrodynamics*

12:15-14:00 **LUNCH**

14:00-16:45 Session VI. Chair: Jean-Paul Blaizot

14:00-14:30 Michal Heller ..... *The approach to hydrodynamics in holographic gauge theories*
14:30-15:00 Edward Shuryak..... *Production and properties of self-interacting string balls and high multiplicity pp/pA collisions*
15:00-15:45 Alfred Mueller ..... *The early stages of ion-ion collisions [blackboard presentation]*

Back to Contents

The Approach to Equilibrium in Strongly Interacting Matter

April 2-4, 2014

Registered Participants

Maximilian Attems	FIAS
Vijay Balasubramanian	University of Pennsylvania
Juergen Berges	Heidelberg University
Jean-Paul Blaizot	CNRS
Kirill Boguslavski	University of Heidelberg
Adam Bzdak	RBRC
Chin-Hao Chen	RBRC
William Christie	BNL
Thomas Epelbaum	IPhT
Stefan Floerchinger	CERN
Hiro Fujii	University of Tokyo
Kenji Fukushima	University of Tokyo
Francois Gelis	CEA Saclay
Vincenzo Greco	University of Catania
Ulrich Heinz	The Ohio State University
Michal Heller	University of Amsterdam
Shengli Huang	Vanderbilt University
Barbara Jacak	Stony Brook University
Yin Jiang	Indiana State University
Dmitri Kharzeev	BNL
Eero Aleksi Kurkela	CERN
Tuomas Lappi	University of Jyvaskyla
Jinfeng Liao	Indiana University / RBRC
Shu Lin	RBRC
Mauricio Martinez Guerrero	The Ohio State University
Larry McLerran	BNL
David Mesterhazy	University of Illinois at Chicago
Akihiko Monnai	RBRC
David Morrison	BNL
Alfred Mueller	Columbia University
Berndt Mueller	BNL
Swagato Mukherjee	BNL
Akira Ohnishi	Yukawa Inst for Theoretical Phys, Kyoto Univ
Jan Pawlowski	University of Heidelberg
Owe Philipsen	University of Frankfurt
Rob Pisarski	BNL
Manju Prakash	Independent Worker
Jianwei Qiu	BNL
Paul Romatschke	Univ of Colorado at Boulder
Marco Ruggieri	University of Catania
Radoslaw Ryblewski	Kent State University
Daisuke Sato	RIKEN
Wilke van der Schee	Utrecht University /Perimeter Institute
Bjoern Schenke	BNL
Soeren Schlichting	BNL
Edward Shuryak	Stony Brook University
Denes Sexty	University of Heidelberg
Michael Strickland	Kent State University
Naoto Tanji	RIKEN
Raju Venugopalan	BNL
Bin Wu	IPhT Saclay
Zhangbu Xu	BNL
Yi Yin	University of Illinois
Bin Zhang	Arkansas State University

Back to Contents

RIKEN BNL Research Center Proceedings

Volume 117 – Lattice Meets Experiment 2013: Beyond the Standard Model, December 5-6, 2013 – BNL-103493-2013
Volume 116 – RBRC Scientific Review Committee Meeting, October 31 - November 1, 2013 – BNL-102596-2013
Volume 115 – Jet Quenching at RHIC vs LHC in Light of Recent dAu vs pPb Controls, April 15-17, 2013 – BNL-100766-2013
Volume 114 – The Physics of p↑+A Collisions at RHIC, January 7-9, 2013 – BNL-99107-2013
Volume 113 – Thermal Radiation Workshop, December 5-7, 2012 – BNL-99088-2013
Volume 112 – RBRC Scientific Review Committee Meeting, November 6-8, 2012 – BNL-99621-2013
Volume 111 – Forward Physics at RHIC, July 30-Aug 1, 2012 – BNL-98400-2012
Volume 110 – P- and CP-odd Effects in Hot and Dense Matter, June 25-27, 2012 – BNL-98398-2012
Volume 109 – New Horizons for Lattice Computations with Chiral Fermions, May 14-18, 2012 – BNL-98392-2012
Volume 108 – Hyperon-Hyperon Interactions and Searches for Exotic Di-Hyperons in Nuclear Collisions, February 29 – March 2, 2012 – BNL-97035-2012
Volume 107 – Future Directions in High Energy QCD, October 20-22, 2011 – BNL-98119-2011
Volume 106 – Fluctuations, Correlations and RHIC Low Energy Runs, October 3-5, 2011 – BNL-96514-2011
Volume 105 – Opportunities for Polarized He-3 in RHIC and EIC, September 28-30, 2011 – BNL-96418-2011
Volume 104 – Brookhaven Summer Program on Quarkonium Production in Elementary and Heavy Ion Collisions, June 6-18, 2011 – BNL-96171-2011
Volume 103 – Opportunities for Drell-Yan Physics at RHIC, May 11-13, 2011 – BNL-95236-2011
Volume 102 – Initial State Fluctuations and Final-State Particle Correlations, February 2-4, 2011 – BNL-94704-2011
Volume 101 – RBRC Scientific Review Committee Meeting, October 27-29, 2010 – BNL-94589-2011
Volume 100 – Summer Program on Nucleon Spin Physics, July 14-27, 2010 – BNL-96163-2011
Volume 99 – The Physics of W and Z Bosons, June 24-25, 2010 – BNL-94287-2010
Volume 98 – Saturation, the Color Glass Condensate and the Glasma: What Have We Learned from RHIC? – May 10-12, 2010 – BNL-94271-2010
Volume 97 – RBRC Scientific Review Committee Meeting, October 21-22, 2009 – BNL-90674-2009
Volume 96 – P- and CP-Odd Effects in Hot and Dense Matter, April 26-30, 2010 – BNL-94237-2010
Volume 95 – Progress in High-pT Physics at RHIC, March 17-19, 2010 – BNL-94214-2010
Volume 94 – Summer Program on Nucleon Spin Physics at LBL, June 1-12, 2009
Volume 93 – PHENIX Spinfest School 2009 at BNL - July 1-31, 2009 – BNL-90343-2009
Link: PHENIXSpinfestSchool2009@BNL
Volume 92 – PKU-RBRC Workshop on Transverse Spin Physics, June 30 - July 4, 2008, Beijing, China – BNL-81685-2008
Volume 91 – RBRC Scientific Review Committee Meeting, November 17-18, 2008 – BNL-81556-2008
Volume 90 – PHENIX Spinfest School 2008 at BNL, August 4-8, 2008 – BNL-81478-2008
Volume 89 – Understanding QGP through Spectral Functions and Euclidean Correlators, April 23-25, 2008 – BNL-81318-2008
Volume 88 – Hydrodynamics in Heavy Ion Collisions and QCD Equation of State, April 21-22, 2008 – BNL-81307-2008
Volume 87 – RBRC Scientific Review Committee Meeting, November 5-6, 2007 – BNL-79570-2007
Volume 86 – Global Analysis of Polarized Parton Distributions in the RHIC Era, October 8, 2007 – BNL-79457-2007
Volume 85 – Parity-Violating Spin Asymmetries at RHIC-BNL, April 26-27, 2007 – BNL-79146-2007
Volume 84 – Domain Wall Fermions at Ten Years, March 15-17, 2007 – BNL 77857-2007
Volume 83 – QCD in Extreme Conditions, July 31 - August 2, 2006 – BNL-76933-2006
Volume 82 – RHIC Physics in the Context of the Standard Model, June 18-23, 2006 – BNL-76863-2006

Back to Contents

Volume 81 – Parton Orbital Angular Momentum (Joint RBRC/University of New Mexico Workshop) February 24-26, 2006 – BNL-75937-2006
Volume 80 – Can We Discover the QCD Critical Point at RHIC?, March 9-10, 2006 – BNL-75692-2006
Volume 79 – Strangeness in Collisions, February 16-17, 2006 – BNL-79763-2008
Volume 78 – Heavy Flavor Productions and Hot/Dense Quark Matter, December 12-14, 2005 – BNL-76915-2006
Volume 77 – RBRC Scientific Review Committee Meeting, October 10-12, 2005 – BNL-52649-2005
Volume 76 – Odderon Searches at RHIC, September 27-29, 2005 – BNL-75092-2005
Volume 75 – Single Spin Asymmetries, June 1-3, 2005 – BNL-74717-2005
Volume 74 – RBRC QCDOC Computer Dedication and Symposium on RBRC QCDOC, May 26, 2005 – BNL-74813-2005
Volume 73 – Jet Correlations at RHIC, March 10-11, 2005 – BNL-73910-2005
Volume 72 – RHIC Spin Collaboration Meetings XXXI, XXXII, XXXIII – BNL-73866-2005
Volume 71 – Classical and Quantum Aspects of the Color Glass Condensate – BNL-73793-2005
Volume 70 – Strongly Coupled Plasmas: Electromagnetic, Nuclear & Atomic – BNL-73867-2005
Volume 69 – RBRC Scientific Review Committee Meeting, November 16-17, 2004 – BNL-73546-2004
Volume 68 – Workshop on the Physics Programme of the RBRC and UKQCD QCDOC Machines – BNL-73604-2004
Volume 67 – High Performance Computing with BlueGene/L and QCDOC Architectures, October 27-28, 2004
Volume 66 – RHIC Spin Collaboration Meeting XXIX, Torino Italy – BNL-73534-2004
Volume 65 – RHIC Spin Collaboration Meetings XXVII, XXVIII, XXX – BNL-73506-2004
Volume 64 – Theory Summer Program on RHIC Physics – BNL-73263-2004
Volume 63 – RHIC Spin Collaboration Meetings XXIV, XXV, XXVI – BNL-72397-2004
Volume 62 – New Discoveries at RHIC, May 14-15, 2004 – BNL-72391-2004
Volume 61 – RIKEN-TODAI Mini Workshop on "Topics in Hadron Physics at RHIC", March 23-24, 2004 – BNL-72336-2004
Volume 60 – Lattice QCD at Finite Temperature and Density – BNL-72083-2004
Volume 59 – RHIC Spin Collaboration Meetings XXI, XXII, XXIII – BNL-72382-2004
Volume 58 – RHIC Spin Collaboration Meeting XX – BNL-71900-2004
Volume 57 – High pt Physics at RHIC, December 2-6, 2003 – BNL-72069-2004
Volume 56 – RBRC Scientific Review Committee Meeting, November 20-21, 2003 – BNL-71899-2003
Volume 55 – Collective Flow and QGP Properties – BNL-71898-2003
Volume 54 – RHIC Spin Collaboration Meetings XVII, XVIII, XIX – BNL-71751-2003
Volume 53 – Theory Studies for Polarized pp Scattering – BNL-71747-2003
Volume 52 – RIKEN School on QCD "Topics on the Proton" – BNL-71694-2003
Volume 51 – RHIC Spin Collaboration Meetings XV, XVI – BNL-71539-2003
Volume 50 – High Performance Computing with QCDOC and BlueGene – BNL-71147-2003
Volume 49 – RBRC Scientific Review Committee Meeting, November 21-22, 2002 – BNL-52679
Volume 48 – RHIC Spin Collaboration Meeting XIV – BNL-71300-2003
Volume 47 – RHIC Spin Collaboration Meetings XII, XIII – BNL-71118-2003
Volume 46 – Large-Scale Computations in Nuclear Physics using the QCDOC – BNL-52678
Volume 45 – Summer Program: Current and Future Directions at RHIC – BNL-71035
Volume 44 – RHIC Spin Collaboration Meetings VIII, IX, X, XI – BNL-71117-2003
Volume 43 – RIKEN Winter School – Quark-Gluon Structure of the Nucleon and QCD – BNL-52672
Volume 42 – Baryon Dynamics at RHIC – BNL-52669
Volume 41 – Hadron Structure from Lattice QCD – BNL-52674
Volume 40 – Theory Studies for RHIC-Spin – BNL-52662
Volume 39 – RHIC Spin Collaboration Meeting VII – BNL-52659

Back to Contents

Volume 38 – RBRC Scientific Review Committee Meeting, November 29-30, 2001 – BNL-52649
Volume 37 – RHIC Spin Collaboration Meeting VI (Part 2) – BNL-52660
Volume 36 – RHIC Spin Collaboration Meeting VI – BNL-52642
Volume 35 – RIKEN Winter School – Quarks, Hadrons and Nuclei – QCD Hard Processes and the Nucleon Spin – BNL-52643
Volume 34 – High Energy QCD: Beyond the Pomeron – BNL-52641
Volume 33 – Spin Physics at RHIC in Year-1 and Beyond – BNL-52635
Volume 32 – RHIC Spin Physics V – BNL-52628
Volume 31 – RHIC Spin Physics III & IV Polarized Partons at High Q^2 Region – BNL-52617
Volume 30 – RBRC Scientific Review Committee Meeting, September 28-29, 2000 – BNL-52603
Volume 29 – Future Transversity Measurements – BNL-52612
Volume 28 – Equilibrium & Non-Equilibrium Aspects of Hot, Dense QCD – BNL-52613
Volume 27 – Predictions and Uncertainties for RHIC Spin Physics & Event Generator for RHIC Spin Physics III – Towards Precision Spin Physics at RHIC – BNL-52596
Volume 26 – Circum-Pan-Pacific RIKEN Symposium on High Energy Spin Physics – BNL-52588
Volume 25 – RHIC Spin – BNL-52581
Volume 24 – Physics Society of Japan Biannual Meeting Symposium on QCD Physics at RIKEN BNL Research Center – BNL-52578
Volume 23 – Coulomb and Pion-Asymmetry Polarimetry and Hadronic Spin Dependence at RHIC Energies – BNL-52589
Volume 22 – OSCAR II: Predictions for RHIC – BNL-52591
Volume 21 – RBRC Scientific Review Committee Meeting, May 27-28, 1999 – BNL-52568
Volume 20 – Gauge-Invariant Variables in Gauge Theories – BNL-52590
Volume 19 – Numerical Algorithms at Non-Zero Chemical Potential – BNL-52573
Volume 18 – Event Generator for RHIC Spin Physics – BNL-52571
Volume 17 – Hard Parton Physics in High-Energy Nuclear Collisions – BNL-52574
Volume 16 – RIKEN Winter School - Structure of Hadrons - Introduction to QCD Hard Processes – BNL-52569
Volume 15 – QCD Phase Transitions – BNL-52561
Volume 14 – Quantum Fields In and Out of Equilibrium – BNL-52560
Volume 13 – Physics of the 1 Teraflop RIKEN-BNL-Columbia QCD Project First Anniversary Celebration – BNL-66299
Volume 12 – Quarkonium Production in Relativistic Nuclear Collisions – BNL-52559
Volume 11 – Event Generator for RHIC Spin Physics – BNL-66116
Volume 10 – Physics of Polarimetry at RHIC – BNL-65926
Volume 9 – High Density Matter in AGS, SPS and RHIC Collisions – BNL-65762
Volume 8 – Fermion Frontiers in Vector Lattice Gauge Theories – BNL-65634
Volume 7 – RHIC Spin Physics – BNL-65615
Volume 6 – Quarks and Gluons in the Nucleon – BNL-65234
Volume 5 – Color Superconductivity, Instantons and Parity (Non?)-Conservation at High Baryon Density – BNL-65105
Volume 4 – Inauguration Ceremony and Non-Equilibrium Many Body Dynamics – BNL-64912
Volume 3 – Hadron Spin-Flip at RHIC Energies – BNL-64724
Volume 2 – Perturbative QCD as a Probe of Hadron Structure – BNL-64723
Volume 1 – Open Standards for Cascade Models for RHIC – BNL-64722

Back to Contents

Li Keran

Nuclei as heavy as bulls
Through collision
Generate new states of matter.
T.D. Lee

©CCASTA

Organizers

Juergen Berges (Heidelberg U)
Jean-Paul Blaizot (Saclay)
Francois Gelis (Saclay)
Jinfeng Liao (IU/RBRC)
Raju Venugopalan (BNL)

RIKEN BNL Research Center
Bldg. 510A, Brookhaven National Laboratory
Upton, NY 11973-5000, USA

April 2014